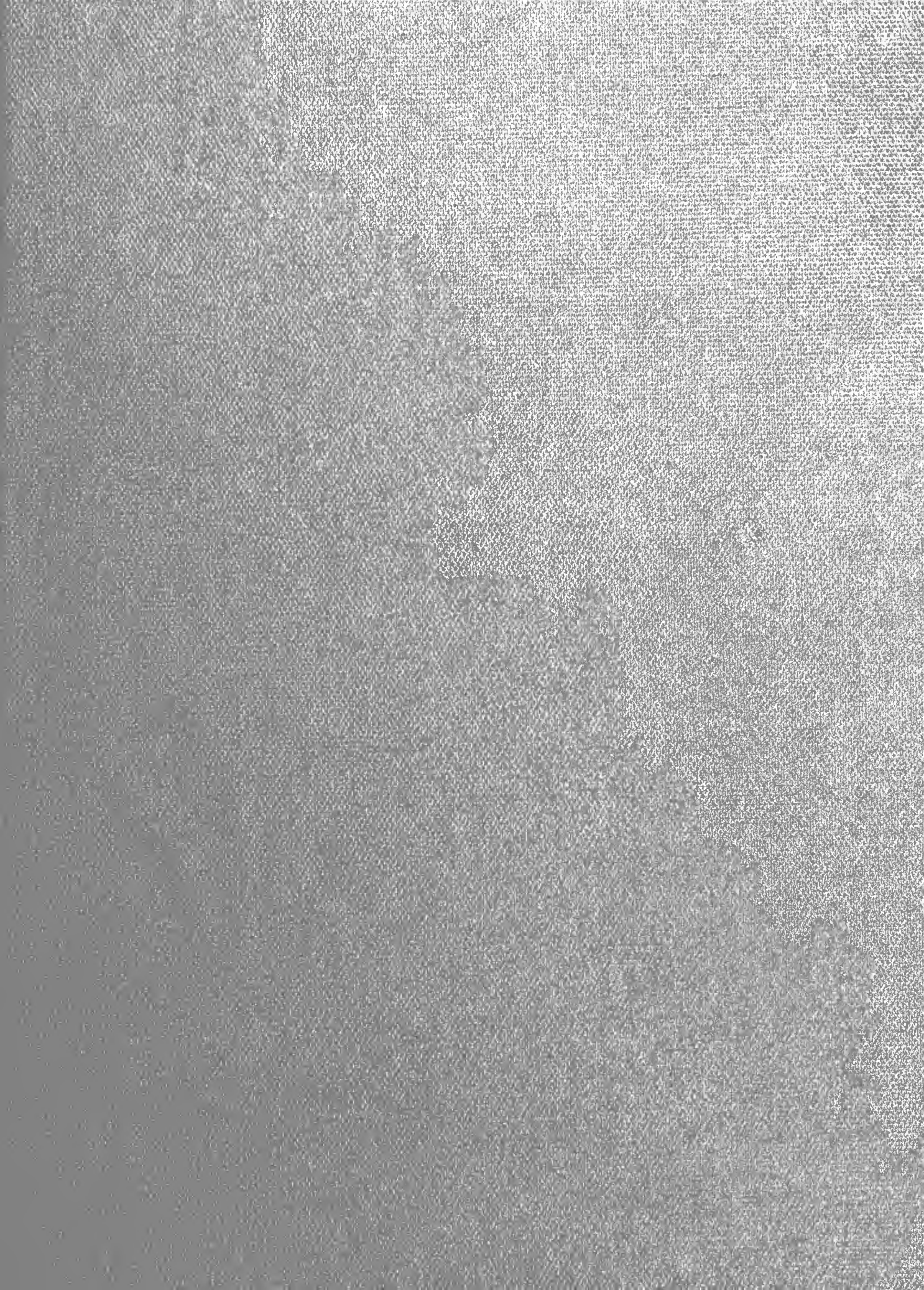

Volume 184 Number 1

THE BIOLOGICAL BULLETIN

FEBRUARY, 1993

Published by the Marine Biological Laboratory

THE BIOLOGICAL BULLETIN

PUBLISHED BY
THE MARINE BIOLOGICAL LABORATORY

FEBRUARY, 1993

Printed and Issued by
LANCASTER PRESS, Inc.
3575 HEMPLAND ROAD
LANCASTER, PA

THE BIOLOGICAL BULLETIN

THE BIOLOGICAL BULLETIN is published six times a year by the Marine Biological Laboratory, MBL Street, Woods Hole, Massachusetts 02543.

Subscriptions and similar matter should be addressed to Subscription Manager, THE BIOLOGICAL BULLETIN, Marine Biological Laboratory, Woods Hole, Massachusetts 02543. Single numbers, $35.00. Subscription per volume (three issues), $87.50 ($175.00 per year for six issues).

Communications relative to manuscripts should be sent to Michael J. Greenberg, Editor-in-Chief, or Pamela L. Clapp, Managing Editor, at the Marine Biological Laboratory, Woods Hole, Massachusetts 02543. Telephone: (508) 548-3705, ext. 428. FAX: 508-540-6902. E-mail: pamcl@hoh.mbl.edu.

POSTMASTER: Send address changes to THE BIOLOGICAL BULLETIN, Marine Biological Laboratory, Woods Hole, MA 02543.

Second-class postage paid at Woods Hole, MA, and additional mailing offices.
ISSN 0006-3185

INSTRUCTIONS TO AUTHORS

The Biological Bulletin accepts outstanding original research reports of general interest to biologists throughout the world. Papers are usually of intermediate length (10–40 manuscript pages). A limited number of solicited review papers may be accepted after formal review. A paper will usually appear within four months after its acceptance.

Very short, especially topical papers (less than 9 manuscript pages including tables, figures, and bibliography) will be published in a separate section entitled "Research Notes." A Research Note in *The Biological Bulletin* follows the format of similar notes in *Nature*. It should open with a summary paragraph of 150 to 200 words comprising the introduction and the conclusions. The rest of the text should continue on without subheadings, and there should be no more than 30 references. References should be referred to in the text by number, and listed in the Literature Cited section in the order that they appear in the text. Unlike references in *Nature*, references in the Research Notes section should conform in punctuation and arrangement to the style of recent issues of *The Biological Bulletin*. Materials and Methods should be incorporated into appropriate figure legends. See the article by Lohmann *et al.* (October 1990, Vol. **179:** 214–218) for sample style. A Research Note will usually appear within two months after its acceptance.

The Editorial Board requests that regular manuscripts conform to the requirements set below; those manuscripts that do not conform will be returned to authors for correction before review.

1. ***Manuscripts.*** Manuscripts, including figures, should be submitted in triplicate. (Xerox copies of photographs are not acceptable for review purposes.) The original manuscript must be typed in no smaller than 12 pitch, using double spacing (*including* figure legends, footnotes, bibliography, etc.) on one side of 16- or 20-lb. bond paper, 8½ by 11 inches. Please, no right justification. Manuscripts should be proofread carefully and errors corrected legibly in black ink. Pages should be numbered consecutively. Margins on all sides should be at least 1 inch (2.5 cm). Manuscripts should conform to the *Council of Biology Editors Style Manual,* 5th Edition (Council of Biology Editors, 1983) and to American spelling. Unusual abbreviations should be kept to a minimum and should be spelled out on first reference as well as defined in a footnote on the title page. Manuscripts should be divided into the following components: Title page, Abstract (of no more than 200 words), Introduction, Materials and Methods, Results, Discussion, Acknowledgments, Literature Cited, Tables, and Figure Legends. In addition, authors should supply a list of words and phrases under which the article should be indexed.

2. ***Title page.*** The title page consists of: a condensed title or running head of no more than 35 letters and spaces, the manuscript title, authors' names and appropriate addresses, and footnotes listing present addresses, acknowledgments or contribution numbers, and explanation of unusual abbreviations.

3. ***Figures.*** The dimensions of the printed page, 7 by 9 inches, should be kept in mind in preparing figures for publication. We recommend that figures be about 1½ times the linear dimensions of the final printing desired, and that the ratio of the largest to the smallest letter or number and of the thickest to the thinnest line not exceed 1:1.5. Explanatory matter generally should be included in legends, although axes should always be identified on the illustration itself. Figures should be prepared for reproduction as either line cuts or halftones. Figures to be reproduced as line cuts should be unmounted glossy photographic reproductions or drawn in black ink on white paper, good-quality tracing cloth or plastic, or blue-lined coordinate paper. Those to be reproduced as halftones should be mounted on board, with both designating numbers or letters and scale bars affixed directly to the figures. All figures should be numbered in consecutive order, with no distinction between text and plate figures. The author's name and an arrow indicating orientation should appear on the reverse side of all figures.

4. ***Tables, footnotes, figure legends, etc.*** Authors should follow the style in a recent issue of *The Biological Bulletin* in preparing table headings, figure legends, and the like. Because of the high cost of setting tabular material in type, authors are asked to limit such material as much as possible. Tables, with their headings and footnotes, should be typed on separate sheets, numbered with consecutive Roman numerals, and placed after

CONTENTS

No. 3, JUNE 1993

REVIEW

DEVELOPMENT AND REPRODUCTION

BIOCHEMISTRY

PHYSIOLOGY

RESEARCH NOTE

VIEWS AND DISCUSSION

the Literature Cited. Figure legends should contain enough information to make the figure intelligible separate from the text. Legends should be typed double spaced, with consecutive Arabic numbers, on a separate sheet at the end of the paper. Footnotes should be limited to authors' current addresses, acknowledgments or contribution numbers, and explanation of unusual abbreviations. All such footnotes should appear on the title page. Footnotes are not normally permitted in the body of the text.

5. ***Literature cited.*** In the text, literature should be cited by the Harvard system, with papers by more than two authors cited as Jones *et al.*, 1980. Personal communications and material in preparation or in press should be cited in the text only, with author's initials and institutions, unless the material has been formally accepted and a volume number can be supplied. The list of references following the text should be headed Literature Cited, and must be typed double spaced on separate pages, conforming in punctuation and arrangement to the style of recent issues of *The Biological Bulletin*. Citations should include complete titles and inclusive pagination. Journal abbreviations should normally follow those of the U. S. A. Standards Institute (USASI), as adopted by BIOLOGICAL ABSTRACTS and CHEMICAL ABSTRACTS, with the minor differences set out below. The most generally useful list of biological journal titles is that published each year by BIOLOGICAL ABSTRACTS (BIOSIS List of Serials; the most recent issue). Foreign authors, and others who are accustomed to using THE WORLD LIST OF SCIENTIFIC PERIODICALS, may find a booklet published by the Biological Council of the U.K. (obtainable from the Institute of Biology, 41 Queen's Gate, London, S.W.7, England, U.K.) useful, since it sets out the WORLD LIST abbreviations for most biological journals with notes of the USASI abbreviations where these differ. CHEMICAL ABSTRACTS publishes quarterly supplements of additional abbreviations. The following points of reference style for THE BIOLOGICAL BULLETIN differ from USASI (or modified WORLD LIST) usage:

A. Journal abbreviations, and book titles, all underlined (for *italics*)

B. All components of abbreviations with initial capitals (not as European usage in WORLD LIST *e.g., J. Cell. Comp. Physiol.* NOT *J. cell. comp. Physiol.*)

C. *All* abbreviated components must be followed by a period, whole word components *must not* (*i.e., J. Cancer Res.*)

D. Space between all components (*e.g., J. Cell. Comp. Physiol.*, not *J.Cell.Comp.Physiol.*)

E. Unusual words in journal titles should be spelled out in full, rather than employing new abbreviations invented by the author. For example, use *Rit Vísindafjélags Islendinga* without abbreviation.

F. All single word journal titles in full (*e.g., Veliger, Ecology, Brain*).

G. The order of abbreviated components should be the same as the word order of the complete title (*i.e., Proc.* and *Trans.* placed where they appear, not transposed as in some BIOLOGICAL ABSTRACTS listings).

H. A few well-known international journals in their preferred forms rather than WORLD LIST or USASI usage (*e.g., Nature, Science, Evolution* NOT *Nature, Lond., Science, N.Y.; Evolution, Lancaster, Pa.*)

6. ***Reprints, page proofs, and charges.*** Authors receive their first 100 reprints (without covers) free of charge. Additional reprints may be ordered at time of publication and normally will be delivered about two to three months after the issue date. Authors (or delegates for foreign authors) will receive page proofs of articles shortly before publication. They will be charged the current cost of printers' time for corrections to these (other than corrections of printers' or editors' errors). Other than these charges for authors' alterations, *The Biological Bulletin* does not have page charges.

Reference: *Biol. Bull.* **184**: 1–5. (February, 1993)

Contact Inhibition: Also a Control for Cell Proliferation in Unicellular Algae?

EDUARDO COSTAS, ANGELES AGUILERA, SONSOLES GONZÁLEZ-GIL, AND VICTORIA LÓPEZ-RODAS

Genética Producción Animal, Facultad de Veterinaria, Universidad Complutense, Madrid, Spain

Abstract. According to traditional views, the proliferation of unicellular algae is controlled primarily by environmental conditions. But as in mammalian cells, other biological mechanisms, such as growth factors, cellular aging, and contact inhibition, might also control algal proliferation. Here we ask whether contact inhibition regulates growth in several species of unicellular algae as it does in mammalian cells. Laboratory cultures of the dinoflagellate *Prorocentrum lima* (Ehrenberg) Dodge show contact inhibition at low cell density, so this would be an autocontrol mechanism of cell proliferation that could also act in natural populations of *P. lima*. But, *Synechocystis spp.*, *Phaeodactylum tricornutum* (Bohlin), *Skeletonema costatum* (Greville), and *Tetraselmis spp.* do not exhibit contact inhibition in laboratory cultures because they are able to grow at high cellular density. Apparently their growth is limited by nutrient depletion or catabolite accumulation instead of contact inhibition. *Spirogyra insignis* (Hassall) Kutz, *Prorocentrum triestinum* Schiller, and *Alexandrium tamarense* (Halim) Balech show a complex response, as they are able to grow in both low and high cell density medium. These results suggest that contact inhibition is more adaptative in benthic unicellular algae.

Introduction

Environmental conditions (light, nutrients, temperature, and turbulence) are thought to be the main controls of proliferation in unicellular algae. Thus, axenic cultures of algae progressively increase in cell number until division slows due to nutrient depletion, the shadowing of some cells by others, or metabolite accumulation. But other mechanisms could play an important role in autocontrol of algal proliferation. In this respect, endogenous rhythms have been proposed as pacemakers of algal proliferation (reviewed by Edmunds, 1988). Also, mucilage production has been considered a mechanism of biological autocontrol in unicellular algae (Margalef, 1989). Recently, Wyatt and Reguera (1989) proposed that the onset of phytoplankton blooms and red tides are due to a mechanism of ecological autocontrol acting at the Gaian level.

Several biological mechanisms that control the cell division cycle in mammalian cells have recently been elucidated. They are based on growth factors, genes, and gene products that respond to growth factors (Baserga *et al.*, 1986; Goustin *et al.*, 1986; Cantley *et al.*, 1991; North, 1991). Although these mechanisms have been interpreted as adaptations for regulating cellular proliferation in multicellular organisms, they are common to all eukaryotic cells, even regulating the cleavage of zygotes (Murray and Kirschner, 1989). Recently, we have proven that the cell division cycle in unicellular algae from different phyla (Cyanophyceae, Dinophyceae, Bacillarophyceae, and Chlorophyceae) are regulated by growth factors just as are mammalian cells (Costas and López-Rodas, 1991a; López-Rodas *et al.*, 1991).

In addition to regulation by growth factors, other mechanisms control the cell proliferation of mammalian cells. For example, some cells are genetically programmed to degenerate and die of old age after a determined number of generations. Also, the unicellular algae *Spirogyra insignis* (Conjugatophyceae) undergoes cellular aging as do mammalian cells (Costas and López-Rodas, 1991b).

In mammals, another important regulator of cellular proliferation is contact inhibition. Mammalian cells grow in monolayers, colonizing the bottom of culture flasks, but they only increase until their growth is inhibited by contact with neighboring cells. Various mechanisms seem to be involved in this complex phenomenon, from growth

Received 26 March 1992; accepted 23 October 1992.

Table I

Characteristics of the species used

Species	Phyla	Characteristic
Synechocystis spp.	Cyanobacteria	unicellular, planktonic
Prorocentrum lima (Ehrenberg) Dodge	Dinophyceae	unicellular, benthic
Prorocentrum triestinum Schiller	Dinophyceae	unicellular, swimming
Alexandrium tamarense (Halim) Balech	Dinophyceae	unicellular, swimming
Tetraselmis spp.	Praxinophyceae	unicellular, swimming
Skeletonema costatum (Greville)	Bacillarophyceae	cenobial filamentous, planktonic
Phaeodactylum tricornutum (Bohlin)	Bacillarophyceae	unicellular, benthic
*Spirogyra insignis** (Hasak) Kutz	Conjugatophyceae	cenobial filamentous, benthic

* *Spirogyra insignis* grows in cenobial filaments anchored to the bottom of the flask by the distal cell. Every cell of the filament can divide (more detail in Costas and López-Rodas, 1991b).

factor competence to cell shape changes related to intercell contacts (review Alberts *et al.*, 1983).

This paper attempts to determine whether contact inhibition can limit the growth of unicellular algae, as is the case in mammalian cells. Several species of unicellular algae from different phyla are analyzed in a combined ecological and evolutionary approach.

Materials and Methods

Cultures

Isolation and culture procedures for the species used were previously described in detail (Costas, 1990; Costas and López-Rodas, 1991a, b, c), so only a brief description is provided here.

The characteristics of the eight species employed are summarized in Table I. Freshwater and marine species were grown, respectively, in Petri dishes with 20 ml of WC medium or f/2 medium (Guillard, 1975), at 22.5 $\pm$ 0.5°C and 80 μmol m^{-2} s^{-1}, 12:12 h light-dark cycle.

Cultures were treated with 150 mg l^{-1} penicillin and 100 mg l^{-1} streptomycin and were, therefore, axenic. Before the experiments were performed, the cultures were tested for the presence of bacteria using epifluorescence procedures as previously described (Costas, 1990). The possible effects of antibiotics on algal proliferation were obviated, because the antibiotic treatment was applied two months before the experiments took place, so the cultures were grown under axenic conditions.

Cultures were maintained by serial transfers of a 500 $\pm$ 30 cell inoculum to fresh medium once every day. The cells grew exponentially for 20–30 days, and then the cultures showed density-dependent inhibition of growth. We determined that a culture reached saturation when its growth rate approached zero and its cell density reached the maximum. Saturation was easily detected because, growth rates and cell densities were determined daily. The experiments took place three days after the cultures were saturated.

Experimental Design

Many factors act in the cell density-dependent inhibition of growth. In this investigation, we attempted to analyze whether contact inhibition also takes part in this process. Clonal cultures of each species were grown until saturation density was reached, and then the following two experiments were performed.

Experiment 1: Cells at saturation density growing in fresh medium. All the cells of each saturated culture were collected (by centrifugation at 1000 rpm for 20 min), and resuspended in the same quantity of fresh medium. In this way we obtained a culture in fresh medium with saturated density of cells. Growth rates and cellular densities were measured during the five following days. Five replicates were performed for each species.

Experiment 2: Cells at low density growing in saturated medium. In the second experiment, the saturated medium, after centrifugation, was filtered through a 0.22 μm pore filter to produce a completely axenic, saturated medium that was free of cells. In this saturated, cell-free medium, a centrifuged inoculum of the same species growing exponentially, was cultured. Growth rates and cellular densities were measured during the five following days. Five replicates were performed for each species.

If inhibition of growth by contact inhibition and other factors are mutually exclusive, then contact inhibition of growth can be detected by this system, according to the following logic. If a species exhibits contact inhibition, then it will probably be able to grow in Experiment 2, but it won't be able to proliferate in Experiment 1. On the contrary, if the growth inhibition is due to other factors (nutrient depletion or catabolite accumulation), then it will probably be able to grow in Experiment 1 but not in Experiment 2. But, if other factors (*i.e.*, soluble factors), as well as contact inhibition affect growth, then the simple two possibility choice won't happen.

To determine whether contact inhibition is a factor in growth inhibition of those algae that grow in monolayers, the following experiment was performed; *i.e.*, the same method used to detect contact inhibition in mammalian cells was applied to algae. The cells from half a Petri dish were removed mechanically from each saturated culture

Table II

Growth rates and percentage increase of cell density in fresh medium at saturation density and in saturated medium at low density

	Exponential growth-rates	Saturated growth-rates	Cells at saturation density in fresh medium: Growth rates	Cells at saturation density in fresh medium: % increase cell density	Cells at low density in saturated medium: Growth rates	Cells at low density in saturated medium: % increase cell density
Synechocystis spp.	0.79 ± 0.01	−0.07 ± 0.006	0.49 ± 0.06**	64 ± 5%	−0.04 ± 0.01**	−4 ± 1%
Prorocentrum lima	0.38 ± 0.03	0.01 ± 0.01	0.03 ± 0.02**	2 ± 1%	0.39 ± 0.07**	47 ± 2%
Prorocentrum triestinum	0.91 ± 0.05	0.01 ± 0.01	0.29 ± 0.02**	33 ± 1%	0.07 ± 0.02**	7 ± 2%
Alexandrium tamarense	0.43 ± 0.03	−0.03 ± 0.02	0.12 ± 0.05*	12 ± 5%	0.07 ± 0.02*	7 ± 1%
Tetraselmis spp.	0.96 ± 0.05	−0.04 ± 0.01	0.87 ± 0.07**	138 ± 6%	0.01 ± 0.01**	1 ± 1%
Skeletonema costatum	1.01 ± 0.07	−0.02 ± 0.03	0.58 ± 0.03**	78 ± 3%	−0.07 ± 0.01**	−6 ± 1%
Phaeodactilum tricornutum	0.88 ± 0.04	0.02 ± 0.01	0.52 ± 0.01**	68 ± 2%	−0.03 ± 0.02**	−2 ± 3%
Spirogyra insignis	0.94 ± 0.05	0.03 ± 0.02	0.18 ± 0.05**	19 ± 4%	0.68 ± 0.05**	97 ± 6%

* Statistically no significant differences were found ($P > 0.05$).

** Statistically significant differences ($P < 0.01$) were found between growth rates of Exp. 1 and Exp. 2.

sample of monolayer species. If contact inhibition exists, the cells on the full side will continue growing into the cell-free half of the dish. Five replicates were performed in each case. A continuous recording by video microscopy helped us to evaluate this experiment.

Control of handling effects

Because some dinoflagellates are very sensitive to shear stress, we performed the following two preliminary experiments to determine whether manipulation would have detectable effects on the analyzed species.

(a) Exponentially growing cells of each species were collected by centrifugation at 1000 rpm for 20 min and resuspended in the same quantity of fresh medium. Their growth rates (5 replicates of each species) were measured during the following five days and compared with the growth rates of uncentrifuged exponentially growing controls (5 replicates of each species). ANOVA analysis showed no significant differences ($P > 0.05$) between growth rates of centrifuged and uncentrifuged cells. Furthermore, the number of dead cells was estimated by the yellow eosine exclusion procedure (more details in Costas, 1986; González-Chavarri, 1991), and ANOVA showed no significant differences ($P > 0.05$) in the rate of cell death between centrifuged and uncentrifuged cells.

(b) A similar procedure was employed with saturated cells, and the same results were obtained; (*i.e.*, there were no significant differences ($P > 0.05$) between centrifuged and uncentrifuged cells). More details about the procedures used to control the effects of handling are set out in Costas (1986) and González-Chavarri (1991).

Table III

Growth rates of Prorocentrum lima *and* Spirogyra insignis *after cells were mechanically removed from half a Petri dish*

	Border where cells had been removed	Zone where cells had not been removed	F
Prorocentrum lima	0.31 ± 0.07	0.01 ± 0.01	$P < 0.01$
Spirogyra insignis	0.47 ± 0.03	0.13 ± 0.02	$P < 0.01$

Experimental evaluation

Once an experiment was initiated for each of the five replicates, both the mean growth rates (during the subsequent five days) and the percentage of cell density increase (during the subsequent 24 h) were determined. Cell density was estimated as the number of cells per square or cubic centimeter in monolayer or suspension cultures, respectively. The number of cells in each culture was determined by counting samples in a hemocytometer. The number of samples counted was determined according to the mean progressive technique (Williams, 1977) to obtain 95% accuracy.

Growth rates were calculated as doublings per day:

$$dd^{-1} = 1/\mathrm{Ln}2\ \mathrm{Ln}(Nt/No)/t,$$

Where Nt = cells at time t; No = cells at time 0; and t = number of days between times t and 0 (more detail in Costas, 1990).

Results and Discussion

Growth inhibition of saturated cultures of unicellular algae is a complex process, influenced by various factors, such as nutrient depletion, catabolite accumulation, shading effects, and possibly by contact inhibition. Because these factors do not act independently, their inter-

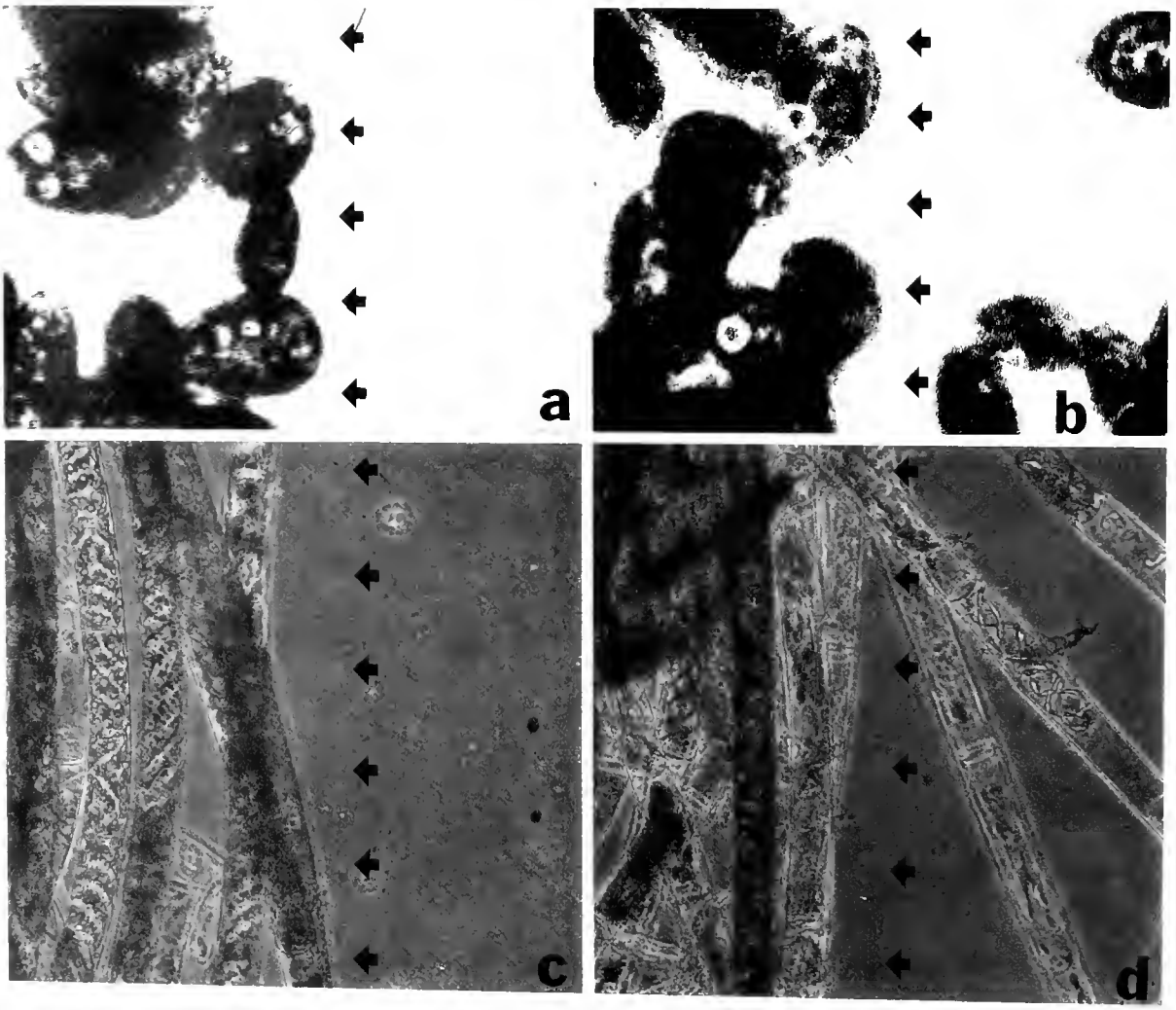

Figure 1. Growth of *Prorocentrum lima* and *Spirogyra insignis* when cells were mechanically removed from half a Petri dish. The arrows represent the border produced in the experiment. Only the cells bordering the cell-free zone were able to grow. (a) Saturated *P. lima* culture at the time of removal. (b) *P. lima* culture 72 h after the removal. New cells have only proliferated into the open half of the plate. (c) Saturated *S. insignis* culture at the time of removal. (d) *S. insignis* culture 72 h after the removal. New cells have only proliferated into the free half of the plate.

actions complicate a precise evaluation of the relative importance of each. Thus, our experimental design was aimed only at detecting whether contact inhibition takes part in cell dependent inhibition of growth.

Table II summarizes the growth rates and the percentage of cell density increases in both fresh and saturated culture media. Apparently, the dinoflagellate *P. lima* showed contact inhibition of growth. Both the growth rates and the cell densities of Experiments 1 and 2 were significantly different ($P < 0.01$). *P. lima* cells were not able to grow at saturation density in fresh medium (Experiment 1), but their growth started again in saturated medium when their cell density decreased (Experiment 2).

In contrast, *Synechocystis spp., Phaeodactilum tricornutum, Skeletonema costatum* and *Tetraselmis spp.* did not exhibit contact inhibition. In all the cases, statistically significant differences ($P < 0.01$) were detected between both the growth rates and the cell densities of Experiments 1 and 2. Apparently, their growth was limited by nutrient depletion or catabolite accumulation; thus they could proliferate at high cellular density in fresh medium (Experiment 1), but were not able to grow in saturated medium at low cell density (Experiment 2).

Contact inhibition of growth may be an important mechanism in *Spirogyra insignis*. Although this species grew slowly at saturation density in fresh medium (Ex-

periment 1), its growth was significantly increased ($P > 0.01$) at low density in saturated medium (Experiment 2). So, in *S. insignis*, the contact inhibition component seems to prevail because proliferation is faster in a saturated medium with low cell density than in fresh medium with high cell density.

In *Prorocentrum triestinum*, however, a nutrient dependent inhibition or catabolite accumulation seemed to be more important than contact inhibition. *P. triestinum* was able to grow in both experiments, although its growth in fresh medium at high cellular density was significantly ($P > 0.01$) faster than that in saturated medium at low cell density. In *Alexandrium tamarense*, all of the factors seemed to slow down proliferation. *A. tamarense* cells were scarcely able to grow in either experiment.

The cells of *P. lima* and *S. insignis* were mechanically removed from half a Petri dish, and the resulting growth rates are summarized in Table III. In agreement with previous experiments, the growth of *P. lima* and *S. insignis* seemed to be inhibited by a contact inhibition mechanism. In particular, only the cells bordering the cell-free zone were able to grow (Fig. 1). This experiment, which employs the traditional method of detecting contact inhibition in mammalian cells (Alberts *et al.*, 1983), supports the hypothesis that contact inhibition takes place in the growth inhibition of *P. lima* and *S. insignis* saturated cultures.

Only two of the three benthic species analyzed seemed to exhibit contact inhibition. These results suggest that contact inhibition is a more adaptative mechanism in benthic unicellular algae.

Contact inhibition is usually thought of as a mechanism developed by animal cells to limit cell division. The results obtained in these experiments suggest an alternative interpretation. The dinoflagellates, which could be considered the earliest group of protist, but which are also far removed from actual eukaryotes (Dodge, 1955; Herzog *et al.*, 1984; Costas and Goyanes, 1988), have developed contact inhibition, thereby suggesting that such a mechanism had already been developed by unicellular organisms in an early era, probably as an autocontrol mechanism regulating natural populations. Nevertheless, contact inhibition has also evolved in the Conjugatophyceae (a recent group of higher algae that are phylogenetically far removed from dinoflagellates), suggesting that such mechanisms may have been developed independently in phylogenetically different groups of unicellular organisms.

Acknowledgments

Supported by DGICYT grants IN89-0163 and PS89-0014.

Literature Cited

Alberts, B., D. Bray, J. Lewis, M. Raff, K. Roberts, and J. D. Watson. 1983. *Molecular Biology of the Cell* Garland Publishing, New York.

Baserga, R., L. Kaczmarek, B. Calabretta, R. Battini, and S. Ferrari. 1986. Cell cycle genes as potential oncogenes. Pp. 3–12 in *Cell Cycle and Oncogenes*, W. Tanner and D. Gallwitz, eds. Springer–Verlag, New York.

Cantley, L. C., K. R. Auger, C. Carpenter, B. Duckworth, A. Graciani, R. Kapeller, and S. Soltoff. 1991. Oncogenes and signal transduction. *Cell* **64**: 281–302.

Costas, E. 1986. *Ultraestructura cromosómica en dinoflagelados. Consideraciones evolutivas* Ph.D. Thesis. Univ. Santiago de Compostela. 240 pp.

Costas, E. 1990. Genetic variability in growth rates of marine dinoflagellates. *Genetica* **83**: 99–102.

Costas, E., and V. J. Goyanes. 1988. Comparative analysis of dinoflagellate chromosomes and nuclei. *Genet (Life Sci. Adv.)* **7**: 15–18.

Costas, E., and V. López–Rodas. 1991a. On growth factors, cell division cycle and the eukaryotic origin. *Endocytobiosis & Cell Res.* **8**: 89–92.

Costas, E., and V. López–Rodas. 1991b. Persistence of cell division synchrony in *Spirogyra insignis* (Gamophyceae): membrane proteoglycans transmitting synchronizing information throughout generations. *Chronobiol. Int.* **8**(2): 85–92.

Costas, E., and V. López–Rodas. 1991c. Evidence for an annual rhythm in cell aging in *Spirogyra insignis* (Chlorophyceae). *Phycologia* **30**(6): 597–599.

Dodge, J. D. 1955. Chromosome structure in the dinoflagellates and the problem of the mesokaryotic cell. *2nd. Internat. Conf. on Protozool. Exc. Med. Inter. Congr. Ser. No.* **91**: 39.

Edmunds, L. N. 1988. *Cellular and molecular basis of biological clocks* Springer-Verlag, New York. 497 pp.

González–Chavarri, E. 1991. *Producción de biomasa a base de microalgas y sus aplicaciones en la producción animal.* Ph.D. Thesis. Universidad Complutense. 142 pp.

Goustin, A. S., E. B. Leof, G. D. Shipley, and H. L. Moses. 1986. Growth factors and cancer. *Cancer Res.* **46**: 1015–1029.

Guillard, R. 1975. Culture of phytoplankton for feeding marine invertebrates. Pp: 26–60 in *Culture of Marine Invertebrate Animals*, W. Smith and M. Chanley, eds. Plenum Publ. Co., New York.

Herzog, M., S. Boletzky, and M. O. Soyer. 1984. Ultrastructural and biochemical nuclear aspects of eukaryote classification: independent evolution of the dinoflagellates as a sister group of the actual eukaryotes. *Origins of Life* **13**: 205–215.

López–Rodas, V., M. Navarro, L. De La Campa, E. González De Chavarri, S. González–Gil, A. Aguilera, R. Segura, and E. Costas. 1991. Tras las pistas de los primeros mecanismos de control de la división celular: Una aproximación evolutiva. Pp. 94–108 in *Cromocancerología.* F. Chavarria, ed. Fundación Cientifica A.E.C.C. Madrid.

Margalef, R. 1989. Condiciones de aparición de la purga de mar y presiones de selección sobre sus componentes. *Cuadernos da Area de Ciencias Marñas* **4**: 13–20.

Murray, A. W., and M. W. Kirschner. 1989. Dominions and clocks: The union of two views of the cell cycle. *Science* **246**: 614–621.

North, G. 1991. Starting and stopping. *Nature* **351**: 604–605.

Williams, M. 1977. Stereological techniques. Pp. 226 in *Practical methods in Electron Microscopy. Vol. VI.* M. Hayat, ed. Elsevier Sci. Publ. Co., New York.

Wyatt, T., and B. Reguera. 1989. ¿Ha alcanzado el cultivo de mejillón en Galicia su masa critica? *Cuadernos da Area de Ciencias Marñas* **4**: 63–71.

Reference: *Biol. Bull.* **184**: 6–14. (February, 1993)

Specific Inhibitors of Protein Synthesis Do Not Block RNA Synthesis or Settlement in Larvae of a Marine Gastropod Mollusk (*Haliotis rufescens*)

GABRIEL FENTEANY[1] AND DANIEL E. MORSE[2]

Department of Biological Sciences and the Marine Biotechnology Center, Marine Science Institute, University of California, Santa Barbara, California 93106

Abstract. Antibiotic inhibitors of protein synthesis were tested for their effectiveness in larvae of the red abalone, *Haliotis rufescens* (gastropod mollusk). Emetine and anisomycin proved highly effective in this system, while cycloheximide, fusidic acid, puromycin, and tetracycline were less effective. Emetine and anisomycin specifically inhibited protein synthesis but not RNA synthesis. The contribution to protein synthesis by chloramphenicol-sensitive prokaryotic contaminants was found to be undetectable, except following the onset of symptoms of toxicity resulting from prolonged exposure to emetine or anisomycin. The induction of larval settlement and plantigrade attachment by γ-aminobutyric acid (GABA), a functional analog of the natural inducer of settlement, occurred even under conditions in which most protein synthesis was inhibited, as expected for a chemosensory system response, whereas subsequent developmental metamorphosis was completely blocked. Because emetine and anisomycin block protein synthesis—including the synthesis of new transcription factors—but do not block early transcription, treatment of marine invertebrate embryos and larvae with these inhibitors can be used to obtain a selective enrichment in the mRNA population of "early gene" transcripts induced directly by GABA and other morphogenetic signals, without dilution by new mRNAs, the appearance of which is dependent on the synthesis of new protein transcription factors.

Received 5 August 1992; accepted 18 November 1992.

Abbreviations: GABA, γ-aminobutyric acid; TCA, trichloroacetic acid; SSC, standard sodium chloride-sodium citrate buffer.

Present address: [1] Program in Cell and Developmental Biology, Harvard Medical School, Boston, Massachusetts 02115.

[2] Author to whom correspondence should be addressed.

Introduction

Developmentally competent larvae (0.2 mm in diameter) of the marine gastropod mollusk *Haliotis rufescens* (red abalone) are induced to settle from the plankton and begin metamorphosis by oligopeptides and proteins associated with the surfaces of crustose red algae (Morse *et al.*, 1979a, b, 1984; Morse and Morse, 1984), and by functional analogs of these natural inducers, such as γ-aminobutyric acid (GABA), muscimol, and baclofen (Morse *et al.*, 1979a,b, 1980a, Morse, 1992). These compounds apparently bind to chemosensory receptors, with subsequent transduction of the signal mediated by the second messengers cyclic AMP and Ca^{++} (Trapido-Rosenthal and Morse, 1986a; Morse, 1992). This transduction pathway culminates in an excitatory depolarization that is apparently triggered by the regulated opening of chloride ion channels (Morse *et al.*, 1980; Baloun and Morse, 1984; Morse, 1990, 1992). The morphogenetic response can be facilitated or amplified by the presence of lysine or lysine analogs (Trapido-Rosenthal and Morse, 1985, 1986b), acting through a separate lysine receptor that, in turn, stimulates a G protein-diacylglycerol signal transduction cascade (Baxter and Morse, 1987, 1992; Wodicka and Morse, 1991; Morse, 1990, 1992). Before we can understand the molecular mechanisms by which these convergent chemosensory pathways regulate larval settlement behavior and the subsequent induction of gene expression controlling cellular differentiation and proliferation (*cf.* Cariolou and Morse, 1988; Groppe and Morse, 1989; Spaulding and Morse, 1991; Degnan and Morse, 1993), we must first determine the requirements for *de novo* protein synthesis in these processes.

Specific inhibitors of protein synthesis, such as cycloheximide and puromycin, have proved invaluable for such

studies in many other systems. Yet these well-known inhibitors were ineffective with larvae of the red abalone (*Haliotis rufescens;* gastropod mollusk) developing in seawater. This finding prompted our search for inhibitors of mRNA translation that would specifically block protein synthesis in abalone larvae in seawater media, while not inhibiting RNA synthesis.

The antibiotic protein synthesis inhibitors emetine and anisomycin exhibit the necessary effectiveness and specificity. These compounds do not inhibit RNA synthesis or the induction of settlement and plantigrade attachment of the planktonic abalone larvae, as would be expected if these processes are mediated by a chemosensory system, but they completely block the subsequent metamorphosis which, as expected, is apparently dependent on *de novo* protein synthesis. These inhibitors should therefore help investigators identify the primary response genes (the transcription of which does not depend on *de novo* protein synthesis) and messenger RNAs responsible for the induction of metamorphosis.

Materials and Methods

Haliotis rufescens broodstock was collected off the coast of Santa Barbara, California, and production and cultivation of larvae conducted as previously described (Morse *et al.*, 1977, 1978, 1979b). Spawning was induced by exposing gravid adults to 10 m*M* hydrogen peroxide. Male and female gametes were collected and washed separately, and then mixed to allow fertilization. Embryos and larvae were maintained in 5 μm-filtered, U.V.-sterilized flowing seawater at 15 ± 1°C.

Antibiotic inhibitors of protein synthesis were purchased from Sigma Chemical Company (St. Louis, Missouri), dissolved to make concentrated stock solutions and used fresh on the day of preparation. Tetracycline was purchased as the hydrochloride, fusidic acid as the sodium salt, and puromycin and emetine as the dihydrochlorides. Stock solutions were prepared in 0.22 μm-filtered distilled water, either alone, or containing the minimum amount of ethanol required to completely solubilize the antibiotic. After addition of antibiotics to experimental samples, no more than 0.2% (v/v) ethanol was present in any seawater sample. Control experiments showed that the presence of 0.3% ethanol had no effect on larval behavior and settlement or on the level of [^{3}H]leucine incorporation into TCA-insoluble material in the larvae; higher concentrations of ethanol (above *ca.* 0.75%) and other organic solvents induced settlement of the larvae, with a rapidity corresponding to the concentration of solvent (data not shown). Similar results were reported earlier by Pennington and Hadfield (1989) for larvae of the nudibranch mollusk *Phestilla sibogae.*

Synthesis of protein and RNA was measured by incorporation of radioactive amino acid or nucleoside into acid-precipitable macromolecules. For each assay *ca.* 2000 larvae were placed in 10 ml of 5 μm-filtered, U.V.-sterilized seawater in 40 ml Oakridge tubes. Rifampicin, a specific inhibitor of bacterial RNA synthesis, was added to a final concentration of 2.4 μ*M* in all samples to limit bacterial growth, except where otherwise noted. After incubations in the presence or absence of inhibitors, either L-[4,5-^{3}H]leucine (150 Ci/mmol; Amersham Corporation, Arlington Heights, Illinois) or [5,6-^{3}H]uridine (42 Ci/mmol; Amersham) was added to 0.1 or 0.2 μCi/ml, as noted in the figure legends. For each treatment at each time point, three larval samples were used. Larvae were kept at 15 ± 1°C, except as noted. To end the labeling, nonradioactive L-leucine or uridine was added to a final concentration of 0.8 m*M* or 0.4 m*M*, respectively. The Oakridge tubes then were centrifuged (16,000 rpm; 4°C) for 5 min (Sorvall RC5 or RC5C Superspeed Centrifuges, Claremont, California); Sorvall SA-600 or SS-34 fixed angle rotors were used to pellet the larvae. The tubes were placed on ice, the water was drained off, 2 ml of cold 1 × SSC was added, and the larvae were re-suspended and homogenized completely in an ice-cold Dounce homogenizer (7 ml Pyrex tissue grinder). One aliquot of 0.5 ml for each sample was removed, placed in a 1.5 ml microfuge tube, and frozen for future quantitation of protein. For each sample, 1.5 ml of the homogenate was then placed into another microfuge tube on ice, and 100% (w/v) trichloroacetic acid (TCA) was added to yield a final concentration of 10% (w/v). After acid precipitation for 30 min at 4°C, each sample was poured through a 2.4 cm glass microfiber filter (GF/C; Whatman International Ltd., Maidstone, UK), washed three times with 5% TCA, then washed twice with 100% ethanol. The filters were completely dried in an oven at 55°C and then placed in liquid scintillation vials; 1 ml of scintillation cocktail (Bio-Safe II; Research Products International, Mount Prospect, IL) was added and radioactivity determined by liquid scintillation. Protein was quantitated by the method of Bradford (1976) according to the protocol of the reagent manufacturer (Bio-Rad Protein Assay; Bio-Rad Laboratories, Richmond, California); assays were conducted in triplicate and evaluated relative to a bovine serum albumin standard measured in parallel. The incorporation data presented are the means of triplicate determinations, with error bars representing one standard deviation.

Assays of settlement and metamorphosis were conducted with larvae in glass scintillation vials (*ca.* 200 larvae in 10 ml of rifampicin-containing 5 μm-filtered, U.V.-sterilized seawater) maintained under low illumination and observed with a dissecting microscope. Each treatment was conducted in triplicate. Larvae also were placed at a density comparable to that used in the incorporation

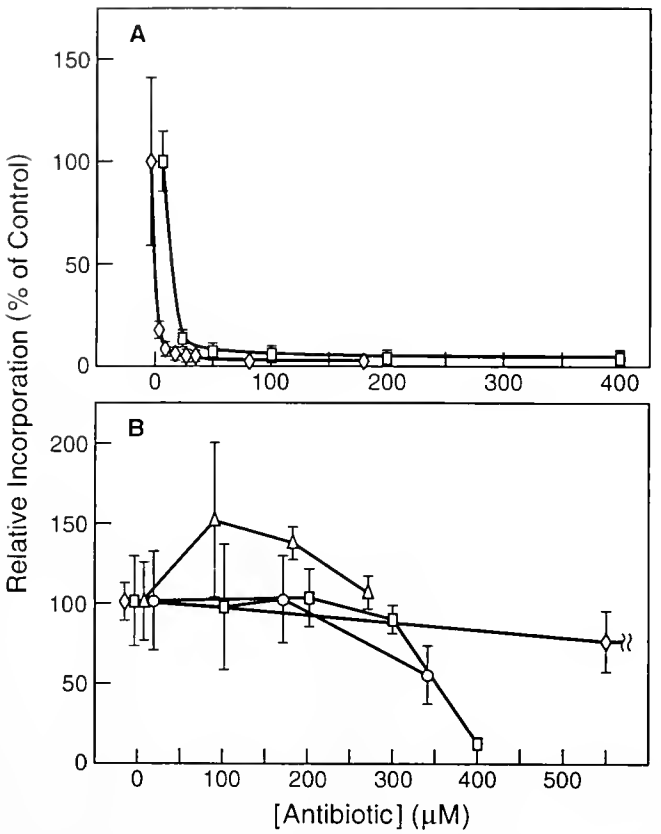

Figure 1. Incorporation of [^{3}H]leucine as a function of the concentration of antibiotic. After incubating 8-10-day-old larvae (*ca.* 2,000 larvae/10 ml rifampicin-containing seawater) for 2 h in the presence or absence of blocker at the concentrations indicated, [^{3}H]leucine was added to 0.1 μCi/ml, and the pulse allowed to proceed for 2 h. Mean control values (representing incorporation in the absence of antibiotic) are displaced on the abscissa for clarity. (A) Incorporation in the presence of emetine (diamonds) or anisomycin (rectangles). (B) Incorporation in the presence of cycloheximide (diamonds), puromycin (rectangles), tetracycline (triangles), or fusidic acid (circles). Details as described in Materials and Methods.

assays (*ca.* 2000 larvae/10 ml seawater), and observed for mortality and other responses to the protein synthesis inhibitors.

Results

Inhibition of protein synthesis

Larvae of *H. rufescens* take up exogenous amino acids from seawater, as demonstrated by these and other investigations (Jaeckle and Manahan, 1989), although these larvae are lecithotrophic. Several commonly used inhibitors of protein synthesis, including cycloheximide, fusidic acid, puromycin, and tetracycline, had little or no inhibitory effect on the overall incorporation of [^{3}H]leucine into TCA-insoluble material at concentrations that were not toxic to the larvae (Fig. 1). In marked contrast, both emetine and anisomycin proved strongly inhibitory in a concentration-dependent manner.

Emetine (9 μ*M*) efficiently blocked the incorporation of [^{3}H]leucine into *Haliotis* larvae under conditions in which 100 μ*M* chloramphenicol (an inhibitor of protein synthesis only in prokaryotes) had no significant effect (Fig. 2A). Identical results were obtained for a range of chloramphenicol concentrations (50–600 μ*M*), both in the presence or absence of 2.4 μ*M* rifampicin (an inhibitor of bacterial RNA polymerase). Thus, in the absence of emetine, prokaryotic incorporation of [^{3}H]leucine was not detectable. Inhibition by emetine was quite rapid; incubation for 10 min with 9 μ*M* emetine prior to addition of radiolabel was sufficient to block incorporation to a level comparable to that produced by an incubation for 2 h (data not shown). The inhibitory effect of a single

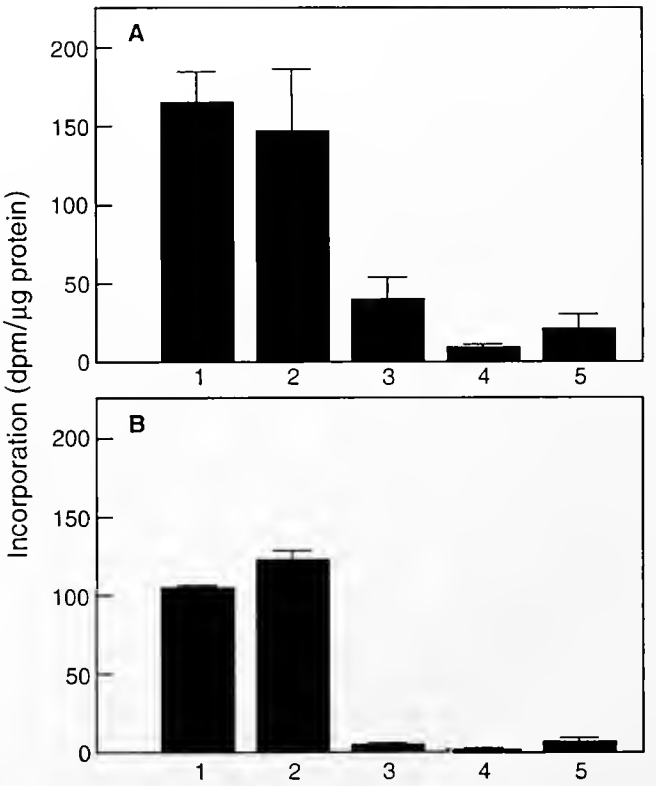

Figure 2. Incorporation of [^{3}H]leucine in 7-day-old larvae in the presence or absence of emetine (9 μ*M*) or anisomycin (200 μ*M*) and chloramphenicol (150 μ*M*). 7-day-old larvae were used. Pulse-labeling at 24 h following the time of initial addition of emetine was for 2 h (0.1 μCi/ml). (A) Treatments: (1) No emetine or chloramphenicol. (2) Chloramphenicol added at 21 h. (3) Emetine added at 0 h. (4) Emetine added at 0 h and chloramphenicol added at 21 h. (5) Emetine added to a concentration of 9 μ*M* at 0 h and the same amount added again at 12 h. (B) Treatments: (1) No anisomycin or chloramphenicol. (2) Chloramphenicol added at 21 h. (3) Anisomycin added at 0 h. (4) Anisomycin added at 0 h and chloramphenicol added at 21 h. (5) Anisomycin added to a concentration of 200 μ*M* at 0 h and the same amount added again at 12 h.

addition of emetine relaxed with time (Fig. 3A), and a second addition of the same amount of emetine at 12 h reduced incorporation slightly further (Fig. 2A). However, following prolonged incubation in the presence of emetine, the addition of chloramphenicol 3 h before labeling led to significantly lower levels of incorporation, particularly at 24 h and 48 h following the addition of emetine (Figs. 2A, 3A). Therefore, some of the apparent relaxation of inhibition by emetine may be due to an increase in the proportion of protein synthesis attributable to contaminating chloramphenicol-sensitive prokaryotes. This is likely to be the result of bacterial growth on the emetine-treated larvae themselves, as these larvae become weaker, although rifampicin (2.4 μM) was present throughout.

The inhibitory effect of a single addition of anisomycin (200 μM) persisted longer than that caused by 9 μM emetine (Figs. 2B, 3B), and a second addition 12 h after the first did not reduce the incorporation of [^{3}H]leucine further (Fig. 2B). In the presence of anisomycin, the addition of chloramphenicol 3 h before pulse-labeling did not lead to significantly lower levels of incorporation up to 24 h (Figs. 2B, 3B). Much of the inhibition of protein synthesis by a single addition of anisomycin was reversed between 24 and 48 h (Fig. 3B). This late apparent relaxation was blocked by chloramphenicol (Fig. 3B), suggesting that it was due to an increase in prokaryotic incorporation.

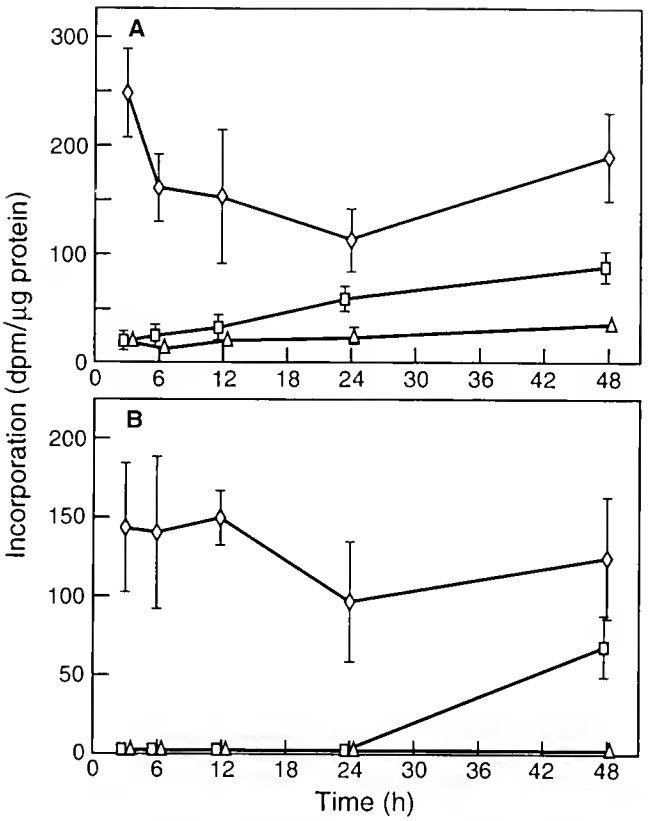

Figure 3. Incorporation of [^{3}H]leucine in the presence or absence of emetine (9 μM) or anisomycin (200 μM) and chloramphenicol (150 μM) as a function of time following addition of emetine. Larvae were pulsed at the times after addition of emetine or anisomycin indicated for 2 h (0.1 μCi/ml). In the chloramphenicol-treated samples, chloramphenicol was added 3 h prior to pulse-labeling. Mean values are displaced slightly on the abscissa for clarity. (A) 4-day-old larvae were used (6 days old by the end of the experiment in the last 3 sets of samples). No antibiotic (diamonds); emetine (rectangles); emetine plus chloramphenicol (triangles). (B) 5-day-old larvae were used (7 days old by the end of the experiment in the last 3 sets of samples). No antibiotic (diamonds); anisomycin (rectangles); anisomycin plus chloramphenicol (triangles).

Effects of emetine and anisomycin on RNA synthesis

To test whether emetine affects RNA synthesis, larvae were pulsed with [^{3}H]uridine both in the presence and absence of 10^{-6} M GABA (added 30 min following the addition of emetine). No significant inhibition of RNA synthesis was observed except at 6 h in the presence of both GABA and 9 μM emetine (Fig. 4A). The presence of emetine (9 μM) may have a stimulatory effect on the incorporation of [^{3}H]uridine in *Haliotis* larvae after 12.5 h. A similar experiment showed that the incorporation of [^{3}H]uridine also was not inhibited by the addition of 200 μM anisomycin (added 60 min before addition of GABA; Fig. 4B).

Effects of emetine and anisomycin on settlement, metamorphosis, and survival

At concentrations sufficient to inhibit most protein synthesis, emetine and anisomycin did not block the initial induction of larval settlement and plantigrade attachment by GABA, although subsequent metamorphosis was completely blocked. Toxicity of these inhibitors was both time- and concentration-dependent. Initial settlement and plantigrade attachment of larvae induced by GABA (10^{-6} M and 10^{-3} M) occurred normally in the presence of 9 μM emetine (Fig. 5A, B). Both in the presence and absence of emetine, larvae ceased their swimming behavior after addition of GABA, and plantigrade attachment followed. Attached larvae exhibited normal pedal locomotion in the presence of emetine. Abscission of the velum was also observed in the presence of emetine and occurred whether GABA (10^{-6} M) was present or not, although at 9 μM emetine abscission occurred at lower levels when GABA was not present. Abscission was often premature or incomplete, particularly at higher concentrations of emetine. By 6 h after the addition of 10^{-6} M GABA, most of the larvae had settled both in the presence and absence of 9 μM emetine (Fig. 5A). New shell growth was not observed in the presence of emetine when larvae were induced to settle with 10^{-6} M GABA, although it was observed normally in settled larvae in the absence of the inhibitor by 48 h. Attachment proceeded more rapidly at the higher

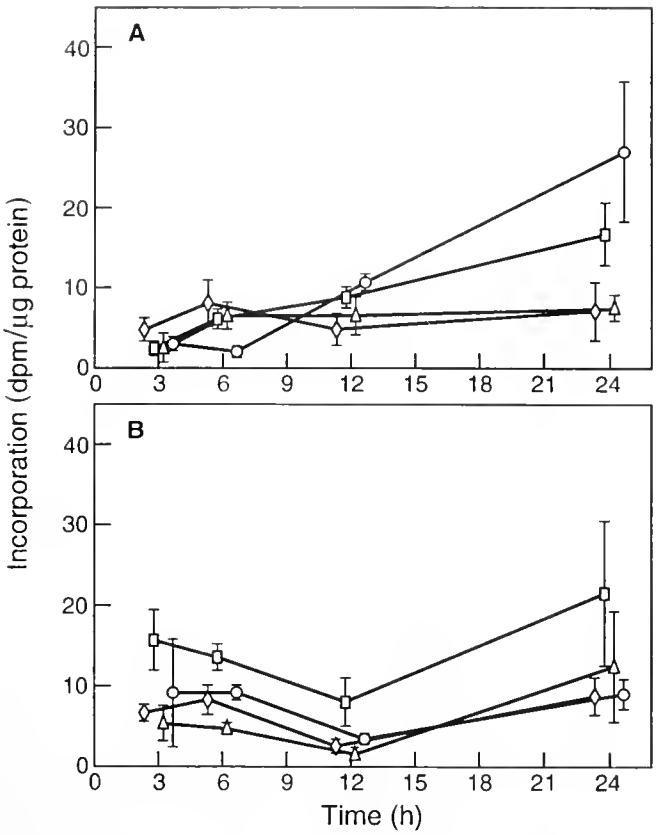

Figure 4. Incorporation of [^{3}H]uridine in the presence or absence of emetine or anisomycin as a function of time after addition of GABA (10^{-6} *M*). The larvae were pulsed for 20 min with radiolabeled nucleoside (0.2 μCi/ml) at the times indicated. Mean values slightly displaced on the abscissa for clarity. (A) 10-day-old larvae were used. Where indicated, emetine (9 μ*M*) was added 30 min prior to the addition of GABA. No emetine or GABA (diamonds); emetine with no GABA (rectangles); no emetine, plus GABA (triangles); emetine plus GABA (circles). (B) 9-day-old larvae were used. Where indicated, anisomycin (200 μ*M*) was added 60 min prior to the addition of GABA. No anisomycin or GABA (diamonds); anisomycin with no GABA (rectangles); no anisomycin, plus GABA (triangles); anisomycin plus GABA, (circles).

concentration of GABA; virtually all of the larvae were attached within 20 min, with no inhibition by emetine (Fig. 5B). Although emetine did not inhibit the initial rate of attachment of the larvae induced by GABA, the larvae failed to maintain their plantigrade attachment (Fig. 5A, B), and progressively more were found on their sides, apparently due to the toxic effect of prolonged exposure to emetine. There also was some attachment in the presence of emetine when GABA was absent (Fig. 5A, B).

Prolonged exposure of larvae to emetine proved lethal. Even before any mortality was observed, larvae treated with 9 μ*M* emetine appeared to spend more time on the bottom of the test vial than larvae in control vials. By 36 h after the addition of emetine (9 μ*M*) both in the presence and absence of GABA (*ca.* 20 larvae/ml), few larvae were swimming and many appeared dead, while in the control vials lacking GABA, many of the larvae remained swimming and virtually all remained alive. All the larvae were dead by 54 h in the presence of 9 μ*M* emetine at *ca.* 20 larvae/ml, and by 72 h at *ca.* 200 larvae/ml. Toxicity was progressively accelerated by higher concentrations, although the initial rate of GABA-induced attachment remained unimpaired below 80 μ*M* emetine; in the presence of 18 μ*M* and 40 μ*M* emetine, virtually all of the larvae were attached within 20 min following the addition of 10^{-3} *M* GABA (data not shown). Exposure to 80 μ*M* or 160 μ*M* emetine produced marked symptoms of toxicity; GABA-induced settlement was reduced, premature abscission of the velum occurred in the presence and absence of GABA, and all of the larvae died within 6–12 h at the low density.

Anisomycin appeared to exert a stimulatory effect on the activity of the larvae, particularly on the movement of the cilia. The level of swimming activity of the larvae was markedly greater in the presence of 200 μ*M* anisomycin than in control or emetine-treated vials, even after only 20 min following addition. This effect appeared to partially antagonize the initial GABA-induced attachment, with the attached larvae abnormally continuing sustained beating of their swimming cilia and displaying little pedal locomotion; plantigrade larvae often were displaced by collision with other swimming larvae, and sometimes began swimming again. The initial rates of settlement and attachment induced by 10^{-3} *M* GABA were relatively unaffected by anisomycin, although long-term attachment was reduced (Fig. 5C, D). [The weak settlement-inducing activity of high concentrations of anisomycin itself (*cf.* Fig. 5C, D) may explain the biphasic settlement observed in the presence of GABA.] Anisomycin also produced concentration-dependent and time-dependent symptoms of toxicity, with complete mortality resulting from prolonged exposure (96 h) of larvae, at high or low density, to 200 μ*M* concentration.

Discussion

Inhibition of protein synthesis

Emetine and anisomycin were found to be highly effective inhibitors of protein synthesis in *Haliotis* larvae, whereas cycloheximide, fusidic acid, puromycin, and tetracycline proved far less effective. Possible reasons for the limited effectiveness of these widely used inhibitors may include their instability or low solubility in seawater, or their inefficient diffusion into the deeper layers of larval tissue. There is some structural evidence supporting the suggestion that membrane permeability may be an important determinant of effectiveness in the marine larval system. Emetine contains four methoxy groups, while anisomycin contains one methoxy and one acetoxy group, all carbon-linked to cyclic nuclei in both of these anti-

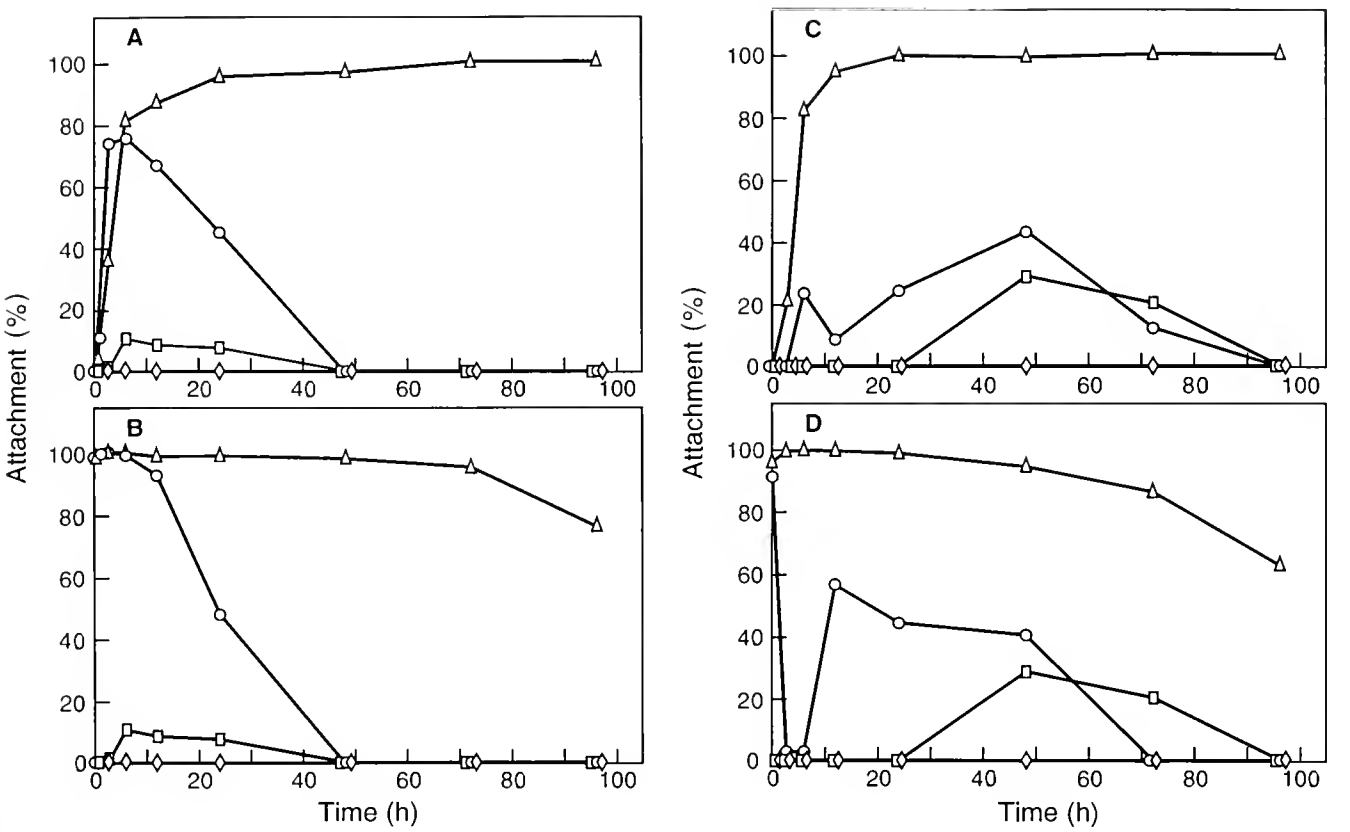

Figure 5. Attachment of larvae in the presence or absence of emetine or anisomycin as a function of time following addition of GABA. *Ca* 200 were placed in 10 ml rifampicin-treated seawater in triplicate, as described in Materials and Methods. Following a 30-min incubation with or without emetine (A and B) or a 2-h incubation with or without anisomycin (C and D), GABA was added to the samples indicated, and the mean percentage of the larvae showing attachment was scored at the times indicated. Standard deviations for all points, assayed in triplicate, were ≤4%. (A) 8-day-old larvae treated with or without 10^{-6} *M* GABA and 9 μM emetine. No emetine or GABA (diamonds); emetine with no GABA (rectangles); no emetine, plus GABA (triangles); emetine plus GABA (circles). (B) 8-day-old larvae treated with or without 10^{-3} *M* GABA and 9 μM emetine. No emetine or GABA (diamonds); emetine with no GABA (rectangles); no emetine, plus GABA (triangles); emetine plus GABA (circles). (C) 10-day-old larvae treated with or without 10^{-6} *M* GABA and 200 μM anisomycin. No anisomycin or GABA (diamonds); anisomycin, with no GABA (rectangles); no anisomycin, plus GABA (triangles); anisomycin plus GABA (circles). (D) 10-day-old larvae treated with or without 10^{-3} *M* GABA and 200 μM anisomycin. No anisomycin or GABA (diamonds); anisomycin with no GABA (rectangles); no anisomycin, plus GABA (triangles); anisomycin plus GABA (circles).

biotics. These lipophilic groups may facilitate entry into cells and diffusion through tissues. This lipid solvent-like effect also might account for the weak settlement-inducing activity of these antibiotics, analogous to that reported by Pennington and Hadfield (1989) for some organic solvents. Puromycin contains only one methoxy group, and fusidic acid contains one acetoxy group.

Puromycin, which was not an effective inhibitor of protein synthesis in *Haliotis* larvae, has been successfully used in sea urchin embryos. Gong and Brandhorst (1988) found puromycin to effectively inhibit most protein synthesis in gastrulae of the sea urchin *Lytechinus pictus* in artificial seawater. On a molar basis, however, it was less effective than emetine, anisomycin, or the less readily available pactamycin. Cycloheximide dissolved in seawater-based media has limited use as a protein synthesis inhibitor in sea urchin eggs (K. Foltz, pers. comm.) and is a poor inhibitor of protein synthesis in sea urchin embryos (Hogan and Gross, 1971). This could be due in part to the fact that cycloheximide is rapidly inactivated in dilute alkali at room temperature, and thus may be unstable at the pH of seawater (*ca.* pH 8). This could also help to explain its lack of effectiveness in *Haliotis* larvae.

Emetine and anisomycin are specific inhibitors of protein synthesis in eukaryotes; they bind to specific sites on eukaryotic ribosomes, and are ineffective in prokaryotes

(Grollman, 1967; Barbacid *et al.*, 1975; Carrasco *et al.*, 1976; Jiménez *et al.*, 1977; Sánchez *et al.*, 1977). Inhibition of protein synthesis by emetine is irreversible (Grollman, 1968), whereas the inhibition by anisomycin is reversible (Barbacid and Vázquez, 1975). Both are effective inhibitors of protein synthesis in the eggs and embryos of several species of sea urchins (Hogan and Gross, 1971; Epel, 1972; Wagenaar and Mazia, 1978; Hille *et al.*, 1981; Wagenaar, 1983; Dubé, 1988; Gong and Brandhorst, 1988; Sluder *et al.*, 1990). Our extension of these findings to the anatomically more complex larvae of the mollusk, *Haliotis rufescens*, suggests that these compounds may be generally useful for inhibiting protein synthesis in marine invertebrate embryos and larvae.

Settlement, metamorphosis, and toxicity

The density of *Haliotis* larvae used in the incorporation assays was about ten-fold higher than in the samples used to investigate the effects on settlement, metamorphosis and survival. This reflected the practical requirements for a large number of larvae needed to obtain reliable values in the isotope incorporation studies, and a low density of larvae needed to make accurate observations of behavior and metamorphosis. Therefore, one would expect that the actual level of inhibition of protein synthesis that occurred in the samples in which settlement and metamorphosis were investigated would be at least equal to and probably greater than the inhibition estimated in the incorporation assays. The survival and behavior of the larvae at the higher density in the presence of the inhibitors nevertheless were found to parallel those at the lower density, although mortality generally was delayed at higher density.

The fact that the larvae initially settle and attach normally in response to GABA in the presence of emetine or anisomycin at concentrations sufficient to block nearly all protein synthesis suggests that the induction of settlement and plantigrade attachment does not require *de novo* protein synthesis, consistent with the notion that these behavioral responses are controlled by a chemosensory mechanism mediated by the preformed larval nervous system. It remains possible, however, that the inhibition of protein synthesis may not have been sufficient to block the synthesis of some new proteins required for this response. While the highest concentrations of emetine tested (80 μM and 160 μM) did interfere with initial settlement, these concentrations rapidly caused acute symptoms of toxicity, and all the larvae died within 6–12 h at *ca.* 20 larvae/ml. The initial high level of induced attachment observed in response to 10^{-3} M GABA in the presence of anisomycin was transitory, and appeared to be antagonized by the stimulatory effect of this compound on swimming activity. Emetine had no such stimulatory effect on the larvae. Anisomycin may directly or indirectly stimulate the movement of the cilia, independently of its effects as an inhibitor of protein synthesis.

Both emetine and anisomycin completely blocked the induction of metamorphosis (in conjunction with their effect on protein synthesis) at concentrations that did not inhibit initial settlement and plantigrade attachment. There was no shell growth, nor were any other landmarks of developmental metamorphosis observed (beyond the abnormal abscission of the velum in the presence of emetine). This may be the direct result of the inhibition of protein synthesis, suggesting that the biosynthesis of new proteins is required even for the early processes of metamorphosis to follow settlement. New proteins made following the induction of metamorphosis in *H. rufescens* have been shown to include a sulfatase (Spaulding and Morse, 1991), a chymotrypsin-like protease (Groppe and Morse, 1989) and a new conchiolin shell matrix protein (Cariolou and Morse, 1988). It also is possible that the failure to progress through metamorphosis may have resulted from other toxic effects of emetine and anisomycin beyond their inhibition of protein synthesis. Emetine has well-documented cardiotoxic effects in vertebrates (for reviews, see Wenzel, 1967; Yang and Dubrick, 1980). The abscission of the velum observed in the presence of emetine, in the presence or absence of GABA, apparently is a result of toxicity of this compound. This suggestion is supported by the facts that this abscission also occurs in the absence of GABA and that similar responses of the larvae to unrelated toxic compounds have been observed previously (Morse *et al.*, 1980). Moreover, the fact that anisomycin, an equally potent but longer-lasting inhibitor of protein synthesis in the larvae, does not induce this abscission and causes less rapid mortality than does emetine at the concentrations used, supports the interpretation that this abscission is the result of toxicity rather than normal morphogenesis. However, whether the inhibition of metamorphosis is a direct result of an inhibition of protein synthesis, or the consequence of other toxic effects of the inhibitors, does not alter the principal conclusion of this study: both the initial induction of larval settlement and attachment and the overall rate of RNA synthesis are not significantly inhibited under conditions in which emetine and anisomycin block nearly all protein synthesis.

Conclusions and prospects

The embryos and larvae of marine invertebrates such as abalones and sea urchins provide highly tractable model systems for analyses of the molecular mechanisms of gene expression and gene regulation controlling behavior, cell function, cellular differentiation, and proliferation. Advantages of these systems include: egg-to-egg cultivation; the large numbers of gametes, embryos, and larvae that are readily obtainable (in some species numbering in the

millions); the ability to trigger development and other responses with high synchrony; and the accessibility of the genes, messenger RNAs and proteins for experimental analysis and manipulation.

The conditions reported here can be used to selectively obtain mRNAs induced in marine invertebrate embryos and larvae by GABA and other morphogenetic signals in the absence of *de novo* protein synthesis. The isolation and characterization of such primary response (or "immediate-early") transcripts will be essential to understand the cascade of gene expression and regulatory events that transduce signals such as those induced by GABA into morphogenetic development in the larvae of *H. rufescens*.

Acknowledgments

This research was supported by grants R01-RR06640 and R01-CA53105 from the National Institutes of Health to D. E. M., and a National Defense Science and Engineering Graduate Fellowship to G. F.

Literature Cited

Baloun, A. J., and D. E. Morse. 1984. Ionic control of settlement and metamorphosis in larval *Haliotis rufescens* (gastropoda). *Biol. Bull.* **167:** 124–138.

Barbacid, M., and D. Vázquez. 1975. Ribosome changes during translation. *J. Mol. Biol.* **93:** 449–463.

Barbacid, M., M. Fresno, and D. Vázquez. 1975. Inhibitors of polypeptide elongation on yeast polysomes. *J. Antibiotics* **28:** 453–462.

Baxter, G., and D. E. Morse. 1987. G protein and diacylglycerol regulate metamorphosis of planktonic molluscan larvae. *Proc. Natl. Acad. Sci. USA* **84:** 1867–1870.

Baxter, G., and D. E. Morse. 1992. Cilia from abalone larvae contain a receptor-dependent G protein transduction system similar to that in mammals. *Biol. Bull.* **183:** 147–154.

Bradford, M. A. 1976. A rapid and sensitive method for the quantitation of microgram quantities of protein utilizing the principle of protein-dye binding. *Anal. Biochem.* **72:** 248–254.

Cariolou, M. A., and D. E. Morse. 1988. Purification and characterization of conchiolin shell peptides from the marine mollusc, *Haliotis rufescens*, as a function of development. *J. Comp. Biochem. Physiol. B* **157:** 717–729.

Carrasco, L., A. Jiménez, and D. Vázquez. 1976. Specific inhibitors of translocation by tubulosine in eukaryotic polysomes. *Europ. J. Biochem.* **64:** 1–5.

Degnan, B. M., and D. E. Morse. 1993. Identification of eight homeobox-containing transcripts expressed during larval development and at metamorphosis in the gastropod mollusc *Haliotis rufescens*. *Molec. Mar. Biol. Biotechnol.* (in press)

Dubé, F. 1988. Effect of reduced protein synthesis on the cell cycle in sea urchin embryos. *J. Cell. Physiol.* **137:** 545–552.

Epel, D. 1972. Activation of Na^+-dependent amino acid transport system upon fertilization of sea urchin eggs. *Exp. Cell Res.* **72:** 74–89.

Gong, Z., and B. P. Brandhorst. 1988. Stabilization of tubulin mRNA by inhibition of protein synthesis in sea urchin embryos. *Mol. Cell. Biol.* **8:** 3518–3525.

Grollman, A. P. 1967. Inhibitors of protein synthesis. II. Mode of action of anisomycin. *J. Biol. Chem.* **242:** 3226–3233.

Grollman, A. P. 1968. Inhibitors of protein synthesis. V. Effects of emetine on protein and nucleic acid biosynthesis in HeLa cells. *J. Biol. Chem.* **243:** 4089–4094.

Groppe, J., and D. E. Morse. 1989. Cloning and sequence analysis of novel serine protease cDNAs from the abalone, *Haliotis rufescens*. Pp. 285–288, in *Current Topics in Marine Biotechnology*, S. Miyachi, I. Karube, and Y. Ishida, eds. Fuji Technology Press, Tokyo.

Hille, M. B., D. C. Hall, Z. Yablonka-Reuveni, M. V. Danilchik, and R. T. Moon. 1981. Translational control in sea urchin eggs and embryos: initiation is rate limiting in blastula stage embryos. *Dev. Biol.* **86:** 241–249.

Hogan, B., and P. R. Gross. 1971. The effect of protein synthesis inhibition on the entry of messenger RNA into the cytoplasm of sea urchin embryos. *J. Cell Biol.* **49:** 692–701.

Jaeckle, W. B., and D. T. Manahan. 1989. Feeding by a "nonfeeding" larva: uptake of dissolved amino acids from seawater by lecithotrophic larvae of the gastropod *Haliotis rufescens*. *Mar. Biol.* **103:** 87–94.

Jiménez, A., L. Carrasco, and D. Vázquez. 1977. Enzymic and non-enzymic translocation by yeast polysomes. Site of action of a number of inhibitors. *Biochemistry* **16:** 4727–4730.

Morse, A. N. C., and D. E. Morse. 1984. Recruitment and metamorphosis of *Haliotis* larvae induced by molecules uniquely available at the surfaces of crustose red algae. *J. Exp. Mar. Biol. Ecol.* **75:** 191–215.

Morse, A. N. C., C. Froyd, and D. E. Morse. 1984. Molecules from cyanobacteria and red algae that induce larval settlement and metamorphosis in the mollusc *Haliotis rufescens*. *Mar. Biol.* **81:** 293–298.

Morse, D. E. 1985. Neurotransmitter-mimetic inducers of larval settlement and metamorphosis. *Bull. Mar. Sci.* **37:** 697–706.

Morse, D. E. 1990. Recent progress in larval settlement and metamorphosis: closing the gaps between molecular biology and ecology. *Bull. Mar. Sci* **46:** 465–483.

Morse, D. E. 1992. Molecular mechanisms controlling larval metamorphosis and recruitment in abalone larvae. Pp. 107–119 in *Abalone of the World*, S. A. Shepherd, M. J. Tegner, and S. Guzman del Proo, eds. Blackwell, Oxford.

Morse, D. E., H. Duncan, N. Hooker, and A. Morse. 1977. Hydrogen peroxide induces spawning in mollusks, with activation of prostaglandin endoperoxide synthetase. *Science* **196:** 298–300.

Morse, D. E., N. Hooker, and A. Morse. 1978. Chemical control of reproduction in bivalve and gastropod molluscs, III: An inexpensive technique for mariculture of many species. *Proc. World Maricult. Soc.* **9:** 543–547.

Morse, D. E., N. Hooker, H. Duncan, and L. Jensen. 1979a. γ-aminobutyric acid, a neurotransmitter, induces planktonic abalone larvae to settle and begin metamorphosis. *Science* **204:** 407–410.

Morse, D. E., N. Hooker, L. Jensen, and H. Duncan. 1979b. Induction of larval abalone settling and metamorphosis by γ-aminobutyric acid and its congeners from crustose red algae, II: Applications to cultivation, seed-production and bioassays; principal causes of mortality and interference. *Proc. World Maricult. Soc.* **10:** 81–91.

Morse, D. E., H. Duncan, N. Hooker, A. Baloun, and G. Young. 1980. GABA induces behavioral and developmental metamorphosis in planktonic molluscan larvae. *Fed. Proc.* **39:** 3237–3241.

Pennington, J. T., and M. G. Hadfield. 1989. Larvae of a nudibranch mollusc (*Phestilla sibogae*) metamorphose when exposed to common organic solvents. *Biol. Bull.* **177:** 350–355.

Sánchez, L., D. Vázquez, and A. Jiménez. 1977. Genetics and biochemistry of cryptopleurine resistance in the yeast *Saccharomyces cerevisiae*. *Mol. Gen. Genetics* **156:** 319–326.

Sluder, G., J. M. Miller, R. Cole, and C. L. Rieder. 1990. Protein synthesis and the cell cycle: Centrosome reproduction in sea urchin eggs is not under translational control. *J. Cell Biol.* **110:** 2025–2032.

Spaulding, D. C., and D. E. Morse. 1991. Purification and characterization of sulfatases from *Haliotis rufescens*. Evidence for changes in synthesis and heterogeneity during development. *J. Comp. Physiol. B* **161:** 498–515.

Trapido-Rosenthal, H. G., and D. E. Morse. 1985. L-α,ω-Diamino acids facilitate GABA induction of larval metamorphosis in a gastropod mollusc (*Haliotis rufescens*). *J. Comp. Physiol. B* **155:** 403–414.

Trapido-Rosenthal, H. G., and D. E. Morse. 1986a. Availability of chemosensory receptors is down-regulated by habituation of larvae to a morphogenetic signal. *Proc. Natl. Acad. Sci. USA* **83:** 7658–7662.

Trapido-Rosenthal, H. G., and D. E. Morse. 1986b. Regulation of receptor-mediated settlement and metamorphosis in larvae of a gastropod mollusc (*Haliotis rufescens*). *Bull. Mar. Sci.* **39:** 383–392.

Wagenaar, E. B. 1983. The timing of synthesis of proteins for mitosis in the cell cycle of the sea urchin embryo. *Exp. Cell Res.* **144:** 393–403.

Wagenaar, E. B., and D. Mazia. 1978. The effect of emetine on first cleavage division in the sea urchin, *Strongylocentrotus purpuratus*. Pp. 539–545 in *Cell Reproduction*, E. R. Dirksen, D. M. Prescott, and C. F. Fox, eds. Academic Press, New York.

Wenzel, D. G. 1967. Drug-induced cardiomyopathies. *J. Pharm. Sci.* **56:** 1209–1224.

Wodicka, L. M., and D. E. Morse. 1991. cDNA sequences reveal mRNAs for two Gα signal transducing proteins from larval cilia. *Biol. Bull.* **180:** 318–327.

Yang, W. C. T., and M. Dubrick. 1980. Mechanism of emetine cardiotoxicity. *Pharm. Ther.* **10:** 15–26.

Reference: *Biol. Bull.* **184**: 15–24. (February, 1993)

Metamorphosis in the Brachiopod *Terebratalia*: Evidence for a Role of Calcium Channel Function and the Dissociation of Shell Formation from Settlement

GARY FREEMAN

Friday Harbor Laboratories of the University of Washington and Center for Developmental Biology, Department of Zoology, University of Texas, Austin, Texas 78712

Abstract. Larvae of *Terebratalia* will not undergo metamorphosis when maintained in a sterile environment unless they are 9–10 days old; under these conditions the frequency of normal metamorphosis is low. Four-day larvae are normally induced to metamorphose when they contact a suitable substrate. They will also undergo metamorphosis when they are treated with high K^+ seawater in the presence of Ca^{2+}. Additional experiments indicate that both substrate-induced and high K^+ seawater-induced metamorphosis may involve the function of voltage-dependent calcium channels.

Metamorphosis involves settlement of the larva followed by formation of the protegulum, the initial shell. In larvae that have been aged in a sterile environment and in larvae treated with high K^+ in seawater with low Ca^{2+}, partial metamorphosis takes place. Under these conditions the larva does not settle, however a protegulum forms. Substrate-induced metamorphosis does not occur in the absence of the distal end of the pedicle lobe of the larva which normally makes contact with the substrate, however, treatment with high K^+ seawater containing Ca^{2+} induces partial metamorphosis in these larvae. These experiments suggest that there are at least two centers in the larva that control metamorphosis.

Introduction

Adult articulate brachiopods are sessile organisms. The larvae of these animals do not feed; they disperse the species as a consequence of their behavior and their ability to settle and metamorphose at appropriate sites. The process of settlement and metamorphosis has been described for several species of articulate brachiopods (See Long and Stricker, 1991, for a review). These events are similar in all of the species examined (Fig. 1). The larva swims close to the substrate for a variable period of time. Settlement begins when the larva orients itself perpendicular to the substrate and becomes attached to it via a secretory product produced by the distal tip of its pedicle lobe. After attachment of the larva to the substrate, the mantle lobe flips so that instead of partially covering the pedicle lobe it now partially covers the apical lobe. In *Terebratalia transversa* the mantle lobe secretes a periostracum prior to flipping (Stricker and Reed, 1985a). Within one day after the mantle lobe moves to its new position, a protegulum (initial shell) containing calcium carbonate is deposited on the periostracum, which lies over the new outer surface of the mantle lobe and part of the pedicle lobe (Stricker and Reed, 1985b). By four days, the post settlement part of the pedicle lobe has secreted a cuticle (Stricker and Reed, 1985c). At an unknown time after settlement the endoderm makes contact with a region of the apical lobe ectoderm, and a mouth is formed giving the metamorphosed individual the capacity to feed.

Virtually nothing is known about the factors that are responsible for the induction of settlement and metamorphosis in brachiopods. In order to induce metamorphosis in *Terebratalia transversa*, investigators have introduced fragments of brachiopod shell, various pelecypod shells or *Sabellaria* tubes into dishes with the larvae. The larvae frequently settle and metamorphose on these substrates. Long and Stricker (1991) state that larvae of *Terebratalia transversa* will not settle on clean glass surfaces or on shell fragments from which diatoms and bacteria have been removed. Long (1964) is cited for this

Received 14 May 1992; accepted 25 October 1992.

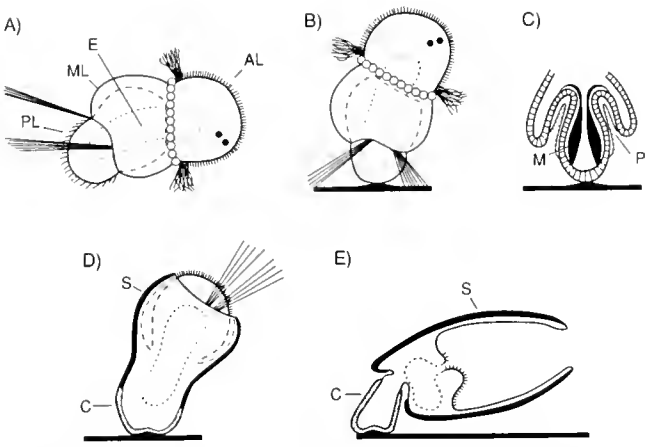

Figure 1. Diagrammatic view of swimming larva and larvae at various stages of substrate induced metamorphosis. (A) Side view of swimming larva. The larva is composed of three lobes. The apical lobe (AL) is at the anterior end of the larva. Behind the apical lobe there is a mantle lobe (ML) that partially covers the pedicle lobe (PL). The pedicle lobe comprises the posterior end of the larva. The apical lobe has a ciliary field that is responsible for larval locomotion. This lobe also has pigmented eye spots at its anterior end and a population of vesicular cells at its distal end bordering the cleft between the apical and mantle lobes. Setae extend from the distal end of the mantle lobe. An internal endodermal mass (E) is present. (B) Larva that has attached to the substrate by its pedicle lobe. (C) Longitudinal section showing the pedicle and part of the mantle lobe of a larva that has attached to a substrate. A periostracum (P) has formed externally between the upper part of the pedicle lobe and the inner surface of the mantle lobe. The inside of the larva has a pair of muscles (M) that insert in the mantle and pedicle lobes. The endodermal mass is not shown. (D) Side view of a larva where the mantle lobe has reversed and partially covers the apical lobe. Note the new position of the setae. A protegulum (S) has been laid down on the periostracum secreted by the mantle and pedicle lobes. The distal part of the pedicle lobe is forming a cuticle (C). (E) Side view of an individual that has completed metamorphosis. The endodermal region has formed a gut which is connected to the mantle cavity by a mouth. Shell has been added to the protegulum by the mantle.

information, however his dissertation does not make these statements.

In some animals the timing of metamorphosis appears to depend on internal signals that are only indirectly influenced by the external environment (*e.g.*, amphibia, White and Nicoll, 1981). In other organisms specific cues from the external environment play a necessary role in inducing metamorphosis (Burke, 1983a). Metamorphosis of larvae in several groups of marine invertebrate animals appears to fit this latter category. One way to distinguish between these two possibilities is to rear larvae in an environment that is devoid of the cues that are thought to induce metamorphosis and to see if metamorphosis will occur spontaneously. Larvae from several groups of animals that are competent to metamorphose will not undergo metamorphosis under these conditions (*e.g.*, Freeman, 1981, for hydrozoans). One aim of this study is to find out if this is the case for brachiopod larvae.

In those cases where specific chemical cues induce metamorphosis, the cues appear to activate receptor cells on the surface of the larva, and the receptor cells then activate a neuro-endocrine pathway that mediates metamorphosis (Morse, 1990). In some cases where metamorphosis is activated by an external chemical cue, this process can also be activated by depolarizing cells that are presumably part of the receptor or neuro-endocrine system that mediates metamorphosis by treating intact larvae with seawater containing excess K^+ (Yool *et al.*, 1986; Cameron *et al.*, 1989). Presumably the K^+ treatment activates membrane potential dependent ion channels such as Ca^{2+} or Na^+ channels. Another aim of this study is to provide evidence that settlement and metamorphosis in *Terebratalia transversa* occurs as a consequence of the opening of voltage-dependent calcium channels.

Metamorphosis involves a number of changes in the larva that occur at specific times after settlement. These changes appear to be coordinated. During the course of this work, larvae regularly have been observed that have not settled and have not reversed their mantle lobe but have secreted a protegulum. This observation indicates that different components of the metamorphic response can be dissociated from each other.

Materials and Methods

The biological material

Terebratalia transversa were dredged or collected by SCUBA at various subtidal localities near San Juan Island, Washington. The animals were maintained in aquaria with running seawater. Artificially inseminated cultures were prepared using the methods outlined in Strathman (1987). Because most *T. transversa* oocytes from a given female do not fertilize, cleavage stage embryos were picked out of the mass culture and washed in several changes of pasteurized seawater (PSW) with 100 units of Streptomycin per ml to dilute out the bacteria and inhibit their growth. Pasteurized seawater was prepared by filtering seawater through a 0.45 μM filter and heating it to 80–90°C. for 15 min followed by cooling and aeration. The embryos were reared in PSW with 100 units of streptomycin per ml in Falcon 1008 35 × 10 mm petri dishes until they had formed larvae. Streptomycin was always added to PSW immediately before use. The PSW with streptomycin and the petri dishes used were changed every other day. All experiments were carried out at 12–13°C.

For some experiments, four-day larvae were produced that had the distal tip of their pedicle removed. This operation was done by placing a larva in a Falcon plastic dish and using an electrolytically sharpened tungsten needle to cut through the pedicle lobe.

The induction of metamorphosis

Two methods were used for eliciting metamorphosis. Larvae were either exposed to natural substrates that induce metamorphosis or they were treated with seawater containing an excess of K^+ for a short time period to depolarize their cells. Natural substrate experiments were carried out in sterile flat bottom 10 × 15 mm Linbro sterile plastic dishes. One ml of cloth-filtered natural seawater was placed in the dishes and about 40 fragments of shell with external surface from a freshly smashed *T. transversa* or sand grains from the outside of a *Sabellaria* tube were added to the dish. About 20 four-day-old larvae were placed in the dish and the dish was incubated in the dark for 1 day. If 50% or more of the larvae had attached and reversed their mantle lobe, all of the animals were removed from the dish and the dish was set aside for subsequent experiments. Between 25 and 50% of the dishes were suitable for experimental purposes. When high K^+ seawater was used to induce metamorphosis, larvae were incubated in the high K^+ seawater for a defined period of time (30 min in most experiments), then washed in several changes of PSW to dilute out the K^+ and set aside in sterile Linbro dishes. They were assayed for metamorphosis at 24 h. In those experiments where larvae were treated with high K^+ in a modified seawater that lacked, or had a lower or a higher than normal amount of a given ion, the larvae were washed several times in the modified seawater before treatment with the high K^+ modified seawater. Table I gives the ionic composition of the different seawaters used.

Histological work

Larvae were fixed in 1% osmium in PSW in the cold for one hour, stored in 70% ethanol, dehydrated through an alcohol series, transferred to propylene oxide and embedded in an Epon equivalent. Sections were cut at 2 μM and stained with methylene blue.

Results

Can metamorphosis occur autonomously?

The first aim of this study was to find out if articulate brachiopod larvae would autonomously settle and undergo metamorphosis when reared in an environment with no external cues. Cohorts of 20 four-day-old larvae were set up in Linbro dishes in PSW with streptomycin. Each day of the experiment all of the larvae were examined for settlement and reversal of the mantle lobe and a cohort of larvae was examined with a compound microscope equipped with polarizing filters for shell mediated birefringence. Every other day, the larvae that were not used for birefringence studies were transferred to new sterile Linbro dishes with PSW containing streptomycin. The results of one of these experiments is presented in Table II.

Normal metamorphosis, settlement, reversal of the mantle lobe and formation of the protegulum was initiated only after larvae had been cultured in a sterile environment for at least 9 days; the percentage of larvae showing normal metamorphosis was low (29% at 10 days). Partial metamorphosis also took place in this experiment. Partial metamorphosis occurs when a larva does not settle and the mantle lobe is not reversed, but a birefringent mass forms in association with the mantle lobe (compare Fig. 2A and B). In a swimming larva, the eye spots in the apical lobe and the retractor muscles inside the pedicle lobe are birefringent. These can easily be distinguished from mantle lobe birefringence which is much stronger. The birefringent mass associated with the mantle lobe can be isolated by placing living larvae in 10% sodium hypochlorite in a 0.1 M phosphate buffer at pH 7 and

Table I

Ionic composition of artificial seawaters (mM)

Salt	Artificial SW	High K^+ SW	Na^+-free SW	High K^+ Na^+-free SW	Ca^{2+}-free SW	High K^+ Ca^{2+}-free SW	Mg^{2+}-free SW	High K^+ Mg^{2+}-free SW
NaCl	425.0	262.5	0.0	0.0	425.0	262.5	425.0	262.5
KCl	9.4	279.5	9.4	280.8	9.4	279.7	9.4	279.5
$CaCl_2 \cdot 2H_2O$	9.0	9.0	9.0	9.0	0.0	0.0	9.0	9.0
$MgCl_2 \cdot H_2O$	22.1	11.1	22.1	11.05	22.1	11.1	0.0	0.0
$MgSO_4$	25.6	12.8	25.6	12.8	25.6	12.8	0.0	0.0
$NaHCO_3$	2.1	1.1	0.0	0.0	2.1	1.1	2.1	1.1
TES buffer	10.0	5.0	10.0	5.0	10.0	5.0	10.0	5.0
Choline Cl			425.0	262.5				
$KHCO_3$			2.1	1.1				
Na_2SO_4							25.0	12.5

All seawaters had their pH adjusted to 7.9; 1M NaOH was used to adjust the pH except in Na^{2+}–free seawater where 1M KOH was used.

Table II

Settlement, normal metamorphosis, and partial metamorphosis in larvae reared under sterile conditions

Experiment number	Days in culture	Number settled	Mantle lobe reflected	Birefringent	Sample of swimming larvae	Percent birefringent
1	5	0/126			19	0
	6	0/102			18	0
	7	0/81			19	0
	8	0/59			17	0
	9	1/40	1	1	18	39
	10	6/21	6	3	15	87
2A	7	0/78			15	0
	8	0/61			14	0
	9	1/47	1	0	13	0
	10	0/31			15	40
	11	0/14			14	50
2B	7	0/76			14	0
	8	0/60			13	0
	9	0/44			13	0
	10	2/29	2	0	14	36
	11	1/14	1	1	13	54

changing the solution at frequent intervals until the organic material that makes up the larva is dissolved. One is left with a birefringent mass (Fig. 2C). When the birefringent mass was transferred to weak acid (0.1 *M* HCl), it effervesced as it dissolved indicating that it was composed of calcium carbonate. Sections through partially metamorphosed larvae showed that the calcium carbonate mass was located on the side of the mantle lobe that covered the pedicle lobe (Fig. 2D). This is the side of the mantle lobe on which the protegulum would have formed. The onset of partial metamorphosis was variable; In Experiment 1 in Table 2 it was observed as early as day nine. In a replica of this experiment with another batch of larvae (data not shown) partial metamorphosis was not observed until day 12 of culture. By the second day after the initial appearance of partial metamorphosis it was seen in 50–75% of the larvae.

A group of larvae may produce enough of a metabolite that induces metamorphosis during a two-day culture period to potentiate group metamorphosis. This possibility was examined in Experiment 2 (Table II). The onset of metamorphosis was compared for larvae from the same batch reared in groups of 16–20 in one ml dishes (Experiment 2A) or individually in one ml dishes (Experiment 2B). There was no difference in the onset of metamorphosis under these two culture conditions.

The ionic induction of metamorphosis: evidence for the involvement of voltage-dependent calcium channels

Four-day-old larvae were treated with high K^+ seawater (Table 1) for 30 min and set aside to see if they would metamorphose. The high K^+ seawater presumably depolarizes the cells of the larvae. In the high K^+ seawater the larvae stop swimming and show signs of sticking to the container. This treatment induces normal metamorphosis and partial metamorphosis in from 25–90% of the larvae, depending on the batch, when metamorphosis is assayed 24 h later (Fig. 3). Among the larvae that respond to high K^+ seawater, 40–90% undergo normal metamorphosis while the remainder undergo partial metamorphosis. Experiments where cohorts of larvae from the same batch were treated with high K^+ seawater for varying periods of time showed that a 5-min incubation in high K^+ seawater will not induce normal or partial metamorphosis while treatment with high K^+ seawater for 15, 30, or 45 min induces normal or partial metamorphosis with the same frequency. Treatment with high K^+ seawater for one or two hours reduces the percentage of larvae undergoing normal or partial metamorphosis (data not shown). While these experiments were done with a seawater with 280 m*M* K^+, artificial seawater with 114 m*M* K^+, 9 m*M* Ca^{2+} and slightly higher concentration of the other salts are equally effective (data not shown). These experiments suggest that the opening of voltage-dependent ion channels in appropriate cells may play a role in inducing metamorphosis.

The most common voltage-dependent ion channels are the calcium, sodium and potassium channels (Hille, 1984). The function of these different ion channels following membrane depolarization can be distinguished using the following criteria. (1) The movement of ions across cell membranes via these channels depends on their concentration in the external medium and the cytosol of

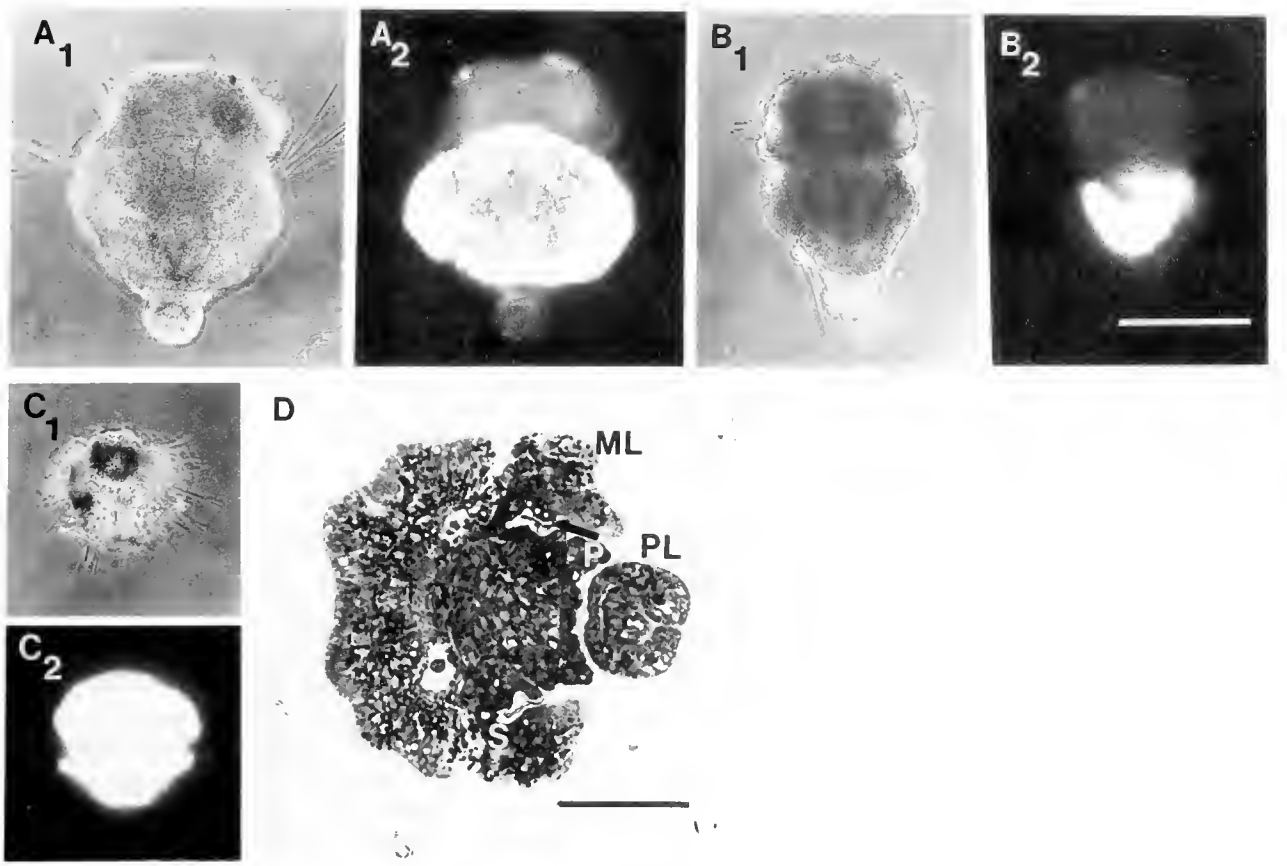

Figure 2. Photographs of larvae that have undergone normal or partial metamorphosis and the protegulum from a larva that has undergone partial metamorphosis. (A_1) Larva undergoing normal metamorphosis. The mantle lobe partly covers the apical lobe. Note the position of the setae and the eye spots of the apical lobe. (A_2) The same larva viewed with polarized light showing its birefringent protegulum and eye spots. (B_1) Partially metamorphosed larva. The mantle lobe partially covers the pedicle lobe and the setae have a position typical of a swimming larva. (B_2) Same larva viewed with polarized light showing the birefringent protegulum and eye spots. (C_1) Isolated protegulum from a partially metamorphosed larva. Note the setae embedded in the protegulum. (C_2) The same protegulum viewed with polarized light showing its birefringence. A–C are at the same magnification; the bar indicates 50 μM (D) Longitudinal section through a partially metamorphosed larva. Note the periostracum (P) between the mantle (ML) and the pedicle lobes (PL) and the space where the calcium carbonate (S) had been deposited. The bar indicates 100 μM

the cell. For example, in Ca^{2+}-free seawater the depolarization of cells should have no effect if internal Ca^{2+} levels must rise via calcium channels to initiate metamorphosis, (2) The function of specific ion channels is inhibited by channel blockers. For example, the ions Mg^{2+} and Co^{2+} and the drug nifedipine block calcium channel functions at concentrations that have no effect on sodium or potassium channel function.

Treatment of four-day-old larvae for 30 min with high K^+ in Na^+–free seawater induces normal and partial metamorphosis with the same frequency that normal and partial metamorphosis are induced in high K^+ seawater (Fig. 3A). Treatment of four-day-old larvae for 30 min with Na^+–free seawater, had no effect on metamorphosis (data not shown). Treatments of four-day-old larvae with high K^+ in Ca^{2+}–free seawater inhibited both normal and partial metamorphosis (Fig. 3B). These larvae were not damaged by the treatment in Ca^{2+}–free seawater because when some of these treated larvae were subsequently treated with high K^+ seawater, they were induced to undergo normal and partial metamorphosis.

The effects of the calcium channel blockers Co^{2+} and nifedipine on high K^+ seawater induced metamorphosis were tested (Fig. 3C, D). The Co^{2+} was prepared as a 360 mM $CoCl_2$ stock solution that was diluted appropriately with high K^+ seawater. The nifedipine was prepared as a 10 mM stock solution in ethanol and diluted appropriately in high K^+ seawater. When four-day-old larvae were inincubated for 30 min in high K^+ seawater with either 50 mM Co^{2+} or 0.2 mM nifedipine, normal and partial

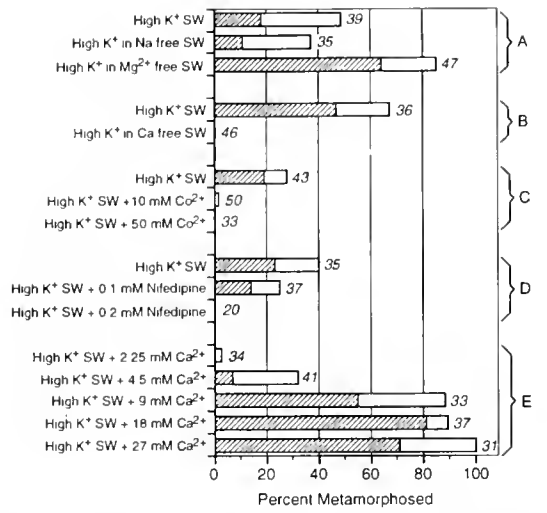

Figure 3. Histograms showing the effect of treatment with high K^+ in seawaters that lack Na^+, Ca^{2+}, or Mg^{2+}, in high K^+ seawater with different concentrations of Ca^{2+} and in high K^+ seawater with calcium channel blockers on metamorphosis. The hatched segment of each bar indicates the proportion of cases that underwent normal metamorphosis. The clear segment of the bar indicates the percentage of cases that underwent partial metamorphosis. The number of cases is indicated at the top of the bar. Experiments A–E were each done with a batch of larvae from a separate female.

metamorphosis was completely inhibited. When four-day-old larvae were incubated for 30 min in high K^+ seawater with the concentration of ethanol used to make the 0.2 m*M* nifedipine solution, metamorphosis was not inhibited (data not shown). The larvae that were treated with 50 m*M* Co^{2+} or 0.2 m*M* nifedipine were not damaged by these treatments because when some of these larvae were subsequently treated with high K^+ seawater in the absence of these calcium blockers, many of them were induced to undergo normal or partial metamorphosis. The calcium channel blocker Mg^{2+} is a normal constituent of seawater. Treatment of four-day-old larvae with high K^+ in Mg^{2+}–free saltwater induces both normal and partial metamorphosis in a higher percentage of cases than in high K^+ seawater (Fig. 3A). Treatment of four-day-old larvae for 30 min with Mg^{2+}–free seawater had no effect on metamorphosis (data not shown). When four-day-old larvae are treated with high K^+ seawater in the presence of the sodium channel blocker tetrodotoxin at a concentration of 20 n*M*, metamorphosis was not inhibited.

In an additional experiment, the effect of varying the external concentration of Ca^{2+} on high K^+ seawater mediated metamorphosis was tested by incubating four-day-old larvae for 30 min in an appropriate high K^+ seawater. The normal Ca^{2+} concentration in seawater is 9 m*M*. Concentrations of Ca^{2+} were used that were lower or higher than the normal concentration (Fig. 3E). At concentrations of 2.25 m*M* Ca^{2+} high K^+ seawater had almost no effect on metamorphosis. At concentrations between 4.5 and 9 m*M* Ca^{2+} the percentage of larvae undergoing metamorphosis increased; between 4.5 and 18 m*M* Ca^{2+} the proportion of larvae showing normal metamorphosis increased. Incubating four-day-old larvae for 30 min in artificial seawater with 18 or 27 m*M* Ca^{2+} had no effect on metamorphosis. The response to high K^+ seawater in the presence of elevated levels of Ca^{2+} was comparable to the responses to high K^+ seawater in the absence of the calcium channel blocker Mg^{2+}. In both cases there was a significant increase in the percentage of larvae that underwent normal as opposed to partial metamorphosis.

Does substrate induced metamorphosis involve putative voltage-dependent calcium channel function?

Substrate induced metamorphosis presumably involves a random walk on the part of the larva until it makes contact with a substrate bound inducer that elicits metamorphosis. These experiments were done to find out if inhibitors of calcium channel function, Co^{2+}, nifedipine, and Ca^{2+}-free seawater, also inhibit substrate induced metamorphosis and if Mg^{2+}-free seawater or high Ca^{2+} seawater, which facilitate calcium channel function, also facilitate substrate induced metamorphosis. Some of these experiments were not feasible. Incubation of larvae in Ca^{2+} or Mg^{2+}-free seawater for 24 h leads to a marked decrease in the adhesive bonds between cells, causing some cell dissociation. It was possible to do experiments in low Ca^{2+} seawater (2.25 m*M*). When larvae were incubated in seawater with 50 m*M* Co^{2+} or 0.2 m*M* nifedipine, both agents caused the larvae to stop swimming after a few hours rendering them unable to sample the substrate. After about 12 h the nifedipine began to come out of solution and form crystals at the air-water interface; as this happened, the larvae began to locomote again. It was possible to incubate larvae in seawater with 10 m*M* Co^{2+}; under these conditions larval locomotion slowed down but did not stop.

Four-day-old larvae were used for these experiments. Substrate induced metamorphosis differs from high K^+ induced metamorphosis in that the larvae either undergo natural metamorphosis, which was assayed 24 h after the experiment had been set up, or they retain their larval character. Very few cases of partial metamorphosis were observed. Over 100 larvae that were swimming after 24 h in the experiments without the channel blocker Co^{2+}, or low or high Ca^{2+} were examined; only three of these cases had a birefringent mantle lobe. Both 10 m*M* Co^{2+} and low Ca^{2+} seawater inhibited substrate induced metamorphosis (Fig. 4A, B). Treatment with Co^{2+} or low Ca^{2+} seawater for 24 h did not damage these larvae because when they were introduced into a dish with a substrate that would induce metamorphosis or treated with high

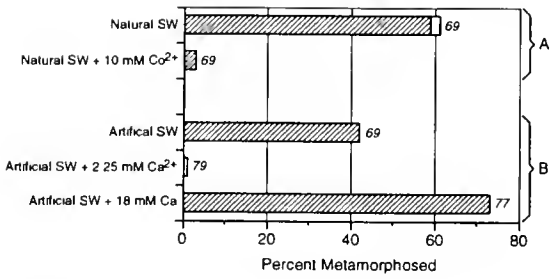

Figure 4. Histograms showing the effect of treatment with seawater with lower than normal or higher than normal concentrations of Ca^{2+} or the calcium channel blocker Co^{2+} on substrate induced metamorphosis. The hatched segment of each bar indicates the proportion of cases that underwent normal metamorphosis. The number of cases is indicated at the top of the bar. Experiments A and B were done with larvae from separate females.

K^+ seawater for 30 min, over half of these larvae underwent metamorphosis. The Co^{2+} and low Ca^{2+} seawater treatments did not alter the ability of the substrate in the Linbro dishes to induce metamorphosis. When the seawater with the Co^{2+} and the low Ca^{2+} seawater was removed from the wells and replaced by natural seawater and a batch of four-day larvae were added to the dish, metamorphosis was induced in more than 50% of the cases at 24 h. When larvae were placed in dishes with a substrate that would induce metamorphosis under conditions where the Ca^{2+} was higher than normal (18 m*M*), a higher proportion of larvae underwent metamorphosis than in dishes of seawater with the normal amount of Ca^{2+} (9 m*M*) (Fig. 4B). These experiments suggest that calcium channel function may also play a role in substrate induced metamorphosis.

The role of the pedicle lobe in metamorphosis

Prior to substrate induced metamorphosis the larva approaches the site where it will settle with its pedicle lobe, makes contact and adheres to the substrate with the distal end of its pedicle lobe. The possibility exists that there are substrate receptor cells in the pedicle that have to be activated to initiate metamorphosis. These may be the same cells that contain putative voltage-dependent calcium channels whose activation is necessary for metamorphosis.

In order to test this hypothesis four-day-old larvae were operated on to remove the distal portion of their pedicle lobe (Fig. 5), and two hours after the operations were completed they were tested to see whether or not they could undergo substrate induced or high K^+ seawater induced metamorphosis (Fig. 6). None of these larvae settled or reversed their mantle lobe. Settling should not be expected because the distal part of the pedicle lobe is missing, and reversal of the mantle lobe is also not expected because

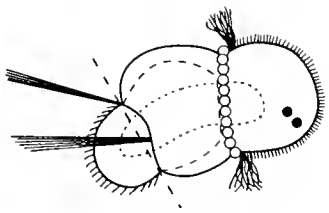

Figure 5. Diagram of a swimming larva showing the operation to remove the distal part of the pedicle lobe.

the retractor muscles that presumably play a role in moving the mantle lobe have been cut (see Discussion). All of the larvae with the distal end of the pedicle lobe missing swam around the Linbro dish among the substrates in a normal manner; at 24 h none of these larvae exhibited mantle birefringence indicating that substrate induced metamorphosis had not occurred. Many of the larvae with the distal end of the pedicle lobe missing that were treated with high K^+ seawater underwent partial metamorphosis when assayed at 24 h; however, the percentage of cases undergoing partial metamorphosis was not as high as it was for intact four-day-old larvae from the same batch. These results suggest that substrate receptors needed for metamorphosis are located in the pedicle lobe and that the removal of the distal region of the pedicle makes the larva unresponsive to substrate mediated cues, however, other cells with putative voltage-dependent calcium channels whose activation is necessary for metamorphosis are located in another region of the larva.

Can larvae that have undergone partial metamorphosis subsequently undergo normal metamorphosis?

It is not clear whether partial metamorphosis is the result of the activation of a metamorphic pathway or an epiphenomenon that is not related to metamorphosis. The strongest evidence that partial metamorphosis is related to normal metamorphosis is that both can be induced with high K^+ seawater and that both can occur spontaneously at the same time in aging larvae reared under

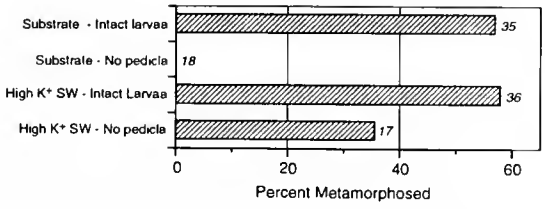

Figure 6. Histograms showing the effect of pedicle removal on substrate or high K^+ seawater induced metamorphosis. Metamorphosis was measured as larvae with birefringent mantle lobes. The number of cases is indicated at the top of the bar. The histograms combine data from two experiments on larvae from separate females.

sterile conditions. To better understand partial metamorphosis, experiments were done to find out if larvae that had undergone partial metamorphosis could respond to substrates that induce metamorphosis or high K^+ seawater by undergoing normal metamorphosis.

A large batch of four-day-old larvae were induced to undergo metamorphosis using high K^+ seawater. Under these conditions some of the larvae underwent normal metamorphosis, some underwent partial metamorphosis and some larvae had not metamorphosed when they were assayed one day later. The five-day-old larvae that had undergone partial metamorphosis and those that had not metamorphosed as a consequence of the high K^+ seawater treatment and five-day-old larvae from the same batch that had not previously been treated with high K^+ seawater were exposed to a substrate that would induce metamorphosis or high K^+ seawater with 18 m*M* Ca^{2+} which induces normal metamorphosis in a high percentage of cases. The results of these experiments (Fig. 7) show that larvae which have already undergone partial metamorphosis will not respond to a natural substrate that induces metamorphosis or to high K^+ seawater with 18 m*M* Ca^{2+} by settling or reversing their mantle. Reversal of the mantle may not be possible for these larvae because of the calcification of their mantle lobe; some movement of the lobe in these partially metamorphosed larvae is possible because when they are stimulated by prodding with a tungsten needle, the setae of the larvae take on a transient position perpendicular to the body. This same kind of movement takes place in normal larvae. There is no obvious reason why partially metamorphosed larvae should not be able to attach to the substrate. When larvae that had been treated with high K^+ seawater that did not undergo normal or partial metamorphosis were treated with a natural substrate that induces metamorphosis or high K^+ seawater with 18 m*M* Ca^{2+}, many of these larvae underwent natural or partial metamorphosis. The percentage of pretreated larvae that underwent metamorphosis was lower than the percentage of larvae metamorphosing that had not been pretreated with high K^+ seawater. This suggests that larvae which have been exposed to a metamorphic stimulus and do not respond, may either be less competent to respond to a metamorphic inducer and have been selected for via the pretreatment, or prior exposure to a metamorphic inducer may render these larvae less competent to respond to a subsequent metamorphic cue even though they have not undergone metamorphosis.

As part of this experiment some larvae that settled, but had not yet undergone mantle reversal, were gently removed from their substrate with a tungsten needle so that their pedicle lobe was not damaged and transferred to PSW in a sterile Linbro dish, while other larvae that had not undergone mantle reversal were left in place. All of the larvae that had not yet undergone mantle reversal and were not disturbed underwent normal metamorphosis by the next day (six cases). The larvae that were removed from their settlement site did not resettle but underwent partial metamorphosis (four out of six cases). This experiment suggests that settlement is necessary for normal metamorphosis.

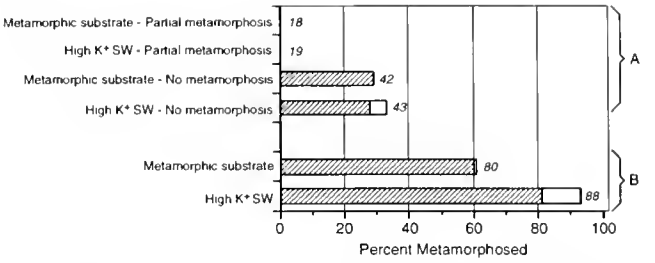

Figure 7. (A) Histograms showing the effect of pretreatment at four days of larvae with high K^+ seawater that either induced partial metamorphosis or no metamorphosis on the ability of these two categories of larvae to undergo metamorphosis after treatment with a metamorphosis substrate or high K^+ seawater at five days. (B) Histograms showing effect of treatment with a metamorphosis substrate or high K^+ seawater at five days on metamorphosis of larvae that had not been pretreated with high K^+ seawater at four days. The hatched segment of each bar indicates the proportion of cases that underwent normal metamorphosis. The clear segment of the bar indicates the percentage of cases that underwent partial metamorphosis. The number of cases is at the top of the bar.

Discussion

The role of voltage-dependent Ca^{2+} channels in metamorphosis

The following lines of evidence indicate that voltage-dependent calcium channels may play a role in metamorphosis: (1) Treatment of larvae with high K^+ seawater which presumably depolarizes the cells of the larva induces metamorphosis and treatment of larvae with high K^+ in Na^+-free seawater is just as effective in inducing metamorphosis, (2) Treatment of larvae with high K^+ in Ca^{2+}-free seawater inhibits metamorphosis, (3) Treatment of larvae with high K^+ in seawater with elevated Ca^{2+} levels or Mg^{2+}-free seawater increases the percentage of cases metamorphosing, (4) Treatment of larvae with high K^+ seawater in the presence of the calcium channel blockers Co^{2+} and Nifedipine inhibits metamorphosis. In order to make this work more convincing one would have to demonstrate electrophysiologically that target cells are not only depolarized but give an action potential which is typical of voltage-dependent Ca^{2+} channels and that Ca^{2+} moves into the target cells from the external environment during depolarization.

The identities of the target cells where voltage-dependent calcium channels function to mediate the metamorphic stimulus is not known. One possible target cell

candidate is a subset of cells in the larval nervous system. There is evidence that the nervous system receives and mediates the metamorphic stimulus in echinoid larvae (Burke, 1983b). Unfortunately, virtually nothing is known about the organization of the nervous system in articulate brachiopod larvae; however, nerve cell processes have been noted in ultrastructural studies done on these larvae for other purposes (Stricker and Reed, 1985a). Another possible set of target cells could be some of the cells that make up the surface epithelium of the larva (*e.g.*, the cells of the distal part of the pedicle lobe). After these cells receive a metamorphic stimulus, it could be transferred to other epithelial cells of the larva by epithelial conduction. There is evidence that epithelial conduction mediates the metamorphic stimulus in hydrozoans (Freeman and Ridgway, 1990).

Both substrate and high K^+ seawater induced metamorphosis appear to depend on calcium channel function. Substrate induced metamorphosis also depends on the pedicle lobe while high K^+ seawater induced metamorphosis does not. The simplest model that accounts for these results is that there is a substrate-induced metamorphosis receptor at the distal end of the pedicle lobe. When this is activated a metamorphic signal is sent from this site to cells outside of the distal region of the pedicle lobe that must have their putative voltage-dependent calcium channels activated in order to spread the metamorphic stimulus (Fig. 8). When the cells outside the distal region of the pedicle lobe are activated, they also send an inhibitory signal to the cells in the distal region of the pedicle lobe preventing them from responding to substrate mediated metamorphic cues (Fig. 7).

The significance of "partially metamorphosed" larvae

The partially metamorphosed larva is most probably the result of an abnormal metamorphic response. This larva is characterized as a larva that forms a protegulum in the absence of mantle reversal and settlement. Because the formation of a protegulum under these conditions probably renders the mantle lobe incapable of reversal and because the mantle lobe does not spread out to occupy a larger area as it does after reversal, this metamorphic response is probably maladaptive. I have made only limited attempts to look for later manifestations of normal metamorphosis in partially metamorphosed larvae. Two partially metamorphosed larvae were fixed and sectioned four days after the initiation of high K^+ seawater induced metamorphosis. Both of these larvae showed suggestions of cuticle deposition by the pedicle. In order to make this point with certainty, it would be necessary to do a study of these larvae at an electron microscope level of resolution. I did not observe any indication of mouth formation in these partial larvae; however, they may not have been cultured long enough.

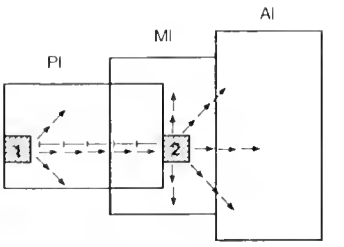

Figure 8. Diagrammatic view of a swimming larva with an apical lobe (AL), mantle lobe (ML), and pedicle lobe (PL). At the distal end of the pedicle lobe there is a postulated center composed of cells (1) which may use voltage-dependent calcium channels to transduce a substrate mediated metamorphic signal. This center sends a stimulatory metamorphic signal to other cells in the larva including center (2) which functions via voltage-dependent calcium channels that acts as a secondary metamorphic center. Here this center is shown in the mantle lobe but it could be any place outside of the distal end of the pedicle lobe. The cells of this secondary metamorphic center send a stimulatory metamorphic signal to other cells of the larva and an inhibitory signal to the cells that transduce the substrate mediated metamorphic signal turning off the metamorphic stimulus from these cells. This model accounts for the experiments described in this paper.

A variety of factors probably play a role in generating the partial metamorphosis phenotype. In larvae that have been reared for a number of days in a sterile environment intrinsic maturational changes may occur so that various parts of the metamorphosis signaling pathway or cells that respond to the signaling pathway may be activated. If the postulated distal pedicle lobe substrate receptor cells were activated, an aged larvae may undergo normal metamorphosis. This happened in a small percentage of cases (Table II). If cells that are part of the metamorphic pathway that reside outside of the distal region of the pedicle lobe are activated or if cells that will form the protegulum are activated, a larva that shows the partial metamorphosis phenotype would be generated. There is evidence that in some species with a bathy-pelagic life cycle that larvae which do not see an appropriate metamorphic cue in nature will metamorphose or partially metamorphose and still continue a pelagic existence (Thorson, 1946; Paine, 1963).

The mechanics of mantle lobe reversal during metamorphosis are not understood. There is a pair of muscles that insert in the mantle lobe and the pedicle lobe that are thought to contract during metamorphosis causing the mantle lobe to flip (Franzen, 1969; Long, 1964). Substrate adhesion by the pedicle lobe may be necessary for these muscles to contract or to cause the pedicle lobe to be compressed in an appropriate way as the muscles contract so that the mantle lobe is reversed. The production of larvae that show partial metamorphosis following substrate detachment could occur because protegulum formation is activated even though mantle reversal is inhibited. The small number of cases where partial metamor-

phosis occurs following the culture of larvae in the presence of substrates that induce metamorphosis can be explained in this way. Partially metamorphosed larvae and the conditions where they are formed provide an insight into the normal metamorphosis process.

Acknowledgments

I am grateful to Dr. A. O. D. Willows and the staff of the Friday Harbor Laboratories for their hospitality. I want to thank Sarah Cohen and her diving companions for collecting animals using SCUBA, Dr. Craig Staude for saving animals for me that were collected on dredging trips, and Drs. Alan Kohn and Patricia Morse for letting me use animals that were dredged for class use. I want to thank Judith Lundelius, Bob Goldstein, and Hyla Sweet for their comments on this manuscript. This work was supported by NSF grant DCB-8904333 and a URI research leave from The University of Texas.

Literature Cited

Burke, R. D. 1983a. The induction of metamorphosis of marine invertebrate larvae: stimulus and response. *Can J Zool.* **61:** 1701–1719.

Burke, R. D. 1983b. Neural control of metamorphosis in *Dendraster excentricus*. *Biol. Bull.* **164:** 176–188.

Cameron, A., T. Tosteson, and V. Hensley. 1989. The control of sea urchin metamorphosis: ionic effects. *Develop. Growth Differ.* **31:** 589–594.

Franzen, A. 1969. On larval development and metamorphosis of *Terebratulina* Brachiopoda. *Zool Bid Uppsala* **38:** 155–174.

Freeman, G. 1981. The role of polarity in the development of the hydrozoan planula larva. *Roux's Arch Dev Biol* **190:** 168–184.

Freeman, G., and E. B. Ridgway. 1990. Cellular and intracellular pathways mediating the metamorphic stimulus in hydrozoan planulae. *Roux's Arch Dev Biol* **199:** 63–79.

Hille, B. 1984. *Ionic Channels and Excitable Membranes.* Sinauer Assoc., Sunderland, MA.

Long, J. A. 1964. The embryology of three species representing three superfamilies of articulate brachiopoda. Ph.D. Dissertation, University of Washington.

Long, J. A., and S. A. Stricker. 1991. Brachiopoda. Pp. 47–84 In *Reproduction in Marine Invertebrates, Vol 6 Echinoderms and Lophophorates*, A. C. Giese, J. S. Pearse, and V. B. Pearse, eds. Boxwood Press, Palo Alto, CA.

Morse, D. E. 1990. Recent progress in larval settlement and metamorphosis: closing the gaps between molecular biology and ecology. *Bull Mar Sci.* **46:** 465–483.

Paine, R. 1963. Ecology of the brachiopod *Glottidia pyramidata*. *Ecol. Monogr* **33:** 187–213.

Strathman, M. 1987. *Reproduction and Development of Marine Invertebrates of the Northern Pacific Coast.* University of Washington Press, Seattle, WA.

Stricker, S. A., and C. G. Reed. 1985a. The ontogeny of shell secretion in *Terebratalia transversa* (Brachiopoda, Articulata) I. Development of the mantle. *J Morphol.* **183:** 233–250.

Stricker, S. A., and C. G. Reed. 1985b. The protegulum and juvenile shell of a recent articulate brachiopod: patterns of growth and chemical composition. *Lethaia* **18:** 295–303.

Stricker, S. A., and C. G. Reed. 1985c. Development of the pedicle in the articulate brachiopod *Terebratalia transversa* (Brachiopoda, Terebratulida) *Zoomorphology* **105:** 253–264.

Thorson, G. 1946. Reproduction and larval development of Danish marine bottom invertebrates. *Medd. Komm. Dan Fisk: Havundersog Ser. Plankton* **4:** 1–523.

White, B. H., and C. S. Nicoll. 1981. Hormonal control of amphibian metamorphosis. Pp. 363–396 in *Metamorphosis: A Problem in Developmental Biology*, L. I. Gilbert and E. Frieden, eds. Plenum, New York.

Yool, A. J., S. M. Green, M. Hadfield, R. Jensen, D. Markell, and D. Morse. 1986. Excess potassium induces larval metamorphosis in four marine invertebrate species. *Biol. Bull.* **170:** 255–266.

Reference: *Biol. Bull.* **184**: 25–35. (February, 1993)

Species Relationships in a Marine Gastropod-Trematode Ecological System

LAWRENCE A. CURTIS[1] AND KAREN M. K. HUBBARD*

University Parallel, School of Life Sciences, and College of Marine Studies, University of Delaware, Newark, Delaware 19716*

Abstract. Individual snails (*Ilyanassa obsoleta*) on Cape Henlopen, Delaware, frequently are host to one or more trematode species. When different species occupy the same host, interactions might be expected. We investigated five species of parasites to determine whether their existence in different combinations would lead to altered within-host distributions or changed numbers of shed cercariae. Snails (32 samples, total = 379) were collected from June to August, in 1989, and microscopically examined. Parasite species and stages present in five sections through each snail were recorded. Before examination, 206 of these snails were held in individual chambers in the field. After two high tides (*ca.* 24 h), the chambers were checked for species and the numbers of cercariae shed. Overall, 22 trematode combinations in single hosts were observed. Analysis revealed that co-occurrence with other species had no significant effects on any trematode. Further, analyses of species richness of infecting assemblages over two distinct intervals failed to show that competition is important in determining assemblage richness. One pair of trematodes (*Himasthla quissetensis* and *Lepocreadium setiferoides*) has been reported not to co-occur. We observed co-occurrences, but so few that the apparent conflict between them could not be statistically demonstrated. We suggest that, in this system, parasites are adapted to the host only; they may interact, but they are not adapted to each other. Chances for a parasite to live free from other parasites seem too great for evolved (adapted) relationships to develop. The host, for similar reasons, is probably not adapted to the parasites.

Received 14 February 1992; accepted 6 October 1992.

[1] Mailing address: Cape Henlopen Laboratory, College of Marine Studies, University of Delaware, Lewes, DE 19958.

Introduction

For one species to be adapted to another, they must interact in such a manner that one consistently exerts a selective pressure on the other. Species interactions may be thought of as a continuum from local to global. A local interaction (as used here) results in genetic changes in restricted parts of a gene pool (and may result in local ecotypes). On the other hand, if an interaction is global, one species can be a source of biotic selective pressure over the whole operating gene pool of another. Reciprocal genetic changes between species amount to coevolution (Futuyma and Slatkin, 1983). This paper considers the species interactions in a marine gastropod–trematode system. Because the host gastropod has a planktonic larva and the trematodes are dispersed by highly mobile definitive hosts, both local and global phenomena must be considered.

The interactions between hosts and parasites have been much discussed (see Moore, 1987 for an extensive review), and the levels at which such discussions may be focussed should be distinguished. In this work, two levels are necessary. The component community includes all parasite species using a particular host species (population). The infracommunity includes all the parasites in a single host (Esch *et al.*, 1990). An individual host, harboring a multispecies parasite assemblage, is a biological unit where parasite–parasite as well as host–parasite interactions can occur.

There are four basic patterns of *evolutionary* relationships that may be found in any host–parasite system (Fig. 1a–d). In scheme a, the parasites are adapted to the host (the minimal condition), whereas in scheme b, the host is also adapted to the parasites. Scheme c illustrates the case where the parasites are adapted to the host and to

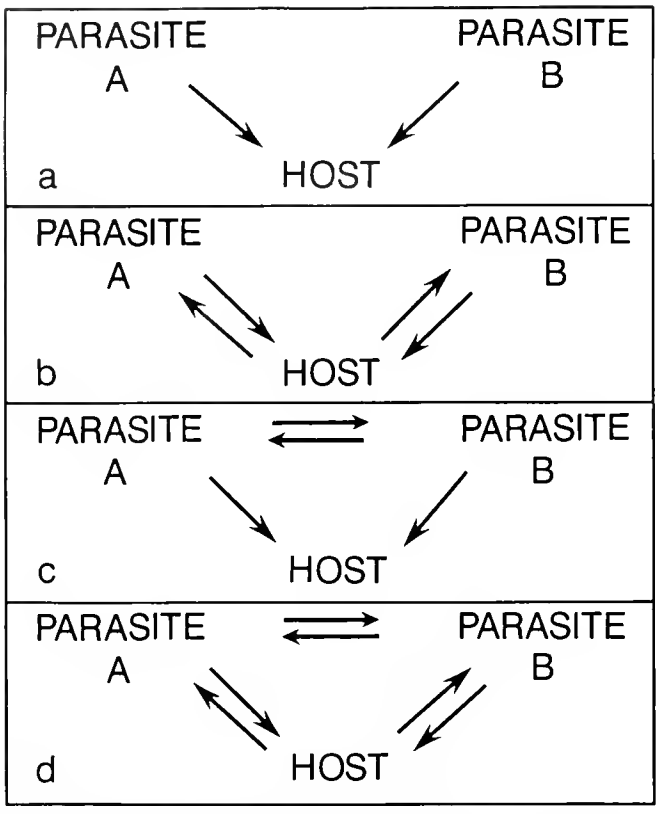

Figure 1. Four models of possible adaptive relationships among species in a snail-trematode system. Parasites A and B may coexist in a single host. An arrow from one participant to another indicates that the participant at the origin of the arrow has evolved adaptations to selection pressures coming from the other (*i.e.*, "PARASITE A → PARASITE B" means A is adapted to B). One-way interactions between parasites (*i.e.*, A adapts to B but not the reverse) are possible, but not figured.

each other. Scheme d shows the case where parasites are coevolved with the host and with each other. There should be evidence of an adaptive relationship between species before it is assumed to exist (Williams, 1966). In this work, we have tested for species interactions among trematodes inhabiting the same gastropod host. The goal is to gather evidence to support the elimination of one or more of the above schemes and thereby improve our understanding of host–parasite systems.

Studies of trematodes infecting gastropod populations have often revealed patterns of species co-occurrence that suggest interactions (see Rohde, 1981 for references). However, few workers have examined trematode assemblages in individual gastropods taken from their natural habitat, to determine whether fitness of certain members is consistently affected by co-occurrence with other members (see DeCoursey and Vernberg, 1974). This is largely because multiply-infected hosts are difficult to obtain in numbers for study. The prevalence of trematodes in the population of *Ilyanassa obsoleta* (Prosobranchia, Neogastropoda) on Cape Henlopen, Delaware Bay is high, and a diversity of multiply-infected snails may be obtained (Curtis, 1985, 1987, 1990; Curtis and Hubbard, 1990). This allowed us to test for species interactions in a variety of trematode ensembles.

Of the nine trematode species in *Ilyanassa obsoleta* observed in Delaware, five are commonly observed in the Cape Henlopen population and figure in this study: *Himasthla quissetensis, Lepocreadium setiferoides, Zoogonus rubellus, Austrobilharzia variglandis,* and *Gynaecotyla adunca.* The snail is the first intermediate host. A variety of second intermediate hosts is used by these species. Various shorebirds serve as definitive hosts for *H. quissetensis, A. variglandis* and *G. adunca,* whereas fish species are used by *L. setiferoides* and *Z. rubellus* (see Stunkard, 1983 for life-cycles and taxonomic matters). Any direct species interactions among these parasites must occur in the snail, the only host they all have in common.

There is no indication that *Ilyanassa obsoleta* lose infections (Curtis and Hurd, 1983), so the ensembles observed in snails probably represent relatively longstanding (period unknown) assemblages. Enduring species assemblages, proximity in a natural habitat unit, and utilization of similar resources (Smyth and Halton, 1983), suggest that strong interspecific interactions might occur.

If competitive interactions are frequent within individual hosts whereby dominant species come to monopolize the host population through time, a pattern should emerge at the component community level. Early on, most snails should have single species infections; as time progresses species accumulate and there should be a preponderance of double and triple infections; and eventually there should be mostly single infections again, as the dominant species evict subordinates (Sousa, 1990). We searched for such a component community pattern among our snails at two time scales, through the summer and over several years.

To examine within-snail parasite interactions, we tested individual species to see whether existence in different assemblages had consequences in terms of (1) alterations of within-snail spatial distributions, (2) complete suppression of cercarial production, and (3) changes in numbers of cercariae released from hosts.

Materials and Methods

One sandbar (Fig. 2), located near the mouth of the Delaware Bay on Cape Henlopen (75° 06′W, 38° 47′N), was chosen as the source for snails. Certain species of trematodes affect the behavior, distribution and temporal occurrence of *Ilyanassa obsoleta* on sandbars (Curtis, 1987, 1990). To avoid over-representing snails harboring particular parasite ensembles, we randomly chose collection sites according to the angle and distance from a reference point at the peak of the sandbar (Fig. 2). Samples

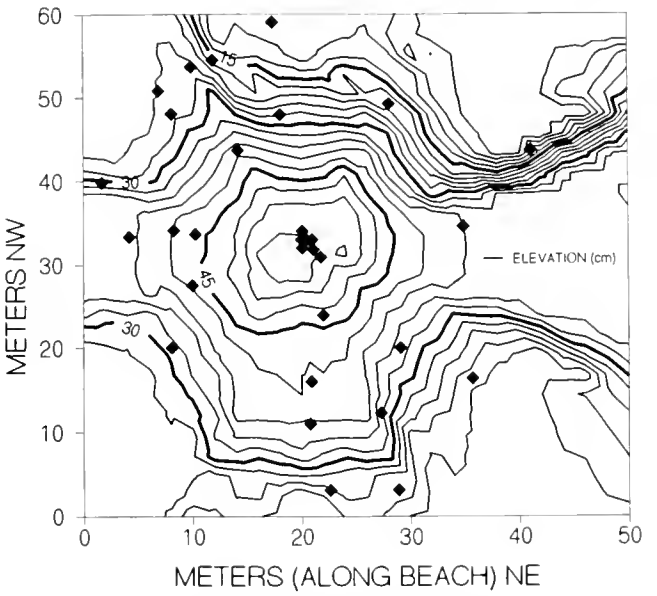

Figure 2. An elevational contour map of the 1989 sandbar on Cape Henlopen, Delaware where samples of *Ilyanassa obsoleta* were collected for this study. The 32 randomly selected sample sites are indicated by filled diamonds. The highest point on the map (the sandbar peak at center) is 56 cm above the lowest.

were taken between 16 June and 17 August 1989 on both day and night low tides. We wanted many multiply-infected snails in the samples, and the 379 snails obtained (Table I) were purposely biased to include them. The snails came from an area where many multiples were likely to be found (*e.g.*, Curtis, 1987), and large snails that were likely to be infected were chosen (Curtis and Hurd, 1983). Usually, two collections of 10 to 13 snails were collected and processed at a time. All the snails were dissected and 206 were also tested for cercarial release.

We were interested in revealing gross within-snail displacements of individual parasite species by other species or combinations of species. Such displacements would be required if dominant species gradually evicted subordinates from the snail. During dissection each snail was removed from its shell and examined in sections to determine how individual parasite species, and stages thereof, were distributed within. Heavily parasitized snails are virtual bags of trematodes; they retain no consistent morphological landmarks that are useable as standard points of reference. Consequently, each snail was pinned to a board and cut crosswise into five equal lengths with a razor blade. Section 1 was the most dorsal portion of the snail (the spire), and section 5 was the most ventral (head and foot). The razor was cleaned between cuts and scrupulous care was taken to prevent contamination of one section with material from another.

Sections were placed separately in small vials containing 5 ml filtered baywater. Each vial was vigorously shaken 50 times to release the contained trematode stages into the water. A small amount of the water was placed on a slide and examined with the aid of dissecting (32×) and compound (100×) microscopes. We took two samples from each vial. The species and stages of the trematodes were recorded for each section of each snail as follows: parental stages (rediae or sporocysts) and cercariae (PC); cercariae only (C); parental stage without mature cercariae (P); or absent (A). Observed cercariae may have been liberated from parental stages during the procedure, but this does not matter as we were only interested in whether formed (mature) cercariae were present. Trematodes were never found in section 5, and after the hundredth snail we stopped examining this section.

Table I

Trematode infections in Ilyanassa obsoleta *collected for this study from a sandbar area (Fig. 2) on Cape Henlopen, Delaware*

Infecting species	n	Mean shell height (mm)	Range shell height (mm)
uninfected	18	21	17–25
singles			
Hq	74	24	20–27
Ls	25	24	20–27
Zr	29	22	20–26
Av	5	23	22–24
Ga	29	22	18–25
doubles			
HL	4	23	22–23
HZ	42	24	20–27
HG	10	23	21–25
LZ	8	24	20–28
LA	1	25	—
LG	32	23	20–26
ZA	1	24	—
ZG	24	23	20–27
AG	10	22	19–24
AD	1	23	—
GD	1	21	—
triples			
HZG	33	24	18–26
LZA	1	28	—
LZG	22	23	17–26
LAG	4	21	20–24
ZAG	5	23	23–25
Total =	379	Overall = 23	17–28

For each infection, number collected (n), and mean and range of shell heights are given. Snails infected by a single species (singles) are represented by the genus and species initials of the trematode (Hq = *Himasthla quissetensis*, Ls = *Lepocreadium setiferoides*, Zr = *Zoogonus rubellus*, Av = *Austrobilharzia variglandis*, Ga = *Gynaecotyla adunca*). Double and triple infections are represented with the generic initials of the species involved (*e.g.*, a snail infected with *H. quissetensis*, *Z. rubellus*, and *G. adunca* goes in the HZG category). *Diplostomum nassa* (D) occurred only in double infections. Shell height = siphonal canal to apex of shell (*e.g.*, 21 = 20.5 to 21.4 mm).

The frequencies of parasite presence or absence in the snails were crosstabulated according to the following criteria: parasite assemblage (those species infecting the snail); snail section (1 – 4); and the stage of the parasite (sporocysts, rediae, cercariae). Contingency table analyses were employed to test for significant displacements of parasite stages within snails. For each parasite, we used log linear models (Sokal and Rohlf, 1981) to calculate the expected frequencies of occurrence of the stages (PC, P, C, or A) in various sections of hosts harboring various trematode ensembles. A saturated log linear model for this kind of analysis includes seven terms: Assemblage; Section; Stage; Assemblage × Section; Assemblage × Stage; Section × Stage; and Assemblage × Section × Stage. The purpose of this analysis is to learn which of these terms are necessary to calculate a set of expected frequencies that do not deviate significantly from the observed frequencies. After unnecessary terms are eliminated, we are left with the accepted model. The accepted model is expressed in hierarchical form. For example, an Assemblage × Section × Stage hierarchical model would nest all seven terms of the full model; and an Assemblage, Section × Stage model would nest all three one-way terms and the Section × Stage two-way term.

If species interactions lead to spatial rearrangements within snails, a 3-way interaction term (*i.e.*, Assemblage × Section × Stage) would be necessary in the accepted model for any displaced species. For example, suppose species "a" were usually distributed throughout the snail from spire to mantle when it occurred alone, but in the presence of species "b" (*i.e.*, assemblage "ab"), "a" were consistently absent from the spire section. The three-way interaction term would be necessary in the accepted model because absence (A) of species "a" from Section 1 would be a consequence of Assemblage composition. That is, the presence of species "b" in Section 1 would change Stage entries for "a" in Section 1 to absent (A) from one of the present categories (PC, P, or C). Therefore, a table of expected frequencies that matched observed frequencies could not be calculated without the Assemblage × Section × Stage term in the accepted model.

We used cercarial release as a measure of fitness to learn whether parasites were affected by within-host interactions with other infecting species. We evaluated cercarial output from assemblages during one short period, and tested similar assemblages throughout the summer. (An alternative, more manipulation laden, approach would be to follow cercarial output from individual assemblages over a longer period of time.) Individual snails were confined in chambers in the natural environment for two high tides (*ca.* 24 h), and the water in which they had been immersed was examined for numbers and species of cercariae. We used 24-h periods to encompass any daily shedding patterns. The procedure is described in more detail in Curtis and Hubbard (1990). We used a Kruskal–Wallis test (Hollander and Wolfe, 1973) to determine, for each species, whether the number of cercariae shed was significantly different when in various co-occurring assemblages of parasites. All statistical calculations were done with the software package, Number Cruncher Statistical System, 5× Series.

Results

A competition model (Sousa, 1990) suggests that trematodes might invade a snail population, accumulate in snails, compete, and eventually complete the process by having dominant trematodes evict subordinates. If true, then over the relevant time we should see infecting species richness start low (mostly single infections), increase (mostly doubles and triples), and then decrease again. We looked for such a pattern within two distinct intervals, over the summer (Table IIA), and over several years (Table IIB). We divided the sampling period into four two-week intervals; the fourth interval was extended to encompass the 25 snails collected on August 17. There were significant changes in richness from one period to the next, but the expected pattern was not seen. In particular, triple infections were quite abundant early in summer and were most abundant in the last sampling period. This would not have been observed if dominant trematodes had defeated subordinates in this period of time.

Using size-classes of snails (Table IIB), the interval can be extended from months to years. At the beginning of its third summer, a snail on Cape Henlopen is about 14–15 mm; by the end of that summer, it has grown to about 17–18 mm (Curtis and Hurd, 1983). This means that the smallest snails we collected (17 mm, Table I) were probably in their fourth summer. If 3 mm/summer is used as an estimate of growth for parasitized snails, then the < =22 group in Table IIB is 4–5 yr old; the 23–25 group is 5–6 yr old; and the 26–28 group is 6–7 yr old. The interval encompassed by Table IIB is about three years using this estimate. Parasitized snails may not grow this rapidly, and the interval is possibly longer. In this years-long interval (size-class range), there were significant changes in infecting species richness. Note (Table IIB) that single infections were more abundant than triple infections in the youngest snails, but that the proportion of triples increased among older snails. This is not the pattern predicted by the competition model.

Occurrence of stages of five trematodes in sections of *Ilyanassa obsoleta* harboring different assemblages is shown in Table III. Recall that section 1 was dorsal (spire) and section 4 ventral (mantle). In Table IV, models for all five species (except *Austrobilharzia variglandis*) require the one-way Assemblage term because of the widely different numbers of snails infected with each assemblage

Table II

Trematode infections in Ilyanassa obsoleta *examined during this work crosstabulated by number of infecting trematode species (richness), time of collection in summer 1989 (A), and size (age) of snail (B)*

	Infecting Species Richness				
	% NI (n = 18)	% Singles (n = 162)	% Doubles (n = 134)	% Triples (n = 65)	n =
A. Time Collected					
16 Jun–29 Jun	0.9	39.8	44.3	15.0	113
30 Jun–13 Jul	15.0	38.7	40.0	6.3	80
14 Jul–27 Jul	1.1	50.0	30.7	18.2	88
28 Jul–17 Aug	4.1	42.9	25.5	27.5	98
B. Size Class (mm)					
< = 22	10.5	43.8	33.3	12.4	153
23–25	1.0	43.6	36.9	18.5	195
26–28	0.0	32.3	35.5	32.3	31
2-way contingency analyses:					
Time × richness, $\chi^2_{(9)} = 43.69$, $P < 0.001$					
Size × richness, $\chi^2_{(6)} = 25.16$, $P < 0.001$					

Size class ranges are in terms of shell height as in Table I.

(see Table III). The frequencies for *Lepocreadium setiferoides* can be modeled by taking into account, beyond the Assemblage term, only the one-way Stage term because most of the stage entries are in the PC category. The rest of the models require the Section × Stage term because there was some specificity as to what sections were likely to harbor which stages. This is clearest for *Zoogonus rubellus* and *Gynaecotyla adunca*. Stages were often (clearly not always) absent (A) from sections 1 and 4. However, this was not significantly correlated with the assemblage of species infecting the snail. For none of the five species tabulated is an Assemblage × Section × Stage (three-way) interaction term necessary in its accepted hierarchical log linear model (Table IV). That is, co-occurring trematodes did not significantly affect the distribution of any of the five species tested. In most snails, parasite stages of all species present occurred throughout.

Parasite species interactions could lead to cercarial suppression in a section rather than species eviction. For example, if the presence of species "a" suppressed cercarial production by species "b", the accepted log linear model for species "b" would have to include the Assemblage × Stage term. This would be necessary because, for species "b" in the presence of species "a", the frequency of the PC category would decrease, while the frequency of the P category would increase as compared to other assemblages involving species "b". Expected values that matched this shift in observed frequencies could not be predicted (modeled) without incorporating the influence of Assemblage on Stage. No species' cercarial production was completely suppressed in this manner (Table IV, lack of Assemblage × Stage terms).

The question now becomes: given that cercariae were being produced, was the number released from snails changed as a function of assemblage composition? To answer this, we used data from cercarial release chambers. Prepatent infections (those with no cercariae present) were eliminated from this analysis because their prepatency was not caused by assemblage composition (Table IV, no Assemblage × Stage terms in the accepted models). Including prepatents would add meaningless variability. Absent cercariae are not germane to this analysis if they are not caused by the presence of other species. Table V describes statistically the cercarial output of each of the five species in various assemblages. The magnitude of variability should be noted.

Table VI presents the results of Kruskal–Wallis tests that were used to determine whether the assemblage composition significantly affected the numbers of cercariae released by particular (patent) assemblage members. The results show that although cercarial output (mean rank) did decrease for all species when additional species were present, there was not a significant depression of cercarial output for any one species.

Finally, because *Himasthla quissetensis* and *Lepocreadium setiferoides* have not previously been observed together, note that in Table V such a co-occurrence is listed, and that both species shed cercariae concurrently. Four snails contained both *H. quissetensis* and *L. setiferoides* (Table I). Based on observations of a few mature (often moribund) *H. quissetensis* rediae and cercariae among many *L. setiferoides* rediae and cercariae, it appeared that *L. setiferoides* was evicting *H. quissetensis* from the snails. There were not enough of these snails to

Table III

Spatial distributions of five trematode species (see Table I for parasite abbreviations) within singly- and multiply-infected Ilyanassa obsoleta. *Observed frequencies of parasite occurrence (by stage*), in snail sections 1–4 (see text), are given for each species*

Infecting trematodes	Species tabulated	Section 1 Stage				2 Stage				3 Stage				4 Stage			
		PC	C	P	A	PC	C	P	A	PC	C	P	A	PC	C	P	A
Hq (n = 74)	Hq	72	1	1	0	73	0	1	0	73	1	0	0	69	2	1	2
HZ (n = 42)	Hq	38	0	2	2	40	0	0	2	40	1	0	1	33	6	2	1
HG (n = 10)	Hq	6	0	3	1	10	0	0	0	9	0	0	1	8	0	1	1
HZG (n = 33)	Hq	30	0	2	1	33	0	0	0	32	0	1	0	27	2	0	4
Ls (n = 25)	Ls	25	0	0	0	25	0	0	0	24	1	0	0	22	3	0	0
LZ (n = 8)	Ls	8	0	0	0	8	0	0	0	8	0	0	0	7	1	0	0
LG (n = 32)	Ls	26	4	2	0	32	0	0	0	30	0	2	0	23	2	3	4
LZG (n = 22)	Ls	19	2	1	0	21	1	0	0	21	1	0	0	17	5	0	0
Zr (n = 29)	Zr	27	0	0	2	27	0	0	2	27	0	0	2	17	0	0	12
HZ	Zr	25	0	0	17	37	0	0	5	38	0	0	4	26	2	0	14
LZ	Zr	4	0	0	4	8	0	0	0	7	1	0	0	2	0	0	6
ZG (n = 24)	Zr	22	0	0	2	24	0	0	0	23	0	0	1	10	0	0	14
HZG	Zr	20	0	0	13	30	0	0	3	32	0	0	1	17	0	0	16
LZG	Zr	12	0	0	10	21	0	0	1	21	0	0	1	8	0	1	13
ZAG (n = 5)	Zr	3	0	0	2	4	0	0	1	5	0	0	0	0	0	0	5
Av (n = 5)	Av	4	1	0	0	5	0	0	0	4	0	0	1	2	0	0	3
AG (n = 10)	Av	7	0	0	3	10	0	0	0	10	0	0	0	2	0	0	8
ZAG (n = 5)	Av	3	0	0	2	5	0	0	0	1	0	0	4	0	0	0	5
Ga (n = 24)	Ga	25	0	0	4	28	0	0	1	26	0	0	3	16	1	0	12
HG	Ga	6	0	0	4	9	0	0	1	10	0	0	0	4	1	0	5
LG	Ga	23	1	1	7	29	0	1	2	29	1	0	2	16	2	0	14
ZG	Ga	20	0	0	4	22	0	0	2	24	0	0	0	15	0	0	9
AG	Ga	9	0	0	1	9	0	0	1	9	0	0	1	8	0	0	2
HZG	Ga	21	0	0	12	28	0	0	5	32	0	0	1	10	0	0	23
ZG	Ga	14	0	0	8	17	0	0	5	21	0	0	1	13	0	0	9
AG	Ga	4	1	0	0	5	0	0	0	5	0	0	0	4	0	0	1

* Stage abbreviations: PC = parental stage (*i.e.*, sporocysts or rediae) plus cercariae; P = parental stage only; C = cercariae only; and A = all stages absent.

Individual species occurred in the context of several different combinations of infecting species (*e.g.*, Hg occurred alone, in HZ and HG doubles, and in HZG triples). For each species, frequencies are tabulated for each context. The number (n) of snails infected by particular trematode assemblages is indicated. Assemblages found in fewer than four snails are not tabulated.

be included in the above log linear or Kruskal–Wallis analyses.

Discussion

Ilyanassa obsoleta is the only shared host in the life-cycles of these trematode species and is, therefore, the only place they might directly interact. They are tightly packed together in the snail, gather resources in similar ways, and are abundant on Cape Henlopen. Antagonistic interactions between trematode assemblage members have been noted by several investigators (*e.g.*, Lie *et al.*, 1965; Basch *et al.*, 1969; DeCoursey and Vernberg, 1974; Kuris, 1990; Sousa, 1990). On such grounds we anticipated that trematodes co-occurring in *I. obsoleta* would interact and most likely compete. A between-snail (component community) analysis indicated that competition within snails was not an important determinant of the number of trematodes infecting individual snails. Further, regarding within-snail phenomena, no effect of assemblage composition on any individual species could be discerned statistically. However, *Himasthla quissetensis* and *Lepocreadium setiferoides* were seen to co-occur in this study for the first time (Tables I, V), and this observation deserves special comment. By virtue of their rare co-occurrence, which eliminated the pair from our statistical analyses, these species apparently do interact negatively when they occur in the same snail.

Our sample of trematode assemblages from the Cape Henlopen sandflat naturally included only those species combinations that can coexist long enough to be observed by the methods used. These included most of the possible

Table IV

Results of loglinear analyses testing the influence of three factors (trematode Assemblage, snail Section, and parasite Stage) on the frequencies of within snail occurrence reported in Table V

Species analyzed	Hierarchical log-linear model accepted	χ^2	d.o.f.	$P = *$
Hq	Assemblage, Section × Stage	54.21	45	0.163
Ls	Assemblage, Stage	67.33	57	0.165
Zr	Assemblage, Section × Stage	63.25	90	0.985
Av	Section × Stage	25.79	32	0.773
Ga	Assemblage, Section × Stage	60.99	105	0.999

* An insignificant χ^2 ($P > 0.05$) without the three-way interaction term means that it is unnecessary; no significant displacement occurred.

If a trematode's stages (*i.e.*, sporocysts, rediae, cercariae) were displaced from one snail section to another by the presence of a co-occurring species or combination of species, the accepted model for that trematode would require the three-way interaction term (*i.e.*, Assemblage × Section × Stage) to calculate expected frequencies without significant deviation from the observed.

assemblages and virtually all that might have been expected to occur. Twenty, of the 32 possible for five species analyzed, were actually observed (Table I). Missing assemblages were the quintuple, the five quadruples, multiples involving the scarce *Austrobilharzia variglandis*, and two triples involving *Himasthla quissetensis* and *Lepocreadium setiferoides*.

A major concern is whether interparasite competitions occur that require considerable time for completion. In the early to middle phases of competition there may be no noticeable effect on any one species. We may have examined most assemblages at a time when coexistence is possible, and erroneously concluded that species do not interact. If such a time-course for competition is involved, how much time is necessary, and was our collection of parasite assemblages (in snails) biased by this? Two possibilities present themselves: competitions could play themselves out over the summer; or over several summers. There was no indication that trematodes assemble in snails, compete, and ultimately evict subordinate species in either the short or the long interval (Table II). To the contrary, species appear to collect in snails as a function of time. Note that older snails, and not either younger group, have the largest proportion of triple infections (Table IIB). Sousa (1990) looked for a hyperbolic relationship between snail size and infecting species richness and similarly did not find one.

Direct measurements of within-snail species dynamics also indicate no interactions among assemblage members. The occurrence of parasitic stages in different sections of variously infected snails is shown in Table III. No species was excluded from sections of snails because of co-occurring species (lack of Assemblage × Section × Stage terms in Table IV). If one species (or combinations of species) leads to gradual eviction of another species from snails, this phenomenon should have been quite common. Neither was cercarial production (from existing parental stages) of any species shut down by co-occurring species (lack of Assemblage × Stage terms in Table IV). Also, there was no indication that cercarial output from hosts (an estimate of fitness) was influenced by co-occurring species. There was no statistically significant reduction of cercarial output of any species as a function of assemblage

Table V

Descriptive statistics associated with numbers of trematode cercariae released per host (Ilyanassa obsoleta) *in 24 h in the field. Information is grouped by species of cercariae being tabulated (see Table I for species abbreviations)*

Infecting trematodes	Cercariae tabulated	Mean #	S.D.	Max.	Med.	Min.
Hq (n = 42)	Hq	527	709	2739	225	0
HL (n = 1)	Hq	18	0	18	18	18
HZ (n = 23)	Hq	211	344	1428	90	0
HG (n = 4)	Hq	696	1135	2388	177	42
HZG (n = 22)	Hq	155	274	1233	60	0
Ls (n = 18)	Ls	319	590	2394	129	0
HL (n = 1)	Ls	567	0	567	567	567
LZ (n = 2)	Ls	130	185	261	131	0
LG (n = 10)	Ls	42	66	165	9	0
LZG (n = 15)	Ls	121	153	483	45	0
LAG (n = 2)	Ls	18	25	36	18	0
Zr (n = 12)	Zr	249	378	1095	15	0
HZ (n = 20)	Zr	68	199	882	1	0
LZ (n = 2)	Zr	0	0	0	0	0
ZA (n = 1)	Zr	1065	0	1065	1065	1065
ZG (n = 8)	Zr	61	67	189	42	0
HZG (n = 19)	Zr	47	73	210	6	0
LZG (n = 13)	Zr	79	138	474	21	0
ZAG (n = 2)	Zr	12	8	18	12	6
Av (n = 3)	Av	0	0	0	0	0
ZA (n = 1)	Av	0	0	0	0	0
AG (n = 5)	Av	9	16	36	0	0
LAG (n = 3)	Av	21	16	33	27	3
ZAG (n = 1)	Av	6	0	6	6	6
Ga (n = 14)	Ga	222	454	1398	0	0
HG (n = 3)	Ga	6	10	18	0	0
LG (n = 8)	Ga	74	168	483	0	0
ZG (n = 6)	Ga	0	0	0	0	0
AG (n = 5)	Ga	3	5	12	0	0
HZG (n = 17)	Ga	2	9	36	0	0
LZG (n = 13)	Ga	27	96	345	0	0
LAG (n = 4)	Ga	6	12	24	0	0
ZAG (n = 1)	Ga	18	0	18	18	18

Only infections that were patent for the species being tabulated are considered (n). For example, there were 33 HZG-infected snails (from Table I); 22 of these were patent for Hq; 19 for Zr; and 17 for Ga. A total of 206 snails were tested for cercarial release.

Table VI

Results of Kruskal-Wallis tests evaluating the null hypothesis for each trematode species (see Table I for species abbreviations), that the number of cercariae shed was unaffected by coexisting species

Effect of coexisting species on fitness of	Infecting species	Mean rank (# cercariae)	d.o.f.	Kruskal-Wallis H	$P =$
Hq	Hq (n = 42)	52.583			
	HZ (n = 23)	41.957			
	HG (n = 4)	53.500			
	HZG (n = 22)	36.295	3	6.454	0.091
Ls	Ls (n = 18)	23.972			
	LG (n = 10)	15.850			
	LZG (n = 15)	23.733	2	3.186	0.203
Zr	Zr (n = 12)	42.417			
	HZ (n = 20)	29.575			
	ZG (n = 8)	42.563			
	HZG (n = 19)	33.763			
	LZG (n = 13)	41.962	4	5.254	0.262
Av	No test				
Ga	Ga (n = 14)	39.536			
	LG (n = 8)	39.688			
	ZG (n = 6)	26.500			
	AG (n = 5)	38.100			
	HZG (n = 17)	28.471			
	LZG (n = 13)	33.537			
	LAG (n = 4)	34.375	6	8.075	0.233

Prepatent infections and trematode assemblages observed fewer than four times were excluded.

composition (Table VI). There was much variation, even in single infections (Table V), suggesting that sources of variability other than co-occurring species control cercarial output.

DeCoursey and Vernberg (1974) studied assemblages of trematodes infecting *Ilyanassa obsoleta* in North and South Carolina. At the level of the component community, they noted that some species co-occur in multiple infections more or less often than would be expected based on the abundance of each in the system. They proposed that such patterns are produced by antagonisms or affinities among assemblage members. About 80 snails were dissected, with 30 of these being serially sectioned. The number of snails examined in each assemblage category is not reported. The authors noted "marked overlap in territory and habitat preferences," as we did in this study. Contrary to our conclusion (based on arbitrary snail sections) that the parasites are not displaced, they concluded that some species are displaced from preferred sites (specific snail organs) by other species. Even if small scale displacements (*i.e.*, from organ to organ within our arbitrary sections) do occur, they would have to result in reductions in cercarial output (fitness) to have evolutionary consequences. Cercarial output was not significantly reduced (Table VI). We also note that, if the interest is in adaptation of one parasite to others (Fig. 1), then sectioning snails along snail organ boundaries confounds adaptation to other parasites with adaptation to the host.

In the laboratory, DeCoursey and Vernberg (1974) also counted the cercariae released from 10 infected snails. Three were infected with *Zoogonus lasius* (=*rubellus*) and five with *Lepocreadium setiferoides*. The remaining two were doubly infected with these same species. The numbers of cercariae released in the laboratory by each species of trematode were averaged and compared. When *Z. rubellus* and *L. setiferoides* occurred alone, they each released approximately 3500 cercariae in 24 h. When the species co-occurred, they released 901 and 1477, respectively. The authors concluded that *L. setiferoides* suppressed cercarial release by *Z. rubellus*. Data show that cercarial production of both species was lower when they co-occurred. In any case, the number of observations precludes meaningful statistical inference.

We are interested in eliminating inoperative models from the four presented in Figure 1. Williams' (1966) distinction between "functions" and "effects" seems useful here. Functions are biological characteristics that are direct products of natural selection (adaptations), whereas effects are characteristics that are a consequence of functions ("side" effects, not directly selected). Holmes (1986) points out that parasitic ". . . interactions should be important [in structuring helminth communities] only when species regularly co-occur at substantial population densities" (p. 203, brackets ours). We note, more specifically, that interactions based on adaptive responses (functions) of one parasite species to another cannot arise unless there is frequent co-occurrence over global gene pools.

We cannot imagine how the parasites under study here could have adapted to one another. Definitive hosts (fish and birds) are highly mobile and scatter parasite eggs widely and unevenly. Consequently, spatial distribution of these trematodes within and among host snail populations is patchy (Curtis and Hurd, 1983; Curtis and Hubbard, 1990), and there are abundant opportunities for trematode species to exist in isolation. The probability of co-occurrence generation after generation, particularly for specific parasites, is very low. Therefore, evolved parasite-parasite relationships are unlikely in this system. If interactions occur, they most likely result from effects, not functions. Our data indicating the lack of interactions among the majority of co-occurring trematodes, and the above considerations, justify eliminating models "c" and "d" (Fig. 1). Any evolved features of this system probably stem ultimately from the evolution of parasites to host, or possibly of host to parasites (models "a" and "b", Fig. 1).

In deciding between models "a" and "b", many of the same arguments apply. Gooch *et al.* (1972) found that

Ilyanassa obsoleta were electrophoretically homogeneous all along the eastern seaboard, pointing to extensive dispersal of larvae as the main cause. The planktonic larvae of *I. obsoleta* would then function analogously to parasite definitive hosts in the dispersal of progeny. Given the heterogeneity of trematode prevalence in *I. obsoleta* populations, many snail larvae would settle where parasites are not a frequent environmental challenge. If a snail were to obtain, by mutation, resistance to infection by one or more trematode species, its fitness probably would be enhanced in parasite-ridden environments such as parts of Cape Henlopen. Yet its progeny would very possibly settle where parasites are infrequent. The mutation, there, would be at best neutral. These considerations suggest that model "a" (Fig. 1) is the operative one—the only adaptive responses between species in the *I. obsoleta* system are most likely those of the parasites to the host.

The negative interaction between *Himasthla quissetensis* and *Lepocreadium setiferoides* in the *Ilyanassa obsoleta* system deserves comment because it seems to counter the proposition that these parasites are not adapted to each other. A lack of co-occurrence of these abundant species in *I. obsoleta* has been reported (Vernberg *et al.*, 1969; Curtis, 1985), but the detailed dissection methods used in this study revealed four co-occurrences (Table 1). Obviously, miracidia of both species reach the same host, and there is a subsequent eviction (apparently of *H. quissctensis*). This eviction is important in terms of determining composition of the infra- and component assemblages observed, but is it based on adaptation of one parasite to another? In keeping with the above reasoning—that parasite co-occurrence is not globally predictable enough to result in adaptations to other parasites—we interpret this negative co-occurrence as based on an effect rather than a function [an exaptation (Gould and Vbra, 1982)] because it results from the way these species have evolved to the host, not to each other. In ecological terms, such a phenomenon is a competitive exclusion. However, in our hypothesis, the exclusion occurs between two species that are adaptively unaware of each other. If species interactions are an evolutionary force driving the structuring of interactive, co-adapted species assemblages, then we should distinguish between function- and effect-based relationships among species. A deeper appreciation of causal relationships in ecological systems will require understanding these relationships.

Factors structuring the assemblage of larval trematodes in populations of the California estuarine snail *Cerithidea californica* have been examined by Sousa (1990) and Kuris (1990). Two direct lines of evidence convinced these authors that competitive exclusions were occurring among *C. californica* trematodes. Sousa (1990) cites personal laboratory observations in which dominant species preyed upon stages of subordinates. Both authors reported trematode species replacements in individual snails periodically reexamined for infection by cercarial release. Kuris (1990) constructed a competitive hierarchy among trematode species in infracommunities, which he concluded would produce component community structure. In the *Ilyanassa obsoleta* system, such cercarial release data would have to be used judiciously because cercariae, even if present, often are not shed (Curtis and Hubbard, 1990). Data are not presented that assess this source of error for the *C. californica* system. In any event, there is considerable heterogeneity in prevalence of trematodes among *C. californica* populations (Kuris, 1990; Sousa, 1990). Parasite progeny are dispersed by definitive hosts similar to those in the *I. obsoleta* system, giving species the same opportunities to exist in isolation. This may mean that, whether they interact or not, parasites are not co-adapted in the *C. californica* system either. Because *C. californica* has direct development (Sousa, 1990)—making populations more insular—the host may have the ability to evolve to its parasites.

Several authors have examined snail–trematode systems for interactions among parasites infecting the same host individual. Some have emphasized direct microscopical observations of antagonisms occurring in freshwater snails (*e.g.*, Lie *et al.*, 1965; Basch *et al.*, 1969; Mouahid and Mone, 1990). Based upon such observations, there can be no doubt that antagonisms between trematodes can and do occur, but their frequencies in natural snail populations are less certain. Other authors have emphasized observations of multiple infections in marine (*e.g.*, Kuris, 1990; Sousa, 1990) and freshwater (*e.g.*, Fernandez and Esch, 1991a, b; Williams and Esch, 1991) gastropods. In no case are multispecies assemblages reported to be particularly frequent. Such species-rich assemblages are more frequent and various in the *Ilyanassa obsoleta* system on Cape Henlopen (Curtis, 1985, 1987, 1990; present study) than in any studied so far (see Cort *et al.* (1937)). The most frequent assemblage observed on Cape Henlopen is *Lepocreadium setiferoides* with *Gynaecotyla adunca*, and it occurred in only 4.4% of snails (n = 4870) examined by dissection (Curtis, unpub. data). Individual occurrence of each was 16.9 and 20.3%, respectively. Thus, even when species can and do co-occur, the probability of co-occurrence is slight. The opportunity to evolve adaptive responses to other particular trematodes seems minimal or nonexistent, which suggests that models "c" and "d" (Fig. 1) may be generally inoperative. The best opportunity for trematode–trematode adaptive responses would be in a situation where all the necessary hosts are confined to one habitat, such as in a freshwater pond, as described by Williams and Esch (1991) and Fernandez and Esch (1991a). However, Williams and Esch (1991) and Fernandez and Esch (1991b) conclude that within-snail trematode interactions in their system are in-

frequent and not the factor structuring the infra- and component communities.

Can the host be adapted to its parasites? The evolution of a host to several parasites is a problem of "overwhelming complexity" (McLennan and Brooks, 1991), and the issue is not resolvable with the data at hand. Dobson and Merenlender (1991) suggest, as we content here, that the probability of such evolutionary responses would depend on host and parasite dispersal abilities. *Ilyanassa obsoleta*, because of its widespread dispersal, is unlikely to evolve to its parasites (model "b"), but it is a possibility with a snail in a more insular system, such as a pond.

How can the coexistence, in a small habitat unit, of several species with similar resource requirements be explained? This study has provided considerable comparative data on the fitness of parasites when they occur in different assemblages. The extensive variation in cercarial output (Table V) is not explainable by looking to presence or absence of other species. Perhaps resources for trematodes living in *Ilyanassa obsoleta* are somehow not limiting. We have suggested that the only adaptations (functions) in the system are those of the parasites enabling them to live in the snail (model "a", Fig. 1). We offer the following possible explanation. Each of these five trematodes has evolved to castrate the host snail. Castration of the host stems from a parasite adaptation to channel energy to the parasite that would otherwise go to the support of host gonadal tissue (Baudoin, 1975). *Ilyanassa obsoleta* is a long-lived host (7 years or more); the largest (oldest) snails are nearly all parasitized where trematodes are prevalent; and they appear not to lose infections (Curtis and Hurd, 1983). The host must survive the rigors of succeeding winters. A trematode adapted to such a host may have been selected to exact intermediate to minimal damage (besides castration) because it could then "farm" the host for many years (see Minchella *et al.* (1985) and Gill and Mock (1985) for similar interpretations of host-parasite systems). We propose that, if the trematodes of *I. obsoleta* operate this way, then they should not singly, or in multiples, drain resources to the extent that they become limiting. In brief, they can coexist if they are all adapted to live well below the level at which the host is stressed.

Acknowledgments

We would like to thank the Undergraduate Research Office and the School of Life Sciences, University of Delaware for a Science and Engineering Scholar grant, and two Peter White Fellowships awarded to support K. H.'s undergraduate thesis, from which this paper is adapted. We thank J. Moore for helpful comments on an earlier version. We are also grateful for the efforts and comments of two anonymous reviewers. This is contribution number 173 from the Program in Ecology, School of Life Sciences.

Literature Cited

Basch, P. F., K. J. Lie, and D. Heyneman. 1969. Antagonistic interaction between strigeid and schistosome sporocysts within a snail host. *J. Parasitol.* **55:** 753–758.

Baudoin, M. 1975. Host castration as a parasitic strategy. *Evolution* **29:** 335–352.

Curtis, L. A. 1985. The influence of sex and trematode parasites on carrion response of the estuarine snail *Ilyanassa obsoleta*. *Biol. Bull.* **169:** 377–390.

Curtis, L. A. 1987. Vertical distribution of an estuarine snail altered by a parasite. *Science* **235:** 1509–1511.

Curtis, L. A. 1990. Parasitism and the movements of intertidal gastropod individuals. *Biol. Bull.* **179:** 105–112.

Curtis, L. A., and K. M. Hubbard. 1990. Trematode infections in a gastropod host misrepresented by observing shed cercariae. *J. Exp. Mar. Biol. Ecol.* **143:** 131–137.

Curtis, L. A., and L. E. Hurd. 1983. Age, sex and parasites: spatial heterogeneity in a sandflat population of *Ilyanassa obsoleta*. *Ecology* **64:** 819–828.

Cort, W. W., D. B. McMullen, and S. Brackett. 1937. Ecological studies on the cercariae in *Stagnicola emarginata angulata* (Sowerby) in the Douglas Lake region, Michigan. *J. Parasitol.* **23:** 504–532.

DeCoursey, P. J., and W. B. Vernberg. 1974. Double infections of larval trematodes: competitive interactions. Pp. 93–109 in *Symbiosis in the Sea*, W. B. Vernberg, ed. University of South Carolina Press, Columbia, SC.

Dobson, A. P., and A. Merenlender. 1991. Coevolution of macroparasites and their hosts. Pp. 83–101 in *Parasite–Host Associations Coexistence or Conflict?* C. A. Toft, A. Aeschlimann, and L. Bolis, eds. Oxford University Press, New York.

Esch, G. W., A. W. Shostak, D. J. Marcogliese, and T. M. Goater. 1990. Patterns and processes in helminth parasite communities: an overview. Pp. 1–19 in *Parasite Communities: Patterns and Processes*, G. Esch, A. Bush, and J. Aho, eds. Chapman and Hall, London.

Fernandez, J., and G. W. Esch. 1991a. Guild structure of larval trematodes in the snail *Helisoma anceps:* patterns and processes at the individual host level. *J. Parasitol.* **77:** 528–539.

Fernandez, J., and G. W. Esch. 1991b. The component community structure of larval trematodes in the pulmonate snail *Helisoma anceps*. *J. Parasitol.* **77:** 540–550.

Futuyma, D. J., and M. Slatkin. 1983. Introduction. Pp. 1–13 in *Coevolution*, D. J. Futuyma and M. Slatkin, eds. Sinauer Associates, Sunderland, MA.

Gill, D. E., and B. A. Mock. 1985. Ecological and evolutionary dynamics of parasites: the case of *Trypanosoma diemyctyli* in the red-spotted newt *Notophthalmus viridescens*. Pp. 157–183 in *Ecology and Genetics of Host–Parasite Interactions*, D. Rollinson and R. M. Anderson, eds. Academic Press, New York.

Gooch, J. L., B. S. Smith, and D. Knupp. 1972. Regional survey of gene frequencies in the mud snail *Nassarius obsoletus*. *Biol. Bull.* **142:** 36–48.

Gould, S. J., and E. Vbra. 1982. Exaptation—a missing term in the science of form. *Paleobiology* **8:** 4–15.

Hollander, M., and D. A. Wolfe. 1973. *Nonparametric Statistical Methods*. John Wiley and Sons, New York.

Holmes, J. C. 1986. The structure of helminth communities. Pp. 203–208 in *Parasitology—Quo vadit?*, M. J. Howell, ed. Proceedings 6th International Congress of Parasitology, Australian Academy of Sciences, Canberra.

Kuris, A. 1990. Guild structure of larval trematodes in molluscan hosts: prevalence, dominance and significance in competition. Pp. 69–100 in *Parasite Communities: Patterns and Processes*, G. Esch, A. Bush, and J. Aho, eds. Chapman and Hall, London.

Lie, K. J., P. F. Basch, and T. Umathevy. 1965. Antagonism between two species of larval trematodes in the same snail. *Nature* **206**: 422–423.

McLennan, D. A., and D. R. Brooks. 1991. Parasites and sexual selection: a macroevolutionary perspective. *Q Rev. Biol* **66**: 255–286.

Minchella, D. J., B. K. Leathers, K. M. Brown, J. M. McNair. 1985. Host and parasite counteradaptations: an example from a freshwater snail. *Am Nat* **126**: 843–854.

Moore, J. 1987. Some roles of parasitic helminths in trophic interactions. A view from North America. *Revista Chilena de Historia Natural* **60**: 159–179.

Mouahid, A., and H. Mone. 1990. Interference of *Echinoparyphium elegans* with the host-parasite system *Bulinus truncatus-Schistosoma bovis* in natural conditions. *Ann Trop. Med Parasitol.* **84**: 341–348.

Rohde, K. 1981. Population dynamics of two snail species, *Planaxis sulcatus* and *Cerithium moniliferum*, and their trematode species at Heron Island, Great Barrier Reef. *Oecologia* **49**: 344–352.

Smyth, J. D., and D. W. Halton. 1983. *The Physiology of Trematodes*, 2nd ed. Cambridge University Press, Cambridge.

Sokal, R. R., and F. J. Rohlf. 1981. *Biometry*, 2nd ed. Freeman and Company, New York.

Sousa, W. P. 1990. Spatial scale and the processes structuring a guild of larval trematode parasites. Pp. 41–67 in *Parasite Communities Patterns and Processes*, G. Esch, A. Bush, and J. Aho, eds. Chapman and Hall, London.

Stunkard, H. W. 1983. The marine cercariae of the Woods Hole, Massachusetts region, a review and a revision. *Biol Bull.* **164**: 143–162.

Vernberg, W. B., F. J. Vernberg, and F. W. Beckerdite. 1969. Larval trematodes: double infections in the common mud-flat snail. *Science* **167**: 1287.

Williams, G. C. 1966. *Adaptation and Natural Selection* Princeton University Press, Princeton, NJ.

Williams, J. A., and G. W. Esch. 1991. Infra- and component community dynamics in the pulmonate snail *Helisoma anceps*, with special emphasis on the hemiurid trematode *Halipegus occidualis*. *J Parasitol.* **77**: 246–253.

Reference: *Biol. Bull.* **184**: 36–51. (February, 1993)

Effects of Marine Bacteria on the Culture of Axenic Oyster *Crassostrea gigas* (Thunberg) Larvae

PHILIPPE DOUILLET[1] AND CHRISTOPHER J. LANGDON

Oregon State University, Department of Fisheries, Hatfield Marine Science Center, Newport, Oregon 97365

Abstract. Bacteria-free oyster larvae (*Crassostrea gigas*) were cultured under aseptic conditions; they were fed axenic algae (*Isochrysis galbana*), and the medium was inoculated with isolated strains of marine bacteria. Twenty-one bacterial strains were tested, and most were detrimental to larval survival and growth. However, additions of strain CA2 consistently enhanced larval survival (21–22%) and growth (16–21%) in comparison with control cultures that were fed only algae. Size-frequency distributions of populations of larvae cultured for 10 days on axenic algae were skewed due to the poor growth of many individuals; whereas size-frequencies from populations of larvae fed axenic algae supplemented with CA2 bacteria were distributed normally. Strain CA2 may therefore make a nutritional contribution to the growth of oyster larvae. *I. galbana* did not grow under the light intensities used for larval culture; thus the improvement in larval growth cannot be attributed to bacterial enhancement of algal growth and, consequently, food availability. Naturally occurring microflora from Yaquina Bay, Oregon, depressed survival or growth of larvae-fed live algae.

Introduction

Bivalve larvae in culture vary substantially in survival and growth (Davis, 1953; Loosanoff, 1954; Walne, 1956a). Between 25% and 50% of the variability in the growth of a single population of mussel larvae (Innes and Haley, 1977), or different populations of larval *Crassostrea virginica* (Newkirk *et al.*, 1977), are due to genetic factors. A significant proportion of the variability in the survival of *C. gigas* larvae was similarly attributed to genetic factors (Lannan, 1980). Exogenous factors, such as temperature (Loosanoff, 1959), salinity (Bayne, 1965), pH (Calabrese and Davis, 1970), food quantity (Walne, 1965), food quality (Davis, 1953), age of the algal food (Dupuy, 1975), larval concentration (Loosanoff *et al.*, 1953), size of container (Dupuy, 1975), silt (Davis and Hidu, 1969), exudates of unfavorable algal species (Bayne, 1965), water quality (Millar and Scott, 1967) and toxicants (Walne, 1970) have been found to contribute significantly to variability in larval growth. Nonetheless, even different cultures of larvae obtained from the same parents and grown under identical conditions of temperature, salinity and ration have been commonly reported to vary in their growth (Bayne, 1983).

The role of bacteria as beneficial or harmful agents in the culture of bivalve larvae has been the subject of many investigations, but this role has not been fully evaluated. Thirteen different isolates of marine bacteria did not support the growth of oyster larvae when provided as the sole source of particulate food (Davis, 1950, 1953). High bacterial densities in cultures of bivalve larvae are generally considered to be deleterious to the larvae (Walne, 1956a, 1956b, 1958), and even innocuous bacteria in large numbers have been reported to depress the rate of algal ingestion (Ukeles and Sweeney, 1969). Some bacterial strains are reportedly able to invade larvae, to produce toxins, or both (Guillard, 1959; Tubiash *et al.*, 1965; Tubiash *et al.*, 1970; Brown, 1973; Di Salvo, 1978; Nottage and Birkbeck, 1986). In contrast, bacteria have also been implicated as a food source for bivalve larvae (Carriker, 1956; Hidu and Tubiash, 1963) or as improving the growth of larvae fed on algae (Martin and Mengus, 1977; Beese, in Prieur *et al.*, 1990).

The elimination of microbial contaminants is prerequisite to a study of the effects of a bacterial strain on an organism in culture. This approach has been used to study the effects of several bacterial strains on cultures of the

Received 3 June 1992; accepted 10 November 1992.

[1] Present address: The University of Texas at Austin, Marine Science Institute, P.O. Box 1267, Port Aransas, Texas 78373.

protozoan *Amoeba nitrophila* (Frosch, 1897 in Luck *et al.*, 1931); the cladoceran *Moina macrocopa* (Stuart *et al.*, 1931); and larvae of the clam *Mercenaria mercenaria* (Guillard, 1959).

In the present study, axenic larval *Crassostrea gigas*, obtained without the use of antibiotics, were used in a series of experiments meant to reveal whether selected strains of marine bacteria can consistently improve the survival and growth of algal-fed oyster larvae.

Materials and Methods

Maintenance of larvae, bacteria and algae

Bacteria-free oyster larvae were obtained according to the method of Langdon (1983). Adult oysters *Crassostrea gigas* were held at 18°C in a recirculating seawater system for a period of 4 to 6 weeks, depending on the initial reproductive condition of the broodstock. After this conditioning period, the oysters were opened and shucked. Using aseptic techniques in a laminar-flow hood, we disinfected the external surface of the gonads of each oyster with a 1% solution of sodium hypochlorite. A small incision was made through the surface of the gonads with a heat-sterilized scalpel, and gametes from each oyster were removed with sterile Pasteur pipettes and transferred to separate sterile flasks containing 0.2 μm-filtered, autoclaved seawater (FSSW). Eggs were fertilized by the addition of a few drops of sperm suspension and then were transferred to Erlenmeyer flasks containing FSSW at a density of 100 eggs ml^{-1}. Eggs were incubated on an orbital shaker at 25°C for 48 h. When the trocophore larvae had developed into veligers (straight-hinged larvae), subsamples of larvae were aseptically withdrawn for axenicity tests, and the remaining larvae were then held at 5°C for 5 days. Axenicity of larvae was determined by epifluorescence microscopy using 4'6-diamidino-2-phenylindole (DAPI) staining techniques (Porter and Feig, 1980). Samples of larvae were also added to 1/10 recommended concentration of Difco marine broth 2216 (3.74 $g\,l^{-1}$, salinity 30 ppt) and incubated at 25°C under aerobic or anaerobic conditions (BBL GasPak Pouch). Larvae from cultures that showed no evidence of microbial contamination from either the epifluorescence test or the 5 day broth incubations were considered adequate for experimentation. To confirm that the larvae were axenic, broth incubations were continued for 30 days. Axenic straight-hinged larvae were transferred to 250 ml Erlenmeyer flasks, each containing 150 ml of FSSW, closed with cotton plugs and capped with aluminum foil. Final larval density was 5 ml^{-1}. Growth experiments were then initiated by the addition to the culture flasks of axenic algae and the different bacterial strains. Shell lengths of 100 randomly selected larvae were measured, either with an optical micrometer fitted to a compound microscope, or with an image analysis system (Zeiss Videoplan 2).

Strains of marine bacteria were isolated from cultures of algae or oyster larvae at the Whiskey Creek Hatchery in Netarts Bay, Oregon. Other bacteria were isolated, either from the guts of adult oysters, or from incubations of protein capsules (Langdon, 1989) suspended in unfiltered seawater. Pure bacterial strains were obtained by the dilution method of Rodina (1972). Strains were grown, at 25°C, on marine agar 2216 or brain heart infusion agar (Difco). Bacteria grown on such solid media for 3 to 5 days were resuspended for 24 h in FSSW; they were then washed by centrifugation at 20,000 × g for 10 min and resuspended in FSSW.

Strains were added to larval cultures at concentrations of 10^5–10^6 cells ml^{-1}. Cell concentrations were derived from equations relating spectrophotometric absorbance (600 nm) and bacterial concentration; the latter value was determined by direct count after staining with DAPI (Porter and Feig, 1980). Such equations were developed and used for each strain tested.

Axenic *Isochrysis galbana* Parke (clone ISO) was obtained from the Culture Collection of Marine Phytoplankton (Maine). Algal cultures were grown at 20°C in 200 ml f/2 medium (Guillard and Ryther, 1962) illuminated by 1000–1500 lux of cool white fluorescent light under a 12 h light/12 h dark photoperiod. Algal axenicity was determined as described above for larvae.

All glassware was washed in 10% nitric acid, rinsed seven times with distilled water, and baked overnight at 450°C. Disodium ethylenediamine-tetraacetate (EDTA) was added at a final concentration of 1 ppm to all seawater to reduce the load of dissolved organic matter (Utting and Helm, 1985). Salinity of seawater after sterilization varied between 28 and 31 ppt. Heat sterilization was carried out for 15 min at 121°C and 1.06 kg cm^2 pressure.

Larvae fed on live algae and bacteria

Twenty-one marine bacterial isolates were tested in three culture experiments for their effects on the survival and growth of larvae fed axenic *Isochrysis galbana*. Experiment I included seven microbial isolates from the Whiskey Creek Hatchery (H1–H7) and five isolates from the guts of adult oysters (G1–G5). Control treatments were either larvae fed only algae or starved larvae.

In Experiment II, two strains (H6, H7) that improved larval growth in Experiment I were tested along with five strains isolated from the Whiskey Creek Hatchery (H8–H12), one strain isolated from the gut of an adult oyster (G6), and three strains isolated from protein capsules incubated in seawater (CA1–CA3). Control treatments included starved larvae and larvae fed only algae. In third control (SW), cultures of larvae were inoculated at the beginning of the experiment with naturally occurring bacteria present in 5 ml samples of 1 μm-filtered seawater collected from Yaquina Bay, Oregon. The larvae in the

third control treatment were fed axenic algae every other day. Experiments I and II were carried out with four replicates per treatment.

Experiment III was designed to retest strains that had enhanced larval survival and growth in Experiment II (H7, CA2). Control treatments similar to those described for Experiment II were included. Experiment III was carried out with eight replicates per treatment.

Cultures of bacteria-free oyster larvae (75.5–82 μm shell length) were inoculated once at the beginning of each experiment with bacterial strains. Bacteria-free algal cells, harvested from cultures in exponential growth phase, were added to the larval cultures every two days. The seawater of the larval cultures was not renewed during the culture period. The concentration of algal cells in each larval culture flask was estimated, as follows, before each feeding. A 2-ml sample of the larval culture medium was aseptically removed from each flask with a pipet; to prevent removal of larvae, the end of the pipet was covered with a 64 μm Nitex screen. Algal cells were preserved with formalin, concentrated by centrifugation, and re-suspended in 100 μl of 0.2 μm-filtered seawater. Algal concentrations in the samples were then determined with a hemocytometer. Fresh algae were then added to larval culture flasks to provide cell concentrations at pre-determined levels. Algal cell concentrations were increased by 15,000 cells ml^{-1}, from 40,000 to 100,000 cells ml^{-1} over a 10 day culture period. To provide uniform food quality during the experiments, algae from a single culture were added at each feeding period, to all larval cultures receiving an algal diet.

Larval culture flasks were placed randomly on orbital shakers in a temperature-controlled room at 25°C. The cultures were exposed to a light intensity of 50–70 lux for 12 h each day. No algal growth occurred at this low light intensity. After 10 days of culture, samples of water were aseptically withdrawn from flasks containing starved larvae or larvae fed only axenic algae; these samples were analyzed for microbial contamination as described above. The experimental data were analyzed only if these control treatments were bacteria-free at the end of the 10 day culture period.

Effects of CA2 bacteria on the growth of algae in larval cultures

Cells of axenic *I. galbana* were initially suspended at a concentration of 40,000 ml^{-1} in f/2 medium and then subdivided in sixteen 250 ml Erlenmeyer flasks. CA2 cells were added at 10^5 cells ml^{-1} (final concentration) to eight flasks, while FSSW was added to the other eight flasks to maintain similar initial algal concentrations in all flasks. The final volume of each algal culture was 200 ml. Four algal cultures inoculated with bacteria and four cultures that had received only FSSW were placed in conditions conducive to the growth of *I. galbana* (1000–1500 lux and 20°C); the remaining algal cultures were exposed to the conditions used for larval culture (50–70 lux and 25°C). The algal cultures were incubated on orbital shakers for three weeks. Every second day, 10 ml samples were removed aseptically from each algal culture, and algal concentrations determined with a Coulter counter (Model ZB1).

Larvae fed on dead algae and bacteria

Interactions between strain CA2 and living *Isochrysis galbana* that could modify algal food quality were not addressed in the previous experiments. To determine whether bacteria could enhance cultures of larvae fed on non-living diets, live *I. galbana* were replaced with dead algae.

In Experiment IV, known concentrations of axenic *I. galbana* were frozen at −5°C. Freezing and thawing broke the cell walls and membranes of the algal cells. Larvae were fed dead freeze-killed algae (FA) every two days according to the same protocol used with live algae. One group of larval cultures fed FA was maintained bacteria-free, and two groups were inoculated at the beginning of the experiment with either strain H6 at 10^5 cells ml^{-1} (final concentration), or with an inoculum of naturally occurring bacteria (SW). The wild strains were added in 5 ml samples of 1 μm-filtered seawater collected from Yaquina Bay, Oregon, at a concentration of 10^5–10^6 cells ml^{-1}. Other larval cultures received on alternate days, either additions of strain H6 (at a final concentration of 10^5 cells ml^{-1}) alone, or naturally occurring bacteria (SW) (5 ml of 1 μm-filtered seawater) alone. Control treatments included starved larvae and larvae fed every second day on live axenic *I. galbana*. Culture conditions and sample treatments were similar to those of experiments carried out with live algae. Four replicates were tested per treatment.

Algal cells were also killed by ^{60}Co-irradiation (5 megarads) at the Radiation Center at Oregon State University. Non-viability of irradiated algae (IA) was evident by the lack of growth of cells in f/2 medium at 20°C under 1000–1500 lux of fluorescent light emitted 12 h a day. The irradiation process also destroyed contaminants, as demonstrated by incubations, at 25°C, of irradiated algae in 1/10 diluted marine broth 2216 (3.74 g l^{-1}, salinity of 30 ppt) under either aerobic or anaerobic conditions (BBL GasPak Pouch). The integrity of the irradiated algal cells was verified by microscopic examination. Cell volumes of irradiated and non-irradiated algae from seven different cultures were determined with a Coulter counter (Model ZB1) equipped with a calibrated Coulter channelyser (Model 256).

To ensure that IA were acceptable to larvae as a food source, the ingestion rates of larvae fed on either IA or

live *Isochrysis galbana* were compared. Ingestion rates were calculated according to the methods described by Checkley (1980). Larval ingestion rates for live and ^{60}Co-irradiated algae were compared with a 2 sample t-test, after verifying homocedasticity by Cochran's test for homogeneity of variances at the 0.05 level of probability (Douillet, 1991).

In Experiment V, oyster larvae were fed IA every second day according to the methods employed with live algae in Experiments I to III. Three groups of larval cultures were fed IA. One group was maintained bacteria-free, while the two others were inoculated at the beginning of the experiment with strains H7 or CA2. Control treatments included starved larvae or larvae fed every two days on live axenic *Isochrysis galbana*. Eight replicates were tested per treatment. Larval survival and growth were determined as described below.

Data collection and analysis

At the end of each experiment, the larvae were carefully transferred to scintillation vials containing buffered formaldehyde (2% final concentration, pH = 8). The larval tissues were stained with rose of Bengal, so that the larvae that were alive could be distinguished from empty shells. The whole larval population in each flask was counted with a dissecting microscope, and the shell lengths of 100 randomly selected larvae were measured, either with an optical micrometer fitted to a compound microscope, or with an image analysis system (Zeiss Videoplan 2). Survival and growth data were transformed to satisfy assumptions of ANOVA. Survival data were transformed as:

$$\text{arcsin (square root (percent survival } 100^{-1}))$$

Growth data were transformed as:

$$\text{arcsin (square root } ((\ln L_t - \ln L_0)t^{-1}))$$

where L_t is the final mean shell length (μm); L_0 is the initial mean shell length (μm); and t is the culture period (10 days).

These transformations were successful in reducing the heterocedasticity of the survival data but not of the growth data (Cochran's test for heterogeneity of variances, at the 0.05 level of probability). Treatment effects on larval survival were tested with one-way ANOVA. Where significant differences were indicated, Tukey's honestly significant difference test (T-HSD) was applied to determine the statistical significance of differences among individual treatments at the 0.05 level of probability. Treatment effects on larval growth were analyzed with the Kruskal-Wallis test (KW). Differences among individual treatments were determined by means of the Games and Howell test (G&H) of equality of means with heterogeneous variances (Sokal and Rohlf, 1981), at the 0.05 level of probability. All tests were performed with the computer program Statistix (NH Analytical Software), except the Games and Howell test which was carried out with the program Biom (Rohlf, 1982).

The size-frequency distributions of populations of algae-fed larvae that were bacteria-free were compared with those fed algae supplemented with CA2 bacteria in Experiments II and III. Skewness coefficients (g1; Sokal and Rohlf, 1981) of larval populations from each replicate flask were calculated and used to compare larval size frequency distributions. A normal size distribution would have a g1 coefficient equal to 0. A skewness coefficient higher than 0 indicates that the size distribution is positively skewed (higher proportion of small-sized individuals), while a coefficient smaller than 0 indicates negative skewness. After confirmation of homocedasticity of g1 values by Cochran's test at the 0.05 probability level, data were analyzed by two-way ANOVA with treatment (algae, algae + CA2) and experiment as factors. As dictated by the results of ANOVA, appropriate multiple comparisons of means were conducted at the 0.05 level of probability using the Student-Newman-Keuls procedure (SNK), controlling for experiment-wide error (Underwood, 1981).

Cryopreservation of bacteria

Bacteria have been described as adaptable chimaeras, the metabolic plasticity of which results from widespread transfer of genetic information though plasmids or prophages (Sonea, 1988). This strategy for adaptation to changing environments may result, during evolution, in the loss of beneficial characteristics of selected bacterial strains. In order to reduce the possibility of changes in bacterial characteristics between successive experiments, selected strains were cryopreserved at −70°C in 10% (V/V) glycerol in sterile 1/10 diluted marine broth 2216.

Identification of strain CA2

The identification of bacterial strain CA2 was based on *Bergey's Manual of Systematic Bacteriology* (Holt, 1984). The methodology used for different procedures followed the *Manual of Methods of General Bacteriology* (Gerhardt *et al.*, 1981). Exponentially growing cells cultured on marine agar 2216 were used for the following tests performed at the Hatfield Marine Science Center, Newport, Oregon. (a) Cells were Gram stained. (b) Motility was determined by observations of wet mounts with light microscopy. (c) Oxidase activity was determined by spreading CA2 cells with sterile cotton swabs over Pathotec cytochrome oxidase test strips (General Diagnostics), which contained a derivative of dimethyl-p-phenylenediamine and α-naphthol. (d) Cultures of CA2 cells were flooded with 3% hydrogen peroxide for catalase testing. (e) Oxidation and fermentation of glucose was assayed with the modified O-F medium of Leifson (1963). (f) Utilization of inorganic

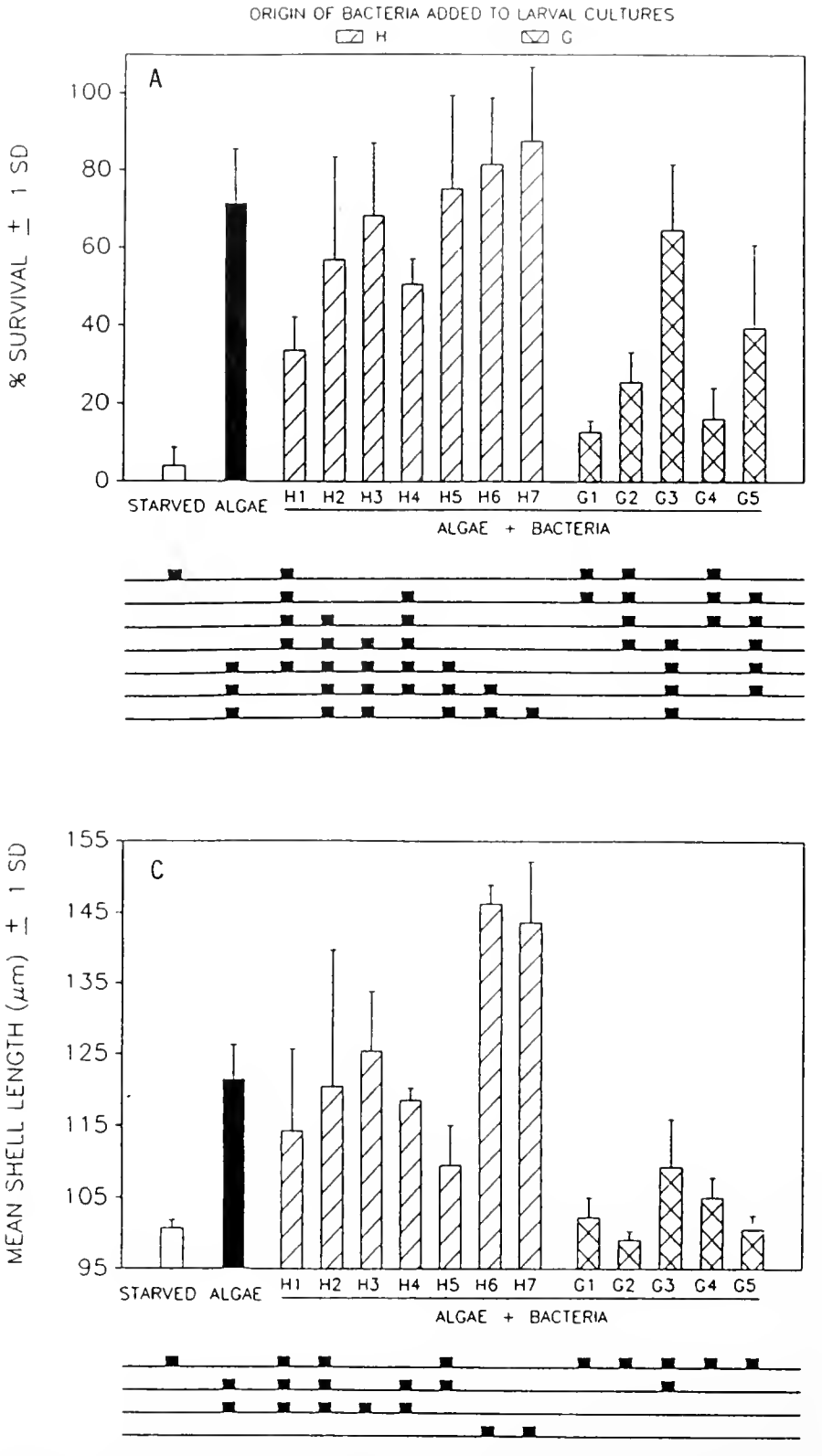

Figure 1. Effects of different bacterial strains on oyster larvae cultured on a diet of axenic *Isochrysis galbana* for 10 days. (A) Survival in Experiment I. (B) Survival in Experiment II. (C) Growth in Experiment I. (D) Growth in Experiment II. Bacteria were isolated from the Whiskey Creek Hatchery, Oregon (H), from the guts of adult oysters (G), from incubations of protein capsules in seawater (CA), or were naturally-occurring in 1 μm-filtered seawater (SW). Larval control treatments were starved or fed axenic *I. galbana*. Results of Tukey's HSD pairwise comparisons and Games and Howell's tests are displayed below the histograms of survival and growth, respectively. Squares that occur together on any one of the horizontal lines indicate mean values that are not different at the 0.05% level of significance.

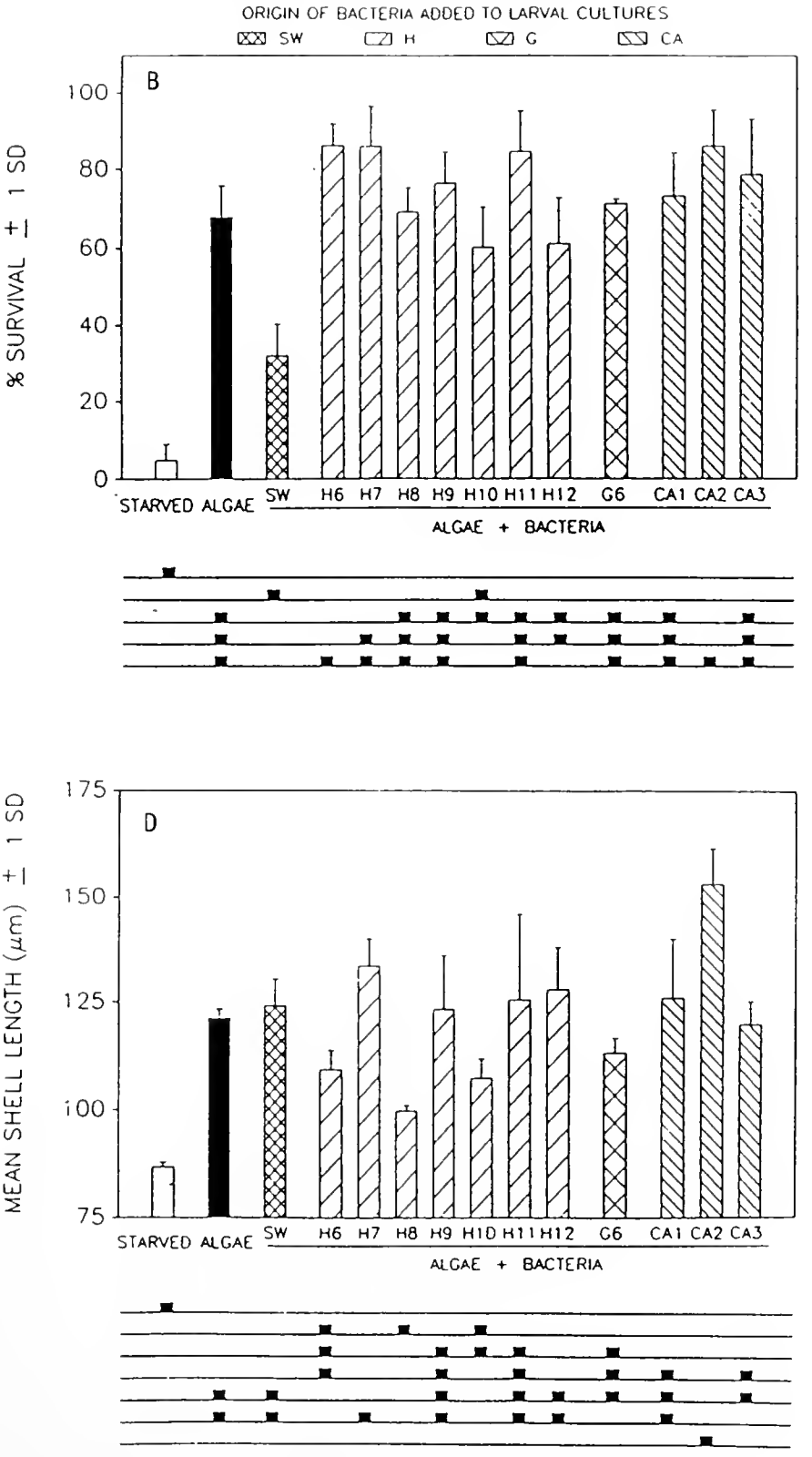

Figure 1. (*Continued*)

sources of nitrogen was evaluated by culturing CA2 cells on media prepared with NH_4Cl or $NaNO_3$ (0.5 g l^{-1}), glucose (0.1 g l^{-1}), Na_2HPO_4 (0.1 g l^{-1}), $FePO_4$ (0.004 g l^{-1}) and 1 ml l^{-1} of f/2 vitamin mix (Guillard and Ryther, 1962). The culture media used as controls were prepared by replacing $NaNO_3$ or NH_4Cl with peptone or tryptone (Difco) at 0.5 g l^{-1}. (g) Anaerobic growth was determined by transferring CA2 cells either into solid media in Petri dishes, or into 25 ml 1/10 diluted marine broth 2216 (3.74 g l^{-1}; salinity 30 ppt) contained in 50 ml Erlenmeyer flasks, placing these cultures in anaerobic GasPak pouches (BBL), and incubating the cells at 20°C for up to one month.

The following tests were carried out by Dr. Ronald Weiner (University of Maryland at College Park). Methodology followed the *Manual of Methods for General Bacteriology* (Gerhardt *et al.*, 1981). (a) Salt requirements were evaluated by culturing CA2 cells in tryptic soy agar (TSA) prepared at different salt concentrations; NaCl was added at 1% increments up to 10% of the control level. (b) As evidence of anaerobic growth and motility, CA2 cells on a straight needle were used to inoculate a tube containing semisolid tryptic soy broth enriched with 0.8% agar and 1% NaCl, and the pattern of growth observed. (c) Flagellar staining was carried out by the Leifson method (Gerhardt *et al.*, 1981). (d) Synthesis of exopolysaccharides was evaluated by the phenol-sulfuric acid reaction (Gerhardt *et al.*, 1981). (e) The mole percent guanine plus cytosine (mol% G + C) in extracted deoxyribonucleic acid (DNA) was determined by the thermal melting (denaturation) methods of Marmur and Doty (1962) with a Gilford UV programmable spectrophotometer. (f) Antibodies of 20 different bacteria strains belonging to the Alteromonas/Shewanella group were tested for reaction with exopolysaccharides of CA2 cells. (g) Fatty acid analyses of strain CA2 were carried out for comparison with profiles of other marine bacteria by Dr. Fred Singleton (Center for Marine Biotechnology, University of Maryland) and by Dr. Warren L. Landry (Food and Drug Administration, Dallas, Texas).

Results

Larvae fed on live algae and bacteria

Single additions of marine bacterial isolates to oyster larvae cultures significantly affected larval survival (ANOVA, $P < 0.01$) and growth (KW, $P < 0.01$) after 10 days of culture in all experiments (Figs. 1, 2). The microbes tested can be divided into categories depending on their effects upon oyster larvae: adverse, neutral, or beneficial. Bacteria belonging to the last category were tested further, and their effects upon oyster larvae were designated as either variable or consistently beneficial.

Adverse strains. Strains G1, G2 and G4 adversely affected larval survival (T-HSD, $P < 0.05$), whereas strains G1, G2, G4, G5, H8, and H10 adversely affected larval growth (G&H, $P < 0.05$). Bacteria present in 5 ml aliquots of 1 μm-filtered seawater depressed larval survival (T-HSD, $P < 0.05$) in Experiment II and larval growth (G&H, $P < 0.05$) in Experiment III.

Neutral strains. A large proportion of the strains (H1, H2, H3, H4, H5, H9, H11, H12, G3, CA1, and CA3) added to cultures of oyster larvae had no significant effect on larval survival (T-HSD, $P > 0.05$) or growth (G&H, $P > 0.05$) compared with cultures fed algae alone.

Variable strains. Addition of strains H6 and H7 to larval cultures caused inconsistent improvements of larval growth. For example, larval growth was enhanced (G&H, $P < 0.05$) in cultures inoculated with strains H6 and H7 in Experiment I, but the enhancement with strain H7 was statistically insignificant in Experiments II and III (G&H, $P > 0.05$). Moreover, larval growth was depressed (G&H, $P < 0.05$) when strain H6 was added to larval cultures in Experiment II.

Beneficial strains. In both Experiments II and III, larvae grown in cultures inoculated with strain CA2 had a significantly greater shell length than control larvae fed only axenic algae (G&H, $P < 0.05$). Larval survival was enhanced in cultures inoculated with strain H7 and CA2, but this enhancement was statistically significant only in Experiment III (T-HSD, $P < 0.05$).

Size frequency distributions of populations of larvae fed axenic algae were skewed compared to those from cultures fed algae supplemented with CA2 bacteria (Fig. 3; Table 1). Analysis of variance indicates a significant interaction between treatment and experimental factors (Table 2). In both Experiments II and III, skewness coefficients for populations of larvae fed axenic algae alone were significantly larger (SNK, $P < 0.05$) that those for populations of larvae fed algae and inoculated with CA2 bacteria. The difference between the skewness coefficients of treatments in Experiment II is larger than that in Experiment III, explaining the significant interaction determined by the two-way ANOVA test.

Effects of CA2 bacteria on the growth of algae in larval cultures

Cells of *Isochrysis galbana*, with or without inoculations of CA2 bacteria, did not grow under the conditions used to culture larvae (Fig. 4). The occurrence of CA2 cells in the culture medium had no effect on algal growth under favorable light intensity (1000–1500 lux) and temperature (20°C).

Larvae fed on dead algae and bacteria

Significant differences among treatments in Experiments IV and V were determined for larval survival (ANOVA, $P < 0.01$) and growth (KW, $P < 0.01$). The survival of larvae cultured on axenic FA or IA alone was significantly lower (T-HSD, $P < 0.05$) than that of larvae

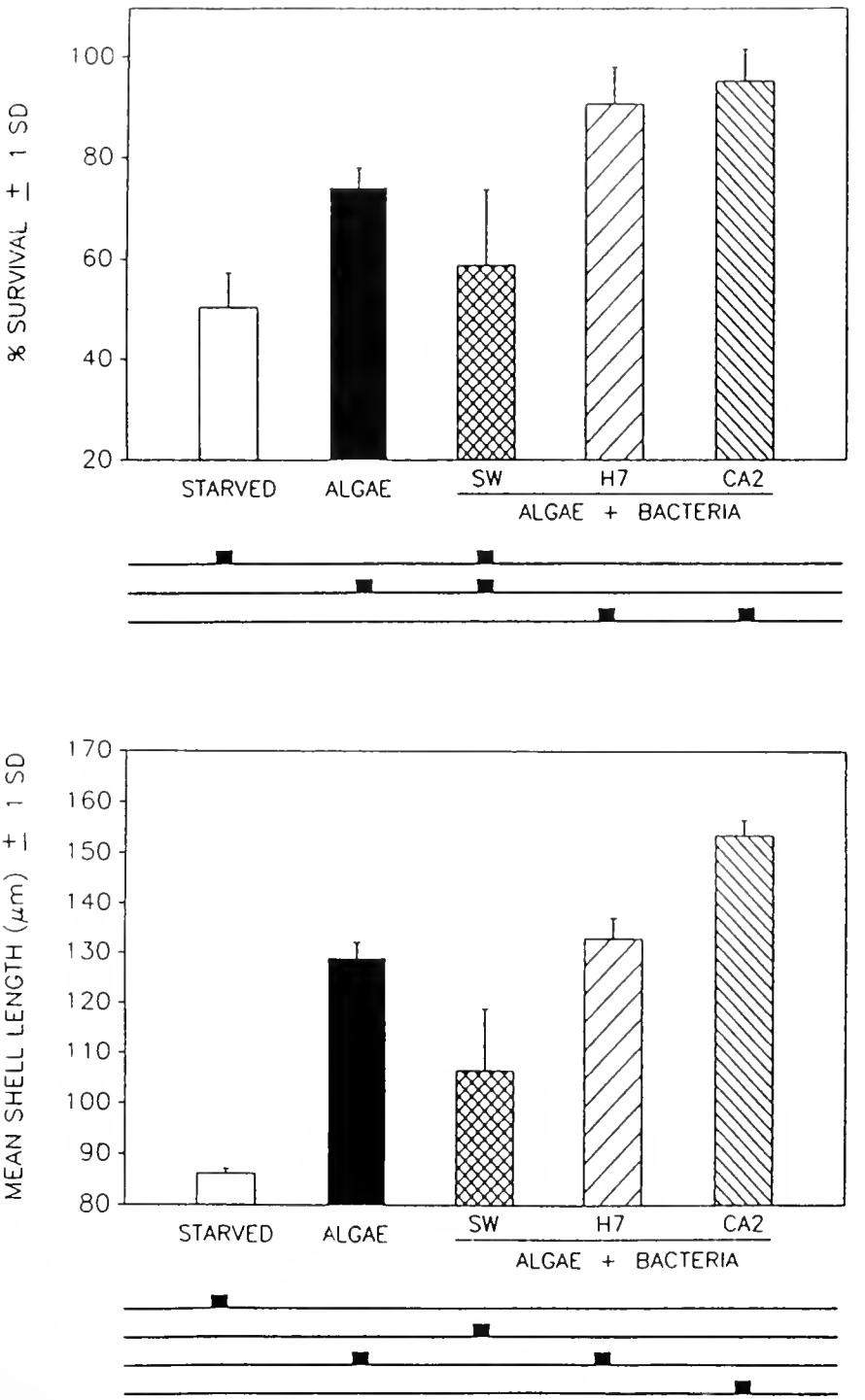

Figure 2. Survival and growth of oyster larvae after 10 days of culture on axenic *Isochrysis galbana* supplemented with different bacterial strains (Experiment III). Bacteria were isolated from the Whiskey Creek Hatchery, Oregon (H) or from incubations of protein capsules in seawater (CA). Naturally-occurring bacteria present in 1 μm-filtered seawater (SW) were added in a control treatment. Other control treatments included larvae fed axenic *I. galbana* or starved. Results of Tukey's HSD pairwise comparisons and Games and Howell's tests are displayed below the histograms of survival and growth, respectively. Squares that occur together on any one of the horizontal lines indicate mean values that are not different at the 0.05% level of significance.

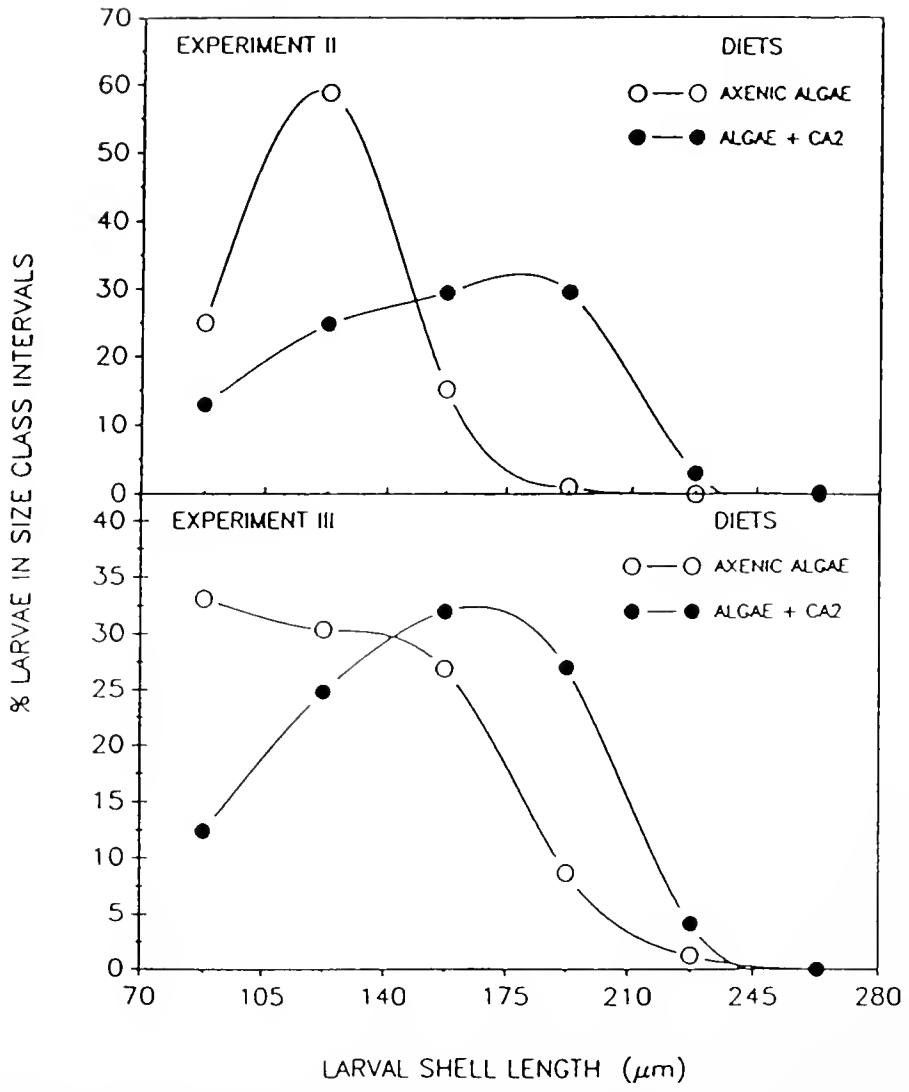

Figure 3. Size frequency distributions of larvae cultured for 10 days on a diet of *Isochrysis galbana* with or without addition of CA2 cells. Points represent percent larvae for each shell length interval of 30 μm. Lines used for illustrative purposes only. Data from Experiments II (n = 400) and III (n = 800) for each treatment.

cultured on live axenic algae alone (Figs. 5, 6). However, the survival of larvae fed FA or IA was higher (T-HSD, $P < 0.05$) than that of starved larvae. In contrast, no significant differences in larval survival were detected between cultures fed live algae and cultures fed FA or IA inoculated with strains H6 and H7, respectively (T-HSD, $P > 0.05$). Survival of larvae fed every two days on bacteria H6 alone was not significantly different (T-HSD, $P > 0.05$) from that of larvae fed live algae, and was significantly higher (T-HSD, $P < 0.05$) than that of starved larvae (Fig. 5). Larvae from cultures inoculated every two days with 5 ml of 1 μm-filtered seawater (SW) also showed higher survival (T-HSD, $P < 0.05$) than that of starved larvae.

Larvae fed on FA or IA were significantly smaller than larvae fed on live axenic algae (G&H, $P < 0.05$), and were not different from the size of starved larvae (G&H, $P > 0.05$) at the end of the experiment (Figs. 5, 6). Additions of single bacterial strains to cultures of larvae fed FA or IA did not improve larval growth compared to larvae fed FA or IA alone (G&H, $P > 0.05$). In contrast, growth of larvae fed FA inoculated with 5 ml of 1 μm-filtered seawater was significantly enhanced (G&H, $P < 0.05$) compared to that of larvae fed FA alone or starved larvae (Fig. 5). Similarly, additions every two days of 5 ml of 1 μm-filtered seawater or strain H6 alone to larval cultures significantly enhanced the growth of larvae (G&H, $P < 0.05$) compared to that of starved larvae.

The poor growth of larvae fed FA may have been due to the rupture of the freeze-killed algal cells. ^{60}Co-irradiation did not affect the integrity of the algal cells but re-

Table I

Skewness coefficients (g1) from size frequency distributions of populations of larvae cultured in Experiments II and III

Experiment	Diet	Average skewness of populations ± 1 S.D.
II	ISO	0.7906 ± 0.2134 (n = 4)
II	ISO + CA2	−0.0605 ± 0.2235 (n = 4)
III	ISO	0.3801 ± 0.1720 (n = 8)
III	ISO + CA2	−0.0466 ± 0.2910 (n = 8)

Larvae were cultured with either axenic *Isochrysis galbana* (ISO) alone or *I. galbana* plus CA2 bacteria.

duced their volume from 44.4 ± 1.92 μm^3 to 26.3 ± 0.59 μm^3 ($\bar{x}$ ± 1 SD; n = 7). A high proportion of irradiated cells remained intact while in suspension in seawater, as demonstrated by the small decrease in cell concentration in control flasks, from 59,043 ± 1,119 cells ml^{-1}, to 58,539 ± 1,505 cells ml^{-1} ($\bar{x}$ ± 1 SD; n = 4) in 105 min. IA cells were ingested by oyster larvae at rates significantly (2 sample t-test, $P < 0.01$) greater than that for live cells.

Identification of strain CA2

Strain CA2 was presumptively identified as *Alteromonas* sp. on the basis of the following characteristics: Gram negative rod; aerobic; oxidase positive; requires 250 n*M* salt; motile with polar flagella; exopolysaccharide synthesis; and guanine plus cytosine 43 mol% (T_m).

The exopolysaccharides of CA2 bacteria did not react with antibodies to 20 species of *Alteromonas*. Furthermore, both analyses of fatty acids revealed a very unusual fatty acid profile with a high proportion of C-14, C-15 fatty acids (Table 3); this is not characteristic of the genus *Alteromonas*. However, the fatty acid profile was not similar to any of the species profiles listed in Dr. Landry's marine library. Therefore, strain CA2 may be an *Alteromonas* species not typical of the genus.

Further characteristics of strain CA2 include yellow pigment production, oxidation and fermentation of glucose, but no gas production, and inability to utilize inorganic sources of nitrogen, such as NH_4Cl or $NaNO_3$ for growth. Catalase was weakly positive.

Discussion

Axenic larval *Crassostrea gigas* were used to determine the effects of additions of single bacterial strains on the survival and growth of larvae cultured with algae. Bacteria can be categorized as adverse, neutral or beneficial, depending on their effects upon oyster larvae. Furthermore, bacteria found beneficial in one experiment were retested in subsequent experiments and could be further categorized as either variable or consistently beneficial strains. Additions of strain CA2 to larval cultures consistently enhanced larval survival (21–22%) and growth (16–21%) compared with that of larvae fed on algae alone.

The specificity of bacterial strains as food for grazers has frequently been reported (Frosch, 1897 in Luck *et al.*, 1931; Stuart *et al.*, 1931; Curds and Vandyke, 1966). Furthermore, Curds and VanDyke (1966) found that one bacterial strain was either slightly toxic, unfavorable, or favorable depending on the ciliate species tested. In contrast, a single bacterial strain (PM-4) was found to promote the growth of both shrimp (*Penaeus monodon*) and crab (*Portunus tridentatus*) larvae (Maeda, 1988; Maeda and Nogami, 1989). Consequently, no generalization about the beneficial effects of specific bacterial strains can be made; *i.e.*, each strain must be tested again with each new target species.

Bacteria may be used directly as a food item by oyster larvae (Douillet, 1991). Starved axenic oyster larvae showed poor survival and did not grow after 10 days of culture. In contrast, larvae in cultures inoculated with single bacterial strains or mixtures of naturally-occurring marine bacteria had higher survival rates than starved larvae, but lower growth rates than larvae fed on algal diets. Consequently, the bacterial strains tested did not provide all the nutritional requirements for larvae, but appeared, at least, to partially satisfy larval metabolic requirements, as demonstrated by the beneficial effects of bacteria on larval survival and growth. Straight-hinged oyster larvae, fed for 10 min on ^{14}C-labeled CA2 cells at 1.5×10^7 cells ml^{-1} and purged of undigested ^{14}C-material, retained enough bacterial carbon to meet over 140% of their active carbon metabolic requirements during a 10 min period (Douillet, 1991). Beese (in Prieur *et al.*, 1990) determined that xenic, starved larval *Crassostrea gigas* grew 60% in size after seven days of culture, whereas starved axenic larvae did not grow. The ability of starved xenic bivalve larvae to grow has been determined to be greater for larvae

Table II

Two-way analysis of variance of skewness coefficients (g1) for size frequency distributions of populations of larvae cultured in Experiments II and III

Source of variation	d.f.	Sum of squares	Mean squares	F-ratio	Sig. level
Experiment (A)	1	0.31468	0.31468	5.79	0.0259
CA2 addition (B)	1	3.2656	3.2656	60.12	0.0000
Interactions (A*B)	1	0.36039	0.36039	6.63	0.0180
Replicates (C)					
Residual (A*B*C)	20	1.0864	0.05432		
Total	23	5.0271			

Larvae were cultured with *Isochrysis galbana* alone or *I. galbana* plus CA2 bacteria.

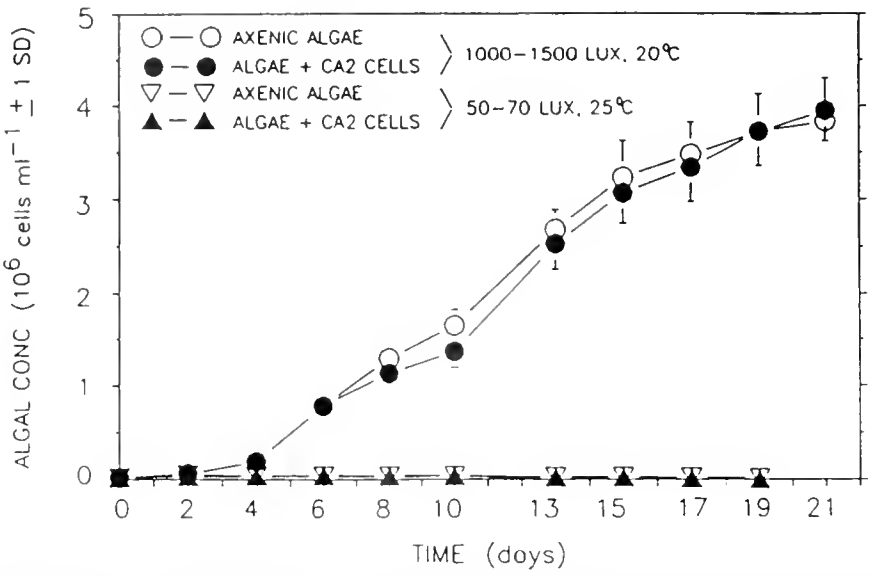

Figure 4. Effects of CA2 bacteria on growth of *Isochrysis galbana* under conditions used to raise larvae (50–70 lux; 25°C) or under conditions found optimal for algal growth (1000–1500 lux; 20°C).

of the mussel *Mytilus edulis* than for larval *C. gigas* (His *et al.*, 1989). But bacteria lack long-chain polyunsaturated fatty acids (PUFA) (Kates, 1964; Perry *et al.*, 1979) and sterols (Lehninger, 1975), both of which may be essential for the growth of marine bivalves (Trider and Castell, 1980; Langdon and Waldock, 1981). This lack of essential nutrients could explain why larvae grew more poorly on a diet of bacteria alone than on a diet of algae alone.

Size-frequency distributions of bacteria-free oyster larvae cultured for 10 days on axenic live algae were always positively skewed due to a high proportion of larvae that exhibited poor growth. Algae were always present in cultures at satisfactory concentrations for larval growth (Breese and Malouf, 1975); therefore, the poor growth of some larvae in populations fed axenic algae could not be due to insufficient algal food. In contrast, additions of CA2 bacteria to cultures of algae-fed larvae consistently normalized larval size-frequency distributions. Larval survival was equal (Experiment II; Fig. 1B, D) or higher (Experiment III; Fig. 2) in cultures inoculated with strain CA2 than in cultures fed algae alone; therefore, changes in size-frequency distributions were not due to the selective death of slow growing larvae in bacterized cultures. Instead, additions of strain CA2 to larvae fed on algae apparently shifted larval size-frequency distributions by promoting the growth of larvae that would grow poorly on an algal diet alone. This result suggests that some oyster larvae in cultured populations require supplements of bacteria in order to grow, and that an algal diet of *Isochrysis galbana* alone is not sufficient to meet their nutritional requirements.

The inability of a single algal food species to support larval growth rates comparable to those obtained on mixtures of algal species suggests that diets of single algal species can be nutritionally inadequate for maximum larval growth (Davis and Guillard, 1958; Walne, 1970). Microbes could provide dietary micronutrients, such as vitamins (Kutsky, 1981) or other growth factors, that could be deficient in algal diets. Vitamin deficiencies in the media used to culture axenic *Artemia* have arrested growth and caused the early mortality of this crustacean (Provasoli and D'Agostino, 1962). Vitamin supplements increased the growth rate of larval *Crassostrea virginica*, when given alone or in combination with *Chlorella* (Davis and Chanley, 1956). The high nutritional value of bacteria is indicated by the success of bacterial supplements in improving the quality of algae (Provasoli *et al.*, 1959), or of dried diets of different chemical composition (Douillet, 1987).

Bacterial enhancement of larval cultures may also have been due to other mechanisms apart from bacterivory. Bacteria could have acted as a symbiont for larvae, contributing to the larva's protein nutrition through nitrogen fixation (Benemann, 1973; Carpenter and Culliney, 1975; Guerinot and Patriquin, 1981), or by aiding in the digestion and assimilation of ingested algae. The bacterial flora of bivalve larvae consists of a high proportion of strains that produce extracellular enzymes, such as proteases and lipases (Prieur, 1982).

Oyster larvae were grown for 10 days with no change in the culture medium; thus metabolites excreted by bivalves (Cockcroft, 1990) and algae (Hellebust, 1974) would accumulate in the larval cultures. Strain CA2 may

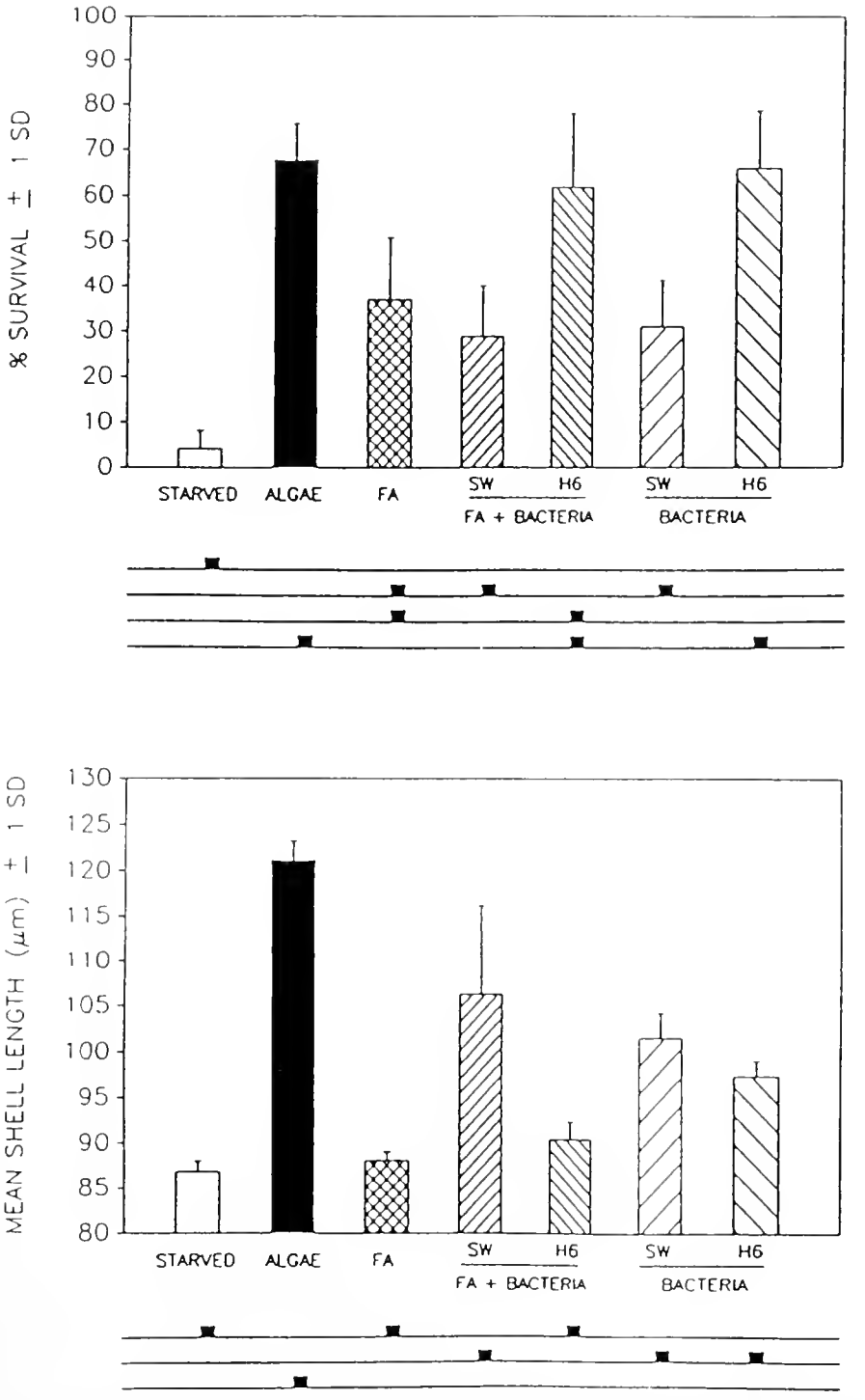

Figure 5. Survival and growth of oyster larvae after 10 days of culture when fed on a diet of either bacteria alone (strain H6, naturally-occurring bacteria present in 1 μm-filtered seawater (SW)) or freeze-killed *Isochrysis galbana* (FA) with or without supplements of bacteria (H6 or SW) (Experiment IV). Control treatments were starved or fed axenic *I. galbana*. Results of Tukey's HSD pairwise comparisons and Games and Howell's tests are displayed below survival and growth histograms, respectively. Squares that occur together on any one of the horizontal lines indicate mean values that are not different at the 0.05% level of significance.

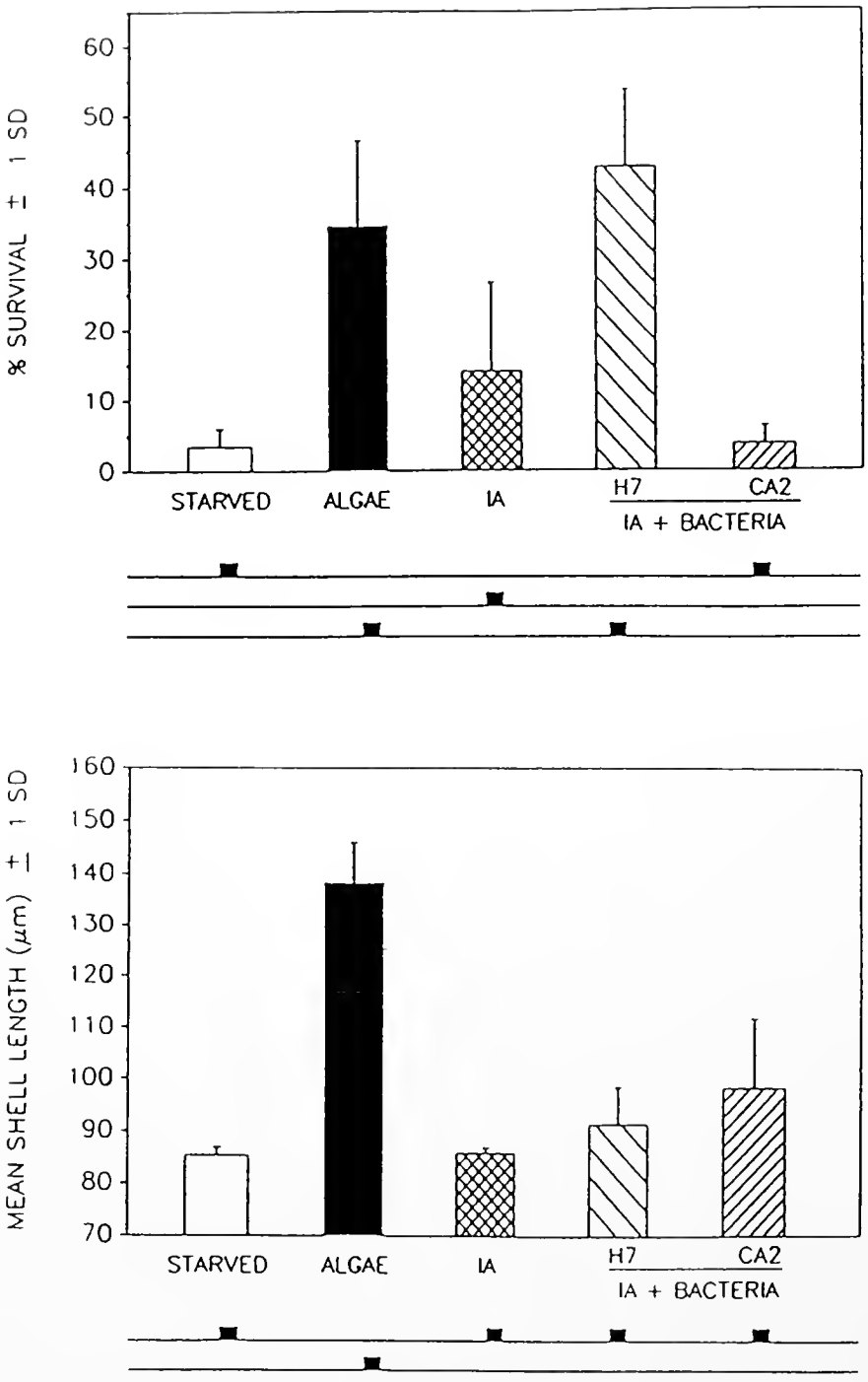

Figure 6. Survival and growth of oyster larvae after 10 days of culture on ^{60}Co-irradiated *Isochrysis galbana* (IA) with or without supplements of H7 and CA2 bacteria (Experiment V). Control treatments were starved or fed axenic *I. galbana*. Results of Tukey's HSD pairwise comparisons and Games and Howell's tests are displayed below survival and growth histograms, respectively. Squares that occur together on any one of the horizontal lines indicate mean values that are not different at the 0.05% level of significance.

have enhanced larval cultures by removing toxic metabolites. This may have stimulated larval growth and may have normalized the size-frequency distribution by promoting the growth of larvae that were more sensitive than others to the adverse growth effects of metabolites. However, the growth of xenic larvae was also enhanced by the addition of CA2 bacteria in cultures where the water was replaced every second day (Douillet, 1991); therefore,

Table III

Fatty acid composition of CA2 bacteria

Fatty acid	% composition
Unknown 11.541	1.73
14:0 ISO	4.17
14:0	0.76
15:1 ISO G	4.99
15:0 ISO	18.99
15:0 ANTEISO	8.07
15:1 B	6.62
15:0	4.66
16:1 ISO H	5.71
16:0 ISO	2.02
16:1 CIS 9	4.08
16:0	0.99
15:0 ISO 3OH	12.44
15:0 3OH	1.89
17:1 C	2.24
16:0 ISO 3OH	15.98
16:0 3OH	1.00
17:0 ISO 3OH	1.78
17:0 2OH	1.21

bacterial removal of toxic metabolites from culture waters is less likely the mechanism of enhancement of larval growth.

Strain CA2 did not indirectly affect larvae by increasing algal growth and food availability in larval cultures, because no enhanced algal growth occurred in the presence of CA2 bacteria.

Larvae did not grow when fed on freeze-killed or ^{60}Co-irradiated *Isochrysis galbana*, and additions of bacteria did not significantly improve the growth of larvae fed on either of the two killed algal diets. ^{60}Co-irradiated algal cells were grazed by larvae at rates that were significantly higher than those for live algal cells (Douillet, 1991). This suggests that the poor growth of larvae fed on killed algal diets was not due to a lack of available particulate matter, but more likely to the destruction or loss of essential nutrients from killed algal cells. Supplements of bacterial strains or mixtures of naturally occurring bacteria did not overcome these possible nutritional deficiencies of the killed algal diets.

The ability of the larvae of some bivalve species to utilize dead algae as food under xenic conditions has been well documented. Larvae of the mussel *Mytilus galloprovincialis* grew at similar rates whether fed on live or frozen *Monochrysis lutherii* (Masson, 1977). Chanley and Normandin (1967) reported that larvae of the clam *Mercenaria mercenaria* grew and survived equally well when fed on either live or frozen cells of *Isochrysis galbana*. However, different species of bivalves appear to have different nutritional requirements, as indicated by the findings of Loosanoff (1954) on the ability of *M. mercenaria* larvae to utilize a greater variety of natural foods than the larvae of the American oyster *Crassostrea virginica*. Larvae of *M. mercenaria* grew when fed on a diet of lyophilized *I. galbana* (Hidu and Ukeles, 1962) or frozen *I. galbana* (Chanley and Normandin, 1967), whereas larval *C. virginica* did not grow when fed either of these nonliving diets. The failure of larval *Crassostrea gigas* to grow when fed on dead algae impeded the evaluation of the direct nutritional contribution by bacteria under conditions where potential bacteria-algal interactions were eliminated by the use of killed, rather than living, algal cells.

In summary, bacteria added as single strains or as natural communities were found to be major sources of variation in cultures of *Crassostrea gigas* larvae. Selection of a consistently beneficial bacterium (strain CA2) for bivalve larval culture offers a valuable tool for research on the role of bacteria in the nutrition and culture of marine invertebrates. In addition, the use of beneficial microbes in aquaculture may contribute to the reduction of undesirable variation in culture success.

Acknowledgments

Support for this research was provided by a Markham Award as well as by the Oregon Sea Grant, NOAA grant #NA 85AA-D-SG095 (to C. J. L.). We are grateful to Drs. A. Robinson, R. Y. Morita, R. Griffiths and C. Dungan for helpful discussions; to Drs. R. Weiner, F. Singleton and W. Landry, for help in the taxonomic identification of bacteria; and to L. Hanson (Whiskey Creek Hatchery, Netarts Bay, Oregon), for encouragement and collaboration throughout the years. This research is part of a doctoral thesis submitted by P. D. to Oregon State University.

Literature Cited

Bayne, B. L. 1965. Growth and the delay of metamorphosis of the larvae of *Mytilus edulis* (1). *Ophelia* **2:** 1–47.

Bayne, B. L. 1983. Physiological ecology of marine molluscan larvae. Pp. 299–343 in *The Mollusca*, Vol. 3, K. M. Wilbur, ed. Academic Press, New York.

Benemann, J. R. 1973. Nitrogen fixation in termites. *Science* **181:** 164–165.

Breese, W. P., and R. E. Malouf. 1975. Hatchery manual for the Pacific oyster. Oregon Agricultural Experiment Station Special Report No. 443, and Oregon State University Sea Grant College Program Publication No. ORESU-H-75-002. 22 pp.

Brown, C. 1973. The effects of some selected bacteria on embryos and larvae of the American oyster, *Crassostrea virginica*. *J. Invert. Pathol.* **21:** 215–223.

Calabrese, A., and H. C. Davis. 1970. Tolerances and requirements of embryos and larvae of bivalve molluscs. *Helgol. Wiss. Meeresunters.* **20:** 553–564.

Carpenter, E. J., and J. L. Culliney. 1975. Nitrogen fixation in marine shipworms. *Science* **187:** 551–552.

Carriker, M. R. 1956. Biology and propagation of young hard clam, *Mercenaria mercenaria*. *J. Elisha Mitchell Sci. Soc.* **72:** 57–60.

Chanley, P., and R. F. Normandin. 1967. Use of artificial foods for larvae of the hard clam, *Mercenaria mercenaria* (L.). *Proc. Natl. Shellfish Ass.* **57:** 31–37.

Checkley, D. M. 1980. The egg production of a marine planktonic copepod in relation to its food supply: laboratory studies. *Limnol. Oceanogr.* **25**(3): 430–446.

Cockcroft, A. C. 1990. Nitrogen excretion by the surf zone bivalves *Donax serra* and *D. sordidus*. *Mar. Ecol. Prog. Ser.* **60:** 57–65.

Curds, C. R., and J. M. Vandyke. 1966. The feeding habits and growth rates of some fresh-water ciliates found in activated-sludge plants. *J. Appl. Ecol.* **3:** 127–137.

Davis, H. C. 1950. On food requirements of larvae of *Ostrea virginica*. *Anat. Rec.* **108:** 132–133.

Davis, H. C. 1953. On food and feeding of larvae of the American oyster, *C. virginica*. *Biol. Bull.* **104:** 334–350.

Davis, H. C., and P. E. Chanley. 1956. Effects of some dissolved substances on bivalve larvae. *Proc. Natl. Shellfish. Assoc.* **46:** 59–74.

Davis, H. C., and R. R. Guillard. 1958. Relative value of ten genera of micro-organisms as foods for oyster and clam larvae. *Fish. Bull.* **58:** 293–304.

Davis, H. C., and H. Hidu. 1969. Effects of turbidity-producing substances in sea water on eggs and larvae of three genera of bivalve molluscs. *Veliger* **11:** 316–323.

Di Salvo, L. H. 1978. *Vibrio anguillarum* and larval mortality in a California coastal shellfish hatchery. *Appl. Environ. Microbiol.* **35**(1): 219–221.

Douillet, P. 1987. Effect of bacteria on the nutrition of the brine shrimp *Artemia* fed on dried diets. Pp. 295–308 in *Artemia Research and Its Applications*, Vol. 3, P. Sorgeloos, D. A. Bengtson, W. Decleir, and E. Jaspers, eds. Universa Press, Wetteren.

Douillet, P. 1991. Beneficial effects of bacteria on the culture of larvae of the Pacific oyster Crassostrea gigas (Thunberg). Ph.D Thesis, Oregon State University, 185 pp.

Dupuy, J. L. 1975. Some physical and nutritional factors which affect the growth and setting of the larvae of the oyster, *Crassostrea virginica*, in the laboratory. Pp. 319–331 in *Physiological Ecology of Estuarine Organisms*, F. J. Vernberg, ed. University of South Carolina Press, Columbia.

Gerhardt, P., R. G. E. Murray, R. N. Costilow, E. W. Nester, W. A. Wood, N. R. Krieg, and G. B. Phillips. 1981. *Manual of methods for general bacteriology*. Am. Soc. Microbiol., Washington DC. 524 pp.

Guerinot, M. L., and D. G. Patriquin. 1981. N_2-fixing vibrios isolated from the gastrointestinal tract of sea urchins. *Can. J. Microbiol.* **27:** 311–317.

Guillard, R. R. L. 1959. Further evidence of the destruction of bivalves larvae by bacteria. *Biol. Bull.* **55:** 260–282.

Guillard, R. R. L., and J. H. Ryther. 1962. Studies on marine planktonic diatoms. I. *Cyclotela nana* Hustedt and *Detonula confervacea* Cleve. *Can. J. Microbiol.* **8:** 229–239.

Hellebust, J. A. 1974. Extracellular products. Pp. 838–963 in *Algal Physiology and Biochemistry*, W. D. Stewart, ed. University of California Press, Berkeley.

Hidu, H. J., and R. Ukeles. 1962. Dried unicellular algae as food for the larvae of the hard shell clam, *Mercenaria mercenaria*. *Proc. Natl. Shellfish Assoc.* **53:** 85–101.

Hidu, H., and H. S. Tubiash. 1963. A bacterial basis for the growth of antibiotic treated bivalve larvae. *Proc. Natl. Shellfish Assoc.* **54:** 25–39.

His, E., R. Robert, and A. Dinet. 1989. Combined effects of temperature and salinity on fed and starved larvae of the Mediterranean mussel *Mytilus galloprovincialis* and the Japanese oyster *Crassostrea gigas*. *Mar. Biol.* **100**(4): 5–463.

Holt, J. G. 1984. *Bergey's Manual of Determinative Bacteriology*. Williams and Wilkins, Baltimore. 964 pp.

Innes, D. J., and L. E. Haley. 1977. Genetic aspects of larval growth under reduced salinity in *Mytilus edulis*. *Biol. Bull.* **153:** 312–321.

Kates, M. 1964. Bacterial lipids. *Adv. Lipid Res.* **2:** 17–90.

Kutsky, R. J. 1981. *Handbook of Vitamins, Minerals, and Hormones*. Van Nostrand Reinhold, New York. 492 pp.

Langdon, C. J. 1983. Growth studies with bacteria-free oyster (*Crassostrea gigas*) larvae fed on semi-defined artificial diets. *Biol. Bull.* **164:** 227–235.

Langdon, C. J. 1989. Preparation and evaluation of protein microcapsules for a marine suspension-feeder, the Pacific oyster *Crassostrea gigas*. *Mar. Biol.* **102:** 217–224.

Langdon, C. J., and M. J. Waldock. 1981. The effect of algal and artificial diets on the growth and fatty acid composition of *Crassostrea gigas* spat. *J. Mar. Biol.* **61:** 431–448.

Lannan, J. E. 1980. Broodstock management of *Crassostrea gigas*. I. Genetic and environmental variation in survival in the larval rearing system. *Aquaculture* **21:** 323–336.

Lehninger, A. L. 1975. *Biochemistry*. Worth Publishers, New York. 1104 pp.

Leifson, E. 1963. Determination of carbohydrate metabolism of marine bacteria. *J. Bacteriol.* **85:** 1183–1184.

Loosanoff, V. L. 1954. New advances in the study of bivalve larvae. *Am. Sci.* **42:** 607–624.

Loosanoff, V. L. 1959. The size and shape of metamorphosing larvae of *Venus (Mercenaria) mercenaria* grown at different temperatures. *Biol. Bull.* **117:** 308–318.

Loosanoff, V. L., H. C. Davis, and P. E. Chanley. 1953. Effect of overcrowding on rate of growth of clam larvae. *Anat. Rec.* **117**(3): 645–646.

Luck, J. M., G. Sheets, and J. O. Thomas. 1931. The role of bacteria in the nutrition of protozoa. *Quart. Rev. Biol.* **6:** 46–58.

Maeda, M. 1988. Microorganisms and protozoa as feed in mariculture. *Prog. Oceanog.* **21:** 201–206.

Maeda, M., and K. Nogami. 1989. Some aspects of the biocontrolling method in aquaculture. Pp. 395–398 in *Current Topics in Marine Biotechnology*, S. Miyachi, I. Karube, and Y. Ishida, eds. Jap. Soc. Mar. Biotechnol, Tokyo.

Marmur, J., and P. Doty. 1962. Determination of the base composition of deoxyribonucleic acid from its thermal denaturation temperature. *J. Mol. Biol.* **5:** 109–118.

Martin, Y. P., and B. M. Mengus. 1977. Utilisation de souches bacteriennes selectionees dans l'alimentation des larves de *Mytilus galloprovincialis* (LMK) (Mollusque bivalve) en elevages experimentaux. *Aquaculture* **10:** 253–262.

Masson, M. 1977. Observations sur la nutrition des larves de *Mytilus galloprovincialis* avec des aliments inertes. *Marine Biology* **40:** 157–164.

Millar, R. H., and J. M. Scott. 1967. Bacteria-free culture of oyster larvae. *Nature* **216:** 1139–1140.

Newkirk, G. F., L. E. Haley, D. L. Waugh, and R. Doyle. 1977. Genetics of larvae and spat growth rate with the oyster *Crassostrea virginica*. *Mar. Biol.* **41:** 49–52.

Nottage, A. S., and T. H. Birkbeck. 1986. Toxicity to marine bivalves of culture supernatant fluids of the bivalve-pathogenic *Vibrio* strain MCNB 1338 and other marine vibrios. *J. Fish. Dis.* **9:** 249–256.

Perry, G. J., J. M. Volkman, R. B. Johns, and H. J. Bavor, Jr. 1979. Fatty acids of bacterial origin in contemporary marine sediments. *Geochim. Cosmochim. Acta.* **43:** 1715–1725.

Porter, K. G., and Y. S. Feig. 1980. The use of DAPI for identifying and counting aquatic microflora. *Limnol. Oceanogr.* **25:** 943–948.

Prieur, D. 1982. Les bactéries héterotrophes dans les élevages experimentaux et industriels de larves de bivalves marins. *Oceanis* **8**(8): 437–457.

Prieur, D., G. Mevel, J.-L. Nicolas, A. Plusquellec, and M. Vigneulle. 1990. Interactions between bivalve molluscs and bacteria in the marine environment. *Oceanogr. Mar. Biol. Annu. Rev.* **28:** 277–352.

Provasoli, L., K. Shiraishi, and J. R. Lance. 1959. Nutritional idiosyncrasies of *Artemia* and *Tigriopus* in monoxenic culture. *Ann New York Acad Sci* **77:** 250–261.

Provasoli, L., and A. D'Agostino. 1962. Vitamin requirements of *Artemia salina* in aseptic culture. *Amer. Zool* **2:** 439.

Rodina, A. G. 1972. *Methods in Aquatic Microbiology* R. R. Colwell and M. S. Zambruski, eds. University Park Press, Baltimore. 461 pp.

Rohlf, F. J. 1982. *Biom. A Package of Statistical Programs to Accompany the Text Biometry.* State University of New York at Stony Brook, New York. 859 pp.

Sokal, R. R., and F. J. Rohlf. 1981. *Biometry.* W. H. Freeman and Co., San Francisco, CA. 859 pp.

Sonea, S. 1988. A bacterial way of life. *Nature* **331:** 216.

Stuart, C. A., M. McPherson, and H. J. Cooper. 1931. Studies on bacteriologically sterile *Monna macrocopa* and their food requirements. *Physiol. Zool* **4:** 87–100.

Trider, D. J., and J. D. Castell. 1980. Effect of dietary lipids on growth, tissue composition and metabolism of the oyster (*Crassostrea virginica*). *J of Nutr* **110**(7): 1303–1309.

Tubiash, H. S., P. E. Chanley, and E. Leifson. 1965. Bacillary necrosis, a disease of larval and juvenile bivalve mollusks. I Etiology and Epizoology. *J. Bact* **90**(4): 1036–1044.

Tubiash, H. S., R. R. Colwell, and R. Sakazaki. 1970. Marine vibrios associated with bacillary necrosis, a disease of larval and juvenile bivalve mollusks. *J Bact* **103**(1): 272–273.

Ukeles, R., and B. M. Sweeney. 1969. Influence of dinoflagellate trichocysts and other factors on the feeding of *Crassostrea virginica* larvae on *Monochrysis lutheri. Limnol Oceanogr* **14**(3): 403–410.

Underwood, A. J. 1981. Techniques of analysis of variance in experimental marine biology and ecology. Oceanogr. *Mar Biol A Rev* **19:** 513–605.

Utting, S. D., and M. M. Helm. 1985. Improvement of sea water quality by physical and chemical pre-treatment in a bivalve hatchery. *Aquaculture* **44:** 133–144

Walne, P. R. 1956a. Experimental rearing of the larvae of *Ostrea edulis* (L.) in the laboratory. Ministry of Agriculture, Fisheries and Food. *Fishery Invest Series II* **20**(9): 22 pp.

Walne, P. R. 1956b. Bacteria in experiments on rearing oyster larvae. *Nature* **178:** 91.

Walne, P. R. 1958. The importance of bacteria in laboratory experiments on rearing the larvae of *Ostrea edulis* (L.). *J. Mar Biol* **37:** 415–425.

Walne, P. R. 1965. Observations on the influence of food supply and temperature on the feeding and growth of the larvae of *Ostrea edulis* L. *Fish Invest , London Ser 2* **24**(1): 1–45.

Walne, P. R. 1970. Present problems in the culture of the larvae of *Ostrea edulis. Helgol Wiss Meeresunters.* **20:** 514–525.

Reference: *Biol. Bull.* **184**: 52–56. (February, 1993)

Patterns of Suspension Feeding in the Freshwater Bryozoan *Plumatella repens*

BETH OKAMURA[1] AND LITA ANN DOOLAN[2]

[1]*Department of Zoology, South Parks Road, Oxford, U. K. OX1 3PS and* [2]*27 Hawthorn Avenue, Headington, Oxford, U. K. OX3 9QJ*

Abstract. Feeding of large and small colonies of *Plumatella repens* was assessed under two flow conditions. Large colonies ingested greater numbers of particles than small colonies and feeding of colonies of both sizes increased with flow. However, the rate of increase depended on colony size. Small colonies increased feeding to a greater degree than large colonies. Mechanisms that may explain these patterns are discussed. These results contrast with an earlier study of feeding in a freshwater bryozoan. The conflicting results may reflect experimental conditions. In the previous study a small volume of still water likely entailed greater food depletion by large colonies. In our study food depletion did not occur and ambient flow carried away filtered water. We discuss how the relatively large, U-shaped lophophores of freshwater bryozoans function to produce powerful feeding currents that are suited to feeding in lotic and lentic habitats.

Introduction

Assemblages of colonial suspension feeders are common to both marine and freshwater habitats. In general, marine assemblages are characterized by high levels of competition for space and food as asexual growth results in numerous interactions (*e.g.*, Stebbing, 1973; Jackson, 1979; Buss, 1980; Kay and Keough, 1981; Rubin, 1982; Okamura, 1988; López Gappa, 1989). By contrast, very little is known about the dynamics of freshwater systems where assemblages of colonial invertebrates such as bryozoans and sponges are common (Bushnell, 1966; Wood, 1973; Frost, 1991; Karlson, 1991; Ricciardi and Lewis, 1991). However, competition for food and space has been shown to influence patterns of distribution and abundance of freshwater insects (*e.g.*, Hildrew and Townsend, 1980; McAuliffe, 1984; Hart, 1985; Chance and Craig, 1986; Lamberti *et al.*, 1987; Ciborowski and Craig, 1989).

Investigations of marine bryozoans have revealed that colony size, neighbors, and ambient flow conditions can influence feeding success (Buss, 1980; Okamura, 1984, 1985, 1988) and subsequent colony growth (Okamura, 1992). Thus patterns of suspension feeding play an important role in the dynamics of these assemblages that are typically limited by space. Unlike their marine counterparts who feed with a circular lophophore (an apical tentacular crown), freshwater bryozoans (Cl: Phylactolaemata) possess a relatively larger and U-shaped lophophore. However, little is known about comparative patterns of feeding in freshwater bryozoans and how these may influence patterns of distribution and abundance of freshwater populations. For these reasons we undertook to characterize how colony size and ambient flow conditions influence suspension feeding in the freshwater bryozoan *Plumatella repens.*

Materials and Methods

Plumatella repens is probably the most common freshwater bryozoan and shows a cosmopolitan distribution (Wood, 1989). As its name implies, colonies are repent, adhering to the substratum as a series of branching zooecial tubes that can spread to cover large areas. Lophophores typically are deployed some distance apart as a result of elongation of zooecial tubes. Colonies are found in lakes, ponds, and streams on a variety of substrata including the undersurfaces of aquatic vegetation (especially lily pads: pers. obs.), submerged branches and roots, and rocks and stones (Wood, 1989).

Colonies for feeding studies were collected from a 47-year-old gravel pit located at Cassington Nurseries in Cassington, Oxfordshire. Pieces of lily pads containing large

Received 26 March 1992; accepted 23 October 1992.

(5–7 cm in diameter) and small (2–3 cm in diameter) colonies were brought to the laboratory where feeding studies were conducted. Lily pads were cut to approximately equal sizes for each treatment (7 cm for large colonies and 5 cm for small colonies; colonies were located centrally).

During feeding trials, cut lily pads containing colonies were floated on the surface of the water in the working area of a recirculating flow tank that contained a suspension of polystyrene particles. Lily pad segments were retained in position with thin lengths of wire. Colonies on the undersurfaces of the lily pads were thus immersed just below the surface of the water as they are in the field.

Polystyrene particles were suspended in distilled water at a concentration of 200 particles $\cdot$ ml^{-1} (SD = 3.95, n = 10). The concentration of particles was estimated by counting 10 haphazardly chosen fields of 10 samples of suspension. Polystyrene particles have been used to study feeding in marine bryozoans (*e.g.*, Okamura, 1984, 1985), and preliminary investigation revealed *Plumatella* would ingest them in large numbers. The diameter of the particles was 19.1 μm (SD = 0.6 μm) (Duke Scientific Corporation, Palo Alto, California) and lies within the size range of normal food items ingested by *Plumatella* (Kaminski, 1984). The concentration of particles was well within the range experienced by suspension feeders in their natural environment (DeMott, 1986).

Two standard flow conditions were created by effecting two known velocities in the mid-channel section of the flow tank (approx. 3–10 cm below the air-water interface, 2 cm in from the sides of the flow tank, and 20 cm long) (total cross section of water in the flow tank was 15 $\times$ 17 cm) during feeding trials. In the slower flow condition, velocity in the mid-channel section was 2.5 cm $\cdot$ s^{-1} (SD = 0.40 cm $\cdot$ s^{-1}, n = 15), and in the faster flow condition it was 5.3 cm $\cdot$ s^{-1} (SD = 0.80 cm $\cdot$ s^{-1}, n = 15). These velocities were determined by timing the passage of particles (hydrated *Artemia* eggs) over a known distance (15 cm) of the mid-channel section. Since lily pads with colonies were floated on the surface of the water, interaction of flow with the air-water interface and with the lily pad substrata would have created a velocity gradient (a boundary layer) during feeding trials (Vogel, 1981). Thus colonies experienced slower ambient flow velocities than those measured at the mid-channel section. Although we did not have the means to characterize flow at the level of lophophores, casual observations indicated that colonies experienced qualitatively different flow conditions during the feeding trials.

Colonies were starved for 24 h and then allowed to feed on particles for 10 min. Feeding trials of longer than 15 min were found to result in the ingestion of too many particles to assure accurate counting. A feeding trial time of 10 min is shorter than the gut passage time of various marine bryozoans (Winston, 1977). As the polystyrene particles were slightly denser than freshwater, a poultry baster was used at two minute intervals to resuspend particles. Immediately after each feeding run, colonies were placed facing down in individual petri dishes containing distilled water. Feces obtained after 12 h were collected and preserved in 80% ethanol until sampling.

Feeding rates were estimated by determining the mean number of particles per fecal pellet. Individual fecal pellets were gently squashed under a cover slip on a microscope slide, and the number of particles was counted using a compound microscope. Forty fecal pellets were sampled per colony when colonies produced large numbers of fecal pellets, otherwise all fecal pellets were sampled. As the relative proportions of actively feeding zooids varied in colonies during feeding trials, the total number of pellets produced per colony is not particularly informative. However, to check that fecal pellets did not vary with colony size, the maximum lengths and widths of 3–5 fecal pellets of large (n = 17) and small (n = 8) colonies were determined (colonies were not used in feeding trials).

Data on mean number of particles per fecal pellet per colony in the different treatments and on fecal pellet size were checked for normality and heterogeneity of variances prior to analysis. F-max tests revealed heterogeneous variances in the number of particles per fecal pellet per colony so data were log-transformed for ANOVA.

Results

Zooids of phylactolaemates produce mucus-encased fecal pellets that appear to be of fairly fixed sizes and regular shapes. Observations suggest that pellet dimensions reflect the dimensions of the packaging region of the hindgut (Okamura, pers. obs.). Data on fecal pellet size collected for small and large colonies support these observations. The mean volume of fecal pellets did not vary with colony size (mean volume of fecal pellets for large colonies was 3.24×10^{-3} mm^3 [SD = 1.8×10^{-3}] and for small colonies was 4.38×10^{-3} mm^3 [SD = 2.67×10^{-3}]; t = 1.264, df = 23, P = 0.219). Furthermore, although the total number of fecal pellets produced by colonies was not determined (since the number of feeding zooids per colony was variable and very difficult to count during feeding trials), fecal pellet production during experiments seemed generally to parallel feeding estimated by the number of particles per fecal pellet per colony. We therefore are confident that the data collected are good estimates of feeding rates.

Two-way ANOVA indicated significant size and flow effects on feeding (as measured by mean number of particles per fecal pellet per colony) (see Table I). The interaction of size and flow was also significant. These effects are shown in Figure 1. Large colonies had greater feeding

Table I

Two-way ANOVA of the effects of flow and colony size on the mean number particles per fecal pellet per colony. Analysis on log-transformed data

Source	df	Sum of squares	Mean square	F-value	*P*-value
Flow	1	1.169	1.169	42.690	0.0001
Size	1	1.820	1.820	66.457	0.0001
Flow × Size	1	0.400	0.400	14.592	0.0006
Residual	32	0.876	0.027		

rates, and feeding increased with flow in colonies of both sizes, however, when feeding from faster flow small colonies increased feeding rates approximately five times, while feeding rates of large colonies increased by a factor of only 1.8.

Discussion

Flow conditions and feeding

Increased feeding of *Plumatella* in conditions of greater flow contrasts with feeding patterns of marine bryozoans. In general, marine bryozoans experience reduced feeding success with increased ambient flow (*e.g.*, Okamura, 1984, 1985, 1988, 1990). The explanation for this difference may relate to the relative sizes and shapes of their lophophores. Phylactolaemate lophophores are large and U-shaped and have numerous ciliated tentacles. For instance, in *Plumatella repens* tentacle number ranges from 40–60 (Lacourt, 1968), while the number of tentacles in various marine bryozoan groups ranges from 8–34 (Winston, 1977). Best and Thorpe (1986) found that the strength of feeding currents related positively to lophophore size in marine bryozoans. This suggests that phylactolaemates should produce relatively more powerful feeding currents. Furthermore, deflection of lophophoral arms in phylactolaemates places cilia lining the arms in relatively closer proximity than the cilia that line the arms of the circular lophophores of marine bryozoans. This closer ciliary proximity should also contribute to creation of stronger feeding currents.

Bishop and Bahr (1973) report feeding currents extending 5 mm from lophophores of the phylactolaemate *Lophopodella carteri* (tentacle number = 50–95; Lacourt, 1968). McKinney *et al.* (1986) observed feeding currents to be effective at a distance of 3 mm in the marine cheilostome *Bugula neritina* (tentacle number = 23; Winston, 1978). (Both observations of feeding currents were in still water.) Greater pumping capacity of phylactolaemates may thus explain why, over the velocity range tested in this study, feeding by large lophophores of *Plumatella* was not constrained. Ultimately, of course, phylactolaemate feeding will be constrained by flow, when feeding currents can no longer overcome friction drag imposed by flow.

Greater feeding rates in the faster flow condition by *Plumatella* may reflect higher concentrations of particles in volumes of water diverted by feeding currents and, consequently, a greater flux of particles through the lophophore. Profiles of particle availability near surfaces can change: as flow increases higher particle concentrations and fluxes can occur closer to surfaces in boundary layer flows (Muschenheim, 1987; Fréchette *et al.*, 1989). Whether this is true for particle profiles near the air–water interface is not known to us (colonies floating on lily segments were situated just below this interface). Alternatively, there may be a greater propensity to feed at increased flow.

These results suggest that phylactolaemates possess powerful lophophores that allow them to feed from lotic and lentic environments (many, including *Plumatella,* occur in both). In diverting fluid from great distances, powerful lophophores may be significant for feeding in still conditions where food-depletion close to surfaces may be common and where lack of flow precludes resource renewal. Powerful lophophores will also be less overwhelmed by friction drag imposed by water moving downstream in lotic environments.

Colony size and feeding

The relatively high feeding rates of large *Plumatella* colonies may be explained by several mechanisms. The many lophophores of large colonies may concertedly pump greater volumes of water under varying flow conditions than can the fewer lophophores of small colonies (*i.e.*, the many lophophores of large colonies may concertedly produce a stronger pump). Alternatively, large

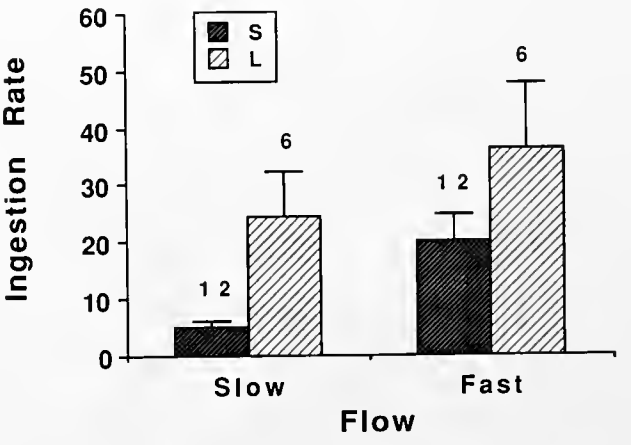

Figure 1. Ingestion rates (mean number of particles per fecal pellet per colony) of small (S) and large (L) colonies in slow and fast ambient flow (numbers above columns indicate number of colonies sampled). Bars represent two standard errors.

colonies may have relatively greater metabolic demands (possibly they invest more in statoblast or larval production per unit mass) than small colonies and therefore have a higher propensity to feed. However, the greater increase in the rate of feeding in small colonies with increased flow (by a factor of five) relative to large colonies (in which feeding increased by a factor of 1.8) (see Fig. 1) suggests that small colonies respond more strongly to increases in particle flux (or flow). Why small colonies should show such a marked response is not apparent. Perhaps small colonies create stronger ciliary currents in response to an abundance of food (particle flux serving as a cue) as has been observed in marine bryozoans (Best and Thorpe, 1983). Concerted pumping in large colonies may preclude the necessity to create individually stronger feeding currents and may provide for a more constant food supply.

Our results contrast with those obtained by Bishop and Bahr (1973) who found that clearance rates of the phylactolaemate *Lophopodella carteri* decreased with colony size. This discrepancy may relate, in part, to differences in colony morphology and growth in the two species, but it also is complicated by comparing feeding studies conducted under static and dynamic conditions and in dissimilar volumes of suspension.

Lophopodella is a higher phylactolaemate, producing gelatinous, globular colonies with no branching (Wood, 1991). Colonies of *Lophopodella* do not grow indefinitely but undergo fission, the resulting colonies slowly creeping apart. Fission in *Lophopodella* may result in avoidance of lophophoral feeding interference that occurs as colonies get bigger, hence maximizing filtering efficiency (Bishop and Bahr, 1973; Hughes, 1989). To some extent, our results for feeding in *Plumatella* support this contention. *Plumatella* does not undergo fission and its feeding does not decrease with increased colony size. The lack of interference in feeding in *Plumatella* may partly reflect its morphology. *Plumatella* colonies are tubular and branching and their lophophores are spaced much further apart than those of *Lophopodella*. However, we also believe it is crucial to consider differing patterns of excurrent flow and food depletion in our experiments and in those of Bishop and Bahr (1973).

In Bishop and Bahr's study (1973), *Lophopodella* colonies were placed in small vials (diameter = 22 mm) that contained 10 ml of an algal suspension. Thus colonies will have had ample opportunity to resample previously filtered water because the total volume of water was small and because, under conditions of still water, previously filtered water was not carried away. Thus, it is not surprising that clearance rates were lower for large colonies. The volume of suspension in our study was large (25 l), and food depletion was not significant. Furthermore, incorporation of ambient flow meant food-depleted water was carried away from colony surfaces.

Conclusion

This study indicates that feeding by freshwater bryozoans is less constrained by increased flow than it is in marine forms. As suggested above, the relatively large lophophores of phylactolaemates create powerful feeding currents that may be beneficial in both lotic and lentic environments. The complex hydrodynamics characteristic of marine habitats (see Denny, 1988) may ensure delivery of food to the level of small, circular lophophores of marine bryozoans. Furthermore, small, circular lophophores maximize the collective surface area for feeding, and colonies can benefit from the larger energy surplus associated with small size (Sebens, 1979, 1982; Ryland and Warner, 1986; Hughes, 1989). Thus lophophore size and shape in marine and freshwater bryozoans may reflect different solutions to different kinds of problems faced by small, colonial suspension feeders in the two sorts of environments. However, the role of phylogenetic constraint in determining lophophore morphology cannot be ruled out (traditional views hold U-shaped lophophores to be primitive). Although the majority of freshwater bryozoans possess large, U-shaped lophophores, small, circular lophophores are found in the phylactolaemate *Fredericella* and in the few gymnolaemates that have invaded freshwater habitats. These exceptions to the rule indicate that the significance of lophophore size and shape in freshwater habitats merits further investigation.

Acknowledgments

We thank Pauline and David Whittington for their friendly interest and kind permission to collect *Plumatella* from their pond at Cassington Nurseries and Mark Brown for technical help. This work was submitted in partial fulfillment for the Zoology Honours Degree in the Department of Zoology, University of Oxford by L. Doolan. The manuscript has been improved by comments from two reviewers.

Literature Cited

Best, M. A., and J. P. Thorpe. 1983. Effects of particle concentration on clearance rate and feeding current velocity in the marine bryozoan *Flustrellidra hispida*. *Mar. Biol.* **77:** 85–92.

Best, M. A., and J. P. Thorpe. 1986. Effects of food particle concentration on feeding current velocity in six species of marine Bryozoa. *Mar. Biol.* **93:** 255–262.

Bishop, J. W., and L. M. Bahr. 1973. Effects of colony size on feeding by *Lophopodella carteri*. Pp. 433–437 in *Animal Colonies: Development and Function through Time*, R. S. Boardman, A. H. Cheetham, and W. A. Oliver, eds. Dowden, Hutchinson and Ross, Stroudsberg, PA.

Bushnell, J. H. 1966. Environmental relations of Michigan Ectoprocta, and dynamics of natural populations of *Plumatella repens*. *Ecol. Monogr.* **36:** 95–123.

Buss, L. W. 1980. Bryozoan overgrowth interactions–the interdependence of competition for space and food. *Nature* **281:** 475–477.

Chance, M. M., and D. A. Craig. 1986. Hydrodynamics and behaviour of Simuliidae larvae (Diptera). *Can. J. Zool.* **64:** 1295–1309.

Ciborowski, J. J. H., and D. A. Craig. 1989. Factors influencing dispersion of larval black flies (Diptera: Simuliidae): effects of current velocity and food concentration. *Can. J. Fish. Aquat. Sci.* **46:** 1329–1341.

DeMott, W. R. 1986. The role of taste in food selection by freshwater zooplankton. *Oecologia* **69:** 334–340.

Denny, M. W. 1988. *Biology and the Mechanics of the Wave-Swept Environment.* Princeton University Press, Princeton, N. J. 329 pp.

Fréchette, M., C. A. Butman, and W. R. Geyer. 1989. The importance of boundary-layer flows in supplying phytoplankton to the benthic suspension feeder, *Mytilus edulis* L. *Limnol. Oceanogr.* **34:** 19–36.

Frost, T. M. 1991. Porifera. Pp. 95–124 in *Ecology and Classification of North American Freshwater Invertebrates.* J. H. Thorp and A. P. Covich, eds. Academic Press, Inc., San Diego, CA.

Hart, D. D. 1985. Causes and consequences of territoriality in a grazing stream insect. *Ecology* **66:** 404–414.

Hildrew, A. G., and C. R. Townsend. 1980. Aggregation, interference, and foraging by larvae of *Plectrocnemia conspersa* (Trichoptera: Polycentropodidae). *Anim. Behav.* **28:** 553–560.

Hughes, R. N. 1989. *A Functional Biology of Clonal Animals.* Chapman and Hall, London. 331 pp.

Jackson, J. B. C. 1979. Overgrowth competition between encrusting cheilostome ectoprocts in a Jamaican cryptic reef environment. *J. Anim. Ecol.* **48:** 805–823.

Kaminski, M. 1984. Food composition of three bryozoan species (Bryozoa, Phylactolaemata) in a mesotrophic lake. *Pol. Arch. Hydrobiol.* **31:** 45–53.

Karlson, R. H. 1991. Recruitment and local persistence of a freshwater bryozoan in stream riffles. *Hydrobiologia* **226:** 91–101.

Kay, A. M., and M. J. Keough. 1981. Occupation of patches in the epifaunal communities on pier pilings and the bivalve *Pinna bicolor* at Edithburgh, South Australia. *Oecologia* **48:** 123–130.

Lacourt, A. W. 1968. A monograph of the freshwater Bryozoa–Phylactolaemata. *Zoologische Verhandelingen* No. 93.

Lamberti, G. A., J. W. Feminella, and V. H. Resh. 1987. Herbivory and intraspecific competition in a stream caddisfly population. *Oecologia* **73:** 75–81.

López Gappa, J. J. 1989. Overgrowth competition in an assemblage of encrusting bryozoans settled on artificial substrata. *Mar. Ecol. Prog. Ser.* **51:** 121–130.

McAuliffe, J. R. 1984. Competition for space, disturbance, and the structure of a benthic stream community. *Ecology* **65:** 894–908.

McKinney, F. K., M. R. A. Listokin, and C. D. Phifer. 1986. Flow and polypide distribution in the cheilostome bryozoan *Bugula* and their inference in *Archimedes*. *Lethaia* **19:** 81–93.

Muschenheim, D. K. 1987. The dynamics of near-bed seston flux and suspension-feeding benthos. *J. Mar. Res.* **45:** 473–496.

Okamura, B. 1984. The effects of ambient flow velocity, colony size, and upstream colonies on the feeding success of Bryozoa. I. *Bugula stolonifera* Ryland, an arborescent species. *J. Exp. Mar. Biol. Ecol.* **83:** 179–193.

Okamura, B. 1985. The effects of ambient flow velocity, colony size, and upstream colonies on the feeding success of Bryozoa. II. *Conopeum reticulum* (Linnaeus), an encrusting species. *J. Exp. Mar. Biol. Ecol.* **89:** 69–80.

Okamura, B. 1988. The influence of neighbors on the feeding of an epifaunal bryozoan. *J. Exp. Mar. Biol. Ecol.* **120:** 105–123.

Okamura, B. 1990. Particle size, flow velocity, and suspension-feeding by the erect bryozoans *Bugula neritina* and *B. stolonifera*. *Mar. Biol.* **105:** 33–38.

Okamura, B. 1992. Microhabitat variation and patterns of colony growth and feeding in a marine bryozoan. *Ecology* **73:** 1502–1513.

Ricciardi, A., and D. J. Lewis. 1991. Occurrence and ecology of *Lophopodella carteri* (Hyatt) and other freshwater Bryozoa in the lower Ottawa River near Montréal, Quebec. *Can. J. Zool.* **69:** 1401–1404.

Rubin, J. S. 1982. The degree of intransitivity and its measurement in an assemblage of encrusting cheilostome Bryozoa. *J. Exp. Mar. Biol. Ecol.* **60:** 119–128.

Ryland, J. S., and G. F. Warner. 1986. Growth and form in modular animals: ideas on the size and arrangement of zooids. *Phil. Trans. R. Soc. Lond. B* **313:** 53–76.

Sebens, K. P. 1979. The energetics of asexual reproduction and colony formation in benthic marine invertebrates. *Am. Zool.* **19:** 683–697.

Sebens, K. P. 1982. The limits to indeterminate growth: an optimal size model applied to passive suspension feeders. *Ecology* **63:** 209–222.

Stebbing, A. R. D. 1973. Competition for space between the epiphytes of *Fucus serratus* L. *J. Mar. Biol. Assoc. U.K.* **53:** 247–261.

Vogel, S. 1981. *Life in Moving Fluids.* Princeton University Press, Princeton, N. J. 352 pp.

Winston, J. E. 1977. Feeding in marine bryozoans. Pp. 233–271 in *Biology of Bryozoans*, R. M. Woollacott and R. L. Zimmer, eds. Academic Press, New York.

Winston, J. E. 1978. Polypide morphology and feeding behavior in marine ectoprocts. *Bull. Mar. Sci.* **28:** 1–31.

Wood, T. S. 1973. Colony development in species of *Plumatella* and *Fredericella* (Ectoprocta: Phylactolaemata). Pp. 395–432 in *Development and Function of Animal Colonies through Time*, R. S. Boardman, A. Cheetham, and J. Oliver, eds. Dowden, Hutchinson & Ross, Stroudsburg, PA.

Wood, T. S. 1989. Ectoproct bryozoans of Ohio. *Ohio Biol. Surv. Bull. New Series* **8**(2): × + 70 pp.

Wood, T. S. 1991. Bryozoans. Pp. 481–499 in *Ecology and Classification of North American Freshwater Invertebrates.* J. H. Thorp and A. P. Covich, eds. Academic Press, Inc., San Diego, CA.

Reference: *Biol. Bull.* **184**: 57–78. (February, 1993)

Aplacophora as Progenetic Aculiferans and the Coelomate Origin of Mollusks as the Sister Taxon of Sipuncula[1]

AMÉLIE H. SCHELTEMA

Woods Hole Oceanographic Institution, Woods Hole, Massachusetts 02543

Abstract. Evidence is presented in support of the following phylogenetic hypotheses: (1) Sipuncula are the sister taxon of Mollusca; (2) the two aplacophoran taxa, Neomeniomorpha (= neomenioids) and Chaetodermomorpha (= chaetoderms), are monophyletic with a common neomenioid-like ancestor, and of the two taxa, Chaetodermomorpha are more derived; (3) Aplacophora and Polyplacophora are sister taxa and form a clade, Aculifera; (4) Aculifera are the sister group of the remaining extant mollusks, Conchifera; and (5) Aplacophora are progenetic Aculifera.

The evidence is based on homologies of early and late embryological development, adult morphologies, and molecular analyses. Embryological development in sipunculans and mollusks shows a close relationship between them, and embryological development of the shell separates Aculifera and Conchifera. Adult morphologies indicate: (1) monophyly of Aplacophora; (2) sister-group relationship between Aplacophora and Polyplacophora; (3) a molluscan plesiomorphy of nonsegmented serial replication of organs; and (4) progenesis in Aplacophora. Molecular evidence supports the embryological and morphological relationships between Sipuncula and Mollusca.

Mollusca are thus hypothesized to be coelomate Eutrochozoa, which share an ancestor that probably had serial replication of organs. Differences in size and structure of the coelom among Eutrochozoa are hypothesized to have been brought about by changes in the timing and the process of cavitation of the mesodermal bands that arise from cell 4d. Through the process of progenesis Aplacophora retained an ovoid embryological shape and several internal structures that, although they appear to be in a primitive state, are actually secondarily derived as is quadrant D specification during early cleavage.

Received 19 August 1992; accepted 25 November 1992.

[1] Contribution Nos. 8205 from the Woods Hole Oceanographic Institution, and 314 from the Smithsonian Marine Station at Link Port.

Introduction

The uniqueness of Aplacophora among Mollusca lies in their derived vermiform body in combination with an internal organization that appears to reflect a primitive molluscan state, especially the simple ladderlike nervous system, serial musculature, distichous radula (two teeth per row) in its plesiomorphic aplacophoran state, simple digestive system, and epidermis that produces an aculiferous cuticle. Their evolutionary significance to the phylum has long been a matter for conjecture. First came the question of whether Aplacophora were even mollusks, as they lack a number of "typical" characters such as a shell, mantle, and kidneys (*e.g.*, Thiele, 1902; H. Hoffmann, 1929-30), but they have more usually been considered to belong within the phylum because of similarities to chitons in their nervous system (Amphineura) and spicules (Aculifera) (*e.g.*, Spengel, 1881; Heath, 1911). Further discussions were concerned with whether aplacophorans were "degraded" or truly "primitive" mollusks (see Hyman, 1967, pp. 68–70 for a historical account).

There have been no current arguments which separate Aplacophora from Mollusca since evidence for a close relationship between Aplacophora and Polyplacophora was published by S. Hoffman (1949), but under present discussion is their origin and position within the phylum (Salvini-Plawen, 1972, 1981a, 1985; Scheltema, 1978, 1988), as well as the origin of the phylum Mollusca itself. Mollusca have been argued either to have a noncoelomate origin and to be the sister taxon of the eucoelomate Annelia-Echiura-Sipuncula (Salvini-Plawen, 1972, 1985 fig. 42), or to be eucoelomates with an ancestor in common

with other coelomates (Wingstrand, 1985; Scheltema, 1988). In either argument, Aplacophora have been considered stem forms and therefore preceded the Monoplacophora with serial replication of organs.

Hypotheses for a noncoelomate origin rest on the argument that the worm-like Aplacophora with replicated lateroventral musculature evolved from a turbellariomorph ancestor, and that consequently the molluscan coelom is not homologous to that in the Eutrochozoa. A coelomate origin has been hypothesized from annelid-mollusk relationships, including the presence of a cell 4d that gives rise to mesoblasts and consequently a homologous coelom, the presence of a trochophore larva, and serial repetition of body parts. Because the molluscan coelom is small and unsegmented, the idea that annelids and mollusks form a clade with a common segmented ancestor is poorly accepted. The dichotomous choice between either a turbellariomorph or an annelid-like ancestor for mollusks has dominated recent thinking about molluscan evolution (*e.g.*, Hyman, 1967; Haszprunar, 1992), and the relationship of mollusks to other Eutrochozoa has not been examined. However, recent molecular data discussed below urge reconsideration of molluscan relationships to other phyla.

Evidence is presented here to support the hypotheses that (1) Mollusca are eucoelomates with their closest living relatives in Sipuncula, their sister group; (2) Aplacophora and Polyplacophora are sister groups in the subphylum Aculifera (contradicting Scheltema, 1978, 1988); (3) Aculifera are the sister group of the remaining living mollusks, Conchifera; (4) the aplacophoran taxa Chaetodermomorpha (= Caudofoveata, here also called chaetoderms) and Neomeniomorpha (= Solenogastres sensu nomine Salvini-Plawen, here also called neomenioids) are monophyletic, sharing a neomenioid-like ancestor; and (5) aplacophorans are progenetic Aculifera. Considered in the discussion is the homology of the eutrochozoan coelom and the evolutionary difference between metamerism, or segmentation as it occurs in the annelids, and serial replication of organs, as found in *Neopilina* and *Vema* (Wingstrand, 1985). The term "metamerism" is used here only to denote a segmented coelom; "serial replication" is used to denote the more general case of serial repetition of organs, whether or not by metameres.

Evidence that Mollusca are Descended from Coelomates

Mollusca have a coelom consisting of gonadal lumina, pericardium, and kidneys, as well as part of the gametoducts in Aplacophora. A noncoelomate ancestry calls for the widening of a pericardial space lined by mesoderm as protection for a heart (Salvini-Plawen, 1968a, 1972; not discussed 1985, 1990) and for gonads separate from the pericardium. This development of coelomic spaces would be a molluscan apomorphy, not homologous with annelid or sipunculan coelom. Alternatively, the molluscan pericardium can be considered as reduced from a large coelomic space homologous to that in other eutrochozoa. The involvement of the pericardial coelom in excretion is unique to mollusks. Ultrafiltration of blood occurs through podocytes that are present in most molluscan classes including Aplacophora (Andrews, 1988; Reynolds and Morse, 1991).

Five independent lines of evidence indicate that reduction of coelom is the case, and that Mollusca are eutrochozoan coelomates: (1) presence of the molluscan cross in mollusks and sipunculans and (2) homology of certain characters in larvae of mollusks and sipunculans indicate that mollusks and sipunculans are sister taxa; (3) a large pericardium among "primitive" mollusks indicates that it is a molluscan plesiomorphy; (4) the embryological development of mesoderm in annelids, mollusks, sipunculans, and nemertines is similar, and the coelom in the four groups is homologous; and (5) molecular data groups mollusks with other eutrochozoans.

Sipunculans as sister taxon of the mollusks

An evolutionary relationship between sipunculans and mollusks lies in their early embryological development and in morphological features of sipunculan pelagosphera and molluscan larvae.

Molluscan cross. The molluscan cross is found in the embryological development of Gastropoda, Polyplacophora, Scaphopoda, and Aplacophora by the end of the 64-cell stage (Verdonk and van den Biggelaar, 1983; Heath, 1899; van Dongen and Geilenkirchen, 1974; Baba, 1951). It is formed by $1a^{12}$–$1d^{12}$ cells and their descendents, with cells $1a^{112}$–$1d^{112}$, called peripheral rosette cells, forming the angle between the arms of the cross (Fig. 1A, B, D, peripheral cells solid black). In Annelida, however, it is cells $1a^{112}$–$1d^{112}$ that form the cross (Fig. 1E, cross cells solid black) (Wilson, 1892). In the 64-cell stage of the neomenioid aplacophoran *Epimenia verrucosa* figured by Baba (1951), a molluscan cross seems apparent from Baba's shading (Fig. 1D), although Salvini-Plawen (1985) found "no definite cross formation" in the same source. Manuscript drawings by G. Gustafson of developing *Chaetoderma nitidulum* eggs likewise show a molluscan cross. In contrast to most mollusks, early cleavage in Pelecypoda is asynchronous and bilateral, and no cross is formed; its absence would seem to be an apomorphy. Likewise, development in Cephalopoda seems an apomorphy of that group, which has telolecithal eggs, early bilateral cleavage, and no molluscan cross.

In Sipuncula, a molluscan—not an annelid—cross is formed, as Rice (1975, 1985) has emphasized and refigured from Gerould (1906), who first described its presence

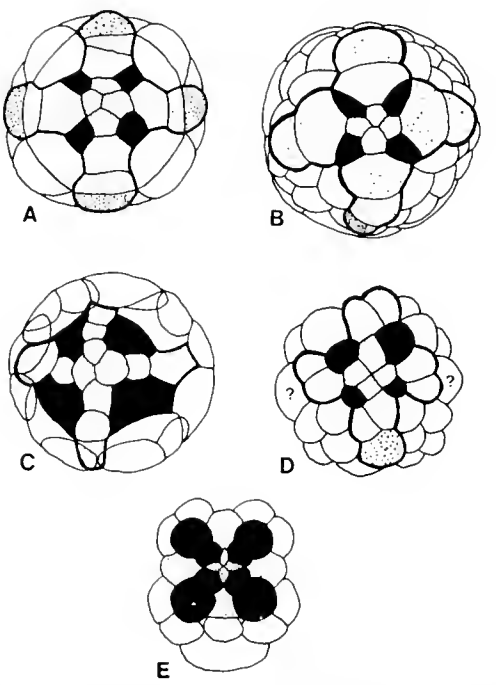

Figure 1. (A-D) The molluscan cross. (A) Gastropoda (*Lymnaea stagnalis*, after Verdonk and van den Biggelaar, 1983, p. 111 fig. 3b); (B) Polyplacophora (*Stenoplax heathiana*, after Heath, 1899, pl. 32, fig. 23); (C) Sipuncula (*Golfingia vulgaris*, after Gerould, 1906, p. 99, fig. D, as published in Rice, 1975, p. 99, fig. 17); (D) Aplacophora (*Epimenia verrucosa*, after Baba, 1951, p. 46, fig. 18). The apical rosette $1a^{111}$–$1d^{111}$ is shown in fine, close stippling; arms of the cross $1a^{12}$–$1d^{12}$ and daughter cells are shown in fine, open stippling; tip cells of cross $2a^{11}$–$2d^{11}$ are shown in coarse stippling; peripheral rosette cells $1a^{112}$–$1d^{112}$ are solid; and trochoblast cells $1a^{2}$–$1d^{2}$ are clear. In *Epimenia* (D), the cleavage stage appears to be earlier than shown in A-C, as the tip cells have not yet separated from $2a^{1}$ and $2c^{1}$ (indicated by question marks), and the arms of the cross are not quite straight, similar to an earlier stage in Polyplacophora (Heath, 1899, pl. 32, fig. 17). In B, only one tip cell was discernible in Heath's illustration, and in C tip cells were not indicated in Gerould's original figure. (E) Annelid cross, Polychaeta (*Nereis*) (after Wilson, 1892, p. 396, diagram II). The apical rosette $1a^{111}$–$1d^{111}$ is shown in fine, close stippling; peripheral cells $1a^{12}$–$1d^{12}$ are shown in fine, open stippling; and the arms of the cross from $1a^{112}$–$1d^{112}$ are solid.

in sipunculan development (Fig. 1C). The presence of a molluscan cross during embryological development is understood here to be of phylogenetic importance, and sipunculans and mollusks share a character not found in either annelids or flatworms (Freeman and Lundelius, 1992). Its presence can be considered apomorphic to the embryonic morphology of turbellarians, which lack a cross.

Similarities between sipunculan and molluscan larvae. Gerould (1906) noticed certain other resemblances to mollusks besides the molluscan cross in the development of sipunculans. In particular, he found similarity between sipunculan pelagosphera and molluscan larvae. The pelagosphera is unique to sipunculans. It is a swimming larva that metamorphoses from a trochophore stage (Rice, 1975, 1985). Gerould noted the resemblance of the pelagosphera lip glands to chiton larval pedal glands, and of the pelagosphera buccal organ to the radula sac in chiton larvae (Figs. 2, 3, 4). Pelagosphera larvae can either swim upright with the large metatroch or creep, head-down, along a solid surface. These activities are lost along with the larval head at metamorphosis. Jägersten (1963) first described creeping in living pelagosphera, and he related it to a creeping gastropod. He also noted that the buccal organ (= pharyngeal bulb, Schlundkopf) was used in feeding. Later Jägersten (1972) proposed a possible, but not certain, homology of the pelagosphera lip, which is the creeping surface posterior to the mouth, and the creeping lobe, or foot, between mouth and anus of molluscan larvae.

Rice (1975, pp. 120–121) described the creeping locomotion of pelagosphera as follows: "The larva is able to . . . glide along with . . . [the] head flattened against the bottom. Frequently the larvae . . . may crawl in the manner of an inchworm, presumably scraping material from the bottom. The continual eversion of the buccal organ during feeding probably aids in the removal of food from the substratum. This tough muscular organ [covered by cuticle, Rice, 1973] is believed to function in breaking up material into small particles for feeding. . ." A mucus-like substance from the lip glands is secreted as the animal moves along a natural substratum (Rice, 1981 and pers. comm.). My own recent observations on living pelagosphera corroborate many of Rice's.

Precise descriptions of the protrusible buccal organ and lip gland have been given by Rice (1973). The buccal organ is a muscular sac, ventral and posterior to a cuticle-lined invagination called the buccal groove that lies below the esophagus. The epithelium of the buccal organ is overlain by the cuticle of the ventral side of the buccal groove and is the area first protruded (Fig. 2). Although the precise innervation of the buccal organ was not demonstrated, the circumesophageal connectives, which arise from the dorsal cerebral ganglion, are closely associated with the organ. Both the topography and function of the buccal organ and groove are remarkably similar to those of the radular apparatus in mollusks: ventral odontophore = buccal organ; ventral radula sac = buccal groove; and ventral cuticular radula = ventral portion of the cuticular buccal groove. Furthermore, the odontophore and probably the buccal organ are innervated through connectives united with the cerebral ganglion. The homology would be more certain if it were known whether the buccal organ musculature is formed from mesoderm, as is the odontophore of mollusks (Raven, 1966), or whether it is myoepithelial as in archiannelids (Jägersten, 1947; Rice, 1973).

The lip gland takes several forms in various pelagosphera, from a bilobed to a paired or four-lobed body

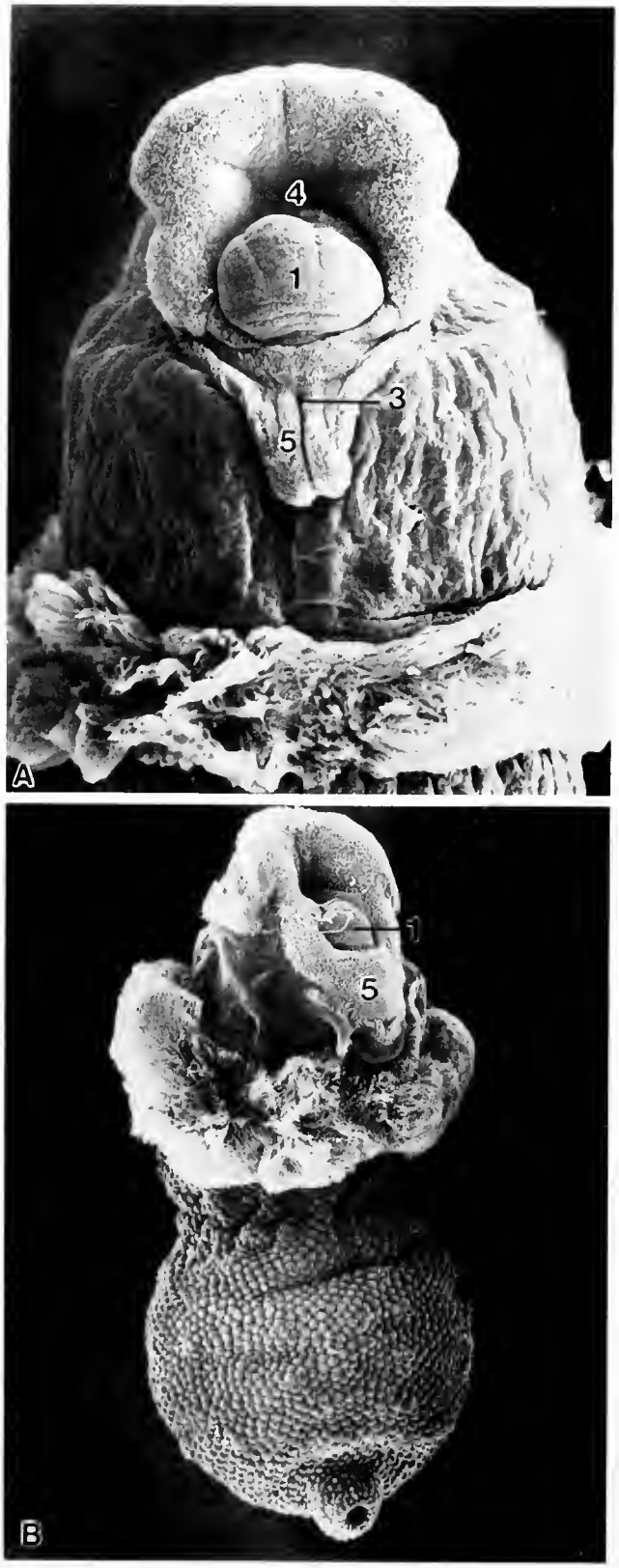

Figure 2. Pelagosphera larvae of Sipuncula. (A) Frontal view of head, *Sipunculus* sp. (from Rice, 1981, fig. 4). (B) Entire larva, *Aspidosiphon* sp. (from Rice, 1981, fig. 6). Numbers as in Figure 3: 1 buccal gland, 3 pore of lip gland, 4 mouth, 5 lip.

which opens either directly, or by way of a ciliated duct or ducts, into the lip pore. In comparison, the anterior pedal gland in larval chitons and in Aplacophora is ductless (*cf.*, Figs. 2A, 4B, 6C). Aplacophora, but not chitons, have a central ciliated pit.

Similarities in form and function in these three structures—lip and foot, lip glands and pedal glands, and buccal organ and radula with its sac—are striking. Their morphologies are particularly clear in sagittal sections of a pelagosphera and a chiton larva (Figs. 3, 4). There are also similarities in their development, as they all arise from posttrochal ectoderm, with these differences: in sipunculans, the origin of all three structures is stomodeal, whereas in mollusks, the ventral somatic plate, usually from cell 2d, gives rise to the foot and its glands, and only the radula sac is stomodeal (Raven, 1966). In Sipuncula as well, cell 2d gives rise to the somatic plate, which forms the ectoderm of the trunk (Rice, 1976). In mollusks, however, the proximity and functional interdependence of the somatic and stomodeal structures are indicated by the pedal contribution to feeding in veliger larvae. An anterior, medial ciliary tract is formed on the foot by which particles unsuitable for ingestion are rejected (Moor, 1983).

Only the head region of the pelagosphera, which is radically altered during metamorphosis to a juvenile sipunculan, can be compared to the Mollusca. The posterior part of the body with its large coelomic sac, nephridia, mid-dorsal anus, and ventral nerve cord, are already definitive adult structures.

Evidence from the presence of the molluscan cross and from locomotary and feeding structures that are similar in mollusks and larval sipunculans is sufficiently strong that the two phyla can be considered as sister groups, and mollusks, therefore, as eucoelomates. Of course, if the primitive mode of sipunculan development should prove to be by way of a nonfeeding, lecithotrophic larva, then the similarities between planktotrophic pelagosphera and molluscan larvae would be convergent. However, Rice (1985) most recently considered evolutionary questions of sipunculan larval development and concluded that a yolky egg and short-lived planktotrophic pelagosphera was the primitive mode of development.

Other considerations. Two further observations can be made to support arguments for a sipunculan-molluscan sister relationship, one embryological, the other paleontological. The first is the embryological development of Echiura (Newby, 1940) compared to that of the sipunculans. Echiurans have traditionally been linked with sipunculans, both having worm- or sac-like, unsegmented coelomate bodies, but echiurans afford a contrast to sipunculans in their closer relationship to annelids. They have an annelid cross rather than a molluscan cross during early cleavage, and as in annelids, the major ciliary band

Figure 3. Midsagittal section of the pelagosphera larva, *Phascolosoma agassizii* (from Rice, 1973, pl. 5). 1 buccal organ, 2 lip gland, 3 pore of lip gland, 4 mouth, 5 lip, 6 stomach, 7 coelom, 8 esophagus.

of older echiuran larvae is the prototroch anterior to the mouth. In sipunculan pelagosphera, the metatroch below the mouth, not the prototroch, is the major swimming organ. Indeed, the region in pelagosphera that forms the head with its locomotory lip, lip gland, and buccal organ, is represented in echiuran larvae by only a few rows of cells between the prototroch and metatroch, and no larval organs are present.

If sipunculans are sister taxon of the Mollusca, they must have arisen, like mollusks, early in the evolution of metazoans. One piece of evidence for an early sipunculan history is the mid-Cambrian genus *Ottoia* from the Burgess Shale. Considered priapulids by Conway Morris (Whittington, 1985) and close to priapulids by Banta and Rice (1976), the genus indicates great diversity of specialized sacciform, coelomate or pseudocoelomate, wormlike animals already in the early Paleozoic. Sipunculans therefore could have a very long, but unobservable and unverified, geologic history. A second piece of evidence is that sipunculans contain hemerythrins, found also only in priapulids, lingulid brachiopods, and some annelids (Curry and Runnegar, 1990). Because lingulids and probably priapulids and annelids are known from the early Cambrian, the presence of hemerythrins indicates a very long history for all forms having these oxygen transport molecules.

Size of the pericardium in "primitive" mollusks

The pericardium is larger relative to the heart in Aplacophora, Monoplacophora, and Polyplacophora than it is in Gastropoda, Pelecypoda, and Cephalopoda (Scheltema, 1973, 1988; Scheltema and Kuzirian, 1991) (Figs. 5, 6A). Ontogenetically, the pericardium is already large before the heart develops from pericardial epithelium in Aplacophora (Baba, 1938), and in Polyplacophora development of the pericardium precedes development of the gonad (Hammersten and Runnström, 1925). Thus the polarity of pericardial size is from large to small in Mollusca, and the continued reduction within the phylum is considered to be a derived condition of the Mollusca.

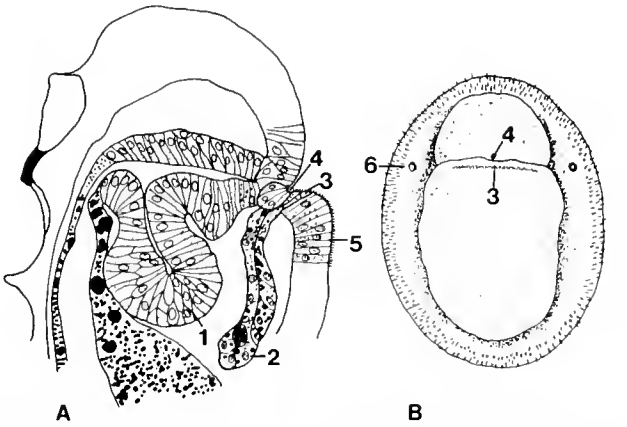

Figure 4. Newly settled larvae of Polyplacophora. (A) Midsagittal section of *Acanthochiton discrepans* (after Hammarsten and Runnström, 1925, fig. E, figure reversed). (B) Ventral view of *Stenoplax heathiana* just after metamorphosis (after Heath, 1899, fig. 59). The opening of the pedal gland (3) lies posterior to the mouth (4); the gland opens through "a series of . . . intercellular channels" rather than a duct (Heath, 1899, p. 631); compare with Figure 6C. 1 radula sac, 2 anterior pedal gland, 3 opening of pedal gland, 4 mouth, 5 foot, 6 larval eye. Structures numbered 1–5 are homologous to structures with the same numbers in Figs. 2, 3.

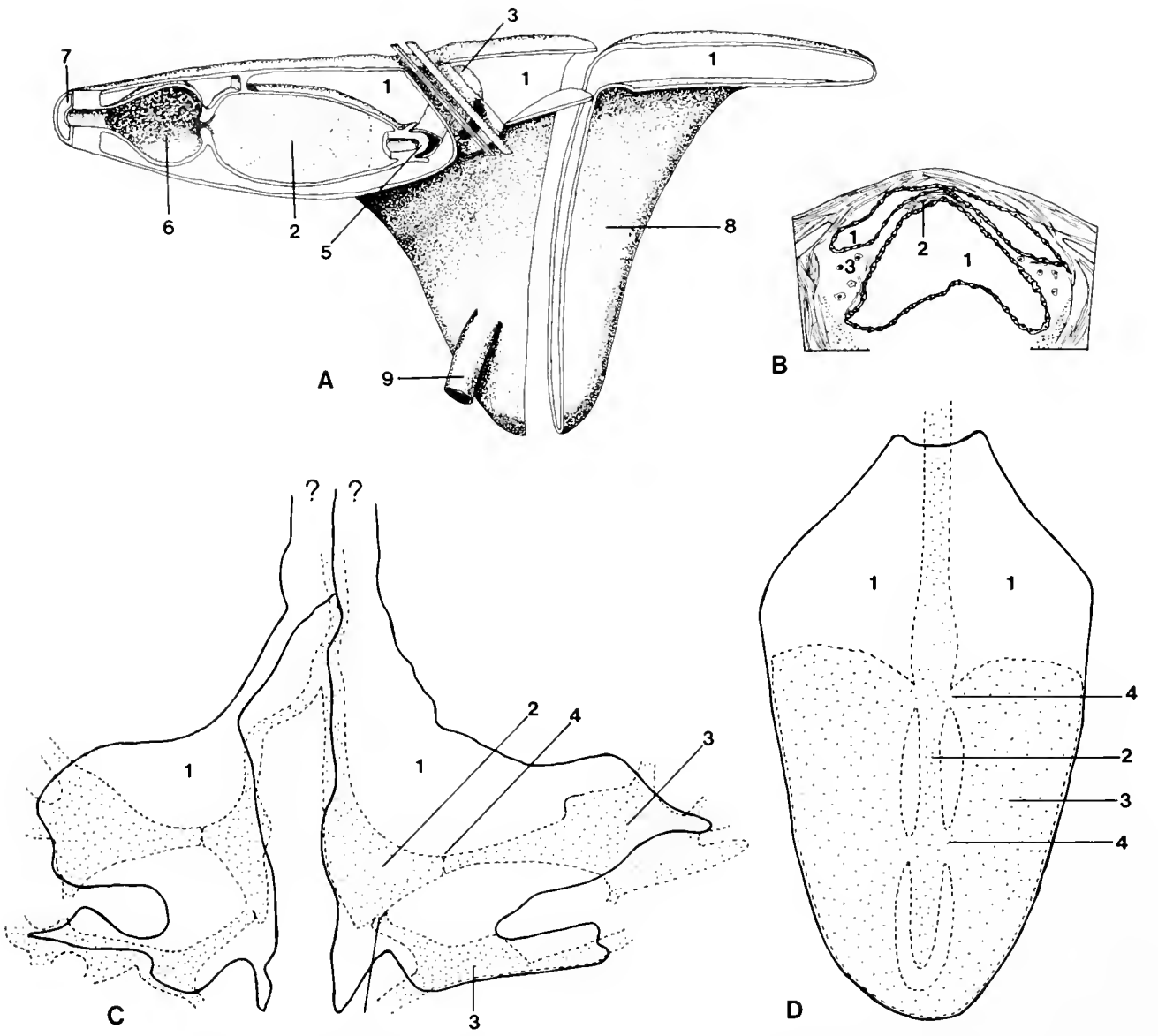

Figure 5. Large pericardial space and heart in primitive molluscs. (A) Aplacophoran, *Chaetoderma nitidulum,* sagittal section. Gametes pass from the gonads through the pericardium with its large, paired, lateral extensions ("horns") and thence into gametoducts leading to the mantle cavity (from Scheltema, 1973, fig. 2, and Scheltema, 1988, fig. 13). (B) Polyplacophoran, *Chiton sinclairi,* cross section (after Wissel, 1904, pl. 24, fig. 49). (C) Monoplacophoran, *Neopilina galathea,* dorsal view, with paired pericardial sacs, paired ventricles, and two pairs of auricles (after Lemche and Wingstrand, 1959, from Scheltema, 1988, fig. 13). (D) Polyplacophoran, *Acanthopleura echinata,* dorsal view, with two pairs of openings between auricles and ventricle (after Plate, 1898, from Scheltema, 1988, fig. 13). 1 pericardium, 2 ventricle, 3 auricle, 4 opening between auricle and ventricle, 5 auriculoventricular valve, 6 aortal bulb, 7 gonopericardial duct, 8 lateral extension of pericardium, 9 gametoduct.

Development of mesoderm

The interpretation that the coelom is reduced in Mollusca assumes that the molluscan pericardium is homologous to the coelom in other spiralian coelomates, namely Annelida and Sipuncula. In all three, the coelom is formed from mesoderm that originates from embryonic cell 4d. This cell gives rise to a pair of mesodermal teloblasts, which migrate inward to a ventrolateral position, one on each side of the midline (Verdonk and van den Biggelaar, 1983; Anderson, 1973; Rice, 1975) and proliferate forward into two lateral mesodermal bands. Mesodermal bands

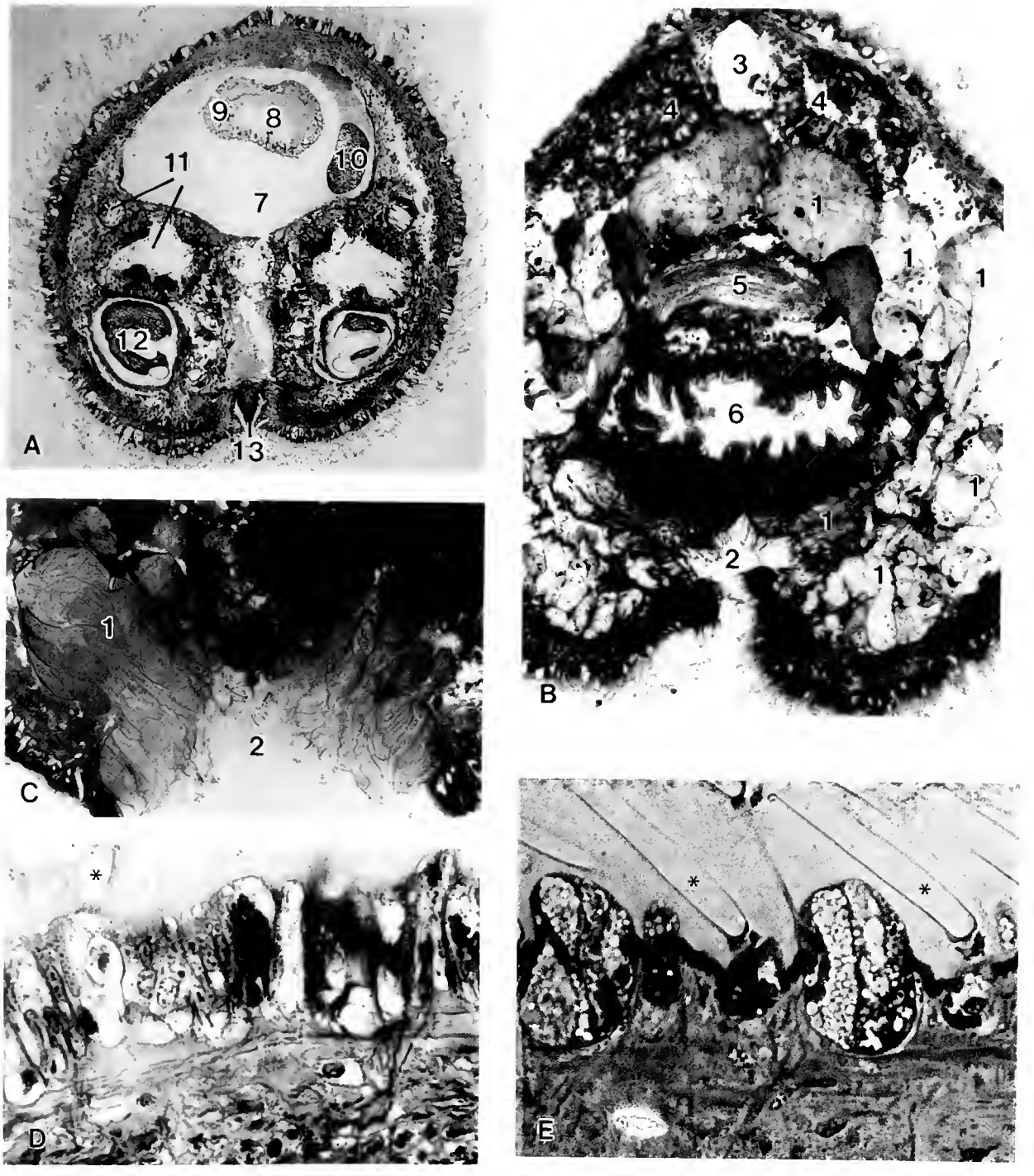

Figure 6. (A) Cross-section through the pericardium of a neomenioid aplacophoran, *Helicoradomenia juani* (from Scheltema and Kuzirian, 1991, fig. 5C). (B) Cross-section through the pedal gland and pedal pit of a neomenioid aplacophoran, *Ocheyoherpia* sp. The voluminous pedal gland occupies most of the head region; the lobes of the gland are in varying stages of secretion. (C) Ciliated pedal pit of *Helicoradomenia juani*. The pedal gland discharges into the pedal pit, not through distinct ducts, but through numerous channels as described for chitons (Fig. 4B). (D) Secretory epidermal papillae of the neomenioid aplacophoran, *Helicoradomena juani* (from Scheltema and Kuzirian, 1991, fig. 2C). (E) Secretory epidermal papillae of the polyplacophoran, *Acanthochiton fasciculatis* (from Fischer *et al.*, 1980, fig. 3). 1 pedal gland, 2 ciliated pedal pit, 3 dorsal blood sinus, 4 dorsal cecum of midgut, 5 cerebral ganglion, 6 oral cavity, 7 pericardium, 8 auricle, 9 ventricle, 10 ovum, 11 U-shaped gametoduct, 12 copulatory spicule pocket, 13 foot. Asterisks in D and E, cavities of dissolved spicules.

are present as well in Nemertini (Turbeville, 1986). In annelids, sipunculans, and nemertines, the coelom is formed by cavitation (schizocoely) of the bands. The coelom constitutes the major body cavity in annelids and sipunculans, but in nemertines it forms only vessels for blood circulation (Turbeville, 1986). In mollusks, the mesodermal bands break up into masses of coelenchyme, from which is formed a solid anlage or pair of anlagen that cavitate to form the pericardium, heart and kidneys (Raven, 1966; Moor, 1983). In some mollusks with paired anlagen, the pericardium begins as paired cavities before becoming united (Raven, 1966). In *Neopilina* the pericardium is still paired (Fig. 5C), and the large pericardial "horns" in some Aplacophora (Fig. 5A) may reflect an ancestral paired condition.

The coelom among the spiralian protostomes described here is interpreted as being homologous because of similarities in early embryological development. Differences in coelom formation among the four phyla apparently arise from variations in the timing of cavitation after the mesodermal bands have formed; but the differences in process are not considered sufficient to deny homology of the coelom. A single pericardium formed by fusion in mollusks other than *Neopilina* is thus an apomorphy.

Molecular evidence

Recent sequencing of 18S ribosomal RNA among 22 classes (not including Aplacophora), in 10 animal phyla, split off acoelomate Platyhelminthes as sister group of the remaining bilaterian taxa, the eucoelomates, which fall into four closely rooted groups (Field *et al.*, 1988). The group termed Eutrochozoa (Ghiselin, 1988) includes five analyzed phyla: Mollusca, Annelida, Brachiopoda, Pogonophora, and Sipuncula. More recently Turbeville *et al.* (1992) have added Nemertini to the Eutrochozoa, basing their results on 18S rRNA and analyzing two Platyhelminthes, in addition to the single flatworm analyzed by Field *et al.* (1988). A re-analysis by Lake (1990) of the 1988 data positioned Sipuncula closest to Mollusca and Brachiopoda, with Annelida and Pogonophora as sister groups. The presence of hemerythrins in Brachiopoda, Sipuncula, and some Annelida affords independent support from molecular data for some of the results of Field *et al.* (Curry and Runnegar, 1990).

The relationships among Sipuncula, Mollusca, and Brachiopoda, however, remain unresolved, and possible synapomorphies of sipunculan and molluscan larval characters were not taken into account by Lake. Although the molecular evidence is still incomplete, it suggests that mollusks have descended from a coelomate ancestor, and that sipunculans are their closest sister group. In proposing that the last common ancestor of the Annelida-Mollusca lineage was hemocoelic and segmented, Lake did not discuss the presence or absence of a coelom. Ghiselin (1988) considered the evolution of Mollusca in light of the molecular evidence given in Field *et al.* (1988), amplifying the data with an analysis of specific nucleotides and a useful history of molluscan phylogenetic hypotheses. Ghiselin favored a segmented, coelomate eutrochozoan ancestor, with loss or reduction of segmentation in the Mollusca. Salvini-Plawen (1990), however, retained a preference for a turbellariomorph molluscan ancestry and refuted the validity of the sequencing by Field *et al.* (1988) and Ghiselin (1988), because "for some selected, traditionally monophyletic groups [including mollusks] euphemistic premises are made" by eliminating some data as convergences. Willmer and Holland (1991) also considered that mollusks had a flatworm origin and suggested that RNA analysis of several Platyhelminthes might show them to be poly- or paraphyletic, but the work of Turbeville *et al.* (1992) indicates that they are monophyletic.

Monophyly of Aplacophora

A proposed homology of the chaetoderm oral shield with the creeping sole of the archimollusk was the basis for separating the two aplacophoran taxa into two classes (Fig. 7B, C; Fig. 8A) (Salvini-Plawen, 1972, 1985, 1990). This homology was based on the innervation of the oral shield (Salvini-Plawen, 1972), the character of the epidermis, and the presumed homology of cuticular structures (Fig. 8C, arrowhead) (S. Hoffman, 1949), but it is not upheld either by light or transmission electron microscopy (Scheltema *et al.*, in press, fig. 9; Tscherkassky, 1989). The oral shield cuticle is continuous with that of the pharynx and is a lip, and the innervation of the shield is cerebral, lying anterior to that part of the anterior nervous system considered "tentacular," and thus part of the head region, by Ivanov (1991). Accordingly the two aplacophoran taxa cannot be separated on the basis of the chaetoderm oral shield, although Salvini-Plawen (1990) recently argued that the homology holds because the foregut and oral-shield epithelia are different, and the presence of the cuticle is secondary. In a schematic drawing through an oral shield, Salvini-Plawen (1990, fig. 7) showed a separation, the "mantle rim," between the oral shield cuticle and body cuticle, but this separation does not exist in my experience (Scheltema *et al.*, in press, fig. 9B). The argument would be clarified if it were known whether the oral shield is stomadeal in origin.

Several synapomorphies suggest that the two aplacophoran taxa are monophyletic. The outgroup for comparison is Polyplacophora.

The tetraneural nervous system, including the cerebral commissure, lateral and ventral nerve cords, and suprarectal commissure, is more heavily ganglionated in both neomenioids and chaetoderms than in chitons. The radula

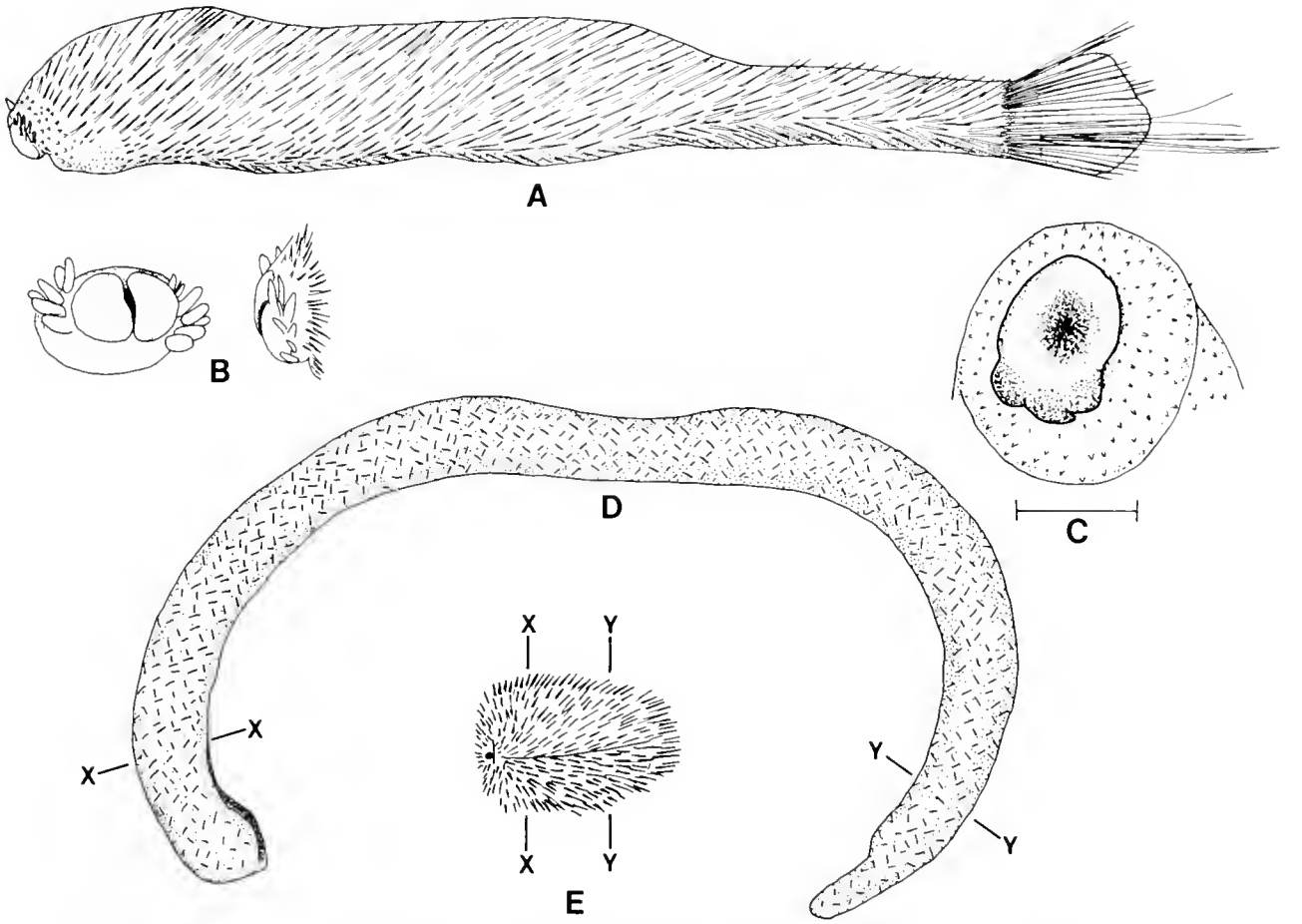

Figure 7. (A-C) Chaetodermomorpha. (A, B) *Chevroderma turnerae*, entire animal (anterior to left) and divided oral shield (from Scheltema, 1985, fig. 3L, O, P). (C) Oral shield of *Scutopus megaradulatus* (*cf.*, Fig. 8A) (from Scheltema, 1988, fig. 6). (D, E) Neomeniomorpha. (D) *Dorymenia* sp. (E) A new neomenioid genus and species in the family Simrothiellidae. D and E are drawn to the same scale, anterior to left; the midgut and gonad lie between X-X and Y-Y.

in its plesiomorphic state in Aplacophora is distichous, that is, only two teeth per row (Scheltema, 1988; Scheltema *et al.*, 1989), a reduction in number from the docoglossate chiton radula. Both neomenioids and chaetoderms have a dorsoterminal sense organ (= dorsocaudal sensory pit), or sometimes several, in the epidermis. It is of unknown function, although homology to the osphradium has been conjectured (Spengel, 1881; Haszprunar, 1987). Whether or not this homology is correct, the position of the dorsoterminal sense organ is an autapomorphy of the Aplacophora, for there is no compelling evidence that this position, postulated to be primitive for the molluscan osphradium (Salvini-Plawen, 1985), is other than an apomorphy shared only by neomenioids and chaetoderms.

The two aplacophoran taxa share a similar reproductive system unique among mollusks. Paired gonads, sometimes fused, open directly into the pericardium, and paired U-shaped gametoducts lead from the posterior end of the pericardium, first anteriorly and then posteriorly, to the mantle cavity (Figs. 5A, 6A, 9D). Separate gonaduct openings in species of *Phyllomenia* (Salvini-Plawen, 1978) are interpreted here as a derived condition of that genus.

The mantle cavity in both neomenioids and chaetoderms is small and posterior, acting as little more than a cloaca. In neomenioids, the groove on either side of the foot-fold can also be considered as reduced mantle grooves (Figs. 6A, 8C). The paired ctenidia in chaetoderms, which fill most of the mantle cavity, is probably a plesiomorphy, with loss in the neomenioids resulting from the space requirements of a secondarily more complicated reproductive system, including sometimes very large copulatory spicules.

Finally, the worm shape itself is here considered a synapomorphy of the Aplacophora, and not separate,

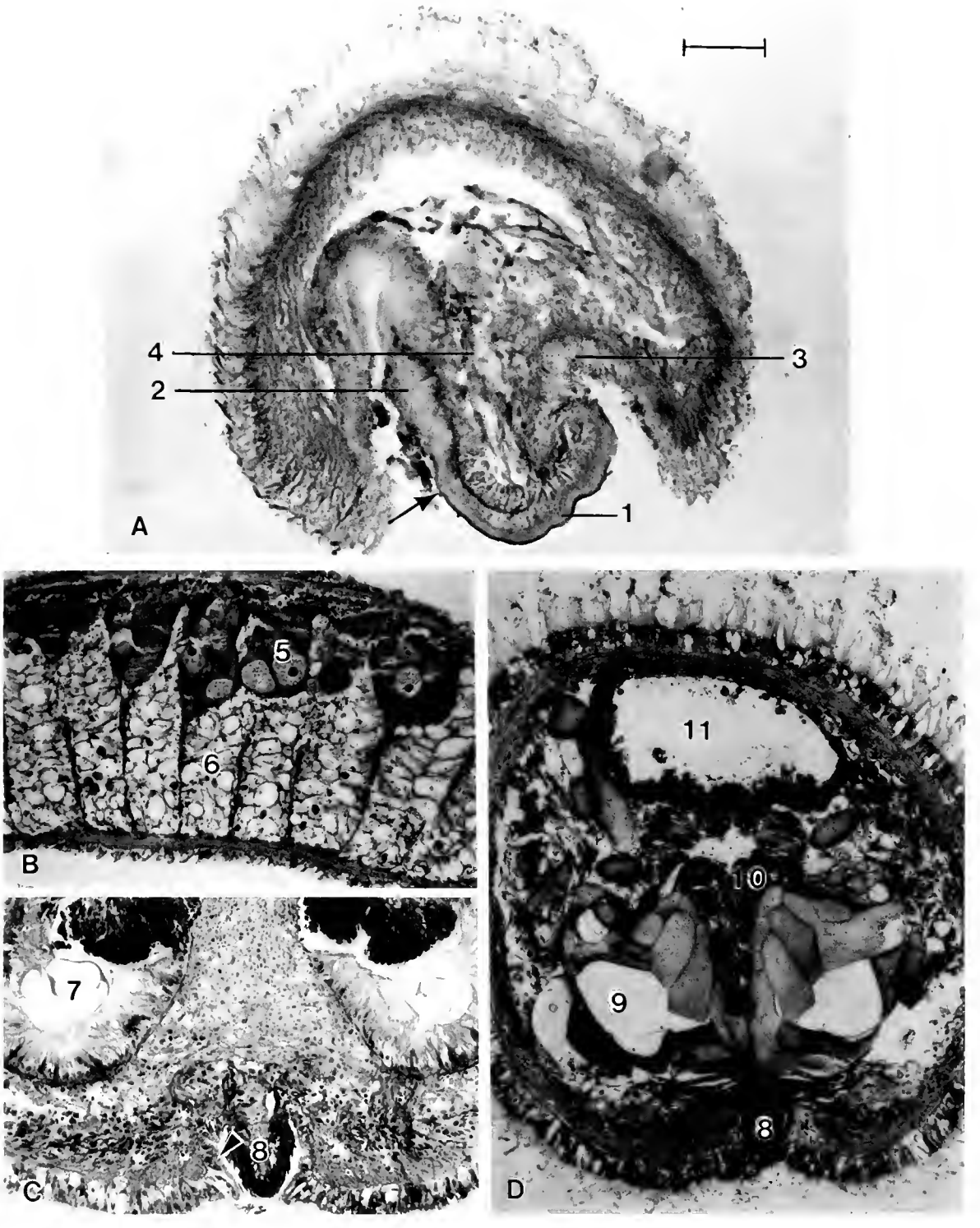

Figure 8. (A) Cross-section through the oral shield of a chaetoderm, *Scutopus megaradulatus*, showing continuity between pharyngeal and oral-shield cuticle. Arrow indicates transition between homogeneous pharyngeal cuticle and more specialized fibrillar oral-shield cuticle with a thickened outer layer (from Scheltema, 1988, fig. 5). (B) Sagittal section through a neomenioid, *Gymnomenia* sp., showing serial lateroventral musculature. (C) Cross-section through the nonmuscular, heavily ciliated foot of a neomenioid, *Helicoradomenia juani*. The arrowhead indicates the nonspiculose cuticle of the mantle cavity extending along each side of the foot groove, which was considered homologous to the chaetoderm oral shield by S. Hoffman (1949). (D) Cross-section through the radula, radula bolsters, and paired, hollow radula vesicles in *Helicoradomenia juani* (from Scheltema and Kuzirian, 1991, fig. 4D). 1 oral-shield cuticle, 2 pharyngeal cuticle, 3 cuticle of body wall, 4 nerve fibers from precerebral ganglion, 5 ovarian region of hermaphroditic gonad, 6 digestive cells of undifferentiated midgut, 7 copulatory spicule pocket, 8 foot, 9 radula vesicle, 10 radula, 11 dorsal cecum of stomach/digestive gland.

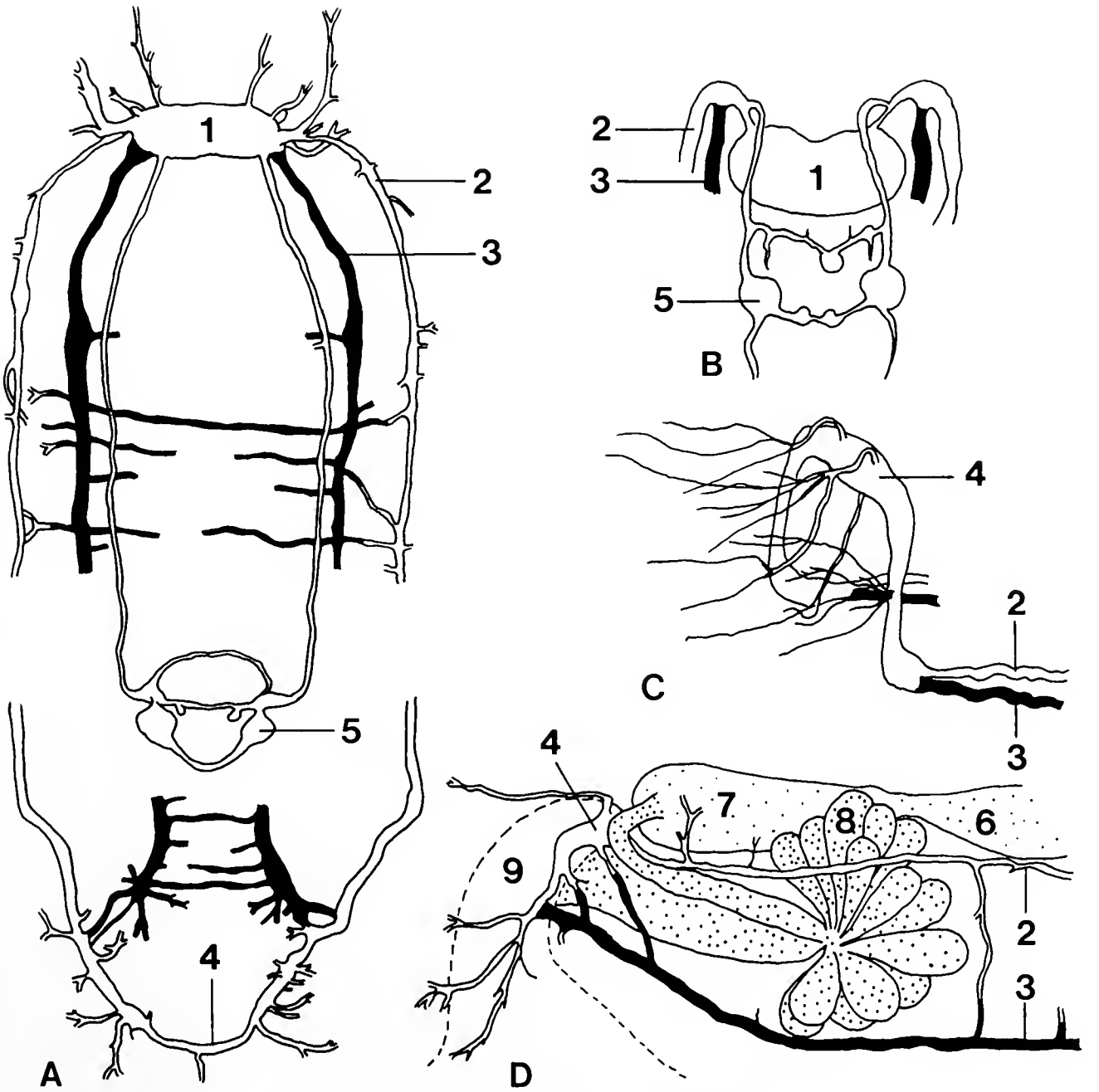

Figure 9. Nervous system and reproductive system in a neomenioid, *Strophomenia scandens* (A, D) and nervous system in a chaetoderm, *Limifossor talpoideus* (B, C). (A) Lateral (= pleural, visceral) cord with its origin in the cerebral ganglion separate from the origin of the ventral (= pedal) cord. Lateral and ventral cords remain separate posteriorly (after Heath, 1904, pl. 27, fig. 2). (B) Anterior end; the lateral and ventral cord have a single origin in the cerebral ganglion (after Heath, 1911, pl. 10, fig. 8). (C) Posterior end; the ventral cord runs close to the lateral cord and fuses with it. The suprarectal commissure is ganglionated (after Heath, 1905, pl. 43, fig. 18). (D) Posterior end; the lateral and ventral cords are well separated, with the separation maintained throughout. The gonad empties into the pericardium, which is shown in fine stippling. The U-shaped gametoduct, with a many-lobed seminal receptacle, is shown in coarse stippling; it runs from the posterior end of the pericardium to the mantle cavity, indicated by dashed lines (after Heath, 1904, pl. 27, fig. 6). 1 cerebral ganglion, 2 lateral cord, 3 pedal cord, 4 suprarectal ganglion/commissure, 5 buccal ganglion, 6 gonad, 7 pericardium, 8 seminal receptacle, 9 mantle cavity.

convergent apomorphies in the two taxa. When this character and those mentioned above are considered together, the Aplacophora clearly emerge as a monophyletic taxon.

Chaetodermomorpha, derived Aplacophorans

Neomeniomorpha are more similar than Chaetodermomorpha to the outgroup, the Polyplacophora, in nervous system (Fig. 9A, D), form of epidermal papillae (Fig. 6D, E), presence of anterior pedal glands (present only in the larvae of chitons) (Figs. 4, 6B), presence of paired pharyngeal glands, serial lateroventral musculature (Fig. 8B), and inequality of height and width dimensions. Several autapomorphies indicate that the burrowing Chaetodermomorpha have been derived from a creeping neomenioid-like ancestor. Criteria for considering a structure to be apomorphic are fusion or elaboration.

Changes in the nervous system are pronounced. In chaetoderms the lateral and ventral cord on each side have a single origin from the cerebral ganglion, whereas in nearly all neomenioids lateral and ventral cords have separate origins (Fig. 9A, B). In chaetoderms, the lateral and ventral cords on each side soon run close to each other, finally fusing into a single cord anterior to the suprarectal ganglion (Fig. 9C). In neomenioids, the cords remain apart and are well separated from each other (Fig. 9A, D). There are few commissures between the ventral cords in chaetoderms, and many in neomenioids. In chaetoderms, the suprarectal commissure and precerebral ganglia are larger and more swollen than in neomenioids.

Related to the loss of the ventral cord commissures, chaetoderms have entirely lost the foot and anterior pedal glands. The homology of mucous glands of the oral shield with pedal glands, proposed by S. Hoffman (1949), does not hold in TEM studies (Scheltema *et al.*, in press, Fig. 9A). In some species of *Scutopus* and *Psilodens*, ventral fusion of the mantle is marked by a longitudinal furrow between the spicules (Salvini-Plawen, 1968b; author's unpub. data).

The gut of chaetoderms is modified from the simple combined stomach-digestive gland midgut of neomenioids to a separate stomach and blind digestive gland. In its most derived state in Chaetodermatidae, there is a gastric shield and style sac with a mucoid rod (Scheltema, 1978; Salvini-Plawen, 1981b).

The serial lateroventral musculature of neomenioids (Fig. 8B) is lost in chaetoderms, although a few vestigial anterior bundles have been reported in a species of *Scutopus* (Salvini-Plawen, 1985). Body form in chaetoderms is circular in cross-section; in neomenioids there is usually a small but measurable difference between height and width. The circulatory system is somewhat better defined in chaetoderms than in neomenioids, with anterior and posterior vertical septa defining hemocoelic sinuses, and with an often thick-walled aorta and aortal bulb (Scheltema, 1973) (Fig. 5A). Finally, the chaetoderm oral shield represents a specialized cuticular structure.

The autapomorphies of Chaetodermomorpha all seem to be related to their form of locomotion—burrowing in muds and silts—and feeding habits, either as carnivores on small benthic organisms, or as detritivores. Autapomorphies also exist in the Neomeniomorpha, particularly the sensory vestibule and rather complicated reproductive system with accompanying loss of mantle cavity ctenidia, but specializations of the Chaetodermomorpha mark them as the more derived of the two taxa.

Relationship of Aplacophora and Polyplacophora

Aplacophora and Polyplacophora are here considered to be sister taxa, the Aculifera, on the basis of shared characters of nervous system, spicules, and epidermal papillae. An attempt is made to determine the polarities of these characters, and other anatomical similarities are noted.

Nervous system

Aplacophora, Polyplacophora, and the monoplacophoran Tryblidiacea *Neopilina* and *Vema* all have a fully developed tetraneury, with paired lateral and pedal nerve cords arising from a cerebral commissure or ganglia and a circumoral or circumesophageal nerve ring. In the monoplacophorans, both cords are joined posteriorly ventral to the rectum, whereas in Aplacophora (Fig. 9) and Polyplacophora, only the lateral cords are joined, and they unite above the rectum in a commissure (chitons) or ganglion (aplacophorans). There is only a single cross-pedal commissure in the monoplacophorans and numerous ones in chitons and neomenioid aplacophorans.

What is the polarity of these two plans, both of which are plesiomorphic to more specialized nervous systems in other mollusks? Obvious outgroups for comparison, Annelida, Echiura, Nemertini, and Sipuncula, appear to have a reduced nervous system and offer no clues. In Annelida there is only a paired ventral cord, except for a secondarily derived tetraneury in Amphinomidae (Gustafson, 1930); in Nemertini there is a pair of lateral cords joined either above or below the rectum; in Echiura, there is a single ventral cord; and in sipunculans there is also a single ventral cord which is paired in the larval pelagosphera of *Phascolosoma agassizii* (Rice, 1973). One might surmise that *Neopilina*, a deep-sea deposit or xenophyophore feeder (Tendal, 1985), is less mobile than either aplacophorans or polyplacophorans and has retained a simpler nervous system, and the aplacophoran-polyplacophoran system is more specialized (derived) owing to habitat (chitons) or to carnivory (aplacophorans). Of course, a secondary loss and shifting of nerve elements in the monoplacophorans might also be considered, and Wingstrand

(1985) and Salvini-Plawen (1972) suggest that the subrectal commissure is an apomorphy. Whichever interpretation is correct, one can say that monoplacophoran and aplacophoran-polyplacophoran nervous systems are each apomorphic to some unknown ancestral state, and the suprarectal ganglion or commissure of the Aplacophora-Polyplacophora serves to relate them phylogenetically and set them apart from the Monoplacophora.

Spicule formation

Spicule formation in aplacophorans and polyplacophorans has most recently been investigated by Haas (1981) (Fig. 10). Spicules in both taxa are aragonite and formed extracellularly within an invagination of a single basal cell, which secretes calcium carbonate within a crystallization chamber sealed by neighboring cells (Scheltema *et al.*, in press, fig. 6D). In chitons, megaspines are formed from a proliferation of the basal cell and do not occur in aplacophorans.

Spicules of the Aculifera are usually considered to be a plesiomorphic state of calcium carbonate formation within Mollusca, since both spines and shell occur in chitons and only spines occur in Aplacophora, both being "primitive" groups in the general sense. However, Monoplacophora, likewise considered primitive, have no spines.

The dorsal, calcium-carbonate-secreting epidermis of Mollusca, in combination with a ventral locomotary surface, is probably an apomorphy. However, the shell-bearing Brachiopoda are rooted with the Mollusca-Annelida group by RNA sequencing (Field *et al.*, 1988), and some boring Sipuncula have calcium carbonate deposits at the dorsal anterior end of the trunk (Rice, 1969). Further comparative work needs to be done to compare calcium carbonate secretion among the Eutrochozoa before homology can be assumed.

It cannot be concluded from outgroup comparison that spicules and shell are homologous structures (and the argument will be made further on that they are not), or that either is the plesiomorphic state. It can be concluded, however, that because of the way in which they are formed, spicules of Aplacophora and Polyplacophora are homologous and can be construed as a synapomorphy.

Epidermal papillae

The epidermis of both chitons and aplacophorans are liberally supplied with secretory papillae (Fig. 6D, E). In chitons, papillae are homologous with aesthetes (Fischer *et al.*, 1980). Although homology with other conchiferan shell-penetrating structures has been suggested (Salvini-Plawen, 1985), the homology was considered spurious by Wingstrand, who reviewed the literature on the subject (1985, pp. 58–59). The presence of these papillae is considered here to be an apomorphy of the Aplacophora-Polyplacophora.

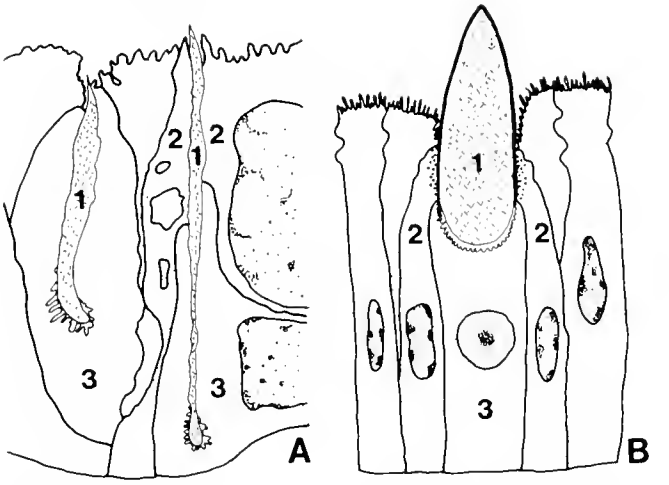

Figure 10. Spicule formation in (A) Aplacophora and (B) Polyplacophora (after Haas, 1981, figs. 6, 12). The spicule is formed within an invagination of a basal cell which secretes $CaCO_3$. The crystallization chamber is sealed by a ring of neighboring cells, which in Polyplacophora produce a pellicle around the spicule. 1 spicule, 2 neighboring cell, 3 $CaCO_3$-secreting basal cell.

Reduced serial replication

Compared to Monoplacophora, there is less serial replication in both Polyplacophora and Aplacophora, but both have greater serial replication than other mollusks. Serial replication appears as regular, lateroventral musculature in Neomeniomorpha (Fig. 8B) and as 8-fold repetition of muscles and shell plates in chitons.

Other anatomical homologies

Aplacophorans and polyplacophorans share certain other anatomical structures that are probably homologous, but they may be plesiomorphies of the Mollusca. Dorsal paired gonads, becoming fused during ontogeny in chitons and most Chaetodermomorpha, lie like sacs more or less free above the gut and digestive gland in the dorsal hemocoel. In *Neopilina*, the gonad is ventral to the digestive system (Lemche and Wingstrand, 1959), and in many other Mollusca the gonad is intermingled closely with lobes of the digestive gland. The circulatory system in both groups is extremely open with posterior paired auricles and a ventricle, a dorsal aorta leading to the head (lacking in many Neomeniomorpha), and open sinuses, the latter more profuse in chitons.

Taken together, the above reasons are sufficient for concluding that Aplacophora and Polyplacophora belong together in a single taxon, the Aculifera, which is therefore a clade, and not a grade.

Aculifera as the Sister Taxon of the Conchifera

Chitons provide evidence that Aculifera are separate from their sister group, the Conchifera. The evidence is based on shell ontogeny, shell structure, and perhaps molecular data.

Shell ontogeny

In Conchifera, the shell originates within an ectodermal invagination, the shell-field invagination, which is covered by an organic pellicle (Eyster and Morse, 1984) (Fig. 11). In *Aeolidia papillosa*, long cytoplasmic processes overlie the pellicle. In chitons, there is no shell field invagination, and shell plate anlagen are deposited within transverse depressions which are sealed, not by a pellicle, but by long, overlapping microvilli that lie beneath a gelatinous mucoid substance (Kniprath, 1980; Haas *et al.*, 1980; Haas, 1981; see Scheltema, 1988, for a more complete discussion). Furthermore, in healthy larvae, shell is not deposited as separate granules, as illustrated by Kowalevsky (1883), but as uninterrupted rods (Kniprath, 1980). This fact conflicts with the hypothesis that chiton shell arose from fused spicules (Salvini-Plawen, 1985, 1990).

Shell structure

The crystallography of chiton shell has been said to indicate an autapomorphy of chitons by Haas (1976), who found that "The . . . c-axis of [the] hypostracum lies in the bisectrix of the crystalline fibers. The whole complex acts crystallographically as a single crystal" (p. 392). If this crystallographic orientation is correct, then no homology exists between polyplacophoran and conchiferan shell. Further differences are a lack of true periostracum in chitons (although Haas [1981] has demonstrated a thin cuticle overlying the shell plates) and a lack of a nacreous layer (for further discussion see Wingstrand, 1985; and Scheltema, 1988). On the other hand, the shell of the tryblidiacean Monoplacophora does not differ from other primitive conchiferan shells (Lemche and Wingstrand, 1959).

Molecular evidence

The evolutionary tree of 18S rRNA has three branches for three classes of mollusks—a nudibranch, two species of clam, and a chiton. This trifurcation of mollusks also appears in Lake's (1990) re-analysis of the data. Further molecular data for all molluscan classes should resolve the branching, but there is a hint of molecular distance between chitons and the two other classes analyzed.

Evidence for Progenesis in Aplacophora

A vermiform body is a character that could have been added rapidly by a small change in a regulatory gene or

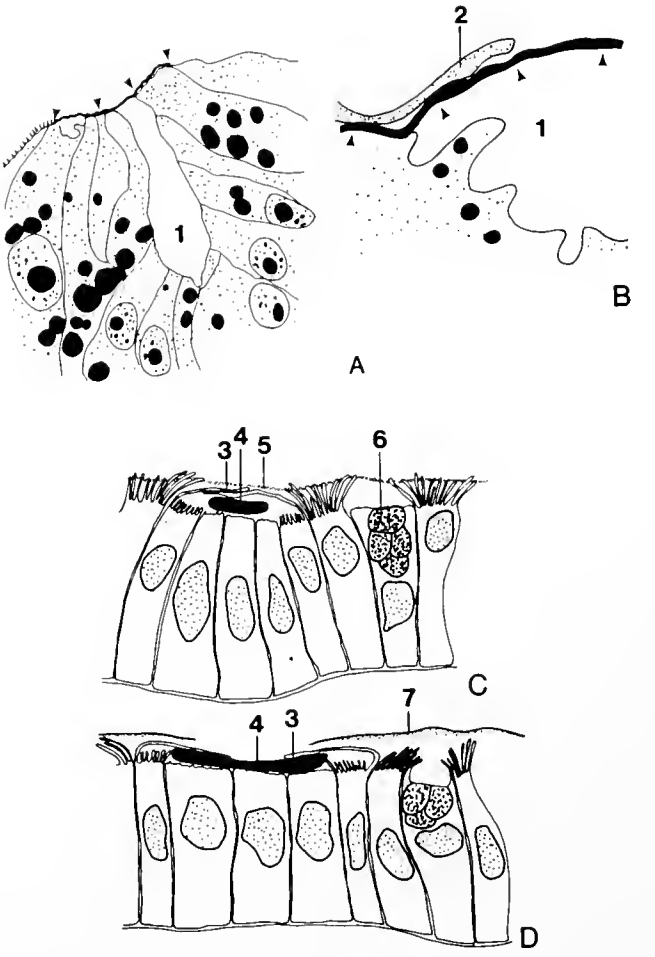

Figure 11. Shell deposition in larvae of Conchifera and Aculifera. (A, B) Gastropod, *Aolidia papillosa*. An organic pellicle (arrowheads) covers the lumen of the shell field invagination; a cytoplasmic extension shown in B seals the edge of the pellicle (after Eyster and Morse, 1984, figs. 1, 2; from Scheltema, 1988, fig. 4). (C, D) Polyplacophoran, *Ischnochiton rissoi*. The shell plate is first secreted beneath microvilli (stragulum) which are covered by a layer of mucus (C); later (D) the microvillar processes have pulled apart and a cuticle begins to form (after Kniprath, 1980, fig. 5, from Scheltema, 1988, fig. 4). Haas (1981) illustrated a similar process except for showing that cuticle covered the stragulum before $CaCO_3$ deposition. 1 shell field invagination, 2 cytoplasmic extension, 3 microvillar process (stragulum), 4 calcium carbonate of shell plate, 5 mucous layer, 6 ?mucous cell, 7 cuticle.

in timing of cell assembly early in the ontogeny of an aculiferan mollusk (for mechanisms and examples see Raff and Kaufman, 1983; McKinney and McNamara, 1991). In the embryological development of the chiton *Lepidopleurus asellus*, swimming larvae are first oval and then become secondarily flattened and sink to the bottom (Christiansen, 1954). Even with development of the foot, chiton larvae remain ovoid for a time (Heath, 1899, Fig. 52; Eernisse, 1988, Fig. 7). One can imagine that larvae of some aculiferan, not necessarily a chiton, might not

have become dorsoventrally flattened through a small change in gene regulation and the worm-like shape arose.

The change to a vermiform shape could have occurred either early in the evolution of Mollusca or late. Recent phylogenies presume that a vermiform shape evolved as an early offshoot of the Mollusca, placing Aplacophora closest to the stem form, either as a monophyletic clade (Scheltema, 1988; Wingstrand, 1985), or as two separate clades, with the Chaetodermomorpha evolving first as the sister-group to all extant Mollusca (Salvini-Plawen, 1972, 1985). Serial replication thus was seen to be an apomorphy. If Aplacophora are closest to the molluscan ancestor, then the imperatives following from that phylogenetic construct fit poorly with the arguments given above, that is: (1) Aplacophora and Polyplacophora are a clade; (2) shell is not formed by fusion of spicules; and (3) chiton shell is not homologous to conchiferan shell. The question of when serial replication evolved in mollusks becomes critical, for it is either a plesiomorphy of mollusks, or not.

Polyplacophora, belonging to Aculifera, have some structures homologous with Monoplacophora, belonging to Conchifera, that are not shared with the Aplacophora (Wingstrand, 1985): radula dentition and radular apparatus including musculature; 8-serial pedal retractors; preoral unpaired fold, or velum; perhaps the heart with two pairs of atria; and coiled intestine. Wingstrand noted that some of these structures "could be plesiomorphic, *i.e.*, could have been present already in some Aplacophoran ancestors" (1985, p. 74), but considered that the radula and radular apparatus, in particular the paired, hollow radula vesicles, are synapomorphies. It was not then known that paired radular vesicles are also present in some neomenioids (Fig. 8D). Here, structures argued to be apomorphic by Wingstrand are considered plesiomorphic with exception of the coiled gut, a character widely convergent among mollusks. Thus, serial replication is here considered a plesiomorphy of Mollusca.

The possibility that a worm shape was acquired by aplacophorans late in aculiferan evolution leads to a wholly different concept of molluscan phylogeny. It calls for progenesis in Aplacophora, wherein nonserial but plesiomorphic-appearing anatomical characters are retained. The following evidence supports the hypothesis that Aplacophora are progenetic; *i.e.*, that they have retained ancestral juvenile characters in adult form through acceleration of sexual maturation (Gould, 1977).

(1) If narrowing of the body by acquisition of a worm shape arose early in aculiferan evolution without progenesis, then this process should be reflected somehow in the internal anatomy, and the more elongate (that is, narrower) the shape, the more pronounced should the internal changes become. Within the Neomeniomorpha, the least derived aplacophoran taxon, there is little organizational difference between short and elongate species in anterior and posterior ends or in musculature. Elongation of external form is accompanied internally by a simple lengthening of the gonad and midgut (Fig. 7D, E). The situation in the more derived chaetoderms differs and does not serve the argument.

A comparison can be made to *Cryptoplax*, a genus of chiton with a derived worm-like shape. In *Cryptoplax* there are at least four specializations of adult characters: (a) the mantle is very thick relative to internal body diameter; (b) there is loss of circulatory pathways; (c) there is loss of shell and shell musculature; and (d) the intestinal tract is remarkably long and complicated, turning back on itself in numerous spirals (Wettstein, 1904; H. Hoffmann, 1929-30). Furthermore, an analysis of the allometric equation defining shape in 408 chiton species in 39 genera indicated great uniformity in allometry, except in the carnivorous *Placiphorella* and in genera of Cryptoplacidae (Watters, 1991). Species of Cryptoplacidae, except those in the most primitive genus, are allometrically similar to each other but have shifted markedly from the allometry of other chitons. Although no allometric studies have been made of neomenioids, the extremes in vermiformity (Fig. 7D, E) do not predict uniformity. Thus there may be an ontogenetic difference in the evolutionary pathway to a worm-like shape taken by the two aculiferan taxa. Progenesis, an intrinsic process, is hypothesized for Aplacophora, and selection working on structural genes, an extrinsic process, for *Cryptoplax*.

(2) Progenesis results in early reproduction (Gould, 1977). One abundant northwestern Atlantic aplacophoran species living at 2000 m, *Prochaetoderma yongei*, is known to mature within one year, a remarkably rapid rate, given the ambient temperature (~3°C) and in comparison with other cold-water mollusks. *P. yongei* is interpreted as being an opportunistic species (Scheltema, 1987), but since it is the only aplacophoran for which even part of the life history is known, one cannot be sure that early reproduction is the usual case in Aplacophora.

(3) Progenesis results in a reduced body size (Gould, 1977), but the size of the nearest ancestor to Aplacophora is, of course, unknown. Most neomenioids are usually less than 5 mm long, and one can only infer from the generally larger size of chitons that the first ancestral aplacophoran was already small. Like some other deep-sea taxa, such as protobranch bivalves (Sanders and Allen, 1973) and isopods (Hessler *et al.*, 1979), aplacophorans have evolved primarily in the deep sea, where they reach their greatest diversity (Scheltema, 1990). Food is limiting there, and small body size of macrobenthic organisms is the norm (Monniot and Monniot, 1978; Allen, 1983; Soetaert and Heip, 1989). Large neomenioids do exist in the deep sea, but they are usually either specialized (giant *Neomenia* species: Baba, 1975; Kaiser, 1976) or live in environments where there is high productivity (*e.g.*, high

latitudes: *Proneomenia sluiteri*, Derjugin, 1915, 1928). Large body size in Aplacophora is probably an apomorphic character because it is found scattered amongst unrelated families, some of which have derived characters such as loss of radula or a thick dermis.

(4) Certain structures in Aplacophora are less developed than homologous structures in Polyplacophora or other mollusks. (a) The organic composition of the cuticle is simpler than in chitons (Beedham and Trueman, 1968). (b) The radula in its plesiomorphic state in neomenioids has only two teeth per row (distichous), a condition found in the early ontogeny of several gastropods (Kerth, 1983; Scheltema, 1988; Scheltema *et al.*, 1989). (c) The aplacophoran mantle cavity, located ventroposterior to posterior, is small, serving as little more than a cloaca (Fig. 7A, D). (d) Both neomenioids and chaetoderms lack kidneys. (e) The foot is developed only as a ciliated ridge without musculature in neomenioids (Fig. 6A). (f) Gonads and pericardium are united in aplacophorans, reflecting the early ontogenic state in chitons, where the gonad originates as an anlage of the pericardium (Hammarsten and Runnström, 1925) (Figs. 5A, 6A, 9D). (g) The gut in neomenioids is simple, with a united stomach and digestive gland; the digestive gland is separate from the stomach in other mollusks.

(5) Aplacophora have retained a structure found in chitons only as larvae. The anterior pedal glands are large and specialized in neomenioids (Fig. 6B, C), but are lost soon after metamorphosis in chitons, where they serve only for early postmetamorphic attachment (Heath, 1899) (Fig. 4B).

Although progenesis results in primitive-appearing structures, they are actually derived. Therefore, some process within the Aculifera should be primitive in the Polyplacophora but derived in the progenetic Aplacophora. Such seems to be the case in early embryological development. Freeman and Lundelius (1992) have proposed that, among the spiralian coelomates Mollusca, Annelida, Sipuncula and Echiura, two mechanisms determine which blastomere is specified as the D quadrant. They hypothesized that the primitive mechanism for D quadrant specification is by induction after the fifth cleavage, when one of the four macromeres has maximum contact with the micromeres. The derived mechanism is by segregation of the cytoplasm into one macromere, which is then specified as the D quadrant; it occurs by the second cleavage. In Polyplacophora, macromeres cleave equally and the D quadrant is specified by induction, the primitive mechanism. But in the cleaving egg of the neomenioid *Epimenia*, a polar body is formed and therefore macromeres of unequal size; thus the D quadrant is specified by cytoplasmic determinants, the derived mechanism (Baba, 1951; Freeman and Lundelius, 1992).

The evidence for progenesis presented here argues for heterochrony in the Aplacophora, but this idea cannot be tested either against fossils, which are unknown, or against a more complete phyletic lineage, as has been done for progenetic meiofaunal forms (Westheide, 1987) and deep-sea tunicates (Monniot and Monniot, 1978). When the early embryological development of aplacophorans is better known, and with further intrataxon comparative studies, the validity of the hypothesis may be clarified.

Phylogeny of the Mollusca

The phylogeny represented in Figure 12 proposes a coelomate molluscan ancestor with serial replication; two separate evolutionary molluscan lineages, the Conchifera and the Aculifera, based on synapomorphies of differences in $CaCO_3$ deposits; and morphologies arising from progenesis in the Aplacophora.

The molluscan ancestor is considered to have had the following plesiomorphies: (1) extracellular $CaCO_3$ deposition by the dorsal epidermis (Mollusca generally); (2) serial replication, probably originally 8-fold (Monoplacophora, Polyplacophora, *Nautilus*, neomenioids, some bivalves); (3) coelom from the 4d cell, paired pericardial cavities (in Monoplacophora, and fused but large in Aplacophora and Polyplacophora); (4) radula, radular apparatus with hollow radula vesicles (Polyplacophora, Monoplacophora, Aplacophora, Fig. 8D); (5) nervous system poorly ganglionated, with cerebral ganglia and commissure, circumenteric ring, and paired lateral and pedal cords with cross-commissures and posterior connection (Monoplacophora in part, Aplacophora and Polyplacophora); (6) dorsoventrally flattened, small size (Cambrian Mollusca: Runnegar and Pojeta, 1985; Haszprunar, 1992; but note that the Cambrian fossil halkierids and *Wiwaxia*, perhaps near relatives of mollusks, are centimeters in length [Conway Morris, 1985; Conway Morris and Peel, 1990]); (7) dorsal cuticle (Aplacophora, Polyplacophora); (8) ventral ciliated locomotory sole (Mollusca generally); (9) head separate from the locomotory sole and with cerebral ganglia (Mollusca generally); (10) a groove between the dorsal and ventral surfaces, the future mantle cavity (Mollusca generally); (11) pre-oral fold; (12) the presence of podocytes in pericardial tissue (mollusks generally); (13) ductless anterior pedal mucous glands (as a glandular epithelium in Monoplacophora; Lemche and Wingstrand, 1959); (14) a one-way gut with mouth, anus, large digestive gland poorly differentiated from stomach (Neomeniomorpha, Monoplacophora); (15) paired pharyngeal diverticula; (16) poorly defined circulatory system; and (17) gonad and pericardium joined at least during ontogeny (Mollusca generally).

The phylogeny presented in Figure 12 requires that the original calcium carbonate deposition in mollusks was

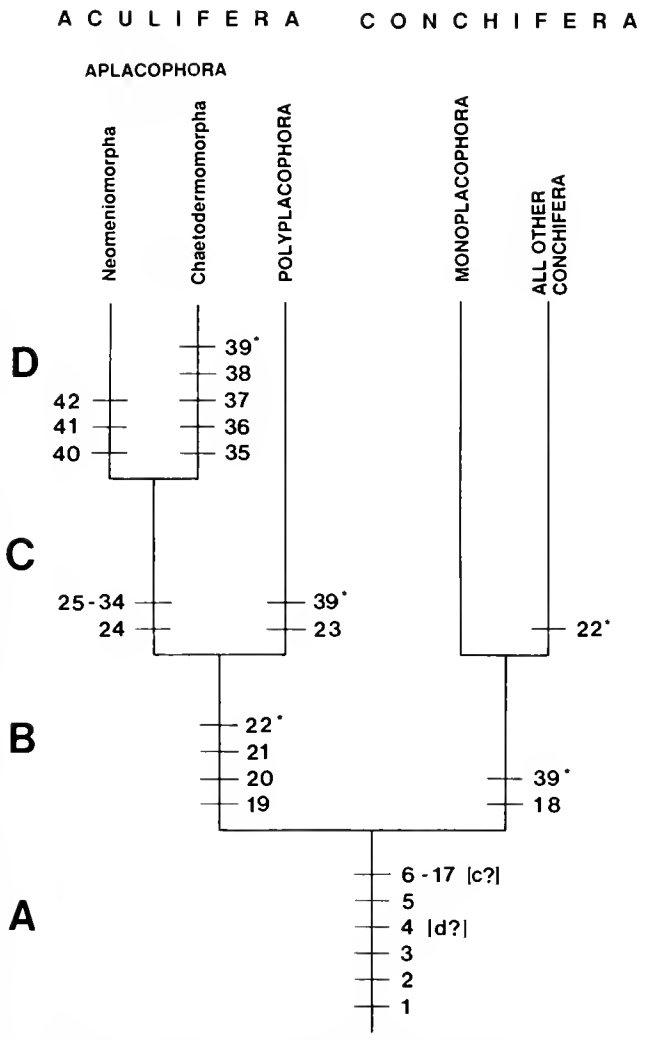

Figure 12. Proposed phylogeny of extant "primitive" Mollusca. (A) Apomorphies of Mollusca: 1 extracellular $CaCO_3$ deposition by dorsal epidermis; 2 eight-fold serial replication; 3 paired coelom, including pericardium; 4 radula; 5 poorly ganglionated tetraneury; 6 small size, dorsoventrally flattened; 7 dorsal cuticle; 8 ventral locomotory sole; 9 head separate from sole; 10 groove between dorsal and ventral surfaces; 11 pre-oral fold; 12 nonsegmented pericardium, pericardial tissue with podocytes; 13 ductless anterior pedal gland; 14 poorly differentiated stomach/digestive gland (model: *Neopilina*); 15 paired pharyngeal diverticula; 16 poorly defined circulatory system; 17 joined gonad/pericardium during early ontogeny. (B) Separation of Conchifera and Aculifera: 18 calcareous shell; 19 spicules; 20 epidermal papillae; 21 suprarectal ganglion/commissure; 22 reduced serial replication and fused pericardium. (C) Separation of Polyplacophora and Aplacophora (24–31 the result of progenesis): 23 eight shell plates; 24 worm shape; 25 reduced foot; 26 reduced mantle cavity; 27 joined gonad/pericardium; 28 kidneys absent; 29 chemically simple cuticle; 30 serial lateroventral musculature; 31 distichous radula; 32 U-shaped gametoducts; 33 ganglionated nervous system; 34 dorsoterminal sense organ. (D) Separation of Chaetodermomorpha and Neomeniomorpha: 35 ventrally fused cuticle, foot lacking; 36 oral shield; 37 fused, reduced nervous system; 38 serial replication absent; 39 stomach separate from digestive gland; 40 large anterior pedal gland; 41 elaborated reproductive system; 42 ctenidia absent. * = convergent morphologies; c? = presence of ctenidia questionable; d? = radula questionably docoglossate.

neither as spicules nor as shell. $CaCO_3$ was first deposited, perhaps, as granules within a dorsal cuticle, which was thereby stiffened. Such a reinforced cuticle could act as the antagonist to the dorsoventral pedal musculature. During chiton ontogeny, the pedal musculature develops earlier than the shell plates (Hammarsten and Runnström, 1925). One can speculate from this fact that, perhaps, the various forms of shell and spicules among mollusks have resulted from selection for different modes of locomotion in various habitats, rather than selection just for protection.

In terms of $CaCO_3$ secretion among phyla, the important synapomorphy for mollusks, which sets them off from other spiralian coelomates, is the locomotary sole in combination with a cuticle- and $CaCO_3$-secreting dorsal epidermis. Certain rock-boring sipunculans also secrete $CaCO_3$ dorsally, forming a plug for their tubes (Rice, 1969), and Brachiopoda, which fall in with spiralian coelomates in molecular analysis, also have calcium carbonate shells. However, animals in neither of these phyla have the combination of dorsally produced $CaCO_3$ and a ventral locomotary surface unique to mollusks.

It is hypothesized that after, or as, Conchifera diverged from the stem line, the mantle deepened and gills developed. Serial replication was retained in Monoplacophora but lost in the rest of the Conchifera, except for serial pedal musculature in some taxa and the renal system in cephalopods. Aculifera may have evolved either at the same time as Conchifera or later. By the Upper Cambrian or Lower Ordovician, the serial shell plates of Polyplacophora had evolved (Runnegar and Pojeta, 1985). This event was preceded by the loss of serial replication other than lateroventral muscles and perhaps by an increase in size. In a separate evolutionary event of progenesis, the Aplacophora evolved with probable reduction in size, further loss of serial replication, loss of nephridia, retention of gonad-pericardial connection, and acquisition of a worm shape with concomitant reduction of the foot. Chaetodermomorpha were derived from the neomenioid-like stem with complete loss of foot, reduction and fusion of the nervous system, and specializations of the gut.

This hypothesized phylogeny does not call for an evolutionary process in which $CaCO_3$ deposits, or the cells that produce them, become fused. Furthermore, it should allow some of the Early Cambrian sclerite-bearing forms now coming to light, such as the shell-bearing, articulated halkieriid described recently from the Lower Cambrian of Greenland (Conway Morris and Peel, 1990), to find their place in relation to the extant Mollusca.

In this phylogeny, the Monoplacophora with clear serial replication are not evolved after Aplacophora, and molluscan serial replication is considered to be a plesiomorphy. As Wingstrand (1985) pointed out, it is difficult to imagine that serial replication evolved after the shell. The

careful and original anatomical analysis of Wingstrand showing close affinities of the monoplacophoran Tryblidiacea and Polyplacophora are upheld here as retained plesiomorphies of the common ancestor. Whether Pruvot's neomenioid larva with its supposed seven rows of spicules actually exists does not change the argument (see Salvini-Plawen, 1972, 1981a, 1985; Scheltema, 1988 for discussions and figures of the larva). Manuscript drawings of *Chaetoderma nitidulum* larvae made by G. Gustafson show eight rows of spicules for this taxon as well. If further observations on aplacophoran development prove that serial rows of spicules do exist, the larva still would not necessarily reflect progressive evolution from spicules to fused shell plate formation, but more likely would indicate a breakdown of plate formation similar to the breakdown of larval chiton shell plates caused experimentally by Kniprath (1980) (See also Scheltema, 1988).

Age of the Aplacophora

If known fossils reflect the actual time of evolutionary events, then the evolution of Polyplacophora late in the Cambrian (Runnegar and Pojeta, 1985) from a continuing line of aculiferous creatures was probable, with increased size and muscles being the determinants of shell plates rather than vice versa (see Hammarsten and Runnström, 1925, p. 276, for ontogenetic development of muscle before shell). Aplacophora, with their highly derived shape and paedomorphic internal organization, give information about the primitive conditions of mollusks without being themselves primitive. A Late Cambrian-Early Ordovician origin from an aculiferan form with a developed mantle groove and posterior mantle cavity is postulated for Aplacophora, with the 8-fold dorsoventral muscles rearranged in neomenioids into a series of indeterminate number.

Cautionary Notes on Convergences

Digestive system

The molluscan gut appears to have evolved similar morphologies more than once (Fig. 12, no. 39). Evidence for convergence lies in presence of the style sac and gastric shield, found in a number of molluscan classes. In the aplacophoran family Chaetodermatidae, one of the most derived of the chaetoderm groups based on radula morphology (Scheltema, 1972, 1981), the gut is the most complicated among chaetoderms, with a gastric shield and a mucoid rod in a style sac (Scheltema, 1978; Salvini-Plawen, 1981b). The polarity of a less to a more complicated gut configuration within the chaetoderms is clear (Scheltema, 1981). Thus, the presence of a style sac and gastric shield is convergent among Mollusca.

Metamerism

Reduction of serial replication (Fig. 12, no. 22) is hypothesized for several molluscan classes—Cephalopoda, Bivalvia, Polyplacophora, and Aplacophora. The evidence from morphology, ontogeny, and molecular analysis seems not to favor the hypothesis that replication originated in annelids. If the altogether unsegmented Sipuncula are sister taxon of the mollusks, then arguments that the molluscan coelom is the result of a reduced annelid-like segmented coelom are not convincing.

Evidence presented here could be interpreted in three ways (Fig. 13, s^1–s^4). (1) A nonsegmented ancestor that had serial replication of organs and a coelom lies at the base of the lineage giving rise to Eutrochozoa (s^1). (2) The eutrochozoan ancestor had no serial replication, which

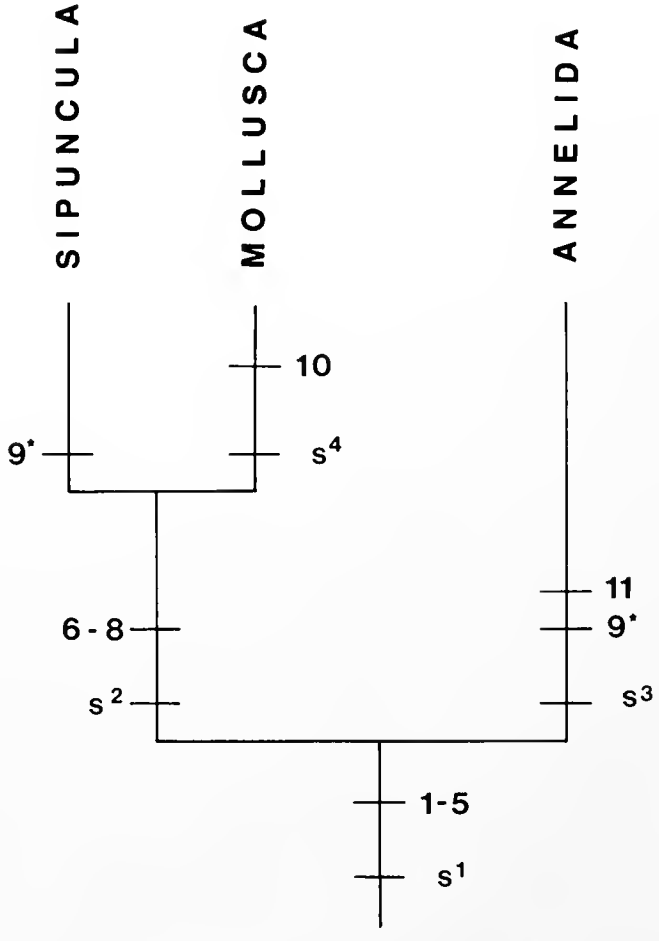

Figure 13. Phylogenetic relationship among Sipuncula, Mollusca, and Annelida. 1 spiral cleavage; 2 paired coelom originating from two teloblasts derived from 4d; 3 trochophore larva (?); 4 tetraneury; 5 ciliated creeping sole; 6 molluscan cross; 7 ventral, cuticular, pharyngeal (stomadeal), protrusible invagination and attendant musculature; 8 anterior pedal gland; 9 fused nerve cords; 10 reduced coelom; 11 loss of creeping sole. s = serial replication: s^1 symplesiomorphic for all three taxa, but lost in Sipuncula; s^2 symplesiomorphic for Sipuncula and Mollusca, but lost in Sipuncula, and convergent with s^3 as metamerism in annelids; s^3 metamerism plesiomorphic for Annelida, convergent with either s^2 or s^4; s^4 plesiomorphic for Mollusca, convergent with s^3. * = convergent morphologies.

later arose de novo twice: once in the stem form leading to mollusks and sipunculans (s^2), which was lost in the latter, and secondly in the ancestral annelid as metamerism (s^3). (3) Molluscan 8-fold serial replication (s^4) evolved after the stem form that gave rise to Sipuncula and Mollusca; and annelidan metamery (s^3) [as in (2)], arose as an unrelated evolutionary event. The first interpretation is perhaps closest to what may actually have occurred and seems the most parsimonious explanation.

Differences in the coelom among eutrochozoan groups can be related to locomotion, a theme emphasized—correctly, I believe—by Salvini-Plawen (*e.g.*, 1972, 1985). Locomotion among Eutrochozoa is most rapid in annelids and mollusks. Serial pedal musculature is related to a creeping locomotion and is the most conservative serial structure in mollusks, present as a plesiomorphy in Monoplacophora, Polyplacophora, Aplacophora, and (much reduced) Pelecypoda and perhaps the neritid Gastropoda. In Annelida, coelom and muscle have combined in the perfection of a hydraulic locomotion (Clark, 1964). Perhaps, then, a re-examination of the relationship of muscles and coelom during ontogeny would be a useful exercise in providing insights into understanding the development of metamerism in Eutrochozoa. For instance, in at least some Annelida, ectodermal segmentation of the three anterior segments precedes segmentation of mesoderm (Anderson, 1973, pp. 36–37).

Radula

Wingstrand (1985) gave a detailed description of the radular apparatus in Polyplacophora and Monoplacophora, demonstrating their great similarity, especially the docoglossate radula and radula vesicles. There are three possibilities: such a radula is a molluscan plesiomorphy; it is an apomorphy of Polyplacophora and Monoplacophora; or it is convergent.

Evidence from Aplacophora and ontogeny of some Gastropoda suggests that the plesiomorphic radula in mollusks was distichous (Kerth, 1983; Scheltema *et al.*, 1989). An outgroup for comparison is the Cambrian sclerite-bearing *Wiwaxia* (Conway Morris, 1985) with two or three rows of teeth which appear much like the plesiomorphic radula in Aplacophora. The phylogenetic position of *Wiwaxia,* however, remains enigmatic, considered either to be close to mollusks (Conway Morris, 1985) or to be an annelid (Butterfield, 1990). If the plesiomorphic radula is distichous, then the docoglossate radula is convergent in Polyplacophora, Monoplacophora, and patellacean Gastropoda. If the docoglossate radula is a molluscan plesiomorphy, it is difficult to imagine how it functioned in a small Cambrian mollusk and what evolutionary steps would be necessary to account for all other molluscan radulae.

The strongest evidence given by Wingstrand (1985) for monophyly of polyplacophorans and conchiferans is presence of a pair of hollow, presumably liquid-filled radula vesicles found at that time only in Polyplacophora and Monoplacophora. None had been reported in Aplacophora. However, a re-examination of the neomenioid *Helicoradomenia juani* and other species in the genus, which have a plesiomorphic aplacophoran radula, has led me to conjecture that paired, elongate, hollow vesicles present in this genus are a homolog to the radula vesicles in Polyplacophora and Monoplacophora (Fig. 8D). Therefore these vesicles are a molluscan plesiomorphy. However, further study of the aplacophoran radula and its apparatus is needed.

Larval forms

The phylogenetic significance of larval forms in Spiralia is not addressed here. There is still no agreement on whether a pelagic organism gave rise to benthic forms (*e.g.*, Nielsen and Norrevang, 1985), or vice versa, and whether the trochophore larva arose once or several times (Ivanova-Kazas, 1985a, b, for careful discussions). Within Mollusca, Salvini-Plawen (1972, 1985) regarded the pericalymma larva, which lacks purely larval organs except the swimming test and is found only in aplacophorans and protobranch bivalves, as the ancestral type. The questions are left here as unresolved and not affecting the arguments for homology of early cell fate among Eutrochozoa, although my preference is indicated by use of the latter term.

Classification of Extant Molluscan Classes

With shell and spicules considered as synapomorphies for Conchifera and Aculifera, respectively, the following classification of extant Mollusca emerges:

Phylum Mollusca
- Subphylum Conchifera
  - Class Monoplacophora
  - Class Bivalvia
  - Class Gastropoda
  - Class Scaphopoda
  - Class Cephalopoda
- Subphylum Aculifera
  - Class Polyplacophora
  - Class Aplacophora
    - Subclass Neomeniomorpha
    - Subclass Chaetodermomorpha

This arrangement is similar to that already proposed in the last century with little knowledge of the soft anatomy of Monoplacophora. Garstang (1896) considered the

Aplacophora as "degraded" from an ancestral chiton-like form, but although he later stressed the importance of paedomorphosis in evolution, he did not see it as pertaining to Aplacophora. It is curious that a classification based on what are here inferred to be synapomorphies and on progenesis should be much the same as classifications of a hundred years ago.

Conclusions

The hypotheses, arguments, and pieces of evidence presented here lead to the conclusions that Mollusca (1) are eucolomates with an ancestry in common with spiralian trochozoans; (2) are related to Annelida, but not as closely as they are to Sipuncula; (3) have a reduced coelom which was never segmented; (4) are not directly descended from an aplacophoran-like or turbellariomorph predecessor; and (5) are descended from an ancestor with serial replication.

Acknowledgments

The idea that aplacophorans may have evolved through progenesis originally came from David R. Lindberg. I have benefitted from critical discussions with Dave and with Carole S. Hickman, Bruce Runnegar, Claus Nielsen, Tom Waller, Douglas Eernisse, and Bertil Åkesson, all of whom also steered me towards relevant literature. Doug Eernisse and Bruce Runnegar read an earlier version of this paper as well. Thanks are also due to Gerhard Haszprunar, who read the manuscript in its present form. Two reviewers most helpfully suggested literature that I had overlooked. I have tried to keep the phylogeny presented here as straightforward as criticisms and discussions suggested, and hopefully there is not too much "story telling." My gratitude goes to each of my critics.

Mary E. Rice opened the way for an understanding of the Sipuncula-Mollusca relationships presented here, and the visit with her at the Smithsonian Marine Station at Link Port, Ft. Pierce, Florida, afforded the opportunity to work with both living pelagosphera larvae and aplacophorans. I thank her deeply, and for prints of the splendid photographs of pelagosphera.

I thank Franz P. Fischer for providing me with a copy of his photograph of polyplacophoran epidermis, and Claus Nielsen for a copy of G. Gustafson's original drawings of *Chaetoderma nitidulum* larvae.

As always, I gratefully acknowledge helpful discussions with Rudolf Scheltema, who has provided me space and who has always taken an energetic interest in my work.

The following credits for previously published illustrations are acknowledged: figures 5A, C, D, 7C, 8A, and 11 from *American Malacological Bulletin* **6** (1988): 57–68, figs. 4, 5, 6, 13; figure 2A, B from *American Zoologist* **21** (1981): 605–619, figs. 4, 6; figure 3 from *Smithsonian Contributions to Zoology* **132** (1973): pl. 5; figures 6A, D, and 8D from *Veliger* **34** (1991): 195–203, figs. 2C, 4D, and 5C; figure 6E from *Zoomorphologie* **94** (1980): 121–131, fig. 3; figure 7A, B from *Biological Bulletin* **169** (1985): 484–529, fig. 3L, O, P.

Note added in proof: Two papers have just been published that have direct bearing on the ideas presented here. (1) Bengston S. 1992. The cap-shaped Cambrian fossil *Maikhanella* and the relationship between coeloscleritophorants and molluscs. *Lethaia* **25:** 401–420. *Maikhanella* is a genus of Lower Cambrian halkieriids with a cap-shaped shell formed of rows of embedded spicules, which were added by marginal accretion. Bengston discusses the possible homology with spicules of extant mollusks and with polyplacophoran shells. (2) Eernissee, D. J., J. S. Albert, and F. E. Anderson. 1992. Annelida and Anthropoda are not sister taxa: a phylogenetic analysis of spiralian and metazoan morphology. *Syst. Biol.* **41:** 331–344. Analysis by maximum parsimony among 141 morphological and embryological characters supports the concept of Eutrochoza, including the Mollusca.

Literature Cited

Allen, J. A. 1983. The ecology of deep-sea molluscs. Pp. 29–75 in *The Mollusca. Vol. 6. Ecology,* W. D. Russell-Hunter, ed. Academic Press, Orlando, FL.

Anderson, D. T. 1973. *Embryology and Phylogeny in Annelids and Arthropods.* Pergamon Press, Oxford and New York. xiv + 495 pp.

Andrews, E. B. 1988. Excretory systems of molluscs. Pp. 381–448 in *The Mollusca, Vol. 11. Form and Function,* E. R. Trueman and M. R. Clarke, eds. Academic Press, San Diego, CA.

Baba, K. 1938. The later development of a Solenogastre, *Epimenia verrucosa* (Nierstrasz). *J. Dept. Agric. Kyusyu Imp. Univ.* **6:** 21–40.

Baba, K. 1951. General sketch of the development in a Solenogastre, *Epimenia verrucosa* (Nierstrasz). *Misc. Repts. Res. Inst. Nat. Res.* **19–21:** 38–46. [In Japanese with English summary.]

Baba, K. 1975. *Neomenia yamamotoi* spec. nov., a gigantic Solenogaster (Mollusca: Class Solenogastres, Family Neomeniidae), occurring in the north-eastern part of Japan. *Publ. Seto Mar. Biol. Lab.* **22**(5): 277–284.

Banta, W. C., and M. E. Rice. 1976. A restudy of the Middle Cambrian Burgess Shale fossil worm, *Ottoia prolifica.* Pp. 79–90 in *Proceedings of the International Symposium on the Biology of the Sipuncula and Echiura,* M. E. Rice and M. Todorović, eds. Institute for Biological Research "Siniš Stanković," Belgrade, and Smithsonian Institution, Washington, DC.

Beedham, G. E., and E. R. Trueman. 1968. The cuticle of the Aplacophora and its evolutionary significance in the Mollusca. *J. Zool.* **154:** 443–451.

Butterfield, N. J. 1990. A reassessment of the enigmatic Burgess Shale fossil *Wiwaxia corrugata* (Matthew) and its relationship to the polychaete *Canadia spinosa* Walcott. *Paleobiology* **16:** 287–303.

Christiansen, M. E. 1954. The life-history of *Lepidopleurus asellus* (Spengler) (Placophora). *Nytt Mag. Zool.* **2:** 52–72.

Clark, R. B. 1964. *Dynamics in Metazoan Evolution: The Origin of the Coelom and Segments.* Clarendon Press, Oxford. 313 pp.

Conway Morris, S. 1985. The Middle Cambrian metazoan *Wiwaxia corrugata* (Matthew) from the Burgess Shale and *Ogygopsis* Shale, British Columbia, Canada. *Phil. Trans. Roy. Soc. London, B* **307:** 507–586.

Conway Morris, S., and J. S. Peel. 1990. Articulated halkieriids from the Lower Cambrian of north Greenland. *Nature* **345:** 802–805.

Curry, G. B., and B. Runnegar. 1990. Partial amino acid sequences of hemerythrins from *Lingula* and a priapulid worm, and the evolution of oxygen transport in early metazoans. No. 4314, *Geol. Soc. Am Abstr.* Dallas, TX.

Derjugin, K. M. 1915. [Fauna of the Kola gulf and its life conditions.]. *Mém. Acad. Imp. Sci. Petrograd* (ser. 8) **34**(1): 1–929, t. 1–14 [Pp. 499–501 Solenogastres]. [In Russian]

Derjugin, K. M. 1928. Fauna des Weissen Meeres und ihre Existenzbedingungen. *Exp. Mers U.R.S.S.* fasc. 7–8, 1–511 [Pp. 294–295, Solenogastres].

Eernisse, D. J. 1988. Reproductive patterns in six species of *Lepidochitona* (Mollusca: Polyplacophora) from the Pacific Coast of North America. *Biol. Bull.* **174:** 287–302.

Eyster, L. S., and M. P. Morse. 1984. Early shell formation during molluscan embryogenesis, with new studies on the surf clam, *Spisula solidissima*. *Am. Zool.* **24:** 871–882.

Field, K. G., G. J. Olsen, D. J. Lane, S. J. Giovannoni, M. T. Ghiselin, E. C. Raff, N. R. Pace, and R. A. Raff. 1988. Molecular phylogeny of the animal kingdom. *Science* **239:** 748–753.

Fischer, F. P., W. Maile, and M. Renner. 1980. Die Mantelpapillen und Stacheln von *Acanthochiton fascicularis* L. (Mollusca, Polyplacophora). *Zoomorphologie* **94:** 121–131.

Freeman, G., and J. W. Lundelius. 1992. Evolutionary implications of the mode of D quadrant specification in coelomates with spiral cleavage. *J. Evol. Biol.* **5:** 205–247.

Garstang, W. 1896. On the aplacophorous Amphineura of the British Seas. *Proc. Malacol. Soc. London* **2:** 123–125.

Gerould, J. H. 1906. The development of *Phascolosoma*. Studies on the embryology of the Sipunculidae I. *Zool. Jahrb., Anat.* **23:** 77–162.

Ghiselin, M. T. 1988. The origin of molluscs in the light of molecular evidence. Pp. 66–95 in *Oxford Surveys in Evolutionary Biology Vol. 5*, P. H. Harvey and L. Partridge, eds. Oxford University Press, Oxford.

Gould, S. J. 1977. *Ontogeny and Phylogeny.* Harvard University Press, Cambridge, MA, and London.

Gustafson, G. 1930. Anatomische Studien über die Polychäten-familien Amphinomidae und Euphrosynidae. *Zool. Bidr. Uppsala* **12:** 305–471.

Haas, W. 1976. Observations of the shell and mantle of the Placophora. Pp. 389–402 in *The Mechanisms of Mineralization in Invertebrates and Plants*, N. Watabe and K. M. Wilbur, eds. Belle W. Baruch Library in Marine Science 5.

Haas, W. 1981. Evolution of calcareous hardparts in primitive molluscs. *Malacologia* **21:** 403–418.

Haas, W., K. Kriesten, and N. Watabe. 1980. Preliminary note on the calcification of the shell plates in chiton larvae (Placophora). Pp. 67–72 in *The Mechanisms of Biomineralization in Animals and Plants*, M. Omori and N. Watabe, eds. Tokai University Press, Tokyo.

Hammarsten, O. D., and J. Runnström. 1925. Zur Embryologie von *Acanthochiton discrepans* Brown. *Zool. Jahrb. Anat.* **47:** 261–318.

Haszprunar, G. 1987. The fine morphology of the osphradial sense organs of the Mollusca. IV. Caudofoveata and Solenogastres. *Phil. Trans. Roy. Soc. London B* **315:** 63–73.

Haszprunar, G. 1992. The first molluscs—small animals. *Boll. Zool.* **59:** 1–16.

Heath, H. 1899. The development of *Ischnochiton*. *Zool. Jahrb., Anat.* **12:** 567–656.

Heath, H. 1904. The nervous system and subradular organ in two genera of Solenogastres. *Zool. Jahrb., Anat.* **20:** 399–408.

Heath, H. 1905. The morphology of a Solenogastre. *Zool. Jahrb. Anat.* **21:** 703–734.

Heath, H. 1911. The Solenogastres. Reports on the scientific results of the expedition to the tropical Pacific . . . by the "Albatross" . . . *Mem. Mus. Comp. Zool.* (Harvard University) **45**(1): 1–179.

Hessler, R. R., G. D. Wilson, and D. Thistle. 1979. The deep-sea isopods: a biogeographic and phylogenetic overview. *Sarsia* **64:** 67–75.

Hoffman, S. 1949. Studien über das Integument der Solenogastren nebst Bemerkungen über die Verwandtschaft zwischen den Solenogastren und Placophoren. *Zool. Bidr. Uppsala* **27:** 293–427.

Hoffmann, H. 1929–30. Aplacophora. Pp. 1–134, 383–453 in *Bronns Klassen und Ordnungen des Tier-Reichs*, Band III, Abt. 1.

Hyman, L. H. 1967. *The Invertebrates.* Vol. VI, *Mollusca I.* McGraw-Hill, Inc., New York. vii + 792 pp.

Ivanov, D. L. 1991. [Tentacular region of the central nervous system of the Mollusca and the homology of the organs of locomotion.] *Ruthenica* **1:** 81–89. [In Russian]

Ivanova-Kazas, O. M. 1985a. Origin and phylogenetic significance of trochophore larvae. *Zool. Zhur.* **64**(4): 485–497. [In Russian. English translation no. 1112119, National Museum of Canada, in manuscript.]

Ivanova-Kazas, O. M. 1985b. Origin and phylogenetic significance of trochophore larvae. *Zool. Zhur.* **64**(5): 650–660. [In Russian. English translation no. 1112120, National Museum of Canada, in manuscript.]

Jägersten, G. 1947. On the structure of the pharynx of the Archiannelida with special reference to there occurring muscle cells of aberrant type. *Zool. Bidr. Uppsala* **25:** 551–570.

Jägersten, G. 1963. On the morphology and behaviour of Pelagosphaera larvae (Sipunculoidea). *Zool. Bidr. Uppsala* **36:** 27–35.

Jägersten, G. 1972. *Evolution of the Metazoan Life Cycle.* Academic Press, London and New York.

Kaiser, P. 1976. *Neomenia herwigi*, sp. n., ein bemerkenswerter Vertreter der Solenogastren (Mollusca, Aculifera) aus Argentinischen Schelfgewässern. *Mitt. Hamb. Zool. Mus. Inst.* **73:** 57–63.

Kerth, K. 1983. Radulaapparat und Radulabildung der Mollusken. II. Zahnbildung, Abbau und Radulawachstum. *Zool. Jahrb., Anat.* **110:** 239–269.

Kniprath, E. 1980. Ontogenetic plate and plate field development in two chitons, *Middendorffia* [= *Lepidochitona*] and *Ischnochiton*. *Wilhelm Roux's Arch. Devel. Biol.* **189:** 97–106.

Kowalevsky, M. A. 1883. Embryogénie du *Chiton polii* Phil., avec quelques remarques sur le développement des autres Chitons. *Ann. Mus. Hist. Nat. Marseille* **1:** 1–46.

Lake, J. A. 1990. Origin of the Metazoa. *Proc. Nat. Acad. Sci. USA* **87:** 763–766.

Lemche, H., and K. G. Wingstrand. 1959. The anatomy of *Neopilina galatheae* Lemche, 1957 (Mollusca Tryblidiacea). *Galathea Rept.* **3:** 9–71.

McKinney, M. L., and K. L. McNamara. 1991. *Heterochrony: the Evolution of Ontogeny.* Plenum Press, New York and London. xix + 437 pp.

Monniot, C., and F. Monniot. 1978. Recent work on the deep-sea tunicates. *Oceanogr. Mar. Biol. Ann. Rev.* **16:** 181–228.

Moor, B. 1983. Organogenesis. Pp. 123–177 in *The Mollusca. Vol. 3, Development*, N. H. Verdonk, J. A. M. van den Biggelaar, and A. S. Tompa, eds. Academic Press, New York.

Newby, W. W. 1940. The embryology of the echiuroid worm *Urechis caupo*. *Mem. Am. Philos. Soc.* **16:** 1–213.

Nielsen, C., and A. Norrevang. 1985. The trochaea theory: an example of life cycle phylogeny. Pp. 28–41 in *The Origins and Relationships of Lower Invertebrates. Syst. Assoc. Spec. Vol. No. 28*, S. Conway Morris, J. D. George, R. Gibson, and H. M. Platt, eds. Clarendon Press, Oxford.

Plate, L. H. 1898. Die Anatomie und Phylogenie der Chitonen. *Zool. Jahrb., Suppl. IV (Fauna Chilensis I):* 1–243.

Raff, R. A., and T. C. Kaufman. 1983. *Embryos, Genes, and Evolution* Macmillan Publishing Co., Inc., New York & Collier Macmillan Publishers, London.

Raven, C. P. 1966. *Morphogenesis: The Analysis of Molluscan Development* 2nd ed. Pergamon Press, Oxford etc. xiii + 365 pp.

Reynolds, P. D., and M. P. Morse. 1991. Morphological evidence for ultrafiltration of blood in the Aplacophora. *Amer. Zool.* **31:** 137A.

Rice, M. E. 1969. Possible boring structures of Sipunculids. *Amer. Zool.* **9:** 803–812.

Rice, M. E. 1973. Morphology, behavior, and histogenesis of the pelagosphera larva of *Phascolosoma agassizii* (Sipuncula). *Smithsonian Contr. Zool.* **132:** 51 pp.

Rice, M. E. 1975. Sipuncula. Pp. 67–127 in *Reproduction of Marine Invertebrates. Vol. 2. Entoprocts and lesser coelomates,* A. Giese, and J. Pearse, eds. Academic Press, New York.

Rice, M. E. 1981. Larvae adrift: Patterns and problems in life histories of sipunculans. *Am. Zool.* **21:** 605–619.

Rice, M. E. 1985. Sipuncula: developmental evidence for phylogenetic inference. Pp. 274–296 in *The Origins and Relationships of Lower Invertebrates,* S. Conway Morris, J. D. George, R. Gibson, and H. M. Platt, eds. Oxford University Press, Oxford.

Runnegar, B., and J. Pojeta, Jr. 1985. Origin and diversification of the Mollusca. Pp. 1–57 in *The Mollusca, Vol 10, Evolution,* E. R. Trueman, and M. R. Clarke, eds. Academic Press, Orlando, FL.

Salvini-Plawen, L. v. 1968a. Die 'Funktions-Coelom Theorie' in der Evolution der Mollusken. *Syst. Zool.* **17:** 192–208.

Salvini-Plawen, L. v. 1968b. Über Lebendbeobachtungen an Caudofoveata (Mollusca, Aculifera), nebst Bemerkungen zum System der Klasse. *Sarsia* **31:** 105–126.

Salvini-Plawen, L. v. 1972. Zur Morphologie und Phylogenie der Mollusken: Die Beziehungen der Caudofoveata und der Solenogastres als Aculifera, als Mollusca und als Spiralia. *Z. wiss. Zool.* **184:** 205–394.

Salvini-Plawen, L. v. 1978. Antarktische und subantarktische Solenogastres (eine Monographie: 1898–1974). *Zoologica* **44:** 1–315.

Salvini-Plawen, L. v. 1981a. On the origin and evolution of the Mollusca. *Att. Convegni Lincei* **49:** 235–293.

Salvini-Plawen, L. v. 1981b. The molluscan digestive system in evolution. *Malacologia* **21:** 371–401.

Salvini-Plawen, L. v. 1985. Early evolution and the primitive groups. Pp. 59–150 in *The Mollusca, Vol. 10. Evolution.* E. R. Trueman, and M. R. Clarke, eds. Academic Press, Orlando, FL.

Salvini-Plawen, L. v. 1990. Origin, phylogeny and classification of the phylum Mollusca. *Iberus* **9:** 1–33.

Sanders, H. L., and J. A. Allen. 1973. Studies on deep-sea Protobranchia (Bivalvia); Prologue and the Pristiglomidae. *Bull. Mus. Comp. Zool.* **145:** 237–262.

Scheltema, A. H. 1972. The radula of the Chaetodermatidae (Mollusca, Aplacophora). *Z. Morph. Tiere* **72:** 361–370.

Scheltema, A. H. 1973. Heart, pericardium, coelomoduct openings, and juvenile gonad in *Chaetoderma nitidulum* and *Falcidens caudatus* (Mollusca, Aplacophora). *Z. Morph. Tiere* **76:** 97–107.

Scheltema, A. H. 1978. Position of the class Aplacophora in the phylum Mollusca. *Malacologia* **17:** 99–109.

Scheltema, A. H. 1981. Comparative morphology of the radula and alimentary tracts in the Aplacophora. *Malacologia* **20:** 361–383.

Scheltema, A. H. 1985. The aplacophoran family Prochaetodermatidae in the North American Basin, including *Chevroderma n.g.* and *Spathoderma n.g.* (Mollusca: Chaetodermomorpha). *Biol. Bull.* **169:** 484–529.

Scheltema, A. H. 1987. Reproduction and rapid growth in a deep-sea aplacophoran mollusc, *Prochaetoderma yongei. Mar. Ecol. Progr. Ser.* **37:** 171–180.

Scheltema, A. H. 1988. Ancestors and descendents: relationships of the Aplacophora and Polyplacophora. *Amer. Malacol. Bull.* **6:** 57–68.

Scheltema, A. H. 1990. Aplacophora as a Tethyan slope taxon: evidence from the Pacific. *Bull. Mar. Sci.* **47:** 50–61.

Scheltema, A. H., K. Kerth, and A. M. Kuzirian. 1989. The primitive molluscan radula. P. 220 in *Unitas Malacologica 10th International Congress,* Tübingen. [Abstract]

Scheltema, A. H., and A. M. Kuzirian. 1991. *Helicoradomenia juani* n.g. n. sp., a Pacific hydrothermal vent Aplacophora (Mollusca, Neomeniomorpha). *Veliger* **34:** 195–203.

Scheltema, A. H., M. Tscherkassky, and A. M. Kuzirian. (In press). Aplacophora. In *Microscopic Anatomy of Invertebrates. Vol. 5. Mollusca: Monoplacophora, Aplacophora, Polyplacophora, and Gastropoda,* F. W. Harrison and A. J. Kohn, eds. Wiley-Liss, New York.

Soetaert, K., and C. Heip. 1989. The size structure of nematode assemblages along a Mediterranean deep-sea transect. *Deep-Sea Res.* **36:** 93–102.

Spengel, J. W. 1881. Die Geruchsorgane und das Nervensystem der Mollusken. *Z. wiss. Zool.* **35:** 333–383.

Tendal, O. S. 1985. Xenophyophores (Protozoa, Sarcodina) in the diet of *Neopilina galatheae* (Mollusca, Monoplacophora). *Galathea Rept.* **16:** 95–98.

Thiele, J. 1902. Die systematische Stellung der Solenogastren und die Phylogenie der Mollusken. *Z. wiss. Zool.* **72:** 249–466.

Tscherkassky, M. 1989. Pedal shield or oral shield in Caudofoveata (Mollusca, Aculifera)? P. 254 in *Unitas Malacologica, Abstracts of 10th International Malacological Congress,* Tübingen. [Abstract]

Turbeville, J. M. 1986. An ultrastructural analysis of coelomogenesis in the hoplonemertine *Prosorhochmus americanus* and the polychaete *Magelona* sp. *J. Morphol.* **187:** 51–60.

Turbeville, J. M., K. G. Field, and R. A. Raff. 1992. Phylogenetic position of phylum Nemertini, inferred from 18S rRNA sequences: molecular data as a test of morphological character homology. *Mol. Biol. Evol.* **9:** 235–249.

van Dongen, C. A. M., and W. L. M. Geilenkirchen. 1974. The development of *Dentalium* with special reference to the significance of the polar lobe. I, II and III. Division chronology and development of the cell pattern in *Dentalium dentale* (Scaphopoda). *Proc. K. Nederl. Akad. Wetens.,* ser. C, **77:** 57–100.

Verdonk, N. H., and J. A. M. van den Biggelaar. 1983. Early development and the formation of the germ layers. Pp. 91–122 in *The Mollusca. Vol. 3. Development,* N. H. Verdonk, J. A. M. van den Biggelaar, and A. S. Tompa, eds. Academic Press, New York.

Watters, G. T. 1991. Utilization of a simple morphospace by polyplacophorans and its evolutionary implications. *Malacologia* **33:** 221–240.

Westheide, W. 1987. Progenesis as a principle in meiofauna evolution. *J. Nat. Hist.* **21:** 843–854.

Wettstein, E. 1904. Anatomie von Cryptoplax. *Jenaische Z. Naturwiss.* **38:** 473–504.

Whittington, H. B. 1985. *The Burgess Shale.* Yale University Press, New Haven and London. xv + 151 pp.

Willmer, P. G., and P. W. H. Holland. 1991. Modern approaches to metazoan relationships. *J. Zool., London,* **224:** 689–694.

Wilson, E. B. 1892. The cell-lineage of Nereis. *J. Morphol.* **6:** 361–480.

Wingstrand, K. G. 1985. On the anatomy and relationships of Recent Monoplacophora. *Galathea Rept.* **16:** 7–94.

Wissel, C. v. 1904. Pacifische Chitonen. *Zool. Jahrb., Syst.* **20:** 591–676.

Reference: *Biol. Bull.* **184**: 79–86. (February, 1993)

A Colonial Invertebrate Species that Displays a Hierarchy of Allorecognition Responses

B. RINKEVICH[1], Y. SAITO[2], AND I. L. WEISSMAN[3]

[1]*Marine Biology Department, Israel Oceanographic & Limnological Research, Tel-Shikmona, P.O.B. 8030, Haifa 31080, Israel,* [2]*Shimoda Marine Research Center, University of Tsukuba, Shimoda 5–10–1, Shizuoka 415, Japan, and* [3]*Howard Hughes Medical Institute, Stanford University Medical Center, B–257, Beckman Center, Stanford, California 94305*

Abstract. When two colonies of the compound ascidian *Botryllus schlosseri* come into contact with each other, they either fuse or reject. This allorecognition is governed genetically by multiple, codominantly expressed alleles at a single, highly polymorphic haplotype called the fusibility/histocompatibility (Fu/HC) locus. Two colonies sharing one or both alleles at this locus can fuse via their extracorporeal tunic blood vessels. Thereafter, in laboratory studies, one partner in the chimera is usually resorbed. The direction of resorption appears to be inherited, as multiple subclones of asexually-derived individuals from colony A always resorb paired subclones from colony B, independent of laboratory conditions or colony age.

We established 121 pairs of chimeric partners by fusions of relatives from four generations within a pedigree, all homozygotes (AA line) at their Fu/HC haplotype. This was carried out by self- and defined-crosses done in the laboratory on two outbred founder colonies (each AB at the fusibility locus) which were taken from the field. We found that the resorption phenomenon is characterized by a linear hierarchy within each generation of colonies, which is expressed by the existence of at least 5 intermediate groups. However, the time for resorption did not correlate with the position in the hierarchy. Analysis of resorption hierarchies between different generations revealed that mother colonies always resorbed their self crossed offspring. More interesting, colonies low in the hierarchy within a specific generation reproducibly resorbed the self crossed offspring of a superior kin. Chimeras between defined-crossed offspring of different generations revealed nontransitive types of hierarchies which were correlated with the relative position of each colony in the linear hierarchy established for the colonies within each generation. We propose that colony resorption in colonial botryllid ascidians is controlled by several allorecognition elements that determine a resorption hierarchy.

Received 24 April 1992; accepted 14 September 1992.

Introduction

The compound ascidian *Botryllus schlosseri* is a cosmopolitan metazoan of the subfamily Botryllinae, inhabiting shallow waters abundantly throughout the world, especially in harbors. Adults are made of several to hundreds of genetically identical units (each one is called a zooid), which are grouped in typical star-shape structures (systems), and are embedded within a translucent, gelatinous matrix, the tunic. All systems, as well as zooids within a single system, are interconnected to each other by a network of blood vessels, which bear spherical to elongate termini (called ampullae) near the surface of the tunic, between the systems and around the borders of the colony.

Colonies originate from a sexually produced tadpole larva. After a short free-swimming phase, the larva attaches to the substrate, resorbs its tail components, and undergoes metamorphosis to a founder individual, the oozooid. Oozooids grow by a typical asexual budding (blastogenesis), a cyclic phenomenon: *i.e.*, every six to seven days all parental zooids in a colony are synchronously resorbed and a new generation of buds matures to the zooid stage. Each adult zooid can give rise to one to four buds per generation (Boyd *et al.*, 1986). At the end of each blastogenic cycle, all of the zooids of one generation are resorbed. This event, called "takeover", is characterized by a massive phagocytosis, and is completed within 24 h (Harp *et al.*, 1988). During takeover, some

buds can be resorbed together with their parent, and thus the total number of zooids in a colony can either increase, remain constant, or decrease.

Allorecognition by complex metazoans can result in a variety of manifestations of histoincompatibility. The most detailed information concerning the genes that encode histocompatibility determinants, and the cells and receptors that recognize these determinants, comes from studies of mouse and man. In these species, as in all vertebrates tested, a single, highly polymorphic haplotype of linked histocompatibility genes—called the major histocompatibility complex (MHC)—is the primary determinant of rapid graft rejection mediated by allospecific T lymphocytes (Klein, 1986). However, when grafts are exchanged between individuals that share both MHC alleles, but are otherwise genetically distinct, a T cell-mediated graft rejection occurs, albeit at a slower pace than when MHC mismatched grafts are applied (Bevan, 1975; Loveland and Simpson, 1986). The genes encoding these determinants—almost certainly proteolytically derived peptides that are embedded in an MHC protein cleft (Bjorkman *et al.*, 1987) and thereby presented to MHC-restricted, allospecific T cells—are called minor histocompatibility (H) antigens. Genetic studies indicate that, with any two distinct mouse strains, the combinatorial association of minor H antigenic peptides with highly polymorphic MHC genes results in the elaboration of tens of alloantigens, encoded by genes residing on all (or nearly all) chromosomes (Bailey, 1978; Johnson, 1981; Zaleski *et al.*, 1983; Klein, 1986).

Allorecognition is also genetically defined in botryllid ascidians, as manifested by several distinct phenomena. Colonies that meet naturally in the wild or under laboratory conditions, very soon after initial contact, either fuse their adjacent extracorporeal tunic blood vessels to form a natural vascular parabiont (cytomictical chimera), or undergo a rapid series of inflammatory phenomena culminating in rejection, and the formation of a fibrous barrier between them (Scofield *et al.*, 1982; Taneda *et al.*, 1985; and literature therein). This colony specificity phenomenon is determined by a single, highly polymorphic fusibility/histocompatibility (Fu/HC) locus (or haplotype). In laboratory experiments, if two individuals sharing a single allele (or both alleles) at this locus fuse at some later time, the genetic colonial descendants (zooids) from one partner in the chimera are all resorbed by massive phagocytosis, leaving the genetic descendants of the other colony intact (Rinkevich and Weissman, 1987a, b, 1989, 1992; Weissman *et al.*, 1990). This phenomenon, called colony resorption, typically occurs at the end of a blastogenic cycle, when the new generation of zooids fails to develop to the mature phase, or does not develop at all (Rinkevich and Weissman, 1987a). Moreover, colony resorption also appears to be controlled genetically, insofar as all subclones from colony A will resorb all subclones from colony B, whatever the laboratory microenvironment in which the subclones are reared. The microenvironmental variables tested include different temperature regimens, types of food, running *versus* standing seawater systems, and the number of asexual generations separating the founder of the colony and the particular subclone tested (Taneda *et al.*, 1985; Rinkevich and Weissman, 1987a, b; 1989, 1992).

Here we provide evidence that the resorption of nonidentical partners in a chimera of the colonial tunicate *Botryllus schlosseri*, from Monterey, California, is at least partly controlled by additional recognition elements unlinked to the Fu/HC haplotype of this species. These colony resorption responses have a hierarchial property in that dominant, intermediate, and inferior responses are maintained through many asexual cycles, independent of environment.

Materials and Methods

Animals

Botryllus schlosseri colonies were kept in 17 l glass tanks supplied with 50–70 ml/min of filtered seawater that had been preconditioned in a large plastic holding tank containing 235 l. The water in each glass tank was aerated with an airstone and maintained at 18°C (with a 50 W aquarium heater). The animals were fed daily with 0.55 gr/tank of powdered Similac (a milk substitute) and subjected to a 14:10 hour light:dark regimen. Colonies were grown on 5 × 7.5 cm glass slides, one colony per slide, and kept vertically in slots of glass staining racks, within the glass tanks.

Colony allorecognition assays (CAAs)

Only large, healthy colonies were used. Small pieces of growing edges (subclones, ramets; containing one to three systems each) were isolated by careful dissection from each colony without injuring their surrounding ampullae. Subclones from two genetically distinct colonies were paired on glass slides, so that they contacted one another with their extended ampullae. They were fastened to the slides by placing them in a moisture chamber for 30–45 min before transferring them into the 17 l running seawater tanks. All of the paired subclones were in the range of size differences which does not affect directionality in the resorption phenomenon (Rinkevich and Weissman, 1987a) and were observed under the binocular stereomicroscope every day until they formed a well-organized chimera (Rinkevich and Weissman, 1987a, 1988, 1989). Thereafter they were observed 2 to 3 times a week. During the observations, colonies were cleaned with soft, small brushes to remove debris, fouling organisms, and trapped food particles. The substrate around the colonies was carefully cleaned with small pieces of razor blade.

Experimental procedures

To analyze further the possible role of heritable elements in colony resorption other than the Fu/HC locus, we carried out self and defined crosses from one of the Fu/HC homozygotic strains that are raised in our laboratory (Boyd *et al.*, 1986), the Monterey AA haplotype. The gencalogical tree relevant to the present study is illustrated in Figure 1, which shows the pedigree of four successive generations.

Two outbred colonies, each AB at the fusibility locus, were taken from the Monterey marina and served as the founders of this strain. The fusibility of each offspring was determined through CAAs by removing subclones from the main colony and placing them with subclones from other colonies (Rinkevich and Weissman, 1988). The present study focuses on the AA strain. Five healthy colonies of the AA strain served as parent colonies for the next generation offspring by self-crosses and defined-crosses. Self-crosses result from the fertilization of the eggs of one subclone (ramet) from a specific colony with the sperm from another ramet from the same colony, in the absence of competing sperm. The fastest growing and healthiest offspring colonies were either used in the experiments, with subclones being taken for fusibility assays (Rinkevich and Weissman, 1988), or they were used to produce the next generation of the AA line. Subclones from the indicated colonies were isolated, placed side-by-side on colony fusion plates, as described previously, and observed closely to record colony resorption (Rinkevich and Weissman, 1987a).

Results

Colony resorption hierarchies within different generations

Thirteen chimeras were derived by fusion between the four surviving AA colonies of generation II (Fig. 2a). In five cases (38.5%), the partners within the chimeras disconnected before resorption was complete (average time for disconnection 64 ± 21 days). Colony P111R was involved in four of these cases.

The resorption between this group of colonies (average time for resorption 48 ± 23 days) is characterized by a linear hierarchy. In this hierarchy, colony P21R is the "superior" partner, in that in the absence of dissociation, it resorbs all other colonies of this generation. In contrast, colony P94R is the "inferior" partner, as it is resorbed by the other three members of this generation (Fig. 2a). The time for resorption does not correlate with position in the hierarchy; subclones from the inferior P94R colony were resorbed by subclones from the superior P21R colony at the same, or even a slower pace than between the subclones of the two intermediate members (P32R and P111R; Fig. 2a). During the phase of chimerism, from the day of fusion up to the day of complete resorption, the superior partners increased in zooid numbers by asexual budding by 35–300%.

Eleven chimeras were derived by fusion between the self-crossed offspring of generation III themselves, the offspring of P111R and P21R (Fig. 1 and the two diagrams on the left of Fig. 2b). Out of 11 cases, one chimera died and one disconnected. Two hierarchies emerged when the resorption patterns were observed. Another hierarchy was

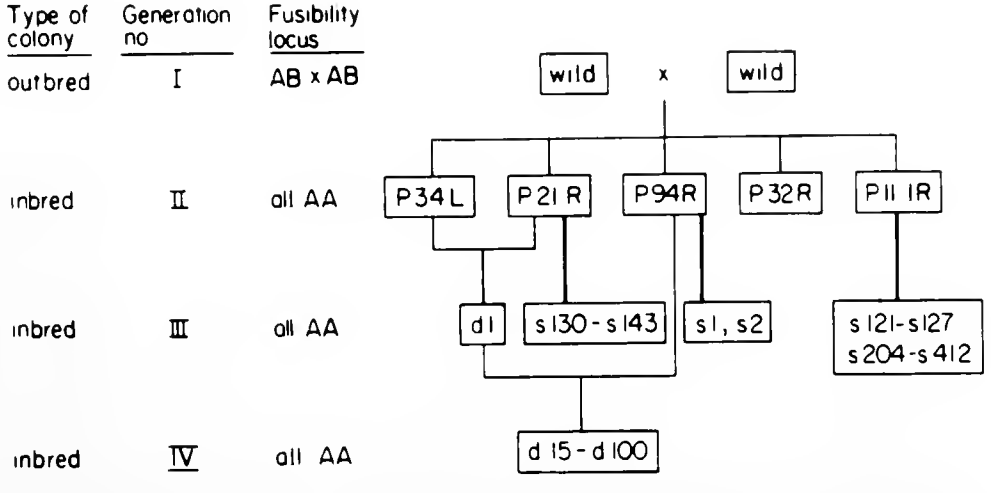

Figure 1. The pedigree of four successive generations of Monterey *Botryllus schlosseri* used in this study. Two independent outbred colonies, typed as Fu/HC AB, were designated generation I and were mated to give rise to generation II of Fu/HC AA colonies. Colonies of generations III and IV (all AA on the Fu/HC haplotype) are designated in running numbers with a preface letter which denotes the type of crossing: d = defined crossed colony; s = self-crossed colony. Heavy lines represent the pedigree of self-crossed colonies.

established by analyzing the outcome of 20 CAAs carried out between the defined-cross offspring of generation IV (right diagram, Fig. 2b). In this set, three chimeras disconnected and one died. The average time for resorption between self-crossed offspring (20 ± 18 days) was significantly shorter than the average time for resorption between defined-cross offspring (69 ± 43 days; $P < 0.001$, t test). As before (Fig. 2a), a linear hierarchy emerged from the analyses of the interactions within generations III and IV (Fig. 2b), and there was no correlation between the time to resorption and level in the hierarchy. The results illustrated in Fig. 2b also indicate the existence of at least five intermediate levels in the resorption hierarchy.

Colony resorption hierarchies between different generations

Fifty chimeras were generated between colonies of generation II and their self-crossed offspring of generation III, by assaying pairs of similar-sized ramets between parents vs. its own offspring, and pairs of generation II colonies vs. offspring of a kin colony (Fig. 2c). Death of the chimera or a disconnection was recorded in eight (16%) of the cases. In the other 42 cases, no matter how large the colonies were at the time of fusion, generation II ramets resorb generation III ramets (average time 42.4 ± 25.9 days). This result was obtained either when parent-offspring chimeras or chimeras of a generation II colony vs. self-crossed offspring from a kin were done. Most interestingly, generation II inferior colonies in the resorption hierarchy reproducibly resorbed the self-crossed offspring of a superior kin, such as the cases of P94R, P111R and P32R vs. offspring of P21R (Fig. 2c). In addition, similar to the cases shown in Fig. 2b, a resorption hierarchy is also found between the self-crossed offspring of colony P94R (Fig. 2c).

Twenty-seven chimeras were established between colonies of generation II and the defined-cross offspring of generation IV (Fig. 2d); 12 of them (44.4%) died or disconnected. The average time to a complete resorption in the other 15 chimeras was 56.1 ± 26.8 days. In this set of experiments, five of the IVth generation colonies resorbed and two (marked by dashed arrows with arrowheads; Fig. 2d) started to resorb colonies of the IInd generation, while in 10 cases, generation II ramets resorbed generation IV ramets (Fig. 2d). A closer examination reveals that colony d20 of generation IV is superior in the hierarchy of resorption to all four generation II colonies (Fig. 2d). This colony was found to be the superior colony within generation IV offspring as well (Fig. 2b). Colony d15 is the most inferior colony in generation IV colonies (Fig. 2b) and is resorbed by generation II colonies as well (Fig. 2d). Colony P94R (the inferior colony of generation II, Fig. 2a) was resorbed in all cases where a successful chimera was followed with generation IV colonies (Fig. 2d), whereas colony P21R (the superior colony of generation II, Fig. 2a) was inferior in the resorption hierarchy only to colony d20 of generation IV colonies (Fig. 2d).

Discussion

The colony resorption phenomenon is limited to individuals that are not genetically identical, since two genetically identical isolates from a single parent colony will meet, fuse, and give rise by asexual budding to growing colonies (Rinkevich and Weissman, 1987a). The studies of tunicate colony resorption reported here and previously (Rinkevich and Weissman, 1987a, b, 1989, 1990, 1992; Weissman *et al.*, 1990) reveal a unique hierarchical organization in *Botryllus schlosseri* chimeras. Fusion in the laboratory between two colonies that are Fu/HC homozygotes (*i.e.*, AA *vs.* AA), but that are not genetically identical or Fu/HC heterozygotes (*i.e.*, any combination of AX *vs.* AY), leads to colony resorption. All ramets from a superior colony will resorb fused ramets of an inferior colony, implying that other resorption elements, most likely encoded at other genetic loci, are responsible. Because the mother colony ramets usually resorb ramets from their more inbred progeny ramets, a simple hierarchy is difficult to explain. Perhaps heterozygotes at these loci are more likely to resorb homozygotes; or perhaps the general "fitness" of progeny of a self-cross allows a weaker resorption locus to emerge superior in colony resorption. The second suggestion is much less plausible, since the "performance" of the studied self-crossed homozygotes (either in survivorship, reproductive outputs, or growth rates) in our laboratory conditions (Boyd *et al.*, 1986) was as good if not better than that of the control, more heterozygotic colonies (Ishizuka and Rinkevich, in prep.).

If the above view is correct, then there may be positive selection for tunicates heterozygous for several allorecognition loci. Allorecognition in colonial tunicates therefore represents a histocompatibility system of considerable genetic sophistication and diversity, rivalling the MHC and minor histocompatibility loci in vertebrates, such as the mouse (Eichwald *et al.*, 1958; Eichwald and Weissman, 1966; Graff *et al.*, 1966; Lappe *et al.*, 1969; Graff, 1978; Klein, 1986; Townsend *et al.*, 1986; Weissman, 1988). These genes provide means by which each individual is likely to be unique in terms of histocompatibility. Whether this elaborate system of histocompatibility and allorecognition in colonial tunicates and vertebrate histocompatibility was derived from the same ancestral genes, or whether the similarities are merely semantic, remains to be determined.

The strength of the chimerism-resorption system, as defined by the period needed for a complete resorption, is extremely variable, from one week to five months (Fig. 2). At least part of the variability in the time for resorption may have been caused by experimental manipulations (such as the length and the structure of the fusion areas,

the numbers of anastomizing blood vessels, etc.; Rinkevich and Weissman, 1989), rather than by genetic factors. A similar characteristic of variability is also found in the murine minor histocompatibility loci (Klein, 1986), where there appear to be at least 50–100 distinct histocompatibility loci, with histocompatibility genes scattered throughout virtually every chromosome.

That the diversity of genetic types in the MHC of the vertebrates is the result of past selection for resistance to different diseases is a persistent speculation (Black and Salzano, 1981; Robertson, 1982; Hedrick and Thomson, 1983). This suggests that an animal heterozygous for the MHC antigens may respond much more efficiently to a wider range of pathogens than a homozygote, and that polymorphism may be maintained by heterozygous advantage or heterosis. In contrast, Flaherty (1988) has proposed that the high degree of mammalian MHC polymorphism has been established and maintained because of a constant, but promiscuous, heterozygote advantage. That is, no particular MHC allele has selective advantage; rather, all heterozygotes are favored over all homozygotes. This promiscuous heterozygote advantage would lead to a large allelic pool, because rare alleles would be favored and lead to more heterozygotes in the population. Other authors have proposed previously that heterozygote advantage might be involved in mammalian MHC evolution (Galton, 1967; Robertson, 1982; Hughes and Nei, 1988).

In general, heterosis refers to allelic combinations in which a heterozygote (*i.e.*, AB) has greater fitness than either of its homozygotes (AA or BB) (reviewed in Grosberg, 1988). We therefore postulate that the phenomena of fusion and chimeric resorption of Fu/HC compatible botryllid ascidians may provide substantial fitness benefits. If the dominant resorption of offspring settling near, and fusing with, maternal colonies (Rinkevich and Weissman, 1987b) is due to heterozygote advantage, then chimeric resorption linked to chromosomally dispersed "resorption" loci may serve to promote chromosomal heterogeneity, and therefore may provide substantial fitness benefits. Indeed, Grosberg and Quinn (1986) have shown in field experiments that sibling larvae of *B. schlosseri* settle non-randomly in aggregations; siblings that cosettle in these clusters share at least one Fu/HC allele, which should lead to the formation of more chimeras, and the resorption of a significant part of the *Botryllus* population. If colony resorption occurs in nature, the survivors would not only be at the top of the resorption hierarchy, but also are more likely to be heterozygotic at the resorption loci; thus colony resorption could contribute to heterosis benefits.

Four classes of benefits: genetic variability, developmental synergism, mate location, and size-specific ecological processes, have been attributed to the chimeric state (Buss, 1982). Despite these proposed benefits and those that heterosis might engender, however, there are potential costs to fusion, as well as mechanisms that could prevent this advantage from being passed on. The result of mixing genetically distant cell lines could result in germ-cell or somatic-cell parasitism when one member of the chimera could parasitize the other (Buss, 1982; Rinkevich and Weissman, 1987c). It has been reported (Sabbadin and Zaniolo, 1979; Rinkevich and Weissman, 1987c) that short-term chimeras of *Botryllus* colonies result in free exchange of germ cells, and that one individual in the chimera may gain a disproportionate share of gametic output even after the separation between both members in the chimera (Sabbadin and Zaniolo, 1979).

Thus, while the "heterosis" concept favors fusion as a pathway for selection against the less vigorous partner (including its soma and the germ line), the "somatic cell parasitism" concept, if reproducible and functional in nature, could lead to the survival of blood cells (especially the totipotent stem cells) from the resorbed partner, in effect cancelling the advantages gained by heterozygote-dominated resorption. In chimeras, therefore, several contradicting processes might play a role in colony survival until complete resorption occurs. However, successful domination of a feeding surface by chimeras should effectively prevent colonization of that surface by other competitor species. Whether the resorption "winner" or "loser" gives rise to the germ line that will successfully give rise to offspring is a critical evolutionary issue. Clearly, much more effort will be needed to elucidate the processes occurring within *Botryllus* chimeras in the field.

The present and previous studies on tunicate resorption (Rinkevich and Weissman, 1987a, b, 1989, 1990, 1992) used non-inbred *Botryllus* colonies. In order to study the individual histocompatibility gene and proteins of the mouse MHC, it was necessary to deal with the problems of multiple histocompatibility loci, extensive H-2 polymorphism and heterozygosity of the H-2 genes. These obstacles were circumvented by the development of three special types of mouse strains: inbred, congenic, and recombinant congenic, which is also the reason why we know the murine histocompatibility system better than in any other vertebrate. Studies on the colonial tunicate *Botryllus schlosseri* have revealed the Fu/HC system which resembles in some ways the vertebrate MHC (Scofield *et al.*, 1982), and a multilevel hierarchial organization of histocompatibility alleles which lead to the resorption of partners within chimeras (this study). The genetic structure of the protochordate histocompatibility system is only now being slowly revealed. Therefore, the analysis of histocompatibility pathways in *Botryllus* inbred lines may elucidate the sophisticated immunological systems of both protochordates and vertebrates, and their evolution.

Acknowledgments

We thank R. Lauzon for critically reading the manuscript, K. Ishizuka and K. Palmeri for their endless care

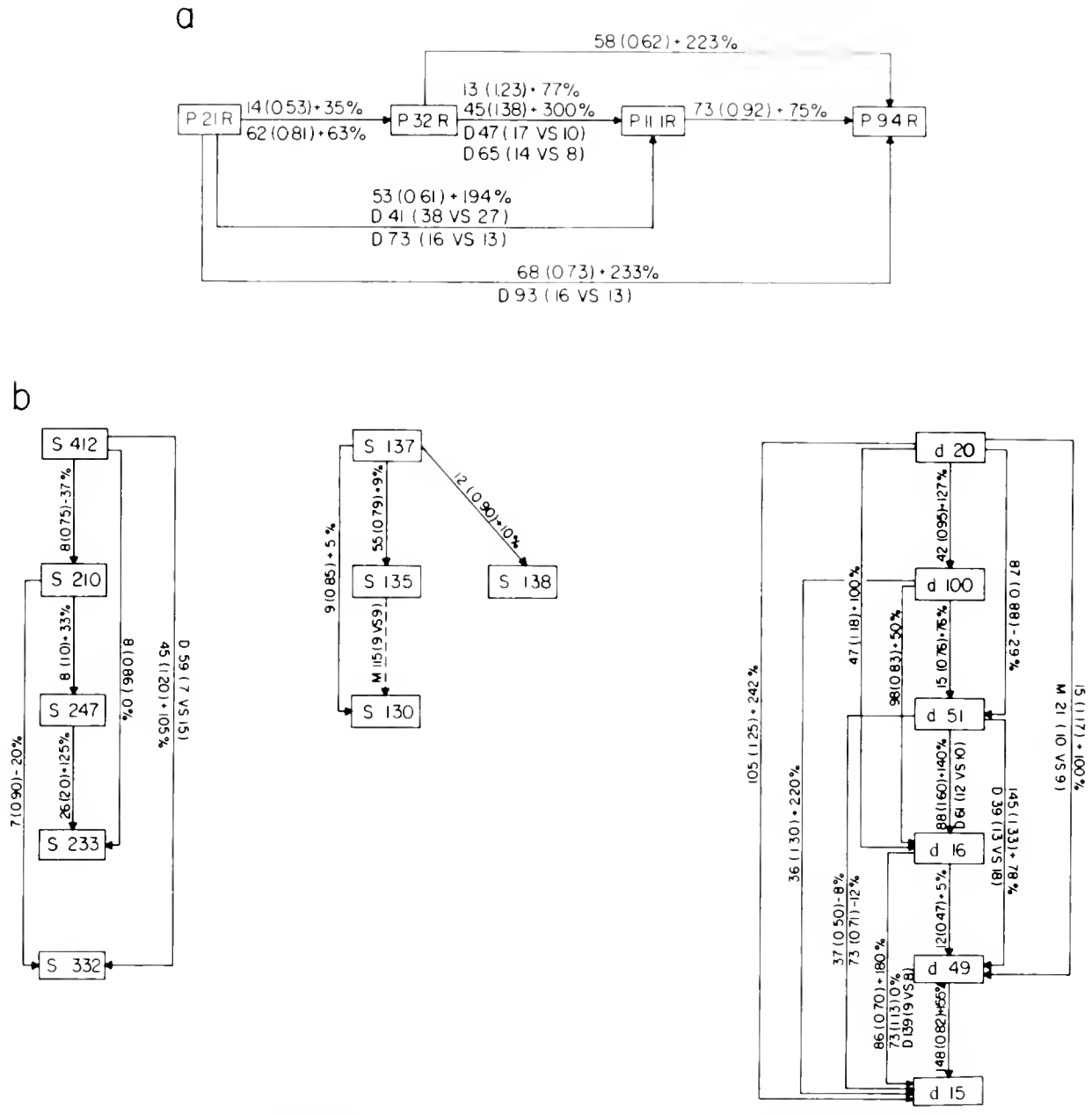

Figure 2. a. A hierarchy in the resorption between four colonies of generation II (refer to Fig. 1). The arrowheads point to the inferior partner. Numbers printed along the arrows refer to, respectively: days for complete resorption, zooid ratio (in parentheses, calculated as: the number of zooids in the inferior/superior partners on the day of fusion), percent increase or decrease of zooids in the superior partner from the day of fusion until a complete resorption of the inferior partner. The letter D refers to a case where a disconnection between the partners in a specific chimera occurs. In that case, the numbers along the arrow indicate: days from fusion to disconnection, number of zooids of the left colony on the day of fusion vs. the number of zooids of the right colony (in parentheses). Disconnection between the partners within a *Botryllus* chimera is one of the variations in the outcome to chimera formation, resulting from unsuccessful fusion (Rinkevich and Weissman, 1989), reciprocal resorption (Rinkevich and Weissman, 1987a, 1989), or from a retreat growth phenomenon (Rinkevich and Weissman, 1988). These physiological-genetic-morphological parameters may lead to early separation between the partners before a complete resorption of the inferior partners in a chimera is obtained (Rinkevich and Weissman, 1988, 1989). The hierarchial tendency in the resorption phenomenon is, in most of the cases, already observed before separation between the candidates cancels this reaction. However, we did not count disconnection even when figuring hierarchy. In each such case, at least one additional chimera, where full resorption was accomplished, is assayed. It should be noted, however, that the incompleted results of disconnections are always in agreement with the results where resorption is completed. Subclone sizes may alter the direction of chimera resorption. However, this occurs only when

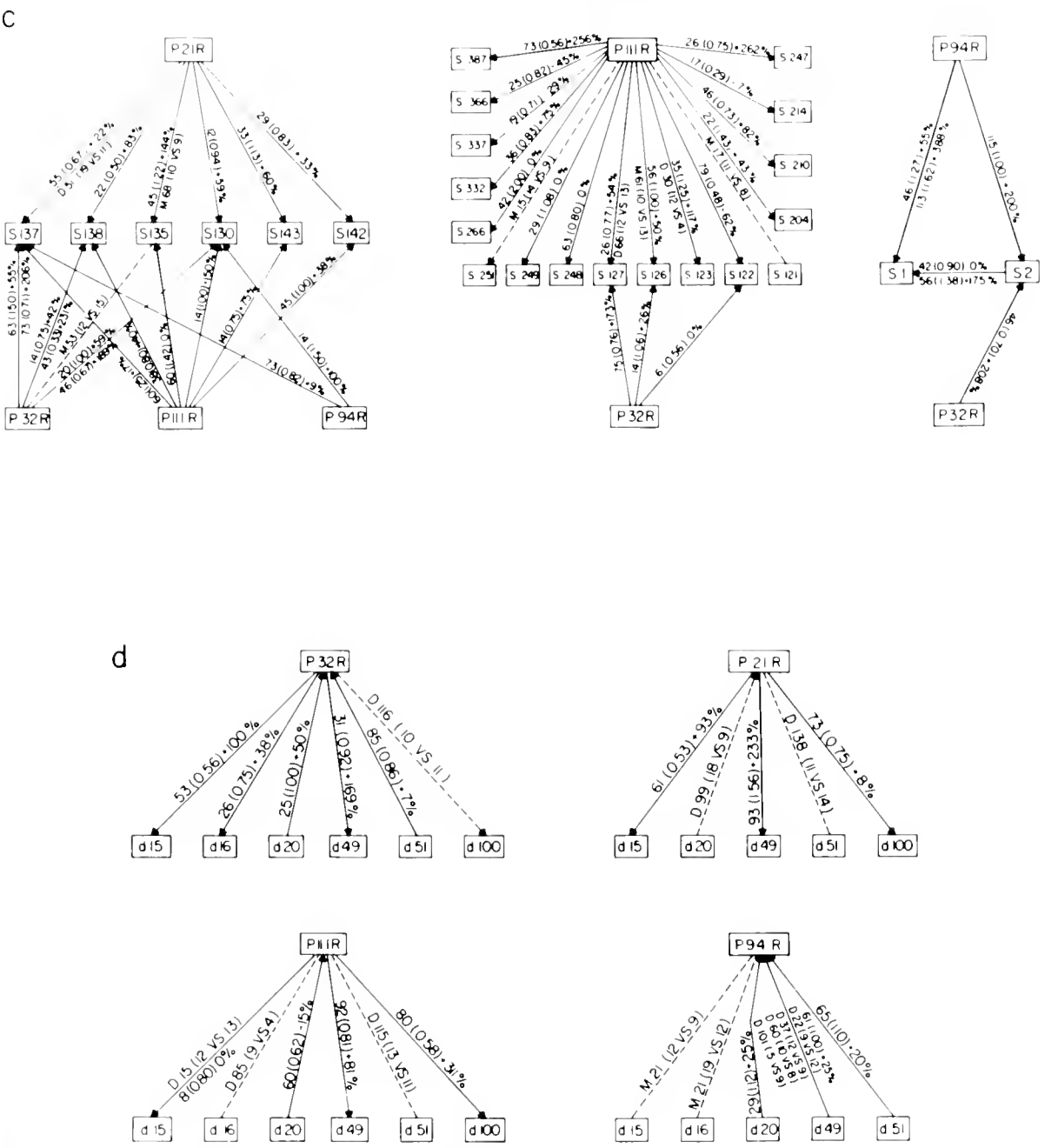

the subordinate partner is much larger than the winner. All subclones used in the present study were matched to pairs with zooid ratios, below that may reverse the direction of resorption. b. Hierarchy in the resorption within the self-crossed offspring of generation III (the two left schemes) and within the defined-cross offspring of generation IV (refer to Fig. 1). The letter M refers to a case where the chimera dies. In that case, the numbers along the arrow indicate: days from fusion until the death of the chimera, number of zooids of the left and the right partners, respectively, on the day of fusion (in parentheses). A dashed arrow with an arrowhead points to a case where the direction of resorption is evident; however, the chimera either died or the partners disconnected before the resorption was completed. Additional subclones for doing new chimeras were absent; therefore, the hierarchy in resorption was not fully determined. c. Hierarchy in the resorption between generation II colonies and the self-crossed offspring of generation III. A dashed arrow without an arrowhead indicates a case where hierarchy is not evident before interactions of the partners in a specific chimera were interrupted by chimera mortality or disconnection. In those cases, no more chimeras were done because of the lack of additional subclones. d. Hierarchy in the resorption between generation II colonies and the defined-cross offspring of generation IV. Dashed arrow with arrowhead indicates two cases where hierarchy became evident before the interactions in the CAAs were interrupted by disconnection.

in maintaining the *Botryllus* colonies, and M. Greenberg for valuable remarks on an earlier version. This study was supported by NCI Grant CA 42551, partly by a grant from the United States-Israel Binational Science Foundation, by a grant from the Basic Research Foundation administered by the Israel Academy of Sciences and Humanities, and by a Career Development Award from the Israel Cancer Research Fund, USA.

Literature Cited

Bailey, D. W. 1978. Sources of subline divergence and their relative importance for sublines of six major inbred strains of mice. Pp. 197–215 in *Origins of Inbred Mice*, H. C. Morse, ed. Academic Press, New York.

Bevan, M. J. 1975. Interaction antigens detected by cytotoxic T cells with the major histocompatibility complex as modifier. *Nature* **256:** 419–421.

Bjorkman, P., M. A. Sapir, B. Samraoui, W. S. Bennett, J. L. Strominger, and D. C. Wiley. 1987. The foreign antigen binding site and T cell recognition regions of class I histocompatibility cell recognition antigens. *Nature* **329:** 512–518.

Black, F. L., and F. M. Salzano. 1981. Evidence for heterosis in the HLA system. *Am. J. Hum. Genet.* **33:** 894–899.

Boyd, H. C., S. K. Brown, J. A. Harp, and I. L. Weissman. 1986. Growth and sexual maturation of laboratory-cultured Monterey *Botryllus schlosseri*. *Biol. Bull.* **170:** 91–109.

Buss, L. W. 1982. Somatic cell parasitism and the evolution of somatic tissue compatibility. *Proc. Natl. Acad. Sci. USA* **79:** 5337–5341.

Eichwald, E. J., and I. L. Weissman. 1966. Weak histocompatibility loci. *Annals N.Y. Acad. Sci.* **129:** 94–101.

Eichwald, E. J., C. R. Silmser, and I. L. Weissman. 1958. Sex linked rejection of normal and neoplastic tissue. I. Distribution and specificity. *J. Natl. Cancer Inst.* **20:** 563–575.

Flaherty, L. 1988. Major histocompatibility complex polymorphism: A non immune theory for selection. *Human Immun.* **21:** 3–13.

Galton, M. 1967. Factors involved in the rejection of skin transplanted across a weak histocompatibility barrier: gene dosage, sex of recipient, and nature of expression of histocompatibility genes. *Transplantation* **5:** 154–168.

Graff, R. J. 1978. Minor histocompatibility genes and their antigens. *Transplant. Proc.* **10:** 701–705.

Graff, R. J., W. K. Silvers, R. E. Billingham, W. H. Hildemann, and G. D. Snell. 1966. The cumulative effect of histocompatibility antigens. *Transplantation* **4:** 605–617.

Grosberg, R. K. 1988. The evolution of allorecognition specificity in clonal invertebrates. *Q. Rev. Biol.* **63:** 377–412.

Grosberg, R. K., and J. F. Quinn. 1986. The genetic control and consequences of kin recognition by the larvae of a colonial marine invertebrate. *Nature* **322:** 456–459.

Harp, J. A., C. B. Tsuchida, I. L. Weissman, and V. L. Scofield. 1988. Autoreactive blood cells and programmed cell death in growth and development of protochordates. *J. Exp. Zool.* **247:** 257–262.

Hedrick, P. W., and G. Thomson. 1983. Evidence for balancing selection at HLA. *Genetics* **104:** 449–456.

Hughes, A. L., and M. Nei. 1988. Pattern of nucleotide substitution at major histocompatibility complex class I loci reveals overdominant selection. *Nature* **335:** 167–170.

Johnson, L. L. 1981. At how many histocompatibility loci do congenic mouse strains differ? Probability estimates and some implications. *J. Hered.* **72:** 27–31.

Klein, J. 1986. *Natural History of the Major Histocompatibility Complex.* John Wiley & Sons, New York.

Lappe, M. A., R. G. Graff, and G. D. Snell. 1969. The importance of target size in the destruction of skin grafts with non H-2 incompatibility. *Transplantation* **7:** 372–377.

Loveland, B., and E. Simpson. 1986. The non-MHC transplantation antigens: neither weak or minor. *Immunol. Today* **7:** 223–224.

Rinkevich, B., and I. L. Weissman. 1987a. A long-term study on fused subclones in the ascidian *Botryllus schlosseri*: The resorption phenomenon (Protochordata: Tunicata). *J. Zool. (Lond.)* **213:** 717–733.

Rinkevich, B., and I. L. Weissman. 1987b. The fate of *Botryllus* (Ascidiacea) larvae cosettled with parental colonies: beneficial or deleterious consequences? *Biol. Bull.* **173:** 474–488.

Rinkevich, B., and I. L. Weissman. 1987c. Chimeras in colonial invertebrates: A synergistic symbiosis or somatic and germ-cell parasitism? *Symbiosis* **4:** 117–134.

Rinkevich, B., and I. L. Weissman. 1988. Retreat growth in the ascidian *Botryllus schlosseri*: A consequence of nonself recognition. Pp. 93–109 in *Invertebrate Historecognition*, R. K. Grosberg, D. Hedgecock, and K. Nelson, eds. Plenum, New York.

Rinkevich, B., and I. L. Weissman. 1989. Variation in the outcomes following chimera formation in the colonial tunicate *Botryllus schlosseri*. *Bull. Mar. Sci.* **45:** 213–222.

Rinkevich, B., and I. L. Weissman. 1990. *Botryllus schlosseri* (Tunicata) whole colony irradiation: do senescent zooid resorption and immunological resorption involve similar recognition events? *J. Exp. Zool.* **253:** 189–201.

Rinkevich, B., and I. L. Weissman. 1992. Allogeneic resorption in colonial protochordates: consequences of nonself recognition. *Dev. Comp. Immun.* **16:** 275–286.

Robertson, M. 1982. The evolutionary past of the major histocompatibility complex and the future of cellular immunology. *Nature* **297:** 629–632.

Sabbadin, A., and G. Zaniolo. 1979. Sexual differentiation and germ cell transfer in the colonial ascidian *Botryllus schlosseri*. *J. Exp. Zool.* **207:** 289–304.

Scofield, V. L., J. M. Schlumpberger, L. A. West, and I. L. Weissman. 1982. Protochordate allorecognition is controlled by an MHC-like gene system. *Nature* **295:** 499–502.

Taneda, Y., Y. Saito, and H. Watanabe. 1985. Self or nonself discrimination in ascidians. *Zool. Sci.* **2:** 433–442.

Townsend, A. R. M., J. Bastin, K. Gould, and G. G. Brownlee. 1986. Cytotoxic T lymphocytes recognize influenza haemagglutinin that lacks a signal sequence. *Nature* **324:** 575–577.

Weissman, I. L. 1988. Was the MHC made for the immune system, or did immunity take advantage of an ancient polymorphic gene family encoding cell surface interaction molecules? A speculative essay. *Int. Rev. Immun.* **3:** 393–416.

Weissman, I. L., Y. Saito, and B. Rinkevich. 1990. Allorecognition histocompatibility in a protochordate species: is the relationship to MHC semantic or structural? *Immunol. Rev.* **113:** 227–241.

Zaleski, M. B., S. Dubiski, E. G. Niles, and R. K. Cunningham. 1983. *Immunogenetics.* Pitman, Boston.

Reference: *Biol Bull* **184:** 87–96. (February, 1993)

Classification and Characterization of Hemocytes in *Styela clava*

TOMOO SAWADA[1], JEFFREY ZHANG[2], AND EDWIN L. COOPER

Department of Anatomy and Cell Biology, School of Medicine, University of California, Los Angeles, California 90024

Abstract. Viable hemocytes of the common tunicate *Styela clava* are classified into four groups designated as eosinophilic granulocytes, basophilic granulocytes, hyaline cells and lymphocyte-like cells. Eosinophilic granulocytes, actively amoeboid, have large refractive granules that stain with neutral red. Basophilic granulocytes do not stain with neutral red and formed couplets or triplets. Hyaline cells, which often contain phagosomes, have electron-dense small vesicles recognizable only by electron microscopy. Hemoblasts have a characteristic large nucleolus which is visible by light microscopy. Eosinophilic granulocytes and hyaline cells actively ingest yeast particles *in vitro*. This classification simplifies former ones by correlating electron microscopy, with light microscopy, and viable with fixed hemocytes. Clearly viable tunicate hemocytes can be identified by simple methods. We have provided clear and more accurate descriptions which will lessen the controversy often associated with assigning hemocyte functions in immunodefense responses both *in vivo* and *in vitro*.

Introduction

The classification of tunicate hemocytes remains confused, not withstanding Wright's attempt (1981) to devise useful categories. Recent progress in tunicate biology, however, requires a precise correlation between various cellular functions and particular types of hemocytes. *Styela clava*, especially, has been used in investigations of immunological responses including those associated with hemocytes: allogeneic reactions (Raftos and Cooper, 1991); cytotoxic reactions (Kelly *et al.*, 1992a); humoral opsonin (Kelly *et al.*, 1992b, 1993a, b, in press); and the production of cytokines (Beck *et al.*, 1989; Raftos *et al.*, 1991). Humoral lectins (Yokozawa *et al.*, 1986; Harada-Azumi *et al.*, 1987), antibacterial substances (Azumi *et al.*, 1990), and a metallo-protease (Azumi *et al.*, 1991) were studied in another species, *Halocynthia roretzi*.

Although the classification of *Styela clava* hemocytes began early (Ohue, 1936) and the site of hemopoiesis is described (Ermak, 1975, 1976), the literature includes descriptive morphologies with a plethora of terms, but relatively little experimental information uniting structure with function. Previous analyses of hemocytes failed to correlate age, season, and cell behavior in a systematic way, and these variables were not related to the various techniques used for examining them (*e.g.*, staining and fixation versus observation of live cells). Recent molecular and cytological studies focusing on the hemocytes and immune system of *Styela* will reveal a more precise picture of the functional contribution of individual effector cells. But this development depends on a thorough and consistent classification of the hemocytes.

To establish an acceptable and predictable classification scheme, we examined hemocytes from *Styela clava* and correlated the morphological and behavioral characteristics of living hemocytes, and compared appearance of viable cells with those analyzed by light and electron microscopy. Our work offers a strategy for classifying hemocytes in any invertebrate, especially tunicates which are becoming increasingly more important as we decipher the nature of effector cell activity during immune responses.

Materials and Methods

Hemocytes

Hemocytes were harvested by severing the stolons of *Styela clava* after rinsing the outside with 70% ethanol.

Received 20 May 1992; accepted 9 November 1992.

Present address: [1] Department of Anatomy, Yamaguchi University School of Medicine, Ube-city, 755 Japan.

[2] Undergraduate under the SRP program at UCLA.

Exuding hemolymph was collected into 0.5 *M* NaCl (NaCl-solution, pH 7.0 by 0.01 N NaOH) in polystyrene tubes; this prevented the nonspecific coagulation of hemocytes and allowed individual hemocytes to be observed. Hemolymph was mixed with the NaCl solution one to one in final volume.

Staining

Hemolymph or hemocyte suspensions in NaCl-solution were loaded onto glass slides. After 10 min, adhering hemocytes were fixed for 15 min and stained with hematoxylin and eosin (H&E). Cold ethanol, cold methanol or 4% paraformaldehyde (0.1 *M* sodium cacodylate buffer, pH 7.0) were used as fixatives, and the morphological preservation was compared. For vital staining, neutral red (NR, 0.01% in final concentration) was added to hemocyte suspensions; 15–30 min later, the hemocytes were loaded onto glass slides and observed.

Correlation of NR-staining with H&E-staining

We photographed NR-stained hemocytes adhering on glass slides, then fixed them for regular light microscopy without moving the slides, and photographed them again under phase-contrast microscopy. After H&E-staining, we found exactly the same cells as in the former two photographs (NR-staining and phase-contrast) to compare their appearance.

Transmission electron microscopy (TEM)

Hemocytes in the hemolymph and inside pharyngeal tissue were examined by TEM. Hemolymph collected into polystyrene tubes was centrifuged (400 × *g* for 5 min) and the pellet fixed. Pieces of pharynx (about 1.5 mm square) were dissected and fixed. Specimens were prefixed in a mixture of 2% glutaraldehyde and 2% paraformaldehyde (0.75 *M* sucrose, 0.2 *M* sodium cacodylate buffer, pH 7.0), then post-fixed with 1% osmium tetroxide in the same buffer. The specimens were dehydrated in ethanol series and embedded in Medcast (Ted Pella, Redding, CA). Propylene oxide was used to infiltrate the resin.

Autonomous fluorescence of viable hemocytes

Hemocytes suspended in NaCl-solution were loaded on glass slides and observed with a Nikon EFD2 fluorescence microscope with blue (420–490 nm)–and ultraviolet (330–380 nm)-illumination.

Composition of hemocytes

Different hemocyte types were counted by light microscopy after H&E or NR-staining, and also by TEM. A sample of hemocytes was taken from 6 animals, and five to ten different viewing fields (110–130 cells in total) from each sample were examined in light microscopy with a 100× objective lens. Five pharyngeal pieces, one each from 5 animals (one TEM-section for each piece), and a hemocyte-pellet from one animal were examined by TEM. About one hundred cells were examined on each section.

Phagocytic activity against yeast particles

Saccharomyces cerevisiae (baker's yeast, type II; Sigma Chemicals, St. Louis, MO) was stained with Congo red and suspended in artificial seawater (approximately 1×10^8 particles/ml), according to Kelly *et al.* (1993a). Hemocyte suspensions in NaCl-solution (100 μl) were loaded on cover slips, and yeast particle suspension (100 μl) was added 5 min later. The hemocytes were incubated for 30 min. After the cover slips were gently rinsed to remove excess yeast particles, 0.01% neutral-red solution was added. Hemocyte types were identified by NR-staining. Types of hemocytes which phagocytized yeast particles were identified.

Results

Light microscopy of hemocytes

Most hemocytes adhered to glass slides, and some of them exhibited amoeboid movement within 5 min. However, many small, transparent cells did not adhere well enough to resist water movement caused by pressure on the cover slip. By phase contrast microscopy, four different types were observed (Table I): (1) hyaline cells, which exhibited significant extensions (15–20 μm in diameter); (2) round cells (basophilic granulocytes, 6–10 μm in diameter), which contained highly refractive small granules and often formed couplets or triplets; (3) amoeboid cells (eosinophilic granulocytes; 8–15 μm in diameter), which contained large granules and exhibited more active amoeboid movement than the other types; and (4) small spherical cells that did not spread (hemoblasts; 4–6 μm in diameter), which contained a small amount of cytoplasm and had a nucleolus clearly visible by light microscopy. The nuclei of hemocytes other than hemoblasts were not visible unless they were spread flat on a glass slide.

Phase contrast microscopy was not sufficient to distinguish all eosinophilic and basophilic granulocytes with certainty. The eosinophilic granulocytes often contained granules as small as those of basophilic granulocytes, and when they were not moving they were just as round as basophilic granulocytes.

We observed large cells that had a hyaline cytoplasm lacking visible granules, but they did contain pigmented or non-pigmented large vacuoles. These cells were also identifiable as hyaline cells because they spread wide and flat. The spreading of hyaline cells was rapid once it began, and these cells did not exhibit active amoeboid movement after they spread.

Table I

Classification and some characteristics of Styela clava *hemocytes*

Type	Eosinophilic granulocytes	Basophilic granulocytes	Hyaline cells	LLC hemoblast
Size	8–15 μm	6–10 μm	15–20 μm	4–6 μm
H&E-staining	Orange	Purple	Very weak purple or pink	Purple
NR-staining	Orange or red-violet	—	Negative or orange at vacuoles	—
Granules in LM	Many refractile	Many small G refractile	—	—
Granules in TEM	Not uniform heterogeneous	Uniform spherical	Small vesicles electron dense	—
Adhesion to glass	++	++	++	±
Phagocytosis	++	+	+++	—
Other characteristics	Active amoeboid movement * Blue fluorecence in red-violet cells	Forming couplets or aggregates	Widely spread (cell fusion?)	Nucleolus visible in LM
Previous classifications	Compartment signet-ring vesiculated morula coarsely granular	Finely granular amoebocyte	Hyaline signet-ring?	Hyaline lymphocyte-like hemoblasts

* Under UV-illumination (330–380 nm).

NR-staining and some characteristics of viable cells

NR mainly stained the cytoplasmic granules of amoeboid cells (Fig. 1). Hyaline cells were usually not stained except for some cases in which small or large cytoplasmic vacuoles were stained (Fig. 1E, F). Two groups of amoeboid cells were positively stained by NR (eosinophilic granulocytes), but the intensity differed. One was stained a dense red-violet, whereas the other was orange (Fig. 1). Both types of cells contained 5–20 large cytoplasmic granules, and they were morula-shaped before starting amoeboid movement. Other granular cells were usually round, unstained by NR, and contained highly refractive small granules (Fig. 1; basophilic granulocytes). Most of the hemoblasts were not stained (Fig. 1), but a few sometimes stained faintly orange.

Following staining with NR, hemocytes were easily distinguished and their characteristic behaviors examined. Both types of NR-positive granulocytes (eosinophilic granulocytes) were active in amoeboid movement, extending many spine-like pseudopodia. NR-negative granular cells (basophilic granulocytes) were less active in amoeboid movement, but extended long pseudopodia. These cells were often observed as couplets (Fig. 1D), triplets or small aggregates composed only of this type of cell, and they did not separate once they came in contact. Occasionally, these cells spread flat after 30–60 min incubation.

H&E-staining

We used three different methods to observe hemocytes with H&E-staining after fixation. Ethanol and methanol significantly modified hemocyte morphology, so only paraformaldehyde fixation was utilized. We observed the same cells with NR-staining and H&E-staining.

Two NR–positive amoeboid cells (red-violet and orange cells) were stained intensely red or pink. Both cells contained various sizes of cytoplasmic granules that stained with eosin, so both cells were classified as eosinophilic granulocytes. The appearance of the cytoplasmic granules was altered by fixation, especially by ethanol and methanol. Cells that were fixed with these agents appeared as vacuolated cells, granular cells, compartment cells or signet-ring cells.

NR-negative amoeboid cells that contain small refractive granules were stained purple with H&E and were designated as basophilic granulocytes. Their cytoplasmic granules were no longer evident after fixation, and cytoplasmic staining was relatively weak after they spread on slides. However, the nuclei of basophilic granulocytes were smaller and more dense than those of hyaline cells.

The cytoplasm of hyaline cells was very thin after spreading so H&E stained them only weakly purple with some orange-stained cytoplasmic vesicles. Phagocytic vacuoles in some of them were stained red. Some hyaline cells contained large cytoplasmic vacuoles and thus appeared as signet-rings. Also their nuclei became larger as they spread.

A few encapsulations of several small cells were observed (small encapsulation; Fig. 2). In addition, small numbers of multinuclear cells were observed in H&E-staining (Fig. 2). These cells spread flat and contained several large nuclei and small vesicles stained with eosin. Finally, hemoblasts stained purple, and their nucleoli became unclear after fixation.

TEM of hemocytes

In centrifuged pellets of hemolymph, we observed five different hemocyte types (Figs. 3, 4): (1) *large cells*

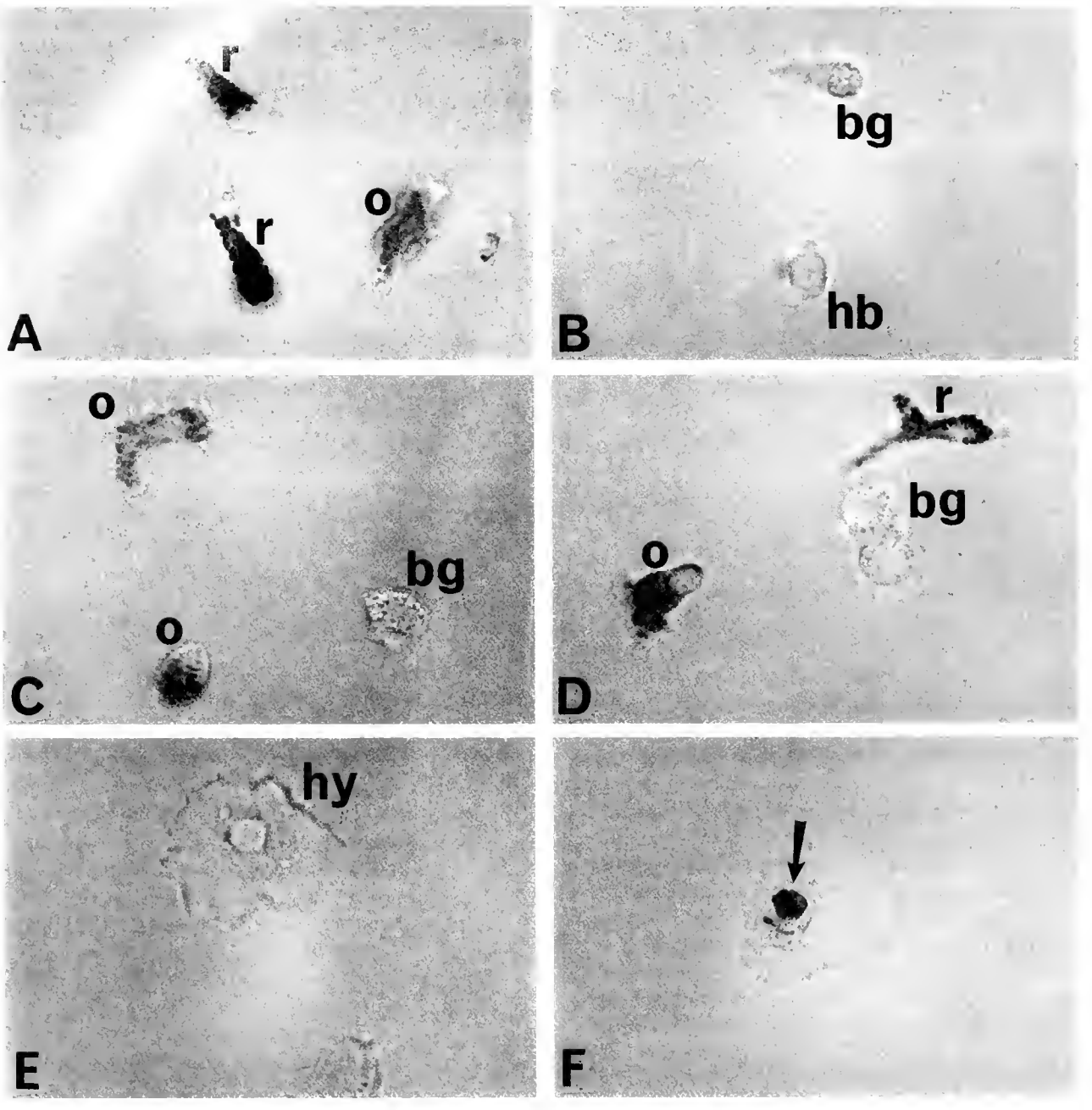

Figure 1. Living hemocytes on glass slides after NR-staining. (A) Eosinophilic granulocytes included two groups of granulocytes that stained in different colors (o = orange and r = red–violet). The sizes of the cytoplasmic granules are variable in each hemocyte. (B) Neither hemoblasts (hb) and basophilic granulocytes (bg) were stained. Nucleoli were evident in hemoblasts. (C) Basophilic granulocytes (bg) contained many refractive granules which were smaller than those of eosinophilic granulocytes (o = orange cells). (D) A couplet of basophilic granulocytes (bg); these were frequently observed. (E) Hyaline cells (hy) spread wide and flat on the glass slide to form a thin cytoplasmic sheet. (F) Some hyaline cells contained granules (arrow) that stained with NR. × 1250

(10–12 μm in diameter: hyaline cells) containing significant amounts of endoplasmic reticulum (ER); (2) *small spherical cells* (5–6 μm in diameter: hemoblasts) with little cytoplasm and large nuclei; (3–5) *three different granulocytes* (6–12 μm in diameter: basophilic and eosinophilic granulocytes) containing abundant cytoplasmic granules. These five types also constituted the entire hemocyte population within the pharyngeal tissue.

The *large cells* contained numerous rough-surfaced and smooth-surfaced ER and also small vesicles (0.1 μm in

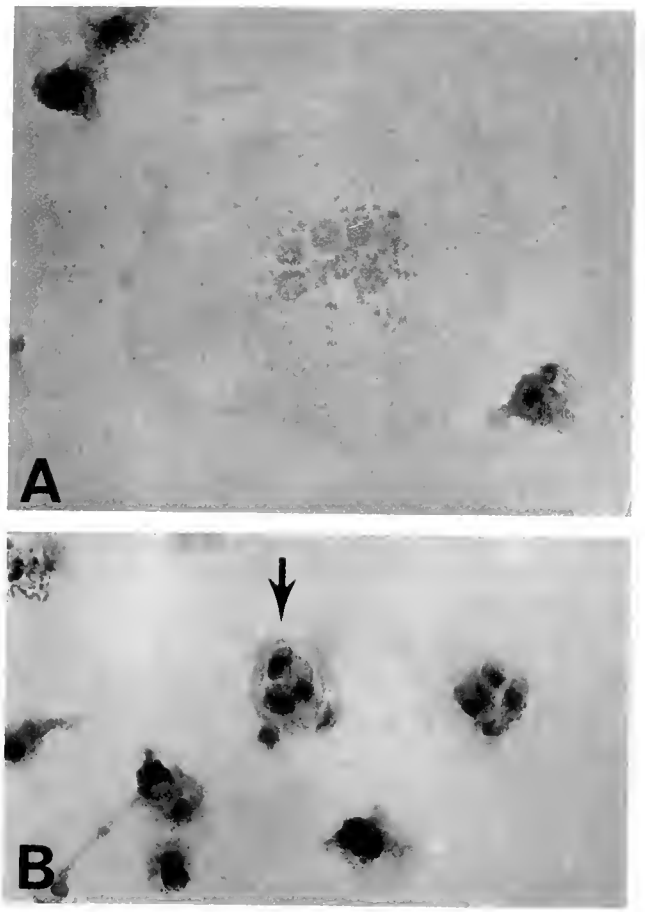

Figure 2. Fixed hemocytes on glass slides with H&E-staining. (A) Multinuclear cells with seven nuclei spread wide and flat. Vesicular structures in the cytoplasm were slightly stained. (B) Small encapsulation (arrow) containing 3–7 small cells; these were sometimes observed in the hemolymph. ×1180

diameter) of high electron density (Fig. 3). A few of these cells contained large vacuoles or phagosomes. Their nuclei often had nucleoli and coarse and uniform euchromatin, although heterochromatin was sometimes observed. These cells corresponded to hyaline cells on the basis of size, phagosomes, and the absence of large cytoplasmic granules.

The *small cells* with little cytoplasm contained mitochondria and small amounts of ER (Fig. 4C). Their nuclei, with characteristic large nucleoli, were usually larger than those of other hemocytes. Chromatin was uniformly distributed and slightly more dense in comparison with hyaline cells. These cells corresponded to hemoblasts in cell size, *i.e.*, little cytoplasm and characteristically large nucleoli.

The *three different granulocytes* (temporarily designated as type 1, 2 and 3 granulocytes according to TEM) had the same nuclear pattern (usually with dense heterochromatin at the periphery and sometimes small nucleoli) but differed in their cytoplasmic granules. *Type 1 granulocytes* (6–10 μm in diameter) contained electron-dense and spherical granules with a diameter range of 0.2–0.5 μm (Fig. 4A). These cells correspond to basophilic granulocytes on the basis of size, the sizes of their cytoplasmic granules (they had smallest granules among granulocytes), and their frequency in the hemolymph. *Type 2 granulocytes* (8–10 μm in diameter) contained irregular-shaped granules that varied in size (0.1–1.3 μm in diameter). The granules contained homogeneous material of intermediate electron-density (Fig. 4B). *Type 3 granulocytes* (8–12 μm in diameter) had cytoplasmic granules that were also irregularly-shaped and remarkably varied in size (0.1–1.5 μm in diameter). These granules were composed of heterogeneous materials—central spheres with high electron density and surrounding material of intermediate electron density (Fig. 4B). Type 2 and 3 granulocytes corresponded to eosinophilic granulocytes on the basis of size, the irregular shape of their cytoplasmic granules, and their frequency of occurrence.

Hemocyte composition

We examined percentages of the various hemocytes in hemolymph by counting each type after NR- and H&E-staining and TEM (Table II). The order of dominance for each type was the same in all cases, but the exact values were somewhat different. The most abundant cells were eosinophilic granulocytes (46.3% in NR-staining); second were the basophilic granulocytes (21.0%); hyaline cells were third (18.5%); and the smallest population was that of the hemoblasts (14.1%).

The percentage of eosinophilic cells in H&E-staining (68.5%) was about the same as the sum of type 2 and 3 granulocytes in the hemocyte pellets observed by TEM (67.8%), but it was larger than the sum of orange- and red-violet cells in NR-staining (46.3%). Many fewer hemoblasts were found in both H&E-staining (2.3%) and TEM (2.0%) than in NR-staining (14.1%). The proportion of hyaline cells ranged from 5.5 to 18.5%, even after the percentages of multinuclear cells and phagocytosis were added. Multinuclear cells (1.2% in H&E-staining) were not found in NR-staining or TEM of pharyngeal tissue.

Autonomous fluorescence of hemocytes

Blue fluorescence was observed in certain granulocytes under ultraviolet-illumination. NR-staining of those fluorescent hemocytes, in the same field of view, revealed that the autonomous fluorescence was from eosinophilic granulocytes which stained in red-violet (Table I). Under blue-illumination, no hemocytes exhibited autonomous fluorescence.

Phagocytosis

Four hemocyte types—*i.e.*, hyaline cells, eosinophilic granulocytes (including red-violet and orange cells in

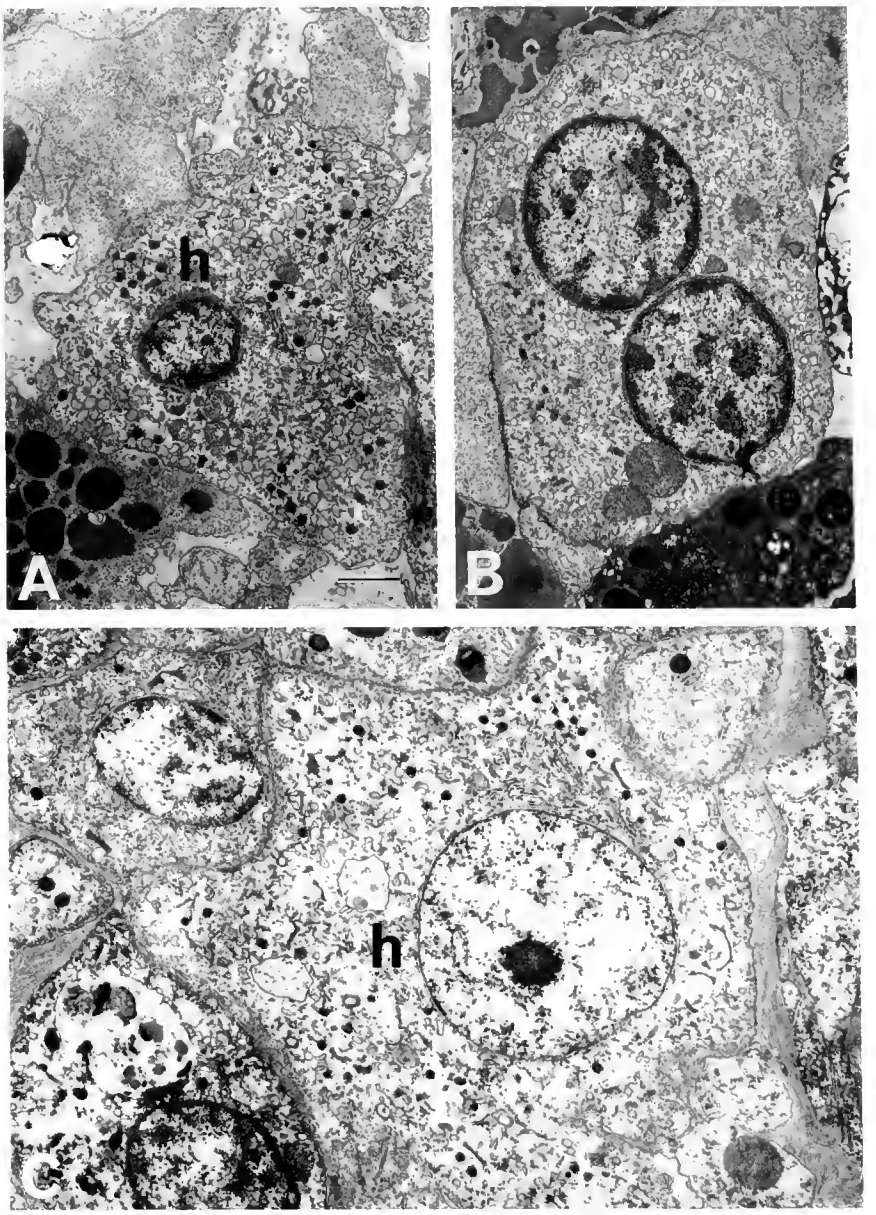

Figure 3. Transmission electron microscopy of hyaline cells and a binuclear cell. (A) Hyaline cell (h) in the centrifuged pellet, with heterochromatin at the nuclear periphery. (B) A binuclear cell in the centrifuged pellet. (C) Hyaline cell (h) in pharyngeal tissue; the nucleus has a large nucleolus and uniform euchromatin. All cells (A, B, C) contained electron-dense small vesicles, numerous vesicular structures, and endoplasmic reticulum. Bar = 1 μm.

NR-staining), and basophilic cells—ingested yeast particles. Among them, hyaline cells and cosinophilic granulocytes had significantly higher activity than basophilic granulocytes (Table III). In the cell population that had ingested yeast particles, hyaline cells (36–42%) were fewer than eosinophilic granulocytes (51–68%), as shown in Table IA. However, phagocytic activity was higher in hyaline cells, because the phagocytic ratios were higher in hyaline cells (32–78%) than in eosinophilic granulocytes (13–35%), as shown in Table IB. Many hyaline cells engulfed 2–5 yeast particles, whereas most eosinophilic granulocytes incorporated only one particle.

Discussion

Classification of hemocytes

Hemocytes from many species of tunicates have been classified by both light and electron microscopy (Ohue, 1936; George, 1939; Endean, 1960; Andrew, 1961, 1962; Overton, 1966; Smith, 1970; Botte and Scippa, 1977;

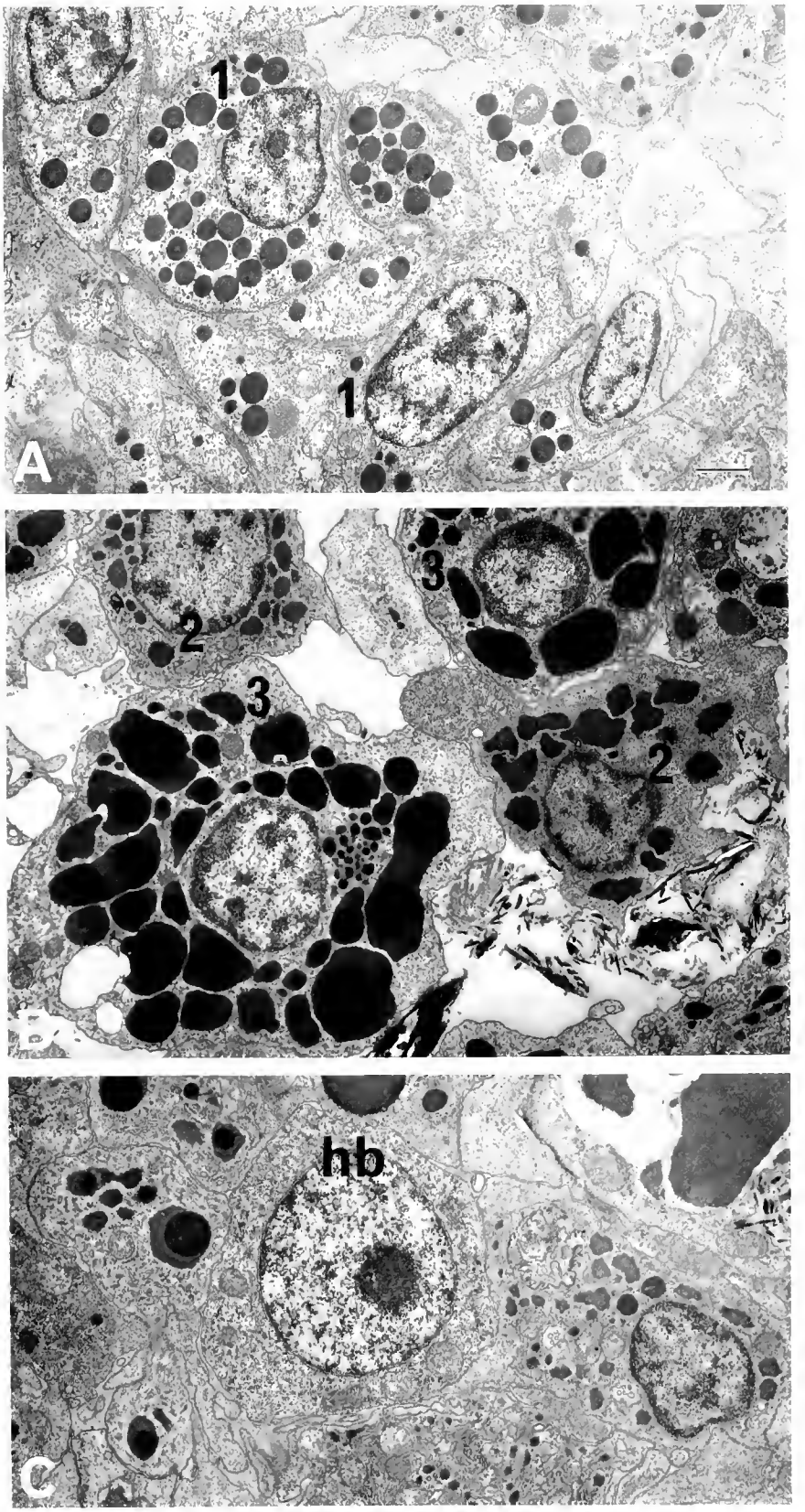

Figure 4. Transmission electron microscopy of hemocytes in the centrifuge pellet of hemolymph. (A) Type 1 granular cells (1 = basophilic granulocytes) containing relatively uniform and spherical granules. (B) Both type 2 (2) and 3 (3) granular cells (eosinophilic granulocytes) containing irregularly shaped granules. The granules of type 3 cells contain electron dense cores. (C) Hemoblast (hb) with little cytoplasm and without cytoplasmic granules, except for mitochondria and vesicles. The relatively large nucleus contains characteristic large nucleolus. Bar = 1 μm.

Table II

Hemocyte composition examined under different conditions

Hemocyte types	Viable cells (NR-staining)	Fixed cells (H&E-staining)	EM (pellet)	EM (pharynx)
Eosinophilic granulocytes	Orange 16.5 ± 5.0%	68.5 ± 5.6%	38.9%	15.8 ± 7.5%
	Red-violet 29.8 ± 8.5		28.9	32.8 ± 11.0
Basophilic granulocytes	21.0 ± 5.1	21.1 ± 4.4	21.0	21.3 ± 7.0
Hyaline cells	18.5 ± 7.9	5.5 ± 2.9	8.0	16.8 ± 3.8
Hemoblasts	14.1 ± 3.2	2.3 ± 2.2	2.0	8.5 ± 6.0
Multinuclear cells	0.0	1.2 ± 1.2	0.2	0.0
Cells of phagocytosis	0.1 ± 0.2	1.4 ± 1.2	1.1	2.3 ± 1.6
No. of individuals examined	6	6	1	5

average ± S.D.

Milanesi and Burighel, 1978; Fuke, 1979, 1980; Rowley, 1981, 1982; Mukai *et al.*, 1990), and in morphological terms, such as vacuolated or granular cells, hyaline cells, hemoblasts or lymphocytes (Wright, 1981), or by *functions* (Freeman, 1964; Fuke, 1980; Fujimoto and Watanabe, 1976; Burighel *et al.*, 1976; Rowley, 1983; Azumi *et al.*, 1990, 1991; Raftos *et al.*, 1990; Raftos and Cooper, 1991). However, the inapplicability of these classifications from one species to the next, and the lack of correspondence between different methods (*e.g.*, light versus electron microscopy) have produced confusion.

Hemocytes of *S. clava* have been classified into morula cells, compartment cells, signet-ring cells, granular amoebocytes, hyaline cells and lymphocyte-like cells (Ohue, 1936; Wright, 1981). But, among fresh and living hemocytes, we observed no signet-ring cells nor any cells with a stable, morula shape. Instead, there were granulocytes that frequently changed their appearance during amoeboid movement. They appeared morula-like when they rounded up, and could be compartment cells or granular amoebocytes after they had become extended and flattened. Fixation, especially with ethanol or methanol, modified hemocyte morphology significantly, and some of the eosinophilic granulocytes and hyaline cells became signet-ring in shape. Therefore, we adopted two cautious guidelines. First, we avoided using such terms as morula, compartment, or signet-ring. Second, we employed no Wright- or Giemsa staining because they require methanol as the fixative. Instead, we preferred to use formaldehyde fixation and H&E-staining.

We identified five different hemocyte types by vital NR-staining and TEM, and four types by H&E-staining of fixed cells. We estimated that the granules of the orange cells in NR-staining contain less dense material, and so correspond to type 2 granulocytes in TEM; similarly red-violet cells in NR-staining correspond to type 3 granulocytes in TEM. The difference between type 2 and 3 cells, or between orange and red-violet cells, is not significant enough to separate them into two cell types. Moreover, both the orange and red-violet cells evidently correspond to eosinophilic granulocytes in H&E-staining. These two granulocytes appear to be similar in amoeboid movement and phagocytic activity. Therefore, we classified both of them into the same group as eosinophilic granulocytes. We suggest that type 2 granulocytes (orange cells) are an earlier stage in cell differentiation than type 3 granulocytes (red-violet cells).

The correspondences between the light microscopical and TEM images of basophilic granulocytes (type 1 granulocytes in TEM), hyaline cells, and hemoblasts were clear on the basis of their morphological characteristics and their frequencies of appearance.

Multinuclear cells were classified as hyaline cells for the following reasons: (1) morphologically multinuclear cells are in all other respects similar to hyaline cells; (2) they sometimes contain large, eosinophilic vacuoles that we assume to be phagosomes; (3) the morphology and behavior of hyaline cells are quite similar to phagocytes type 1 (p1-cells) of *Halocynthia roretzi* (*H. roretzi*), which evidently fuse together and form multinuclear cell sheets (Sawada *et al.*, 1991). But, we have no strong evidence for cell fusion between the hyaline cells of *S. clava*. Moreover, the frequency of multinuclear cells in fresh hemolymph is not clear, because they could be identified only after spreading on glass. Both of these points require further investigation.

In this study, therefore, we have identified four hemocyte types in *S. clava*. (1) Eosinophilic granulocytes contain several refractive vacuoles that appeared red in neutral red vital stain, red by H&E, and exhibit active amoeboid

Table III

Phagocytosis of yeast particles by hemocytes from three different individuals

(A) Composition of hemocytes which ingested yeast particles

Animals	Eosinophilic granulocytes (red–violet)*[1]	Eosinophilic granulocytes (orange)*[1]	Basophilic granulocytes	Hyaline cells	Hemoblasts	Total cells examined
a*[2]	29.2%	22.1%	6.2%	42.5%	0.0%	113
b	41.0	11.0	10.0	38.0	0.0	100
c	41.6	16.8	5.0	36.6	0.0	101

(B) Phagocytosis against yeast particles within each hemocyte type

Hemocyte types	Animals	Ingesting cells	Non-ingesting cells	Total cells examined
eosinophilic granulocytes	a*[2]	19.4%	80.6%	108
(red–violet)	b	30.8	69.2	52
	c	12.9	87.1	101
(orange)	a	16.4	83.6	110
	b	ND*[3]	ND	ND
	c	1.6	98.4	61
basophilic granulocytes	a	7.3	92.7	124
	b	3.8	96.2	53
	c	0.0	100	57
hyaline cells	a	78.0	22.0	100
	b	63.6	36.4	22
	c	32.8	67.2	61

*[1] Two sub-populations of eosinophilic granulocytes different in colors of NR-staining are indicated in parenthesis.
*[2] Animals (a, b, c) in Table A correspond to the animals in Table B.
*[3] No data.

movement and phagocytosis. (2) Basophilic granulocytes contain numerous small granules that do not stain with neutral red, are purple in H&E, and form specific aggregations with the same cell type. (3) Hyaline cells contain fine electron-dense granules in TEM, occasionally contain phagosomes that stain red with neutral red and H&E, and extend into thin circular sheets on glass. (4) Hemoblasts possessed little cytoplasm, large nucleoli visible by light microscopy, but adhere only weakly to glass. Possible correspondence between former classifications are shown in Table I.

Functions and characteristic behavior of each hemocyte type

Phagocytosis, as is well known, is a ubiquitous and important immuno-defense response found throughout the animal kingdom. Hyaline cells exhibited the highest phagocytic activity, and some of them engulfed more than five yeast particles. Eosinophilic granulocytes were less active than hyaline cells, but they accounted for the largest population because of their abundance and active motility.

Hyaline cells were the most likely candidates for effecting encapsulation of larger particles by their ability to spread and form flat sheets and to fuse together into larger multinuclear sheets. Hemoblasts have been referred to as lymphocyte-like cells (Wright, 1981) and as proliferative stem cells (Ermak, 1976). We also observed the characteristically large nucleolus also in viable cells and confirmed their equivalents by light (Wright, 1981) and electron microscopy (Ermak, 1976).

Motility was also an important and definitive, behavioral characteristic. Only eosinophilic granulocytes exhibited active movement. In contrast, the basophilic granulocytes did not separate after once contacting others, which resulted in the formation of couplets or triplets. This behavior continues when augmented, resulting in small aggregates. Similar behavior was also observed on g1-cells of *H. roretzi* (Sawada *et al.*, 1991), and we suggest the presence of common granulocytes that can form specific aggregates within the same cell type.

Correspondence to the hemocytes in other tunicate species

Hemocyte types found in many species have been categorized into several groups by Wright (1981). However, the hemocytes of a single category often include several different types. In addition, certain hemocytes of one species are apparently absent in other species. It would not be instructive to compare only morphological aspects of hemocytes, and only under a single condition, such as in paraffin

sections. Observations of living hemocytes, under different conditions and stained with simple dye, coupled with functional analysis, *e.g.*, of phagocytosis, would be more useful.

In such a manner, we compared the hemocytes of *Styela clava* and *Halocynthia roretzi* which have also been classified in the living state (Sawada *et al.*, 1991), and found interesting correspondences between types. Hyaline cells and basophilic granulocytes were similar to the p1-cells and g1-cells of *Halocynthia roretzi*, respectively, in morphological and behavioral aspects. Hemoblasts, as the candidate for hematopoietic stem cells, may correspond to the ly-cells of *Halocynthia roretzi*, but their function as the stem cells has not been established in either species. Eosinophilic granulocytes seemed to be similar to the v3- and v4-cells of *Halocynthia roretzi* in that refractive vacuoles occupy most of the cell volume, and active amoeboid movement and acidphilic staining occur. But eosinophilic granulocytes of *Styela clava* were evidently more phagocytic. The correspondence between these species of at least two to three cell types may be consistent with their phylogeny.

Acknowledgments

We thank Sharon Sampogna and Monica Eiserling for technical help in light and electron microscopy. This study was supported by the National Science Foundation (Grant #DCB 90 05061).

Literature Cited

Andrew, W. 1961. Phase microscope studies of living blood-cells of the tunicates under normal and experimental conditions, with a description of a new type of motile cell appendage. *Q. J. Micr. Sci.* **102:** 89–105.

Andrew, W. 1962. Cells of the blood and coelomic fluids of tunicates and echinoderms. *Am. Zool.* **2:** 285–297.

Azumi, K., H. Yokozawa, and S. Ishii. 1990. Halocyamines: novel antimicrobial tetrapeptide-like substances isolated from the hemocytes of the solitary ascidian, *Halocynthia roretzi*. *Biochemistry* **29:** 159–165.

Azumi, K., H. Yokozawa, and S. Ishii. 1991. Lipopolysaccharide induces release of a metallo-protease from hemocytes of the ascidian, *Halocynthia roretzi*. *Dev. Comp. Immunol.* **15:** 1–7.

Beck, G., G. R. Vasta, J. J. Marchalonis, and G. S. Habicht. 1989. Characterization of interleukin-1 activity in tunicates. *Comp. Biochem. Physiol.* **92B:** 93–98.

Botte, L., and S. Scippa. 1977. Ultrastructural study of vanadocytes in *Ascidia malaca*. *Experientia* **33:** 80–81.

Burighel, P., R. Brunetti, and G. Zaniolo. 1976. Hibernation of the colonial ascidian *Botrylloides leachi* (Savigny): histological observations. *Boll. Zool.* **43:** 293–301.

Endean, R. 1960. The blood-cells of the ascidian, *Phallusia mammilata*. *Q. J. Micr. Sci.* **101:** 177–197.

Ermak, T. H. 1975. An autoradiographic demonstration of blood cell renewal in *Styela clava* (Urochordata: Ascidiacea). *Experientia* **31:** 837–839.

Ermak, T. H. 1976. The hematogenic tissue of tunicates. Pp. 45–56 in *Phylogeny of Thymus and Bone Marrow–bursa Cells*, R. K. Wright and E. L. Cooper, eds. Elsevier/North–Holland, Amsterdam.

Freeman, G. 1964. The role of blood cells in the process of asexual reproduction in the tunicate *Perophora viridis*. *J. Exp. Zool.* **156:** 157–183.

Fujimoto, H., and H. Watanabe. 1976. The characterization of granular amoebocytes and their possible roles in the asexual reproduction of the polystyelid ascidian, *Polyzoa vesiculiphora*. *J. Morphol.* **150:** 623–638.

Fuke, M. T. 1979. Studies on the coelomic cells of some Japanese ascidians. *Bull. Mar. Biol. Stn.* Asamushi, Tohoku University **16:** 143–159.

Fuke, M. T. 1980. "Contact reactions" between xenogeneic or allogeneic coelomic cells of solitary ascidians. *Biol. Bull.* **158:** 304–315.

George, W. C. 1939. A comparative study of the blood of the tunicates. *Quart. J. Micr. Sci.* **81:** 391–431.

Harada-Azumi, K., H. Yokozawa, and S. Ishii. 1987. N-acetyl-galactosamine-specific lectin, a novel lectin in the hemolymph of the ascidian *Halocynthia roretzi*: Isolation, characterization and comparison with galactose-specific lectin. *Com. Biochem. Physiol.* **88B:** 375–381.

Kelly, K. L., E. L. Cooper, and D. A. Raftos. 1992a. In vitro allogeneic cytotoxicity in the solitary urochordates. *J. Exp. Zool.* **262:** 202–208.

Kelly, K. L., E. L. Cooper, and D. A. Raftos. 1993a. A humoral opsonin from the solitary urochordate *Styela clava*. *Dev. Comp. Immunol.* **17:** (in press).

Kelly, K. L., E. L. Cooper, and D. A. Raftos. 1992b. Purification and characterization of a humoral opsonin from the *Styela clava*. *Comp. Biochem. Physiol.* **103B:** 749–753.

Kelly, K. L., E. L. Cooper, and D. A. Raftos. 1993b. Cytokine-like activities of a humoral opsonin from *Styela clava*. *Zool. Sci.* (in press).

Milanesi, C., and P. Burighel. 1978. Blood cell ultrastructure of the ascidian *Botryllus schlosseri*. I. Hemoblast, granulocytes macrophage, morula cell and nephrocyte. *Acta Zool.* **59:** 135–147.

Mukai, H., K. Hashimoto, and H. Watanabe. 1990. Tunic cords, glomerulocytes, and eosinophilic bodies in a styelid ascidian, *Polyandrocarpa misakiensis*. *J. Morphol.* **206:** 197–210.

Ohue, T. 1936. On the coelomic corpuscles in the body fluid of some invertebrates. III. The histology of the blood of some Japanese ascidians. *Sci. Rep. Tohoku Univ.* **11:** 191–206.

Overton, J. 1966. The fine structure of blood cells in the ascidian *Perophora viridis*. *J. Morph.* **119:** 305–326.

Raftos, D. A., D. L. Stillman, and E. L. Cooper. 1990. *In vitro* culture of tissue from the tunicate *Styela clava*. In Vitro *Cell Dev. Biol.* **26:** 962–970.

Raftos, D. A., and E. L. Cooper. 1991. Proliferation of lymphocyte-like cells from the solitary tunicate, *Styela clava*, in response to allogeneic stimuli. *J. Exp. Zool.* **260:** 391–400.

Raftos, D. A., E. L. Cooper, G. S. Habicht, and G. Beck. 1991. Invertebrate cytokines—Tunicate cell proliferation stimulated by an interleukin-1-like molecule. *Proc. Nat. Acad. Sci. USA.* **88:** 9518–9522.

Rowley, A. F. 1981. The blood cells of the sea squirt, *Ciona intestinalis*: morphology, differential counts and *in vitro* phagocytic activity. *J. Invertebr. Pathol.* **37:** 91–200.

Rowley, A. F. 1982. Ultrastructural and cytochemical studies on the blood cells of the sea squirt, *Ciona intestinalis*. I. Stem cells and amoebocytes. *Cell Tissue Res.* **223:** 403–414.

Rowley, A. F. 1983. Preliminary investigations on the possible antimicrobial properties of tunicate blood cell vanadium. *J. Exp. Zool.* **27:** 319–323.

Sawada, T., Y. Fujikura, S. Tomonaga, and T. Fukumoto. 1991. Classification and characterization of ten types of hemocytes in tunicate *Halocynthia roretzi*. *Zool. Sci.* **8:** 939–950.

Smith, M. J. 1970. The blood cells and tunic of the ascidian *Halocynthia aurantium* (Pallas). I. Hematology, tunic morphology and partition of cells between blood and tunic. *Biol. Bull.* **138:** 354–378.

Wright, R. K. 1981. Urochordates. Pp. 565–626 in *Invertebrate Blood Cells 2*, N. A. Ratcliffe and A. F. Rowley, eds. Academic Press, London.

Yokozawa, H., K. Harada, K. Igarashi, Y. Abe, K. Takahashi, and S. Ishii. 1986. Galactose-specific lectin in the hemolymph of solitary ascidian, *Halocynthia roretzi*. Molecular, binding and functional properties. *Biochim. Biophys. Acta.* **870:** 242–247.

Reference: *Biol. Bull.* **184**: 97–104. (February, 1993)

Effects of Cations on the Volume and Elemental Composition of Nematocysts Isolated from Acontia of the Sea Anemone *Calliactis polypus*

MICHIO HIDAKA AND KIWAMU AFUSO

Department of Biology, University of the Ryukyus, Nishihara Okinawa, 903-01 Japan

Abstract. The hypothesis that exchange of intracapsular divalent cations with Na^+ in seawater increases the internal osmotic pressure during discharge of nematocysts of marine cnidarians was tested by examining effects of externally applied cations on the volume and elemental composition of nematocysts isolated from acontia of the sea anemone *Calliactis polypus*. The volume of isolated nematocysts increased with increasing concentrations of cations if the cation was monovalent but appeared to decrease if the cation was divalent. Ca^{2+} reduced the internal osmotic pressure of the nematocysts more efficiently than Mg^{2+}. X-ray microanalysis of nematocysts incubated in 1 *M* solutions of various salts showed that Ca^{2+} in isolated nematocysts was only partially replaced, if at all, by externally applied Na^+ and Mg^{2+} while most Mg^{2+} was replaced by Na^+ and Ca^{2+}. The present results suggest that exchange of intracapsular divalent cations with external monovalent cations increases the internal osmotic pressure, and that selective binding of Ca^{2+} to polyanions in the capsule decreases it. Whether the increase in the internal osmotic pressure caused by the cation exchange is large enough to trigger discharge remains to be investigated.

Introduction

Lubbock and his colleagues proposed that loss of Ca^{2+} from a nematocyst increases the osmotic pressure of the intracapsular fluid and thus causes discharge of the nematocyst (Lubbock and Amos, 1981; Lubbock *et al.*, 1981; Gupta and Hall, 1984). They proposed that polypeptides in undischarged nematocysts are crosslinked by Ca^{2+} to form polypeptide chains and that the release of calcium from the nematocyst dissociates the polypeptide chains, thereby increasing the number of osmotically active molecules. Because of this report, Ca^{2+} has been considered to play a major role in nematocyst discharge.

Recently Weber (1989) demonstrated that naturally occurring cations of *Hydra* nematocysts can be replaced by externally applied cations. Nematocysts loaded with other cations generally retain discharge capabilities. Gerke *et al.* (1991) found that *in situ* nematocysts of *Hydra* contained high concentrations of potassium (K) instead of calcium (Ca). These observations suggest that Ca^{2+} is not indispensable for the discharge of certain kinds of nematocysts.

Weber (1989) proposed that *Hydra* nematocysts can be considered as Donnan-equilibrium dominated osmotic systems and that cations associated with polyanions in the capsule, rather than polyanions themselves, contribute to high intracapsular osmotic pressure. Because *Hydra* nematocysts contain high concentrations of K (Gerke *et al.*, 1991) and are surrounded by a membrane that might serve as a diffusion barrier against ions of low molecular weight (Lubbock *et al.*, 1981), nematocysts of *Hydra* might be in equilibrium with high concentrations of K^+. If such nematocysts are exposed to freshwater as a result of exocytosis, the osmotic pressure difference across the capsule wall would increase, leading to the discharge of the nematocysts. Indeed, isolated *Hydra* nematocysts immersed in concentrated NaCl or KCl solutions swell up to 115% of the original volume and tend to discharge when the external concentration of the salts is lowered (Weber, 1989).

The above process, however, may not account for the discharge of nematocysts of marine cnidarians, because nematocysts of marine cnidarians must discharge in seawater, which contains high concentrations of salts. X-ray

Received 14 May 1992; accepted 20 October 1992.

microanalysis of frozen sections of various marine cnidarians show that the predominant cation of nematocysts *in situ* is either Ca^{2+}, Mg^{2+}, or K^+ (Tardent *et al.*, 1990). If nematocysts of marine cnidarians also behave as Donnan-equilibrium dominated systems, exchange of intracapsular cations with cations in seawater will occur when nematocysts are exposed to seawater as a result of exocytosis. In Ca- or Mg-containing nematocysts, the exchange of divalent cations in the capsule with monovalent cations such as Na^+ in seawater might increase the internal osmotic pressure, since one divalent cation is replaced by two monovalent cations to maintain electroneutrality. If the increase in the internal osmotic pressure is large enough, the nematocysts would discharge.

The purpose of the present study is to examine the hypothesis of divalent-monovalent cation exchange. Undischarged nematocysts isolated from various cnidarians contain high concentrations of Ca and Mg (Weber *et al.*, 1987; Mariscal, 1988; Hidaka, 1993). These isolated nematocysts provide a useful model for studying the responses of Ca- and/or Mg-containing nematocysts to various cations. We determined the effects of mono- and divalent cations on the volume of nematocysts isolated from acontia of the sea anemone *Calliactis polypus*. We also studied whether Ca^{2+} and Mg^{2+} found in the isolated nematocysts could be replaced by externally applied cations as in *Hydra* nematocysts (Weber, 1989).

Materials and Methods

Specimens of *Calliactis polypus* on the shells of hermit crabs belonging to the genus *Dardanus*, were collected from the reef around the Okinawa island, and maintained in an aquarium supplied with a subgravel filter. The hermit crabs were fed with chopped *Tapes* every 2–4 days. The anemones were used as a source of acontial nematocysts 1–3 days after feeding. Acontial filaments were obtained by prodding the sea anemone with blunt-tipped forceps.

Undischarged basitrichous isorhiza nematocysts were isolated either in artificial seawater (ASW) or in distilled water (DW), since nematocysts isolated in ASW and those isolated in DW display different discharge capabilities (Hidaka and Mariscal, 1988). A piece of acontium was placed in a drop of ASW or DW on a glass slide. The glass slide was treated with a drop of a 0.1% solution of poly-l-lysine (Sigma; approx. mol. wt. 90,000) in distilled water for 10 min in a wet chamber prior to use (Mazia *et al.*, 1975). Two strips of thin adhesive tape (Scotch 3M) were placed on both sides of the drop to make a narrow space between the glass slide and a cover slip, and to make it easy to replace the solution in this space. When nematocysts were isolated in ASW, the acontium was squashed under a cover slip. Only a small percentage (about 5%) of nematocysts discharged during this procedure, and most of them only partially discharged—eversion of the tubule stopped halfway. Cellular debris and partially discharged nematocysts were removed by washing the squashed acontium with a few drops of ASW. Most of the nematocysts isolated in this manner from acontia of *Calliactis tricolor* discharged when immersed in 5 m*M* EGTA (Hidaka and Mariscal, 1988), suggesting that the isolated nematocysts are functional. When nematocysts were isolated in DW, the acontium was immersed in a drop of DW for 5 min and then the remaining acontium was removed. The extruded undischarged nematocysts were allowed to settle onto the glass slide for 10 min. Then, the isolated nematocysts were washed with more than five drops of ASW or DW to remove unattached nematocysts.

Photomicrographs of nematocysts were taken in ASW or DW using a plan objective lens (×100). Then, test solutions were applied by perfusing the nematocysts with at least eight drops of each test solution (Hidaka and Mariscal, 1988). Nematocysts isolated in ASW were treated with decreasing concentrations of salt solutions, that is, 1000, 100, 10, 1, and 0 m*M* solutions. Nematocysts isolated in DW were treated with increasing concentrations of salt solutions. Nematocysts were immersed in each test solution for 10 min, because changes in the volume of isolated nematocysts in solutions with or without Ca^{2+} were completed within 10 min (Hidaka, 1992). After 10 min a pair of photomicrographs of the nematocysts was taken for each test solution. The length and diameter of nematocysts capsules were measured to the nearest 0.1 mm (corresponding to 0.05 μm) on two photomicrograph prints using calipers. The average value was used for each capsule. The volume was calculated assuming that the capsule was an ellipsoid. The volume of nematocysts immersed in test solutions was normalized by the original volume of the nematocysts in ASW or DW, and expressed as relative volume. The original volume (mean ± SD) was 117.7 ± 18.8 μm^3 (n = 37) in ASW-isolated nematocysts and 100.7 ± 10.1 μm^3 (n = 37) in DW-isolated nematocysts. For each salt solution, three or four experiments were performed and at least seven nematocysts were measured. The significance of regression of the relative volume of nematocysts on log (salt concentration) was tested in each salt solution. When the regression was not significant, the relative volume at 1 *M* salt concentration was compared with that at 1 m*M* using Duncan's multiple range test. The difference in the relative volume of nematocysts was tested among pairs of cations at 1 *M* salt concentration using the multiple range test.

For substitution experiments, nematocysts were isolated by immersing 20 acontia in 5 ml of DW for 5–10 min. Remaining acontial tissues were removed by filtering the nematocyst suspension through 60 μm nylon mesh. Aliquots (0.8 ml) of the filtrate were placed in each of six

microtubes and centrifuged at 1940 × *g* for 5 min. One ml of each test solution was added to the pellet. Nematocysts were resuspended in the test solutions and allowed to stand for 10 min. Test solutions were ASW and 1 *M* solutions of NaCl, KCl, $CaCl_2$, $MgCl_2$, and $SrCl_2$. Next, the nematocysts were washed in DW by centrifuging at 1940 × *g* for 5 min and by resuspending the nematocysts in 1 ml of DW. The nematocysts were washed in DW and collected by centrifugation three times. Finally, the nematocysts were resuspended in 150 μl of DW. Aliquots (20 μl) of the nematocyst suspension were placed on meshes with formval or collodion membranes that had been coated with carbon and treated with poly-l-lysine. The nematocysts were allowed to settle on the membrane for 1 h, then air-dried after the remaining solution was soaked up with a piece of filter paper. Specimens were observed under a scanning transmission electron microscope (JEOL JEM-2000EX) equipped with an energy dispersive spectrometer (TN 421J). X-ray spectra were acquired at an acceleration voltage of 100 kV. Semiquantitative elemental analyses were performed using an application software (Noran Instruments Inc. SMTF) on 4–6 nematocysts for each test solution. The software, which was designed for standardless semiquantitative analysis of metallurgical thin films, removes background and integrates peak areas. The peak intensities were converted to ratios of element concentrations by multiplying by calculated K-factors. Correction for absorption was not made.

The ASW contained (in m*M*): NaCl, 480; KCl, 10; $CaCl_2$, 10; $MgCl_2$, 26; $MgSO_4$, 29; and was adjusted to pH 8.0 with 10 m*M* HEPES. All the salt solutions and DW were buffered to pH 8.0 with 10 m*M* HEPES, and all the experiments were done at room temperature (23–26°C).

Results

Nematocysts isolated from acontia of *Calliactis polypus* in ASW swelled in concentrated solutions of monovalent cations (Fig. 1). There was a significant positive regression between the volume of nematocysts and the concentration of Na^+ and K^+ (regression analysis, $P < 0.05$). Though there was no significant regression between the volume of nematocysts and the concentration of divalent cations, the volume of nematocysts was significantly smaller in 1 *M* $MgCl_2$ and $SrCl_2$ than in 1 m*M* solutions (Duncan's multiple range test, $P < 0.01$). At 1 *M* concentration, nematocysts immersed in divalent cations were significantly smaller than those immersed in monovalent cations (Duncan's multiple range test, $P < 0.01$). When nematocysts that had been immersed in various salt solutions were immersed in a buffer solution without added salts, there was no significant difference in the mean volume

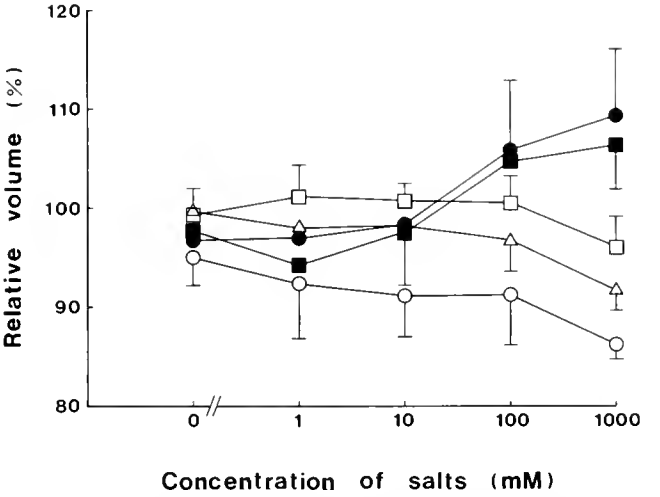

Figure 1. Effects of cations of various concentrations on the volume of nematocysts isolated from acontia of *Calliactis polypus* in ASW. Nematocysts isolated in ASW were immersed successively in salt solutions of decreasing concentrations. The salt solutions examined were NaCl (●), KCl (■), $CaCl_2$ (○), $SrCl_2$ (△), and $MgCl_2$ (□). The volume of nematocysts in each solution is expressed as a percentage of the original volume of nematocysts in ASW. Vertical bars represent standard deviations; some SD bars are omitted for clarity.

(one-way ANOVA, $P > 0.25$). Thus the volume of the nematocysts increased with increasing concentration of cations if the cation was monovalent, but decreased if the cation was Mg^{2+} or Sr^{2+}. The volume of the nematocysts was smaller in 1 *M* $CaCl_2$ than in 1 *M* $MgCl_2$ ($P < 0.01$).

The volumetric behavior of nematocysts isolated in DW was almost the same as that of nematocysts isolated in ASW (Fig. 2). When the concentration of external K^+ was increased, the volume of isolated nematocysts increased (regression analysis, $P < 0.05$). Though regression between the volume of nematocysts and concentration of Na^+ was not significant, nematocysts immersed in 1 *M* NaCl were larger than those immersed in 1 m*M* NaCl (Duncan's multiple range test, $P < 0.05$). Nematocysts immersed in 1 *M* $CaCl_2$ and $SrCl_2$ were smaller than those immersed in 1 m*M* solutions ($P < 0.01$). Nematocysts immersed in 1 *M* $CaCl_2$ or $SrCl_2$ were smaller than those immersed in 1 *M* $MgCl_2$ ($P < 0.01$).

A scanning electron micrograph of a nematocyst sample prepared for X-ray microanalysis is shown in Figure 3. X-ray spectra of nematocysts were different depending on the incubation solutions (Fig. 4). The major elements of nematocysts incubated in ASW were Ca and Mg in addition to sulfur (S), though a small Na-peak was present (Fig. 4A). When nematocysts were incubated in 1 *M* NaCl, the Na-peak increased, the Ca-peak remained high but the Mg-peak disappeared (Fig. 4B). When nematocysts were immersed in 1 *M* KCl, a small K-peak appeared, but the peaks of the other elements were not affected (Fig.

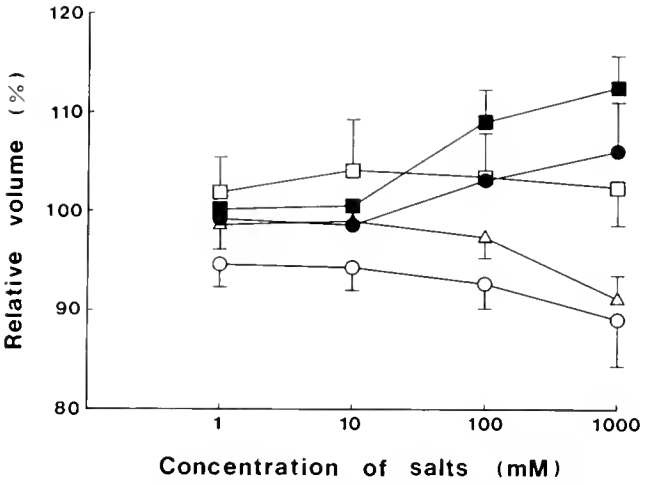

Figure 2. Effects of cations of various concentrations on the volume of nematocysts isolated from acontia of *Calliactis polypus* in DW. Nematocysts isolated in DW were immersed successively in salt solutions of increasing concentrations. The symbols are the same as in Figure 1. The volume of nematocysts in each solution is expressed as a percentage of the original volume of the nematocysts in DW. The vertical bars represent standard deviations; some SD bars are omitted for clarity.

4C). Nematocysts incubated in 1 *M* $CaCl_2$ showed large Ca- and small Na-peaks in addition to the S-peak (Fig. 4D). When nematocysts were incubated in 1 *M* $MgCl_2$, the Mg-peak increased (Fig. 4E). Nematocysts incubated in 1 *M* $SrCl_2$ showed large Sr- and small Ca-peaks in addition to the S-peak (Fig. 4F). When discharged nematocysts were analyzed, peaks of metals were absent regardless of the incubation solutions.

Table I shows the relative abundance of metal cations in undischarged nematocysts that were isolated in DW and then incubated in various salt solutions. Ca accounted for about 50% of the metals in nematocysts immersed in ASW or 1 *M* $MgCl_2$ and more than 50% in nematocysts immersed in 1 *M* NaCl or KCl. Ca was replaced substantially only by strontium (Sr). Most of the Mg disappeared when nematocysts were immersed in 1 *M* NaCl, $CaCl_2$, and $SrCl_2$. Only a small amount of K was present in nematocysts incubated in 1 *M* KCl.

Discussion

Weber (1989) studied the volumetric behavior of isolated stenoteles of *Hydra* under different ionic conditions. He showed that nematocysts immersed in 1 *M* solutions of various salts swell when the concentration of salts is lowered, regardless of whether the cations are monovalent or divalent. The volumetric behavior of isolated nematocysts of the sea anemone *Calliactis polypus* was different from that of *Hydra* nematocysts. *Calliactis* nematocysts appeared to shrink in concentrated solutions of divalent cations as in *Hydra* nematocysts, but swelled in concentrated solutions of monovalent cations. Thus the volumetric behaviors of the marine anemone nematocysts and the freshwater *Hydra* nematocysts are different in solutions of monovalent cations.

Weber (1989) showed that the volumetric behavior of *Hydra* nematocysts immersed in salt solutions of various concentrations can be accounted for by a Donnan-equilibrium model. The Donnan potential generates an asymmetrical distribution of ions across the capsule wall. According to Weber's simulation studies, the difference in total ion concentration between the inside and outside of the capsule increases as the external salt concentration is lowered from 3 *M* to 0.1–0.01 *M*. When the external salt concentration is further lowered, the osmolarity difference drops due to protonation of polyanions, unless the external pH is high. The volume of *Calliactis* nematocysts, however, decreased as the external concentration of monovalent cations was lowered from 1 to 0 *M*. Thus the volumetric response of the sea anemone nematocysts to monovalent cations cannot be accounted for by the simple Donnan-equilibrium model.

Weber (1989) showed that naturally occurring cations in *Hydra* nematocysts can be replaced by externally applied cations. If this is true for nematocysts of marine cnidarians, cations contained in the isolated capsule might be replaced by external cations when nematocysts are immersed in various salt solutions. Isolated *Calliactis* nematocysts contained predominantly Ca^{2+} and Mg^{2+} (Hidaka, 1993). If Ca^{2+} and Mg^{2+} in the isolated nematocysts are replaced by monovalent cations, the internal osmotic pressure would increase as one divalent cation is replaced by the two monovalent cations required to maintain electroneutrality. The swelling of the sea anemone nemato-

Figure 3. Scanning electron micrograph of isolated nematocysts used for X-ray microanalysis. The white spot represents the site irradiated with an electron beam during the acquisition of spectra. These nematocysts were isolated in DW and incubated in 1 *M* $MgCl_2$ for 10 min.

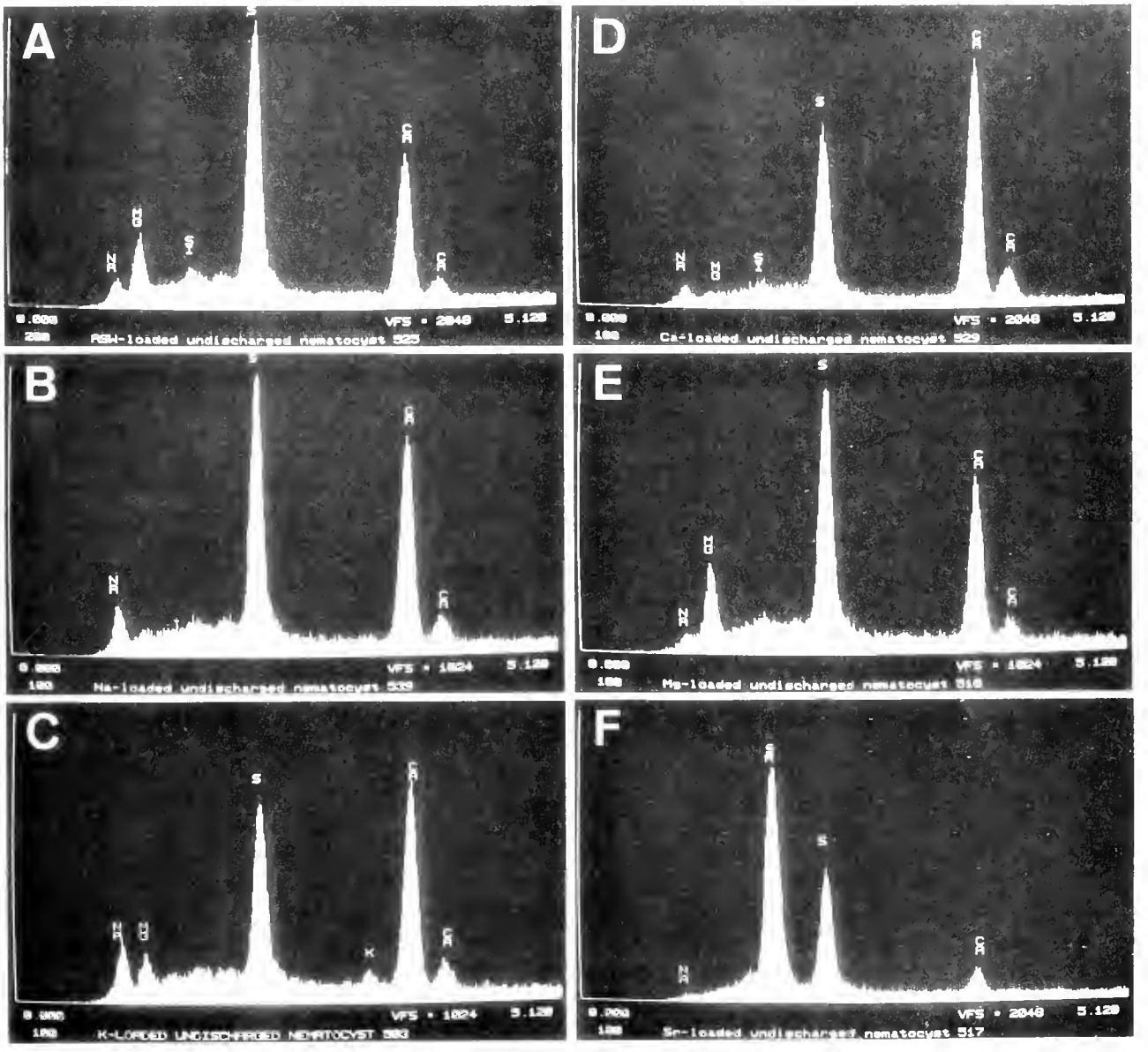

Figure 4. X-ray spectra of nematocysts incubated in various salt solutions. Nematocysts isolated in DW were incubated in ASW or 1 *M* solutions of various salts for 10 min. A, ASW; B, NaCl; C, KCl; D, $CaCl_2$; E, $MgCl_2$; F, $SrCl_2$.

cysts in 1 *M* NaCl or KCl might be partly due to an exchange of intracapsular divalent cations with monovalent cations in the bathing solution.

X-ray microanalysis of *Calliactis* nematocysts incubated in 1 *M* solutions of various salts for 10 min showed that the predominant cation in the nematocysts was not necessarily the cation in the incubation medium. The predominant cation in nematocysts incubated in 1 *M* NaCl, KCl, $MgCl_2$ and $CaCl_2$ was Ca^{2+}. Beside Ca^{2+}, Sr^{2+} is the only cation that replaced most of the cations in isolated nematocysts and accounted for about 90% of the cations contained in the nematocysts. This implies that Ca^{2+} in isolated nematocysts was replaced only partially, if at all, by externally applied cations. This contrasts with the observation that Ca^{2+} and Mg^{2+} found in isolated *Hydra* nematocysts can be replaced almost completely by externally applied cations (Weber, 1989). On the other hand, most of the Mg^{2+} in isolated nematocysts is replaced by externally applied Na^{2+}, since Mg^{2+} almost disappeared after incubation in 1 *M* NaCl.

However, it was difficult in this experiment to estimate what percentage of Ca^{2+} and Mg^{2+} in isolated nematocysts was actually replaced by externally applied cations. The present semiquantitative analyses do not provide a mea-

Table I

Relative abundance of metal elements in isolated Calliactis polypus *nematocysts incubated in various salt solutions*[1]

Solutions	Na	K	Ca	Mg	Sr	N[2]
ASW	10.9 ± 5.8	1.4 ± 0.4	52.5 ± 4.7	35.2 ± 2.4	0	5
1 *M* NaCl	26.6 ± 8.3	1.5 ± 0.2	71.7 ± 8.4	0.3 ± 0.4	0	4
1 *M* KCl	23.2 ± 7.1	2.6 ± 1.8	61.3 ± 7.1	13.0 ± 1.9	0	4
1 *M* $CaCl_2$	6.5 ± 6.1	1.6 ± 0.3	91.7 ± 6.3	0.2 ± 0.3	0	6
1 *M* $MgCl_2$	5.9 ± 5.9	0.8 ± 0.4	48.7 ± 5.7	44.5 ± 3.2	0	5
1 *M* $SrCl_2$	0	0	8.4 ± 0.3	0.7 ± 0.5	90.1 ± 0.3	4

[1] The relative abundance of each metal element is shown as a percentage of total metal elements listed. Means ± SD.
[2] Number of nematocysts analyzed.

sure of the absolute concentration of each metal but only their relative abundances. Some of the cations that have lower affinity for polyanions in the capsule might be lost during washing in DW. If this is the case, the actual concentration of Na^+ and K^+ in the nematocysts immersed in 1 *M* solutions of these monovalent cations must have been much higher than estimated. It is likely that most of the Mg^{2+} and some of the Ca^{2+} in isolated nematocysts are replaced by Na^+ or K^+ when the nematocysts are immersed in 1 *M* NaCl or KCl. Such divalent cation-monovalent cation exchange might at least partly account for the swelling of nematocysts in solutions containing high concentrations of monovalent cations.

Nematocysts isolated in ASW and those isolated in DW responded similarly to changes in external salt concentration. Nematocysts isolated in DW swelled as the external concentration of monovalent cations was increased. This is probably because a greater percentage of the divalent cations was replaced by monovalent cations as the concentration of external monovalent cations was raised. The volume of nematocysts isolated in ASW decreased as the concentration of external monovalent cations was lowered. It is unlikely that the decrease in the nematocyst volume was due to an exchange of intracapsular monovalent cations with external divalent cations, since the external solutions did not contain divalent cations. The affinity of divalent cations for polyanions might have become higher, and negative charges on the polyanions might have become neutralized, by tightly bound divalent cations as the ionic strength decreased. This might account for the decrease in the volume of the nematocysts at low monovalent cation concentrations.

Since Ca^{2+} reduced the volume of isolated nematocysts to a greater extent than Mg^{2+}, Ca^{2+} might have a higher affinity for polyanions than Mg^{2+}. The substitution experiments also show that Ca^{2+} had a higher affinity for polyanions than Mg^{2+}. Binding of Ca^{2+} to polyanions may mask some of the negative charges on the polyanions and thus reduce the number of osmotically active cations within the capsule. It is also possible that Ca^{2+} cross-links polyanions to reduce the number of osmotically active particles, as suggested by Lubbock *et al.* (1981). Thus, the osmotic pressure of the intracapsular fluid is determined not only by the Donnan-equilibrium, but also by the selective binding of Ca^{2+} to polyanions in the capsule. The present observations suggest that not only divalent-monovalent cation exchange but also exchange of intracapsular Ca^{2+} with Mg^{2+} in seawater will increase the internal osmotic pressure when Ca-containing nematocysts come into contact with seawater.

Lubbock *et al.* (1981) found high concentrations of Ca in undischarged holotrichous isorhiza nematocysts by X-ray microanalysis of frozen sections of mesenterial filaments of the sea anemone *Rhodactis rhodostoma* and acrorhagi of *Anthopleura elegantissima.* They observed that an influx of Na accompanies the efflux of Ca during discharge. Their observation is consistent with the above hypothesis that the osmotic pressure of the sea anemone nematocysts increases due to the exchange of intracapsular divalent cations with Na^+ in seawater. Lubbock *et al.* (1981) suggested that nematocysts become exposed to seawater at the time of discharge—after exocytotic fusion of the nematocyst membrane with the cell membrane. Robson (1973) observed that nematocysts of *Rhodactis rhodostoma* swell up to 150% of their original size when they are exposed to seawater immediately before discharge. This observation suggests that the osmotic pressure of sea anemone nematocysts increases when nematocysts are exposed to seawater.

Weber (1990, 1991) found that polyanions contained in nematocysts of *Hydra* and various marine cnidarians are poly(γ-glutamic acid)s with various degrees of polymerization. As for the cations associated with the polyanions, there are differences between species and between types of nematocysts. Tardent *et al.* (1990) reported that the predominant cation of marine cnidarian nematocysts is either Ca^{2+}, Mg^{2+} or K^+. The predominant cation of the tentacular and acontial nematocysts of *Calliactis par-*

asitica is K^+ as in *Hydra* nematocysts. The tentacular nematocysts of *Anthopleura elegantissima* and *Actinia equina* contain Mg^{2+} while the acrorhagial nematocysts of these species contain predominantly Ca^{2+} (Tardent *et al.*, 1990). The differences in the dominant cation among nematocysts of marine cnidarians suggest that the hypothesis of divalent-monovalent cation exchange is not applicable to all nematocysts of marine cnidarians but only to those that contain predominantly Ca^{2+} and/or Mg^{2+}.

Potassium was almost absent even in nematocysts incubated in 1 *M* KCl, indicating that K^+ had the lowest affinity for polyanions. This means that K^+ is the ideal cation to generate a high internal osmotic pressure if ionic distribution across the capsule wall is determined by a Donnan-equilibrium. K-containing nematocysts may encounter an osmotic pressure difference large enough to trigger discharge when they come into contact with seawater. If they fail to discharge, the internal osmotic pressure would decrease due to the exchange of intracapsular K^+ with Ca^{2+} and Mg^{2+} in seawater.

The problem with the hypothesis of divalent-monovalent cation exchange, is that exposure of nematocysts to seawater alone does not elicit discharge of the nematocysts, as shown by the fact that undischarged nematocysts can be isolated from marine cnidarians in ASW (*e.g.*, Hidaka and Mariscal, 1988). Yanagita (1959), however, found that nematocysts isolated from acontia of the sea anemone *Haliplanella luciae* in 1 *M* glycerol, discharged when immersed in concentrated salt solutions such as seawater and isotonic NaCl. He also reported that when nematocysts isolated in 1 *M* glycerol are immersed in diluted salt solutions such as 0.03 *M* $CaCl_2$, the nematocysts become unresponsive to concentrated salt solutions that would otherwise elicit discharge of the nematocysts. This suggests that the isolated nematocysts can remain undischarged if the salt concentration of the surrounding medium is increased gradually. During artificial isolation of nematocysts in ASW, changes in the ionic composition of the surrounding medium might be too slow to cause nematocyst discharge. Yanagita (1959) also noted that nematocysts liberated into a salt solution through cytolytic disintegration of acontia often remain undischarged.

Furthermore, nematocysts isolated in ASW did not discharge in 1 *M* NaCl or KCl. This suggests that the increase in the internal osmotic pressure caused by cation exchange may not be large enough to trigger discharge. However, the possibility remains that the rate of change in the ionic composition of the surrounding medium was too slow to trigger discharge, because solution exchange was performed by perfusing the test solution drop by drop. If the "stopper" (a sealing structure of nematocysts) is made of viscoelastic material, whether it fractures or not depends on the rate of deformation. Nematocysts would discharge only when the rate of increase in the internal osmotic pressure exceeds a certain limit. When nematocysts incubated in 1 *M* $CaCl_2$ were treated with 1 *M* NaCl using the present perfusion method, the volume of the nematocysts increased by 18% and 3–5% of them discharged (Hidaka and Afuso, unpub. ob.). It is likely that more nematocysts would discharge if the surrounding medium is changed more rapidly. The observation that isolated nematocysts did not discharge in 1 *M* NaCl or KCl does not necessarily contradict the hypothesis of divalent-monovalent cation exchange.

Nematocysts can be induced to discharge in media that contain no or only small amounts of monovalent cations by reagents that rupture disulfide bonds or chelate calcium (Hidaka, 1993). These reagents seem to induce discharge of nematocysts by weakening the nematocyst "stopper." The question of whether such weakening of the "stopper" is involved in the *in situ* mechanism of nematocyst discharge remains to be investigated.

The present results show that the volumetric behavior of isolated *Calliactis* nematocysts immersed in various salt solutions can be explained by the exchange of intracapsular divalent cations with cations in the external medium and by the selective binding of Ca^{2+} to polyanions in the capsule. It remains unknown whether the increase in the internal osmotic pressure caused by the cation exchange is large enough to trigger discharge, or whether nematocyst discharge involves biochemical modification of structural components such as the nematocyst "stopper."

Acknowledgments

The authors would like to thank Drs. R. A. Kinzie, III and M. J. Grygier for critically reading this manuscript.

Literature Cited

Gerke, I., K. Zierold, J. Weber, and P. Tardent. 1991. The spatial distribution of cations in nematocytes of *Hydra vulgaris*. *Hydrobiologia* **216/217:** 661–669.

Gupta, B. L., and T. A. Hall. 1984. Role of high concentration of Ca, Cu, and Zn in the maturation and discharge *in situ* of sea anemone nematocysts as shown by X-ray microanalysis of cryosections. Pp. 77–95 In *Toxins, Drugs, and Pollutants in Marine Animals*, L. Bolis, J. Zadunaisky, and R. Gilles, eds. Springer-Verlag, Berlin, Heidelberg.

Hidaka, M. 1992. Effects of Ca^{2+} on the volume of nematocysts isolated from acontia of the sea anemone *Calliactis tricolor*. *Comp. Biochem. Physiol.* **101A:** 737–741.

Hidaka, M. 1993. Mechanism of nematocyst discharge and its cellular control. *Adv. Comp. Envir. Physiol.* (in press)

Hidaka, M., and R. N. Mariscal. 1988. Effects of ions on nematocysts isolated from acontia of the sea anemone *Calliactis tricolor* by different methods. *J. Exp. Biol.* **136:** 23–34.

Lubbock, R., and W. B. Amos. 1981. Removal of bound calcium from nematocyst contents causes discharge. *Nature* **290:** 500–501.

Lubbock, R., B. L. Gupta, and T. A. Hall. 1981. Novel role of calcium in exocytosis: mechanism of nematocyst discharge as shown by X-ray microanalysis. *Proc. Natl. Acad. Sci. USA* **78:** 3624–3628.

Mariscal, R. N. 1988. X-ray microanalysis and perspectives on the role of calcium and other elements in cnidae. Pp. 95–113 in *The Biology of Nematocysts*, D. A. Hessinger and H. M. Lenhoff, eds. Academic Press, San Diego, New York.

Mazia, D., G. Schatten, and W. Sale. 1975. Adhesion of cells to surfaces coated with polylysine. Application to electron microscopy. *J. Cell Biol.* **66:** 198–200.

Robson, E. A. 1973. The discharge of nematocysts in relation to properties of the capsule. *Publ. Seto Mar. Biol. Lab.* **20:** 653–665.

Tardent, P., K. Zierold, M. Klug, and J. Weber. 1990. X-ray microanalysis of elements present in the matrix of cnidarian nematocysts. *Tissue Cell* **22:** 629–643.

Weber, J. 1989. Nematocysts (stinging capsules of Cnidaria) as Donnan-potential-dominated osmotic systems. *Eur. J. Biochem.* **184:** 465–476.

Weber, J. 1990. Poly(γ-glutamic acid)s are the major constituents of nematocysts in *Hydra* (Hydrozoa, Cnidaria). *J. Biol. Chem.* **265:** 9664–9669.

Weber, J. 1991. A novel kind of polyanions as principal components of cnidarian nematocysts. *Comp. Biochem. Physiol.* **98A:** 285–291.

Weber, J., M. Klug, and P. Tardent. 1987. Detection of high concentrations of Mg and Ca in the nematocysts of various cnidarians. *Experientia* **43:** 1022–1025.

Yanagita, T. M. 1959. Physiological mechanisms of nematocyst responses in sea-anemone II. Effects of electrolyte ions upon the isolated cnidae. *J. Fac. Sci. Univ. Tokyo Sect. IV* **8:** 381–400.

Reference: *Biol. Bull* **184:** 105–113. (February, 1993)

Hemocyanin Subunit Composition and Oxygen Binding in Two Species of the Lobster Genus *Homarus* and Their Hybrids

CHARLOTTE P. MANGUM

Bodega Marine Laboratory, University of California, P. O. Box 247, Bodega Bay, California 94923[1]

Abstract. The monomeric subunit composition and O_2 binding properties of the hemocyanins (Hcs) of *Homarus americanus, H. gammarus* and their hybrids are very similar, though not identical. *H. americanus* Hc has six major electrophoretically separable polypeptide chains; *H. gammarus* Hc has four major and two minor chains; and the hybrid Hc has four major and one minor chain. Four chains co-migrate in all three groups, and the fifth chain in the hybrid co-migrates with a fifth chain in *H. gammarus*. Thus, qualitatively, the hybrid Hc is more like that of *H. gammarus* than *H. americanus*, a similarity reflected in respiratory properties. Although the O_2 affinity of the hybrid hemocyanin appears to lie intermediate between that of the two parent hemocyanins at 25°C, in fact it is significantly different from that of *H. americanus* but not *H. gammarus*. The cooperativity of the hybrid Hc also differs significantly from that of *H. americanus* but not *H. gammarus* Hc. The distinctive properties of *H. americanus* hemocyanin at 25°C are believed to be due to either or both of two chains: a unique and also invariant chain in *H. americanus*, and one that is present in *H. gammarus* and the hybrids but not in *H. americanus*. *H. americanus* Hc also appears to be slightly less sensitive to the allosteric modulator L-lactate. No difference in $CaCl_2$ sensitivity was found. At lower temperatures respiratory properties are indistinguishable. In adult *H. americanus* that had been held under identical conditions for long periods, variation in subunit pattern was not entirely absent, but it was smaller than that found in natural populations of other species. No differences in O_2 binding at 25°C were found in morphs differing qualitatively in one chain and quantitatively in two others. No effect of a combination of rearing temperature and diet was found on the Hc subunit composition of juveniles.

Received 3 June 1992; accepted 8 October 1992.

Permanent address: [1]Department of Biology, College of William & Mary, Williamsburg, VA 23185-8795.

Introduction

The arthropod hemocyanins (Hcs) are multiples of hexamers built of 70–80 kDa polypeptide chains. Often the 2×6-mers predominate in the bloods of adult decapod crustaceans, including the lobster *Homarus americanus* (Olson *et al.*, 1988). The number of different monomers is usually large, with a dozen or more found in several species of *Uca* (Sullivan *et al.*, 1983; Callicott and Mangum, 1992; Mangum, 1992 and unpub. data). The monomers have been grouped into one of four categories on the basis of their electrophoretic mobilities, immunological reactions and roles in oligomer assembly (Markl, 1986). Within a species, the monomeric heterogeneity also plays a functional role in respiratory adaptation during the adult stage (Mason *et al.*, 1983; Mangum and Rainer, 1988; deFur *et al.*, 1990; Mangum *et al.*, 1991). By comparing morphs, the functional differences have been attributed to particular electrophoretic bands (Mangum and Rainer, 1988; Mangum *et al.*, 1991; Mangum, 1992).

The role of Hc subunit composition in bringing about functional differences between species is less clear. A survey of forty-two species of various degrees of taxonomic relatedness suggests a high degree of specificity (Reese and Mangum, 1992). More intensive investigation of the Hcs of seven species of the genus *Uca*, which are extremely polymorphic as well as heterogeneous, supports the inference of species specificity (Callicott and Mangum, 1992; Mangum, 1992; C. P. Mangum, unpub. data). In every case, including sibling species such as *U. panacea* and *pugilator*, even low frequency Hc morphs of a species can be readily distinguished from those of another. Functional

properties can also differ in sibling congeners with different latitudinal ranges. In comparisons of congeners that are less closely related, however, functional properties are more clearly related to environmental factors than to phylogenetic affinity or subunit composition (Reese and Mangum, 1992).

In the only two species in which the effect of laboratory acclimation has been examined, the subunit phenotype of an adult individual is not fixed (Mason *et al.*, 1983; deFur *et al.*, 1990; Callicott and Mangum, 1992). In *Callinectes sapidus,* moreover, the variation both in the laboratory and in nature can be related to environmental factors such as salinity and hypoxia (Mangum, 1990; Pihl *et al.*, 1991; C. P. Mangum and S. P. Baden, unpub. obs.). Thus the members of the highly polymorphic samples of natural populations may have been acclimated to different environmental (or nutritional) conditions.

Here I report data for the monomeric subunit composition and oxygen binding of the Hcs of the adults of two species of lobsters in the genus *Homarus* and the hybrid progeny of their spontaneous matings. The two parent species had been brought from their native Atlantic habitats to the Bodega Marine Laboratory, where they were held under identical conditions for periods far longer than the species investigated previously. They are known to be highly homozygous at 41 loci and, at most loci, the allozymic phenotypes of the two are either extremely similar or identical. It is believed that the two speciated allopatrically when isolated for the first time during the Pleistocene (Hedgecock *et al.*, 1977). In one species, I also examined the Hc subunit composition of juveniles which had been reared on either of two diets, and at different temperatures.

Materials and Methods

The sample

All available adults, a total of 36, were examined; they were large (28–42 cm from rostrum to tail), intermolt individuals. Two (one of each sex) belong to *Homarus gammarus* (Linnaeus), formerly known as *H. vulgaris;* they were collected near Iona, Scotland in 1975. They are the sole survivors of the larger sample characterized by Hedgecock *et al.* in 1977. Twenty-five adults (16 females, 9 males) are members of *Homarus americanus* H. Milne Edwards. All but one were caught on various dates in 1988–92 in waters surrounding Martha's Vineyard, Massachusetts, and had been held in the mariculture facility at the Bodega Marine Laboratory for periods ranging from three months (1 individual) to more than three years (3 individuals). One individual of *H. americanus* (age > 6 years) was born in the Bodega Marine Laboratory. Nine hybrid adults (7 fertile females, 2 infertile males) were progeny of spontaneous matings between *H. gammarus* and *americanus.* Most were produced in 1983 by a female *H. gammarus* and a male *H. americanus;* one, of unknown parentage, was born in 1978.

All adults had been fed the same diet of surf fish and shrimp, and had been held under identical photoperiods in the running seawater system of the Bodega Marine Laboratory. A seven year compilation of data (1985–91) indicates that the water temperature ranges from 10 to 15°C, and usually varies within about two degrees; over the four month period of sampling the salinity varied from 32.5–33.5‰, which is typical.

The Hc subunit composition of 14 juvenile *H. americanus* (8–10 cm length, both sexes), which had hatched in the Bodega Marine Laboratory 20–22 months earlier, was also examined. Half of these animals, which were their natural color, had been fed since stage IV a diet of brine shrimp, fish and crabs, and had been held at the seawater system temperature. The other half, phenotypic albinos, had been fed a diet based on casein; for the past year they had been held at room temperature (*ca.*, 23°C). The diets, rearing conditions and molt history of animals such as these were described in detail by Baum (1990).

Preparation of material and electrophoresis

Blood was taken from the base of the last leg and serum expressed from the clot in a tissue grinder. After centrifugation an aliquot of the material was dissociated to its monomers by dilution with 0.01 mol l^{-1} EDTA + 0.05 mol l^{-1} Tris (pH 8.9), to reduce light scattering; Hc concentration was estimated from the absorbance of dissociated material at 338 nm (Bausch & Lomb Spectronic 2000 spectrophotometer), using the extinction coefficient reported by Nickerson and van Holde (1971). An additional aliquot was diluted (1:10 or 1:30, depending on concentration) with the dissociating buffer for electrophoresis, and the remainder frozen for future use. Absorbance of the material from several individuals, detailed below, was compared at 280 and 338 nm.

PAGE electrophoresis of native monomers was carried out at constant current according to Hames and Rickwood (1985). Following determination of the Hc phenotype in each individual, the variants among *H. americanus* were examined several times in adjacent lanes on the same gels. Representatives of each of the three groups were also compared many times on the same gels. Finally, gels were overloaded with six times the usual amount of material, the presence of Cu was determined according to Bruyninckx *et al.* (1978), and then the gels were stained as usual with Coomassie Blue.

Oxygen binding

On the basis of the PAGE, particular individuals were selected for a second bleeding, performed within a week

of the final phenotype determination. Serum was dialyzed overnight, against seawater for most of the measurements or against a Tris maleate buffered salt for the experiments on inorganic ion sensitivity. Oxygen binding was determined within a few days, using the cell respiration method (Mangum and Lykkeboe, 1979).

Data analysis

Bohr plots of the values for P_{50} (oxygen affinity) were described by regression lines and their 95% confidence intervals compared. Mean values for n_{50} (cooperativity) and Hc concentration were compared by Student's *t*-test. The data for O_2 binding as a function of [$CaCl_2$] were analyzed similarly. However, the nonlinearity of the response of P_{50} to [NaCl] and [Na_2SO_4] precluded statistical analysis.

Results

Hemocyanin concentration

Adults of *Homarus americanus* had significantly ($P = .02$) higher levels of Hc [6.11 (±0.41 S.E.) g 100ml^{-1}] than the hybrids [4.18 (±0.70 S.E.) g 100 ml^{-1}]. The values for the two members of *H. gammarus* (2.75 and 4.84 g 100 ml^{-1}) also fall below the 95% confidence interval around the mean of the *H. americanus* sample. In the *H. americanus* data there is no clear trend with length of time in the laboratory, suggesting that the nutritional state of the animals was good. The juveniles of this species had considerably lower Hc concentrations [1.02 (±0.15) g 100 ml^{-1}], which were unrelated to diet.

Monomeric subunit composition

The two adult *Homarus gammarus* had identical Hc phenotypes, which were also the same as that of one of the two individuals examined two years earlier (C. P. Mangum, unpub. obs.). Four high density (or major) and two intermediate density (or minor) electrophoretic bands separated by charge (Fig. 1). All six were positive for Cu.

The 25 adults of *H. americanus* exhibited very similar but not identical Hc phenotypes (Fig. 1). As many as eight bands separated on the lower third of the gels, four of which had co-migrants in *H. gammarus* (Fig. 1). The two most anodic bands (1 and 2) were always present in trace quantities, if at all. Material at their position appeared to quench the fluorescence of bathocuproine sulfonate, indicating the presence of Cu. However, it was not possible to ascertain the site of the quenching more precisely; only one of the two may contain Cu. These bands had no co-migrants in *H. gammarus* or the hybrids.

In *H. americanus* bands 3–8 could reach high concentrations. The gels on which the best separation was obtained exhibited less density in the middle of the material designated as bands 3 and 4, suggesting the presence of two chains that are similar in charge and extremely difficult to resolve. Moreover, the leading edge of this material clearly co-migrated with bands 2 in the hybrid and 3 in *H. gammarus*, whereas the trailing edge clearly lagged behind. Thus I assigned two numbers (3 and 4) to this position of the *H. americanus* material, even though the separation was not great enough to photograph. In addition, I was not able to decide whether the trailing material was present in all 25 individuals. The quantities of chains 6 and 7 in *H. americanus* are similar to the corresponding ones in *H. gammarus*, but chains 4 and 8 always occurred in higher levels in *H. americanus* than *H. gammarus* (Fig. 1).

In the early PAGE, band 5 in *H. americanus* did not appear to be sharply delineated at its leading and trailing edges. It was the only high density band that clearly varied qualitatively as well as quantitatively, ranging from absent (3 adults) to low concentration (5) to high concentration (17). Since I suspected that this band might not be a Hc chain, I examined the ratio of the absorbance at the protein peak (280 nm) and the active site (338 nm). According to this index, however, the total Cu content of *H. americanus* samples containing maximal levels of band 5 did not clearly differ from those that lacked it; nor did it differ from the samples from *H. gammarus* and the hybrids, none of which contained co-migratory material. In addition, on subsequent gels band 5 was as sharply delineated as the rest (Fig. 1).

Bands 6 and 8 varied quantitatively, though the magnitude was not great. They decreased concomitantly to intermediate levels in two of the 25 animals; band 8 was intermediate in two additional individuals in which band 6 remained maximal. Band 7 appeared to be absent in a single individual in which 6 and 8 were maximal. This female, from which larvae had hatched two months earlier, had been in the laboratory for only three months. All other individuals had maximal levels of these three chains.

Although I did not investigate material held at temperatures above freezing, there was no correlation between phenotype and age of frozen preparations; this has been true in my experience with Hcs from all species examined thus far. In the present case the same banding pattern was observed before and after four months. Finally, material prepared on a second occasion from four of the same individuals three months after the first bleeding showed no change in phenotype.

The hybrids, all adults, exhibited a single phenotype which did not vary quantitatively or qualitatively. With the exception of the higher levels of band 2, it resembles the phenotype of *H. gammarus* more than that of *H. americanus* (Fig. 1). The hybrid Hc has four major chains and one minor chain, all of which correspond in mobility

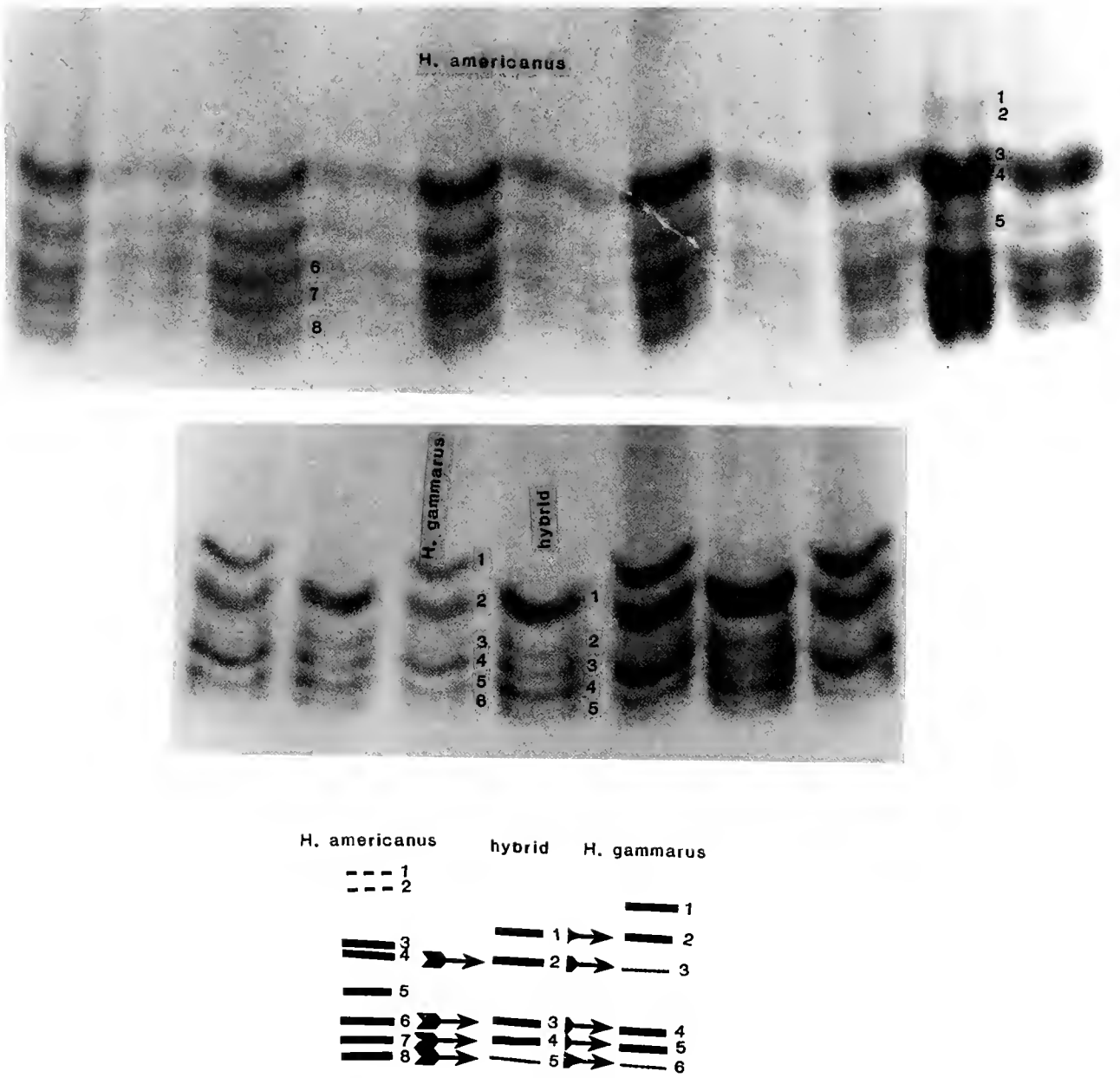

Figure 1. Banding patterns of the dissociated hemocyanins of the two parent species of *Homarus* and their hybrids, and a diagram illustrating the correspondence (arrows) of band positions. The anode is at the top. In the gel for *H. americanus*, each pair of lanes shows a sample from a different individual in higher (left) and lower (right) concentrations. The lanes on the far right were overloaded to show the anodic material (numbered 1 and 2) that occurs in trace quantities. The cathodic triplet of bands in this species is more clearly shown in lanes that were not overloaded. The middle panel shows *H. gammarus* (1 individual) and the hybrid Hc (1 individual) in alternating lanes.

to one of the six chains of *H. gammarus*. The hybrids differ from both parents, but from *H. gammarus* only in the absence of the most anodic band (*H. gammarus* band 1) and the higher levels of hybrid band 2. They differ from *H. americanus* in the absence of its three most anodic bands (*H. americanus* bands 1–3), in the absence of *H. americanus* band 5, in the consistently lower quantity of their most cathodic chain (hybrid band 5) and in the presence of a distinctive band 1.

As in all other species I have examined (*e.g.*, Mangum *et al.*, 1985; Mangum, 1992), the phenotypes of males and females in each of the three groups were indistinguishable—no sex specific material was present.

The juvenile *H. americanus* were indistinguishable from the adults. Six of the seven members of each dietary-thermal group had the maximum number of bands. One in each group lacked chain 5. Chains 6–8 were invariably present in maximal concentrations.

Oxygen binding

First, the intraspecific variation in *H. americanus* was examined. One adult lacked band 5 and also had minimal (=intermediate) levels of chains 6 and 8; at 25°C, however, the oxygen binding properties of its Hc (stripped of organic co-factors) were indistinguishable from those of another individual containing maximal amounts of all eight bands. Therefore the data have been combined for presentation. The coefficient of determination (r^2) for the regression line describing P_{50} in Figure 2 is 0.962, further affirming the absence of a perceptible effect of phenotype. The single individual with low quantities of band 7 had been sacrificed at the time the O_2 binding measurements were performed.

Second, the Hcs of the two parent species were compared. At all but the lowest pH investigated, Hc O_2 affinity at 25°C is significantly lower in *H. gammarus* than *H. americanus*, though the difference is fairly small (Fig. 2). Third, the hybrid Hc was compared with each of the parent Hcs. Whereas the data for the hybrid Hc appear to be intermediate between those for the two parent species, the difference from *H. gammarus* is not significant even in the middle of the pH range investigated. In contrast, the difference between the hybrid and *H. americanus* is significant throughout most of the pH range examined (>7.2).

The mean value for cooperativity is somewhat smaller (P = .001) in *H. americanus* (3.24 ± .11 S.E.) than *H. gammarus* and the hybrids (3.95 ± .13), which do not differ from one another (P = .15). Thus the respiratory properties of the hybrid Hc are also more like those of *H. gammarus* than *H. americanus*.

At lower temperatures, the significant differences disappear completely. Ninety-five percent confidence intervals around regression lines fit to the O_2 affinity data in Figure 3 overlap fully throughout the pH range investigated. Often this is true because the numerical values diminish and are thus more difficult to distinguish, but in this example there is not even an apparent trend. Mean values for cooperativity do not differ (P = .2–.8). As a result, *H. americanus* Hc is less temperature sensitive than the other two Hcs, though only in the 15–25°C range. For that range, the apparent heat of oxygenation (ΔH) is only −2.4 kcal mol^{-1} for *H. americanus* Hc (pH 7.6), whereas the value for the hybrid Hc is −5.6, and the value for *H. gammarus* Hc is −6.6. For the range 5–15°C the value of ΔH for all three Hcs is −9.4 kcal mol^{-1} (same pH).

H. americanus Hc is slightly less sensitive to the allosteric effector L-lactate (Fig. 4) than *H. gammarus* Hc; once again, the sensitivity of the hybrid Hc appears to be intermediate. At pH 7.6 the addition of 10 mmol l^{-1} lactate changes log P_{50} of *H. americanus* Hc by 0.166, *H. gammarus* Hc by 0.232, and the hybrid Hc by 0.203. However, O_2 affinity in *H. gammarus* and the hybrids is

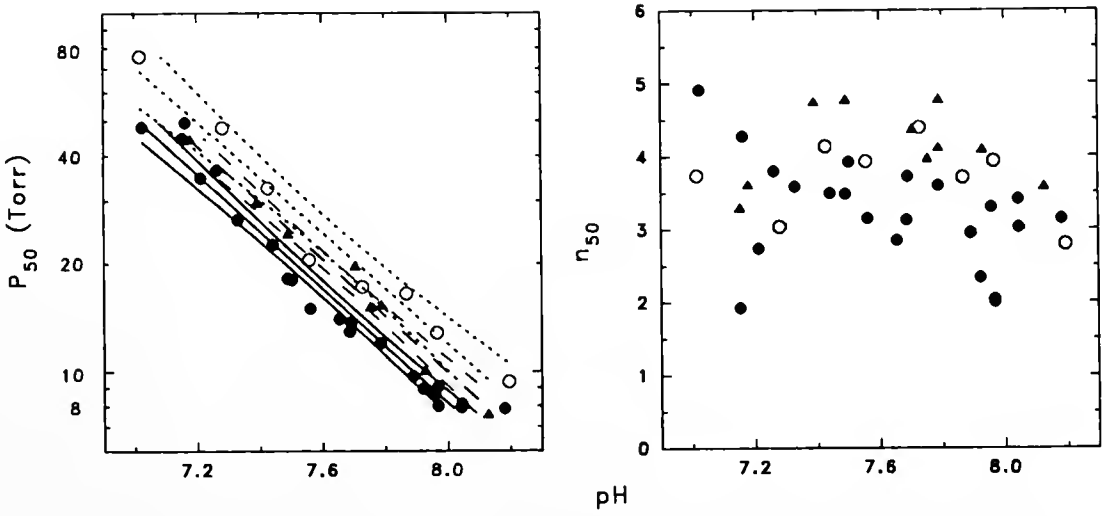

Figure 2. Oxygen binding at 25°C of *Homarus americanus* (closed circles, solid lines), *H. gammarus* (open circles, dotted lines) and their hybrid (triangles, dashed lines) hemocyanins. The curves are fitted regression lines ± 95% confidence intervals. 0.05 mol l^{-1} Tris maleate buffered seawater. Material obtained from two individuals of *H. americanus* was used (see text), whereas *H. gammarus* and the hybrids are represented by a single individual.

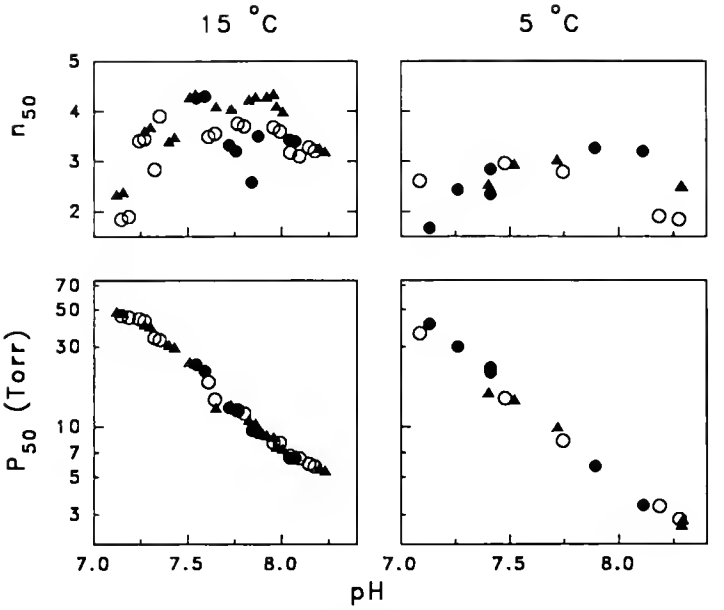

Figure 3. Oxygen binding at 15 and 5°C of *H. americanus* (closed circles), *H. gammarus* (open circles) and their hybrid (triangles) hemocyanins. The regression lines and confidence intervals were omitted for clarity. 0.05 mol l^{-1} Tris maleate buffered seawater. Origin of material as in Figure 2.

not quite significantly different in the presence of lactate, even in the middle of the pH range. In the presence of lactate, O_2 affinity of *H. gammarus* Hc remains significantly lower than that of *H. americanus* throughout the pH range investigated. In contrast, the hybrid Hc has a significantly lower O_2 affinity than that of *H. americanus* Hc only at high pH. In all three groups cooperativity is significantly diminished in the presence of lactate. The mean value drops from 3.2 to 2.86 ± .05 S.E. (P = .05) for *H. americanus* Hc, from almost 4 to 3.06 ± .24 (P = .05) for *H. gammarus* Hc, and from almost 4 to 2.95 ± .29 (P = .002) for the hybrid Hc.

The sensitivity of the three Hcs to $CaCl_2$ is indistinguishable (Fig. 5). Regression lines and their 95% confidence intervals overlap fully throughout the concentration range investigated. Mean values for cooperativity do not differ (P = .50–.75).

NaCl clearly raises Hc O_2 affinity and lowers cooperativity of *H. americanus* Hc (Fig. 5). Once again, however, the different morphs were indistinguishable, and the data were combined for presentation. In contrast to the allosteric effect of Ca^{2+}, the relationship between P_{50} and NaCl is nonlinear on logarithmic coordinates. I used high concentrations of Na_2SO_4, prepared from the decahydrate,

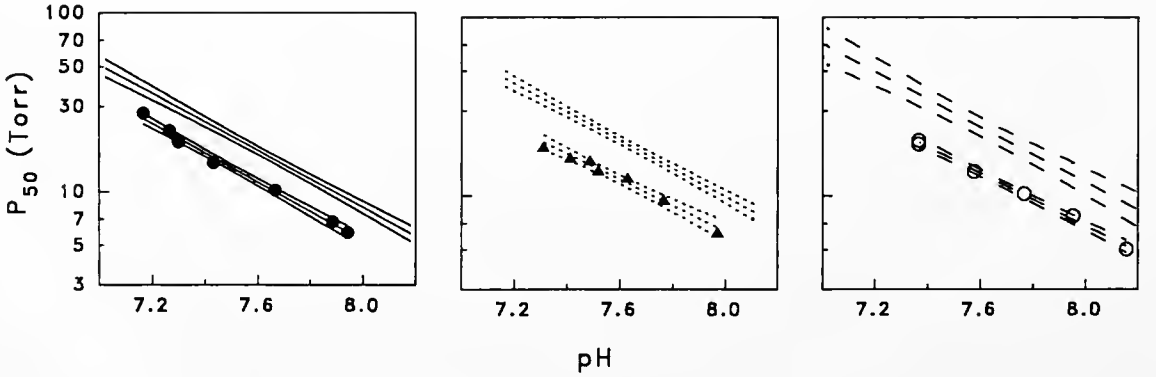

Figure 4. Lactate sensitivity of *H. americanus* (left panel: closed circles, solid regression lines ± 95% confidence intervals), *H. gammarus* (right panel: open circles, dotted lines) and their hybrid (middle panel: triangles, dashed lines) hemocyanins. Origin of material as in Figure 2. Control curves reproduced in each panel from Figure 2. 25°C, 0.05 mol l^{-1} Tris maleate buffered seawater.

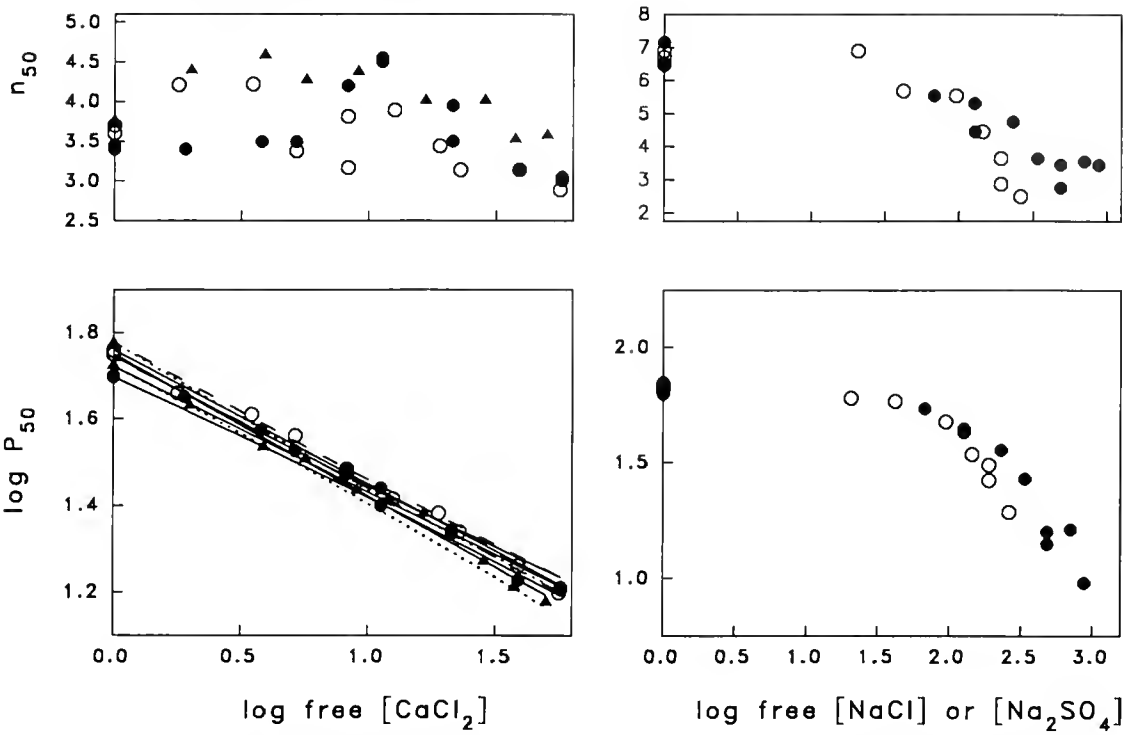

Figure 5. Inorganic ion sensitivities of lobster hemocyanins. The units of free ion concentrations (antilogs) are mmol l^{-1}. Left panels: *H. americanus* (closed circles, solid lines), *H. gammarus* (open circles, dashes) and their hybrids (triangles, dots). 0.05 mol l^{-1} Tris maleate buffer (pH 7.7) + 0.1 mol l^{-1} NaCl. Right panels: the response of *H. americanus* Hc to NaCl (closed circles) and Na_2SO_4 (open circles). 0.05 mol l^{-1} Tris maleate + 0.01 mol l^{-1} $CaCl_2$, 25°C. Origin of material as in Figure 2.

to examine specificity. The response differed very little from that of NaCl (Fig. 5), and the apparent difference may lie within the error of preparing an accurate solution of a highly hydrated salt (especially at a marine laboratory).

Discussion

The essentially non-specific sensitivity of *Homarus americanus* Hc to NaCl is further evidence that the inorganic ion responses of the crustacean Hcs are not all alike. The response of this Hc differs from that of portunid crab Hcs (Truchot, 1975; Mason *et al.*, 1983), which are insensitive to NaCl, but resembles that of penaid shrimp Hcs (Brouwer *et al.*, 1978; Mangum and Burnett, 1985). From a physiological point of view, however, NaCl sensitivity is unlikely to be important in *H. americanus*, a stenohaline species.

According to Hedgecock *et al.* (1977 and pers. comm.), the genetic distance between the two parent species of *Homarus*, though significant, is so small that the numerical value is closer to expectation for subspecies than species. Thus it is of particular interest that the present findings support the inference of species specificity of Hc subunit composition (Reese and Mangum, 1992). Although *H. gammarus* is monomorphic for the common *H. americanus* allele at 30 allozymic loci, neither of the two parent Hcs in the present sample could be confused with the other. As in the sibling species of *Uca* (Mangum, 1992 and unpub. obs.), this inference is true in spite of intraspecific variation. In *H. americanus*, band 3 is both diagnostic of the species and, at least in the present sample, invariant. Material that co-migrates with chains 1 and 2 of *H. gammarus* is clearly absent from *H. americanus*. Furthermore, the hybrid Hc is structurally distinct from either parent.

The present findings also support the inference of little interspecific genetic distance. Even though they are not identical, the two parent Hcs are more similar than any of the *ca.* 50 Hcs we have examined thus far, with the exception of *Menippe adina* and *M. mercenaria* Hcs (Reese 1989). Like the lobsters, these two sibling species of stone crabs are also believed to have speciated recently, and they also hybridize spontaneously (Bert, 1986).

In both structural and functional properties the hybrid Hc resembles that of one parent more than the other. It has only one less chain than *H. gammarus* Hc but several fewer than *H. americanus* Hc. The electrophoretic be-

havior of each of the five hybrid chains is identical to that of some one of the *H. gammarus* chains, whereas hybrid chain 1 has no co-migrant in *H. americanus*. These relationships are reflected in the O_2 binding of the Hcs in a complete saline, though only at high temperature.

In stage IV through adult *H. americanus*, SDS PAGE separates three Hc chains (Olson *et al.*, 1988; Olson and McDowell, 1989). As is often the case (*e.g.*, Sullivan *et al.*, 1983), additional bands are revealed when the separation is made by charge.

In neither juveniles nor adults of this species can the Hc be categorized as strictly monomorphic at the level of quaternary structure, despite prolonged acclimation of the donors. Moreover, in juveniles the variation is distinctive of neither the stage nor the thermal-nutritional history. In both stages, however, the variation is much smaller than in samples of natural populations of several species of brachyuran crabs (Mangum, 1990, 1992; Callicott and Mangum, 1992). This generalization is true of respiratory properties of the adults as well. Although the sample size is much smaller in the present investigation, the inference remains unchanged when the comparison is made with, for example, the 14–20 individuals of *Callinectes sapidus* investigated by Mangum *et al.* in 1991.

I emphasize that the small amount of Hc variation found here may not accurately represent natural populations of *H. americanus* (much less *H. gammarus*). Nor is it clear that the lack of variation results from prolonged acclimation rather than limited genetic diversity, as found at other loci (Tracey *et al.*, 1975; Hedgecock *et al.*, 1977). However, I note that the inference of allozymic similarity in the species was made from samples of populations on either side of Cape Cod but not Cape Hatteras, the greater geographic barrier (*e.g.*, Friedrich, 1973; National Geographic Society, 1985).

The present findings suggest that, given the common acclimation, the differences observed both within *H. americanus*, and between this species and the other two groups, represent a fixed condition in an adult individual. Although only intermolt animals were investigated here, the finding of no change with molt stage in *Callinectes sapidus* (Mangum *et al.*, 1985) has recently been confirmed in *H. americanus* (N. B. Terwilliger, pers. comm.). More important in the present context, the virtual identity of most respiratory properties of the three Hcs appears to reflect the notable similarity of the electrophoretic phenotypes. Conversely, it is reasonable to suggest that the slightly higher O_2 affinity and lower cooperativity of *H. americanus* Hc at high temperature are due to the chains that are unique to one of the three groups. Perhaps the most likely candidate is chain 2 in *H. gammarus* (=1 in the hybrids), which is absent in *H. americanus*. However, the possibility that band 3 is invariant as well as unique to *H. americanus* cannot be excluded. Bands 1 and 2 are never present in *H. americanus* in more than trace quantities, and morphs containing or lacking chain 5 did not differ in O_2 binding. The latter inference would be unwarranted only if the effect of chain 5 was exactly compensated by an equal and opposite effect of chains 6 and 8, which were also variables in the comparison.

Acknowledgments

Supported by NSF DCB 88-16172 (Physiological Processes). I am extremely grateful to the University of California for a Research Fellowship and to the Bodega Marine Laboratory for its unfailing hospitality.

Literature Cited

Baum, N. A. 1990. Studies on the role of dietary protein and lecithin in molting and cholesterol transport in juvenile lobsters, *Homarus* sp. M. A. Thesis, Sonoma State University, Rohnert Park, Cal., 65 pp.

Bert, T. M. 1986. Speciation in western Atlantic stone crabs (genus *Menippe*): the role of geologic processes and climatic events in the formation and distribution of species. *Mar. Biol.* **93:** 157–170.

Brouwer, M., C. Bonaventura, and J. Bonaventura. 1978. Analysis of the effect of three different allosteric ligands on oxygen binding by hemocyanin of the shrimp *Penaeus setiferus*. *Biochem.* **17:** 2148–2154.

Bruyninckx, W. J., S. Gutteridge, and H. S. Mason. 1978. Detection of copper on polyacrylamide gels. *Analyt. Biochem.* **89:** 174–177.

Callicott, K. A., and C. P. Mangum. 1992. Phenotypic variation and lability of the subunit composition of the hemocyanin of *Uca pugilator*. *J. Exp. Mar. Biol. Ecol.* (in press).

deFur, P. L., C. P. Mangum, and J. E. Reese. 1990. Respiratory responses of the blue crab *Callinectes sapidus* to longterm hypoxia. *Biol. Bull.* **178:** 46–54.

Friedrich, H. 1973. *Marine Biology*. University of Washington Press, United Kingdom. 474 pp.

Hames, B. D., and D. Rickwood. 1985. Gel Electrophoresis of Proteins. IRL Press, Oxford. 290 pp.

Hedgecock, D., K. Nelson, J. Simons, and R. Shleser. 1977. Genic similarity of American and European species of the lobster genus *Homarus*. *Biol. Bull.* **152:** 41–50.

Mangum, C. P. 1990. Inducible O_2 carriers in the crustaceans. Pp. 92–103 in *Animal Nutrition and Transport Processes. 2. Transport, Respiration and Excretion: Comparative and Environmental Aspects*, J.-P. Truchot and B. Lalou, eds. Karger, Basel, Switzerland.

Mangum, C. P. 1992. Structural and functional polymorphism of the hemocyanin O_2 transport system of the sand fiddler crab, *Uca pugilator*. *J. Exp. Mar. Biol. Ecol.* (in press).

Mangum, C. P., and L. E. Burnett. 1986. The CO_2 sensitivity of the hemocyanins and its relationship to Cl^- sensitivity. *Biol. Bull.* **171:** 248–263.

Mangum, C. P., and G. Lykkeboe. 1979. The influence of inorganic ions and pH on the oxygenation properties of the blood in the gastropod mollusc *Busycon canaliculatum*. *J. Exp. Zool.* **207:** 417–430.

Mangum, C. P., and J. S. Rainer. 1988. The relationship between subunit composition and oxygen binding of blue crab hemocyanin. *Biol. Bull.* **174:** 77–82.

Mangum, C. P., J. Greaves, and J. S. Rainer. 1991. Oligomer composition and oxygen binding of the hemocyanin of the blue crab *Callinectes sapidus*. *Biol. Bull.* **181:** 453–458.

Mangum, C. P., B. A. McMahon, P. L. deFur, and M. I. Wheatly. 1985. Gas exchange, acid-base balance and the oxygen supply to

tissues during a molt of the blue crab, *Callinectes sapidus* Rathbun. *J. Crust. Biol.* **5:** 207–215.

Mason, R. P., C. P. Mangum, and G. Godette. 1983. The influence of inorganic ions and acclimation salinity on hemocyanin–oxygen binding in the blue crab *Callinectes sapidus*. *Biol. Bull.* **164:** 104–123.

Markl, J. 1986. Evolution and function of structurally diverse subunits in the respiratory protein hemocyanin from arthropods. *Biol. Bull.* **171:** 90–115.

National Geographic Society. 1985. *Atlas of North America.* Washington, DC. Pp. 66–67.

Nickerson, K. W., and K. E. van Holde. 1971. A comparison of molluscan and arthropod hemocyanin. I. Circular dichroism and absorption spectra. *Comp. Biochem. Physiol.* **39B:** 855–872.

Olson, K., N. B. Terwilliger, and J. McDowell Capuzzo. 1988. Structure of hemocyanin in larval and adult lobsters. *Am. Zool.* **28:** 47A.

Olson, K. S., and J. McDowell. 1989. Structure and function of hemocyanin in American lobsters. *Am. Zool.* **29:** 20A.

Pihl, L., S. P. Baden, and R. J. Diaz. 1991. Effects of periodic hypoxia on distribution of demersal fish and crustaceans. *Mar. Biol.* **108:** 349–360.

Reese, J. E. 1989. Structure and function of crustacean hemocyanins. MA Thesis, College of William and Mary, Williamsburg, VA. 75 pp.

Sullivan, B., L. Pennell, B. Hutchison, and R. Hutchings. 1983. Genetics and evolution of the hemocyanin multigene-I. Genetic variability in *Uca pugilator* from Beaufort, NC. *Comp. Biochem. Physiol.* **76B:** 615–618.

Tracey, M. L., K. Nelson, D. Hedgecock, R. A. Shleser, and M. L. Pressiek. 1975. Biochemical genetics of lobsters: Genetic variation and the structure of American lobsters (*Homarus americanus*) populations. *J. Fish. Res. Board Can.* **32:** 2091–2101.

Truchot, J.-P. 1975. Factors controlling the *in vitro* and *in vivo* oxygen affinity of the hemocyanin of the crab, *Carcinus meanas*. *Resp. Physiol.* **24:** 173–189.

CONTENTS

Volume 184 Number 2

THE BIOLOGICAL BULLETIN

APRIL, 1993

Published by the Marine Biological Laboratory

1993 LATE SUMMER COURSES AT THE MBL

History of Biology: Human Genetics in the Twentieth Century
(AUGUST 1-AUGUST 11, 1993)
APPLICATION DEADLINE: MAY 21, 1993
Open to students from a wide variety of backgrounds and ranks who share an interest in the history and philosophy of human genetics and eugenics. This course will focus on the history of human genetics in the United States, Great Britain, France, Germany and Russia in the twentieth century. Themes will include clinical and eugenic aspects of human genetic studies, the history of efforts to control human evolution, ethical questions arising from present as well as past attempts at such control, and the social construction of scientific knowledge. ***Directors: Garland Allen, Washington University; John Beatty, University of Minnesota; and Jane Maienschein, Arizona State University.***

Methods in Computational Neuroscience *(AUGUST 3-AUGUST 31, 1993)*
APPLICATION DEADLINE: MAY 21, 1993
This intensive, four week computer laboratory and lecture course for 23 advanced graduate students, postdoctoral fellows and faculty, will examine how the biophysical and biochemical properties of neurons and synapses, together with the architecture of neural circuits, produce observed animal behavior. Lecture material will include the dynamics of individual neurons and synapses; the use of exact models of single cells versus reduced neural models in analysis of networks; the coding and processing of external stimuli within nervous systems; development of the nervous system; and applied mathematics. In the laboratory, specific aspects of nervous systems will be modeled using a UNIX graphic-color workstation and software designed for the analysis of both single-cell dynamics and large network properties. ***Directors: David Kleinfeld and David W. Tank, Biological Computation Research Department, Bell Laboratories, Murray Hill, NJ.***

Molecular Evolution *(AUGUST 8-AUGUST 20, 1993)*
APPLICATION DEADLINE: JUNE 1, 1993
A series of lectures and discussions exploring multiple approaches to molecular evolution, and a computer laboratory for phylogenetic and sequence analysis. Designed for a class of 60 established investigators, postdoctoral fellows, and advanced graduate students, this two week program will provide a forum for exchange of information among organismic and molecular biologists and ecologists. ***Director: Mitchell L. Sogin, Marine Biological Laboratory.***

Cellular and Molecular Neurobiology and Development of the Leech
(AUGUST 8-AUGUST 28, 1993)
APPLICATION DEADLINE: JUNE 1, 1993
This course is for 12 graduate and postdoctoral students and independent investigators interested in applying diverse experimental approaches (electrophysiology, biophysics, cellular and molecular biology) to the study of the nervous system and development of a single organism. Students will learn techniques and concepts of modern experimental embryology, including lineage tracing, cell cycle analysis and the analysis of gene expression by in situ hybridization and immunohistochemical procedures. Students will also use patch clamp techniques to study whole cell and single channel transmembrane currents in situ and in isolated neurons in culture . ***Directors: Pierre Drapeau, McGill University; and David Weisblat, University of California, Berkeley.***

Pathogenesis of Neuroimmunologic Diseases *(AUGUST 15-AUGUST 27, 1993)*
APPLICATION DEADLINE: MAY 4, 1993
This course for 30 advanced graduate students, postdoctoral fellows, and junior faculty in neurosciences and immunology, and for residents in neurology, neurosurgery or psychiatry, will consist of lectures and discussions describing the application of genetic, molecular, and cell physiologic concepts and techniques in current use in immunology and neurophysiology to the analysis of pathogenesis in the better known neurologic and psychiatric diseases thought to have an immunologic basis. ***Directors: J. Murdoch Ritchie, Yale University; and Byron H. Waksman, Harvard and New York Universities.***

Optical Microscopy and Imaging in the Biomedical Sciences
(OCTOBER 20-OCTOBER 28, 1993)
APPLICATION DEADLINE: JULY 19, 1993
Designed for 22 research scientists, physicians, postdoctoral trainees, and advanced graduate students in animal, plant, medical, and material sciences, as well as non-biologists seeking a comprehensive introduction to microscopy and video-imaging. The course consists of lectures, laboratory exercises, demonstrations, and discussions that will enable the participant to obtain and interpret microscope images of high quality, to perform quantitative optical measurements, and to produce photographic and video records for documentation and analysis. Instruction on state-of-the-art equipment will be provided by experienced staff from universities and industry. ***Director: Colin S. Izzard, State University of New York at Albany.***

FOR FURTHER INFORMATION AND APPLICATION FORMS contact:
Ms. Dorianne Chrysler, Admissions Coordinator, **Marine Biological Laboratory**, Woods Hole, MA 02543, USA; (508) 548-3705, ext. 401.

THE
BIOLOGICAL BULLETIN

PUBLISHED BY
THE MARINE BIOLOGICAL LABORATORY

APRIL, 1993

Printed and Issued by
LANCASTER PRESS, Inc.
3575 HEMPLAND ROAD
LANCASTER, PA

THE BIOLOGICAL BULLETIN is published six times a year by the Marine Biological Laboratory, MBL Street, Woods Hole, Massachusetts 02543.

Subscriptions and similar matter should be addressed to Subscription Manager, THE BIOLOGICAL BULLETIN, Marine Biological Laboratory, Woods Hole, Massachusetts 02543. Single numbers, $35.00. Subscription per volume (three issues), $87.50 ($175.00 per year for six issues).

Communications relative to manuscripts should be sent to Michael J. Greenberg, Editor-in-Chief, or Pamela L. Clapp, Managing Editor, at the Marine Biological Laboratory, Woods Hole, Massachusetts 02543. Telephone: (508) 548-3705, ext. 428. FAX: 508-540-6902. E-mail: pamel@hoh.mbl.edu.

POSTMASTER: Send address changes to THE BIOLOGICAL BULLETIN, Marine Biological Laboratory, Woods Hole, MA 02543.

Second-class postage paid at Woods Hole, MA, and additional mailing offices.
ISSN 0006-3185

INSTRUCTIONS TO AUTHORS

The Biological Bulletin accepts outstanding original research reports of general interest to biologists throughout the world. Papers are usually of intermediate length (10–40 manuscript pages). A limited number of solicited review papers may be accepted after formal review. A paper will usually appear within four months after its acceptance.

Very short, especially topical papers (less than 9 manuscript pages including tables, figures, and bibliography) will be published in a separate section entitled "Research Notes." A Research Note in *The Biological Bulletin* follows the format of similar notes in *Nature*. It should open with a summary paragraph of 150 to 200 words comprising the introduction and the conclusions. The rest of the text should continue on without subheadings, and there should be no more than 30 references. References should be referred to in the text by number, and listed in the Literature Cited section in the order that they appear in the text. Unlike references in *Nature*, references in the Research Notes section should conform in punctuation and arrangement to the style of recent issues of *The Biological Bulletin*. Materials and Methods should be incorporated into appropriate figure legends. See the article by Lohmann *et al.* (October 1990, Vol. **179**: 214–218) for sample style. A Research Note will usually appear within two months after its acceptance.

The Editorial Board requests that regular manuscripts conform to the requirements set below; those manuscripts that do not conform will be returned to authors for correction before review.

1. ***Manuscripts.*** Manuscripts, including figures, should be submitted in triplicate. (Xerox copies of photographs are not acceptable for review purposes.) The original manuscript must be typed in no smaller than 12 pitch, using double spacing (*including* figure legends, footnotes, bibliography, etc.) on one side of 16- or 20-lb. bond paper, 8½ by 11 inches. Please, no right justification. Manuscripts should be proofread carefully and errors corrected legibly in black ink. Pages should be numbered consecutively. Margins on all sides should be at least 1 inch (2.5 cm). Manuscripts should conform to the *Council of Biology Editors Style Manual*, 5th Edition (Council of Biology Editors, 1983) and to American spelling. Unusual abbreviations should be kept to a minimum and should be spelled out on first reference as well as defined in a footnote on the title page. Manuscripts should be divided into the following components: Title page, Abstract (of no more than 200 words), Introduction, Materials and Methods, Results, Discussion, Acknowledgments, Literature Cited, Tables, and Figure Legends. In addition, authors should supply a list of words and phrases under which the article should be indexed.

2. ***Title page.*** The title page consists of: a condensed title or running head of no more than 35 letters and spaces, the manuscript title, authors' names and appropriate addresses, and footnotes listing present addresses, acknowledgments or contribution numbers, and explanation of unusual abbreviations.

3. ***Figures.*** The dimensions of the printed page, 7 by 9 inches, should be kept in mind in preparing figures for publication. We recommend that figures be about 1½ times the linear dimensions of the final printing desired, and that the ratio of the largest to the smallest letter or number and of the thickest to the thinnest line not exceed 1:1.5. Explanatory matter generally should be included in legends, although axes should always be identified on the illustration itself. Figures should be prepared for reproduction as either line cuts or halftones. Figures to be reproduced as line cuts should be unmounted glossy photographic reproductions or drawn in black ink on white paper, good-quality tracing cloth or plastic, or blue-lined coordinate paper. Those to be reproduced as halftones should be mounted on board, with both designating numbers or letters and scale bars affixed directly to the figures. All figures should be numbered in consecutive order, with no distinction between text and plate figures. The author's name and an arrow indicating orientation should appear on the reverse side of all figures.

4. ***Tables, footnotes, figure legends, etc.*** Authors should follow the style in a recent issue of *The Biological Bulletin* in preparing table headings, figure legends, and the like. Because of the high cost of setting tabular material in type, authors are asked to limit such material as much as possible. Tables, with their headings and footnotes, should be typed on separate sheets, numbered with consecutive Roman numerals, and placed after

the Literature Cited. Figure legends should contain enough information to make the figure intelligible separate from the text. Legends should be typed double spaced, with consecutive Arabic numbers, on a separate sheet at the end of the paper. Footnotes should be limited to authors' current addresses, acknowledgments or contribution numbers, and explanation of unusual abbreviations. All such footnotes should appear on the title page. Footnotes are not normally permitted in the body of the text.

5. ***Literature cited.*** In the text, literature should be cited by the Harvard system, with papers by more than two authors cited as Jones *et al.*, 1980. Personal communications and material in preparation or in press should be cited in the text only, with author's initials and institutions, unless the material has been formally accepted and a volume number can be supplied. The list of references following the text should be headed Literature Cited, and must be typed double spaced on separate pages, conforming in punctuation and arrangement to the style of recent issues of *The Biological Bulletin*. Citations should include complete titles and inclusive pagination. Journal abbreviations should normally follow those of the U. S. A. Standards Institute (USASI), as adopted by BIOLOGICAL ABSTRACTS and CHEMICAL ABSTRACTS, with the minor differences set out below. The most generally useful list of biological journal titles is that published each year by BIOLOGICAL ABSTRACTS (BIOSIS List of Serials; the most recent issue). Foreign authors, and others who are accustomed to using THE WORLD LIST OF SCIENTIFIC PERIODICALS, may find a booklet published by the Biological Council of the U.K. (obtainable from the Institute of Biology, 41 Queen's Gate, London, S.W.7, England, U.K.) useful, since it sets out the WORLD LIST abbreviations for most biological journals with notes of the USASI abbreviations where these differ. CHEMICAL ABSTRACTS publishes quarterly supplements of additional abbreviations. The following points of reference style for THE BIOLOGICAL BULLETIN differ from USASI (or modified WORLD LIST) usage:

A. Journal abbreviations, and book titles, all underlined (for *italics*)

B. All components of abbreviations with initial capitals (not as European usage in WORLD LIST *e.g., J. Cell. Comp. Physiol.* NOT *J. cell. comp. Physiol.*)

C. *All* abbreviated components must be followed by a period, whole word components *must not* (*i.e., J. Cancer Res.*)

D. Space between all components (*e.g., J Cell. Comp. Physiol.*, not *J.Cell.Comp.Physiol.*)

E. Unusual words in journal titles should be spelled out in full, rather than employing new abbreviations invented by the author. For example, use *Rit Vísindafjélags Islendinga* without abbreviation.

F. All single word journal titles in full (*e.g., Veliger, Ecology, Brain*).

G. The order of abbreviated components should be the same as the word order of the complete title (*i.e., Proc.* and *Trans.* placed where they appear, not transposed as in some BIOLOGICAL ABSTRACTS listings).

H. A few well-known international journals in their preferred forms rather than WORLD LIST or USASI usage (*e.g., Nature, Science, Evolution* NOT *Nature, Lond., Science, N.Y.; Evolution, Lancaster, Pa.*)

6. ***Reprints, page proofs, and charges.*** Authors receive their first 100 reprints (without covers) free of charge. Additional reprints may be ordered at time of publication and normally will be delivered about two to three months after the issue date. Authors (or delegates for foreign authors) will receive page proofs of articles shortly before publication. They will be charged the current cost of printers' time for corrections to these (other than corrections of printers' or editors' errors). Other than these charges for authors' alterations, *The Biological Bulletin* does not have page charges.

Reference: *Biol. Bull.* **184:** 115–124. (April, 1993)

Ooplasmic Segregation in the Medaka (*Oryzias latipes*) Egg

VIVEK C. ABRAHAM, SUNITA GUPTA, AND RICHARD A. FLUCK

Department of Biology, Franklin and Marshall College, P.O. Box 3003, Lancaster, Pennsylvania 17604-3003

Abstract. Using time-lapse video microscopy, we found that ooplasmic inclusions in the fertilized medaka egg displayed two types of movement during ooplasmic segregation. The first manifested itself as the movement of many inclusions (diameter = 1.5–11 μm) toward the animal pole at about 2.2 μm min^{-1}; this type of movement appeared to be streaming. The second type of movement was faster (about 44 μm min^{-1}) and saltatory; inclusions displaying this type of movement were smaller (diameter $\leq$ 1.0 μm) and moved toward the vegetal pole. The movement of oil droplets toward the vegetal pole of the egg may represent a third type of motion. All these movements began only after a strong contraction of the ooplasm toward the animal pole, which at 25°C began 10–12 min after fertilization and <3 min after formation of the second polar body.

In eggs treated with microtubule poisons—colchicine, colcemid, or nocodazole—oil droplets did not move toward the vegetal pole, saltatory motion toward the vegetal pole was absent, and the growth of the blastodisc was slowed. Eggs treated with β-lumicolchicine, an inactive derivative of colchicine, showed normal movements. Colchicine, while not inhibiting formation of the second polar body, did inhibit pronuclear migration. These results suggest that microtubules are involved in the movement of some ooplasmic inclusions, including oil droplets, toward the vegetal pole; the movement of ooplasmic inclusions toward the animal pole; and pronuclear migration.

Introduction

Eggs of many animal species display a remarkable variety of movements soon after they are fertilized. Many of these movements, known collectively as ooplasmic segregation, are important for the rearrangement of egg cytoplasm during the minutes and hours following fertilization. In some animals, amphibians and ascidians for example, these movements lead to cytoplasmic localization of morphogenetic determinants, which are subsequently segregated to specific cells during cleavage and ultimately affect gene expression in the cells that incorporate them (Reverberi, 1971; Davidson, 1976; Illmensee *et al.*, 1976; Jeffery, 1984; Speksnijder *et al.*, 1990a).

In contrast to a relatively detailed understanding of ooplasmic segregation in eggs of ascidians, annelids, and amphibians (Vacquier, 1981), relatively little is known about it in fish eggs. Except for Roosen-Runge's (1938) classic study in which time-lapse cinemicrography was used to monitor ooplasmic segregation in the zebrafish egg (*Brachydanio rerio*), there have been no published reports of the use of time-lapse microscopy to monitor segregation in a fish egg. Given the increasing use of fish embryos as model systems in the study of development (Kimmel, 1989; Powers, 1989; Kimmel *et al.*, 1990; Schindler, 1991), it is important to examine segregation in this group of organisms more closely.

Microtubules are required for ooplasmic movements in several taxa of animals, including amphibians (Wakahara, 1989; Houliston and Elinson, 1991; Peter *et al.*, 1991), ascidians (Zalokar, 1974; Sawada, 1988; Sawada and Schatten, 1989), and annelids (Eckberg, 1981; Shimizu, 1982; Astrow *et al.*, 1989). Microtubule poisons—drugs that block either assembly or disassembly of microtubules—have been useful tools in these studies (Zalokar, 1974; Eckberg, 1981; Shimizu, 1982; Astrow *et al.*, 1989; Sawada and Schatten, 1989), in which a role for microtubules is presumed when a particular movement is inhibited by one or more of these poisons. Because these poisons can have cytotoxic effects unrelated to their effects on microtubules, many studies have compared the

Received 18 May 1992; accepted 25 January 1993.

effects of more than one such class of these poisons and, also, have used as controls chemically similar derivatives that have low affinity for tubulin, the protein subunit of microtubules. For example, β-lumicolchicine, a derivative of colchicine (Wilson and Friedkin, 1967), can be used as a control for colchicine (Sabnis, 1981; Achler *et al.*, 1989; Peter *et al.*, 1991).

We have studied ooplasmic segregation in the egg of the medaka (*Oryzias latipes*). This large (diameter = 1.2 mm) clear egg, with its thin peripheral layer of ooplasm surrounding a central yolk vacuole, permits microscopic study of both the gross movements of ooplasm as well as the movement of ooplasmic inclusions. The objectives of the present study were (1) to describe the movements of ooplasmic inclusions, and (2) to monitor the effects on these movements of three drugs that block microtubule assembly (Wilson *et al.*, 1974; Dustin, 1984, ch. 5; Bray, 1992, p. 207).

A preliminary account of these findings has been published (Abraham and Fluck, 1991).

Materials and Methods

We removed gonads from breeding medaka (Yamamoto, 1967; Kirchen and West, 1976; Fluck, 1978) and placed them in a balanced saline solution (BSS: 111 m*M* NaCl; 5.37 m*M* KCl; 1.0 m*M* $CaCl_2$; 0.6 m*M* $MgSO_4$; HEPES, pH 7.3). Eggs were removed from the ovary, and the long chorionic fibers at the vegetal pole were removed with scissors. Eggs were fertilized in BSS (Yamamoto, 1967) and transferred to a microscope slide on which a cover glass was supported by four pillars of petroleum jelly. The cover glass was then pressed gently against the chorion to flatten a small region of the egg near its equator. Such flattening facilitated optical studies and also enabled us to roll the egg to achieve the desired orientation. All procedures were performed at room temperature (23–26°C in most experiments); in this temperature range, the first cell division begins after about 70 min. Because the rate of development varies inversely with temperature, we have reported the timing of events not only as "minutes after fertilization" but also as "normalized time" (t_n), where $t_n = 1.0$ is the time at which cytokinesis begins.

We monitored the movements of ooplasmic inclusions (or parcels) with time-lapse video microscopy, using a Nikon Optiphot or Diaphot microscope equipped with phase-contrast optics and connected through a Dage/MTI camera to a Panasonic NV-8050 time-lapse video cassette recorder. Using a 40× phase-contrast objective lens, we usually focused on a patch of ooplasm near the equator of the just-fertilized egg; with the Optiphot, the field of view was approximately 140 μm × 200 μm (total magnification = 882×) and with the Diaphot it was approximately 225 μm × 325 μm (total magnification = 542×). We measured the diameters of inclusions on the screen of the video monitor and corrected for scale. To measure the speed and direction of movement of the inclusions, we placed a transparent plastic sheet over the video monitor during playback and mapped the paths of randomly chosen inclusions at regular time intervals; the length of the time interval chosen, usually either 20 s or 40 s, depended on the average speed of the inclusions at the time.

To measure the thickness of the blastodisc, we viewed it in profile from the side, measured its thickness along the animal-vegetal axis, and corrected for scale. To measure the volume of the blastodisc, we viewed it in profile from the side and used an image analysis program (Microcomp Planar Morphometry, Southern Micro Instruments, Atlanta, Georgia) to measure three parameters (area, centroid x, and projected x) of one-half of the blastodisc, after drawing a line that bisected the image along the animal-vegetal axis. We then calculated its volume, using the following equation: volume = (2π) (area) (centroid x-projected x). The validity of this method was established by measuring standard objects. To measure the thickness of ooplasm elsewhere on the egg, we measured its thickness *en face* in the Z axis of the objective lens, using the presence of inclusions as a marker for ooplasm.

We used two methods to monitor the timing of the second meiotic division. In the first, we fixed eggs in 3.7% formaldehyde in BSS at regular intervals after fertilization. After rinsing away the fixative and staining the nuclei with Hoechst 33258 (10 μg ml^{-1} in BSS containing 1% Triton X-100), we examined the eggs with epifluorescence optics. In the second method, we microinjected Hoechst 33258 (100 μg ml^{-1}, dissolved in 50 m*M* K_2SO_4 and 10 m*M* HEPES, pH 7.2) into unfertilized eggs, injecting approximately 1.5 nl into the ooplasm at about 45° latitude from the animal pole. The method for microinjection was similar to that used by Fluck *et al.* (1991), except we used a high pressure microinjection system (Narashige IM-200). The injection process parthenogenetically activated the eggs, while Hoechst 33258 stained the maternal nuclear DNA. After placing these eggs between a coverglass and slide, we recorded movements of the ooplasmic inclusions, using a SIT camera coupled to the VCR, and monitored the second meiotic division by examining the eggs at regular intervals with epifluorescence optics. Room temperature was 19.5°C in this latter series of experiments.

Microtubule poisons

Stock solutions of colchicine (1 m*M* in BSS), β-lumicolchicine (1 m*M* in BSS), colcemid (0.35 m*M* in BSS), and nocodazole (2 mg ml^{-1}) in DMSO were diluted into BSS to make working solutions. Working solutions of nocodazole also contained 1% DMSO, which had no ap-

parent effect on the eggs. In preliminary experiments, we monitored the effects of several concentrations of each drug on the movement of oil droplets during ooplasmic segregation and found the minimum effective concentrations that disrupted their normal movement to be 100 μM colchicine, 0.35 μM colcemid, and 0.17 μM nocodazole; we used these concentrations in subsequent experiments. Eggs were generally incubated with the drugs for 1 h before fertilization and then fertilized in the same medium; however, in some experiments, eggs were incubated with the drugs for 1.5 h or 2 h before they were fertilized. In each experiment, we monitored one egg with time-lapse video microscopy and monitored an additional 15–20 eggs with a stereomicroscope.

To monitor the effect of colchicine on formation of the second polar body and migration of the pronuclei, control eggs (nine eggs from two females) and eggs treated with 100 μM colchicine (eight eggs from two females) were fixed in 3.7% formaldehyde in BSS at $t_n = 0.45$. After washing away the fixative, the eggs were stained with Hoechst 33258 and examined with epifluorescence optics.

Chemicals

Colcemid, colchicine, Hoechst 33258, β-lumicolchicine, and nocodazole were obtained from Sigma (St. Louis, Missouri) and formaldehyde from Electron Microscopy Sciences (Fort Washington, Pennsylvania).

Results

An early sign of egg activation was the cortical granule reaction, which spread as a wave from the animal pole to the vegetal pole in about 90 sec at 26°C, a result consistent with the time reported by Gilkey *et al.* (1978). After the cortical granule reaction, the ooplasm became relatively transparent (Fig. 1A), and several types of inclusions could be seen in it (Fig. 2). One class of inclusions were oil droplets, which with phase-contrast optics appeared as white spheres with diameters from <1.0–100 μm. That these spheres were oil droplets was confirmed by staining them with a lipophilic fluorescent dye, nile red (data not shown). About 1 min after the beginning of the cortical granule reaction, there was a strong contraction of the ooplasm, marked by the movement of all ooplasmic inclusions toward the animal pole; this fertilization contraction lasted about 1.5 min and thus was over within 2.5 min after fertilization, times also consistent with Gilkey *et al.* (1978). Our detailed study of the movement of ooplasmic inclusions began after the fertilization contraction.

At 10–12 min after fertilization (at $t_n \approx 0.16$ at 25°C), a second contraction occurred (Fig. 3), in which all ooplasmic inclusions, including oil droplets, again moved toward the animal pole. After this second contraction, most inclusions continued to move toward the animal pole; however, oil droplets (Fig. 1C–F) and some smaller inclusions began to move toward the vegetal pole. Accumulation of ooplasm at the animal pole and the movement of oil droplets and other inclusions toward the vegetal pole proceeded simultaneously for ≈70 min, at which time the blastodisc underwent its first division (Fig. 1F). By this time, there were fewer, larger oil droplets, a result of their fusion with each other during their movement toward the vegetal pole.

The timing of the second meiotic division was approximated by examining fixed eggs and was confirmed by injecting Hoechst 33258 into live eggs. At 19.5°C the second polar body formed by 13.8 ± 3.3 min ($\bar{X}$ ± S.D., n = 4; $t_n \approx 0.12$) after activation, and the second contraction began about 3 min later at 16.7 ± 1.2 min ($\bar{X}$ ± S.D., n = 6; $t_n \approx 0.15$; Fig. 2). In all cases, polar body formation preceded the second contraction.

In the following three sections, we describe (1) the streaming movement of inclusions toward the animal pole, (2) the saltatory movement of inclusions toward the vegetal pole, and (3) the movement of oil droplets toward the vegetal pole. The data presented in Figures 4 and 5 were collected from a single egg at $t_n \approx 0.43$. The movements seen in this egg were confirmed in 41 other eggs studied between the second contraction and the first cell division, and an additional 15 eggs were used to obtain the data summarized in Figure 2.

Streaming

Essentially all the inclusions in Figure 2 appeared to be streaming toward the animal pole. The diameters of these inclusions were in the range 1.5–11 μm, and they appeared to be distributed throughout the depth of the ooplasm. By "streaming" we mean that the movements of the individual inclusions did not appear to be independent of each other; in other words, all inclusions moved at nearly the same speed and in the same direction. The motion of three such inclusions, moving at about 1.5 μm min^{-1}, is summarized in Fig. 4A. Though this speed was typical of streaming motion (2.2 ± 0.8 μm min^{-1}, $\bar{X}$ ± S.D., n = 31 inclusions from 5 eggs), the speed sometimes increased to as high as 8.2 μm min^{-1} for periods lasting up to 10 min and sometimes decreased to near zero for periods lasting up to 12 min.

Saltatory movement

The circled inclusion in Figure 2 is one that by its size, shape, and appearance (phase-dark) would be expected to exhibit saltatory movement. The number of inclusions showing such movement was usually not more than three per microscopic field. These inclusions were in the same optical section as those showing streaming movement

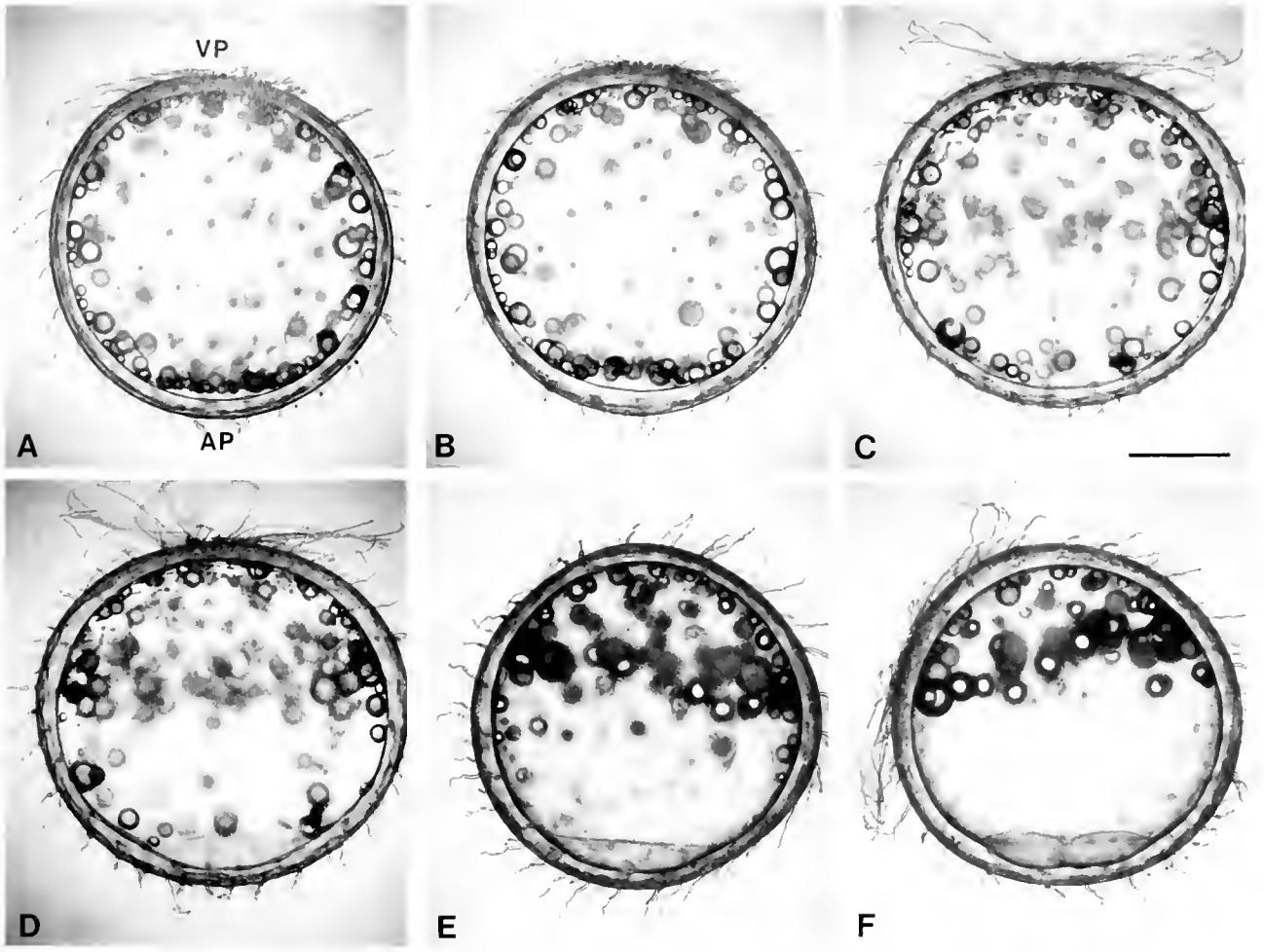

Figure 1. Ooplasmic segregation in the medaka egg. (A) $t_n = 0.07$. The just-fertilized egg consists of a chorion covered with hairs, a large yolk vacuole, and a thin peripheral layer of ooplasm between the yolk membrane and plasma membrane. Oil droplets are present throughout the ooplasm, and a thin blastodisc is visible at the animal pole (AP). (B) $t_n = 0.25$. The thickness of the blastodisc has increased, but oil droplet movement toward the vegetal pole has not yet begun. (C) $t_n = 0.53$. The thickness of the blastodisc has increased even more, and oil droplets have begun to move toward the vegetal pole. (D) $t_n = 0.69$. A biconvex blastodisc has formed, and many oil droplets have left the animal hemisphere. (E) $t_n = 0.81$. The blastodisc has become plano-convex, and oil droplet movement continues. (F) $t_n = 1.00$ (about 70 min at 23°C). The blastodisc has begun to undergo cytokinesis, and most of the oil droplets have formed a crude cap over the vegetal hemisphere. Scale bar, 500 μm.

toward the animal pole. The movement of such inclusions (Fig. 4B) differed from those that streamed in the following ways: (1) Their motion was intermittent, hence the designation "saltatory." An inclusion showing saltatory motion typically moved at a constant rate for 15–120 sec, paused for 5–20 sec and then began moving again. (2) Their velocity (44.4 ± 13.8 μm min^{-1}, $\bar{X}$ ± S.D., n = 17 inclusions from 9 eggs) was about 20-fold higher than that of streaming inclusions. (3) They moved toward the vegetal pole, not the animal pole. (4) Whereas streaming inclusions appeared to move directly toward the animal pole, the paths of these inclusions, though generally directed toward the vegetal pole, were more zig-zagged.

Movement of oil droplets

Immediately after the second contraction, oil droplets, like saltatory inclusions, began to move toward the vegetal pole (Fig. 1B–E). Unlike saltatory inclusions, however, oil droplets appeared to move directly toward the vegetal pole. Moreover, oil droplets moved more slowly than sal-

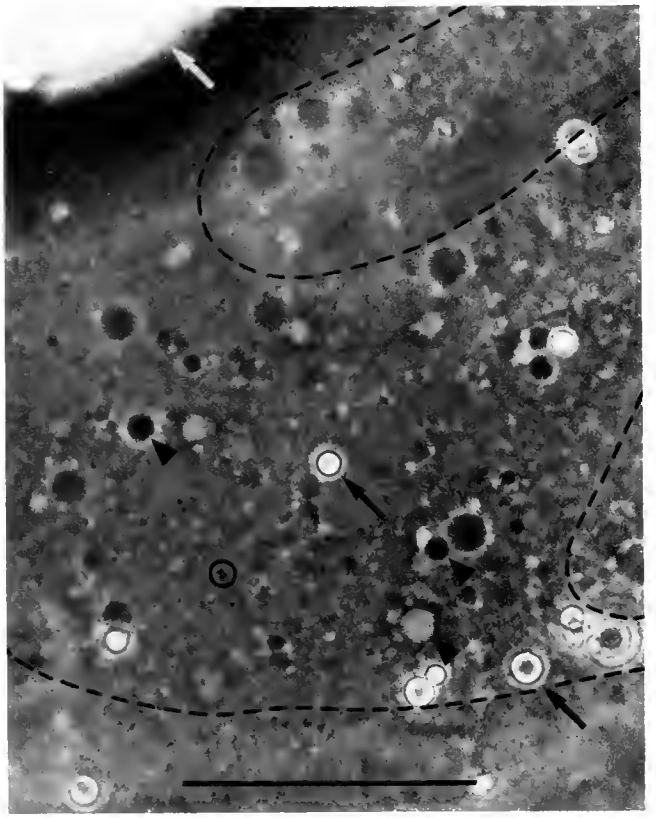

Figure 2. Phase-contrast image of a typical microscopic field near the equator of a fertilized egg at $t_n = 0.43$. Ooplasmic inclusions include some that streamed toward the animal pole (arrowheads), oil droplets of various sizes (arrows), and inclusions that moved saltatorily toward the vegetal pole (encircled parcel). The out-of-focus image of chorionic hairs distorts the image in places (outlined by dashed lines). Scale bar, 50 μm.

tatory inclusions (17.0 ± 5.7 μm min^{-1}, $\bar{X}$ ± S.D., n = 15 droplets in 3 eggs), and their speed varied more than that of saltatory inclusions during a given stretch in which they were moving continuously (Fig. 4C).

Second contraction complex

We monitored this contraction by observing either oil droplet movement at low magnification (at which the entire egg could be seen simultaneously) or the movements of inclusions at higher magnification. In all 18 eggs (from 8 females) in which we analyzed the second contraction, it was composed of at least two components: (1) a movement of ooplasmic inclusions, including oil droplets, toward the vegetal pole, and (2) a subsequent pronounced movement of the inclusions toward the animal pole (Fig. 5A, B). In 5 of the 18 eggs we observed, the movement toward the vegetal pole was preceded by a weaker movement toward the animal pole (data not shown).

Effects of microtubule poisons

Colchicine, colcemid, and nocodazole had the same effects on the eggs, while eggs treated with β-lumicolchicine behaved as untreated (control) eggs. No effect of these poisons was apparent until after the second contraction, even in eggs that were incubated in the microtubule poisons for 1.5 h or 2 h before fertilization: The cortical granule reaction (in 96% of the drug-treated eggs vs. 97% of the controls), the fertilization contraction, elevation of the fertilization membrane, and the second contraction occurred normally in these eggs.

However, these drugs had dramatic effects on the subsequent movement of ooplasmic inclusions toward the poles of the egg. The most obvious effect was on the oil droplets, which floated to the top of the egg instead of moving toward the vegetal pole (Fig. 6B). Moreover, saltatory motion toward the vegetal pole was absent from drug-treated eggs. All three poisons also slowed the rate of growth of the blastodisc (Figs. 6B; 7). The volume of the blastodisc of control eggs at $t_n \approx 0.85$–1.0 was 21.3 ± 4.0 nl ($\bar{X}$ ± S.D., n = 7), while that in eggs treated with microtubule poisons was 11.6 ± 2.6 nl (n = 12). Moreover, in poisoned eggs the blastodisc did not undergo the changes in shape seen in control eggs—from meniscus to biconvex to planoconvex (Fig. 1); instead the blastodisc appeared only to enlarge while maintaining its meniscus form. The microtubule poisons also caused a decrease in the velocity of streaming inclusions [2.2 ± 0.2 μm min^{-1} ($\bar{X}$ ± S.E.M., n = 3 eggs) *versus* 2.9 ± 0.5 (n = 3 eggs) in control eggs]. When we looked at the direction of movement of inclusions during a 10-min period, we found that

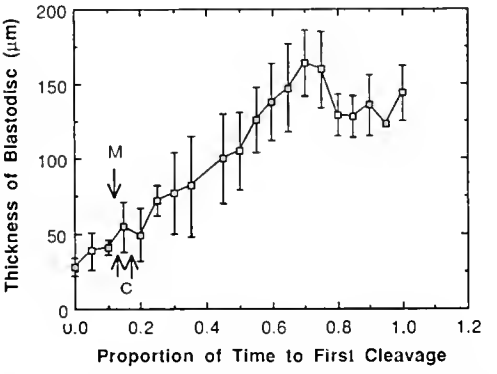

Figure 3. Change in thickness of the blastodisc during ooplasmic segregation. Data from 15 eggs, grown at 14°C–24°C, were used to construct this figure; shown are $\bar{X}$ ± S.D. Arrows mark the times of occurrence of the second meiotic division (M) and the beginning and end of the second contraction (C). The thickness of the blastodisc increased from ≈40 μm in the just-fertilized egg ($t_n = 0.05$) to ≈160 μm at $t_n = 0.7$, by which time the blastodisc was biconvex (Fig. 1D). The decrease in the thickness at $t_n > 0.7$ was caused by a change in the shape of the blastodisc from biconvex to plano-convex before the first mitotic division (Fig. 1D, E).

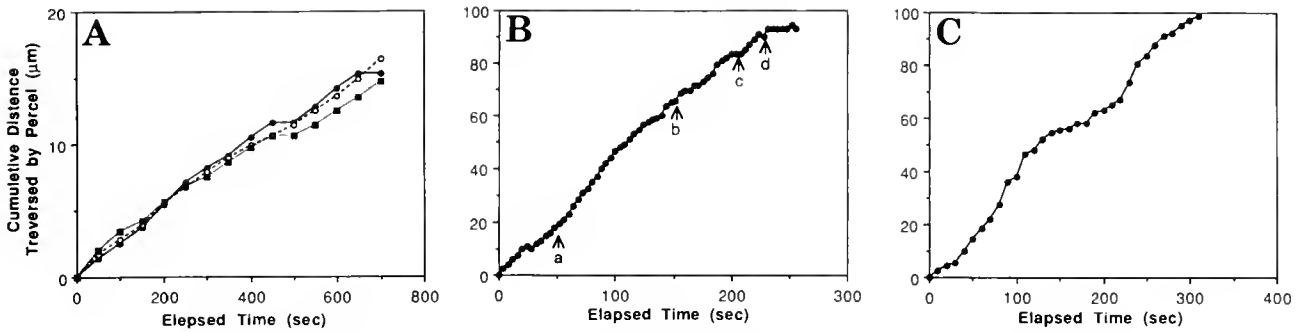

Figure 4. Graphic summary of the movements of ooplasmic inclusions. The movements of five inclusions in a single egg are shown, beginning at $t_n \approx 0.4$. (A) Streaming of inclusions toward the animal pole. Throughout most of this 11+ minute period, the speed of the inclusions was ≈ 1.5 μm min^{-1}. (B) Saltatory motion of an inclusion toward the vegetal pole. Movement was intermittent, *i.e.*, the inclusion sometimes moved rapidly (a → b) and sometimes paused (c). Occasionally such inclusions reversed their direction (d). The velocity of the inclusion between $t \approx 28$ s and $t \approx 200$ s was ≈ 25.7 μm min^{-1}. (C) Movement of an oil droplet toward the vegetal pole. The motion summarized here is that of a small oil droplet (diam. ≈ 6 μm). The speed of the droplet was about 30 μm min^{-1} at 50–100 s and about 9 μm min^{-1} at 125–225 s.

whereas inclusions in control eggs moved in essentially the same direction (3.7° ± 10.6° departure from the animal-vegetal axis, $\bar{X}$ ± S.D., n = 30 inclusions; note the small standard deviation), inclusions in poisoned eggs varied substantially in their direction of movement (10.9° ± 55.7°, $\bar{X}$ ± S.D., n = 52 inclusions; note the large standard deviation).

Hoechst 33258 stained three bodies in control eggs fixed at $t_n = 0.45$. One was inferred to be the second polar body (Fig. 8A) on the basis of its protrusion from the surface of the egg, its size, and the presence of a halo of membrane ruffles around it (Brummett *et al.*, 1985). The other two, the male and female pronuclei, were about 5 μm from each other and 51.8 ± 10.2 μm ($\bar{X}$ ± S.D., n = 9) from the polar body (Fig. 8B, C). As in control eggs, Hoechst 33258 stained three bodies in eggs treated with 100 μ*M* colchicine and fixed at $t_n = 0.45$, one of which was the second polar body (Fig. 8D). However, in contrast to the

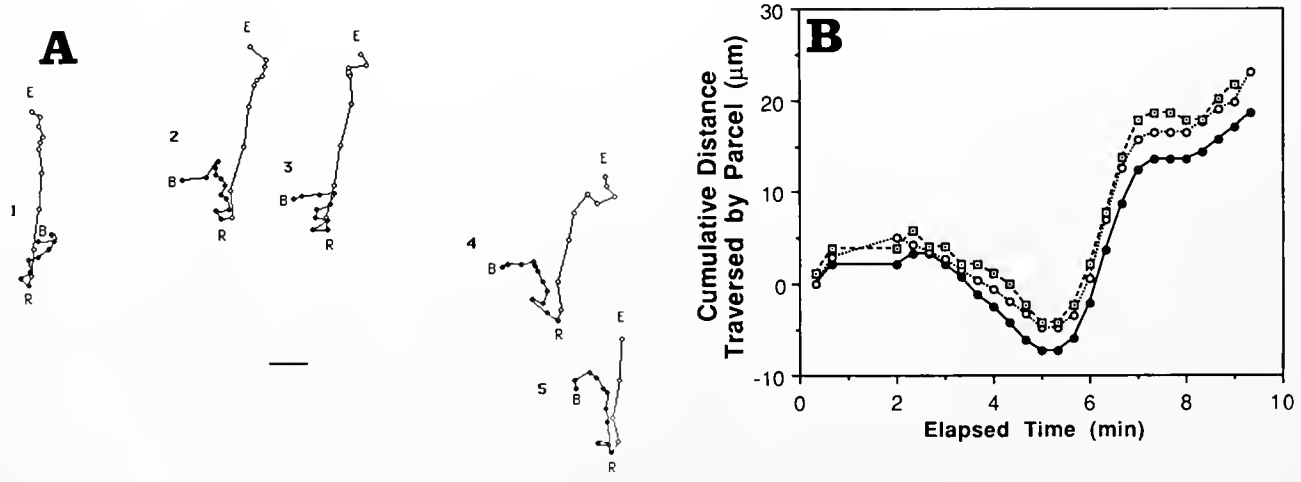

Figure 5. The second contraction. (A) The "tracks" of five inclusions during the second contraction in an egg growing at 21°C. The circles represent the positions of the inclusions at 20 sec intervals, beginning at "B" (6 min after fertilization; $t_n = 0.06$) and ending about 9.5 min later at "E" (at $t_n = 0.15$). The parcels first moved toward the vegetal pole ("down" in this figure; ●—●), and then reversed their direction at "R" and began to move toward the animal pole (o-o). Note that the movement toward the animal pole was rapid at first and then slowed. Scale bar, 5.65 μm. (B) Graphic summary of the movement of parcels #1–3 in Figure 5A. The parcels moved hardly at all for 2 min, began to move toward the vegetal pole (down in this figure) after about 3 min (at $t_n = 0.09$), and then reversed their direction after 5 min ($> t_n = 0.11$) and began to move toward the animal pole (up in this figure).

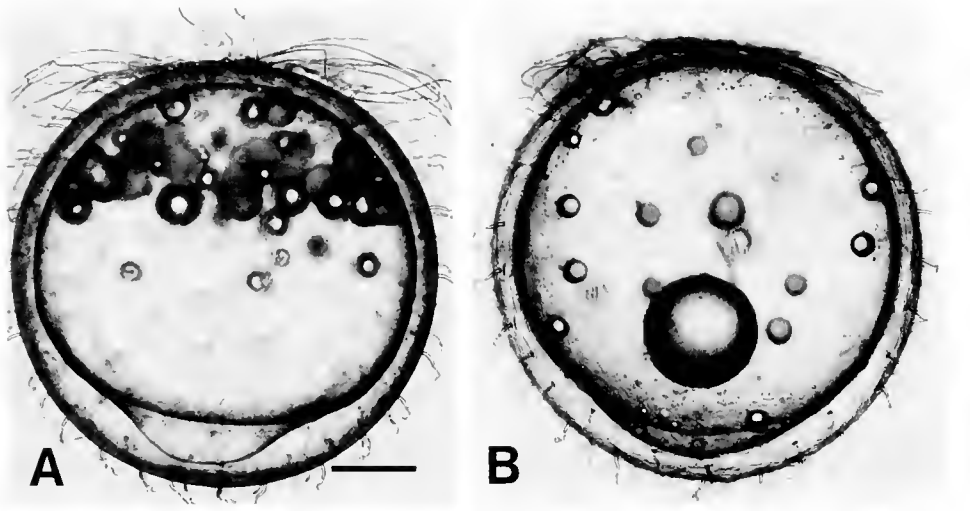

Figure 6. Effects of nocodazole on ooplasmic segregation. (A) Control egg, $t_n = 0.84$. A large blastodisc has formed at the animal pole, and oil droplets have formed a cap over the vegetal hemisphere. (B) Egg treated with 0.17 μM nocodazole, $t_n = 0.80$. The blastodisc is smaller than in the control egg, and most of the oil droplets, instead of moving toward the vegetal pole, have floated to the top of the egg (*i.e.*, toward the viewer, whose perspective is from above the egg) and coalesced into one large droplet there. Scale bar, 250 μm.

situation in control eggs, in which the male and female pronuclei were within 5 μm of each other, the male and female pronuclei in colchicine-treated eggs were far apart (132.2 ± 54.8 μm; $\bar{X}$ ± S.D., n = 8; Fig. 8E).

Discussion

All three microtubule poisons used in this study—colchicine, colcemid, and nocodazole—affected the movement of ooplasmic inclusions during segregation in the medaka egg. That the poisons acted specifically as microtubule poisons is a reasonable inference because (1) their effective concentrations were similar to those used in previous studies (Zalokar, 1974; Eckberg, 1981; Shimizu, 1982; Astrow *et al.*, 1989; Sawada and Schatten, 1989); (2) poisons from two classes of microtubule poisons (Bray, 1992, p. 207) had similar effects on the eggs; and (3) 100 μM β-lumicolchicine had no apparent effect on the eggs. The results of the present study differ from those of Katow (1983), who reported that the blastodisc formed normally in zebrafish eggs treated with colchicine. This difference could be due to the lower concentration of colchicine used in the earlier study (2.5 μM vs. 100 μM in the present study) or to a lower permeability of the zebrafish egg to colchicine. It is possible (but unlikely, we believe) that microtubules are not required for ooplasmic segregation in the zebrafish egg.

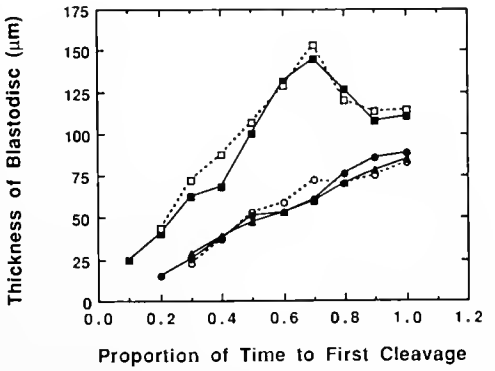

Figure 7. Effect of microtubule poisons on the growth of the blastodisc. The thickness of the blastodisc along the animal-vegetal axis was measured in untreated eggs (— ■ —, four eggs) and in eggs treated with 100 μM β-lumicolchicine (— □ —, three eggs), 100 μM colchicine (— ● —, four eggs), 0.35 μM colcemid (— ○ —, three eggs), or 0.17 μM nocodazole (— ▲ —, five eggs). Shown are the mean values; over all the treatments and times, the standard deviation averaged 12% of the mean. Colcemid, colchicine, and nocodazole all slowed the growth of the blastodisc, while eggs treated with β-lulmicolchicine behaved as untreated eggs. The volume of the blastodisc in control eggs and poisoned eggs at $t_n \approx 0.85$–1.0 was 21.3 ± 4.0 nl and 11.6 ± 2.6 nl ($\bar{X}$ ± SD), respectively.

Saltatory movement similar to that observed in the present study is often associated with microtubules (Hayden *et al.*, 1983; Brady and Pfister, 1991). Similarities include the intermittent nature of the movement, its inhibition by microtubule poisons, and the speed of moving particles (Hamaguchi *et al.*, 1986; Shimizu *et al.*, 1991). These similarities suggest that in the medaka egg some ooplasmic inclusions move toward the vegetal pole via microtubules oriented approximately along the animal-vegetal axis.

The normal movement of oil droplets was also affected by the poisons, suggesting that microtubules are also involved in the movement of these droplets. Such an in-

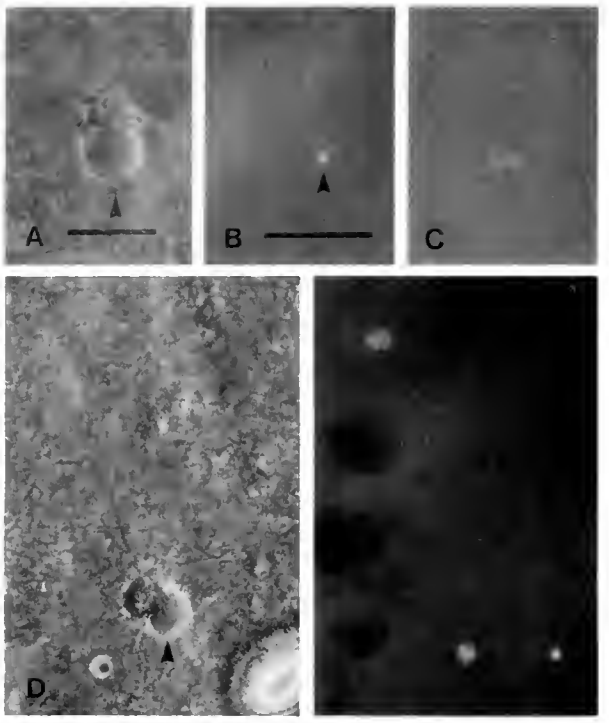

Figure 8. Formation of second polar body and pronuclear migration. Untreated eggs (A–C) and eggs treated with 100 μM colchicine (D–E) were fixed at $t_n = 0.45$, subsequently stained with Hoechst 33258, and viewed with either phase contrast (A, D) or epifluorescence (B, C, E) optics. The second polar body (arrowhead) could be seen near the animal pole in both untreated eggs (A) and in eggs treated with 100 μM colchicine (D). Of the three fluorescent bodies present in this region of the egg, one corresponded to the polar body (arrowhead in B, E), and the other two were the male and female pronuclei (C, E). In the untreated egg shown here, the polar body and pronuclei were recorded in separate photographs (B, C) because their focal planes were separated by about 25 μm. The two pronuclei were close to each other and were about 37 μm from the polar body. In eggs treated with colchicine, the pronuclei were much farther apart (E). Scale bars, A, D, 10 μm; B, C, E, 50 μm.

volvement would seem to require the presence of a unit membrane at the surface of the oil droplets to provide a site of attachment for a kinesin-like molecule. Whether such a membrane is present around these droplets is not known. In other types of cells, unit membranes are present around some lipid droplets but not others (Wake, 1974; Nedergard and Lindberg, 1982). An alternative explanation for the effect of these poisons on oil droplet movement is that in control eggs a dynamic network of microtubules holds the oil droplets in place; in the presence of these microtubule poisons, such a dynamic network would eventually disappear as disassembly continues in the absence of assembly. This question will require further study.

The movement of ooplasm toward the animal pole in fish embryos has been previously described as streaming (Roosen-Runge, 1938; Beams *et al.*, 1985) or bulk flow (Gilkey, 1981); our results confirm these reports. Microtubule poisons slowed both the movement of inclusions toward the animal pole and the growth of the blastodisc, but they did not inhibit either process entirely, suggesting that more than one mechanism is responsible for these phenomena. In ascidians (Sawada and Osanai, 1981, 1984, 1985; Jeffery, 1984; Bates and Jeffery, 1988) and an oligochaete (Shimizu, 1982, 1984), actin microfilaments form a cortical network that contracts toward one pole of the egg, pulling with it both cortical and subcortical components of the ooplasm. F-actin is present in the cortex and subcortex (Beams *et al.*, 1985; Wolenski and Hart, 1987; Chang, 1991) of the zebrafish egg, and an actomyosin-like ATPase has been identified in cortical preparations of fish eggs (Jorgensen, 1972). Moreover, cytochalasins (Katow, 1983; Ivanenkov *et al.*, 1987; Fluck, unpub.) and DNase I (Ivanenkov *et al.*, 1987) inhibit formation of the blastodisc in fish embryos. Thus, both microtubules and microfilaments may be involved in the movement of ooplasm and its inclusions toward the animal pole in the medaka egg.

Calcium ion may both trigger and organize such a contraction in the medaka egg just as it does in ascidian egg (Jeffery, 1982; Sardet *et al.*, 1986; Speksnijder *et al.*, 1990a, b; see also Cheer *et al.*, 1987). Cytosolic [Ca^{2+}] is elevated at the animal and vegetal poles of the medaka egg during ooplasmic segregation (Fluck *et al.*, 1992b), and injection of the weak calcium buffer, dibromo-BAPTA (Speksnijder *et al.*, 1989), into the medaka egg inhibits formation of the blastodisc (Fluck *et al.*, 1992a).

In eggs treated with microtubule poisons, the ooplasm appeared to be solated compared to that in control eggs because oil droplets floated to the top of the egg instead of moving toward the vegetal pole. Moreover, the movement of inclusions toward the animal pole of the egg was more disorganized. Both of these effects could be the result of the disruption of a dynamic network of microtubules in the ooplasm by the microtubule poisons.

All three of the movements described in this report—streaming toward the animal pole, saltatory movement toward the vegetal pole, and movement of oil droplets toward the vegetal pole–began only after formation of the second polar body and the second contraction; this was true for both control eggs and for eggs treated with microtubule poisons. These events thus heralded a radical change in the structure and/or activity of the cytoskeleton of the egg. Though the present study is the first to describe this phenomenon as a contraction (or series of contractions), both Sakai (1965) and Iwamatsu (1973) reported that oil droplets in the medaka egg oscillate along the animal-vegetal axis at this time.

In addition to its effect on ooplasmic segregation, colchicine inhibited the migration of the pronuclei after formation of the second polar body, which apparently formed normally. In its insensitivity to a microtubule poison, the

medaka egg is like that of the ascidian *Phallusia mammillata* (Zalokar, 1974) and the polychaete *Chaetopterus pergamentaceus* (Eckberg, 1981), but unlike that of the leech *Helobdella triserialis* (Astrow *et al.*, 1989) and the oligochaete *Tubifex hattai* (Shimizu, 1982). In contrast to their variable effects on polar body formation, microtubule poisons consistently inhibit pronuclear migration (Zalokar, 1974; Hiramoto *et al.*, 1984; Hamaguchi and Hiramoto, 1986; Sawada and Schatten, 1989). The results of the present study are consistent with these earlier studies.

These results suggest that in the medaka egg microtubules are necessary for the movement of some components of the ooplasm to the vegetal pole and of others to the animal pole. Such movement in an animal egg is generally considered to constitute "ooplasmic segregation," but whether it also constitutes "cytoplasmic localization" (Davidson, 1976) remains to be seen. These movements in the medaka egg, especially the saltatory ones, may simply reflect the need of this large, polarized cell to sustain its polarity in the same way that epithelial cells (Rindler *et al.*, 1987; Achler *et al.*, 1989; Breitfeld *et al.*, 1990) and other eggs (Peter *et al.*, 1991) do.

Acknowledgments

Doug Antonioli, Jesse Fluck, and Justine Fluck assisted in the studies summarized in Figure 3; Justine Fluck in the analysis of that data and the preparation of Figure 3; and Minerva Medina in the studies of the timing of the second meiotic division. We thank Dr. Lionel Jaffe and Dr. Andrew Miller for helpful discussions of these phenomena; Dr. Jaffe for helping us improve the text of the manuscript; and Dr. George Rosenstein and Dr. Gene Johnson for their help in measuring the volume of the blastodisc. Supported by NSF DCB-9017210 and Franklin and Marshall College's Hackman Scholar Program and STEP program.

Literature Cited

Abraham, V., and R. A. Fluck. 1991. Ooplasmic segregation in the fertilized egg of *Oryzias latipes* (medaka). *J. Cell Biol.* **115:** 56a.

Achler, C., D. Filmer, C. Merte, and D. Drenckhahn. 1989. Role of microtubules in polarized delivery of apical membrane proteins to the brush border of the intestinal epithelium. *J. Cell Biol.* **109:** 179–189.

Astrow, S. H., B. Holton, and D. A. Donovan. 1989. Teloplasm formation in a leech, *Helobdella triserialis*, is a microtubule-dependent process. *Dev. Biol.* **135:** 306–319.

Bates, W. R., and W. R. Jeffery. 1988. Polarization of ooplasmic segregation and dorsal-ventral axis determination in ascidian embryos. *Dev. Biol.* **130:** 98–107.

Beams, H. W., R. K. Kessel, C. Y. Shih, and H. N. Tung. 1985. Scanning electron microscope studies on blastodisc formation in the zebrafish, *Brachydanio rerio*. *J. Morphol.* **184:** 41–49.

Brady, S. T., and K. K. Pfister. 1991. Kinesin interactions with membrane bounded organelles *in vivo* and *in vitro*. *J. Cell Sci. Suppl.* **14:** 103–108.

Bray, D. 1992. *Cell Movements*, Garland Publishing, Inc., New York.

Breitfield, P. P., W. C. McKinnon, and K. E. Mostov. 1990. Effect of nocodazole on vesicular traffic to the apical and basolateral surfaces of polarized MDCK cells. *J. Cell Biol.* **111:** 2365–2373.

Brummett, A. R., J. N. Dumont, and C. S. Richter. 1985. Later stages of sperm penetration and second polar body and blastodisc formation in the egg of *Fundulus heteroclitus*. *J. Exp. Zool.* **234:** 423–439.

Chang, D. C. 1991. Structures of actin in zebra fish embryos studied by confocal microscopy. *Biophys. J.* **59:** 55a.

Cheer, A., J.-P. Vincent, R. Nuccitelli, and G. Oster. 1987. Cortical activity in vertebrate eggs. I. The activation waves. *J. Theor. Biol.* **124:** 377–404.

Davidson, E. H. 1976. Pp. 245–248 in *Gene Activity in Early Development*, 2nd ed., Academic Press, New York.

Dustin, P. 1984. *Microtubules*, 2nd ed. Springer-Verlag, Berlin.

Eckberg, W. R. 1981. The effects of cytoskeleton inhibitors on cytoplasmic localization in *Chaetopterus pergamentaceus*. *Differentiation* **19:** 55–58.

Fluck, R. A. 1978. Acetylcholine and acetylcholinesterase activity in early embryos of the medaka *Oryzias latipes*, a teleost. *Dev. Growth Differ.* **20:** 17–25.

Fluck, R. A., V. C. Abraham, A. L. Miller, and L. F. Jaffe. 1992a. Calcium buffer injections block ooplasmic segregation in *Oryzias latipes* (medaka) eggs. *Biol. Bull.* **183:** 371–372.

Fluck, R. A., A. L. Miller, and L. F. Jaffe. 1991. Slow calcium waves accompany cytokinesis in medaka fish eggs. *J. Cell Biol.* **115:** 1259–1265.

Fluck, R. A., A. L. Miller, and L. F. Jaffe. 1992b. High calcium zones at the poles of developing medaka eggs. *Biol. Bull.* **183:** 70–77.

Gilkey, J. C. 1981. Mechanisms of fertilization in fishes. *Am. Zool.* **21:** 359–375.

Gilkey, J. C., L. F. Jaffe, E. B. Ridgway, and G. T. Reynolds. 1978. A free calcium wave traverses the activating egg of the medaka, *Oryzias latipes*. *J. Cell Biol.* **76:** 448–466.

Hamaguchi, M. S., Y. Hamaguchi, and Y. Hiramoto. 1986. Microinjected polystyrene beads move along astral rays in sand dollar eggs. *Dev. Growth Differ.* **28:** 461–470.

Hamaguchi, M. S., and Y. Hiramoto. 1986. Analysis of the role of astral rays in pronuclear migration in sand dollar eggs by the colcemid-UV method. *Dev. Growth Differ.* **28:** 143–156.

Hayden, J. H., R. D. Allen, and R. D. Goldman. 1983. Cytoplasmic transport in keratocytes: direct visualization of particle translocation along microtubules. *Cell Motil.* **3:** 1–19.

Hiramoto, Y., M. S. Hamaguchi, Y. Nakano, and Y. Shoji. 1984. Colcemid uv-irradiation method for analyzing the role of microtubules in pronuclear migration and chromosome movement in sand-dollar eggs. *Zool. Sci.* **1:** 29–34.

Houliston, E., and R. P. Elinson. 1991. Patterns of microtubule polymerization relating to cortical rotation in *Xenopus laevis* eggs. *Development* **112:** 107–117.

Illmensee, K., A. P. Mahowald, and M. R. Loomis. 1976. The ontogeny of germ plasm during oogenesis in *Drosophila*. *Dev. Biol.* **49:** 40–65.

Ivanenkov, V. V., A. A. Minin, V. N. Meshcheryakov, and L. E. Martynova. 1987. The effect of local microfilament disorganization on ooplasmic segregation in the loach (*Misgurnus fossilis*) egg. *Cell Differ.* **22:** 19–28.

Iwamatsu, T. 1973. On the mechanism of ooplasmic segregation upon fertilization in *Oryzias latipes*. *Jpn. J. Ichthyol.* **20:** 273–278.

Jeffery, W. R. 1982. Calcium ionophore polarizes ooplasmic segregation in ascidian eggs. *Science* **216:** 545–547.

Jeffery, W. R. 1984. Pattern formation by ooplasmic segregation in ascidian eggs. *Biol. Bull.* **166:** 277–298.

Jorgensen, N.-C. 1972. Actomyosin-like ATPase activity at the surface of fish eggs. *Exp. Cell Res.* **71:** 460–464.

Katow, H. 1983. Obstruction of blastodisc formation by cytochalasin B in the zebrafish, *Brachydanio rerio*. *Dev. Growth Differ.* **25:** 477–484.

Kimmel, C. B. 1989. Genetics and early development of zebrafish. *Trends Genet.* **5:** 283–288.

Kimmel, C. B., R. M. Warga, and T. F. Schilling. 1990. Origin and organization of the zebrafish fate map. *Development* **108:** 581–594.

Kirchen, R. V., and W. R. West. 1976. *The Japanese Medaka: Its Care and Development.* Carolina Biological Supply Company, Burlington, North Carolina.

Nedergard, J., and O. Lindberg. 1982. The brown fat cell. *Int. Rev. Cytol.* **74:** 187–286.

Peter, A. B., J. C. Schittny, V. Niggli, H. Reuter, and E. Sigel. 1991. The polarized distribution of poly(A^+)-mRNA-induced functional ion channels in *Xenopus* oocyte plasma membrane is prevented by anticytoskeletal drugs. *J. Cell Biol.* **114:** 455–464.

Powers, D. A. 1989. Fish as model systems. *Science* **246:** 352–358.

Reverberi, G. 1971. Ascidians. Pp. 529–532 in *Experimental Embryology of Marine and Freshwater Invertebrates*, G. Reverberi, ed. North Holland, Amsterdam.

Rindler, M. J., I. E. Ivanov, and D. D. Sabatini. 1987. Microtubule-acting drugs lead to the nonpolarized delivery of the influenza hemagglutinin to the cell surface of polarized Madin-Darby canine kidney cells. *J. Cell Biol.* **104:** 231–241.

Roosen-Runge, E. C. 1938. On the early development—bipolar differentiation and cleavage—of the zebra fish, *Brachydanio rerio*. *Biol. Bull.* **75:** 119–133.

Sabnis, D. D. 1981. Lumicolchicine as a tool in the study of plant microtubules: some biological effects of sequential products formed during phototransformation of colchicine. *J. Exp. Bot.* **32:** 271–278.

Sakai, Y. T. 1965. Studies on the ooplasmic segregation in the egg of the fish *Oryzias latipes*. III. Analysis of the movement of oil droplets during the process of ooplasmic segregation. *Biol. Bull.* **129:** 189–198.

Sardet, C., S. Inoué, L. F. Jaffe, and J. E. Speksnijder. 1986. Surface and internal movements in fertilizing *Phallusia* eggs. *Biol. Bull.* **171:** 488.

Sawada, T. 1988. The mechanism of ooplasmic segregation in the ascidian egg. *Zool. Sci.* **5:** 667–675.

Sawada, T., and K. Osanai. 1981. The cortical contraction related to the ooplasmic segregation in *Ciona intestinalis* eggs. *Wilhelm Roux's Arch. Dev. Biol.* **190:** 208–214.

Sawada, T., and K. Osanai. 1984. Cortical contraction and ooplasmic movement in centrifuged or artificially constricted eggs of *Ciona intestinalis* eggs. *Wilhelm Roux's Arch. Dev. Biol.* **193:** 127–132.

Sawada, T., and K. Osanai. 1985. Distribution of actin filaments in fertilized eggs of the ascidian *Ciona intestinalis*. *Dev. Biol.* **111:** 260–265.

Sawada, T., and G. Schatten. 1989. Effects of cytoskeletal inhibitors on ooplasmic segregation and microtubule organization during fertilization and early development in the ascidian *Molgula occidentalis*. *Dev. Biol.* **132:** 331–342.

Schindler, J. M. 1991. Zebrafish: *Drosophila* with a spine (but can they fly?). *New Biol.* **3:** 47–49.

Shimizu, T. 1982. Ooplasmic segregation in the *Tubifex* egg: mode of pole plasma accumulation and possible involvement of microfilaments. *Wilhelm Roux's Arch. Dev. Biol.* **191:** 246–256.

Shimizu, T. 1984. Dynamics of the actin microfilament system in the *Tubifex* egg during ooplasmic segregation. *Dev. Biol.* **106:** 414–426.

Shimizu, T., K. Furusawa, S. Ohashi, Y. Y. Toyoshima, M. Okuno, F. Malik, and R. D. Vale. 1991. Nucleotide specificity of the enzymatic and motile activities of dynein, kinesin, and heavy meromyosin. *J. Cell Biol.* **112:** 1189–1197.

Speksnijder, J. E., A. L. Miller, M. H. Weisenseel, T.-H. Chen, and L. F. Jaffe. 1989. Calcium buffer injections block fucoid egg development by facilitating calcium diffusion. *Proc. Natl. Acad. Sci. USA* **86:** 6607–6611.

Speksnijder, J. E., C. Sardet, and L. F. Jaffe. 1990a. The activation wave of calcium in the ascidian egg and its role in ooplasmic segregation. *J. Cell Biol.* **110:** 1589–1598.

Speksnijder, J. E., C. Sardet, and L. F. Jaffe. 1990b. Periodic calcium waves cross ascidian eggs after fertilization. *Dev. Biol.* **142:** 246–249.

Vacquier, V. D. 1981. Dynamic changes of the egg cortex. *Dev. Biol.* **84:** 1–26.

Wakahara, M. 1989. Specification and establishment of dorsal-ventral polarity in eggs and embryos of *Xenopus laevis*. *Dev. Growth Differ.* **31:** 197–207.

Wake, K. 1974. Development of vitamin A-rich lipid droplets in multivesicular bodies of rat liver stellate cells. *J. Cell Biol.* **63:** 683–691.

Wilson, L., J. R. Bamburg, S. B. Mizel, L. M. Grisham, and K. M. Creswell. 1974. Interaction of drugs with microtubule proteins. *Fed. Proc.* **33:** 158–166.

Wilson, L., and M. Friedkin. 1967. The biochemical events of mitosis. II. The *in vivo* and *in vitro* binding of colchicine in grasshopper embryos and its possible relation to inhibition of mitosis. *Biochemistry* **6:** 3126–3135.

Wolenski, J. S., and N. H. Hart. 1987. Visualization of actin with rhodamine phalloidin in the zebrafish egg. *Biol. Bull.* **173:** 573a.

Yamamoto, T. 1967. Medaka. Pp. 101–111 in *Methods in Developmental Biology*, F. M. Wilt and N. K. Wessells, eds. Thomas Y. Crowell Company, New York.

Zalokar, M. 1974. Effect of colchicine and cytochalasin B on ooplasmic segregation of ascidian eggs. *Wilhelm Roux's Archiv. Dev. Biol.* **175:** 243–248.

Reference: *Biol Bull* **184**: 125–143. (April, 1993)

Gametogenesis and Spawning of the Sea Cucumber *Psolus fabricii* (Duben and Koren)

JEAN-FRANÇOIS HAMEL[1], JOHN H. HIMMELMAN[1], AND LOUISE DUFRESNE[2]

[1]*Département de Biologie and GIROQ (Groupe Interuniversitaire de Recherches Océanographiques du Québec), Université Laval, Québec, Canada G1K 7P4 and* [2]*Département d'Océanographie, Université du Québec à Rimouski and Centre Océanographique de Rimouski, Rimouski, Canada G5L 3A1*

Abstract. The reproductive cycle of the sea cucumber *Psolus fabricii* was studied in a population from the St. Lawrence Estuary in eastern Canada from May 1988 through August 1989. The gonad consists of numerous germinal tubules which vary greatly in size. The mean diameter of the tubules and gonadal mass follow annual cycles, increasing from early winter through spring, and dropping abruptly during spawning in the summer. Gametogenesis is generally a prolonged process and begins in small tubules in January. By summer the ovarian tubules contain oocytes with a modal diameter of 400–600 μm, and the testicular tubules contain an abundance of early spermatogenic stages, but rarely spermatozoa. These small tubules of the gonad do not spawn until the following year, and there is little gametogenic activity within them until January, when oocyte growth and the production of later spermatogenic stages resumes. The latter production continues until summer and results in a marked increase in the diameter of the tubules. Then, during spawning, these now large fecund tubules are transformed into small tubules. Following spawning, the predominant activity within the spent tubules is phagocytosis of the residual gametes. The active phase of gametogenesis (January to summer) coincides with an increasing photoperiod regime, and an accelerated gametogenesis occurs in March when temperature and food availability begin to increase. Spawning was one month later in 1989 than in 1988 and did not show a consistent relationship with either temperature or light conditions. However, in both years, spawning coincided with a decrease in the freshwater run-off into the Estuary and with the predicted annual increase in phytoplankton.

Received 2 April 1992; accepted 25 January 1993.

Introduction

If we want to describe the reproductive cycle of an invertebrate, we need information about the gonad (structure and development) and gametogenesis (with respect to biometry) (Smiley *et al.*, 1991), and about environmental factors that control these events (Giese and Pearse, 1974; Himmelman, 1981). We are interested in reproduction in echinoderms and particularly in holothurians. The gonad of many holothurians is unusual in that it consists of numerous germinal tubules (Théel, 1882; Tyler and Gage, 1983; Smiley and Cloney, 1985; Smiley, 1988) that can vary markedly in size and state of gametogenic development (Théel, 1901; Kille, 1939, 1942; Smiley and Cloney, 1985; Smiley, 1988; Smiley *et al.*, 1991). Smiley (1988) shows that, in female *Stichopus californicus,* fecund tubules are attached to the posterior part of the gonad. He suggests that this arrangement may be a general characteristic of holothurians. Because of the complex gonadal morphology, seasonal changes in gametogenesis are more difficult to quantify in holothurians than in invertebrates that have a globular gonad. Another problem in studying holothurian reproductive cycles is that body size can vary drastically due to water uptake and loss (Edwards, 1910) so that body component indices are not as constant and reliable as they are for many other invertebrates. The principal studies on holothuroid reproduction are those by Tanaka (1958), Krishnaswamy and Krishnan (1967), Rutherford (1973), Green (1978), Engstrom (1980), Conand (1981, 1982), Tyler and Gage (1983), Costelloe (1985), Smiley and Cloney (1985), Cameron and Fankboner (1986), Tyler and Billett (1988), Smiley (1988), Bulteel *et al.* (1992), and Sewell (1992).

The role of environmental factors in controlling gametogenesis and spawning in marine invertebrates has

been well investigated. Temperature, food availability, and photoperiod have often been suggested as environmental cues based on correlative evidence (Giese and Pearse, 1974; Himmelman, 1981; Todd and Doyle, 1981; Giese and Kanatani, 1987). Laboratory experiments in conjunction with field observations have demonstrated that specific environmental changes coordinate certain reproductive events in echinoderms. For example, photoperiod has been shown to be the primary factor controlling gametogenesis in the urchin *Strongylocentrotus purpuratus* and the seastar *Pisaster ochraceus* (Pearse and Eernisse, 1982; Pearse *et al.*, 1986). In addition, spawning in several echinoderms as well as molluscs, seems to be triggered by the spring phytoplankton increase (Himmelman, 1975, 1981; Starr, 1990; Starr *et al.*, 1990, 1992). Temperature (Tanaka, 1958), light intensity (Conand, 1982; Cameron and Fankboner, 1986), water turbulence (Engstrom, 1980), salinity (Krishnaswamy and Krisnan, 1967), a combination of temperature and light intensity (Costelloe, 1985), and phytoplankton blooms (Cameron and Fankboner, 1986) have all been suggested as potential spawning cues particularly for holothurians, but experiments demonstrating such a role have yet to be performed.

In this study we examined the reproductive cycle of the holothuroid *Psolus fabricii* (Duben and Koren) in relation to environmental conditions for a period of 16 months. This species was chosen because it possesses the complex system of gonadal tubules characteristic of holothurians, and because it can be readily collected since it is abundant on rocky faces in the subtidal zone in our region. First, we developed techniques for quantifying changes in the gonads and associated body organs. Because of the marked variation in the size and state of development of the germinal tubules, we decided to quantify the gametogenic events in large and small tubules separately, so as to clarify the extent to which tubule size affects interpretation. Although previous studies on holothurians report differences in gametogenetic development in tubules of different size, this is the first study quantifying the rate of gametogenic development in different-sized male and female tubules at frequent intervals throughout the year.

Materials and Methods

Study site

The population studied was at Anse à Robitaille (48°32′ N: 69°41′ W), 2.5 km from Les Escoumins on the north shore of the lower St. Lawrence Estuary. Samples of 35–40 individuals were collected at monthly or bimonthly intervals between May 1988 and August 1989, from a bedrock face (45°–60°) at a depth of about 10 m below the lowest water of spring tides. Because the animals could not be dissected immediately, they were preserved in 10% neutralized formalin in seawater and dissected about a month later. By this time, changes due to the preservation should have stabilized (Pitmann and Munroe, 1982).

Determination of indices of the gonad, respiratory tree, and intestine (including its contents)

The dry mass of the body wall, including the aquapharyngeal bulb, longitudinal muscle bands, and cloacal muscles (Fig. 1A), was chosen as a denominator for body component indices because calculating these indices as a proportion of the wet body wall mass would have markedly increased the confidence intervals (by 12–25% for the gonadal index, 9–18% for the intestinal index, and 16–22% for the respiratory tree index). Moreover, seasonal variations in dry body wall mass were probably small since the calcareous plates accounted for ≈87% of this mass. All masses were recorded to the nearest 0.01 g, and dry masses were determined after drying at 55°C for 96 h.

The intestine (with contents) was removed from the posterior end of the stomach to the beginning of the cloaca, the gonad from its point of attachment to the gonoduct, and the respiratory tree from its point of attachment to the cloaca. Intestinal and gonadal indices were calculated as the ratio of their wet mass to dry body wall mass (this permitted an examination of the intestinal contents and gonadal histology), whereas the respiratory tree index was calculated as its dry mass relative to the dry body wall mass. For each collection date, the various indices were determined for 15 males and 15 females, ranging from 25 to 34 g in dry body wall mass (equivalent to 5.7–6.1 cm in the distance from the mouth to the anus).

In order to compare them with the evolution of the gonadal indices, seasonal changes in the diameter of the gonadal tubules were quantified as follows: The gonads were spread out in a shallow container, and the tubule diameter was measured at random points with a binocular scope (12×). Fifteen measurements for each of 15 males and 15 females were made for each sampling date.

Gametogenesis

Gonads from preserved individuals were removed and transferred to Bouin's fixative for four weeks and then processed according to standard embedding technique (Junqueira *et al.*, 1986). To determine the variation due to differences in tubule size, separate examinations were made of small (<1.9 mm) and large tubules (>1.9 mm). To prevent the loss of tubule contents during embedding, the tubule sections were cut well beyond the segment selected for sectioning. For each individual, six 5 μm-microtome sections were cut from both the small and large tubules. These sections were first placed on gelatin coated slides (the gelatin was heated to 42°C) and then transferred

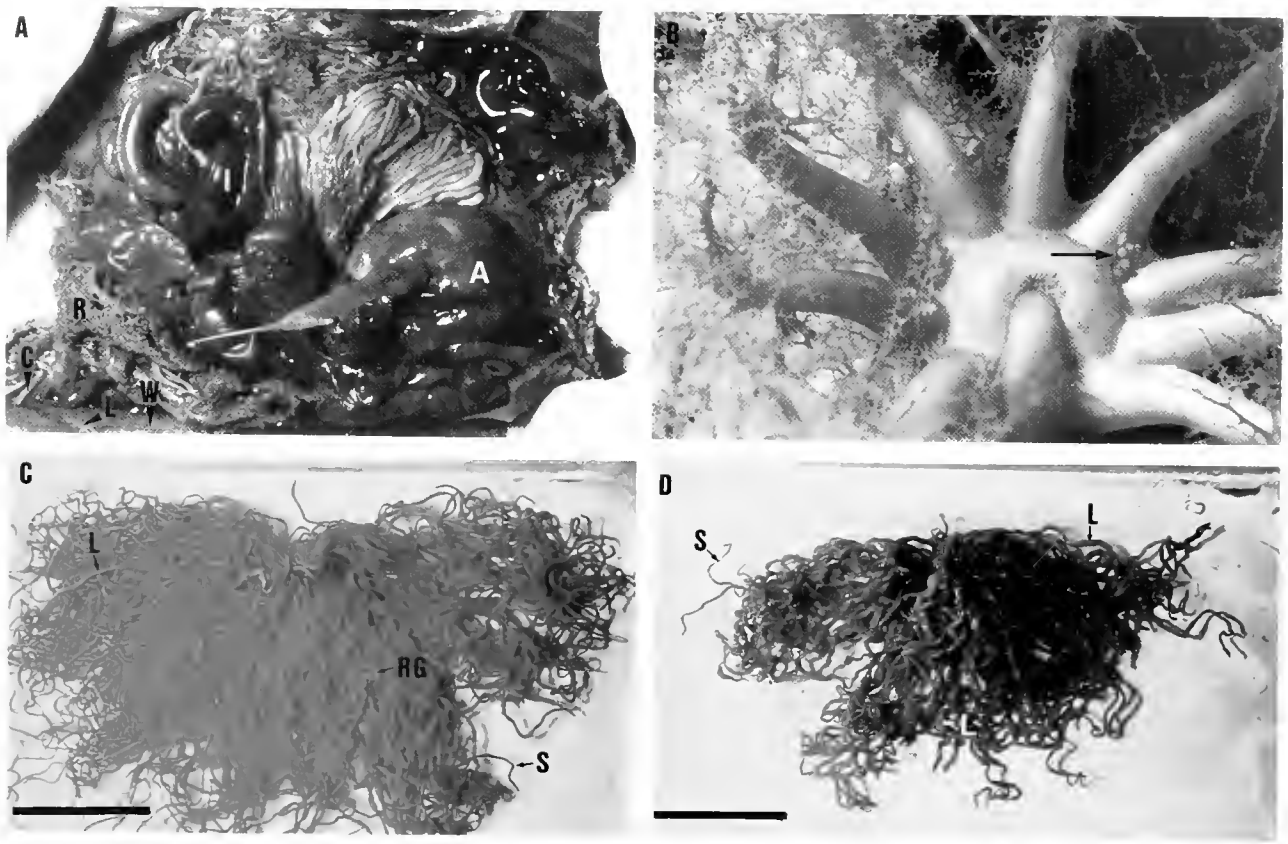

Figure 1. *Psolus fabricii.* (A) Dissected male showing the respiratory tree (R), intestine (I), body wall (W), aquapharyngeal bulb (A), cloacal muscles (C), longitudinal muscles (L), and testis (G). (B) Photograph of the mouth region showing the feeding podia, one of which is in the mouth and the others extended, and papillae surrounding the gonopore (arrow). Photographs of a testis (C) and an ovary (D) just after spawning showing the large tubules (L), small tubules (S), and tubules with swellings containing residual gametes (RG). The horizontal bars in photographs C and D represent 50 mm.

to an oven at 37°C for 1 h. This technique usually prevented the breaking of the fragile tubules and the loss of gametes. The slides were stained with eosine and hematoxylin, as described by Galigher and Kozloff (1971), and good resolution of the various cell types was achieved. A second series of slides was stained with the periodic acid-Schiff (PAS) reaction (Humason, 1981) to identify polysaccharides (glycogen).

Gonadal development was classified into five stages (post-spawning, recovery, growth, advanced growth, and mature stage) that were adapted from the earlier studies of holothurians (Tanaka, 1958; Costelloe, 1985; Cameron and Fankboner, 1986). For each male, we made 15 random measurements of the thickness of the gonadal tubule wall from slides of both small and large tubules. Only intact areas were used in this assay. For each female and for both small and large tubules, we determined the diameters of 200 relatively unbroken oocytes that showed a well-centered germinal vesicle.

Size of the gonad at sexual maturity

A sample of 132 individuals was collected on 4 May 1988. For each of these individuals, we measured the gonadal index and made histological sections to determine whether mature gametes were present. We also determined the total number of tubules in each individual, as well as the length of 15 randomly selected tubules, and the length of the intestine.

Environmental factors

Continuous temperature measurements at the study site at Anse à Robitaille were made during most of our study using a Peabody Ryan thermograph placed at 10 m in depth. Data on day length and minimum daily sunshine were obtained from the weather station at the Québec Airport (Environment Canada, Atmospheric Environment Service). Data on freshwater run-off were provided by Environment Canada (Climatologic Services) by

using the combined discharges from the Montmorency, Bastiscan, Saint-Anne and Chaudière rivers.

Phytoplankton cells abundance control the spawning of a number of marine invertebrates in the Estuary, but regular phytoplankton measurements could not be made during our study. As an indirect signal of the spring phytoplankton bloom, we determined, in 1989, the time of spawning in the green sea urchin *Strongylocentrotus drobachiensis*. This species spawns when the adults detect the rapid growth of phytoplankton during the spring bloom (Himmelman, 1981; Starr, 1990; Starr *et al.*, 1990, 1992). Thus, from March to August, when spawning was anticipated, gonadal indices (percentage gonadal mass) were determined for 15 adult urchins (4.0–6.5 cm in diameter) of both sexes at each sampling date.

We used two approaches to examine seasonal changes in the intestinal contents of *Psolus fabricii*. First, for each date, the contents of the first centimeter of the intestine of each of the 30 individuals were suspended in 5 ml of 10% formalin, and the various types of undecomposed organisms present in a 1 ml subsample were identified and counted with a hemacytometer. Large cells were examined under white illumination, and the presence of small phytoplankton cells was determined by the fluorometric method of Yentsch and Menzel (1963). Second, the contents of the following 30 g portion of the digestive tract was emptied into a Petrie dish, examined with a binocular scope, and the proportion of living phytoplankton cells (green in color) to non living materials (decomposed cells and inorganic materials) was estimated. The phytoplankton cells in the first centimeter of the intestine seemed virtually undigested (green in color and intact).

Buoyancy of oocytes

Forty oocytes were collected from five mature females (measuring 25–34 g in dry body wall mass) collected on 14 July 1990. The oocytes were placed in natural seawater to provoke breakdown of the germinal vesicle.

The oocytes were then placed in a 500 ml graduated cylinder (5 cm in diameter) at 7–8°C and the rate of upward vertical movement was recorded (Fig. 8). This movement was taken as a measure of buoyancy.

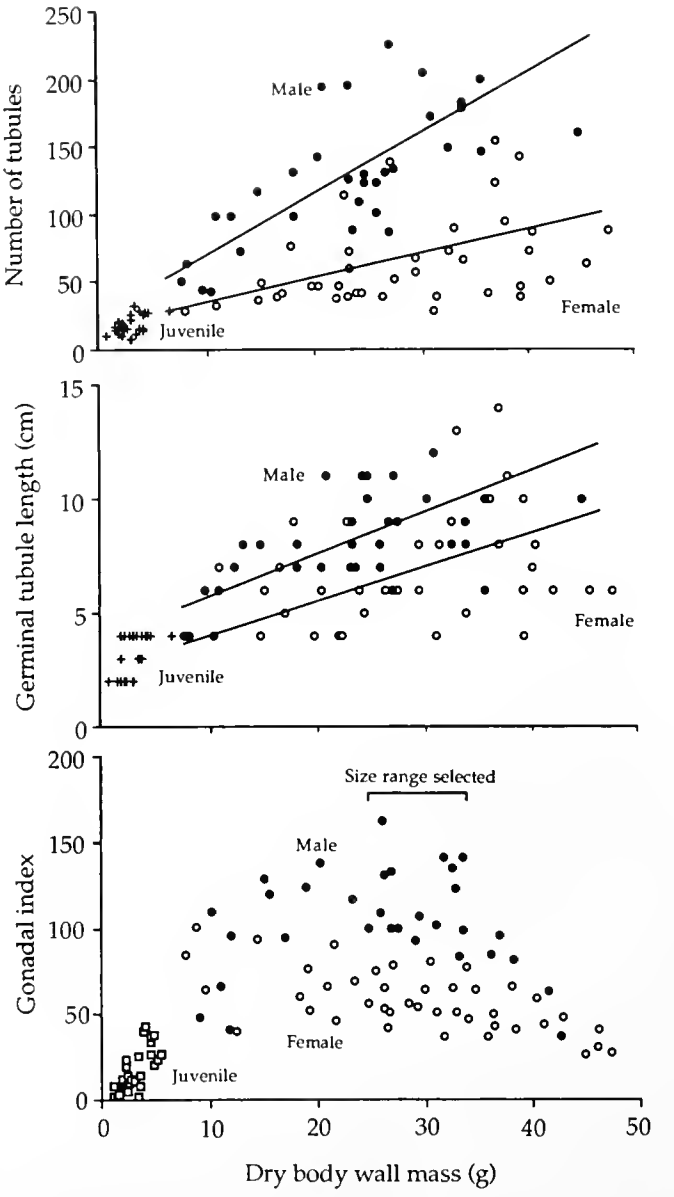

Figure 2. *Psolus fabricii*. The relation of the number of germinal tubules (A) and of germinal tubules length (B) to dry body wall mass for juvenile and adult males and females in May 1988 (n = 132). (C) The relation of the gonadal index to dry body wall mass (n = 132) in May 1988. The bracket indicates the size range used for gonadal index determinations.

Results

Gonadal morphology and size at sexual maturity

The gonads of *Psolus fabricii* consist of a large number of rarely branched germinal tubules distributed throughout the perivisceral cavity (Fig. 1C, D). The tubules join at a single gonoduct which exits through a gonopore located between the feeding podia (Fig. 1B). The number of tubules is greater for males than for females (Fig. 2A, Z test, $P < 0.01$, Tessier's slope analysis, Tessier, 1948), whereas tubule length does not vary significantly between the sexes (Fig. 2B, Z test, $P > 0.05$). In some very large males and females, the terminal ends of some tubules were necrotic, and at times these ends were found floating free in the coelomic fluid.

The size of the gonad at sexual maturity was determined from the 132 individuals collected on 4 May 1988 (Fig. 2C). Gonadal tubules were present in every individual examined that had a dry body wall mass of at least 1.2 g

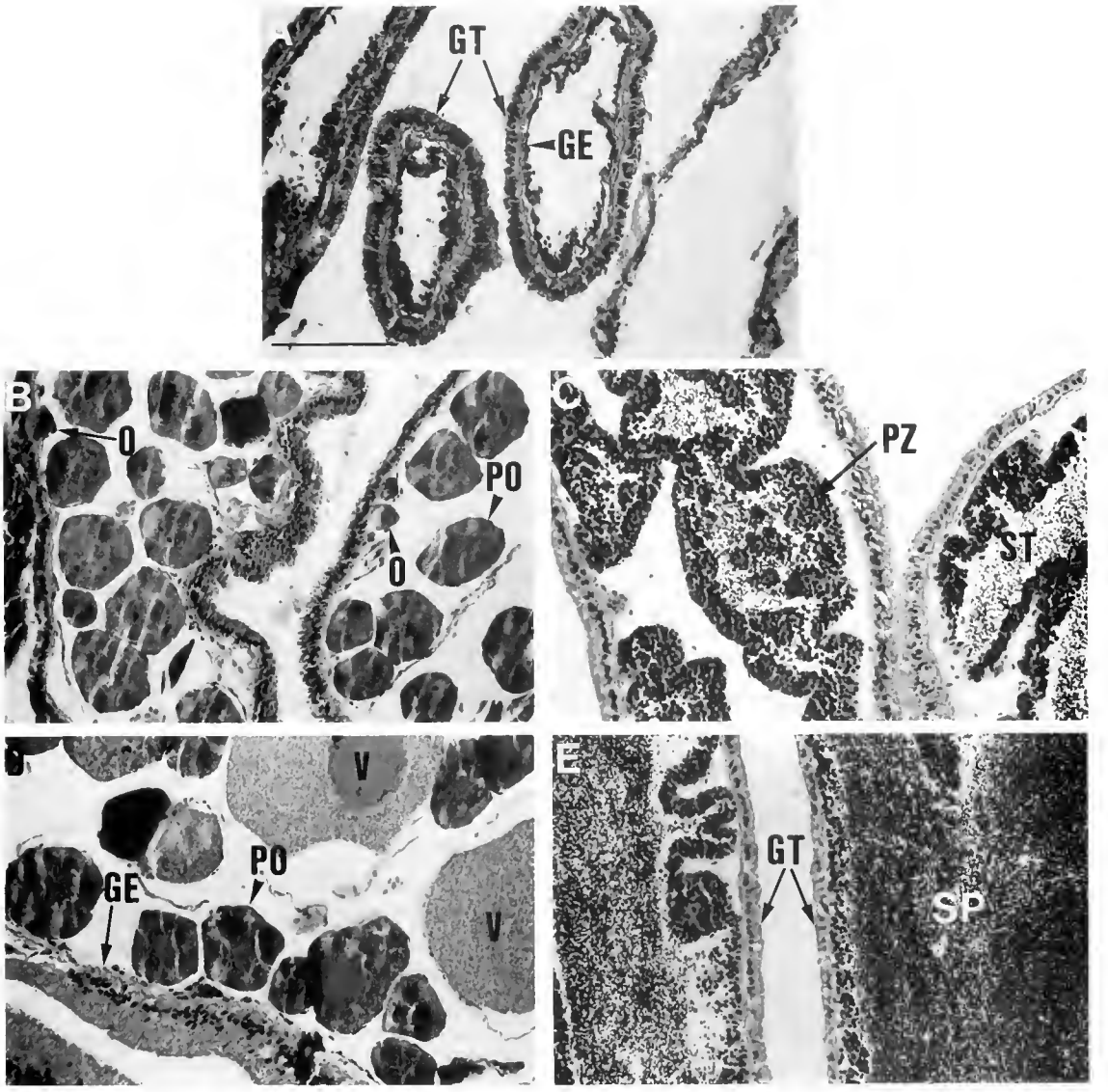

Figure 3. *Psolus fabricii.* Light micrographs of sections of gonads of juveniles. (A) Immature gonad (from an individual weighing <5.5 g in dry body wall mass) showing the germinal epithelium (GE) and an absence of identifiable precursor cells for two germinal tubules (GT); (B) Immature female (between 5.6–10 g) with oogonia (O), primary oocytes (PR), but an absence of more advanced stages; (C) Immature male (between 5.6–10 g) showing the proliferation zone (PZ) and the lumen containing only a few spermatozoa (SP); (D) Young female (≈10 g) showing the germinal epithelium (GE), primary oocytes (PO) and a few vitellogenic oocytes (V); (E) Young male (≈10 g) showing two distinct germinal tubules (GT) and numerous spermatozoa (SP) in the lumen. The horizontal bar in photograph A represents 800 μm and applies to all of the photographs.

(equivalent to ≈0.7 cm in distance mouth-anus). The relative size of the gonads increased sharply as the dry body wall mass rose from 3 to 10 g (Fig. 2C). The size of testis and ovary overlapped greatly up to a body wall mass of ≈15 g, but the testis was generally larger than the ovary for larger individuals (Kruskal-Wallis, analysis of variance, $P < 0.01$, followed by a non-parametric multiple-range test, $P < 0.05$; Sokal and Rolph, 1981). The variation in gonadal size was relatively small between 20 and 34 g (5.5 to 6.1 cm); beyond that range the relative gonadal size dropped.

Histological preparations showed that only undifferentiated precursor cells are present along the germinal epithelium of individuals weighing <5.5 g (≈3.2 cm) (Fig. 3A). The sex of larger individuals could be identified by the presence of oogonia and young oocytes in females, and spermatogonic stages in males (Fig. 3B, C). Beginning at 6.5–7.9 g (4.0–4.6 cm), the sexes were readily recognized

from gonadal smears (Fig. 2C), although histological examination showed that only individuals weighing >10 g (≈4.8 cm) contained mature gametes with the same morphology and reaction to PAS and hematoxylin and eosine as for very large individuals (Fig. 3D, E). Immature gonads were cream in color, whereas the mature testis was pink, and the mature ovary reddish brown (individuals > 10 g). Thus, *Psolus fabricii* starts to produce mature gametes at 10 g, but the gonads only attain a plateau in size at 15–20 g (Fig. 2C). Individuals weighing 25 to 34 g showed no variation due to body size and were used in following the gonadal index cycle.

No significant departure from a sex ratio of 1:1 was observed in any of the samples, and the ratio for all of the samples together was 595 males to 607 females (df = 14, $\chi^2 = 1.44$, $P > 0.05$). No external differences were observed between the sexes, and hermaphrodites were not encountered.

Seasonal changes in body component indices

Throughout the study, the mean gonadal index of males was more than twice that of females (Kruskal-Wallis, $P < 0.01$), and on no date did the maximum value for any given female attain the minimum observed for the males (Fig. 4). Nevertheless, the two sexes showed parallel seasonal cycles in gonadal size. The index for males and females dropped significantly between 14 May and 12 June 1988 (Kruskal-Wallis, $P < 0.01$), suggesting the release of gametes. The gonads showed no further significant change in size until the end of the following winter (in March 1989 for males and April 1989 for females), when a significant growth was evident (Kruskall-Wallis, $P < 0.01$). Both testicular and ovarian indices attained a peak in mid July 1989 and then dropped abruptly by 5 August 1989, suggesting a second spawning.

The diameter of the germinal tubules showed a similar pattern, although the annual cycle was more pronounced (Fig. 4). In both years, the mean diameter attained a maximum just before spawning (higher in 1989 than in 1988) and dropped precipitously during spawning (Kruskal-Wallis, $P < 0.01$). The decrease was by ≈24% in 1988 compared with ≈80% in 1989. The diameter of any given tubule was relatively uniform, except after spawning when some tubules had swollen sections containing unspawned gametes. The mean diameter of male tubules was consistently larger than that of females during May through August (Kruskal-Wallis, $P < 0.01$), but not during autumn and winter (Kruskal-Wallis, $P > 0.05$). In spite of the distinct seasonal pattern in mean tubule size, extremes in tubule size were always evident, and every gonad contained tubules ranging from small to large.

The 1989 spawning was also observed directly by persons diving in our study site on 22 July (Normand Piché and Andréa Cantin, pers. comm.). Numerous females were seen releasing eggs. Spawning was probably widespread and massive in the lower St. Lawrence Estuary because on 25 and 26 July 1989 other divers observed an abundance of *Psolus fabricii* oocytes and embryos throughout the first 3 m of the water column over a long section (≥5 km) of the southern side of the Estuary near Rimouski (Lucie Bossé, Institut Maurice-Lamontagne, pers. comm.).

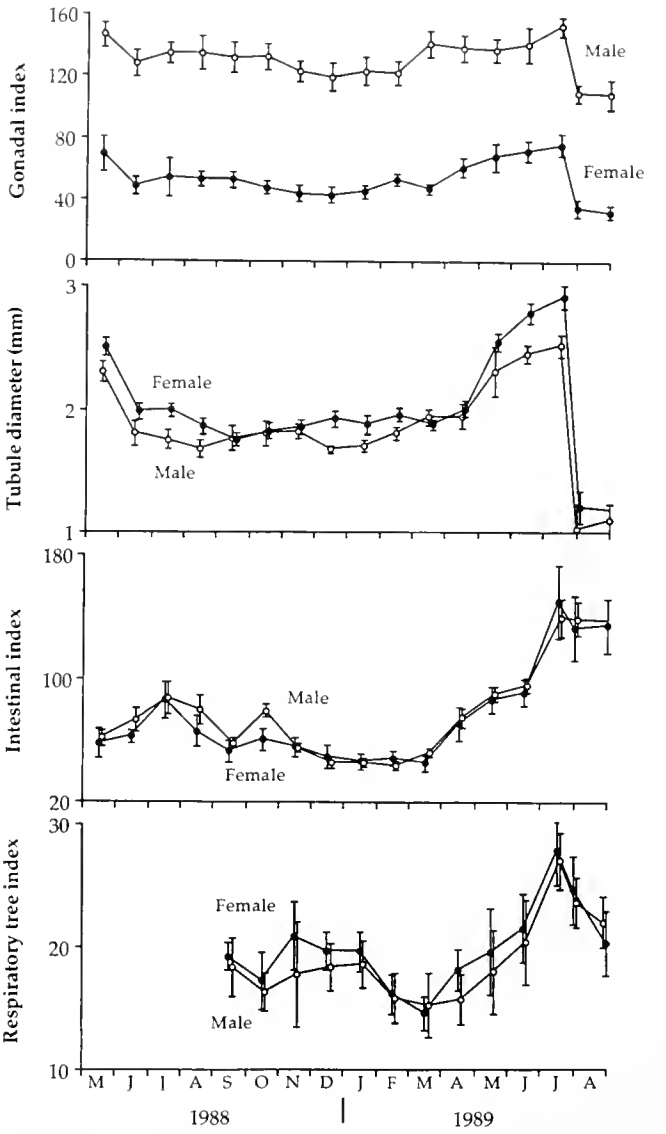

Figure 4. *Psolus fabricii*. Seasonal changes in the mean gonadal, intestinal and respiratory tree indices and in the diameter of the germinal tubules for males and females from May 1988 to August 1989. Vertical lines indicate the 95% confidence intervals.

Variations in the intestinal index were largely attributable to changes in the intestinal contents: the mass of the wall of the first centimeter of the intestine varied by <2% throughout the study (and no significant seasonal

changes were detected, Kruskal-Wallis, $P > 0.05$), whereas the mass of its contents varied by $\approx 37\%$ (Kruskal-Wallis, $P < 0.01$). The intestinal index showed intermediate values during the summer of 1988, a minimum between December 1988 to March 1989, and then a sharp increase to a maximum in July 1989. The maximum attained in 1989 was much greater than in 1988 (Fig. 4). The respiratory tree decreased during the winter of 1988–89, started to growth in April 1989, and reached a peak in mid July 1989 (Fig. 4).

Female reproductive cycle

Oogenesis. The development of gametes in *Psolus fabricii* was transversal, starting at the surface of the germinal epithelium and progressing towards the lumen of the tubule. In addition, it proceeded in a relatively uniform fashion along all surfaces of any tubule. Along the surface of the germinal epithelium, oogonia occurred in groups at numerous points, whereas primary oocytes (<100 μm) were dispersed. The small oocytes (<250 μm) were surrounded by follicular cells which persisted until spawning. The germinal vesicle is central and also persisted until spawning. The small oocytes have a PAS-negative basophilic cytoplasm which becomes slightly PAS-positive upon attaining 300 μm (indicating the beginning of glycogen accumulation), and increasingly positive as vitellogenesis progressed. The morphology and histological staining indicated that the oocytes were mature at ≈ 800 μm, although they could attain up to 1400 μm in diameter. Nutritive phagocytes were associated with the tubules that had released gametes. For both males and females, the tubule wall became more and more PAS-positive after spawning until January-February, and then progressively PAS-negative until the following spawning period. The following five stages of oogenic development were used to quantify the seasonal oogenic changes (Fig. 5).

(1) Post-spawning (Fig. 5A). The gonadal tubule wall is thin and extremely convoluted. Although some residual or unspawned oocytes, measuring 400–800 μm, remained in the tubules, the majority of oocytes measured <300 μm and are generally PAS-negative. Striking elongated empty areas are seen in the tubules, suggesting the passage of oocytes along the length of the tubule during spawning. Nutritive phagocytes begin to appear and are always inside of the follicular cells that surround the residual oocytes. The follicular cells around the residual oocytes were degenerated.

(2) Recovery (Fig. 5B, C). The gonadal tubule wall is very thick. The germinal epithelium is convoluted, and beds of small oocytes (<200 μm in diameter) are present along the epithelium. Nutritive phagocytes are closely associated with nearly all of the residual oocytes and the follicular cells are poorly defined.

(3) Growth (Fig. 5D). The thickness of the tubule wall reaches its maximum. Along the surface of the germinal epithelium, many small oocytes (<200 μm, PAS-negative) and some previtellogenic oocytes (300–600 μm, PAS-positive) are present and nutritive phagocytes are virtually absent.

(4) Advanced growth (Fig. 5E). The tubule wall is thinner, and the diameter of the tubules is increased. In the lumen of the tubules, well-defined follicular cells are associated with large PAS-positive previtellogenic (400–600 μm) and vitellogenic (>600 μm, PAS-positive) oocytes. The vitellogenic oocytes are reddish orange. Numerous small oocytes (<400 μm) are present along the germinal epithelium.

(5) Mature (Fig. 5F). The tubules are highly dilated, their walls thin and not convoluted, and they are almost completely filled with mature oocytes (>800 μm). Each oocyte contains one to four nucleoli and a well-defined germinal vesicle, which occupies 30–50% of the surface of the oocyte in the histological preparations. Immature oocytes are virtually absent.

Seasonal changes in the oogenesis. Advanced oogenic stages (advanced growth and mature stages) predominate in the large tubules, and earlier stages (post-spawning, recovery and growth stages) in the small tubules (Fig. 6). Nevertheless, both categories of tubules showed a seasonal pattern that is correlated with the gonadal index cycle. In the large tubules, the post-spawning and recovery stages are almost always absent, and the major evidence of the June 1988 and July 1989 spawnings was the decrease in the mature stage. In contrast, the mature stage in the small tubules is rare before spawning and absent in other periods, and the major evidence of spawning was a sharp increase in the post-spawning stage (from 0 to 80%). These observations suggest that the release of mature oocytes during spawning transforms large fecund tubules into small tubules in post-spawning condition. This change coincides with a sharp drop in the mean diameter of tubules (Fig. 4). Following spawning there is a period of inactivity until mid January; then oocyte development resumes. In small tubules, a progressive increase in the frequency of the growth stage occurred between January and July 1989 coincident with a decrease, first in the post-spawning stage, and then in the recovery stage. Meanwhile, the large tubules show an increase in the advanced growth and mature stages (Fig. 6).

Size of oocytes. The seasonal pattern in the size structure of oocytes varies markedly between large and small tubules (Fig. 7). In large tubules, a striking change in the oocyte population occurred during the 1988 spawning. Prior to spawning, most oocytes measured >800 μm, whereas after spawning in June 1988, 500–700 μm oocytes predominated. Following this, the oocyte population in the large tubules was stable. Then in January 1989, renewed oocyte

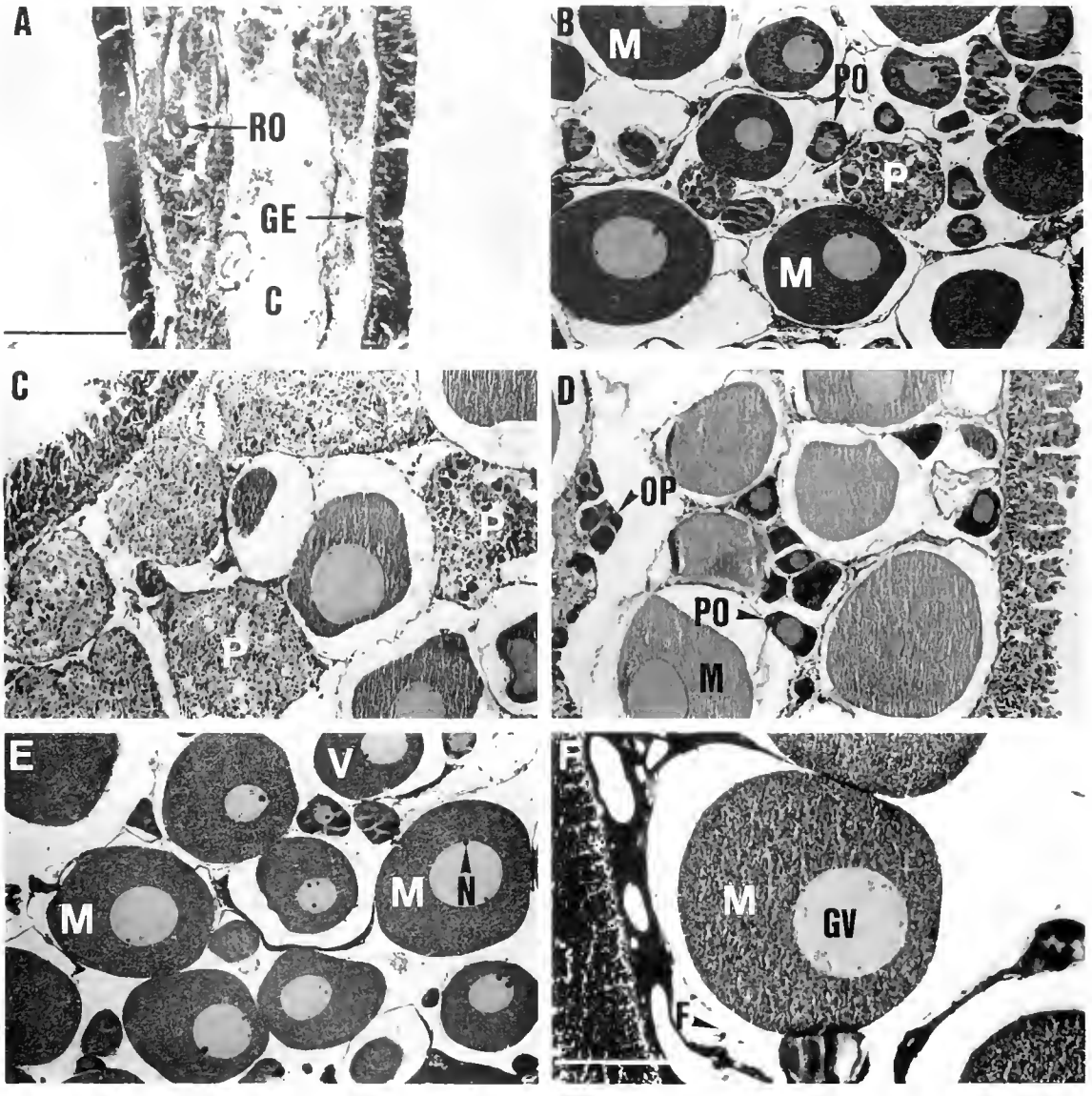

Figure 5. *Psolus fabricii* Light micrographs of ovarian sections illustrating the oogenic cycle. (A) Portion of a post-spawning ovary showing the germinal epithelium (GE), residual oocytes (RO), and a channel created by the expulsion of eggs during spawning (C); (B) Early recovery stage showing primary oocytes (PO), mature oocytes (M), and nutritive phagocytes (P) surrounded by follicular cells. (This section was across a swelling containing residual gametes in a spent tubule); (C) Late recovery stage showing an abundance of nutritive phagocytes (P); (D) Growth stage showing sites of oogonial proliferation (OP), primary oocytes (PO), and mature oocytes (M); (E) Advanced-growth stage showing an abundance of both vitellogenic oocytes (V) and mature oocytes (M) with nucleoli (N); (F) Mature stage showing large mature oocytes (M) containing the germinal vesicle (GV) and surrounded by follicular cells (F). The bar in photograph A represents 800 μm and applies to photographs B, C, D and E, whereas the bar in photograph F represents 400 μm.

growth was evident, and the predominant mode of oocytes attained a peak of 1100 to 1300 μm in mid July 1989. These mature oocytes largely disappeared during the July 1989 spawning, and on 5 August the modal oocyte class was again 500–700 μm. Although the loss of large oocytes (>800 μm) during spawning was expected, the presence of a strong cohort of intermediate oogenic stages (500–700 μm) in the large tubules after spawning seemed at first surprising. This was because spawning transformed the large tubules into small tubules. Thus, the small tubules in June 1988, which were characterized by a strong mode of oocytes measuring <300 μm, were probably those which had just spawned. They contained residual oocytes that were being attacked by nutritive phagocytes, whereas

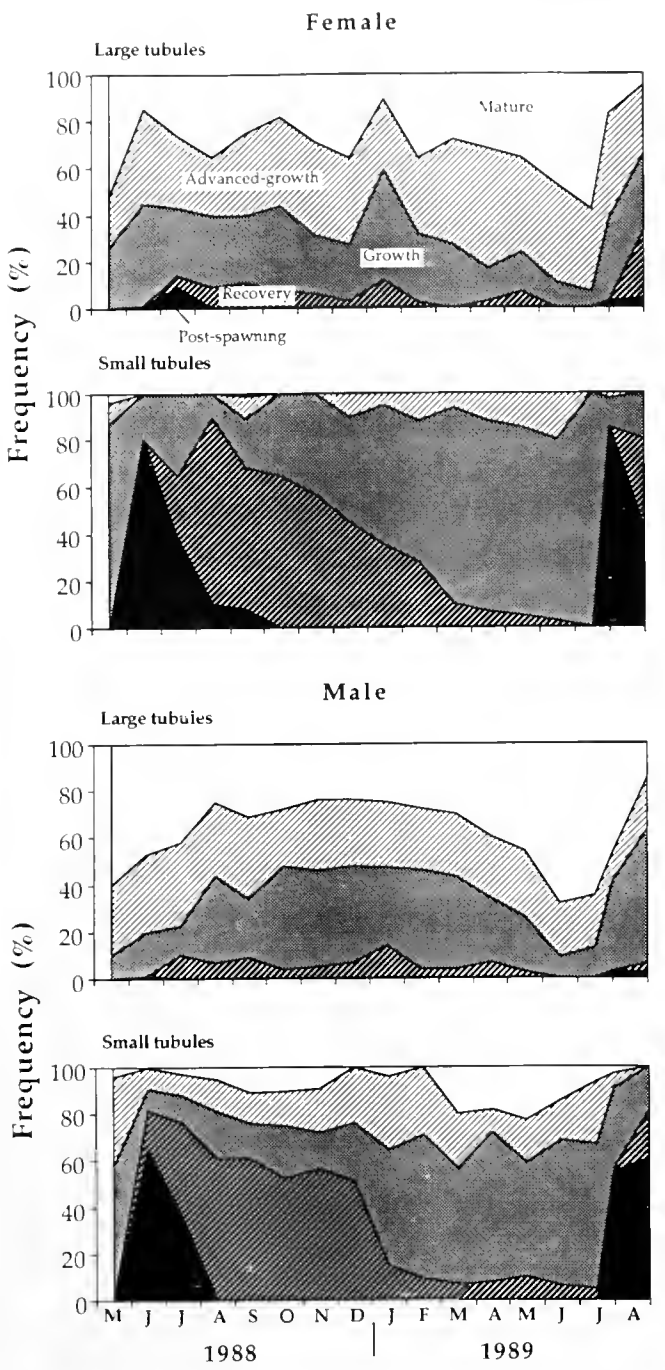

Figure 6. *Psolus fabricii.* Relative frequency of different gametogenic stages (as defined in the Materials and Methods section) in small and large, female and male, tubules for the period from May 1988 to August 1989.

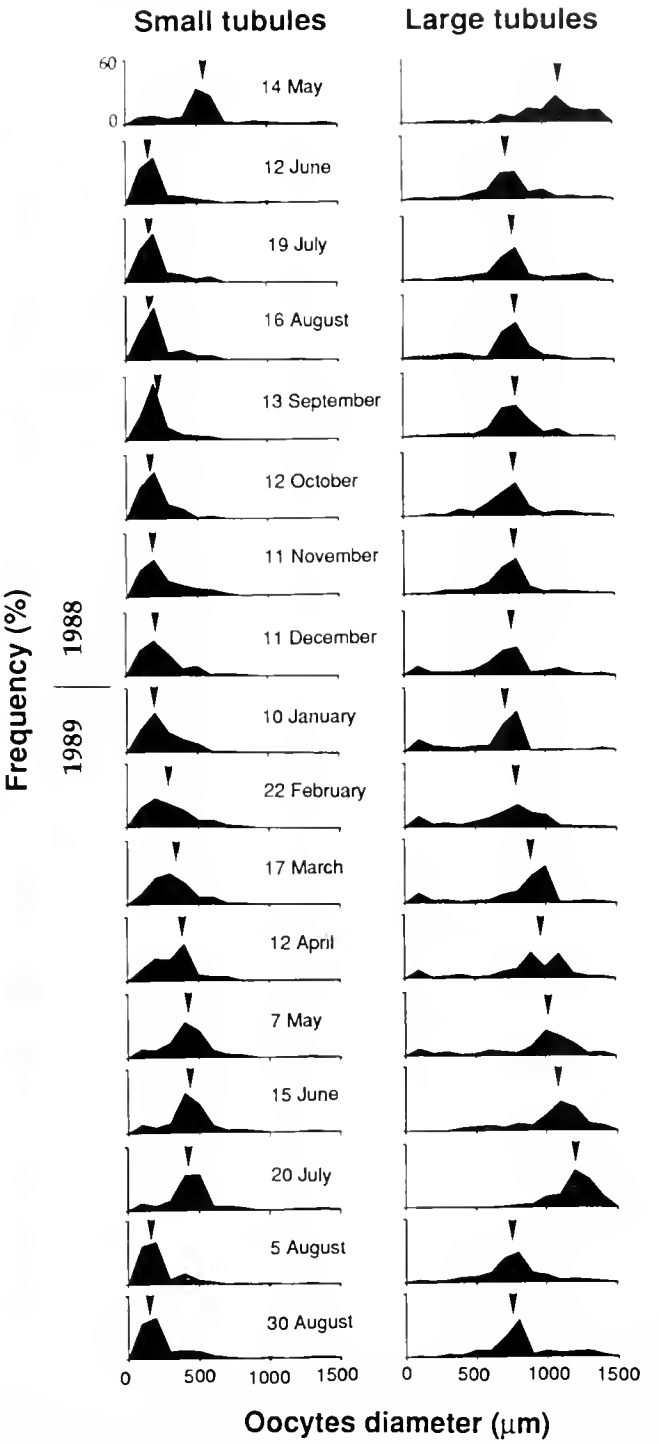

Figure 7. *Psolus fabricii.* Oocyte diameter distributions for small and large tubules for the period from April 1988 to August 1989. For each distribution the vertical axis is from 0 to 60% and the mean oocyte diameter is indicated by an arrow.

at the same time, the large tubules contained an abundance of intermediate stages, and nutritive phagocytes were rare. Most oocytes in the small tubules in mid May 1988 measured 400–600 μm, whereas those in the large tubules in June 1988 measured 600–800 μm. The similarity in size distributions for these two samples suggested the transition from small to large tubules during spawning. Following spawning, until mid December 1988, the oocyte

distributions for the small tubules showed little change. However, a marked increase in the total number of cells per surface of germinal tubule was noted in January 1989. Thereafter, oocyte size and number progressively increased in the small tubules until 20 July 1989 when the size structure was virtually identical to that of the small tubules prior to spawning in 1988. The sharp reduction in >800 μm oocytes in the large tubules during the 1989 spawning closely followed the changes in the large tubules during the 1988 spawning.

Buoyancy of oocytes. Thirty three of the oocytes showed a positive floatability which clearly increased with diameter (Spearman rank correlation coefficient, r = 0.67, df: 32, $P < 0.01$). This indicated that 1.2 mm oocytes would move upward at a rate of 20–30 mm · min^{-1}. The other four oocytes showed a slightly negative floatability, and we suspect that they were damaged (possibly the egg membrane was not intact) (Fig. 8). These observations indicate that spawned eggs will move to the surface of the water column. This agrees with the abundance of developing *Psolus fabricii* embryos near the surface, as observed by divers during the 1989 spawning.

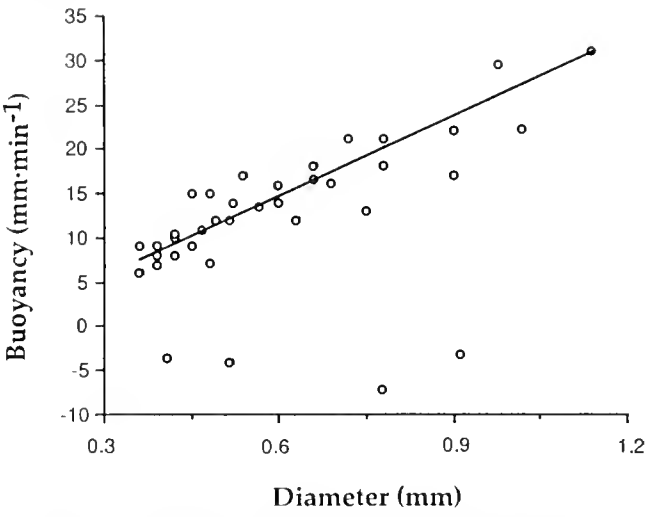

Figure 8. *Psolus fabricii.* Relation of buoyancy to diameter for oocytes dissected for mature females and activated by being placed in seawater. The regression line is based only on oocytes with positive buoyancy.

Male reproductive cycle

Spermiogenesis. The following five stages of spermiogenesis are used to quantify the seasonal changes in the small and large tubules (Fig. 9).

(1) Post-spawning (Fig. 9A). The thickness of the tubule wall is at its minimum. In the sections, we observed elongated empty areas along the length of the tubules, suggesting the passage of gametes during spawning. A few residual spermatozoa are present, and no proliferating zone (containing spermatogonia, spermatocytes and spermatids) was present.

(2) Recovery. The tubule wall is extremely thick and highly convoluted. The tubules contain small quantities of spermatozoa and scattered nutritive phagocytes.

(3) Growth (Fig. 9B, C). The gonadal tubule wall is beginning to decrease in thickness but is still convoluted. Spermatogonia are abundant along the surface of the germinal epithelium. Progressing towards the lumen, there is a layer of spermatocytes, one of spermatids, and finally a small number of spermatozoa in the lumen.

(4) Advanced growth (Fig. 9D, E). The tubule wall is thinner and slightly convoluted, and the lumen is filled with spermatozoa.

(5) Mature (Fig. 9F). The tubules are stretched to their maximum diameter and completely filled with spermatozoa. The tubule wall is nearly smooth, and earlier spermatogenetic stages are absent.

Psolus fabricii spermatozoa are flagellated with a round head measuring 5–6 μm. Microscopic observation of a sperm suspension in seawater, just prior to spawning, revealed a low motility of the spermatozoa.

Seasonal changes in spermatogenesis. In May and June 1988 and again in July and August 1989, advanced stages (advanced growth and mature stages) were found in >85% of the large tubules, whereas earlier stages (post-spawning, recovery and growth stages) predominated in the small tubules (Fig. 6). The most striking evidence of the spawnings in June 1988 and August 1989 was the abrupt appearance of post-spawning stages in the small tubules. The tubules classified as large after spawning were characterized by an abundance of early spermatogenetic stages and few spermatozoa. These observations suggested, first, that the release of spermatozoa from the large tubules during spawning diminish their size, so that after spawning they were considered as small tubules. Moreover, the tubules that were selected as large were those that had recently attained a diameter of 1.9 mm (the lower limit for large tubules). Thus a pattern parallel to that observed for the females was found. The post-spawning stage, found only in the small tubules, disappeared by late summer and was replaced largely by the recovery and growth stages. Subsequently, the advanced growth and mature stages became more common and attained a peak a few month prior to spawning.

Thickness of the gonadal tubule wall. In males, the distributions for gonadal tubule wall thickness were virtually always skewed rather than being symmetrical (Fig. 10). Further, all size classes up to 140–160 μm were present in both small and large tubules throughout the study, except for four dates near the time of spawning, when the largest classes were absent. In both the small and large tubules, changes in the distributions followed an annual pattern. Just before spawning in May 1988, the mean thickness was 20–40 μm; after spawning it decreased

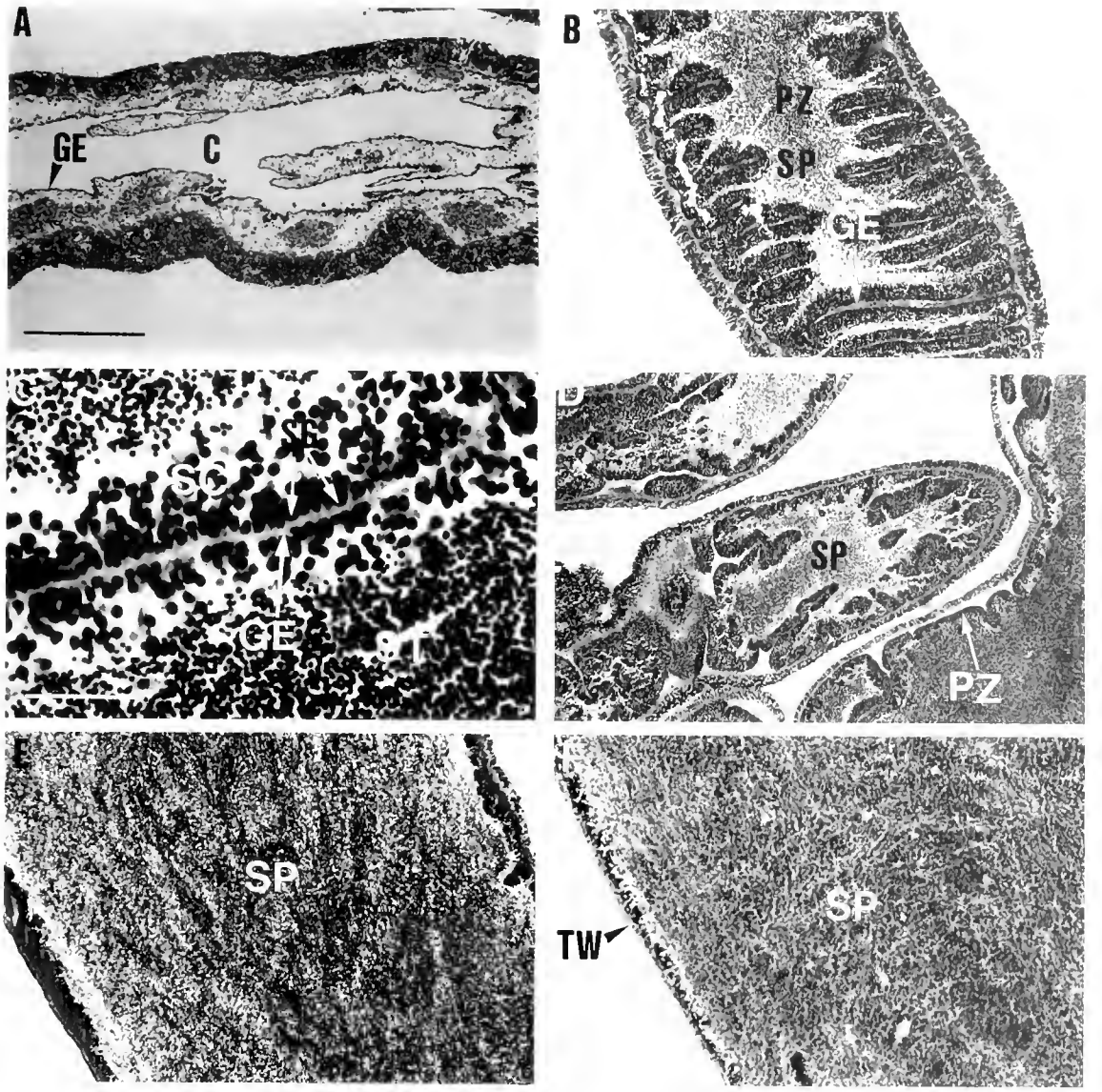

Figure 9. *Psolus fabricii.* Light micrographs of testicular sections illustrating the spermatogenic cycle. (A) Post-spawning testis showing the germinal epithelium (GE) and channels where sperm passed during spawning (C); (B) Growth stage showing the highly convoluted germinal epithelium (GE) and the proliferation zone (PZ); (C) Growth stage showing the germinal epithelium, spermatogonia (SG), spermatocytes (SC) spermatids (ST) and spermatozoa (SP) in successive layers progressing towards the lumen; (D) Early advanced-growth stage showing the proliferating zone (PZ) and spermatozoa (SP); (E) Late advanced-growth stage showing the thin gonadal tubule wall and an abundance of spermatozoa (SP); (F) Mature stage showing the thin tubule wall (TW), absence of the proliferation zone, and great numbers of spermatozoa (SP) in the lumen. The bar in photograph A represents 800 μm and applies to photographs B, D, E and F, whereas the bar in photograph C represents 300 μm.

slightly. Subsequently, the thickness of the tubule wall progressively increased, although the pattern varied depending on tubule size. Thus, the large tubules grew more rapidly and attained a peak ($\approx$120 μm) in November 1988, whereas the small tubules did not attain a peak ($\approx$140 μm) until February 1989. Subsequently, the size of the modal size class again decreased to 20–40 μm following the 1989 spawning (Fig. 10).

Environmental factors

Temperature. The mid May to mid June spawning, in 1988, coincided with the spring warming period, and temperatures attained about 5°C at the time of spawning (Fig. 11). However, temperatures fluctuated markedly during this period. An increase from 4 to 6°C was observed between 20 and 23 May 1988, and a drop of 6.7

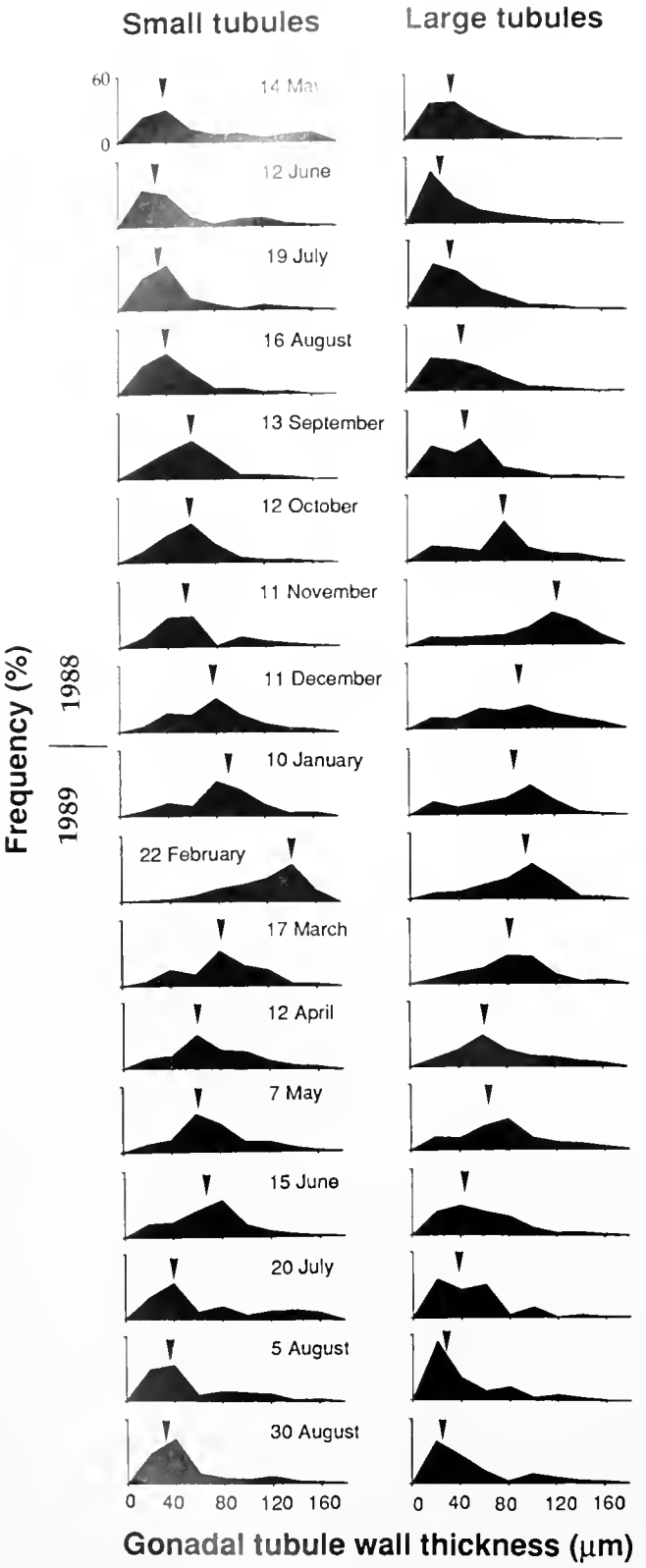

Figure 10. *Psolus fabricii.* Frequency distributions (10 μm size classes) of the thickness of the gonadal tubule wall for small and large tubules for males collected from May 1988 to August 1989. The arrows indicate the mean thickness for each sampling date.

to 4.4°C between 5 and 6 June. These variations were due to the semidurnal tides in the Estuary (Demers *et al.*, 1986). During 1988, the maximum temperature was reached in mid July, and the autumnal decrease began in late August.

In 1989, warming began in March, attained a peak in late June, and then varied around 6°C until the end of the study (2–4°C daily fluctuations were frequent). The accelerated gonadal growth, which began in March or April, occurred at about the time that the vernal warming began. There was no spawning, either during the warming phase or during marked temperature variations in May and June; rather, spawning occurred in late July when temperatures were more stable. Thus, although spawning occurred at about the same temperature in the two years (5–6°C), the point in the temperature cycle was quite different (Fig. 11).

Photoperiod. In our study, the renewal of gametogenesis in January coincided with the period when day length and daily bright sunshine were beginning to increase, and the gonadal peak was attained at the photoperiod maximum (Fig. 11). Although *Psolus fabricii* spawned near the photoperiod maximum in both years, the 1988 spawning occurred at the beginning of this maximum and the 1989 spawning one month later, when photoperiod was just beginning to decline.

Freshwater run-off and the predicted timing of the phytoplankton bloom. The period during which freshwater run-off decreased in the Estuary was much later in 1989 (July) than in 1988 (late May) (Fig. 11). Nevertheless, spawning in both years coincided with this event, suggesting a relationship between the two. 1989 was an exceptional year in that the run-off was markedly greater and more delayed than in the five previous years. It was also unusual in that spawning of the green sea urchin *Strongylocentrotus droebachiensis*, a signal of the phytoplankton increase, was much later than in the previous years. The urchin spawned abruptly between 14 July and 5 August, exactly the same period during which *Psolus fabricii* spawned (Fig. 11). In contrast, when urchins were studied in the Estuary in the previous years, spawning occurred prior to mid June (Starr, 1990).

Intestinal contents. The intestine of adult *Psolus fabricii* contains two types of materials: (1) non living particles and (2) phytoplanktonic cells; the major species of plankton are the diatoms *Thalassiosira* sp., *Coscinodiscus* sp., *Chaetoceros* sp., and *Skeletonema* sp. (Fig. 11). During the autumn and winter, only 20–50% of the contents were phytoplanktonic cells, and this increased during the spring, attaining virtually 100% in the summer (Fig. 11).

A marked seasonal pattern was evident for the diatoms present in the intestines. Most cells in the first samples in May and June 1988 were *Coscinodiscus* sp., *Thalassiosira* sp., and *Skeletonema* sp., suggesting a diatom bloom at

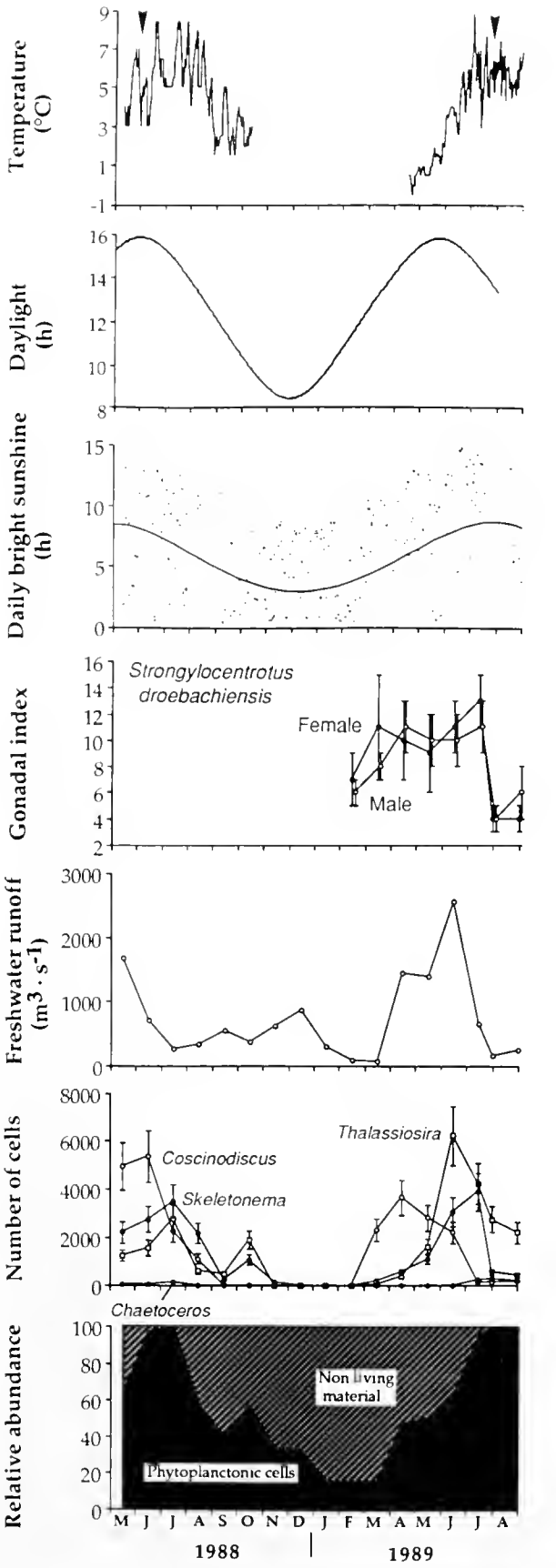

this time. Subsequently, there was a progressive decrease to the winter minimum. In 1989, *Coscinodiscus* sp. showed an increase during March and April, and *Thalassiosira* sp. and *Skeletonema* sp. an increase in June (Fig. 11). The latter two species increased further to the highest level for the study in late July. This suggested an intensive bloom at this time. Whereas the above large diatom species typically occur in chains in the water column, they were always present as individual cells in the intestines. No animal structures were observed in *Psolus fabricii* intestines.

Discussion

Morphological comparisons with other holothurians

Non-branched germinal tubules, such as are found in *Psolus fabricii*, also occur in *Cucumaria lubrica* and *Ypsilothuria talismani* (Atwood and Chia, 1974; Tyler and Gage, 1983), but branched tubules have been reported in other holothurians (Atwood, 1974; Smiley and Cloney, 1985; Cameron and Fankboner, 1986; Tyler and Billett, 1987). The increase in the number of gonadal tubules with size in *P. fabricii* (Fig. 2A) is in contrasts with *Aslia lefevrei*, where tubule number is highly variable and not related to size (Costelloe, 1985).

Throughout the year, the gonad of *Psolus fabricii* is larger in males than in females, and this is primarily due to the number of tubules in the testis rather than to tubule length or diameter (Fig. 2A, B). This, together with the greater drop in gonadal mass during spawning (Fig. 4), suggests that males have a greater reproductive output. A larger male gonad is not a general holothurian characteristic, since the inverse is the case for *Stichopus californicus* (Cameron and Fankboner, 1986), and equal-sized gonads are reported for *Cucumaria pseudocurata* (Rutherford, 1973). A sex ratio of 1:1 has been reported for several holothurians in addition to *P. fabricii* (Cameron and Fankboner, 1986; Jespersen and Lutzen, 1971; Conand, 1982; Engstrom, 1982; Mosher, 1982), but numerous others have a ratio favoring males (Lawrence, 1987).

Necrotic fragments of germinal tubules as found in *Psolus fabricii* have previously been described for *Sticho-*

Figure 11. Seasonal variations in temperature, daylight, daily bright sunshine, and freshwater run-off, as well as the relative proportion of living and non-living materials in a ≈30 g portion of the intestinal mass and the absolute abundance of the four major phytoplankton species, in the first centimeter of the intestine of *Psolus fabricii*, during the period from May 1988 to August 1989. The gonadal index cycle of the urchin *Strongylocentrotus droebachiensis* was quantified in 1989, and the drop in the index between 20 July and 5 August suggests that there was a phytoplankton bloom at this time. The vertical lines indicate the 95% confidence intervals. The arrows above the temperature cycle indicate when *P. fabricii* spawned.

pus californicus by Cameron and Fankboner (1986), but only for males. In both sexes of *P. fabricii*, necrotic tubules were most common in large individuals and thus may be related to the decrease in relative gonadal size in very large individuals. Aerobic metabolism furnishes most of the energy requirements of echinoderms (Ellington, 1982; Lawrence and Lane, 1982; Shick, 1983; Féral and Magniez, 1985), and Hopcroft *et al.* (1985) demonstrate that 75% of oxygen required by *P. fabricii* (individuals weighing 80 g in wet mass) is obtained through the respiratory tree. Thus, the increase in the size of the respiratory tree as the gonads grow may indicate its role in supplying oxygen for gametogenesis (Fig. 4).

The follicular cells associated with developing oocytes in echinoderms supply nutriments to the oocytes and also control the environment around them (Hirai and Kanatani, 1971). In *Psolus fabricii*, the follicular cells are closely associated with the oocytes as they migrate into the lumen during maturation, and they may surround the oocyte during spawning as reported for *Cucumaria elongata* (Chia and Buchanan, 1969). This contrasts with *Stichopus californicus* in which the follicular cells stay attached to the epithelium as the oocytes migrate into the lumen (Smiley and Cloney, 1985). The clearly stratified spermatogenesis of *P. fabricii* (Fig. 9) contrasts with that in *Leptosynapta clarki* and *C. lubrica*, in which spermatogonia and spermatids are erratically distributed throughout the lumen (Atwood, 1973, 1974).

Gametogenesis

In *Psolus fabricii*, oogenesis begins with the production of precursor cells in the small tubules in January. Progressively through the winter and spring these cells are transformed into oogonia and primary oocytes, and by mid summer 400–600 μm cells are most abundant (Fig. 7). These stages in small tubules do not contribute to spawning. After spawning, some small tubules attain >1.9 mm, a diameter sufficient to be classified as large tubules. During the autumn, the oocyte distributions in the tubules classified as large, remain virtually static, indicating a period of inactivity; then in January, oocytes growth and tubule enlargement resumes. This growth continues until the following summer when most oocytes measure >800 μm and the tubules attain their maximum diameter (Fig. 4). Finally, the release of these large oocytes during spawning results in a drop in the size of the tubules. From the time of spawning until the following January, nutritive phagocytes are active in destroying the residual oocytes (Fig. 5).

Our study also indicates a prolonged spermatogenesis. As with oogenesis, it begins with the production of precursor cells in the small tubules in mid winter, although a prior accumulation of reserves in these tubules is indicated by the thickening of the gonadal tubule wall during the previous autumn (Fig. 10). In late winter and spring, as the thickness of the germinal wall decreases, spermatogonia, spermatocytes, and spermatids progressively accumulate in the tubules (Figs. 9, 10). Since these tubules contain only small amounts of spermatozoa, they probably do not participate in spawning. During and after spawning they progressively attain the size of large tubules. The major change after spawning in what are now the large tubules is the thickening of the gonadal tubule wall and this peaks in February (Fig. 10). At about the same time, the production of spermatozoa increases, and this amplifies until a peak just prior to spawning (Fig. 6). Finally, with the release of sperm during spawning, these large tubules become small; after spawning nutritive phagocytes become abundant. This is the first report of the testicular cycle taking longer than a year in holothurians.

Although the examination of large and small tubules indicates that gametogenesis is prolonged, studies with radioactive markers are needed to determine its duration precisely. Our observations suggest that the production of the majority of gametes begins in winter and terminates 15–18 months later (two summers later). In some tubules, however, this process may be much longer or, at times, shorter.

That gametogenesis in *Psolus fabricii* generally takes more than a year was revealed from the separate histological studies of small and large tubules. Smiley and Cloney (1985) and Smiley (1988) examined the gonads of female *Stichopus californicus* collected in different seasons. Their observations of three size groups of tubules, with the most advanced stages of oogenesis only being present in the largest tubules, similarly led them to conclude that oogenesis was a long process. In contrast to *P. fabricii*, the various sized ovarian tubules of *S. californicus* are not intermixed. Rather they are arranged in order, the large fecund tubules being located posteriorly. Smiley and Cloney (1985) report that the large tubules are completely reabsorbed once the oocytes are released. Based on these observations, they propose that the tubules are produced at the anterior of the gonad and migrate posteriorly as they increase in size and state of development. Reabsorption does not occur in *P. fabricii*, since a new group of oocytes is evident in the fecund tubules at the time of spawning and persists in spent tubules during the autumn when residual gametes are being phagocytised. Thus, the pattern of tubule and gamete production in *S. californicus* contrasts markedly with that in *P. fabricii*. Resorption of tubules has also been noted in *Mesothuria intestinalis* (Théel, 1901) and *Ypsilothuria talismani* (Tyler and Gage, 1983), but probably does not occur in *S. japonicus* (Tanaka, 1958) and three species of sea cucumber examined by Conand (1981).

Gametogenesis in another holothurian, *Aslia lefrevrei*, in the same family as *Psolus fabricii* (Dendrochirotida), follows still another pattern. The tubules are of uniform width, and gametogenesis follows an annual pattern that is highly synchronized amongst the tubules (Costelloe, 1985). For example, during numerous periods in the year, all of the tubules are at the same stage of gametogenetic development. As in *P. fabricii*, the tubules are not reabsorbed after spawning, the growth continues for a subsequent year, oocytes (<200 μm) appearing prior to spawning. The above observations indicate that the pattern of gametogenesis varies markedly even within closely related holothurian species. Future studies should therefore consider the pattern of production of the tubules as well as the gametogenesis within the tubules.

Control of gametogenesis

The active phase of gametogenesis in *Psolus fabricii* begins in January and continues until spawning. In small tubules of both males and females, early gametogenetic stages proliferate. And in the large tubules, oocyte growth increases in females, and more advanced spermatogenic stages are produced in males. This renewed gametogenesis occurs when water temperatures are near freezing (≈ -1°C, Therriault, 1973; Ouellet-Larose, 1973), and an increase does not occur until several months later (March-April). Further, food conditions are minimal as evidenced by the near absence of phytoplankton cells in the intestines. The first increase in phytoplanktonic cells in the intestine is in mid March (Fig. 11). The only notable environmental change during the mid-winter renewal of gametogenesis is the return to increasing photoperiod. In fact, virtually the entire gametogenetic period coincides with the period of increasing day length and daily bright sunshine, and peak maturity is attained at the maximal photoperiod. These observations suggest that an increasing photoperiod controls gametogenesis. Photoperiod has been experimentally shown to control gametogenesis in numerous taxa including echinoderms (Pearse *et al.*, 1986; McClintock *et al.*, 1990). *P. fabricii* occurs where annual changes in temperature and food availability are pronounced, certainly more so than the habitats of other echinoderms that have been used to study the photoperiod control of gametogenesis. Nevertheless, the activation of gametogenesis well before the increase of temperature and food from their annual minima suggests the potential importance of photoperiod for *P. fabricii*.

The increased growth in tubule diameter and gonadal mass observed in March or April (Fig. 4) suggests a second point that may be controlled by environmental factors. At this time, photoperiod has been increasing for several months, and the most notable environmental change is the first increase of phytoplanktonic cells in the intestines (Fig. 11). Phytoplankton are probably not abundant at this time, but abundant enough that the feeding mechanism of *Psolus fabricii* can filter cells from the water column, contributing to gonadal production. An influence of food availability on gonad development is also suggested by numerous studies on other invertebrates (Sastry and Blake, 1971; Gimazane, 1972; Bayne, 1975). The vernal warming is another potential environmental change at this time, and our temperature record, which began in mid April in 1989, indicates that warming had occurred in April.

Role of nutritive phagocytes and the gonadal tubule wall in supporting gametogenesis

The appearance of nutritive phagocytes and their role in eliminating residual gametes is well documented in studies of holothurians (Tanaka, 1958; Costelloe, 1985; Smiley and Cloney, 1985) and other echinoderms (Liebman, 1950; Holland and Giese, 1965; Fenaux, 1972). In echinoids, nutritive phagocytes have been shown to transform reserves to dissolved compounds which are later used for gamete production (Holland and Giese, 1965). This may occur in *Psolus fabricii*, but since the phagocytes disappear before the active gametogenic period, these substances would have to be stored for their eventual use in gametogenesis.

In *Psolus fabricii*, the gonadal tubule wall thickens during the period of gametogenic inactivity, from autumn to mid winter (Fig. 10). This growth, coincident with the autumnal decrease in food availability, falling temperatures, and short photoperiod, appears to be a priority in the use of energetic reserves of the animal at this time. In a variety of echinoderms, gametogenesis is similarly preceded by a thickening of the tubule wall, and this is thought to represent an accumulation of reserves for gametogenesis (Pearse, 1969; Gonor, 1973). Costelloe (1985) suggests that certain increases in gonadal size in the sea cucumber *Aslia lefrevrei* are due to the storage of materials in the tubule wall, but *P. fabricii* does not show an increase in gonadal mass as the tubule wall thickened. The earlier growth of the tubular wall in the large tubules, compared with the small tubules, suggests that resources are channeled preferentially to the large tubules. This could be because the later stages of gametogenesis in the large tubules require more resources than the earlier stages in the small tubules (Fig. 10). In the small tubules, the massive proliferation of the earlier gametogenetic stages during January and February precedes the thinning of the wall that begins in March. This suggests that the proliferation does not require large amounts of reserves.

External spawning cues

A massive loss of gametes over a short period strongly suggests that spawning is controlled by external factors

(Himmelman, 1981; Giese and Kanatani, 1987; Starr, 1990; Starr *et al.*, 1990, 1992). In both years of our study, the gonadal indices, measurements of tubule diameter, and histological observations indicated an abrupt spawning between two successive sampling dates (a 4-weeks interval in 1988, and 2 weeks in 1989). Temperature more than any factor has been suggested as a spawning signal in invertebrates (Orton, 1914; Brown, 1984; Bricelij *et al.*, 1987), but we did not observe a consistent relationship between temperature and spawning in *Psolus fabricii*. Similar conclusions have been reported for other holothurians (Costelloe, 1985; Cameron and Fankboner, 1986). The only study suggesting that temperature might control spawning in holothurians is that of Tanaka (1958). That spawning time of *P. fabricii* varies between years suggests that spawning is not controlled by photoperiod.

Our data suggests that spawning in *Psolus fabricii* may be signaled by the phytoplankton increase. Therriault and Levasseur (1985, 1986) demonstrate that the phytoplankton bloom in the Estuary is always delayed relative to that of the Gulf of St. Lawrence because of freshwater run-off: the bloom only develops after the surface layer has stabilized, which occurs when the spring run-off drops. In both 1988 and 1989, spawning in *P. fabricii* coincided with the predicted onset of the bloom, based in turn on the decrease in freshwater run-off (Fig. 11). Such a synchrony is further indicated by the coincidence of the spawning dates of *P. fabricii* with those of the green sea urchin, whose spawning is triggered by phytoplankton (Himmelman, 1975; Starr *et al.*, 1990, 1992). Cameron and Fankboner (1986) indicated that phytoplankton may also initiate spawning in *Stichopus californicus*. They noted that spawning individuals in the field were almost only observed after periods of bright sunshine ($\geq$5 h d-1 for >4 d), and further that phytoplankton was abundant during some spawnings.

The spawning in 1989 resulted in the release of a larger amount of gametes than in 1988 (Fig. 4). Possibly more gametes attained maturity in 1989 because of the delay in spawning. We suggest this because the mean tubule diameter attained a higher value in 1989 than in 1988, and the difference was largely due to the growth that occurred during June and July (Fig. 4). The longer period before spawning may have permitted the completion of gametogenesis in additional tubules, tubules that might otherwise not have matured until the following year. In addition, the gonadal index and tubule diameter did not fall as low in 1988 as in 1989. This again suggests that fewer gametes were mature when the spawning cue was detected in 1988. This discontinuation of gamete production after the early 1988 spawning suggests that physiological mechanisms prevent further gamete maturation and secondary spawnings once spawning has occurred. For the urchin, for which phytoplankton has been shown to be the spawning cue, spawning in the laboratory increases with plankton abundance (Starr *et al.*, 1990). If this is true for *Psolus fabricii*, a more intense phytoplankton bloom in 1989 might account for the more massive spawning in that year. The greater mass of intestinal contents of *P. fabricii* in 1989 suggests there was a more intense bloom in that year (Fig. 11).

Planktonic stages of Psolus fabricii

Holothurians with small eggs usually have a larval stage, whereas species with large eggs usually develop directly into juveniles (Tanaka, 1958; Rutherford, 1973; Green, 1978; Tyler and Billett, 1988). *Psolus fabricii* has exceptionally large eggs, sometimes attaining 1400 μm in diameter, and lacks a larval phase (pers. obs.). Nevertheless, the juvenile stage is pelagic. Probably, as Tyler and Billett (1987) indicate for elasipodid holothurians, the abundant nutritive reserves in the egg account for the high degree of floatability of the pelagic stage. Warmer temperatures near the surface may enhance the rate of development, and in addition the pelagic juveniles may further benefit from increased food resources, either in the form of dissolved substances or planktonic cells. The feeding podia are well developed around the mouth of the pelagic juveniles of *P. fabricii* (pers. obs.), which suggests that they are capable of feeding on suspended particles.

Feeding

Some holothurians feed on organic material at the water-sediment interphase (Hyman, 1955; Reese, 1966; Ferguson, 1969) whereas others feed on planktonic particles (MacGinitie and MacGinitie, 1949; Brumbaugh, 1965). *Psolus fabricii* is a highly selective feeder. For example, although numerous phytoplankton and zooplankton species are common in the region where we collected *P. fabricii* (Côté, 1972; Cardinal and Lafleur, 1977; Fortier *et al.*, 1978; Maranda and Lacroix, 1983; Therriault and Levasseur, 1985, 1986), the intestines contained almost exclusively four species of diatoms. The proportion of these items decreases in abundance in the intestine as productivity drops in late autumn and winter and is replaced by nonliving matter. *P. chitonoides* (Fish, 1967) and *Cucumaria elongata* (Fankboner, 1978) similarly feed primarily on suspended living particles. That dendrochirotes are most abundant in temperate and subtropical waters, and rare in tropical areas and at great depths (Pawson, 1966; Hansen, 1975; Lawrence, 1987), suggests that they require the abundance of small living particles such as found in shallow water northern areas (Lawrence, 1987). Nonliving matter or detritus has been suggested to be an important source of food in the diet of suspension feeders (Baier, 1935; Newell, 1965; Kirby-Smith, 1976) and could provide nutritional resources for *P. fabricii*

during the winter. The long intestine of dendrochirotides may be an adaptation for digesting vegetal matter (Lawrence, 1987). *P. fabricii* has a remarkably long intestine relative to its body size (intestinal length = −1.68 + 4.52 dry body wall mass; r = 0.95, n = 37). For example, an adult measuring 6.1 cm in distance mouth-anus, (34 g) has a 152 cm intestine. This unusually long intestine may be an adaptation to its diet of diatoms which are protected by siliceous frustules.

Acknowledgments

We are greatly indebted to N. Piché for his help in collecting the samples and for the underwater photographs of *Psolus fabricii*. The aid of S. Paradis, M. Claereboudt, A. Duval, E. Bourget, A. Cantin, A. Cardinal, H. Guderley, L.-P. Hamel, O. Hamel, B. Laganière, and A. Tremblay at various points in the project is also gratefully acknowledged. Thanks are also due to A. Pusterla (Département de Pathologie, Université Laval) and A. J. Collet (Département d'Anatomie, Université Laval) and the Département d'Océanographie (Université du Québec à Rimouski) for the histological preparations. The first author was supported by a FCAR scholarship and the research was supported by NSERC funding to J. H. H. and L. D.

Literature Cited

Atwood, D. G. 1973. Ultrastructure of the gonad wall of the sea cucumber *Leptosynapta clarki*. *Z. Zellforsch* **141:** 319–330.

Atwood, D. G. 1974. Fine structure of the spermatogonia, spermatocytes and spermatids of the sea-cucumber (Echinodermata: Holothuroidea). *Can. J. Zool.* **52:** 1389–1396.

Atwood, D. G., and F.-S. Chia. 1974. Fine structure of an unusual spermatozoan of a brooding sea cucumber, *Cucumaria lubrica*. *Can. J. Zool.* **52:** 519–523.

Baier, C. R. 1935. Studien zur hydro-backteriologie stehenden Binnengerwasser. *Arch. Hydrobiol.* **29:** 183–264.

Bayne, B. L. 1975. Reproduction of bivalve molluscs under environmental stress. Pp. 259–277 in *Physiological Ecology of Estuarine Organisms*, F. J. Vernberg, ed. University of South Carolina.

Bricelij, V. M., J. Epp, and R. E. Malouf. 1987. Intraspecific variation in reproductive and somatic growth cycles of bay scallops *Argopecten irradians*. *Mar. Ecol. Prog. Ser.* **36:** 123–137.

Brown, R. A. 1984. Geographical variations in the reproduction of the horse mussel *Modiolus modiolus* (Mollusca: Bivalvia). *J. Mar. Biol. Assoc. U. K.* **64:** 751–770.

Brumbaugh, J. H. 1965. The anatomy, diet, and tentacular feeding mechanism of the dendrochirote holothurian *Cucumaria curata* Cowles 1907. Ph.D. thesis, Stanford University, California. 119 pp.

Bulteel, P., M. Jangoux, and P. Coulon. 1992. Biometry, bathymetric distribution and reproductive cycle of the holothuroid *Holothuria tubulosa* (Echinodermata) from Mediterranean seagrass beds. *Mar. Ecol.* **13:** 52–62.

Cameron, J. L., and P. V. Fankboner. 1986. Reproductive biology of the sea cucumber *Parastichopus californicus* (Stimpson) (Echinodermata: Holothuroidea). I. Reproductive periodicity and spawning behavior. *Can. J. Zool.* **64:** 168–175.

Cardinal, A., and P.-E. Lafleur. 1977. Le phytoplancton estival de l'estuaire du Saint-Laurent. *Soc. Phycol. France Bull.* **22:** 150–160.

Chia, F.-S., and J. B. Buchanan. 1969. Larval development of *Cucumaria elongata* (Echinodermata: Holothuroidea). *J. Mar. Biol. Assoc. U. K.* **49:** 151–158.

Conand, C. 1981. Sexual cycle of the three commercially important holothurian species (Echinodermata) from the lagoon of New Caledonia. *Bull. Mar. Sci.* **31:** 523–543.

Conand, C. 1982. Reproductive cycle and biometric relations in a population of *Actinopyga echinites* (Echinodermata: Holothuroidea) from the lagoon of New Caledonia, western tropical Pacific. Pp. 437–442 in *Proceeding of the International Conference on Echinoderms, Tampa Bay*, J. M. Lawrence, ed. A. A. Balkema, Rotterdam.

Costelloe, J. 1985. The annual reproductive cycle of the holothurian *Ashia lefèvrei* (Dendrochirota: Echinodermata). *Mar. Biol.* **88:** 155–165.

Côté, R. 1972. Influence d'un mélange intensif de différents types d'eau sur la distribution spatiale et temporelle du zooplancton de l'estuaire du Saint-Laurent. Ph.D. thesis, Université Laval, Québec. 251 pp.

Demers, S., L. Legendre, and J.-C. Therriault. 1986. Phytoplankton response to vertical tidal mixing. Pp. 1–40 in *Tidal Mixing and Plankton Dynamics*, J. Bowman, C. M. Yentsh, and W. T. Peterson, eds. Springer-Verlag, New York.

Edwards, C. L. 1910. Revision of the Holothuroidea. I. *Cucumaria frondoda* (Gunner) 1767. *Zool. Jahrb. Abt. Syst. Ockol. Geogr., Tiere* **29:** 334–357.

Ellington, W. R. 1982. Intermediary metabolism. Pp. 395–415 in *Echinoderm Nutrition*, M. Jangoux and J. M. Lawrence, eds. A. A. Balkema, Rotterdam.

Engstrom, N. A. 1980. Reproductive cycles of *Holothuria floridana, H. (H.) mexicana* and their hybrids (Echinodermata: Holothuroidea) in southern Florida. *Int. J. Invert. Reprod.* **2:** 237–244.

Engstrom, N. A. 1982. Brooding behavior and reproductive biology of sub-tidal Puget Sound sea cucumber, *Cucumaria lubrica* (Clark, 1901) (Echinodermata: Holothuroidea). Pp. 447–450 in *Proceedings of the International Conference on Echinoderms, Tampa Bay*, J. M. Lawrence, ed. A. A. Balkema, Rotterdam.

Fankboner, P. V. 1978. Suspension-feeding mechanisms of the armoured sea cucumber *Psolus chitonoides* Clark. *J. Exp. Mar. Biol. Ecol.* **31:** 11–25.

Fenaux, L. 1972. Modalités de la ponte chez l'oursin *Sphaerechinus granularis* (Lamarck). *Revue Ges. Hydrobiol.* **57:** 551–558.

Féral, J. P., and P. Magniez. 1985. Level, content and energetic equivalent of the main biochemical constituents of the subantarctic moladid holothurian *Eumolpadia violacea* at two seasons of the year. *Comp. Biochem. Physiol.* **81:** 415–422.

Ferguson, J. C. 1969. Feeding, digestion, and nutrition in Echinodermata. Pp. 71–100 in *Chemical Zoology, Vol III*, M. Florkin and B. T. Scheer, eds. Academic Press, New York.

Fish, J. D. 1967. The biology of *Cucumaria elongata* (Echinodermata: Holothuroidea). *J. Mar. Biol. Assoc. U. K.* **47:** 129–143.

Fortier, L., L. Legendre, A. Cardinal, and C. C. Trump. 1978. Variabilité à court terme du phytoplancton de l'estuaire du Saint-Laurent. *Mar. Biol.* **46:** 349–354.

Galigher, A. E., and E. N. Kozloff. 1971. *Essentials of Practical Microtechniques*. Lea and Febiger, Philadelphia, PA.

Giese, A. C., and H. Kanatani. 1987. Maturation and spawning. Pp. 251–313 in *Reproduction of Marine Invertebrates, Vol. 9, General Aspect: Seeking Unity in Diversity*, A. C. Giese and J. S. Pearse, eds. Blackwell Scientific Publications, California.

Giese, A. C., and J. S. Pearse. 1974. Introduction: general principles. Pp. 1–49 in *Reproduction of Marine Invertebrates: Acoelomate and Pseudocoelomate Metazoans*, Vol. 1. A. C. Giese and J. S. Pearse, eds. Academic Press, New York.

Gimazane, J. P. 1972. Étude expérimentale de l'action de quelques facteurs externes sur la reprise de l'activité génitale de la coque, *Cerastoderma edule* L. Mollusque bivalve. *C. R. Soc. Biol.* **166:** 587–589.

Gonor, J. J. 1973. Sex ratio and hemaphroditism in Oregon intertidal populations of the echinoid *Strongylocentrotus purpuratus*. *Mar. Biol.* **19:** 278–280.

Green, J. D. 1978. The annual reproductive cycle of the apodus holothurian *Leptosynapta tenuis*: a bimodal breeding season. *Biol. Bull.* **154:** 68–78.

Hansen, B. 1975. Systematics and biology of the deep-sea holothurians. *Galathea* Reports. 13 pp.

Himmelman, J. H. 1975. Phytoplankton as a stimulus for spawning in three marine invertebrates. *J. Exp. Mar. Biol. Ecol.* **20:** 199–214.

Himmelman, J. H. 1981. Synchronization of spawning in marine invertebrates by phytoplankton. Pp. 3–19 in *Advances in Invertebrate Reproduction*, W. H. Clark, Jr. and T. S. Adams, eds. Elsevier/North-Holland, New York.

Hirai, S., and H. Kanatani. 1971. Site of production of meiosis-inducing substance in ovary of starfish. *Exp. Cell. Res.* **67:** 224–227.

Holland, N. D., and A. C. Giese. 1965. An autoradiographic investigation of the gonads of the purple sea urchin (*Strongylocentrotus purpuratus*). *Biol. Bull.* **128:** 241–258.

Hopcroft, R. R., B. D. Ward, and J. C. Roff. 1985. The relative significance of body surface and cloacal respiration in *Psolus fabricii* (Holothuroidea: Echinodermata). *Can. J. Zool.* **63:** 2878–2881.

Humason, G. L. 1981. *Animal Tissue Techniques*. W. H. Freeman, San Francisco.

Hyman, L. H. 1955. *The Invertebrates. Echinodermata. Vol IV.* McGraw-Hill Book Co., New York. 763 pp.

Jespersen, A., and J. Lützen. 1971. On the ecology of the aspidochirote sea cucumber *Stichopus tremulus* (Gunnerus). *Norw. J. Zool.* **19:** 117–132.

Junqueira, L. C., J. Carneiro, and J. A. Long. 1986. *Basic Histology, Fifth edition*, Lange Medical Publications. Los Altos, CA. 529 pp.

Kille, F. R. 1939. Regeneration of gonad tubules following extripation in the sea cucumber *Thyone briareus*. *Biol. Bull.* **76:** 70–79.

Kille, F. R. 1942. Regeneration of the reproductive system following binary fission in the sea cucumber *Holothuria parvula*. *Biol. Bull.* **83:** 55–66.

Kirby-Smith, W. W. 1976. The detritus problem and the feeding and digestion of an estuarine organism. Pp. 469–479 in *Estuarine Processes*, Vol. 1. M. L. Wiley, ed. New York.

Krishnaswamy, S., and S. Krishnan. 1967. A report of reproductive cycle of the holothurian *Holothuria scabra* Jaeger. *Curr. Sci.* **36:** 155–156.

Lawrence, J. M. 1987. *A Functional Biology of Echinoderms*. Croom Helm Ltd., Australia. 339 pp.

Lawrence, J. M., and J. M. Lane. 1982. The utilization of nutrients by post-metamorphic echinoderms. Pp. 331–371 in *Echinoderm Nutrition*, M. Jangoux and J. M. Lawrence, eds. A. A. Balkema, Rotterdam.

Liebman, E. 1950. The leucocytes of *Arabacia punctulata*. *Biol. Bull.* **98:** 46–59.

MacGinitie, G. E., and N. MacGinitie. 1949. *Natural History of Marine Animals*. McGraw-Hill Co., New York. 473 pp.

Maranda, Y., and G. Lacroix. 1983. Temporal variability of zooplankton biomass (ATP content and dry mass) in the St. Lawrence Estuary: advective phenomena during neap tide. *Mar. Biol.* **73:** 247–255.

McClintock, J. B., and A. W. Stephen. 1990. The effects of photoperiod on gametogenesis in the tropical sea urchin *Eucidaris tribuloides* (Lamarck) (Echinodermata: Echinoidea). *J. Exp. Mar. Biol. Ecol.* **139:** 175–184.

Mosher, C. 1982. Spawning behavior of aspidochirote holothurian *Holothuria mexicana* Ludwig. Pp. 467–469 in *Proceedings of the International Conference on Echinoderms, Tampa Bay*, J. M. Lawrence, ed. A. A. Balkema, Rotterdam.

Newell, R. C. 1965. *Biology of Intertidal Animals*. Am. Elsevier, New York. 254 pp.

Orton, J. H. 1914. On some Plymouth holothurians. *J. Mar. Biol. Assoc. U. K.* **10:** 211–235.

Ouellet-Larose, D. 1973. Influence des marées sur les fluctuations à court terme des biomasses planctoniques dans l'estuaire. Masters thesis, Université Laval, Québec. 231 pp.

Pawson, D. L. 1966. *Ecology of holothurians. Pp. 63–71 in Physiology of Echinodermata*. R. A. Boolootian, ed. Wiley Interscience, New York.

Pearse, J. S. 1969. Reproductive periodicities of Indo-Pacific invertebrates in the Gulf of Suez. II. The echinoid *Echinometra mathaei* (de Blainville). *Bull. Mar. Sci.* **19:** 580–613.

Pearse, J. S., and D. J. Eernisse. 1982. Photoperiodic regulation of gametogenesis and gonadal growth in the sea star *Pisaster ochraceus*. *Mar. Biol.* **67:** 212–125.

Pearse, J. S., V. B. Pearse, and K. K. Davis. 1986. Photoperiodic regulation of gametogenesis and gonadal growth in the sea urchin *Strongylocentrotus purpuratus*. *J. Exp. Zool.* **237:** 107–118.

Pittman, B., and B. Monroe. 1982. Effect of preservation on the mass of marine benthic invertebrates. *Can. J. Fish. Aquat. Sci.* **39:** 220–224.

Reese, E. S. 1966. The complex behavior of echinoderms. Pp. 157–218 in *Physiology of Echinodermata*, R. A. Boolootian, ed. Interscience Publishers, New York.

Rutherford, J. C. 1973. Reproduction, growth and mortality of the holothurian *Cucumaria pseudocurata*. *Mar. Biol.* **22:** 167–176.

Sastry, A. N., and N. J. Blake. 1971. Regulation of gonadal development in the bay scallop, *Aequipecten irradians* Lamarck. *Biol. Bull.* **140:** 274–283.

Sewell, M. A. 1992. Reproduction of the temperate Aspidochirote *Stichopus mollis* (Echinodermata: Holothuroides) in New Zealand. *Ophelia* **35:** 103–121.

Shick, J. M. 1983. Respiratory gas exchange in echinoderms. Pp. 67–110 in *Echinoderm Studies I*. M. Jangoux and J. M. Lawrence, eds. Balkema, Rotterdam.

Smiley, S. 1988. The dynamics of oogenesis and the annual ovarian cycle of *Stichopus californicus* (Echinodermata: Holothuroidea). *Biol. Bull.* **175:** 79–93.

Smiley, S., and R. A. Cloney. 1985. Ovulation and the fine structure of the *Stichopus californicus* (Echinodermata: Holothuroidea) fecund ovarian tubules. *Biol. Bull.* **169:** 342–364.

Smiley, S., F. S. McEuen, C. Chaffee, and S. Krishnan. 1991. Echinodermata: Holothuroidea. Pp. 663–750 in *Reproduction of Marine Invertebrates. Lophophorates, Echinoderms, Vol. VI*, Giese and Pearse, eds. Boxwood Press, California.

Sokal, R. R., and F. J. Rohlf. 1981. *Biometry*. Freeman, San Francisco. 776 pp.

Starr, M. 1990. Mécanismes de coordination entre la ponte de certains invertébrés marins et la poussée printanière du phytoplancton. Ph.D. thesis, Université Laval, Québec, Canada. 133 pp.

Starr, M., J. H. Himmelman, and J. C. Therriault. 1990. Direct coupling of marine invertebrates spawning with phytoplankton blooms. *Science* **247:** 1071–1074.

Starr, M., J. H. Himmelman, and J. C. Therriault. 1992. Isolation and properties of a substance from the diatom *Phaeodactylum tricornutum* which induces spawning in the sea urchin *Strongylocentrotus droebachiensis*. *Mar. Ecol. Prog. Ser.* **79:** 275–287.

Tanaka, Y. 1958. Seasonal changes in the gonad of *Stichopus japonicus*. *Bull. Fac. Fish. Hokkaido Univ.* **9:** 29–36.

Tessier, G. 1948. La relation d'allométrie: sa signification statistique et biologique. *Biometrics* **4:** 14–48.

Therriault, J.-C. 1973. Variations des propriétés physico-chimiques et biologiques d'une zone de melange de l'estuaire du Saint-Laurent. Masters thesis. Université Laval, Québec. 155 pp.

Therriault, J.-C., and M. Levasseur. 1985. Control of phytoplankton production in the lower St. Lawrence Estuary: light and freshwater run-off. *Nat. Can.* **112:** 77–96.

Therriault, J.-C., and M. Levasseur. 1986. Freshwater run-off control of spatio-temporal distribution of phytoplankton in the lower St. Lawrence Estuary (Canada). Pp. 251–260 in *Proceedings of the NATO Freshwater, Sea Workshop, Bodo, Norway*, S. Skresled, ed. NATO ASI Series. Vol. G7. Springer-Verlag, New York.

Théel, H. 1882. *Report on the Holothuroidea by H. M. S. Challenger During the Years 1873-1876.* Part 1. Report of the Scientific Results of the Voyage of the Challenger (Zoology) **4:** 1–176.

Théel, P. A. 1901. A singular case of hermaphroditism in holothuroids. *Bihang till Kungl. Svenska Vetensk. Acad. Handl.* **27:** Afd. 4, No. 6.

Todd, C. D., and R. W. Doyle. 1981. Reproductive strategies of marine benthic invertebrates: settlement-timing hypothesis. *Mar. Ecol. Prog. Ecol.* **23:** 55–69.

Tyler, H., and J. D. Gage. 1983. The reproductive biology of *Ypsilothuria talismani* from the northeast Atlantic. *J. Mar. Biol. Assoc. U.K.* **63:** 609–616.

Tyler, P. A., and D. S. M. Billett. 1988. The reproductive ecology of elasipodid holothurians from the N. E. Atlantic. *Biol. Oceanogr.* **5:** 273–296.

Yentsh, C. S., and D. W. Menzel. 1963. A method for the determination of phytoplankton chlorophyll and phaeophytin by fluorescence. *Deep Sea Res.* **10:** 221–231.

Reference: *Biol Bull* **184**: 144–152. (April, 1993)

Reproductive Investment in Four Developmental Morphs of *Streblospio* (Polychaeta: Spionidae)

TODD S. BRIDGES*

Department of Marine, Earth, and Atmospheric Sciences, North Carolina State University, Raleigh, North Carolina 27695-8208

Abstract. Per brood and per offspring C and N investment were examined in four developmental morphs of the spionid polychaete *Streblospio: S. shrubsolii* (direct development, D), *S. benedicti* (lecithotrophic, L), *S. benedicti* (planktotrophic, P), and *Streblospio* n. sp. (planktotrophic, P). Large differences were apparent among these morphs in fecundity and embryo size. *S. shrubsolii* (D) and *S. benedicti* (L) invested about 10 × more C and N in each offspring and 30% more C and N in each brood than did the morphs with planktotrophic development. C and N concentration (μg per unit volume) was significantly greater in *S. benedicti* (L) than in the other morphs, though no general relationship with embryo size was evident. The C:N ratio of offspring did not differ among the four morphs. Comparisons of estimated lifetime reproductive investment made by the two developmental types of *S. benedicti* indicated that lecithotrophic development involved twice the C and N investment in reproduction. Positive, significant regressions were evident between embryo C and N content and embryo volume at the intermorph level. Significant intra-morph regressions were evident in all morphs but *Streblospio* n. sp. (P). However, the large amount of variation unaccounted for by embryo volume calls into question the use of embryo size as a predictor of parental investment in offspring.

Introduction

Three modes of development, strongly correlated with egg size and fecundity (Thorson, 1946, 1950), are recognized among marine invertebrates. Planktotrophic development is descriptive of the production of a relatively large number of larvae, developed from small eggs, which acquire the necessary energy for growth by feeding on particulate matter during planktonic life. Lecithotrophic larvae are produced from fewer, but larger, eggs. These larvae do not feed on particulate matter but subsist, at least in part, on the energy supplied by the mother in the form of yolk during oogenesis. During direct development, offspring complete their development without a planktonic phase, usually within the mother or an egg mass; the energy for development is supplied by the mother (Thorson, 1950; Grahame and Branch, 1985).

The adaptive significance of development mode has received extensive consideration. Selection pressures such as predation, starvation, and dispersal have been proposed for development mode evolution (Thorson, 1950; Chia, 1974; Strathmann, 1985). Quantitative modeling approaches have been employed in an effort to identify the selection pressures and processes of importance in life history and development mode evolution in marine invertebrates (Vance, 1973a, b; Christiansen and Fenchel, 1979; Caswell, 1981; Grant, 1983).

One fundamental assumption of the models of Vance (1973a, b) and Christiansen and Fenchel (1979) concerns the relationship between an egg's size and its energy content. It is assumed that a positive correlation exists between an egg's measured or estimated size and the investment in material or energy that egg represents. This seemingly reasonable assumption enables the models to make use of the large amount of data on egg size and development mode available for marine invertebrates.

Interspecific comparisons of egg size and organic content including a broad range of taxa have shown the expected positive relationship to exist (Strathmann and Vedder, 1977). However, the use of interspecies comparisons to justify the assumed relationship between egg size and organic content appears invalid. McEdward and Car-

Received 13 March 1992; accepted 25 January 1993.

* Current address: USAE Waterways Experiment Station, WES-ES-F, 3909 Halls Ferry Road, Vicksburg, Mississippi 39180.

son (1987) and McEdward and Coulter (1987) have pointed out that for models describing evolutionary processes, the relevant level of variation to examine occurs within a single species. For the species of asteroids studied by McEdward, Carson and Coulter, egg size was found to be a poor predictor of organic content when examined intraspecifically due to the large amount of variation in organic content unaccounted for by egg size. Likewise, Qian (1991) found that egg size was not correlated with egg energy content within three populations of the polychaete *Capitella* sp. Variation in egg organic composition may also make egg size an unreliable predictor of an egg's energetic value (Turner and Lawrence, 1979).

To date, the relationship between egg size and egg organic content has been examined in only a small number of taxa (mostly echinoderms). One of the questions addressed in this paper concerns the extent to which the pattern identified in echinoderms is present in other taxa, specifically spionid polychaetes.

Inter- and intraspecific comparisons of reproductive and per offspring investment in organisms with different development modes have proved to be useful in identifying the ecological consequences of development mode as well as the potential evolutionary forces shaping these patterns (Menge, 1974; Perron, 1986; Levin *et al.*, 1991). The spionid polychaete genus *Streblospio*, which exhibits developmental variation both within and between species (Levin, 1984; Cazaux, 1985), offers a highly suitable system for examining questions concerning egg size and egg organic content and the consequences of development mode. Six reproductive variants are known for *Streblospio*, comprising three or more species (Levin, 1984; Cazaux, 1985; Rice, 1991; Levin and Eckelbarger, pers. comm.).

To assess the nature of reproductive costs associated with development mode patterns in *Streblospio*, both reproductive expenditure per offspring and per brood were examined in four reproductive variants. These variants are similar in body size and ecology but are distinguishable in a number of reproductive characteristics (Dean, 1965; Levin, 1984; Cazaux, 1985). Two reproductive morphs of *S. benedicti* have been identified from the Atlantic coast of the United States (Levin, 1984; Levin *et al.*, 1991). Females with planktotrophic development produce a large number (100–600) of small eggs (70–90 μm dia.) which develop into planktotrophic larvae. Lecithotrophic morphs of this species produce a smaller number (10–100) of large eggs (100–200 μm dia.) and lecithotrophic larvae (Levin, 1984). *Streblospio* n. sp. from the Gulf of Mexico also has planktotrophic development and produces a large number (100–700) of small eggs (60–70 μm dia.) (Levin, 1984; Rice and Levin, in prep.). *S. shrubsolii* with direct development from near-shore habitats in France produces a very small number (20–50) of large eggs (200–230 μm dia.) which develop directly into crawl away juveniles (Cazaux, 1985).

Materials and Methods

Animals used during this study were obtained from three sources. *S. benedicti* with both planktotrophic and lecithotrophic development were initially collected from intertidal salt marsh habitats in Bogue Sound, North Carolina. Worms with lecithotrophic development represented second generation laboratory animals whose parents were collected in September, 1990 from natural populations at Pivers Island near Duke Marine Lab in Beaufort, North Carolina. Individuals with planktotrophic development were collected at Tar Landing Bay, North Carolina in June 1991. Individuals of *Streblospio* n. sp. were settled in the lab by S. Rice from plankton samples made in the Hillsborough River, Tampa Bay, Florida in July 1991. Individuals of *S. shrubsolii* were taken from laboratory cultures established by L. Levin in 1986 from samples collected by C. Cazaux in Arcachon, France.

Males and females of each variant were incubated in pairs at 20°C in culture dishes of sieved marsh sediment and 34–36‰ seawater, according to the techniques outlined in Levin and Creed (1986). To make observations of multiple broods from the same female it was necessary to collect recently fertilized embryos rather than eggs. Embryos are brooded on the dorsal surface in all reproductive variants and are more accessible than maturing eggs which occur within the body coelom. Embryos were always collected within 24 h of fertilization and were composed of between one (zygotes) and approximately 250 cells. The developmental stage of sampled embryos, estimated from the number of blastomeres present, was used as a covariate in data analyses.

Once embryos were separated from females they were collected by pipet, counted, and placed in a dish of filtered (0.45 μm) seawater. Two perpendicular (maximum length and width) measures of embryo diameter were made with a compound microscope and ocular micrometer for approximately 20 embryos within a brood. Embryo volume was calculated using the mean radius and the formula $\frac{4}{3}\pi r^3$ since the embryos were more spherical than prolate or oblate in form.

Entire broods, produced by a single female, were collected for C and N analysis by depositing all the embryos onto a small square of previously combusted Whatman GF/F (glass-fiber) filter paper. A minimum of approximately 15 embryos of *S. shrubsolii* (direct developer) or *S. benedicti* (lecithotrophic) and 200 embryos of *S. benedicti* (planktotrophic) or *Streblospio* n. sp. (planktotrophic) were needed to meet the detection limits of the analysis (2–3 μg of C or N). Broods smaller than these minimum sizes were not analyzed. Samples were dried

Table I

Summary of the reproductive characteristics of the four developmental morphs of Streblospio

Characters	*S. shrubsolii* (D) $\bar{x}$	SD	n	*S. benedicti* (L) $\bar{x}$	SD	n	*S. benedicti* (P) $\bar{x}$	SD	n	*Streblospio* n. sp. (P) $\bar{x}$	SD	n	df	F	*P*
Embryos/Blood	34.33^{a}	8.15	24	50.49^{a}	20.41	100	276.04^{b}	93.27	26	315.20^{b}	132.11	20	3, 103	168.93	0.0001
μg C/Brood	37.53^{a}	12.76	24	41.15^{a}	13.26	100	30.79^{b}	13.83	26	26.80^{b}	9.00	20	3, 103	8.81	0.0001
μg N/Brood	$7.77^{a/b}$	1.63	19	8.50^{a}	2.80	90	6.75^{b}	2.22	21	5.14^{b}	1.55	20	3, 86	8.99	0.0001
Embryo Volume ($\mu l \times 10^{-3}$)	4.67^{a}	0.78	24	3.08^{b}	0.44	100	0.495^{c}	0.057	26	0.366^{d}	0.041	20	3, 103	1395.	0.0001
μg C/Embryo	1.09^{a}	0.25	24	0.85^{b}	0.14	100	0.108^{c}	0.026	26	0.091^{d}	0.031	20	3, 103	725.4	0.0001
μg N/Embryo	0.229^{a}	0.048	19	0.174^{b}	0.026	90	0.023^{c}	0.0033	21	0.017^{d}	0.0051	20	3, 86	949.0	0.0001
C conc. (μg/μl)	233.3^{a}	34.50	24	279.7^{b}	51.54	100	217.2^{a}	48.02	26	248.9^{a}	79.7	20	3, 102	12.60	0.0001
N conc. (μg/μl)	48.67^{a}	5.57	19	57.62^{b}	10.19	90	45.72^{a}	4.67	21	47.47^{a}	12.62	20	3, 85	13.58	0.0001
C:N Ratio	4.83^{a}	0.54	19	4.88^{a}	0.28	90	4.97^{a}	0.69	21	5.17^{a}	0.48	20	3, 85	2.40	0.0767

Data on embryo volume was obtained by calculating volume ($4/3\pi r^3$) using a mean radius determined from two perpendicular estimates of diameter. C and N data were obtained from elemental analysis of entire broods of early embryos. Degrees of freedom (df), F, and *P* values are listed for the ANOVA results for each character. Superscripted letters denote those values within a row which are significantly different.

in an oven at 50°C for approximately 24 h, then stored in a vacuum desiccator prior to analysis. Appropriate blank samples, without eggs, were prepared to distinguish background C and N values associated with the collection technique. The amount of C and N in each brood was determined by use of a Carlo Erba Elemental Analyzer (model E.A. 1108).

All statistical analyses of data were performed with SAS (version 5.18). All data were log transformed to remove heteroscedasticity and normalize distributions. When significant differences ($P < 0.05$) were found among the four reproductive variants, an *a-posteriori* Least Significant Difference (LSD) test was performed on means of the four reproductive types ($\alpha = 0.05$). A multiple linear regression model was used to examine the relationship between embryo volume and C and N content. Given the repeated measures structure of the data, two covariates were included in the model to distinguish between among-female and within-female variation. Covariate 1 (cov 1), representing mean values of embryo volume for each female, allowed the relationship between either C or N content and embryo volume to be examined. Covariate 2 (cov 2) was formed by subtracting the mean embryo volume of all broods produced by a female during the experiment from the mean embryo volume of each individual brood. These deviations permitted testing for a relationship between embryo C and N content and volume for multiple broods from a given female.

Results

Reproductive and offspring investment

Per brood measures of fecundity in *S. shrubsolii* (D) and *S. benedicti* (L) were significantly lower than *S. benedicti* (P) and *Streblospio* n. sp. (P), where (L), (P), and (D) designate lecithotrophic, planktotrophic and direct development, respectively (Table I). The differences in fecundity among reproductive morphs were accompanied by differences in embryo volume. *S. shrubsolii* (D) embryos, which were the largest of the four types (4.67×10^{-3} μl), were 12.7 × the volume of *Streblospio* n. sp. (P) embryos, 9.4 × the volume of *S. benedicti* (P) embryos, and 1.5 × the volume of embryos of *S. benedicti* (L) (Table I). Embryo volume increased with developmental stage ($P = 0.0021$).

Comparisons of the C and N investment made to individual offspring produced by each reproductive type revealed differences similar to those found for embryo volume (Table I). *S. shrubsolii* (D) made the largest average investment in each offspring (1.09 μg C, 0.229 μg N) followed by *S. benedicti* (L) (0.851 μg C, 0.174 μg N), *S. benedicti* (P) (0.108 μg C, 0.023 μg N), and *Streblospio* n. sp. (0.091 μg C, 0.017 μg N).

In terms of C and N, the lecithotrophic and direct developer made a greater material investment in each brood than did the morphs with planktotrophic development (Table I). Significant differences were present in μg C per brood between *S. shrubsolii* (D) and both planktotrophic developers, and in μg C and N per brood between *S. benedicti* (L) and both planktotrophic morphs (Table I). Even though the planktotrophic morphs produced much larger numbers of embryos, the lecithotrophic and direct developers were found to have made a 30% greater C and N investment in each brood.

The C:N ratio of brooded offspring was similar among the reproductive variants, ranging from 4.83 in *S. shrubsolii* (D) to 5.17 in *Streblospio* n. sp. (P) (Table I). The C:N ratio of embryos decreased with developmental stage ($P = 0.0112$).

S. benedicti (L) exhibited significantly greater C and N concentration (μg C and μg N per μl) than the other re-

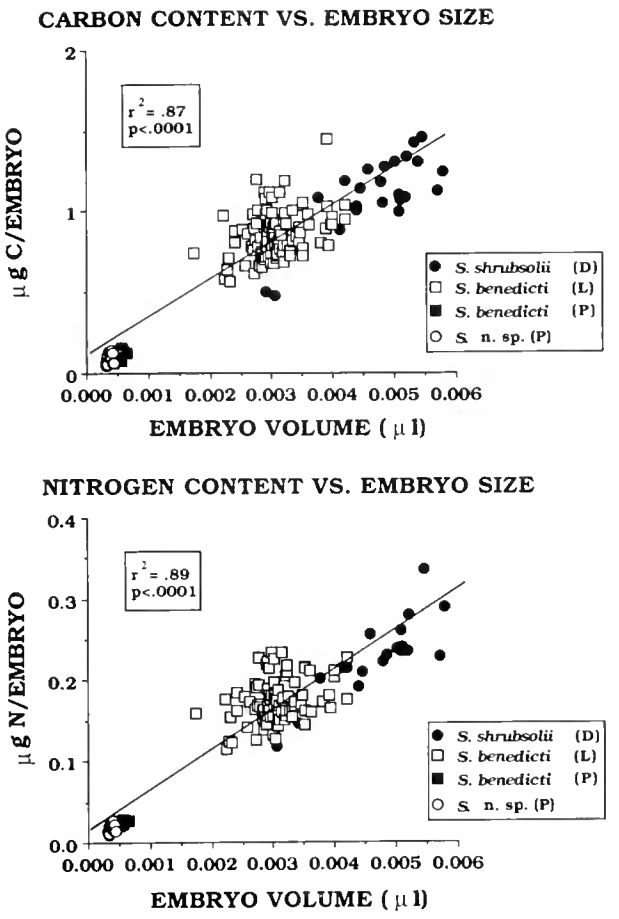

Figure 1. Scatter plots describing the relationship between μg C/embryo (A) and μg N/embryo (B) and embryo volume for all reproductive morphs. Both regressions are highly significant ($P < 0.0001$).

productive types (Table I). Both C ($P = 0.0306$) and N ($P = 0.0794$) concentrations decreased with developmental stage.

Embryo C and N content versus embryo volume

Significant, positive correlations were found between μg C per embryo and embryo volume ($r^2 = 0.87$, $P < 0.0001$) and μg N per embryo and embryo volume ($r^2 = 0.89$, $P < 0.0001$) across reproductive variants of *Streblospio* (Fig. 1). The regression model incorporating cov 1 and cov 2 used in analyzing the relationship between μg C (or μg N) per embryo and embryo volume explained 95% of the C variation and 97% of the N variation. A strong relationship was evident between C and N content and embryo volume across reproductive types as indicated by the significance of cov 1 in the models (C ANCOVA: $F_{1,102} = 82.34$; $P < 0.0001$; N ANCOVA: $F_{1,185} = 56.38$; $P < 0.0001$). However, the relationships between μg C and N per embryo and embryo volume within each reproductive type were not identical. The significance of reproductive type (C ANCOVA: $F_{3,102} = 646.84$; $P < 0.0001$; N ANCOVA: $F_{3,85} = 823.51$; $P < 0.0001$) in the models indicated that differences existed among the four morphs in the nature of the regressions, specifically the y-intercept. No differences could be detected in the slope of the lines among the four types as seen by the lack of significance in the cov 1 × type interaction in both models (C ANCOVA: $F_{3,102} = 1.85$; $P = 0.1478$; N ANCOVA: $F_{3,85} = 2.29$; $P = 0.0884$). Cov 2 was significant only in the case of the N model (C ANCOVA: $F_{1,102} = 1.98$; $P = 0.1626$; N ANCOVA: $F_{1,85} = 4.37$; $P = 0.0395$), indicating that the relationship between N content and embryo volume could be detected with data from individual females sampled more than once.

Differences were evident among the four variants in the strength of the relationship between embryo C and N content and embryo volume within each morph. Significant, positive correlations existed between μg C and μg N per embryo and embryo volume for *S. shrubsolii* (D), *S. benedicti* (L), and *S. benedicti* (P), but not for *Streblospio* n. sp. (P) (Table II, Figs. 2, 3). The specific regression parameters for each of the relationships are listed in Table II. The amount of variation accounted for by the regressions, and therefore the strength of the relationship, was highest for *S. shrubsolii* (D) (71% for N content and 66% for C content). A much smaller amount of variation was accounted for by the regressions for *S. benedicti* (L)

Table II

Slope and y-intercept estimates for the regression equations of μg C and μg N/embryo versus embryo volume for Streblospio *(all morphs) and each morph separately*

Variants	y-intercept	SE	Slope	SE	*P*
		μg C/Embryo versus Embryo Volume			
Streblospio (all morphs)	0.0431	0.0213	0.247	0.00713	0.0001
S. shrubsolii (D)	−0.102	0.187	0.256	0.0395	0.0001
S. benedicti (L)	0.489	0.0950	0.118	0.0305	0.0002
S. benedicti (P)	0.00382	0.0414	0.210	0.0831	0.0187
S. n sp. (P)	−0.00732	0.0627	0.269	0.170	0.1306
		μg N/Embryo versus Embryo Volume			
Streblospio (all morphs)	0.00812	0.00431	0.0513	0.00147	0.0001
S. shrubsolii (D)	−0.0276	0.0406	0.0548	0.00855	0.0001
S. benedicti (L)	0.112	0.0187	0.0203	0.00607	0.0012
S. benedicti (P)	0.00271	0.00421	0.0402	0.00847	0.0001
S. n sp. (P)	−0.000504	0.00995	0.0489	0.027	0.0869

Estimates and standard errors (SE) are listed for the slope and y-intercept of the overall regression for *Streblospio*, including all morphs, as well as the specific regressions for each morph. *P* denotes the significance for each relationship.

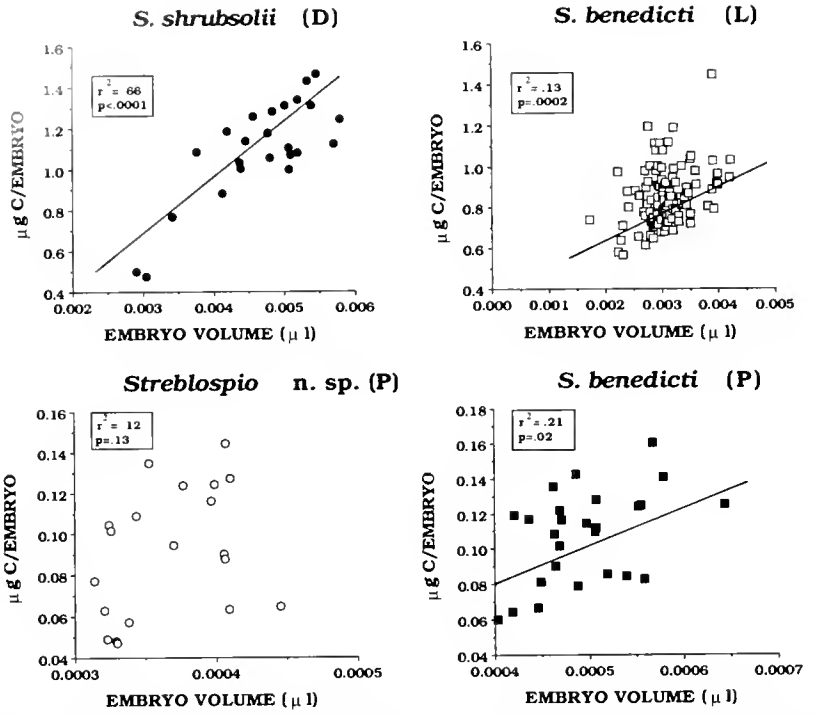

Figure 2. Scatter plots describing the relationship between μg C/embryo and embryo volume for each reproductive morph of *Streblospio*

(11% for C and 13% for N) and *S. benedicti* (P) (21% for C and 51% for N).

A more meaningful estimate of the strength of the three significant regressions can be made by examining confidence limits for predicted embryo C and N content. Predictions of embryo C and N content using each morph's regression parameters and a single value of embryo size (each morph's mean) produced the following predicted values (±95% confidence limits): *S. shrubsolii* (D), C = 1.10 μg ± 0.31, N = 0.228 μg ± 0.058; *S. benedicti* (L), C = 0.851 ± 0.268, N = 0.174 ± 0.050; *S. benedicti* (P), C = 0.108 ± 0.050, N = 0.023 ± 0.005. These confidence intervals envelop a large portion of the range of actual values for embryo C and N content found in each of these morphs, between 53% and 99%. The large amount of variation about these regressions, which results in such large confidence intervals, makes it difficult, if not impossible, to make significantly different predictions of embryo C or N content from embryo volume within each morph.

Discussion

Offspring investment

The negative relationship between offspring size and number described for many marine invertebrate taxa (Thorson, 1946, 1950; Emlet *et al.*, 1987) including polychaetes (Hermans, 1979; Levin *et al.*, 1991), was also found in this study (Table I). This tradeoff can be explained by assuming there to be a finite and limited amount of energy available for reproduction (Vance, 1973a; Smith and Fretwell, 1974; Stearns, 1976), an assumption more easily justified among closely related species which accumulate and apportion nutrients in a similar fashion. Levin *et al.* (1991) observed a negative genetic correlation between fecundity and egg size in *S. benedicti* reared in the lab, suggesting that evolutionary forces may influence this tradeoff.

The potential evolutionary forces driving differences in per offspring investment and development mode are of particular interest. One of the key preadaptations allowing for the evolution of direct from indirect development may be the evolution of a large yolk-filled egg (Wray and Raff, 1991). However, experimental embryology has demonstrated that in species developing directly, development can proceed normally at half the egg size, in a size range similar to forms with indirect development (Okazaki and Dan, 1954; Henry and Raff, 1990; Wray and Raff, 1991).

If direct development or lecithotrophy could be accomplished in *Streblospio* with only a five-fold increase over planktotrophy in per offspring investment (instead of the 10-fold increase in investment reported here), and the remaining C and N was allocated to increased fecundity, the resulting fecundity benefit could make such a

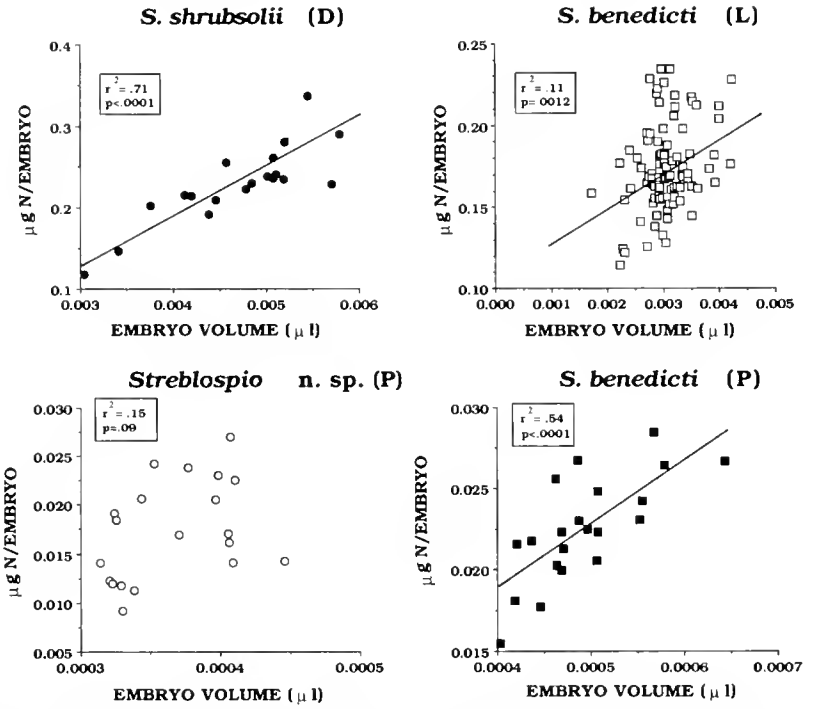

Figure 3. Scatter plots describing the relationship between μg N/embryo and embryo volume for each reproductive morph of *Streblospio*.

strategy adaptive (Table 1). However, greater per offspring investment in *S. shrubsolii* (D) and *S. benedicti* (L), in addition to developmental changes, also produces a larger offspring. *S. shrubsolii* (D) produces a 1000 μm long crawl away juvenile (Cazaux, 1985). Larvae of *S. benedicti* (L) are released and settle at half the size of *S. shrubsolii* (D) (about 550–650 μm) (Levin, 1984). Planktotrophic larvae of *S. benedicti* and *Streblospio* n. sp. are released at about 250–350 μm in length and appear to settle at a size comparable to or smaller than *S. benedicti* with lecithotrophic development (Levin, 1984).

Selection for increased offspring size may have been an important factor in development mode evolution in *Streblospio*. A shift toward larger offspring size in *Streblospio* offspring with a planktonic phase may be adaptive in the face of size-selective planktonic predation (Kerfoot, 1977; Greene, 1985; Rumrill *et al.*, 1985; Pennington *et al.*, 1986). The presumed predator avoidance behavior of some planktotrophic spionid polychaete larvae, including *S. benedicti* (P), that increase their effective size by flaring long swimming setae, is consistent with the importance of size-selective predation in this species. Larger size at settlement in *S. benedicti* (L) and at release from the female in *S. shrubsolii* (D) may also benefit offspring subject to negative interactions with permanent meiofauna or macrofauna by accelerating passage through vulnerable size ranges (Bell and Coull, 1980; Watzin, 1983, 1986). Juvenile *S. benedicti* are sensitive to interactions with macrofauna (McCann and Levin, 1989). Levin and Huggett (1990) reported a larval and juvenile survivorship advantage in *S. benedicti* (L) (relative to *S. benedicti* (P)) during a field study of populations of *S. benedicti* with lecithotrophic and planktotrophic development.

Offspring composition

Even though morphological distinctions are evident in yolk granules of *S. benedicti* with lecithotrophic and planktotrophic development, differences in gross measures of organic composition were not evident in this study (Eckelbarger, 1980, 1986). Offspring C:N ratios of the four reproductive types could not be distinguished statistically, suggesting that the relative proportion of protein to non-nitrogen containing compounds is the same among the four morphs (Table 1). Turner and Lawrence (1979) also found that organic composition did not change with egg size in the echinoderms they studied. Lawrence *et al.* (1984) concluded, due to the compositional similarity of eggs of different sizes and development modes, that the significance of larger eggs was not to accommodate differences in the energetic demands of development, but to create a larger offspring. One would expect to see a higher proportion of lipid in larger eggs if the change in development involved a greater energetic demand (Lawrence *et al.*, 1984). Increased per offspring investment in *Streblospio* may have similar importance, *i.e.*, the production of larger offspring.

C and N concentration ($\mu g/\mu l$) was similar among the embryos of three of the four *Streblospio* reproductive morphs, and no consistent trend with embryo size was noted (Table I). Qian and Chia (1992) found that egg energy concentration was similar in lecithotrophic and planktotrophic *Capitella* sp. Strathmann and Vedder (1977) reported that organic matter per unit volume decreased with egg size in echinoderms with feeding larvae. Such a trend has not been observed in echinoderms with larger eggs, including pelagic lecithotrophs (Turner and Lawrence, 1979; McEdward and Chia, 1991). Energy concentration does appear to be significantly greater in eggs of echinoderms with nonfeeding larvae than those with feeding larvae (Emlet *et al.*, 1987; McEdward, pers. comm.); this observation is consistent with data presented by Needham (1963). Thus, important fundamental differences may exist among the eggs of echinoderms with different developmental modes. More data are required before such trends can be discerned for polychaetes.

Reproductive investment

The lecithotrophic and direct developers made greater material investments in each brood than either planktotrophic developer. In addition to investing more C and N in each offspring, *S. benedicti* (L) was also found to have invested 33% more C and 26% more N in each brood than did *S. benedicti* (P). However, these values are minimum estimates of the difference in reproductive investment since *S. benedicti* (P) produced more broods that were too small to be analyzed for their C and N content. Lifetime investment levels can be estimated by combining data on per offspring investment made in this study with lifetime fecundity data made by Levin *et al.* (1987), where worms were raised under the same experimental conditions. Using these data, *S. benedicti* (P) (1324.32 eggs/lifetime) would have a calculated lifetime reproductive investment level of 143.03 μg C and 30.46 μg N, and *S. benedicti* (L) (336.6 eggs/lifetime) would have invested 286.45 μg C and 58.57 μg N. Based on these calculated values, *S. benedicti* (L) makes a two-fold higher investment in reproduction than *S. benedicti* (P). These estimates do not technically represent reproductive effort since reproductive effort is defined as the proportion of resources devoted to reproduction (Havenhand and Todd, 1989). However, the similarity of these two morphs in size as well as ecology (Levin *et al.*, 1987; Levin and Huggett, 1990), would suggest that such estimates may represent a first approximation of reproductive effort, though some caution is warranted (Grahame, 1982). Efforts at determining which reproductive pattern, planktotrophy or lecithotrophy, is more energetically expensive have yielded equivocal results (Grahame and Branch, 1985; Strathmann, 1985).

Differences in apportionment of energy to growth and development in *S. benedicti* with planktotrophic and lecithotrophic development may partially account for the difference in reproductive investment. *S. benedicti* with planktotrophic development reaches sexual maturity (first reproduction) earlier and at a larger size than the lecithotrophic morph, indicating that growth and developmental rates are accelerated in planktotrophs compared to lecithotrophs (Levin *et al.*, 1987; Levin *et al.*, 1991). The importance of accelerated growth and development in planktotrophic *S. benedicti* is further suggested by demographic analyses of the two developmental morphs. Similarity in estimated population growth rates (λ) in the two morphs were the result of a balance between a larval and juvenile survivorship advantage in lecithotrophs and increased fecundity in early adult stages in planktotrophs (Levin *et al.*, 1987; Levin and Huggett, 1990). Given the effect of age at first reproduction and early fecundity on population growth rates (Stearns, 1976), females with planktotrophic development may be investing in future offspring both through energy committed to eggs directly and through enhanced early growth and development. The evolutionary shift from planktotrophy to lecithotrophy may involve not only changes in offspring size and investment, but also age and size at maturity in *S. benedicti*.

Embryo size versus C and N content

Significant, positive relationships have been found between egg size and organic content using data from a number of species in this study (Fig. 1) as well as others (Strathmann and Vedder, 1977; Turner and Lawrence, 1979; McEdward and Chia, 1991). In general, the strength of this relationship when examined at the interspecific level, as reflected by r^2 values, appears to be high (present study; McEdward and Chia, 1991). However, large errors in prediction may result when using regression equations formulated with interspecific data to predict values of per offspring investment from intraspecific and intra-morph data on embryo size (Bridges, 1992). The strength of intramorph relationships between embryo C and N content and embryo volume ranged from *S. shrubsolii* (D), where the regressions accounted for 66% of the variation in C and 71% of the variation in N to *Streblospio* n. sp. (P), where significant relationships could not be detected (Figs. 2, 3). Even in the three morphs where significant regressions were evident, the size of 95% confidence intervals on predicted values of C and N content would preclude making significantly different predictions of C and N content from embryos of different size within developmental morphs. Observations in this study of lecithotrophic and planktotrophic polychaetes are similar to those in echinoderms with lecithotrophic development where variation

among species in the nature and strength of the relationship between egg size and organic content has been found (McEdward and Carson, 1987; McEdward and Coulter, 1987; McEdward and Chia, 1991). Given that egg or embryo size accounts for minimal variation in organic content within species, considerable caution should be taken in presuming egg or embryo size as an accurate measure of per offspring investment.

Acknowledgments

I would like to thank G. Plaia and N. Blair for providing assistance and advice with elemental analysis and C. Brownie for help with the statistics. Cultures of *Streblospio* were graciously supplied by L. Levin, S. Rice, and C. Cazaux. I would also like to thank F. Gould, J. Garlich, D. Checkley, D. Wolcott, and three anonymous reviewers for their comments on earlier versions of this manuscript. Special thanks must go to L. Levin for her conscientious advising and critical examination of earlier versions of this paper. This project was supported in part by funds from EPA grant R81-72-52-010 to L. Levin.

Literature Cited

Bell, S. S., and B. C. Coull. 1980. Experimental evidence for a model of juvenile macrofauna-meiofauna interactions. Pp. 179–192 in *Marine Benthic Dynamics*, K. R. Tenore and B. C. Coull, eds. University of South Carolina Press, Columbia, SC.

Bridges, T. S. 1992. Effects of development mode, contaminated sediments, and maternal characteristics on growth and reproduction in the polychaetes *Streblospio benedicti* (Spionidae) and *Capitella* sp. I (Capitellidae). Ph.D. thesis, North Carolina State University.

Caswell, H. 1981. The evolution of "mixed" life histories in marine invertebrates and elsewhere. *Am. Nat.* **117:** 529–536.

Cazaux, C. 1985. Reproduction et developpement larvaire de l'annelide polychete saumatre *Streblospio shrubsolii* (Buchanan, 1980). *Cah. Biol. Mar.* **26:** 207–221.

Chia, F.-S. 1974. Classification and adaptive significance of developmental patterns in marine invertebrates. *Thalass. Jugoslav.* **10:** 121–130.

Christiansen, F. B., and T. M. Fenchel. 1979. Evolution of marine invertebrate reproductive pattern. *Theor. Pop. Biol.* **16:** 267–282.

Dean, D. 1965. On reproduction and larval development of *Streblospio benedicti*. *Biol. Bull.* **128:** 67–76.

Eckelbarger, K. J. 1980. An ultrastructural study of oogenesis in *Streblospio benedicti* (Spionidae), with remarks on the diversity of vitellogenic mechanisms in Polychaeta. *Zoomorphologie* **94:** 241–263.

Eckelbarger, K. J. 1986. Vitellogenic mechanisms and the allocation of energy to offspring in polychaetes. *Bull. Mar. Sci.* **39:** 426–443.

Emlet, R. B., L. R. McEdward, and R. R. Strathmann. 1987. Echinoderm larval ecology viewed from the egg. Pp. 55–136 in *Echinoderm Studies vol. 2*, M. Jangoux and J. M. Lawrence, eds. A. A. Balkema, Rotterdam.

Grahame, J. 1982. Energy flow and breeding in two species of *Lacuna*: comparative costs of egg production and maintenance. *Int. J. Invert. Repro.* **5:** 91–99.

Grahame, J., and G. Branch. 1985. Reproductive patterns of marine invertebrates. *Oceanogr. Mar. Biol. Ann. Rev.* **23:** 373–398.

Grant, A. 1983. On the evolution of brood protection in marine benthic invertebrates. *Am. Nat.* **122:** 549–555.

Greene, C. H. 1985. Planktivore functional groups and patterns of prey selection in pelagic communities. *J. Plank. Res.* **7:** 35–40.

Havenhand, J. N., and C. D. Todd. 1989. Reproductive effort of the nudibranch molluscs *Idalaria proxima* (Adler & Hancock) and *Onchidoris muricata* (Muller): an evaluation of techniques. *Func. Ecol.* **3:** 153–163.

Henry, J. J., and R. A. Raff. 1990. Evolutionary change in the process of dorsoventral axis determination in the direct developing sea urchin, *Heliocidaris erythrogramma*. *Dev. Biol.* **141:** 55–69.

Hermans, C. O. 1979. Egg size and energetics: polychaete egg sizes, life histories and phylogeny. Pp. 1–9 in *Reproductive Ecology of Marine Invertebrates*, S. E. Stancyk, ed. University of South Carolina Press, Columbia, SC.

Kerfoot, W. C. 1977. Implications of copepod predation. *Limnol. Oceanogr.* **22:** 316–325.

Lawrence, J. M., J. B. McClintock, and A. Guille. 1984. Organic level and caloric content of eggs of brooding asteroids and an echinoid (Echinodermata) from Kerguelen (South Indian Ocean). *Int. J. Invert. Repro. Dev.* **7:** 249–257.

Levin, L. A. 1984. Multiple patterns of development in *Streblospio benedicti* Webster (Spionidae) from three coasts of North America. *Biol. Bull.* **166:** 494–508.

Levin, L. A., H. Caswell, K. D. DePatra, and E. L. Creed. 1987. Demographic consequences of larval development mode: planktotrophy vs. lecithotrophy in *Streblospio benedicti*. *Ecology* **68:** 1877–1886.

Levin, L. A., and E. L. Creed. 1986. Effect of temperature and food availability on reproductive responses of *Streblospio benedicti* (Polychaeta:Spionidae) with planktotrophic or lecithotrophic development. *Mar. Biol.* **92:** 103–113.

Levin, L. A., and D. V. Hugget. 1990. Implications of alternative reproductive modes for seasonality and demography in an estuarine polychaete. *Ecology* **71:** 2191–2208.

Levin, L. A., J. Zhu, and E. L. Creed. 1991. The genetic basis of life-history characters in a polychaete exhibiting planktotrophy and lecithotrophy. *Evolution* **45:** 380–397.

McCann, L. D., and L. A. Levin. 1989. Oligochaete influence on settlement, growth and reproduction in a surface-deposit-feeding polychaete. *J. Exp. Mar. Biol. Ecol.* **131:** 233–253.

McEdward, L. R., and S. F. Carson. 1987. Variation in egg organic content and its relationship with egg size in the starfish *Solaster stimpsoni*. *Mar. Ecol. Prog. Ser.* **37:** 159–169.

McEdward, L. R., and F.-S. Chia. 1991. Size and energy content of eggs from echinoderms with pelagic lecithotrophic development. *J. Exp. Mar. Biol. Ecol.* **147:** 95–102.

McEdward, L. R., and L. K. Coulter. 1987. Egg volume and energetic content are not correlated among sibling offspring of starfish: implications for life-history theory. *Evolution* **41:** 914–917.

Menge, B. A. 1974. Effect of wave action and competition on brooding and reproductive effort in the seastar, *Leptasterias hexactis*. *Ecology* **55:** 84–93.

Needham, J. 1963. *Chemical Embryology, I*, Hafner, New York. 613 pp.

Okazaki, K., and K. Dan. 1954. The metamorphosis of partial larvae of *Peronella japonica* Mortensen, a sand dollar. *Biol. Bull.* **106:** 83–99.

Pennington, J. T., S. S. Rumrill, and F.-S. Chia. 1986. Stage-specific predation upon embryos and larvae of the Pacific sand dollar, *Dendraster excentricus*, by 11 species of common zooplanktonic predators. *Bull. Mar. Sci.* **39:** 234–240.

Perron, F. E. 1986. Life history consequences of differences in developmental mode among gastropods in the genus *Conus*. *Bull. Mar. Sci.* **39:** 485–497.

Qian, P. Y. 1991. Impact of environmental factors on life history strategies of the marine polychaete *Capitella* sp. Ph.D. thesis, University of Alberta.

Qian, P. Y., and F.-S. Chia. 1992. Effects of diet type on the demographics of *Capitella* sp. (Annelida; Polychaeta): lecithotrophic development vs. planktotrophic development. *J. Exp. Mar. Biol. Ecol.* **157:** 159–179.

Rice, S. A. 1991. Reproductive isolation in the *Polydora ligni* complex and *Streblospio benedicti* complex (Polychaeta: Spionidae). *Bull. Mar. Sci.* **48:** 432–447.

Rumrill, S. S., J. L. Pennington, and F.-S. Chia. 1985. Differential susceptibility of marine invertebrate larvae: laboratory predation of sand dollar, *Dendraster excentricus* (Eschscholtz), embryos and larvae by zoeae of the red crab, *Cancer productus* Randall. *J. Exp. Mar. Biol. Ecol.* **90:** 193–208.

Smith, C. C., and S. D. Fretwell. 1974. The optimal balance between size and number of offspring. *Am. Nat.* **108:** 499–506.

Stearns, S. C. 1976. Life-history tactics: a review of the ideas. *Q. Rev. Biol.* **51:** 3–47.

Strathmann, R. R. 1985. Feeding and nonfeeding larval development and life-history evolution in marine invertebrates. *Ann. Rev. Ecol. Syst.* **16:** 339–361.

Strathmann, R. R., and K. Vedder. 1977. Size and organic content of eggs of echinoderms and other invertebrates as related to developmental strategies and egg eating. *Mar. Biol.* **39:** 305–309.

Thorson, G. 1946. Reproduction and larval development of Danish marine bottom invertebrates with special reference to the planktonic larvae of the Sound (Oresund). *Medd. Komm. For Danm. Fisker-Og Havunders. Ser. Plankton* **4:** 1–523.

Thorson, G. 1950. Reproduction and larval ecology of marine bottom invertebrates. *Biol. Rev.* **25:** 1–45.

Turner, R. L., and J. M. Lawrence. 1979. Volume and composition of echinoderm eggs: implications for the use of egg size in life-history models. Pp. 25–40 in *Reproductive Ecology of Marine Invertebrates*, S. E. Stancyk, ed. University of South Carolina Press, Columbia, SC.

Vance, R. R. 1973a. On reproductive strategies in marine benthic invertebrates. *Am. Nat.* **107:** 339–352.

Vance, R. R. 1973b. More on reproductive strategies in marine benthic invertebrates. *Am. Nat.* **107:** 353–361.

Watzin, M. C. 1983. The effects of meiofauna on settling macrofauna: meiofauna may structure macrofauna communities. *Oecologia* **59:** 163–166.

Watzin, M. C. 1986. Larval settlement into marine soft-sediment systems: interactions with the meiofauna. *J. Exp. Mar. Biol. Ecol.* **98:** 65–113.

Wray, G. A., and R. A. Raff. 1991. The evolution of developmental strategies in marine invertebrates. *Trends Ecol. Evol.* **6:** 45–50.

Reference: *Biol. Bull.* **184:** 153–185. (April, 1993)

On Antarctic Entoprocta: Nematocyst-like Organs in a Loxosomatid, Adaptive Developmental Strategies, Host Specificity, and Bipolar Occurrence of Species*

PETER EMSCHERMANN

Fakultät für Biologie der Universität Freiburg i.Br., Biologie für Mediziner, Schänzlestraße 1, 7800 Freiburg i.Br. BRD

Abstract. In the southern Weddell Sea and the Bransfield Strait a total of eight species of entoproets were found: four Loxosomatidae, originally known to be common in the Northern Polar Sea and the Atlantic sector of the subaretic region (*Loxosomella antedonis* Mortensen, 1911, *L. compressa* Nielsen and Ryland, 1961, *L. varians* Nielsen, 1964, and *L. antarctica* Franzén, 1973); three new species of loxosomatids (*L. brochobola* spec. nov., *L. seiryoini* spec. nov., and *L. tonsoria* spec. nov.); and one single colonial entoproet *Barentsia discreta* (Busk, 1886) which is distributed worldwide. *Loxosomella brachystipes*, described by Franzén in 1973 from South Georgia, is shown to be synonymous with *L. varians* Nielsen, 1964. The microscopic investigation of the above species revealed several morphological characters, previously unknown, that add to our knowledge of the Entoprocta in general, and also help in characterizing species. The first of these novel characters, observed in *L. brochobola* spec. nov., are extruding organs similar to cnidarian spirocysts. This is the first description of such organs in entoproets. *Loxosomella antarctica* is capable of calyx regeneration and thereby becomes the only solitary entoproct known to have such a regeneration capacity. Finally, the formation of special resting buds in *Barentsia discreta* is described. The range of morphological variation of these species, the question of host specificity in the Loxosomatidae, and the bipolar occurrence of some of these species is discussed.

Introduction

Reports on Antarctic Entoprocta are scarce. Until 1973 only five colonial forms had been recorded from the Southern Ocean, predominantly from the subantarctic region: *Pedicellina australis* Ridley, 1881 was reported from the Magellan Strait, at the Patagonian coast and the Falkland Islands (Islas Malvinas); *Barentsia capitata* Calvet, 1904, and *Barentsia variabilis* Calvet, 1904 were reported from South Georgia and the Falkland Islands; and *Barentsia aggregata*[1] Johnston and Angel, 1940 from Macquarie, Heard, Marion, and the Kerguelen Islands. These latter three species are probably synonymous. Finally, *Barentsia discreta* (Busk, 1886), common circumantarctically in subantarctic latitudes (Johnston and Angel, 1940; Rogick, 1956; Waters, 1904) as well as on the Antarctic shelf itself, was reported in the Commonwealth Bay (Johnston and Angel, 1940) and from the northernmost tip of the Antarctic Peninsula (Franzén, 1973). In 1973, Franzén augmented these reports with observations of older samples from the 1901-03 Swedish Antarctic expedition. He added *Pedicellina cernua* (Pallas, 1774) and four Loxosomatidae to the list of entoproets from Antarctic waters: *Loxosomella compressa* Nielsen and Ryland, 1961 var. antarctica; *Loxosomella murmanica* (Nilus, 1909); *Loxosomella antarctica* spec. nov.; and *Loxosomella brachystipes* spec. nov. There have been no more recent studies of the Antarctic entoproctan fauna.

During the Antarctic summer 1989–90, in the course of a survey of the Antarctic benthos supported by the Deutsche Forschungsgemeinschaft, the entoproctan fauna of the Weddell Sea and the Bransfield Strait were investigated aboard the German research vessels PFS POLAR-

Received 31 August 1992; accepted 25 January 1993.

* These investigations have been supported by the Deutsche Forschungsgemeinschaft.

[1] A sample of barentsiid colonies from the Californian coast near Santa Cruz, sent me by Kerstin Wasson (University of California, Santa Cruz), proved to consist not only of colonies of *Barentsia ramosa*, being common there, but also of Barentsia aggregata J. and A., which had previously been believed to occur only in the subantarctic region.

STERN and FFS METEOR. Benthic samples were taken in the Weddell Sea at 26 locations along the shelf from its northeastern most edge down to the base of the Antarctic Peninsula. Forty-five hauls were taken with both an Agassiz trawl and an epibenthic sledge (Fig. 1, Table 1). Except at three stations in the 600–1100 m depth range, most samples were taken between 100 and 500 m (see Table I and Fig. 1). The benthic fauna, especially the associations of ciliary-feeders, was generally richer, both in abundance and species diversity, in the eastern part of the Weddell Sea where the steep slope is more exposed to the Weddell Sea current than the fauna of the western Weddell Sea where bottoms are less sloped and less exposed to the current.

In the Bransfield Strait a total of 22 hauls were evaluated, nine from a quadrangular dredge and 13 from a Van Veen Grab, taken at a depth range between 120 and 400 m at 15 locations between Elephant Island to the north and Adelaide Island to the south. (Fig. 2, Table II).

Altogether, eight entoproctan species were found. Four of them occurred in both areas and one species was found only in the Weddell Sea. Three new species were described: two from the Weddell Sea and one from the Bransfield Strait.

As a general trend, the abundance and population density of Entoprocta in the Bransfield Strait was much higher than in the Weddell Sea—presumably because of the higher primary production and consequently higher nutrient supply in this area. Of special zoogeographical interest is that four of the species found to be common in the Antarctic region also occur in the North Atlantic and the Arctic Polar Sea, but seem to be absent from the mid-Atlantic coasts.

Sampling Methods and Treatment of Samples

The trawling times of the sampling gear varied between about 30 and 90 min, according to the bottom structure and ice conditions. To obtain undamaged living samples for laboratory observations and culture experiments, the hauls were immediately subject to rough presorting. Appropriate growth substrates for entoprocts, such as bryozoan and hydroid colonies, bivalve shells, small sponges and stones, as well as potential entoproctan hosts such as errant and sedentary polychaetes with their tubes, sipunculids, echiurans, priapulids, ophiuroids and, occasionally, crinoids, were collected as soon as possible and placed in separate plastic tubs with running fresh seawater of outside

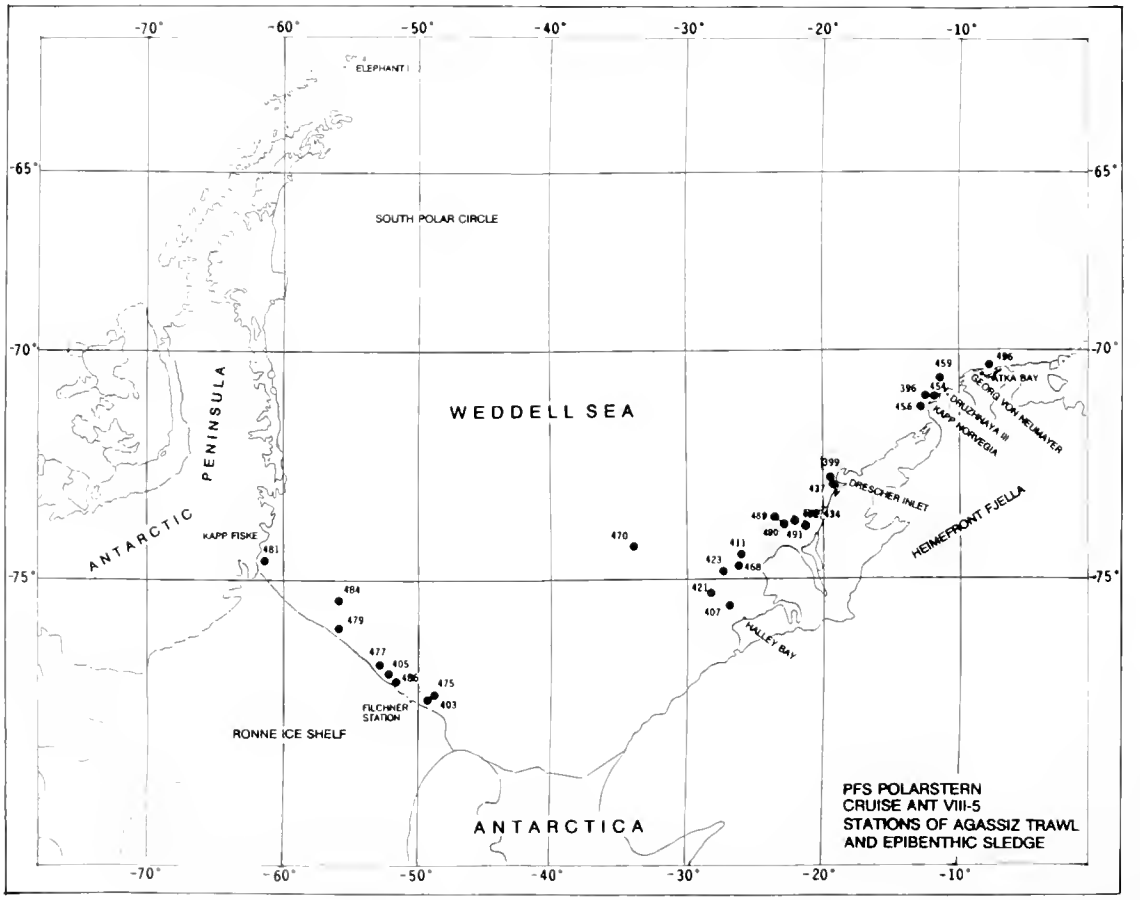

Figure 1. Station map of the POLARSTERN cruise ANT VIII-5 in the Weddell Sea.

Table I

Station List I. Polarstern-Cruise ANT VIII-5 in the Weddell Sea

Station	Position	Depth (m)	Date	Gear	Bottom	Predominant fauna
16-396	S 71,08°; W 11,77°	360-320	29/12/89	A	St	Sponges, Bryozoa
-399	S 72,86°; W 19,30°	380-390	30/12/89	A	St, Sf	Sponges, Bryozoa, Ascidia
-403	S 76,94°; W 49,81°	220-250	06/01/90	A	Cb, G	Bryozoa, Holothuria
-405	S 76,52°; W 52,63°	380-390	07/01/90	A	S	Ascidia, Pennatulids,
	S 76,53°; W 52,72°					Gorgonia, Sponges:
	S 76,52°; W 52,78°					Bryozoa
-407	S 75,46°; W 27,02°	240-250	12/01/90	E, A	Sf	Sponges, Holothuria
-411	S 74,54°; W 25,75°	520-530	14/01/90	E, A	S, St	Crinoids, Holothuria, Nemerteans, Prawns
-421	S 75,21°; W 27,80°	430-400	17/01/90	E, A	S, G	Pennat., Crinoids, Echin., Ophiur., Holothur., Prawns, Fishes
-423	S 74,84°; W 27,56°	460-470	17/01/90	A, E	S, St	Sponges, Pennat., Ophiur., Prawns
-434	S 73,69°; W 21,75°	260-270	20/01/90	E, A	Cb, St	Bryoz., Holoth., Prawns
-437	S 72,84°; S 19,40°	390-420	21/01/90	E	Cb, St	Bryoz., Ophiur., Amphip.
-454	S 71,08°; W 11,69°	210-280	26/01/90	E, A	Sf	Sponges, Gorgon., Fishes
-456	S 71,25°; W 21,01°	200-250	26/01/90	A, E	Sf	Sponges, Ascid., Amphip., Fishes
-459	S 70,69°; W 11,19°	350-390	28/01/90	E, A	G, St, Cb	Sponges, Pennat., Crinoids, Amphipods
-468	S 74,74°; W 26,36°	480-460	09/02/90	E, A	S, G	Pennat., Amphip., Prawns, Fishes
-470	S 74,28°; W 34,09°	1050-960	10/02/90	E, A	Cb	Stylasterids, Ophiur., Ascid., Sponges, Polychaetes
-475	S 76,85°; W 49,45°	280	13/02/90	E, A	S	Sponges, Echin., Ascid., Crin.
-477	S 76,45°; W 53,15°	430-450	14/02/90	A, E	S	Pennat., Echin., Prawns
-479	S 75,68°; W 56,72°	340-360	14/02/90	E, A	S, Sf	Crin., Ophiur., Prawns, Pantop.
-481	S 74,71°; W 61,14°	640-620	15/02/90	A, E	St	Ophiur., Amphip., Prawns
-484	S 75,28°; W 55,98°	450-440	16/02/90	E, A	S	Pennatul., Ascid., Ophiur., Polychaetes, Brachiopods
-486	S 76,50°; W 52,15°	340-330	17/02/90	E	Cb	Spong., Bryoz., Pennat., Ascid.
-489	S 73,68°; W 23,13°	980-990	21/02/90	A	St	Ophiuroids, Prawns
-490	S 73,70°; W 22,66°	630-610	21/02/90	E	Sf	Crin., Holothur., Echin., Prawns
-491	S 73,69°; W 22,42°	390-370	21/02/90	E	S, G	Crinoids, Pantopods, Amphip.
-492	S 73,69°; W 21,74°	250	21/02/90	A	Cb	Crin., Bryoz., Spong., Ophiur.
-496	S 70,63°; W 08,09°	80	27/02/90	A, E	Cb	Bryozoa, Holothuria

Benthos stations: Gear, sediments, and predominant fauna

Gear: A, Agassiz trawl; E, epibenthic sledge; Bottoms: Cb, calcareous bryozoan shells; G, sand and coarse gravel; S, sandy silt and mud; Sf, felt of sponge needles; St, larger stones and rocks.

temperature (−1 to +0.5°C). The presorted substrates were subsequently checked for entoprocts under the dissection microscope. About half of the zooids of each species found were kept alive, whereas the rest of them were preserved, some after narcotization, some without such a pretreatment.

Narcotization and fixation

A 4% formaldehyde solution in seawater proved to be the best fixation medium, yielding usable results even for electron microscopical purposes. For fast narcotization, especially when specimens were treated while still on their host, the gradual addition of an isosmotic solution of $MgSO_4$ gave acceptable results. But the local anesthetic amylocaine-hydrochloride [Stovaine^R Rhone Poulenc: 1-(dimethylamino)-2-methyl-2-butanol-benzoate hydrochloride] was more effective, particularly for small samples or single specimens in a small amount of water. By far the best results were obtained with a two-step narcotization: 8–10 crystals of amylocaine-hydrochloride were gradually added to a small sample of specimens in about 2 ml of seawater until the animals were completely expanded and showed no reaction to mechanical stimulation (about 10 min). Subsequently, some crystals of $MgSO_4$ were added. After 5 min the sample could be fixed by the addition of 0.2 ml of 4% formaldehyde.

Treatment of living samples

Living samples for later culture experiments and observations aboard were kept in 5–10 l aquaria under running seawater at 0–0.5°C on their original substrates or hosts. They were fed by the moderate addition of fresh nanoplankton samples, chiefly diatoms. Only the colonial *Barentsia discreta* could be cultured successfully and brought home to the laboratory still alive. None of the solitary loxosomatids could be kept alive and actively budding for more than three to four weeks, even when left on their original hosts.

Measurements and sketches

Measurements of a representative number of living specimens (30–50 if possible) from every locality were

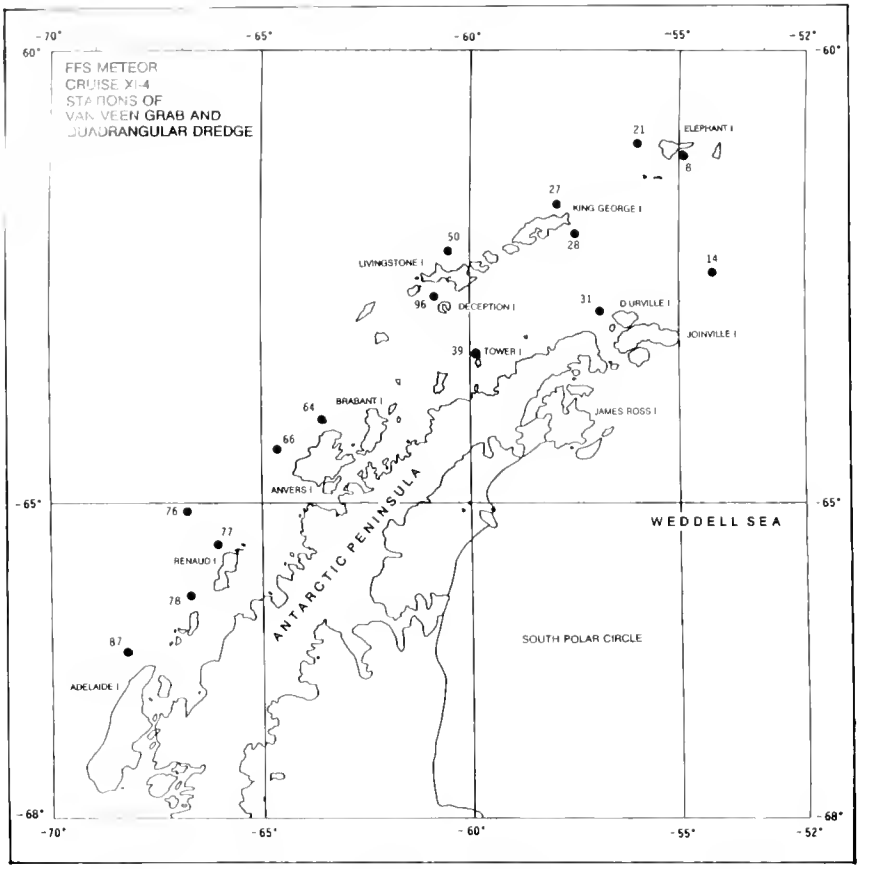

Figure 2. Station map of the Meteor cruise XI-4 in the Bransfield Strait.

taken aboard and, later on, compared with those of random samples of preserved specimens. These groups of measurements were not significantly different. Freehand sketches were made of living specimens. When ship conditions allowed, micrographs of living specimens were taken through the dissection microscope. Higher magnification micrographs were made from preserved material in the home laboratory.

Some Remarks on Species Determination and the Description of New Species in Entoprocta

Entoprocta in general, and most Loxosomatidae in particular, have a scarcity of reliable species characters. The majority of morphological parameters, such as size, number of tentacles, body proportions, shape of stomach, and even conspicuous structures like cuticular pores, and spines, and body appendices, exhibit great intraspecific variability, and there is often overlap between species. Because of this deficiency of reliable morphological features, attempts have often been made to use the host or the locality of an entoproct as an aid for identifying its species. But neither the number of true species and their variation, nor their geographical distribution and possible spectrum of hosts, are sufficiently well-known to be useful in species identification.

A rigorous biological species characterization by demonstration of their genetic isolation has not been possible for the great majority of entoproct species. Therefore, any species determination, especially any description of new species, founded on the evaluation of a few morphological characteristics, should be based on an intimate knowledge of all comparable species and, if possible, a comparison of the specimens in question with the type material of all similar species or, at least, with definitively identified samples of the latter. The description of a new species is not of value in itself; the demonstration of the real distribution range of a species is much more important.

Any description of specimens new to an area should be illustrated with precise drawings in frontal and lateral view, and, if possible, in the contracted as well as the expanded state. Additional micrographs are often very helpful. Proof samples or types should be preserved both in contracted and expanded state. Because of insufficient description and unsatisfactory preservation of type material, not one Loxosomatidae described by Harmer (1915) from the Siboga samples can be reidentified.

Table II

Station List 2. Meteor-Cruise VI-4 to the Bransfield Strait

Station	Position	Depth (m)	Date	Gear	Bottom
08-90	S 61.25° W 55.05°	125	29/01/90	VG	S
14-90	S 62.53°; W 54.15°	400	29/12/90	VG, D	St
21-90	S 61.00°; W 56.00°	337-426	30/12/90	VG	S
27-90	S 61.75°; W 57.89°	340	01/01/90	VG	S
28-90	S 62.09°; W 57.64°	286-383	01/01/90	VG	S
31-90	S 62.99°; W 56.99°	80	02/01/90	VG, D	St, S
39-90	S 63.42°; W 59.86°	155	03/01/90	VG, D	St
50-90	S 62.25°; W 60.57°	167-147	05/01/90	VG, D	S
64-90a	S 64.15°; W 63.55°	135-150	08/01/90	VG, D	St
66-90	S 64.47°; W 64.77°	356	08/01/90	VG, D	St, S
76-90	S 65.06°; W 66.98°	220	10/01/90	D	St
77-90	S 65.39°; W 66.18°	330-370	10/01/90	VG	St
78-90	S 65.91°; W 66.85°	75	11/01/90	D	St
87-90	S 66.57°; W 68.57°	450	12/01/90	VG, D	S, St
96-90	S 62.77°; W 60.90°	150	16/01/90	VG, D	S, St

Benthos stations: gear and sediments

Gear: VG, Van Veen grab; D, rectangular dredge; Bottom: Cb, calcareous bryozoan shells; G, sand and coarse gravel, S, silt and mud; Sf, felt of sponge needles; St, larger stones and rocks.

Because of our limited knowledge of the intraspecific variability and geographic distribution of most entoproctan species, every describer of a new entoproctan species should be wary that his new species may turn out to be synonymous with a species long known, even if all precautions have been taken. The following descriptions of new species must be seen in this light.

Description and Discussion of Species

Loxosomella brochobola *spec. nov.*

Holotype. Collected by the author on 20 January 1990 at the type locality, stat. 16-434 ANT VIII-5 (73.69°S; 21.75°W) at a depth of 260–270 m from sandy and rocky bottoms with abundant calcareous Bryozoa; the entoproctan species was growing exclusively on the inner, abfrontal surface of tube-shaped *Porella malouinensis* colonies (Bryozoa).

Syntypes. Deposited in the British Museum of Natural History, London (No. 1992.12.14.1) and the Zoologisk Museum, Kobenhavn.

Name. From Greek: $\beta\rho o\chi o\zeta$-snare and $\beta\alpha\lambda\lambda\epsilon\iota\nu$-discharge, referring to the sticky threads that can be ejected by nematocyst-like extrusive organs—a unique character of this species.

Description. This is a tall Loxosomella species, about 1300 μm in length, the individuals resemble at first glance a *Pedicellina* zooid (Figs. 3a–c; 4). The bulgy goblet-shaped calyx is sharply delineated from the long, slender, and highly motile stalk. The large tentacular crown with 14–20 slim tentacles is oriented straight up. In the expanded state, the calyx is slightly laterally depressed, but is nearly globular when contracted. The rectum bulges out between the aboral pair of tentacles, and the anus opens immediately anterior to the aboral ends of the horseshoe-shaped periatrial ciliary rim (Fig. 4f, i). The peduncle is slender, cylindrical and one and a half to twice as long as the calyx. About halfway down there is usually a slight "waist." The basal attachment area is narrower than the average diameter of the peduncle and animals are not fixed very strongly to their substratum, but can be removed easily without damage. Remnants of the foot gland normally persist as a plug of globular cells in the base of the stalk. As often observed in loxosomatids, the perikarya of the peduncular epithelial cells are arranged in longitudinal rows between the muscle strands.

The stomach is voluminous and globular with wide lateral pouches bulging out at either side (Fig. 4k). The longitudinal musculature of the oral side consists of a dense layer of fibers running downwards from the oral and orolateral calyx wall to nearly the base of the peduncle, while at the aboral side and laterally in the upper portion of the stalk, only 2–3 single strands at either side are developed. Basalwards these aboral muscle fibers increase in number, thus forming—together with the oral fibers—a closed muscular tube in the lower portion of the peduncle.

Living specimens in normal expanded posture have the peduncle slightly curved, the aboral side of the calyx inclined downwards, the oral side up (Fig. 4f). Seen from above in this position, four large whitish blue, opaque blister-like structures are conspicuously visible at either side between the bases of each of the second and third, as well as the third and fourth, oral tentacle. Upon irritation, or sometimes spontaneously, 300–400 μm long delicate, helically twisted threads can be ejected from these enigmatic organs (Figs. 3d–h; 4b–d, n–g), which resemble

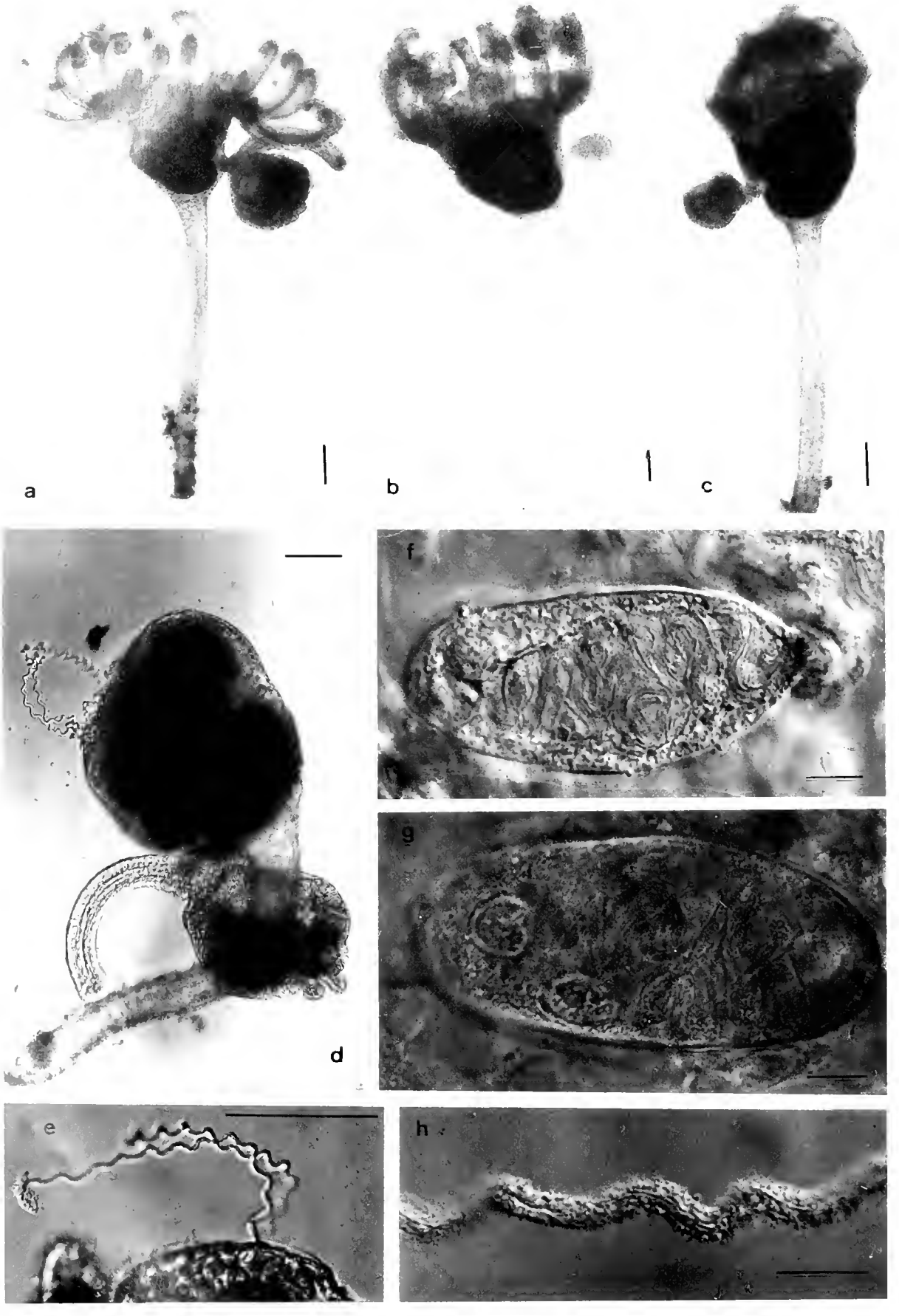
a
b
c
d
e
f
g
h

cnidarian spiro- or nematocysts. The sticky threads are as long, or somewhat longer than the tentacles, and remain anchored with their proximal ends in the epithelial cells from which they originate, floating with their distal ends, outside the tentacular crown. At higher magnification these extrusive organs each consist of an enlarged barrel-shaped and plurinuclear epithelial capsule, about 80 μm long and 45 μm in diameter. In the unexploded state, it is filled with an invaginated highly coiled tubule, roughly square in cross section. The nuclei, generally four, are situated basally in a narrow area of marginal plasma. When ejected, the evaginated tubule, about 3 μm in diameter, has an X-shaped cross section and is covered by a thin mucous coat. *Loxosomella brochobola* is the only entoproct known to have such extrusive organs.

The function of these organs is obscure, but defense seems unlikely. Possibly these extrusive threads are connected with a specialized method of feeding; their arrangement around the mouth supports such a presumption. The extrusive threads could act as a kind of "fly paper" in a marine biotope poor in suspended matter. They would collect small particles attached to the substratum and inaccessible to the ciliary feeding apparatus, and from time to time would be swallowed together with any adhering material. But this kind of activity has, so far, not been observed.

From their genesis, the extruding organs are surely true kamptozoan organs, not "kleptocnides" somehow acquired from hydroids growing in their immediate vicinity, such as *Halecium*. Moreover, in both their overall structure and extrusion mechanism, they are distinct from similar cnidarian organs. Unlike the tubules of cnidarian nematocysts, they do not evaginate by turning inside out, like a glove finger, but rather they are ejected simply by the unfolding of the curled introverted thread through a rupture of the extruding capsule at its proximal tip. (An ultrastructural investigation of these peculiar organs is in progress and will be published separately.)

Buds, normally two to three on either side, develop orolaterally, level with the basal half of the stomach. They are fixed to the parent, not by the aboral tip of the foot, but by a junctional zone situated basally at the aboral side of the calyx, as is known from *Loxosomella kefersteini* (Figs. 3a, d; 4a–e, l). The long, sickle-shaped glandular foot of the bud points upwards. The main body of the foot gland is situated just below the stomach. From there, a narrow glandular groove bordered by large secreting cells runs all along the foot to its aboral tip. After the bud has detached from the parent, the foot does not degenerate totally, but develops into the basal portion of the adult peduncle. The aboral tip of the foot becomes the attachment site for settling on the substrate. The upper portion of the adult stalk above the "slight waist" consequently develops by stretching the zone between the calyx base and the proximal part of the foot.

Gonads in different stages of development were observed in nearly all specimens examined: Immature and mature testes were developed only in undetached buds and newly settled specimens, while mature ovaries were found exclusively in larger animals, usually with 1–2 eggs on either side. The testes are positioned laterally to the stomach; the ovaries lie more distally, in the space between stomach, esophagus and the atrial bottom. In a few specimens unhatched larvae lacking eyespots were observed (Fig. 4m).

Measurements. Total length: 1200 μm (994–1350 μm); length of calyx: 380 μm (260–493 μm); length of stalk: 800 μm (423–978 μm); width of calyx: 335 μm (239–408 μm); thickness of calyx: 400 μm (245–554 μm); diameter of stalk: 90 μm (65–114 μm); number of tentacles: 18 (12–20), in buds: 12.

Habitat and distribution. Though its bryozoan host is abundant all over the Weddell Sea, *Loxosomella brochobola* has been found at only two locations in the eastern Weddell Sea (stations ANT-VIII-5 16-396; 16-434; 16-491; and 16-492). *L. brochobola* grows exclusively on the inner, abfrontal surface of the tube-shaped colonies of *Porella malouinensis* (Bryozoa) which is sometimes associated with young colonies of an undetermined species of *Halecium* (Hydroida). At the type locality *L. brochobola* was growing in small groups of 20–30 specimens/cm^2, specially on younger host colonies settled only sparsely by other epizoans.

Discussion of the species. The loxosomatid described above is the only entoproct known to possess nematocyst-like organs. These may be homologous to and derived from pearl-like glandular cells or cell complexes, which have been found to be more or less regularly scattered around the margin of the tentacular crown in a number of loxosomatids. These organs alone are a striking species character. To date only four other loxosomatids are known which show the budding pattern described above: *Loxosomella kefersteini* Claparède, 1867, *L. pseudocompressa* Konno, 1977, *L. annulata* Harmer, 1915, and *L. mepse* du Bois-Raymond-Marcus, 1957. In its general appear-

Figure 3. *Loxosomella brochobola* spec. nov. a–c: living specimens in abfrontal (a) and lateral view (b, c); d: contracted specimen with large bud and ejected sticky threads; e: ejected sticky thread; f: extrusion organ in Nomarski contrast, the coiled ejectable tubule is visible (bar 10 μm); g: the same organ, two of four nuclei are visible at the left side (bar: 10 μm); h: part of an ejected tubule [bar in all micrographs 100 μm unless otherwise indicated].

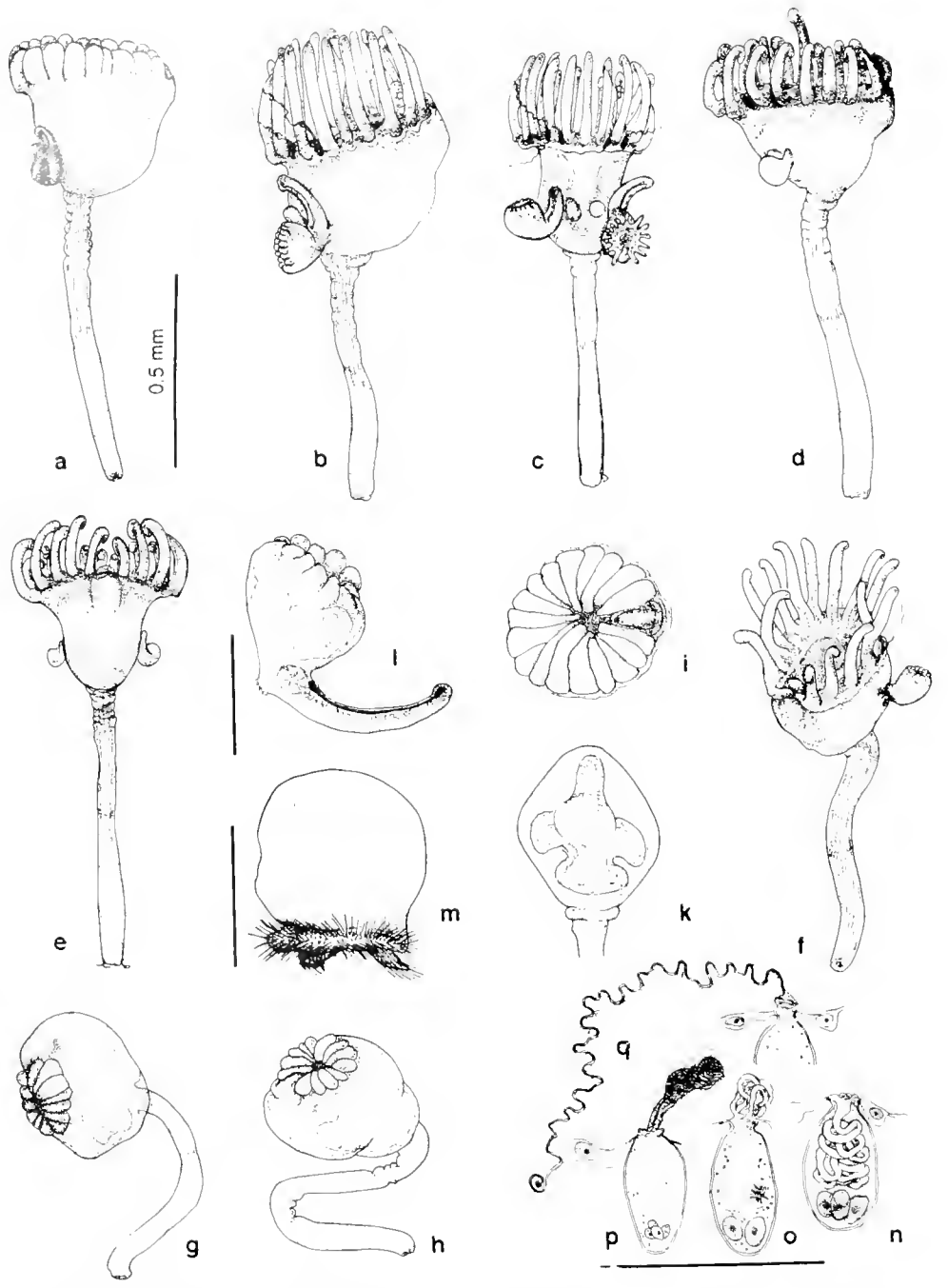

Figure 4. *Loxosomella brochobola* spec. nov. a: contracted zooid from fixed sample; b–e: two expanded zooids (b/c; d/e), in lateral-frontal, and lateral-abfrontal view, respectively, with buds and, partly, ejected extrusion organ; f: living expanded zooid in normal posture; g, h: bending movements of a zooid after irritation; i: contracted tentacular crown seen from above, the rectum bulging out between the aboral tentacles; k: calyx seen from the aboral side; lateral pouches of the stomach are visible; l: newly detached bud, the navel being visible at the abfrontal side of the calyx base; m: young larva before hatching; n–q: extrusive organs in different stages of ejecting the sticky thread (from preserved specimens).

ance, only the latter shows some similarities to the Weddell Sea specimens; but the smaller size and average number of tentacles of *L. mepse*, the shape of its stomach not being trilobed, the shorter foot of its buds not being sickle-shaped, and most of all, the lack of the conspicuous extrusive organs clearly distinguishes this species from the Weddell Sea specimens. In conclusion, *Loxosomella brochobola* is a reliable new species.

Loxosomella seiryoini *spec. nov.*

Holotype. Collected by the author on 17 January 1990 at the type locality, station 16-421 ANT-VIII-5 (75.21°S; 27.56°W) at a depth of 430–470 m from a silty and muddy bottom; specimens were growing in dense populations on the rear end of the body and the anterior part of the proboscis of *Golfingia margaritacea* (Sipunculida). Four of eight specimens of this particular sipunculan species, depending on their size, were host to 20 to several hundred loxosomatids.

Syntypes. Deposited in the British Museum of Natural History (no. 1992.12.14.2) and in the Zoologisk Museum København.

Name. The species name is given in honor and remembrance of a Japanese friend and colleague who passed away.

Description. Loxosomella seiryoini is a small species, with club-shaped individuals about 700 μm long. The calyx, almost circular in cross section, gradually transforms into a peduncle of half to one times the calyx length, tapering slightly towards its base and affixed to the substratum by an enlarged attachment disc (Figs. 5a–e; 6). The tentacular crown, with eight short, stoutish tentacles, is inclined oralwards in an angle of about 45°, both in contracted and expanded state, and is surrounded by a broad peritentacular membrane resembling a Stuart-collar in expanded animals. In living specimens, this collar is much more conspicuous than in preserved ones, where it is manifested merely as a swelling of the lophophoral rim (Fig. 6a, c).

The calyx tapers gradually into the stalk when expanded, but in strongly contracted specimens a deep fold demarcates the transition between calyx and peduncle, and the latter becomes bulgy and barrel-shaped. The footplate is fixed very firmly to the substratum by a thin brownish layer of the foot gland secretion, and in some cases a small remnant of this gland persists as a small globular pit in the middle of the adhesive disc (Fig. 5e).

Specimens settling on the introvert of the host usually are enclosed by a felty and stiff cuirass of adhering detritus particles which are permanently agglutinated with the cuticle, leaving only the lophophoral area and the oral side uncovered (Fig. 6i–k). Such individuals have a considerably reduced capacity for expansion, and they have a more sturdy, globular shape with a short bulging peduncle.

The stomach is globular in outline and lacks lateral pouches. The longitudinal musculature consists of about 12 coarse muscle strands running down from the oral calyx wall to the foot plate, as well as some more delicate lateral and aboral fibers. In the basal portion of the peduncle, particularly in contracted specimens, 10 to 12 additional delicate spirally arranged fibers can be observed (with polarized light!); these fibers crisscross in opposite directions, forming a helical lattice. The buds—usually one at either side of the calyx—develop orolaterally, in line with the base of the stomach. When mature enough to become detached, they have only a short, boat-shaped foot-gland (Figs. 5c; 6d).

In most specimens, gonads in different maturation stages are present: immature testes in undetached or newly detached buds, ovaries in older specimens and, sometimes, embryos and larvae in the brood pouches (Fig. 6f, g). Occasionally, ovaries with eggs as well as degenerating testes were observed in the same specimen, indicating that this species, like other loxosomatids, is protandric.

Measurements. Total length: 700 μm (560–780 μm); length of calyx: 400 μm (318–415 μm); length of peduncle: 270 μm (163–318 μm); width of calyx: 280 μm (160–350 μm); thickness of calyx: 290 μm (254–349 μm); diameter of peduncle: about 124 μm above, tapering to 100 μm at its base; number of tentacles: 8.

In one single, older, not very well preserved sample (stat. 224, Ant VII/4, 71°15'S; 13°07'W) on a specimen of *Golfingia margaritacea*, a number of loxosomatids were found that are similar to *L. seiryoini* in most characters (calyx shape, swollen lophophoral rim, the helical muscular lattice, and remnants of the foot-gland in the peduncular base) except that they have a long, slender peduncle (about 1000–1400 μm) and thus achieve a total length of 1400–2000 μm. Whether *L. seiryoini* really attains such a size, or whether these specimens were artificially stretched by rude handling during sorting and preserving, is unclear.

Habitat and distribution. Loxosomella seiryoini has been found exclusively on *Golfingia margaritacea* in the Weddell Sea, never on other sipunculans of the same size occuring at the same sites. West of the Antarctic Peninsula this loxosomatid seems to be absent, although the host is as common in this region as in the Weddell Sea. This *Loxosomella* preferably settles at the rear of its host and around the foremost part of the introvert where, in most cases, it is difficult to detect. Especially at the latter site, it can form crowded aggregations.

Discussion of the species. This loxosomatid is one of numerous medium-sized species, that lack striking species characters. Quite a list of such species with 8 tentacles and a more or less club-shaped form exists in the literature. Most of these species cannot be reidentified due to the poor quality of the original description—based in some cases on only a single specimen—and due to the insufficient preservation, or the complete lack of any type material. This applies to: *Loxosomella breve* and *L. loricatum* (Harmer, 1915) from the Siboga samples; *Loxosomella minuta* Osburn, 1910, described from the Woods Hole region as growing on sipunculids; *Loxosoma* (*Loxosomella?*) *cingulata, L. infundibuliformis,* and *L. rotunda,* described by Kluge (1946) from the Arctic Polar Sea; and *Loxosoma* (*Loxosomella?*) *singulare* Barrois, 1877 and *L. singulare* Hincks, 1880. However, Harmer mentions small lateral sensory papillae present in the Siboga specimens; so they seem to be different from our species.

Among the more recently described species, *Loxosomella fauveli* Bobin and Prenant, 1953, *L. globosa* Bobin and Prenant, 1953, and *L. varians* Nielsen, 1964, look similar to the Weddell Sea form. But even if one does not attach too great significance to their smaller size and divergent hosts, a number of other characters differ considerably from *L. seiryoini:* they all lack the conspicuous

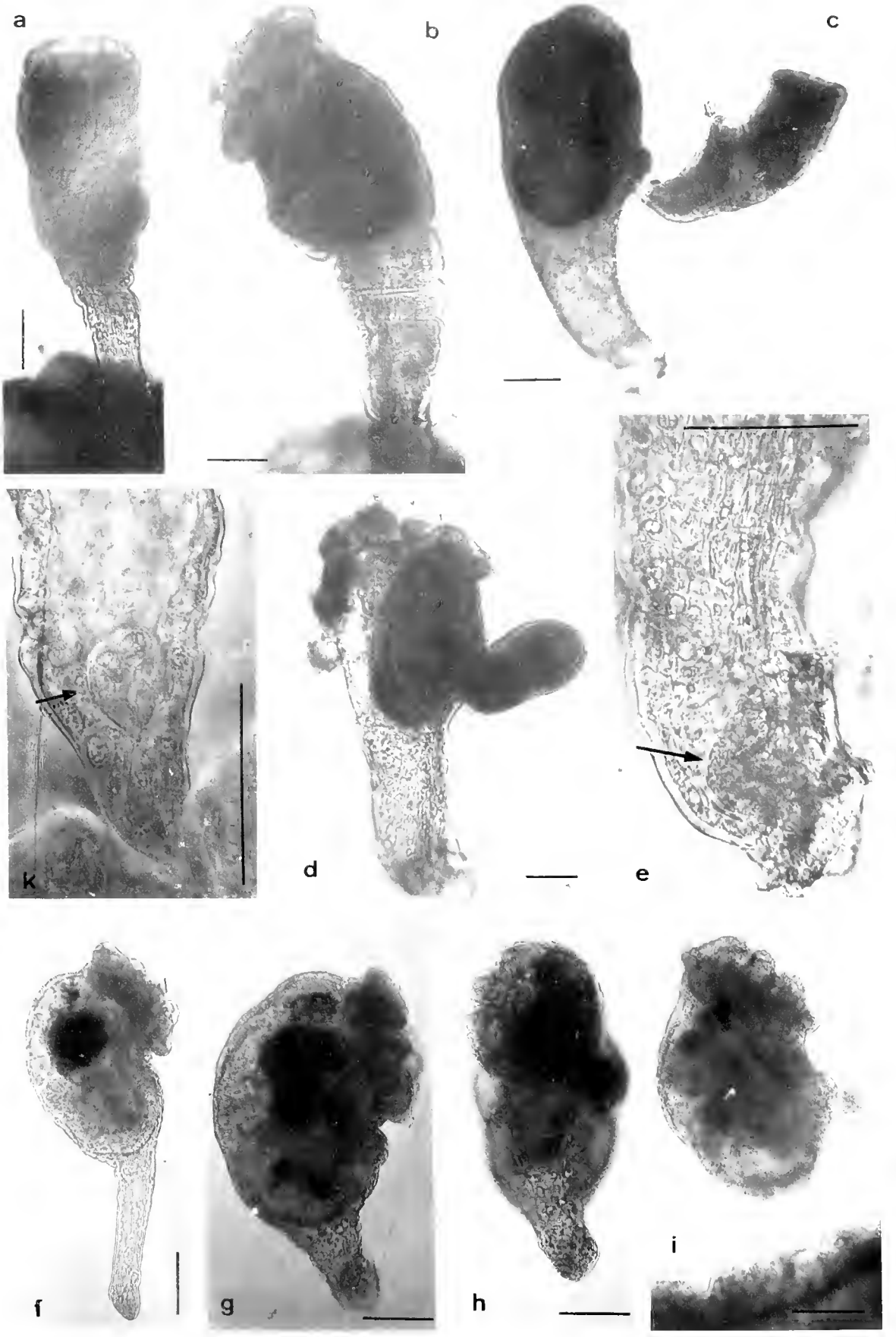
a
b
c
k
d
e
f
g
h
i

collar-like peritentacular membrane; all normally have more than 8 tentacles, except *L. varians;* and the buds of only the latter have a small, partly reduced foot-gland. *L. seiryoini* and *L. varians* on the other hand differ in the shape of the extended adult foot plate, which is bordered by conspicuously large cells in *L. varians,* but which are lacking in *L. seiryoini.* Furthermore, the helically arranged muscle strands in the basal portion of the peduncle of the latter seem to be absent in *L. varians.* So at present, *Loxosomella seiryoini* may be regarded as a new species.

Loxosomella tonsoria *spec. nov.*

Holotype. Specimens were collected by Dr. U. Wirth on 8 January 1990 at the type locality, station 66/90 Meteor XI-4 (64°30'S; 64°45'W) at a depth of 320 m from a stony and muddy bottom, growing in small numbers (10 specimens) dorsally on the anterior segments and gills of an ampharetid polychaete (*cf. Glyphanostomum spec.,* Fig. 7a, b).

Name. From Latin: tonsorius-shaver, because of the gibbous appearance of the calyx, which in lateral profile resembles an old Norelco® electric shaver (*e.g.,* Fig. 5f).

Description. A medium-sized species, 600–800 μm in length, with a characteristic gibbous calyx, a short and thin peduncle of about 0.5–0.7 times the calyx length. The comparatively large tentacular crown with 8 short and stout tentacles faces towards the oral side (Figs. 5f–i; 7c–f).

The calyx is slightly laterally depressed (width/thickness ratio 0.8). Below the stomach, the calyx constricts abruptly into the thin peduncle, which tapers somewhat towards its base and terminates in a small attachment area. The latter consists of a small epithelial invagination representing a remnant of the genuine foot-gland (Figs. 5k; 7h, i). The animals are not fixed very firmly to their substratum and can be easily removed without damage; they fall off easily after fixation. The stomach is almost globular, and as a result of the humpbacked calyx, the rectum is an unusually long tube.

The longitudinal musculature consists of only a few muscle strands: frontally and at either side 2 to 3 fibers each run from the calyx wall down to the base of the peduncle. Buds develop orolaterally in line with the upper half of the stomach. Only two of the specimens had developed very young buds, however, since these did not show any trace of a foot-gland, nothing is known of its structure.

Mature gonads (Fig. 7g, f) were present in all specimens; the majority contained ovaries with 3–4 eggs in different maturation stages. In one single case, testes filled with sperms were observed and in another specimen, the remnants of degenerating testes were visible below the ovaries. This indicates a protandric hermaphroditism also in this species.

Measurements. Total length: 600 μm (366–795 μm); length of calyx: 370 μm (223–461 μm); length of peduncle: 197 μm (95–350); width of calyx: 200 μm (111–240 μm); thickness of calyx: 243 μm (223–254 μm); diameter of peduncle: 95 μm (above) to 64 μm (below); number of tentacles: 8.

Habitat and distribution. Only 10 specimens of this loxosomatid were found on the gills and the dorsal side of the first segments of an ampharetid polychaete from silty and rocky bottom, west of Anvers Island at a depth of 320 m.

Discussion of the species. Since a small foot-gland is present even in adult specimens (Figs. 5k; 7h, i)—a remnant of a presumably larger gland in the buds—the above specimens belong to the genus *Loxosomella.* The rudimentary attachment gland seems to remain active throughout life. Any conspicuous circular muscle fibers in the peduncle base, which would indicate a sucker-like function of the basal glandular pit, as is characteristic for the genus *Loxosoma,* are lacking. The body shape is quite distinctive: no other loxosomatid so far described has such a gibbous calyx with the expanded tentacular crown facing exactly towards the front. The species characterization is based on only a few individuals; additional examination of the foot-gland structure in older buds, as well as an investigation of the variation range of this species from more numerous samples is highly desirable. The data available at present suggest that the specimens described above constitute a new species.

While nothing is known so far about the distribution of the above new species beyond their type localities, the species described below seem to be distributed not only in the whole Atlantic sector of the Antarctic and subantarctic sea, but also in the arctic and subarctic region of the northern hemisphere.

Loxosomella antarctica *Franzén 1973*

Material. Collected by the author in the Weddell Sea at stations ANT VIII-5/16-396, 16-411, 16-421, and 16-434, growing on the brittle star *Ophiurolepis gelida* as well as on the aphroditid polychaete *Laetmonice producta* at stations 16-411 and 16-489. In the Bransfield Strait the species has been found by Dr. U. Wirth at the stations Met. XI-4/31-90, 39-90, and 64-90 growing on the same hosts with an apparent preference for *Ophiurolepis gelida.*

The original description of this species given by Franzén (1973) was based on preserved specimens from samples

Figure 5. *Loxosomella seiryoini* spec. nov. a–e: contracted preserved specimens in frontal view (a), and lateral view (b); c: specimen with large bud; d: contracted specimen with a small bud; e: stalk of the latter with basally visible remnants of the foot-gland (arrow); f–k: *Loxosomella tonsoria* spec. nov., preserved specimens in lateral and frontal view; i: with a small bud; k: stalk of i with basal remnant of the foot-gland (arrow) [bar 100 μm].

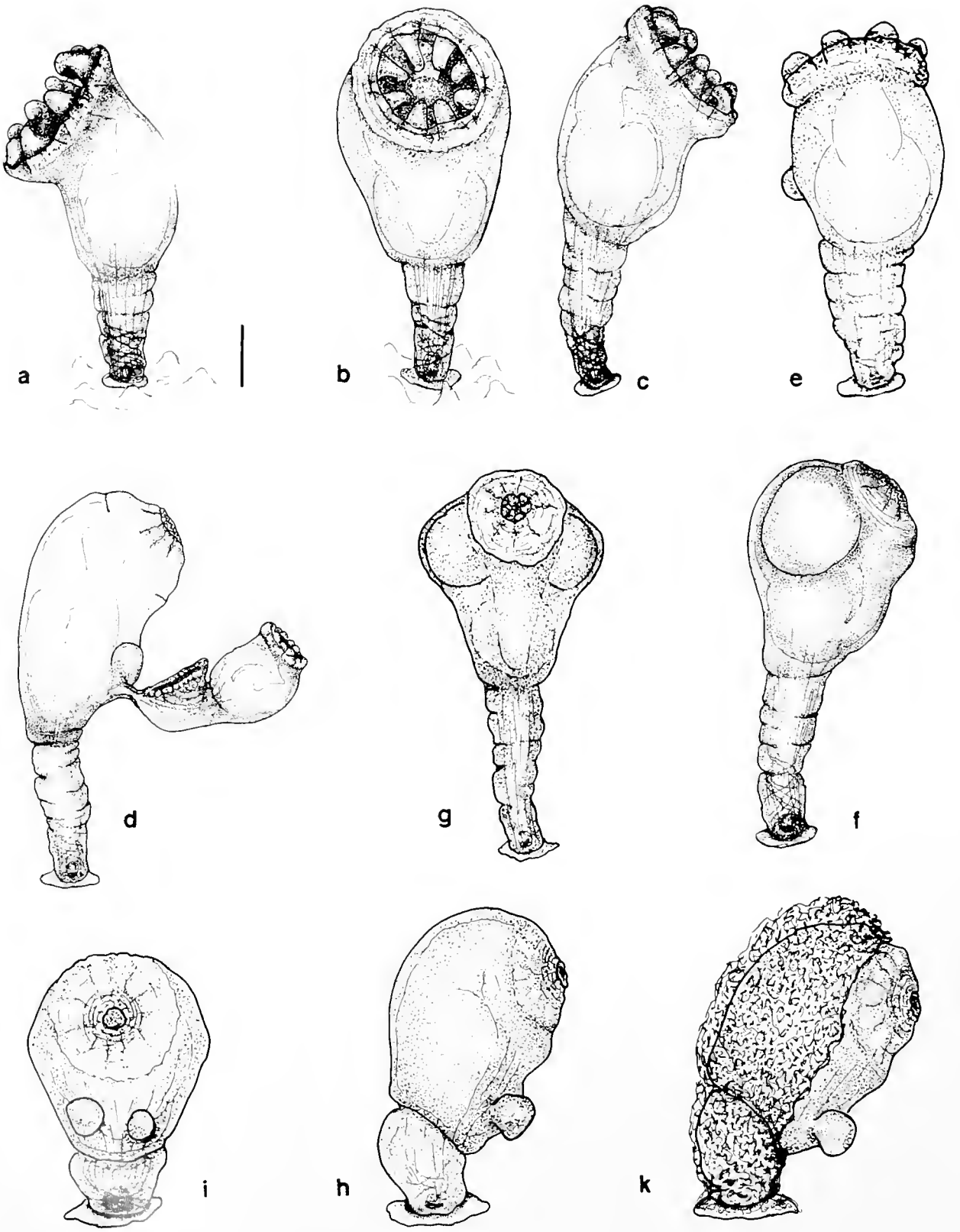

Figure 6. *Loxosomella seiryonini* spec. nov. a–g: different zooids from the rear end of *Golfingia margaritacea*. a: living specimen with the conspicuous peritentacular collar; b and c: preserved specimens; d: contracted specimen with large bud; e: specimen in semiexpanded state, in abfrontal view; f and g: specimens with larvae in their brood pouches in lateral and frontal view, respectively; h–k: different specimens from the introvert of the host. k with a robust "lorica" out of detritus particles covering the abfrontal part of calyx and stalk. In the foot plates of all specimens remnants of the foot-gland are visible.

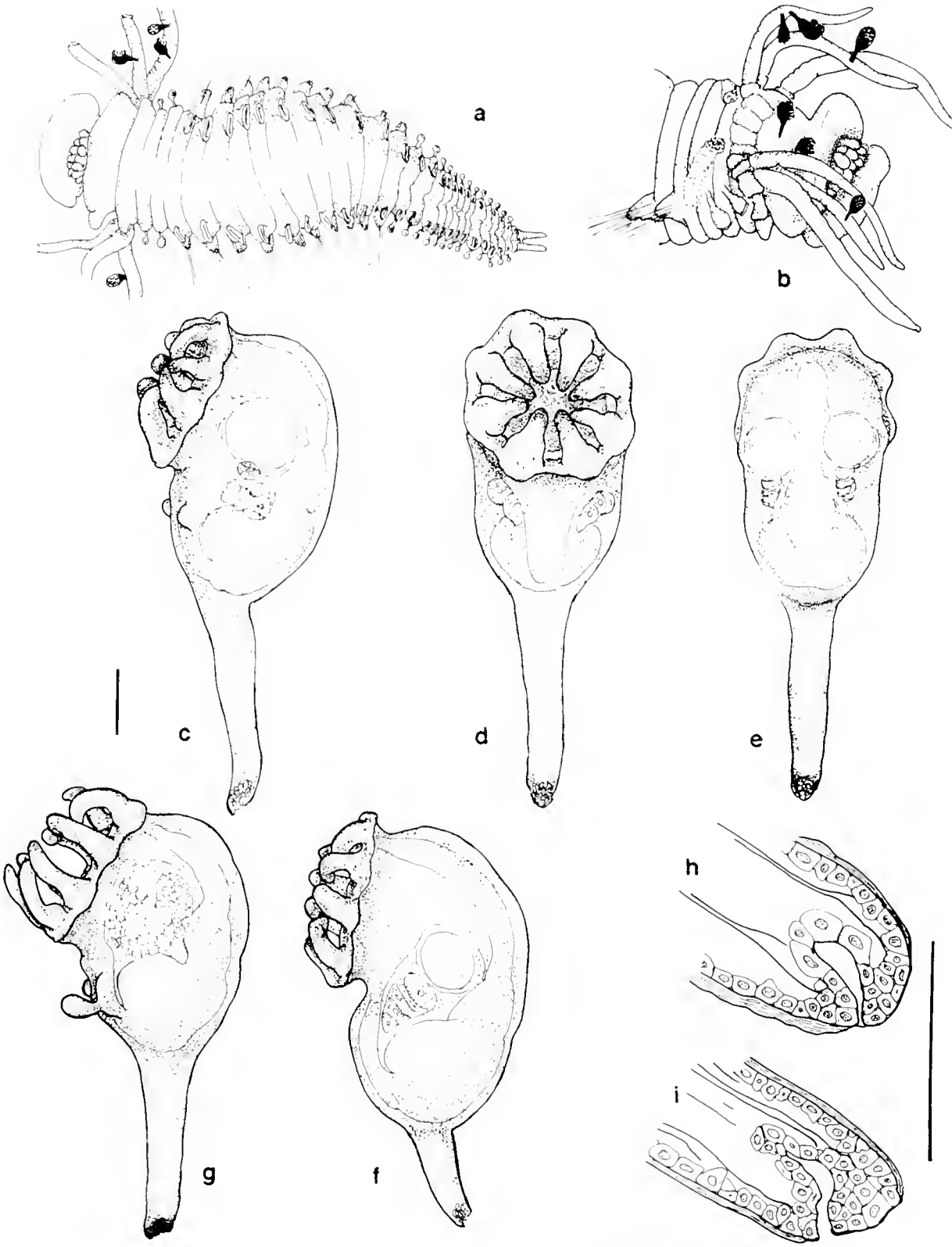

Figure 7. *Loxosomella tonsoria* spec. nov. a: host polychaete *Glyphanostomum spec.*; b: head region of the latter with loxosomatids settling on the cirri and the prostomium; c–e: preserved expanded specimen with mature ovaries, in lateral, frontal, and abfrontal view, respectively; f and g: preserved specimens in lateral view with mature ovary (f) and mature testes (g); h–i: basal tip of the stalk with remnants of the foot-gland.

of the 1902 Swedish Antarctic Expedition; these samples were dredged west of the northernmost tip of the Antarctic Peninsula. Franzén's description will be supplemented by my recent observations on living specimens.

Description. Loxosomella antarctica is a tall species, up to 2 mm in length, with a high goblet-shaped calyx, almost lyriform when seen from the oral side, and nearly circular in cross section. Only in a strongly contracted state is it at times somewhat flattened (Figs. 8a–f; 9a–g). In the expanded state, the large tentacular crown, generally with 12 slender tentacles (only 10 in newly detached buds), is inclined to the oral side at an angle of about 45°; when contracted it faces more or less orally. The peduncle of large budding specimens varies in length from ⅔ to 3 times the calyx length. Basally, below a conspicuous constriction, it terminates in an enlarged foot-plate.

The stomach is variable in shape, voluminous and globular to inversely triangular, but in contracted specimens, transversely oval. The cuticle is comparatively robust; in younger specimens it is smooth, but in older individuals, especially in the basal portion of their peduncle, broadly wrinkled. The body musculature is well developed. Longitudinal fibers run upwards from the peduncular base, fanning out into the calyx where, at either side of the esophagus and intestine, they insert into the frontal and aboral body walls. The muscular layer, compact at the oral side, thins out towards the aboral side into loose bundles of single fibers.

Depending on the nutritional conditions, 1–3 buds appear at either side (Fig. 9f), developing anterolaterally in line with the middle of the stomach. The glandular foot of the bud has a long posterior extension and only a knob-like frontal protuberance (Figs. 8e; 9h). This is one of the striking differences between this species and the similar-looking *Loxosomella antedonis* (Fig. 14e), which is difficult to distinguish from younger specimens of *L. antarctica*. But in the buds of the former, the foot is inversely T-shaped, extending to a conspicuous anterior as well as a posterior, process. Immature and mature gonads are present in most specimens—testes exclusively in buds and newly detached specimens, and ovaries only in older zooids.

So far the Weddell Sea and Bransfield Strait samples agree quite well with Franzén's description and illustrations. But the variability in the ecological conditions of the Weddell Sea, and, consequently, in the size and body shape of the Weddell Sea specimens, is much higher than in the type samples. While the average size of Weddell Sea specimens is about 1000 μm (600–1750 μm), the Bransfield Strait samples average 1500 μm (640–2100 μm), and both are smaller than Franzén's specimens. The calyx of the latter is, in most cases, distinctly marked off from the peduncle, but in some Weddell Sea populations it transforms gradually into the stalk. In these samples, the stalk usually tapers towards its base to about half of its original diameter (Figs. 9i–l; 10c, d), while in Franzén's samples, the stalk was cylindrical throughout its length. According to Franzén, *Loxosomella antarctica* lacks any lateral sensory papillae. But in two Weddell Sea populations (stat. 16-422 and 16-439), in a number of specimens growing on *Ophiurolepis gelida*, very small sensory papillae were present on either side of the calyx, in line with the second pair of oral tentacles (Figs. 9i–l; 10c, d). Usually these delicate "sensory spots" are only visible under higher microscopical magnification as pointed cuticular protrusions equipped with 1 to 3 stiff cilia (Fig. 10e, inset) that protrude from an intraepithelial cluster of sensory cells. I have never found such sensory organs in buds and young individuals. Most remarkable is the ability of *L. antarctica* to shed and regenerate a calyx (Figs. 11; 12)—a regenerative capacity unique to this species amongst loxosomatids.

Measurements. Weddell Sea specimens: Total length: 1000 μm (595–1750 μm); length of calyx: 400 μm (380–636 μm); length of peduncle: 680 μm (240–1130 μm); width of calyx: 315 μm (208–414 μm); thickness of calyx: 317 μm (178–477 μm); diameter of peduncle: 133 μm (85–180 μm); diameter of peduncle in specimens with tapering peduncle: above 155 μm (127–180 μm), basally 104 μm (87–135 μm); number of tentacles: 12 (10–12). *Bransfield Strait specimens:* Total length: 1524 μm (636–2142 μm); length of calyx: 490 μm (318–625 μm); length of peduncle: 1074 μm (318–1525 μm); width of calyx: 280 μm (143–357 μm); thickness of calyx: 290 μm (159–318 μm); diameter of peduncle: 133 μm (95–220 μm); number of tentacles: 12 (10–12).

Habitat and distribution. In the Weddell Sea, *L. antarctica* has been found repeatedly at depths ranging from 100 to 400 m, growing in moderate numbers on the oral disc and the arms of the brittle star *Ophiurolepis gelida* (Fig. 8a), and, occasionally, in small numbers, on the dorsalmost fine setae (Fig. 10a, b) of the polychaete *Laetmonice producta* (Aphroditidae).

In the Bransfield Strait, *Loxosomella antarctica* is the most common loxosomatid, and grows on the same hosts; but it exhibits a conspicuous preference for the brittle star. Usually the ventral body surface and the arms of this host, as well as the dorsal side of the disc, are occupied by crowded populations of the loxosomatid at a density of about 4–6 individuals per mm^2.

Beyond its Antarctic occurrence, the same species possibly has a second area of distribution in the Arctic Polar Sea. In the collections of the British Museum, a small sample of a loxosomatide (no. 31.7.3.1.70) was deposited which was collected from an *Epizoanthus arborescens* colony near Bear Island (Greenland). Although the preservation state of these specimens is not the best, and they are identified by Mortensen himself as *Loxosomella antedonis*, it is evident that they lack bilateral sensory papillae, one of the striking species characters of the latter species (*cf.* p. #). Therefore, these Arctic specimens may also belong to *Loxosomella antarctica* Franzén, 1973. Especially with respect to the bipolar distribution of a number of entoprocts, a critical review of museum samples, as well as some new investigations in arctic waters, would be desirable.

Discussion of the species and the possibility of hybridization. Specimens from different hosts usually did not differ significantly, but samples from the Weddell Sea and

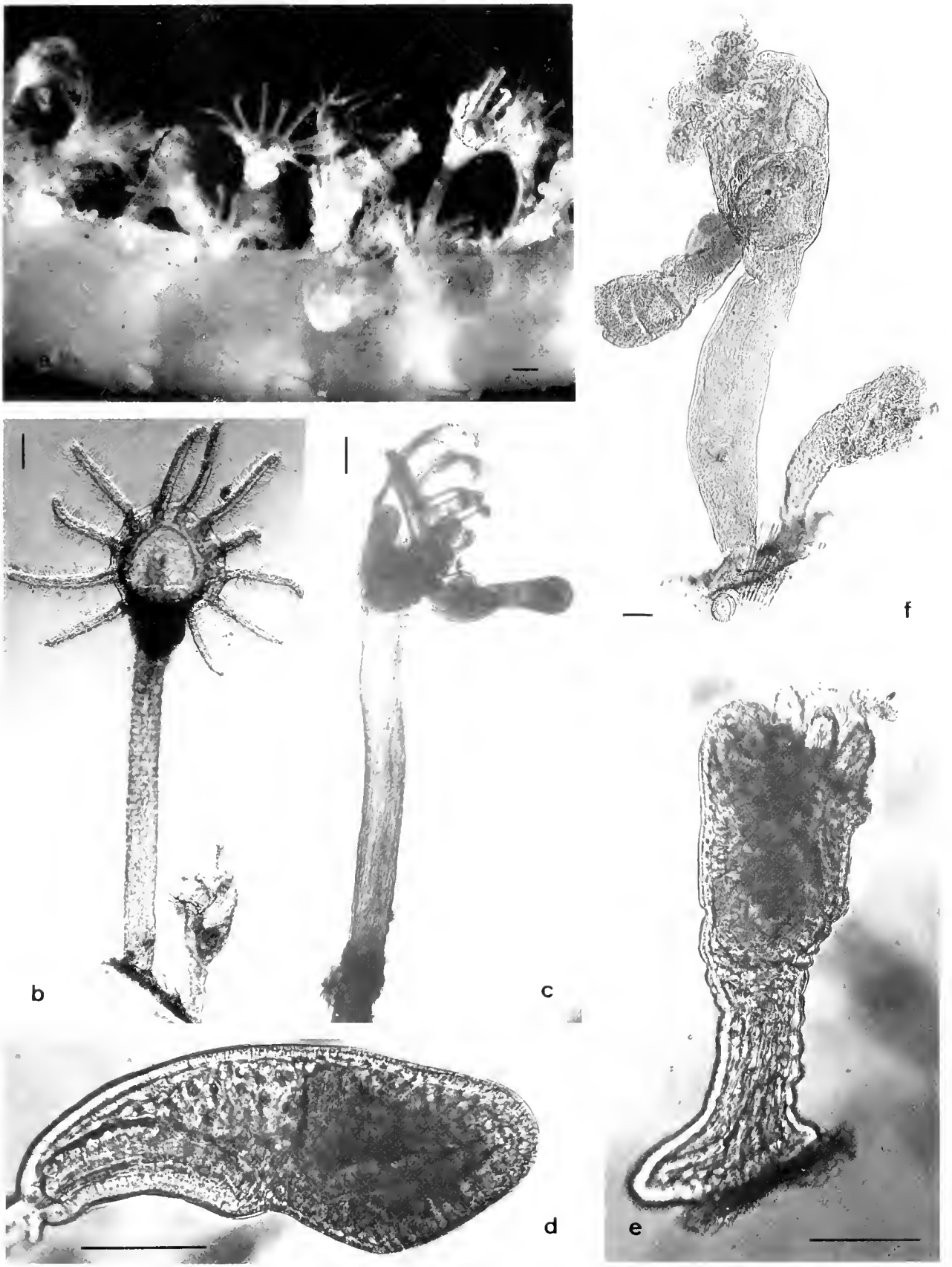

Figure 8. *Loxosomella antarctica* a: Zooids settling tightly on an *Ophiurolepis* arm (scale 1 mm); b and c: living specimens in frontal and lateral view, respectively; d and e: young bud and newly detached bud; f: specimen from Franzén's type sample (bar 100 μm).

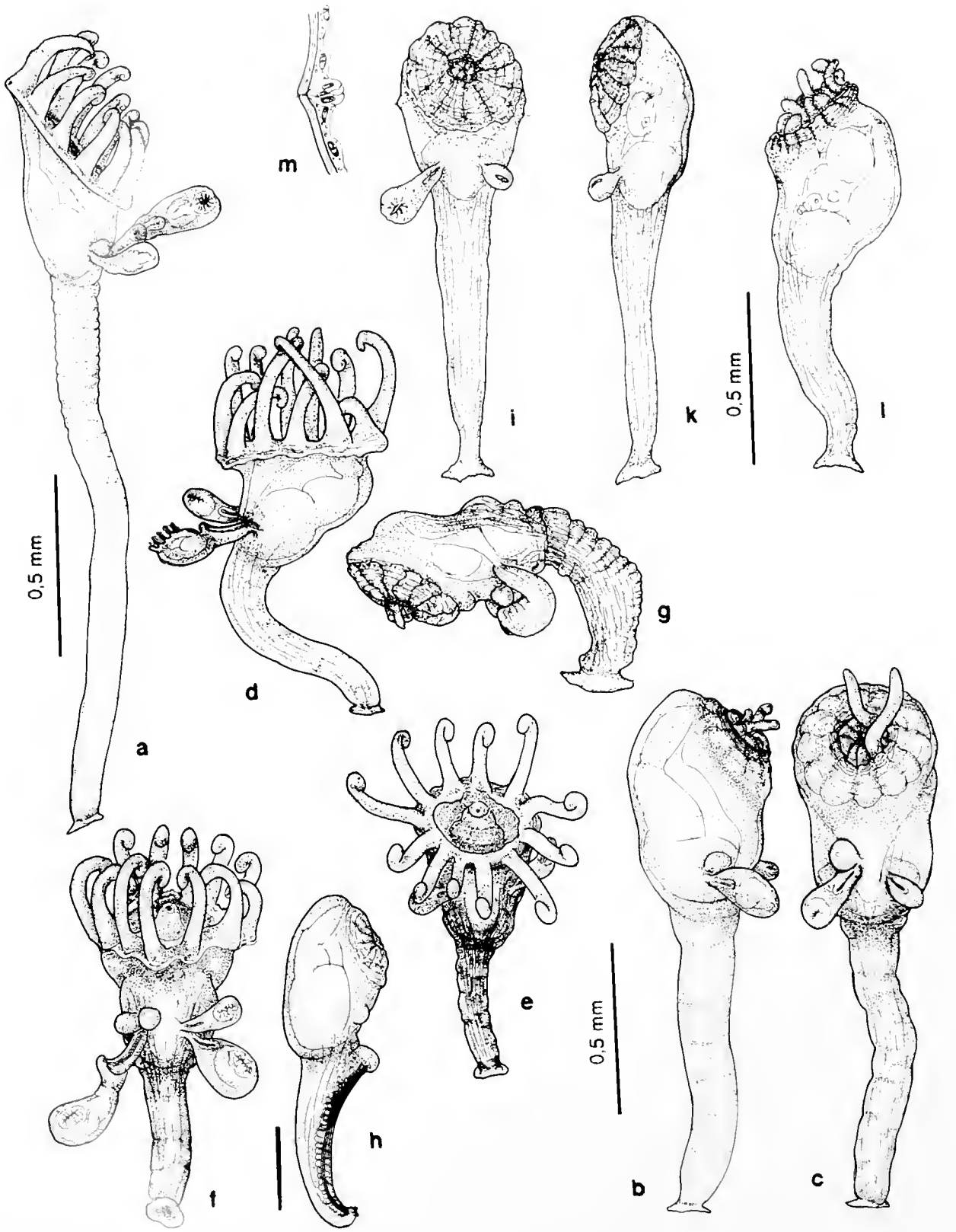

Figure 9. *Loxosomella antarctica*. a–c: expanded and contracted specimens from the Bransfield Strait; a: expanded specimen from *Ophiurolepis* (from life); b–c: preserved contracted specimens from *Laetmonice*; d–g: expanded and contracted specimens from the Weddell Sea (from life); d and e: from *Ophiurolepis*; f and g: from *Laetmonice*; h: newly detached bud; i–l: contracted Weddell Sea specimens from *Ophiurolepis* with tiny sensory spots (m) at either side.

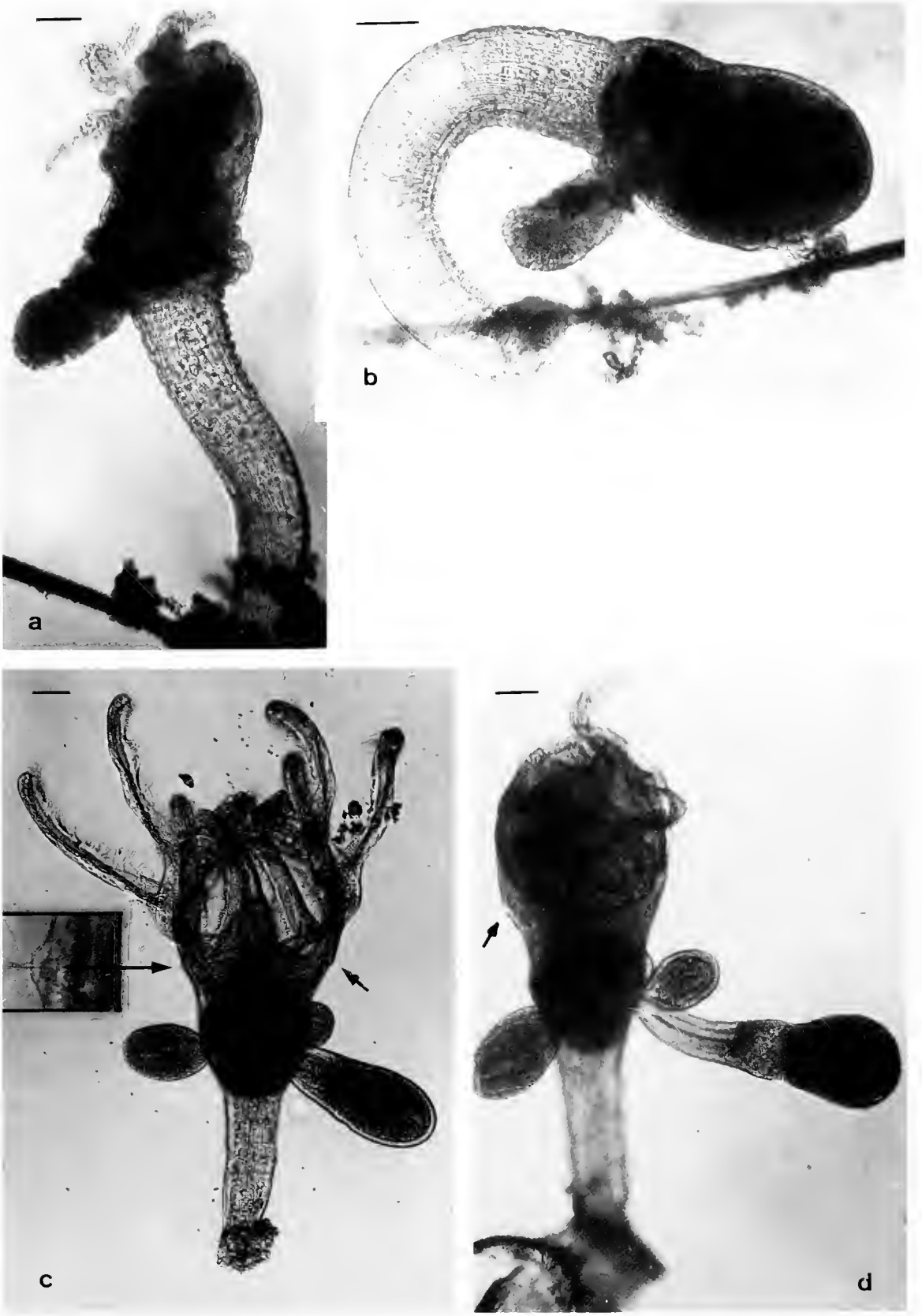

Figure 10. *Loxosomella antarctica.* a and b: Preserved Weddell Sea specimens from the setae of *Lactmonice products;* c and d: expanded and contracted Weddell Sea specimens from *Ophiurolepis gelida* with minute lateral sensory spots (arrows, inset) [bar 100 μm].

the Bransfield Strait differ markedly in their average sizes. This may result from the conspicuous differences in the nutritional conditions in these regions; primary production, predominantly consisting of diatoms, is much richer in the Bransfield Strait than in the Weddell Sea.

A discontinuous presence of lateral sensory spots, which was observed in some rare cases in Weddell Sea specimens of *L. antarctica*, has been reported likewise for *Loxosomella claviformis* and *L. phascolosomata* (Vogt, 1876); but the latter observations are not well established. Since all other characters of such Weddell Sea specimens with small lateral sensory papillae were within the normal range of variation of *L. antarctica*, and since such specimens were always found mixed with a majority of "normal" *antarctica*-zooids, they are considered to belong to the same species. Of course, such cases could also be produced by hybridization between *L. antarctica* and another species, such as *L. antedonis*, that is equipped with lateral sensory papillae.

At the one location in the Weddell Sea (stat. 16-369), where both of these species, *L. antarctica* and *L. antedonis*, occurred, they settled on different hosts and only in small numbers: *L. antarctica* on *Ophiurolepis* and *L. antedonis* on *Laetmonice*. Where *Loxosomella antarctica* occurred abundantly on both the ophiurid and (in smaller numbers) the polychaete, *L. antedonis* seemed to be generally absent. It was exactly under these conditions, amidst a majority of "normal" *Antarctica*-zooids, that zooids with tiny lateral sensory papillae were detected.

These findings are strongly suggestive of hybridization between these species, especially since, within the abundant *L. antarctica* populations of the Bransfield Strait where *L. antedonis* appeared to be generally lacking, no specimens with sensory papillae were detected. In fact, if hybridization between *Loxosomella antarctica* and *Loxosomella antedonis* is possible at all, then small disseminated populations of *L. antedonis* may well be absorbed by hybridization with the *antarctica* populations wherever the latter species is dominating. A sporadic appearanee of *antedonis* characters in such hybridized populations must be expected. Both species can maintain themselves unhybridized only in macrobiotopes where they live as small populations that are spatially separated, *e.g.*, on different hosts.

Regeneration. Loxosomella antarctica is the only solitary entoproet, for which the ability to regenerate a calyx has been demonstrated (Figs. 11; 12). Usually in Loxosomatidae the regenerative capacity is limited to the repair of single injured tentacles.

In abundantly growing populations of *Loxosomella antarctica* on *Ophiurolepis* from the Bransfield Strait, amidst great numbers of large active zooids, sporadic headless (no calyx) stalks were found. These stalks were still intact and were actively twisting and bending. At their headless apical end, they were sealed with a cuticular cap,

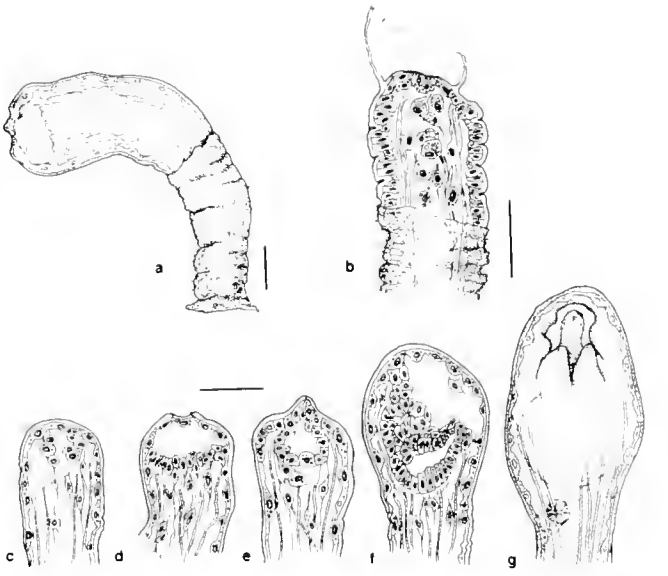

Figure 11. *Loxosomella antarctica* stages of calkyx regeneration. a: headless stalk in total view; b: apical region of a regenerating stalk with adhering remnants of the calyx cuticle; c–g: apical portions of several stalks in different regeneration stages: the beginning invagination and formation of the primary atrial vesicle (c, d), the initial gut formation (e), and differentiation of esophagus, stomach, intestine, and rectum (f), and (g) the atrial opening, newly broken through, and formation of the first oral tentacles (drawn after preserved samples).

and sometimes remnants of the cuticle of the shed calyx were still present. The basal portion of these peduncles is, in general, sharply delineated from the apical part by a different structure of the cuticle; basally, it is roughly wrinkled and coated by detritus particles, while apically it is thinner, smooth, and translucent (Figs. 11a, b; 12a, c). The same was observed in the stalks of many large active zooids—presumably an indication of successive growth periods.

Under the microscope, headless peduncles were observed in different stages of calyx regeneration. The earliest, least differentiated stages, have a thickened body wall epithelium throughout. At their distal ends they are contracted by the fibers of the well-developed longitudinal musculature, the remaining wound of the shed calyx being sealed off by a plug of epithelial cells and covered by a newly secreted cuticular cap (Figs. 11b–d; 12a, b). The innermost strands of the muscular layer are partly disintegrating, and the body cavity is filled with voluminous parenchyma cells containing many granules and vesicles, presumably storage proteins from phagocytized muscle cells. This picture resembles the muscular joints of barentsiid stalks when transforming into resting buds.

It can be inferred from the different stages observed that the subsequent regeneration of a calyx proceeds in the same way as in colonial entoproets (Figs. 11b–g; 12b, d, e): (1) A primary atrial vesicle is formed by an apical invagination of body wall cells. (2) Gut and atrial floor

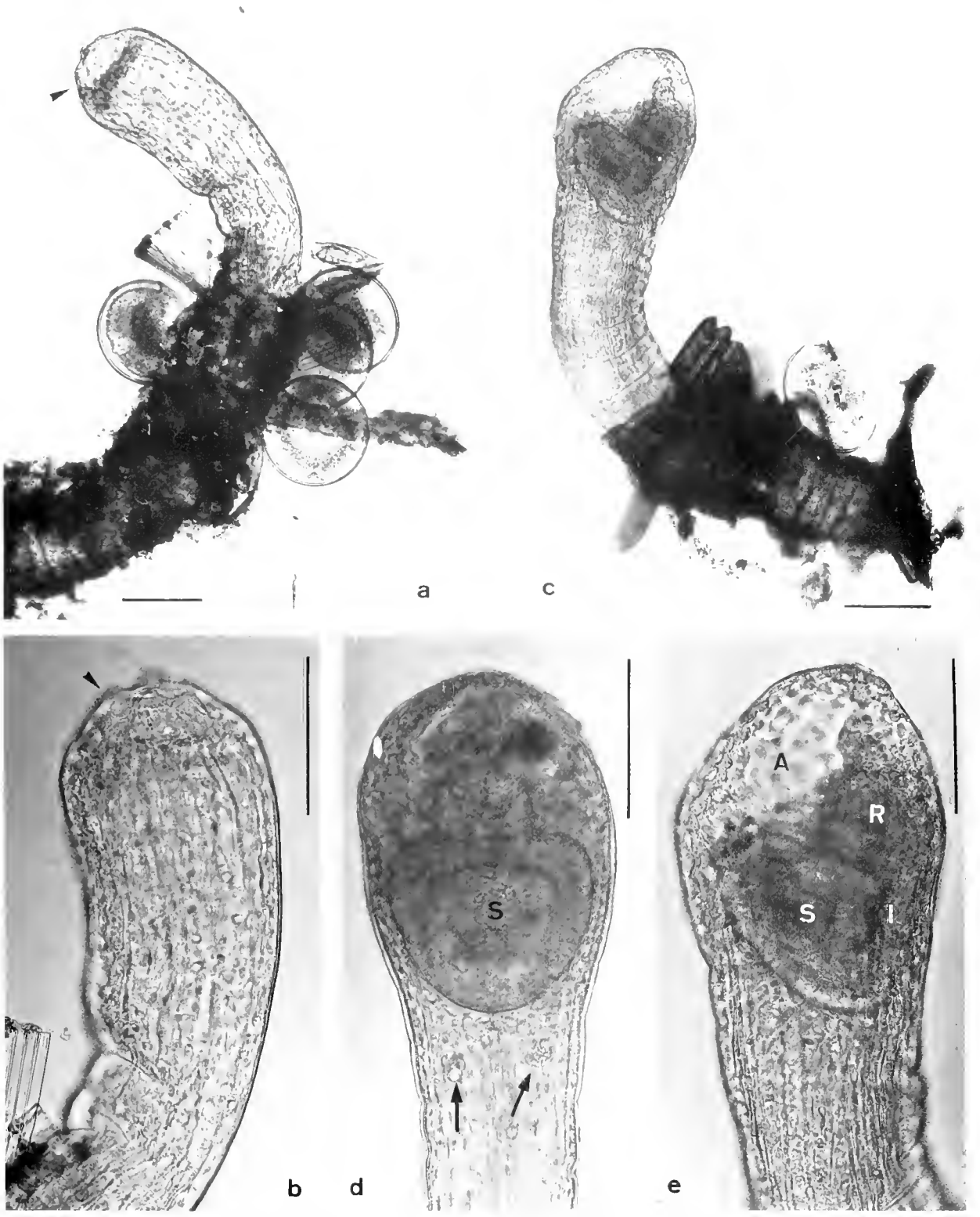

Figure 12. *Loxosomella antarctica*, calyx regenerating stalks; a and b: heavily cuticularized stalk with germinating tip; a primary atrial vesicle has formed (arrowhead); b–d: formation of the gut, the atrial opening not yet broken through; c and e: in lateral view; d: in frontal view; A - atrial cavity; I - intestine; R - "anlage" of the rectum; S - stomach; arrows - residual storage cells (bar 100 μm).

differentiate out of a basal cluster of the invaginated cells. (3) After the atrial opening has been broken through, the tentacles develop along the atrial rim beginning at the oral side.

The size of the headless peduncles, and their obviously successive stages of differentiation, preclude the possibility that they could merely be young metamorphosing specimens or old zooids in the course of degeneration. The former would be expected to be considerably smaller and in any case devoid of adhering apical cuticular remnants (Fig. 11b), whereas the atrium of the latter would never be completely closed (Figs. 11f; 12c–e).

Whether this calyx regeneration takes place as a consequence of external injury to the calyces, or is due to a periodic transformation of peduncles into resting buds under unfavorable environmental conditions, is presently indeterminable. All other loxosomatids examined in this respect under normal temperatures have an individual life span of hardly more than 6–10 weeks. During this time, depending on the nutritive supply, they continuously develop and release buds. Simultaneously, they pass through a short protandric male phase and a subsequent longer female phase. After having released about 10–20 larvae, the zooids degenerate. The larvae require at least about a week for metamorphosis.

The presence of apparently older basal portions and younger distal parts of the peduncles in larger zooids indicates a life span being extended over several growth periods. Such an increased ability to regenerate is obviously an adaptation to extremely short growth periods diminishing the chance of sexual reproduction. Under such circumstances an extension of the life span by an optional inactive resting phase is advantageous.

Loxosomella antedonis *Mortensen 1911*

Material. Collected by the author in the Weddell Sea at stations ANT VIII-5, 16-396 and 16-405 in depths of 300–400 m growing in moderate numbers on the dorsalmost fine setae of *Laetmonice producta* (Polychaeta, Aphroditidae).

The species was originally described by Mortensen (1911) from the northeast coast of Greenland, growing on the cirri of the feather star *Antedon prolixa*, and has been redescribed by Ryland and Austin (1960) from settlement panels off Swansea. I found it again in 1964, growing abundantly for a brief period on rocks and other solid substrates at the rocky shore around Helgoland. The species is very similar to young specimens of *Loxosomella antarctica*, but does not attain the length of the latter.

Description. The Antarctic specimens are 700 to maximally 1200 μm long, the slender, almost cylindrical peduncle being as long, or 1.5 times as long, as the calyx (Figs. 13a–d; 14a–e). The calyx, seen from the oral side, is inversely triangular in outline and slightly depressed in the oral-anal axis. In the expanded state, the calyx transforms gradually into the stalk. The large tentacular crown, with 12–16 tentacles, when expanded, is conspicuously inclined to the oral side. In the contracted state the calyx is racket-shaped, flattened, with the lophophore facing frontally. The stomach is oval to inversely triangular with somewhat projecting lateral lobes. The peduncle, which bears longitudinal musculature that is not as strongly developed as in *L. antarctica*, terminates in an enlarged adhesive disc.

As a striking character, this species possesses at either side of the calyx, just beneath the lophophore and level with the stomach roof, a prominent, non-retractile sensory papilla, about 20–30 μm long, with a tuft of stiff bristles (Figs. 13b–d; 14b–d). Buds develop orolaterally in line with the upper half of the stomach. In contrast to those of most other loxosomatids, they have a very distinct T-shaped foot with a long anterior and posterior process, the peduncle inserting in the middle (Fig. 14e). Sometimes several fine sensory bristles are visible at the anterior tip of the foot.

Measurements. Total length: 900 μm (690–1450 μm); length of calyx: 420 μm (336–548 μm); length of peduncle: 508 μm (361–651 μm); width of calyx: 265 μm (233–308 μm); thickness of calyx: 185 μm (169–189 μm); diameter of peduncle: 107 μm (93–117 μm); number of tentacles: 14–16; length of sensory papillae: 20–30 μm.

Habitat and distribution. In Antarctic waters, the species has been found only in the Weddell Sea, growing exclusively on *Laetmonice producta*. West of the Antarctic Peninsula it seems to be absent. The actual distribution of *Loxosomella antedonis* probably consists of the arctic and subarctic region, where it settles on various living as well as dead substrates, showing no host specificity.

Additional remarks to the species. The Weddell Sea specimens agree quite well with Mortensen's original description of *Loxosomella antedonis*, as well as with Ryland's and my own specimens from the Irish- and the North Sea. Though the original type specimens have been lost, the conspicuous lateral sensory organs, mentioned and figured by Mortensen, present a striking species character. A sample of specimens without such papillae, deposited in the British Museum (*cf.* p. #) and identified by the late Mortensen as *Loxosmella antedonis*, is definitely different from this species.

Loxosomella compressa *Nielsen and Ryland 1961*

Synonym. Loxosomella compressa var. *antarctica* Franzén, 1973.

Material. This species was abundant at depths from 100 to 400 m at almost all stations in the Weddell Sea, but was absent at depths greater than 500 m. In the Bransfield Strait it was found at one single location (Met. XI-4/39-90), at a depth of 160 m, generally growing on the dorsal setae of a great variety of polynoid polychaetes.

Loxosomella compressa, first described by Nielsen and Ryland from the Norwegian coast, growing on the notopodial setae of several polynoids, turned out to be the most common entoproct in the Weddell Sea. In this area, it apparently prefers the same hosts as in its northern area of distribution.

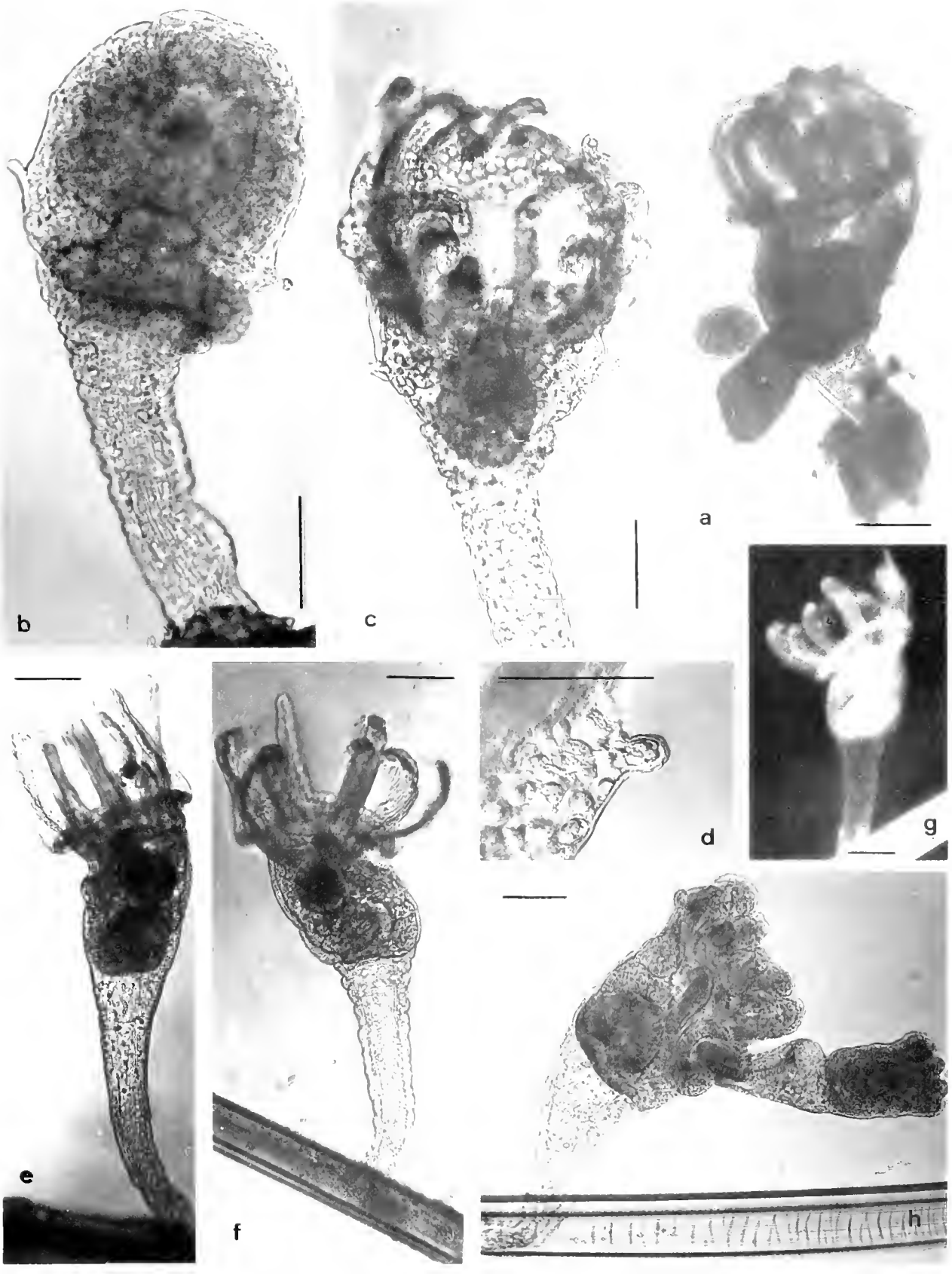

Figure 13. a–d: *Loxosomella antedonis* from the Weddell Sea. a: living expanded specimen; b–c: preserved specimens, the large sensory papillae (d) are conspicuously visible; e–h: *Loxosomella compressa*, preserved expanded specimens (e–f) and living specimen (g) in natural posture on polynoidan setae; h: preserved specimen with large bud (bar 100 μm).

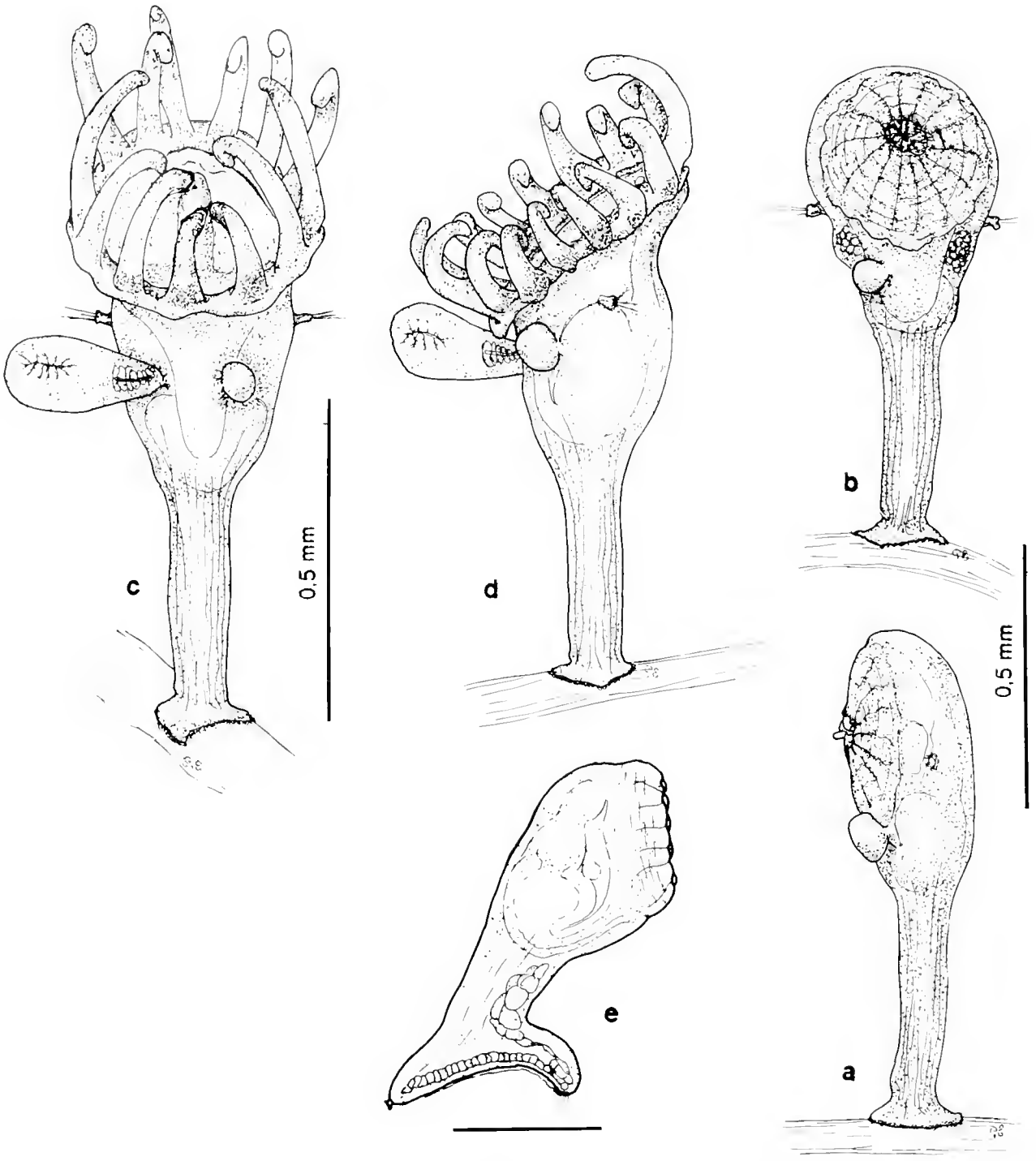

Figure 14. *Loxosomella antedonis* from the Weddell Sea. a–b: contracted specimens from the Weddell Sea (preserved material); c–d: expanded specimens from life, the large sensory papillae being conspicuous in all specimens; e: newly detached bud with its typical T-shaped foot.

Description. A medium size species, easily recognized by its peculiar laterally depressed calyx and by the formation of its buds almost medially, level with the stomach roof, and perched on a console-like protuberance of the oral calyx wall.

The total length of mature, budding Weddell Sea specimens varied between 500 and 750 μm. Seen from the side the calyx is goblet-shaped, with a kind of "paunch" below the budding zone (Figs. 13e–h; 15b–e). With no conspicuous demarcation, it transforms into the slender

stalk, which ends in a small attachment disc. Seen from the frontal side, the calyx is slim, and of the same diameter as the upper part of the peduncle which tapers downwards. The comparably large lophophore with 8 tentacles faces nearly straight up, both in the expanded and contracted state.

The stomach is large and globular. The buds, rarely more than one at either side, are normally oriented in an upright position, rather than hanging downwards (Figs. 13h; 15c). They have a very short stalk and a well-developed, posteriorly extended foot, with a glandular groove along its whole length (Fig. 15f). The latter is lined with large glandular cells. The main portion of the gland is situated just below the stomach. Gonads were observed in detached animals only. Smaller specimens contained both immature testes as well as young ovaries, while larger specimens exclusively contained mature ovaries and brood pouches with embryos and larvae in different developmental stages.

Measurements Total length: 640 μm (540–750 μm) (Nielsen: 500 μm, max. 700 μm; Franzén: 870 μm); length of calyx: 290 μm (240–348 μm) (Nielsen: 178 μm; Franzén: 457 μm); length of stalk: 360 μm (300–460 μm) (Nielsen: 267 μm; Franzén: 411 μm); width of calyx: 183 μm (180–190 μm) (Nielsen: 78 μm; Franzén: 195 μm); thickness of calyx: 215 μm (176–246 μm) (Nielsen: 120 μm; Franzén: 257 μm); diameter of peduncle: above 137 μm (101–168 μm), below: 60 μm (53–75 μm); number of tentacles: 8 (Nielsen: 8–9; Franzén: 8).

Habitat and distribution. Loxosomella compressa was found exclusively perched on the notopodial setae of a broad spectrum of Polynoidae (Fig. 15a). It was never found on other hosts, although about a thousand specimens of a great number of other polychaete species occurring in the same locations were searched for epizoans. Predominantly smaller polynoids (4–10 cm) are chosen as hosts, and species with short and thick notopodial setae covered by the elytrae are preferred; the loxosomellae are attached at the setal bases. On average, 2–4 individuals were found per parapodium, but at several locations offering exceptional nutritional conditions, up to 8 individuals per parapodium were counted. Under such conditions of extreme scarcity of unoccupied substrate, other polynoid species with dense bunches of thinner notopodial setae, or with dorsal setae not covered by the elytrae, *e.g., Hermadion ferox*, served as hosts for *Loxosomella compressa*.

In culture experiments aboard ship, *L. compressa* could be kept actively budding for about 3–4 weeks. In aquaria containing some polynoid hosts with their epizoans, newly detached buds were found to settle and become themselves actively budding on diverse solid substrates, such as stones and small settlement panels.

In the Weddell Sea, *Loxosomella compressa* is the most common entoproct occurring at depths from 100 and 500 m all along the Antarctic shelf from its northeastern edge to Kap Fiske, at the base of the Antarctic Peninsula. West of the peninsula, in contrast, this species seems to be rare, having been found there at only a single location north of Tower Island (stat. 39-90) and in very small numbers. Moreover, this species is also distributed in the Indic sector of the Antarctic Ocean. I detected it in several samples taken by Russian and Soviet Antarctic expeditions: in 1903 at the Alasheyev Bight, off today's Soviet station Molodeshnaya, in 1956 at the Budd Coast, in 1957 off the Lars Kristensen Coast, and in 1965 at the Tokarjev Island, growing on *Harmothoe molluscum* and *H. gourdoni*.

Franzén reports this species from the subantarctic region as occurring abundantly in samples taken in 1902 at the northernmost tip of the Antarctic Peninsula (Seymour Island), as well as from the Falkland Islands (Islas Malvinas), and from South Georgia where it reaches a size of 800–900 μm.

In the northern hemisphere, *Loxosomella compressa* is common in the whole arctic and subarctic regions, where it is reported to occur abundantly on several polynoids (*Lagisca extenuata, Gattyana cirrhosa, Acanthiolepis asperrima,* and *Harmothoe haliaeti*). It also occurs along the English and Norwegian coasts, in the Skagerrak and Kattegatt (Nielsen and Ryland, 1961; Nielsen, 1964a-b; Eggleston, 1965, 1969; Eggleston and Bull, 1966; Jones, 1963), as well as all along the shelf to the Arctic Polar Sea, from the Barents to the Kara Sea, living on the polynoids *Harmothoe imbricata, Antinoella badia, A. sarsi* and *Eunoe hartmannae* (Emschermann, unpub.). In the entire mid-Atlantic, as well as in the Pacific, this species seems to be absent.

Loxosomella varians *Nielsen 1964*

Synonym. Loxosomella brachystipes Franzén 1973.

Material. Collected in the Weddell Sea by the author (stations ANT VIII-5, 16-396 and 16-454), at depths from 270 to 400 m on stony bottoms and in the Bransfield Strait by Dr. U. Wirth (stations Met.XI-4, stat. 8-90, 39-90, and 96-90) at depths from 100 to 150 m on muddy grounds, this species grew in moderate numbers on the gills (Fig. 17a) of *Aglaophamus foliosus* (Polychaeta, Nephthyidae). The species was originally described by Nielsen as common in the North as well as in the Baltic Sea living on the gills of several nephthyid polychaetes.

Description. The specimens from the Weddell Sea, as well as from the Bransfield Strait, are in good agreement with Nielsen's description: a small variable species of about 300–500 μm total length, with a bulgy goblet-shaped calyx on an almost short, sturdy peduncle, distinctly marked off from the calyx, and terminating in a more or less extended foot plate of variable form (Figs. 16; 17; 18a–h).

The calyx is laterally depressed; the comparatively large tentacular crown with its 8 slender tentacles faces upwards, slightly inclined to the oral side. The stomach is large and globular. Buds are formed at the oral side in two adjacent paramedial areas in line with the roof of the stomach. Under favorable conditions, they can build up a crowded

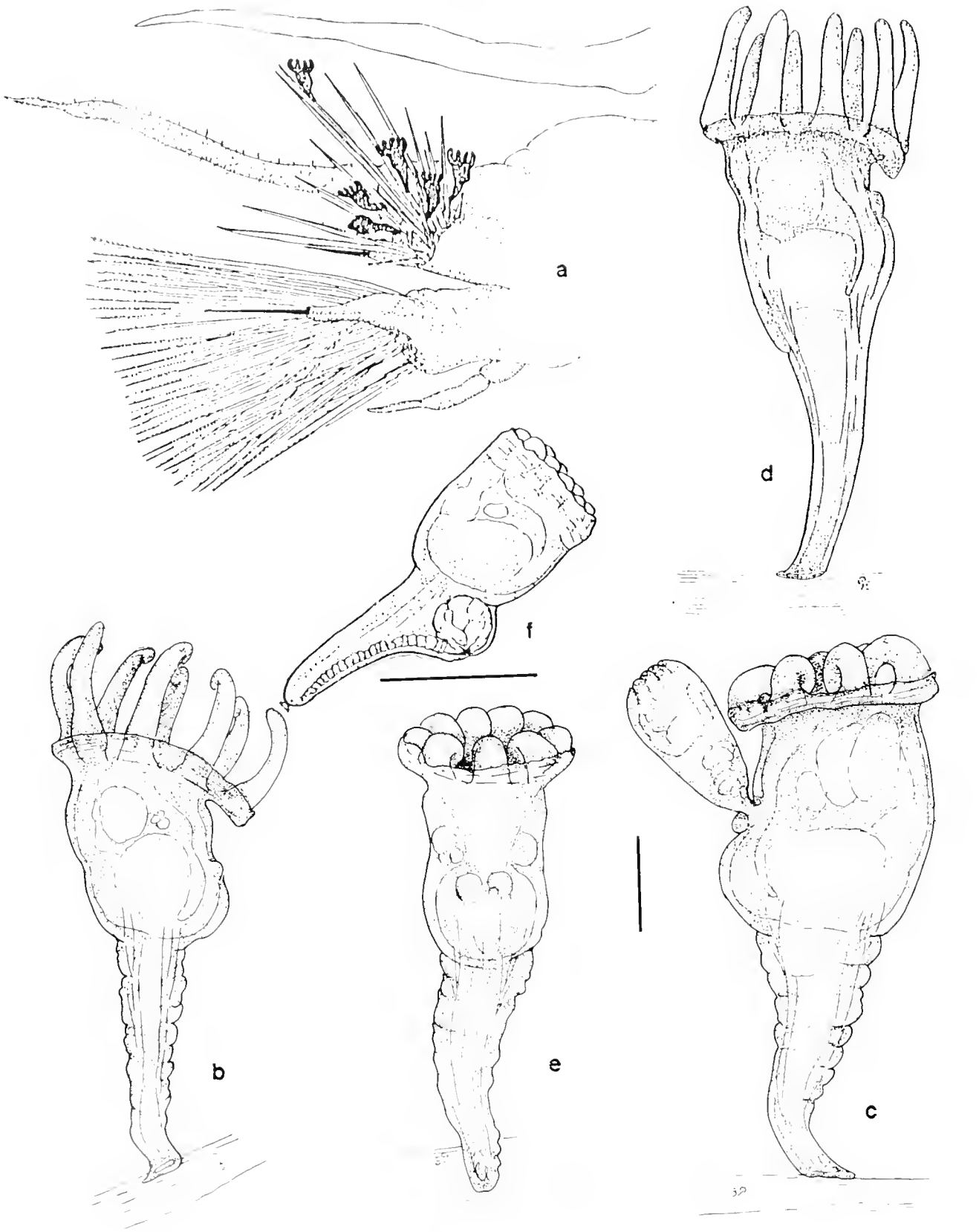

Figure 15. *Loxosomella compressa* a: polynoid parapodium with loxosomatid specimens on the notopodial setae; b–c: living expanded and contracted specimens in lateral and frontal view; d: preserved specimen in expanded state, seen from lateral; f: newly detached bud.

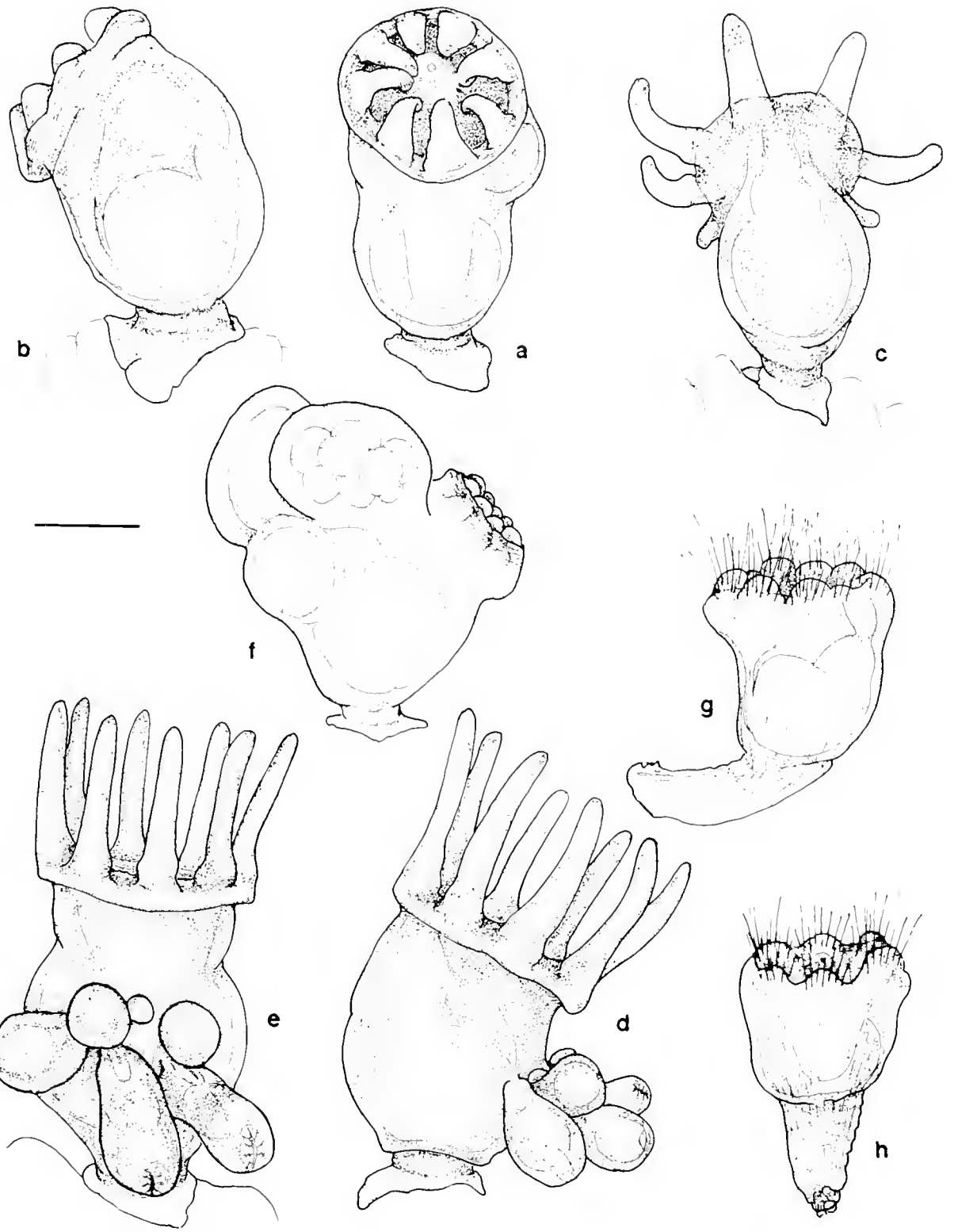

Figure 16. *Loxosomella varians*. a–c: two more or less expanded Weddell Sea specimens in frontal, lateral, and abfrontal view, respectively; d–e: specimen from the Bransfield Strait with a total of six buds in two paramedian clusters, in lateral and frontal view, respectively; f: preserved specimen with larvae in the brood pouches at either side; g–h: abnormal newly detached buds.

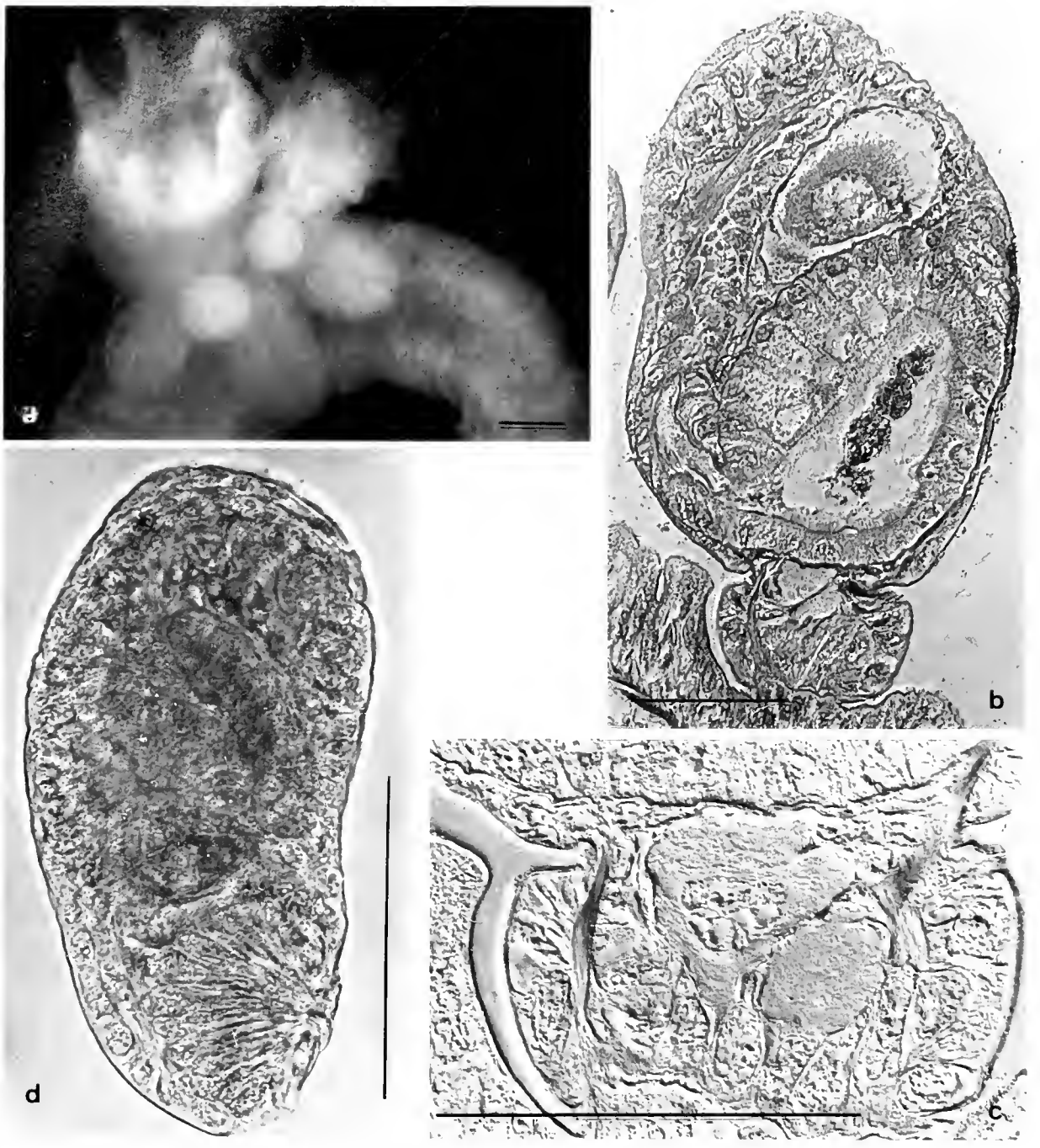

Figure 17. *Loxosomella varians* from the Weddell Sea, specimen with a cluster of 7 buds of different age on a parapodial cirrus of its host, *Aglaophamus foliosus*: b–c: Type specimen of *Loxosomella brachystipes* Franzén (c: foot of b enlarged); d: young bud from Franzén's type specimens with the clearly visible foot-gland (bar 100 μm).

cluster of eight and more buds which appear to originate from a single medial budding area (Figs. 16e, d; 17a).

The foot-gland in young buds forms a small groove; in older ones a slit-like invagination is bordered by densely arranged, elongated, club-shaped gland cells (Figs. 17d; 18i–m). In the adult foot plate, parts of the adhesive gland usually persist as a row of marginal large cells around the rim of the basal disc. Sometimes an additional plug of epithelial cells is formed in the middle of the foot (Fig. 18e, o–p).

Most specimens contained immature and mature ovaries, whereas testes were seen only in older undetached buds. In animals bearing larger embryos or larvae, the aboral calyx wall at either side, just below the tentacular

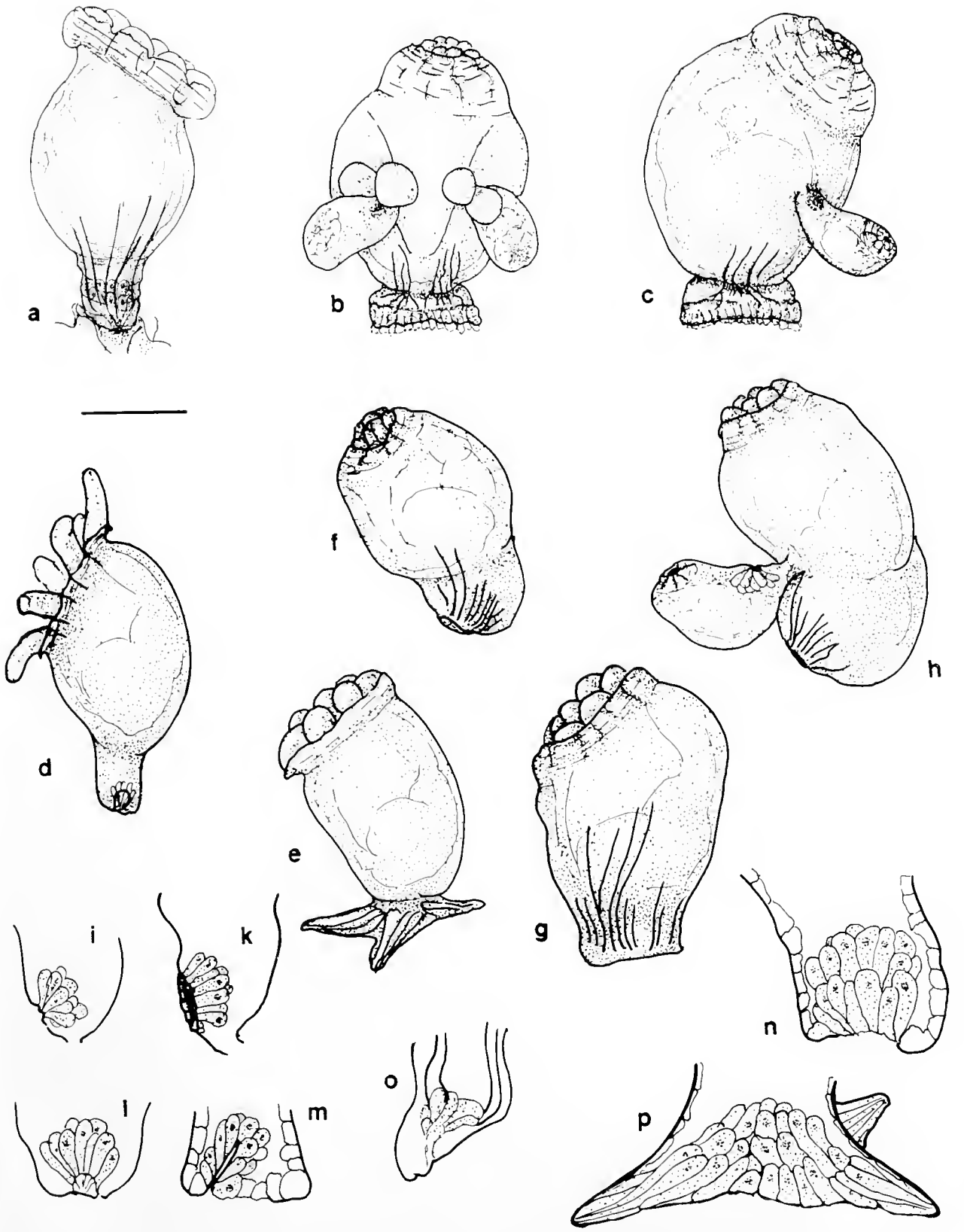

Figure 18. *Loxosomella varians.* Comparison of a Bransfield Strait specimen (a) with type specimens of *Loxosomella brachystipes* Franzén (b–c) and paratypes of *L. varians* Nielsen from the Kattegat (d–h); i–n: shape of the foot-gland in buds (i from Franzén's, k from Nielsen's samples) and in newly detached specimens (l–n); o–p: adhesive plates in adult specimens from Nielsen's paratype material.

crown, bulged out due to the enlarged brood pouches, like a clumsy rucksack almost equal in size to the entire normal calyx (Fig. 16f).

Measurements. Total length: 370 μm (300–485 μm) (Nielsen 392 μm; Franzén: 426 μm); Length of calyx: 305 μm (175–325 μm) (Nielsen: 285 μm; Franzén: 375 μm); length of stalk: 65 μm (32–111 μm) (Nielsen: 107 μm; Franzen: 51 μm); width of calyx: 223 μm (191–254 μm) (Nielsen: 200 μm; Franzén: 292 μm); thickness of calyx: 290 μm (175–461 μm) (Nielsen: 205 μm; Franzén: 332 μm); number of tentacles: 8 (Nielsen: 8, Franzén: 8); maximal number of buds: 8 (Nielsen: 15).

Additional remarks on the variability of this species. Although highly variable, especially with respect to the length of the stalk and shape of the foot plate, the species is well-defined by its general body shape, the crowded buds, and the paramedial budding areas, as well as by the small groove-like foot-gland in the buds.

In 1973, Franzén described a new loxosomatid found in small numbers on the gills of *Aglaophamus virginis* (Polychaeta, Nephthyidae), from old samples collected northeast of South Georgia during the 1902 Swedish Antarctic expedition; he named it *Loxosomella brachystipes* (Figs. 17b, c; 18b, c). This species, in most instances, looks like *Loxosomella varians*, but according to Franzén, the shape of the foot is markedly different in these two forms. However, judging from the present samples, both of these forms must be considered identical, because they cover the whole range from *L. varians*- to *L. brachystipes*- type specimens. So, in agreement with Franzén, they must be considered synonymous (see Fig. 18 regarding the variability of this species).

Habitat and distribution. Loxosomella varians has been found living on the gills of a broad spectrum of nephtydid polychaetes, never on hosts belonging to other polychaete families. In the Atlantic sector of the subantarctic and Antarctic Sea, this species is widespread from South Georgia, south to the eastern Weddell Sea, and along the western coast of the Antarctic Peninsula. In the northern hemisphere, *Loxosomella varians* is reportedly common in the North and Baltic Seas, but it seems to be absent from the midatlantic region and the Pacific Ocean.

Barentsia discreta *(Busk 1886)*

Synonyms Ascopodaria discreta Busk, 1886; Kluge, 1946; Thornely, 1905; *Ascopodaria macropus* Ehlers, 1890; Robertson, 1900; *Barentsia antarctica* Johnston and Angel, 1940; *Barentsia discreta* Annandale, 1915; O'Donoghue, 1920; Emschermann, 1985; Franzén, 1973; Harmer, 1915; Hutchins, 1945; Johnston and Angel 1940; Kirkpatrick 1888; Konno 1971; Marcus, 1922, 1937, 1953; Maturo, 1957; Mukai and Makioka, 1980; Okada and Mawatari, 1938; Osburn, 1912, 1914, 1932, 1944, 1953; Rogick, 1956; Toriumi, 1949, 1951; Vigeland, 1937/38; Waters, 1904; *Barentsia gracilis* Norman, 1907/10; *Barentsia intermedia* Johnston and Angel, 1940; *Barentsia musakiensis* Oka, 1895; *Barentsia timida* Verrill, 1900.

Material. In the Weddell Sea, small colonies were found on diverse solid substrates from three locations (ANT VIII-5/16-396 and 16-456, and additionally in older samples collected at 76° 36,0'S; 30° 33,3'W). In the Bransfield Strait, samples were found at all stations, except 66-90, in a depth range of 80 to 400 m.

Description. Living colonies of *Barentsia discreta* (Fig. 19) can immediately be recognized macroscopically by the vivid bending and twisting movements of the tall, 4–6 mm-long zooids arising from large, cylindrical, and delicately annulated basal sockets. The slender and predominantly rigid stalk bears a broad, cup-shaped calyx with the circle of 20–24 long tentacles facing straight up. The rigid part of the stalk, depending on the growth conditions, may be the same diameter over its entire length, or may widen slightly distally. Its smooth, yellowish to brownish cuticle is usually perforated by more or less numerous, minute, pore-like openings of subcuticular epithelial organs; the latter are presumably ion regulating cells homologous to protonephridia (Emschermann, 1972, 1982). As is normal for Barentsiidae, the rigid portion of the stalk distally, just below the calyx, turns into a short muscular segment with a wrinkled flexible cuticle. This distal

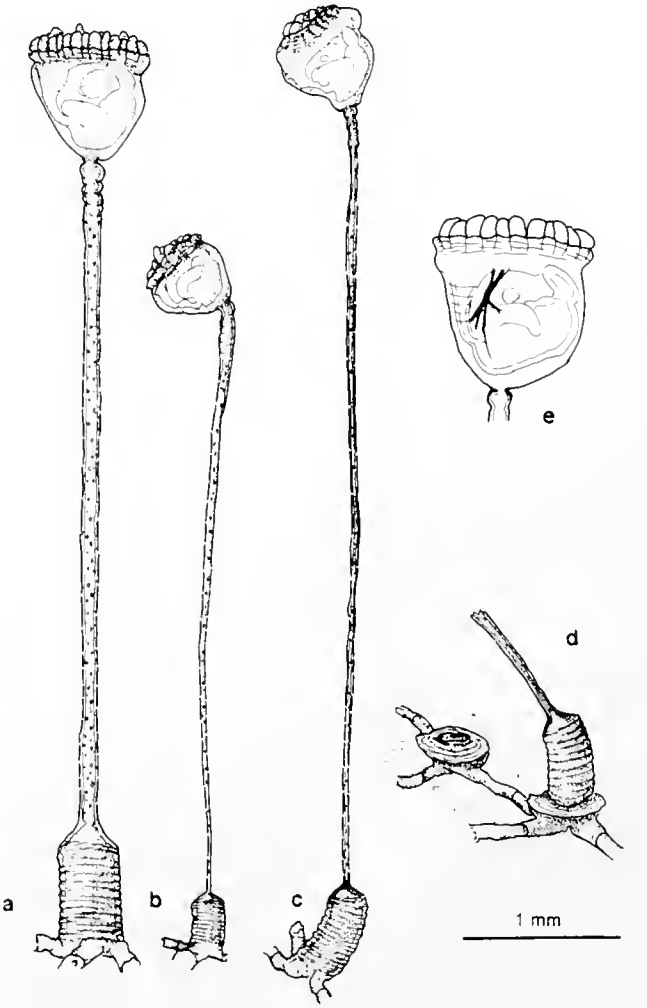

Figure 19. *Barentsia discreta.* a–c: three zooids from the Bransfield Strait (a) and the Weddell Sea (b, c); d: basal socket with a disc-shaped resting bud below it (part of a colony from the Bransfield Strait); e: calyx with the characteristic atrial retractor muscle indicated.

stalk segment has the capacity for calyx regeneration. Under favorable growth conditions, after degeneration of a calyx, and before its regeneration, the muscular section may give rise to a second stalk segment, consisting in turn of a proximal stiff and a distal muscular portion. The primary muscular swelling in such a case persists as an intercalating muscular joint, separated from the next segment by a cuticular hemiseptum. A stack of 8 to 10 star-shaped transverse muscle cells ("star cells" Emschermann, 1969) forms a sort of diaphragm between stalk and calyx.

In older well-fed colonies, a cup-shaped secondary inflation can develop below the bases of the zooid muscular sockets (Fig. 19d); the inflation is filled with storage cells and is separated by a diaphragm from the zooid base. These basal inflations function as resting buds, being resistant to mechanical damage, as well as temperatures up to 25°C, and even against being embedded in ice or drying for at least a week. They give rise to new zooids after the primary ones have been damaged or have died.

The structure of the calyx musculature, in particular the shape of the paired atrial retractor muscles, is a useful and reliable species character (Fig. 19e), as in most Barentsiidae (Emschermann, unpub.). In *Barentsia discreta*, three fine muscular strands on either side originate from the atrial floor just behind the mouth. Running downwards, in line with the roof of the stomach, they unite to form a short muscular ribbon. This in turn bifurcates again into an anterior and a posterior branch, each splitting into 2 to 5 fine single fibers, which insert in the lateral calyx walls at either side of esophagal entrance into the stomach. These atrial retractors can best be visualized in contracted calyces with polarized light or Nomarski interference contrast.

In the Antarctic samples, sexually mature zooids with both ovaries and, more rarely, testes were found.

Measurements. Total length of zooids: 4–6 mm; length of muscular base: 0.8–1.1 mm; diameter of muscular base: 0.3–0.44 mm; length of the distal muscular portion of the stalk: 180–330 μm; length of calyx: 580–700 μm; number of tentacles: 20–24.

Additional remarks about the species. Barentsia discreta has been found worldwide, the size of the zooids varying considerably, not only from location to location, but also under different nutritive conditions at the same locality. The cylindrical (but never barrel-shaped), annulated muscular base, the stalk-rigid over nearly its entire length with only a short muscular portion below the cup-shaped calyx, and the typical structure of the atrial retractor muscles are reliable, if only morphological, species characters. In colonies of different origin (California, Florida, and the Mediterranean Sea) cultured in the laboratory under the same conditions, no significant morphological differences between the specimens of different origin were found (Emschermann, unpub.). Their range of variation falls within that of the Antarctic material. Interbreeding between different populations can be observed in culture to the extent that the experimental populations are able to be active and become sexually mature under the same environmental conditions. In their physiological tolerance to environmental conditions, such as temperature, populations from different parts of the world can differ markedly. An Antarctic colony in my laboratory cultures did not remain active at temperatures above 4–5°C, but in an inactive state, it tolerated temperatures up to 15°C for several weeks. On the other hand, populations from temperate climates are able to tolerate low temperatures nearly to freezing, but they do not develop gonads under these conditions. To date, no long term attempts to gradually adapt colonies of different origin to lower or higher temperatures, have been carried out).

Therefore the genetic exchange between the Antarctic populations and others may be considerably reduced, but not interrupted. Their morphological conformity can be seen as an indication that they are not genetically isolated, and the populations of *Barentsia discreta* reported worldwide may be thought of as belonging to the same species (*cf.* Franzén, 1973, p. 185).

Habitat and distribution. In the Weddell Sea, especially in the eastern part, *Barentsia discreta* is found regularly, but never abundantly, at depths between 200 and 400 m. This species grows on every solid substrate, preferably on primary or secondary hard bottoms, basally on the stems of erect hydrozoan and bryozoan colonies, as well as on stones, shells, and even on brittle stars. But in the Bransfield Strait, the species occurred abundantly everywhere at depths from 80 to 500 m, presumably because of the more favorable nutrient conditions throughout the year in this region.

In general, this species is distributed worldwide, missing only from the Atlantic-subarctic European coasts. Furthermore, it is reported circumantarctically, along the shelves of Antarctica itself and the subantarctic islands (Busk, 1886; Franzén, 1973; Johnston and Angel, 1940; Rogick, 1956; Vigeland, 1937/38; Waters, 1904). Along the South and North American coasts, its distribution extends, on the Atlantic side, from Tierra del Fuego, along the Argentinian and Brazilian coasts (Marcus, 1937, 1953), the Caribbean Sea (Osburn, 1914, 1940; Emschermann, unpub.), and Florida (Nielsen, pers. comm.), up to the Massachusetts Bay in the north (Hutchins, 1945; Maturo, 1957; Osburn, 1912, 1932, 1944); on the Pacific side, it extends from southern Chile and along the coast of Central America (Osburn, 1953), to California (Robertson, 1900; Emschermann, 1985).

In the Atlantic region, and along the European coasts, the species is reported from the Bermuda Islands (Verrill, 1900; Maturo and Schopf, 1968), from Madeira (Norman, 1907/10; Emschermann, unpub.) and the Azores (Emschermann, unpub.), and from the Mediterranean Sea (Ehlers, 1890; Zirpolo, 1927; Emschermann, unpub.).

In the Indo-Pacific region, *Barentsia discreta* seems to be common everywhere, from South Africa (O'Donoghue, 1920), the Indian Ocean (Annandale, 1915; Harmer, 1899; Kirkpatrick, 1888; Thornely, 1905) and South-Pacific (Mareus, 1922), to the Chinese- and Japanese Sea (Konno, 1971; Oka, 1895; Okada and Mawatari, 1938; Toriumi, 1949, 1951; Yamada, 1956). Finally the species was reported by Kluge (1946) from the Laptev Sea (Siberian Polar Sea).

Some General Concluding Considerations

Besides representing merely a faunistical survey, four particular aspects of the above results are of special interest: (1) the detection of nematocyst-like organs in an entoproct; (2) the ability of a loxosomatid to regenerate its calyx; (3) some additional observations on the nature of host preference or host specificity of the Loxosomatidae; and (4) the bipolar occurance of several *Loxosomella* species.

(1) The detection of *extruding organs* in an entoproct raises questions about their comparative morphological importance and their phylogenetic significance. Comparable, usually unicellular, extrusive glandular organs, which produce clearly structured secretions, have been described in quite a number of invertebrate phyla, in addition to coelenterates: in Platyhelminthes (only in Turbellaria; Reisinger and Kelbertz, 1964; Smith *et al.*, 1982), Gastrotricha (Rieger *et al.*, 1974), Nemertini (Jennings and Gibson, 1969), Gnathostomulida (Rieger and Meinitz, 1977), and the Archiannelida among the annelids (Martin, 1978). Except in the Cnidaria, Ctenophora, and Turbellaria, these extrusion organs do not represent typical characters of the above animal taxa, but occur in isolation in one or another species. Only in Cnidaria and Ctenophora do the extrusive organs eject harpoonlike, poisonous or sticky threads. In all of the other above taxa the extrusive gland cells produce rod-like mucous secretions of the rhabdiite type. The probably syncytial plurinuclear extrusive capsules of *Loxosomella brochobola* seem, at present, to be unique in the animal kingdom and to differ remarkably, in development, structure, and extrusion mechanism, from comparable organs in other groups. Thus they must be considered as an isolated apomorphic character of this particular entoproctan species, rather than a character of phylogenetic significance. Probably they are derived, in a highly specialized form, from conspicuous uni- or pluricellular mucous glands of unknown function, which occur in a number of loxosomatids around the margin of the tentacular crown.

(2) The *ability to regenerate calyces* in *Loxosomella antarctica* is unusual for solitary entoprocts. Distinct from *Loxokalypus socialis* (Emschermann, 1972)—another entoproct species with an enhanced regenerative capacity, and in which the budding zone has shifted from the calyx wall down to the stalk as a first evolutionary step towards the colonial growth pattern–normal asexual budding in *Loxosomella antarctica* proceeds as usual in two paired budding areas on the oral wall of the calyx. Therefore, the enhanced regeneration capacity of the distalmost tip of the stalk epithelum in *L. antarctica* (Figs. 11; 12) is an isolated secondary adaptation to the conditions of Antarctic life. This is important to the biology of entoprocts, but is without phylogenetic significance.

(3) A marked *host specificity* is thought by several authors to be characteristic of, most of the epizoic Loxosomatidae. For example, Nielsen (1966) describes *Loxosoma davenporti* as normally settling inside the tubes of the maldanid polychaete *Clymenella zonalis*, but as completely absent from the tubes of the closely related *Clymenella torquata*, which is found much more frequently than *Clymenella zonalis* on the same sandy bottoms. Consequently, many authors consider the host a sufficient species character for the identification of loxosomatids. But the host can only be employed as a reliable species character if its relationship with the loxosomatid is specific; *i.e.*, determined by a strict physiological dependence. A shared preference of the host and its epizoan for the same microenvironment, or some structural feature of the host that offers the epizoan an ideal complex of life conditions (*e.g.*, a combination of mechanical shelter and a water current supplying food and oxygen and removing detritus) are situations in which host specificity is not a reliable species character. A majority of the guest-host relations in the loxosomatids seem to be of this latter type.

Only three of the loxosomatids discussed above are known to show a preference for specific hosts independent of the respective localities: *Loxosomella varians* for nephtyid polychaetes, *Loxosomella antarctica* for the brittle star *Ophiurolepis gelida*, and *Loxosomella compressa* for errant polychaetes of the family Polynoidae. The latter two loxosomatids were very abundant at many locations. *Loxosomella antarctica* is found predominantly on silty bottoms, on the oral disk between the arms of *Ophiurolepis gelida*, never on other ophiurids abundant in the same place. If nutrients are abundant, it also builds up crowded aggregations on the aboral side of its host and laterally along its arms. At adequate sites, where *Ophiurolepis* is lacking or very rare, *Loxosomella antarctica* does not switch to an other ophiurid, but rather to an aphroditid polychaete, *Laetmonice producta*. On this second host, it occupies exclusively the tips of the dorsalmost notopodial setae in the first segments as well as the posterior dozen body segments.

The large robust zooids of *Loxosomella antarctica* are quite resistant to mechanical lesions (*cf.* regeneration capacity), as well as low oxygen supply. As can be seen from their stomach contents, consisting mainly of detritus particles and some larger ciliates mixed with fine mineral material, they are sediment feeders. Their requirements

are for a nutrient-rich fine sediment and a solid settling substrate offering a certain protection against predators and against being buried irreversibly under sediments. So this species thrives on hosts like *Ophiurolepis* and *Laetmonice* which creep on, or dwell in, the upper sediment layer.

Loxosomella compressa on arctic and subarctic shelves as well as in antarctic waters was detected exclusively on polychaetes of the family Polynoidae, attached basally to the notopodial setae of their hosts. A more detailed analysis of the microhabitat of *L. compressa* reveals that the only polynoidan species infested by this epizoan guest are those with notopodial setae that are thick and short, not too densely arranged, and covered by the elytrae. This loxosomatid has only exceptionally been found on polynoids with bushy, thinner notopodial setae or with parapodia not covered by the elytrae. Usually only smaller species, up to 10 cm in length, or younger specimens of larger polynoids are chosen as hosts. In culture experiments, the newly detached buds also settled on diverse non-living substrates (*cf.* p. #) exposed to the current.

Loxosomella compressa is smaller and less resistant to mechanical injury and low oxygen supply than *L. antarctica*. As can be demonstrated by an examination of its stomach contents, its diet consists mainly of small algae; predominantly small pennate diatoms. Consequently, its delicate zooids can grow only in a microhabitat that offers shelter against predators as well as against mechanical injury, but which also exposes them to a continuous water current and provides enough space for optimal feeding positions. Such conditions are preferably offered by smaller polynoid polychaetes, not dwelling in the sediment, but creeping on the exposed surface of sponges and on erect bryozoan and hydroid colonies. Other habitats, offering comparable physical conditions, may also be chosen as a substrate by *L. antarctica* and *L. compressa*. But the small loxosomatids are not easily detected amidst the bulk of possible substrates in dredged material; presumably they are usually overlooked during sorting. But when the hosts were kept for a while in well aerated aquaria, the loxosomatids were also found on various other non-living substrates.

From these observations, one can speculate that the choice of settling substrate, at least for these loxosomatid species, is determined by the physical structure of the microhabitat and the supply of an appropriate diet, rather than by specific physiological properties of the host itself. Thus, although most loxosomatids have preferred hosts, these can only be regarded as weak species characters.

(4) The observed *bipolar occurrence* of *Loxosomella antedonis*, *L. compressa*, and *L. varians* in coastal waters suggests, at first glance, a discontinuous, exclusively *bipolar distribution* of these species. Their northern distribution in the litoral and sublitoral of the continental coasts stretches from Greenland (*L. antedonis*) and the Eurasian polar shelf (*L. compressa* and *L. varians*), along the northern European coasts, south to about 54°N in the southeastern North Sea. In the South Atlantic and the Atlantic sector of the Antarctic Ocean, these three species are common from the Weddell Sea, and north to the Islas Malvinas and South Georgia (about 54°S). To date, none of them has been found along the eastern or western mid-Atlantic coasts, although the entoproctan fauna of the Central European shelf, in particular, as well as of the Caribbean, Argentinean and Chilean coasts have been well investigated. At present, however, nothing is known about the depth range of these species and their possible distribution along the Atlantic deep sea ridges.

Comparable examples of a suggested bipolar distribution of a single species are extremely rare and still controversial, the best known being the bipolar occurrence of *Priapulus caudatus* (Ekman, 1935; van der Land, 1970). A discontinuous distribution of taxa above the species level can be explained by the break-up of an originally continuous area of distribution by geomorphic events, such as continental drift, and long term climatic changes. At the species level, on the other hand, it seems unlikely that populations separated over geological periods could remain uniform in their specific characters unless at least a limited amount of genetic exchange were maintained between them.

But how can such an exchange take place in the present case? Under the conditions of an exclusively bipolar distribution, such a genetic exchange between the North and South Atlantic populations of the above loxosomatids must be excluded, because the life span of individual loxosomatid zooids does not exceed 4–6 weeks, and the mobile larval phase lasts scarcely more than 8 days.

Neither passive drifting with currents, nor transport by fast swimming hypothetical hosts such as whales could proceed quickly enough to maintain a sufficient exchange between populations of the North and South Atlantic. Nor can the considerable increase of the shipping traffic in the past decades be responsible for this distribution. One might postulate that the Antarctic faunal region had been colonized only recently by these species. But at least for *Loxosomalle compressa* and *L. varians*, their distributions in both the Arctic and Antarctic regions were already established in the 19th century, as documented by the evaluation of several samples from the turn of the century (Franzén 1973; this paper).

Thus a recent *continuous distribution* by colonization along the Atlantic ridges, and possibly the deep sea basins, must be postulated as being responsible for the *bipolar occurrence* of these loxosomatids in shallow coastal waters. More deep sea samples should be obtained and evaluated so that this hypothesis can be tested.

As far as can be judged to date, the three loxosomatid species mentioned above are distributed in the Atlantic sector of the Antarctic Sea only, and they seem to be ab-

sent from the Pacific sector. The faunal connection between the North and South Atlantic must, therefore, be much more intense than the circum-Antarctic faunal migrations.

Acknowledgments

I thank Dr. Claus Nielsen (Kobenhavn) and Professor Åke Franzén (Stockholm) for their helpful critical remarks regarding my species determinations and the newly described species as well as for having placed at my disposal their type specimens and comparison samples. Also, I wish to thank Dr. E. Androsova (Leningrad) for giving me the chance to check the entoproctan samples from Soviet Arctic and Antarctic expeditions. I am grateful as well to Kerstin Wasson (Santa Cruz, CA) for critically reading and correcting the English in this manuscript.

Literature Cited

Annandale, N. 1915. Fauna of the Chilka Lake and of brackish water in the Gangetic Delta. *Mem. Ind. Mus. Calcutta*, V: 119–134.

Barrois, J. 1877. Récherches sur l'embryologie des Bryozoaires. *Trav. Stn. Zool. Wimereux* **1**:1–205 (also: *These Fac. Sci. Paris* **396**).

Bobin, G., and M. Prenant. 1953a. La classification des Loxosomes selon Mortensen et le *Loxosoma singulare* de Kéferstein et de Claparède. *Bull. Soc. Zool. France.* **78:** 84–96.

Bobin, G., and M. Prenant. 1953b. Sur trois Loxopsomes méditerranéens. *Bull. Inst. Océanogr. (Monaco)* **50:** 1–9.

Busk, G. 1886. Report on the Polyzoa collected by H.M.S. Challenger during the years 1873–76. Pt. II: The Cyclostomata, Ctenostomata and Pedicellinea. In: *Report on the Sci. Res. Voy. H.M.S. Challenger. Zool.* **XVII**:1–47. Evre & Spattiswood, London.

Calvet, L. 1904. Diagnoses de quelques éspèces de Bryozoaires nouvelles ou incomplètement décrites de la région subantarctique de l'Ocean atlantique. *Bull. Soc. Zool. France* **XXIX:** 50–59.

Calvet, L. 1904. *Ergebnisse der Magalhaensischen Sammelreise 1892/93, III: Bryozoen und Würmer* L. Friedrichsen & Co, Hamburg. Pp. 1–45.

Claparède, E. 1867. Sur le Loxosoma kéfersteini, Bryozoaire mou du Golfe de Naples. *Ann. Sci. Nat. (Paris), sér. 5, Zoologie*, **VIII:** 28–30.

du Bois-Raymond-Marcus, E. 1957. Neue Entoprocten aus der Gegend von Santos. *Zool. Anz.* **159:** 68–75.

Eggleston, D. 1965. The Loxosomatidae of the Isle of Man. *Proc. Zool. Soc. London* **145:** 529–547.

Eggleston, D. 1969. Marine Fauna of the Isle of Man: Revised lists of Phylum Entoprocta (= Kamptozoa) and Phylum Ectoprocta (= Bryozoa). *Rep. Mar. Biol. Stn. Port Erin* **81:** 57–80.

Eggleston, D., and H. O. Buill, 1966. The Marine Fauna of the Cullercoats District. 3a: Entoprocta. *Rep. Dove Mar. Lab.* (3 ser) **15**:5–10.

Ehlers, E. 1890. Zur Kenntnis der Pedicellineen. *Abhandlungen der phys. Klasse der kgl. Ges. Wissensch. Göttingen.* **36:** 1–200.

Ekman, S. 1935. *Tiergeographie des Meeres*, Akad. Verlagsges, Leipzig. 542 pp.

Emschermann, P. 1969. Ein Kreislauforgan bei Kamptozoen. *Z. Zellforsch* **97:** 576–607.

Emschermann, P. 1972a. Cuticular pores and spines in the Pedicellinidae and Barentsiidae (Entoprocta), their relationship, ultrastructure, and suggested function, and their phylogenetic evidence. *Sarsia* **5:** 7–16.

Emschermann, P. 1972b. *Loxokalypus socialis* gen. and spec. nov. (Kamptozoa, Loxokalypodidae fam nov.), ein neuer Kamptozoentyp aus dem nördlichen Pazifischen Ozean. Ein Vorschlag zur Neufassung der Kamptozoensystematik. *Marine Biology* **12:** 237–254.

Emschermann, P. 1982. Les Kamptozoaires. État actuel de nos connaisssances sur leur anatomie, leur développement, leur biologie et leur position phylogénetique. *Bull. Soc. Zool. France* **107:** 317–344.

Emschermann, P. 1985. Factors inducing sexual maturation and influencing the sex determination of *Barentsia discreta* Busk (Entoprocta Barentsiidae). Pp. 101–108 in *Bryozoa Ordovician to Recent*, C. Nielsen and G. P. Larwood, eds. Olsen and Olsen, Fredensborg, Denmark.

Franzén, Å. 1973. Some Antarctic Entoprocta with notes on morphology and taxonomy in the Entoprocta in General. *Zool. Sci.* **2:** 183–195.

Harmer, S. 1885. On the structure and development of Loxosoma. *Q. J. Microsc. Sci. N.S.* **25:** 261–337.

Harmer, S. 1915 The Polyzoa of the Siboga Expedition. Part 1. Entoprocta, Ctenostomata and Cyclostomata. *Siboga Exped. Rep.* **28a:** 1–180.

Hincks, Th. 1880a. On New Hydroida and Polyzoa from Barents Sea. *Ann. Mag. Nat. Hist. (5 ser.)* **6:** 277–286.

Hincks, Th. 1880b. *History of the British Marine Polyzoa*, 2 Vols. John van Voorst, London.

Hutchins, L. W. 1886. An annotated check-list of the salt water Bryozoa of Long Island Sound. *Trans. Connecticut Acad. Arts Sci.* **3:** 533–551.

Jennings, J., and R. Gibson 1969. Observations of the nutrition of seven species Rhynchocoelan Worms. *Biol. Bull* **136:** 405–433.

Johnston, T. H., and L. M. Angel. 1940. Endoprocta. Pp. 215–231 in *B.A.N.Z. Antarctic Research Expedition 1929–1931.* Report Series B (Zoology and Botany). IV, part 7, Adelaide, Australia.

Jones, N. S. 1963. Phylum Kamptozoa (= Polyzoa). Pp. 224–225 in *Marine Fauna of the Isle of Man*, 2nd edition, J. R. Bruce, J. S. Coleman, and N. S. Jones eds., Liverpool University Press, Liverpool.

Kirkpatrick, R. 1888. Reports on the Zoological Collections Made in Torres Straits by Professor A. C. Haddon 1888–1889. Hydroida and Polyzoa. *Sci. Proc. R. Dublin Soc. (N.S.)* **6:** 603–626.

Kluge, G. A. 1946a. Kamptozoa from the Arctic Ocean. *Trudy Droyfuyush. Exped. Glavsev. Na Ledok. Parochode "G. Sedov" God. 1937–1940.* 3:149–156 (in Russian with Engl. summary).

Kluge, G. A. 1946b. New and little known species of Bryozoa from the Arctic Ocean. *Trudy Droyfuyush. Exped. Glavsev. Na Ledok. "G. Sedov" God. 1937–1940.* 3:194–223 (in Russian with Engl. summary).

Konno, K. 1971. On some entoprocts found at Fukaura, Aomori Prefecture. *Rep. Fukaura Mar.Biol. Lab.*, **3:** 2–9.

Konno, K. 1977. Studies on Japanese Entoprocta VII. On two new species of Loxosomatidae. *Sci. Rep. Hirosaki Univers.* **24:** 81–84.

Land, J. van der 1970. Systematics, zoogeography, and ecology of the Priapulida. *Zool. Verhandelingen (Leiden)* **112:** 1–118.

Marcus, E. 1922. Papers from Dr. Th. Mortensen's Pacific Expedition 1914–1916 VI: Bryozoen von den Auckland- and Campbell-Inseln. *Videnskabelige Meddelser fra Dansk Naturhist. Forening Kobenhavn* **173:** 85–121.

Marcus, E. 1937. Bryozoarios marinhos Brasileiros I. *Bol. Fac. Phil. Ciênc. Letr. Univ. São Paulo 1, Zoologia* **1:** 1–224.

Marcus, E. 1953. Notas sobre briozoos marinhos brasileiros. *Arquivos do Mus. Nacional (Rio de Janaro)* **42:** 273–342.

Martin, G. E. 1978. A new finding of Rhabdites: Mucus production for ciliary gliding. *Zoomorphology* **91:** 235–248.

Maturo, F. J. S. 1957. A study of the Bryozoa of Beaufort, North Carolina, and vicinity. *J. Elisha Mitchell Scient. Soc.* **73:** 11–68.

Maturo, F. J. S., and Th. J. M. Schopf. 1968. Ectoproct and Entoproct type material: Reexamination of species from New England and Ber-

muda named by A. E. Verrill, J. W. Dawson and E. Desor. *Postilla (New Haven)* **120:** 1–95.

Mortensen, Th. 1911. A new species of Entoprocta, *Loxosomella antedonis*, from North-east Greenland. *Danmark-Ekspeditionen til Grønlands Nordostkyst 1906–1908* **5**(8): 399–406.

Mukai, H., and T. Makioka. 1980. Some observations on the sex determination of an Entoproct, *Barentsia discreta* (Busk). *J. Exp. Zool.* **21:** 45–59.

Nielsen, C. 1964a. Studies on Danish Entoprocta. *Ophelia* **1:** 1–76.

Nielsen, C. 1964b. Entoprocta from the Bergen Area. *Sarsia* **17:** 1–6.

Nielsen, C. 1966. Some Loxosomatidae (Entoprocta) from the Atlantic Coast of the United States. *Ophelia* **3:** 249–275.

Nielsen, C., and J. Ryland. 1961. Three new species of Entoprocta from West Norway. *Sarsia* **1:** 39–45.

Nilus, G. 1909. Notiz über *Loxosoma murmanica* und *Loxosoma brumpti*. sp. n. *Trav. Soc. Impér. Nat. St. Pétersbourg* **40**(1): 157–169.

Norman, A. M. 1907/10. The Polyzoa of Madeira and the Neighbouring Islands. *J. Linn. Soc. (London)* **30:** 275–277.

O'Donoghue, Ch. 1920. The Bryozoa (Polyzioa) collected by the S. S. "Pickle". *Fish. and Mar. Biol. Survey (Cape Town) rept.* **1:** 1–61.

Oka, A. 1895. Sur la *Barentsia murakiensis*. *Zool. Mag.* **7:** 1–10.

Okada, Y., and S. Mawatari. 1938. On the collection of Bryozoa along the coast of Wakayama-ken, the middle part of Honsyu, Japan. *Imper. Zool. Japan* **17:** 445–448.

Osburn, R. 1912. The Bryozoa of the Woods Hole Region. *Bull. Bur. Fish. (Washington)* **30:** 212–214.

Osburn, R. 1914. The Bryozoa of the Tortugas Islands, Florida. *Papers from the Tortugas Lab. Carnegie Inst. of Washington* **5:** 183–222.

Osburn, R. 1932. Bryozoa from Chesapeake Bay. *Ohio J. Sci.* **3:** 441–446.

Osburn, R. 1944. A Survey of the Bryozoa of the Chesapeake Bay. *Publ. Chesapeake Biol. Lab.* **63:** 1–55.

Osburn, R. 1940. Bryozoa of Puerto Rico with a résumé of the West Indian Bryozoan Fauna. Pp. 321–486 in *Sci. Survey of Puerto Rico and the Virgin Island*, vol 16, New York.

Osburn, R. 1953. Bryozoa of the Pacific Coast of America, Pt. 3: Cyclostomata, Ctenostomata, Entoprocta and Addenda. *Allan hancock Pacific Expeditions* **14:** 613–822.

Pallas, P. 1774. *Spicilegia Zoologica, quibus novae et imprimis obscurae animalium species iconibus, descriptionibus atque commentariis illustrantur*. vol. 1, fasc. 10. Gottlieb August Lange, Berlin.

Reger, J. 1969. Studies on the fine structure of muscle fibers and contained crystalloids in basal socket muscle of the Entoproct, *Barentsia gracilis*. *J. Cell. Sci.* **4:** 305–325.

Reisinger, E., and S. Kelbertz. 1964. Feinbau und Entladungsmechanismus der Rhabditen. *Z. wiss. Mikrosk. Tech.* **65:** 472–508.

Ridley, St. O. 1881. Polyzoa. In: Account of the Zoological Collections made during the survey of H. M. S. "Alert" in the Straits of Magellan and on the Coast of Patagonia. *Proc. Zool. Soc. (London)* **1881:** 44–61.

Rieger, R. M., and M. Mainitz. 1977. Comparative fine structure study of the body wall in Gnathostomulida and their phylogenetic position between Platyhelminthes and Aschelminthes. *Zool. Syst. Evolutionsforsch.* **15:** 9–34.

Rieger, R. M., E. Ruppert, G. E. Rieger, and C. Schoepfer-Sterrer. 1974. On the fine structure of gastrotrichs with description of *Chordodasys antennatus* sp.n. *Zool. Scr.* **3:** 219–237.

Robertson, A. 1900. Studies in Pacific Coast Entoprocta. *Proc. Calif. Acad. Sci. 3rd ser. Zool.* **2:** 323–349.

Rogick, M. D. 1956. Bryozoa of the United States Navy's 1947–1948 Antarctic Expedition, 1–4. *Proc. U. S. Natl. Mus.* **105:** 221–317.

Rogick, M. D. 1965. Bryozoa of the Antarctic. Pp. 401–413 in *Biogeography and Ecology in Antarctica*, P. Van Oye and J. van Mieghem, eds. W. Junk, den Haag.

Ryland, J., and A. P. Austin. 1960. Three species of Kamptozoa new to Britain. *Proc. Zool. Soc. London* **133:** 423–433.

Smith, J., S. Thyler, M. B. Thomas, and R. M. Rieger. 1982. The morphology of Turbellarian Rhabdites: Phylogenetic implications. *Trans. Amer. Soc.* **101:** 109–228.

Thornely, L. R. 1905. Report on the Polyzoa collected by Professor Herdman, at Ceylon in 1902. *Ceylon Pearl Oyster Fisheries, pt. 4. suppl. rep.* **26:** 107–130.

Toriumi, M. 1949. On some Entoprocta from Japan. *Sci. Rep. Tohoku Univ., 4th ser. (Biology)* **18:** 223–227.

Toriumi, M. 1951. Some Entoprocts found in Matsushima Bay. *Sci. Rep. Tohoku Univ. 4th ser. (Biology)* **19:** 17–22.

Verrill, A. E. 1900. Additions to the Tunicata and Molluscoidea of the Bermudas. *Trans. Connect. Acad. Sci.* **10:** 588–598.

Vigeland, I. 1937/38. Bryozoa of Tristan da Cunha. *Res. Norweg. Sci. Exped. to Tristan da Cunha 1937–1938* **44:** 9–18. W. Nygaard, Oslo.

Voigt, C. 1876. Le Loxosome des Phascolosomes (*Loxosoma phascolosomatum*) *Zool. Exp. et Gén. (Paris)* **5:** 305–356.

Waters, A. W. 1904. Bryozoa. Pp. 1–113 in *Res. Voy. du S. Y. Belgica en 1897–1899*, J. E. Buschmann, Anvers.

Yamada, M. 1956. The Fauna of Akkeshi Bay: 24. Entoprocta. *J. Fac. Sci. Hokkaido Univers.* **12:** 237–243.

Zirpolo, G. 1927. Sulla presenza della *Barentsia discreta* Busk nel Golfo di Napoli. *Boll. Soc. Nat. Napoli* **39:** 413–419.

Reference: *Biol. Bull.* **184**: 186–202. (April, 1993)

Control of Hatching in an Estuarine Terrestrial Crab. II. Exchange of a Cluster of Embryos Between Two Females

MASAYUKI SAIGUSA

Okayama University, College of Liberal Arts and Sciences, Tsushima 2-1-1, Okayama 700, Japan

Abstract. The eggs of an estuarine terrestrial crab, *Sesarma haematocheir* (akate-gani), are incubated by the female for about one month. In estuarine crabs larval hatching is synchronized with the nocturnal high tide. To investigate whether the female or the embryo controls the actual timing of the hatching, one cluster of embryos was detached from each of two ovigerous females and reciprocally transplanted. Hatching of the transplanted embryos was divided into the following three patterns according to the number of nights until either (or both) of the females released their larvae. In *Pattern I*, the transplanted clusters both hatched on the same night that the donor females released their larvae. In *Pattern II*, the hatching of one of the transplanted clusters was not controlled by the host female, whereas hatching of the other transplanted cluster was obviously induced. Finally, in *Pattern III*, not only the induction of hatching, but also the time of hatching, was controlled by the female. Hatching profiles of transplanted embryos transferred to aerated conditions indicated that hatching requires *three nights*, and that each embryo also has an endogenous rhythm for hatching. The female seems to play two roles in hatching: *i.e.*, initiation of the hatching process, and enhancement of hatching synchrony in each embryo. A plausible hypothesis explaining the mechanism of induction and the synchronization of hatching is presented.

Introduction

Clearly demarcated rhythmicities are often observed in the reproductive behaviors of both marine and terrestrial animals. A persistent question in reproductive rhythm research is whether the female or the embryo controls the actual timing of these behaviors. Rhythms of spawning (*i.e.*, shedding of gametes or fertilized eggs) or oviposition following gametogenesis must be controlled by the female alone. Examples of this phenomenon are the circadian rhythm of oviposition in the pink bollworm *Pectinophora gossypiella* (Pittendrigh and Minis, 1971), egg laying in the teleost *Oryzias latipes* (Egami, 1954; Ueda and Oishi, 1982), and the daily, tidal and lunar rhythms of spawning in many kinds of marine invertebrates (Korringa, 1947; Pearse, 1990).

Embryonic development proceeds within the eggs oviposited by the female, and hatching occurs after a certain period. A circadian rhythm of hatching appears in the bollworm *P. gossypiella*. Eggs of this species, maintained at 20°C, hatched 10–13 days after they were oviposited; the eggs were transferred from constant light (LL) to constant darkness (DD) every 5.5 h during embryonic development, and hatching was monitored (Minis and Pittendrigh, 1968). This experiment suggested that a circadian pacemaker controlling hatching is differentiated at least around the midpoint of embryogenesis, *i.e.*, 6–7 days after oviposition.

Obvious rhythmic patterns are also observed in the hatching of marine crustaceans (Sastry, 1983; DeCoursey, 1983). But eggs of most marine and freshwater crustaceans are incubated by the female until hatching occurs. This phenomenon complicates the control of the larval hatching rhythm. Indeed, the timing of larval hatching is synchronized with day-night, tidal, and lunar cycles, but whether it is the female or the embryo that controls the actual timing of hatching remains unclear.

This question has only been investigated with respect to eggs already detached from the female (Saigusa, 1992c), the role of the female is still unknown. This paper focuses on the female control of larval hatching in an estuarine

Received 28 May 1991; accepted 25 January 1993.

terrestrial crab, *Sesarma haematocheir*, and reports on an embryonic exchange method that was used in the investigation. Eggs of this species consist of eight clusters. Two of such clusters, one from each of two ovigerous females, were detached and exchanged by reciprocal transplantation. The transplanted eggs survived on the host females, and most of them successfully hatched. Hatching in the transplanted eggs was clearly divided into *three patterns* depending upon the number of nights intervening between the exchange and the occurrence of hatching in both or either of the females.

These results suggest that the female triggers the hatching process in each embryo, but that each embryo has also an endogenous rhythm of hatching. In response to some (unknown) stimuli released from the female, each embryo must initiate its hatching process around the time of nocturnal high tides, and hatching occurs 48–49.5 h later. Since all of the female-attached embryos hatch within a very short time, the female should have some mechanism for enhancing hatching synchrony just before the larval release.

This paper provides evidence that the control of hatching involves cooperation between female and embryo. Based on the data reported here, I present a hypothesis that explains the mechanism controlling the daily timing of larval hatching in *Sesarma haematocheir*.

Materials and Methods

Maintenance of crabs and monitoring of larval release in experimental rooms

Experimental animals were ovigerous females of the terrestrial red-handed crab (akate-gani) *Sesarma haematocheir*, randomly collected on 9, 19, 31 July, 16 August 1990, 19 July, and 8 August 1991 from the thicket along a small estuary at Kasaoka, Okayama Prefecture. The crabs were immediately brought into the experimental rooms in the laboratory, and were kept in plastic containers (70 cm long, 40 cm wide, and 25 cm high) with shallow water (1 cm deep) at the bottom, and with hiding spaces above it. Light and temperature in the experimental rooms were controlled. A 15-h light: 9-h dark photoperiod, the same phase as that in the field (light-off at 20:00 and light-off at 5:00), was employed for all experiments. The intensity of illumination in the light phase was 700–1200 lux at the floor, and in the dark phase, less than 0.05 lux. Temperature was constant at 23 ± 1.5°C and the crabs were fed every few days.

A female of *S. haematocheir* incubates 20,000–50,000 eggs on her abdomen. When embryonic development is complete, all of the larvae hatch simultaneously. Hatching is completed within a very short time, within 5–30 min in the laboratory (Saigusa, 1992c). As soon as hatching is finished, the female releases her larvae into the water. The time of day of larval release can easily be monitored by the photoelectric-switch method (Saigusa, 1992a). Under the above-mentioned light conditions, larval release activity shows a circa-tidal rhythm, the phase of which coincides roughly with nocturnal high waters.

Exchange of egg clusters between two females

The females of *S. haematocheir* incubate their eggs for about one month. During this time, the color of the embryos changes from dark brown to brownish green, according to the stage of development which can, therefore, be estimated by visual inspection. In these experiments, females with mature embryos (brownish green color) or near mature embryos (light brown color) were used.

The reciprocal exchange of a cluster of embryos between paired females is carried out as follows. Two females with similar carapace sizes were taken from containers. The walking legs and body, except the portion where the embryos are incubated, were wrapped in a paper towel, and the claws were then secured with a rubber band (Fig. 1A, upper panel). To prevent the crabs from removing the

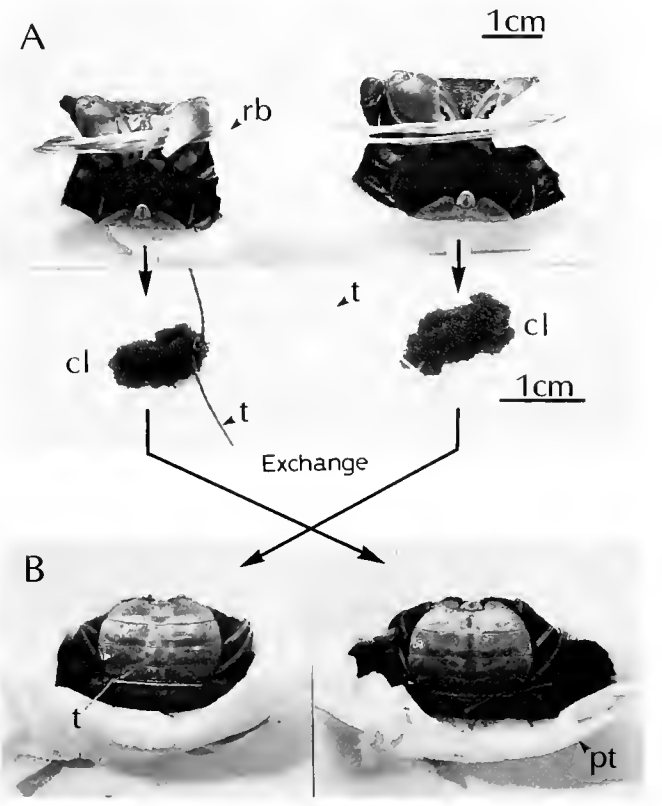

Figure 1. Embryo exchange between two females. (A) Upper photo: females with their chelae and walking legs restrained with a rubber band (*rb*). Lower photo: a cluster of embryos (*cl*) detached from each female. The base of the ovigerous seta is tied with a thread (*t*). (B) Females after the embryo exchange: a view from behind. *pt:* paper towel.

exchanged cluster, 2–3 mm of one of the (paired) tips of both claws was removed with scissors (see the female at the left side of Figure 1A). Bleeding was stopped with a small soldering iron.

Females of *S. haematocheir* have four pairs of abdominal appendages, each of them consisting of plumose and non-plumose setae (Fig. 2). The eggs are attached, just like grapes (8 clusters in all), to ovigerous hairs that grow from the non-plumose setae, and are ventilated by the female during development. The number of attached embryos in a cluster is 2000–6000. The first non-plumose seta on the right side was cut with scissors (Fig. 2), because it is the most convenient place to bind an exchanged cluster from another female. The excision of the egg cluster caused a small amount of bleeding from the base of the non-plumose seta, but hemostasis was induced with a sharpened soldering iron. These procedures, including the removal of an egg cluster, were applied in rapid succession to both females.

Each cluster of removed eggs was tied at the cut end of its seta to the center of a long thread (Fig. 1A, lower panel). Each tied cluster was then put into the space where the reciprocal cluster had been detached, and the free ends of the thread were passed around to the dorsal side of the abdomen and knotted at the articulation between the abdomen and the thorax (Fig. 1B). This prevented the transplanted cluster from being squeezed out of the egg mass being incubated by the host female. There was no exchange of blood between the transplanted non-plumose seta and the female.

Paralleling the exchange of a cluster of embryos, another small embryo cluster (200–500 eggs) was removed from each female and placed in the glass beaker with aeration (Saigusa, 1992b). Under such conditions, embryos that were detached less than 48–49.5 h before the larval release, all hatch on the same night as the eggs incubated by the female; moreover, they develop and are able to swim. In contrast, embryos separated earlier than 48–49.5 h before the release, do not hatch during the experimental period. After more than a week of aeration, these embryos gradually hatch as larvae with no ability to swim (*i.e.*, the prezoea) (Saigusa, 1992c). To determine whether the hatching of transplanted embryos is triggered by the host female, hatching of the embryos detached from the female was monitored (*i.e.*, control experiment).

The time required for the removal and exchange of a pair of egg clusters was about 15–20 min. In addition, preparation of the control experiment—*i.e.*, detachment of a small egg mass, binding it with thread, and then setting it onto the apparatus for aeration—took only about 5 min. To avoid nocturnal light, procedures were carried out in experimental rooms with a light phase of 24-h LD cycle.

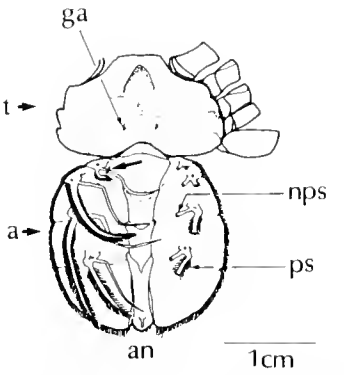

Figure 2. Abdominal appendages of *Sesarma haematocheir* female. The abdomen is opened and drawn from the ventral aspect. (*t.* thorax, *a.* abdomen, *an:* anus, *ps:* plumose seta, *nps:* non-plumose seta, *ga.* genital aperture). Ovigerous hairs growing from the non-plumose seta are omitted from the drawing. The unlabeled black arrow shows the place where the cluster of embryos is cut off with scissors.

Inspections of hatching in transplanted embryos

When the exchange of a cluster of embryos had been completed, the females were put into individual plastic cages with small holes in their sides. (These cages were either 11 cm in diameter and 10.5 cm in height, or 7 cm in diameter and 14 cm in height.) Each cage was then placed in a beaker containing 10‰ clean seawater. The time of larval release was monitored with a photoelectric device; details of this apparatus have already been described elsewhere (Saigusa, 1992a).

One of the most important questions in the present study was whether the transplanted cluster of embryos (Fig. 3A) would successfully hatch, and if so, whether this would occur simultaneously with the 7 clusters of female-attached eggs. For this purpose, hatching was also monitored, not only with the photoelectric apparatus, but also by visual inspections, described in detail below (Fig. 4A, B).

In intact females of *S. haematocheir* (*i.e.*, females without embryo exchange), hatching occurs synchronously, possibly within 5–30 min in the laboratory. Eggs were frequently found to be wet from the diluted seawater in the beaker due to the female's movements within the cage. When the hatching started, several zoea larvae were observed swimming in the beaker (Fig. 4A, middle). As soon as hatching was completed, the female released all the larvae into the water within 3–5 s (Fig. 4A, right). This quick release is associated with an abdominal fanning behavior, which triggers the photoelectric switch. Thus, if the seawater in the beaker is frequently checked, an obvious sign of hatching (*i.e.*, several swimming zoeas) will be noticed about 30 min before the larval release for most specimens. Such visual inspections were also applied to females with a transplanted cluster of embryos.

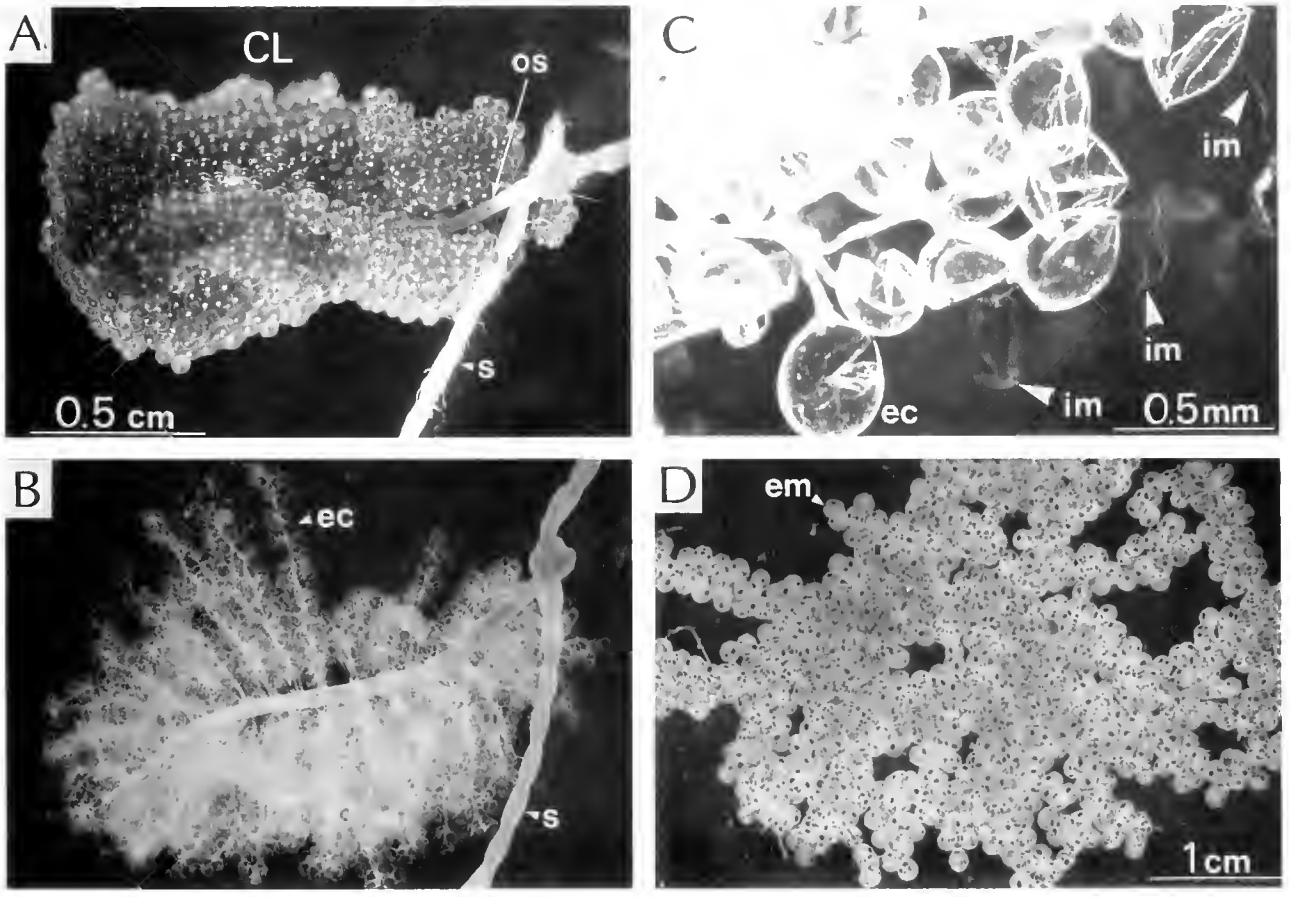

Figure 3. Eggs of *S. haematocheir* and their hatching. (A) a cluster of embryos (*CL*) the cut base of which is tied with a fine thread (*s*). *os*: ovigerous seta. (B) empty egg-cases (*ec*) remaining after larval release by the female. (C) very thin membranes (*im*) protruding from the egg-case upon the liberation of hatched larva. This membrane invests the embryo before hatching [described as the "third membrane" by Sagusa (1992b), but probably the cephalic portion of the so-called embryonic cuticle]. (D) embryos (*em*) dropped from ovigerous hairs without hatching. Diameter of each egg, about 330–350 μm.

Observations were made every 15–30 min throughout the night, using a hand-held light (or head lamp) covered with a few sheets of red cellophane. (These red lights were used for all of the observations and manipulations carried out in the experimental rooms during the dark phase.) When several zoeas were found swimming, the beaker was examined more frequently, *i.e.*, at intervals of 5–10 min.

As the upper diagram of Figure 4B indicates, when the photoelectric switch monitoring one of the paired females with a transplanted cluster operated (*i.e.*, the sign of larval release), the female was taken out of the cage. The thread was cut, and the transplanted cluster was carefully removed from the female's abdomen. Since empty egg cases remain attached to the ovigerous hairs, as they do after a normal larval release, it was easy to determine whether all of the transplanted embryos had hatched. (The judgment as to whether all the eggs hatched at the same time as the other embryos carried by the female is described in the Results section.) This observation was made under normal light, outside of the experimental room, because a female that had completed larval release was never used for further experiments. If hatching had not yet occurred, the cluster was quickly transferred into vigorously aerated seawater (10‰), and examined for the subsequent occurrence of hatching. Some of the aerated clusters were monitored for hatching every hour in constant darkness (DD) or in 24-h light-dark (LD) conditions; the hatching of other clusters was sought during the light phase of the 24-h LD cycle.

Just after the observations and manipulations mentioned above, the *other female* was also checked to examine whether her transplanted cluster had also hatched. This was done by observing the water in the beaker under red light. As indicated in the middle diagram of Figure 4B, when hundreds of zoeas were seen swimming in the beaker, the transplanted cluster was removed and its

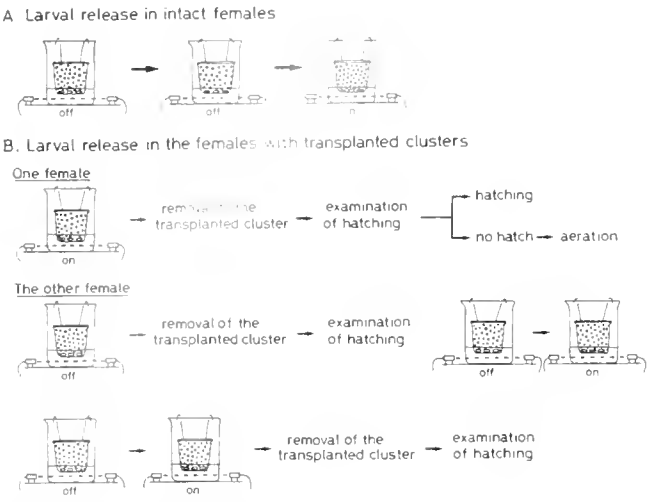

Figure 4. Experimental procedures used to examine hatching in intact females and females with transplanted clusters. The female crabs (not depicted) are in perforated cages suspended in beakers containing dilute seawater (10‰). A photoelectric device monitors the seawater for the presence of zoeas (see text). (A) The sign of hatching and larval release by intact females. Before larval release, the photoelectric switch is "off." Upon larval release, the switch operates ("on"); threshold of response: 10,000–20,000 zoeas in the beaker. (B) Examination of the transplanted clusters removed from host females. *Upper diagram:* Larval release occurs in *one* of the paired females, and the procedures indicated are followed to monitor hatching in the transplanted cluster (described in Materials and Methods section). *Middle diagram:* The cluster transplanted to the *other* female has hatched, indicated by hundreds of zoeas swimming in the beaker; (observed visually—the switch is "off"). The transplanted cluster is removed and examined, and the female is reset in the recording apparatus. *Lower diagram:* No zoeas are seen in the beaker. The female is removed from the cage *after* the release of her larvae, and the transplanted cluster is then examined.

hatching was confirmed; a stereo-microscope was used as necessary. The beaker was then replaced with another, and the female was reset to the recording apparatus. On the other hand, as shown in the lower diagram (Fig. 4B), there were many cases where no zoeas were seen swimming. In these cases, when the female finally released larvae, the transplanted cluster was removed and its hatching was examined.

Notice that the transplanted clusters were examined under normal light to determine whether hatching had occurred. This was no problem when all of the embryos had already hatched. But a question remained in the other cases as to whether this light might have affected the timing of hatching. To reduce the effect of light, some of the transplanted clusters were removed from the female in the experimental room under red light and transferred into a vigorously aerated medium. The latter experiments were carried out in 1991 as specified in the figures. The embryo exchange experiments involving 51 pairs of females were all done in 1990, although the year is not identified in the figures. Animals were never used for more than one experiment.

Results

Ovigerous females with a transplanted cluster released their zoea larvae between the night of embryo exchange (*e.g.*, Fig. 5A-a) and 11 days after. The release behavior was the same as that of intact animals. The results are clearly divided into the following three patterns (*Pattern I, Pattern II,* and *Pattern III*), which are related to the number of nights until larval release occurred.

Pattern I (Fig. 5A)

Both females released their larvae *within two nights* after the embryo exchange. The detached eggs of the control experiment and the transplanted embryos, all hatched on the same night that the *donor* females released their larvae. The results of this data can be further divided into three sub-patterns.

Sub-pattern I-1 (1 pair). As shown in Figure 5A-a, larval release of both females (F-1 and F-2) occurred on the night following embryo exchange. As soon as the release of one of the females (F-1) was recorded, the transplanted eggs (cl:F-2) were removed. Almost all eggs remained unhatched, and were quickly transferred to aerated conditions and monitored. As shown in Figure 5B-a, all of the embryos had hatched by about 6:00 on 18 August. On the other hand, the larval release of the paired female (F-2) occurred 50 min later than F-1 (Fig. 5A-a). When the implanted cluster (cl:F-1) was removed from F-2, it had already hatched. The eggs detached from both females (*i.e.*, ae:F-1 and ae:F-2) also hatched during the same night.

Sub-pattern I-2 (6 pairs). Larval release of these females occurred on the first and second nights after embryo exchange, respectively (Fig. 5A-b). The egg mass of the control experiment (ae:F-3 and ae:F-4) hatched on the same night that the donor females released their larvae. The transplanted eggs (cl:F-4) were removed from the female (F-3) immediately after larval release. No eggs hatched, and this cluster was monitored under constant darkness. Hatching occurred on the following night (Fig. 5B-b), corresponding to the release of the donor female (F-4). On the other hand, in the beaker where the female F-4 was confined, swimming zoeas emerged around the time of larval release of female F-3. These larvae had clearly hatched from the implanted cluster (cl:F-3). When this cluster was removed from the host female F-4, almost every embryo had already hatched. The remaining embryos hatched within a few hours under aerated conditions.

Sub-pattern I-3 (1 pair). In only one instance did both females release larvae two nights after the embryo exchange (Fig. 5A-c). The embryos in the control exper-

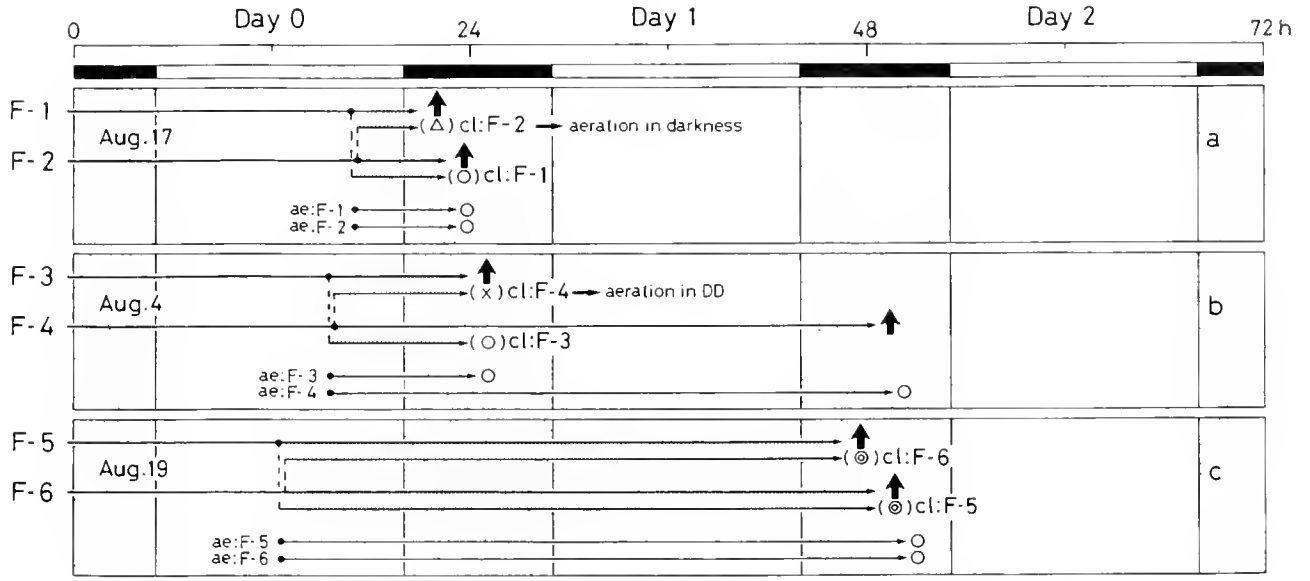

Figure 5A. Hatching of transplanted clusters: *Pattern I* (*a*) *Sub-pattern I-1* F-1 and F-2 designate the paired females that were set into recording apparatuses. Excision and exchange of embryos occurred at 16:55–17:15 on 17 August. Upward black arrows show the time of day of larval release of these females (at 23:00 for F-1, and at 23:50 for F-2). cl:F-2 and cl:F-1 are the transplanted clusters. ae:F-1 and ae:F-2 are the control egg masses kept in vigorous aeration. ○: Hatching of the egg-cluster or egg mass. △: Partial hatching of the egg cluster. (*b*) *Sub-pattern I-2.* Detachment and exchange of eggs, 15:20–15:40 on 4 August. F-3: Larval release at 1:00 on 5 August; F-4: at 1:40 on 6 August. ×: No eggs hatched from the transplanted cluster when it was removed from the host female. (*c*) *Sub-pattern I-3* Detachment and exchange of eggs: 12:55–13:10 on 19 August. F-5: Larval release at 23:50 on 20 August; F-6: at 0:50 on 21 August. ◎: These transplanted egg-clusters hatched at the same time as the female-attached eggs. Other symbols as in Fig. 5A-a and 5A-b.

iment (ae:F-5 and ae:F-6) both hatched on the second night after the embryo exchange. A feature of this case was that hatching of the transplanted cluster (cl:F-6) seemed to be *synchronized* with that of the host female (F-5). On the other hand, no swimming zoeas were observed in the beaker of the female F-6 around the time of the release of F-5, although the beaker was checked often. Female F-6 released her larvae before the transplanted cluster (cl:F-5) was removed. When this cluster was examined, all the egg cases were already empty (Fig. 3B). Thus, hatching of this transplanted cluster also seemed to be synchronized with that of the female-attached eggs.

Pattern II (Figs. 6A and 7A)

In this pattern, only one of the paired females released her larvae *within one or two nights* after the embryo exchange. The embryos of the control experiment all hatched on the same night as the release of the donor female. In contrast, the paired females released their larvae *more than three nights* after the embryo exchange. The control egg masses taken from these females did not hatch at all. A remarkable feature was that the hatching of the transplanted cluster was apparently induced by the donor female. The results were further divided into the following two sub-patterns.

Sub-pattern II-1 (11 pairs). The first pattern occurred when one of the females released larvae on the *first night* after embryo exchange. Five instances are summarized in Figure 6A. For example, in Figure 6A-a, larval release of F-7 occurred on the night of embryo exchange. The transplanted cluster of embryos (cl:F-8) was removed from the female 10 min after the release of F-7, but no eggs had yet hatched. This cluster was quickly transferred to aerated conditions, and was monitored every hour (Fig. 6B-a).

The reciprocal cluster (cl:F-7), which had been transplanted to the female F-8, hatched on the same night that the donor female (F-7) released her larvae. When the beaker of F-8 was observed with the red light shortly after the larval release of F-7, hundreds of zoea larvae were swimming. The transplanted cluster (cl:F-7) was quickly removed from F-8 under red light, and examined. The zoea larvae remaining attached to broken egg cases began to swim when the cluster was shaken by hand several times in the seawater, and hatching was completed within

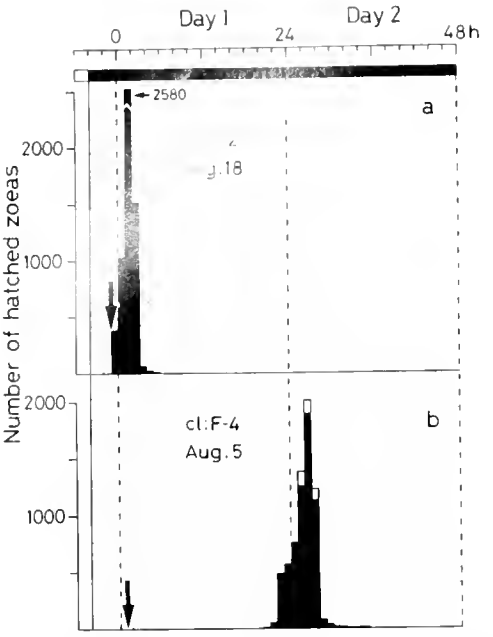

Figure 5B. Hatching of the transplanted egg-clusters. (*a*) Hatching of the cluster (cl:F-2) removed from the host female (F-1). Downward black arrow: time of larval release of the host female (F-1). (*b*) Hatching of the cluster (cl:F-4) removed from F-3. Open areas in histogram indicate the number of premature zoeas (prezoeas) that could not swim and thus sank to the bottom of the beaker.

a few hours. The beaker of F-8 was replaced with another one containing 10‰ seawater, and larval release of this female was monitored.

The control egg mass (ae:F-8) never hatched even after five days (Fig. 6A-a). In contrast, the cluster of embryos (cl:F-8) successfully hatched two nights after the start of aeration (Fig. 6B-a), and all eggs hatched by noon on 10 August. Obviously, hatching of the transplanted embryos (cl:F-8) was *induced* by the host female (F-2).

As four additional cases show (Fig. 6A-b-e), hatching of the transplanted clusters (cl:F-10, cl:F-12, cl:F-14, cl:F-16) was induced by the host females. Moreover, when these embryos were transferred into aerated conditions, they always hatched *two nights* after the removal from the host female (compare Fig. 6A and 6B). The pattern of hatching was similar, whether the clusters were monitored in constant darkness (Fig. 6B-a-b), or in LD cycles (Fig. 6B-c-e).

Sub-pattern II-2 (7 pairs). In these cases (Fig. 7A), the *first* larval release occurred on the *second night* after the embryo exchange. The control egg mass detached from these females hatched on the same night. For example (Fig. 7A-a), female F-17 released her larvae first. The cluster transplanted to this female (*i.e.*, cl:F-18) was quickly removed and examined with the stereo-microscope. No hatching had occurred, so this cluster was transferred into aerated conditions and monitored. After about 24 h, it had completely hatched (Fig. 7B-a).

At about the time that F-17 was releasing her larvae, zoeas were observed swimming in the beaker of female F-18 (Fig. 7A-a). The cluster transplanted to this female (cl:F-17) was removed and examined. Most egg cases were already empty and the remaining embryos all hatched within a few hours in aerated dilute seawater. Female F-18 was replaced in 10‰ seawater, and monitored until the time of larval release (day 3; Fig. 7A-a).

Other transplanted clusters put into aerated conditions (*i.e.*, cl:F-20, cl:F-22, cl:F-24, cl:F-26) also hatched about 24 h after the larval release of their host females. In the first three experiments (Fig. 7A-a-c), the transplanted clusters (*i.e.*, cl:F-18, cl:F-20, and cl:F-22) hatched on the same night as the larval release of the donor females (*i.e.*, F-18, F-20, F-22). But in the other two instances (*d* and *e*), the donor females (F-24 and F-26) released their larvae two or three nights later than their complementary pairs (F-23 and F-25). These results further indicate that hatching of the transplanted clusters is induced by the host female.

Pattern III (Fig. 8)

In these experiments (25 pairs), *both* females released their larvae *more than three nights* after the embryo exchange. In these cases, none of the control egg masses ever hatched during the experiment. Five instances of hatching by the transplanted clusters are summarized in Figure 8. For example, one of the females (F-29) released her larvae five nights after the embryo exchange (Fig. 8-b). Within a few minutes after the photoelectric switch had operated, the transplanted cluster was removed from female F-29 and examined resulting in the discovery that all the embryos had already hatched (Fig. 3B). The beaker containing the paired female (F-30) was frequently checked on the night that female F-29 released, but no swimming larvae were seen, and larval release occurred on the following night. Female F-30 was removed from the cage 5 min after the release, and the transplanted cluster was examined. Again, it was observed that hatching was complete. Similar results were obtained from the other experiments shown in Figure 8-a and 8-c-e.

The following evidence suggests that all of the transplanted clusters in *Pattern III* hatched simultaneously with the attached clusters that had been incubated by the donor female. (1) In intact females, a small number of zoea larvae begins to swim in the beaker around 20–30 min before the larval release. Animals with transplanted embryos exhibited the same phenomenon. (2) When the transplanted cluster of eggs was examined just after the larval release of the host female, hatching had already been complete. (3) The date of larval release for the complementary

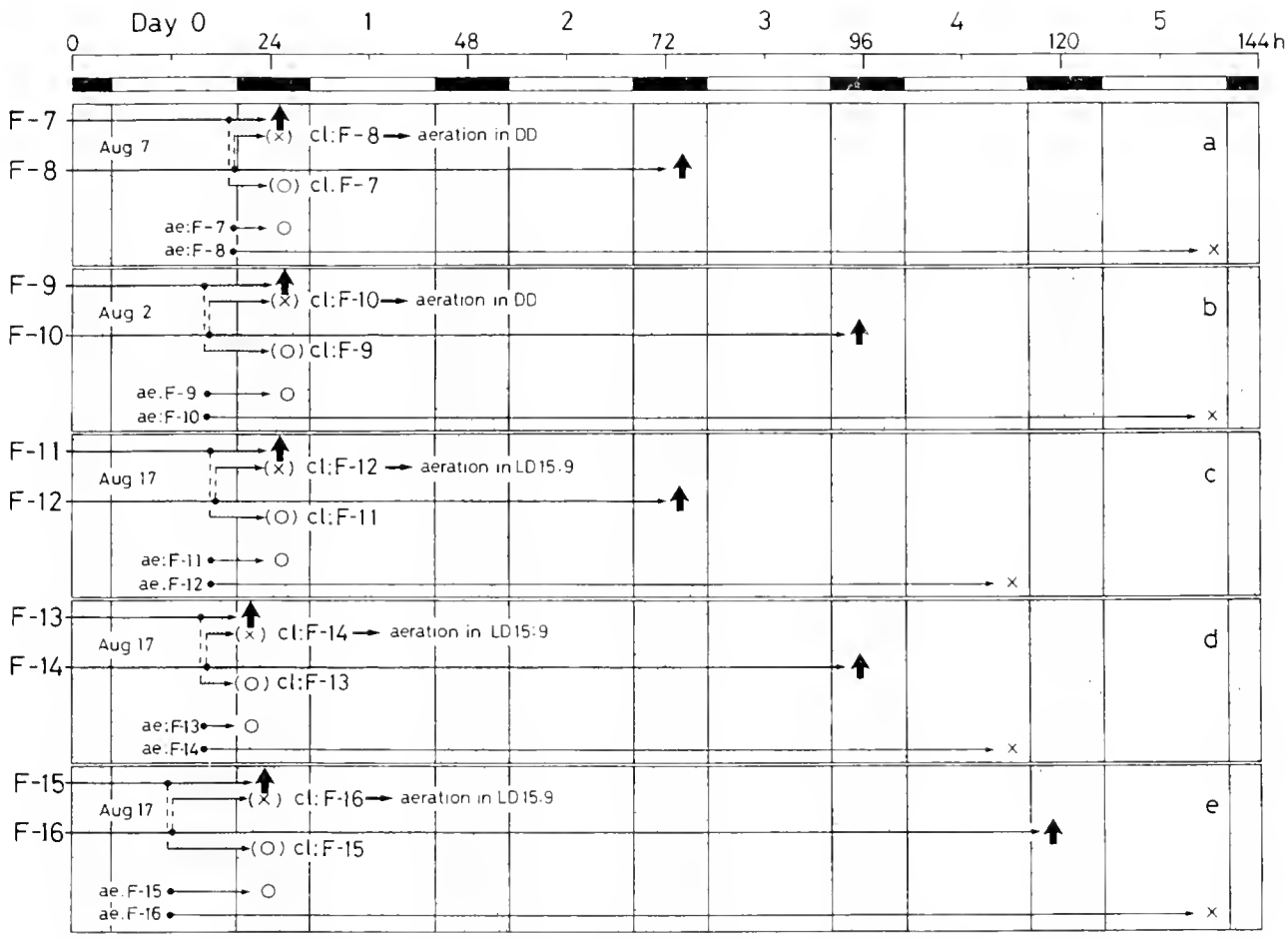

Figure 6A. Induction of hatching in the transplanted cluster of embryos: *Sub-pattern II-1* (*a*) Embryo exchange between females F-7 and F-8. Detachment and exchange of clusters: 19:20–19:40 on 7 August. Larval release: F-7, at 1:00 on 8 August; F-8, at 2:00 on 10 August. (*b*) Embryo exchange between F-9 and F-10. Detachment and exchange of clusters: 15:50–16:20 on 2 August. Larval release: F-9, at 1:50 on 3 August; F-10, at 23:45 on 5 August. (*c*) Embryo exchange between F-11 and F-12 at 17:50–18:10 on 17 August. Larval release: F-11, at 1:00 on 18 August; F-12, at 1:25 on 20 August. (*d*) Embryo exchange between F-13 and F-14 at 16:10–16:30 on 17 August. Larval release: F-13, at 21:45 on 17 August; F-14, at 23:40 on 20 August. (*e*) Embryo exchange between F-15 and F-16 at 11:40–12:00 on 17 August. Larval release: F-15, at 23:40 on 17 August; F-16, at 22:40 on 21 August. The transplanted clusters (cl:F-7, cl:F-9, cl:F-11, cl:F-13, cl:F-15) all hatched on the same night as the larval release of the donor females. Symbols are the same as in Fig. 5A.

females was usually different. If these females carried their eggs for three nights or more after the embryo exchange, no swimming larvae appeared until the host female released her larvae. (4) When the transplanted cluster was examined with the stereo-microscope, a very thin membrane that invests the embryo had emerged from the egg case (Fig. 3C). Emergence of this membrane always accompanies hatching in this species (Saigusa, 1992b), so its appearance signifies that larvae had just emerged. Eventually this membrane is lost, and the inside of the empty egg cases are contaminated with fine detritus.

To prove that the transplanted clusters hatched simultaneously with the clusters attached to the host female, it was necessary to make direct observations of the female releasing larvae. Such observations were only meaningful if the females could be sampled within 30 min after the larval release was monitored in the event recorder (44 females). Shortly after larval release, the females unfold their abdomens and begin eating the empty egg cases that remain attached to the ovigerous hairs. Thus, six females that were examined more than 30 min after release had already eaten most of the empty egg cases, or the cases had dropped to the bottom of the beaker, so the time of hatching of either the transplanted or attached clusters could not be determined.

In *Pattern III*, there were only three instances in which

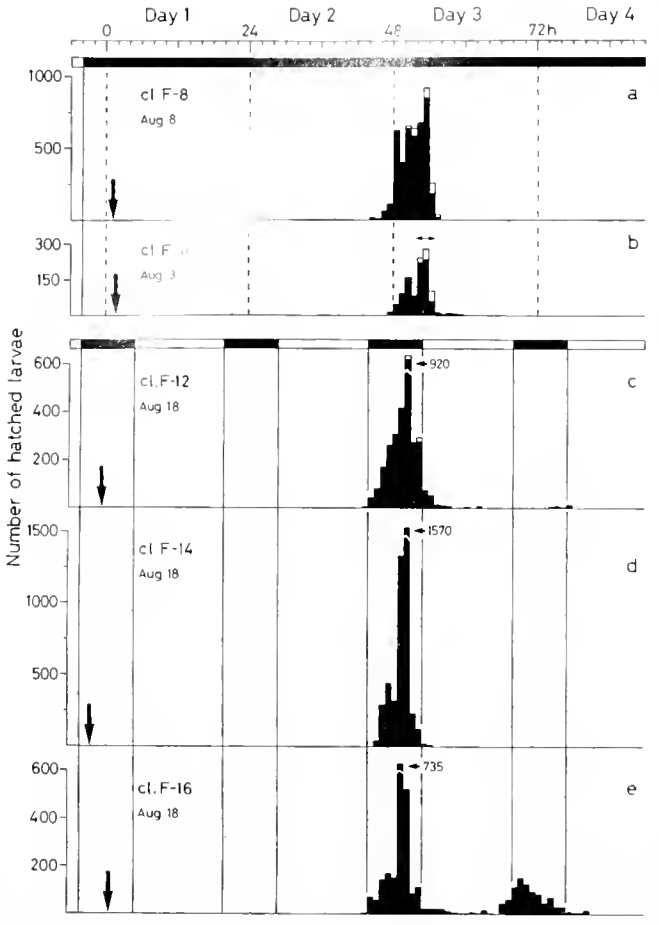

Figure 6B. Hatching of the transplanted egg-clusters in vigorous aeration. In the upper two panels (*a* and *b*), the cluster was monitored in constant darkness. In the lower three panels (*c*, *d*, and *e*), hatching was recorded in 24-h light-dark cycles. Note that the embryos hatch around 48 h after the larval release of the host females (downward black arrows). The horizontal arrow in panel *b* indicates that the egg masses dropped from cluster cl:F-10 during aeration, so the hatching was not fully monitored.

a portion of the transplanted cluster did not hatch, but remained attached to ovigerous hairs. These clusters were shaken by hand several times in 10‰ seawater to remove adherent zoeas, and were quickly transferred to continuously dark (DD) conditions and monitored under aerated conditions. These eggs all hatched with peak hatching occurring about 24 h later (not illustrated).

Loss of the egg sponge by the incubating female

Figure 9A indicates an example of egg loss, a curious phenomenon not usually seen in intact females, either in the laboratory or the field. In this experiment, one of the paired females (F-37) released her larvae on the night of embryo exchange. The egg cluster transplanted to this female (cl:F-38) was quickly removed and transferred into an aerated medium where it hatched about 48 h later. However, the reciprocally transplanted cluster (cl:F-37) was not removed quickly, therefore the egg sponge of the other female (F-38) dropped from her abdomen during the daytime of 2 August. At the time they were dropped, the embryos were still alive (Fig. 3D).

Thus, if a transplanted cluster *hatched* and was not removed soon thereafter, the host female's own attached eggs often dropped within a few days; indeed, 7 out of 52 females dropped all of their eggs without hatching. This phenomenon appears to be due to a substance released outside of the egg membrane and associated with hatching (Saigusa, submitted). Nevertheless, as shown in Figure 9A, the control egg mass (*i.e.*, ae:F-38) never hatched. So we can presume that female F-38 would have released larvae more than three nights after the embryo exchange. These results clearly belong to *Pattern II-1*. Eggs were lost only by females of *Pattern I* and *Pattern II*, and never in females of *Pattern III*. This is indirect evidence that, in *Pattern III*, transplanted embryos hatch on the same night as do the female-attached eggs.

Influence of the light used in monitoring on the hatching of the transplanted clusters

Hatching of transplanted embryos can be induced, if they are incubated by a host female that releases her larvae within two nights (Figs. 6B, 7B). Indeed, all of the transplanted clusters were removed from the host female under red light in the experimental chamber. But the determination of hatching was carried out under the normal light outside of the experimental room, although the time required for this observation was only 5 min. Hence, we must question the influence of this light on the hatching of these embryos.

To address this issue, the hatching profile of egg clusters exposed to normal light was compared with the profile of those exposed to red light. In this experiment, the transplanted cluster was removed from the host female just after larval release, and was kept under the light for 5 min. This cluster was then transferred into aerated conditions and was monitored every hour. In two other experiments, the transplanted clusters were also quickly removed from the host females just after larval release, but they were not exposed to the light outside of the experimental room. Instead they were tied to nylon thread under *red light* and monitored for hatching.

The hatching profiles of the cluster treated with normal light showed that hatching occurred two nights after the transfer into aeration (data not shown). The other two clusters, which had been treated with red light, also hatched two nights after the aeration. Furthermore, a small peak of hatching was also observed on the third night for

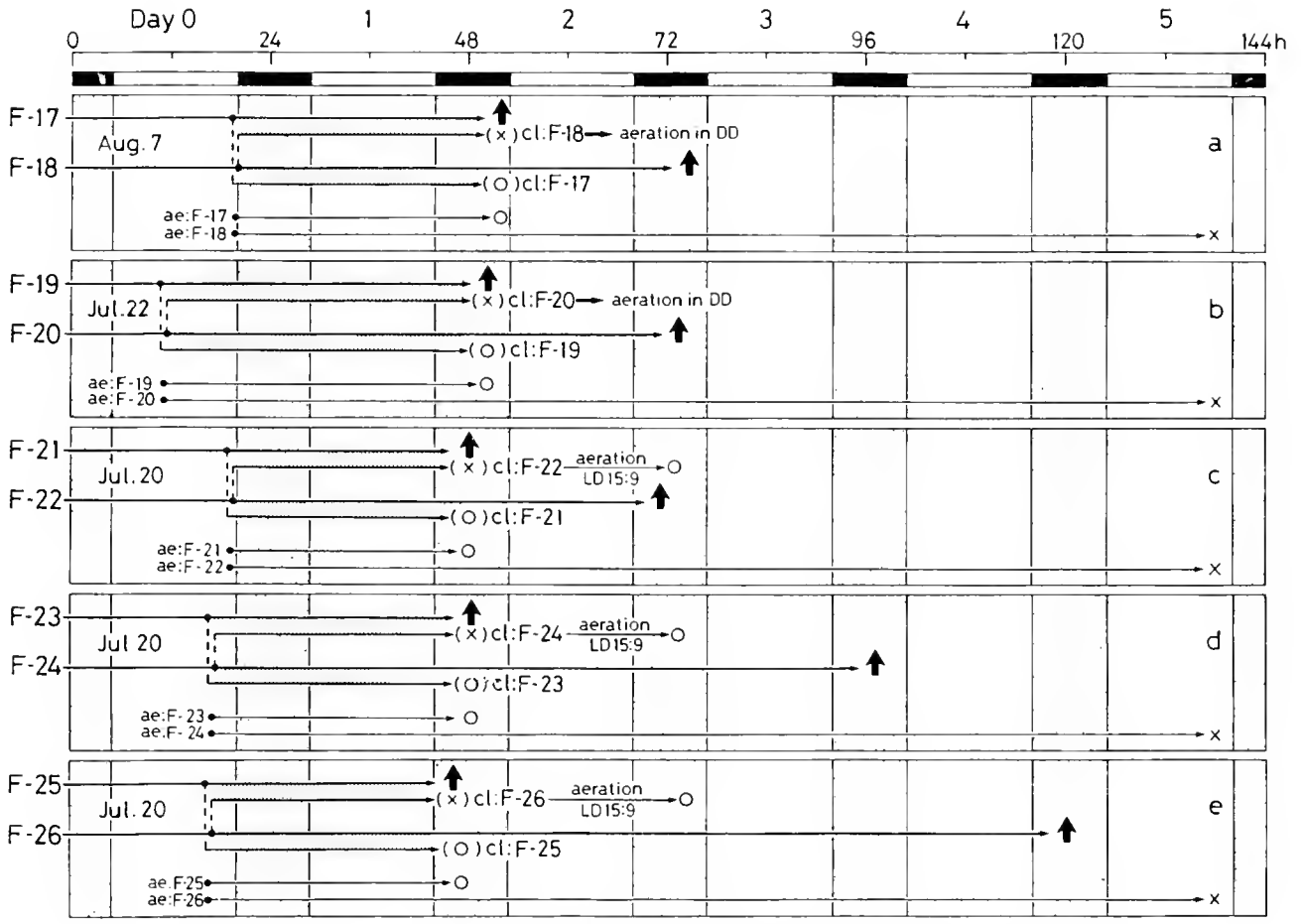

Figure 7A. Induction of hatching in the transplanted cluster of embryos: *Sub-pattern II-2*. (*a*) Embryo exchange between F-17 and F-18 at 19:45–20:00 on 7 August. Larval release: F-17, at 4:00 on 9 August; F-18, at 2:40 on 10 August. (*b*) Embryo exchange between F-19 and F-20 at 11:30–12:00 on 22 July. Larval release: F-19, at 2:30 on 24 July; F-20, at 1:30 on 25 July. (*c*) Embryo exchange between F-21 and F-22 at 18:30–19:00 on 20 July. Larval release: F-21, at 0:10 on 22 July; F-22, at 23:20 on 22 July. (*d*) Embryo exchange between F-23 and F-24 at 16:30–17:00 on 20 July. Larval release: F-23, at 0:20 on 22 July; F-24, at 1:10 on 24 July. (*e*) Embryo exchange between F-25 and F-26 at 17:10–17:40 on 20 July. Larval release: F-25, at 22:30 on 21 July; F-26, at 23:50 on 24 July. For hatching of egg-clusters (cl:F-18, cl:F-20) after they were removed, see Figure 7B-a and 7B-b. The other transplanted clusters (cl:F-22, cl:F-24, cl:F-26) hatched during one night later (hourly data not obtained).

one of these clusters. Such a secondary peak of hatching was often observed in other experiments treated with normal light (*e.g.*, Fig. 6B-e), so it cannot be attributed to the influence of red light (data not shown).

Some experiments related to the induction of hatching by the female

In two instances, the implanted egg-cluster did not hatch at all. Although egg loss occurred in both experiments, these results clearly belong to *Pattern II-1* (see Fig. 9B for the result of one of these experiments). A feature common to these two experiments is that the interval between the embryo exchange and the larval release of the host female was very short. The transplanted clusters were incubated by the host females for 4 h and 4.5 h, respectively. In every case of induced hatching, the minimum period was 5.5 h (*e.g.*, Fig. 6A-d). These results suggest that at least 5–6 hours are required to induce hatching of the transplanted cluster.

The possibility that some stimulus of hatching in the female-attached eggs induced the hatching of transplanted clusters was also examined. For this purpose, the transplanted cluster was removed from the host female some hours before the larval release (Fig. 9C). In this experiment, the clusters were incubated by the host females for about 17 h, and were then transferred into aeration. The cluster (cl:F-41) hatched on the same night that the donor

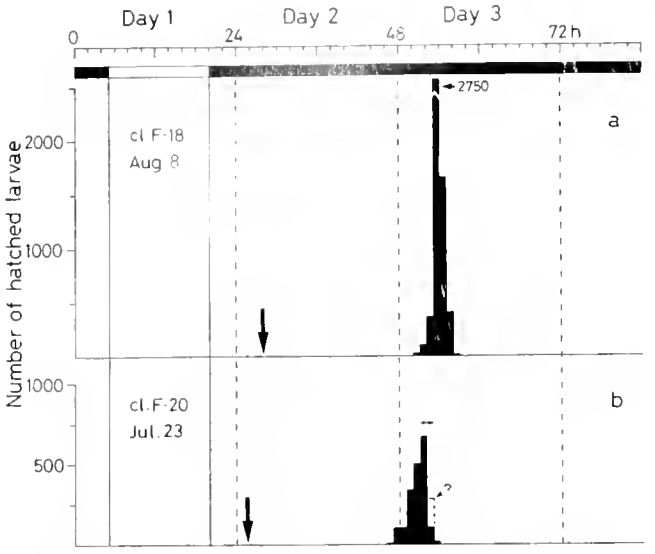

Figure 7B. Distribution of hatching in the transplanted embryos in vigorous aeration: (*a*) cl:F-18; (*b*) cl:F-20. The release of larvae by the host females (F-17, F-19) is shown by a downward arrow. (Egg masses dropped from the cluster at the time indicated by the horizontal arrow, and hatching could not be perfectly monitored during this period.) The other transplanted clusters from Figure 7A (cl:F-22, cl:F-24, cl:F-26) hatched one night later (hourly data not obtained).

female (F-41) released their larvae. The cluster (cl:F-42) also hatched two nights after the aeration. Since no hatching was observed in the control experiment (ae:F-42), hatching of cl:F-42 can be regarded as having been induced by the host female (F-41).

The possibility that egg-clusters kept under aerated conditions for more than three nights after detachment may lose their ability to hatch was then tested. In Figure 9D, a cluster (cl:F-43) was detached from a female and placed in aeration for five days. This cluster was then transplanted to another female (F-44). This cluster hatched in synchrony with the attached eggs of the host female F-44. Similar results were obtained in another experiment (not illustrated). Thus, eggs that were detached and transferred into aeration retained their ability to hatch. Hatching was obviously inhibited under aerated conditions.

The interaction between the female and transplanted embryos was also examined. A few clusters were covered with a skirt made of thin cellophane. This skirt was open at the bottom, ensuring an interchange of water at the surface of the eggs. As seen in Figure 10, the transplanted clusters were induced to hatch (upper left in each panel). But the hatching profiles of the egg-clusters that were transferred into aeration (Fig. 10) showed a somewhat different pattern. In these three experiments, the cluster hatched in two peaks, about 24 h apart. Almost all of the eggs hatched in one experiment (Fig. 10-a), but many eggs failed to hatch in the other two (Fig. 10-b-c). These results are difficult to interpret; one possible explanation is that the stimuli recognized by the embryos are attenuated by the cellophane, which caused the occurrence of two peaks and the decrease of the number of larvae hatched. In any event, such a splitting of the hatching pattern has never been observed in intact females.

Does the hatching of transplanted clusters affect the day or the time of hatching of eggs attached to the host female? For example, the hatching of the transplanted cluster (Figs. 5A, 6A) might release a stimulus that acts on the female to disturb the time of hatching or to advance the day of hatching of the female-attached eggs. To examine the former possibility, the time of day of larval release by host females (except the females whose eggs had dropped) was monitored with the event recorder. As shown in Figure 11, the larval release of these females coincided roughly with the time of night high water in the field, showing a clear circa-tidal rhythm. This suggests that at least the daily timing of egg hatching was not disturbed, either by the exchange of embryos or by the hatching of the transplanted eggs.

To examine whether the hatching of transplanted egg-clusters advances the date of hatching in the host female, the number of nights between the larval release of paired females was compared with respect to differences between *Pattern II* and *Pattern III*. The range was 0–9 days in *Pattern III* (25 pairs), but only 0–4 days in *Pattern II* (19 pairs with no egg loss). Since the experimental crabs were chosen randomly, this difference might suggest that hatching of the transplanted cluster can advance the day of hatching in the host female.

Discussion

The embryos of most marine crustaceans are incubated by the female for a certain period before hatching. An endogenous factor has been suggested as operating in the hatching rhythms of many kinds of marine animals (Saigusa, 1992c). But does the endogenous component controlling rhythmicity occur within the embryo, its mother, or both? To answer this question, larval hatching must be examined, not only in the embryo, but also in the female. Although the embryos of crustaceans are attached to non-plumose setae by a funiculus that is possibly composed of chorion, there is no circulation of blood between embryo and mother (Yonge, 1937, 1946; Cheung, 1966; Goudeau and Lachaise, 1983). Thus, the embryo exchange experiments were aimed at revealing the site of the endogenous clock.

An endogenous clock times hatching in each embryo

The present experiments were primarily aimed at determining whether the implanted embryos would hatch

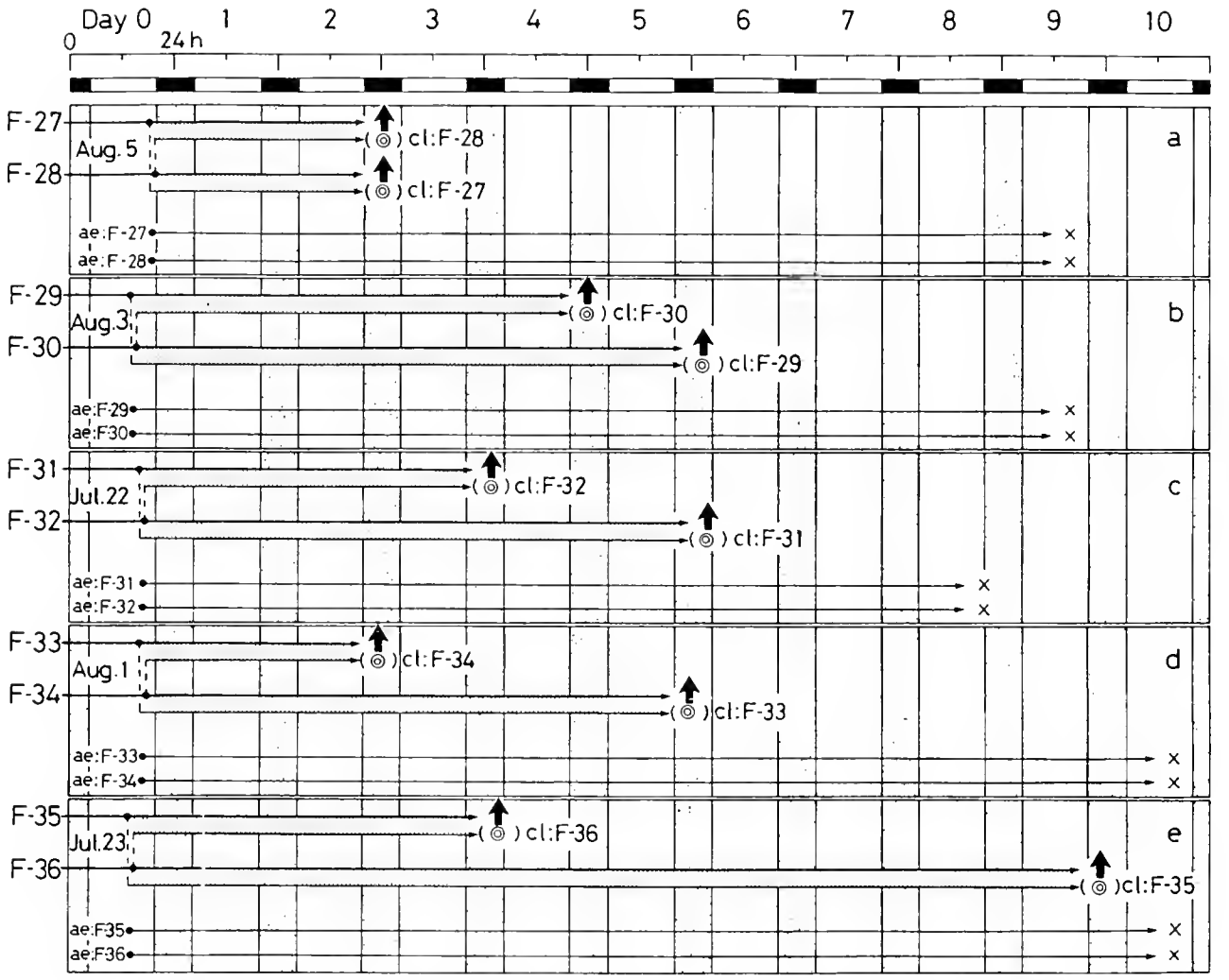

Figure 8. Induction of hatching in the transplanted cluster of embryos; *Pattern III* (*a*) Embryo exchange between females F-27 and F-28. Detachment and exchange of clusters: 19:20–19:40 on 5 August. Larval release: F-27, at 0:30 on 8 August; F-28, at 0:40 on 8 August. (*b*) Embryo exchange between F-29 and F-30 at 14:45–15:10 on 3 August. Larval release: F-29, at 0:35 on 8 August; F-30, at 3:05 on 9 August. (*c*) Embryo exchange between F-31 and F-32 at 16:30–17:00 on 22 July. Larval release: F-31, at 2:10 on 26 July; F-32, at 3:20 on 28 July. (*d*) Embryo exchange between F-33 and F-34 at 16:25–16:45 on 1 August. Larval release: F-33, at 23:35 on 3 August; F-34, at 23:50 on 6 August. (*e*) Embryo exchange between F-35 and F-36 at 14:15–14:40 on 23 July. Larval release: F-35, at 3:40 on 27 July; F-36, at 22:40 on 1 August. Symbols the same as in Figure 5A.

synchronously with the attached embryos of the host female. A potential procedural problem remaining is that the transplanted embryos were exposed to light, although for only 5 min, to determine whether hatching had occurred. Hatching could have been induced by the direct influence of this light, *e.g.*, like the oviposition of the teleost *Oryzias* (Egami, 1954; Ueda and Oishi, 1982). To reduce the effect of light, transplanted clusters were removed from the female, and subsequent procedures involving aeration were carried out under red light. The hatching pattern under red light was similar to that of an egg-cluster exposed to normal light. Furthermore, the peak of hatching occurred about 24 or 48 h after the transplanted egg-clusters had been transferred into aeration, even in constant darkness (Figs. 5B-b, 6B-a-b, 7B-a-b). These peaks must have been induced by an *endogenous* rhythm existed in embryo itself, and not caused by the light used during examination of hatching or by 24-h LD cycles.

Like hatching, pupation, and emergence, many aspects of development occur only once in the life cycle of an animal (Saunders, 1976). Whether the timing of those phenomena is controlled by an endogenous pacemaker can be examined in a population of mixed age *e.g.*, the

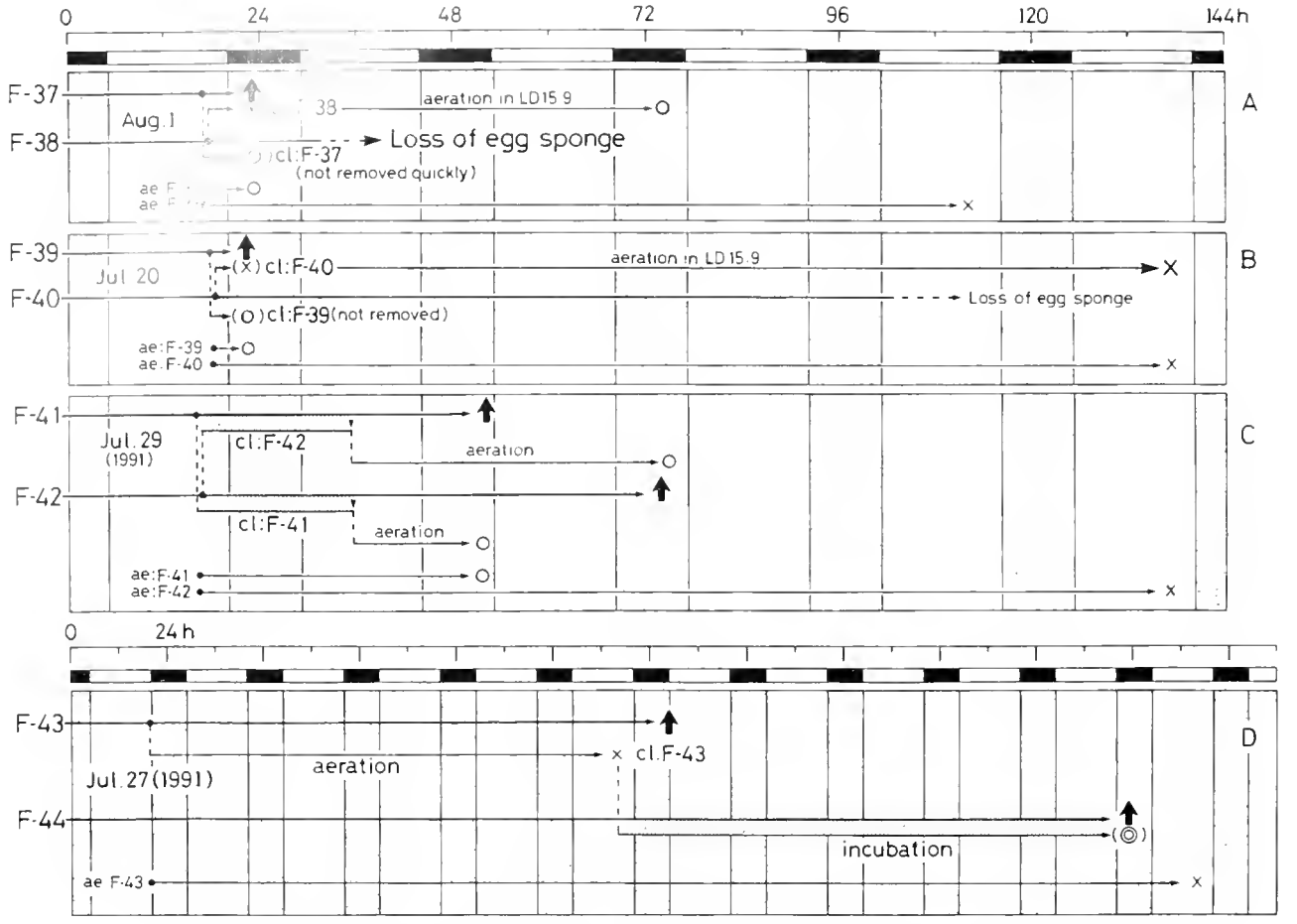

Figure 9. Hatching profile of transplanted clusters. (*A*) Loss of the egg sponge by the host female. Embryo exchange between females F-37 and F-38 at 16:10–16:25 on 1 August. Larval release: F-37, at 23:35 on 1 August. (*B*) Failure to induce hatching. Embryo exchange between females F-39 and F-40 at 17:50–18:20 on 20 July. Larval release: F-39, at 22:30 on 20 July. (*C*) Removal of the transplanted cluster before the release of the host female. Embryo exchange between females F-41 and F-42 at 16:05–16:25 on 29 July. Larval release: F-41, at 3:45 on 31 July; F-42, at 1:35 on 1 August. (*D*) Hatching of the egg-cluster kept in aeration for five days. Detachment of cl:F-43, at 19:50 on 27 July; binding to F-44, at 16:20 on 1 August. Larval release: F-43, at 4:55 on 2 August; F-44, at 23:10 on 6 August.

circadian rhythm of emergence in the fly *Drosophila* (Pittendrigh and Bruce, 1959). But the validity of using such a population to demonstrate a circadian rhythm has been questioned (Saunders, 1976, chapter 3). So Pittendrigh and Skopik (1970) used populations that were developmentally synchronous at pupation to study the emergence rhythm in the fly *Drosophila pseudoobuscura*, and suggested that a circadian pacemaker in each developing fly dictates the circadian time of *emergence*, but not that of the intermediate developmental stages, such as head eversion and eye pigmentation.

The eggs of *Sesarma haematocheir* are oviposited within a short time. So the developmental embryos incubated by a female clearly do not constitute a mixed-age population. Like the data presented by Pittendrigh and Skopik (1970), the hatching of the egg clusters removed from the host females was often split into two distinct peaks almost 24 h apart (Figs. 6b-e, 10a-c). To explain such a splitting of hatching pattern, we can assume an *allowed* zone (see Pittendrigh and Skopik, 1970) related to hatching in the endogenous pacemaker of each embryo. In Figure 12, this zone is expressed by the acrophase (shown by a dot) in the embryo's pacemaker. The preceding paper (Saigusa, 1992c) indicated that each embryo undergoes a hatching process that continues for 48–49.5 h prior to egg-membrane breakage. If the embryos were detached from the female early enough that this time interval were exceeded, hatching would not occur. One speculation is that, in the larval hatching rhythm in *Sesarma*, a gated phenomenon occurs at the start of the

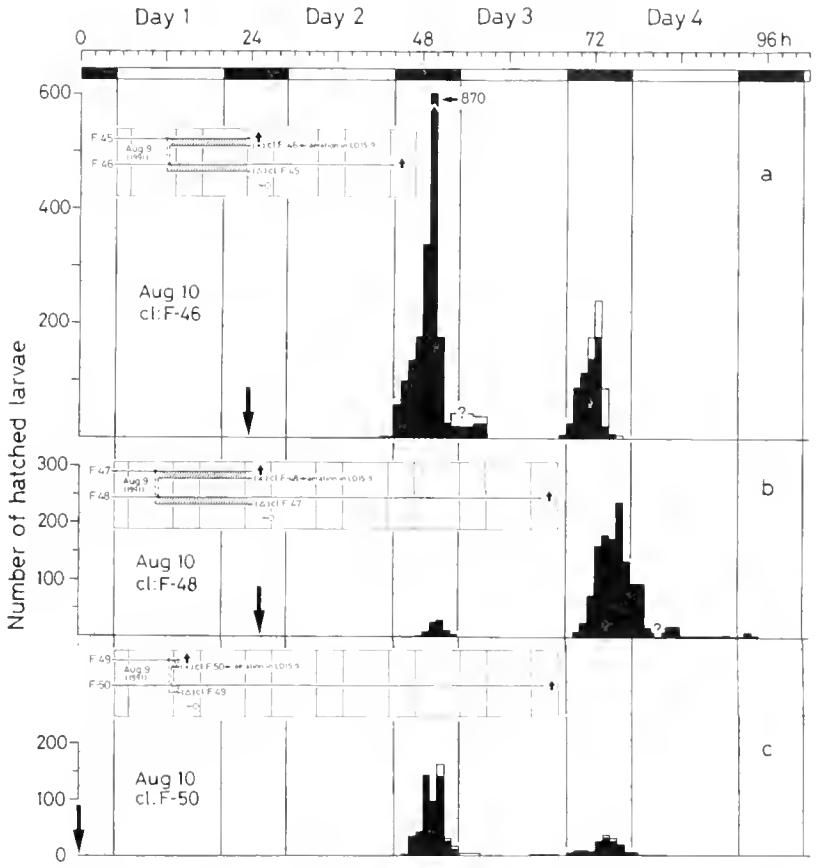

Figure 10. Hatching of egg-clusters from which the cellophane skirt was removed before transfer into aeration. (*a*) Hatching of cl:F-46. Embryo exchange between F-45 and F-46 at 17:25–17:40 on 9 August. Larval release: F-45, at 23:45 on 10 August; F-46, at 23:50 on 12 August. (*b*) Hatching of cl:F-48. Embryo exchange between F-47 and F-48 at 14:25–14:35 on 9 August. Larval release: F-47, at 1:30 on 11 August; F-48, at 1:50 on 15 August. (*c*) Hatching of cl:F-50. Embryo exchange between F-49 and F-50 at 19:10–19:20 on 9 August. Larval release: F-49, at 0:20 on 10 August; F-50, at 2:20 on 15 August. Downward arrows indicate time of day of release by the host females.

hatching process, and not hatching itself. If the hatching process is not initiated at a certain acrophase (Fig. 12), the embryos must wait until the next allowed zone to start the process.

Induction of hatching in the transplanted cluster

While each embryo has an endogenous rhythm of hatching, the present study indicates that the hatching of exchanged clusters is *induced* by the host female, provided that the incubation was longer than 5–6 h (compare Figs. 6A, 7A and 9B). Since the start of the hatching process may be a gated event, it is reasonable to speculate that this process begins 48–49.5 h before the hatching, responding to some signal to each embryo. But we do not know *what* stimuli trigger the hatching process in each embryo. One possibility is mechanical stimuli generated by the female—perhaps some special movements of the abdomen or ovigerous setae as the embryonic development is completed. Another possibility is a hatch-inducing substance, produced by the female and recognized by the embryos. We also do not know *when* hatch-inducing stimuli are released from the female. Females could generate such stimuli at any time of day, or at a particular phase of her circatidal rhythm (see the question mark on the female pacemaker in Fig. 12).

Synchronization of hatching between transplanted embryos and female-attached embryos

For most intertidal and estuarine crustaceans, female-attached eggs hatch within a very short period, although the exact duration cannot be determined because of the mass. In *S. haematocheir*, hatching is completed in 5–30 min in each female (Saigusa, 1992b). Because the hatching synchrony of the embryos detached from the female is perturbed (Saigusa, 1992c), some mechanism must underlie the highly-synchronous hatching in female-attached eggs. This cannot be an endogenous clock in each embryo;

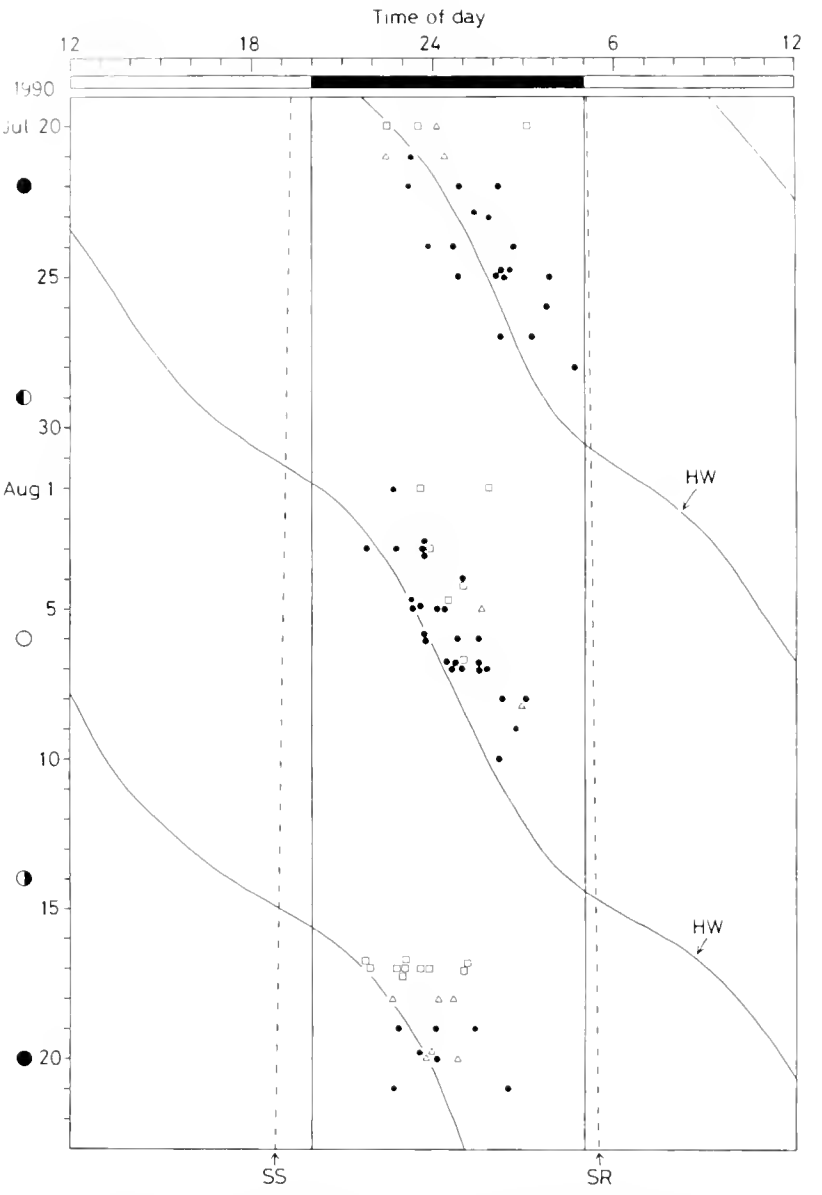

Figure 11. Time of day of larval release by females carrying an exchanged cluster and by females from which the cluster had been removed. Records were made in the laboratory under 24-h LD cycle, but under no tidal influence. Solid diagonal lines connect the times of high water (*HW*) in the field. □: larval release on the first night of embryo exchange. △: larval release on the second night after embryo exchange. ●: larval release occurs more than three nights after the embryo exchange. *ss* and *sr* connect the times of sunset and sunrise, respectively.

the female must produce some unknown stimulus that enhances synchronous hatching.

Females of *S. haematocheir* release their larvae with vigorous abdominal movements. This same behavior is observed in other terrestrial crabs (Saigusa, 1981). In species that release their larvae under the water, the release is effected by the pumping behavior of the abdomen (DeCoursey, 1979; Forward *et al.*, 1982; Saigusa, 1992a). Forward and Lohmann (1983) suggested that this behavior enhances hatching synchrony. In contrast, hatching in terrestrial species occurs prior to larval release. Clearly, larval release behavior itself does not enhance the hatching synchrony in female-attached embryos. One possible mechanism is that the female kneads the egg-clusters several times around the time of night high tide. In addition to such physical stimuli, the hatching of a few embryos might release a substance like the hatching enzyme suggested by De Vries and Forward (1991), and thus stimulate the hatching of the remaining embryos.

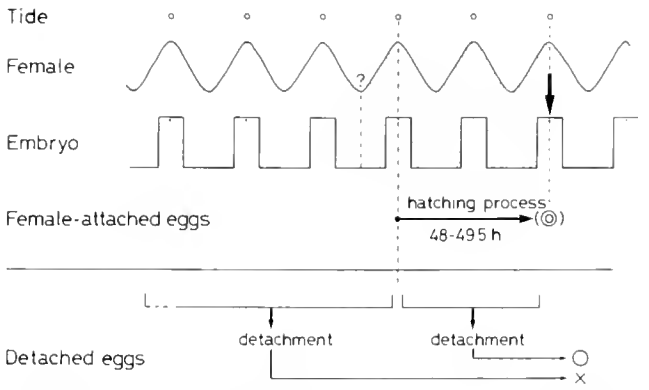

Figure 12. Proposed mechanism of induction of hatching and synchronization of hatching with nocturnal high water. Endogenous pacemakers related to hatching are shown with by a sine curve (female) and a rectangle (embryo). Small circle above the female's pacemaker indicates time of nocturnal high water. Stippled area: stimuli that induce the hatching process in each embryo are released during this period. The heavy downward arrow represents stimuli by the female to enhance hatching synchrony among embryos. The success of hatching in detached embryos is shown under the horizontal line. See the text for details.

Timing mechanism of hatching: a hypothesis (Fig. 12)

As in most other decapods, the oviposited eggs of *S. haematocheir* are incubated by the female until hatching occurs. Most of this period is probably related to embryonic development. But hatching does not immediately follow the completion of development; *i.e.*, embryos wait for stimuli that initiate the hatching process. So when the eggs are detached from the female during this period, hatching should be inhibited. As demonstrated in this study, one or more hatch-inducing stimuli are produced by the female. But once these signals have been received, the start of the hatching process would be determined by an endogenous clock within each embryo.

We can assume that a self-sustained oscillation underlies most endogenous rhythms (Pittendrigh and Bruce, 1959). As shown in Figure 12, we can express the embryo's pacemaker for hatching as a rectangular wave with 24.5-h period. Similarly, females would also have 24.5-h pacemaker for hatching and larval release. Both pacemakers would be synchronized with nocturnal high tide in the field. Since eggs that are detached from the female more than 48–49.5 h before hatching of the female-attached eggs do not hatch, the "allowed zone" related to the start of this process should be positioned at the phase corresponding to the time of nocturnal high tide, *i.e.*, the acrophase of the embryo's pacemaker in Figure 12. When some (unknown) stimuli (stippled area in Fig. 12) have been transmitted to the embryos for several hours (at least more than 5–6 h), the hatching process starts at this phase, and zoeas hatch 48–49.5 h later; *i.e.*, around the time of nocturnal high tide. If the stimuli from the female are insufficient to start the hatching process, embryos must wait for the next acrophase. This would have resulted in the split hatching peaks seen in vigorously aerated dilute seawater (Figs. 6B-e and 10 a-c).

As shown in the lower diagram of Figure 12, if the embryos are detached from a female before the hatching process, they would not hatch at all. If they are separated from a female while the hatching process is in progress, then those embryos will hatch at about the same time as the embryos that remain attached to the female. But hatching synchrony is perturbed in this condition, so the process is extended by several hours (Saigusa, 1992c). Since female-attached eggs hatch synchronously, the females must have some mechanism (a downward arrow in Fig. 12) for enhancing hatching synchrony while they are still on the hillside awaiting the time of hatching.

Acknowledgments

The zoea larvae found after hatching were counted by Mr. A. Shiomi and Miss H. Yunoki, students of Okayama University. They also helped with some of the daytime procedures, such as exchanging clusters, placing females in the recording apparatuses, and collecting ovigerous females. Supported by a Grant-in-Aid for Scientific Research (C) (No. 02640582) from the Ministry of Education, Science and Culture.

Literature Cited

Cheung, T. S. 1966. The development of egg-membranes and egg attachment in the shore crab, *Carcinus maenas*, and some related decapods. *J. Mar. Biol. Assoc. U.K.* **46:** 373–400.

DeCoursey, P. J. 1979. Egg-hatching rhythms in three species of fiddler crabs. Pp. 399–406 in *Cyclic Phenomena in Marine Plants and Animals*, E. Naylor and R. G. Hartnoll, eds. Pergamon Press, Oxford.

DeCoursey, P. J. 1983. Biological timing. Pp. 107–162 in *The Biology of Crustacea VII. Behavior and Ecology*, F. J. Vernberg and W. B. Vernberg, eds. Academic Press, New York.

De Vries, M. C., and R. B. Forward, Jr. 1991. Mechanisms of crustacean egg hatching: evidence for enzyme release by crab embryos. *Mar. Biol.* **110:** 281–291.

Egami, N. 1954. Effect of artificial photoperiodicity on time of oviposition in the fish, *Oryzias latipes*. *Annot. Zool. Jpn.* **27:** 57–62.

Forward, R. B., Jr., K. Lohmann, and T. W. Cronin. 1982. Rhythms in larval release by an estuarine crab (*Rhithropanopeus harrisii*). *Biol. Bull.* **163:** 287–300.

Forward, R. B., Jr., and K. J. Lohmann. 1983. Control of egg hatching in the crab *Rhithropanopeus harrisii* (Gould). *Biol. Bull.* **165:** 154–166.

Goudeau, M., and F. Lachaise. 1983. Structure of the egg funiculus and deposition of embryonic envelopes in a crab. *Tissue Cell* **15:** 47–62.

Korringa, P. 1947. Relations between the moon and periodicity in the breeding of marine animals. *Ecol. Monogr.* **17:** 347–381.

Minis, D. H., and C. S. Pittendrigh. 1968. Circadian oscillation controlling hatching: its ontogeny during embryogenesis of a moth. *Science* **159:** 534–536.

Pearse, J. S. 1990. Lunar reproductive rhythms in marine invertebrates: maximizing fertilization? Pp. 311–316 in *Advances in Invertebrate*

Reproduction 5, M. Hoshi and O. Yamashita, eds. Elsevier Science Publishers B. V.

Pittendrigh, C. S., and V. G. Bruce. 1959. Daily rhythms as coupled oscillator systems and their relation to thermoperiodism and photoperiodism. Pp. 475–505 in *Photoperiodism and Related Phenomena in Plants and Animals*, R. B. Withrow, ed. American Association for the Advancement of Science, Washington, DC.

Pittendrigh, C. S., and S. D. Skopik. 1970. Circadian systems, V. The driving oscillation and the temporal sequence of development. *Proc. Natl. Acad. Sci. U.S.A.* **65:** 500–507.

Pittendrigh, C. S., and D. H. Minis. 1971. The photoperiodic time measurement in *Pectinophora gossypiella* and its relation to the circadian system in that species. Pp. 212–250 in *Biochronometry*, M. Menaker, ed. National Academy of Sciences, Washington.

Saigusa, M. 1981. Adaptive significance of a semilunar rhythm in the terrestrial crab *Sesarma*. *Biol. Bull.* **160:** 311–321.

Saigusa, M. 1992a. Phase shift of a tidal rhythm by light-dark cycles in the semi-terrestrial crab *Sesarma pictum*. *Biol. Bull.* **182:** 257–264.

Saigusa, M. 1992b. Observations on egg hatching in the estuarine crab *Sesarma haematocheir*. *Pac. Sci.* **46:** 484–494.

Saigusa, M. 1992c. Control of hatching in an estuarine terrestrial crab. I. Hatching of embryos detached from the female and emergence of mature larvae. *Biol. Bull.* **183:** 401–408.

Sastry, A. N. 1983. Pelagic larval ecology and development. Pp. 213–282 in *The Biology of Crustacea, Vol. VII. Behavior and Ecology*, F. J. Vernberg and W. B. Vernberg, eds. Academic Press, New York.

Saunders, C. S. 1976. *Insect Clocks*, Pergamon Press, Oxford. 279 pp.

Ueda, M., and T. Oishi. 1982. Circadian oviposition rhythm and locomotor activity in the medaka, *Oryzias latipes*. *J. Interdiscipl. Cycle Res.* **13:** 97–104.

Yonge, C. M. 1937. The nature and significance of the membranes surrounding the developing eggs of *Homarus vulgaris* and other Decapoda. *Proc. Zool. Soc. Lond., Ser. A* **107:** 499–517 (plus 1 plate page).

Yonge, C. M. 1946. Permeability and properties of the membranes surrounding the developing egg of *Homarus vulgaris*. *J. Mar. Biol. Assoc. U.K.* **26:** 432–438.

Reference: *Biol. Bull* **184**: 203–208. (April, 1993)

Asymmetry in Male Fiddler Crabs is Related to the Basic Pattern of Claw-waving Display

SATOSHI TAKEDA[1] AND MINORU MURAI[2]

[1]*Marine Biological Station, Tohoku University, Asamushi, Aomori 039-34, Japan and* [2]*Department of Biology, Faculty of Science, Kyushu University, Hakozaki, Fukuoka 812, Japan*

Abstract. Morphological asymmetry was correlated with the pattern of claw-waving display in males from five species of fiddler crabs: three vertical wavers (*Uca urvillei, U. dussumieri, U. vocans*), a lateral waver (*U. annulipes*), and an intermediate waver (*U. tetragonon*). On the first, second and third ambulatory legs of male lateral waver crabs, the distance between the inner edge of the basis and the outer edge of the merus was larger on the side bearing the major cheliped than it was on the side with the minor cheliped. A similar asymmetry was observed in male intermediate waver crabs, but only the first ambulatory leg was involved. This morphological asymmetry is clearly related to the style of waving adopted by these crabs. When lateral wavers display, the weight of the major cheliped (which forms about one-third of the total body weight) is carried largely by the anterior ambulatory legs on the same side of the body, but the imbalance of weight during display is less in the intermediate waver. In the vertical waver crab horizontal motion of the major cheliped occurs relatively rarely; thus there is hardly any additional load on the ambulatory legs, which showed no asymmetry.

However, the total length of the five sterna bearing thoracic legs tended to be larger on vertical waver males than on the female crabs. Thus the sterna of male crabs bulge outwards more than those of female crabs, and the angle between the sternum bearing the cheliped and the ground surface is larger in male crabs than in females. This may be an adaption enabling the cheliped of the male to be raised higher during the waving display.

Introduction

A characteristic feature of the genus *Uca* (Ocypodidae; Brachyura) is hypertrophy of one of the male chelipeds, resulting in a striking asymmetry (Crane, 1975). The hypertrophic, or major, cheliped plays a very important role in antagonistic and courtship behaviors (Crane, 1957, 1975), especially as a distinctive indicator of the male sex during the breeding season (Salmon and Stout, 1962).

The mechanism determining which of the chelipeds becomes hypertrophic has been examined in some species (Morgan, 1923, 1924; Yamaguchi, 1977; Ahmed, 1978), and the development of the asymmetry has been analyzed by monitoring the growth rate of the major cheliped relative to that of the carapace (Huxley and Callow, 1933; Tazelaar, 1933; Miller, 1973). In addition, the first and second ambulatory legs are longer on the side bearing the major cheliped than they are on the contralateral side in male *U. pugilator* (Yerkes, 1901; Duncker, 1903; Huxley and Callow, 1933; Miller, 1973), and in *U. pugnax* (Yerkes, 1901; Tazelaar, 1933) in North America. This asymmetry of the ambulatory legs was thought to help in raising the major cheliped higher, thus displaying it to more crabs (Miller, 1973).

Crane (1957, 1975) divided *Uca* into two groups based on the male's claw-waving display; *i.e.,* into vertical and lateral waving species. *U. pugilator* and *U. pugnax,* with asymmetry of the ambulatory legs as well as the chelipeds, form the lateral waving group (Crane, 1957, 1975). On the other hand, the ambulatory legs of male crabs of the vertical waving group have not yet been examined for possible asymmetries.

In this study, the degree of asymmetry of certain morphological characters, including the length of the ambulatory legs, was determined and compared among five species of *Uca* with different patterns of claw-waving display. Three of the five species were vertical wavers, one species was a lateral waver, and one exhibited an intermediate type of waving display.

Received 5 November 1992; accepted 25 January 1993.

Materials and Methods

Crabs of five species, *U. urvillei*, *U. dussumieri*, *U. vocans*, *U. tetragonon* and *U. annulipes*, were collected on the seashores in Thailand (Table I). Larger individuals were selected for examination, since the degree of asymmetry in male fiddler crabs increases with body growth (Miller, 1973). Crabs lacking thoracic legs or those with degenerate, atypical thoracic legs were excluded.

U. urvillei, *U. dussumieri* and *U. vocans* are vertical wavers, *U. annulipes* is a lateral waver, and *U. tetragonon* is an intermediate (Crane, 1957, 1975). The proportion of right-handed and left-handed male crabs was nearly equal in *U. urvillei*, *U. dussumieri* and *U. annulipes*, and almost all male *U. vocans* and *U. tetragonon* are right-handed (Takeda and Yamaguchi, 1973; Frith and Frith, 1977).

Two indices of body-size were measured: carapace width (Fig. 1A); and the whole body wet-weight. The wet weight of the cheliped cut off between ischium and basis was also measured. Several morphological measurements were made (Fig. 1). These measurements on the right and left side of each individual include: three dimensions on the minor cheliped or ambulatory leg (Fig. 1B); body depth (Fig. 1A); carapace depth (Fig. 1A); and the length of each sternum bearing thoracic legs (Fig. 1C).

These measured values were normalized with respect to the wet-weight or carapace width. To determine the degree of asymmetry, the ratio of the values on the major cheliped side to the values on the opposite side in male crabs, and the ratio of the values on the right side to those on the left side in female crabs, were calculated for each individual. These data were examined for significance with Student's *t*-test.

Results

The carapace width and body wet-weight of individuals differed among the five species of *Uca* (Table II).

The weight of the major cheliped relative to the whole body wet-weight increased in the following order: *U. tetragonon* ≦ *U. dussumieri* ≦ *U. urvillei* ≦ *U. annulipes* ≦ *U. vocans* (Table III). The relative weight did not differ widely among the species of vertical, intermediate, and lateral wavers. The relative weight of the minor cheliped did not differ significantly ($P > 0.05$) among individuals of the same sex in four species, but *U. tetragonon* had a larger minor cheliped than the other four species ($P < 0.05$).

The relative dimensions of the minor chelipeds were larger in female crabs than in male crabs in each species ($P < 0.05$). The smaller values in male crabs resulted from their larger whole body wet-weight, which included the weight of the major cheliped.

The chelipeds of male crabs had a remarkable asymmetry ($P < 0.001$), and the ratio of major cheliped weight to minor cheliped weight increased in the order of *U. tetragonon* < *U. annulipes* ≦ *U. dussumieri* ≦ *U. urvillei* ≦ *U. vocans*. The smaller ratio in male crabs of *U. tetragonon* ($P < 0.05$) was caused by their having heavier minor chelipeds than the other four species. However, the intensity of asymmetry did not differ among the species with the different display patterns. In female crabs of all five species, the asymmetry ratio was near 1.0, which indicates the chelipeds were the same size.

Considering the total length of the ambulatory legs, which was calculated by adding the lengths of the I, II and III-sections of each ambulatory leg (Fig. 1B), asymmetry was perceptible ($P < 0.05$) only in first (ratio = 1.04 ± 0.02 (mean ± the 95% confidence interval)) and second ambulatory legs (ratio = 1.02 ± 0.01) of male *U. annulipes* (Fig. 2), and the ambulatory legs of the side bearing the major cheliped were longer than those of the opposite side. Moreover, for each section of the ambulatory legs, asymmetry was present in the I-section of the first, second and third ambulatory legs of male *U.*

Table I

Materials, display form and handedness in Uca *spp.*

Species	Display	Handedness	Specimens	Location	Date
U. urvillei	vertical	random	6 males 7 females	Ao Nam Bor[1]	1990. Sep.
U. dussumieri	vertical	random	9 males 9 females	Smare Kaow[2]	1987. Oct.
U. vocans	vertical	right	8 males 6 females	Ao Nam Bor[1]	1990. Sep.
U. tetragonon	intermediate	right	11 males 9 females	Ao Tang Khen[3]	1990. Sep.
U. annulipes	lateral	random	10 males 6 females	Ao Nam Bor[1] Ao Tang Khen[3]	1990. Sep. 1991. Jan.

[1] 7°50′ N; 98°24′ E
[2] 13°28′ N; 100°55′ E
[3] 7°44′ N; 98°25′ E

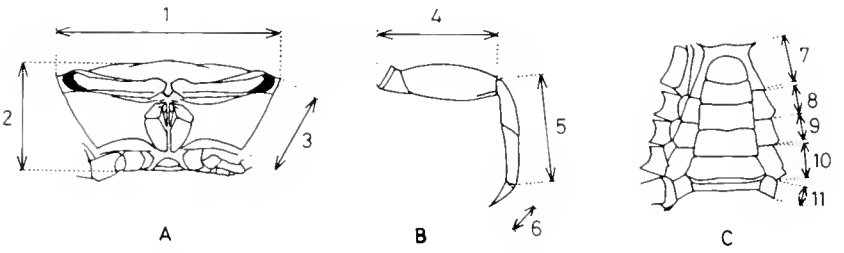

Figure 1. Diagrams of frontal view of carapace (A), ventral surface of left ambulatory leg (B), ventral view of male crab (C), and dimensions measured in this study. (1) carapace width: the minimum distance between both tips of the anterolateral angles. (2) body depth: the minimum distance between the carapace and a straight line in contact with the plane of the sterna with the first and second ambulatory legs. (3) carapace depth: the minimum distance between the tip of one anterolateral angle and the edge of the buccal region on the side of the Milne-Edwards opening. (4) I-section: the minimum distance between the inner edge of the basis and the outer edge of the merus of the thoracic legs. (5) II-section: the minimum distance between the inner edge of the carpus and the outer tip of the propodus of the thoracic legs. (6) III-section: the minimum distance between the inner edge and the tip of the dactylus of the ambulatory legs. (7), (8), (9), (10), and (11) the length of each sternum with cheliped, first, second, third and fourth ambulatory leg, respectively.

annulipes ($P < 0.001$), and in the I-section of the first ambulatory legs only of male *U. tetragonon* ($P < 0.01$). The asymmetry ratios of *U. annulipes* male crabs were 1.09 ± 0.01, 1.06 ± 0.02 and 1.05 ± 0.02, and the degree of asymmetry decreased posteriorly. The ratio for male *U. tetragonon* was 1.02 ± 0.01.

Total lengths of the minor cheliped and the first ambulatory leg on minor cheliped side tended to be greater in males than in females, and the difference was significant ($P < 0.05$) in *U. dussumieri*, *U. tetragonon* and *U. annulipes* for the minor chelipeds, and in *U. dussumieri* and *U. tetragonon* for the first ambulatory legs (Fig. 2). In addition, the same tendency ($P > 0.05$) was observed for the total length of the second ambulatory leg in the four species other than *U. annulipes*. The total length of the third ambulatory legs did not differ between male and female crabs. The total length of the fourth ambulatory leg was greater in female *U. tetragonon* than in male crabs ($P < 0.05$).

The body depths of male crabs were larger on the major cheliped side than on the other side ($P < 0.001$) (Table IV). The asymmetry ratios were between 1.05 and 1.07 for all species, indicating no difference between the species. The body depths of female crabs of all five species were symmetrical ($P < 0.05$).

The relative body depths on the major cheliped side of male crabs were larger than those of female crabs ($P < 0.05$). The relative body depth on the side bearing the minor cheliped in male crabs showed a similar tendency, especially in *U. dussumieri* and *U. tetragonon* ($P < 0.05$).

Table II

Carapace width and wet weight in Uca *spp.*

Species	Carapace width (mm)		Wet weight (g)	
	Male	Female	Male	Female
U. urvillei	25.19 ± 1.43 (23.40–26.75)	23.07 ± 1.49 (20.85–25.35)	5.030 ± 0.709 (4.115–6.169)	2.989 ± 0.604 (2.309–4.136)
U. dussumieri	29.80 ± 1.18 (27.65–32.85)	23.31 ± 1.03 (21.70–24.95)	9.273 ± 1.161 (7.371–12.553)	3.490 ± 0.508 (2.680–4.646)
U. vocans	23.05 ± 0.63 (22.15–24.55)	17.17 ± 0.66 (16.15–18.05)	5.503 ± 0.298 (4.865–5.930)	1.487 ± 0.294 (1.191–1.955)
U. tetragonon	21.00 ± 0.87 (19.40–23.35)	21.03 ± 0.93 (19.10–22.95)	3.754 ± 0.563 (2.956–5.465)	3.090 ± 0.339 (2.333–3.605)
U. annulipes	15.49 ± 0.79 (14.35–17.50)	11.98 ± 0.60 (10.95–12.50)	1.319 ± 0.229 (0.978–1.910)	0.437 ± 0.048 (0.355–0.495)

Mean ± the 95% confidence interval.
Numbers in parentheses indicate the range.

Table III

Weight of chelipeds relative to whole body wet-weight in Uca *spp.*

Species	Male crab		Female crab	
	Major side	Minor side	Right side	Left side
U. urvillei	0.366 ± 0.047 (31.48 ± 7.15)*	0.012 ± 0.001	0.016 ± 0.001 (1.02 ± 0.04)	0.016 ± 0.001
U. dussumieri	0.358 ± 0.015 (31.07 ± 2.12)*	0.012 ± 0.001	0.015 ± 0.001 (1.01 ± 0.07)	0.015 ± 0.001
U. vocans	0.432 ± 0.034 (40.18 ± 4.35)*	0.011 ± 0.000	0.015 ± 0.002 (0.98 ± 0.04)	0.016 ± 0.001
U. tetragonon	0.340 ± 0.013 (17.58 ± 1.13)*	0.019 ± 0.001	0.022 ± 0.001 (1.01 ± 0.02)	0.022 ± 0.001
U. annulipes	0.380 ± 0.032 (28.41 ± 4.41)*	0.014 ± 0.001	0.018 ± 0.001 (1.00 ± 0.00)	0.018 ± 0.001

* Student's *t*-test, $P < 0.001$.
Mean ± the 95% confidence interval.
Numbers in parentheses (mean ± the 95% confidence interval) indicate the asymmetry ratio based on weight (male crab = major cheliped side/minor cheliped side; female crab = right side/left side).

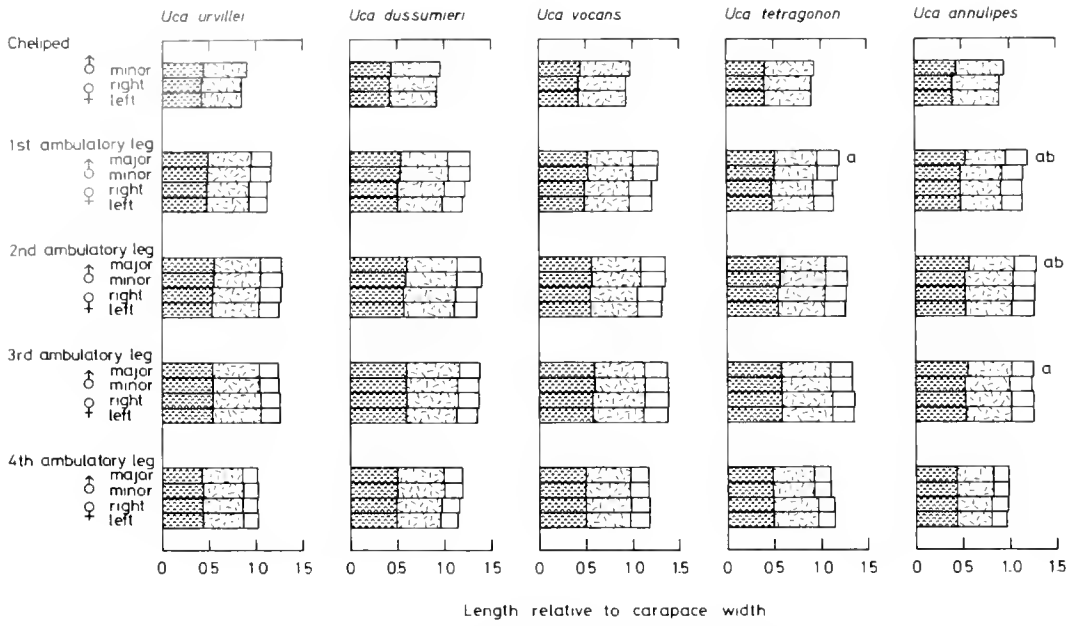

Figure 2. Length of the three sections of the thoracic leg relative to carapace width in *Uca* spp. Each bar shows the relative length of the I-, II- and III-section (Fig. 1B) from the left. (a), (b): asymmetry in the length of I-section of the thoracic leg and in the total length of the thoracic leg, respectively.

The carapace depths of crabs was symmetrical ($P < 0.05$) in both sexes of the four species other than in male *U. vocans* (Table V).

In the male crabs of all species, the sternum bearing the major cheliped was larger than that bearing the minor cheliped ($P < 0.001$), and the asymmetry ratios were between 1.16 and 1.19 (Fig. 3). The asymmetry is probably due to the hypertrophy of the coxa of the major cheliped, as indicated by the remarkable development of the propodus of the major cheliped (see Fig. 1C). In the male crabs of all species, the total length of the five sterna with thoracic legs was greater on the major cheliped side than it was on the opposite side, showing significant asymmetry ($P < 0.05$).

Male crabs of *U. urvillei*, *U. dussumieri* and *U. vocans* had larger major cheliped-bearing sterna than did female crabs of the same species ($P < 0.05$). But, there was no significant difference between male and female crabs of *U. tetragonon* and *U. annulipes* ($P > 0.05$).

The total length of the five sterna on the minor cheliped

Table IV

Length of body depth relative to carapace width in Uca *spp.*

Species	Male crab		Female crab	
	Major side	Minor side	Right side	Left side
U. urvillei	0.53 ± 0.01 (1.06 ± 0.01)*	0.50 ± 0.01	0.48 ± 0.01 (1.00 ± 0.01)	0.48 ± 0.01
U. dussumieri	0.58 ± 0.01 (1.07 ± 0.01)*	0.55 ± 0.01	0.52 ± 0.01 (1.00 ± 0.01)	0.52 ± 0.01
U. vocans	0.56 ± 0.01 (1.07 ± 0.01)*	0.53 ± 0.01	0.49 ± 0.02 (1.00 ± 0.01)	0.49 ± 0.03
U. tetragonon	0.56 ± 0.01 (1.05 ± 0.00)*	0.54 ± 0.01	0.51 ± 0.01 (1.00 ± 0.00)	0.51 ± 0.01
U. annulipes	0.55 ± 0.01 (1.05 ± 0.01)*	0.53 ± 0.01	0.52 ± 0.02 (1.00 ± 0.02)	0.52 ± 0.01

* Student's *t*-test, $P < 0.001$.

Mean ± the 95% confidence interval

Numbers in parentheses (mean ± the 95% confidence interval) indicate the asymmetry ratio (male crab = major cheliped side/minor cheliped side; female crab = right side/left side).

Table V

Length of carapace depth relative to carapace width in Uca *spp.*

Species	Male crab		Female crab	
	Major side	Minor side	Right side	Left side
U. urvillei	0.34 ± 0.01 (1.02 ± 0.02)	0.34 ± 0.01	0.32 ± 0.01 (1.00 ± 0.01)	0.33 ± 0.01
U. dussumieri	0.33 ± 0.01 (1.01 ± 0.01)	0.33 ± 0.01	0.32 ± 0.01 (1.00 ± 0.01)	0.32 ± 0.01
U. vocans	0.31 ± 0.01 (0.98 ± 0.01)*	0.32 ± 0.01	0.31 ± 0.01 (0.99 ± 0.01)	0.31 ± 0.01
U. tetragonon	0.31 ± 0.00 (1.00 ± 0.01)	0.32 ± 0.00	0.30 ± 0.00 (1.00 ± 0.00)	0.31 ± 0.00
U. annulipes	0.33 ± 0.00 (1.00 ± 0.01)	0.33 ± 0.00	0.32 ± 0.01 (1.00 ± 0.01	0.32 ± 0.00

* Student's *t*-test, $P < 0.05$.

Mean ± the 95% confidence interval.

Numbers in parentheses (mean ± the 95% confidence interval) indicate the asymmetry ratio (male crab = major cheliped side/minor cheliped side; female crab = right side/left side).

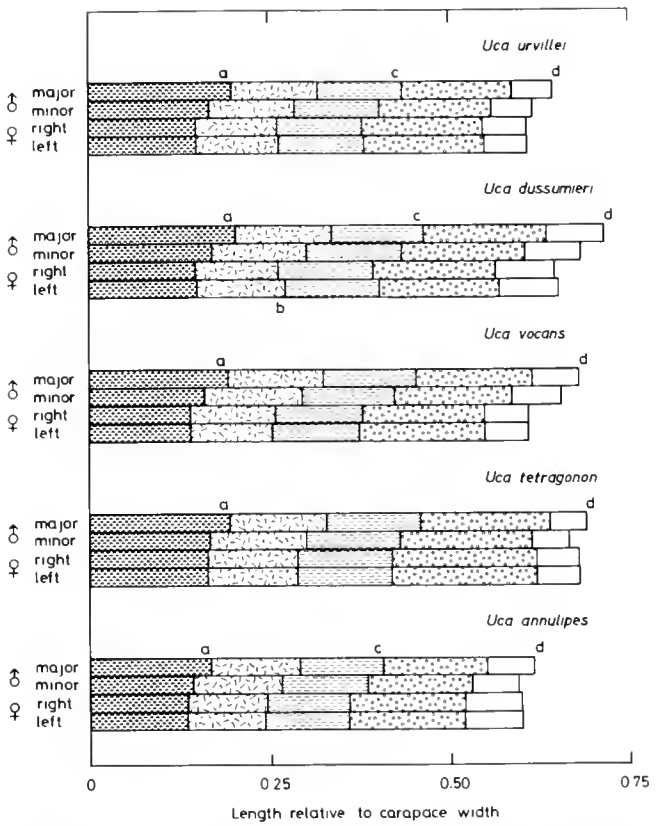

Figure 3. Length of each sternum bearing thoracic legs relative to carapace width in *Uca* spp. Each bar shows the relative length of the sternum bearing (from left to right) the cheliped, first, second, third and fourth ambulatory leg (Fig. 1C). (a), (b), (c), and (d) indicate asymmetry in the length of the sternum bearing the cheliped, first and second ambulatory leg, and in the total length of five sterna with thoracic legs, respectively.

side of male *U. dussumieri* and *U. vocans* tended to be larger than those of female crabs, and a similar, though weaker, tendency was observed in *U. urvillei*. The differences between the male and female crabs of *U. dussumieri* and *U. vocans* were caused by the male crabs having more extensive sterna bearing the cheliped and first ambulatory leg. The slight difference in the total length of the sterna of male and female *U. urvillei* was due to the smaller degree of enlargement of the sternum with the first ambulatory leg in male *U. urvillei*, compared with that of male *U. dussumieri* and *U. vocans*. On the other hand, female *U. tetragonon* and *U. annulipes* tended to have slightly longer sterna than the male crabs. This was because the sternum bearing the third ambulatory leg is remarkably larger in female crabs than in males, although the male crabs tended to have a larger sternum bearing the first ambulatory leg than did the female crabs.

Discussion

Male crabs of *U. annulipes*, which display with lateral waving, had longer first and second ambulatory legs on the major cheliped side than on the other side (Fig. 2), corresponding with the asymmetry reported for the lateral waver males of *U. pugilator* (Yerkes, 1901; Duncker, 1903; Huxley and Callow, 1933; Miller, 1973) and *U. pugnax* (Yerkes, 1901; Tazelaar, 1933). Moreover, comparing the major and minor cheliped sides, the l-sections of the first, second and third ambulatory legs were longer on the major cheliped side, resulting in asymmetry of total lengths of, especially, the first and second ambulatory legs. Male *U. tetragonon* have a form of display intermediate between the lateral and vertical waving types, and the l-section of their first ambulatory leg showed only asymmetry similar to that of the male *U. annulipes*. Asymmetry of the ambulatory legs was not seen in *U. urvillei*, *U. dussumieri* and *U. vocans* males, which display in the vertical form, or in females of any of the five species.

The sequence of the display performed by *U. annulipes* male crabs is as follows: the major cheliped, normally flexed in front of the buccal region, is extended laterally and subsequently raised, then flexed and brought down to the starting position from above the eyes and buccal region (Crane, 1957, 1975). The major cheliped constitutes about one-third of the whole body weight (Table III), and during such a display the proportion of its weight supported by each pair of ambulatory legs will change according to the angular position of the major cheliped. That is, while the flexed major cheliped is moving toward the side, its weight is borne on the anterior ambulatory legs and then on the ambulatory legs on the same side as the major cheliped. When the major cheliped is fully extended laterally, it achieves its maximum loading weight. Subsequently, during the raising of the unflexed major cheliped and its return to the starting position, the weight carried on the side of the body bearing the major cheliped will decrease gradually. The degree of asymmetry in the l-section of the ambulatory legs was greatest for the first ambulatory leg, and decreased gradually until no asymmetry was apparent for the fourth ambulatory legs (Fig. 2). Thus, the distances between the dactylus tips of each pair of ambulatory legs are greater anteriorly, especially on the side bearing the major cheliped, since waving males hold the l-section horizontally rather than vertically (Crane, 1975, Fig. 92). In addition, the distance between the dactylus tips of the first and fourth ambulatory legs is greater on the major cheliped side than on the other side, since the ambulatory legs of both sides were extended in the antero-posterior direction during display. The increased horizontal distance on the major cheliped side may be a morphological adaptation to bearing most of the weight of the major cheliped as it moves laterally from the anterior position during display.

On the other hand, in the sequence of the display of male *U. urvillei*, *U. dussumieri* and *U. vocans*, the major cheliped initially remains flexed in front of the buccal region, and is moved up and slightly forward, without

unflexing (Crane, 1957, 1975). In such a display, the horizontal component of the motion of the major cheliped will be very small in both the antero-posterior direction and laterally, compared with the display of the lateral wavers. Therefore, the crab does not have to bear an additional load on the side of the major cheliped during waving. Vertical wavers, therefore, do not have an elongated l-section of the ambulatory legs on the major cheliped side.

The display performed by male *U. tetragonon* is intermediate between the lateral and vertical waving types (Crane, 1957, 1975). That is, the major cheliped, flexed in front of the buccal region, is incompletely extended forward at an acute angle. Subsequently, the semi-flexed cheliped is raised so that its tip barely reaches to the eye. In such a display, the crab does not have to bear a load on the ambulatory legs of the major cheliped side, as the lateral wavers do.

The asymmetry in the total length of the ambulatory legs or in the length of each section of the ambulatory leg was not seen in *U. vocans*, in which right-handed males are predominant (Takeda and Yamaguchi, 1973), or in male *U. urvillei* and *U. dussumieri* in which the ratio of left and right handedness is similar (Fig. 2). These facts suggest that the asymmetry of the ambulatory legs corresponds with differences in the form of display, rather than with differences in the mechanism inducing hypertrophy of one of the chelipeds, whether innate or random.

The ratio of body depth to carapace width was greater on the side bearing the major cheliped than it was on the opposite side, in male crabs of all species (Table IV). However, the relative carapace depth, which is considered to be related directly to the body depth, was the same on the two sides of the body (Table V). On the other hand, the length of the sternum bearing cheliped was much greater on the major cheliped side than it was on the minor cheliped side, resulting in the asymmetry of the body depth. Because the body depth was measured as the minimum distance between the carapace and a straight line in contact with the planes of the sterna bearing the first and second ambulatory legs (Fig. 1A), the excessive increase in the body depth on the major cheliped side, resulting from the excessive enlargement of the sternum bearing the major cheliped, means that the plane of the sternum with the major cheliped was inclined more vertically than was that of the opposing sternum. This more vertical sternum position probably contributes to the smoother motion of the major cheliped in a vertical direction.

The total length of the five sterna on the side with the minor cheliped in male *U. urvillei, U. dussumieri* and *U. vocans* tended to be greater than that of the female crabs (Fig. 3). But, there was no such sexual dimorphism in *U. tetragonon* and *U. annulipes*. These results indicate that the sterna on the minor cheliped side of males extend further laterally, like those on the major cheliped side, and that the plane of the sternum bearing the minor cheliped becomes more vertical than is the case in females of the vertically waving species.

Acknowledgments

We thank the Phuket Marine Biological Center and the National Research Council of Thailand for providing facilities for this research in Thailand. We thank Dr. M. Matsumasa, Department of Biology, School of Liberal Arts and Sciences, Iwate Medical University and Mr. T. Koga and Mr. T. Kosuge, Faculty of Science, Kyushu University, for their field assistance. This study was partially supported by Grants-in-Aid for International Scientific Research for the Japanese Ministry of Education, Science and Culture (Nos. 62042019 and 01041069).

Literature Cited

Ahmed, M. 1978. Development of asymmetry in the fiddler crab *Uca camulanta* Crane, 1943 (Decapoda, Brachyura). *Crustaceana* **34:** 294–300.

Crane, J. 1957. Basic patterns of display in fiddler crabs (Ocypodidae, Genus *Uca*). *Zoologica* **42:** 69–82.

Crane, J. 1975. *Fiddler Crabs of the World. Ocypodidae: Genus Uca.* Princeton University Press, New Zealand. 736 pp.

Duncker, V. G. 1903. Über Asymmetrie bei *Gelasimus pugilator* Latr. *Biometrika* **2:** 307–320.

Frith, D. W., and C. B. Frith. 1977. Observations on fiddler crabs (Ocypodidae: Genus *Uca*) on Surin Island, western peninsular Thailand, with particular reference to *Uca tetragonon* (Herbst). *Phuket Mar. Biol. Center Res. Bull.* **18:** 1–14.

Huxley, J. S., and F. S. Callow. 1933. A note on the asymmetry of male fiddler-crabs (*Uca pugilator*). *W. Roux Arch. Entwicklungsmech.* **129:** 379–392.

Miller, D. C. 1973. Growth in *Uca*, 1. Ontogeny of asymmetry in *Uca pugilator* (Bosc) (Decapoda, Ocypodidae). *Crustaceana* **24:** 119–131.

Morgan, T. H. 1923. The development of asymmetry in the fiddler crab. *Am. Nat.* **57:** 269–273.

Morgan, T. H. 1924. The artificial induction of symmetrical claws in male fiddler crabs. *Am. Nat.* **58:** 289–295.

Salmon, M., and J. F. Stout. 1962. Sexual discrimination and sound production in *Uca pugilator* Bosc. *Zoologica* **47:** 15–21.

Takeda, M., and T. Yamaguchi. 1973. Occurrences of abnormal males in a fiddler crab *Uca marionis* (Desmarest), with notes on asymmetry of chelipeds. *Proc. Jpn. Soc. Syst. Zool.* **9:** 13–20.

Tazelaar, M. A. 1933. A study of relative growth in *Uca pugnax*. *W. Roux Arch. Entwicklungsmech.* **129:** 393–401.

Yamaguchi, T. 1977. Studies on the handedness of the fiddler crab, *Uca lactea*. *Biol. Bull.* **152:** 424–436.

Yerkes, R. M. 1901. A study of variation in the fiddler crab *Gelasimus pugilator* Latr. *Proc. Am. Acad. Arts Sci.* **36:** 417–442.

Reference: *Biol. Bull.* **184**: 209–215. (April, 1993)

Studies of Intracellular pH Regulation in Cardiac Myocytes From the Marine Bivalve Mollusk, *Mercenaria campechiensis*

W. ROSS ELLINGTON

Department of Biological Science, B-157, Florida State University, Tallahassee, Florida 32306

Abstract. Myocytes were isolated from the ventricle of the marine clam *Mercenaria campechiensis* by enzymatic dispersion procedures. Intracellular pH (pH_i) was measured via fluorescence imaging techniques using an inverted microscope interfaced with a high sensitivity television camera. Myocyte pH_i was similar to values observed in other molluscan muscles measured by weak acid distribution and nuclear magnetic resonance (NMR) techniques. Myocytes displayed a good capacity for defending pH_i against changes in extracellular pH (pH_e) as the pH_i remained unchanged in the pH_e range of 7.1 to 8.0, but gradually declined at lower pH_e values. Myocytes had a relatively high non-bicarbonate intracellular buffering capacity. Further, these cells showed recovery from imposed acid loads. This recovery was accelerated by increasing HCO_3^- concentrations, was not dependent on external Na^+ and was blocked by a stilbene transport inhibitor, suggesting that a HCO_3^-:Cl^- transporter plays a central role in regulation of pH_i. Collectively, these data show that ventricular myocytes of *M. campechiensis* have a relatively high capacity for dealing with potential metabolic proton loads associated with environmental anaerobiosis.

Introduction

Environmental hypoxia or anoxia imposes important energetic and acid/base stresses on marine invertebrates. When anaerobic energy yielding processes prevail, there appears to be an uncoupling of proton production and consumption. The extent of excess production of protons is dependent on the specific pathways operating (Pörtner *et al.*, 1984a; Pörtner, 1987a, 1989). The major evolutionary trajectory in highly anoxia-tolerant marine invertebrates (bivalve/gastropod mollusks and certain worm groups) is the development and use of anaerobic metabolic pathways with a lower H^+/ATP ratio, the ratio of proton release to ATP produced (Gnaiger, 1980).

Because proton production will continue throughout anoxia, it is readily apparent that specific mechanisms are present in these organisms to minimize reductions in intracellular pH (pH_i). Rates of intracellular acidification during anoxia (or air exposure) are generally quite low in the muscles of bivalves (Barrow *et al.*, 1980; Ellington, 1983a; Walsh *et al.*, 1984) and gastropods (Ellington, 1983b; Graham and Ellington, 1985). This is also true of the sipunculid *Sipunculus nudus* (Pörtner *et al.*, 1984b; Pörtner, 1987b). Muscles of many of these species have moderately high non-bicarbonate intracellular buffering capacities (β_{NB}) (Eberlee and Storey, 1984; Morris and Baldwin, 1984; Pörtner *et al.*, 1984a; Wiseman and Ellington, 1989). Furthermore, there is good evidence for ion exchange of acid/base equivalents between the intra- and extracellular compartments. For instance, in *S. nudus* Pörtner and coworkers (Pörtner *et al.*, 1984b; Pörtner, 1987b) have shown that the extracellular compartment serves as sink during anoxia for metabolically produced protons. This is also true of bivalves where the calcareous shell serves as an external buffering agent (Crenshaw and Neff, 1969; Booth *et al.*, 1984). In terms of ion exchange processes in marine invertebrates, a sodium-dependent Cl^--HCO_3^- exchanger appears to be the predominant effector of regulation of pH_i in two well-studied systems—squid giant axon (Boron and Russell, 1983) and the giant muscle fibers of barnacles (Boron *et al.*, 1979). These exchangers are blocked by stilbene derivatives and have low Kms for HCO_3^- (around 2–3 m*M*). Recently, it has been shown that bivalve anterior byssus retractor muscle (ABRM) has a stilbene-sensitive anion exchanger (Zange *et al.*, 1990).

Received 13 November 1992; accepted 25 January 1993.

In the present study, regulation of pH_i has been investigated in myocytes isolated from the ventricle of the marine bivalve *Mercenaria campechiensis*. This study uses fluorescent ratio imaging technology, which permits the observation of the dynamics of change in pH_i in individual myocytes. Experiments focus on the measurement of β_{NB} and observation of defense of pH_i after exposure of cells to acid/base stress.

Materials and Methods

Animals and materials

Specimens of *M. campechiensis* were collected via a dredge by a commercial fisherman from St. Joseph's Bay, Gulf County, Florida, and were transported to the Florida State University Marine Laboratory within a few hours after collection. Animals were maintained in raw (unfiltered, unsettled), continuously flowing seawater. Prior to experiments, animals were transported to the main university campus and maintained in recirculating aquaria 20 ± 1.5°C under a 12:12 (L:D) photoperiod.

Dispersion enzymes and buffers were purchased from Sigma Chemical Co. (St. Louis, Missouri). Nigericin (free acid), 2′,7′-bi-(2-carboxyethyl)-5-(and -6)-carboxyfluorescein-acetoxymethyl ester (BCECF/AM) and BCECF (free acid) were purchased from Molecular Probes (Eugene, Oregon). The anion transport inhibitor, 4-acetamido-4′-isothiocyanatostilbene-2, 2′-disulfonic acid (SITS), was obtained from Sigma Chemical Co. All other chemicals were of reagent grade quality.

Isolation of myocytes

Procedures for myocyte dispersion were adapted from suggestions made by C. Bruce (Department of Pharmacology, University of British Columbia, Vancouver, BC). Ventricles were dissected from 3 to 5 specimens of *M. campechiensis*. After removal of the intestine, tissue was cut into very small pieces (1 mm^3), suspended in 45 ml myocyte artificial seawater (MASW, 440 m*M* NaCl, 10 m*M* KCl, 7.5 m*M* $CaCl_2$, 23 m*M* $MgCl_2$, 25 m*M* $MgSO_4$ and 10 m*M* HEPES adjusted to pH 7.75 with NaOH), and gently washed in a rotary shaker for 1 h. The suspension was placed in a 50 ml conical centrifuge tube and the tissue pieces were allowed to settle by gravity for a few minutes. After aspirating off the MASW, tissue was resuspended in 20 ml 0.1% protease VIII (Sigma) in MASW and incubated with gentle agitation for 30 min. The tissue was again placed in a 50 ml centrifuge tube followed by 30 ml MASW. After settling of the tissue, the MASW was aspirated off and 50 ml MASW added. After settling and aspiration, the tissue pieces were resuspended in 20 ml 0.1% collagenase (type 2, Sigma) and incubated with agitation for 90 min. Periodically during incubation, tissue was gently sucked in and out of a flame-polished Pasteur pipette. After incubation, the cell suspension was centrifuged for 45 s at low speed (400 rpm) in a clinical centrifuge. The supernatant was carefully decanted without disturbing the loose pellet and centrifuged for 4 min as above. The supernatant was discarded and the pellet resuspended in MASW and centrifuged for 4 min. The final pellets were resuspended in a small volume of MASW. Cells were seeded on circular coverslips (Nicholson Precision Instruments, Gaithersburg, Maryland) which were immersed in 15 ml MASW in 10 cm plastic culture dishes. Coverslips had been previously washed in acid, rinsed exhaustively and then polished with ethanol using lens paper. Dishes were placed in a humidified culture chamber. Cells were always prepared during the afternoon and then used for imaging the following morning. All isolation and incubation procedures were conducted at 18–21°C.

Fluorescent ratio imaging

The overall rationale and approach for BCECF imaging has been previously described (Rink *et al.*, 1982; Bright *et al.*, 1987). Cells were loaded with 5 μM BCECF/AM for 45 min. After washing, the coverslip was mounted in a Dorvak-Stottler chamber (Nicholson Precision Instruments) which was attached to a Peltier device (Physitemp, Clifton, New Jersey) mounted on the stage of a Zeiss IM-35 inverted microscope. Cells were superfused (0.1 ml/min) by gravity flow from a manifold device consisting of a Hamilton (Reno, Nevada) eight-way valve, microbore tubing and eight reservoir chambers. Temperature was controlled at 20°C.

A xenon lamp (Optiquip, Highland Mills, New York) provided illumination. Fluorescence excitation was controlled via a dual filter wheel/shutter assembly (Ludl, Hawthorne, New York). One wheel contained excitation filters (490, 450 nm) while the other had a range of neutral density filters. A dichroic (530 nm) was positioned on the fluorescence emission side. All filters were from Omega Optical (Brattleboro, Vermont). Phase and fluorescence images were obtained using an Achrostigmat LD 32X/.4 PH1 objective with light passing onto an iCCD camera (QUANTEX, Sunnyvale, California). Video signals were digitized and processed by IMAGE 1/FL software from Universal Imaging Corp. (Westchester, Pennsylvania) using a 486-based computer with output on a color monitor (Trinitron, SONY). Software controlled the operation of the filterwheel/shutter system.

Isolated myocytes did not display any auto-fluorescence. Preliminary experiments showed that BCECF-loaded myocytes went into contracture when illuminated with intense monochromatic light (490 or 450 nm). Unloaded cells did not respond to light in this way. Furthermore, the ability to regulate pH_i was impaired in

loaded cells at high light intensities. Thus, during all experiments we used high range neutral density filters to reduce light intensities compensating for the reduced fluorescence by employing high camera gain and intensity settings. Furthermore, the period of irradiation of cells with monochromatic light was reduced to a minimum consistent with camera lag. Images were acquired using shade (shade "mask" obtained using 25 μl of 25 μM BCECF sandwiched between coverslip and slide) and background correction capabilities of the IMAGE 1/FL software. Image pairs were acquired at specific time intervals (usually every 20 s). Individual cells were selected and fluorescence ratios (I_{490}/I_{450}) for each cell *versus* time were stored in a spread-sheet data base. Numerical data were transferred as ASCII files to a Macintosh IIci and processed and analyzed using Sigmaplot (Jandel, San Rafael, California).

In vivo *calibration of ratios*

Fluorescent ratios with respect to pH were calibrated by the nigericin pH clamp approach of Thomas *et al.* (1979). The calibration solution was identical to MASW except that it contained 290 mM NaCl, 160 mM KCl and nigericin (5 μg/ml). The concentration of KCl chosen brackets values for intracellular K^+ as determined in the muscles of marine mollusks (Potts, 1958; Robertson, 1965; Burton, 1983). Cells were allowed to equilibrate with each solution until ratios stabilized (generally <5 min). In routine experiments, pH_i was estimated for individual myocytes. Mean values for acid-base measurements in each physiological treatment represent data from individual cells from up to two independent cell dispersions.

Figure 1. Cardiac myocyte from the ventricle of the clam *Mercenaria campechiensis*. Photograph was taken with Kodak TMAX 100 film. Bar corresponds to 100 μm.

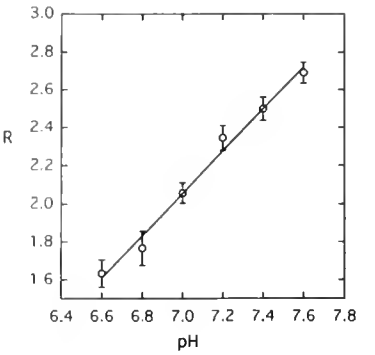

Figure 2. Relationship between the fluorescence intensity ratio ($R = I_{490}/I_{450}$) and pH obtained using the nigericin approach with cardiac myocytes from *Mercenaria campechiensis*. Each value corresponds to a mean ± 1 SD (n ranges from 8 to 12).

Results

Myocytes

Dispersion procedures produced a very high yield of myocytes. Cells were generally long and spindly (50–400 $\mu \times 10\ \mu$) (Fig. 1). Immediately after dispersion, a large fraction of cells showed spontaneous contractile activity but were generally quiescent after 12 h. Dispersed cells excluded trypan blue and were responsive to addition of 10^{-5} M 5-hydroxytryptamine (5-HT). In fact, many cells remained viable and responded to 5-HT up to 7 days after isolation. The addition of antibiotics (penicillin G, bacitricin) and 5 mM D-glucose did not enhance survival in the short term nor influence results of pH_i determinations. Thus, these components were not added to MASW. Ventricles of the congeneric clam *Mercenaria mercenaria* have extremely high glycogen levels, on the order of 240 μmoles/g wet wgt (Ellington, 1985). Thus, it is clear that there is a sufficient endogenous reserve of metabolic fuels in these myocytes for the period over which they were used (15–18 h).

Nigericin pH clamp

Myocytes were subjected to a nigericin pH clamp protocol encompassing the range of pH from 6.6 to 7.6 in 0.2-unit increments. Typically, most cells responded to the clamping medium by contracting to approximately 60% of their initial length and remained so throughout the protocol. Fluorescence ratios varied linearly with pH (Fig. 2). A regression equation was calculated (RATIO = 1.111 pH −5.724, R = 0.994) and used to transform all ratios from the ratio *versus* time spreadsheets to pH_i. The compressed ratio range was due to differential

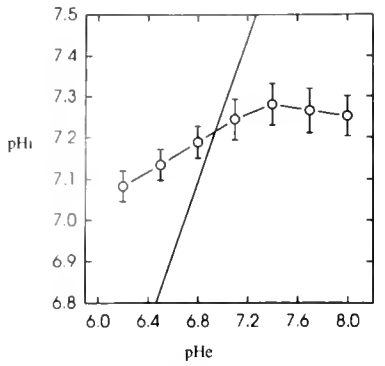

Figure 3. The relationship between pH_i and pH_e in cardiac myocytes from *Mercenaria campechiensis*. The continuous diagonal line corresponds to the iso-pH line. Each value corresponds to a mean ± 1 SD (n = 11).

gain/level adjustments of the analog-digital converter at the two excitation wavelengths as well as the fact that the neutral density filter at 490 nm was higher than the one used at 450 nm. Under routine superfusion conditions, pH_i of myocytes was observed to be 7.22 ± 0.08 (mean ± 1 SD, n = 20).

Relationship between intracellular and extracellular pH

Cells were superfused with MASW (containing 20 m*M* HEPES) adjusted to various pH values (pH_e). Media were equilibrated with air. Ratios were observed for 15–20 min at each pH. pH_i was essentially constant in the pH_e range from 7.1 to 8.0 (Fig. 3). At lower pH_e values, the pH_i declined linearly but still was considerably above the iso-pH line indicating good capacity for defense of pH_i against pH_e (Fig. 3).

Non-bicarbonate buffering capacity (β_{NB})

Non-bicarbonate buffering capacity was estimated by the NH_4Cl prepulse method of Boron (1977). Myocytes were superfused with MASW and then subjected to a pulse of 15 m*M* NH_4Cl-MASW (pH 7.75). After peak alkalinization, myocytes were superfused with MASW resulting in a pronounced acidification. β_{NB} values were calculated as described by Boron (1977). Buffering capacity is expressed as Slykes (dH^+/dpH). Since the MASW was equilibrated in air, $[HCO_3^-]$ was low (around 0.7 m*M*) so the contribution of this species to total buffering capacity is negligible. Figure 4 is an example of a typical pre-pulse experiment. Following alkalinization, there was a gradual decline in pH_i. After NH_4Cl wash-out, there was a characteristic alkalinization back towards the initial condition (Fig. 4). β_{NB} values for individual myocytes were somewhat variable ranging from 22 to 65 Slykes with a mean of 39.98 ± 8.86 (±1 SD, n = 31). The inherent limitation of the NH_4Cl prepulse approach is that some recovery of pH_i could occur during the early phase of the wash-out therebye producing an overestimate of β_{NB} (Boron, 1977). In the present study, wash-out was extremely

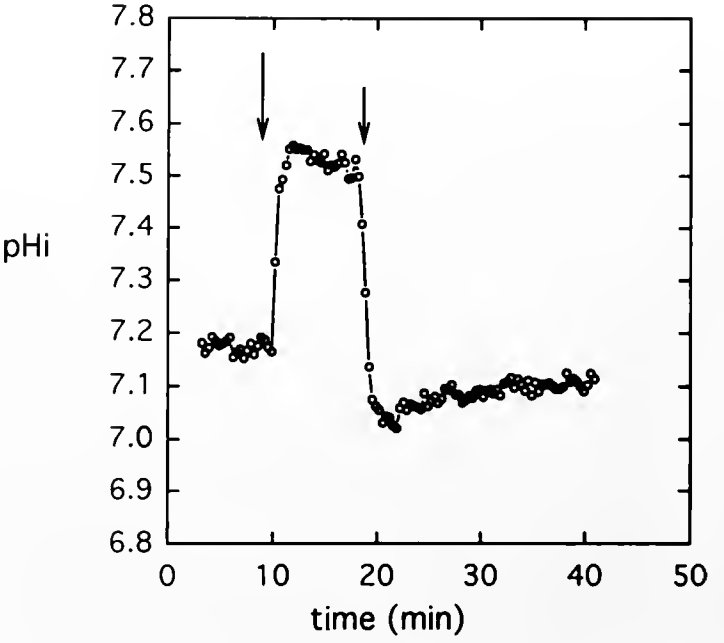

Figure 4. Time course of changes in pH_i in a single *Mercenaria campechiensis* cardiac myocyte during a typical NH_4Cl pre-pulse experiment. The first arrow indicates the onset of superfusion with 15 m*M* NH_4Cl-MASW. The second arrow indicates the onset of washing with MASW.

rapid as the peak acidosis occurred within 3 min (Fig. 4). Thus, it is likely that pH_i recovery processes would potentially produce only minor errors in β_{NB} determination in this system.

Recovery from acid loading

Isolated myocytes regulate pH_i after acid-loading as evidenced by the slow alkalinization following NH_4Cl wash-out using normal MASW ($[HCO_3^-]$ approximately 0.7 m*M*) (Fig. 5A; Table 1). However, the rate of alkalinization was greatly accelerated during wash-out using 0.3% CO_2/4 m*M* HCO_3^- MASW (Fig. 5B; Table I). Recovery from acid loading did not appear to be dependent on external Na^+, as the recovery rate was essentially the same for MASW and Na^+-free MASW (Table I). SITS completely blocked recovery. In fact, there was a gradual reduction in pH_i once the plateau acidification after wash-out had been attained (Table I). Collectively, these results show that it is likely that a SITS-sensitive HCO_3^-:Cl^- exchanger plays a major role in recovery from acid loading in *M. campechiensis* myocytes.

Table I

Recovery from acid loading in myocytes from Mercenaria campechiensis

Washing medium	dpH/dt (pH units/min)	Acid/base transport (μmoles/min)	n
MASW	0.0040 ± 0.0018	0.157 ± 0.055	10
MASW-0.3% CO_2: 4 m*M* HCO_3^-	0.0152 ± 0.0012	0.576 ± 0.115	9
Na^+-free MASW	0.0054 ± 0.0030	0.236 ± 0.159	9
MASW-0.5 m*M* SITS	No Recovery (−0.0073 ± 0.0056)	Not estimated	10

Myocytes were superfused with MASW followed by 15 m*M* NH_4Cl-MASW. After the plateau alkalinization was acheived, myocytes were washed with various media. The rate of recovery (dpH/dt) was calculated using a regression (Sigma Plot) of the initial, linear portion of the recovery curve after NH_4Cl wash-out. Buffering capacity values (dH^+/dpH) were calculated according to Boron (1977). Rates of acid/base equivalent transport (μmoles/min) were calculated for each myocyte by multiplying the measured individual β_{NB} value times the corresponding dpH/dt value (μmoles/min = β_{NB} · dpH/min). Each value represents a mean ± 1 SD. Sample size (n) is indicated.

MASW-0.3% CO_2: 4 m*M* HCO_3^- was prepared by gassing MASW with 0.3% CO_2 (balance air), addition of solid $NaHCO_3$ followed by adjustment of pH. The reservoir was continuously gassed with hydrated 0.3% CO_2 in air and the superfusion line was contained within a gas jacket. Concentrations were calculated using appropriate apparent dissociation (Mehrbach *et al.*, 1973) and solubility (Riley and Skirrow, 1975) constants. Na^+-free MASW was prepared by replacing NaCl with three times crystallized choline chloride (Sigma Chemical Co.). SITS solutions were shielded from light to prevent photodecomposition.

Discussion

Molluscan myocytes have been used on a number of occasions as experimental systems for investigating physiological phenomena ranging from ion channels (Brezden *et al.*, 1986) to changes in intracellular Ca^{2+} concentrations during contraction (Ishii *et al.*, 1989). In this regard, cardiac myocytes from *M. campechiensis* appear to be an ideal model system for studies of regulation of pH_i in that these cells are easily isolated, retain viability for extended time periods and, of course, can maintain acid-base balance in spite of extracellular and intracellular pH disturbances. The average pH_i of 7.22 in these cells as determined by BCECF-imaging is comparable to values observed in various marine gastropod muscles (Ellington, 1983b; Graham and Ellington, 1985; Wiseman and Ellington, 1989) and is slightly lower (0.1–0.2 units) than what has been observed for squid giant axon (Boron and Russell, 1983) and various tissues of the mussel *Mytilus edulis* (Walsh *et al.*, 1984; Zange *et al.*, 1990). The above data on other species were obtained by a variety of techniques including NMR, weak acid distribution and microelectrode methods.

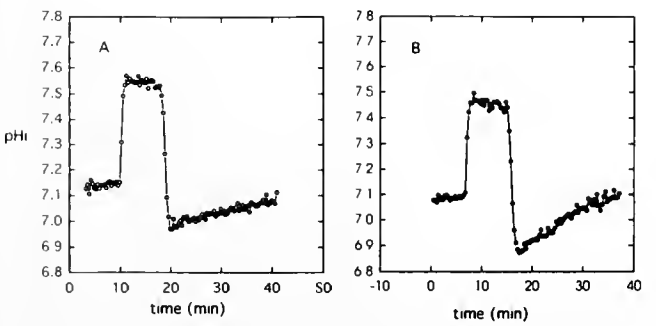

Figure 5. Typical records of change of pH_i in single *Mercenaria campechiensis* myocytes during NH_4Cl pre-pulse experiments when MASW (A) or 0.3% CO_2:4 m*M* HCO_3^--MASW (B) were used in washing.

Changes in pH_e have minimal effect on the pH_i of *M. campechiensis* myocytes over what can be viewed as a physiologically realistic range of pH_es (7.1–8.0). A similar high capacity for defending pH_i against changes in pH_e has been observed in *M. edulis* ABRM preparations (Zange *et al.*, 1990) as well as in hemocytes from the squid *Sepiateuthis lessoniana* (Hemming *et al.*, 1990). In the present study, we have further seen that clam myocytes display recovery from experimentally imposed acid-base disturbances. Walsh and Milligan (1989) have pointed out that there are three potential avenues of regulation of pH_i available to cells—(a) intracellular physico-chemical buffering, (b) ion exchange of acids/bases between intra- and extracellular compartments, and (c) metabolic production or consumption of acids and bases. The present results with *M. campechiensis* myocytes provide strong

evidence for operation of the first two of these mechanisms.

The presence of non-bicarbonate intracellular buffers constitutes the first line of defense against acid/base stress in cells (see reviews by Burton, 1978, and Roos and Boron, 1981). In vertebrate muscles, there appears to be a general correlation between the magnitude of the β_{NB} and the potential for anaerobic function (Castellini and Somero, 1981). This general correlation has been suggested for molluscan muscles (Eberlee and Storey, 1984; Morris and Baldwin, 1984), however, the validity of these conclusions is somewhat in doubt due to the artifacts imposed by homogenate titration methods used for β_{NB} determinations (Wiseman and Ellington, 1989; Pörtner, 1990). In the present study we used the NH_4Cl-prepulse approach and obtained a value of 40 Slykes, which is in the range of values determined by NMR-prepulse for whelk radula muscle (33 Slykes; Wiseman and Ellington, 1989) and mussel ABRM (26.5 Slykes; Zange *et al.*, 1990), both of which have impressive capacities for anaerobic metabolism. In contrast to these observations, the average β_{NB} for squid giant axons was 11.2 (Boron and Russell, 1983). Thus, it is clear that *M. campechiensis* myocytes have a relatively high β_{NB}, which is consistent with the natural history of this species where exposure to hypoxic stress may be a regular phenomenon.

The pH_e in bivalves is alkaline relative to pH_i under normal conditions (Booth *et al.*, 1984). Given a slightly alkaline pH_e, the pH_i of 7.22, and the undoubtedly negative sign of the membrane potential in *M. campechiensis* myocytes, it is clear that protons are not at equilibrium. These cells must continuously export protons or bring in base equivalents to maintain pH_i. This problem becomes greatly exacerbated when the pH_e is reduced (therebye decreasing or even reversing the transmembrane proton gradient) or when acid or base loads are imposed on the cells. The relative constancy of pH_i with pH_e and recovery from experimentally imposed acidosis in clam myocytes clearly show that such ion exchange processes are operating in these cells.

Our results show that *M. campechiensis* myocytes appear to regulate pH_i via a SITS-sensitive ion exchanger which does not have a requirement for external Na^+. Most likely, this transporter is a HCO_3^-:Cl^- exchanger as has been seen in *M. edulis* ABRM (Zange *et al.*, 1990). Under the routine, normocapnic conditions in the present study the concentration of HCO_3^- was estimated to be around 0.7 m*M*, which appears to be sufficient to promote recovery of pH_i after acidosis. However, recovery was greatly accelerated when HCO_3^- concentration was increased to around 4 m*M*. Booth *et al.* (1984) estimated that [HCO_3^-] in *M. edulis* hemolymph was 1.8 m*M* in normoxia and rose to nearly 3 m*M* during hypoxic stress. It is likely that physiological [HCO_3^-] in *M. campechiensis* spans a higher range that 0.7 m*M*, implying greater overall transport rates *in vivo*. The above results are in contrast to the work of Boron and Russell (1983) who found that there was an absolute Na^+ requirement (Km = 77 m*M*) for HCO_3^-:Cl^- exchange in squid axons. However, Hemming *et al.* (1990) found that acid recovery in squid hemocytes was Na^+-independent. Zange *et al.* (1990) found that addition of 5-hydroxytryptamine (5-HT) elicited activation of a Na^+:H^+ exchanger in *M. edulis* ABRM. It was not possible to investigate this possibility in *M. campechiensis* myocytes, as addition of 5-HT caused rather violent contractions of myocytes, which interfered with imaging experiments.

The present results show that myocytes from the clam *M. campechiensis* have a good capacity for regulation of pH_i. This capacity is based a relatively high β_{NB} and the presence of a SITS-sensitive anion exchanger. Clam myocytes also appear to be excellent candidates for long-term primary culture. Thus, future studies will focus on potential phenotypic plasticity of β_{NB} and ion exchange capacity in cells cultured under conditions which might induce such changes (altered pH_e, hyper- or hypo-capnia or hypoxia).

Acknowledgments

I wish to heartily thank Ms. Carolyn Bruce (University of British Columbia) for advice and encouragement in the development of the myocyte isolation protocol. I am also very grateful to Leavins Seafood, Inc. (Apalachicola, Florida) for providing animals. This research was supported by NSF grants DIR-9014510 (Instrument and Instrument Development Program) and IBN-9104548 (Functional and Physiological Ecology Program).

Literature Cited

Barrow, K. D., D. D. Jamieson, and R. S. Norton. 1980. ^{31}P nuclear magnetic resonance studies of energy metabolism in tissue from the marine mollusc *Tapes watlingi*. *Eur. J. Biochem.* **103:** 289–297.

Booth, C. E., D. G. McDonald, and P. J. Walsh. 1984. Acid-base balance in the sea mussel *Mytilus edulis*. I. Effects of hypoxia and air-exposure on the hemolymph acid-base status. *Mar. Biol. Lett.* **5:** 347–358.

Boron, W. F. 1977. Intracellular pH transients in giant barnacle muscle fibers. *Am. J. Physiol.* **233:** C61–C73.

Boron, W. F., and J. M. Russell. 1983. Stoichiometry and ion dependencies of the intracellular-pH-regulating mechanism in squid giant axons. *J. Gen. Physiol.* **81:** 373–399.

Boron, W. F., W. C. McCormick, and A. Roos. 1979. pH regulation in barnacle muscle fibers: dependence on intracellular and extracellular pH. *Am. J. Physiol.* **237:** C185–C193.

Brezden, B. L., D. R. Gardner, and G. E. Morris. 1986. A potassium-selective channel in isolated *Lymnaea stagnalis* heart muscle cells. *J. Exp. Biol.* **123:** 175–189.

Bright, G. R., G. W. Fisher, J. Rogowska, and D. L. Taylor. 1987. Fluorescence ratio imaging microscopy: temporal and spatial measurements of cytoplasmic pH. *J. Cell Biol.* **104:** 1019–1033.

Burton, R. F. 1978. Intracellular buffering. *Resp. Physiol* **33:** 51–58.

Burton, R. F. 1983. Ionic regulation and water balance. Pp. 291–352 in *The Mollusca*, Vol 5, A. S. M. Saleudin and K. M. Wilbur, eds. Academic Press, New York.

Castellini, M. A., and G. N. Somero. 1981. Buffering capacity of vertebrate muscle: correlations with potentials for anaerobic function. *J. Comp. Physiol* **143:** 191–198.

Crenshaw, M. A., and J. M. Neff. 1969. Decalcification at the mantle-shell interface in molluscs. *Am. Zool* **9:** 881–889.

Eberlee, J. C., and K. B. Storey. 1984. Buffering capacities of the tissues of marine molluscs. *Physiol. Zool.* **57:** 567–572.

Ellington, W. R. 1983a. The extent of intracellular acidification during anoxia in catch muscle of two bivalve molluscs. *J. Exp. Zool* **227:** 313–317.

Ellington, W. R. 1983b. Phosphorus nuclear magnetic resonance studies of energy metabolism in molluscan tissues: effect of anoxia and ischemia on intracellular pH and high energy phosphates in the ventricle of the whelk, *Busycon contrarium*. *J. Comp. Physiol.* **153:** 159–166.

Ellington, W. R. 1985. Cardiac energy metabolism in relation to work demand and habitat in bivalve and gastropod molluscs. Pp. 356–366 in *Circulation, Respiration and Metabolism*, R. Gilles, ed. Springer Verlag, Berlin.

Gnaiger, E. 1980. Das Kalorische Aquivalent des ATP-Umstazes im aeroben und anoxischen metabolismus. *Thermochim. Acta* **40:** 195–223.

Graham, R. A., and W. R. Ellington. 1985. Phosphorus nuclear magnetic resonance studies of energy metabolism in molluscan tissues: intracellular pH change and the qualitative nature of anaerobic end products. *Physiol. Zool.* **58:** 478–490.

Hemming, T. A., C. O. Vanoye, S. E. S. Brown, and A. Bidani. 1990. Cytoplasmic pH recovery in acid-loaded haemocytes of squid (*Sepioteuthis lessoniana*). *J. Exp. Biol.* **148:** 385–394.

Ishii, N., A. W. M. Simpson, and C. C. Ashley. 1989. Free calcium at rest during "catch" in single smooth muscle cells. *Science* **243:** 1367–1368.

Mehrbach, C., C. H. Culberson, J. E. Hawley, and R. M. Pytkowicz. 1973. Measurement of the apparent dissociation constants of carbonic acid in seawater at atmospheric pressure. *Limnol. Oceanogr.* **18:** 897–907.

Morris, G. M., and J. Baldwin. 1984. pH buffering capacity of invertebrate muscle: correlations with anaerobic muscle work. *Molec. Physiol.* **5:** 61–70.

Pörtner, H.-O. 1987a. Contributions of anaerobic metabolism to pH regulation in animal tissues-theory. *J. Exp. Biol.* **131:** 69–87.

Pörtner, H.-O. 1987b. Anaerobic metabolism and changes in acid-base status: quantitative interrelationships and pH regulation in the marine worm *Sipunculus nudus*. *J. Exp. Biol* **131:** 89–105.

Pörtner, H.-O. 1989. The importance of metabolism in acid-base regulation and acid-base methodology. *Can. J. Zool.* **67:** 3005–3017.

Pörtner, H.-O. 1990. Determination of intracellular buffer values after metabolic inhibition with fluoride and nitrilotriacetic acid. *Resp. Physiol* **81:** 275–288.

Pörtner, H.-O., N. Heisler, and M. K. Grieshaber. 1984a. Anaerobiosis and acid-base status in marine invertebrates: a theoretical analysis of proton generation by anaerobic metabolism. *J. Comp. Physiol.* **155:** 1–12.

Pörtner, H.-O., M. K. Grieshaber, and N. Heisler. 1984b. Anaerobiosis and acid-base status in marine invertebrates: effect of environmental hypoxia on extracellular and intracellular pH in *Sipunculus nudus* L. *J. Comp. Physiol* **155:** 13–20.

Potts, W. T. W. 1958. The inorganic and amino acid composition of some lamellibranch muscles. *J. Exp. Biol.* **35:** 749–764.

Riley, J. P., and G. Skirrow. 1975. *Chemical Oceanography*. Academic Press, New York.

Rink, T. J., R. Y. Tsien, and T. Pozzan. 1982. Cytoplasmic pH and free Mg^{2+} in lymphocytes. *J. Cell Biol.* **95:** 189–196.

Robertson, J. D. 1965. Studies on the chemical composition of muscle tissue. III. The mantle muscle of cephalopods. *J. Exp. Biol.* **42:** 153–175.

Roos, A., and W. F. Boron. 1981. Intracellular pH. *Physiol. Rev.* **61:** 296–434.

Thomas, J. A., R. N. Buschbaum, A. Zimniak, and E. Racker. 1979. Intracellular pH measurements in Ehrlich ascites tumor cells utilizing spectroscopic probes generated *in situ*. *Biochemistry* **18:** 2210–2218.

Walsh, P. J., D. G. McDonald, and C. E. Booth. 1984. Acid-base balance in the sea mussel *Mytilus edulis* II. Effects of hypoxia and air exposure on intracellular acid-base status. *Mar. Biol. Lett.* **5:** 359–369.

Walsh, P. J., and C. L. Milligan. 1989. Coordination of metabolism and intracellular acid-base status: ionic regulation and metabolic consequences. *Can. J. Zool.* **67:** 2994–3004.

Wiseman, R. W., and W. R. Ellington. 1989. Intracellular buffering in molluscan muscle: superfused muscle *versus* homogenates. *Physiol. Zool.* **62:** 541–558.

Zange, J., M. K. Grieshaber, and A. W. H. Jans. 1990. The regulation of intracellular pH estimated by ^{31}P-NMR spectroscopy in the anterior byssus retractor muscle of *Mytilus edulis* L. *J. Exp. Biol.* **150:** 95–109.

Reference: *Biol Bull* **184**: 216–222. (April, 1993)

Two S-Iamide Peptides, AKSGFVRIamide and VSSFVRIamide, Isolated from an Annelid, *Perinereis vancaurica*

O. MATSUSHIMA[1], T. TAKAHASHI[1], F. MORISHITA[1], M. FUJIMOTO[1], T. IKEDA[2], I. KUBOTA[3], T. NOSE[4], AND W. MIKI[4]

[1]*Zoological Institute, Faculty of Science, Hiroshima University, Higashi-hiroshima 724, Japan,* [2]*Physiological Laboratory, Faculty of Integrated Arts and Sciences, Hiroshima University, Hiroshima 730, Japan,* [3]*Suntory Bio-Pharma Tech Center, Gunma 370-05, Japan, and* [4]*Marine Biotechnology Institute, Shimizu 424, Japan*

Abstract. Two peptides, H-Ala-Lys-Ser-Gly-Phe-Val-Arg-Ile-NH_2 (AKSGFVRIamide), and H-Val-Ser-Ser-Phe-Val-Arg-Ile-NH_2 (VSSFVRIamide) were isolated from a polychaete annelid, *Perinereis vancaurica.* Both the peptides evoked rhythmic contractions in the esophagus of *Perinereis* with a threshold as low as 10^{-10}–10^{-9} *M*, suggesting that the peptides may be involved in the regulation of gut motility of the animal. The sequences of these peptides are very similar to those of other S-Iamide family peptides which have been previously isolated from an echiuroid worm and some molluscs. In particular, the sequence of VSSFVRIamide is identical to that of an echiuroid S-Iamide peptide. All of the molluscan and echiuroid S-Iamide peptides, as well as the annelid peptides, were found to produce contractions in the esophagus of *Perinereis.* On the other hand, the annelid S-Iamide peptides, as well as the molluscan and echiuroid peptides, were found to inhibit or potentiate contractions elicited by electrical stimulation in echiuroid and molluscan muscles. S-Iamide peptides may be a typical neuropeptide family distributed interphyletically in the Protostomia.

Introduction

In annelids, pharmacological studies have been extensively done on the actions of classical transmitters such as 5-hydroxytryptamine, epinephrine, norepinephrine and dopamine mainly on somatic muscles, and these substances have been suggested to be present in the central and peripheral nervous systems (for review, Tashiro and Kuriyama, 1978). In addition, bioactive peptides found in vertebrates and other phyla of invertebrates have been suggested to be present in annelids (Carraway *et al.,* 1982; Engelhardt *et al.,* 1982; Dhainaut-Courtois *et al.,* 1985; Diaz-Miranda *et al.,* 1991, 1992).

Many peptides are known in vertebrates, especially in mammals which control the motility of the gut (Holmgren, 1989). However, few gut motility-controlling peptides have been reported for invertebrates. Immunohistochemical or immunochemical studies have suggested that some vertebrate neuropeptides, such as enkephalin, β-endorphin (Alumets *et al.,* 1979), substance P (Dhainaut-Courtois *et al.,* 1985; Kaloustian and Edmands, 1986), cholecystokinin/gastrin, β-MSH (Engelhardt *et al.,* 1982; Dhainaut-Courtois *et al.,* 1985) and neurotensin (Carraway *et al.,* 1982) may be present in annelids. Kaloustian and Edmands (1986) reported that substance P stimulated the rate of spontaneous contraction of intestinal tissues of the earthworm *Lumbricus terrestris.* It has also been shown that a tetrapeptide (WMDFamide) related to cholecystokinin/gastrin has excitatory effects on the anterior intestine of a polychaete, *Chaetopterus variopedatus* (Anctil *et al.,* 1984). Apart from immunocytochemical and pharmacological studies, most investigations of bioactive peptides in annelids have centered on those involved in reproductive events (Thorndyke, 1989). Thus, reports on authentic bioactive peptides involved in the regulation of gut-motility of annelids are very few in number.

Received 6 October 1992, accepted 25 January 1993.

Recently, Krajniak and Price (1990) showed the presence of FMRFamide which was first identified in a mollusc as a cardioexcitatory neuropeptide in the polychaete *Nereis virens* (Price and Greenberg, 1977). Krajniak and Greenberg (1992) showed that immunoreactive FMRFamide was present in various tissues including the gut in *Nereis*, and that FMRFamide had a relaxing action on both the spontaneously active and electrically stimulated esophagus, suggesting the involvement of the tetrapeptide in the control of gut-motility. Furthermore, FMRFamide and its related peptides have been shown to be present in other annelid species such as *Nereis diversicolor* (Baratte *et al.*, 1991) and *Hirudo medicinalis* (Evans *et al.*, 1991).

In the present study, we isolated and sequenced two bioactive peptides, AKSGFVRIamide and VSSFVRIamide, from the polychaete *Perinereis vancaurica*, which induced contraction of the isolated esophagus of the animal. These peptides were found to be members of the S-Iamide peptide family (Ikeda *et al.*, 1991; Muneoka and Kobayashi, 1992). The name S-Iamide peptide was given after the common structure, -SSFVRIamide. Kuroki *et al.* (1992) first isolated one of the S-Iamide peptides, LSSFVRIamide, from the prosobranch mollusc *Fusinus ferrugineus*, and up to the present, S-Iamide peptides have been found not only in molluscs but also in an echiuroid worm (Ikeda *et al.*, 1991). We also examined the effects of several S-Iamide peptides on some invertebrate muscle tissues including the esophagus of *Perinereis*.

Materials and Methods

Purification

Perinereis vancaurica tetradentata are commercially available as fishing bait. Approximately 380 worms (500 g) were rinsed twice with artificial seawater (ASW), blotted lightly with tissue paper and boiled for 10 min in 4 volumes of 4% acetic acid (21). The animals were homogenized in 4% acetic acid by using a Waring blender and a Polytron. The homogenate was centrifuged (15,000 × *g*, 40 min, 4°C), and the resulting precipitate was again homogenized and centrifuged. The two supernatants were pooled and concentrated to a volume of about 100 ml by using a rotary evaporator (40°C). To the concentrated supernatant, 1/10 volume of 1 *N* HCl was added, and the precipitated material was centrifuged off (15,000 × *g*, 40 min, 4°C). Next, the supernatant was forced through two disposable C-18 cartridges in series (Mega Bond-Elut, Varian). The retained material was eluted with 50% methanol. The eluate was concentrated, loaded on a C-18 reversed phase HPLC column (CAPCELL-PAK, Shiseido; 10 mm × 250 mm), and eluted with a linear gradient of 0–60% acetonitrile (ACN) in 0.1% trifluoroacetic acid (TFA) for 120 min at a flow rate of 1 ml/min. The chromatography was monitored at 220 nm. Aliquots of 2 ml-fractions were evaporated to dryness, and the residues were dissolved in ASW and bioassayed on an isolated esophagus of *Perinereis* as described below. Two contractile peaks were detected. The fractions of each active peak were concentrated and subjected to HPLC using another C-18 reversed phase column (ODS-80TM, Tosoh; 4.6 mm × 150 mm) with a linear gradient of 10–20% ACN for one activity and 15–25% ACN for the other in 0.1% TFA (0.5 ml/min). Active fractions obtained from each HPLC were then loaded onto a cation-exchange column (SP-5PW, Tosoh; 7.5 mm × 75 mm) and eluted in a linear gradient of 0–0.7 *M* NaCl in 10 m*M* phosphate buffer (pH 7.1) for 70 min at a flow rate of 0.5 ml/min. Then, the active substances identified as single peaks on the cation-exchange HPLC were chromatographed on the ODS-80TM column with a linear gradient of 10–16% ACN and 15–25% ACN, respectively, and finally purified on the same column with an isocratic elution of 17% and 19% ACN.

The two purified substances were subjected to amino acid sequence analysis by automated Edman degradation with a gas-phase sequencer (Shimazu PSQ-1). The results of the chemical analyses suggested that the substances were members of the S-Iamide peptide family. Therefore, the two peptides having the suggested structures were synthesized by a manual method followed by an HF-anisol cleavage and purified by reversed-phase HPLC. Then, the synthetic peptides were compared with native ones in the behavior on HPLC and in the bioactivity on the *Perinereis* esophagus.

Bioassay

The contractile activities of the native and synthetic substances were examined on the isolated esophagus of *Perinereis*. The method for contraction recording was essentially the same as that reported by Krajniak and Greenberg (1992). Both ends of the isolated esophagus were ligated with two cotton threads, one being secured to a stationary rod at the bottom of a trough (2 ml) and the other connected to a force-displacement transducer (NEC San-ei Instruments).

The saline in the trough was constantly aerated through a syringe needle connected with an air pump to ensure uniform distribution of applied substances (dissolved in 0.1 ml saline) in the trough. In the present study, we did not apply electrical stimulation but just monitored inductivity of spontaneous contractions of the esophagus by test substances. For examination of the bioactivity of the material retained by the C-18 cartridges, two more assay systems, the inner circular body-wall muscle of an echiuroid worm *Urechis unicinctus* (Ikeda *et al.*, 1991), and the radula retractor muscle of a prosobranch mollusc

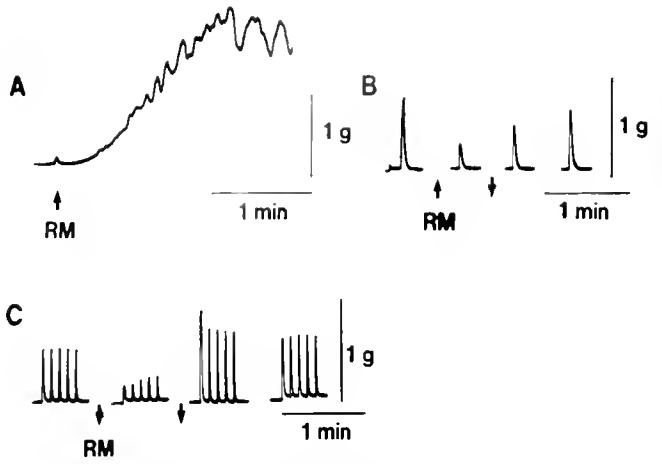

Figure 1. Effects of the retained materials (RM) on the three muscle systems. (A) the esophagus of *Perinereis*. (B) twitch contractions of the inner circular body-wall muscle of *Urechis*. The twitch contraction was produced by an electrical pulse (20 V, 3 ms). (C) twitch contractions of the radula retractor of *Rapana* The twitch contractions were produced by a train of electrical pulses (15 V, 1 ms, 0.2 Hz, 5 pulses). In each case, 1/1000 of total RM, which corresponded with extracts from 0.4 worm, was applied to the assay system. The upward arrows indicate application of RM to the tissue. The downward arrows indicate washing-out of the RM.

Rapana thomasiana (Muneoka *et al.*, 1991), were employed. In these cases, electrical pulses of stimulation were applied to the preparations.

Pharmacology

The methods used in the pharmacological experiments were basically the same as those in the bioassay experiments. In these experiments, we used three kinds of muscles, the esophagus of *Perinereis*, the anterior byssus retractor muscle (ABRM) of the bivalve mollusc *Mytilus edulis* and the radula retractor muscle of the prosobranch mollusc *Fusinus ferrugineus*.

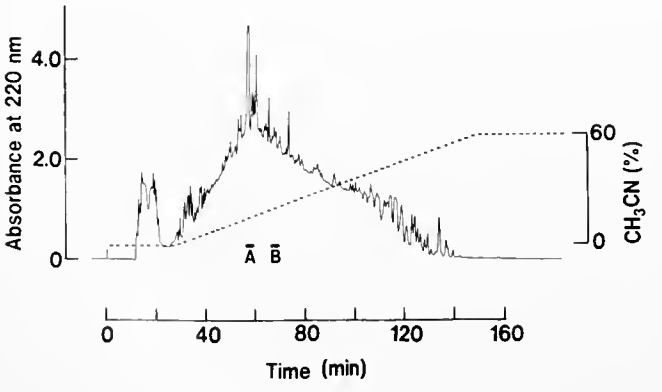

Figure 2. HPLC profile of the retained materials (RM) on a reversed phase column. The RM loaded onto the column was eluted with a linear gradient of ACN concentration (0–60%/120 min) in 0.1% TFA (pH 2.2) at a flow rate of 1 ml/min and collected in 60 fractions of 2 ml each. Aliquots (10 μl = 1/200) of each fraction were evaporated to dryness, dissolved in ASW and applied to the *Perinereis* esophagus. The contractile peaks were indicated by the horizontal bars (A and B).

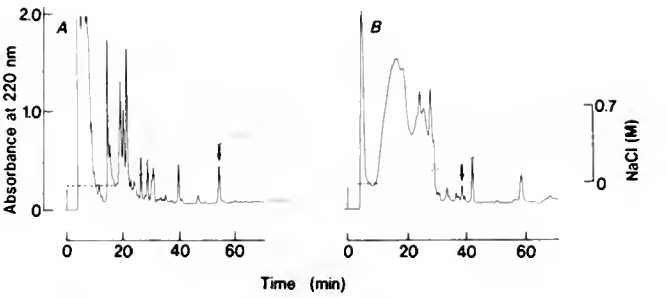

Figure 3. HPLC profiles of active fractions (A and B in Fig. 2) on a cation-exchange column. Elution was performed in a 70-min linear gradient of 0–0.7 *M* NaCl in 10 m*M* phosphate buffer (pH 7.1) at a flow rate of 0.5 ml/min (collected in 1-ml fractions). The activities (A and B) were detected in respective peaks indicated by arrows.

Salines

The saline used for *Perinereis* and *Urechis* muscles was ASW of the following composition: 445 m*M* NaCl, 55 m*M* $MgCl_2$, 10 m*M* $CaCl_2$, 10 m*M* KCl, 10 m*M* Tris-HCl; pH 7.6. For the *Rapana* and *Fusinus* muscles, low Mg-ASW (20 m*M* $MgCl_2$) was used. The low-Mg ASW was prepared by replacing a part of $MgCl_2$ in the normal ASW with osmotically equivalent NaCl.

Results

The retained material (RM) eluted with 50% methanol was examined for its biological action on three muscle systems, the esophagus of *Perinereis*, the inner circular body-wall muscle of *Urechis* and the radula retractor muscle of *Rapana* (Fig. 1). The RM elevated a basal tone with rhythmic small contractions in the esophagus of *Perinereis* and exerted inhibitory effects on twitch contractions evoked by electrical stimulations in the latter two muscles. After the test solution was replaced with normal ASW, the contractions of *Rapana* radula retractor became greater than the control contractions and then returned to the control level. We decided to purify at first the substance which elicited contractions of the *Perinereis* esophagus.

At the first step of HPLC, two contractile peaks (peak A and B) were found. They were eluted at approximately 15% and 20% ACN, respectively (Fig. 2). At the second step, active substances of peak A and B were eluted at 13% ACN and 19% ACN, respectively (data not shown). Then, the fractions containing active substance A and B were respectively subjected to the cation-exchange HPLC

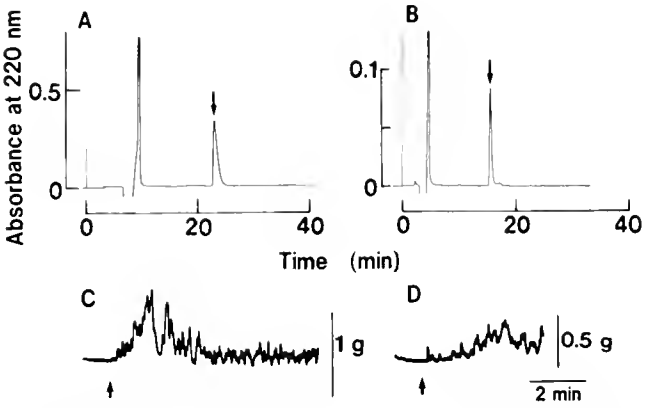

Figure 4. Final purification by HPLC using a reversed-phase column (A, B) and the action of each purified substance on the *Perinereis* esophagus (C, D). Isocratic elution with 17% ACN (A) and 19% ACN (B) in 0.1% TFA at a flow rate of 0.3 ml/min. Aliquots (1/100) of the purified substances were dissolved in ASW and applied to the isolated esophagus at the time indicated by arrows (C, D).

(Fig. 3). The active substances appeared to be eluted as single peaks around 0.35 *M* NaCl (A) and 0.25 *M* NaCl (B). The final purification was performed on the C-18 column with an isocratic elution of 17% ACN (A) and 19% ACN (B) (Fig. 4). The respective single peaks with OD at 220 nm of 0.303 (A) and 0.085 (B) were eluted at 23 min and 16 min after injection. The purified substances (1/100) elicited rhythmic contractions of the esophagus (Fig. 4C, D).

Amino acid sequence analysis of the purified substances (A and B) revealed the structure to be the octapeptide Ala (216)-Lys (43.3)-Ser (8.7)-Gly (7.0)-Phe (5.9)-Val (1.7)-Arg (1.3)-Ile (+) and the heptapeptide Val (181.5)-Ser (66.0)-Ser (45.8)-Phe (118.6)-Val (150.2)-Arg (28.2)-Ile (0.9), respectively (the figures are expressed in pmoles). The peptides of the respective sequences with C-terminus amidated were synthesized, and HPLC profiles of the synthetic peptides were compared with those of native ones. The synthetic and native peptides showed identical retention times on the C-18 reversed-phase column and the cation-exchange column (data not shown). Furthermore, the mixture of the synthetic and native peptides was eluted as a single peak on each column (Fig. 5). The respective synthetic peptides evoked contraction of the *Perinereis* esophagus in the similar manner to the corresponding native peptides (Figs. 6, 7). The threshold concentrations for the synthetic peptides to evoke contraction were found to be between 10^{-10} *M* and 10^{-9} *M* for both peptides.

Thus, the structures of substance A and B were concluded to be AKSGFVRIamide and VSSFVRIamide, respectively. Both AKSGFVRIamide and VSSFVRIamide were members of S-Iamide peptides which had been purified from one echiuroid and four mollusks (Table 1).

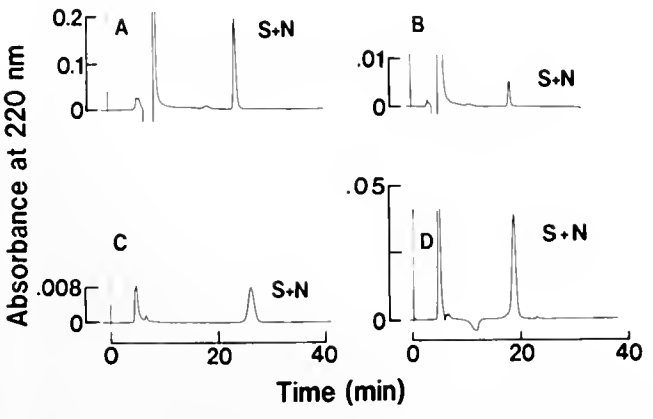

Figure 5. HPLC profiles of mixtures of native and synthetic peptides. AKSGFVRIamide (A) and VSSFVRIamide (B) on a reversed phase column with an isocratic elution of 17% ACN and 19% ACN at a flow rate of 0.3 ml/min. AKSGFVRIamide (C) and VSSFVRIamide (D) on a cation-exchange column with an isocratic elution of 0.27 *M* NaCl and 0.14 *M* NaCl in 10 m*M* phosphate buffer (pH 7.1) at a flow rate of 0.5 ml/min.

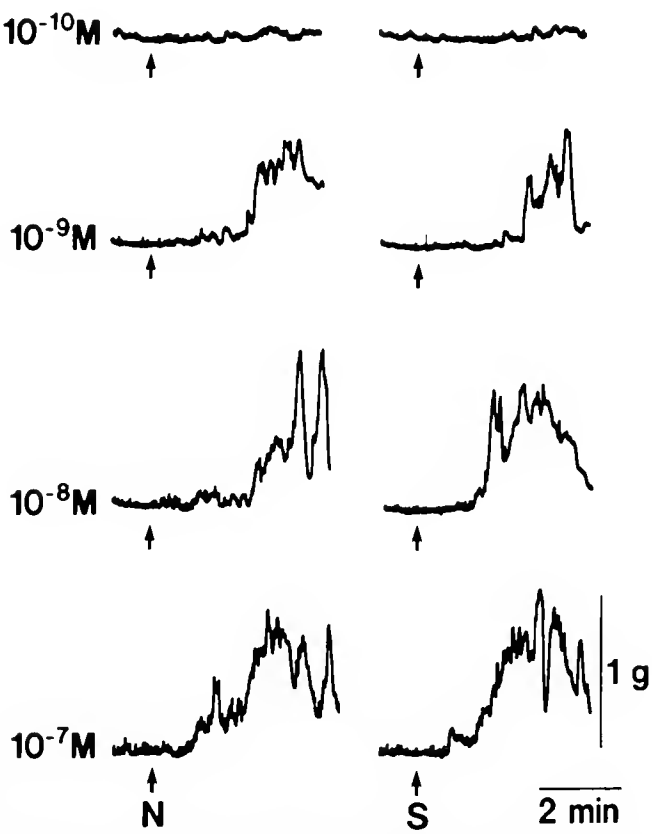

Figure 6. Comparison of the bioactivities of the native (N) and synthetic (S) peptides (AKSGFVRIamide) on the isolated esophagus of *Perinereis*. The peptide solutions were applied at the time indicated by arrows. The concentration of the native peptide was estimated by comparing its peak height on HPLC with that of the synthetic peptide.

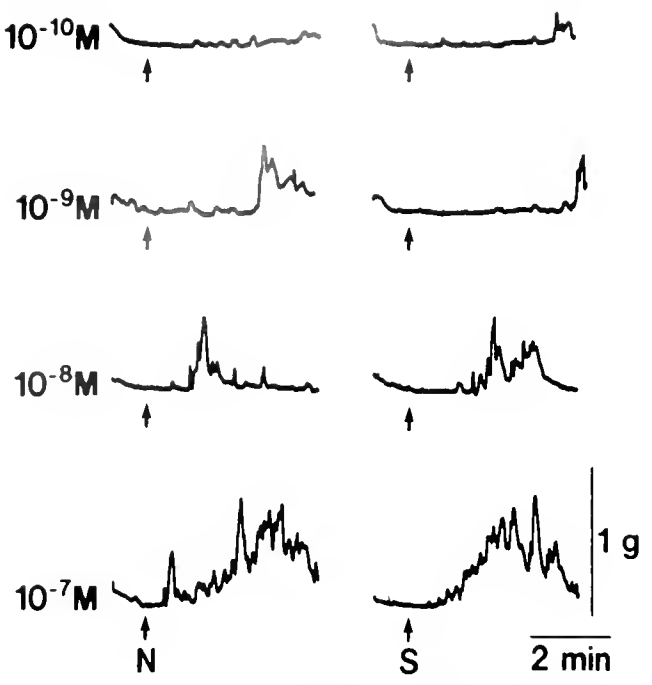

Figure 7. Comparison of the bioactivities of the native (N) and synthetic (S) peptides (VSSFVRIamide) on the isolated esophagus of *Perinereis*. The peptide solutions were applied at the time indicated by arrows. The concentration of the native peptide was estimated by comparing its peak height on HPLC with that of the synthetic peptide.

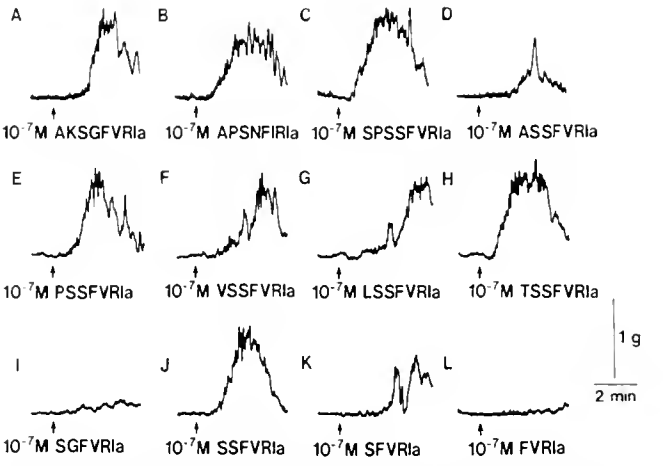

Figure 8. The actions of 10^{-7} *M* of various S-lamide peptides and some fragment peptides on the isolated *Perinereis* esophagus. Each peptide was applied at the time indicated by arrows.

These S-lamide peptides and some fragment peptides were examined on the *Perinereis* esophagus (Fig. 8). All of the S-lamide family peptides and the fragment peptides more or less elicited rhythmic contractions of the esophagus at 10^{-7} *M*.

The biological activities of the two S-lamide peptides isolated from *Perinereis* were examined on three muscle systems, the inner circular body-wall muscle of *Urechis* (Fig. 9), the ABRM of *Mytilus* (Fig. 10) and the radula retractor muscle of *Fusinus* (Fig. 11). In the *Urechis* muscle, the twitch contraction evoked by electrical stimulation was inhibited by the S-lamide peptides; AKSGFVRIamide was less potent than VSSFVRIamide (Fig. 9). The phasic contraction of the *Mytilus* ABRM evoked by repetitive electrical stimulation was inhibited by the peptides (Fig. 10). The effects of these two peptides on *Fusinus* muscle were somewhat complicated. AKSGFVRIamide potentiated twitch contractions at the concentration of 10^{-7} *M*, but inhibited at 10^{-5} *M*. VSSFVRIamide, on the other hand, did not show any augmentation of the twitch contraction, but inhibited at concentrations higher than 10^{-6} *M* (Fig. 11).

Table I

S-lamide peptides

Phyla	Species	Structures
Annelida	*Perinereis vancaurica*	AKSGFVRIamide
		VSSFVRIamide
Echiura	*Urechis unicinctus*	ASSFVRIamide
		PSSFVRIamide
		VSSFVRIamide
Mollusca	*Fusinus ferrugineus*	LSSFVRIamide
	Helix pomatia	TSSFVRIamide
	Achatina fulica	SPSSFVRIamide
		APSNFIRIamide
	Anodonta cygnea	SGFVRIamide

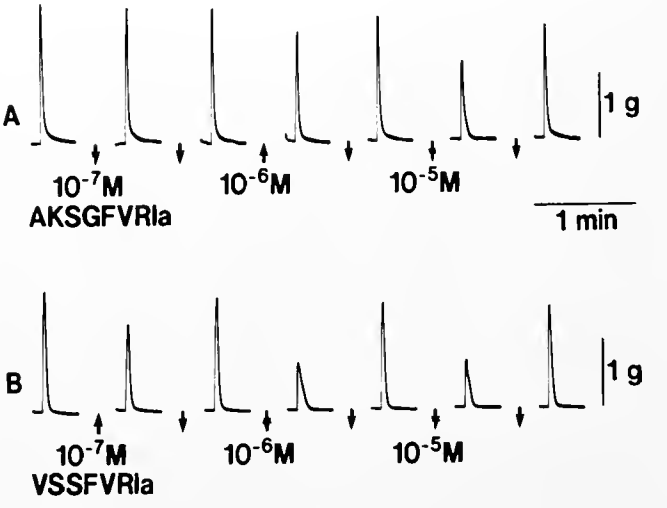

Figure 9. Effects of AKSGFVRIamide and VSSFVRIamide on twitch contraction of the inner circular muscle of the body wall of *Urechis*. The upward arrows indicate application of the peptides. The downward arrows indicate washing-out of the peptides. The twitch contraction was evoked by an electrical pulse (20 V, 3 msec).

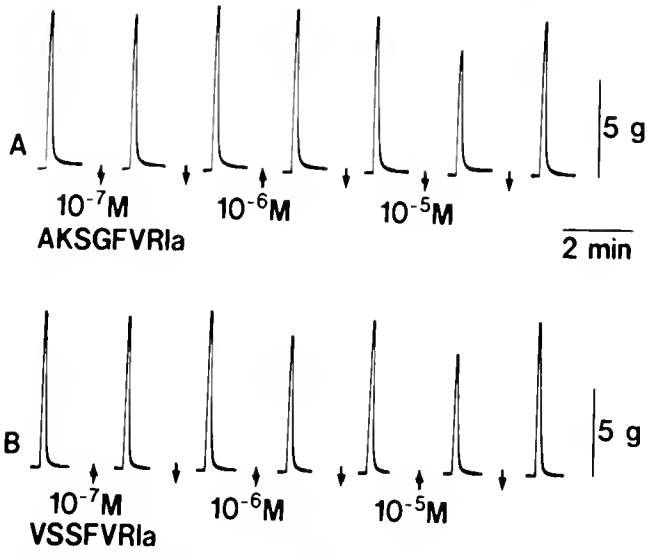

Figure 10. Effects of AKSGFVRIamide and VSSFVRIamide on phasic contraction of the ABRM of *Mytilus*. The upward arrows indicate application of the peptides. The downward arrows indicate washing-out of the peptides. The phasic contraction was evoked by repetitive electrical pulses (15 V, 3 msec, 10 Hz, 50 pulses).

Discussion

The principal aim of this study was to find out authentic bioactive peptides in annelids. We isolated two S-lamide family peptides, AKSGFVRIamide and VSSFVRIamide, from the polychaete annelid, *Perinereis*. Both the peptides showed a contractile effect on the esophagus of the animal. AKSGFVRIamide is the novel peptide, and VSSFVRIamide has previously been found in the ventral nerve cord of the echiuroid worm, *Urechis*. S-lamide peptides have been found so far in one species of Echiura and four species of Mollusca (Ikeda *et al.*, 1991; Kuroki *et al.*, 1992; Muneoka and Kobayashi, 1992; in prep. for *Anodonta* S-lamide peptide), as listed in Table I. Thus, S-lamide peptides have been proven to be distributed among at least three invertebrate phyla and may range throughout the Protostomia.

The C-termini of the two S-lamide peptides identified in the current study were concluded to be amidated, though the purified substances were not subjected to fast atom bombardment mass spectrometry. Since the C-termini of all the S-lamide peptides so far isolated from the echiuroid and molluscs have been known to be amidated, we synthesized AKSGFVRIamide and VSSFVRIamide and compared their behavior on HPLC and contractile activity with those of the purified native peptides. As a result, the identical properties of the native and synthesized peptides were confirmed.

The synthetic tetra- and pentapeptides, FVRIamide and SFVRIamide, showed only a slight activity for induction of the spontaneous contraction in the esophagus of *Perinereis*. However, the synthetic hexapeptide, SSFVRIamide (a common structure for most of the S-lamide peptides), was active, suggesting that at least six amino acid residues would be important for the expression of the activity of S-lamide peptides. However, SGFVRIamide which has been isolated from *Anodonta* showed weak contractile activity in the esophagus. The substitution of the amino acid residue, Ser, with Gly seems to be deleterious for contractile activity, and the N-terminal elongation of SGFVRIamide by Ala-Lys might cancel the deleteriousness.

The effect of AKSGFVRIamide on twitch contractions of the radula retractor of *Fusinus* was somewhat complicated. That is, the peptide potentiated the contractions at 10^{-7} *M*, but inhibited at 10^{-5} *M*. The well-known molluscan neuropeptide FMRFamide has been known to potentiate the contractions of the same muscles (Kuroki *et al.*, 1992). Since the C-terminal tetrapeptide sequence of the S-lamide peptide, -FVRIamide, is closely related to that of FMRFamide, the potentiating effect of 10^{-7} *M* AKSGFVRIamide may be attributable to the FMRFamide-like action of the S-lamide peptide. The inhibition of the twitch contractions by 10^{-5} *M* of AKSGFVRIamide is probably the original action of the S-lamide peptide. In this connection, Kuroki *et al.* (1992) reported that another S-lamide peptide, LSSFVRIamide, isolated from the ganglia of *Fusinus* showed the same dose-dependent actions on the contractions as did AKSGFVRIamide.

The physiological role of AKSGFVRIamide and VSSFVRIamide in *Perinereis* is not elucidated at present. The threshold concentrations of these two S-lamide peptides to induce contraction of the esophagus were between

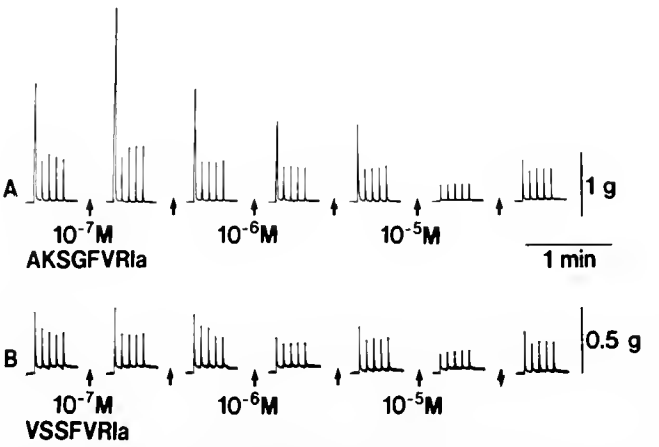

Figure 11. Effects of AKSGFVRIamide and VSSFVRIamide on twitch contractions of the radula retractor muscle of *Fusinus*. The upward arrows indicate application of the peptides. The downward arrows indicate washing-out of the peptides. The twitch contractions were evoked by a train of electrical pulses (15 V, 1 msec, 0.2 Hz, 5 pulses).

10^{-10} *M* and 10^{-9} *M*. It seems to be probable that these S-lamide peptides are neuropeptides which regulate the gut-motility in the annelid. It has been demonstrated that FMRFamide is present in annelids such as *Nereis virens* (Krajniak and Price, 1990), *Nereis diversicolor* (Baratte *et al.*, 1991) and *Hirudo medicinalis* (Evans *et al.*, 1991) and that the tetrapeptide relaxed spontaneous and electrically-induced contractions of the esophagus (Krajniak and Greenberg, 1992). Thus, the action of FMRFamide on the esophagus of polychaete annelid is opposite to those of the S-lamide peptides. This was also the case for most of the molluscan muscles examined (Muneoka and Kobayashi, 1992). Therefore, FMRFamide and the S-lamide peptides may regulate the esophagus-motility in an antagonistic manner, and this regulatory relation may be also applied to the molluscan muscles.

The classical neurotransmitters such as norepinephrine, epinephrine, acetylcholine, 5-hydroxytryptamine and γ-aminobutyric acid also seem to regulate gut-motility in the polychaete annelid, *Chaetopterus variopedatus* (Anctil *et al.*, 1984), and the presence of catecholamines (dopamine, norepinephrine and epinephrine) has been reported in the nervous and intestinal tissues of the same species (Anctil *et al.*, 1990). Thus, peptides such as FMRFamide and the S-lamide peptides, and classical transmitters seem to regulate the gut-motility harmoniously in annelids. Further study is necessary to reveal the relationship between the physiological role of classical transmitters and peptides.

Acknowledgments

The authors wish to express their thanks to Professor Yojiro Muneoka (Hiroshima University) for his kind advice regarding the present study.

Literature Cited

Alumets, J., R. Hakanson, F. Sundler, and T. Thorell. 1979. Neuronal localisation of immunoreactive enkephalin and β-endorphin in the earthworm. *Nature* **279:** 805–806.

Anctil, M., M. Laberge, and N. Martin. 1984. Neuromuscular pharmacology of the anterior intestine of *Chaetopterus variopedatus*, a filter-feeding polychaete. *Comp. Biochem. Physiol.* **79:** 343–351.

Anctil, M., J.-P. De Waele, M.-J. Miron, and A. K. Pani. 1990. Monoamines in the nervous system of the tube-worm *Chaetopterus variopedatus* (Polychaeta): Biochemical detection and serotonin immunoreactivity. *Cell Tissue Res.* **259:** 81–92.

Baratte, B., H. Gras-Masse, G. Ricart, P. Bulet, and N. Dhainaut-Courtois. 1991. Isolation and characterization of authentic Phe-Met-Arg-Phe-NH_2 and the novel Phe-Thr-Arg-Phe-NH_2 peptide from *Nereis diversicolor*. *Eur. J. Biochem.* **198:** 627–633.

Carraway, R., S. E. Ruane, and H. R. Kim. 1982. Distribution and immunochemical character of neurotensin-like material in representative vertebrates and invertebrates: Apparent conservation of the COOH-terminal region during evolution. *Peptides* **3:** 115–123.

Dhainaut-Courtois, N., M. P. Dubois, G. Tramu, and M. Masson. 1985. Occurrence and coexistence in *Nereis diversicolor* O. F. Muller (Annelida Polychaeta) of substances immunologically related to vertebrate neuropeptides. *Cell Tissue Res.* **242:** 97–108.

Diaz-Miranda, L., G. Escalona de Motta, and J. E. Garcia-Arraras. 1991. Localization of neuropeptides in the nervous system of the marine annelid *Sabellastarte magnifica*. *Cell Tissue Res.* **266:** 209–217.

Diaz-Miranda, L., G. Escalona de Motta, and J. E. Garcia-Arraras. 1992. Monoamines and neuropeptides as transmitters in the sedentary polychaete *Sabellastarte magnifica*: Actions on the longitudinal muscle of the body wall. *J. Exp. Zool.* **263:** 54–67.

Engelhardt, R. P., N. Dhainaut-Coutois, and G. Tramu. 1982. Immunohistochemical demonstration of a CCK-like peptide in the nervous system of a marine annelid worm, *Nereis diversicolor* O. F. Muller. *Cell Tissue Res.* **227:** 401–411.

Evans, B. D., J. Pohl, N. A. Kartsonis, and R. L. Calabrese. 1991. Identification of RFamide neuropeptides in the medicinal leech. *Peptides* **12:** 897–908.

Holmgren, S. 1989. Gut motility. Pp. 231–255 in *The Comparative Physiology of Regulatory Peptides*, S. Holmgren, ed., Chapman and Hall, New York.

Ikeda, T., I. Kubota, Y. Kitajima, and Y. Muneoka. 1991. Structures and actions of neuropeptides isolated from an echiuroid worm, *Urechis unicinctus*. Pp. 29–41 in *Comparative Aspects of Neuropeptide Function*, E. Florey and G. B. Stefano, eds., Manchester University Press, Manchester.

Ikeda, T., Y. Kuroki, I. Kubota, H. Minakata, K. Nomoto, W. Miki, T. Kiss, L. Hiripi, and Y. Muneoka. 1991. SSFVRIamide peptides—A new family of neuropeptides distributed interphyletically. Pp. 65–70 in *Peptide Chemistry*, A. Suzuki, ed., Protein Research Foundation, Osaka, Japan.

Kaloustian, K. V., and J. A. Edmands. 1986. Immunochemical evidence for substance P-like peptide in tissues of the earthworm *Lumbricus terrestris*: Action on intestinal contraction. *Comp. Biochem. Physiol.* **83C:** 329–333.

Krajniak, K., and D. A. Price. 1990. Authentic FMRFamide is present in the polychaete *Nereis virens*. *Peptides* **11:** 75–77.

Krajniak, K., and M. J. Greenberg. 1992. The localization of FMRFamide in the nervous and somatic tissues of *Nereis virens* and its effects upon the isolated esophagus. *Comp. Biochem. Physiol.* **101C:** 93–100.

Kuroki, Y., T. Kanda, I. Kubota, T. Ikeda, Y. Fujisawa, H. Minakata, and Y. Muneoka. 1992. FMRFamide-related peptides isolated from the prosobranch mollusc *Fusinus ferrugineus*. *J. Biol. Hung.* **43:** 491–494.

Muneoka, Y., and M. Kobayashi. 1992. Comparative aspects of structure and action of molluscan neuropeptides. *Experientia* **48:** 448–456.

Muneoka, Y., Y. Kuroki, H. Minakata, T. Ikeda, Y. Fujisawa, K. Nomoto, and I. Kubota. 1991. Structure and pharmacological characterization of a molluscan neuropeptide related to the crustacean RPCH. Pp. 274–279 in *Molluscan Neurobiology*, K. S. Kits, H. H. Boer, and J. Joose, eds. North Holland, Amsterdam.

Price, D. A., and M. J. Greenberg. 1977. Structure of a molluscan cardioexcitatory neuropeptide. *Science* **197:** 670–671.

Tashiro, N., and H. Kuriyama. 1978. Neurosecretion and pharmacology of the nervous system. Pp. 207–242 in *Physiology of Annelids*, P. J. Mill, ed. Academic Press, London.

Thorndyke, M. C. 1989. Peptides in invertebrates. Pp. 203–228 in *The Comparative Physiology of Regulatory Peptides*, S. Holmgren, ed. Chapman and Hall, New York.

Reference: *Biol. Bull.* **184**: 223–229. (April, 1993)

Photosynthesis and Retention of Zooxanthellae and Zoochlorellae Within the Aeolid Nudibranch *Aeolidia papillosa*

F. K. McFARLAND AND G. MULLER-PARKER[1]

Shannon Point Marine Center, Western Washington University, 1900 Shannon Point Road, Anacortes, Washington 98221

Abstract. Both zooxanthellae and zoochlorellae are found in the cerata of *Aeolidia papillosa* after it has ingested symbiotic *Anthopleura elegantissima* containing these algae. High rates of photosynthesis were found in algae present in the cerata and in algae isolated from nudibranch feces. For algal cells present in the cerata of nudibranchs collected in June 1991, carbon fixation by zooxanthellae (1.18 ± 0.36 pg C/cell/h) was significantly greater than carbon fixation by zoochlorellae (0.55 ± 0.32 pg C/cell/h). Algal densities within the cerata of laboratory fed nudibranchs were significantly greater for zoochlorellae (175 ± 82 cells/μg protein, light treatment; 131 ± 106 cells/μg protein, dark treatment) than for zooxanthellae (38 ± 18 cells/μg protein, light; 53 ± 30 cells/μg protein, dark). Ceratal densities of zooxanthellae (16 ± 8 cells/μg protein) in the field during January 1992 were low in comparison to ceratal densities in the laboratory—several of the nudibranchs in the field lacked any symbiotic algae, and zoochlorellae were always absent. Nudibranch algal densities were not stable and dropped rapidly if the nudibranchs were starved. Both zoochlorella and zooxanthella densities dropped to 0 cells/μg protein within 11 days of starvation. While these results show that the relationship between *A. papillosa* and the two algae is not a stable symbiosis, the photosynthetic activity of the algae in the cerata suggests that the nudibranch and/or the algae may benefit from the association while it lasts.

Introduction

Several aeolid nudibranchs, as well as other nudibranchs with cerata, contain zooxanthellae of the genus *Symbiodinium* (Rudman, 1981a, b, 1982; Kempf, 1984, 1991). Each ceras contains a diverticulum of the digestive gland within which the algal symbionts are both extra- and intracellularly located (Rudman, 1982; Kempf, 1984, 1991). Many of these nudibranchs obtain their algae through ingestion of marine cnidarians which are symbiotic with zooxanthellae. Zooxanthellae in the cnidarian host fix carbon through photosynthesis, and then translocate much of this carbon to the animal's tissue (*e.g.*, Trench, 1979). The carbon available for translocation may represent as much as 95% of the amount fixed (Muscatine *et al.*, 1984), and is used by the host for respiration, growth, and reproduction (Kevin and Hudson, 1979; Davies, 1984; Rinkevich, 1989).

The ability of zooxanthellae to fix and translocate carbon in nudibranchs, as well as the benefits of such an association to the nudibranchs, have been described for several relationships. Crossland and Kempf (1985) reported that zooxanthellae in the tropical nudibranch *Melibe pilosa* fixed large amounts of carbon (5.85 mg C/mg chlorophyll *a*/h), and that fixed carbon was translocated to the nudibranch for growth and reproduction. Kempf (1990) reported that the aeolid nudibranch *Berghia verrucicornis* produced 1.7 times more eggs when in a symbiotic relationship with zooxanthellae than when algae-free. At high densities, zooxanthellae in the temperate nudibranch *Pteraeolidia ianthina* can supply carbon well in excess of the nudibranch's respiratory demand during the spring and summer (Høegh-Guldberg and Hinde, 1986; Hoegh-Guldberg *et al.*, 1986). With the exception of the nudibranch *Pteraeolidia ianthina*, only tropical species have been studied, and all the studies have focused on species with zooxanthellae symbionts.

Received 6 July 1992; accepted 25 January 1993.

[1] Author to whom reprint requests should be addressed.

The temperate nudibranch *Aeolidia papillosa* is found within the intertidal zone of the northeastern Pacific (Kozloff, 1983) where one of its preferred prey species is the symbiotic anemone *Anthopleura elegantissima* (Waters, 1973; Edmunds *et al.*, 1974; McDonald and Nybakken, 1978). *A. elegantissima* forms symbiotic relationships with both zooxanthellae and the unicellular green algae called zoochlorellae (Muscatine, 1971). Fixation and translocation of carbon by zooxanthellae in *A. elegantissima* is substantial (Trench 1971a, b), and the contribution of these anemones to intertidal gross primary production is equal to that of temperate intertidal seaweed populations on an areal basis (Fitt *et al.*, 1982). Zoochlorellae found in *A. elegantissima* and *A. xanthogrammica* are also photosynthetically active (Muscatine, 1971; O'Brien, 1980). While both zooxanthellae and zoochlorellae fix carbon in their host species, zooxanthellae translocate much more of their fixed carbon to their host than do zoochlorellae. Zooxanthellae translocate on the order of 50% of the carbon fixed while zoochlorellae translocate less than 5% (Muscatine, 1971; O'Brien, 1980).

High densities of zooxanthellae and zoochlorellae are found in the cerata of *A. papillosa* after it has been fed symbiotic anemones containing these algae (Kellett and Wiederspohn, pers. comm.). The following study considers the nature of the symbiotic relationship formed between *A. papillosa* and both zooxanthellae and zoochlorellae, particularly the photosynthetic activity of these algae and the stability of their populations within the nudibranchs' cerata.

Materials and Methods

Collection and maintenance of nudibranchs and anemones

Specimens of *A. papillosa* were collected from the San Juan Islands, WA in June 1991 and from the Port Orchard side of the Sinclair Inlet, WA in January 1992. All anemones used to feed the nudibranchs were collected from Skyline beach in Burrows Bay at Anacortes, WA. No nudibranchs were found on this beach. Individual nudibranchs were maintained in separate plastic mesh containers submerged in flow-through seawater tables at Shannon Point Marine Center (Anacortes, WA). Seawater tables were cleaned twice weekly. The temperature of the water during June 1991 ranged from 10.7°C to 13.0°C with a mean of 11.6°C. During January 1992 the temperature ranged from 7.5°C to 9.2°C with a mean of 8.4°C, and during February 1992 the temperature ranged from 8.2°C to 10.9°C with a mean of 9.1°C. The average salinity during the study was 29 ‰.

Specimens of *A. papillosa* collected in June 1991 were used to determine the productivity of symbiotic algae. Continuous light provided to nudibranchs by a bank of two fluorescent lamps averaged 28 μmol photons/m^2/s at the water's surface (LiCor cosine quantum sensor, 400–700 nm PAR). One group of nudibranchs was fed brown *A. elegantissima* containing zooxanthellae, another group was fed green *A. elegantissima* containing zoochlorellae, and the control group was fed white (algae-free) *A. elegantissima*. Personal experience has shown that brown anemones always contain at least 98% zooxanthellae (on a cell basis) and green anemones contain at least 98% zoochlorellae. This was confirmed during the experiment by periodic microscopic examinations of tentacle squashes from brown and green anemones.

Specimens of *A. papillosa* collected in January were separated into two groups of twelve to examine retention of zooxanthellae and zoochlorellae in the cerata. The initial algal complement of field nudibranchs was determined by sampling two cerata from each nudibranch within 24 h of collection. One group was maintained in continuous darkness, and the other group was maintained under 12 h light/12 h dark. During the light cycle, irradiance at the water's surface averaged 33 μmol photons/m^2/s. Each group in the light and the dark treatments was further separated into three treatments of 4 nudibranchs each. One group was fed brown anemones for 28 days, then had its diet switched to green anemones for 13 days, and was then starved. Another group was fed green anemones for 28 days and was then switched to a diet of brown anemones. The third group was fed brown anemones for 28 days and was then starved. Each fed nudibranch was given 5 anemones per week, provided individually on separate days. Fed nudibranchs had no more than two consecutive days without feeding.

Productivity of symbiotic algae

Algae within the cerata. To determine whether zooxanthellae and zoochlorellae remain photosynthetically active within the cerata of the nudibranchs, 3 cerata (one anterior, one middle, and one posterior) were removed from each nudibranch and incubated whole with ^{14}C in 20 ml glass scintillation vials. 2.0 ml of filtered seawater (FSW) and 0.1 μCi ^{14}C bicarbonate were added to each vial. The cerata were incubated at room temperature (20–24°C) at 249 μmol photons/m^2/s for 50–120 min. Control vials for dark carbon fixation were also maintained for each ^{14}C experiment. Replicate vials of each treatment were wrapped with black electrical tape and incubated under the same conditions as light vials. The dark vials were used to correct for dark carbon fixation. To determine total activity (TA), 100 μl was subsampled from each vial and placed in a 7 ml plastic scintillation vial with 5 ml of Ecolume (ICN) scintillation fluid. Incubations were terminated by removing the cerata and washing them with several rinses of FSW. The cerata were then homogenized

in 1.5 ml of FSW using a 5-ml Wheaton tissue grinder. Two 500 μl subsamples were taken from each homogenate solution and placed in separate plastic scintillation vials. All unfixed $^{14}CO_2$ was evolved from the homogenate subsamples by adding 300 μl of 6N HCl and then placing the vials under a heat lamp in a fume hood for 1 h. The subsamples were neutralized with 300 μl 6N NaOH prior to the addition of 5 ml scintillation fluid. The homogenate subsamples were counted along with the TA subsamples in a Packard TR 1900 scintillation counter using the automatic DPM mode. The remaining homogenate suspension was used for algal cell counts and then frozen for future protein analysis.

Algae isolated from nudibranch feces. Nudibranchs fed symbiotic *A. elegantissima* produced green or brown fecal pellets consisting mainly of intact symbiotic algae. Fresh fecal pellets were collected from nudibranchs and were suspended in FSW. Fecal algae were washed three times in FSW by centrifugation and resuspension. The final suspension was sequentially filtered through 73 μm and 20 μm Nitex screening to remove debris. After initial cell counts algal densities were adjusted to 4–6 × 10^5 cells/ml. The productivity of fecal algae was measured using a protocol similar to that described for the cerata with the following exceptions: 2.0 ml of either the green or the brown fecal algae suspension was placed in each 20 ml glass vial and the algal cells were allowed to incubate for 30 min at room temperature (20–24°C). Incubations were at an average irradiance of 249 μmol photons/m^2/s.

Algae freshly isolated from anemones. The productivity of algae isolated directly from *A. elegantissima* was also determined. The oral disk and tentacles of individual anemones were excised and homogenized using a tissue grinder. Algal cell suspensions were washed and filtered as described above. Final algal densities ranged from 2.5–6 × 10^5 cells/ml. Incubations were performed as above except that cells were allowed to incubate for up to 1 h at an average irradiance of 102 μmol photons/m^2/s.

Algal densities and replacement within the cerata

Algal population density within the cerata was measured twice each week by removing 2 cerata (one posterior and one anterior) from each experimental nudibranch during January and February 1992. The cerata were homogenized in 1.5 ml of cold FSW using a 2-ml Wheaton tissue grinder. Algal cell counts of the homogenate solutions were determined using a hemocytometer, and the remaining homogenate solutions were frozen for future protein analysis. Protein analysis was performed using the Lowry method (Lowry *et al.*, 1951) and bovine serum albumin (BSA) standards with the modification that the homogenates and standards were pre-treated at 30°C for 30 min in 0.1 N NaOH to solubilize the proteins. Cell counts and protein content were used to determine cell densities within the cerata of nudibranchs fed green and brown *A. elegantissima.*

Statistical analyses

Comparison of photosynthetic rates. Photosynthesis data for algae in *A. papillosa* cerata, algae freshly isolated from *A. papillosa* feces, and freshly isolated from *A. elegantissima* were analyzed to determine if there was a significant difference in the rates of carbon fixation for zooxanthellae and zoochlorellae. Zooxanthellae rates of carbon fixation were compared to zoochlorellae carbon fixation rates using two-sample t-tests. Algae in cerata, algae from feces, and algae from anemones were all compared separately. Comparisons were also made of the photosynthetic rates of zooxanthellae and zoochlorellae between the different treatments.

Comparison of algal densities. Algal densities in *A. papillosa* cerata after 28 days of feeding the nudibranch either brown or green anemones were analyzed using two-sample t-tests to determine if there was a significant difference in the densities of zooxanthellae and zoochlorellae found in the nudibranchs both under light and dark conditions. When zooxanthellar densities were compared to zoochlorellar densities, the data were logarithmically transformed to correct for differences in variance between the algal types. The effect of light versus dark on zooxanthellar and zoochlorellar densities was also analyzed using two-sample t-tests.

Comparison of treatment effect on algal replacement. Repeated-measures analysis of variance (Potvin and Lechowicz, 1990) was used to analyze the effect of light versus dark on the replacement (after switching diets) and expulsion (during starvation) of algae in the cerata. Zooxanthellae data for the replacement of zoochlorellae with zooxanthellae and the expulsion of zooxanthellae were logarithmically transformed to correct for differences in variance between the light and dark treatments.

Results

Productivity of symbiotic algae

Both zooxanthellae and zoochlorellae remain photosynthetically active within the nudibranch cerata (Fig. 1), where the mean rate of carbon fixation by zooxanthellae is significantly greater ($P = 0.0216$) than that of zoochlorellae. Cerata used for determining the photosynthetic rate of zooxanthellae contained 99.9% zooxanthellae on a cell basis. Cerata used for determining photosynthetic rate of zoochlorellae contained 99.5% zoochlorellae.

Figure 1 also shows that algal symbionts isolated from nudibranch feces also had high photosynthetic rates. There is no significant difference ($P = 0.0781$) between the pho-

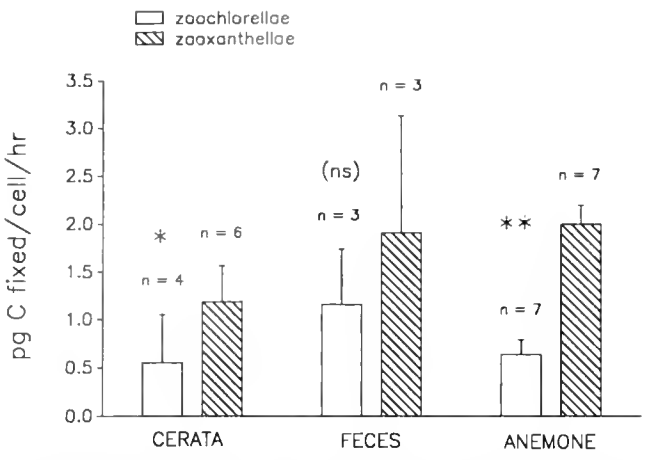

Figure 1. Mean rates of photosynthesis for algae incubated within whole cerata (*A. papillosa*) and for algae isolated from *A. papillosa* feces and from symbiotic anemones (*A. elegantissima*). Photosynthesis was determined in July 1991 at an average irradiance of 249 μmol/m^2/s for cerata and fecal algae and in May 1991 at an average irradiance of 102 μmol/m^2/s for anemone algae. Vertical lines represent 95% confidence intervals. Numbers above each bar represent treatment size. *, $P < 0.05$; **, $P < 0.0001$.

tosynthetic rate of zooxanthellae and that of zoochlorellae isolated from the nudibranch feces. But there is a significant difference ($P < 0.0001$) between the photosynthetic rate of zooxanthellae and the photosynthetic rate of zoochlorellae isolated from *A. elegantissima*.

In cross comparisons, photosynthesis by fecal zoochlorellae is significantly higher than photosynthesis of both zoochlorellae in the cerata ($P = 0.0369$) and zoochlorellae from the anemone ($P = 0.0033$). Photosynthetic rates are not significantly different between zoochlorellae in the cerata and zoochlorellae isolated from the anemone ($P = 0.5493$). For zooxanthellae, photosynthesis in the cerata is significantly lower than photosynthesis by both fecal zooxanthellae ($P = 0.0375$) and anemone zooxanthellae ($P = 0.0003$). The latter two are not significantly different from each other ($P = 0.6772$).

Algal densities within the cerata

Algal densities in freshly collected nudibranchs (field) during January 1992 averaged 16 zooxanthellae/μg protein and ranged from 0 to 69 zooxanthellae/μg protein. Only zooxanthellae were found within the cerata of the 24 nudibranchs collected from one beach on the Sinclair Inlet during a single low tide. No symbiotic algae were found in the cerata of nudibranchs collected in June 1991. These nudibranchs were collected from beaches where symbiotic anemones were not available as a food source. The algal densities in the cerata of field nudibranchs were low in comparison to those of nudibranchs regularly fed symbiotic anemones in the laboratory. These nudibranchs ingested an average of 4.5 anemones each per week regardless of whether they were fed anemones with zooxanthellae or zoochlorellae.

Comparisons of algal densities between the light and dark treatments showed no effect from light on the densities of zooxanthellae or zoochlorellae in nudibranchs fed brown or green anemones, respectively. Zooxanthellae densities in nudibranchs maintained in the light (38 ± 18 cells/μg protein) were not significantly different ($P = 0.3063$) from those in nudibranchs maintained in the dark (53 ± 30 cells/μg protein). Zoochlorellae densities in the light treatment (175 ± 82 cells/μg protein) were not significantly different ($P = 0.3339$) from those in the dark treatment (131 ± 106 cells/μg protein).

Nudibranchs fed green anemones contained significantly higher algal densities than nudibranchs fed brown anemones ($P = 0.0004$ for nudibranchs maintained in the light; $P = 0.0152$ for nudibranchs maintained in the dark). After 28 days of feeding on one type of anemone, the cerata of nudibranchs fed brown anemones contained 99.9% zooxanthellae and the cerata of nudibranchs fed green anemones contained 99.0% zoochlorellae.

Replacement of algal populations in the cerata

Algal densities within the cerata do not remain constant over time and depend on the algal complement of the food source. When the nudibranchs were switched from a diet of anemones containing zoochlorellae to a diet of anemones containing zooxanthellae, the zoochlorellae within the cerata were completely replaced by zooxanthellae within 24 days (Fig. 2), after approximately 15 anemones containing zooxanthellae had been ingested per nudibranch. There is no significant difference between the light and dark treatments in either the loss of zoochlorellae ($P = 0.8338$) or the gain of zooxanthellae ($P = 0.0561$).

The replacement of zooxanthellae with zoochlorellae in the cerata required even less time. Upon switching the diet of nudibranchs from anemones containing zooxanthellae to anemones containing zoochlorellae, the zooxanthellae were replaced by zoochlorellae within 13 days (Fig. 3), after approximately 8 anemones with zoochlorellae had been ingested per nudibranch. Again, there is no significant difference between light and dark treatments in either the loss of zooxanthellae ($P = 0.7988$) or the gain of zoochlorellae ($P = 0.6664$).

The time it took for each type of alga to be completely expelled from the cerata upon starvation was even less than the algal replacement times. All algae disappeared from the cerata within 11 days when nudibranchs containing either zooxanthellae or zoochlorellae were starved (Figs. 3, 4). There is no significant difference between light and dark treatments in either the expulsion of zooxan-

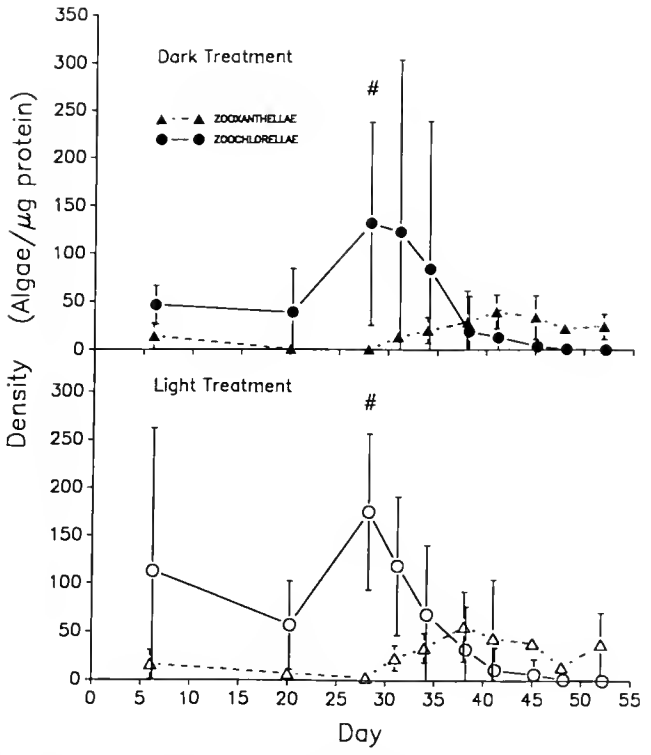

Figure 2. Mean algal densities in the cerata of nudibranchs initially fed anemones containing zoochlorellae, and then switched to anemones containing zooxanthellae on day 28 of the experiment. Closed symbols represent dark treatments and open symbols represent light treatments. △ = zooxanthellae; ○ = zoochlorellae. Vertical lines represent 95% confidence intervals. The size of each treatment was 4 nudibranchs. # = day diet switched.

thellae ($P = 0.6674$) or the expulsion of zoochlorellae ($P = 0.1337$) during starvation.

Discussion

Since both zooxanthellae and zoochlorellae obtained by the ingestion of *Anthopleura elegantissima* remain photosynthetically active within the cerata (Fig. 1), it is likely that *Aeolidia papillosa* derives some benefit from these algae. Because of the higher density of zoochlorellae than zooxanthellae in the cerata, the actual amount of carbon fixed per ceras is not as different as the algal productivities would imply. The lack of any significant difference between the photosynthetic rates of fecal zooxanthellae and zoochlorellae may be due simply to the limited number of replicates. Although incubations were carried out at different irradiances (249 μmol photons/m^2/s for cerata and fecal algae, 102 μmol photons/m^2/s for anemone algae), and algae in cerata are likely to receive lower light during incubations than the isolated algae, both irradiances are well above the I_k value determined for zooxanthellae and zoochlorellae (I_k = 50 μmol photons/m^2/s) in independent experiments also conducted during the summer (Aagaard and Muller-Parker, unpub.).

Zooxanthellae release much more of their photosynthate than do zoochlorellae within their primary hosts *A. elegantissima* and *A. xanthogrammica* (Muscatine, 1971; O'Brien, 1980). If this is also true within the nudibranch's cerata, there may be an energetic advantage to the selection of prey anemones containing zooxanthellae. *A. papillosa* does not appear to selectively retain one alga over the other since the expulsion of algae upon starvation was the same for both algae (Figs. 3, 4). The replacement of zoochlorellae with zooxanthellae took longer than the reverse. This may have been due in part to the size difference of the algae; the larger zooxanthellae may have restricted the exit of smaller zoochlorellae from the diverticula within the cerata.

Any benefits to the nudibranch of containing photosynthetically active algae would be most evident under light conditions. Therefore, if the nudibranch had the ability to control expulsion rates, algae should be retained longer under light than under dark conditions, especially

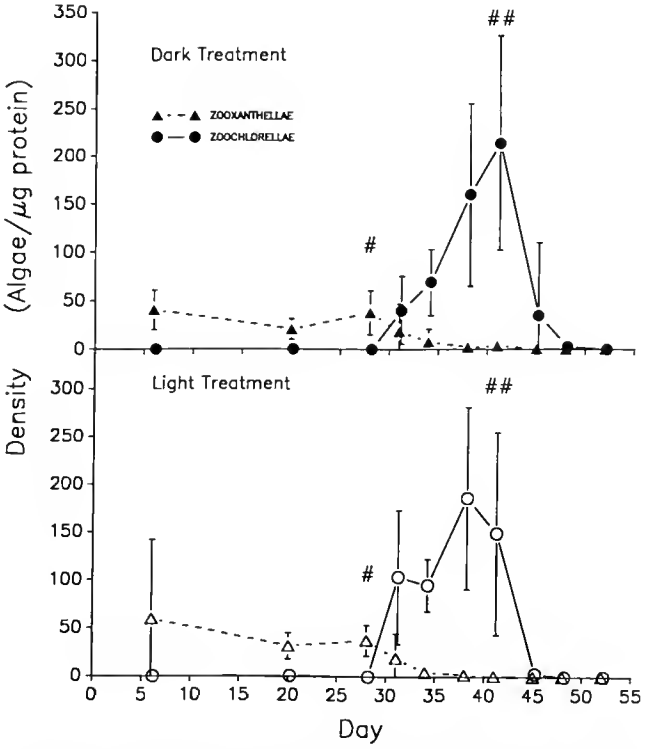

Figure 3. Mean algal densities in the cerata of nudibranchs initially fed anemones containing zooxanthellae, then switched to anemones containing zoochlorellae on day 28 of the experiment, and then starved after day 41 of the experiment. Closed symbols represent dark treatments and open symbols represent light treatments. △ = zooxanthellae; ○ = zoochlorellae. Vertical lines represent 95% confidence intervals. The size of each treatment was 4 nudibranchs. # = day diet switched; ## = day began starving.

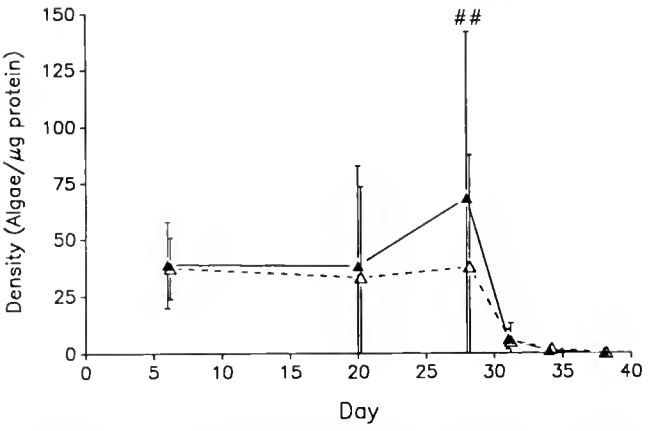

Figure 4. Mean zooxanthellae densities in the cerata of nudibranchs initially fed anemones containing zooxanthellae, and then starved after day 28 of the experiment. Closed symbols represent dark treatments and open symbols represent light treatments. Vertical lines represent 95% confidence intervals. The size of each treatment was 4 nudibranchs. ## = day began starving.

if the nudibranch is starved. The rapid expulsion of algae under both light and dark conditions suggests that *A. papillosa* has little control over the retention or expulsion of algae from its cerata, even when starved.

The large numbers of healthy algal cells present in fecal pellets and the photosynthetic rates of the fecal algae (Fig. 1) indicate that at least a portion of the algae consumed by the nudibranch pass unharmed through the digestive tract. Kempf (1984) found evidence of algal breakdown within the tissues of three tropical nudibranchs, but no evidence of active digestion in two additional species (Kempf 1984, 1991). Whether *A. papillosa* digests some of the ingested symbiotic algae is unknown, but at least a large number of the algae remain unaffected by passage through the nudibranch. Thus, the fecal material of *A. papillosa* may be important in the dispersal of algae and reinfection of temperate anemones as has been suggested for *Berghia major*, a tropical nudibranch that also feeds on symbiotic anemones (Muller Parker, 1984).

Another possibility is that the algae are heterotrophic in the nudibranch and thus represent a liability. Zooxanthellae isolated from the sea anemone *Aiptasia pulchella* are capable of heterotrophic growth under low light levels (Steen, 1987). The possibility of zoochlorellae being parasitic in *A. elegantissima* has been suggested by Muscatine (1971). Because of the generally low light levels in the Northeastern Pacific region, especially during winter months, algae within the cerata of the nudibranch may not be able to meet their carbon requirements photosynthetically. As such, it is possible that algae in *A. papillosa* are a benefit during the summer and a liability during the winter.

Kempf (1990, 1991) suggested that the nudibranch *Berghia verrucicornis* has a primitive mutualistic symbiosis with zooxanthellae based on the following observations. Relatively high concentrations of zooxanthellae are found in all *B. verrucicornis* from the field. The zooxanthellae (1) reside in peri-algal vacuoles within the nudibranch's digestive cells, (2) do not appear to be digested along with their primary host *Aiptasia pallida*, (3) remain photosynthetically active within the nudibranch, and (4) appear to benefit the nudibranch in its reproductive effort. Kempf terms the relationship primitive because the symbiosis is not permanent. The zooxanthellae are eventually exocytosed back into the gut and defecated in a healthy state when nudibranchs are starved in the laboratory.

The relationship between zooxanthellae, zoochlorellae, and *A. papillosa* may also be a primitive form of symbiosis, possibly corresponding to a Type IV association as described by Kempf (1991). Both algae are photosynthetically active within the nudibranch's cerata (Fig. 1). Rapid reduction in the density of each alga when it is no longer available in the nudibranch's food shows that frequent ingestion of symbiotic anemones is required to maintain the association. But *A. papillosa* does not appear to be obligately dependent on either alga at any period of the year. Several of the *A. papillosa* collected in the Sinclair Inlet lacked symbiotic algae in their cerata, and all of the *A. papillosa* collected in June 1991 on beaches where symbiotic *Anthopleura sp.* were not available, lacked symbiotic algae in their cerata. Ultrastructural investigations are needed to determine whether the algae are intracellular, and whether they reproduce while in the cerata. Translocation experiments to determine whether fixed carbon is utilized by the nudibranch for growth or reproduction will help to explain the nature of this relationship. Our work to date suggests that *A. papillosa* will be a good model system for comparing and contrasting the symbiotic relationships between zooxanthellae and zoochlorellae and their animal host.

Acknowledgments

A portion of this study was supported by an NSF Research Experience for Undergraduates Site grant (OCE-9000676) to Shannon Point Marine Center and an NSF Instrumentation and Laboratory Improvement Program award (USE-9051180). The technical assistance of Katie McFarland was critical to the successful completion of the project. The initial work on the symbiotic relationships of *A. papillosa* by Michael Kellett and David Wiederspohn (WWU undergraduates) provided the inspiration for this project. M. Kellett's assistance with collection of nudibranchs is greatly appreciated. Brian Bingham provided invaluable assistance with the statistical analysis of the data. The suggestions of anonymous reviewers are also appreciated.

Literature Cited

Crossland, C. J., and S. C. Kempf. 1985. Carbon fixation and compartmentation in the zooxanthellae containing nudibranchs, *Melibe pilosa* and *Melibe sp.* Proceedings of the Fifth International Coral Reef Congress, Tahiti. Vol. 6: 125–130.

Davies, P. S. 1984. The role of zooxanthellae in the nutritional energy requirements of *Pocillopora eydouxi*. *Coral Reefs* **2:** 181–186.

Edmunds, M., G. W. Potts, R. C. Swinfen, and V. L. Waters. 1974. The feeding preference of *Aeolidia papillosa* (L.) (Mollusca, Nudibranchia). *J. Mar. Biol. Ass. U.K.* **54:** 939–947.

Fitt, W. K., R. L. Pardy, and M. M. Littler. 1982. Photosynthesis, respiration, and contribution to community productivity of the symbiotic sea anemone *Anthopleura elegantissima* (Brandt, 1835). *J. Exp. Mar. Biol. Ecol.* **61:** 213–232.

Hoegh-Guldberg, O., and R. Hinde. 1986. Studies on a nudibranch that contains zooxanthellae. I. Photosynthesis, respiration and the translocation of newly fixed carbon by zooxanthellae in *Pteraeolidia ianthina*. *Proc. R. Soc. Lond. B.* **228:** 493–509.

Hoegh-Guldberg, O., R. Hinde, and L. Muscatine. 1986. Studies on a nudibranch that contains zooxanthellae. II. Contribution of zooxanthellae to animal respiration (CZAR) in *Pteraeolidia ianthina* with high and low densities of zooxanthellae. *Proc. R. Soc. Lond. B* **228:** 511–521.

Kempf, S. C. 1984. Symbiosis between the zooxanthella *Symbiodinium* (=*Gymnodinium*) *microadriaticum* (Freudenthal) and four species of nudibranchs. *Biol. Bull.* **166:** 110–126.

Kempf, S. C. 1990. Is the association between the aeolid nudibranch *Berghia verrucicornis* and a zooxanthella a true symbiosis? *Am. Zool.* **30:** 99A.

Kempf, S. C. 1991. A 'primitive' symbiosis between the aeolid nudibranch *Berghia verrucicornis* (A. Costa, 1987) and zooxanthellae. *J. Moll. Stud.* **57:** 75–85.

Kevin, K. M., and R. C. L. Hudson. 1979. The role of zooxanthellae in the hermatypic coral *Plesiastrea urvillea* (Milne-Edwards & Haime) from cold waters. *J. Exp. Mar. Biol. Ecol.* **36:** 157–170.

Kozloff, E. N. 1983. Pp. 186 and 246 in *Seashore Life of the Northern Pacific Coast*, University of Washington Press, Seattle, WA.

Lowry, O. H., N. J. Rosebrough, A. L. Farr, and R. J. Randall. 1951. Protein measurement with the Folin phenol reagent. *J. Biol. Chem.* **193:** 265–275.

McDonald, G. R., and J. W. Nybakken. 1978. Additional notes on the food of some California nudibranchs with a summary of known food habits of California species. *Veliger* **21:** 110–119.

Muller-Parker, G. 1984. Dispersal of zooxanthellae on coral reefs by predators on cnidarians. *Biol. Bull.* **167:** 159–167.

Muscatine, L. 1971. Experiments on green algae coexistent with zooxanthellae in sea anemones. *Pac. Sci.* **25:** 13–21.

Muscatine, L., P. G. Falkowski, J. W. Porter, and Z. Dubinsky. 1984. Fate of photosynthetic carbon in light- and shade-adapted colonies of the symbiotic coral *Stylophora pistillata*. *Proc. R. Soc. Lond. B* **222:** 181–202.

O'Brien, T. L. 1980. The symbiotic association between intracellular zoochlorellae (Chlorophyceae) and the coelenterate *Anthopleura xanthogrammica*. *J. Exp. Zool.* **211:** 343–355.

Potvin, C., and M. J. Lechowicz. 1990. The statistical analysis of ecophysiological response curves obtained from experiments involving repeated measures. *Ecology* **71**(4): 1389–1400.

Rinkevich, B. 1989. The contribution of photosynthetic products to coral reproduction. *Mar. Biol.* **101:** 259–263.

Rudman, W. B. 1981a. Further studies on the anatomy and ecology of opisthobranch molluscs feeding on the scleractinian coral *Porites*. *Zool. J. Linn. Soc.* **71:** 373–412.

Rudman, W. B. 1981b. The anatomy and biology of alcyonarian-feeding aeolid opisthobranch molluscs and their development of symbiosis with zooxanthellae. *Zool. J. Linn. Soc.* **72:** 219–262.

Rudman, W. B. 1982. The taxonomy and biology of further aeolidacean and arminacean nudibranch molluscs with symbiotic zooxanthellae. *Zool. J. Linn. Soc.* **74:** 147–196.

Steen, R. G. 1987. Evidence for facultative heterotrophy in cultured zooxanthellae. *Mar. Biol.* **95:** 15–23.

Trench, R. K. 1971a. The physiology and biochemistry of zooxanthellae symbiotic with marine coelenterates. I. The assimilation of photosynthetic products of zooxanthellae by two marine coelenterates. *Proc. R. Soc. Lond. B* **177:** 225–235.

Trench, R. K. 1971b. The physiology and biochemistry of zooxanthellae symbiotic with marine coelenterates. II. Liberation of fixed ^{14}C by zooxanthellae *in vitro*. *Proc. R. Soc. Lond. B* **177:** 237–250.

Trench, R. K. 1979. The cell biology of plant-animal symbiosis. *Ann. Rev. Pl. Physiol.* **30:** 485–531.

Waters, V. L. 1973. Food-preference of the nudibranch *Aeolidia papillosa*, and the effect of the defenses of the prey on predation. *Veliger* **15:** 174–192.

Reference: *Biol. Bull* **184**: 230–242. (April, 1993)

Biochemical Correlates of Estivation Tolerance in the Mountainsnail *Oreohelix* (Pulmonata: Oreohelicidae)

BERNARD B. REES[1] AND STEVEN C. HAND

Department of Environmental, Population and Organismic Biology, University of Colorado, Boulder, Colorado 80309-0334

Abstract. Biochemical changes occurring over 7 months of estivation were studied in two species of land snail, *Oreohelix strigosa* (Gould) and *O. subrudis* (Reeve), to determine whether differential mortality during estivation is related to different energetic strategies. Laboratory-maintained snails, which were fed *ad libitum* prior to estivation, were compared with snails collected from the field and induced to estivate without augmenting their energy reserves. In all groups, polysaccharide was catabolized early in estivation, and protein was the primary metabolic substrate after polysaccharide reserves were depleted. Lipid was catabolized at a low rate throughout estivation. Rates of catabolism were largely statistically equivalent between species. Urea and purine bases accumulated during estivation as a result of protein catabolism, with the former being quantitatively more important. In both laboratory-maintained and field-collected snails, the rate of urea accumulation was greater in *O. subrudis*, resulting in higher tissue urea contents in this species at the end of the 7-month experiment. The tissue concentrations of urea at 7 months ranged from about 150 to 300 m*M* and were positively correlated ($r = 0.99$, $P = 0.006$) with mortality in these snails. Methylamine compounds, a class of compounds that can offset disruptive effects of elevated urea, were measured in one group of *O. strigosa* at 7 months of estivation and found to be low relative to urea levels. We suggest, therefore, that in the absence of elevated levels of counteracting compounds, urea may reach toxic levels and may be one factor limiting the duration of estivation that is survived by these land snails.

Received 2 June 1992; accepted 9 December 1992.

[1] Present address: Hopkins Marine Station, Department of Biological Sciences, Stanford University, Pacific Grove, CA 93950.

Introduction

The success of gastropod mollusks in terrestrial habitats has been due to various structural, physiological, and behavioral specializations (Riddle, 1983). One specialization that is well developed among the pulmonate land snails is the capacity to enter the dormant state of estivation during periods of hot and dry environmental conditions. By entering estivation, snails are able to endure potentially desiccating climatic conditions until the return of more favorable conditions. Some species are capable of estivating for remarkable periods of time, ranging up to several years in duration (Stearns, 1877; Machin, 1967).

There are limits to the duration of estivation that can be tolerated, though, and mortality eventually increases as estivation is prolonged. Because there is no intake of foodstuffs during estivation, the period of estivation that can be survived may be limited by the exhaustion of endogenous energy reserves (Pomeroy, 1969; Schmidt-Nielsen *et al.*, 1971). Metabolic rate reduction, which would serve to prolong the energy stores of the animal, occurs during estivation, and desert-dwelling species display lower rates than species from more mesic environments (Schmidt-Nielsen *et al.*, 1971; Herreid, 1977; Rees and Hand, 1990). These observations have been taken as supporting the idea that energy reserves are limiting. But since the rates of metabolism and evaporative water loss are highly correlated in land snails (Barnhart, 1986), the reduction of metabolic rate may reflect an adaptation to conserve water rather than energy. A comparison of survivorship in snails with differing levels of energy reserves prior to estivation would more clearly address the question of energy limitation.

The duration of estivation may also be limited by the accumulation of noxious end-products of protein catabolism. Depending upon the species and activity pattern,

land snails can dispose of nitrogen derived from protein catabolism in the form of uric acid and other purines, urea or gaseous ammonia (Bishop *et al.*, 1983). In species that produce urea, this compound can reach very high levels in the tissues during estivation: levels of 260 μmol g^{-1} wet mass (*ca.* 300 m*M*) have been measured in the tissues of *Bulimulus dealbatus* (Horne, 1971), and 440 m*M* in the blood of *Strophocheilus oblongus* (Tramell and Campbell, 1972). At these levels, urea can have significant deleterious effects on the function of several biological processes (Yancey *et al.*, 1982; Yancey, 1985; Yancey and Berg, 1990). In other organisms displaying elevated tissue contents of urea, methylamine compounds, which can offset the disruptive effects of urea, are commonly accumulated. It is not known whether methylamines accumulate during estivation in snails with high urea. If not, then urea could reach toxic levels and be a factor limiting the duration of estivation.

In the present study, we have investigated the extent to which the exhaustion of energy reserves and the accumulation of nitrogenous compounds correlate with mortality differences observed during laboratory estivation in two species of the mountainsnail *Oreohelix*. We measured the biochemical composition of *O. strigosa* and *O. subrudis* over a 7-month period of laboratory estivation. From these data we have estimated rates of catabolism of protein, polysaccharide, and lipid. We compared snails that had been fed *ad libitum* prior to estivation with snails that had been collected from the field and induced to estivate without feeding to ascertain the effects of elevated energy stores. We also measured the accumulation of nitrogenous end-products of protein catabolism. Estivating snails were found to accumulate large quantities of urea, and we measured the tissue content of methylamines to address the possible counteraction of urea effects by these compounds.

Finally, tolerance to desiccation under laboratory conditions has been correlated with the distribution of a variety of land snail species in nature, with the more tolerant species occurring in drier habitats (Machin, 1967; Cameron, 1970; Arad *et al.*, 1989). The genus *Oreohelix* is widely distributed in western North America, ranging from mesic riparian areas to semi-arid habitats (Bequaert and Miller, 1973; Rees, 1988). In the present study, we have characterized the climatic conditions prevailing at three collection sites in western Colorado, and we have evaluated the distribution of *O. strigosa* and *O. subrudis* at these sites in light of their differing capacities for prolonged laboratory estivation.

Materials and Methods

Collection sites

Oreohelix spp. were collected in western Colorado along Mitchell and East Rifle Creeks. The snails from the Mitchell Creek drainage were collected along the east bank of the creek, approximately 100 m downstream of the Mitchell Creek Fish Hatchery (39°42′, 107°22′W; 1850 m), near Glenwood Springs, Colorado. Along the East Rifle Creek, snails were collected from areas located approximately 1 km upstream and 3 km downstream of the Rifle Falls Fish Hatchery (39°42′, 107°42′W; 2100 m). The upstream site was about 25 m west of the creek among rock slide rubble in Rifle Gorge, and the downstream site was adjacent to the creek at the Rifle Falls campground. The three collection locales will be referred to as the Mitchell Creek, Rifle Gorge, and Rifle Falls sites. The Mitchell Creek site has previously been referred to as the Glenwood Springs collection site (Rees, 1988).

The climatic conditions prevailing during the summer months in the Mitchell Creek and East Rifle Creek drainages are shown in Table 1. Further information on the conditions at the two Rifle sites was obtained with a handheld temperature-humidity sensor on several days during the summers of 1990 and 1991. Measurements were made 2–5 cm above the ground between 06:00 and 08:00, and again between 13:00 and 16:00 h. On average, the early morning humidity was 4% higher, and the mid-day humidity was 5% higher, at the Rifle Falls than at the Rifle Gorge site. Taken together, these data illustrate that moisture availability at the three collection sites decreases in the order Mitchell Creek > Rifle Falls > Rifle Gorge.

Animals and species identification

Snails were collected in June and August of 1987 and in November of 1989. They were either sacrificed immediately for determination of the biochemical composition of animals in the field, or brought into the laboratory and used for estivation studies (see below). The average shell-free tissue mass of snails prior to estivation in the laboratory was 0.453 ± 0.014 g (SEM, n = 63) for *O. strigosa* and 0.394 ± 0.013 g for *O. subrudis* (n = 41). Both species are hermaphroditic and bear live young. Only individuals without developing young in their oviducts were used in this study.

After the snails had been sacrificed for biochemical analyses (see below), the species was determined by starch gel electrophoresis of proteins (Rees, 1988). During the present study, additional, faster-migrating alleles were resolved in *O. strigosa* at the phosphoglucomutase and phosphoglucose isomerase loci. This finding does not compromise the utility of this technique in species determination, however, as the occurrence of the slow alleles at these loci remains diagnostic of *O. subrudis*. Individuals that were not electrophoretically genotyped (snails collected in June 1987 and those which died during the estivation series) were separated into species by their shell morphology (Rees, 1988).

Table 1

Climatic conditions during the summer of 1990 in the Mitchell Creek and East Rifle Creek drainages

Site	Month	Daily low temp (°C)	Daily high temp (°C)	Daily low RH (%)	Daily high RH (%)	Rainfall (mm)	Normal rainfall (mm)
Mitchell Creek	June	8 ± 2	25 ± 4	30 ± 8	70 ± 6	22	31
	July	11 ± 2	23 ± 2	37 ± 8	75 ± 6	48	30
	August	10 ± 2	23 ± 3	36 ± 9	72 ± 8	15	36
	June-Aug	10 ± 2	23 ± 3	35 ± 9	72 ± 7	85	97
East Rifle Creek	June	11 ± 3	28 ± 5	26 ± 6	52 ± 15	18	21
	July	13 ± 2	28 ± 2	31 ± 6	65 ± 15	31	19
	August	12 ± 2	27 ± 4	30 ± 7	61 ± 17	7	32
	June-Aug	12 ± 2	28 ± 4	29 ± 7	60 ± 17	56	72

Temperature and humidity readings were made continuously with hygrothermographs located at the Mitchell Creek and Rifle Falls Fish Hatcheries. Hygrothermographs were enclosed in Stevenson-style temperature cabinets approximately 10 cm above the ground and were calibrated against a hand-held temperature-humidity sensor that had been certified by the National Bureau of Standards. The data reported for June were recorded between June 5 and June 30; data for July and August are from all days in these months. Temperature and humidity are reported as the means and one standard deviation of the daily values. All monthly temperature and relative humidity averages are significantly different between field sites, except for June daily low relative humidity (t-test, $P < 0.05$). Monthly rainfall data for 1990 and normal rainfall (averages for the years 1951–1980) were recorded in the nearby communities of Glenwood Springs and Rifle (*ca.*, 5 and 20 km from fish hatcheries, respectively) and are taken from *Climatological Data*, Colorado (U.S. Department of Commerce).

Estivation series

Two experiments were carried out to assess the effects of estivation on the biochemical composition of these snails. One was performed with snails collected in November of 1989 and fed *ad libitum* for 2 months prior to estivation. These snails were kept in damp terraria and fed lettuce and carrots. Chalkboard chalk was provided as a source of calcium. This feeding regime was designed to saturate the energy reserves of the snails prior to estivation and to minimize the variation in nutritional status due to differing conditions at the collection sites. After 2 months, these snails were transferred to dry terraria without food, which induced estivation. These snails are referred to as the laboratory-maintained group. In the other experiment, snails collected in August 1987 were brought into the lab and induced to estivate immediately by placement in dry terraria. In this experiment, we wanted to determine the effect of estivation on snails that did not have their energy reserves augmented by laboratory feeding. These snails are referred to as the field-collected snails. In both series, snails were maintained at room temperature (23–28°C) and humidity (*ca.* 20–60%) for the duration of the experiment. Under these conditions, snails were inactive within 2 days after being transferred to dry conditions, and there was no indication that any of the animals became active again once they had entered quiescence. Photoperiod was not controlled.

Preparation of snails for chemical analyses

Snail extracts were prepared and maintained at 0–4°C unless otherwise stated. Chemicals and biochemicals were of reagent grade, and water was purified with a Milli-Q Reagent Water System (Continental Water Systems, Inc.).

At the start of the experiments and at 1, 2, 4, and 7 months following entry into estivation, snails were sampled randomly from the terraria. An additional sampling interval at 10 days was included in the experiment with the field-collected snails. The shell diameter of each individual was measured, and the snails were then dissected from their shells, briefly blotted, and frozen in liquid nitrogen. Tissues were kept at −70°C until biochemical analyses could be performed, at which time a small portion (5–15 mg) of the digestive gland was removed for electrophoresis, and the remainder of the tissue was lyophilized to a constant dry mass. The difference between fresh tissue mass and dry tissue mass was recorded as tissue water. Dry tissues were then pulverized with a mortar and pestle and divided into two subsamples: one fraction (approximately 40 mg) was used for determination of protein, DNA, polysaccharide, urea, and for the lab-maintained snails, purines; and the other fraction (10–25 mg) was kept for lipid analysis. At the later time points in the estivation series, individuals were commonly less than 50 mg dry mass. This small amount of dry tissue could not be divided, so lipid was not measured in these individuals.

Extracts for the determination of protein, DNA, polysaccharide, urea and purines were prepared as follows. Dry tissues were homogenized in 1.0 ml of ice cold 1 N perchloric acid with a glass homogenizer. Two 50 μl aliquots of the perchloric acid homogenate were removed: one was combined with 0.95 ml 0.5 *N* NaOH and saved at −70°C for protein assays; and the other was combined with 0.95 ml 0.5% (w/v) lithium carbonate and saved at

−70°C for purine analysis. The remainder of the perchloric acid extract was centrifuged at 10,000 × *g* for 15 min. The pellets were washed once with 0.7–0.8 ml of 1 *N* perchloric acid and centrifuged as above. The perchloric acid insoluble material was saved for DNA measurement. Perchloric acid supernatants for each individual were pooled, neutralized with 5 *M* K_2CO_3, and centrifuged at 10,000 × *g* for 10 min to remove perchlorate salts. Two hundred to 400 μl of the neutralized extract was combined with two volumes of 95% ethanol and stored at −70°C for polysaccharide assays, and the remainder was saved at −70°C for urea measurements.

Biochemical analyses

Protein was measured by the method of Lowry *et al.* (1951), as modified by Peterson (1977), with bovine serum albumin as the standard. For calculations of nitrogen balance, it was necessary to determine the mass of nitrogen in snail protein. The protein in a perchloric acid homogenate was recovered by centrifugation after the nucleic acids had been digested by heating (see below). Lipid was removed by washing the PCA-insoluble material with methanol. The amount of nitrogen in the PCA-insoluble fraction was determined by a micro-Kjeldahl procedure that includes direct nesslerization of ammonia following digestion of the proteins (Koch and McMeekin, 1924). The Nessler reagent was obtained from Sigma Chemical Company. The amount of nitrogen in protein determined in this manner was not different in the two species and was found to account for 16.8 ± 0.9% (S.D., n = 4) of the protein mass measured by the Lowry assay.

DNA was determined by the diphenylamine assay of Burton (1956) with modifications suggested by Giles and Myers (1965). Briefly, perchloric acid insoluble material was suspended in 1.0 ml 1.5 *N* perchloric acid and heated at 70°C for 20 min. Following centrifugation at 10,000 × *g* for 20 min, an aliquot (50–100 μl) of the supernatant was brought to 2.5 ml with 1.5 *N* perchloric acid and combined with 1.5 ml 4% (w/v) diphenylamine made in glacial acetic acid and 0.1 ml 0.16 mg ml^{-1} acetaldehyde made in water. The color was allowed to develop for 20 h in the dark at room temperature. To correct for nonspecific color development, an absorbance difference (A_{600} − A_{700}) was determined for each sample. Calf thymus DNA was the standard.

Polysaccharide (glycogen plus galatogen), which precipitated in the ethanolic extract, was collected by centrifugation at 10,000 × *g* for 20 min, washed once with 1.0 ml 95% ethanol and centrifuged again. The pellets were air-dried and redissolved in 1.0 ml water by heating at 70°C. Polysaccharide was measured by the anthrone method described by Jermyn (1975), except that the additions of hydrochloric and formic acid to the samples were omitted. Polysaccharide content was expressed as 0.9 × glucose mass.

For urea analysis, samples were thawed and clarified by centrifugation at 10,000 × *g* for 10 min. Urea was measured colorimetrically as ammonia after treatment of the samples with urease (Sigma Diagnostic Kit No. 640). Blanks without urease were subtracted from each sample.

Purine bases were analyzed with high performance liquid chromatography essentially as described by Simmonds and Harkness (1981). A LDC/Milton Roy HPLC system was employed in conjunction with a Waters μBondapak C-18 column (30 cm × 3.9 mm i.d.). The lithium carbonate solutions were thawed, diluted, neutralized, and filtered through Gelman Supor 0.45 μm membrane filters. Twenty μl were injected onto the column, and purines were eluted isocratically with a buffer of 4 m*M* potassium phosphate (pH 3.6) containing 1% (v/v) methanol. Absorbance was monitored at 265 nm, and uric acid, guanine and xanthine were quantified by integration of peak area.

Total lipid was determined after extraction of the tissues in chloroform:methanol (Folch *et al.*, 1957; Ways and Hanahan, 1964). For each snail, lyophilized tissues were homogenized in 4 ml chloroform:methanol (2:1) with a Virtis micro-ultrashear apparatus for 1 min and filtered through a fritted disc funnel. The residue was rehomogenized in 4 ml chloroform:methanol and filtered. The residue was finally washed with another 2 ml of chloroform:methanol and the filtrates combined. The filtered chloroform:methanol homogenate was mixed with 0.25 volume 0.88% (w/v) KCl in water, and after separation, the aqueous phase was aspirated. The remaining organic phase was mixed with 0.25 volume methanol:water (1:1), and the aqueous phase was aspirated after separation. The organic phase was then decanted into a pre-weighed aluminum planchet and evaporated to dryness under a stream of nitrogen. The dried lipid was held over Drierite a further 24 h and weighed to the nearest 0.1 mg.

In one group of estivating snails, methylamine compounds were measured by reineckate precipitation protocol modified from Kermack *et al.* (1955). Lyophilized tissues from a whole snail were homogenized in 30 volumes of 40% ethanol and centrifuged at 20,000 × *g* for 15 min. The pellet was washed with another 30 volumes of 40% ethanol, and the combined supernatants were boiled for 10 min to precipitate proteins. The ethanolic extract was centrifuged at 10,000 × *g* for 20 min, lyophilized, and redissolved in 1.0 ml 0.1 *N* HCl. Saturated ammonium reineckate, prepared in water and titrated to pH 1 with 5.0 N HCl, was added to the each sample in the ratio 3:1 (reineckate:sample). Reineckate salts were allowed to precipitate at 4°C overnight and were collected by filtration on polycarbonate membrane filters (Nucleopore, 0.2 μm). After washing the precipitate three times with 3 ml diethyl ether, the precipitate and membrane

Table II

Biochemical composition of laboratory maintained Oreohelix

Compound	*O. strigosa*		*O. subrudis*	
	mg g^{-1} dry mass	% dry mass	mg g^{-1} dry mass	% dry mass
Protein	512.6 ± 19.2	51.3	509.4 ± 13.7	50.9
Polysaccharide	216.2 ± 11.3	21.6	230.1 ± 8.8	23.0
Lipid	70.3 ± 1.4*	7.0	78.2 ± 1.9	7.8
DNA	14.9 ± 0.3	1.5	16.7 ± 0.5	1.7
	μmol g^{-1} dry mass	% dry mass	μmol g^{-1} dry mass	% dry mass
Urea	0.98 ± 0.29*	<0.1	2.20 ± 0.76	<0.1
Uric acid	55.1 ± 3.9	0.9	45.1 ± 4.0	0.8
Guanine	17.1 ± 1.9	0.3	10.3 ± 1.2	0.2
Xanthine	7.1 ± 0.6	0.1	8.2 ± 0.9	0.1
Total dry mass accounted for		82.7		84.5

Values are given as the mean and standard error of the mean. The sample sizes were 27 *O. strigosa* and 21 *O. subrudis*, except for the lipid analyses, where sample sizes were 18 and 12 for *O. strigosa* and *O. subrudis*, respectively. Asterisks indicate that species means for these biochemical constituents are significantly different.

were dissolved in 70% acetone, and the absorbance was read at 520 nm. Betaine was the standard.

Following the above protocols, the recoveries of known quantities of protein, DNA, urea, uric acid, guanine, xanthine, and lipid were >88%, and we did not correct the results for differences in recovery. In the case of polysaccharide, this protocol led to a 77 ± 2.5% (S.D., n = 4) recovery of glycogen standards, and the polysaccharide content of snails was corrected accordingly.

Data analysis

Examination of the total tissue contents of various biochemical compounds revealed a large degree of variation due to size differences among individuals. For snails prior to estivation (both laboratory-maintained and field-collected), biochemical constituents were expressed in terms of dry mass in order to standardize for size differences. Equality of sample variances was tested with Bartlett's Box-F (Zar, 1984), and differences among group means were evaluated with parametric or nonparametric analyses of variance accordingly (Zar, 1984). *A posteriori* testing was done with Scheffé's or Dunn's multiple comparison tests (Zar, 1984).

During estivation, considerable dry mass was lost, so some variable other than dry mass was required as an index of snail size for standardization of biochemical composition. Data from non-estivating, laboratory-maintained snails showed that the relationship between shell diameter and snail size was quite good: coefficients of determination (r^2) for regressions of whole tissue and dry tissue mass versus shell diameter were 0.763 and 0.784, respectively. Furthermore, when all snails were considered, there was no effect of duration of estivation on shell diameter (analysis of variance, $P = 0.969$), suggesting that shell diameter neither increases nor decreases during estivation. Therefore, tissue mass, water, and biochemical contents of estivating snails were adjusted to a snail of average shell diameter (15.63 mm) based upon the slopes of regression equations describing the relationship between each component and shell diameter. For each species, the rates of change in these adjusted values during various intervals of estivation were then determined by regression analysis. Differences between species-specific rates of change were evaluated with the test for homogeneity of slopes in an analysis of covariance package (Zar, 1984).

Correlations between various biochemical measurements and mortality at 7 months of estivation were analyzed with Pearson's product-moment correlation. All statistical analyses were performed with SPSS-X, version 4 (SPSS, Inc.), and a probability ≤ 0.05 was considered as statistically significant. Unless otherwise stated, data are presented as means and one standard error of the mean (SEM).

Results

Biochemical composition of laboratory-maintained Oreohelix

Laboratory-maintained *Oreohelix strigosa* and *O. subrudis* were composed of approximately 51% protein, 22–23% polysaccharide, 7–8% lipid, and about 1.5% DNA (Table II). The levels of urea and purine bases were low prior to estivation. Urea averaged 1–2 μmol g^{-1} dry mass, comparable to the level reported in *Bulimulus dealbatus* prior to estivation (Horne, 1971). The levels of purine

bases totaled to 64–79 μmol g^{-1} dry tissue, similar to the tissue contents of other non-estivating snails (Jezewska *et al.*, 1963; Horne, 1971). On a molar basis, uric acid accounted for about 70% of the total purine, with guanine and xanthine accounting for approximately 20 and 10% of the total purine, respectively, in both *O. strigosa* and *O. subrudis*. Hypoxanthine was not found in the tissues of these snails. Taken together, these compounds account for more than 80% of the dry mass of these snails. The unaccounted fraction is presumed to be other low molecular weight organic compounds (*e.g.*, amino acids) and inorganic ash.

Biochemical composition of field-collected Oreohelix

Compared with the values obtained for laboratory-maintained snails, both *O. strigosa* and *O. subrudis* displayed lower polysaccharide levels in the field-collected groups (Fig. 1A). Protein constituted a correspondingly larger portion of the dry mass in both species (Fig. 1B), and lipid was somewhat higher in *O. strigosa* collected in the late summer (Fig. 1C). These differences in biochemical composition reflect the effects of *ad libitum* feeding in the laboratory-maintained group and suggest that snails feed less regularly or on food of differing qualities in the field. Of the snails collected in the late summer, *O. strigosa* displayed significantly higher levels of polysaccharide than *O. subrudis*. Differences in polysaccharide content may influence the capacity of these snails for long-term estivation (see Discussion).

Snails of either species collected late in the summer demonstrated much more variable urea contents than snails in the laboratory-maintained or early summer groups (Fig. 1D). Among the laboratory-maintained snails, only 17% had urea contents greater than 1 μmol g^{-1} dry mass, and among the snails collected early in the summer, this percentage was 22%. In these groups, the highest urea content measured was 11.7 μmol g^{-1} dry mass. Among the snails collected later in the summer, urea was higher than 1 μmol g^{-1} dry mass in 33% of the snails, and the highest value was 93.0 μmol g^{-1} dry mass. Since urea accumulates during estivation (see below), the occurrence of elevated urea in snails collected late in the summer suggests that many of these animals had been estivating in the field.

Mortality during estivation

Both species of *Oreohelix* experienced mortality during the later months of estivation. In the group of snails that had been maintained in the laboratory prior to estivation, 1 of the remaining 13 *O. strigosa* had died at 7 months, whereas 9 of 30 *O. subrudis* had died. For snails that were brought in from the field, the mortality at 7 months in both species was higher: 10 of 24 *O. strigosa* had died, whereas 28 of 34 *O. subrudis* had died. Among the field-collected snails, the proportion of dead *O. subrudis* at 7 months was significantly greater than the proportion in *O. strigosa* (G-test, $P < 0.05$). These results demonstrate that *O. strigosa* tolerates extended periods of estivation in the laboratory better than *O. subrudis*.

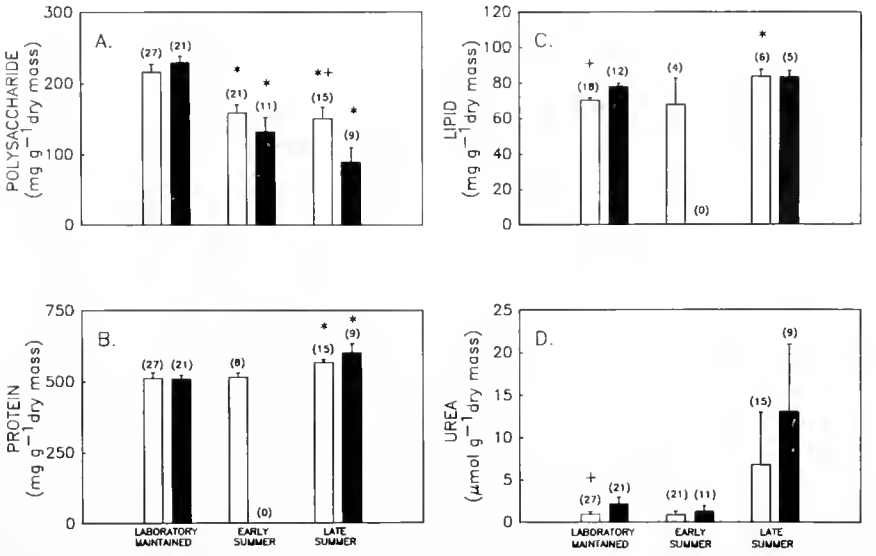

Figure 1. Biochemical composition of laboratory-maintained and field-collected *O. strigosa* (open bars) and *O. subrudis* (solid bars). A. Polysaccharide content. B. Protein content. C. Lipid content. D. Urea content. Error bars indicate one standard error of the mean. Asterisks indicate that the content of this constituent is significantly different from that measured in laboratory-maintained snails of the same species, and the crosses indicate that species means are significantly different for that sampling interval.

Analysis of changes during estivation

We were interested in whether the two species have different rates of substrate depletion or end-product accumulation during estivation. Because variation in the size of individuals among the sampling intervals and between species would tend to obscure these rates, we have normalized the tissue mass, water content, and the content of biochemical constituents to an average snail size based upon shell diameter (see Materials and Methods). Note that, since dry mass, water content, and biochemical composition can be determined only once for any individual, the rates of change described below reflect average rates of loss or accumulation among groups of individuals rather than rates of change within individual snails. Furthermore, shell diameters were not measured on the field-collected snails sacrificed prior to estivation (day 0), and consequently the data for this group begin at 10 days of estivation.

Loss of tissue mass and water during estivation

Fresh tissue mass, dry tissue mass, and water decreased significantly in both species of *Oreohelix* during estivation. When tissue mass and water content data were corrected for size differences among individuals, rates of loss in the two species were not significantly different. The loss of tissue was characterized by parallel decreases in both dry tissue mass and tissue water. These losses were biphasic, occurring more quickly at the onset of estivation as the snails entered estivation, and then reaching a steady slower rate after the initial drop. By 7 months of estivation, the tissue mass and water content of snails were reduced by approximately 35% in all groups.

The loss of tissue water from estivating *Oreohelix* was not reflected in a decrease in the percent tissue water because the dry mass decreased proportionately. The percentage of tissue water remained between 78 and 81% for both species in both experimental series. In fact, among the laboratory-maintained snails, there was a slight but statistically significant increase in the percent tissue water over the 7 months of estivation despite the overall loss of water. Thus a constant percentage tissue water cannot be interpreted as indicating no loss of water, as has been assumed previously for other species of estivating snails (Schmidt-Nielsen *et al.*, 1971).

Catabolism of energy reserves during estivation

Polysaccharide, protein, and lipid were all catabolized during estivation, but the substrates that were utilized changed as estivation proceeded (Figs. 2–4, Table III). Polysaccharide was the primary metabolic fuel for the initial months of estivation (Fig. 2). Snails that had been maintained in the laboratory began the estivation period with large polysaccharide stores, and in these snails, catabolism of this substrate continued for the first 4 months of estivation (Fig. 2A). During the first month of estivation, the rate of polysaccharide depletion was significantly faster in *O. subrudis* (Table III). Between 1 and 4 months, carbohydrate catabolism continued at moderate rates that were similar in the two species. After 4 months, the polysaccharide content of the snails was much reduced and its rate of utilization was correspondingly low. In the field-collected snails, the polysaccharide stores were smaller, and consequently they were depleted earlier (Fig. 2B). Although the initial rates of utilization were similar in the two species, carbohydrate lasted longer in *O. strigosa*, which had begun estivation with larger stores. As in the estivation series begun with laboratory-maintained snails, rates of polysaccharide utilization were much reduced during the later phases of estivation and statistically equivalent between species.

Upon depletion of the polysaccharide stores, net protein catabolism occurred (Fig. 3). In the laboratory-maintained snails, the onset of net protein depletion occurred at about 2 months of estivation (Fig. 3A). Before this time, no net

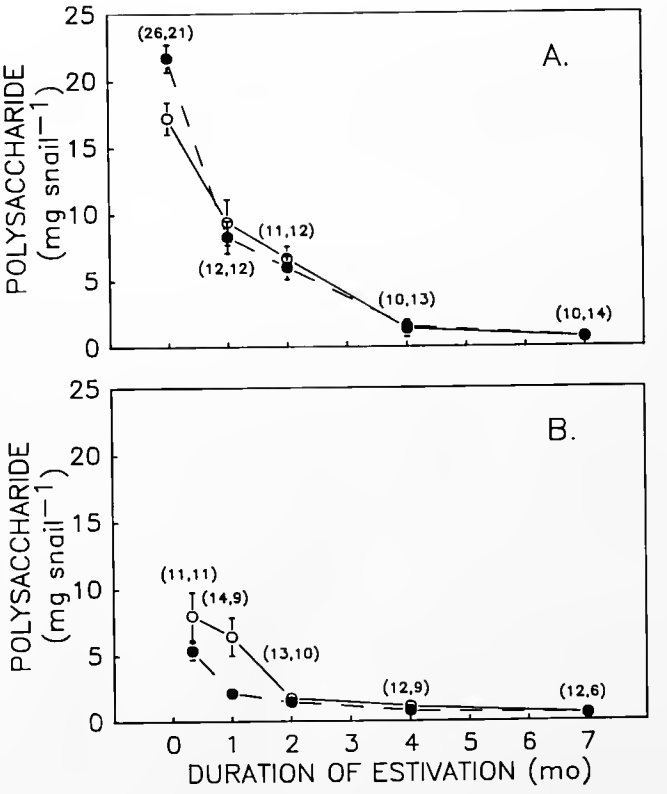

Figure 2. Polysaccharide content during estivation in *O. strigosa* (○) and *O. subrudis* (●). All values have been adjusted to a snail of average size based upon shell diameter. A. Laboratory-maintained snails. B. Field-collected snails. Sample sizes are given in parentheses with the value for *O. strigosa* appearing first. Bars indicate one standard error of the mean.

Table III

Rates of polysaccharide, protein, and lipid catabolism and urea and purine accumulation in Oreohelix *spp. during estivation*

Compound	Experiment	Interval	*O. strigosa*	*O. subrudis*	*P*
Polysaccharide	A	0–1 month	−7.81 ± 2.16	−13.45 ± 1.71	0.05
	A	1–4 months	−2.66 ± 0.59	−2.23 ± 0.41	0.54
	A	4–7 months	−0.23 ± 0.22^{NS}	−0.27 ± 0.12	0.84
	B	10 days–2 months	−3.84 ± 1.14	−2.25 ± 0.45	0.23
	B	2–7 months	−0.23 ± 0.08	−0.18 ± 0.04	0.64
Protein	A	0–2 months	−0.72 ± 1.56^{NS}	0.95 ± 0.97^{NS}	0.37
	A	2–7 months	−1.95 ± 0.63	−2.73 ± 0.35	0.26
	B	10 days–7 months	−2.14 ± 0.58	−3.03 ± 0.43	0.26
Lipid	A	0–7 months	−0.33 ± 0.06	−0.36 ± 0.07	0.78
	B	10 days–7 months	−0.11 ± 0.12^{NS}	−0.67 ± 0.21	0.06
Urea	A	0–2 months	0.98 ± 0.21	1.25 ± 0.32	0.47
	A	2–7 months	6.20 ± 0.87	8.66 ± 0.67	0.03
	B	10 days–7 months	5.52 ± 0.59	8.75 ± 0.53	<0.01
Uric acid	A	0–7 months	0.43 ± 0.12	0.56 ± 0.08	0.36
Guanine	A	0–7 months	0.11 ± 0.04	0.15 ± 0.02	0.40
Xanthine	A	0–7 months	0.03 ± 0.02^{NS}	0.05 ± 0.02	0.51

Experiment A was done with snails after laboratory maintenance and experiment B with field-collected snails without prior laboratory maintenance. Values for rates of catabolism (negative values) and accumulation (positive values) are slopes and their standard errors from regression equations of the adjusted tissue content of each compound versus length of estivation over the intervals indicated (see also Figs. 2–6). Units are mg snail^{-1} mo^{-1} for polysaccharide, protein and lipid and μmol snail^{-1} mo^{-1} for urea, uric acid, guanine and xanthine. All slopes were significantly different from zero, except where indicated (NS). *P* values are from tests of equality of species-specific slopes.

protein catabolism occurred in either species, as indicated by the slopes of regression lines not significantly different from zero (Table III). After the onset of net protein catabolism, the rates of utilization were fairly linear throughout the remainder of the estivation period. Among the field-collected snails, significant protein catabolism occurred from the beginning of estivation (Fig. 3B). While species-specific rates were not significantly different, there was a trend toward lower rates of protein catabolism in *O. strigosa* in both experimental series (Table III)—a trend that likely influenced the rates of end-product accumulation (see below).

Lipid was catabolized at a low rate throughout the duration of estivation in both experimental series (Fig. 4). The rates of lipid utilization in the two species were not significantly different during the 7-month estivation experiments (Table III).

Accumulation of nitrogenous end-products and nitrogen balance

With the onset of protein catabolism, the nitrogenous end-products, urea and purine bases, accumulated in the tissues of estivating snails (Figs. 5–6, Table III). The tissue levels of urea increased dramatically in both species of *Oreohelix* (Fig. 5). In the laboratory-maintained snails, protein was not catabolized early in estivation, and hence urea began to accumulate only after 2 months of estivation (Fig. 5A). Between 2 and 7 months of estivation, the rate of accumulation was higher in *O. subrudis* than in *O. strigosa* (Table III). By 7 months of estivation, urea was 32.9 ± 4.5 μmol snail^{-1} in *O. strigosa* (n = 10) and 43.7 ± 3.1 μmol snail^{-1} in *O. subrudis* (n = 14). In the field-collected snails, urea began to increase almost immediately upon the commencement of estivation, reflecting the early dependence upon protein catabolism (Fig. 5B). Between 10 days and 7 months, the rate of urea accumulation in *O. subrudis* was again greater than in *O. strigosa* (Table III). The tissue urea contents of these snails after 7 months of laboratory estivation were 36.4 ± 4.3 μmol snail^{-1} in *O. strigosa* (n = 12) and 58.2 ± 6.1 μmol snail^{-1} in *O. subrudis* (n = 6).

The accumulation of purine bases was only measured in snails that had been maintained in the laboratory, and their patterns of change are shown in Figure 6. Over 7 months of estivation, uric acid increased by 3 to 4 μmol snail^{-1} (Fig. 6A), guanine increased by approximately 1 μmol snail^{-1} (Fig. 6B), and xanthine increased by less than 0.5 μmol snail^{-1} (Fig. 6C). Hence the sum of the purines increased by only 5 to 6 μmol snail^{-1}. Over the 7-month estivation period, the rates for uric acid, guanine and xanthine accumulation were not statistically different between the two species (Table III).

Ammonia production was measured as described by Speeg and Campbell (1968), except that estivating snails were kept in a closed chamber for a period of two days.

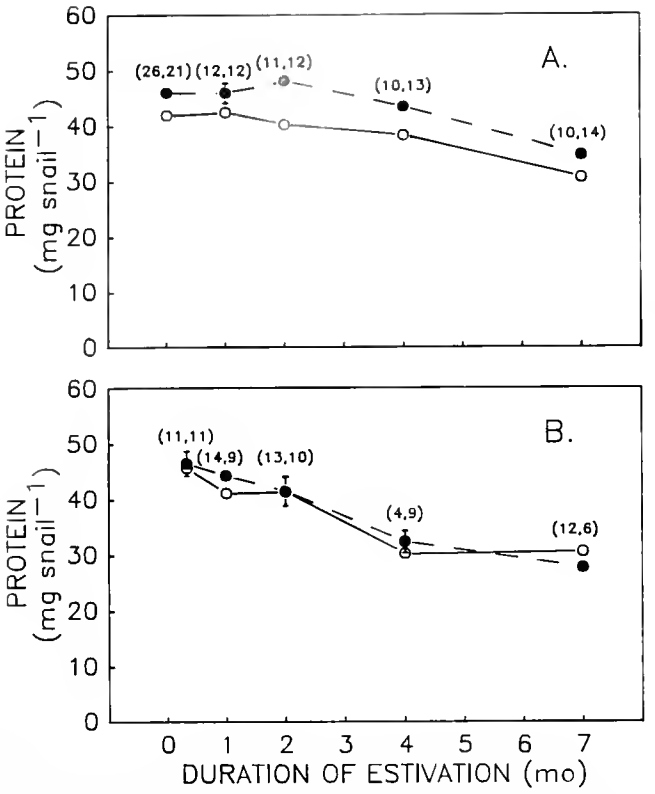

Figure 3. Protein content during estivation in *O. strigosa* (○) and *O. subrudis* (●). All values have been adjusted to a snail of average size based upon shell diameter. A. Laboratory-maintained snails. B. Field-collected snails. Sample sizes are given in parentheses with the value for *O. strigosa* appearing first. Bars indicate one standard error of the mean.

Over this period, the amount of ammonia produced by 8 snails of either species was below the limit of detection (0.02 μmole).

Levels of urea-counteracting solutes

Methylamine compounds were measured in one group of field-collected *O. strigosa* after 7 months of estivation and found to be 2.68 ± 0.27 μmol snail^{-1} (n = 5). HPLC analyses of selected extracts of both species have shown that betaine is the predominant methylamine compound, and that polyhydric alcohols, another class of protective compounds, do not significantly accumulate in snail tissues during estivation (data not shown).

Discussion

In the present study, we undertook an analysis of the biochemical changes that occur in *Oreohelix strigosa* and *O. subrudis* during a period of laboratory estivation. The temporal nature of substrate utilization and nitrogenous end-product accumulation were described for the first time in congeneric species of land snails that are dissimilar in their capacity for long-term estivation. Differences in the patterns of biochemical changes may account, in part, for the observed difference in mortality. Below, we evaluate the relationships between mortality and both the exhaustion of energy stores and the accumulation of nitrogenous end-products of protein catabolism. We also discuss the distributions of these *Oreohelix* species in the field in light of their different survivorship during desiccation stress.

Mortality and exhaustion of energy stores

If the duration of estivation is limited by the depletion of energy storage compounds during estivation, then snails with larger stores prior to estivation would be predicted to survive estivation proportionately longer. We were able to elevate the level of polysaccharide, the primary metabolic substrate during early estivation, by feeding snails *ad libitum* in the laboratory prior to estivation. Subsequently, when these snails were allowed to estivate, polysaccharide stores lasted longer, and mortality in both species was lower than when snails collected from the field

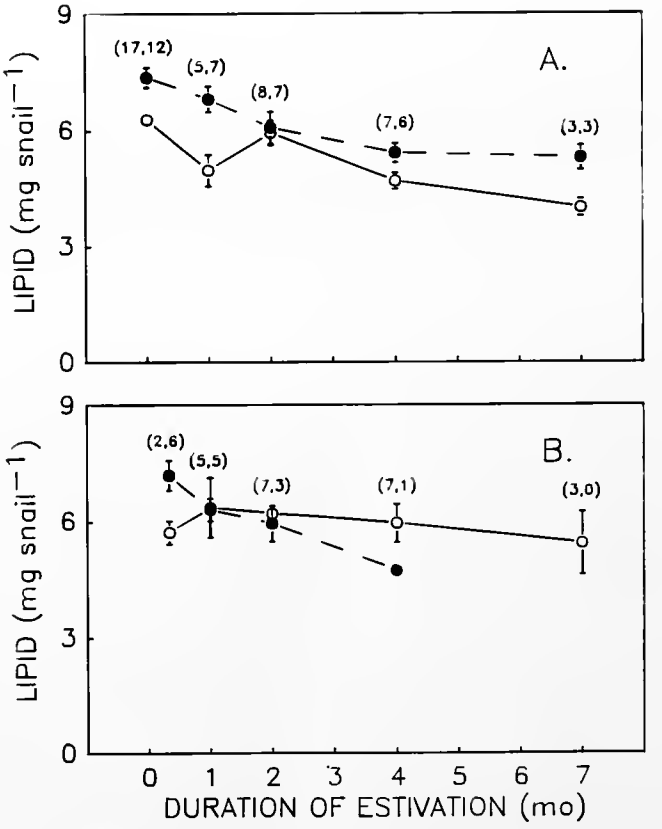

Figure 4. Lipid content during estivation in *O. strigosa* (○) and *O. subrudis* (●). All values have been adjusted to a snail of average size based upon shell diameter. A. Laboratory-maintained snails. B. Field-collected snails. Sample sizes are given in parentheses with the value for *O. strigosa* appearing first. Bars indicate one standard error of the mean.

estivated without prior laboratory feeding. In addition, among the field-collected snails, *O. strigosa* began with higher polysaccharide levels than *O. subrudis*, and the former displayed only half the mortality by 7 months of estivation. With data from four groups of snails (2 species × 2 experimental series), we tested the correlation between pre-estivation polysaccharide stores and percent mortality at 7 months of estivation. Since snails with higher polysaccharide stores were predicted to survive estivation better (*i.e.*, show lower mortality), the test was one-tailed. The negative correlation between pre-estivation polysaccharide stores and mortality was statistically significant ($r = -0.91$, $P = 0.045$). The observation that polysaccharide stores were exhausted several months prior to the onset of mortality, however, suggests that mortality is not due to the depletion of this substrate *in sensu stricto*. Rather, the correlation between polysaccharide stores and mortality likely reflects other biochemical changes that are initiated upon the depletion of the polysaccharide reserves (see below).

Mortality and the accumulation of nitrogenous end-products

Upon the exhaustion of polysaccharide, protein was catabolized, and both *O. strigosa* and *O. subrudis* were found to accumulate urea as the major product of protein metabolism. Based upon rates of protein catabolism and end-product accumulation during the estivation interval of net protein depletion (2–7 months for laboratory-maintained snails and 10 days–7 months for field-collected snails), urea accumulation in the tissues accounted for approximately 50% of the nitrogen derived from protein catabolism, whereas the accumulation of purines only accounted for about 10% of the protein nitrogen. Ammonia production was below measurable levels, corresponding to less than 1% of the calculated nitrogen liberated from protein catabolism. A portion of the unaccounted fraction of nitrogen was probably lost during sample preparation (blotting of hemolymph can account for the loss of up to 25% of the urea nitrogen), and nitrogen may have accumulated in compounds not measured in this study (*e.g.*, amino acids; *c.f.*, Wieser and Schuster, 1975). Further studies of nitrogenous compounds in hemolymph of estivating snails may elucidate the nature of the missing nitrogen fraction.

In both experimental series, the rate of tissue urea accumulation was found to be faster in *O. subrudis* than in *O. strigosa*, resulting in higher urea contents in the former species. Because urea can easily cross most cell membranes (Forster and Goldstein, 1976), the urea measured in extracts of whole snails is likely to be uniformly distributed throughout the tissues of the snails. This assumption was supported by measuring urea in hemolymph, foot muscle and digestive gland of two laboratory-maintained *O. strigosa* after 7 months of estivation. In one snail, the urea concentrations were 131, 126, and 130 m*M* in hemolymph, foot muscle, and digestive gland, respectively, and the other snail had urea concentrations of 211, 155, and 198 m*M* in these tissues. When urea concentrations were calculated for all snails based upon a uniform distribution in the total tissue water, urea was found to rise from less than 1 m*M* prior to estivation to levels exceeding 150 m*M* by 7 months. The average urea concentrations in snails that had been estivating for 7 months were: 152 ± 24 m*M* (n = 10) and 204 ± 14 m*M* (n = 14) in laboratory-maintained *O. strigosa* and *O. subrudis*, respectively, and 203 ± 15 m*M* (n = 12) and 288 ± 27 m*M* (n = 6) in the two species when field-collected snails were used. When tested with correlation analysis, a significant positive correlation was found between tissue urea concentration and mortality at 7 months in the four groups of snails ($r = 0.99$, $P = 0.006$). In a recent study of mammalian cells in culture, Yancey and Burg (1990) showed a dramatic decrease in viability as the urea concentration

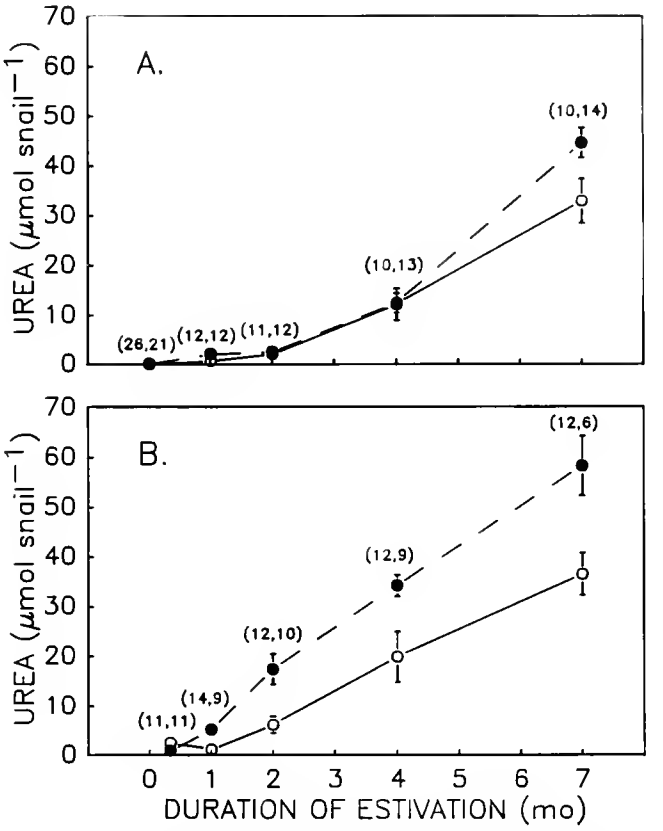

Figure 5. Urea content during estivation in *O. strigosa* (○) and *O. subrudis* (●). All values have been adjusted to a snail of average size based upon shell diameter. A. Laboratory-maintained snails. B. Field-collected snails. Sample sizes are given in parentheses with the value for *O. strigosa* appearing first. Bars indicate one standard error of the mean.

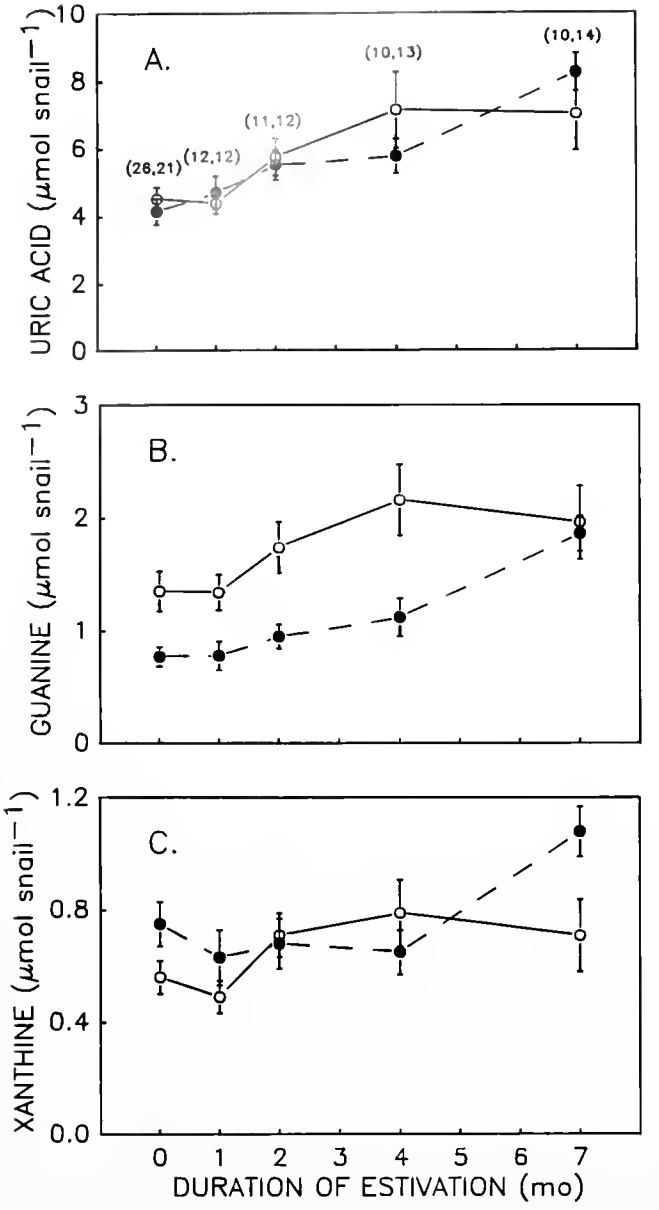

Figure 6. Purine content during estivation in *O. strigosa* (○) and *O subrudis* (●). Measurements were only made with snails that had been maintained in the laboratory prior to estivation. All values have been adjusted to a snail of average size based upon shell diameter. A. Urate content. B. Guanine content. C. Xanthine content. Sample sizes are given in 6A in parentheses with the value for *O strigosa* appearing first. Bars indicate one standard error of the mean.

in the medium increased from 150 to 300 m*M*, the same range of concentrations across which survivorship decreased sharply in *Oreohelix*.

In other organisms that accumulate high levels of urea, there are also high levels of compounds that are capable of counteracting the potentially deleterious effects of urea (Yancey *et al.*, 1982; Yancey, 1985). For example, in elasmobranch fish, which display a tissue concentration of urea in this range, methylamine compounds occur in a 1:2 proportion with urea. At this ratio, methylamines are able to counteract the disruptive effects of high urea *in vitro* and are presumed to act this way *in vivo*. The methylamine content of estivating *O. strigosa* was low relative to urea. If methylamines were distributed uniformly in the tissue water, then their concentration would correspond to 12.2 ± 1.9 m*M*. If methylamine compounds are concentrated intracellularly, as suggested by work with mammalian cells (Yancey and Burg, 1990), the intracellular concentration can approach 25 m*M*. Relative to the urea measured at this point in estivation, however, even 25 m*M* methylamines is far below the ratio of 1:2 at which methylamine effects counteract the perturbation of macromolecules by urea.

Thus, we offer the hypothesis that urea toxicity is a factor that limits the duration of estivation that can be tolerated by these two species of land snail. While higher levels of urea have been reported in other species of land snail (DeJorge and Peterson, 1970; Horne, 1971; Trammel and Campbell, 1972), in the absence of data on mortality and methylamine concentrations, we cannot evaluate the applicability of this hypothesis to these species. This hypothesis does not exclude the involvement of other factors (*e.g.*, blood gases, pH or osmolarity) in setting the upper limit to estivation in these or other snails.

Biological rationale for urea accumulation

If urea does reach toxic levels, then it raises the question: why do estivating snails synthesize urea? One explanation is that the high tissue concentration of urea aids in water retention in arid environments (Horne, 1971). This explanation is unlikely, though, for two reasons. First, urea concentrations of 300 m*M* only contribute a trivial amount to the gradient for water movement between the tissues and dry air (Machin, 1975). Secondly, urea accumulates faster in humid environments than in dry ones (Horne, 1973a). The osmotic effect of elevated urea could be beneficial in the uptake of water when conditions of high humidity return (Riddle, 1983).

Alternatively, the synthesis of urea may simply serve as a means of ammonia detoxification. The LD_{50} for ammonia in the land snail *Bulimulus dealbatus* is approximately 16 μmol g^{-1} wet weight (Horne, 1973b). Based upon rates of protein catabolism measured for *Oreohelix* species during estivation, this amount of ammonia is generated within 8 days. Clearly, if these snails are similarly sensitive to ammonia toxicity, then during prolonged periods of high protein catabolism, ammonia must be removed. By producing the moderately less toxic urea, snails may be able to carry out protein catabolism for a longer period. But *O. strigosa* and *O. subrudis*, as well as other

species that accumulate urea during estivation, appear to have the capacity to synthesize purines as nitrogenous wastes, a class of compounds considered completely innocuous. It is a paradox that urea synthesis, rather than purine synthesis, is the primary pathway for ammonia detoxification in these snails during estivation. Perhaps urea synthesis is a compromise between the toxicity of the terminal end-product and the loss of organic carbon and energy equivalents, both of which are greater in purine synthesis.

Ecological implications of differential mortality during laboratory estivation

Previous studies have demonstrated that species of land snail that are more tolerant of desiccation under laboratory conditions are typically found in more arid habitats in nature (Machin, 1967; Cameron, 1970; Arad *et al.*, 1989). While the ecologies of *O. strigosa* and *O. subrudis* have not been studied in depth, our data describe the climatic conditions and the species distributions at three sites in western Colorado. Based upon summer temperatures, relative humidities, and precipitation, moisture availability at these three sites decreases in the order Mitchell Creek > Rifle Falls > Rifle Gorge (see Materials and Methods; Table I). At the driest site, *O. strigosa* constitutes more than 60% of the snails collected (Fig. 7), suggesting that tolerance to prolonged estivation may influence the distribution of these species of land snail in nature. While *O. strigosa* is the predominant species at the Rifle Gorge site, *O. subrudis* does constitute nearly 40% of the snails collected at this dry site. The survival of *O. subrudis*, despite its lower tolerance to estivation under laboratory conditions, may be related to selection of moister microhabitats, as described for land snail species of the Middle Eastern deserts (Arad *et al.*, 1989).

The other two sites were more mesic, and they were dominated by either *O. strigosa* (Mitchell Creek) or *O. subrudis* (Rifle Falls) (Fig. 7). Because the potential for desiccation stress is probably lowest at the Mitchell Creek site, the low abundance of *O. subrudis* at this site cannot be attributed to a lower tolerance of desiccation. Rather, other factors, either physical (*e.g.*, calcium availability) or biological (*e.g.*, differential predation, different food preferences, or random effects associated with founding the colony), may explain their low numbers at the Mitchell Creek site. Similarly, factors other than desiccation tolerance must be responsible for the low abundance of *O. strigosa* at the Rifle Falls site.

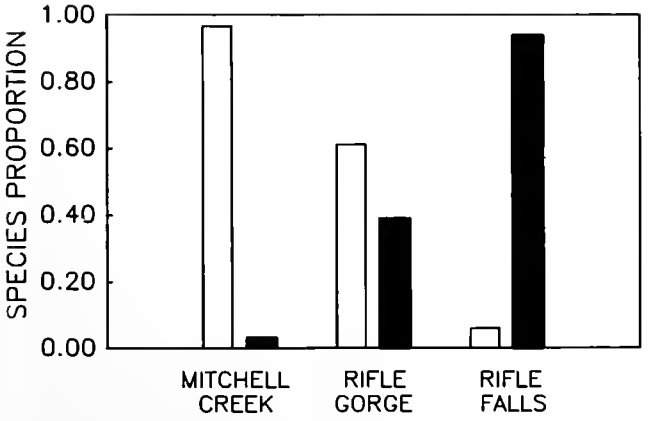

Figure 7. Distribution of *O. strigosa* (open bars) and *O. subrudis* (solid bars) at three collection sites in western Colorado. Data from the present study have been pooled with previous work (Rees, 1988; and unpub. obs.). Sample sizes were 157, 103, and 115 snails from the Mitchell Creek, Rifle Gorge, and Rifle Falls collection sites. At each site, the species proportions are significantly different from a uniform distribution (G-tests, $P < 0.05$).

Acknowledgments

We would like to thank Mark Losleben (University of Colorado Mountain Research Station) and Drs. Jeffry Mitton and Cynthia Carey (Department of Environmental, Population and Organismic Biology) for the loan of various pieces of equipment used in this study. We are grateful to the staff of the Mitchell Creek and Rifle Falls Fish Hatcheries for allowing us to record climatic conditions at their facilities. Dr. Paul Yancey (Whitman College) is acknowledged for kindly performing the HPLC analyses of methylamine and polyol compounds. We also thank Dr. Michael Grant (EPO Biology) for statistical advice and Dr. Shi-Kuei Wu (University of Colorado Museum) for his help in locating populations of *Oreohelix strigosa* and *O. subrudis*. Financial support for this research was provided by the Kathy-Lichty Award for Graduate Student Research and a National Science Foundation Graduate Fellowship to BBR and NSF grants DCB-8702615 and DCB-9018579 to SCH.

Literature Cited

Arad, Z., S. Goldenberg, and J. Heller. 1989. Resistance to desiccation and distribution patterns in the land snail *Sphincterochila*. *J. Zool. Lond* **218:** 353–364.

Barnhart, M. C. 1986. Respiratory gas tensions and gas exchange in active and dormant land snails, *Otala lactea*. *Physiol. Zool.* **59:** 733–745.

Bequaert, J. C., and W. B. Miller. 1973. *The Mollusks of the Arid Southwest*. University of Arizona Press, Tucson, AZ.

Bishop, S. H., L. L. Ellis, and J. M. Burcham. 1983. Amino acid metabolism in Molluscs. Pp. 243–327 in *The Mollusca, vol. 1*, P. W. Hochachka, ed. Academic Press, NY.

Burton, K. 1956. A study of the conditions and mechanism of the diphenylamine reaction for the colorimetric estimation of deoxyribonucleic acid. *Biochem. J.* **62:** 315–323.

Cameron, R. A. D. 1970. The survival, weight-loss and behaviour of three species of land snail in conditions of low humidity. *J. Zool. Lond.* **160:** 143–157.

DeJorge, F. B., and J. A. Peterson. 1970. Urea and uric acid contents in the hepatopancreas, kidney and lung of active and dormant snails, *Strophocheilus* and *Thaumastus* (Pulmonata, Mollusca). *Comp. Biochem. Physiol.* **35:** 211–219.

Folch, J., M. Lees, and G. H. S. Stanley. 1957. A simple method for the isolation and purification of total lipides from animal tissues. *J. Biol. Chem.* **226:** 497–509.

Forster, R. P., and L. Goldstein. 1976. Intracellular osmoregulatory role of amino acids and urea in marine elasmobranchs. *Am. J. Physiol.* **230:** 925–931.

Giles, K. W., and A. Myers. 1965. An improved diphenylamine method for the estimation of deoxyribonucleic acid. *Nature* **206:** 93.

Herreid, C. F., III. 1977. Metabolism of land snails (*Otala lactea*) during dormancy, arousal, and activity. *Comp. Biochem. Physiol.* **56A:** 211–215.

Horne, F. R. 1971. The accumulation of urea by a pulmonate snail during estivation. *Comp. Biochem. Physiol.* **38A:** 565–570.

Horne, F. R. 1973a. The utilization of foodstuffs and urea production by a land snail during estivation. *Biol. Bull.* **144:** 321–330.

Horne, F. R. 1973b. Urea metabolism in an estivating terrestrial snail *Bulimulus dealbatus*. *Am. J. Physiol.* **224:** 781–787.

Jermyn, M. A. 1975. Increasing the sensitivity of the anthrone method for carbohydrate. *Anal. Biochem.* **68:** 332–335.

Jezewska, M. M., B. Gorzkowski, and J. Heller. 1963. Nitrogen compounds in snail *Helix pomatia* excretion. *Acta Biochim. Polonica* **10:** 55–64.

Kermack, W. O., H. Lees, and J. D. Wood. 1955. Some non-protein constituents of the tissues of the lobster. *Biochem. J.* **60:** 424–428.

Koch, F. C., and T. L. McMeekin. 1924. A new direct nesslerization micro-Kjeldahl method and a modification of the Nessler-Folin reagent for ammonia. *J. Am. Chem. Soc.* **46:** 2066–2069.

Lowry, O. H., N. J. Rosebrough, A. L. Farr, and R. J. Randall. 1951. Protein measurement with the Folin phenol reagent. *J. Biol. Chem.* **193:** 265–275.

Machin, J. 1967. Structural adaptation for reducing water-loss in three species of terrestrial snail. *J. Zool. Lond.* **152:** 55–65.

Machin, J. 1975. Water relationships. Pp. 105–163 in *The Pulmonates, vol. 1*, V. Fretter and J. Peake, eds. Academic Press, NY.

Peterson, G. L. 1977. A simplification of the protein assay method of Lowry *et al.* which is generally more applicable. *Anal. Biochem.* **83:** 346–356.

Pomeroy, D. E. 1969. Some aspects of the ecology of the land snail, *Helicella virgata*, in South Australia. *Aust. J. Zool.* **17:** 495–514.

Rees, B. B. 1988. Electrophoretic and morphological characteristics of two species of *Oreohelix*, the Mountain Snail. *Malacol. Rev.* **21:** 129–132.

Rees, B. B., and S. C. Hand. 1990. Heat dissipation, gas exchange and acid-base status in the land snail *Oreohelix* during short-term estivation. *J. Exp. Biol.* **152:** 77–92.

Riddle, W. A. 1983. Physiological ecology of land snails and slugs. Pp. 431–461 in *The Mollusca, vol. 6*, W. D. Russell-Hunter, ed. Academic Press, NY.

Schmidt-Nielsen, K., C. R. Taylor, and A. Shkolnik. 1971. Desert snails: problems of heat, water and food. *J. Exp. Biol.* **55:** 385–398.

Simmonds, R. J., and R. A. Harkness. 1981. High-performance liquid chromatography for base and nucleoside analysis in extracellular fluids and in cells. *J. Chromatog.* **226:** 369–381.

Speeg, K. V., Jr., and J. W. Campbell. 1968. Formation and volatilization of ammonia gas by terrestrial snails. *Am. J. Physiol.* **214:** 1392–1402.

Stearns, R. E. C. 1877. On the vitality of certain land mollusks. *Am. Nat.* **2:** 100–102.

Trammel, P. R., and J. W. Campbell. 1972. Arginine and urea metabolism in the South American land snail, *Strophocheilus oblongus*. *Comp. Biochem. Physiol.* **42B:** 439–449.

Ways, P., and D. J. Hanahan. 1964. Characterization and quantification of red cell lipids in normal man. *J. Lipid Res.* **5:** 318–328.

Wieser, W., and M. Schuster. 1975. The relationship between water content, activity, and free amino acids in *Helix pomatia*. *J. Comp. Physiol.* **98:** 169–181.

Yancey, P. H. 1985. Organic osmotic effectors in cartilaginous fishes. Pp. 424–436 in *Transport Processes, Iono- and Osmoregulation*, R. Gilles and M. Gilles-Baillien, eds. Springer-Verlag, Berlin.

Yancey, P. H., M. E. Clark, S. C. Hand, R. D. Bowlus, and G. N. Somero. 1982. Living with water stress: evolution of osmolyte systems. *Science* **217:** 1214–1222.

Yancey, P. H., and M. B. Burg. 1990. Counteracting effects of urea and betaine in mammalian cells in culture. *Am. J. Physiol.* **258:** R198–R204.

Zar, J. H. 1984. *Biostatistical Analysis.* Prentice-Hall, Inc., Englewood Cliffs, NJ.

Reference: *Biol. Bull.* **184**: 243–253. (April, 1993)

Atmospheric Water Absorption and the Water Budget of Terrestrial Isopods (Crustacea, Isopoda, Oniscidea)

JONATHAN C. WRIGHT AND JOHN MACHIN

Department of Zoology, University of Toronto, 25 Harbord Street, Toronto, Ontario, Canada M5S 1A1

Abstract. Studies of terrestrial isopods (Crustacea, Isopoda, Oniscidea) have revealed a capacity for active water vapor absorption (WVA) in the taxonomic sections Crinocheta and Diplocheta but not in Synocheta. Uptake thresholds in Crinocheta are modest by comparison with other vapor absorbers, but standardized uptake fluxes are among the highest recorded and are probably an adaptive requirement to counter the high transpiratory losses. Comparative data for uptake fluxes, thresholds, and transpiratory losses allows the compilation of water budgets in hypothetical temperature and humidity regimes. Given a 12-h light-dark cycle, with saturated ambient activities for diurnal WVA, all species could recover water losses incurred during nocturnal foraging in an ambient water activity of 0.75, and xeric species could forage in activities below 0.30. Xeric trends based on these models agree closely with predictions from ecotypic surveys. In the littoral *Ligia oceanica* (Diplocheta) haemolymph hyperosmosis and periodic submergence provide additional means of water balance regulation. It is proposed that WVA in *Ligia* provides an essentially solute-free water source to counteract salt-loading in the splash-zone. The absence of WVA in synochetes, together with their cryptozoic habits, reflects an alternative terrestrial strategy to those of other oniscideans.

Introduction

Atmospheric water vapor absorption (WVA) is an active process enabling certain terrestrial organisms to exploit a physical state of water which is often spatially and temporally more abundant than liquid sources. A capacity for WVA has been described in several insect groups: lepismatid Thysanura (Noble-Nesbitt, 1970; Okasha, 1972); Blattodea (Edney, 1966; O'Donnell, 1977, 1981, 1982); Siphonaptera (Knulle, 1967; Rudolph and Knulle, 1982); Psocoptera and Mallophaga (Knulle and Spadafora, 1969; Rudolph, 1982a, b, 1983); tenebrionid larvae (Mellanby, 1932; Ramsay, 1964; Grimstone *et al.*, 1968; Machin, 1975); and lepidopteran larvae (Chauvin and Vannier, 1980). Other major exponents of vapor absorption include certain acarine families (Lees, 1946; Rudolph and Knulle, 1979; Knulle and Rudolph, 1982). Recently, WVA has been demonstrated in the oniscidean isopods (Wright and Machin, 1990), the only crustaceans having attained major ecotypic diversification on land. Adaptations for WVA have yet to be demonstrated in myriapods and the non-acarine arachnids. There is one described case of vapor absorption in a desert plant *Nolana mollis*, a succulent shrub from the Atacama (Mooney *et al.*, 1980).

Our understanding of the physiological processes involved in vapor absorption is fragmentary. Any mechanism does, however, have basic prerequisites. A water-collecting surface must be brought into contact with the humid air and must contain fluids of depressed water vapor pressure, and hence depressed water activity (= relative humidity/100) such that water vapor moves thermodynamically into the collecting fluid. The collected fluid must then be moved internally, by imbibition or co-transport with solutes. The minimum water activity (a_w) generated by the collecting fluid constitutes the minimum activity of water vapor, or ambient activity (Aa_w), from which absorption is possible, defined as the uptake threshold (Machin, 1979a). The activity at which vapor absorption balances passive losses is referred to as the critical equilibrium activity or CEA (after Knulle and Wharton, 1964); a net gain in water is thus possible in ambient activities above the CEA. Physical principles of vapor-liquid transitions and energetic considerations are dis-

Received 27 July 1992; accepted 25 January 1993.

cussed by Wharton and Richards (1978), Machin (1979a), and O'Donnell and Machin (1988).

Vapor absorption systems based on colligative lowering of vapor-pressure require a compartment, isolated from the haemolymph, in which solutes can be accumulated by active transport. Hyperosmotic fluids have been identified in the cryptonephridial systems of tenebrionid larvae (Ramsay, 1964; Machin, 1979b; O'Donnell and Machin, 1991; Machin and O'Donnell, 1991), creating an activity gradient between the rectal lumen and the peripheral Malpighian tubules. They have also recently been described in the salivary secretions of ticks (Sigal *et al.*, 1991), although conflicting data is presented by Gaede (1989). Deeply folded apical and basal membranes with densely packed mitochondria suggest ion transport compatible with production/resorption of hyperosmotic fluids in the recta of flea larvae (Bernotat-Dalielowski and Knulle, 1986) and thysanurans (Noirot and Noirot-Timothee, 1971).

The hypopharyngeal bladders of the desert cockroach *Arenivaga* appear to exploit a different absorption mechanism (O'Donnell, 1981, 1982). The bladders are covered in hydrophilic hairs which are moistened by the cyclical secretion of a fluid comparable in ionic strength to the haemolymph. It is proposed that, by altering the iso-electric point of the cuticular chitin and/or protein, this fluid reduces water affinity and the hairs release water which is subsequently imbibed. Condensation onto the bladder surfaces reverses the trend, decreasing the ionic concentration of the remaining frontal body fluid, and increasing the water affinity of the cutaneous hairs. The process is thus self-sustaining and the hairs absorb water until it is released by the next pulse of uptake fluid. A similar mechanism may operate in the Psocoptera and Mallophaga, based on alterations in the iso-electric point of protein polymers secreted onto the lingual sclerites (Rudolph, 1982b, 1983; O'Donnell and Machin, 1988).

Blocking experiments have established that vapor uptake in oniscidean isopods occurs in the pleon with water possibly being absorbed across the pleopodal endopods (Wright and Machin, 1990; Wright and Machin, 1993). Prior to absorption, a strongly hyperosmotic fluid consisting mostly of Na^+ and Cl^- is secreted into the 'pleoventralraum' (PV) (Wright and O'Donnell, 1992), the cavity formed between the imbricate pleopodal exopods and the pleon sternites. A few minutes later, the pleopods begin a metachronal ventilatory rhythm and the fluid volume declines. There is a simultaneous drop in the fluid osmolality such that its vapor pressure increases to levels only slightly below that of the ambient air (Wright and O'Donnell, 1992). Since pleopodal ventilation is invariably associated with WVA in gravimetric studies, and has only otherwise been observed during maxillary urination, the dilution of uptake fluid is attributed to the onset of vapor condensation. Pleopodal ventilation presumably functions to circulate air over the uptake fluid and may be involved in fluid transport and dissemination.

This explanation for the absorption mechanism requires modification at vapor activities close to the uptake threshold. Under these conditions, pleon fluid osmolalities will sometimes equate with water vapor pressures above those of the ambient air, and are thus incompatible with uptake by direct condensation. It has been proposed (Wright and O'Donnell, 1992) that cyclical compression of air within the PV serves to increase the vapor density and hence increase water activity above that of the uptake fluid. Intermittent compression of air during pleopodal ventilations is suggested by visible pulses of displaced fluid at the pleopodal margins. Such 'pressure cycling' has subsequently been confirmed by monitoring pressure changes coincident with pleopodal ventilations (Wright and Machin, 1993). Interventions of pressure cycling are also detectable gravimetrically as sharp deviations from the typical linear uptake kinetics when net flux is plotted against Aa_w. Such plots indicate that the pressure changes involved are relatively small: 3.65–6.38 kPa for seven common, temperate Crinocheta. It provides a supplement to the usual colligative absorption mechanism, allowing animals to boost uptake in near-threshold activities. The feasibility of pressure cycling as a means of water recovery was first noted by Maddrell (1971). It has subsequently been suggested as a widespread means of water conservation in insect tracheal systems, and to play a role in the vapor absorption mechanism of lepismatids and siphonapterans (Corbet, 1988).

The described uptake thresholds for oniscideans are approximately $a_w = 0.90$ (Wright and Machin, 1990), modest by comparison with many other vapor absorbers. The pyroglyphid dust mite *Dermatophagoides farinae* Hughes, for example, has a critical equilibrium activity 0.70 (Arlian and Wharton, 1974). Psocoptera and Mallophaga display uptake thresholds below 0.50 (Rudolph, 1982a, b, 1983) and respective thresholds of 0.45 and 0.43 have been demonstrated for *Thermobia* (Lepismatidae) (Noble-Nesbitt, 1969) and larvae of *Lasioderma* (Anobiidae) (Knulle and Spadafora, 1970). Uptake fluids based on the major cellular electrolytes (Na^+, K^+, Cl^-) are limited in colligative vapor pressure lowering by saturation: NaCl saturates at an activity of 0.75 and KCl at 0.85 (Winston and Bates, 1960). However, it has been proposed that larvae of the tenebrionid *Onymacris plana* exploit supersaturation of KCl to depress the threshold down to 0.81 (Machin and O'Donnell, 1991). Avoidance of crystallization may depend on 'supersaturation proteins' which bind to crystal surfaces, presenting conformations incompatible with crystal growth. Analogous 'antifreeze proteins' are widely documented in freeze-resistant or-

ganisms and serve to block the growth of ice crystals during supercooling (Davies and Hew, 1990).

Uptake thresholds and absorption kinetics are clearly the main factors determining the physiological and ecological significance of WVA in different groups. Together, these determine the humidity range over which absorption is possible and the water deficits which can be recovered in a given time. The ecological significance of equilibrium humidities in arthropods has been discussed by Knulle and Wharton (1964), with particular reference to acarines. The new finding of WVA in oniscideans is particularly interesting in this regard since, unlike other documented vapor absorbers, oniscideans are typically mesic-hygric arthropods, usually considered poorly adapted to xeric habitats (Cloudsley-Thompson, 1956; Edney, 1968). Here we report results of a comparative study of thresholds and uptake kinetics in the Oniscidea. Such information serves both to establish the range of vapor-absorbing abilities across the sub-order, and to provide a means for assessing ecotypic consequences of WVA.

Materials and Methods

Oniscideans were collected from diverse localities in England and Ontario and maintained in laboratory cultures with deciduous litter. Moistened paper towels served to regulate the culture humidities between 95% and 98% and provided a locally saturated microclimate. The following species were selected for study:

Section Crinocheta
- *Oniscus asellus* Linnaeus, 1758
- *Philoscia muscorum* (Scopoli, 1763)
- *Armadillidium vulgare* (Latreille, 1804)
- *Eluma purpurascens* Budde-Lund, 1885
- *Cylisticus convexus* (De Geer, 1778)
- *Porcellio dilatatus* Brandt, 1833
- *Porcellio laevis* Latreille, 1804
- *Porcellio scaber* Latreille, 1804
- *Porcellio spinicornis* Say, 1818
- *Porcellionides pruinosus* (Brandt, 1833)
- *Trachelipus rathkei* (Brandt, 1833)

Section Synocheta
- *Androniscus dentiger* Verhoeff, 1908
- *Haplophthalmus danicus* Budde-Lund, 1880
- *Trichoniscus pusillus* Brandt, 1833

Section Diplocheta
- *Ligia oceanica* (Linnaeus, 1767)

The littoral species *Ligia oceanica* was maintained in an aereated tank of artificial seawater (Marine Enterprises Inc., Baltimore, MD) and fed on *Enteromorpha sp.* Emergent rocks allowed animals to move freely between air and water.

Water vapor absorption was determined gravimetrically by monitoring mass-changes of isopods in different water activities. Individual animals were contained within 10 mm × 25 mm cylindrical cages constructed from 1 mm or 2 mm mesh aluminum gauze. They were weighed in a moving air stream (1 cm s^{-1}) in a continuous-recording Sartorius 4410 digital microbalance (Sartorius GMBH, Gottingen) sensitive to 10 μg. The balance and weighing chambers were enclosed in temperature-regulated water jackets permitting accurate control of temperature and humidity of the air stream. These parameters were regulated by means of a Hewlett-Packard 71B computer and 3421A data-acquisition unit; details are given in Machin (1976). All experiments were conducted at 20.0°C.

Determinations of net flux in different ambient activities permitted the quantification of passive losses and uptake fluxes during WVA. Passive fluxes were standardized for surface area assuming the formula of Edney (1977):

$$\text{Surface area (cm}^2) = 12\ \text{Mass (grams)}^{0.67}$$

Uptake fluxes were standardized for surface area assuming a net pleoventral absorbing area of 0.05 cm^2 for a 100 mg animal (Wright and Machin, 1993). The net surface area of such an animal computes at 2.57 cm^2, so we may assume the pleoventral area to comprise a proportional area of 0.05/2.57 = 0.0195. Incorporating this factor into Edney's equation gives:

$$\text{Pleoventral area for WVA} = 0.234\ M^{0.67}$$

Fluxes were also standardized for vapor pressure difference between ambient air and haemolymph. For passive fluxes, this assumed a haemolymph osmolality of 700 mosmol l^{-1} for Crinocheta and Synocheta (Little, 1983; J. C. Wright, unpub. data) and 1157 mosmol l^{-1} for *Ligia oceanica* (Parry, 1953). Since water activity is approximately equal to solvent mole fraction (as follows from Raoult's Law) and the molar concentration of liquid water at 20.0°C is 55.5 mol l^{-1}, the haemolymph water activity for Crinocheta and Synocheta is given as:

$$55.5/[55.5 + 0.700] = 0.988$$

Multiplying this value by the saturation vapor pressure of water at 20.0°C (2339 Pa) gives the haemolymph vapor pressure in Pascals.

For uptake fluxes, standardization was based on the absorption threshold activities for each species, and thus assumed initial secretion of uptake fluid at this activity. Justifications for this analysis are discussed in a separate paper (Wright and Machin, 1993). Unless otherwise mentioned, the term 'standardized flux' indicates flux standardized for both area and vapor pressure difference (*i.e.*, μg h^{-1} cm^{-2} Pa^{-1}).

Results

Oniscideans display considerable variation in their ability to restrict passive water losses. Since there are multiple components to water losses in this group (Lindqvist, 1971; Hadley and Quinlan, 1984; Wright and Machin, unpub. data), cumulative mass losses over time do not strictly reflect cutaneous transpiration. However, with continuous gravimetric monitoring it is possible to identify and exclude the irregular bouts of maxillary urination (Wright *et al.*, in prep.). Losses from the moist pleopodal endopods can be estimated using blocking techniques and account for less than 5% of total losses in all species investigated (Hadley and Quinlan, 1984; Wright and Machin, unpub. data). Whole-animal losses have also been shown, using an Al_2O_3 humidity sensor, to be in good agreement with losses measured across isolated cuticle (Hadley and Quinlan, 1984). Finally, carbon in respiratory CO_2 is a source of net mass-loss. Assuming a typical resting metabolism of 200 μl g^{-1} h^{-1} for Crinocheta (Wieser, 1984), and a respiratory quotient of 1, the net mass-loss attributable to respiration is 3.7 $\mu g\ h^{-1}$ for a representative 70 mg animal. This is below 5% of measured losses for ambient activities below 0.97, and typically below 1% of losses for ambient activities below 0.85. For lower respiratory quotients, as with significant lipid metabolism, the respiratory mass-losses are negligible. Analysis of gravimetric losses can thus provide a close approximation of passive cutaneous transpiration.

Mean standardized loss fluxes are listed in Table I for the species studied. Pressure-standardized loss fluxes are also expressed as proportional losses (percent hydrated mass per hour per unit activity). Species fall broadly into three physiologieal categories, corresponding to the different taxonomic sections. The Synocheta and Diplocheta both reveal higher cuticle fluxes than Crinocheta but proportional losses differ markedly owing to size variation. Synocheta thus sustain approximately 50% mass-loss—equivalent to approximately 65% water-loss (lethal)—within 1 h in dry air. *Ligia oceanica* (Diplocheta), in contrast, suffers only 8.5% mass-loss in the same conditions. The Crinocheta reveal the lowest standardized fluxes with the least permeable species (*Armadillidium vulgare, Porcellionides pruinosus*) possessing comparable waterproofing to mesic-hygric insects (Edney, 1977). Proportional mass-losses range from 11.63% $M\ h^{-1}\ a_w^{-1}$ (*Philoscia muscorum*) to 2.88% $M\ h^{-1}\ a_w^{-1}$ (*A. vulgare*).

A capacity for WVA was confirmed for all representatives of the Crinocheta and for *Ligia oceanica*. This extends the number of Crinocheta for which WVA has been demonstrated to 12, and provides the first evidence of WVA in the Diplocheta. Despite repeated studies with both continuous and intermittent weighing, it has not been possible to identify vapor absorption in the Synocheta.

Table I

Mean masses and integumental water fluxes of Oniscidea

Species	Mean M (mg)	n	Standardized flux ($\mu g\ h^{-1}\ cm^{-2}\ Pa^{-1}$)	SE	Proportional flux (%M $h^{-1}\ a_w^{-1}$)
Diplocheta					
L. oceanica	162.76	7	1.664	0.084	8.512
Synocheta					
I. denticr	2.23	4	2.862	0.062	59.39
H. danicus	1.18	9	1.529	0.085	43.93
T. pusillus	2.85	10	2.929	0.229	56.86
Crinocheta					
A. vulgare	112.08	23	0.491	0.035	2.879
C. convexus	58.69	3	1.555	0.139	11.107
E. purpurascens	24.9	1	1.067	—	10.112
O. asellus	78.18	7	1.477	0.088	9.566
P. muscorum	16.5	2	1.069	0.111	11.63
P. dilatatus	89.25	3	0.800	0.034	4.670
P. laevis	55.25	2	0.740	0.035	5.389
P. scaber	54.35	10	0.719	0.075	5.694
P. spinicornis	42.17	18	0.690	0.066	5.733
Ps. pruinosus	26.89	8	0.581	0.037	5.677
T. rathkei	45.11	11	0.901	0.064	7.202

Data were gathered from sections of Diplocheta, Synocheta, and Crinocheta measured at 20°C. Integumental fluxes are expressed as 'standardized flux' ($\mu g\ h^{-1}\ cm^{-2}\ Pa^{-1}$) and as 'proportional flux'—the percentage of the hydrated mass lost per hour per unit activity deficit between haemolymph and ambient.

All species studied died within 24 h when transferred to a 10 ml vial containing saturated $K_2SO_{4(aq)}$ to regulate the humidity at 98.0%; animals survived long after the period required for approximate humidity equilibration (RH > 97.0% in 20–30 min) so there appears to be good evidence to discount WVA in this section.

The kinetics of WVA in Crinocheta have been described before (Wright and Machin, 1990; Wright and Machin, 1993) but a brief account is included here. The description also applies to absorption in *Ligia oceanica*. Plots of net flux against ambient activity reveal a linear curve for passive losses and a capacity for variable rates of vapor uptake above a threshold activity (Fig. 1). Maximum uptake fluxes vary with ambient activity according to approximate linear kinetics, excepting augmented fluxes in near-threshold activities attributable to pressure cycling.

Plots such as Figure 1 allow the determination of regression lines for net uptake and loss fluxes, omitting sub-maximal uptake fluxes and interventions of pressure cycling. The intersection of these curves marks the uptake threshold and the intersection of the uptake curve with the ordinate of zero net flux marks the critical equilibrium activity. Slopes ($\mu g\ h^{-1}\ a_w^{-1}$) are corrected for vapor pressure by dividing by the saturated vapor pressure of water at 20.0°C (2339 Pa). True uptake fluxes ($\mu g\ h^{-1}$) are obtained by subtracting the slope of the loss curve from that of the net uptake curve and can be standardized for surface area and vapor pressure in the usual way.

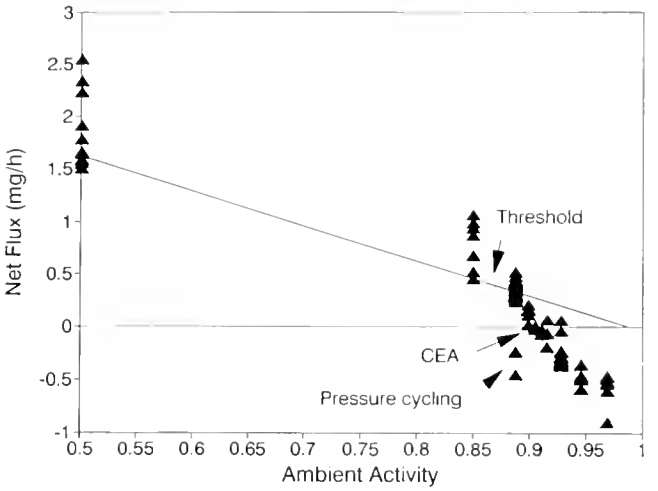

Figure 1. Example plot of net flux against ambient water activity for a vapor-absorbing oniscidean (*A. vulgare*). Each point represents the mean flux measured over a 20 or 30 min period. Passive losses (indicated as positive fluxes) decrease approximately linearly with increasing Aa_w, ceasing where this equals the haemolymph a_w (0.988). Deviations from this curve attributable to active water vapour absorption (WVA) are evident in activities above the uptake threshold, with uptake maxima showing approximate linear kinetics with Aa_w. Uptake fluxes can be modulated in any given Aa_w to balance passive losses or generate maximal uptake as required. They can also be boosted in lower activities by pressure cycling, evident in two recording periods, where compression of air within the pleoventral cavity is used to increase the activity gradient for uptake (Wright and Machin, submitted).

Uptake thresholds and critical equilibrium activities for Crinocheta and Diplocheta are listed in Table II. Species for which insufficient uptake data were available are excluded. Thresholds vary from 0.866 for *Armadillidium vulgare* to 0.927 for *Oniscus asellus*. Product-moment correlation analysis reveals a significant positive relationship between uptake thresholds and standardized loss fluxes ($P < 0.01$; Fig. 2). Species with lower uptake thresholds for WVA thus display lower integumental permeabilities, both constituting xeric adaptations. If the Crinocheta are ranked in ascending order of thresholds and CEAs, the sequence agrees closely with xeric trends based on the most comprehensive ecotypic surveys (Harding and Sutton, 1985; Sutton *et al.*, 1984).

Means and standard errors for vapor-pressure-standardized, as well as vapor-pressure and area-standardized, uptake fluxes for Crinocheta and Diplocheta are listed in Table III. This table also lists net uptake fluxes expressed as percentage of hydrated mass. Corresponding values are given for other vapor absorbers, derived from data in the literature. The most striking observation is the superior efficacy of the oniscidean uptake mechanism, with standardized uptake fluxes an order of magnitude higher than in other vapor absorbers. The Oniscidea are also among the most efficient absorbers when net uptake is expressed

Table II

Mean uptake thresholds and critical equilibrium activities for Crinocheta and Diplocheta

	Threshold	SE	CEA	n
A. vulgare	0.866	0.0046	0.882	5
C. convexus	0.905	0.0035	0.931	2
P. dilatatus	0.892	—	0.910	1
P. scaber	0.889	0.0046	0.913	5
P. spinicornis	0.872	0.0056	0.901	4
Ps. pruinosus	0.872	0.0009	0.899	3
O. asellus	0.927	0.0085	0.946	3
T. rathkei	0.893	0.0073	0.905	2
L. oceanica	0.900	0.0071	0.937	3

Mean uptake thresholds include standard errors.

Information was determined from vapor absorption plots such as seen in Figure 1.

per unit body mass. Since uptake flux is proportional to the area of the absorbing surface, it is expected to scale with body mass according to the relationship:

$$\text{Flux } (\mu\text{g h}^{-1}\ \text{Pa}^{-1}) = \text{a.Mass}^{0.67}$$

Hence:

$$\text{Log Flux} = \log \text{a} + \log \text{Mass} \times 0.67$$

The log:log plot is illustrated in Figure 3 for the species listed in Table III and illustrates the superior uptake fluxes in the Oniscidea. The regression line has an x coefficient of 0.692 indicating a close fit to the predicted scaling. However, the corresponding allometric scaling for the

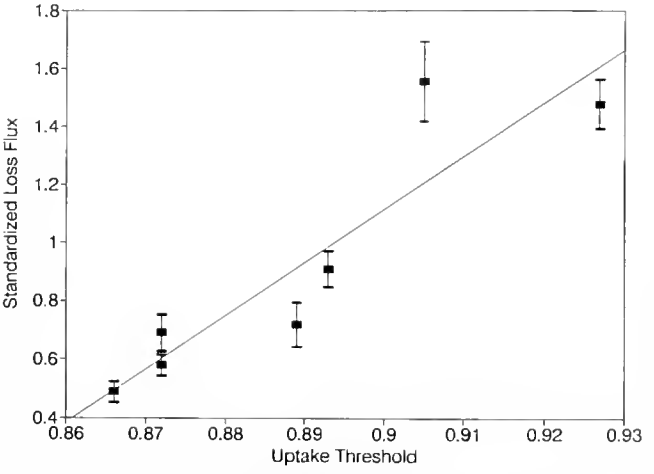

Figure 2. Plot of mean standardized loss flux (μg h^{-1} cm^{-2} Pa^{-1}) against mean uptake threshold for species of Crinocheta. Error bars are indicated for standardized flux only. The relationship reveals a significant positive correlation ($r = 0.907$, $P < 0.01$) indicating parallel selective trends towards low permeability and depressed uptake threshold in xeric species.

Table III

Inward water fluxes measured during WVA in oniscideans and other vapor absorbers

	Uptake flux ($\mu g\ h^{-1}\ cm^{-2}\ Pa^{-1}$)	SE	Uptake flux ($\mu g\ h^{-1}\ Pa^{-1}$)	SE	%M/12h	SE
A. vulgare	126.77	25.86	6.742	1.118	24.67	6.21
C. convexus	222.03	—	6.722	—	39.68	—
O. asellus	257.61	11.09	11.455	1.153	29.20	0.75
P. dilatatus	152.02	—	7.601	—	25.13	—
P. scaber	156.40	17.91	7.820	0.896	24.96	2.86
P. spinicornis	194.14	29.76	5.739	1.201	48.10	6.97
Ps. prunosus	126.84	30.52	3.162	0.757	33.52	6.95
T. rathkei	241.62	49.12	6.710	1.364	50.45	7.25
L. oceanica	290.54	46.25	19.71	2.733	19.34	3.62
Arenivaga	2.70	—	0.136	—	0.126	—
Thermobia	18.93	—	0.379	—	29.16	—
Tenebrio	33.80	—	2.10	—	6.67	—
Onymacris	24.70	—	2.50	—	12.68	—
Liposcelis	2.67	—	0.0086	—	137.69	—

See previous references for sources of data. Uptake fluxes are standardized for both absorbing surface area and vapor pressure deficit ($\mu g\ h^{-1}\ cm^{-2}\ Pa^{-1}$), and for vapor pressure deficit only ($\mu g\ h^{-1}\ Pa^{-1}$). They are also expressed as proportional gains in saturated air (% hydrated mass per 12 h). Standardized uptake fluxes reveal capacities for vapor absorption in the Oniscidea to be an order of magnitude higher than in other groups.

Oniscidea reveals a much lower coefficient of 0.519 indicating a relative increase in uptake flux in smaller animals. This may be achieved by a proportional enlargement of the absorbing endopods in early instars and smaller species, or by other mechanisms such as proportional changes in ventilatory patterns and rates of coupled water transport. We have no current explanation for why such a low scaling coefficient should be adaptive.

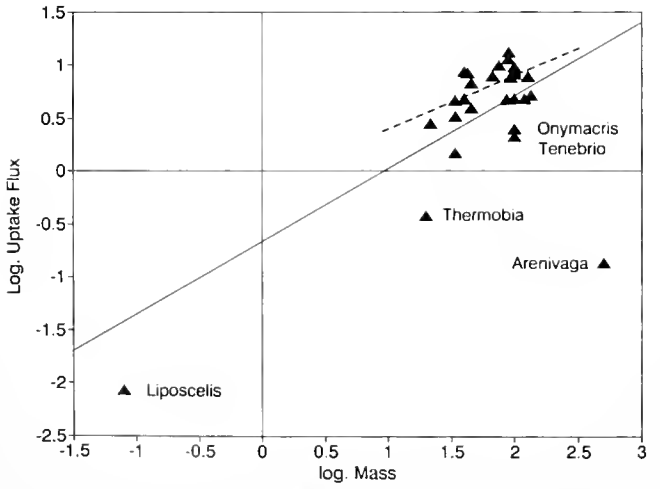

Figure 3. Log-log plot of uptake flux (in $\mu g\ h^{-1}\ Pa^{-1}$) against mass (mg) for a selection of vapor absorbers, based on the values listed in Table 3. The regression line has a slope of 0.692 indicating a scaling approximately in proportion to surface area (flux = a.mass$^{0.67}$). Oniscidea, however, display a different scaling (dotted line) with a slope of 0.519. This indicates mechanisms for increasing relative uptake fluxes in smaller species. For example, proportionally larger absorbing surfaces or more efficient coupled water transport.

The relationships between standardized uptake flux and other physiological parameters reflecting water-balance efficacy are peculiar. Mean standardized uptake flux increases significantly as a function of both uptake threshold and standardized loss flux in the Crinocheta ($P < 0.02$ for both analyses; product-moment correlation). Hygric species such as *Oniscus asellus*, with high integumental permeabilities and high uptake thresholds, thus possess the most efficient uptake mechanisms. This apparently anomalous situation is considered further in the discussion.

Comparative data for passive losses, uptake fluxes and absorption thresholds permits analysis of water budgets in given nocturnal and diurnal regimes. Consider a 12-h light-dark cycle, isopods foraging nocturnally and resting in humid microhabitats diurnally in accordance with typical activity patterns (Brereton, 1957; Sutton *et al.*, 1984; Warburg *et al.*, 1984). Using pressure-standardized net uptake fluxes ($\mu g\ h^{-1}\ Pa^{-1}$), we can calculate the maximum mass of water an isopod could recover by WVA in a diurnal retreat of known ambient activity at 20°C (saturated V.P. = 2339 Pa):

$$\text{Net water-gain (mg)} = \text{Net uptake flux (mg h}^{-1}\ \text{Pa}^{-1}\text{)} \times \text{absorption period (12 h)} \times [(Aa_w - \text{Threshold } a_w) \times 2339]$$

Similarly, since we know loss fluxes for the same species, we can now predict the mean ambient activity in which it would incur a corresponding water debt during nocturnal foraging. It is thus possible to compile water budget curves relating ambient activities during nocturnal for-

aging to the minimum ambient activities required for diurnal replenishment of the resultant water losses. Such water budget curves are illustrated in Figure 4 for the species studied, assuming a uniform diel temperature of 20°C. The nocturnal water debt could not exceed lethal dehydration levels. Data gathered for a range of Crinocheta (5 species, cumulative n = 14) indicate a lethal dehydration level of 34.7% hydrated mass ± 2.4% SE. The low variance and absence of outliers suggests this as a useful approximate value for the section (*ca.* 50% water-loss). Mean nocturnal activities in which the study species would sustain 34.7% desiccation in 12 h are listed in Table IV. For most species, these are below the minimum mean foraging a_w exploitable, given access to saturated air for diurnal WVA; that is to say, the maximum water recovered by WVA could not exceed 34.7% hydrated mass in 12 h. The magnitude of water deficits incurred during nocturnal foraging is thus limited by the capacity for replenishment by WVA, rather than short-term (nocturnal) desiccation tolerance. The major exceptions are *P. spinicornis* and *T. rathkei* in which the desiccation-limited foraging a_w exceeds the WVA-limited a_w.

The most striking revelation of this analysis is the low foraging activities which many species could exploit given even modest activities (0.94, 0.96) for diurnal WVA. With access to a saturated diurnal refuge, all species could exploit mean foraging activities below 0.75 and maintain their long-term water budget. The curves reveal clear interspecific differences, *Porcellio spinicornis* and *Armadillidium vulgare* showing the greatest capacity to tolerate low activities, and *Oniscus asellus* and *Cylisticus convexus* requiring the highest activities. Xeric trends could be manifested primarily in either diurnal or nocturnal habitat selection. The assumptions of this analysis are considered further in the discussion.

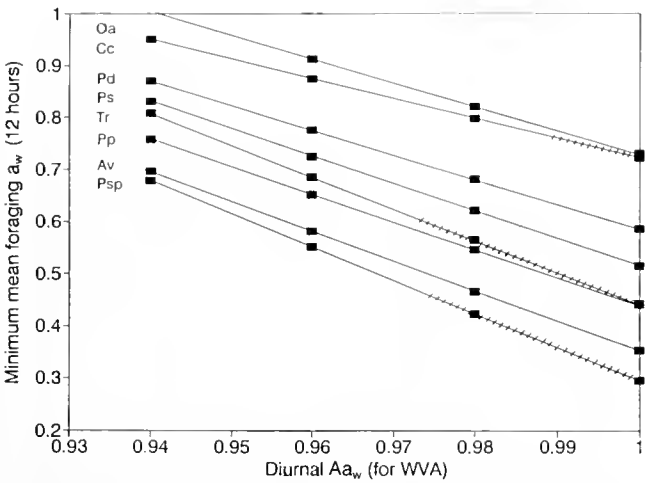

Figure 4. Plots of minimum mean ambient activities in which Crinocheta could forage nocturnally given different ambient activities for diurnal WVA. The analysis assumes a 12-h light-dark cycle. Species initials are indicated beside their respective water budget curves. For each diurnal Aa_w, the maximum attainable water-gain is calculated, knowing thresholds, uptake fluxes, and simultaneous loss fluxes for each species. The nocturnal activity in which a corresponding water-deficit would be sustained is then determined from the standardized loss fluxes. Foraging activities which would result in lethal desiccation within a 12-h period are indicated by hatched bars. All species could theoretically forage in activities below 0.75 given saturated air for diurnal WVA, and xeric species (*A. vulgare, P. spinicornis, Ps. pruinosus*) could forage in mean activities below 0.50.

Table IV

Lower lethal ambient activities for nocturnal foraging in Oniscidea at 20°C

	Aa_w (lethal)	WVA-limited foraging Aa_w
A. vulgare	—	0.305
C. convexus	0.758	0.733
O. asellus	0.690	0.735
P. dilatatus	0.404	0.589
P. scaber	0.322	0.517
P. spinicornis	0.464	0.296
Ps. pruinosus	0.413	0.454
T. rathkei	0.612	0.454
L. oceanica	0.657	0.811

Data were determined by: (a) the activity required to effect lethal desiccation (34.7% hydrated mass) in 12 h; (b) the activity which would result in a cumulative 12-h water loss equal to that which could be recovered by WVA in a saturated diurnal refuge over the same period.

Discussion

The comparative studies of Edney and Cloudsley-Thompson have drawn particular attention to the adaptive constraints limiting terrestrial success in the Oniscidea. These include the relatively inefficient integumental water barriers, the retention of maxillary urination and ammonotely as the major means of nitrogenous excretion, and the need to maintain a fluid film over the pleopodal endopods for respiratory exchange. The picture emerging from these studies is that terrestrial diversification of oniscideans has primarily been the result of behavioral rather than physiological adaptations (Cloudsley-Thompson, 1956, 1974; Den Boer, 1961; Edney, 1954, 1960, 1968; Lindqvist, 1972; Little, 1983). It is perhaps appropriate to reassess this standpoint in the light of the present study.

Three main terrestrial strategies can be differentiated among the Oniscidea. An amphibious, hygrophile strategy is characteristic of the Diplocheta, generally restricted to hygric (*Ligidium*) or littoral habitats (*Ligia*). *Ligia oceanica* can tolerate indefinite periods of submersion, as well as substantial desiccation (Parry, 1953). The latter is offset,

in part, by the large size (and hence low surface area: volume ratio) and extreme osmotic tolerance. An ability to withstand haemolymph hyperosmosis up to 2000 mosmol kg^{-1} (Parry, 1953) allows *Ligia oceanica* to attain thermodynamic equilibrium with an ambient water activity of 0.965. Provided these adaptations can maintain sub-lethal hydration levels through the 12-hourly tidal cycle, water replenishment is then available. The surprising discovery of WVA in this species provides yet another means by which it can regulate water balance. *Ligia* frequently inhabits splash-zone and supra-littoral habitats (Harding and Sutton, 1985) where water supplies are restricted to spray or pools flushed only by spring tides. As such, it may face severe salt-loading and dangers of hyperosmosis. Vapor absorption in littoral and supra-littoral habitats may serve primarily to provide a salt-free water source for osmoregulatory purposes rather than providing a source of water *per se*. This suggests a possible evolutionary scenario, with the pleon initially serving in active salt secretion in salt-loaded littoral species. Hyperosmotic NaCl in pleon fluids would constitute a preadaptation for colligative WVA, allowing animals to compensate for evaporative concentration of body fluids as well as dietary salt-loading. This would then confer obvious preadaptive benefits for the colonization of terrestrial habitats where liquid water supplies are absent or infrequent. Such a scenario is compatible with the known capacity for certain *Ligia* spp. to hyporegulate (Wilson, 1970), demonstrations of high ATPase activity and ion-transport activity by the pleopodal endopods of oniscideans (Dr. C. W. Holliday, pers. comm.; Wright *et al.*, unpub. data), and several lines of evidence suggesting a marine ancestry for the Oniscidea and the ancestral status of the Diplocheta with respect to Crinocheta (Vandel, 1943, 1965; Edney, 1968; Little, 1983; Hoese, 1981, 1982, 1984). It would be interesting to obtain data for WVA and osmoregulation in more terrestrial Diplocheta such as *Ligidium hypnorum* (Cuvier) where close convergence with the Crinocheta might be expected. The occurrence of WVA in both Diplocheta and Crinocheta, but not in Synocheta, concurs with Vandel's (1960, 1965) classification, uniting the former sections in the Ligian series, separate from the Trichoniscian (containing Synocheta) and Tylian series. However, further studies are required to determine whether WVA is an ancestral or derived condition within the Diplocheta.

The Synocheta employ a cryptozoic or 'endogean' strategy, seldom foraging in the open (Harding and Sutton, 1985; Sutton *et al.*, 1984). These species follow high ambient activities by vertical migration, avoiding desiccation behaviorally (Sutton *et al.*, 1984). Physiological adaptations to desiccating conditions are poorly developed. Cuticle permeabilities of the three species monitored in the present study are similar to or somewhat higher than those of *Ligia oceanica*. Combined with the animals' unfavorable surface area/volume ratios, these result in proportional loss fluxes of approximately 50% hydrated mass h^{-1} a_w^{-1}, equating with lethal desiccation times of approximately 7 h in 90% RH, and within 1 h in humidities below 30% RH. Nano-osmometric studies (J. C. Wright, unpub. data) indicate haemolymph osmolalities for *Trichoniscus pusillus* to be in the order of 680 mosmol kg^{-1}. Even on the assumption that dehydration is accompanied by osmotic tolerance rather than haemolymph osmoregulation, this would only induce hyperosmosis to 1.36 osmol kg^{-1} at lethal desiccation. This represents a water activity of 0.976, which may therefore be taken to represent the minimum activity (=97.6% RH) in which *T. pusillus*, and probably other Synocheta, could maintain long-term survival. The characteristically mural/lapidary habitats of *Androniscus dentiger* (Harding and Sutton, 1985) suggest unexpectedly water-stressed diurnal microclimates for a synochete and would repay further investigation.

Only the Crinocheta display substantial independence from liquid water or high ambient activities and thereby colonize mesic-xeric biotopes. Their 'physiological strategy' involves several adaptations to reduce water losses (lowered cuticle permeability, reduction or loss of the maxillary/WS excretory avenue, substitution of respiratory pleopodal endopods with exopodal lungs) and the ability to replenish water-debts above the CEA using vapor absorption. Like *Ligia* spp., Crinocheta can therefore alternate between periods of sustained desiccation and bouts of water recovery. It is well established that activity patterns of Crinocheta are intermittent and primarily nocturnal (Cloudsley-Thompson, 1952; Brereton, 1957; Den Boer, 1961; Paris, 1963, 1965). We predict, from the high efficacy of their vapor absorption, that the Crinocheta routinely sustain large water debts during nocturnal foraging. This supposition requires confirmation from field studies but gains preliminary support from the significant activity of several species in depressed humidities (Brereton, 1957; Den Boer, 1961; Paris, 1963, 1965). Such behavior has been suggested to subserve in the transpiratory loss of excess water accumulated during the day (Den Boer, 1961). Den Boer measured substantial diurnal water gains in *P. scaber* in aspen woods, though he assumed these were attributable to passive, not active absorption. This possibility can be dismissed since, for an isopod with a hydrated haemolymph water activity of 0.988, the activity gradient for integumental water gain in a saturated diurnal microclimate ($Aa_w = 1$) is only 0.012 (28.0 Pa at 20°C) and would only induce a minuscule inward water flux of 30–80 $\mu g\ h^{-1}$ (*ca.* 0.1% body mass h^{-1}) for calculated integumental permeabilities of the study species. Waterlogged habitats, on the other hand, present a serious danger to isopods owing to the hydrophilic ventral cuticle and permeable pleopodal endopods. Drowning has been

shown to constitute a major cause of mortality in grassland populations of *A. vulgare* (Paris, 1963). Even larger species regularly die within an hour when immersed, presumably from anoxia or from ion-loss and hypo-osmosis. The characteristic behavior of emerging onto the surface of soil and litter during precipitation is equally apparent in other permeable soil invertebrates (pulmonates, oligochaetes) and is generally regarded as an evasive response to waterlogging.

Interspecific differences in WVA thresholds, uptake fluxes, and integumental permeabilities reflect adaptive responses to differing xeric stresses. The strong positive correlation between uptake threshold and standardized loss flux reflects parallel adaptive trends in vapor absorption and permeability reduction. Low thresholds and high uptake fluxes will both increase water recovery in sub-saturated diurnal habitats. The ability of *C. convexus, P. spinicornis* and *T. rathkei* to recover maximum tolerable water deficits in sub-saturated diurnal activities (0.991, 0.975, and 0.983, respectively) over a 12-h period may reflect their frequently mesic-xeric diurnal habitats (Van Name, 1936; Harding and Sutton, 1985). However, the significant positive correlations between standardized uptake flux and threshold, and between standardized uptake flux and standardized loss flux, both suggest compensatory adaptive solutions to the problem of water recovery. Permeable species require higher uptake fluxes to counter their greater simultaneous losses. Similarly, species with high thresholds require greater uptake fluxes to compensate for the modest activity gradients they are able to generate. Unlike most vapor absorbers, oniscideans face water stress primarily as a result of relatively inefficient water barriers, not severely xeric habitats. Their remarkably high uptake fluxes are necessary to compensate for high simultaneous losses and relatively high thresholds.

It is clear from the present study that the traditional description of oniscideans as hygric, drought-shunning arthropods, possessing only modest adaptations for terrestriality, requires a fundamental revision in the case of the Crinocheta. By means of highly efficient water vapor absorption, they can routinely sustain large water-debts during nocturnal foraging and thereby tolerate low foraging activities for extended periods. The water budget analyses in this study, based on a 12-h light-dark diel cycle, are a conservative model for oniscideans in temperate latitudes since species are typically quiescent between the September and March equinoxes and are restricted to correspondingly shorter foraging periods. This means that water-debts will be more modest, and periods available for WVA will be more extensive. In addition, the analysis excludes interventions of pressure cycling in lower humidities which, though generally infrequent, can greatly boost uptake fluxes (Wright and Machin, 1993). Behavioral adaptations to limit desiccation are likely to be of minor significance during foraging outings, particularly if these occupy restricted periods during the night (Den Boer, 1961). However, orienting kineses to temperature and humidity, as well as thigmokinesis, will serve a critical role in the selection of diurnal microhabitats compatible with WVA. Although uptake fluxes are likely to increase with temperature, WVA being an energy-dependent process (Machin, 1979a), and passive transpiration in *P. laevis* has been shown to increase linearly with ambient temperature over a biological range (Hadley and Quinlan, 1984), there is currently insufficient data available to allow predictions of the effect of temperature on the overall water budget. Excessive water vapor pressure deficits associated with diurnal temperatures may constitute the major selection pressure restricting Crinocheta to a predominantly nocturnal habit.

Acknowledgments

This study was made possible through the financial assistance of the Leverhulme Trust, U.K. (JCW) and NSERC (JM). We extend our thanks to Gloria Lampert, Mike O'Donnell, and Berry Smith for helpful discussions at various stages of this work.

Literature Cited

Arlian, L. G., and G. W. Wharton. 1974. Kinetics of active and passive components of water exchange between the air and a mite *Dermatophagoides farinae*. *J. Insect Physiol.* **20:** 335–347.

Bernotat-Dalielowski, S., and W. Knulle. 1986. Ultrastructure of the rectal sac, the site of uptake of water vapour from the atmosphere in larvae of the oriental rat flea *Xenopsylla chaeopis*. *Tissue Cell* **18:** 437–455.

Brereton, J. Le G. 1957. The distribution of woodland isopods. *Oikos* **8:** 85–106.

Chauvin, G., and G. Vannier. 1980. Absorption of water vapour by the larvae of *Tinea pellionella* L. (Lepidoptera: Tineidae). *Experientia* **36:** 87–88.

Cloudsley-Thompson, J. L. 1952. Studies in diurnal rhythms II. Changes in the physiological responses of the woodlouse *Oniscus asellus* to environmental stimuli. *J. Exp. Biol.* **29:** 295–303.

Cloudsley-Thompson, J. L. 1956. Studies in diurnal rhythms VII. Humidity responses and nocturnal activity in woodlice (Isopoda). *J. Exp. Biol.* **33:** 576–582.

Cloudsley-Thompson, J. L. 1974. Climatic effect affecting the nocturnal emergence of woodlice and other arthropods. *Ent. Mon. Mag.* **109:** 123–124.

Cloudsley-Thompson, J. L., and M. Gupta. 1960. The effect of wind on the nocturnal emergence of woodlice and other arthropods. *Ent. Mon. Mag.* **95:** 167–168.

Corbet, S. A. 1988. Pressure cycling and the water economy of insects. Review. *Phil. Trans. R. Soc. Lond. B* **318:** 377–407.

Davis, P. L., and C. L. Hew. 1990. Biochemistry of fish antifreeze proteins. *FASEB Journal* **4:** 2460–2468.

Den Boer, P. J. 1961. The ecological significance of activity patterns in the woodlouse *Porcellio scaber* Latr. (Isopoda). *Archs. Neerl. Zool.* **14:** 283–409.

Edney, E. B. 1954. Woodlice and the land habitat. *Biol. Rev.* **29:** 185–219.

Edney, E. B. 1960. Terrestrial adaptations. Pp. 367–393 in *The Physiology of Crustacea*, T. H. Waterman, ed. Academic Press, New York.

Edney, E. B. 1966. Absorption of water vapor from unsaturated air by *Arenivaga sp* (Polyphagidae, Dictyoptera). *Comp. Biochem Physiol* **19:** 387–408.

Edney, E. B. 1968. The transition from water to land in isopod Crustacea. *Am. Zool.* 8: 309–326.

Edney, E. B. 1977. *Water balance in land arthropods.* Springer-Verlag, Berlin.

Gaede, K. 1989. Vergleichende Untersuchungen zur Wasserdampfsorptionsfähigkeit bei Insekten and Milben unter besonderer Berucksichtigung der Merostigmata. Ph.D. Thesis, Free University of Berlin.

Grimstone, A. V., A. M. Mullinger, and J. A. Ramsay. 1968. Further studies on the rectal complex of the mealworm, *Tenebrio molitor* L. (Coleoptera, Tenebrionidae). *Proc. R. Soc. Lond. B* **253:** 343–382.

Hadley, N. F., and M. C. Quinlan. 1984. Cuticular transpiration in the isopod *Porcellio laevis*: chemical and morphological factors involved in its control. *Symp. Zool. Soc. Lond.* **53:** 97–107.

Harding, P. T., and S. L. Sutton. 1985. *Woodlice in Britain and Ireland: Distribution and Habitat.* Natural Environment Research Council, Institute of Terrestrial Ecology, Huntingdon.

Hoese, B. 1981. Morphologie und Funktion des Wasserleitungssystems der terrestrichen Isopoden (Crustacea, Isopoda, Oniscidea). *Zoomorphol.* **98:** 135–167.

Hoese, B. 1982. Der *Ligia*-Typ des Wassedrleitungssystems bei terrestrichen Isopoden und seine Entwicklung in der Familie Ligiidae (Crustacea, Isopoda, Oniscoidea). *Zool. Jb. Anat.* **108:** 223–261.

Hoese, B. 1984. The Marsupium in terrestrial isopods. *Symp. Zool. Soc. Lond.* **53:** 65–76.

Knulle, W., and D. Rudolph. 1982. Humidity relationships and water balance of ticks. Pp. 43–70 in *Physiology of Ticks*, F. D. Obenchain and R. L. Galun, eds. Pergamon Press, Oxford, New York.

Knulle, W. 1967. Physiological properties and biological implications of the water vapor sorption mechanism in larvae of the Oriental rat flea *Xenopsylla cheopis* (Roths.). *J. Insect Physiol.* **13:** 333–357.

Knulle, W., and R. R. Spadafora. 1970. Occurrence of water vapor sorption from the atmosphere in larvae of some stored-produce beetles. *J. Econ. Entomol.* **4:** 1069–1070.

Knulle, W., and G. W. Wharton. 1964. Equilibrium humidities in arthropods and their ecological significance. *Acarologia* **6:** 299–306.

Lees, A. D. 1946. The water balance in *Ixodes ricinus* L. and certain other species of ticks. *Parasitology* **37:** 1–20.

Lindqvist, O. V. 1971. Evaporation in terrestrial isopods is determined by oral and anal discharge. *Experientia* **27:** 1496–1498.

Lindqvist, O. V. 1972. Humidity reactions of the young of the terrestrial isopods *Porcellio scaber* Latr. and *Trachaeoniscus rathkei* (Brandt). *Ann. Zool. Fennici* **9:** 10–14.

Little, C. 1983. *The Colonisation of Land.* Cambridge University Press.

Machin, J. 1975. Water balance in *Tenebrio molitor* L. larvae; the effect of atmospheric water absorption. *J. Comp. Physiol.* **101:** 121–132.

Machin, J. 1976. Positive exchange during water vapour absorption in mealworms (Tenebrio molitor): a new approach to studying the phenomenon. *J. Exp. Biol.* **65:** 603–615.

Machin, J. 1979a. Atmospheric water vapor absorption in arthropods. *Adv. Insect Physiol.* **14:** 1–48.

Machin, J. 1979b. Compartmental osmotic pressure in the rectal complex of *Tenebrio* larvae: evidence for a single tubular pumping site. *J. Exp. Biol.* **82:** 123–137.

Machin, J., and M. J. O'Donnell. 1991. Rectal complex ion activities and electrochemical gradients in larvae of the desert beetle *Onymacris*: comparisons with *Tenebrio*. *J. Insect Physiol.* **37:** 829–838.

Maddrell, S. H. P. 1971. The mechanism of insect excretory systems. *Adv. Insect Physiol.* **8:** 199–331.

Mellanby, K. 1932. The effect of atmospheric humidity on the metabolism of the fasting mealworm (*Tenebrio molitor* L. Coleoptera). *Proc. R. Soc. Lond. B* **111:** 376–390.

Mooney, H. A., S. L. Gulmon, J. Ehleringer, and P. W. Rundel. 1980. Atmospheric water uptake by an Atacama desert shrub. *Science* **209:** 693–694.

Noble-Nesbitt, J. 1969. Water balance in the firebrat *Thermobia domestica* (Packard): exchanges of water with the atmosphere. *J. Exp. Biol.* **50:** 475–469.

Noble-Nesbitt, J. 1970. Water balance in the firebrat *Thermobia domestica* (Packard): the site of water uptake from the atmosphere. *J. Exp. Biol* **52:** 193–200.

Noirot, C., and C. Noirot-Timothee. 1971. Ultrastructure du proctodeum chez le *Lepismodes inquilinus* Newman (= *Thermobia domestica* Packard) II. Le sac anal. *J. Ultrastr. Res.* **37:** 335–350.

O'Donnell, M. J. 1977. Site of water vapor absorption in the desert cockroach *Arenivaga investigata*. *Proc. Natl. Acad. Sci., U.S.A.* **74:** 1757–1760.

O'Donnell, M. J. 1981. Frontal bodies: novel structures involved in water vapor absorption in the desert burrowing cockroach *Arenivaga investigata*. *Tissue Cell* **13:** 541–555.

O'Donnell, M. J. 1982. Hydrophilic cuticle: The basis for water vapour absorption by the desert burrowing cockroach *Arenivaga investigata*. *J. Exp. Biol.* **99:** 43–60.

O'Donnell, M. J., and J. Machin. 1988. Water vapor absorption by terrestrial organisms. Pp. 47–107 in *Advances in Comparative and Environmental Physiology* Vol. 2, Springer-Verlag, Berlin.

O'Donnell, M. J., and J. Machin. 1991. Ion activities and electrochemical gradients in the mealworm rectal complex. *J. Exp. Biol.* **155:** 375–402.

Okasha, A. Y. K. 1972. Water relations in an insect *Thermobia domestica* II. Relationships between water content, water uptake from subsaturated atmospheres and water loss. *J. Exp. Biol.* **57:** 285–296.

Paris, O. H. 1963. The ecology of *Armadillidium vulgare* in California grassland: Food, enemies and weather. *Ecol. Monog.* **33:** 1–22.

Paris, O. H. 1965. Vaglity of P^{32}-labeled isopods in grassland. *Ecology* **36:** 635–648.

Parry, G. 1953. Osmotic and ionic regulation in the isopod crustacean *Ligia oceanica*. *J. Exp. Biol.* **30:** 567–574.

Ramsay, J. A. 1964. The rectal complex of the mealworm *Tenebrio molitor* L. (Coleoptera, Tenebrionidae). *Phil. Trans. R. Soc. B* **248:** 279–314.

Rudolph, D. 1982a. Occurrence, properties and biological implications of the active uptake of water vapor from the atmosphere in Psocoptera. *J. Insect Physiol.* **28:** 111–121.

Rudolph, D. 1982b. Site, process and mechanisms of active uptake of water vapor from the atmosphere in the Psocoptera. *J. Insect Physiol.* **28:** 205–212.

Rudolph, D. 1983. The water vapor uptake system of the Pthiraptera. *J. Insect Physiol.* **29:** 15–25.

Rudolph, D., and W. Knulle. 1979. Mechanisms contributing to water balance in non-feeding ticks and ecological implications. Pp. 375–383 in *Recent Advances in Acarology*, Vol. 1, J. G. Rodriguez, ed. Academic Press, London, New York.

Rudolph, D., and W. Knulle. 1982. Novel uptake systems for atmospheric water vapour among insects. *J. Exp. Zool.* **222:** 321–333.

Sigal, M. D., J. Machin, and G. R. Needham. 1991. Hyperosmotic oral fluid secretions during active water vapour absorption and during desiccation-induced storage excretion by the unfed female tick *Amblyomma americanum*. *J. Exp. Biol.* **157:** 585–591.

Sutton, S. L., M. Hassall, R. Willows, R. C. Davis, A. Grundy, and K. D. Sunderland. 1984. Life histories of terrestrial isopods: a study

of intra and inter-specific variation. *Symp Zool Soc Lond* **53:** 269–294.

Van Name, W. G. 1936. The American land and freshwater isopod Crustacea. *Bull Am Mus Nat Hist* **71:** 1–535.

Vandel, A. 1943. Essai sur l'origine, l'evolution et la classification des Oniscoidea (isopodes terrestres). *Bull biol Fr Belg* (suppl.) **30:** 1–143.

Vandel, A. 1960. *Isopodes Terrestres. Faune de France,* Vol. 64. Librairie de la Faculte de Sciences, Paris.

Vandel, A. 1965. Sur l'existence d'oniscoides très primitifs menant une vie aquatique et sur le polyphyletisme des isopodes terrestres. *Inn Spelcologie* **20:** 489–518.

Warburg, M. R., K. E. Linsenmair, and K. Berkovitz. 1984. The effect of climate on the distribution and abundance of isopods. *Symp Zool Soc Lond* **53:** 339–367.

Wharton, G. W., and A. G. Richards. 1978. Water vapor exchange kinetics in insects and acarines. *Ann Rev Entomol* **23:** 309–328.

Wieser, W. 1984. Ecophysiological adaptations of terrestrial isopods: a brief review. *Symp Zool Soc Lond* **53:** 247–265.

Wilson, W. J. 1970. Osmoregulatory capabilities in isopods: *Ligia occidentalis* and *Ligia pallasii*. *Biol. Bull* **138:** 196–198.

Winston, P. W., and D. H. Bates. 1960. Saturated solutions for the control of humidity in biological research. *Ecology* **41:** 232–237.

Wright, J. C., and J. Machin. 1990. Water vapour absorption in terrestrial isopods. *J Exp Biol* **154:** 13–30.

Wright, J. C., and J. Machin. 1993. Energy-dependent water vapor absorption in the pleoventral cavity of terrestrial isopods (Crustacea, Isopoda, Oniscidea): evidence for pressure cycling as a supplement to the colligative uptake mechanism. *Physiol Zool* In press.

Wright, J. C., and M. J. O'Donnell. 1992. Osmolality and electrolyte composition of pleon fluid in *Porcellio scaber* (Crustacea, Isopoda, Oniscidea): implications for water vapour absorption. *J Exp Biol* **164:** 189–203.

CONTENTS

Volume 184 Number 3

THE BIOLOGICAL BULLETIN

JUNE, 1993

Published by the Marine Biological Laboratory

THE
BIOLOGICAL BULLETIN

PUBLISHED BY
THE MARINE BIOLOGICAL LABORATORY

JUNE, 1993

Printed and Issued by
LANCASTER PRESS, Inc.
3575 HEMPLAND ROAD
LANCASTER, PA

THE BIOLOGICAL BULLETIN

THE BIOLOGICAL BULLETIN is published six times a year by the Marine Biological Laboratory, MBL Street, Woods Hole, Massachusetts 02543.

Subscriptions and similar matter should be addressed to Subscription Manager, THE BIOLOGICAL BULLETIN, Marine Biological Laboratory, Woods Hole, Massachusetts 02543. Single numbers, $35.00. Subscription per volume (three issues), $87.50 ($175.00 per year for six issues).

Communications relative to manuscripts should be sent to Michael J. Greenberg, Editor-in-Chief, or Pamela L. Clapp, Managing Editor, at the Marine Biological Laboratory, Woods Hole, Massachusetts 02543. Telephone: (508) 548-3705, ext. 428. FAX: 508-540-6902. E-mail: pamcl@hoh.mbl.edu.

POSTMASTER: Send address changes to THE BIOLOGICAL BULLETIN, Marine Biological Laboratory, Woods Hole, MA 02543.

Second-class postage paid at Woods Hole, MA, and additional mailing offices.
ISSN 0006-3185

INSTRUCTIONS TO AUTHORS

The Biological Bulletin accepts outstanding original research reports of general interest to biologists throughout the world. Papers are usually of intermediate length (10–40 manuscript pages). A limited number of solicited review papers may be accepted after formal review. A paper will usually appear within four months after its acceptance.

Very short, especially topical papers (less than 9 manuscript pages including tables, figures, and bibliography) will be published in a separate section entitled "Research Notes." A Research Note in *The Biological Bulletin* follows the format of similar notes in *Nature*. It should open with a summary paragraph of 150 to 200 words comprising the introduction and the conclusions. The rest of the text should continue on without subheadings, and there should be no more than 30 references. References should be referred to in the text by number, and listed in the Literature Cited section in the order that they appear in the text. Unlike references in *Nature*, references in the Research Notes section should conform in punctuation and arrangement to the style of recent issues of *The Biological Bulletin*. Materials and Methods should be incorporated into appropriate figure legends. See the article by Lohmann *et al.* (October 1990, Vol. **179**: 214–218) for sample style. A Research Note will usually appear within two months after its acceptance.

The Editorial Board requests that regular manuscripts conform to the requirements set below; those manuscripts that do not conform will be returned to authors for correction before review.

1. ***Manuscripts.*** Manuscripts, including figures, should be submitted in triplicate. (Xerox copies of photographs are not acceptable for review purposes.) The original manuscript must be typed in no smaller than 12 pitch, using double spacing (*including* figure legends, footnotes, bibliography, etc.) on one side of 16- or 20-lb. bond paper, 8½ by 11 inches. Please, no right justification. Manuscripts should be proofread carefully and errors corrected legibly in black ink. Pages should be numbered consecutively. Margins on all sides should be at least 1 inch (2.5 cm). Manuscripts should conform to the *Council of Biology Editors Style Manual*, 5th Edition (Council of Biology Editors, 1983) and to American spelling. Unusual abbreviations should be kept to a minimum and should be spelled out on first reference as well as defined in a footnote on the title page. Manuscripts should be divided into the following components: Title page, Abstract (of no more than 200 words), Introduction, Materials and Methods, Results, Discussion, Acknowledgments, Literature Cited, Tables, and Figure Legends. In addition, authors should supply a list of words and phrases under which the article should be indexed.

2. ***Title page.*** The title page consists of: a condensed title or running head of no more than 35 letters and spaces, the manuscript title, authors' names and appropriate addresses, and footnotes listing present addresses, acknowledgments or contribution numbers, and explanation of unusual abbreviations.

3. ***Figures.*** The dimensions of the printed page, 7 by 9 inches, should be kept in mind in preparing figures for publication. We recommend that figures be about 1½ times the linear dimensions of the final printing desired, and that the ratio of the largest to the smallest letter or number and of the thickest to the thinnest line not exceed 1:1.5. Explanatory matter generally should be included in legends, although axes should always be identified on the illustration itself. Figures should be prepared for reproduction as either line cuts or halftones. Figures to be reproduced as line cuts should be unmounted glossy photographic reproductions or drawn in black ink on white paper, good-quality tracing cloth or plastic, or blue-lined coordinate paper. Those to be reproduced as halftones should be mounted on board, with both designating numbers or letters and scale bars affixed directly to the figures. All figures should be numbered in consecutive order, with no distinction between text and plate figures. The author's name and an arrow indicating orientation should appear on the reverse side of all figures.

4. ***Tables, footnotes, figure legends, etc.*** Authors should follow the style in a recent issue of *The Biological Bulletin* in preparing table headings, figure legends, and the like. Because of the high cost of setting tabular material in type, authors are asked to limit such material as much as possible. Tables, with their headings and footnotes, should be typed on separate sheets, numbered with consecutive Roman numerals, and placed after

the Literature Cited. Figure legends should contain enough information to make the figure intelligible separate from the text. Legends should be typed double spaced, with consecutive Arabic numbers, on a separate sheet at the end of the paper. Footnotes should be limited to authors' current addresses, acknowledgments or contribution numbers, and explanation of unusual abbreviations. All such footnotes should appear on the title page. Footnotes are not normally permitted in the body of the text.

5. ***Literature cited.*** In the text, literature should be cited by the Harvard system, with papers by more than two authors cited as Jones *et al.*, 1980. Personal communications and material in preparation or in press should be cited in the text only, with author's initials and institutions, unless the material has been formally accepted and a volume number can be supplied. The list of references following the text should be headed Literature Cited, and must be typed double spaced on separate pages, conforming in punctuation and arrangement to the style of recent issues of *The Biological Bulletin*. Citations should include complete titles and inclusive pagination. Journal abbreviations should normally follow those of the U. S. A. Standards Institute (USASI), as adopted by BIOLOGICAL ABSTRACTS and CHEMICAL ABSTRACTS, with the minor differences set out below. The most generally useful list of biological journal titles is that published each year by BIOLOGICAL ABSTRACTS (BIOSIS List of Serials; the most recent issue). Foreign authors, and others who are accustomed to using THE WORLD LIST OF SCIENTIFIC PERIODICALS, may find a booklet published by the Biological Council of the U.K. (obtainable from the Institute of Biology, 41 Queen's Gate, London, S.W.7, England, U.K.) useful, since it sets out the WORLD LIST abbreviations for most biological journals with notes of the USASI abbreviations where these differ. CHEMICAL ABSTRACTS publishes quarterly supplements of additional abbreviations. The following points of reference style for THE BIOLOGICAL BULLETIN differ from USASI (or modified WORLD LIST) usage:

A. Journal abbreviations, and book titles, all underlined (for *italics*)

B. All components of abbreviations with initial capitals (not as European usage in WORLD LIST *e.g., J. Cell. Comp. Physiol.* NOT *J. cell. comp. Physiol.*)

C. *All* abbreviated components must be followed by a period, whole word components *must not* (*i.e., J. Cancer Res.*)

D. Space between all components (*e.g., J. Cell. Comp. Physiol.*, not *J Cell.Comp.Physiol.*)

E. Unusual words in journal titles should be spelled out in full, rather than employing new abbreviations invented by the author. For example, use *Rit Vísindafjélags Islendinga* without abbreviation.

F. All single word journal titles in full (*e.g., Veliger, Ecology, Brain*).

G. The order of abbreviated components should be the same as the word order of the complete title (*i.e., Proc.* and *Trans.* placed where they appear, not transposed as in some BIOLOGICAL ABSTRACTS listings).

H. A few well-known international journals in their preferred forms rather than WORLD LIST or USASI usage (*e.g., Nature, Science, Evolution* NOT *Nature, Lond., Science, N.Y.; Evolution, Lancaster, Pa.*)

6. ***Reprints, page proofs, and charges.*** Authors receive their first 100 reprints (without covers) free of charge. Additional reprints may be ordered at time of publication and normally will be delivered about two to three months after the issue date. Authors (or delegates for foreign authors) will receive page proofs of articles shortly before publication. They will be charged the current cost of printers' time for corrections to these (other than corrections of printers' or editors' errors). Other than these charges for authors' alterations, *The Biological Bulletin* does not have page charges.

Reference: *Biol. Bull.* **184**: 255–268. (June, 1993)

Life Cycle Evolution in Asteroids: What is a Larva?

LARRY R. McEDWARD AND DANIEL A. JANIES

University of Florida, Department of Zoology, 223 Bartram Hall, Gainesville, Florida 32611-2009

Abstract. The diversity of larval forms and developmental patterns in asteroid echinoderms has become increasingly apparent over the past 10–15 years. However, the classification of developmental patterns has been ambiguous because the patterns have not been defined as unique sets of ecological and developmental character states. In addition, character states have not been defined consistently. Thus attempts to understand the evolutionary changes in development (*e.g.*, heterochrony and heterotopy in morphogenesis) that underlie larval diversity have been hampered. We propose a multifactor classification of asteroid developmental patterns that uses an explicit set of characters that provide information on habitat (*e.g.*, pelagic or benthic) and mode of nutrition (*e.g.*, feeding or nonfeeding) of the developing young, as well as the type of morphological development (indirect = larval; direct = nonlarval). We conclude that direct development is exceptionally rare. All asteroids whose development has been studied, except *Pteraster tesselatus*, have the indirect type of development. We also propose definitions of some important terms that have been used inconsistently in the literature (*e.g.*, larva, metamorphosis, indirect development, and direct development). Our definitions take into account the continuous nature of development and the evolutionary diversification of ontogenetic sequences. These definitions are intended to provide a clear conceptual basis for analyzing asteroid life cycle evolution. We argue that the ancestral asteroid life cycle involved pelagic larval development with both bipinnarian and brachiolarian stages. We then present a series of hypotheses for six types of evolutionary transitions in development that can account for the diversity of larval forms and developmental patterns in starfish.

Patterns of Development in Asteroids

Different schemes for classifying the patterns of development of marine benthic invertebrates have been applied to asteroids. In general, four different patterns (Table 1) have been identified: (1) planktotrophy, (2) pelagic lecithotrophy, (3) demersal development, and (4) brooding (including viviparity) (Thorson, 1950; Mileikovsky, 1971, 1974; Chia, 1974; Jablonski and Lutz, 1983; Grahme and Branch, 1985). These patterns are distinguished largely on the basis of ecological characteristics, such as habitat or source of nutrition. The following descriptions of these major patterns of development outline the features that apply specifically to asteroids.

In the planktotrophic pattern, development involves a pelagic larva that feeds on suspended particles from the water column (*e.g.*, *Asterias rubens*, Gemmill, 1914; *Porania pulvillus*, Gemmill, 1915; *Astropecten aranciacus*, Hörstadius, 1939; *Astropecten scoparius*, Oguro *et al.*, 1976; *Patiriella regularis*, Byrne and Barker, 1991; see Emlet *et al.*, 1987, for an extensive list of asteroid species and patterns of development). Feeding larvae often have complex morphology and behavior associated with particle capture (Strathmann, 1974, 1987). A universal characteristic of species with planktotrophic development is the production of small eggs ($\approx$100–250 μm) that contain insufficient nutritional reserves to support larval development to metamorphosis. Correlated with the very low levels of parental investment per offspring are extraordinarily high fecundities (ranging up to hundreds of millions of eggs per female per year). Because successful larval feeding is obligatory in species with the planktotrophic pattern of development, the duration of the larval period is often quite long (weeks to months), providing considerable potential for larval dispersal.

Pelagic lecithotrophy involves development via a pelagic nonfeeding larva (*e.g.*, *Solaster endeca*, Gemmill, 1912; *Crossaster papposus*, Gemmill, 1920; *Pteraster tesselatus*, Chia, 1966; McEdward, 1992; *Mediaster aequalis*, Birkeland *et al.*, 1971; *Astropecten gisselbrechti*, Komatsu and Nojima, 1985). Lecithotrophic larvae are morphologically simpler than related planktotrophic larvae, in that they lack feeding structures, such as ciliated bands

Received 24 November 1992; accepted 23 March 1993.

Table I

Traditional classification of developmental patterns in asteroids with characteristics and examples

	Characters			
Name of pattern	Development[1]	Habitat	Nutrition[2]	Asteroid examples[3]
Planktotrophy	Indirect	Pelagic	Feeding	*Asterias rubens* *Astropecten scoparius*
Pelagic lecithotrophy	Indirect or direct	Pelagic	Nonfeeding	*Solaster endeca* *Astropecten gisselbrechti* *Pteraster tesselatus*
Demersal development	Indirect	Benthic	Nonfeeding or feeding	*Asterina minor* *Odontaster validus?*
Brooding	Indirect or direct	Benthic	Nonfeeding	*Leptasterias hexactis* *Pteraster militaris*

[1] Indirect and direct development are defined by the presence or absence, respectively, of a larval stage in development. These types of development are defined here using the restricted definition of a larva (see text).

[2] Feeding means that particulate nutrition is acquired from the seawater. Nonfeeding means that nutrition is acquired only from the mother.

[3] The examples provide a cross reference to those cited in the body of the paper.

or a mouth. In many cases, the only specialized structures that nonfeeding larvae possess are swimming structures or attachment organs for settlement to the benthos. Lecithotrophic larvae typically develop from much larger eggs than do planktotrophic larvae. As a consequence, species with lecithotrophic development have substantially lower fecundity relative to reproductive effort. These large eggs ($\approx$300–1500 μm) contain sufficient material to fuel development without larval feeding. In fact, most lecithotrophic larvae do not have a functional gut and are incapable of feeding. The pelagic period (days to weeks) provides the potential for at least some, and often considerable, dispersal from the parental site (Palmer and Strathmann, 1981).

Demersal development involves free-swimming larvae that remain very close to, or on, the benthos (*e.g., Asterina gibbosa,* MacBride, 1896; *Asterina minor,* Komatsu *et al.,* 1979; *Ophidiaster granifer,* Yamaguchi and Lucas, 1984; and perhaps *Odontaster validus,* Pearse and Bosch, 1986). Most species with demersal development have nonfeeding larvae that develop from relatively large eggs. Although the demersal period can be several months long (*e.g., Porania* sp., Bosch, 1989), the offspring are probably not dispersed great distances from the parental site. It is not yet known whether demersal larvae experience reduced predation risk compared with pelagic larvae.

Brooding involves the retention of the young by the parent on the benthos throughout development to the juvenile stage (*e.g., Leptasterias hexactis,* Chia, 1968; *Pteraster militaris,* Kaufman, 1968). Brooding is accomplished in a tremendous variety of ways, especially with respect to the degree of parental care and the location of the young. Offspring can be brooded internally in the stomach, in a specialized brood chamber (*e.g.,* under the supradorsal membrane of pterasterids), in the coelom, or in the gonad or externally under the oral surface or among the spines on the aboral surface. Several characteristics are common to all brooders. First, the lack of a pelagic phase in the life cycle greatly limits the potential for larval dispersal. Second, all brooded offspring rely exclusively on maternally provided nutrition. There is the potential for the transfer of nutritional materials from the parent to the offspring during the period of brooded development in some cases where the young are retained within the body of the parent (*e.g., Patiriella vivipera,* Chia, 1969; Byrne, 1991; *Pteraster militaris,* McClary and Mladenov, 1990; *Asterina pseudoexigua pacifica,* Komatsu *et al.,* 1990). Post-fertilization investment of resources by the parent complicates the picture, but in general, brooders produce eggs as large as, or larger than, related species with pelagic lecithotrophic development (Emlet *et al.,* 1987). Brooding is often correlated with small adult size and hermaphroditism (Strathmann and Strathmann, 1982).

The Problem

A developmental pattern is a complex entity that consists of a set of characters (*e.g.,* development, habitat, and nutrition) that describe the embryonic and larval stages of the life cycle. As discussed in the previous section, the character states of developmental patterns in asteroids are not perfectly correlated. For example, pelagic development can be associated with either feeding or nonfeeding development. Likewise, nonfeeding development can be associated with either indirect or direct development. Any effective classification of developmental patterns must be multifactorial in order to distinguish among the various possible combinations of the character states. There are eight patterns possible, based on three characters each with two states.

In the traditional classification, patterns are named and defined on the basis of the states of one (or at most two) characters. For example, demersal development is defined solely on the basis of habitat state (benthic). Consequently, there are two major problems: ambiguity and inconsistency. Ambiguity arises because only four patterns in the traditional classification attempt to encompass all of the possible combinations of the character states that describe a developmental pattern. Therefore the four traditional patterns do not distinguish unique sets of character states. Demersal development (Table 1) is an ambiguous definition of a developmental pattern because it does not distinguish between different nutritional (*i.e.*, feeding or nonfeeding) or developmental states (direct or indirect development).

The traditional classification scheme is also inconsistent because some patterns, such as planktotrophy, are defined and named on the basis of one character (nutrition), whereas others, such as brooding, are defined on the basis of a different character (habitat). Inconsistency in the classification of developmental patterns also arises from the variable definition of character states (*e.g.*, direct or indirect development; see below) by different authors. The result of ambiguity and inconsistency is that the patterns of development described by the traditional classification cannot be mutually exclusive, and the classification must fail to adequately distinguish the existing patterns.

We think that there is an additional difficulty with the traditional classification. The definitions of developmental patterns emphasize ecological characteristics (habitat and nutrition) with little attention to the morphological nature of development (direct or indirect). As pointed out by Bonar (1978, p. 179), ecological descriptions of development have tended to mask the basic similarity of morphogenesis in many taxa. Conversely, they have also hampered the recognition of fundamental differences in morphogenesis (*e.g.*, *Pteraster tesselatus*, McEdward, 1992; Janies and McEdward, in review). To illustrate these points, we will survey the larval diversity and developmental characteristics in asteroid echinoderms. We will then propose explicit definitions of important terms and outline a multifactor classification scheme for developmental patterns.

Asteroid Larval Types

Starfish have two characteristic larval types: the bipinnaria and the brachiolaria (see Fell, 1967, p.S68). A bipinnarian larva (Fig. 1A) is characterized by the bilateral arrangement of the pre- and post-oral ciliated swimming and feeding bands that are borne on arms (MacBride, 1914, p.464; Kume and Dan, 1968, p.306). Bipinnarian arms are hollow extensions of the body wall; they contain blastocoelic space, but are not supported by calcareous skeletal rods. Although the number and size of bipinnarian arms varies among species, the arms can be identified by their anatomical location using the nomenclature designated by Mortensen (1898, pp: 6–7). The bipinnaria is a feeding larva and it occurs in the life cycle of all asteroids with planktotrophic larval development (*e.g.*, *Asterias forbesi*, *A. vulgaris*, Agassiz, 1877; *Luidia sarsi*, Wilson, 1978; *Patiriella regularis*, Byrne and Barker, 1991). A brachiolarian larva (Fig. 1B) is defined by the presence of specialized attachment structures on the preoral lobe: the brachiolar arms and attachment disk. Brachiolar arms are hollow, but contain extensions of the larval anterior coelom, and are thereby distinguished from bipinnarian arms (Gemmill, 1914; Barker, 1978). Brachiolar arms are used by larvae to test the substratum and provide initial, temporary adhesion during settlement. The adhesive disk secretes cement and provides more permanent attachment for metamorphosis. In asteroids with planktotrophic development, the brachiolarian stage only occurs after the bipinnaria (*e.g.*, *Asterias rubens*, Gemmill, 1914). Although these larvae are given different names, they are not independently evolved types of larvae, but rather sequential developmental stages.

Since the discovery of these asteroid larvae by Sars and Müller, several other larval types have been discovered. Some asteroids (*e.g.*, *Crossaster papposus*, Gemmill, 1920; *Echinaster echinophorus*, Atwood, 1973) develop via a nonfeeding pelagic brachiolarian larva (Fig. 1C). Nonfeeding brachiolarian larvae are morphologically simpler than planktotrophic brachiolarian larvae because they lack the ciliated band feeding structures, bipinnarian arms, and a functional gut. The most conspicuous larval structures that characterize both feeding and nonfeeding brachiolarian larvae are the attachment structures (brachiolar arms and attachment disk) and bilateral symmetry. Some asteroids develop via a benthic brachiolaria that has reduced brachiolar structures. For example, in *Asterina gibbosa*, the brachiolar arms are reduced to nonfunctional bulbs on a simple ciliated preoral lobe, but a functional adhesive disk remains (Fig. 1D) (Ludwig, 1882; MacBride, 1896). More typically, brooded brachiolaria retain well-developed and functional brachiolar arms and adhesive disks (*e.g.*, *Henricia sanguinolenta*, Masterman, 1902; *Leptasterias hexactis*, Osterud, 1918; Chia, 1968; *Henricia* sp., Chia and Walker, 1991; [= variety F, *H. leviuscula*, Fisher, 1911; p.282, according to Strathmann *et al.*, 1988]). Barrel-shaped larvae (Fig. 1E) occur in some species of paxillosids (*e.g.*, *Astropecten latespinosus*, Komatsu, 1975; Komatsu *et al.*, 1988, *Ctenopleura fisheri*, Komatsu, 1982; *Astropecten gisselbrechti*, Komatsu and Nojima, 1985). Barrel-shaped larvae are pelagic lecithotrophic larvae with abbreviated development and simplified morphology. *Pteraster tesselatus* has an unusual type of nonbrachiolarian pelagic lecithotrophic development (Chia, 1966; McEdward, 1992). A similar type of nonbrachio-

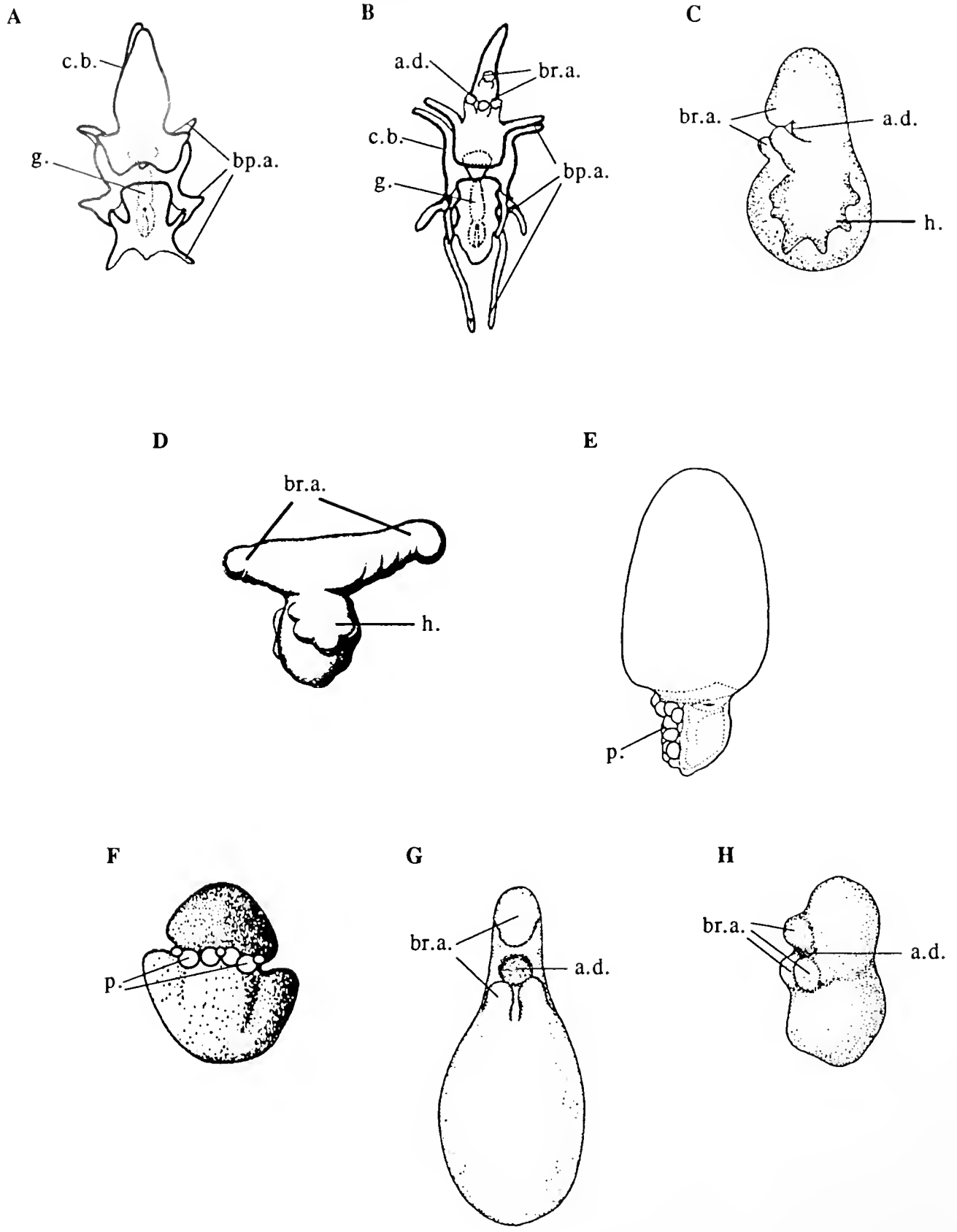
A
c.b.
g.
bp.a.
B
a.d.
br.a.
c.b.
g.
bp.a.
C
br.a.
a.d.
h.
D
br.a.
h.
E
p.
F
p.
G
br.a.
a.d.
H
br.a.
a.d.

larian development also occurs in a brooder (Fig. 1F) (*Pteraster militaris*, Kaufman, 1968).

Appreciation of asteroid developmental diversity has increased over the past 10–15 years with the discovery of new larval types (*e.g.*, barrel-shaped larvae) and new developmental patterns [*e.g.*, demersal development, *Porania* sp., Bosch, 1989 (Fig. 1G); intragonadal ovoviviparity, *Asterina pseudoexigua pacifica*, Komatsu *et al.*, 1990 (Fig. 1H); and viviparity, *Pteraster militaris*, McClary and Mladenov, 1990]. This diversity has been described and classified largely according to the patterns outlined above (*e.g.*, planktotrophy, lecithotrophy, brooding, demersal development). The ambiguity and inconsistency inherent in the traditional classification scheme has hampered attempts to understand the evolutionary changes in development that underlie larval diversity. For example, the lack of correspondence between larval type and the traditional classification of developmental patterns in starfish is shown in Table II; the traditional classification scheme, cannot predict unambiguously the pattern of development, given the type of larva. Clearly the ecological and morphological characters of developmental patterns have evolved independently (*e.g.*, brachiolar attachment structures are often retained in brooded young).

Table II

Relationships between types of asteroid larvae and traditional patterns of development

Larval type	Developmental pattern
Bipinnaria	Planktotrophy
	Demersal development
Brachiolaria	Planktotrophy
	Pelagic lecithotrophy
	Demersal development
	Brooding
Paxillosid barrel-shaped larva	Pelagic lecithotrophy
Pterasterid nonbrachiolaria	Pelagic lecithotrophy
	Brooding
Developmental pattern	**Larval type**
Planktotrophy	Bipinnaria
	Brachiolaria
Pelagic Lecithotrophy	Brachiolaria
	Paxillosid barrel-shaped larva
	Pterasterid nonbrachiolaria
Demersal development	Bipinnaria
	Brachiolaria
Brooding	Brachiolaria
	Pterasterid nonbrachiolaria

Life Cycle Terminology

Many apparently simple terms are used to describe and interpret the diversity of development in asteroids. However, a consensus for the definition these terms does not exist. The problem stems in large part from the different contexts (*i.e.*, ecological or morphological) inherent in considerations of the evolution of marine invertebrate larvae. The discussion of terminology that follows is an attempt to provide a clear conceptual basis for analyzing evolutionary changes in asteroid life cycles. The application of these terms to specific developmental patterns and the resulting multifactor classification is discussed in the next sections.

Embryo

In general, embryos can be defined morphologically as cleavage stages, the blastula, and the gastrula. These are recognizable stages in the development of all animals, and in fact, the blastula and gastrula stages are defining features of the Metazoa (Buss, 1987; Bonner, 1988; Margulis, 1990). Hatching in asteroids occurs at various stages of development (blastula, gastrula, or later) and can therefore define neither the end of the embryonic period nor the beginning of the larval period. In the course of morphogenesis, structures specific to each group of organisms appear and gradually produce a definitive form (larval or juvenile). It is the seamless transition between the onset of morphogenesis and the achievement of a definitive form that makes the distinction between late embryo and early larva, or early juvenile, impossible to identify with precision. For this reason, the term "embryo" is best restricted to the stages of development that are of universal occurrence (cleavage, blastula, and gastrula) and should not be used to refer to the subsequent transitional period.

Larva

In spite of numerous attempts, no one has provided a precise and generally accepted definition of the term

Figure 1. Diagrams of various asteroid larval types. A. Complex feeding, pelagic bipinnaria (unidentified luidiid, *e.g.*, *Luidia foliolata;* modified from Strathmann, 1974, p.324); B. Complex feeding, pelagic brachiolaria (unidentified asteriid, *e.g.*, *Pisaster ochraceus;* modified from Strathmann, 1974, p.324); C. Simple nonfeeding, pelagic brachiolaria (*Solaster endeca*, modified from Hyman, 1955, p.298); D. Simple nonfeeding, benthic brachiolaria (*Asterina gibbosa*, modified from MacBride, 1896, pl. 18); E. Nonfeeding, pelagic barrel-shaped larva (*Ctenopleura fisheri*, modified from Komatsu, 1982, p.202); F. Simple nonfeeding, benthic nonbrachiolarian stage (*Pteraster militaris*, modified from Kaufman, 1968, p.508). G. Simple nonfeeding, benthic brachiolaria (*Porania* sp., modified from Bosch, 1989, p.80); H. Simple nonfeeding, benthic brachiolaria (*Asterina pseudoexigua pacifica*, modified from Komatsu *et al.*, 1990, p.259). Abbreviations: a.d., adhesive disk; bp.a., bipinnarian arm; br.a., brachiolar arm; c.b., ciliated band; g., gut; h., hydrocoel; p., podia.

"larva." We believe that such a definition is impossible for two reasons: (1) the continuous nature of development, and (2) the evolutionary diversification of development. First, "larva" refers to a stage (or series of stages) in a developmental sequence. In asteroids, development does not progress as a sequence of discrete instars but rather involves continuous changes in morphology. Stages cannot be precisely defined, because they do not begin and end with unambiguously identifiable developmental events. The larval form is produced by morphogenetic processes that gradually transform the embryo into a more complex shape. Larval stages transform into juvenile stages during metamorphosis, which can be rapid and drastic or prolonged and gradual. Second, developmental sequences may have been greatly modified (accelerated, retarded, and condensed), and the stages within those sequences may have undergone evolutionary modification. Given the tremendous morphological, ecological, and taxonomic diversity of marine invertebrates, it is not surprising that a single definition fails to be universally applicable.

For evolutionary studies, we maintain that a larva should be defined as an intermediate stage in the life cycle that is produced by post-embryonic morphogenesis and is eliminated by the metamorphic transition to the juvenile; in addition, this intermediate stage must possess transitory structural features that are not developmentally necessary for morphogenesis of the juvenile. Transitory larval features may be specialized for independent existence during development, or be reduced in derived modes of development.

Juvenile

The term "juvenile" has been used in a very broad sense. At one extreme, it refers to the "post-larval" stages, either immediately following abrupt metamorphosis from a definitive larval stage, or at some ill-defined point during a prolonged, gradual metamorphosis. At the other extreme, juveniles are "pre-adults" that have the definitive adult morphology, but are small or at least not sexually mature. For the present discussion, it is more important to establish criteria for defining the earliest juvenile stage. We suggest that a juvenile has attained the adult body plan (symmetry, general body shape), and the major systems are functional (especially locomotion and feeding, but not reproduction). This definition intentionally excludes the transitional period during metamorphosis.

Metamorphosis

This literally means a change in morphology. But as was stated above, the entire developmental process produces continuous changes in form. "Metamorphosis" has often been restricted to cases where there is a drastic and rapid change in morphology. However, it is more useful to consider metamorphosis as the transition from the larval body plan to the juvenile body plan, regardless of the rate or magnitude of the change. Metamorphosis then requires a definitive larval stage in the life cycle, and its occurrence thus defines the indirect pattern of development.

Indirect development

This refers to a pattern of development in which the embryo is followed by intermediate stages with structural features that are not directly involved in the morphogenesis of the juvenile (Fig. 2). These intermediate stages are larvae and by virtue of having a specialized structure and a transitory body plan must undergo a metamorphosis to the juvenile body plan. The construction of larval morphology (*e.g.*, specific organs or overall body symmetry) defines the indirect nature of a developmental sequence. Larval structures might, but need not be functional during development. A brooded larva that does not swim in the water column or settle to the benthos may still possess the structures for swimming and settlement.

Direct development

This refers to a pattern of development wherein the embryonic stages are followed by the morphogenesis of the juvenile, without an intervening larval stage. The idealized life cycles in Figure 2 illustrate the importance of the larval stage in distinguishing between direct and

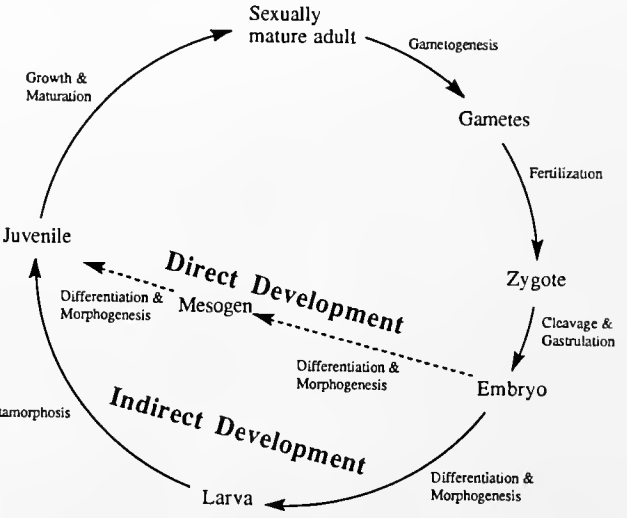

Figure 2. Diagram of an idealized Metazoan life cycle. Small typeface identifies the major life cycle processes (*e.g.*, Differentiation & Morphogenesis); medium-sized typeface identifies the major life cycle stages (*e.g.*, Juvenile); large typeface indicates the two alternative types of development in the life cycle (*e.g.*, Direct Development). See the text sections Life Cycle Terminology, Direct and Indirect Development in Asteroids, and What is a Larva, and What is Not? for definitions and explanations of life cycle features in asteroids.

indirect development. Direct modes of development can involve short, simple ontogenetic sequences or long, complex ones. All that is required for direct development is that larval stages be absent from the life cycle. If larval stages are absent, then metamorphosis does not occur because there is not a definitive morphological stage to be transformed into the juvenile. Thus, direct development, as defined here, is equivalent to "ametamorphic" development (Bonar, 1978). In contrast to indirect development, the juvenile develops progressively (directly) from the embryo, through a series of intermediate stages, all of which are transitional towards the juvenile and without morphogenesis of any larval structures. Since there is not a generally accepted term to apply to these intermediate ontogenetic stages and the term "larva" only refers to a specialized stage in the indirect pattern of development, it seems useful to introduce the term "mesogen" (≈middle stage) to refer to the developmental stages that occur between the embryo and the juvenile in the direct pattern of development. This recognizes that even with direct development there can be a prolonged period of development before the definitive juvenile stage is reached. This term is especially useful where stages of direct development are free-living (*e.g., Pteraster tesselatus*, McEdward, 1992).

Direct and Indirect Development in Asteroids

The distinction between direct and indirect development has been widely used to characterize asteroid developmental patterns. This is potentially useful for the study of evolutionary changes in development because it involves only morphological criteria, rather than ecological ones. However, inconsistent application of these terms (Table III) has led to considerable confusion.

Originally, development via a larval stage was termed indirect and development without a larval stage was described as direct. Habitat and nutrition were not considered relevant to the distinction. Masterman described the brooded development of *Henricia sanguinolenta* as ". . . enabling development to proceed independently of the capture or acquirement of food. But although this is the case, there is to be discerned no essential difference in the course of development which would justify the application of a term like 'direct' development. . . . The presence of lecithal nutrition, like that of haemal nutrition in viviparous forms, no doubt accounts for certain marked adaptations not unlike those characteristics of parasites, such as loss of alimentation, sensory and motor organs, but there can be little question that the larval 'entity' is evident both in space and time in these demersal forms equally with the pelagic" (Masterman, 1902, p.384). *Henricia sanguinolenta* has a brachiolarian stage that remains within a brood protected by the parent during development. However, because it possesses purely larval structures (brachiolar arms, bilateral symmetry), development is indirect.

Table III

Varying application of the terms direct and indirect development in asteroids

Reference	Indirect	Direct
Chia (1968)	Feeding, pelagic development	Nonfeeding development
Mileikovsky (1974)	Pelagic or demersal development	Benthic development
Komatsu (1975)	Bipinnaria + brachiolaria	Brachiolaria only
Oguro *et al.* (1988)	Bipinnaria + brachiolaria[1]	Brachiolaria only[1]
McEdward and Janies	Possesses larval structures	Lacks larval structures

[1] The paxillosids, which have a bipinnaria only or a barrel-shaped larva, were considered as having neither direct nor indirect development, but were placed in a third category, nonbrachiolarian development.

Vestigial larval structures or larval bilateral symmetry are sufficient to characterize asteroid development as indirect. Fell (1945, p.88) stated that "We have now reached the critical point in development at which the forms with direct development diverge from the forms with a larval stage or with a vestige of a larva. Whereas the former proceed to adopt radial symmetry immediately after the conclusion of gastrulation, the latter begin to assume bilateral symmetry, and retain it for a greater or lesser period till it is finally obliterated by radial symmetry." Fell's interest was in the evolution of echinoderm development (especially ophiuroids) and he used an exclusively morphological criterion for direct development.

A significant change occurred when Chia (1968, p.363; see also pp: 359–361) introduced an ecological criterion for indirect development: "Larval nutrition was used as a major criteria to define the types of development. Animals undergoing indirect development are those who have planktotrophic larva resulting from small and less yolky eggs, while animals undergoing direct development are those who have lecithotrophic larva resulting from large and yolky eggs." This change probably reflected two things: (1) an attempt to distinguish between the complex larval morphology characteristic of feeding development and the simpler larval morphology of nonfeeding development; and (2) an attempt to distinguish major patterns of development on the basis of important ecological differences. Whatever the intention, the effect was to introduce considerable confusion into the dichotomy between direct and indirect development. Mileikovsky (1971, 1974, p.172, 175) proposed an ecologically based scheme for classification of developmental patterns in marine invertebrates. He listed four major patterns: pelagic development, demersal development, direct development, and viviparity, and defined direct development solely on the basis of habitat: "Direct development. Larva develops

within the egg-spawn until hatching into a fully formed juvenile bottom form. Therefore, larval development of the species is completely under the protection of the egg-envelopes and the spawn-substances. (Pelagic larval phase is omitted)." Mileikovsky (1974, p.172). In these examples, different and inconsistent sets of criteria were used to define these patterns, thus effectively removing any meaningful morphological interpretation of direct development.

Indirect development is usually restricted to cases of feeding larval development (*e.g.*, Wray and Raff, 1991, p.45). This is particularly true for asteroids (Komatsu, 1975; Oguro *et al.*, 1976, 1988). "Development having brachiolaria only, irrespective of whether it is pelagic or benthic, is called the direct type. Development which passes through both the bipinnaria and the brachiolaria is called the indirect type." (Oguro *et al.*, 1976, p.571).

Differing criteria for direct and indirect development create a problem because these patterns of development are intimately tied to the definition of a larva. Does this mean that nonfeeding or benthic larvae are not really larvae after all? Chia argued that ". . . it is indirect development when there is a larval stage and it is direct development when a larval stage is lacking. This definition seems clear and simple but in practice there has been much confusion. The main problem, as I see it, lies in differences of defining what is a larva and much confusion would be reduced if the term 'larva' is clarified" (Chia, 1974, p.121).

What is a Larva, and What is Not?

Chia (1974) proposed a definition for the term "larva." "Larva is a developmental stage, occupying the period from post embryonic stage to metamorphosis, and it differs from the adult in morphology, nutrition, or habitat. In this definition, post embryonic designates the time after emerging (hatching) from the primary egg membrane; prior to that it is considered as embryonic stage" (Chia, 1974, p.122). Chia explicitly rejected the idea that a larva had to possess purely "larval" structures. This was necessary to encompass the ecological sense of a larva as a dispersive propagule. In this regard, Chia was following Vannucci (1959), who had reviewed the various definitions of the term larva that had been used previously and had rejected the common definition of a larva as a developmental stage that had transitory or larval organs. Vannucci's intention was "to use the word larva in a very broad sense, and will thus include many organisms that would not be considered a larva by authors giving to this word a restricted meaning" (Vannucci, 1959, p.7). He cited as examples of organisms that had larvae only by the ecological criterion, the planula, actinula, and ephyrae of cnidarians. Vannucci (1959) defined larva as "a developmental stage, as a rule sexually immature, which may or may not be endowed with special larval organs and which always differs sensibly from the adult" (p.9). The rationale for this broad definition of the term larva was a practical one: the preparation of a comprehensive catalogue of marine larvae (*i.e.*, pelagic dispersive propagules). At the time that it was proposed, the broad, ecological definition of a larva was recognized as "a point of dispute" (Vannucci, 1959, p.7). Chia (1974) improved on Vannucci's definition by making the language less ambiguous. He maintained the ecological sense of a larva by making morphology, nutrition, and habitat alternative criteria by which to define a larva. The advantage of this broader definition is that it recognizes the important ecological roles played by many "larvae" (*i.e.*, feeding and dispersal). This was consistent with the current emphasis on larval ecology and the adaptive significance of developmental patterns in marine benthic invertebrates.

The disadvantage of such an expanded definition of a larva is that by allowing three alternative characters to define a larva (morphology or nutrition or habitat) the definition becomes ambiguous. Under this broad definition, nutritional type or habitat could suffice to define a larva (indirect development), without regard to the nature of morphological development. In addition, numerous applications of the ecological characterization of a larva have involved logical errors, in that negation of only one of the criteria (morphology *or* nutrition *or* habitat), rather than all of the criteria (morphology *and* nutrition *and* habitat), have been used to designate development as nonlarval (*i.e.*, direct).

The problem is seen clearly with regard to brooded development in which young stages can be larval by morphological and developmental criteria (indirect development) but do not live in the plankton and thus do not provide larval dispersal (*e.g., Leptasterias hexactis,* Chia, 1968; *Asterina pseudoexigua pacifica,* Komatsu *et al.*, 1990; *Henricia* sp., Chia and Walker, 1991). On the other hand, there are pelagic propagules that undergo direct development and thus qualify as larvae only in the sense that they are dispersed by water movements (*e.g., Pteraster tesselatus,* McEdward, 1992).

Of the four ecological patterns of development described above (Table 1), which necessarily have or do not have larval stages and which can potentially have larvae? Planktotrophic development must include a larval stage in order to possess the structures necessary for food particle capture. In the other four patterns, indirect or direct development are evolutionary options. Pelagic lecithotrophy generally involves larval stages with specialized swimming or settlement structures, but direct development could occur in the plankton via a pelagic mesogen. Demersal development could involve feeding or nonfeeding larvae, as well as direct-developing mesogens. Benthic brooding often involves well-developed larval stages, some brooded young have simplified larval features, but brooding rarely

proceeds by strictly direct development. In numerous cases, brooding involves stages with larval structures (sometimes reduced but often functional). This makes the classification of developmental stages as larvae or mesogens difficult; however it is important to realize that there cannot be an absolute distinction between larvae and mesogens, because the evolution from indirect to direct development usually involves the successive reduction and elimination of larval structures. The closest approximation to truly direct development in the asteroids is in the highly derived pterasterids which lack all larval structures, as well as bilateral symmetry, and are thus fundamentally different from all other starfish (McEdward, 1992; McEdward, in prep.; Janies and McEdward, in review).

To answer the question raised in the heading to this section, only a larva (in the strictest morphological and developmental sense) is a larva, and everything else—including a mesogen—is not.

Classification of Developmental Patterns of Asteroids

We propose a multifactor classification scheme for asteroid developmental patterns (Table IV). There are three completely independent characters by which developmental patterns are classified. First, the morphological nature of development can be described using the distinction between indirect and direct development, in the strict sense outlined above. In our scheme, all indirect types have larvae and all direct types do not, regardless of habitat or mode of nutrition during development. Second, developmental patterns can be distinguished by habitat, using the pelagic or benthic distinction. Third, the distinction between feeding and nonfeeding development provides information about nutrition. All three characters must be used to unambiguously describe or classify a developmental pattern.

Eight different developmental patterns can potentially be described when three characters exist, each with two alternative states. Of these eight potential patterns, only six are known to occur in asteroids (Table IV). Indirect development via pelagic feeding larvae is common in asteroids, and it can involve either bipinnarian and brachiolarian stages (*e.g., Asterias rubens,* Gemmill, 1914) or only bipinnarian stages (*e.g., Astropecten scoparius,* Oguro *et al.,* 1976). Indirect development via pelagic nonfeeding larvae can involve a simplified brachiolaria or the barrel-shaped larva. Indirect development on the benthos with a feeding larva possibly occurs in the Antarctic asteroid *Odontaster validus,* but this is uncertain (Pearse and Bosch, 1986). Indirect development via a benthic nonfeeding larva is common among brooding asteroids (*e.g., Ctenodiscus australis,* Lieberkind, 1926; *Henricia sanguinolenta,* Masterman, 1902; *Leptasterias hexactis,* Chia, 1968). Strict direct development is extremely rare in asteroids. Pelagic nonfeeding direct development occurs only in *Pteraster tesselatus* (McEdward, 1992). Benthic nonfeeding direct development has not been reported, but we infer it for the brooding pterasterid, *Pteraster militaris* (Kaufman, 1968; McClary and Mladenov, 1990), based on similarities with *P. tesselatus* (McEdward, in prep.). Construction of the proposed multifactor classification scheme was stimulated, in large part, by the need to clarify the developmental differences between pterasterids and other asteroids with nonfeeding patterns of development. Direct development involving feeding has not been reported for asteroids. Given the predatory nature of most juvenile and adult asteroids, it is unlikely that transitional developmental stages (meso-

Table IV

Multifactor classification of asteroid development patterns

Developmental pattern				
Characters				
Type	Habitat	Nutrition	Developmental stage and morphology	Asteroid examples[1]
Indirect	Pelagic	Feeding	Complex bipinnarian + brachiolarian larva	*Asterias rubens*
			Complex bipinnarian larva	*Astropecten scoparius*
Indirect	Pelagic	Nonfeeding	Simple brachiolarian larva	*Solaster endeca*
			Simple barrel-shaped larva	*Astropecten gisselbrechti*
Indirect	Benthic	Feeding	Complex bipinnarian + brachiolarian larva	*Odontaster validus?*
Indirect	Benthic	Nonfeeding	Simple brachiolarian larva	*Lepasterias hexactis*
				Asterina minor
Direct	Pelagic	Feeding	—	none known
Direct	Pelagic	Nonfeeding	Simple nonbrachiolarian mesogen	*Pteraster tesselatus*
Direct	Benthic	Feeding	—	none known
Direct	Benthic	Nonfeeding	Simple nonbrachiolarian mesogen	*Pteraster militaris*

[1] The examples provide a cross reference to those cited in the body of the paper. These examples are not exhaustive but were chosen because the references provide good documentation of the various characters used.

gens) could acquire particulate food without the use of specialized (*i.e.*, larval) feeding structures. Direct development, with feeding seems to be an unlikely evolutionary option for starfish.

Evolution of Developmental Patterns in Asteroids

Although indirect development with a complex, feeding, pelagic larva is considered the ancestral condition for echinoderms (Jägersten, 1972; Strathmann, 1978), there has been considerable debate over the nature of the ancestral asteroid life cycle (Bather 1921a, b, 1923; MacBride, 1921, 1923a, b; Mortensen, 1922, 1923). Until recently, it was widely accepted that indirect development via a pelagic feeding bipinnaria with complex larval morphology, but without a brachiolaria stage, characterized the original developmental pattern of asteroids (Fell, 1967, p.S71; Oguro *et al.*, 1988). This argument was first developed by Mortensen (1921, p.219–220), and it was largely based on the absence of the brachiolarian stage in the paxillosids (esp. Luidiidae and Astropectinidae). Paxillosids were considered to be the most primitive of the starfish orders, so the lack of a brachiolarian larval stage was interpreted as the original condition for the asteroids (Oguro *et al.*, 1988). The brachiolaria was thought to have evolved later, at about the same time as the appearance of suckered podia (Fell, 1967, p.S71). The importance of the taxonomic position of the paxillosids in this argument was clearly pointed out by Mortensen (1923, p.323): "I have no direct interest in maintaining the Brachiolaria to be a secondarily specialized larval type. If conclusive proof is given that the Brachiolaria is the primitive, the Astropectinid-larva the specialized form, I shall not hesitate to drop my present view. But I must maintain that this view is not unjustified by the facts so far known." In contrast, MacBride (1921, 1923b) argued that paxillosids were specialized, not primitive, and he explained the lack of a brachiolarian larva as an adaptation for life on soft substrata. This view was strengthened by the discovery that some paxillosids have suckered podia for a short period immediately after metamorphosis (*Astropecten latespinosus*, Komatsu, 1975, p.53; *Astropecten scoparius*, Oguro *et al.*, 1976, p.567). The recent analyses of paxillosid biology by Blake (1987, 1988) have provided convincing support to the view that paxillosids are highly derived asteroids with body form, digestive, podial, as well as developmental, specializations for life in sandy and muddy habitats. We accept this view and consider the original asteroid life cycle to have consisted of pelagic feeding indirect development via a complex bipinnaria and a complex brachiolaria (Fig. 1A, B, 3, 4).

All of the other developmental patterns that occur in asteroids (Table IV) can be derived by means of six different evolutionary transitions (Fig. 3). Loss of larval feeding (transition A) eliminated the bipinnaria from the life cycle and resulted in a pelagic, nonfeeding brachiolaria. Associated with the loss of larval feeding structures, such as ciliated bands, bipinnarian arms, and a functional gut, the morphology of the brachiolaria was greatly simplified (Fig. 1C). However, the larva retained bilateral symmetry, brachiolar arms, and many features of internal development (*e.g.*, coelom formation) characteristic of the more complex bipinnarian and brachiolarian forms. This has occurred at least 6–9 times in the asteroids (Strathmann, 1978). Indirect development via a simple brachiolarian larva is known to occur in four orders: Forcipulatida, Valvatida, Spinulosida, and Velatida (Fig. 4). From this pelagic, nonfeeding pattern of development, a second evolutionary change (transition B, Fig. 3) eliminated the pelagic phase of development and resulted in benthic development via brooding, or a free-living demersal larva. This resulted in an indirect pattern of development with a nonfeeding brachiolarian larva and is known from the orders Forcipulatida, Valvatida, Spinulosida, and Velatida (Fig. 4).

Direct development, in the strict sense that we use the term, is known among asteroids only in the family Pterasteridae. We postulate that direct development evolved in a lineage of brooders within the order Velatida (Fig. 4). Brooding is rare in solasterids, but is presumed to be the predominant mode of development in the other velatid families: Korethrasteridae, Caymanostellidae, Myxasteridae, and Pterasteridae. Unfortunately, because these are mostly deep-sea organisms, very little is known about their development (Clark and Downey, 1992). Larval attachment structures were likely lost in the pterasterids as the lineage became specialized in the deep-sea and evolved brooded young. Direct development was probably the result of selection for general developmental efficiency (*i.e.*, the discontinuance of vestigial larval programs) during a long history of brooding. Extreme simplification of development (transition C, Fig. 3), eliminated all of the larval features (*e.g.*, brachiolar arms, bilateral symmetry) from the life cycle and produced an ontogenetic sequence leading directly from the embryo to the juvenile (Fig. 2). Intermediate developmental stages represent mesogens (Fig. 1F) that are brooded by the parent. The developmental pattern is benthic, nonfeeding, and direct (Table IV) and it is known for only a single species, *Pteraster militaris* (Kaufman, 1968; McEdward, in prep.) (Fig. 4). A subsequent modification of this pattern of direct development involved the re-evolution of a pelagic period during development (transition D, Fig. 3). This produced the unique type of pelagic, nonfeeding "larva" of *Pteraster tesselatus* (McEdward, 1992). This pelagic developmental stage is a mesogen (*not* a larva) and the pattern of development is direct, pelagic, and nonfeeding (Table IV). The pelagic mesogen of *Pteraster tesselatus* is fundamentally different from the pelagic, nonfeeding brachiolarian larva of other starfish. Important differences include: absence of bra-

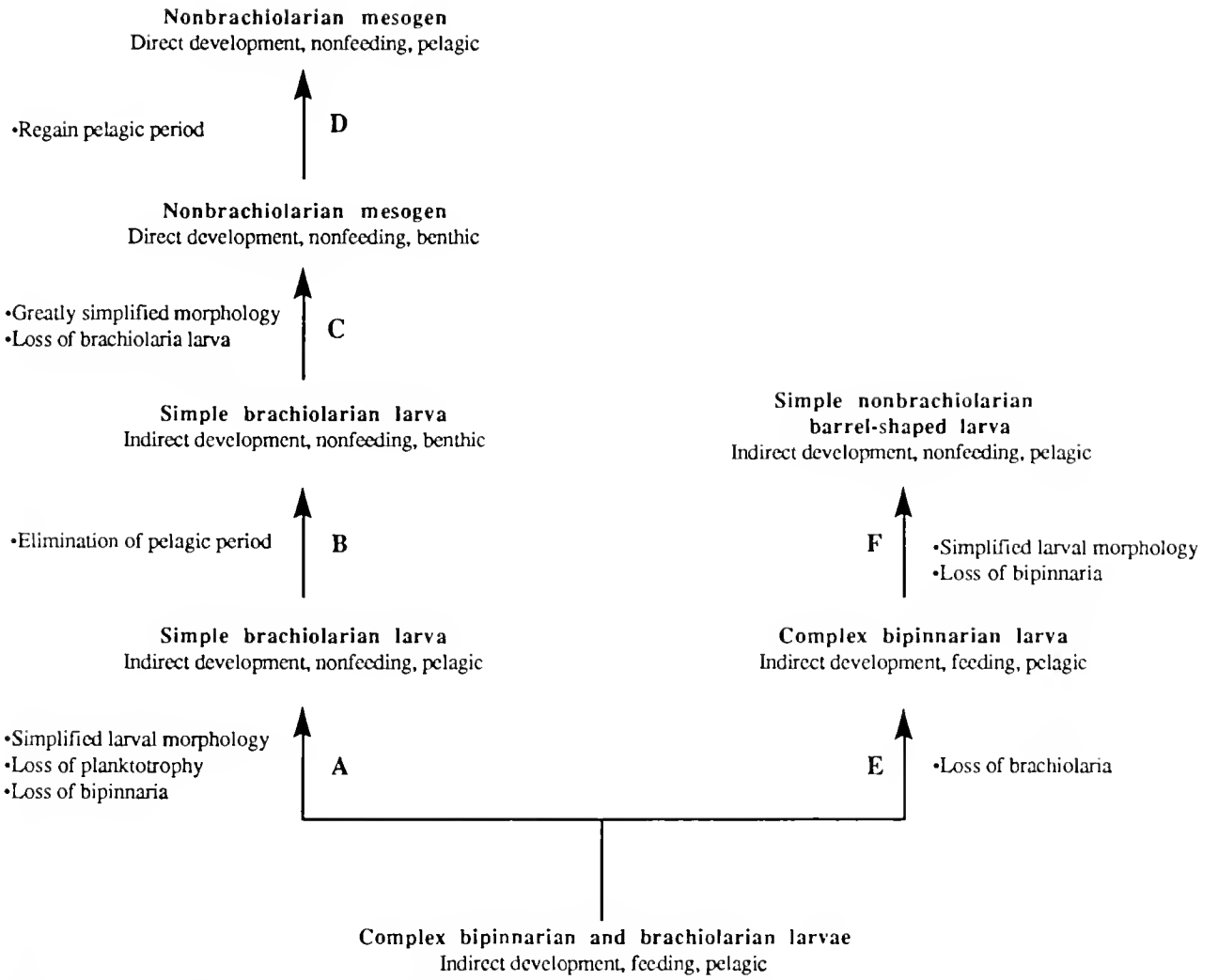

Figure 3. Postulated sequences of evolutionary transitions in asteroid life cycles that account for the diversity of larval types and developmental patterns. Bold typeface identifies the larval types (*e.g.*, Complex bipinnarian larva); associated plain typeface indicates the developmental pattern (*e.g.*, Indirect development, feeding, pelagic; see Table IV); bulleted lists and bold typeface uppercase letters identify the changes in development associated with each evolutionary transition (*e.g.*, E; •Loss of brachiolaria).

chiolar arms and attachment disk, use of podia for attachment at settlement, a novel pattern of coelom formation and water-vascular morphogenesis, radial rather than bilateral symmetry, parallel embryonic, mesogen, and adult axes of symmetry, and a transverse orientation of the juvenile disk (Janies and McEdward, in review; McEdward, 1992). Note that our interpretation of the development of *P. tesselatus* is radically different from the currently accepted view. Chia (1966, pp.507–508) originally described this species as developing via a nonfeeding bipinnaria. Others have interpreted the pelagic stage as a modified lecithotrophic brachiolaria (Fell, 1967, p.S71; Oguro *et al.*, 1988, p.242). Detailed evidence supporting our interpretation will be presented elsewhere (McEdward, in prep.; Janies and McEdward, in review).

An entirely unrelated sequence of evolutionary changes has occurred in the paxillosids. All paxillosids lack the brachiolaria (Fig. 4). The pattern of development involving only a complex feeding bipinnarian larva (Table IV) evolved from the ancestral asteroid life cycle by loss of the brachiolarian stage (transition E, Fig. 3). This interpretation is different from that of Oguro *et al.* (1988, p.243) who claim that "the bipinnaria is the original or primitive type of sea-star larva." This view that the ancestral asteroid life cycle lacked the brachiolaria stage is inconsistent with the recent analysis of the paxillosids as a highly derived group of asteroids (see above). Loss of the brachiolaria was undoubtedly associated with specialization for life on soft substrata by the paxillosids; adhesive structures would not provide anchorage for settle-

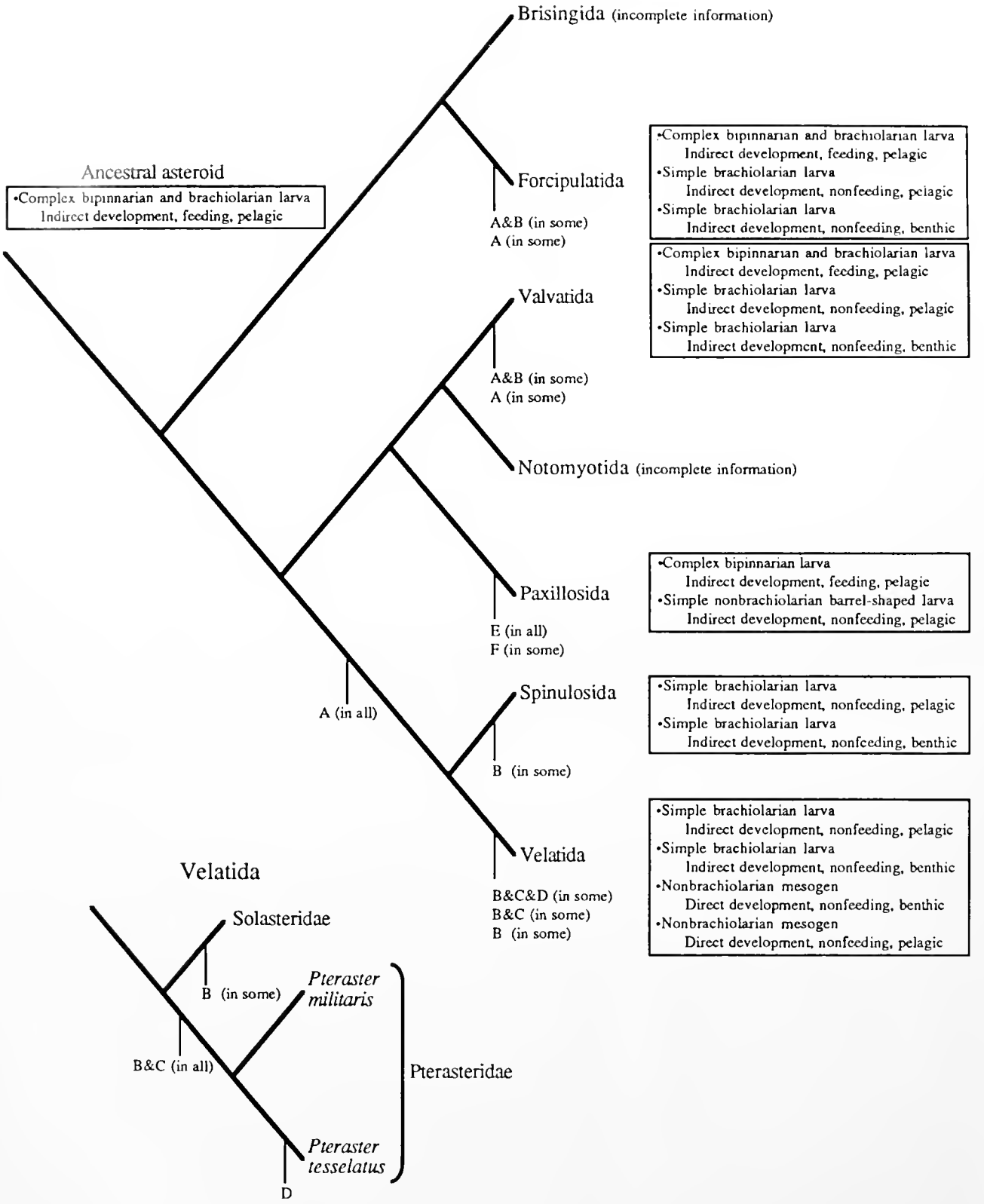

Figure 4. Phylogenetic distribution of larval types and developmental patterns among asteroid orders (large cladogram) and within selected groups of velatids (small cladogram). Phylogenetic relationships are based on Blake (1987). Boxed text lists the different larval types and developmental patterns for each clade (*e.g.*, •Complex bipinnarian and brachiolarian larva; Indirect development, feeding, pelagic; see Table IV). See text for examples and references. Uppercase letters on the branches of the cladograms indicate probable occurrences of evolutionary transitions that can account for the distribution of larval types and developmental patterns (*e.g.*, A & B; see Fig. 3).

ment on mud or sand. Evolutionary loss of larval feeding and the resulting morphological simplification (transition F, Fig. 3) produced the barrel-shaped larva (Fig. 1G). This is the only type of nonfeeding development known in the paxillosids (Fig. 4). The barrel-shaped larva is clearly modified from the bipinnaria (Komatsu *et al.*, 1988).

Summary

Explicit definitions of life cycle terminology and our multifactor classification scheme for developmental patterns help focus attention on the morphological features of development. We believe that this provides a clearer conceptual basis for the analysis of asteroid life cycle evolution. Our hypothesis for the evolutionary transitions in development can account for the diversity of larval forms and developmental patterns in starfish. More importantly, we hope that they stimulate further exploration, analysis, and discussion of the evolution of asteroid development.

Acknowledgments

We are grateful for the assistance of M. Strathmann and many colleagues at the North American Echinoderm Conference and the Chris Reed Memorial Symposium who discussed the ideas presented in this paper with us. M. Greenberg, R. Strathmann, M. Strathmann, J. Herrera, M. Allard, S. McWeeney, and several anonymous reviewers helped improve the manuscript. This work was supported by grant OCE-9115549 from the National Science Foundation to L. R. McEdward.

Literature Cited

Agassiz, A. 1877. Embryology of the starfish. *Mem. Mus. Comp. Zool.* **5:** 1–83.

Atwood, D. G. 1973. Larval development of the asteroid, *Echinaster echinophorus*. *Biol. Bull.* **144:** 1–11.

Barker, M. F. 1978. Structure of the organs of attachment of brachiolaria larvae of *Stichaster australis* (Verril) and *Coscinasterias calamaria* (Gray) (Echinodermata: Asteriodea). *J. Exp. Mar. Biol. Ecol.* **33:** 1–36.

Bather, F. A. 1921a. Echinoderm larvae and their bearing on classification. *Nature* **108:** 459–460.

Bather, F. A. 1921b. Echinoderm larvae and their bearing on classification. *Nature* **108:** 530.

Bather, F. A. 1923. Echinoderm larvae and their bearing on classification. *Nature* **111:** 397.

Birkeland, C., F.-S. Chia, and R. R. Strathmann. 1971. Development, substratum selection, delay of metamorphosis and growth in the seastar, *Mediaster aequalis* Stimpson. *Biol. Bull.* **141:** 99–108.

Blake, D. B. 1987. A classification and phylogeny of post-Palaeozoic sea stars (Asteroidea: Echinodermata). *J. Nat. Hist.* **21:** 481–528.

Blake, D. B. 1988. Paxillosidans are not primitive asteroids: a hypothesis based on functional considerations. Pp. 309–314 in *Echinoderm Biology*, R. D. Burke, P. V. Mladenov, P. Lambert, and R. L. Parsley, eds. A. A. Balkema, Rotterdam.

Bonar, D. B. 1978. Morphogenesis at metamorphosis in opisthobranch molluscs. Pp. 177–196 in *Settlement and Metamorphosis of Marine Invertebrate Larvae*, F.-S. Chia and M. E. Rice eds. Elsevier-North Holland, Amsterdam.

Bonner, J. T. 1988. *The Evolution of Complexity.* Princeton University Press, Princeton.

Bosch, I. 1989. Contrasting modes of reproduction in two Antarctic asteroids of the genus *Porania*, with a description of unusual feeding and non-feeding larval types. *Biol. Bull.* **177:** 77–82.

Buss, L. W. 1987. *The Evolution of Individuality.* Princeton University Press, Princeton.

Byrne, M. 1991. Developmental diversity in the starfish genus *Patiriella* (Asteroidea: Asterinidae). Pp. 499–508 in *Biology of Echinodermata*, T. Yanagisawa, I. Yasumasu, C. Oguro, N. Suzuki, and T. Motokawa eds. A. A. Balkema, Rotterdam.

Byrne, M., and M. F. Barker. 1991. Embryogenesis and larval development of the asteroid *Patiriella regularis* viewed by light and scanning electron microscopy. *Biol. Bull.* **180:** 332–345.

Chia, F.-S. 1966. Development of a deep-sea cusion star, *Pteraster tesselatus*. *Proc. Cal. Acad. Sci.* **34:** 505–510.

Chia, F.-S. 1968. The embyrology of a brooding starfish, *Leptasterias hexactis* (Stimpson). *Acta Zool.* **49:** 321–364.

Chia, F.-S. 1969. Reproductive biology of an intraovarian brooding starfish, *Patiriella vivipera* Dartnall. *Am. Zool.* **16:** 181.

Chia, F.-S. 1974. Classification and adaptive significance of developmental patterns in marine invertebrates. *Thalassia Jugoslav.* **10:** 121–130.

Chia, F.-S., and C. W. Walker. 1991. Echinodermata: Asteroidea. Pp. 301–353 in *Reproduction of Marine Invertebrates*, Vol. VI, *Echinoderms and Lophophorates*, A. C. Giese, J. S. Pearse, and V. B. Pearse eds. Boxwood Press, Pacific Grove, CA.

Clark, A. M., and M. E. Downey. 1992. *Starfishes of the Atlantic.* Chapman and Hall, New York.

Emlet, R. B., L. R. McEdward, and R. R. Strathmann. 1987. Echinoderm larval ecology viewed from the egg. Pp. 55–136 in *Echinoderm Studies*, M. Jangoux, and J. M. Lawrence, eds. A. A. Balkema, Rotterdam.

Fell, H. B. 1945. A revision of the current theory of echinoderm embryology. *Trans. R. Soc. N. Z.* **75:** 73–101.

Fell, H. B. 1967. Echinoderm ontogeny. Pp. 60–85 in *Treatise on Invertebrate Paleontology, Part S, Echinodermata*, R. C. Moore, ed. GSA and University of Kansas Press, Lawrence.

Fisher, W. K. 1911. Asteroidea of the North Pacific and adjacent waters. *U. S. Natl. Mus. Bull.* **76:** 1–405.

Gemmill, J. F. 1912. The development of the starfish *Solaster endeca* Forbes. *Trans. Zool. Soc. Lond.* **20:** 1–71.

Gemmill, J. F. 1914. The development and certain points in the adult structure of the starfish *Asterias rubens*. L. *Phil. Trans. R. Soc. Lond.* **205B:** 213–294.

Gemmill, J. F. 1915. The larva of the starfish *Porania pulvillus* (O.F.M.). *Q. J. Microsc. Sci.* **61:** 27–50.

Gemmill, J. F. 1920. The development of the starfish *Crossaster papposus*, Müller and Troschel. *Q. J. Microsc. Sci.* **64:** 155–190.

Grahme, J., and G. M. Branch. 1985. Reproductive patterns of marine invertebrates. *Oceanog. Mar. Biol. Ann. Rev.* **23:** 373–398.

Hörstadius, S. 1939. Uber die Entwicklung von *Astropecten aranciacus*. *L. Pubbl. Staz. Zool. Napoli.* **17:** 221–312.

Hyman, L. H. 1955. *The Invertebrates.* Vol. IV. *Echinodermata.* McGraw-Hill, NY.

Jablonski, D., and R. A. Lutz. 1983. Larval ecology of marine benthic invertebrates: paleobiological implications. *Biol. Rev.* **58:** 21–89.

Jägersten, G. 1972. *The Evolution of the Metazoan Life Cycle, A Comprehensive Theory.* Academic Press, London and New York.

Kaufman, Z. S. 1968. The postembryonic period of development of some White Sea starfish. *Dolkady Biol. Sci.* **181:** 507–510.

Komatsu, M. 1975. On the development of the sea-star, *Astropecten latespinosus* Meissner. *Biol. Bull.* **148:** 49–59.

Komatsu, M. 1982. Development of the sea-star *Ctenopleura fisheri*. *Mar. Biol.* **66:** 199–205.

Komatsu, M., and S. Nojima. 1985. Development of the seastar, *Astropecten gisselbrechti* Doderlein. *Pac. Sci.* **39:** 274–282.

Komatsu, M., M. Murase, and C. Oguro. 1988. Morphology of the barrel-shaped larva of the sea-star, *Astropecten latespinosus*. Pp. 267–272 in *Echinoderm Biology*, R. D. Burke, P. V. Mladenov, P. Lambert, and R. L. Parsley, eds. A. A. Balkema, Rotterdam.

Komatsu, M., Y. T. Kano, H. Yoshizawa, S. Akabane, and C. Oguro. 1979. Reproduction and development of the hermaphroditic sea-star, *Asterina minor* Hayashi. *Biol. Bull.* **157:** 258–274.

Komatsu, M., Y. T. Kano, and C. Oguro. 1990. Development of a true ovoviviparous sea star, *Asterina pseudoexigua pacifica* Hayashi. *Biol. Bull.* **179:** 254–263.

Kume, M., and K. Dan. 1968. *Invertebrate Embrology*. National Technical Information Services, Springfield, VA.

Lieberkind, I. 1926. *Ctenodiscus australis* Lütken. A brood-protection asteroid. *Vid. Medd. Dansk. Hist. Foren.* **82:** 184–196.

Ludwig, H. 1882. Entwicklungsgeschichte der Asterina gibbosa Forbes. *Zeitschrift Zool.* **37:** 1–98.

MacBride, E. W. 1896. The development of *Asterina gibbosa*. *Q. J. Microsc. Sci.* **38:** 339–411.

MacBride, E. W. 1914. *Textbook of Embryology, Vol. I, Invertebrata*. MacMillan and Co, London.

MacBride, E. W. 1921. Echinoderm larvae and their bearing on classification. *Nature* **108:** 529–530.

MacBride, E. W. 1923a. Echinoderm larvae and their bearing on classification. *Nature* **111:** 47.

MacBride, E. W. 1923b. Echinoderm larvae and their bearing on classification. *Nature* **111:** 323–324.

Margulis, L. 1990. Kingdom Animalia: the zoological malaise from a microbial perspective. *Am. Zool.* **30:** 861–875.

Masterman, A. T. 1902. The early development of *Cribrella oculata* (Forbes) with remarks on echinoderm development. *Trans. R. Soc. Edin.* **40:** 373–418.

McClary, D. J., and P. V. Mladenov. 1990. Brooding biololgy of the sea star *Pteraster militaris* (O. F. Müller): energetic and histological evidence for nutrient translocation to brooded juveniles. *J. Exp. Mar. Biol. Ecol.* **142:** 183–199.

McEdward, L. R. 1992. Morphology and development of a unique type of pelagic larva in the starfish *Pteraster tesselatus* (Echinodermata; Asteroidea). *Biol. Bull.* **182:** 177–187.

Mileikovsky, S. A. 1971. Types of larval development in marine bottom invertebrates, their distribution and ecological significance: a re-evaluation. *Mar. Biol.* **10:** 193–213.

Mileikovsky, S. A. 1974. Types of larval development in marine bottom invertebrates: an integrated ecological scheme. *Thalassia Jugoslav.* **10:** 171–179.

Mortensen, T. 1898. Die echinodermenlarven der plankton-expedition. *Ergebnisse der Plankton-Expedition der Humbolt-Stiftung*. Bd. II. J. Verlag von Lipsius and Tischer, Kiel and Leipzig.

Mortensen, T. 1921. *Studies on the Development and Larval Forms of Echinoderms*. G. E. C. Gad, Copenhagen.

Mortensen, T. 1922. Echinoderm larvae and their bearing on classification. *Nature* **110:** 806–807.

Mortensen, T. 1923. Echinoderm larvae and their bearing on classification. *Nature* **111:** 322–323.

Oguro, C., M. Komatsu, and Y. Kano. 1976. Development and metamorphosis of the sea star *Astropecten scoparius* Valenciennes. *Biol. Bull.* **151:** 560–573.

Oguro, C., M. Komatsu, and Y. Kano. 1988. Significance of the non-brachiolarian type of development in sea stars. Pp. 241–246 in *Echinoderm Biology*, R. D. Burke, P. V. Mladenov, P. Lambert, and R. L. Parsley, eds. A. A. Balkema, Rotterdam.

Osterud, H. L. 1918. Preliminary observations on the development of *Leptasterias hexactis*. *Publ. Puget Sound Biol. Sta.* **2:** 1–15.

Palmer, A. R., and R. R. Strathmann. 1981. Scale of dispersal in varying environments and its implications for life histories of marine invertebrates. *Oecologia* **48:** 308–318.

Pearse, J. S., and I. Bosch. 1986. Are the feeding larvae of the commonest antarctic asteroid really demersal? *Bull. Mar. Sci.* **39:** 477–484.

Strathmann, M. F. 1987. *Reproduction and Development of the Marine Invertebrates of the Northern Pacific Coast*. University of Washington Press, Seattle.

Strathmann, R. R. 1974. Introduction to function and adaptation in Echinoderm larvae. *Thalassia Jugoslav.* **10:** 321–339.

Strathmann, R. R. 1978. The evolution and loss of feeding larval stages of marine invertebrates. *Evolution* **32:** 894–906.

Strathmann, R. R., and M. F. Strathmann. 1982. The relationship between adult size and brooding in marine invertebrates. *Am. Nat.* **119:** 91–101.

Strathmann, M. F., R. R. Strathmann, and D. J. Eernisse. 1988. A new species of *Henricia*, Gray 1840, in the Northeastern Pacific. P. 813 in *Echinoderm Biology*, R. D. Burke, P. V. Mladenov, P. Lambert, and R. L. Parsley, eds. A. A. Balkema, Rotterdam.

Thorson, G. 1950. Reproductive and larval ecology of marine bottom invertebrates. *Biol. Rev.* **25:** 1–45.

Vannucci, M. 1959. Catalogue of marine larvae. Universidade de Sao Paulo. Instituto Oceanografico. 7-11.

Wilson, D. P. 1978. Some observations on bipinnariae and juveniles of the starfish genus *Luidia*. *J. Mar. Biol. Assoc.* (U.K.). **58:** 467–478.

Wray, G. A., and R. A. Raff. 1991. The evolution of developmental strategy in marine invertebrates. *T. R. E. E.* **6:** 45–50.

Yamaguchi, M., and J. S. Lucas. 1984. Natural parthenogenesis, larval and juvenile development, and geographical distribution of the coral reef asteroid *Ophidiaster granifer*. *Mar. Biol.* **83:** 33–42.

Reference: *Biol. Bull* **184**: 269–276. (June, 1993)

Hull Cupules of Chiton Eggs: Parachute Structures and Sperm Focusing Devices?

JOHN BUCKLAND-NICKS

Department of Biology, Box 7, St. Francis Xavier University, Antigonish, Nova Scotia, Canada, B2G 1C0

Abstract. The extracellular hull of chiton eggs is often elaborated into cupules or spines that may be open or closed to the external environment. Scanning electron microscopy was used to examine the location of fertilizing sperm in eggs that had been exposed to a dilute sperm suspension to create natural fertilization or to a sperm concentrate to induce polyspermic egg penetration. The effect of cupules on sinking rates was tested in cupulous (free-spawning) and non-cupulous (brooding) species, by timing descent of eggs over a fixed distance in a large container of seawater. Densities of eggs were compared on Percoll gradients and found to be similar. It was found that hull cupules focus the sperm to specific regions of the egg surface in both brooding and free-spawning species. Furthermore, protruding cupules act as parachute structures that can significantly reduce sinking rates.

Introduction

In a majority of chitons, the extracellular egg hull is elaborated into complex cupules or spines that project outwards from the surface of the egg (see review by Pearse, 1979). The mechanism of sperm entry was misunderstood for many years, partly because hull elaborations made it difficult to visualize sperm-egg interactions, and partly because accumulated ultrastructural evidence favored the lack of an acrosome, and there was no obvious means of sperm entry (Pearse and Woollacott, 1979; Russell-Pinto *et al.*, 1983, 1984; Sakker, 1984; Al-Hajj, 1987; Hodgson *et al.*, 1988). The discovery of a tiny acrosome at the tip of the nuclear filament in *Tonicella lineata* (Buckland-Nicks *et al.*, 1988a), the documentation of fertilization in this species (Buckland-Nicks *et al.*, 1988b), and the subsequent demonstration that similar acrosomes are present in five different sub-families of chitons (Buckland-Nicks *et al.*, 1990), indicated that with the exception of one primitive sub-family (Hodgson *et al.*, 1988), there is a common mechanism of fertilization among most chitons. However, there are striking differences in the structure of the egg hull of chitons. For example, hull cupules may be open or closed to the external environment; they may be blunt or spinous, reduced to plates or bumps, or be totally absent (see reviews by Pearse, 1979; Eernisse and Reynolds, 1993).

In *T. lineata*, the cupules are opened by follicle cell retraction when the eggs ripen and sperm are attracted inside the cupules to fertilize each egg (Buckland-Nicks *et al.*, 1988b); but where do the sperm enter in closed cupule species? In brooding forms such as *Lepidochitona fernaldi* and *L. thomasi*, the cupules are of the closed type; furthermore, they are reduced in these species to flattened plates (Eernisse, 1988). This variation in cupule size, shape, and structure may have profound influences on the site and mechanism of fertilization, the sinking rates, adhesion, and cohesion of eggs, as well as the numbers of eggs that can be brooded by brooding species. This study examines the role of hull cupules in focusing sperm to a particular region of the egg surface, as well as their influence on sinking rates in free-spawning *versus* brooding species.

Materials and Methods

Specimens of the free-spawning species *Mopalia lignosa* (Gould, 1846), *Mopalia ciliata* (Sowerby, 1840), *Mopalia muscosa* (Gould, 1846), and *Lepidochitona dentiens* (Gould, 1846) were obtained in May 1989 and 1990 from tidepools and beneath rocks in the intertidal zone at

Received 18 November 1992; accepted 25 March 1993.

Portions of this work were presented as a poster at the EMSA/MSC meetings in Boston, August 1992.

Eagle's Cove, San Juan Island, Washington. Specimens of the brooding species *L. fernaldi* (Eernisse, 1986) were obtained in May 1990 from tidepools in association with the barnacle *Semibalanus cariosus* (Pallas, 1788) and the sea anemone, *Anthopleura elegantissima* (Brandt, 1835), at Deadman Bay on the west coast of San Juan Island. Specimens of *Chaetopleura apiculata* (Say, 1834) were purchased from Gulf Specimen Co., Panacea, Florida, and shipped to San Juan Island in early June 1990. Animals were maintained at Friday Harbor Labs in separate dishes on a running seawater table at about 10°C until spawning occurred naturally. No attempt was made to induce spawning artificially. Some individuals of a species were kept in the same tank to encourage natural fertilization. When polyspermy was required, unfertilized eggs of *M. lignosa, M. muscosa, M. ciliata, C. apiculata* and *L. dentiens* were collected and fertilized with sperm dissected from males of the same species. Eggs of *L. fernaldi* were dissected from the ovary or removed from the pallial groove with a toothpick following spawning. Eggs were washed in two changes of 0.45 μm millipore-filtered seawater prior to sedimentation experiments, to remove mucus.

Scanning electron microscopy

For scanning electron microscopy fertilized eggs were fixed in cold 2.5% glutaraldehyde in 0.45 μm millipore-filtered seawater at pH 8.0 (adjusted by adding 1 *N* NaOH to 25% glutaraldehyde prior to mixing 1:9 with seawater) for 3 h followed by a rinse in 2.5% sodium bicarbonate buffer at pH 7.2 and post-fixation with cold 1% osmium tetroxide in 1.25% sodium bicarbonate buffer at pH 7.2 (final concentrations). Eggs were washed in distilled water and dehydrated in a graded ethanol series to 100% ethanol. The ethanol was gradually replaced by amyl acetate to 100%, with three changes in pure amyl acetate, prior to critical point drying in teflon "microporous specimen capsules" (S.P.I. supplies). Eggs were tapped out onto aluminum stubs coated with double-sided sticky tabs. Some eggs were rolled on the sticky tab to remove cupules and reveal internal structure and sperm-egg interactions. Following these pre-treatments, the eggs were sputter-coated with gold and examined in a Cambridge S250 or S150 scanning electron microscope.

Sedimentation velocity

Sinking rates of eggs of *M. ciliata* and *L. fernaldi* were tested by dropping individual eggs into the center of a 5-l beaker of 1 μm filtered seawater and timing their descent over a distance of 25 cm between two marks on the side of the beaker. The upper mark was approximately two inches below the surface of the water, which allowed eggs to reach terminal velocity before timing began. Wall effects were assumed to be minimal and in any case would cancel out in comparisons between species.

Percoll gradients

Densities of eggs of *M. ciliata* and *L. fernaldi* were compared empirically by centrifugation on paired Percoll (Pharmacia, Sweden) gradients. Ten milliliter aliquots of different concentrations of Percoll ranging from 10 to 70% Percoll were made up in 0.45 μm millipore-filtered seawater. Beginning with 70% Percoll, each aliquot was drawn up into a 10 ml disposable plastic pipette using a pi-pump (Fisher), and 5 ml of it was gently layered into each of two slanting, 50-ml capacity, pyrex centrifuge tubes. The final result was a Percoll gradient ranging from 70% at the bottom of the tube to 10% at the top. Samples of eggs in 5 ml of 0.45 μm millipore-filtered seawater were pipetted on top of each gradient, and the gradients were transferred to a bench top centrifuge (being very careful to avoid bumping the tubes) and spun at 400 G's for 10 min. Five replicates were done for each species (eggs were recovered and re-used for *L. fernaldi*) with equivalent results each time. In one instance the centrifuge was stopped and the tubes examined after 2 min. The resulting distribution of eggs was photographed against a white background with Kodak 2415 Technical Pan film.

Results

Evidence for the influence of hull cupules on the site of fertilization

In ripe eggs of *Mopalia* spp. the hull cupules are open to the external environment (Figs. 1, 3). Sperm rapidly located the open cupules and swam inside one of seven channels, at the base of which they penetrated the hull (Figs. 2, 4). The fact that this is the main site of fertilization in this species was demonstrated by exposing eggs to high sperm concentrations which induced polyspermic egg penetration. When these eggs were rolled on sticky tape to remove cupules, numerous sperm were found penetrating the hull inside the cupules, but very few were seen penetrating in the intercupule area (Fig. 4).

Figures 1–4: Scanning electron micrographs of fertilized eggs of *Mopalia* spp.

Figure 1. Fertilized egg of *M. ciliata*, demonstrating open cupules. Scale bar = 50 μm.

Figure 2. Naturally fertilized egg of *M. lignosa* rolled on sticky tape to remove some cupules and demonstrate subdivision of each cupule into seven channels. Sperm (arrow) can be seen penetrating the hull within some channels. Scale bar = 20 μm.

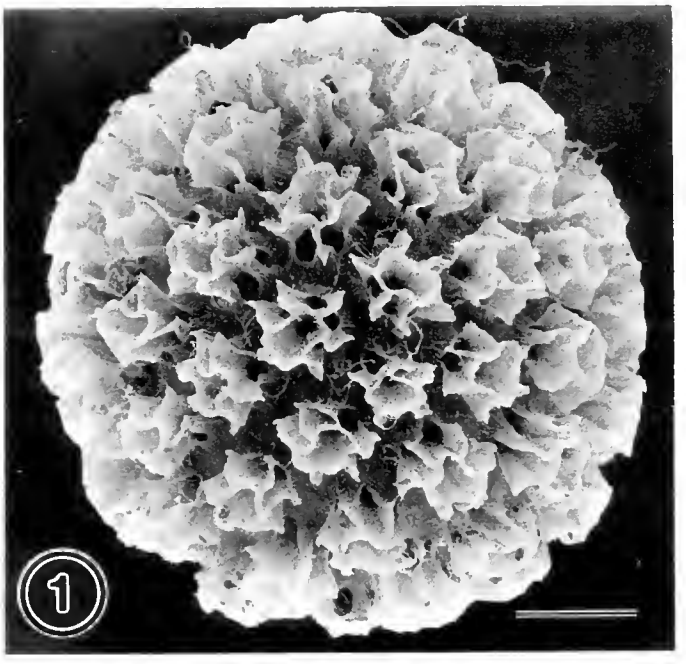

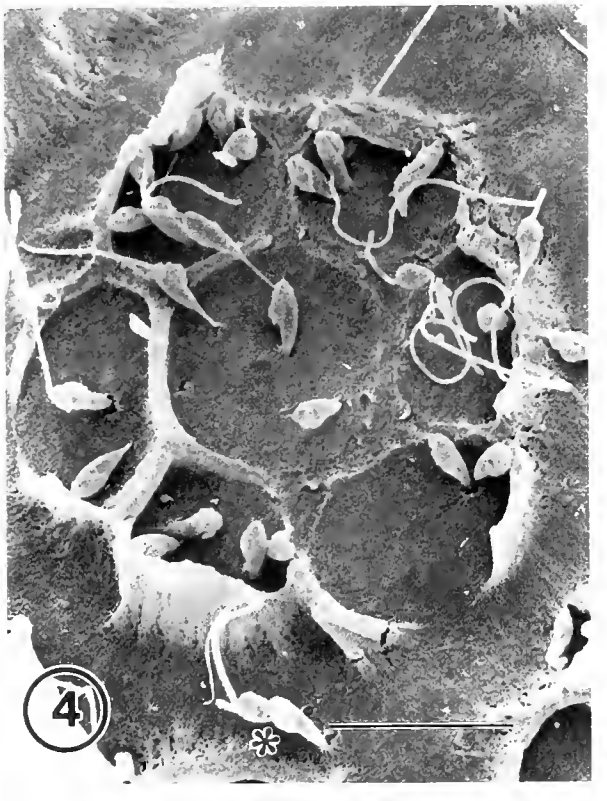

Figure 3. Hull cupules of naturally fertilized egg of *M. muscosa*. Note sperm inside cupule (arrows), and few sperm between cupules that are not penetrating the hull (asterisks). Scale bar = 15 μm.

Figure 4. Egg of *M. lignosa* artificially fertilized with sperm concentrate to create polyspermy. Few sperm have penetrated hull between cupules (asterisk) but numerous sperm can be seen penetrating within cupules. Scale bar = 10 μm.

The ripe eggs of *Lepidochitona dentiens* are permanently closed (Fig. 5), blocking sperm entry. Instead, sperm were focused to the intercupule area which represents roughly 20% of the egg surface. The removal of cupules in this species revealed that sperm did not gain access to the inside of cupules (Fig. 6). Instead, sperm were found in abundance in the intercupule area (Fig. 7). On closer examination, the intercupule area was found to be characterized by a series of micropores. Sperm appeared to penetrate the hull via individual micropores (Fig. 8). Micropores were not found in the intercupule area of *M. muscosa* (Fig. 3) or *M. lignosa* eggs (Fig. 4), but they were found in this region in eggs of the brooder *L. fernaldi* (Fig. 9), which, like *L. dentiens*, has closed hull cupules. Furthermore, occasional elongate microvilli were seen projecting from the micropores (Fig. 10).

Preliminary examination of spinous-hulled eggs of *Chaetopleura apiculata* (Fig. 11), showed that after the spines had unwound during maturation of the egg (Fig. 12), they remained closed to the external environment, yet hollow inside (Fig. 13). This condition resembles that of the closed-cupule species, *L. dentiens*. Sperm did not gain access to the inside of the spines. Unfortunately, most eggs were damaged and it was not possible to view the intercupule area to assess sperm binding or penetration in this region, nor to discover the presence or absence of micropores.

Evidence for the influence of hull cupules on sinking rates

Sinking rates of eggs of *M. ciliata* and *L. fernaldi* were measured by dropping individually 20 eggs of each species into the center of a 5-l beaker of seawater and timing their sinking rates between two marks, 25 cm apart. The mean sinking rate for *M. ciliata* was 330 μm/s (S.E. = 0.48); and for *L. fernaldi* was 1930 μm/s (S.E. = 0.10) $\{P < 0.0001\}$. Eggs of the open cupule species sank almost six times more slowly than eggs of the brooding species.

To test whether this was due largely to differences in overall density, the eggs of *L. fernaldi* and *M. ciliata* were centrifuged on Percoll gradients for 10 min at 400 G's. However, the results presented in Figure 14 show that egg density was roughly the same. What was interesting was that if the centrifuge was stopped after 2 min, eggs of *L. fernaldi* had already reached their final level in the gradient, whereas those of *M. ciliata* had only migrated a fraction of this distance (Fig. 14). After 10 min, eggs of both species had reached the same level in the gradient, which did not change with longer centrifugation times.

The diameter of the egg core (248 μm), excluding the hull, of an *L. fernaldi* egg, was slightly larger than that of *M. ciliata* (231 μm). However, the total diameter, taking into account the hull and hull cupules, was 25% less in *L. fernaldi* eggs (292 μm) than those of *M. ciliata* (363 μm). The actual volume of eggs was calculated to be approximately 9.27×10^{-3} mm^3 for *L. fernaldi* and 8.04×10^{-3} mm^3 for *M. ciliata* (volume of cupules was calculated by estimating the volume of a single cupule compressed into a rectangle of known dimensions and multiplying by the number of cupules on the egg). Thus the cupulous egg of *M. ciliata* has a smaller actual volume, which is distributed over a larger effective volume.

Discussion

Do hull elaborations focus the sperm?

In the majority of chitons, the egg hull is elaborated into a series of cupules or spines which cover much of the egg surface. This covering of cupules restricts sperm access to some parts of the egg in some species, while focusing sperm to particular regions in other species. Cupules may be open or closed at maturity. In open cupule species, the inside of the cupule is exposed when the follicle cell covering it has retracted (Buckland-Nicks *et al.*, 1988b, and this study). The sperm are attracted inside the cupules and penetrate the egg at the base of these cupules. Sperm are not attracted to individual cupules when still covered by follicle cells, and infrequently penetrate the hull in the intercupule area (Buckland-Nicks *et al.*, 1988b; and this study). Miller (1977) has shown that a sperm chemoattractant is released by some chiton eggs, including *Mopalia* spp. My observations suggest that this chemoattractant is probably released from within hull cupules, following follicle cell retraction. The result is that sperm are focused to a restricted area of the egg surface inside the cupules.

Micropores provide direct access to the vitelline layer

In the two closed cupule species studied (*L. fernaldi* and *L. dentiens*), the area covered by the cupules is unavailable to the sperm, thus focusing them on the intercupule area, where an array of micropores provides direct access to the vitelline layer. Micropores were not found elsewhere on the egg surface. Once again the area available for the fertilizing sperm is only a fraction of the total egg surface.

Spinous hull species have not been studied in detail but preliminary observations in this study suggest that they are equivalent to closed cupule species. The spines of *Chaetopleura apiculata* are hollow and closed to the outside. Observations of hull formation in *Sypharochiton septentriones* (Ashby) (concluded from: Selwood, 1970) also showed the spines to be hollow and closed. Furthermore, Eernisse (1984) has observed closed spines in several spinous hull species, including *Stenoplax fallax* (Carpenter in Pilsbry, 1892).

How do sperm penetrate the egg?

The presence of an acrosome is probably universal among chitons (Buckland-Nicks *et al.*, 1990), although

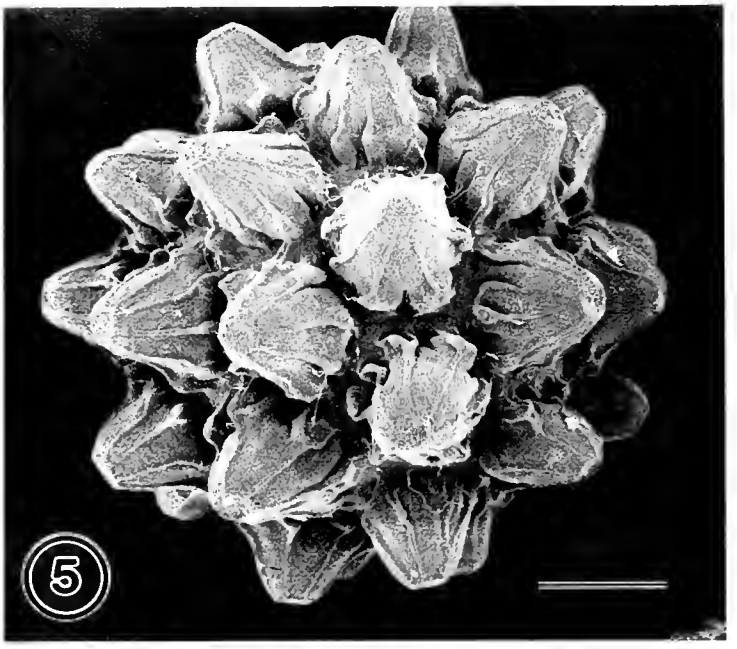

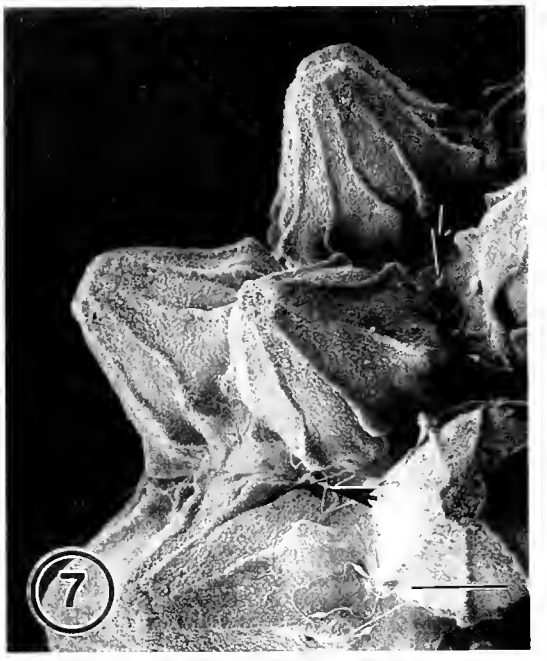

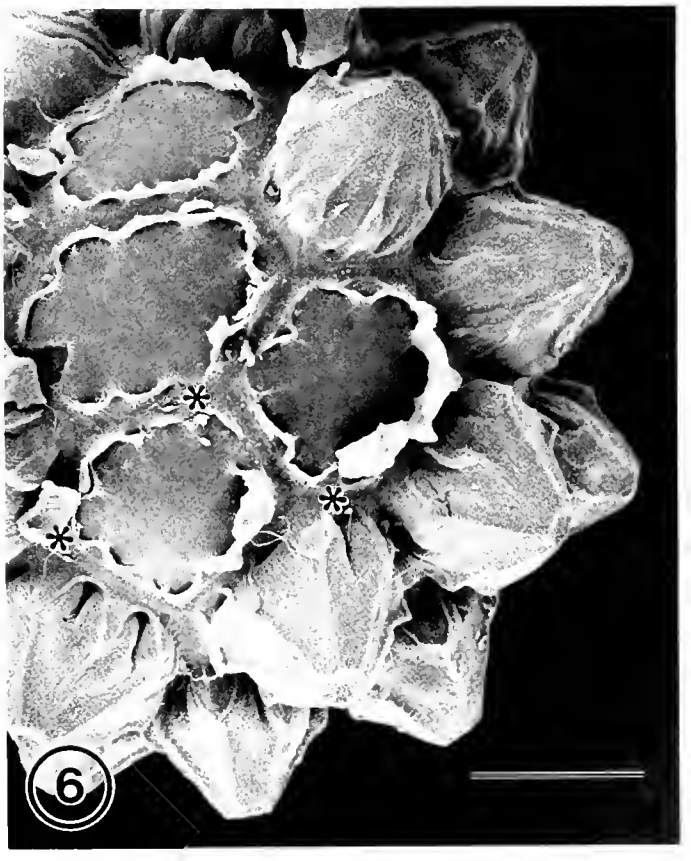

Figures 5–8: Scanning electron micrographs of fertilized eggs of *Lepidochitona dentiens*

Figure 5. Fertilized egg of *L. dentiens* demonstrating closed cupules. Scale bar = 40 μm.

Figure 6. Fertilized egg of *L. dentiens* with some cupules removed. No sperm are found inside cupules. Note sperm penetrating hull between cupules (asterisks). Scale bar = 40 μm.

Figure 7. Fertilized egg of *L. dentiens* showing sperm in intercupule area (arrows). Scale bar = 20 μm.

Figure 8. Sperm penetration of *L. dentiens* egg. Sperm anterior filament has entered micropore in intercupule region. Scale bar = 2 μm.

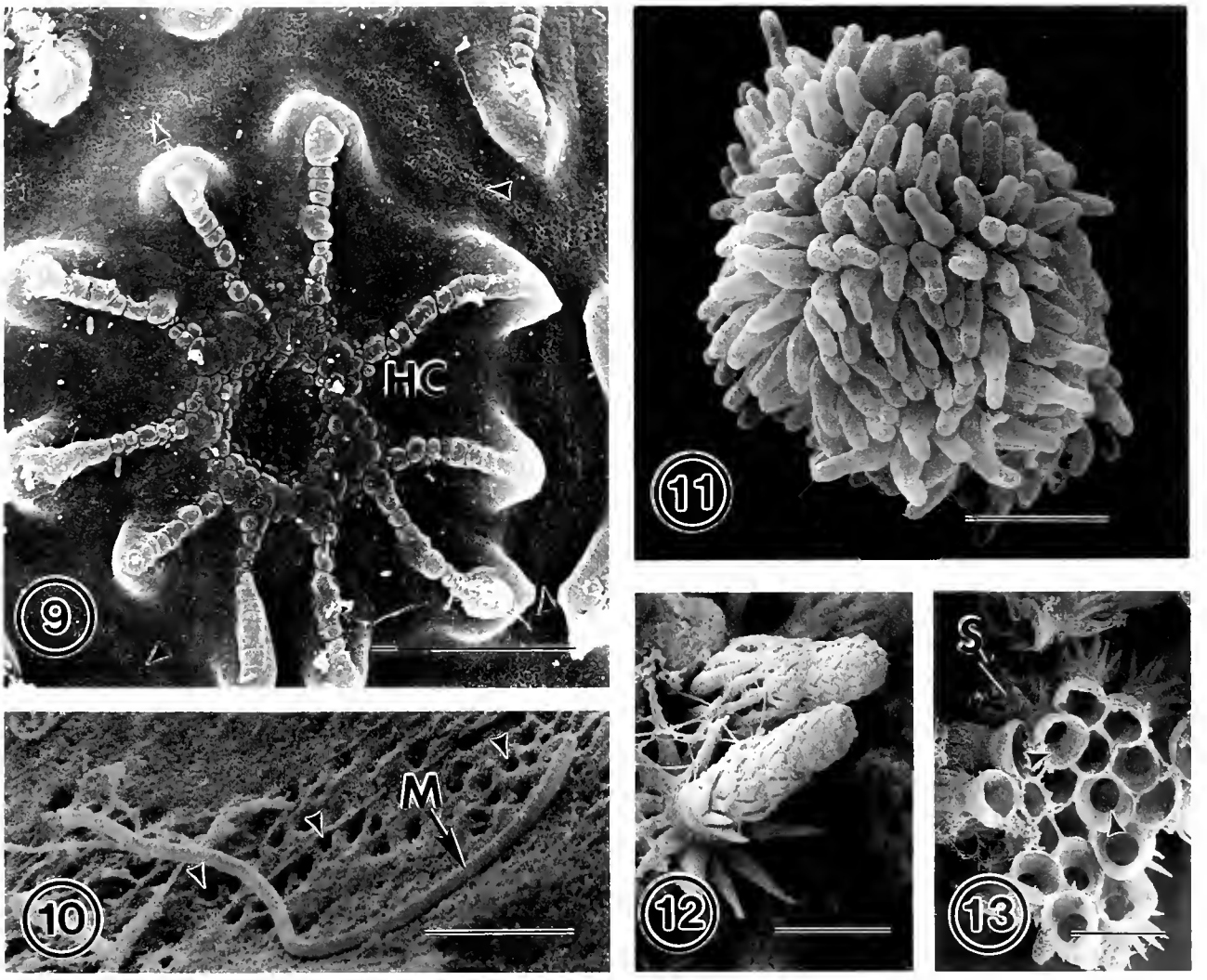

Figure 9. S.E.M. of closed hull cupule (HC) of *Lepidochitona fernaldi* egg, showing reduction typical of brooders. Regular series of micropores is visible in intercupule area (arrowheads). Scale bar = 20 μm.

Figure 10. S.E.M. of *L. fernaldi* egg showing elongate microvillus (arrow), extending from one of a series of micropores in the intercupule region (arrowheads). Scale bar = 2 μm.

Figure 11. S.E.M. of *Chaetopleura apiculata* egg showing spinous hull. Scale bar = 100 μm.

Figure 12. S.E.M. of spine of mature egg of *C. apiculata*. Spines are effectively closed, blocking sperm entry. Scale bar = 20 μm.

Figure 13. S.E.M. of spines of mature egg of *C. apiculata* viewed from the base, showing that they are hollow internally (arrowheads). Note sperm visible only on external surface (S). Scale bar = 40 μm.

the highly reduced form found in the majority of chitons differs markedly from the large, more typical molluscan acrosome found in the primitive Lepidopleurina (Hodgson *et al.*, 1988). Furthermore, there may be key differences in the structure of acrosomes in open and closed cupule species. In the open cupule species *Tonicella lineata*, sperm penetration of hull and vitelline layer apparently involves sequential exhaustion of two Golgi-derived granules in the acrosome (Buckland-Nicks *et al.*, 1988). The apical granule is used up during passage through the hull, whereas the basal granule is used up during passage through the vitelline layer. Any exposed area of the hull, but apparently not the hull cupules themselves, can be penetrated by the sperm; although the majority of sperm are attracted inside the hull cupules. Conversely, in closed cupule species, I have not found sperm penetrating the hull anywhere except in the region of micropores, which enable the sperm to bi-pass the hull and gain direct access to the vitelline layer; although it is not certain yet that sperm are unable to penetrate the hull directly, between micropores. Upon re-examination of the acrosomes of *Chaetopleura apiculata, L. dentiens, L. fer-*

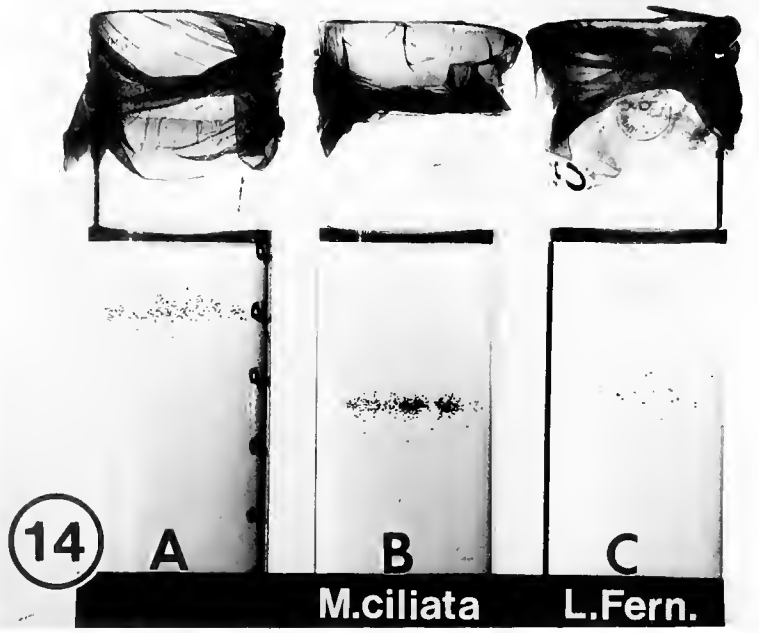

Figure 14. Photograph of eggs of *Lepidochitona fernaldi* and *Mopalia ciliata* centrifuged at 400 G's on Percoll gradients in pyrex tubes. A. *M. ciliata* eggs after 2 min centrifugation. B. *M. ciliata* eggs after 10 min centrifugation. C. *L. fernaldi* eggs after 10 min centrifugation.

naldi, and *L. caverna*, I could only resolve a single granule in the acrosome. This could explain the lack of sperm penetration of the hull except in the region of micropores in *L. fernaldi* and *L. dentiens* (Buckland-Nicks and Eernisse, 1992). Further study will be required to confirm the substructure of acrosomes in open and closed cupule species. Improved fixation methods will have to be devised to clarify these distinctions.

The presence or absence of micropores and the structure of the acrosomes in spinous hull species remain to be discovered.

Specializations of the egg membrane

The direct involvement of microvilli in the fertilization of animals has been documented in vertebrates (Bedford, 1982; Ohta, 1991), as well as many different invertebrates (Longo, 1983; Sato and Osanai, 1983; Fukumoto, 1988), including chitons (Buckland-Nicks *et al.*, 1988b). Richter (1976) and Selwood (1970) point out that elongate microvilli are intimately involved with the secretion of the egg hull in chitons and one would expect to find them within the hull elaborations of all species, during this process. However, the location of elongate microvilli in mature eggs appears to be different in open and closed cupule species, and it may be linked with fertilization. In open cupule species, elongate microvilli are found directly below hull cupules in mature eggs and extend upwards into the vitelline layer and sometimes into the hull (Richter, 1976; Buckland-Nicks *et al.*, 1988b).

In closed cupule species, elongate microvilli are found below the intercupule area. No spinous hull species has been studied in detail with S.E.M., but a photograph taken by D. Eernisse (1984) of the unfertilized egg of *Stenoplax fallax* shows numerous microvilli projecting above the hull in the intercupule area. These and other exposed microvilli likely retract prior to fertilization, and may give rise to the micropores we see in the intercupule area in closed cupule species. Differences in the location of specialized microvilli may indicate variation in the site and mechanism of fertilization in the different chiton groups.

Do hull elaborations act as parachute structures in free-spawners?

Sinking rates of the eggs of *M. ciliata* were much slower than those of *L. fernaldi*. This was not due to differences in overall density, as egg densities were found to be similar. The eggs of *M. ciliata* had a smaller actual volume and a larger effective volume than eggs of *L. fernaldi*. Since density is mass per unit volume, and densities were the same, this indicates that the mass of the *L. fernaldi* egg was slightly greater. I conclude that hull cupules in *M. ciliata* distribute the mass of the egg over a larger effective volume and by doing so they trap a layer of seawater around the egg that reduces effective density and slows sinking rate.

In this manner, the hull cupules are acting as parachute structures (Vogel, 1981).

Some other factors also may influence sinking rates. For example, there may be differential density in eggs, with hull cupules being less dense than the egg core, or perhaps the egg is secreting a low density compound into the cupules, such as a sperm chemoattractant (Miller, 1977). Some ascidians secrete ammonium ions into the cupules, resulting in the production of gas bubbles, which act as a flotation device (Lambert and Lambert, 1978). However, no gas bubbles were observed within the cupules of chiton eggs.

In species where spawned eggs are not dispersed immediately, hull cupules may have other functions such as linking eggs together in chains held by mucus, or sticking eggs on the substrate by their spines (Eernisse, 1988; Eernisse and Reynolds, 1993). In some species, eggs are embedded in a gelatinous mass on the substrate and hull cupules are sometimes reduced, but also they may be retained (Eernisse and Reynolds, 1993). In brooding species, cupules invariably are reduced, sometimes to flattened plates, as in *L. fernaldi* and *L. thomasi* (Eernisse, 1988). Brooding chitons are frequently small, with a restricted space (the pallial grooves) in which to store developing embryos. The reduction in cupule size may correlate with increased potential for brooding, as presumably then more eggs could be packed into such a restricted brood chamber.

Acknowledgments

Thanks are due to Doug Eernisse for assisting in preparation of some tissues for electron microscopy, to Steven Vogel for help with understanding the fluid dynamics of passive sinking (any misconceptions are mine!), to Edwin DeMont for helpful discussions, and to Professor A.O.D. Willows for the use of research facilities at the Friday Harbor Labs. This study was supported by an NSERC of Canada grant to J.B-N.

Literature Cited

Al-Hajj, H. A. 1987. Ultrastructural study of spermiogenesis in the chiton *Acanthopleura haddoni* from the Gulf of Aqaba (Red Sea). *Int. J. Invert. Reprod. Dev.* **12:** 295–308.

Bedford, J. M. 1982. Fertilization. Pp. 128–163 in *Reproduction in Mammals, Book 1: Germ Cells and Fertilization,* C. R. Austin and R. V. Short, eds. 2nd ed. Cambridge University Press, Cambridge.

Buckland-Nicks, J., R. Koss, and F.-S. Chia. 1988a. The elusive acrosome of chiton sperm. *Int. J. Invert. Reprod. Dev.* **13:** 193–198.

Buckland-Nicks, J., R. Koss, and F.-S. Chia. 1988b. Fertilization in a chiton: acrosome-mediated sperm-egg fusion. *Gamete Res.* **21:** 199–212.

Buckland-Nicks, J., F.-S. Chia, and R. Koss. 1990. Spermiogenesis in Polyplacophora, with special reference to acrosome formation (Mollusca). *Zoomorphology* **109:** 179–188.

Buckland-Nicks, J., and D. J. Eernisse. 1993. Ultrastructure of mature sperm and eggs of the brooding hermaphroditic chiton, *Lepidochitona fernaldi* Eernisse 1986, with special reference to the mechanism of fertilization. *J. Exp. Zool.* **265:**567–574.

Eernisse, D. J. 1984. *Lepidochitona* Gray, 1821 (Mollusca: Polyplacophora), from the Pacific Coast of the United States: Systematics and Reproduction. Ph.D. Dissertation. University of California, Santa Cruz. 358 pp.

Eernisse, D. J. 1988. Reproductive patterns in six species of *Lepidochitona* (Mollusca: Polyplacophora) from the Pacific Coast of North America. *Biol. Bull.* **174:** 287–302.

Eernisse, D. J., and P. D. Reynolds. 1993. Polyplacophora. In *Microscopical Anatomy of Invertebrates, vol 5,* F. W. Harrison and A. J. Kohn, eds. Wiley-Liss, New York (In press).

Fukumoto, M. 1988. Fertilization in ascidians: apical processes and gamete fusion in *Ciona intestinalis* spermatozoa. *J. Cell Sci.* **89:** 189–196.

Hodgson, A. N., J. M. Baxter, M. G. Sturrock, and R. T. F. Bernard. 1988. Comparative spermatology of 11 species of Polyplacophora (Mollusca) from the suborders Lepidopleurina, Chitonina and Acanthochitonina. *Proc. R. Soc. London Ser. B* **235:** 161–177.

Lambert, C., and G. Lambert. 1978. Tunicate eggs utilize ammonium ions for flotation. *Science* **200:** 64–65.

Longo, F. J. 1983. Meiotic maturation and fertilization. Pp. 49–89 in *The Mollusca vol. 3, Development,* N. H. Verdonk, J. A. M. van den Biggelaar, and A. S. Tompa, eds. Academic Press, New York.

Miller, R. L. 1977. Chemotactic behavior of the sperm of chitons (Mollusca: Polyplacophora). *J. Exp. Zool.* **202:** 203–212.

Ohta, T. 1991. Initial stages of sperm-egg fusion in the freshwater teleost, *Rhodeus ocellatus ocellatus. Anat. Rec.* **229:** 195–202.

Pearse, J. S. 1979. Polyplacophora. Pp. 27–85 in *Reproduction of Marine Invertebrates, Vol 5, Molluscs: Pelecypods and Lesser Classes,* A. C. Giese and J. S. Pearse, eds. Academic Press, New York.

Pearse, J. S., and R. M. Woollacott. 1979. Chiton sperm: no acrosome? *Am. Zool.* **19:** 956 (abs).

Richter, H-P. 1976. Feinstrukturelle Untersuchungen zur Oogenese der Käferschnecke *Lepidochitona cinereus* (Mollusca, Polyplacophora). *Helgol. Wiss. Meeresunters.* **28:** 250–303.

Russell-Pinto, F., C. Azevedo, and T. Barandela. 1983. Fine structure of the spermatozoa of *Chiton marginatus* (Mollusca: Amphineura), with special reference to nucleus maturation. *Gamete Res.* **8:** 345–355.

Russell-Pinto, F., C. Azevedo, and E. Oliveira. 1984. Comparative ultrastructural studies of spermiogenesis and spermatozoa in some species of Polyplacophora (Mollusca). *Int. J. Invert. Reprod. Dev.* **7:** 267–277.

Sakker, E. R. 1984. Sperm morphology, spermatogenesis and spermiogenesis of three species of chitons (Mollusca, Polyplacophora). *Zoomorphology* **104:** 111–121.

Sato, M., and K. Osanai. 1983. Sperm attachment and acrosome reaction on the surface of the polychaete, *Tylorrhynchus heterochaetus. Biol. Bull.* **178:** 101–110.

Selwood (née Bedford), L. 1970. The role of the follicle cells during oogenesis in the chiton *Sypharochiton septentriones* (Ashby) (Polyplacophora, Mollusca). *Z. Zellforsch.* **104:** 178–192.

Vogel, S. 1989. *Life in Moving Fluids: The Physical Biology of Flow,* 3rd ed. Princeton University Press, New Jersey. 352 pp.

Reference: *Biol. Bull.* **184**: 277–285. (June, 1993)

The Patterns of Bromodeoxyuridine Incorporation in the Nervous System of a Larval Ascidian, *Ciona intestinalis*

TOMAS BOLLNER[1,2,*] AND I. A. MEINERTZHAGEN[2]

[1]*Department of Zoology, Stockholm University, 106 91 Stockholm, Sweden, and* [2]*Neuroscience Institute, Life Sciences Centre, Dalhousie University, Halifax, Nova Scotia, Canada B3H 4J1*

Abstract. The fates of cells from the anterior region of the ascidian neural plate are described either as neural or as mixed neural and non-neural. In *Ciona intestinalis*, all cellular progeny are accounted for until a time 60% between the onset of embryonic development and larval hatching. To resolve the issue of their fates in this species, we have examined the later mitotic history of neural-plate cells. Because cessation of cell division in the neural plate has been claimed to occur at 70% of embryonic development, we need to account for cell production from 60% onward, to determine whether more cells are produced than populate the larval CNS, allowing some to adopt non-neural fates. The embryonic incorporation of bromodeoxyuridine (BrdU), 500 μM in seawater, was monitored in 1-h larvae by anti-BrdU immunocytochemistry. The pattern of incorporations indicates that all larval neurons are born before 70% of embryonic development, but that cell division unexpectedly continues to generate ependymal cells until at least 95%. Divisions in the neurohypophysis continue throughout embryonic development. The total number of cells produced appears sufficient only to complete the complement of larval CNS cells, denying non-neural fates for anteriorly migrating neural plate cells, and indicating a general absence of cell death. Consistent numbers of incorporations after the same exposure in different larvae provide evidence for determinacy of neural plate lineages. The last three conclusions confirm those reached previously (Nicol and Meinertzhagen, 1988b).

Received 2 June 1992; accepted 26 February 1993.

* Present address: Department of Biology, Royal Holloway and Bedford New College (London University), Egham, Surrey TW20 OBX, UK.

Introduction

Ascidians or sea-squirts have long attracted interest because, as urochordates, they are considered to be closely related to the common ancestor of all chordates (Garstang, 1928; Berrill, 1955; Bone, 1972). It is not the sessile adult, however, but rather the short-lived larval stage that exhibits some of the typical features of a chordate. These include a dorsal tubular central nervous system (CNS), and the fact that this arises from an embryonic neural plate. On the other hand, the number of cells within the larval CNS is approximately 370 and is apparently fixed, at least within narrow limits, in closely related offspring of the mutual fertilization of two hermaphrodite adults (Nicol and Meinertzhagen, 1991). Such cell constancy, or eutely, is not an invariably identifiable feature of chordate nervous systems (Williams and Herrup, 1988), but rather is usually associated with invertebrate animals. Most of the cells constitute the functional larval nervous system, which consists of an anterior sensory vesicle, the visceral ganglion in the posterior part of the trunk, and the nerve cord in the tail (Nicol and Meinertzhagen, 1991; Fig. 1). The formation of this CNS follows the pattern in other chordate embryos (Nicol and Meinertzhagen, 1988a), with neurulation following the formation of the neural plate.

Two current ideas exist about the fate of the cells in the embryonic neural plate. Descriptive studies in *Ciona* (Nicol and Meinertzhagen, 1988a,b) indicate that all neural plate progeny contribute to the CNS, and thus offer an orthodox view of the fate of this structure in ascidians. On the other hand, injections of horseradish peroxidase (HRP) into seventh and eighth generation neural-plate blastomeres in *Halocynthia* (Nishida and Satoh, 1985; Nishida, 1987) imply that some anterior neural plate cells

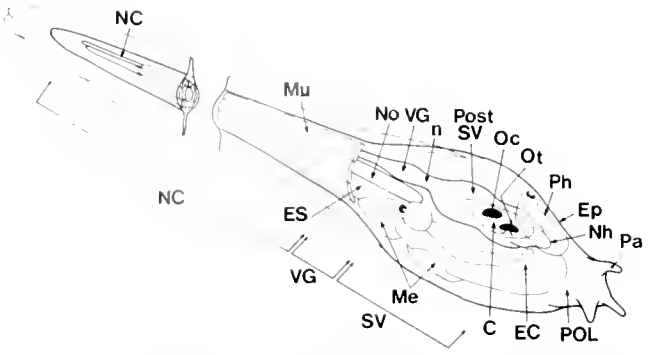

Figure 1. Diagram of the entire larva, from the right rostral side. Abbreviations: Nervous system. C: cavity of the sensory vesicle; n: neck; NC: nerve cord; Nh: neurohypophysis; Oc: ocellus; Ot: otolith; PostSV: posterior sensory vesicle; SV: sensory vesicle; VG: visceral ganglion. Other systems: EC: endodermal cavity; Ep: epithelium; ES: endodermal strand; Me: mesenchyme; Mu: muscle band; No: notochord; Pa: papilla; Ph: pharynx; POL: pre-oral lobe. (From Nicol and Meinertzhagen, 1991.)

migrate anteriorly, away from the CNS, where they acquire non-neural fates either in the pharyngeal region or in the epidermal adhesive papillae. If migration of neural plate cells were also to occur in *Ciona*, it must, according to the results of Nicol and Meinertzhagen (1988b), occur later than the 60.5% developmental stage (where 100% is the period of embryonic development required to attain larval hatching), because this was the last record of these workers. If migration were to occur, it would further require that extra cell divisions occur to replace the migrating cells (Nicol and Meinertzhagen, 1988b). The resolution of this issue hinges on an accurate determination of the time at which the last cell divisions take place.

When does cell division actually cease? Reliable information about the actual time for cessation of cell divisions in the CNS is lacking. Berrill (1935) suggests, but without clear documentation, that the onset of pigment differentiation in the ocellus and otolith (70% of embryonic development) marks the end of neural proliferation, and this claim was used to arbitrate the differences between neural-plate fates in *Ciona* and *Halocynthia* (Nicol and Meinertzhagen, 1988b). Cell counts in *Ciona*, however, indicate that this is not accurately the case (Fig. 2). At 70%, some 300 cells exist in the CNS (Nicol, 1987), while at hatching there are 371 or so, implying that further proliferation must occur between 70–100%. Previous cell counts have indicated that 88% of the final cell complement in one larva was attained by about 73% (Balinsky, 1931), and thus confirm this picture. Our study was designed to address the question of whether later mitoses do actually occur in the neural plate, as these figures suggest. If these mitoses do occur, then our aim was to identify the location, if not the fate, of the resultant progeny. To do this, we have exploited the incorporation of a substituted nucleotide, 5-bromodeoxyuridine (BrdU), to expose late cell divisions in the neural tube. Our observations build on the only precedent in this direction (Reverberi *et al.*, 1960), a previous study in which thymidine incorporations were examined, but only at earlier stages in neurulation.

Materials and Methods

Adult *Ciona intestinalis* were obtained from the Marine Resources Department of the Marine Biological Laboratory, Woods Hole, Massachusetts, or from Tjärnö Marine Biological Laboratory, Sweden, and maintained in running seawater. Gametes collected from the gonoducts of two individuals were mixed to produce cross-fertilized embryos, which were then raised in plastic petri dishes floating on a water bath at 16°C.

DNA synthesis was monitored by the incorporation of BrdU (Sigma), and revealed by a monoclonal antibody directed against BrdU (Gratzner, 1982). Incorporations occurred when embryos were immersed in BrdU dissolved in Millipore-filtered seawater. Initially, three concentrations, 250 μM, 500 μM, and 1 mM, were tested. The lowest concentration produced less clear immuno-staining. Although the two higher concentrations both gave equally strong immuno-labeling, the lower of the two, 500 μM, was chosen. It exceeded the detection threshold for

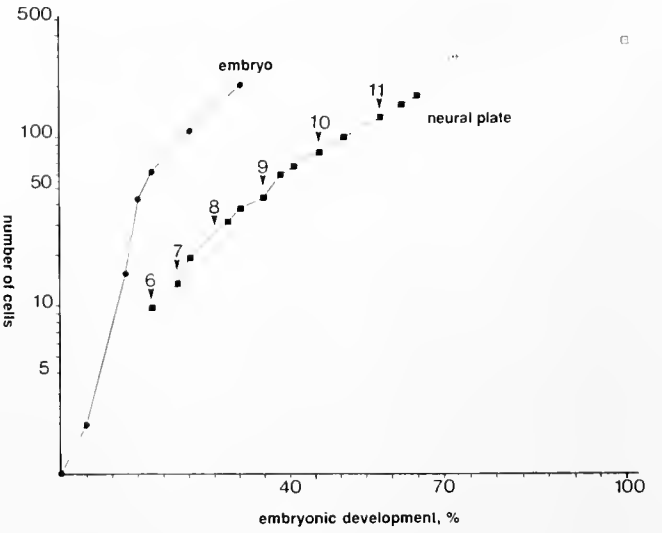

Figure 2. Cell proliferation at different stages in the neural plate revealed from cell counts (ordinate: square symbols, data plotted from Nicol and Meinertzhagen, 1988a, b), compared with cell number in the entire embryo (circles, data from Conklin, 1905; Nicol and Meinertzhagen 1988a). Arrowheads indicate the generation number of the cells at that stage. The increase in the number of neural plate cells is roughly exponential, as shown by their linear progression in this plot, and attains the cell complement of the swimming larva (100%, open square, data from Nicol and Meinertzhagen, 1991) only at a time projected to occur later than 70% (open square, data from Nicol, 1987).

dividing cells in adult *Ciona* (Bollner *et al.*, 1991), but avoided an unnecessarily high concentration, which could have disturbed embryonic development. This type of perturbation has been previously reported for *Ciona* (Cusimano, 1961) and is also widely known in other embryos, such as, for example, insects (Truman and Bate, 1988).

Two strategies for BrdU incorporation were used (Fig. 3). In the first, incorporations resulting from long-pulse exposures to BrdU which started at 60% of embryonic development or later, and ended when the larva hatched, were used to reveal all cells that were not already postmitotic before these times. Long-pulse exposures were started at 60%, 70%, 72.5%, 75%, and so on, and were extended in 2.5% increments up to 95%. In the second strategy, short-pulse BrdU incorporations of 30 min (about 2.5%) were also administered, starting at 70% and then at the same intervals as for the long pulses, but with the embryos transferred to fresh seawater after the pulse. Short-pulse incorporations were used to reveal the regional and temporal distribution of mitoses. In all cases, larvae were fixed 1 h after hatching.

Fixation for pre-embedding immunocytochemistry was carried out in 0.1 *M* phosphate buffer (pH 7.2) containing 4% paraformaldehyde, for 4–12 h at 4°C. After fixation, the specimens were washed in the same buffer and treated with 2 *N* HCl in phosphate-buffered saline (PBS) for 45 min, and then rinsed in PBS (pH 7.2) containing 0.1% Triton X-100 (Sigma) (PBS-TX). To improve tissue penetration of antibodies, the fixed larvae were treated with 1% Triton X-100 PBS for 24 h at 4°C. After two washes in PBS-TX, samples were incubated for 48 h at 4°C in anti-BrdU (Becton and Dickinson, Mountain View, California) diluted 1:200 in PBS-TX with 0.5% bovine serum albumin (BSA). The preparations were incubated overnight at 4°C in rabbit anti-mouse secondary antibody (Dakopatts) diluted 1:50 in PBS-TX BSA, followed by mouse PAP-complex (Dakopatts) diluted 1:100 in PBS-TX BSA, before further processing using 0.03% DAB as a chromogen. The preparations were washed in PBS-TX between all steps. Finally, the material was dehydrated and embedded, either in Historesin (LKB) or in Durcupan ACM (Fluka), viewed either as wholemounts or as 1–3-μm sections cut on glass knives, and photographed with differential interference contrast optics.

For post-embedding immunocytochemistry, specimens were fixed either in methanol for 20 min at −20°C, followed by ethanol under the same conditions, or in cold Bouin's fluid for a minimum of 3 h to a maximum of overnight. All specimens were stained with eosin dissolved in 70% alcohol, dehydrated in a routine ethanol series, and embedded in paraffin wax. Sections were cut either transversely or sagittally at 4–5 μm and mounted on poly L-lysine coated slides. The preparations were then dewaxed, rehydrated, and treated with 2 *N* HCl for 30 min, prior to overnight incubation in anti-BrdU 1:200. The same secondary antiserum and PAP-complex were used as for the wholemounts, and preparations were incubated for 1 h and 30 min, respectively. The DAB reaction was enhanced by adding $NiCl_2$ to a final concentration of 0.015%.

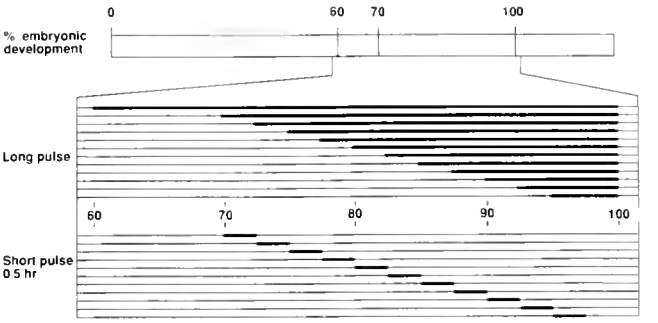

Figure 3. Diagrammatic representation of the two types of BrdU exposure used. Long-pulse exposures (heavy lines) commence during the final 40% of embryonic development and continue until hatching of the larva. Short-pulse exposures (heavy lines) distributed throughout the same period, but in abutting intervals of 30 min.

Results

The larval ascidian CNS is divided into three main regions (Fig. 1), which, in sequence, consist of the anterior sensory vesicle, with 215 cells, separated by a neck region of 6 cells from the visceral ganglion of 45 cells, which lies in the posterior part of the trunk, and the nerve cord of 65–66 cells in the tail. The sensory vesicle is situated rostrally in the trunk with its anterior left portion overlain by the pharynx and the so-called neurohypophysis, the primordium of the adult neural complex with some 40 or so cells. These cell numbers derive mostly from one larva (L4) in Nicol and Meinertzhagen (1991), but are supported by others reported by these authors and by Nicol (1987). Only some cells are neuronal. Roughly 68% have been classified as ependymal, a specialized non-neuronal cell peculiar to embryonic and larval chordates, from their position lining the cavities of the neural tube's elaborations or from clear similarities in the cytological appearance to those that do (Nicol and Meinertzhagen, 1991).

Initially, long pulse exposures were used to establish how late in embryonic development cells of the CNS incorporated BrdU. Larvae were examined in wholemounts, after being immersed in BrdU from 70% of embryonic development and allowed to develop in this medium until they hatched as free-swimming larvae (Fig. 3). Embryos of the correct developmental stage were selected according to the time since their fertilization expressed as a proportion of the time until hatching, which for most batches was attained after 20 h at 16°C. In addition, the devel-

opment of a batch of embryos was calibrated by two further criteria. The first was that 60% of embryonic development has occurred when the length of the tail bud equals that of the trunk, and the second was that 70% has occurred when pigment cells first appear in the sensory vesicle.

Long pulse BrdU exposures starting at 70% of embryonic development produced labeled nuclei in all parts of the CNS within the trunk, but not in the nerve cord (Fig. 4a). It is thus immediately clear that mitotic activity in the CNS extends beyond 70%. With a single short BrdU pulse administered from 72.5% to 75%, labeled nuclei were detected in both the dorsal part of the sensory vesicle and the neurohypophysis (Fig. 4b). A long BrdU pulse starting from 85% and continuing to 100% (Fig. 4c) gave labeled nuclei in the sensory vesicle as well as in the neurohypophysis, while a short BrdU pulse starting from the same stage, 85%, produced labeled nuclei in the ependymal lining of the nerve cord and in the neurohypophysis (Fig. 4d). Thus the cells in the sensory vesicle must have had their S-phase after the period of the short pulse, *i.e.*, later than 87.5%.

BrdU exposure still produced labeled nuclei in the CNS at 95% of embryonic development. At this late stage, a few labeled nuclei were found in, or in close association with, the caudal part of the sensory vesicle or the neck (Figs. 4e, 5). These cells may have been part of the ependymal lining of the nerve cord. Mitotic activity was also evident in the neurohypophysis at this stage (Figs. 4e, 5).

Some idea of the extent of mitotic activity can be gained from the numbers of labeled nuclei. Counts in the CNS of long-pulse larvae, which were incubated in BrdU starting at 60, 70, or 85% and continued until hatching, are shown in Table I.

When the long BrdU pulse started at 60% embryonic development approximately 50 nuclei (53, 50) showed staining in the larval CNS, excluding the neurohypophysis. These included cells in the sensory vesicle, the neck, and the visceral ganglion. Some of the labeled cells in the sensory vesicle were deemed to be neurons from their location, whereas all other labeled cells at this stage were thought to be ependymal (Fig. 6a). Most labeled cells in the visceral ganglion were members of bilateral pairs forming the ependymal lining of the nerve cord.

When the long BrdU pulse started later, at 70% embryonic development, fewer labeled nuclei appeared in the CNS (31, 34 cells: Table I), most of which were in the sensory vesicle (Fig. 6b). The larva with 31 labeled nuclei had only 6 that could be assigned to the visceral ganglion. On the other hand, the second larva possibly had eight incorporations in its visceral ganglion, but because the visceral ganglion and surrounding mesenchymal cells were difficult to distinguish in this larva, some of the eight may not have been part of the CNS. In both larvae, some labeled cells in the posterior part of the sensory vesicle and others in the anterior visceral ganglion might have been neck cells, but this could not be ascertained.

Very few cells were labeled from long-pulse BrdU exposures starting at 85% of embryonic development and extending until hatching (Table I). In one case, seven labeled cells were found in the CNS, while in the second case, the nine cells in the CNS were found in the sensory vesicle and none was found in the visceral ganglion. Of the nine, at least five could be assigned as ependymal cells lining the nerve cord. The identity of the remaining four was unclear, although they were found close to the wall of the sensory vesicle (Fig. 6c), an area where most of the cells are also thought to be ependymal (Nicol and Meinertzhagen, 1991).

These results are summarized in Figure 7. In all the examined groups, BrdU incorporations were detected in the neurohypophysis, which thus seemed to continue to proliferate throughout the entire period investigated.

Discussion

The primary conclusion of this study is that far from ceasing at the time of pigment differentiation at 70%, as Berrill (1935) has suggested, cell division in the nervous system continues throughout the remaining period of embryonic development. In principle, therefore, cells could arise in excess of those surviving in the CNS, and this excess could allow for some to migrate anteriorly, as current evidence indicates must happen in *Halocynthia* (Nishida, 1987). The production of surplus cells had previously been thought unlikely because the progressive increase in the duration of the cell cycle seemed to preclude the possibility for there to be sufficient time for additional rounds of cell division before 70% (Nicol and Meinertzhagen, 1988b).

Is there in fact sufficient time to generate an excess of cells? The observed patterns of divisions within the neural plate concluded with 84 progeny in the posterior region of the neural plate and 85 in the anterior at 60.5% (Nicol and Meinertzhagen, 1988b). Nicol (1987) predicted from the pattern of their previous divisions that these cells will soon generate a total of 109 11th and 12th generation cells in the posterior part of the neural plate, and 158 such cells in the anterior (of which only the pigment cells are still in their 9th generation). She predicted that these would occur before 70%, although some additional divisions must also be required to make up the total number of 300 cells counted at that stage (Nicol, 1987). This means that 130 divisions are required between 60% and 70%, an interval corresponding to 2 h at 16°C. Most of the 170 neural plate cells recorded at 60.5% (Nicol and Meinertzhagen, 1988b: their 13.3 h) were already born 48 min earlier at 57% which, considering a cell cycle time

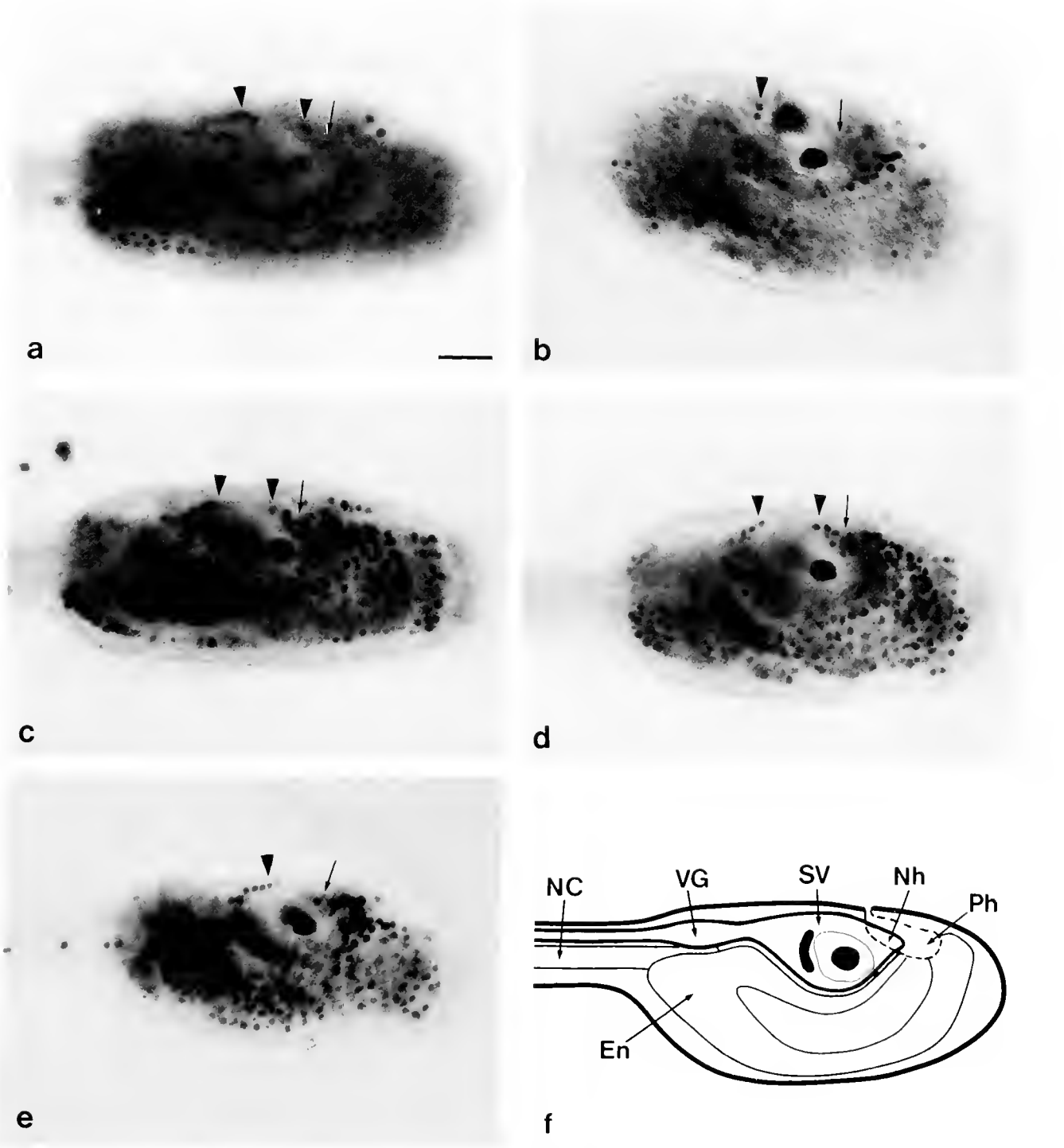

Figure 4. Larval wholemount preparations showing the pattern of incorporations when the embryo is exposed to the BrdU label at different ages. Incorporations occur in nuclei in the sensory vesicle (arrowheads) and neurohypophysis (arrows); scale bar: 30 μm. (a) Long-pulse embryo exposed through the period from 70% to hatching. Labeled nuclei appear in the dorsal and caudal parts of the sensory vesicle, in cells associated with the neck between the sensory vesicle and visceral ganglion, and in the neurohypophysis. (b) A short BrdU pulse at 72.5% (Fig. 3B) labeled nuclei in the posterior part of the sensory vesicle and the neurohypophysis (out of focus). (c) A long BrdU pulse starting at 85% labeled nuclei in the posterior part of the sensory vesicle, along the nerve cord, and in the neurohypophysis. (d) A single BrdU pulse at 85% of embryonic development gave labeled nuclei in the neurohypophysis and along the dorsal nerve cord. (e) A single pulse at 95% incorporated in nuclei of the dorsal posterior sensory vesicle. (f) Diagram of the trunk shown with the same orientation as (a–e), identifying the positions of the major components: endoderm (En), neurohypophysis (Nh), pharynx (Ph), and sensory vesicle (SV).

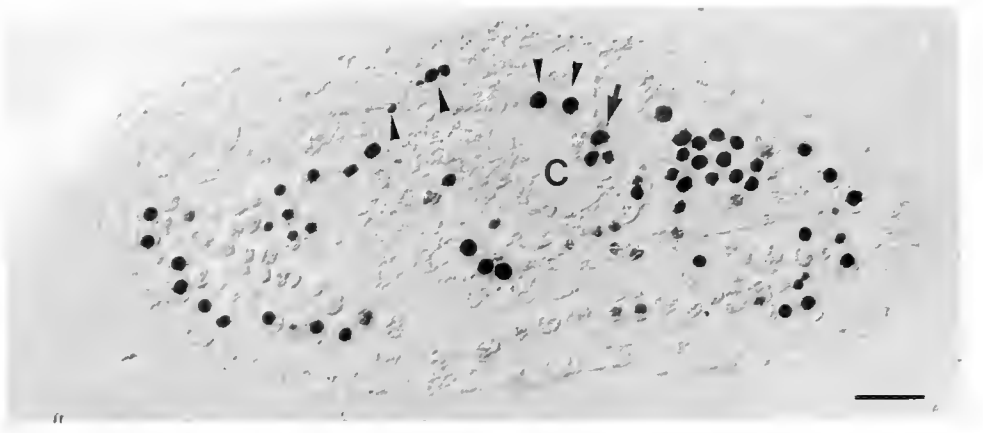

Figure 5. A single BrdU pulse at 95% showing labeled nuclei abutting the cavity (C) of the sensory vesicle, in cells of the caudal part of the sensory vesicle (arrowheads), as well as in the neurohypophysis (arrows) of a wholemount section. Bar = 20 μm.

of 2.5–2.9 h (Nicol and Meinertzhagen, 1988b), gives sufficient time for the 130 divisions needed to reach a total of 300 cells by 70% (15.3 h).

The numbers of cells predicted by Nicol (1987) compare closely in the posterior part of the neural plate with those found in the final larva (65–66 cells in the nerve cord + 45 cells in the visceral ganglion: Nicol and Meinertzhagen, 1991). On the other hand, for the anterior part where 221 cells exist in the larva (266 trunk cells–45 cells in the visceral ganglion of larva L4, in Nicol and Meinertzhagen, 1991), 63 cells (=221–158) would have to divide again just to generate the numbers of larval CNS cells, without excess. Other larvae may have slightly differing cell counts. The number of extra divisions for the four larvae in Nicol and Meinertzhagen (1991) would, for example, range from 56 to 65. These numbers, moreover, take no account of the neurohypophysis, which requires approximately another 40 cell divisions, for a total of 103 divisions.

Are more than 103 BrdU incorporations in fact seen in the period between 60% and hatching, for any excess cells to be created? The 53 or so labeled cells that have been counted in the larval CNS from long-pulse exposure at 60% would seem quite clearly to indicate not an excess of divisions, but an insufficiency. On the other hand, if Nicol's (1987) record of 300 CNS cells at 70% is correct, we can account for the remaining divisions: approximately 30 cells are born from 70% to hatching (Table I) which together with 40 or so cells in the neurohypophysis produces a total of 370. The inconsistency between our data and the predictions arising from Nicol's data (Nicol, 1987) stems, then, from the small number of BrdU incorporations seen in our long-pulse animals at 60%.

There are several possible reasons for these small numbers. (1) The staging of our embryos might have differed from those of Nicol, so that the BrdU pulses actually commenced later than 60%. Since many of the neural plate cells at this stage had been in their 11th generation for some time, it is not impossible that they were about to enter their next generation at about the 60% stage. Fewer incorporations than expected could then have resulted if the pulse were, through slightly inconsistent staging of embryos in the two studies, administered a little later than 60%. The fact that incorporations counted from larvae exposed at 60% derived from a different batch of animals than those used to count incorporations in older larvae (Table I) provides a possible explanation for the internal discrepancy in our study between the 60% batch and the 70 and 85% batches if, once again, the youngest batch had in fact actually been somewhat older than 60%.

(2) We also do not know the details of the cell-cycle. It is therefore possible that although cells were pre-mitotic, they had already passed, or were at least in a late part of their S-phase and were consequently unable to incorporate sufficient BrdU to be detected.

(3) A third possibility is that embryonic development was slightly inhibited from the 60% stage by the concen-

Table I

Number of CNS cells labeled with BrdU[1]

Stage	Larva 1	Larva 2
60–100%	53	50
70–100%	31	34
85–100%	9	7

[1] Two larvae counted at each stage. The older larvae were all from the same two adults and were processed together, while those labeled from 60% were larvae of two adults which received an identical BrdU treatment, but on a different day.

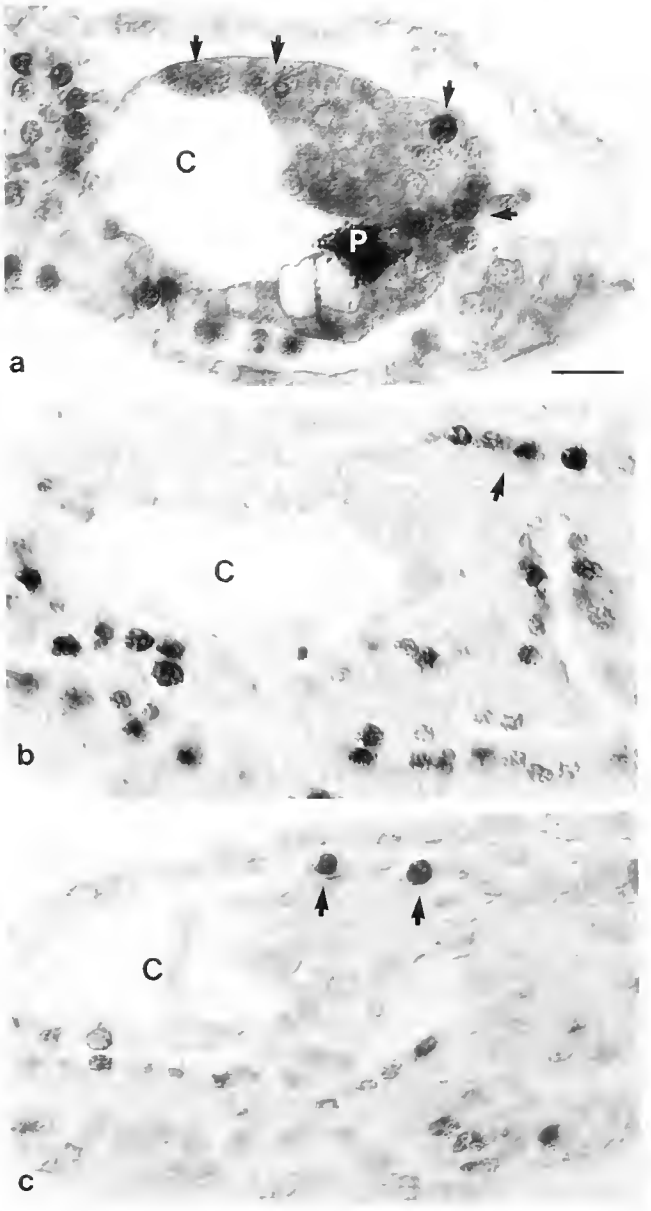

Figure 6. Sections through the sensory vesicle of long-pulse larvae exposed to BrdU from 60 to 85%. (a) 60%. Incorporations occur in the sensory vesicle wall and a group posterior to the pigment cup. (b) 70%. Incorporations occur in ependymal cells lining the dorsal nerve cord. (c) 85%. Incorporations occur in two labeled nuclei in the ependymal lining of the nerve cord. Positions of labeled nuclei are indicated by arrows. C: sensory vesicle cavity; P: pigment cup. Bar = 10 μm.

tration of BrdU we used. Cusimano (1961) reports that after exposing embryos to 500 μM deoxuridine from early cleavage stages onward, 90% of normal larvae emerged, whereas exposure to 1 mM was clearly toxic. Equivalent data to these are lacking for BrdU, which we suggest has no effect on normal development at 500 μM. Not only were the periods for which our embryos were immersed in BrdU much shorter than in Cusimano's study, but all the resultant larvae arising from such treatment also looked normal. It is nevertheless possible that their cell division had been slowed or inhibited by long-pulse exposure to BrdU, but that this was undetectable externally, and that as a result the number of incorporations was smaller than the normal number of divisions. In that case, the effect upon embryos at 70% might be less than at 60% because of the shorter cumulative period of exposure and because the susceptibility of embryos starts at the neurula stage (Cusimano, 1961). We were not able to avoid the possibility of this problem by using BrdU at a lower concentration (250 μM), because that would have diminished the staining intensity and run the risk of recording too few incorporations.

Thus, with these provisos, the evidence supports a mode of neural plate proliferation which at most attains constancy of cell number by addition (Williams and Herrup, 1988), possibly by a lineage dependent mechanism. This proliferation continues, moreover, until the final stage of embryonic development, because the latest stages investigated (95%) still revealed incorporations in the CNS. The cells produced at this late stage are thought to be ependymal rather than neuronal, as indeed is true for most

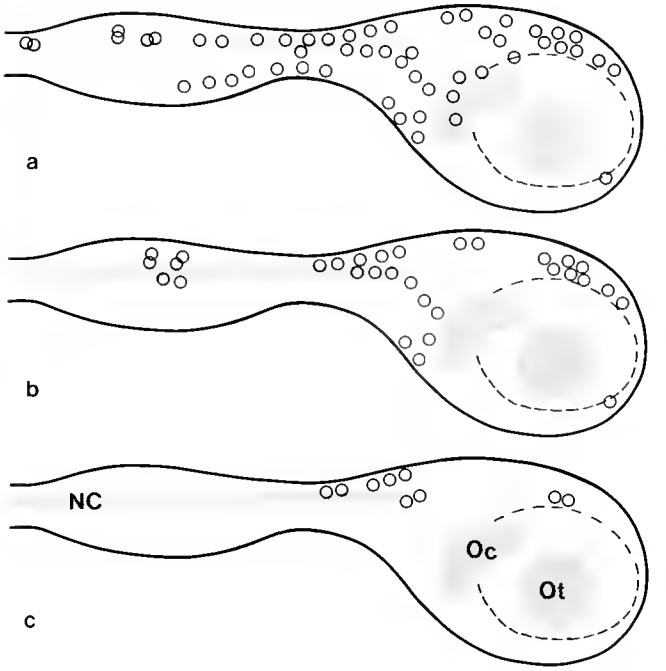

Figure 7. Schematic representation of the positions of labeled nuclei in three counted stages, made by superimposing *camera lucida* drawings. (a) Long-pulse larva labeled at 60%. (b) Long-pulse larva labeled at 70%. (c) Long-pulse larva labeled at 85%. Nuclei are shown with equal sizes; compare their positions with maps of neuronal nuclei (Nicol and Meinertzhagen, 1991: their Figs. 16, 17). Ot: otolith; Oc: ocellus; NC: nerve cord.

BrdU labeled nuclei found in the larval CNS after 60%. This diagnosis is based on the locations of the nuclei relative to published maps (Nicol and Meinertzhagen, 1991), rather than the appearance of the nuclei themselves, which did not distinguish ependymal cells from neurons. Our data thus indicate that all neurons in the larval CNS are born before 70% of embryonic development, and that only ependymal cell incorporations are revealed thereafter, at least outside the neurohypophysis. The neurohypophysis itself continues to proliferate right throughout the period of embryonic development, and thus behaves differently from the cells of the larval CNS proper.

What happens to the cells produced from divisions between 70 and 100% of embryonic development? Three possibilities concerning their fate exist in the light of our new evidence.

The first and by far most likely possibility is that the late divisions of neural plate cells are the final rounds required for the constructive generation of the cells of the CNS by a mechanism of addition (Williams and Herrup, 1988), topping up the complement of neural plate cells to the final total, which, including roughly 40 cells in the neurohypophysis, is about 370 (Nicol and Meinertzhagen, 1991). The only way in which a fixed number of larval CNS cells could then be produced would be by regulating the number of progeny of each neural plate cell, since the total number of such cells in the neural plate is fixed (Nicol and Meinertzhagen, 1988b). If, on the other hand, a small surplus of cells were produced, if for example we were unable to record all incorporations successfully, two further possibilities on the fate of the cells can be entertained.

First, they may migrate away from the neural plate. The late migration of cells to other regions is implied by Nishida's (1987) results on *Halocynthia*, but because incorporations were not found in the adhesive papillae in *Ciona*, and because this was a clear site of their localization in *Halocynthia* (Nishida, 1987), these two species must differ in at least this one important respect, reinforcing the only conclusion reached previously on their comparison (Nicol and Meinertzhagen, 1988b). Migration to sites other than the papillae is at least theoretically possible. For example, we see pharyngeal incorporations, as Nishida (1987) found in *Halocynthia*, but these need not be of migrating cells. Moreover, from BrdU immunocytochemistry we cannot distinguish them from incorporations in the neurohypophysis, because the neurohypophysis is located close to the pharynx and we lack probes to its yet undifferentiated cells.

Finally, surplus cells may be later eliminated by cell death. This has been ruled out for the early stages of neurogenesis (Nicol and Meinertzhagen, 1988b) and is most unlikely for later stages. At least in the nerve cord of the tail, cell death apparently does not occur. Cell complement at 60% has already attained that of the mature larva (Nicol and Meinertzhagen, 1988b, 1991) and we find no BrdU incorporations at this site, so that all postmitotic cells must survive into the larva. To rule out cell death may seem a trivial distinction in the case of the nerve cord, however, given that its cells will in any case degenerate with the onset of metamorphosis, soon after larval hatching (Cloney, 1978), and because probably all such cells are ependymal not neuronal. Nevertheless, the absence of cell death is a cardinal difference seen when we invoke the other major example of chordate neurogenesis, the formation of the CNS in vertebrates (Oppenheim, 1991).

We are therefore confident that our results support all of the following: the absence of migration to the papillae from the neural plate, the birth of all neurons before 70% but continued ependymal cell production until at least 95%, the lack of over-production of neural plate progeny and the consequent absence of neuronal cell death, and the attainment of final cell number by the regulated control of the number of cell divisions. Evidence for the latter comes clearly from consistency among the numbers of incorporations seen in larvae after exposure to BrdU at a particular embryonic stage. Thus, larvae exposed at the same times between 60 and 100% differ by only two to three incorporations (Table I). We take the small range of the differences between two animals at any one larval age to reflect either minor differences in the staging of the larvae or in the timing of their mitoses, and to indicate a determinacy of cell lineage amongst neural plate cells which has been seen previously (Nicol and Meinertzhagen, 1988b). Put another way, if we assume the existence of lineage determinacy, consistency in the number of BrdU incorporations provides assurance that developmental staging and immunocytochemical detection is also consistent between embryos.

Acknowledgments

We are grateful to The Royal Swedish Academy of Sciences and the Foundation "Lars Hiertas minne" for financial support to T.B. We also gratefully acknowledge the help of the staff and the use of the excellent facilities at the Marine Biological Laboratory, Woods Hole, Massachusetts, and the Marine Biological Laboratory at Tjärnö. Supported by NSERC grant A 0065 (to I.A.M.).

Literature Cited

Balinsky, B. I. 1931. Über den Teilungsrhythmus bei der Entwicklung des Eies der Ascidie *Ciona intestinalis*. *Wilhelm Roux' Arch. Entw. Mech. Org.* **125:** 155–175.

Berrill, N. J. 1935. VIII. Studies in tunicate development. Part III.—Differential retardation and acceleration. *Phil. Trans. R. Soc. Lond. Ser. B* **225:** 255–326.

Berrill, N. J. 1955. *The Origin of Vertebrates.* Clarendon Press, Oxford.

Bollner, T., P. W. Beesley, and M. C. Thorndyke. 1991. Birth-dates and differentiation of cells during neural complex regeneration in the ascidian *Ciona intestinalis*. *Reg. Peptides* **35:** 227.

Bone, Q. 1972. *The Origin of Chordates.* Oxford University Press, London.

Cloney, R. A. 1978. Ascidian metamorphosis: review and analysis. Pp. 255–282 in *Settlement and Metamorphosis of Marine Invertebrate Larvae*, F.-S. Chia and M. E. Rice, eds. Elsevier, New York.

Conklin, E. G. 1905. Organization and cell-lineage of the ascidian egg. *J. Acad. Nat. Sci. Philadelphia* **13:** 1–119.

Cusimano, T. 1961. L'azione di alcuni nucleosidi sullo sviluppo dell'uovo di ascidie. *Acta Embryol. Morphol. Exp.* **4:** 62–69.

Garstang, W. 1928. The morphology of the Tunicata, and its bearings on the phylogeny of the Chordata. *Q. J. Microsc. Sci.* **72:** 51–187.

Gratzner, H. G. 1982. Monoclonal antibody to 5-bromo- and 5-iododeoxyuridine: a new reagent for detection of DNA replication. *Science* **218:** 474–475.

Nicol, D. 1987. Development of the larval nervous system in the ascidian, *Ciona intestinalis*. Ph.D. thesis, Dalhousie Univ., Halifax, Nova Scotia. 199 pp.

Nicol, D., and J. A. Meinertzhagen. 1988a. Development of the central nervous system of the larva of the ascidian, *Ciona intestinalis* L. I. The early lineages of the neural plate. *Dev. Biol.* **130:** 721–736.

Nicol, D., and J. A. Meinertzhagen. 1988b. Development of the central nervous system of the larva of the ascidian, *Ciona intestinalis* L. II. Neural plate morphogenesis and cell lineages during neurulation. *Dev. Biol.* **130:** 737–766.

Nicol, D., and J. A. Meinertzhagen. 1991. Cell counts and maps in the larval central nervous system of the ascidian *Ciona intestinalis* (L.). *J. Comp. Neurol.* **309:** 415–429.

Nishida, H. 1987. Cell lineage analysis in ascidian embryos by intracellular injection of a tracer enzyme. III. Up to the tissue restricted stage. *Dev. Biol.* **121:** 526–541.

Nishida, H., and N. Satoh. 1985. Cell lineage analysis in ascidian embryos by intracellular injection of a tracer enzyme. II. The 16- and 32-cell stages. *Dev. Biol.* **110:** 440–454.

Oppenheim, R. W. 1991. Cell death during development of the nervous system. *Ann. Rev. Neurosci.* **14:** 453–501.

Reverberi, G., W. G. Verly, C. Mansueto, and T. D'Anna. 1960. An analysis of the ascidian development by the use of radio-isotopes. *Acta Embryol. Morphol. Exp.* **3:** 202–212.

Truman, J. W., and M. Bate. 1988. Spatial and temporal patterns of neurogenesis in the central nervous system of *Drosophila melanogaster*. *Dev. Biol.* **125:** 145–157.

Williams, R. W., and K. Herrup. 1988. The control of neuron number. *Ann. Rev. Neurosci.* **11:** 423–453.

Reference: *Biol. Bull.* **184**: 286–295. (June, 1993)

Experimental Induction of Localized Reproduction in a Marine Bryozoan

C. DREW HARVELL AND RICHARD HELLING

Section of Ecology and Systematics, Division of Biological Sciences, Cornell University, Ithaca, New York 14853

Abstract. The control of reproduction and growth rate within colonies of marine invertebrates is often conditional and can be very localized. We demonstrate experimentally large and localized shifts in the timing and pattern of reproduction within colonies of a temperate bryozoan (*Membranipora membranacea*) in response to simulated damage by predators and crowding by conspecifics. In these protandrously hermaphrodite colonies, zooids on the damaged side of a colony reproduced sooner than in unmanipulated regions of the same colony. To examine the influence of the pattern of edge damage on localized reproduction, we damaged the perimeter of circular colonies in two patterns: (1) a continuous half of the edge was trimmed (1/2-Damage) and (2) the edge was trimmed in four alternating one-eighth sections (4/8-Damage). The 1/2-damage treatment triggered localized reproduction, and the more localized four-eighths-damage did not. These experiments demonstrate that the configuration rather than the total amount of edge damage affects the localization of reproduction. In parallel experiments, conspecifics were allowed to crowd half the perimeter of experimental colonies. This treatment also resulted in localized and accelerated reproduction near the contact zone adjacent to a conspecific. Not only do patterns of reproduction change in crowded or damaged colonies, but obstructed colonies also compensate for reduced growth at an obstructed edge by extending the adjacent unobstructed perimeter edge at a greater rate.

One model to explain the sort of local cues governing the observed shifts in reproduction and growth rate is a source-sink model. A similar mechanism is proposed to underly growth and reproductive allocation in plants. We suggest that the balance between growth and onset of reproduction in zooids is determined by the rate of translocate moving through each zooid. The rate of translocate movement through zooids is, in turn, affected by the strength and proximity of sinks for that translocate, such as the growing edge of the colony. We propose a simple source-sink model of carbon flow to explain our experimental results. This model would account for the induction of localized reproduction in 1/2 damaged colonies and the lack of localization in 4/8 damaged colonies.

Received 30 November 1992; accepted 22 February 1993.

Introduction

Many organisms do not have fixed life history patterns and are instead plastic in the timing and quantity of metabolites allocated to growth and reproduction (Cohen, 1971; Hickman, 1975; Ryland, 1981; King and Roughgarden, 1982; Schlichting, 1986; Stearns and Koella, 1986; Harvell and Grosberg, 1988; Stearns, 1989). In colonial invertebrates, zooidal responses to biotic and abiotic factors are highly variable because they can be modified, sometimes in a very localized region of a colony, by both intrinsic and extrinsic stimuli (Hughes and Cancino, 1985; Harvell and Grosberg, 1988; Harvell, 1991). In fact, the ability to adjust the shape of modules and the allocation of resources among modules are central characteristics of coloniality (Mackie, 1986; Harvell, 1991). For example, the localized induction of defensive spines or disruption of a growing edge by damage can induce reproduction in a marine bryozoan (Harvell and Grosberg, 1988; Harvell and Padilla, 1990; Harvell, 1991, 1992). In hydrozoan (Cnidaria) colonies, a number of extrinsic stimuli accelerate the onset of reproduction, such as crowding (Loomis and Lenhoff, 1956; Braverman, 1974; Stebbing, 1980) and high carbon dioxide concentration (Crowell, 1957; Braverman, 1974). Despite the ubiquity of resource sharing among modules of colonial invertebrates (Mackie, 1986), there is no theory linking rates or patterns of translocation

there is no theory linking rates or patterns of translocation and resource allocation to growth and reproduction in these organisms.

In other modular organisms such as plants, studies on resource allocation and carbon budgets have revealed the importance of an internal balance of carbon use in determining rates of translocation and subsequent allocation to growth and reproduction (Lang and Thorpe, 1983; Bloom *et al.*, 1985; Chiarello *et al.*, 1989; Chapman *et al.*, 1990; Marshall, 1990). This has led to the development of a source-sink model, which forms the paradigm for carbon (and other metabolite) transport within plants (Chiarello *et al.*, 1989; Marshall, 1990). In bryozoans, translocation of metabolites from central to peripheral zooids has been demonstrated (Best and Thorpe, 1985), but the relationship between translocation patterns and allocation to growth and reproduction remains unknown. Our information on resource allocation within colonies has been largely limited to patterns of reproductive timing rather than experimental investigations of underlying processes.

In this paper, we experimentally investigate how environmental factors such as damage and crowding affect the allocation to reproduction and growth in the marine bryozoan, *Membranipora membranacea*. We examine the applicability of a source-sink model of resource allocation by analyzing how localized disruptions to a growth sink result in localized shifts in the onset of reproduction within colonies. Specifically, we ask how damaging or crowding the colonies' growing edge affects the timing of reproduction of zooids proximal to that edge and how this local disruption affects the growth rate on adjacent undamaged edges. To examine the role that sink strength may play in the observed allocation shifts, we vary the magnitude of damage by cutting different lengths of colony margin in several experiments. Finally, we use our results to develop a source-sink model of rate of carbon flow and resource allocation within a colony to aid in the process of further hypothesis-testing about processes of resource allocation within colonial marine invertebrates.

Materials and Methods

Timing of reproduction

To establish the unmanipulated pattern of onset of reproduction in undamaged and uncrowded colonies, we mapped the distribution of onset of reproduction for zooids within colonies of *Membranipora* through time. Previous attempts to describe the onset of reproduction in colonial invertebrates have proceeded with a descriptive, bulk colony approach (reviewed in Harvell and Grosberg, 1988; but see Dyrynda, 1981; Wahle, 1983, 1984; Brazeau and Lasker, 1990). Colonies of *Membranipora* are sub-annual, protandrous hermaphrodites; each zooid proceeds from non-reproductive to sperm producing to sperm and oocyte producing to only oocyte producing (Harvell and Grosberg, 1988). As reproduction begins within the colony, the number of zooids with gametes and the density of gametes per zooid is low. This is most evident at the onset of oocyte production, because oocytes can be readily counted. Through time, more zooids develop a greater density of gametes. Thus increases in the density of reproductive zooids per colony and oocytes per zooid occur as part of the maturation process. In our experiments, we will equate a greater density of reproductive zooids with a more advanced reproductive state, because there is no indication from previous studies (Harvell and Grosberg, 1988; Harvell, 1992) that our experiments should affect the quantity of gametes produced. To determine whether the timing of reproductive transitions varied within different aged regions of undisturbed colonies, we monitored the reproductive states of zooids from approximately 40-day-old colonies (n = 11). From previous studies we knew that 40 days is the approximate age when undisturbed colonies begin producing sperm (Harvell and Grosberg, 1988; Harvell *et al.*, 1990). We could age colonies because we monitored their settlement and growth on lucite panels on which they had naturally settled, which were suspended underneath the Friday Harbor (FHL) breakwater (see Harvell and Grosberg, 1988, for methods). Colonies on these panel were sampled at three, approximately eight-day intervals in mid July 1987.

The lucite substrates were easily manipulated and could be brought from their storage locations in the field to the lab for monitoring. Panels were maintained in a running seawater system for the 2–5 h they were in the lab, and during the approximately 20 min sampling were kept submerged in cool water under the dissecting microscope. Reproductive states were monitored under 12× with a Wild dissecting microscope and fiber optic lights. Within-colony variation in reproductive state was measured by determining the reproductive state of five haphazardly chosen zooids within each of three regions of the colony. Depending upon the size of a colony, each of these regions might be populated by greater than a hundred zooids. Nonetheless, the variance in reproductive state among the five sampled zooids was low. The sampling was truly haphazard because the reproductive state of a zooid could not be determined prior to scrutinizing with a dissecting microscope and zooids were sampled from all parts of the particular region. The configuration of regions sampled from each approximately circular colony was three concentric bands of equal diameter, but decreasing age: ancestrula region (A) (the founding, morphologically distinct "twinned" zooid is at the approximate center of the colony

and is called an ancestrula), mid region (M), and edge or new growth region (E) (Fig. 1). The width of these regions was determined by counting the total number of rows containing developed zooids in the colony and dividing by three. Reproductive states were easily assigned because both sperm and oocytes were visible under microscopic magnification through the transparent frontal membrane of the zooids. Each zooid was assigned a numerical value for its reproductive state from 0 to 4, and the median of the five values was analyzed in subsequent statistical analyses. A colony was classified as non-reproductive if the median state was 0 or 1 and as reproductive if those measures equalled or exceeded 2. Stage 2 was an unambiguous indicator of active reproduction because the sperm are actively moving and refract light, showing bright birefringence.

0 = non-reproductive
1 = sperm morulae present and visible on the underside of the frontal membrane
2 = mature spermatozeugmata present (bundles of actively moving and light refractive sperm)
3 = oocytes present (and sperm also)
4 = only oocytes present.

Partial damage experiments

New zooids are produced at the outer periphery of a colony and develop from buds to feeding zooids over several days. Colonies of *Membranipora* are indeterminate growers and continue to expand at the periphery by producing new buds until the colonies begin to senesce in late summer (Harvell and Grosberg, 1988; Harvell *et al.*, 1990). Although we had previously shown that damage to the margin of a colony accelerates the sexual development of the zooids proximal to the margin (Harvell and Grosberg, 1988), the degree of localization of this effect was unknown and we did not consider how subsequent growth of zooids would be affected by damage. Could the onset of reproduction be accelerated in one part of the colony in response to localized cues and remain unaffected in another part of the colony? It also appeared that growth of a colony was accelerated on a side away from damage, so we also tested the hypothesis that compensatory growth occurred in response to damage.

Working with single colonies naturally settled to lucite panels, we trimmed the outer edge buds back approximately one millimeter (equivalent of one zooid row) with a razor along half the perimeter of 14 colonies and monitored them from 13 to 24 July 1987 (1/2 damage treatment). We monitored 13 other undamaged colonies as controls. At two-day intervals, we determined the reproductive state of five zooids from three regions (A, M, E) on both the damaged and undamaged half of a colony. Colony areas were determined from tracings of the colonies made at 2-day intervals during the 11-day duration of the study. To test the hypothesis that compensatory growth occurred on the undamaged side of the colony in response to damage, the linear rate of growth was measured on controls and damaged colonies as the distance from the ancestrula to each opposite edge and the areal growth as the total area added to colonies. These were analyzed with linear regression of area and growth distance against original colony size. A linear model was used because both the control and damaged colony data fit this model well over the range for which we have data.

To determine how localized the stimuli triggering reproduction could be, we also divided 15 moderate-size (approximately 2000 mm^2) colonies into eighths and damaged alternating one-eighth lengths of the perimeter (4/8-damage treatment; see Fig. 4 below) and monitored growth and reproduction of the zooids proximal to damaged and undamaged regions. This set of experiments was performed on equal-sized, uncrowded colonies growing naturally on kelp blades and returned to lines off the breakwater after trimming. The colonies were sampled once, 16 days after trimming. For experimental colonies, reproductive states were recorded for five zooids 2–4 mm proximal to each of the four damaged and four undamaged sections of the colony edge. Eight corresponding regions were sampled on undamaged control colonies from the same kelp blades.

Effects of crowding by conspecifics

Harvell and Grosberg (1988) showed that the onset of reproduction was accelerated in colonies that were completely surrounded by conspecifics. In the current study, we designed experiments where colonies were only crowded on one side with a single conspecific to assess whether the crowding-induced reproduction was localized like the response to damage. We investigated both the influence of size and partial crowding on timing of reproduction. We grew 23 pairs of unequally sized (and aged) colonies on lucite panels. This size asymmetry was engineered by removing all colonies settled on the plate except those of particular sizes and distances apart. The size asymmetry was of no particular importance to this study, but it was important for data taken from the same experiment and reported in Harvell and Padilla (1990). At the start of the experiment, the small colony of each pair was an average size of 500 mm^2 and the large colony was an average size of 2500 mm^2. Because growth stops along the common border after contact, we designated zones to sample as in the 1/2-damage treatment. Colonies were sampled on alternate days for 13 days following contact. Data were pooled into three intervals: <8 days, 8–9, and

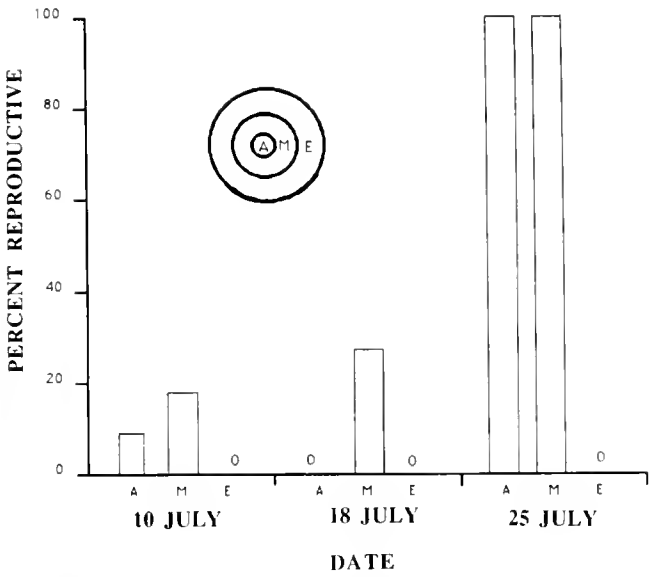

Figure 1. Percentage of control colonies producing spermatocytes or oocytes at three dates. Median percentages were calculated from five zooids haphazardly sampled from each of three regions in 11 colonies (A, M, E = Ancestral, Mid, and Edge regions). Both within-colony location ($\chi^2 = 10.49$, $P = 0.005$) and date ($\chi^2 = 7.91$, $P = 0.02$) significantly affect the frequency of reproductive colonies.

10–13 days after contact. Five zooids were again sampled from each region, and the median of those values analyzed. Because the shapes of colonies became so distorted in the crowding treatment due to compensatory growth away from the interaction, it was impossible to consistently sample the same three regions as on the controls (A, M, E). We therefore divided the crowded colonies into regions of two (M, E) instead of three equal radii for sampling.

Results

Timing of reproduction

Under normal, good-growth, field conditions, colonies begin reproduction as males at an age of approximately 40–60 days and would be approximately 2500 mm^2 in area (Harvell, 1992). The pattern of reproduction in unmanipulated colonies is for older zooids near the ancestrula and in the mid regions of colonies to reproduce first (Fig. 1). Most zooids are producing spermatocytes and oocytes by late July.

The significant results of the log-linear test reflect the transition in ancestral and mid regions of colonies from a non-reproductive to reproductive state between 18 and 25 July (Fig. 1). By 25 July, the percentage of ancestral and mid-colony regions that are reproductive has increased from 0 to 25%, respectively, to 100%. These data do not allow us to differentiate timing of reproductive events in ancestral and mid-colony regions because both regions became equally reproductive; zooids from the edge were still not reproductive (Fig. 1).

Partial damage experiments

In the 1/2-damage experiment, the damaged side produced both sperm and eggs sooner than the non-damaged side (Fig. 2). Reproduction began on the damaged side approximately 5–6 days after trimming (Fig. 2). Unlike control colonies and undamaged sides of the experimental colonies, reproduction was greater at the edge relative to the ancestral regions on damaged halves. This pattern is also evident 8–9 days after trimming: more colonies are reproducing on the damaged side and more colonies are reproducing at the edge than nearer the ancestrula.

Eight to nine days after damage (18 July) the effects of location within the colony are significant, but the effects of proximity to damage are not (Fig. 2). The location effect is a result of the mid and perhaps edge regions beginning to reproduce, but the center not (Fig. 2).

Three days later (11–12 days after damage) the effects of proximity to damage are pronounced (Fig. 2). The within-colony location term is no longer significant, although inspection of Figure 2 does reveal a tendency for reproduction to vary with location within the colony.

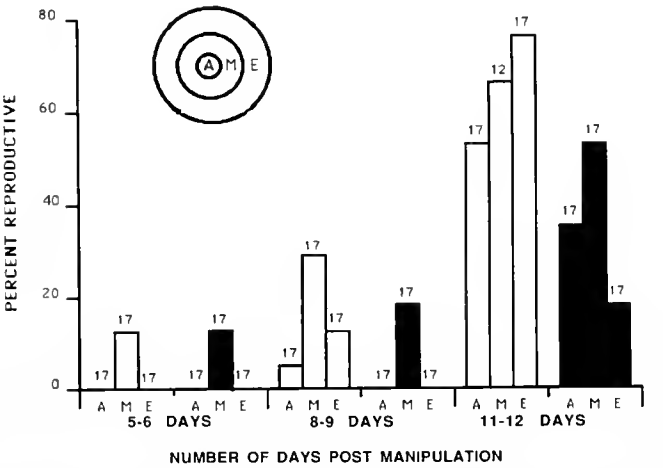

Figure 2. 1/2-damage Experiment: median percentage of colonies producing oocytes or spermatocytes. Reproductive states were tabulated for damaged (open bars) and undamaged (shaded bars) halves of colonies and three regions within each colony (A, M, E). Sample size at top of each bar. At 5-6 days the frequency of reproductive colonies is identical for damaged and control colonies. At 8-9 days, within-colony location affects the frequency of reproductive colonies ($\chi^2 = 7.12$, $P < 0.03$) but proximity to damage does not ($\chi^2 = 2.59$, $P = 0.11$). At 11-12 days, proximity to damage affects the frequency of reproductive colonies ($\chi^2 = 9.05$, $P = 0.003$), but within colony location does not ($\chi^2 = 2.22$, $P = 0.33$).

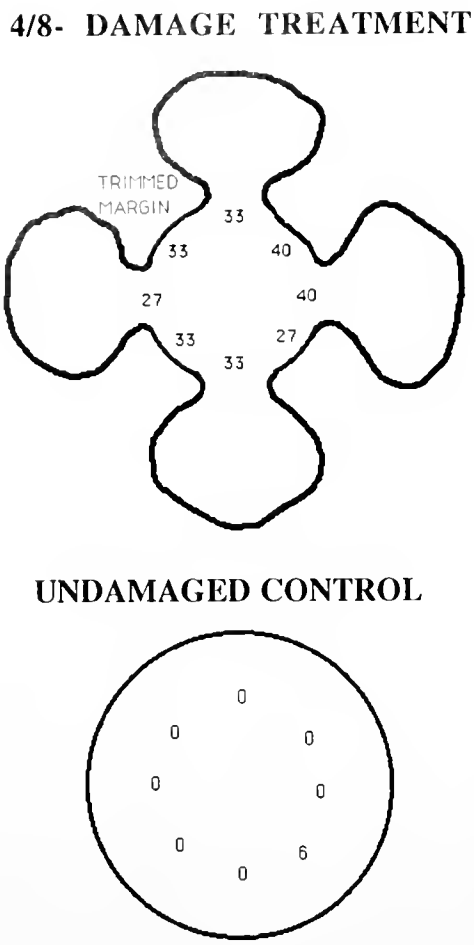

Figure 3. 4/8-damage Experiment: median percentage of colony regions producing oocytes or spermatocytes in 4/8-trim and control colonies 16 days after damage. Numbers are the median percentage of colonies producing spermatocytes or oocytes. The frequency of reproductive colonies varies in 4/8 damaged colonies relative to control colonies ($\chi^2 = 28.41$, $P = 0.00$); proximity to damage does not significantly affect reproductive timing ($\chi^2 = 0.03$, $P = 0.86$).

Proximity to damage is clearly a strong effect, the median percent of reproductive colonies is double adjacent to the damaged edge in comparison to the undamaged sides of the colony (Fig. 2).

The pattern of reproduction in the 4/8-damaged colonies was different from the 1/2-damaged colonies. All the colonies were sampled 16 days after the edge was trimmed. Although a higher proportion of trimmed colonies than untrimmed were reproductive, there was no regionalization of reproduction within the damaged colonies (Fig. 3). Our expectation was that, like the 1/2-damaged colonies, reproduction would be localized and proximal to the trimmed edges. Instead, reproduction was uniformly accelerated in all zooids sampled, irrespective of their proximity to the damaged edge. The log-linear test comparing the 4/8-damage and their controls detected no significant differences in the within colony variation, but a highly significant treatment effect, confirming a generalized increase in reproductive activity in the 4/8 damage colonies (Fig. 3).

Effects of crowding by conspecifics

In paired colonies sharing a crowded edge, the response of colonies was analogous to the 1/2-damage experiment. Zooids on the obstructed side of a colony showed a higher median percent reproduction than zooids from the unobstructed side of the colony at 8–9 days (Fig. 4). For colonies in contact for less than eight days, there were no significant differences in reproduction (Fig. 4). At 8–9 days, colonies crowded with a single conspecific began to reproduce locally near the contact point. In the log-linear test of frequencies at 8–9 days, the within colony location and the proximity terms were significant (Fig. 4).

The pattern was different at 10–13 days after contact. The frequency of reproduction was still higher on the contact side than the non-contact side. The within colony localization term was clearly significant, with the edge region in both treatments showing the highest reproduction (Fig. 4).

Compensatory growth

Patterns and rates of growth on untrimmed halves of colonies were also affected by the manipulation. We

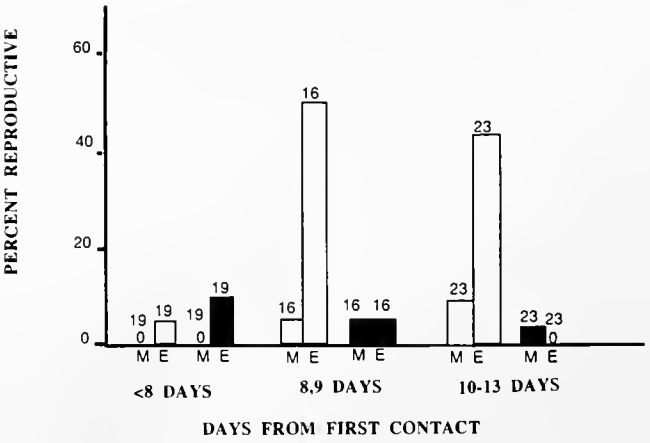

Figure 4. Crowding Experiment: median percentage of colonies producing oocytes or spermatocytes on obstructed and unobstructed sides. Open bars are obstructed sides, closed bars are unobstructed sides of colonies. Sample size at top of each bar. At <8 days post contact, neither location within colony ($\chi^2 = 0.00$, $P = 0.95$) nor proximity to conspecifics ($\chi^2 = 0.35$, $P = 0.55$) affected frequency of reproductive colonies. At 8, 9 days post contact, both location within colony ($\chi^2 = 4.99$, $P = 0.02$) and proximity to conspecific ($\chi^2 = 4.99$, $P = 0.02$) significantly affected the frequency of reproductive colonies. At 10–13 days post contact, both location within colony ($\chi^2 = 4.49$, $P = 0.03$) and proximity to conspecifics ($\chi^2 = 7.14$, $P = 0.007$) significantly affected the frequency of reproductive colonies.

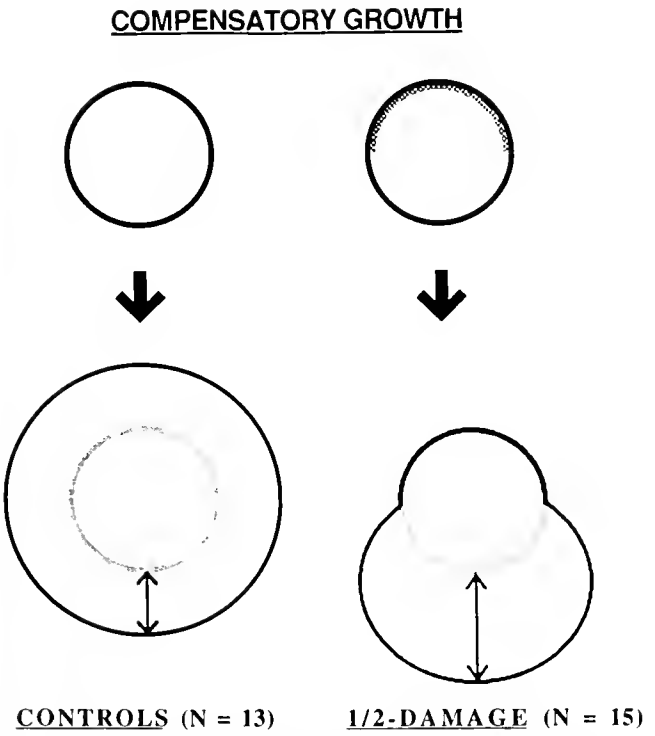

Figure 5. Diagrammatic depiction of the appearance of compensatory growth in the 1/2-damage treatment. The shaded area on the initial half-damage colonies indicates where the edge was trimmed. The compensatory growth of the half-damaged colonies was detected as a greater edge extension rate relative to an undamaged control colony.

monitored growth in the damage experiments and found that colonies responded to localized damage by directed, compensatory growth. Figure 5 shows a representation of compensatory growth defined as an increased area-specific edge extension rate. The increase in edge extension was detected on the undamaged side of 1/2-damaged colonies relative to control colonies (Fig. 6a). When growth was disrupted by trimming on one side, intact sides of the colony responded with an elevated edge extension rate. The size-specific rate of extension of a normal colony was less than the rate of extension of the untrimmed half of an experimental colony, as indicated by the difference in intercepts of the regressions of edge extension on initial area (Fig. 6a). This indicates that the undamaged edge was growing faster on damaged than on undamaged colonies. The analysis of covariance [ANCOVA] revealed a significant effect of the covariate (initial area) in the model and no significant difference in the slopes (included in the initial area*damage term) (Table Ia). The damage treatment significantly affected the intercept when the insignificant slope term was dropped from the model. Thus irrespective of colony size, the rate of edge extension is greater for previously damaged than control, undamaged colonies.

We also compared the area added to the 1/2-damage and control colonies over the same time interval. The total area added to damaged colonies was less than that added to undamaged colonies, as indicated by differences in slope of the initial area against area added plot (Fig. 6b). The ANCOVA showed significant effects of the covariate and slope differences between the two treatments (Table Ib). There was no effect of damage on the intercept in the area analysis. Colonies thus responded to trimming by not only accelerating the onset of reproduction in the damaged half, but also by accelerating growth in a direction away from the damage.

Discussion

Despite a widespread recognition that the population dynamics and biology of modular organisms differ from those of unitary organisms, on which most ecological theory is based (Harper, 1981; Jackson *et al.*, 1985; Harper *et al.*, 1986), many fundamental aspects of their biology are little studied. These aspects include the physiological integration of colonial invertebrates, the nature of the interaction between zooid and colony level processes, and particularly inter-zooid allocation phenomena. Wahle

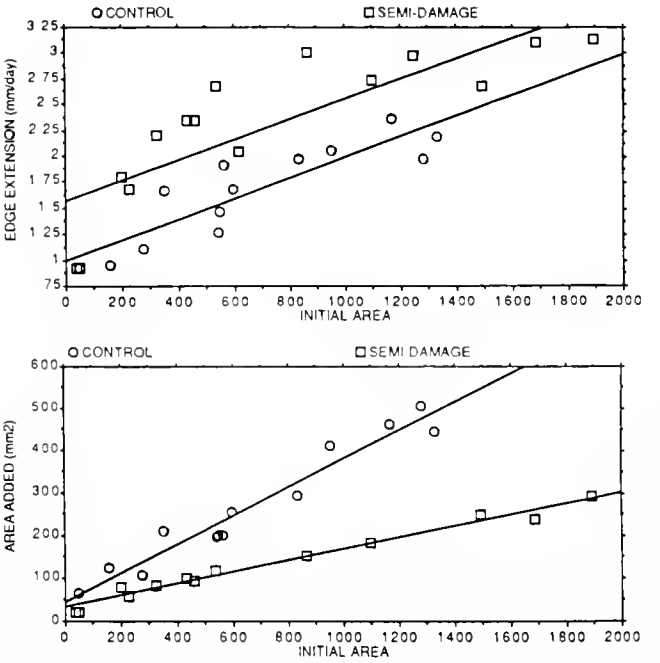

Figure 6. (Top) Compensatory growth measured as an increase in the linear extension rate in 1/2-damaged colonies. Linear regression for control colonies is $Y = 0.0001X + 0.991$ ($r^2 = .783$) and for experimental colonies is $Y = 0.00098X + 1.566$ ($r^2 = .691$). (Bottom) Compensatory growth measured as area added to 1/2-damaged and undamaged colonies. Linear equation for control colonies is $Y = 0.336X + 44.289$ ($r^2 = .972$) and for experimental colonies is $Y = 0.135X + 33.089$ ($r^2 = .978$).

Table I

Analysis of covariance [ANCOVA] on compensatory growth

SOURCE	DF	TYPE III SS	MS	F	*P*
EDGE EXTENSION					
INITAREA	1	5.110	5.110	34.97	0.000
DAMAGE	1	0.352	0.352	2.41	0.133
INITAREA*DAMAGE	1	0.075	0.075	0.52	0.478
INITAREA	1	6.389	6.389	44.58	0.000
DAMAGE	1	1.819	1.819	12.69	0.001
AREA ADDED					
INITAREA	1	326748.148	326748.148	449.62	0.000
DAMAGE	1	273.040	273.040	0.38	0.546
INITAREA*DAMAGE	1	59380.424	59380.424	81.71	0.000

The first ANCOVA result is for the data plotted in Figure 5a, the edge extension rate by colony size for damaged and undamaged colonies. Because the slope was not significantly different, the interaction term [INITAREA*DAMAGE] was deleted from the model. In the second run of the edge extension analysis, the effects of damage on the intercept are significant. The second ANCOVA result is for the data plotted in Figure 6b, the daily area added by colony size for damaged and control colonies.

(1983, 1984) showed experimentally that rates of regeneration vary in different regions within colonies of tropical gorgonians and that timing of reproduction is dependent upon colony size. Similarly, Brazeau and Lasker (1990) found gradients in the distribution of reproductive function within gorgonian colonies. Physiological and reproductive gradients have also been reported from colonies of bryozoans (Dyrynda, 1981; Harvell, 1984). However, none of these studies attempted to explain processes underlying the observed patterns. We have therefore taken the logical step of experimentally manipulating colonies to examine hypotheses about these underlying allocation processes.

Coloniality and self-regulating processes

The modular, often hierarchical, construction of colonial invertebrates permits varying degrees of integration and autonomy among the component zooids. This type of organization allows the operation of self-regulating processes among the zooids within colonies, adjusted in response to local physiological cues (Harvell, 1991). Because many colonies are large relative to the spatial grain of their environment (*e.g.,* a single colony can simultaneously experience multiple environments), the use of local cues permits partitioning of function within a colony in response to environmental variation. In plants, the flow of resources from sources to sinks provides a mechanism by which local processes such as variation in growth rate or disruption of a metabolite sink can govern the timing and location of growth and reproduction (Watson and Caspar, 1984; Marshall, 1990). In *Membranipora,* a disruption of the colony growing edge appears to accelerate the onset of reproduction in zooids proximal to that edge. We suggest that the mechanisms underlying this transition are based on a change in the strength of the sink at the distal edge of the colony. Normally, the edge, which has no actively feeding zooids and so must be subsidized by translocated metabolites from more proximal zooids, functions as a sink. Each feeding zooid must acquire carbon both for its own maintenance and for colony maintenance tasks such as growth of the margin or regeneration of lost zooids. We hypothesize that zooids reproduce proximal to a disrupted sink because they are now able to directly use more of the share of carbon normally translocated to the edge of the colony. When net carbon input to a zooid exceeds that required for maintenance, the zooid becomes reproductive. This is a simple self-organizing principle that could explain the observation of localized reproduction proximal to disrupted growth sinks within a colony.

Colony architecture and the source-sink model

In bryozoans, metabolites are transported through the funicular system, a strand of nutritive and nervous tissues that joins successive zooids in the colony (Bobin, 1977; Lutaud, 1977; Best and Thorpe, 1985). The funicular system connects adjoining zooids through pore-plate cellular junctions between the zooids. The special cells in the pore plates are morphologically polarized, suggesting that lipids are preferentially transported from proximal to distal (Bobin, 1977). Each *Membranipora* zooid is pierced by 12 communication pores, so that it is connected with each of the six zooids surrounding it. Little is known about the directions and rates of nutrient translocation in cheilostome bryozoans, but transport from central regions of the colony to the edge has been confirmed with radioisotope

tracer studies (Best and Thorpe, 1985; Miles, Harvell, Griggs, and Eisner, unpub.). Furthermore, even colonies fed near the growing edge only translocate to the nearest edge, confirming that transport is unidirectional (Miles, Harvell, Griggs, and Eisner, unpub.).

The simplest model of translocation assumes equal transport through all pores of a zooid, with rates determined by sink strength. Because axial pore plates are slightly different than lateral plates morphologically, it is not unreasonable to hypothesize higher transport axially than laterally. Both because of a bias to axial transport and because the growing margin of a colony is a strong carbon sink, transport rates should be greatest in a distal direction. In Figure 7 a hypothetical model of the direction and quantity of carbon flow through zooids for each of the sink disruption treatments is shown. Although transport is normally polarized in a proximo-distal direction, this polarity can presumably be reversed to support regrowth in proximal regions of the colony when these are damaged (Jackson and Palumbi, 1979; Harvell, 1984). When the edge sink is disrupted, the polarity of translocation should change and the flow of carbon either be redirected to the next most active sink or zooids at the edge should reproduce with the surplus carbon. In the case of the 1/2-damage treatment, the next sink is on the other side of the colony and so the response might be reverse translocation. Because the sink is so distant, the translocation is expected to be weak and zooids keep most of the carbon they take in (Fig. 7B). In the case of the 4/8-damage treatment, the next sink is adjacent to the short length of disrupted edge and is still in close proximity to zooids via the lateral pores (Fig. 7C). Thus we hypothesize that the zooids in the 4/8-damage experiment remained nonreproductive because active sinks close by continued to use metabolites. Such a mechanism would produce the results we observed: (1) the onset of reproduction in parts of the half-damage colonies, (2) the lack of regionalization in the 4/8-damage experiment, and (3) the compensatory growth observed in the 1/2-damage experiment. Although colonies in the 4/8-damage treatment showed no regionalization in timing reproduction, there was a slight increase in reproduction throughout the colony relative to the controls. This is consistent with our model; removing half the perimeter slowed down diffusion of metabolites throughout the entire colony, but no region was far enough from a sink to show localization.

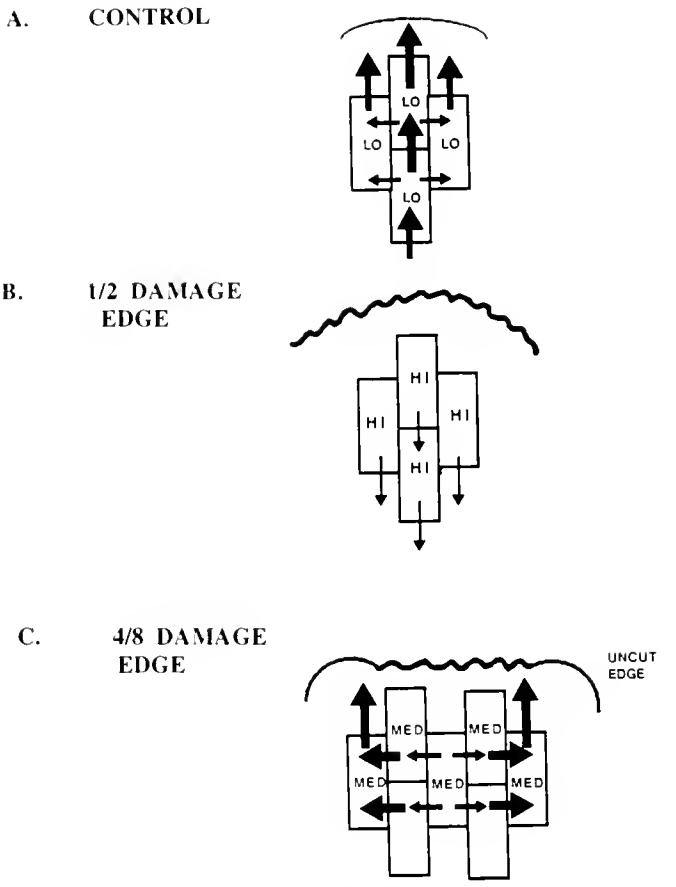

Figure 7. The source-sink model of carbon allocation in cheilostome bryozoans. The hypothesized allocation of translocate is depicted for the three experimental treatments described in this paper. A: Control, B: 1/2-damage (one half the perimeter of a colony removed in a continuous section), C: 4/8-damage (one half the perimeter of a colony removed in four alternating sections separated by four sections of undamaged perimeter). The thickness of the arrows is proportional to the quantity of carbon transported across zooidal boundaries. The labels, Lo, Med, Hi designate the relative amount of translocate retained by a zooid. Thus for control colonies, only a low proportion of the carbon is retained by a zooid. In contrast, when the sink is disrupted as in the half-damage treatment, and there is no close replacement sink, the carbon is not translocated and zooids retain a high proportion. The higher proportion of retained carbon could be used to grow gametes, thus accounting for localized reproduction in zooids adjacent to disrupted sinks. In the 4/8-damage, the original sink is disrupted but an adjacent sink still strongly affects zooid translocation.

We have demonstrated not only localized accelerations of reproduction within colonies, but also an associated and localized acceleration in edge extension rate in nondamaged regions of trimmed colonies. To our knowledge, such compensatory growth (an increased area-specific edge extension rate) has not been shown previously for colonial invertebrates. In this case, the increased edge extension rate was not sufficient to allow the damaged colonies to add the same area as the undamaged colonies of the same size. A localized increase in edge extension adjacent to an obstructed edge once again suggests an extremely plastic, colony-wide source-sink allocation budget. We hypothesize the following mechanism to account for the shift. Because the edge of the colony is normally subsidized by proximal zooids and thus represents a sink for metab-

olites, removing the edge disrupts the flow of metabolites. Some of the carbon is used locally by zooids for reproduction and some of the carbon is redirected to the nearest sink—the undamaged edge. In this situation, the undamaged edge adjacent to damage can grow more rapidly, because it is supplemented by more zooids than normal. This also suggests that normal colony growth rates are limited by metabolite availability and that if more internal zooids could be added to subsidize the edge then the colony would extend across the substrate at a greater rate.

An important consequence of modularity may be the ability to continually re-allocate the priority of resource transport among the units of a colony as the environment changes. The existence of thresholds within zooids that determine major shifts in physiology from growth to reproduction, permit zooid specialization, depending upon their location within the colony. The nutrient flow patterns we have proposed remain hypothetical, but are testable using radioisotopes to trace the fate of newly acquired carbon (Best and Thorpe, 1985; Miles, Harvell, Griggs and Eisner, unpub.). We propose that these allocation capabilities are general for cheilostome bryozoans and, in some form, for all colonial invertebrates. Further experimental work is needed to test models of energy flow through colonies in relation to taxonomic identity and levels of physiological integration.

Acknowledgments

This work was supported by NSF OCE-8796230 and OCE-8817498. Assistance with the field sampling was provided by D. K. Padilla, with data analysis by C. Griggs, and with statistical analysis by M. Geber. The manuscript was improved by comments from D. Shapiro, M. Geber, M. Bertness.

Literature Cited

Best, M. A., and J. P. Thorpe. 1985. Autoradiographic study of feeding and the colonial transport of metabolites in the marine bryozoan *Membranipora membranacea*. *Mar. Biol.* **84:** 295–300.

Bloom, A. J., F. S. Chapin, and H. A. Mooney. 1985. Resource limitation in plants—an economic analogy. *Ann. Rev. Ecol. Syst.* **16:** 363–392.

Bobin, G. 1977. Interzooecial communications and the funicular system. Pp. 307–333 in *Biology of Bryozoans*, R. M. Woollacott and R. L. Zimmer, eds. Academic Press, New York.

Braverman, M. 1974. The cellular basis of morphogenesis and morphostasis in hydroids. *Oceanogr. Mar. Biol.* **12:** 129–221.

Brazeau, D. A., and H. R. Lasker. 1990. Sexual reproduction and external brooding by the Caribbean gorgonian, *Briareum asbestinum*. *Mar. Biol.* **104:** 465–474.

Chapman, D. F., M. J. Robson, and R. W. Snaydon. 1990. Short-term effects of manipulating the source-sink ratio of white clover (*Trifolium repens* L.) plants on export of carbon from and morphology of, developing leaves. *Physiol. Plant* **80:** 262–266.

Chiarello, N. R., H. A. Mooney, and K. Williams. 1989. Growth, carbon allocation and cost of plant tissues. In *Plant Physiological Ecology: Field Methods and Instrumentation*, R. W. Peary, J. R. Ehleringer, H. A. Mooney and P. W. Rundel, eds. Chapman and Hall.

Cohen, D. 1971. Maximizing final yield when growth is limited by time or by limiting resources. *J. Theoret. Biol.* **33:** 299–307.

Crowell, S. 1957 Differential responses of growth zones to nutritive level, age, and temperature in the colonial hydroid *Campanularia*. *J. Exp. Zool.* **134:** 63–90.

Dyrynda, P. E. J. 1981. A preliminary study of polypide generation-degeneration in marine cheilostome bryozoa. In Recent and Fossil Bryozoa, G. P. Larwood and C. Nielsen, eds. Olsen and Olsen, Fredenburg, Denmark. P. 79.

Harper, J. L. 1981. The concept of population in modular organisms. Pp. 53–77 in *Theoretical Ecology: Principles and Applications*, R. M. May, ed. Sinauer Press, Sunderland, MA.

Harper, J. L., B. R. Rosen, and J. White, eds. 1986. The growth and form of modular organisms. *Phil. Trans. Royal Soc. Ser. B* **313.**

Harvell, C. D. 1984. Why nudibranchs are partial predators: intracolonial variation in bryozoan palatability. *Ecology* **65:** 716–724.

Harvell, C. D. 1991. Coloniality and inducible polymorphism. *Am. Nat.* **138:** 1–14.

Harvell, C. D. 1992. Inducible defenses and allocation shifts in a marine bryozoan. *Ecology* **73:** 1567–1576.

Harvell, C. D., and R. K. Grosberg. 1988. The timing of sexual maturity in clonal animals. *Ecology* **69:** 1855–1864.

Harvell, C. D., H. Caswell, and P. Simpson. 1990. Density effects in a colonial monoculture: experimental studies with a marine bryozoan (*Membranipora membranacea* L.). *Oecologia* **82:** 227–237.

Harvell, C. D., and D. K. Padilla. 1990. Inducible morphology, heterochrony, and size hierarchies in a colonial monoculture. *Proc. Natl. Acad. Sci* **87:** 508–512.

Hickman, C. J. 1975. Environmental unpredictability and plastic allocation strategies in the annual *Polygonum cascadense* (Polygonacea). *J. Ecol.* **63:** 684–701.

Hughes, R. N., and J. M. Cancino. 1985. An ecological overview of cloning in metazoa. Pp. 153–186 in *Population Biology and Evolution of Clonal Organisms*, J. B. C. Jackson, L. W. Buss, and R. E. Cook, eds. Yale University Press, New Haven, CT.

Jackson, J. B. C., L. W. Buss, and R. E. Cook, eds. 1985. *Population Biology and Evolution of Clonal Organisms.* Yale University Press, New Haven, CT.

Jackson, J. B. C., and S. R. Palumbi. 1979. Regeneration and partial predation in cryptic coral reef environments: preliminary experiments on sponges and ectoprocts. Pp. 303–309 in *Biologie des Spongiares*, Claude Levi and N. Bourg-Esnault, eds. Centre National de la Recherche Scientifique, Paris, France.

King, D., and J. Roughgarden. 1982. Multiple switches between vegetative and reproductive growth in annual plants. *Theoret. Pop. Biol.* **21:** 194–204.

Lang, A., and M. R. Thorpe. 1983. Analysing partitioning in plants. *Plant Cell, Environ.* **6:** 267–274.

Lutaud, G. 1977. The bryozoan nervous system. Pp. 377–410 in *Biology of Bryozoans*, R. M. Woollacott and R. L. Zimmer, eds. Academic Press, New York.

Loomis, W. F., and H. M. Lenhoff. 1956. Growth and sexual differentiation of *Hydra* in mass culture. *J. Exp. Zool.* **132:** 555–568.

Mackie, G. O. 1986. From aggregates to integrates: physiological aspects of modularity in colonial animals. Pp. 175–196 in The Growth and Form of Modular Organisms, J. L. Harper, B. R. Rosen, and J. White, eds. The Royal Society, London.

Marshall, C. 1990. Source-sink relations of interconnected ramets. In *Clonal Growth in Plants: Regulation and Function*, J. van Groenendaal and H. de Kroon, eds. Academic Publishing, The Hague, The Netherlands.

Ryland, J. S. 1981. Colonies, growth and reproduction. Pp. 221–226 in *Recent and Fossil Bryozoa*, G. P. Larwood and C. Nielsen, eds. Olsen and Olsen, Fredensburg.

Schlichting, C. D. 1986. The evolution of phenotypic plasticity in plants. *Ann. Rev. Ecol. Syst.* **17:** 667–693.

Stearns, S. C. 1989. The evolutionary significance of phenotypic plasticity. *Bioscience* **39:** 436–446.

Stearns, S. C., and J. C. Koella. 1986. The evolution of phenotypic plasticity in life history traits: predictions of reaction norms for age and size at maturity. *Evolution* **40:** 893–913.

Stebbing, A. R. D. 1980. Increases in gonozooid frequency as an adaptive response to stress in *Campanularia flexuosa*. Pp. 27–32 in *Developmental and Cellular Biology of Coelenterates*, P. Tardent and R. Tardent, (eds.). Elsevier, New York.

Wahle, C. M. 1983. Regeneration of injuries among jamaican gorgonians: the roles of colony physiology and environment. *Biol. Bull.* **165:** 778–790.

Wahle, C. M. 1984. Scaling problems in the ecology of colonial invertebrates: injury, mortality, and colony integration in gorgonian octocorals. Ph.D. Dissertation, Johns Hopkins University, Baltimore, MD.

Watson, M. A., and B. B. Caspar. 1984. Morphogenetic constraints on patterns of carbon distribution in plants. *Ann. Rev. Ecol. Syst.* **15:** 233–258

Reference: *Biol. Bull.* **184**: 296–308. (June, 1993)

Embryonic Development of the Light Organ of the Sepiolid Squid *Euprymna scolopes* Berry

MARY K. MONTGOMERY AND MARGARET McFALL-NGAI*

Department of Biological Sciences, University Park, University of Southern California, Los Angeles, California 90089-0371

Abstract. The sepiolid squid *Euprymna scolopes* maintains luminous bacterial symbionts of the species *Vibrio fischeri* in a bilobed light organ partially embedded in the ventral surface of the ink sac. Anatomical and ultrastructural observations of the light organ during embryogenesis indicate that the organ begins development as a paired proliferation of the mesoderm of the hindgut-ink sac complex. Three-dimensional reconstruction of the incipient light organ of a newly hatched juvenile revealed the presence of three pairs of sacculate crypts, each crypt joined to a pore on the surface of the light organ by a ciliated duct. The crypts, which become populated with bacterial symbionts within hours after the juvenile hatches, appear to result from sequential paired invaginations of the surface epithelium of the hindgut-ink sac complex during embryogenesis. A pair of anterior and a pair of posterior ciliated epithelial appendages, which may facilitate infection of the incipient light organ with symbiotic bacteria, develop by extension and growth of the surface epithelium. The ink sac and reflector develop dorsal to the crypts and together function to direct luminescence ventrally. These two accessory tissues are present at the time of hatching, although changes in their overall structure accompany growth and maturation of the light organ. A third accessory tissue, the muscle-derived lens, appears during post-hatch maturation of the light organ.

Introduction

The presence in cephalopods of light organs that harbor luminous bacterial symbionts has been reported in at least 26 species from 5 genera of sepiolids (*Euprymna, Inioteuthis, Rondeletiola, Semirossia* and *Sepiola*) and in at least 5 species from 2 genera of loliginids (*Loligo* and *Uroteuthis*) (Herring, 1988). Although the light organs may have evolved independently in these two families (Sepiolidae and Loliginidae), they are all associated with the ink sac, which is located in the center of the mantle cavity. These organs are typically large and in certain species may have a length equal to 30% that of mantle length (Herring *et al.*, 1981). The bacterially produced light emitted from the organ is thought to function in counterillumination, a behavior whereby the animal emits light of the same wavelength and intensity as downwelling light to camouflage its silhouette from predators below (Herring *et al.*, 1981). Although these light organs occupy a substantial portion of the mantle cavity and are important in the animal's behavior, little is known about their embryonic development.

Euprymna scolopes, a small benthic squid (average mantle length of adults = 22 mm) indigenous to Hawaii (Berry, 1912; Singley, 1983), maintains luminous bacterial symbionts of the species *Vibrio fischeri* (Boettcher and Ruby, 1990) in a bilobed light organ (Wei and Young, 1989; McFall-Ngai and Montgomery, 1990). The mature light organ of *E. scolopes* and of other closely related sepiolids is embedded in the ventral surface of the ink sac and is composed of several host tissues that include a reflector, a muscle-derived lens, and a core of tissue that houses the bacteria (Herring *et al.*, 1981; McFall-Ngai and Montgomery, 1990). This tissue that contains the symbionts is composed of cavities lined with epithelial cells, in which the bacteria are maintained, and supportive connective and vascular tissue.

Several aspects of the reproductive biology of *Euprymna scolopes* make this species particularly amenable to developmental studies. Adult females, which mature in four to six months (Singley, 1983), are present in the field throughout the year. Mature squids readily mate in cap-

Received 30 November 1992; accepted 25 March 1993.

* Corresponding author.

tivity, and females maintained in the laboratory typically lay clutches of 50 to 200 eggs on pieces of dead coral or on the walls of their tanks (Singley, 1983). Females of *E. scolopes* may lay several clutches of eggs at intervals of several days to a few weeks, unlike many cephalopod species in which the female dies soon after a single reproductive effort. Embryonic development of *E. scolopes* is temperature dependent, and juveniles typically hatch 21–22 days after eggs are layed when maintained at 23°C (Wei and Young, 1989; pers. obs.) and within 20 days at 24°C (Arnold *et al.*, 1972).

The light organ of a newly hatched *Euprymna scolopes* does not contain bacterial symbionts but becomes infected within hours post-hatch by symbiotic bacteria present in seawater that is pumped through the mantle cavity in the normal ventilatory process (Wei and Young, 1989; McFall-Ngai and Ruby, 1991). Symbionts enter the incipient light organ through several pores and, within 24 hours post-infection, populate cavities lined by epithelial cells (McFall-Ngai and Ruby, 1991). During initiation and establishment of the symbiotic association, the light organ undergoes a series of morphogenetic events that results in a fully differentiated structure in which the bacterial symbionts are presumably maintained under steady state conditions (McFall-Ngai and Ruby, 1991; Ruby and McFall-Ngai, 1992). Previous work indicates that the light organ of juveniles remains in a state of arrested morphogenesis until it is exposed to, and inoculated with, a competent strain of symbiotic bacteria (McFall-Ngai and Ruby, 1991; Montgomery and McFall-Ngai, 1991).

Although the general embryonic development of *Euprymna scolopes* has been described (Arnold *et al.*, 1972), development of the light organ has remained undescribed. Light organ development in *E. scolopes* appears similar to that described by Pierantoni (1918) for *Sepiola intermedia* Naef, a closely related species found in the Mediterranean. Pierantoni reported that the light organ rudiment developed from the outer epithelium and underlying tissues of the ink sac-hindgut complex. The present paper provides the first ultrastructural study of cephalopod light organ development and offers a basis of comparison between development in the Hawaiian sepiolid squid, *E. scolopes*, and that in the Mediterranean species, *S. intermedia*, described by Pierantoni 75 years ago. Additionally, by providing an understanding of the embryonic development of the tissues that comprise the juvenile light organ, we will be better able to ascertain the effect of the bacterial symbionts on post-hatch morphogenesis.

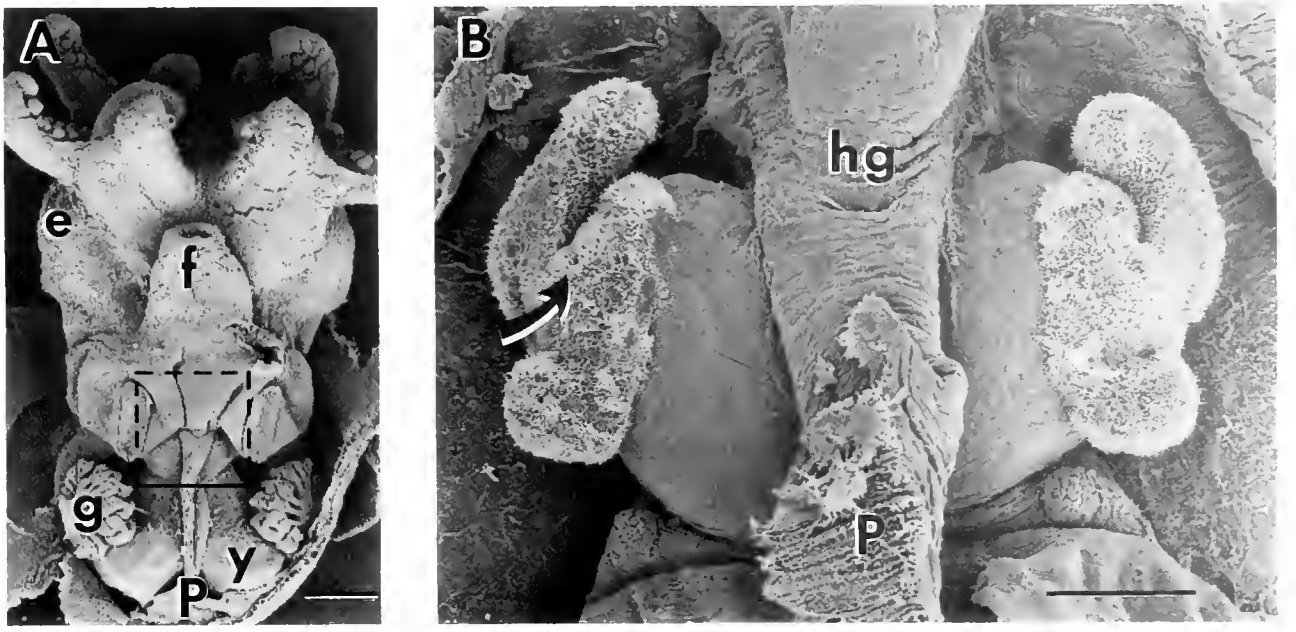

Figure 1. Scanning electron micrographs of juvenile *Euprymna scolopes*. A. Ventral view of a newly hatched squid, in which the mantle has been removed to expose the mantle cavity. Most of the light organ (within dashed box) is located inside the funnel so that seawater circulates through the mantle cavity and passes over the light organ before exiting. Scale bar = 250 μm. B. Ventral view of the light organ of a newly hatched squid (both the mantle and funnel have been removed). The lateral face of each side of the light organ is ciliated. Paired anterior and posterior epithelial appendages extend into the mantle cavity. The arrow indicates the direction of flow of seawater over the organ and points to one of the pores, located near the base of the appendages, that open into the interior of the organ. The hindgut lies directly on top of the organ. Bar scale = 100 μm. (e, eye; f, funnel; g, gill; hg, hindgut; y, internal yolk sac; P, posterior).

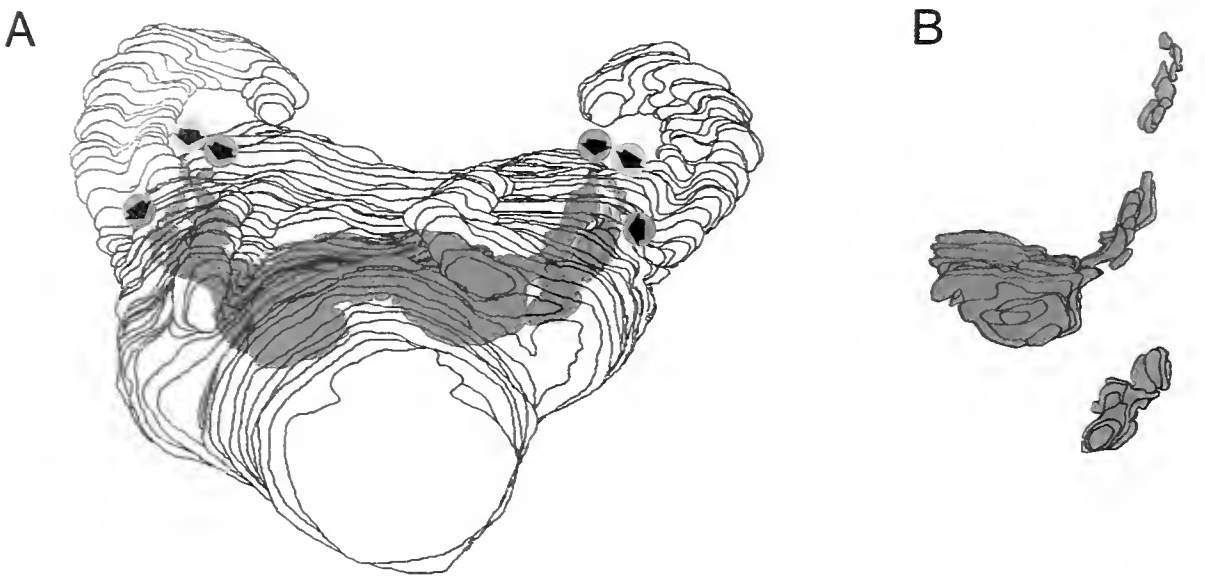

Figure 2. Three-dimensional reconstruction of the light organ of a newly hatched juvenile. A. The light organ is shown in ventral view, anterior end at top. The black lines represent the contours of the surface of the organ. Lying within the organ are three pairs of crypts, represented by three separate colors (blue, red, and green). Each crypt communicates with the mantle cavity through a pore (arrows) present on the ventral surface of the organ near the base of the ciliated arms. B. Exploded view of the crypts from one half of the light organ shown at left. The crypts are differently sized with the smallest one, represented in blue, located anterior to the two larger crypts. The medium-sized crypt, represented in green, is located posterior to the other two crypts, whereas the largest crypt, represented in red, is located in the middle.

Materials and Methods

Adult specimens of *Euprymna scolopes* were collected by dipnet from shallow sandflats in Kaneohe Bay, Oahu in Hawaii throughout 1990 and 1991. The animals were maintained either in running seawater aquaria or in a 250 l recirculating aquarium and on a 12 h light:12 h dark cycle. Mating pairs were placed in individual tanks and females were provided with pieces of dead coral on which to lay eggs. Clutches were removed from the large recirculating aquarium soon after being laid and were placed in smaller aquaria in which the temperature was maintained at 23°C. At various stages of development, embryos were taken from the clutch for analyses.

Embryos and newly hatched juveniles were fixed for light microscopy in 10% formaldehyde in 0.5 *M* sodium phosphate buffer (pH 7.4) at room temperature for 24 h. The embryos were removed from their egg capsule, jelly coats, and chorion with forceps before fixation. Embryos and juvenile squids were fixed for transmission electron microscopy (TEM) in 2.5% glutaraldehyde in 0.1 *M* sodium cacodylate buffer with 0.45 *M* NaCl (pH 7.4) at room temperature for 12 h and post-fixed for 1 h in 1.0% osmium tetroxide in the same buffer as the primary fixative. Following fixation, specimens were rinsed, dehydrated through an ethanol series, cleared with propylene oxide, and embedded in Spurr's resin as previously described (Spurr, 1969; McFall-Ngai and Montgomery, 1990). Ultrathin sections were cut on a Porter Blum MT2-B ultramicrotome with a diamond knife, mounted onto uncoated copper mesh grids, stained with aqueous uranyl acetate and lead citrate, and examined with a JEOL CX-100 transmission electron microscope at 80 kV. Histological sections, 1 to 1.5 μm in thickness, were cut on the same microtrome and stained with Richardson's stain (Richardson *et al.*, 1960).

Embryos and newly hatched juveniles were fixed for scanning electron microscopy (SEM) in 5% formaldehyde in filtered seawater (FSW) at room temperature for 24 h. Specimens were rinsed in FSW, dehydrated through an ethanol series, and dried by the critical point method. Before sputter coating with gold, the ventral portion of the mantle and any other overlying structures (such as the funnel and gills) were carefully removed to expose the underlying light organ rudiment. Specimens were examined with a Cambridge 360 scanning electron microscope.

Three-dimensional images of light organs from embryos and juveniles fixed for light microscopy were constructed using a computer program (PC3D Three-Dimensional Reconstruction Software, Jandel Scientific, Corte Madera,

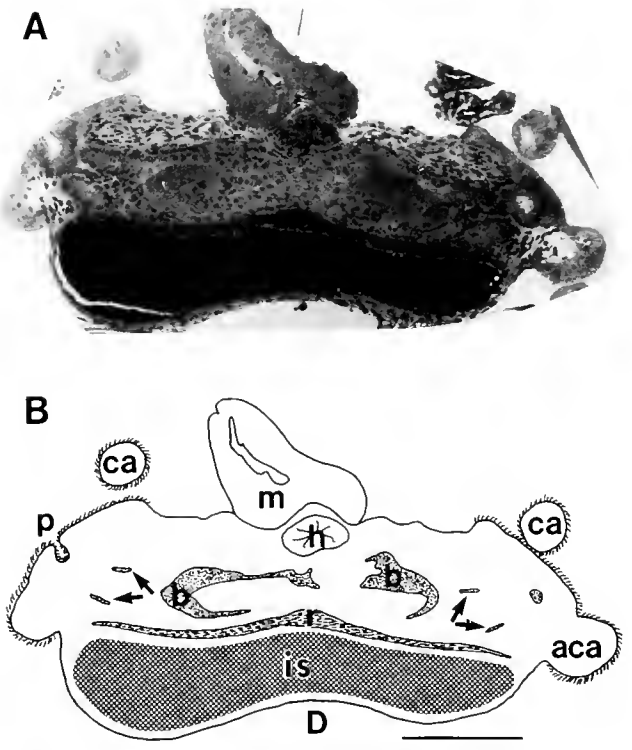

Figure 3. Cross section through the light organ of a juvenile 24 h post-hatch. A. Light micrograph of 1.5 μm section. B. Diagram to indicate the relationships among the light organ components. One of the six pores on the ventral surface of the organ is shown; each pore opens into a ciliated duct that leads to an epithelium-lined cavity or crypt. Each crypt (arrows, b) is populated with luminous bacterial symbionts that infected the juvenile squid shortly after it hatched. Scale bar = 100 μm. (aca, anterior ciliated epithelial appendage; b, bacteria; ca, [posterior] ciliated epithelial appendage; D, dorsal; h, hindgut; is, ink sac; m, muscle; p, pore; r, reflector).

California). Serial cross sections 1.0 or 1.5 μm thick of epoxy-embedded material were used for the reconstructions. Either every second or fourth section, depending on the thickness of the sections and the stage of development, was photographed using a Zeiss RA-16 compound microscope with an Olympus photosystem. From the photographs, the outlines of major tissues and structures, such as the surface epithelium, the ink sac, and the lumen of the crypts were digitized with a Numonics 2210 digitizing tablet. The PC3D software stacked the outlines of specific components from each section, producing a three-dimensional (3-D) representation of the light organ rudiment that could be viewed in any orientation. The PC3D software allowed the calculation of the volumes of specific light organ components. The 3-D images shown were plotted on a Hewlett-Packard HP 7475 A plotter.

Light organ length and mantle length (ML) of newly hatched juveniles were measured using an ocular micrometer on a Wild M5 dissecting scope. ML was measured as defined by Young and Harman (1989) for octopodid paralarvae; light organ length as defined here is the distance from the posterior tip of the ink sac to the anterior tip of the ink sac. The developmental stages referred to here (*e.g.*, A25) are those of Arnold *et al.* (1972).

Results

Reproductive biology

Similar to a previous report (Singley, 1982), individuals of *Euprymna scolopes* under laboratory conditions were nocturnally active and usually remained buried in sand during daylight hours. Adult males were observed mating with females on several nights. Each female laid one to several clutches of eggs, all at night with the exception of one case. In this case, a female layed eggs during daylight hours, which allowed observations of the egg laying process. The female layed the clutch on the side of a piece of dead coral. Each egg was laid down one at a time at approximately one-minute intervals. Between the laying of each egg, the female used her fins to blow sand grains into the space between her arms. Each egg was expelled out the mantle and into the space between the female's arms, where the egg was coated with the sand grains. The egg was slowly moved between the female's extended arms to near the tips; it was then positioned on the clutch. The female appeared to place the eggs fairly randomly on the clutch. If this process is typical of egg laying in this species, then it takes over three hours for a female *E. scolopes* to lay a clutch of 200 eggs.

Following Arnold *et al.* (1972), fertilization was assumed to take place at the time of egg laying, which was designated Day 1. *E. scolopes* individuals reared at 23°C and in a 12 h light:12 h dark regime typically hatched on Day 21. Newly hatched juveniles had an average ML of 1.6 ± 0.1 mm (±S.D., n = 12).

General description of the light organ of newly hatched juveniles

To facilitate an understanding of the embryonic development of the various components of the light organ, the structure of these components as they appear in the light organ of a newly hatched juvenile is described first. The light organ of newly hatched juveniles is located in the center of the mantle cavity, largely within the funnel (Fig. 1A). Based on measurements of live specimens (n = 12), the light organ of newly hatched juveniles averaged 500 ± 45 μm (±S.D.) in light organ width and 390 ± 48 μm (±S.D.) in anterior-posterior length, which was equal to 24 ± 2.5% ML (±S.D.). Scanning electron microscopy revealed that the light organ of the newly hatched juvenile includes a pair of posterior and a pair of anterior ciliated epithelial appendages (Fig. 1B). The anterior appendages are approximately 500 μm in length and 50 μm in width

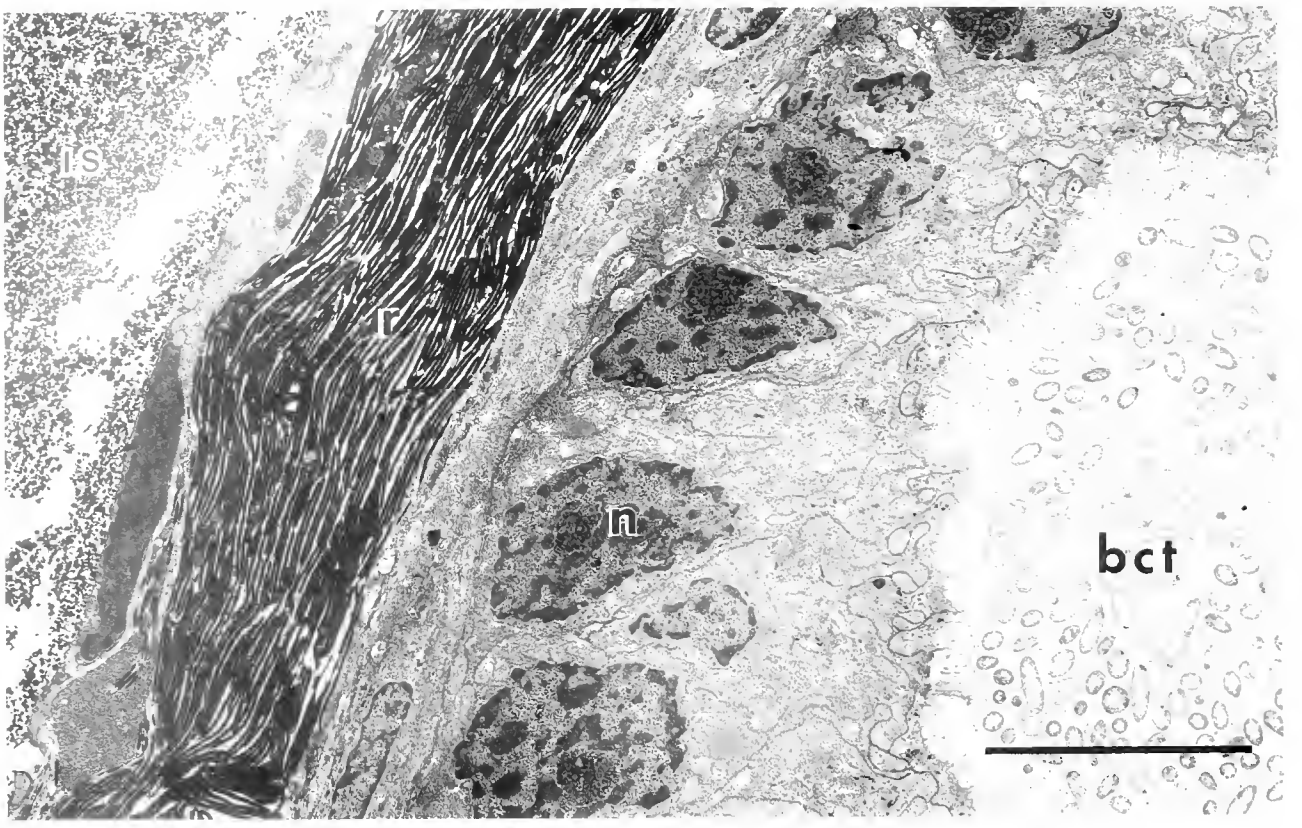

Figure 4. Transmission electron micrograph of the light organ of a juvenile 24 h post-hatch. The crypts, populated with bacterial symbionts, are lined with a simple cuboidal epithelium whose apical surface bears an extensive brush border of microvilli. This epithelial cell layer is surrounded by a layer of blood vessels and connective tissue. The reflector is composed of several layers of electron-dense platelets, and is immediately adjacent to the ink sac whose inner surface is composed of a simple squamous epithelium. Scale bar = 10 μm. (bct, bacteria; is, ink sac; n, nucleus of epithelial cell; r, reflector).

based on measurements of live specimens with a compound microscope. (Tissue shrinkage with SEM is 25–30% in the linear dimension.) TEM revealed that the appendages and surrounding ciliated surface are formed from cells of the surface epithelium, each cell possessing numerous cilia averaging 20 μm in length and 300 nm in width. Each cilium is surrounded by several microvilli 1–2 μm in length and 70–115 nm in width, whereas microvilli on adjacent non-ciliated surface epithelium were considerably shorter, ranging from 0.3 to 0.6 μm in length. On the surface of the light organ are several pores (3 on each side), ranging from 5 to 15 μm in diameter, that lead into the interior of the organ (Fig. 1B).

Three-dimensional reconstruction of the light organ of a newly hatched juvenile revealed that each pore leads into a separate epithelium-lined cavity or crypt (Fig. 2A); these pores, present on the ventral surface of the organ near the base of the epithelial appendages, connect the crypts to the mantle cavity. The three pairs of crypts, which are roughly bilaterally symmetrical, are different in size. On each side of the incipient light organ the smallest crypt is located most anterior, the medium-sized crypt is most posterior, and the largest crypt is situated between the two smaller ones (Fig. 2B). This pattern of number, size, and position of the crypts was similar in all juveniles examined (n = 14).

The bacterial symbionts populate the extracellular lumen of the crypts following infection of the light organ (Fig. 3). A ciliated duct connects each crypt with a pore on the surface of the organ (Fig. 3). A simple cuboidal epithelium forms the crypt; these epithelial cells contain numerous mitochondria in the region between the basally located nucleus and the apical surface, which, like the appendages, possesses extensive microvilli 1–2 μm in length (Fig. 4). A cell layer of endothelium and connective tissue underlies the epithelium.

The entire dorsal surface of the bacteria-containing tissue is covered by a reflector and the ink sac (Fig. 4), which function together to control light emission from the organ and to direct the bacterially produced light ventrally. The reflector is composed of iridosomal platelets, which are produced by cells known as iridophores (Arnold, 1967).

Table I

Developmental events of the light organ of Euprymna scolopes *during embryogenesis**

Stage	Embryological day	Developmental event
A25	10	paired lateral mesoderm of hindgut-ink sac complex begins to proliferate
A26	13	anterior epithelial appendage begins to form; first pair of crypts begins formation
A27	15	anterior and posterior appendages are evident and partially ciliated; epithelial cells of crypts form extensive brush borders; cells toward site of future ducts form cilia; reflector cells begin to differentiate
A28	17	second pair of crypts begins formation; epithelial cells forming crypts appear fully differentiated; many reflector cells differentiated; ink cells are functional
A29	19	third pair of crypts begins formation
A30	21	three crypts are present on each side; entire lateral surface of each side of light organ is ciliated

* Embryos incubated at 23°C; stages according to Arnold *et al.* (1972).

The reflector in the light organ of a newly hatched juvenile is typically 20 to 30 platelets in thickness. The inner lining of the ink sac is composed of a simple squamous epithelium; this epithelium, with the exception of the ventral surface where the crypts of the light organ are situated, is surrounded by mesodermally derived connective tissue and muscle cells, and an outer epidermally derived epithelium. The lens is not yet differentiated in the newly hatched juvenile.

Embryonic development

The light organ begins to develop by stage A25/Day 10, three days after the onset of organogenesis (Table I). At this stage of development, the embryo is 600 μm in total length and only 200 μm in ML. The light organ rudiment appears as a paired proliferation of the mesoderm of the ink sac-hindgut complex (Fig. 5). The ink sac appears as a relatively small outpocketing of the hindgut, in which one or two folds of the ink sac inner epithelium mark the beginning of ink sac gland formation.

The epithelial appendages. The epithelial appendages form by extension and growth of the outer surface epithelium of the light organ rudiment. Scanning electron microscopy revealed that the anterior epithelial appendages begin to form by stage A26/Day 12 (Fig. 6A). In addition, a pore on the surface of the light organ rudiment is apparent and signals the onset of formation of the first pair of crypts (Fig. 6B). By stage A27/Day 15, both appendages are evident and both bear cilia, although much of the rest of the lateral surface of the light organ remains without cilia (Fig. 6C). By stage A29/Day 19, the entire lateral surface of each side of the light organ rudiment is covered with cilia. Small blood sinuses and a few mesodermal cells are evident by Day 17 (stage A28) in cross sections of these appendages (Fig. 6E).

The crypts. Three-dimensional reconstructions of the light organ rudiments of embryos (one per stage) indicate

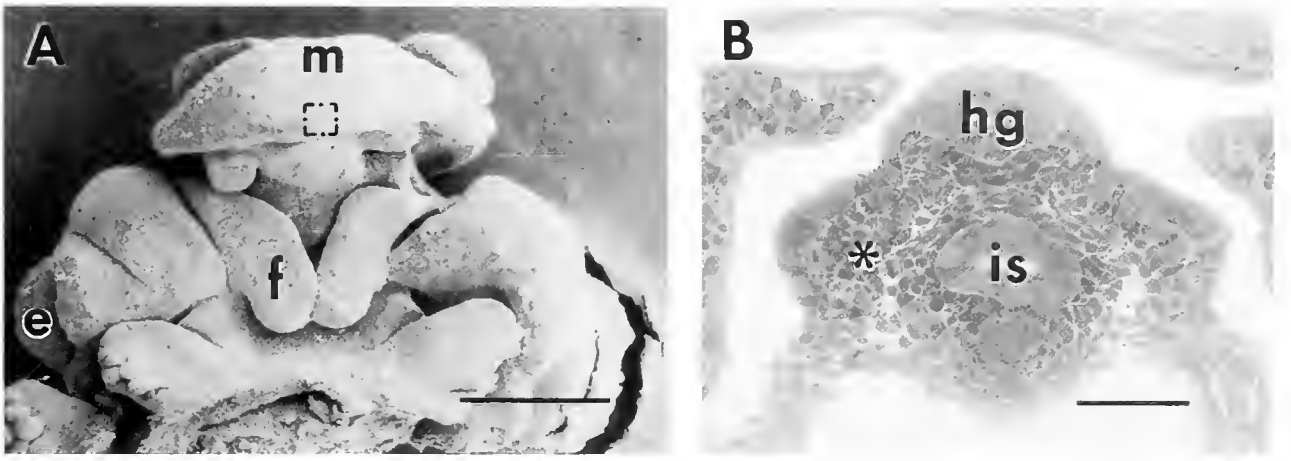

Figure 5. *Euprymna scolopes* at embryonic stage A25/Day 10. A. Scanning electron micrograph of the ventral surface of an embryo, animal pole at top. The eyes and funnel folds are prominent. Although the mantle is small relative to the rest of the embryo, the fin primordia and the gill primordia are evident (just visible under the mantle). The dashed box represents the site of the light organ rudiment hidden by the mantle. Scale bar = 100 μm. B. Light micrograph of a histological cross section through the light organ rudiment, which begins development at this stage as a paired proliferation of the mesoderm (*) of the hindgut-ink sac complex. Scale bar = 20 μm. (e, eye; f, funnel fold; hg, hindgut; is, ink sac; m, mantle).

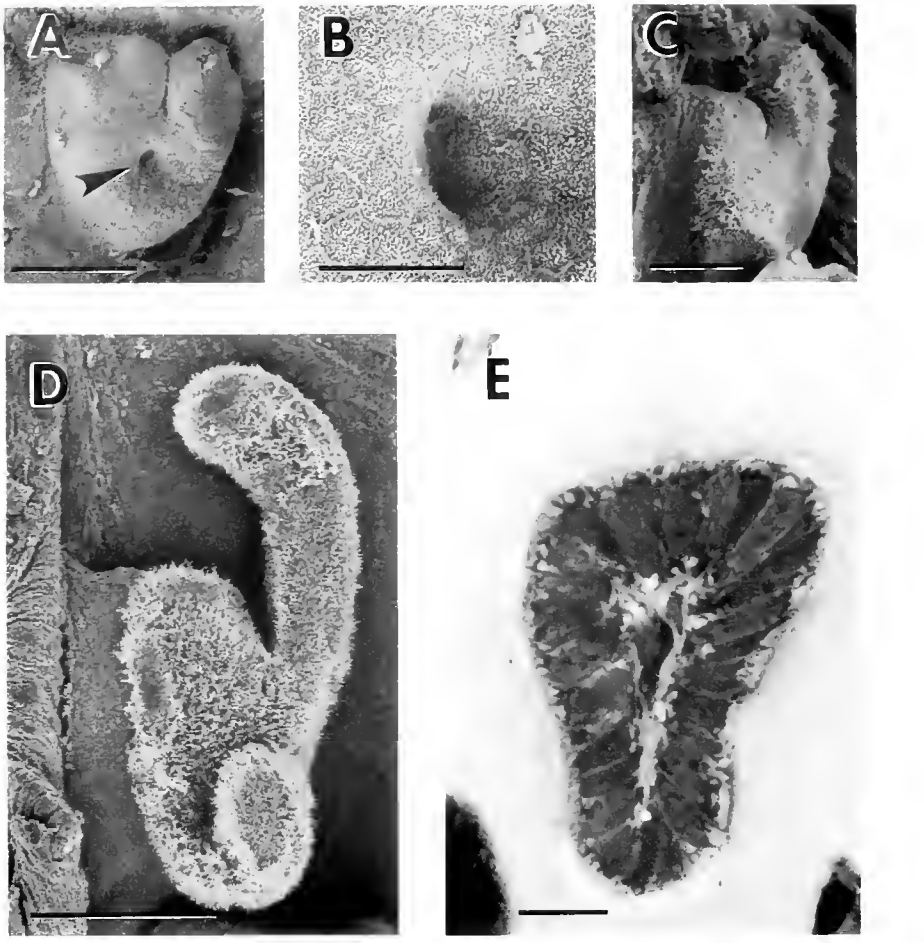

Figure 6. Development of the ciliated epithelial appendages on the light organ of *Euprymna scolopes*. A. Scanning electron micrograph (SEM) of one side of the light organ rudiment from a 12-day embryo (stage A26). The anterior appendage is just beginning to form, although the surface is not yet ciliated. The surface epithelium is beginning to invaginate (arrow), leading to the formation of the first crypt. Scale bar = 50 μm. B. High magnification SEM of the pore shown in "A." Scale bar = 10 μm. C. SEM of one side of the light organ rudiment from a 15-day embryo at stage A27. Scale bar = 50 μm. D. SEM of one side of the light organ rudiment from a newly hatched juvenile (stage A30). Scale bar = 100 μm. E. Histological cross section through the epithelial appendage of a 17-day embryo at stage A28. Scale bar = 10 μm.

that the first pair of crypts appears by stage A27/Day 15 (Fig. 7). Two days later (stage A28), the second pair of crypts has begun to form; but, not until stage A29/Day 19 does the third pair appear as two small pits in the surface of the light organ rudiment. The crypts continue to enlarge throughout embryonic development, resulting in a total volume of almost 750 pl in a newly hatched juvenile (Table II); because tissue shrinkage due to fixation has occurred, the actual lengths and volumes of these light organ components may be substantially larger. Measurements of ML of 10 fixed and embedded specimens averaged 1.3 ± 0.1 mm (±S.D.); light organ length of these specimens averaged 310 ± 51 μm (±S.D.), and light organ width averaged 409 ± 48 μm (±S.D.). Thus, compared to measurements of live specimens (see *General description of light organ of newly hatched juvenile*), shrinkage in the linear dimension is approximately 20%. Assuming that the volumes of the crypts and other light organ components shrink accordingly, then the volume calculations may underestimate true volumes by as much as 50%.

The crypts begin formation relatively late in embryonic development and undergo an exponential increase in volume, as compared to light organ length, which increases linearly (Table II; Fig. 8). The apparent growth rate of the crypts is three to four times that of the whole light organ (Fig. 8b). Even when the total volume of the crypts is normalized against ink sac volume to control for variation in size, there is an apparently exponential increase between stage A28/Day 17 and stage A29/Day 19 (Table II).

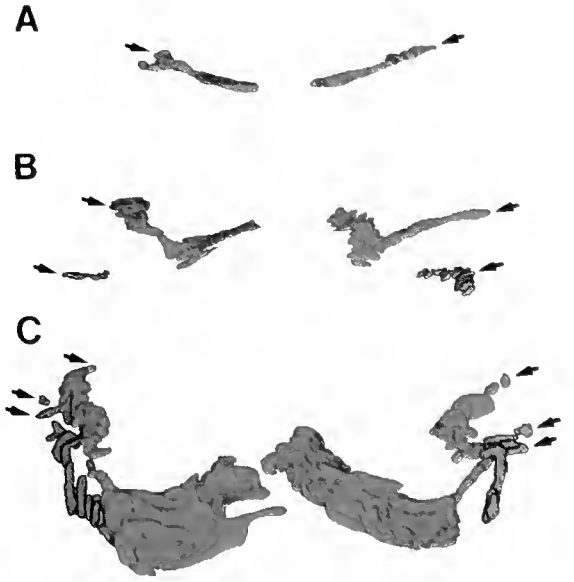

Figure 7. Growth in size and number of the crypts of the light organ during embryogenesis as revealed by three-dimensional reconstructions. A. Embryonic stage A27/Day 15. The first pair of crypts (red) is evident as a pair of thin channels. B. Embryonic stage A28/Day 17. The first pair of crypts (red) has enlarged and a second pair (green) posterior to the first is beginning to form. C. Embryonic stage A29/Day 19. The first two pairs of crypts (red, green) continue to enlarge while the third pair of crypts (blue) is just evident as two pits in the surface epithelium. (arrows, pores).

The epithelium lining the crypts is well differentiated by Day 16 (*ca.* stage A28) (Fig. 9). The cells of the epithelium, although columnar in shape, are similar to those from the light organs of newly hatched juveniles. They are polarized with basally located nuclei and an extensive brush border at the apical surface. Numerous mitochondria are located in the apical region of these cells.

The accessory tissues. The ink sac is apparent by stage A25/Day 10 as an outpocketing of the hindgut. The iridosomal platelets of the reflector are first evident at stage A26/Day 14 (Fig. 10A, B). The iridophores develop from cells immediately adjacent to the ink sac epithelium (Fig. 10A); the iridosomal platelets appear to form from the condensation of electron-dense material (Fig. 10B). At this stage the epithelial cells lining the inner surface of the ink sac are roughly cuboidal and are not yet producing ink. By stage A27/Day 16 (Fig. 9A), the reflector is several platelets thick, and ink is accumulating. By stage A29/Day 19, two to three days prior to hatching, the inner lining of the ink sac (Fig. 10C) resembles the typical squamous epithelium of the ink sac of a mature animal. The reflector of living specimens, when viewed directly, is visible as a silver lining on the ventral surface of the ink sac, and is 20 to 30 platelets in width, each platelet between 100 and 150 nm in thickness (Fig. 10D). The light organ lens is not yet present when the juvenile hatches.

Discussion

Embryogenesis in *Euprymna scolopes* results in a light organ that appears primarily structured to facilitate initiation of the symbiosis with *Vibrio fischeri*, whereas the mature light organ primarily functions to maintain the bacterial symbionts and control luminescence. The light organ develops from the recruitment and elaboration of tissues associated with the hindgut-ink sac complex. Tissues that will directly interact with symbiotic bacteria are well developed at the time the juvenile squid hatches, whereas accessory tissues are either not differentiated or not fully elaborated.

Early light organ development

Our observations indicate that light organ development during embryogenesis in *Euprymna scolopes* is similar to light organ development in the closely related sepiolid, *Sepiola intermedia*, as described by Pierantoni (1918). However, our study reveals differences in the order and interpretation of certain developmental events. In both species, the light organ rudiment begins development approximately halfway between the time of fertilization and hatching as a paired proliferation of the mesoderm within the hindgut-ink sac complex. At this stage (A25/Day 10), the ink sac is just beginning to form as a small outpocketing of the hindgut. (For a review of midgut and hindgut development in cephalopods, see Boletzky, 1967, and Raven, 1958.) Pierantoni (1918) reported that the first evidence of light organ development in *S. intermedia* is the presence of two ciliated zones in the epithelium surrounding the visceral sac in the mantle cavity latero-ventral to the anal opening. Although the light organ in *E. scolopes* begins to develop at a similar site, the light organ rudiment has undergone significant development prior to the appearance of cilia. Both the epithelial appendages and the first pair of crypts begin to develop two to three days prior to the appearance of cilia.

The epithelial appendages

The ciliated epithelial appendages comprise a large portion of the incipient light organ of newly hatched *Euprymna scolopes*. Pierantoni (1918) reported the presence of ciliated "zones" on the surface epithelium of the light organ rudiment in *Sepiola intermedia*, although he does not describe their structure or the presence of appendages that extend into the mantle cavity. The epithelial appendages of the light organ of *E. scolopes*, which consist of a longer anterior pair and a shorter posterior pair, may

Table II

Measurements of developing light organs and light organ components based on three-dimensional reconstructions

	Embryonic Stage of Development			
	A27	A28	A29	A30 (newly hatched)
Anterior-posterior length of light organ (μm)	150	210	275	325
Relative light organ length (%)	46.2	64.6	84.6	100.0
Absolute volume (picoliters)				
Total light organ	1177	3920	5133	13,200
Lumen of crypts, Total	1.5	8.1	132.0	741
Crypt pair 1	1.5	7.0	123.0	622
Crypt pair 2	0.0	1.1	8.5	102
Crypt pair 3	0.0	0.0	0.5	17
Relative volume (%)				
Lumen of crypts, Total (as % of ink sac)	0.6	0.9	12.6	14.1
(as % of total crypts from newly hatched juvenile)	0.2	1.1	17.8	100.0
Total light organ	8.9	29.7	38.9	100.0

aid in the infection process (McFall-Ngai and Ruby, 1991). The appendages develop by extension and growth of the outer surface epithelium which originates from the single cell-layered ectoderm.

The cells of tissues that appear to directly interact with the symbiotic bacteria, *i.e.*, the epithelial appendages and the epithelial cells that form the crypts, contain numerous microvilli that are two to three times longer than in epithelial cells immediately adjacent. These microvilli from cells lining the cavities are also two to three times longer than those of secretory epithelial cells of the dorsal epidermis in *Euprymna scolopes* (Singley, 1982), but are similar in size to microvilli in mammalian intestinal epithelium (Fawcett, 1986). Although the cilia on the appendages apparently function to facilitate transport of bacteria toward the pores (see McFall-Ngai and Ruby, 1991), the function of the microvilli is uncertain. It is possible that the microvilli on the cells of the appendages increase cell surface contact with potential symbiotic bacteria and may function in recognition and specificity during the infection process.

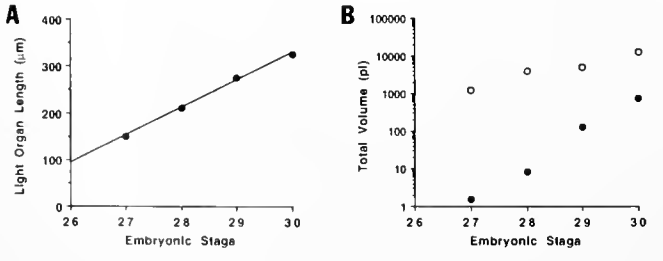

Figure 8. A. Changes in light organ length during embryonic development. Measurements based on fixed specimens used for three-dimensional reconstructions. B. Changes in volume of total light organ (open circle) and total crypts within a light organ (closed circles) during embryonic development. Volumes based on calculations from three-dimensional reconstructions (see text).

The crypts

Pierantoni (1918) described invaginations of the ciliated surface epithelium of the light organ in *Sepiola intermedia* that give rise to the tubules that eventually house the bacterial symbionts. Our observations of light organ development in *Euprymna scolopes* also indicate that the crypts form from invaginations of the surface epithelium; crypts observed were always joined to a pore on the surface of the organ, even in the earliest stages of development when they were present as simple pits in the outer epithelium (Fig. 7). The pattern (number, size and position) of the crypts in the light organs of newly hatched juveniles is remarkably consistent. The differences in the sizes of the crypts appear to be the result of each pair beginning formation several days apart, so that the largest pair of crypts begins formation approximately eight to ten days (stage A26) before hatching, whereas the smallest pair does not begin formation until just one to two days before hatching (stage A29). Whether the smallest pair, whose volume is little more than 2% that of the largest pair (Table I), serves any function during initiation of the symbiosis is unclear. Nonetheless, if the same growth rate for the crypts is maintained post-hatch, the size of each crypt may double almost daily. Pieratoni (1918) does not report on the numbers of pores or tubules present in the light organs of newly hatched *S. intermedia*. He indicates that the surface epithelium first becomes ciliated before formation of the tubules (*i.e.*, crypts). In contrast, our observations of *E. scolopes* indicate that the first pair of crypts begins to

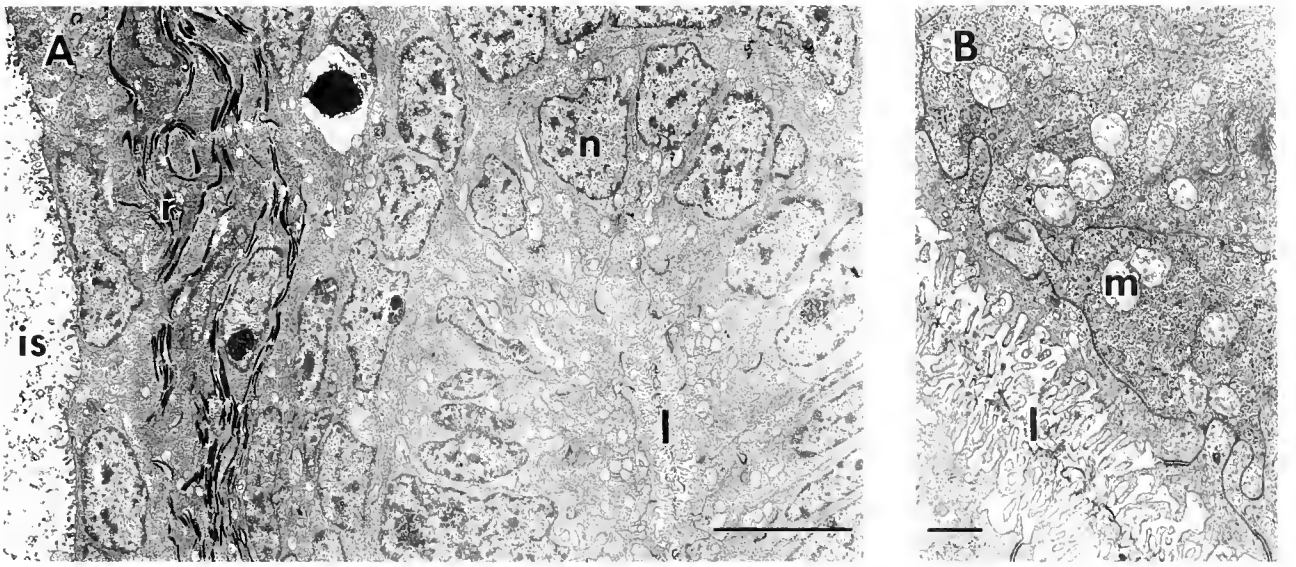

Figure 9. Transmission electron micrographs of the light organ rudiment from a 16-day embryo (*ca.* stage A28). A. Low magnification view of the epithelium forming the crypts and of surrounding cell layers. The epithelium at this stage is well differentiated, with polarized cells that are similar to those from the light organs of newly hatched juveniles. The nuclei are located toward the basal region of these cells, whereas the apical portion contains numerous mitochondria and bears an extensive brush border. Scale bar = 10 μm. B. High magnification view of the epithelial cells of the same tissue shown in "A" revealing the typical structure of the microvilli and the numerous mitochondria present in the apical portions of these cells. Scale bar = 1 μm. (is, ink sac; l, lumen of crypt; m, mitochondrion; n, nucleus of epithelial cell; r, reflector).

form two to three days before any surface epithelial cells are ciliated.

The accessory tissues

Development of the light organ rudiment from the hindgut-ink sac complex results in its central position in the mantle cavity, largely within the funnel. This location may facilitate a rapid infection by maximizing the rudiment's exposure to bacteria in the seawater that circulates through the mantle cavity. The ink sac is also able to function as an accessory structure of the light organ, which uses tissues from the ink bladder and reflective wall to direct and control light emission.

Pierantoni (1918) reported that the reflector in *Sepiola intermedia* develops from muscle tissue. However, our observations of *Euprymna scolopes* indicate that the reflector cells, or iridophores, do not develop from muscle. Pierantoni's observations did not benefit from the use of electron microscopy, and he may have interpreted the laminate structure of the reflector as the striated appearance of muscle cells, which it superficially resembles. The composition of the iridosomal platelets remains unknown, although there is evidence that they are composed largely of protein (Brocco, 1977; Cooper *et al.*, 1990). The wall of the ink sac in many squids and cuttlefishes is highly reflective, so that the ink is camouflaged and not visible through the mantle (Arnold, 1967). Photophores of deep sea squids have also been shown to contain iridiphores that function to reflect bioluminescent light (Arnold *et al.*, 1974). The reflective function is due to the presence of numerous iridophores, similar to those present in the iris and skin (Arnold, 1967). The ink sac wall of *E. scolopes*, a nocturnal animal that remains buried in the sand during the day, is highly reflective only on those portions of the ventral surface that abut the bacteria-containing tissue. However, the ink sac wall does have some reflective material over its entire surface; iridosomal platelets that appear morphologically identical to those in the reflector are present underneath most of the outer epithelium of the ink sac, but are rarely present in numbers greater than two or three. Thus the reflector, which functions to direct the bacterially produced light ventrally, appears to be an augmentation of a primitive feature of the ink sac. The iridosomal platelets, which appear to be membrane-bound, probably form in a manner similar to that described by Arnold (1967) for the iridosomal platelets of the iris and ink sac wall in *Loligo pealei* and *Octopus vulgaris*.

Pierantoni (1918) reported that, in newly hatched *Sepiola intermedia*, the lens has begun to develop from connective tissue underlying the surface epithelium. Previous work on *Euprymna scolopes* (McFall-Ngai and Montgomery, 1990) and other related sepiolids (Herring *et al.*, 1981) has provided evidence that the light organ lens is derived from muscle. Further, although the site of lens

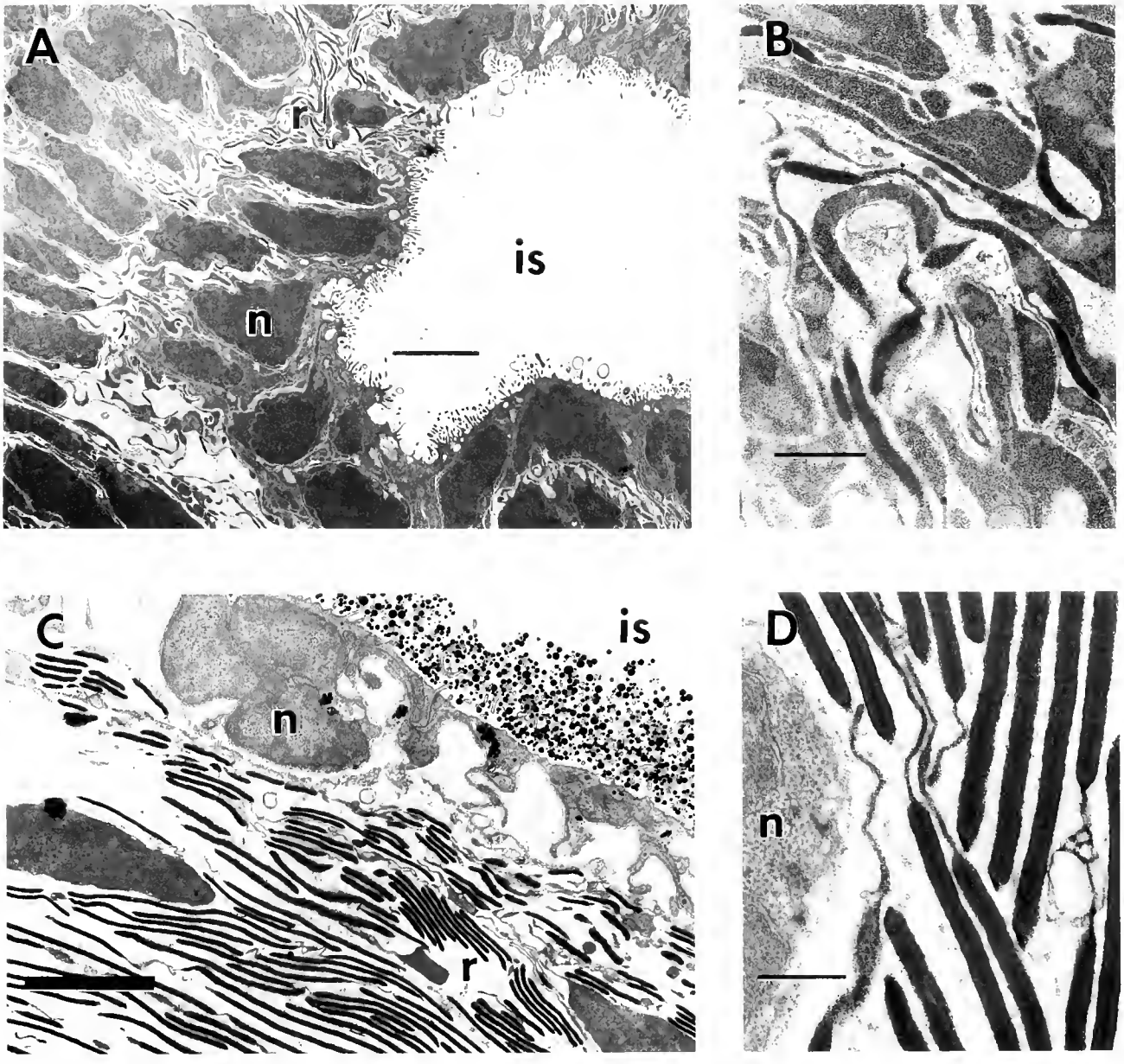

Figure 10. Transmission electron micrographs illustrating the development of the accessory tissues of the light organ. A. Low magnification view of the developing reflector and ink sac from the light organ rudiment of a 14-day-old embryo (stage A26). Scale bar = 5 μm. B. High magnification view of the developing reflector platelets from the same specimen shown in "A." Scale bar = 1 μm. C. Low magnification view of the reflector and ink sac from the light organ rudiment of a stage A29/19-day embryo. The reflector is composed of differentiated iridophores containing several stacks of platelets that are roughly aligned parallel with the surface of the ink sac. The typical squamous epithelium of the ink sac is present; the cells are functional, producing and secreting ink into the lumen of the ink gland. Scale bar = 5 μm. D. High magnification view of the reflector platelets shown in "C." Scale bar = 0.5 μm. (is, ink sac; n, nucleus; r, reflector).

development in *S. intermedia* described by Pierantoni is similar in *E. scolopes*, this tissue is mesodermal at the time juvenile *E. scolopes* hatches, and does not begin to differentiate into the lens until seven to ten days post-hatch (Weis *et al.*, 1993).

Evolutionary relationship with the accessory nidamental gland

The early developmental stages of the light organ strongly resemble the development of the accessory nidamental gland (ANG), another symbiotic organ in ceph-

alopods (Pierantoni, 1918). Although the development of the bacteria-containing tissue of the light organ appears similar to the early morphogenetic events of the ANG, the light organ does not develop ontogenetically from the ANG as suggested by Herring (1988). Development of these two organs is separated by both time and space. In squid species that have symbiotic light organs, including *Euprymna scolopes* and other closely related sepiolids, mature females have both an ANG and a light organ whereas males have only a light organ (see Buchner, 1965, for review). Further, in *Sepiola intermedia* (Pierantoni, 1918) and in *E. scolopes*, the light organ, which develops from the same set of tissues that gives rise to the hindgut-ink sac complex, begins formation during embryogenesis, whereas the ANG, which is adjacent to but separate from the ink sac, does not begin development until several weeks post-hatch.

However, both the apparent primitive nature of the accessory nidamental gland (ANG) relative to the light organ, and similarities in the development of the two organs suggest that the light organ may have evolved from the ANG. The symbiotic state of the light organ, which is monospecific, differs from that of the ANG, which contains several different strains of pigmented and, typically, non-luminous bacteria (Buchner, 1965). Bloodgood's report (1977) on the ANG of *Loligo pealei* provides evidence that each individual tubule of the ANG is populated with a single strain of bacteria, although the same strain may populate several tubules. Possibly, luminous bacteria established a symbiotic association within specialized tubules of the ANG of one or more ancestral species of squid. Symbiotic luminous organs may have evolved by the separation of luminous bacteria-containing tubules from the ANG, the latter being displaced posteriorly, with a concomitant reduction and specialization of the ink sac as a light organ accessory structure. Such a scenario involving "exaptation" (see Gould and Vrba, 1982) of the ANG and of the ink sac in a common ancestor would explain why all symbiotic luminous organs known in cephalopods are associated with the ink sac. The ANG is closely associated with the ink sac in most species that do not have symbiotic luminous organs. Further, one species of squid, *Rondeletiola minor* (Pierantoni, 1914; Naef, 1923; Herfurth, 1936), possesses a luminous organ and an ANG that are both closely associated with the ink sac, such that the luminous organ and ink sac appear to be embedded within the ANG. Female *Semirossia* (a representative of the sepiolid subfamily Rossiinae) sometimes show a duct uniting the light organs with the ANG instead of a light organ with a duct opening directly into the mantle cavity (Boletzky, 1970). Regardless of whether the light organ evolved directly from the ANG, both organs appear to have developed from similar tissues that are susceptible to interactions with bacteria.

Conclusions

The light organ of *Euprymna scolopes* begins development from the hindgut-ink sac complex at stage A25/Day 10, halfway between the time of fertilization and hatching. The incipient light organ of newly hatched juveniles appears "poised" for infection by symbiotic bacteria. A large portion of the surface area of the light organ is allocated to structures that most likely aid in the infection process, and in fact these structures regress within a few days following infection when they are presumably no longer needed (McFall-Ngai and Ruby, 1991). Accessory structures, such as the ink sac and reflector, develop during embryogenesis, but change in shape during post-hatch growth and maturation of the light organ. A third accessory structure, the lens, is not yet differentiated in newly hatched juveniles. Thus, the development of the light organ may be divided into three stages that correlate with the state of the symbiotic association: (i) embryonic development, during which the light organ rudiment first forms and the stage is set for initiation of the symbiosis; (ii) early post-hatch development, during which the light organ undergoes morphological and biochemical changes that accompany infection with and subsequent growth of the bacterial symbionts; and (iii) late post-hatch development, which results (within two weeks) in a fully differentiated light organ that primarily functions to maintain the symbiosis and control light emission.

Acknowledgments

We thank R. Zimmer for help with light photomicroscopy. We thank R. Young and J. Arnold for helpful discussions and E. G. Ruby, M. Snow, R. Wood, and R. Zimmer for helpful comments on the manuscript. We also thank the administrators and staff at the Hawaii Institute of Marine Biology (HIMB) for their support. This is HIMB contribution #900. This work was supported by NSF Grant No. DCB-8917293 (to MM-N and EG Ruby), an ONR Grant No. N00014-91-J-1357 (to MM-N), an NIH Biomedical Grant (to MM-N and MKM) and the ARCS Foundation (to MKM).

Literature Cited

Arnold, J. M. 1967. Organellogenesis of the cephalopod iridophore: cytomembranes in development. *J Ultrastruct. Res.* **20:** 410–421.

Arnold, J., C. Singley, and L. Williams-Arnold. 1972. Embryonic development and post-hatch survival of the sepiolid squid *Euprymna scolopes* under laboratory conditions. *Veliger* **14:** 361–364.

Arnold, J. M., R. E. Young, and M. V. King. 1974. Ultrastructure of a cephalopod photophore. II. Iridiphores as reflectors and transmitters. *Biol. Bull.* **147:** 522–534.

Berry, S. 1912. The Cephalopoda of the Hawaiian Islands. *Bull U.S. Bur. Fish.* **32:** 255–362.

Bloodgood, R. A. 1977. The squid accessory nidamental gland: ultrastructure and association with bacteria. *Tissue Cell* **9:** 197–208.

Boletzky, S. von. 1967. Die embryonale Ausgestaltung der frühen Mitteldarmanlage von *Octopus vulgaris* Lam. *Rev. Suisse Zool.* **74:** 555–562.

Boletzky, S. von. 1970. On the presence of light organs in *Semirossia* Steenstrup, 1887. *Bull. Mar. Sci.* **20:** 374–388.

Boettcher, K., and E. G. Ruby. 1990. Depressed light emission by symbiotic *Vibrio fischeri* of the sepiolid squid *Euprymna scolopes*. *J. Bacteriol.* **172:** 3701–3706.

Brocco, S. L. 1977. The ultrastructure of the epidermis, dermis, iridophores, leucophores and chromatophores of *Octopus dofleini martini* (Cephalopoda: Octopoda). PhD Thesis, University of Washington, Seattle.

Buchner, P. 1965. Symbiosis in luminous animals. Pp. 543–571 in *Endosymbiosis of Animals with Plant Microorganisms*, P. Buchner, ed. Interscience Publishers, New York.

Cooper, K. M., R. T. Hanlon, and B. U. Budelmann. 1990. Physiological color change in squid iridophores. II. Ultrastructural mechanisms in *Lolliguncula brevis*. *Cell Tissue Res.* **259:** 15–24.

Fawcett, D. W. 1986. *A Textbook of Histology*. W. B. Saunders Company, Philadelphia, PA.

Gould, S. J., and E. S. Vrba. 1982. Exaptation—a missing term in the science of form. *Paleobiology* **8:** 4–15.

Herfurth, A. H. 1936. Beitrage zur Kenntnis der Bakterien-symbiose der Cephalopoden. *Z. Morphol. Okol. Tiere* **31:** 562–607.

Herring, P. J. 1988. Luminescent organs. Pp. 449–489 in *The Mollusca*, Vol. 11. Academic Press, London.

Herring, P. J., M. Clarke, S. Boletzky, and K. Ryan. 1981. The light organs of *Sepiola atlantica* and *Spirula spirula* (Mollusca:Cephalopoda): bacterial and intrinsic systems in the order Sepiodea. *J. Mar. Biol. Assoc. U.K.* **61:** 901–916.

McFall-Ngai, M., and M. K. Montgomery. 1990. The anatomy and morphology of the adult bacterial light organ of *Euprymna scolopes* Berry (Cephalopoda:Sepiolidae). *Biol. Bull.* **179:** 332–339.

McFall-Ngai, M., and E. G. Ruby. 1991. Symbiont recognition and subsequent morphogenesis as early events in an animal-bacterial mutualism. *Science* **254:** 1491–1494.

Montgomery, M. K., and M. McFall-Ngai. 1991. The influence of bacterial symbionts on early morphogenesis of the light organ of the sepiolid squid *Euprymna scolopes*. *Am. Zool.* **31:** 15A.

Naef, A. 1923. Die Cephalopoden. *Fauna Flora Golf. Neapel* **35:** 1–863.

Pierantoni, U. 1914. La luce degli insetti luminosi e la simbi ereditorria. *R. C. Accad. Napoli* **20:** 15–21.

Pierantoni, U. 1918. Gli organi simbiotici e la luminescenza batterica dei Cefalopodi. *Publ. Stazione Zool. Napoli* **2:** 105–146.

Raven, C. P. 1958. *Morphogenesis: The Analysis of Molluscan Development*. Pergamon Press, New York.

Richardson, K. C., L. Jarrett, and E. H. Finke. 1960. Embedding in epoxy resin for ultrathin sectioning in electron microscopy. *Stain Technol.* **35:** 313–323.

Ruby, E. G., and M. J. McFall-Ngai. 1992. Examining the development of an animal/bacterial mutualism. *J. Bacteriol.* **174:** 4865–4870.

Singley, C. T. 1982. Histochemistry and fine structure of the ectodermal epithelium of the sepiolid squid *Euprymna scolopes*. *Malacologia* **23:** 177–192.

Singley, C. T. 1983. *Euprymna scolopes*. Pp. 69–74 in *Cephalopod Life Cycles*, Vol. 1. Academic Press, London.

Spurr, A. 1969. A low-viscosity epoxy resin embedding medium for electron microscopy. *J. Ultrastruct. Res.* **26:** 31–43.

Wei, S., and R. E. Young. 1989. Development of a symbiotic bacterial bioluminescence in a nearshore cephalopod, *Euprymna scolopes*. *Mar. Biol.* **103:** 541–546.

Weis, V. M., M. K. Montgomery, and M. J. McFall-Ngai. 1993. Enhanced production of ALDH-like protein in the bacterial light organ of the sepiolid squid *Euprymna scolopes*. *Biol. Bull.* **184:** 309–321.

Young, R. E., and R. F. Harman. 1989. Octopodid paralarvae from Hawaiian waters. *Veliger* **32:** 152–165.

Reference: *Biol Bull* **184**: 309–321. (June, 1993)

Enhanced Production of ALDH-Like Protein in the Bacterial Light Organ of the Sepiolid Squid *Euprymna scolopes*

VIRGINIA M. WEIS, MARY K. MONTGOMERY, AND MARGARET J. McFALL-NGAI

Department of Biological Sciences, University of Southern California, Los Angeles, California 90089-0371

Abstract. We localized one or more aldehyde dehydrogenase (ALDH)-like proteins in the bacterially bioluminescent light organ of the sepiolid squid *Euprymna scolopes*, and determined the temporal changes in expression through normal light organ development. Our previous studies have revealed that 70% of the total protein in the light organ lens of adult animals is comprised of an ALDH-like protein, which we called L-crystallin. In the present study, antibodies raised to this protein were used in immunocytochemical analyses which showed that, in adult light organ lens cells, ALDH-like protein was localized to the cytoplasm, but not to the nuclei or mitochondria. Labeling in adult tissue was also found in moderate abundance in the ciliated duct epithelium, a tissue that is in direct contact with the bacterial symbionts.

To determine the spatial and temporal onset of expression of ALDH-like protein(s), we examined light organs from juveniles at developmental stages before and after the differentiation of lens cells, which begins approximately 7–10 days after hatching. In 5-day symbiotic juvenile light organs, ALDH-like protein was not detected at levels significantly above those in non-symbiotic tissue of the same animals. However, expression of ALDH-like protein began within 10 days after hatching, seen first in a few cells of the ciliated duct, adjacent to the symbiont-containing tissue and in a few differentiated cells of the anterior presumptive light organ lens. These data suggest that, during normal development, induction of one or more ALDH-like proteins occurs simultaneously in both the lens and ciliated duct soon after the differentiation of lens cells.

Received 24 November 1992; accepted 29 March 1993.
Abbreviations: ALDH, aldehyde dehydrogenase.

Introduction

Mutualistic associations between prokaryotes and higher eukaryotes are widespread in many ecosystems (Margulis and Fester, 1991). Many of these associations are characterized by symbiosis-specific organs or tissues, such as nodules in leguminous plants, bacteriomes in several orders of insects, and light organs in some species of bioluminescent fishes and squids (*e.g.*, Hastings *et al.*, 1987; Herring, 1988; Ishikawa, 1990; Nap and Bisseling, 1991). Studies of plant/bacterial associations have shown that the morphogenesis of symbiotic organs involves both the evolution of new proteins that occur only in the symbiotic organ, as well as enhanced expression of genes already present in the host genome (*e.g.*, Sanchez *et al.*, 1991; Verma *et al.*, 1992). In contrast, little is known about such cellular and molecular integration and regulation between the partners of animal/bacterial symbioses during the infection and maintenance of the symbiotic state. Thus, studies directed toward an examination of symbiosis-induced changes in gene expression and the patterns of protein occurrence are essential to reveal the nature of communication that must occur in these highly orchestrated associations.

The symbiosis between the Hawaiian sepiolid squid *Euprymna scolopes* and its luminous bacterial partner *Vibrio fischeri* is well suited as a model association for the study of host-symbiont interactions at this level (McFall-Ngai and Ruby, 1991; Ruby and McFall-Ngai, 1992). Both host and symbiont can be independently raised in the laboratory, a feature that permits the experimental examination of the influence of the symbiotic state on host and bacterial gene expression. The host squid harbors a culture of *V. fischeri* in a complex bilobed organ in the mantle cavity (McFall-Ngai and Ruby, 1991) and is

thought to use its bacterially produced luminescence in anti-predatory behaviors (Moynihan, 1983). The bacteria-containing tissue consists of a network of epithelial cells lining crypts that house the bacteria (Fig. 1a; McFall-Ngai and Montgomery, 1990). Ciliated ducts are contiguous with these crypts and connect them with the outside of the light organ (the mantle cavity) by two pores. The bacteria-containing tissue is surrounded by a reflector and the ink sac, which serve to direct light ventrally. Finally, a thick pad of transparent tissue overlies the ventral surface of the organ and functions as a lens to refract light from the bacterial source into the environment.

During normal development, newly hatched squids become infected by free-living *V. fischeri* within hours after hatching (McFall-Ngai and Ruby, 1991). At the time of hatching, all components of the light organ, except the light organ lens, are differentiated and are simply elaborated during the further maturation of the light organ (Montgomery and McFall-Ngai, 1993). In contrast, the light organ lens cells first begin to differentiate approximately 7 to 10 days after hatching (Montgomery, pers. obs.).

Previous studies of the biochemical nature of the light organ of the adult squid have revealed that a significant portion (approximately 50%) of the total protein occurs as a 54 kD species, which was designated L-crystallin (Montgomery and McFall-Ngai, 1992). We found that the vast majority of this protein occurs in the light organ lens, which is protein rich to refract bioluminescent light effectively. Sequences of tryptic peptides derived from this protein, which had been purified from light organ lens, had a high sequence similarity to human cytosolic aldehyde dehydrogenase (ALDH, EC 1.2.1.3), a member of a large group of related enzymes that catalyze the conversion of aldehydes to carboxylic acids. Although L-crystallin apparently lacks ALDH activity, a polyclonal antibody raised against L-crystallin cross-reacted with 54 kD proteins, a characteristic size for ALDH subunits, from both cephalopods and mammals (Montgomery and McFall-Ngai, 1992). Anti-L-crystallin is therefore specific to ALDH-like proteins and not L-crystallin alone.

The high abundance of ALDH-like protein(s) provides a dramatic example of a gene product whose production is enhanced in a symbiotic organ. In this study, to determine where immunoreactive protein occurs during the maintenance of the symbiotic state, we examined the spatial pattern of their production in the adult light organ. Further, to determine how this pattern is achieved, we examined the temporal nature of protein production during normal development. Our results indicate that one or more of these proteins occurs in abundance not only in the light organ lens, but also in the ciliated duct, a tissue directly in contact with bacterial symbionts. During development, increased levels of these ALDH-like proteins are first seen simultaneously in the ciliated ducts and in newly differentiating lens cells. By following the occurrence of this group of proteins through the establishment and maintenance of the association, we might ultimately better understand how bacterial infection affects host gene expression in the light organ.

Materials and Methods

Maintenance of experimental organisms

Specimens of *E. scolopes* were collected from Kaneohe Bay on Oahu, Hawaii, in May, July, and November of 1991. The animals were kept in running seawater tables at the Hawaii Institute of Marine Biology (University of Hawaii) in Kaneohe Bay before being transported to 24°C recirculating seawater aquaria at the University of Southern California in Los Angeles. The animals were fed a variety of freshwater shrimp daily and kept on a 12 h light/dark cycle.

Clutches of eggs laid by captive females were removed to small recirculating aquaria, also at 24°C. Immediately upon hatching, juveniles were placed in small bowls of seawater from aquaria containing adult animals which regularly shed light organ symbionts. In this water, the juveniles became infected with *V. fischeri* within 12 h (Wei and Young, 1989; McFall-Ngai and Ruby, 1991). Juveniles could be maintained in good condition with daily water changes for up to 6 days. At the end of an incubation period, animals were either processed immediately or frozen in liquid N_2 and stored at −80°C.

Tissue fixation and embedding

To localize the ALDH-like proteins in the *E. scolopes* light organ, organs from both juvenile and adult squids were prepared for immunocytochemistry. *E. scolopes* were anesthetized with a 2:1 0.37 *M* $MgCl_2$:seawater mix for 5 min before dissection or processing. In adults, which range in size from 12 to 20 mm in mantle length, the ventral mantle and funnel were slit open to reveal the light organ, which could be easily removed. Juveniles, which are smaller than 4 mm in mantle length, were treated whole. The fixation protocol was modified from Erickson *et al.* (1987). Tissues were fixed for 1 h at room temperature in 1% paraformaldehyde and 1% glutaraldehyde in 0.1 *M* sodium phosphate buffer containing 0.45 *M* sodium chloride, pH 7.2, washed three times for 10 min each in a 0.1 *M* sodium phosphate buffer containing 0.45 *M* sodium chloride, dehydrated in 15, 30, and 50% methanol (MeOH) for 10 min each. The samples were fixed in a 2% uranyl acetate, 70% MeOH solution for 1 h, and further dehydrated for 10 min each in 85, 95, and 100% MeOH. The light organs were infiltrated with a 1:1 ratio of 100% MeOH and LR White resin (Ted Pella

Inc.) for 12 h at 4°C on a turntable. Subsequently, the specimens were rotated in 100% LR White for 72 h, transferred to fresh 100% LR White in gelatin capsules and allowed to polymerize for two days at 52°C.

Some light organs were also fixed for transmission electron microscopy to provide micrographs of well preserved tissues for orientation. These light organs were fixed for 12 h in 2.5% glutaraldehyde in 0.1 *M* sodium cacodylate, 0.45 *M* sodium chloride (NaCl), pH 7.4. Samples were post-fixed in 1% osmium tetroxide in the fixative buffer and further processed for histology as described in McFall-Ngai and Montgomery (1990).

Light microscopy

The antiserum used to locate ALDH-like proteins was made against a purified fraction of the light organ lens, designated L-crystallin, by Montgomery and McFall-Ngai (1992). The antiserum cross-reacts with ALDH-like proteins from both cephalopods and mammals.

Histological cross sections of light organs were cut with glass knives for light microscopy and dried onto gelatin-coated glass slides. The antibody incubation procedure was modified for light microscopy from the methods of Erickson *et al.* (1987). First, to block non-specific adsorption and binding, the 1-μm sections were incubated for 30 min in a blocking solution consisting of a 1:50 ratio of non-immune goat serum (Sigma, the same species as the secondary antiserum without the antibody) to a 10 m*M* sodium phosphate buffer, containing 150 m*M* NaCl, 0.05% NaN_3 and 0.5% bovine serum albumin (PBS/BSA). The slides were gently rinsed with PBS/BSA and then flooded with a 1:2000 dilution of primary (1°) antiserum: rabbit anti-L-crystallin in PBS/BSA for 2 h. The sections were rinsed twice in PBS/BSA for 10 min, then flooded with the secondary (2°) antibody solution, consisting of a 1:50 dilution of goat anti-rabbit IgG complexed to 15 nm colloidal gold spheres (Ted Pella Inc.) in PBS/BSA. The sections were then rinsed with deionized water (DH_2O) and stained with a silver enhancement kit (Sigma), which allows for the visualization of the immune complex with light microscopy due to the precipitation of silver granules in the presence of colloidal gold. Finally, the sections were counterstained with 1% acid fuchsin for 20 min, rinsed in water, dried, and mounted in heavy immersion oil.

In controls, to determine the degree of non-specific binding of the 2° antibody solution, a 1:2000 dilution of a pre-immune serum, obtained from the same rabbit as the immune serum before injection with L-crystallin, was substituted for the 1° antibody incubation. These sections were designated pre-immune preparations. Some untreated sections were stained with Richardson's stain (Richardson *et al.*, 1960) to provide companion histological sections for orientation and comparison.

Electron microscopy

Ultrathin sections of the light organs were cut with a diamond knife using a Porter Blumm MT2-B ultramicrotome and placed on nickel grids. For all incubations, grids were floated section-side down in solutions in 500 μl wells. The incubation procedure was the same as that described above for 1 μm sections except that grids were rinsed dropwise with PBS/BSA between antibody incubations. After the 2° antibody incubation and DH_2O rinse, grids were stained in 3% uranyl acetate and Reynolds lead citrate for 10 min each. As with the 1 μm sections, pre-immune grids were prepared to control for non-specific binding of the 2° antibody solution.

Sections of light organs were examined at 20,000× to look for the presence of 15 nm gold spheres on a JEOL 100CX transmission electron microscope at 80 kV. To quantify gold spheres in the tissues of the light organ from both immune and pre-immune incubations, spheres were counted in micrographs taken at 40,000× (n = 5; area = 4 μm^2) of each tissue.

Electrophoresis and immunoblotting

To look for the onset of ALDH-like protein production in *E. scolopes*, light organs from newly hatched juveniles and 5-day symbiotic juveniles were dissected and prepared for electrophoresis. Light organs and mantles from approximately 50 previously frozen juveniles per treatment were removed under a dissection microscope and homogenized in a Wheaton ground glass micro-tissue homogenizer in 50 μl of 50 m*M* sodium phosphate, 0.1 *M* NaCl, pH 7.0. Homogenates were spun at 15,000 × *g* for 15 min at 4°C in a Sorvall superspeed RC-5B centrifuge. The supernatants were decanted and kept at 4°C. A homogenate from adult light organs was used as a positive control for the presence of ALDH-like protein (Montgomery and McFall-Ngai, 1992). Concentration (mg/ml) of the soluble protein in each homogenate was determined spectrophotometrically (Whitaker and Granum, 1980).

Polyacrylamide gel electrophoresis in the presence of sodium dodecyl sulfate was carried out using a 12.5% resolving gel on a Hoefer SE 250 slab gel apparatus (techniques modified from Laemmli, 1970). Gels were run at a constant current (20 mA/gel) and stained with Coomassie blue. Eight μg of protein were loaded for all juvenile samples and a range of quantities, from 1 to 200 ng, was loaded for the adult light organ lens positive control.

For immunoblotting, proteins were electrophoretically transferred from unstained gels onto nitrocellulose membrane in a Hoefer TE 22 transfer apparatus for 2 h at 12°C at a constant current (200 mA) in a 25 m*M* Tris, 192 m*M* glycine, 20% methanol, 0.1% SDS buffer, pH 8.3. (modified from Towbin *et al.*, 1979). Immunoblots were performed using an amplified, streptavidin/biotin,

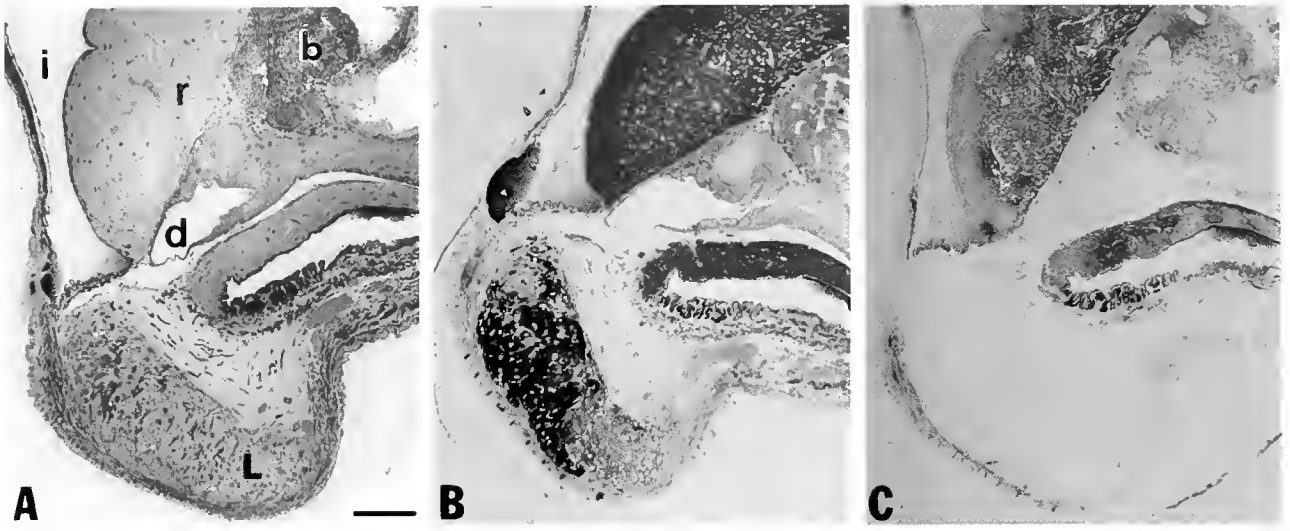

Figure 1. Cross sections through an adult *Euprymna scolopes* light organ. (A) Richardson's stained section: b, the inner bacteria-containing epithelium; d, the ciliated duct with its surrounding epithelium (duct does not reach the pore in this section); r, the reflector; i, the ink sac; and L, the light organ lens. Bar = 50 μm. (B) Silver-enhanced immune section, counter-stained with acid fuchsin. The silver granules indicate the presence of L-crystallin in the light organ lens (dense black) and of an ALDH-like protein in the ciliated duct epithelium (gray). The ink in the ink sac appears brown. (C) A pre-immune section lacks any dense black stain in the lens or duct epithelium.

alkaline phosphatase immune blot kit (BioRad), which was designed to detect as little as 10 pg of antigen. The membrane was incubated in a 1:1000 dilution of the 1° antiserum for 2 h and subsequently incubated and developed according to the manufacturer's directions.

Results

Localization of ALDH-like protein in adult light organs

To determine the location of ALDH-like protein in the adult *E. scolopes* light organ, immunocytochemistry, using anti-L-crystallin, was performed on cross sections of light organs at both the light microscopic and electron microscopic levels. In the 1 μm thick sections, L-crystallin was localized in very high concentrations in the lens of the light organ as evidenced by the dense black silver nitrate granules visible against the pink acid fuchsin background stain (Fig. 1b, see Fig. 1a for orientation). No such black precipitate was present in the pre-immune incubation (Fig. 1c). Residual ink, present in the ink sac, appeared brown in the immune and pre-immune sections. Although not as dramatic as the staining in the lens, silver nitrate granules were also present in the epithelial cells of the ciliated duct in the immune (Fig. 1b) but not in the pre-immune (Fig. 1c) preparations. In some sections, the medial portion of the lens stained more lightly than the lateral portion (Fig. 1b), however in other sections the lens appeared to stain uniformally along this axis.

Silver nitrate granules only precipitated over the cytoplasm of lens cells that stained lightly with Richardson's stain (Fig. 2a, b). The outer epithelial layer surrounding the lens, and muscle cells, shown in longitudinal section running through the lens and in cross section on the edge of the lens, lacked silver granules. Higher magnifications of ciliated duct showed the silver nitrate granules only in the cytoplasm of the epithelial cells, not in the cell nuclei or in the duct itself (Fig. 2c, d).

Ultrastructural examination of the *E. scolopes* light organ confirmed the patterns described in the histological sections. Colloidal gold spheres were found in high numbers in the lens of the light organ, in intermediate numbers in the ciliated duct, and in very low numbers (not significantly above background levels) in the ink sac, reflector, and bacteria-containing epithelial tissue (Table I).

Lens tissue is comprised largely of cells containing nuclei, mitochondria, and a diffuse cytoplasm containing numerous, thinly aligned elements, but lacking any fibrous muscle structure, obvious endoplasmic reticulum or Golgi complexes (Fig. 3a; McFall-Ngai and Montgomery, 1990). It was these cells in which high concentrations of colloidal gold spheres were found in immune (Fig. 3b) compared to pre-immune (Fig. 3c) preparations. The spheres were localized only in the diffuse cytoplasm, not in the mitochondria (Fig. 3d) or cell nuclei (Fig. 3e). There was no gradient of sphere numbers throughout the center of the lens or on the outside margin where gold spheres evenly covered the diffuse lens cells but were absent from muscle cells immediately adjacent to them (Fig. 4a). However, the cells at the inside margin contained a patchy distri-

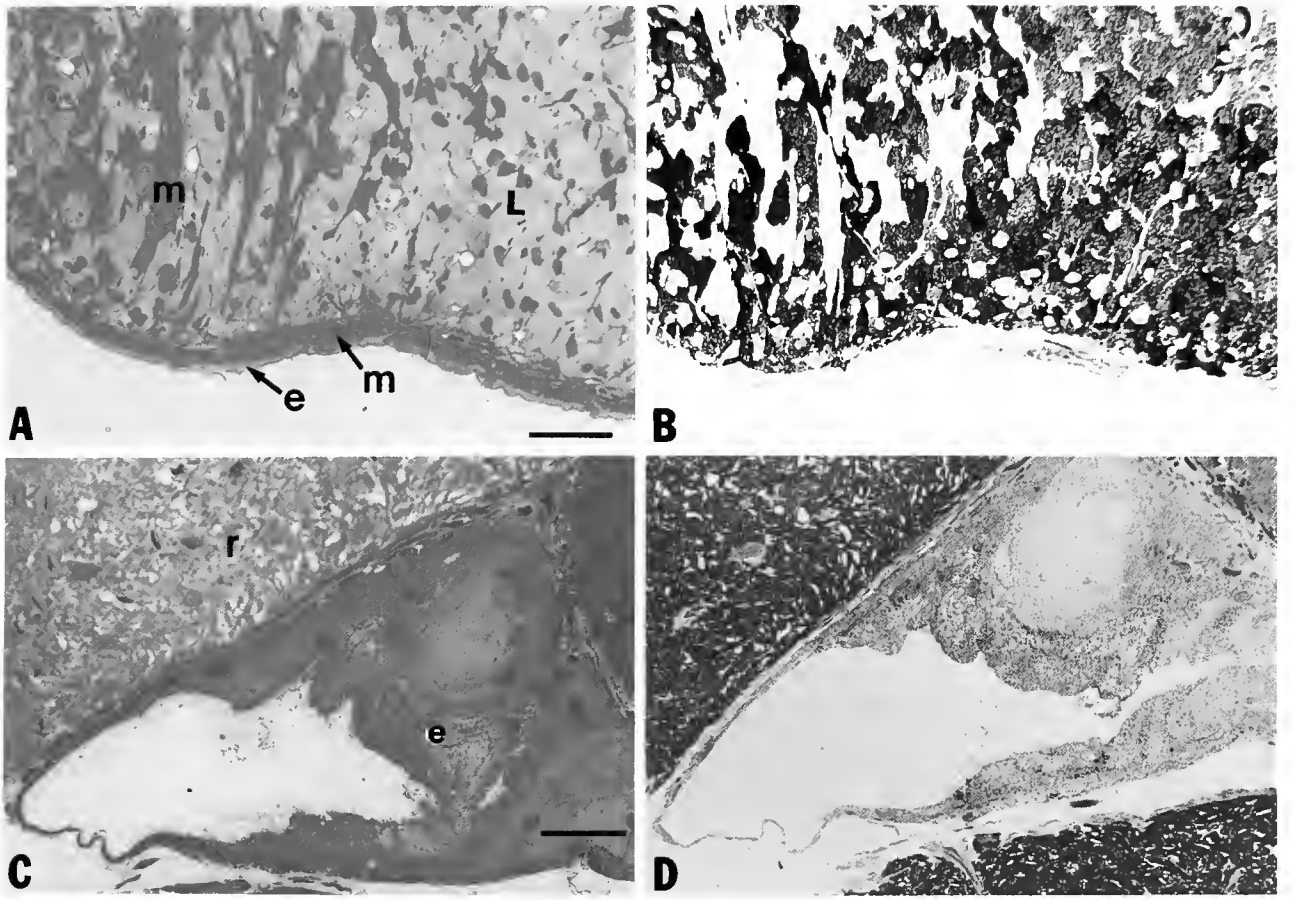

Figure 2. Detail of cross sections from Figure 1. (A) Richardson's stained light organ lens: e, outer epithelial layer; L, lightly staining lens cells comprising the majority of the lens; m, muscle cells running through the lens in longitudinal section and in cross section at the arrow. (B) Immune-treated light organ lens counter-stained with acid fuchsin. Only the cytoplasm of lens cells contains silver granules. Lens cell nuclei, and muscle and epithelial cells lack the black precipitate. (C) Richardson's stained area around the ciliated duct: e, epithelial cells lining the duct and r, reflector tissue. (D) Immune-treated ciliated duct epithelium counter-stained with acid fuchsin. The cytoplasm of the epithelium contains some silver granules. Bars = 20 μm.

bution of spheres where large areas of the diffuse cytoplasm were unlabeled (Fig. 4b).

The epithelial cells lining the duct, which connects the bacteria-containing crypts to the outside of the light organ, contain several cilia and prominent root hairs per cell (Fig. 5a, b). As in the lens cells, immune preparations of epithelial cells in the ciliated duct contained high numbers of gold spheres in the cytoplasm (Fig. 5c) compared to pre-immune preparations (Fig. 5d). Only background levels of spheres were found on the cilia, in the cell nuclei, and in the duct itself.

Localization of ALDH-like protein in E. scolopes *through development*

To determine the onset of ALDH-like protein production and to examine the pattern of production through development, light organs from animals of different sizes were tested for the presence of these proteins. Juvenile animals, collected from the field, with mantle lengths of 4.2, 3.0, 2.3, 2.0, and 1.8 mm were examined. In the 4.2 mm and 3.0 mm animals, the staining pattern was the same as it had been in adult light organs: the developing lens tissues stained a very dense black and the ciliated duct epithelial cells stained a light, more diffuse gray (data not shown). In the 2.3 and 2.0 mm animals, both the lens and the ciliated duct epithelium were positive for these proteins, but the lens, consisting of only a thin layer of differentiated cells at this stage (Fig. 6a), stained gray instead of a dense black (Fig. 6b). In some cases, staining in the ciliated duct was actually more intense than in the developing lens cells.

In the anterior ventral portion of the light organ of the 1.8 mm juvenile, a few dozen lens cells appeared to have

Table I

Number of colloidal gold spheres present in different tissues of the adult E. scolopes *light organ*

Cell type	Number of spheres per micrograph: immune	pre-immune	*P* value
Lens	314.2* (74.4)	2.4 (0.9)	<.001
Ciliated duct epithelium	157.4* (24.4)	1.6 (1.1)	<.0005
Bacteria-containing tissue	1.2 (0.8)	1.0 (1.0)	>.1

* Number of spheres in lens and ciliated duct are different by $P < .05$.

Each micrograph, taken at a magnification of 40,000× corresponds to 4 μm^2. Numbers are means ± (S.D.), n = 5 for each treatment. *P* values are results of two-tailed paired *t*-test.

differentiated from a pad of mesodermal cells (presumptive lens). In light microscopic immune preparations, these cells stained a dark gray, whereas the ciliated duct and posterior presumptive lens were completely free of silver nitrate precipitate. Examination at the ultrastructural level revealed that the number of colloidal gold spheres per 4 μm^2 of these differentiated lens cells was 146.4 ± 58.5 (n = 5) whereas pre-immune preparations averaged only 1.6 ± 1.1 (n = 5; averages different by *t*-test, $P < 0.001$). The level of ALDH-like protein occurrence in these recently differentiated lens cells is significantly lower than that in adult lens cells (*t*-test, $P < 0.05$), and is more similar to protein occurrence in adult ciliated duct (see Table I). Low numbers of colloidal gold spheres (27.0 ± 3.2 per 4 μm^2, n = 5) were detected in a few duct epithelial cells upon examination at the ultrastructural level; but these numbers were significantly above those found in pre-immune preparations (2.6 ± 0.6 per 4 μm^2 n = 5; immune and pre-immune averages different by $P < 0.001$). These cells were located at the interface between the bacteria-containing non-ciliated crypts and the ciliated duct (Fig. 7). Cells in the more distal portion of the duct contained only background levels of spheres.

To further examine the temporal pattern of ALDH-like protein occurrence in early juvenile development and its relation to infection by symbiotic bacteria, newly hatched animals, 5-day symbiotic juveniles (average mantle length = 1.5), and a field caught juvenile measuring 1.6 mm in mantle length were tested for the presence of immunoreactive protein. The size and morphology of this field-caught juvenile suggests that it was between three and five days old at the time of fixation. Ultrastructural examination of the light organ of this animal showed it to be infected with bacterial symbionts. In all of these juveniles, both at the histological and ultrastructural levels, no ALDH-like protein was detected either in the ciliated duct or in presumptive lens tissue (data not shown). No cells were present that resembled the large, lightly staining cells typical of adult lens and which stained positive for these proteins in the adult and older juveniles. Further, in all of these animals, including the 1.6 mm field-caught juvenile, three separate pores opened into three ciliated ducts on each side of the light organ; none of the epithelial cells in these ducts appeared to express ALDH-like protein at this stage of development. The presence of three ducts per side is typical of newly hatched and very young juveniles (Montgomery and McFall-Ngai, 1991). The slightly larger and older juvenile, 1.8 mm in mantle length, contained only one duct on each side of its light organ; the size of this juvenile and the presence of one duct indicate that this animal was approximately one week to ten days old at the time of fixation.

Because detection of the ALDH-like protein induction in a small area of the juvenile light organ might be missed with immunocytochemistry, anti-L-crystallin immunoblots of juvenile light organs were compared to further search for a temporal pattern of induction and its relation to bacterial infection. Light organs and mantles from newly hatched and 5-day symbiotic juveniles were compared, and in all cases only very slight bands at 54 kD, the apparent molecular mass of denatured L-crystallin (Montgomery and McFall-Ngai, 1992) were detected (data not shown). Further, the 54 kD bands in the light organ lanes were weaker than those in mantle lanes, which suggests that levels of the proteins in the light organs were not significantly above baseline levels expressed in all tissues. The amplified immunoblot kit was able to detect L-crystallin in adult light organ lens, which is comprised chiefly of L-crystallin (Montgomery and McFall-Ngai, 1992), when as little as 1 ng of protein was loaded. Therefore, if the very slight positive band in both juvenile preparations represents approximately 1 ng of total soluble protein, and 8 μg of protein were loaded, ALDH-like protein comprises less than 0.02% of the juvenile light organ soluble protein compared to approximately 50% in the adult organ (Montgomery, unpub. data).

Discussion

Our investigation localizes ALDH-like proteins in the adult *E. scolopes* light organ: (1) in high abundance in the cytoplasm of lens cells and (2) in moderate abundance in the cytoplasm of the epithelial cells lining the ciliated duct. Further, we explore the onset of ALDH-like protein occurrence in juvenile light organs and show that these proteins: (1) are not detectable in light organs from either newly hatched or 5-day symbiotic juveniles; (2) are first expressed simultaneously in ciliated duct epithelium and in newly differentiating lens

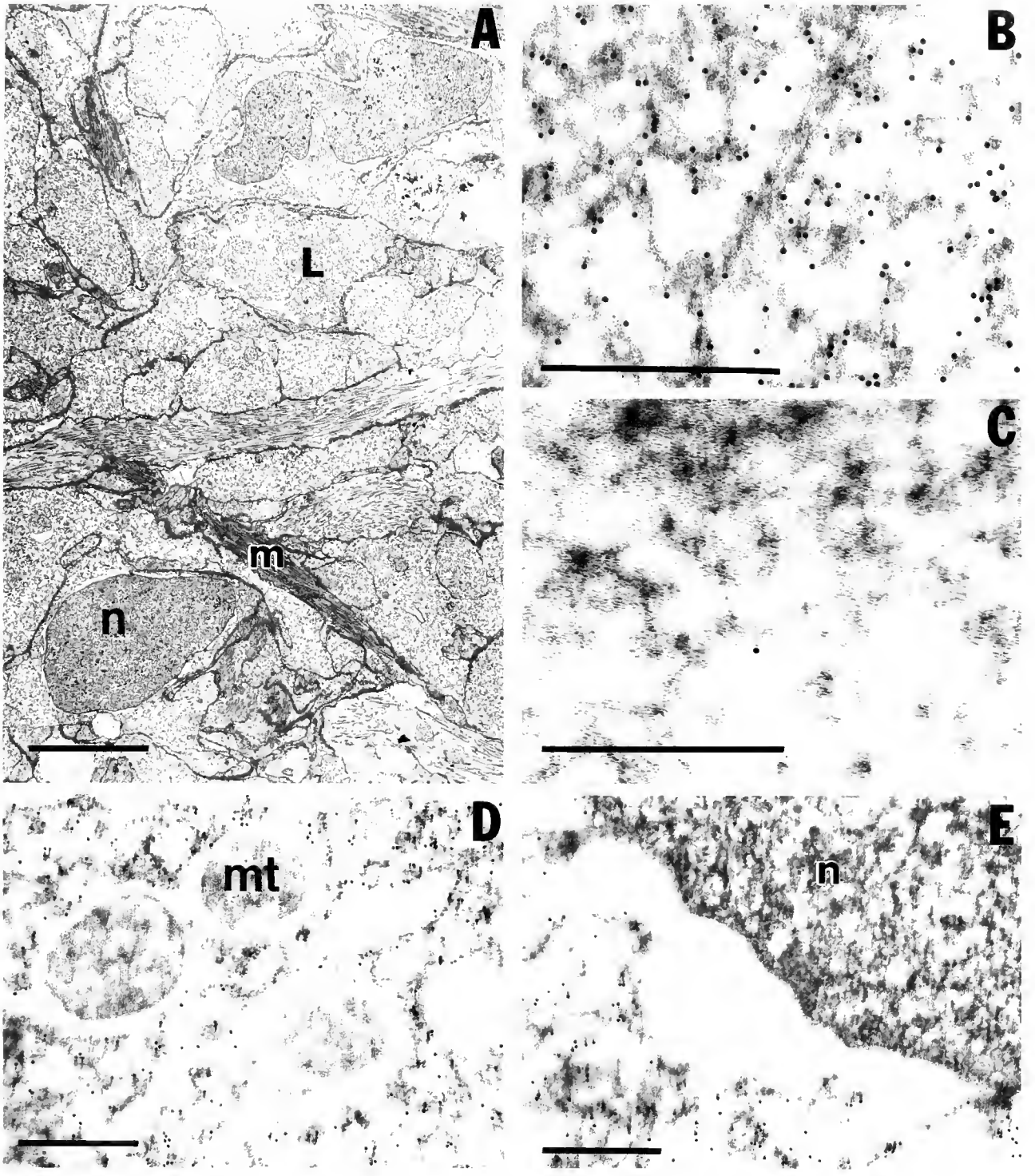

Figure 3. Electron micrographs of immune and pre-immune treatments of the light organ lens. (A) Low magnification of the light organ lens showing that the lightly staining lens cells comprise the majority of the lens (fixed for TEM, not for immunocytochemistry, as described in Methods). L, lens cells with diffuse cytoplasm and lacking any fibrous muscle structure; m, longitudinal section of a muscle fiber; and n, nucleus of a lens cell. Bar = 5 μm. (B) High magnification of immune-treated lens cell cytoplasm revealing numerous 15 nm gold spheres. Bar = 0.5 μm. (C) High magnification of pre-immune-treated lens cell cytoplasm revealing few 15 nm gold spheres. Bar = 0.5 μm. (D) High magnification of immune-treated lens cell cytoplasm containing 3 mitochondria (mt). Gold spheres are present in the cytoplasm but not in the mitochondria. Bar = 0.5 μm. (E) High magnification of immune-treated lens cell cytoplasm and nucleus (n). Gold spheres are present in the cytoplasm but not in the nucleus. Bar = 0.5 μm.

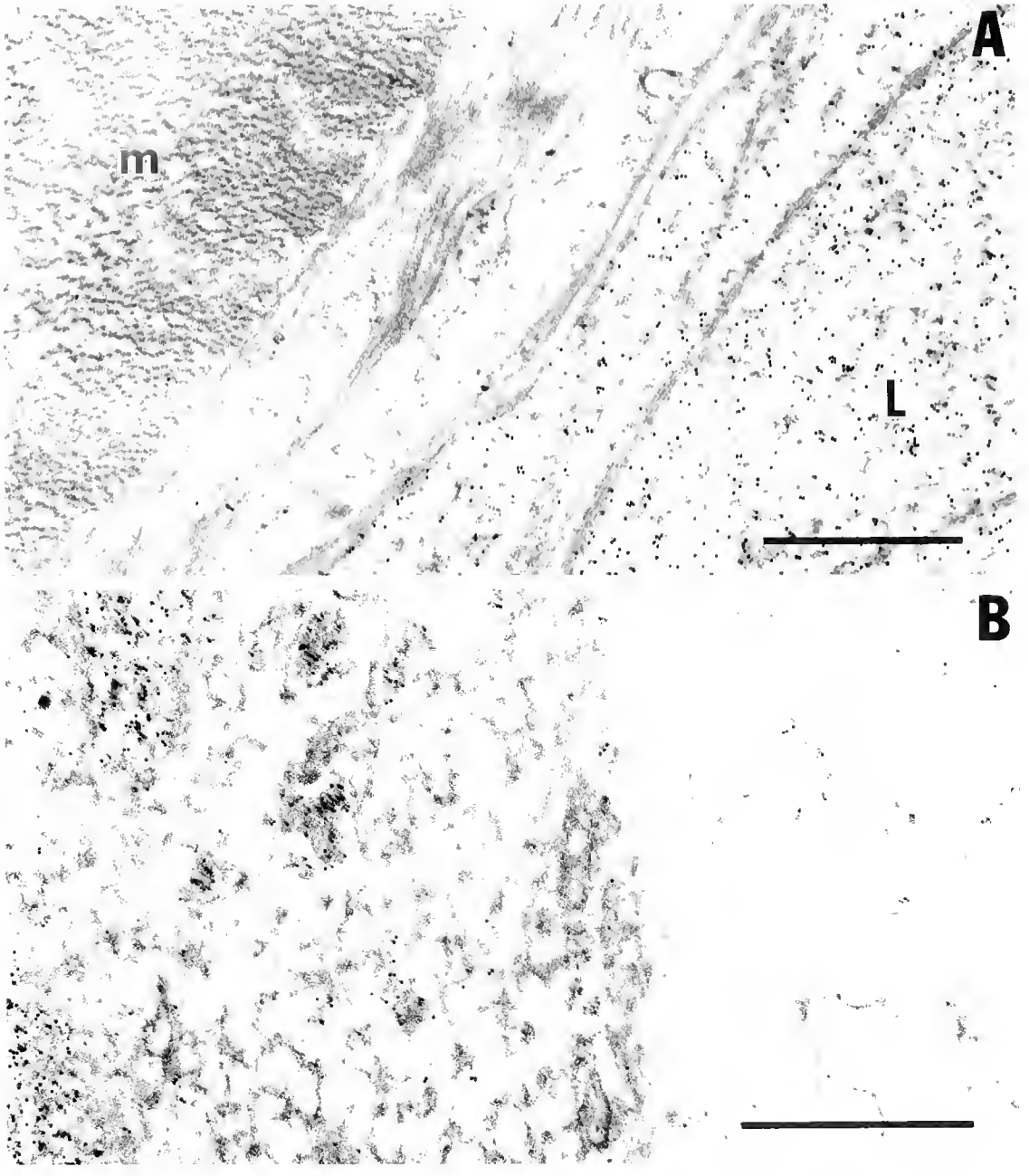

Figure 4. Electron micrographs of the light organ lens margins. (A) Outer lens margin where lightly staining lens cell (L) on right abuts a muscle cell (m) on left. Gold spheres are evenly distributed throughout the lens cell cytoplasm. (B) Inner lens margin where lightly staining lens cell on left abuts acellular connective tissue on right. Gold spheres appear in loose aggregations in the lens cell cytoplasm. Bar = 0.5 μm.

cells in juveniles; and (3) are only expressed in lens cells after lens cell differentiation from mesodermal tissue.

ALDH-like protein occurrence in adult light organ lens

Like the transparent epidermally derived ocular lens tissue of vertebrates and cephalopods, which are comprised chiefly of one or several lens crystallins, the muscle-derived light organ lens has a simple protein profile, in which L-crystallin accounts for 70% of the soluble protein (Montgomery and McFall-Ngai, 1992). Further, L-crystallin is located in the cytoplasm of the large, lightly staining cells, which comprise the vast majority of the lens, but is absent from lens epithelium and muscle (Figs. 1,

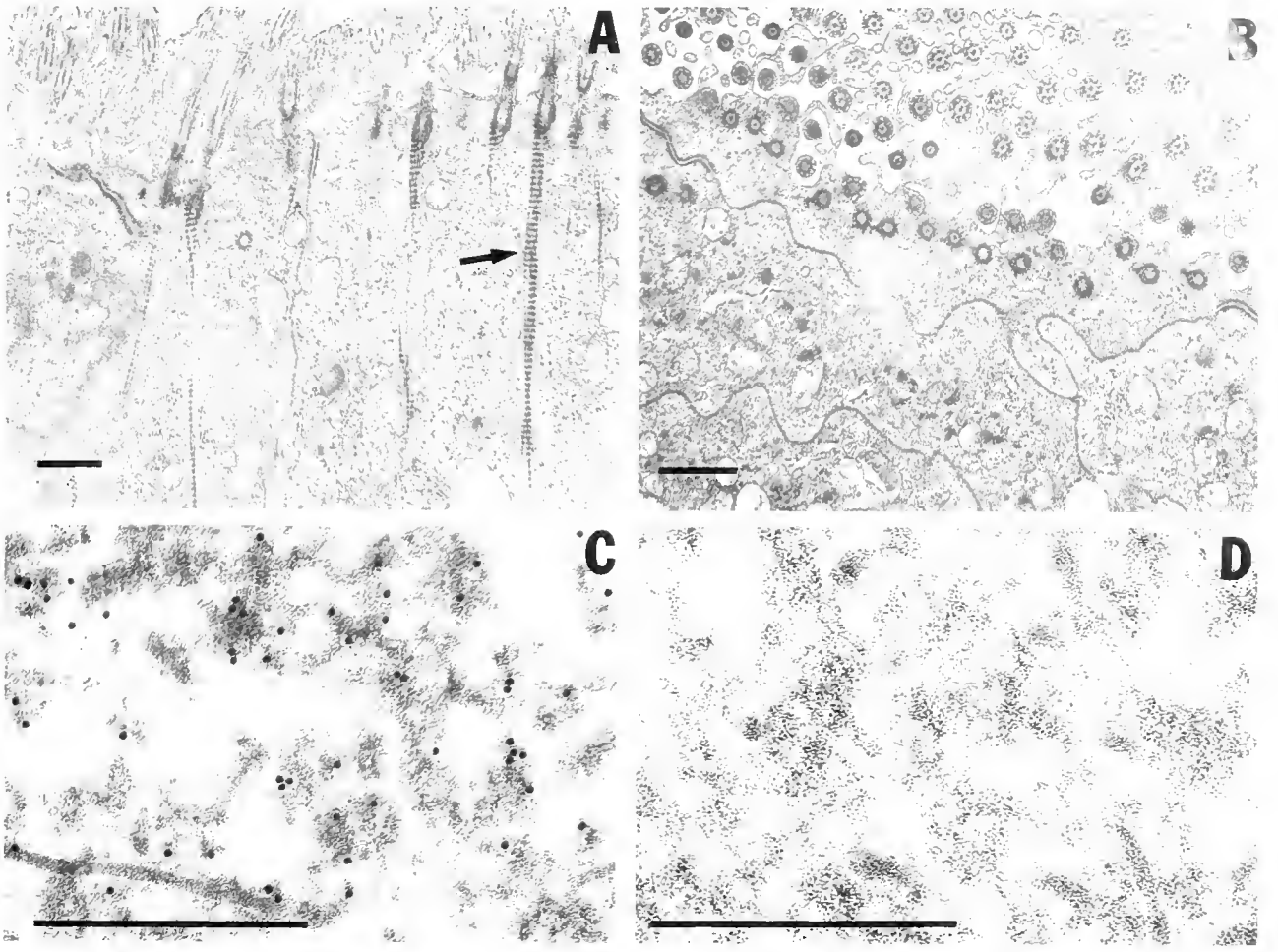

Figure 5. Electron micrographs of immune and pre-immune treatments of ciliated duct epithelium. (A & B) Low magnification of the ciliated duct epithelium in: (A) longitudinal section, and (B) cross section, showing numerous cilia and ciliary root hairs (arrow) (fixed for TEM, not for immunocytochemistry, as described in Methods). Bars = 1 μm. (C) High magnification of immune-treated duct epithelium cytoplasm revealing numerous 15 nm gold spheres. Bar = 0.5 μm (D) High magnification of pre-immune-treated duct epithelium cytoplasm revealing few 15 nm gold spheres. Bar = 0.5 μm.

2). Such a high abundance of L-crystallin together with an apparent reduction in the production of proteins typical of a muscle tissue, such as actin and myosin (Montgomery and McFall-Ngai, 1992) and a lack of subcellular structure (Fig. 3; McFall-Ngai and Montgomery, 1990) in this predominant cell type suggests that these cells do little else than synthesize and retain L-crystallin. As with ocular lens tissue, the over-production of one or a few proteins in specialized lens cells is thought to result in a tissue with a high refractive index, which results in increased transparency (Bloemendal, 1981).

L-crystallin abundance appears to vary along the medial/lateral axis in some sections (Fig. 1b), but not in others. The lighter staining lateral portion of the lens could indicate a differential abundance of L-crystallin along this axis in some areas of the lens, or could be due to uneven fixation of the tissue. L-crystallin occurrence is uniform through the lens along the dorsal/ventral axis, except for the dorsal lens margin where lens cells appear to give way to acellular connective tissue (Fig. 4b). The pockets of cytoplasm that contain high numbers of colloidal gold spheres, surrounded by areas with no spheres, might be sites of L-crystallin production. However, this packaging effect might also be explained by poor fixation and/or infiltration in the far interior of the lens. From these localization results, it is not possible to determine the location of continued lens cell differentiation or new L-crystallin production in the adult lens. In continuing studies, we have been able to isolate only minute quantities of poly A+ RNA from light organ lens tissue from adults (Weis and McFall-Ngai, unpub. data), which suggests that both L-crystallin turnover and synthesis in the adult lens are very low.

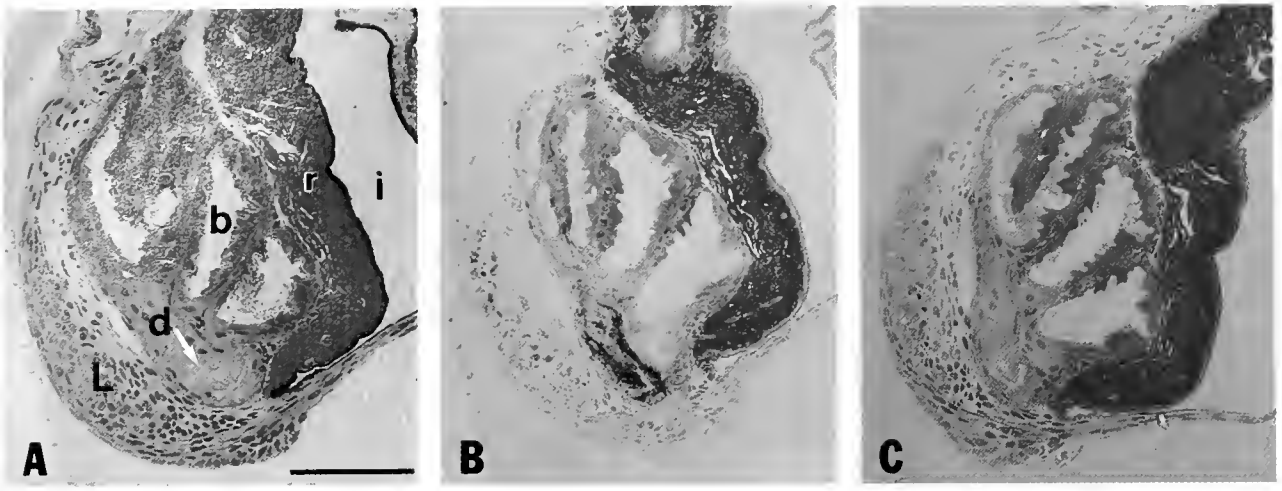

Figure 6. Cross sections through the light organ of a juvenile *Euprymna scolopes* (2.0 mm in mantle length). (A) Richardson's stained section: b, the inner bacteria-containing epithelium; d, the ciliated duct with its surrounding epithelium (duct does not reach the pore in this section); r, the reflector; i, the ink sac; and L, the light organ lens. Bar = 100 μm. (B) Silver-enhanced immune section, counter-stained with acid fuchsin. The silver granules indicate the presence of an ALDH-like protein in the ciliated duct epithelium and the light organ lens. The ink in the ink sac appears brown. (C) A pre-immune section lacks any dense black stain in the lens or duct epithelium.

We have found a 54% amino acid sequence identity between three peptides of L-crystallin and human ALDH1, an enzyme that has been localized in the cell cytosol of mammalian liver and other organs (Kitabatake *et al.*, 1981; Montgomery and McFall-Ngai, 1992). Because of its substantial sequence identity to a known enzyme, L-crystallin has been added to the list of enzyme/crystallins, a group of structural proteins in ocular lenses of vertebrates and cephalopods that have a high sequence identity to various enzymes (Piatigorsky and Wistow, 1991). Although L-crystallin and ALDH1 share a common location within the cell, and ALDH1 cross-reacts with the polyclonal antiserum to L-crystallin, they do not show high enough sequence identity to suggest that they are closely related isozymes.

ALDH isozymes have been localized in a wide variety of tissues using several techniques. In addition to its occurrence in the light organ as L-crystallin, we have found an immunoreactive ALDH-like protein in the *E. scolopes* eye lens in moderate levels, using immunoblot analysis (Montgomery and McFall-Ngai, 1992). This protein species likely functions as an enzyme/crystallin. Like L-crystallin, the ALDH enzyme/crystallins, which have been described in the eye lenses of elephant shrew (η-crystallin, Wistow and Kim, 1991) and octopus (Ω-crystallin, Tomarev *et al.*, 1991) are presumed to be present in the cell cytosol, based on immunoblot analyses. Many studies in various other mammalian tissues localize ALDH to various subcellular fractions using differential centrifugation (*e.g.*, Kitabataki *et al.*, 1981; Lindahl and Evees, 1984; Weiner *et al.*, 1987). In addition, there are ample examples of histochemical localization of mammalian ALDH in several tissues including liver, brain, retina, and respiratory tract which employ both immunological (*e.g.*, Maeda *et al.*, 1988; McCaffery *et al.*, 1991, 1992) and activity staining techniques (*e.g.*, Lindahl *et al.*, 1983; Watabiki *et al.*, 1989; Motavkin *et al.*, 1990).

The ultrastructure of lens cells and the location of the lens crystallins in ocular lenses of vertebrates and the light organ of *E. scolopes* share some common features. Crystallins in vertebrate eye lenses are highly expressed in terminally differentiated fiber cells, which lack nuclei, mitochondria, endoplasmic reticulum, and Golgi complexes (Maisel *et al.*, 1981). Similarly, although light organ lens cells retain their nuclei and mitochondria, they too lose other organelles upon differentiation (Fig. 4; McFall-Ngai and Montgomery, 1990). Further, like L-crystallin in the *E. scolopes* light organ lens, crystallins in vertebrate ocular lenses are localized in the cell cytosol (Bloemendal, 1981).

ALDH-like protein occurrence in adult ciliated duct epithelium

ALDH-like protein was also localized in moderate abundance in the epithelial cells lining the ciliated duct (Figs. 1, 2c, d; Table I). Because lens and ciliated duct are unrelated ontogenetically (Montgomery and McFall-Ngai, 1993), it is unlikely that duct epithelium expressing one or more of these proteins is the source of ALDH-like proteins in the muscle-derived lens cells or visa versa. It is possible that the protein species in the duct epithelium is functioning as an enzyme rather than a structural protein.

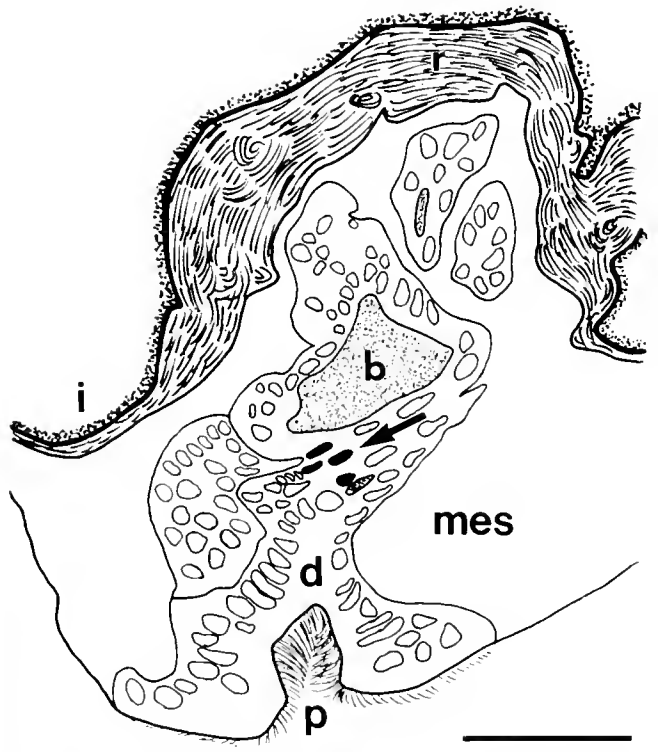

Figure 7. Diagrammatic reconstruction of a light organ from a 1.8 mm juvenile (estimated to be between 7 and 10 days old), illustrating the area where ALDH-like protein is first detected in the ciliated duct epithelium. Arrow points to darkened nuclei, representing cells within the ciliated duct epithelium which contain colloidal gold spheres, immediately adjacent to non-ciliated epithelium, lining the bacteria-containing crypts. All other epithelial cells, represented by clear nuclei, both in the bacteria-containing inner area and in the ciliated duct, lack colloidal gold spheres. b, bacteria-containing crypts; d, ciliated duct epithelium; i, ink sac; mes, mesodermal tissue, the site of the presumptive lens; p, the pore connecting the ciliated duct with the outside of the light organ; and r, reflector. Bar = 50 μm.

We have tested light organ lenses extensively for ALDH activity and found none (Montgomery and McFall-Ngai, 1992), but we have detected very low activities in whole light organs (Montgomery, unpub. data). Activity stains (see above) in the light organ might be a useful technique to further explore the function of the ALDH-like protein species in the ciliated duct epithelium. A positive stain in this tissue would suggest an enzymatic role for this protein.

Unlike lens cells, ciliated duct epithelium comes in direct contact with symbiotic bacteria and possibly other bacteria that enter the light organ through the pores. Some ALDH isozymes function in the detoxification of various biogenic aldehydes that are produced under certain conditions, such as during lipid peroxidation (Holmes *et al.*, 1989) and oxidative stress (Jedziniak *et al.*, 1987; Abedinia *et al.*, 1990). Such conditions have been proposed for several symbioses (Dykens and Shick, 1982; Blum and Fridovich, 1984). It is possible that an enzymatically active ALDH, and thus a form that is biochemically distinct from L-crystallin, could be functioning in a similar capacity in the ciliated duct to detoxify substances from foreign pathogenic microbes or even from symbiotic *V. fischeri* especially in juvenile light organs during the establishment of a stable mutualism.

From our studies, we cannot determine the relation of L-crystallin in the lens with the ALDH-like protein found in the ciliated duct epithelium. Anti-L-crystallin cross-reacts with several ALDH-like proteins, all with 54 kD subunits, from both cephalopods and mammals, but not with other proteins at other molecular masses (Montgomery and McFall-Ngai, 1992). Therefore, anti-L-crystallin is specific to ALDH-like proteins, and not to L-crystallin alone. It can therefore be used to identify ALDH-like proteins in general, but not L-crystallin specifically. Further, we have no sequence information from other ALDH-like proteins in other squid tissues, such as ocular lens and ciliated duct epithelium, with which to infer lineages between the squid ALDH isozymes.

ALDH-like protein localization in juvenile light organs

The examination of ALDH-like protein in juvenile light organs revealed both qualitative and quantitative changes in occurrence through time. Levels of the protein(s) were not significantly above baseline levels, present in all cells, in newly hatched and 5-day symbiotic juveniles and in the 1.6 mm field-caught animal, as shown both with immunocytochemistry and immunoblots. These findings suggest that ALDH-like proteins are neither constitutively expressed in high quantities at the time of hatching nor immediately induced upon infection by bacteria. Based on the size of the 1.8 mm field-caught animal, which was the smallest to stain positive for ALDH-like proteins, we estimate that the age of first induction in juvenile light organs occurs between 7 and 10 days, according to a study by Singley (1983) which correlates size with age in juvenile *E. scolopes* maintained in the laboratory. By comparison, animals hatched under laboratory conditions average 1.6 $\pm$ 0.1 mm mantle length (Montgomery and McFall-Ngai, 1993).

Immunolocalization of field-caught juveniles revealed that ALDH-like protein occurrence in the ciliated duct epithelium and anterior lens precedes that in other portions of the light organ. Further, the onset of expression seems to be related to fundamental changes in light organ morphology. Each side of the newly hatched juvenile light organ possesses three ciliated ducts that lead into three separate crypts. These ducts ultimately coalesce into a single branching duct that leads to a single large pore in symbiotic animals that are more than one week old (Montgomery and McFall-Ngai, 1991). Our data suggest that ALDH-like protein is not expressed in ciliated duct

epithelium until the single duct is formed. Immunoreactive protein was not found in any of the duct epithelial cells in juvenile light organs still containing three ducts per side. However, it was found in a few cells in the duct epithelium in the 1.8 mm juvenile, which had only one duct and pore on each side of the light organ. Because of the small number of cells expressing ALDH-like protein and the relatively low number of spheres within these positive cells, less than one fifth that of adult duct epithelial cells, it appears that these proteins were only just beginning to be synthesized in these cells at this stage of development. Further, expression first occurs in duct epithelial cells that are immediately adjacent to non-ciliated epithelial cells that line the bacteria-containing crypts (Fig. 7). It is in the juvenile light organ that the process of recognition and establishment of symbiotic bacterial strains occurs (McFall-Ngai and Ruby, 1991). High expression of ALDH-like proteins in a tissue in close proximity to the bacteria could indicate that their function is related to bacterial infection.

L-crystallin in developing lens tissue was only detected when clearly differentiated lens cells were present, which suggests that lens cell differentiation occurs before L-crystallin expression. This situation is again analogous to the epidermally derived vertebrate eye lenses where expression of some types of crystallin genes in fiber cells begins only after terminal differentiation (Ramaekers and Bloemendal, 1981). For this reason, the production of certain crystallins is used as a differentiation marker in lens cell tissue culture (Ramaekers and Bloemendal, 1981). Light organ lens cells appear to first differentiate in the anterior portion of the light organ. In the smallest juvenile in which differentiated lens cells were apparent, L-crystallin was found present only in lens cells anterior to the ciliated duct and several cell layers ventral to the crypts. L-crystallin was present in these cells at levels about one half that found in adult lens cells, which suggests that these cells had probably just recently differentiated. The lens cells appear to differentiate from a pad of mesodermal cells that are present ventral and lateral to the bacteria-containing crypts.

Patterns of host gene expression in prokaryote/eukaryote mutualisms

Despite the prevalence of prokaryote/eukaryote symbioses, very little is known about their complex cellular and molecular integration and regulation. One exception is the root nodule symbiosis between the nitrogen-fixing bacterium *Rhizobium* and leguminous plants. There are now many studies that have examined questions of regulation and communication in this highly integrated mutualism. There are a number of plant gene products, nodulins, that are induced or enhanced in the symbiotic organ. The comparison of ALDH-like protein patterns through light organ development with patterns of host gene expression described in symbiotic legumes reveals some interesting parallels. For example, ALDH-like protein is not induced immediately upon infection with bacteria, but is expressed in developing lens only after mesodermal cells differentiate into lens cells. Similarly, induction of leghemaglobin, a nodulin that is thought to aid in creating an oxygen-free environment for bacterial nitrogen fixation, does not occur immediately upon infection, but rather later after the bacteria have invaded the developing nodule (Sanchez *et al.*, 1991). Further, ALDH-like protein induction in the lens occurs far from the site of infection, which suggests that there is a signalling pathway between the lens and the site of bacterial infection. In symbiotic legume roots, similar distances separate the nodule primordia, where early nodulins are induced soon after infection, and the root hairs, the sites of bacterial infection (see Sanchez *et al.*, 1991, and Verma *et al.*, 1992, for reviews).

In future studies we plan to use nucleic acid probes for L-crystallin to examine both the patterns and location of ALDH-like gene expression. Further, we will examine the induction of L-crystallin and other ALDH-like proteins in the juvenile *E. scolopes* light organ. Experimental data will reveal whether (1) over evolutionary time, the symbiosis has resulted in a developmental timetable that includes induction of ALDH-like protein at a prescribed time, regardless of exposure to symbionts or (2) induction of these proteins is a direct result of interactions with the symbiotic bacteria during the infection process.

Acknowledgments

We thank Alicia Thompson for technical support. This work was supported by DCB-8917293 from the National Science Foundation (to M.M.-N.) and N00014-91-J-1357 from the Office of Naval Research (to M.M.-N.) and the ARCS Foundation (to M.K.M.).

Literature Cited

Abedinia, M., T. Pain, E. Algar, and R. Holmes. 1990. Bovine corneal aldehyde dehydrogenase: the major soluble corneal protein with a possible dual protective role for the eye. *Exp. Eye Res.* **51(4):** 419–426.

Bloemendal, H. 1981. The lens proteins. Ch. 1 in *Molecular and Cellular Biology of the Eye Lens,* H. Bloemendal, ed. John Wiley and Sons, New York.

Blum, J., and I. Fridovich. 1984. Enzymatic defenses against oxygen toxicity in the hydrothermal vent animals *Riftia pachyptila* and *Calyptogena magnifica*. *Arch. Biochem. Biophys.* **228(2):** 617–620.

Dykens, J. A., and J. M. Shick. 1982. Oxygen production by endosymbiotic algae controls superoxide dismutase activity in their animal host. *Nature* **297:** 579–580.

Erickson, P. A., D. H. Anderson, and S. K. Fisher. 1987. Use of uranyl acetate en bloc to improve tissue preservation and labeling for post-

embedding immunoelectron microscopy. *J Elec. Micros. Technol* **5**: 303–314.

Hastings, J. W., J. Makemson, and P. V. Dunlap. 1987. How are growth and luminescence regulated independently in light organ symbionts? *Symbiosis* **4**: 3–24.

Herring, P. J. 1988. Luminescent organs. Pp 449–489 in *The Mollusca*, Vol 11. Academic Press, London.

Holmes, R., B. Cheung, and J. VandeBerg. 1989. Isoelectric focusing studies of aldehyde dehydrogenases, alcohol dehydrogenases and oxidases from mammalian anterior eye tissues. *Comp. Biochem. Physiol* **93B**: 271–277.

Ishikawa, H. 1990. A synthesis: the types of interaction system between bacteria and insects. Pp 355–360 in *Endocytobiology IV: 4th International Colloquium on Endocytobiology and Symbiosis*, P. Nardon, V. Gianinazzi-Pearson, A. Grenier, L. Margulis and D. Smith, eds. INRA Service des Publications, Versailles, France.

Jedziniak, J., M. Arredondo, and U. Andley. 1987. Oxidative damage to human eye lenses. *Curr. Eye Res.* **6**: 345–349.

Kitabatake, N., R. Sasaki, and H. Chiba. 1981. Localization of bovine liver aldehyde dehydrogenase isozymes and their immunological properties. *J. Biochem.* **89**: 1223–1229.

Laemmli, U. K. 1970. Cleavage of structural proteins during the assembly of the head of bacteriophage T4. *Nature* **227**: 680–685.

Lindahl, R., R. Clark, and S. Evecs. 1983. Histochemical localization of aldehyde dehydrogenase during rat hepatocarcinogensis. *Cancer Res.* **43**: 5972–5977.

Lindahl, R., and S. Evecs. 1984. Comparative subcellular distribution of aldehyde dehydrogenase in rat, mouse and rabbit liver. *Biochem. Pharmacol.* **33**: 3383–3389.

Maeda, M., Y. Hasumaura, and J. Takeuchi. 1988. Localization of cytoplasmic and mitochondrial aldehyde dehydrogenase isozymes in human liver. *Lab. Invest.* **59**: 75–81.

Maisel, H., C. V. Harding, J. Alcala, J. Kuszak, and R. Bradley. 1981. The morphology of the lens. Ch. 2 in *Molecular and Cellular Biology of the Eye Lens*, H. Bloemendal, ed. John Wiley and Sons, New York.

Margulis, L., and R. Fester. 1991. *Symbiosis as a Source of Evolutionary Innovation.* MIT Press, Cambridge, MA.

McCaffery, P., M. Lee, M. Wagner, N. Sladek, and U. Drager. 1992. Asymmetrical retinoic acid synthesis in the dorsoventral axis of the retina. *Development* **115**: 371–382.

McCaffery, P., P. Tempst, G. Lara, and U. Drager. 1991. Aldehyde dehydrogenase is a positional marker in the retina. *Development* **112**: 693–702.

McFall-Ngai, M., and M. Montgomery. 1990. The anatomy and morphology of the adult bacterial light organ of *Euprymna scolopes* Berry (Cephalopoda:Sepiolidae). *Biol. Bull.* **179**: 332–339.

McFall-Ngai, M., and E. Ruby. 1991. Symbiont recognition and subsequent morphogenesis as early events in an animal-bacterial mutualism. *Science* **254**: 1491–1494.

Montgomery, M., and M. McFall-Ngai. 1991. The influence of bacterial symbionts on early morphogenesis of the light organ of the sepiolid squid *Euprymna scolopes*. *Am. Zool.* **31**: 15A.

Montgomery, M., and M. McFall-Ngai. 1992. The muscle-derived lens of a squid bioluminescent organ is biochemically convergent with the ocular lens. Evidence for recruitment of aldehyde dehydrogenase as a predominant structural protein. *J Biol. Chem* **276(29)**: 20999–21003.

Montgomery, M., and M. McFall-Ngai. 1993. Embryonic development of the light organ of the sepiolid squid *Euprymna scolopes* Berry. *Biol Bull* **184**: 296–308.

Motavkin, P., V. Okhotin, O. Konovko, and S. Zimatkin. 1990. Localization of alcohol- and aldehyde dehydrogenase in the human spinal cord. *Neurosci. Behav. Physiol* **20**: 79–84.

Mnynihan, M. 1983. Notes on the behavior of *Euprymna scolopes* (Cephalopoda:Sepiolidae). *Behavior* **85**: 25–41.

Nap, J. P., and T. Bisseling. 1991. Developmental biology of a plant-prokaryote symbiosis: the legume root nodule. *Science* **250**: 948–954.

Piatigorsky, J., and G. Wistow. 1991. The recruitment of crystallins: new functions precede gene duplication. *Science* **252**: 1078–1079.

Ramaekers, F., and H. Bloemendal. 1981. Cytoskeletal and contractile structures in lens cell differentiation. Ch. 3 in *Molecular and Cellular Biology of the Eye Lens*, H. Bloemendal, ed. John Wiley and Sons, New York.

Richardson, K. C., L. Jarrett, and E. H. Finke. 1960. Embedding in epoxy resin for ultrathin section in electron microscopy. *Stain Technol.* **35**: 313–323.

Ruby, E., and M. McFall-Ngai. 1992. A squid that glows in the night: development of an animal-bacterial mutualism. *J Bacteriol.* **174(15)**: 4865–4870.

Sanchez, F., J. E. Padilla, H. Perez, and M. Lara. 1991. Control of nodulin genes in root-nodule development and metabolism. *Ann. Rev. Plant Physiol.* **42**: 507–528.

Singley, C. 1983. *Euprymna scolopes*. Pp 69–74 in *Cephalopod Life Cycles, Vol 1*. Academic Press, London.

Tomarev, S., R. Zinovieva, and J. Piatigorsky. 1991. Crystallins of the octopus lens. Recruitment from detoxification enzymes. *J. Biol Chem.* **266**: 24226–24231.

Towbin, H., T. Staehelin, and J. Gordon. 1979. Electrophoretic transfer of proteins from polyacrylamide gels to nitrocellulose sheets: Procedure and some applications. *Proc. Natl. Acad. Sci.* **76(9)**: 4350–4354.

Verma, D., C.-A. Hu, and M. Zhang. 1992. Root nodule development: origin, function and regulation of nodulin genes. *Physiol. Plant* **85**: 253–265.

Watabiki, T., T. Tokiyasu, N. Ishida, and K. Ogawa. 1989. Histochemical localization of aldehyde dehydrogenase activity in the mouse liver by the copper ferrocyanide method. *Acta Histochem. Cytochem.* **22**: 397–400.

Wei, S., and R. E. Young. 1989. Development of a symbiotic bacterial bioluminescence in a nearshore cephalopod *Euprymna scolopes*. *Mar. Biol.* **103**: 541–546.

Weiner, H., M. McMichael, E. Lindahl-Hellstrom, and G. Tu. 1987. Use of polyclonal antibodies to study properties of mammalian aldehyde dehydrogenase. *Alcohol. Alcohol.* **Suppl. 1**: 187–191.

Whitaker, J., and P. Granum. 1980. An absolute method for protein determination based on difference in absorbance at 235 and 280 nm. *Anal. Biochem.* **109**: 156–159.

Wistow, G., and H. Kim. 1991. Lens protein expression in mammals: taxon-specificity and the recruitment of crystallins. *J. Mol. Evol.* **32**: 262–269.

Reference: *Biol. Bull* **184**: 322–329. (June, 1993)

The Sequences of Five Neuropeptides Isolated from *Limulus* using Antisera to FMRFamide

GABRIELE GAUS[1], KAREN E. DOBLE[2], DAVID A. PRICE[2], MICHAEL J. GREENBERG[2], TERRY D. LEE[3], AND BARBARA-ANNE BATTELLE[2]

[1]*Institut fur Biologie II (Zoologie), RWTH Aachen, 5100 Aachen, Germany,* [2]*The Whitney Laboratory, St. Augustine, Florida 32086, and* [3]*Division of Immunology, Beckman Research Institute of the City of Hope, Duarte, California 91010*

Abstract. Five neuropeptides were isolated from CNS extracts of the horseshoe crab *Limulus polyphemus* by high pressure liquid chromatography (HPLC). The peptides were identified by radioimmunoassays (RIAs) based on two antisera raised to FMRFamide-related peptides (FaRPs). The purified peptides were analyzed by automated sequencing and mass spectrometry, and the following sequences were obtained: DEGHKMLYFamide, GHSLLHFamide, PDHHMMYFamide, DHGNMLYFamide, and GGRSPSLRLRFamide. The first four peptides are members of a novel family with virtually no relationship to FMRFamide. GGRSPSLRLRFamide, on the basis of structural similarity, becomes the second member of a class of FaRPs known previously only from a peptide isolated from mosquito heads. At least one member of the novel family (GHSLLHFamide) inhibits the isolated heart of *Limulus*.

Introduction

The large set of peptides related—by one or more traits, and to a greater or lesser extent in each—to the molluscan peptide FMRFamide (Phe-Met-Arg-Phe-NH_2) is distributed throughout the animal kingdom, and FMRFamide-like immunoreactivity, as revealed by immunocytochemistry, is seemingly ubiquitous as well (for review see Price and Greenberg, 1989; Greenberg and Price, 1992).

In the horseshoe crab *Limulus polyphemus,* prominent FMRFamide-like immunoreactivity occurs in the brain, cardiac ganglion, and ventral nerve cord (Watson *et al.,* 1984; Watson and Groome, 1989; Groome, 1991). In addition, efferent axons that project to the lateral eyes of *Limulus* also contain FMRFamide-like immunoreactivity (Lewandowski *et al.,* 1989), though these fibers seem to be part of a general epidermal innervation rather than being restricted to the ommatidia. In any event, none of the peptides responsible for this immunoreactivity in *Limulus* have been sequenced.

Biological activity by FMRFamide-related peptides (FaRPs) has also been demonstrated in the horseshoe crab. In particular, two peptides isolated from the lobster (*Homarus americanus*)—F1 (Thr-Asn-Arg-Asn-Phe-Leu-Arg-Phe-NH_2; TNRNFLRFamide) and F2 (Ser-Asp-Arg-Asn-Phe-Leu-Arg-Phe-NH_2, SDRNFLRFamide; Trimmer *et al.,* 1987)—increased both the amplitude and rate of beat of isolated *Limulus* hearts. These effects were similar to those of a partially purified *Limulus* brain extract (Groome, 1991).

Because analogs of F1 and F2 occur in other crustaceans and in insects (Greenberg and Price, 1992), one might suppose that the FMRFamide-like immunoreactivity and cardioactivity in *Limulus* is due to similar peptides. But arthropods contain more than one class of FMRFamide-related peptides. Indeed, in insects, which have been much more extensively and intensively studied, each species appears to have at least four distinct classes of FaRPs (Table I). Moreover, members of the different classes have different biological effects. For example, leucosulfakinin excites the cockroach hindgut while leucomyosuppressin inhibits it (Nachman *et al.,* 1986; Holman *et al.,* 1986); similarly, leucomyosuppressin and its locust homolog SchistoFLRFamide inhibit the semi-isolated heart of *Schistocerca,* whereas F1 and FMRFamide itself are car-

Received 7 December 1992; accepted 29 March 1993.

Table I

*Representatives of four classes of FMRFamide-related peptides present in dipteran insects**

Class	Sequence	Reference
FaGRPs[a]	Asp-Pro-Lys-Gln-Asp-Phe-Met-Arg-Phe-NH_2	(Schneider and Taghert, 1988)
Myosuppressins[b]	Thr-Asp-Val-Asp-His-Val-Phe-Leu-Arg-Phe-NH_2	(Nichols, 1992)
Sulfakinins[c]	pGlu-Ser-Asp-Asp-Tyr-Gly-His-Met-Arg-Phe-NH_2	(Nichols *et al.*, 1988)
Head peptides[d]	pGlu-Arg-Pro-Pro-Ser-Leu-Lys-Thr-Arg-Phe-NH_2	(Matsumoto *et al.*, 1989)

* The first three peptides in the list were isolated from *Drosophila melanogaster*; the fourth is from *Aedes aegypti*.

[a] FMRFamide-gene-related peptides; multiple, variable copies processed from a precursor.

[b] Similar C-terminal tetrapeptide, but not encoded on any known FMRFamide gene; peptide shown is *Drosophila* myosuppressin; type of the class is leucomyosuppressin from *Leucophaea maderae*.

[c] Only C-terminal tripeptide is analogous to FaGRPs; peptide shown is drosulfakinin; type of the class is leucosulfakinin.

[d] Only C-terminal dipeptide is analogous to FaGRPs.

dioexcitatory (Cuthbert and Evans, 1989; Robb *et al.*, 1989).

We therefore isolated the FMRFamide-like immunoreactivity in *Limulus* brains and circumesophageal rings and report here the sequences of five neuropeptides that were identified. One is homologous to an insect head peptide and is only the second member of what may be an arthropodan class of FaRPs. The other four are apparently homologs in a novel peptide family of uncertain phyletic relations. One peptide from this novel group was synthesized and tested on the isolated *Limulus* heart; it is not only a potent cardioinhibitor, but also occurs in heart extracts. We speculate, therefore, that this peptide functions as a cardioregulatory neurotransmitter.

Materials and Methods

Animals

Adult *Limulus polyphemus*, in intermolt and measuring 15–25 cm across the carapace, were collected in the Indian River near Cape Canaveral, Florida. The animals were maintained in running natural seawater (15–18°C) and fed once a week.

Peptide extraction and purification

Brains (including both the protocerebrum and the circumesophageal ring) were collected from horseshoe crabs over several months as the animals were used for visual system studies. Each excised piece of tissue was weighed and then added to a flask of acetone (40 ml) that was kept at −20°C between successive additions. When 9–10 g had been accumulated, the extract was further processed as outlined below. Heart (12.9 g) and lateral eye (3.5 g) were treated similarly.

The acetone extracts were decanted from the pieces of tissue, then clarified by centrifugation, and reduced in volume on a rotary evaporator. The latter step removed most of the acetone and left an aqueous phase consisting of water derived from the tissue. After the addition of 50 ml aqueous 0.1% trifluoroacetic acid (TFA), the extract was again clarified by centrifugation and by filtration through a nylon filter (0.45 μm pore size). The clarified liquid was pumped onto an HPLC column (Brownlee C8 RP-300, 4.6 mm × 220 mm) at 2 ml/min, and this flow rate was maintained throughout the run. After the column had been loaded, it was washed with 0.1% aqueous TFA until the absorbance returned close to the baseline. The solvent composition was then stepped to 16% acetonitrile (ACN) in aqueous 0.1% TFA, and a linear gradient (0.8%/min increase in ACN concentration) was begun when the solvent front reached the detector as indicated by a rapid increase in absorbance. Fractions were collected by time (0.5 min), and an aliquot (2 μl) of each fraction was taken for radioimmunoassay (RIA).

Further purifications of immunoreactive fractions were performed on a smaller diameter column containing the same packing as that used for the initial run (Brownlee C8 RP-300; 2.1 × 220 mm), but with two additional solvent systems: 80% ACN containing 0.05% heptafluorobutyric acid (HFBA), or phosphate buffer (5 m*M*) containing 60% ACN, pH 7.0. The gradients were 0–30, 10–40, or 20–50% of the respective organic solvent, over 30 min, at a flow rate of 0.5 ml/min. The pooled immunoreactive fractions from one run were diluted with an aliquot of aqueous solvent and pumped onto the column at 0.5 ml/min for the next run. Once a peak was substantially pure, we attempted to oxidize the contained peptide and thereby shift its elution time; this maneuver was meant to achieve a further purification, and to help in the characterization. We oxidized the peptide by addition of hydrogen peroxide (50 μl/ml of a 30% solution) directly to the immunoreactive fraction in a TFA- or HFBA-containing solvent; this converts methionine almost

exclusively to methionine sulfoxide. The reaction was terminated after 15 min by the addition of 1–2 ml aqueous solvent, and the sample was loaded onto the HPLC column.

Radioimmunoassay (RIA)

RIAs were carried out as previously described (*e.g.*, Price, 1982; Price *et al.*, 1987, 1990). Two antisera that had been raised in rabbits to thyroglobulin-peptide conjugates were used in these assays: antiserum S253 raised to YGGFMRFamide, and Q2 raised to pGluDPFLRFamide and AspDPFLRFamide. Iodinated pQYPFLRFamide was the trace for both assays.

Mass spectrometry and sequencing

The molecular ions and, in some cases, fragment ions of purified immunoreactive fractions were analyzed by fast atom bombardment mass spectrometry (FABms), as described previously (Bulloch *et al.*, 1988). Fractions were also subjected to automated Edman sequencing (Applied Biosystems Inc. sequencer, Model 470A) with automatic, online HPLC analyses of the phenylthiohydantoin (PTH) amino acids released at each cycle (performed by B. Parten, University of Florida Interdisciplinary Center for Biotechnology Research, Protein Chemistry Core Facility, Gainesville. See Díaz-Miranda *et al.*, 1992, for details).

Synthetic peptides

Peptide resins (GHSLLHFamide and GGRSPSLRLRFamide) were synthesized by the Protein Chemistry Laboratory of the University of Florida's Interdisciplinary Center for Biotechnology Research on an Applied Biosystems 430A peptide synthesizer, starting with MBHA resin and utilizing the protecting groups recommended by Applied Biosystems for use with the trifluoromethanesulfonic acid (TFMSA) deprotection and cleavage system. The peptides were deprotected and cleaved from the resin at the Whitney Laboratory (with TFMSA), purified by HPLC, and quantified by amino acid analysis (Hitachi 835 analyzer).

Bioassay

The heart with its associated cardiac ganglion was removed from the animal and suspended lengthwise in a glass chamber (25 ml) containing natural seawater that was aerated continuously. One end of the heart was fixed near the bottom of the chamber, and the opposite end was hooked to a force-displacement transducer (Grass Model FT .03C). The amplitude and frequency of heartbeat was displayed on an ink-writing oscillograph (Grass Model 7 Polygraph).

Synthetic peptides (GGRSPSLRLRFamide and GHSLLHFamide) were dissolved in an aliquot of seawater (200 μl) which was added directly to the chamber; concentrations are expressed as moles per liter in the bath. The amplitude of beat was measured at the point of maximal response, about 2–3 min after the dose of peptide was added. This measurement, expressed as a percentage of the beat amplitude before treatment, was taken as the response.

Results

Identification of peptides from the CNS

Two CNS extracts were chromatographed by HPLC, and the fractions were assayed with both the Q2 and S253 antisera. The fractions constituting corresponding immunoreactive peaks from each chromatographic run were combined and further purified. In the end, six peaks that were immunoreactive with the Q2 antiserum were isolated.

One of these peaks showed slight immunoreactivity with the S253 antiserum (in addition to that with Q2), did not undergo a shift in elution time after oxidation, and showed very little UV absorbance at 280 nm. We had sufficient material to obtain both a molecular ion and sequence data from this peak. From the protonated molecular ion, which had an m/z ratio of 1244.6, and the sequence Gly-Gly-Arg-Ser-Pro-Ser-Leu-Arg-Leu-Arg-Phe, we deduced the full structure GGRSPSLRLRFamide. This sequence is very similar to that of Aea-HP, the mosquito head peptide (Matsumoto *et al.*, 1989; see Table I), so we will refer to it henceforth as the *Limulus* head peptide (Lip-HP)*.

A second immunoreactive peak (LP1)—after oxidation—eluted about 3 min earlier and showed significant UV absorbance at 280 nm. This peak yielded a partial sequence XEGHKMLYF (X-Glu-Gly-His-Lys-Met-Leu-Tyr-Phe), where X could have been Ala, Asp, or Ser. Although this sequence did contain the methionine and aromatic amino acid (tyrosine, Y) expected from the properties of the immunoreactive peptide in peak LP1, it remained ambiguous, not only because of the free amino acid contamination, but also because no prominent molecular ion was found.

Analysis of the third peak (LP2) revealed a prominent monoisotopic, protonated ion at an m/z ratio of 809.4, and subsequent sequencing of the peak yielded the peptide

* Of course *Limulus* lacks a head, but we retain the name "head peptide" for the sake of continuity and a modest reduction in confusion. The species designation, as with some insect peptides, is derived from the first two letters of the genus and the first letter of the species; hence "Lip" from *Li*mulus *p*olyphemus.

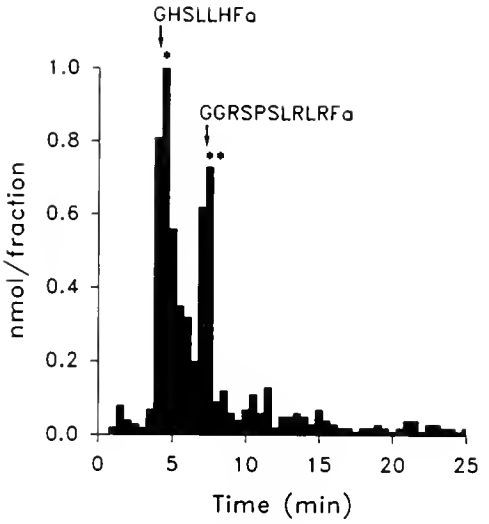

Figure 1. RIA analysis of the initial HPLC fractionation of a *Limulus* CNS extract (second experiment). Half-minute fractions were collected, and 2-μl aliquots were taken from each fraction for the RIA using the Q2 antiserum. The immunoreactive peaks containing peptides LP1-LP4 are indicated: * (LP1, LP2, LP3); ** (LP4). In a previous purification, the *Limulus* head peptide (Lip-HP) was isolated from the second peak (**). The elution times of LP2 (GHSLLHFamide) and Lip-HP (GGRSPSLRLRFamide) are indicated with arrows. The sequences and molecular ions of all of the peptides are listed in Table II.

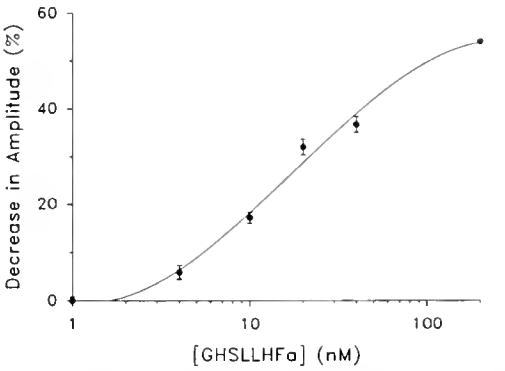

Figure 2. Dose-response relationship of the effect of GHSLLHFamide (LP2) on the isolated *Limulus* heart. LP2 decreases the amplitude of the beat with a threshold of 4 nM (Nine or ten determinations on five different hearts; SEM < 2%). The measurement of the response, the percentage of amplitude relative to that of the control beat, is described in Materials and Methods.

sequence GHSLLHF. This sequence is in agreement with the calculated molecular weight of 808 for GHSLLHF, assuming an amidated carboxyl terminus (Gly-His-Ser-Leu-Leu-His-Phe-NH_2).

The remaining three peaks contained insufficient material for either microsequencing or FABms. We therefore prepared a new extract to resolve the ambiguities left by the first experiment.

The first HPLC fractionation of this new CNS extract, after RIA analysis with the Q2 antiserum, showed immunoreactive peaks (Fig. 1) similar to those in the RIA profile obtained from the earlier CNS extracts. When the S253 antiserum was used, some peaks were more clearly defined than in the previous experiment. Two peptides (LP3 and LP4) that reacted only with the Q2, and that had not been identified earlier, were isolated and identified. In addition, the identification of LP1 was completed with the new extract. The details of these findings are set out below.

After oxidation, peak LP3 eluted almost 8 min earlier; shifts of this magnitude are indicative of more than one methionyl residue. A prominent monoisotopic protonated ion was found at an m/z ratio of 1109.2, and automated Edman degradation of 125 pmol of peptide yielded the sequence PDHHMMYF (Pro-Asp-His-His-Met-Met-Tyr-Phe). This sequence is consistent with the calculated molecular weight of 1108 for LP3, assuming an amidated carboxyl terminus and both methionyl residues as the sulfoxides.

The elution time of LP4 also shifted after oxidation, though not as much as that of LP3. FABms analysis of the immunoreactive peak revealed a prominent protonated molecular ion at an m/z ratio of 1011.2. Further analysis of the fragment ions yielded the sequence DHGNMLYFamide (Asp-His-Gly-Asn-Met-Leu-Tyr-Phe-NH_2).

Finally, the molecular ion for LP1 was obtained (1155.8), and fragment ions indicative of an N-terminal aspartic acid residue were also found. So the sequence of this peptide was deduced to be: DEGHKMLYFamide.

Peptide synthesis

The synthetic peptides GGRSPSLRLRFamide and GHSLLHFamide were purified by HPLC. Amino acid

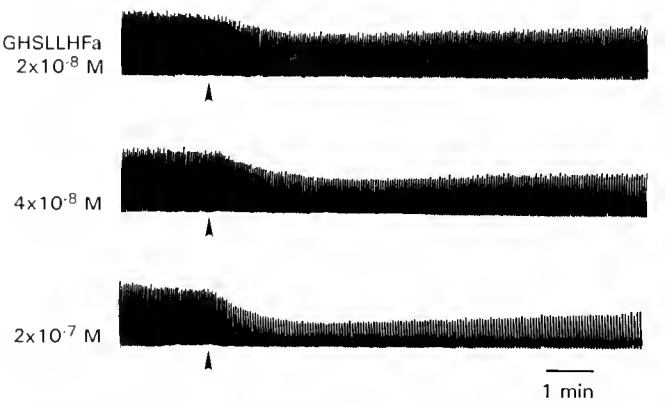

Figure 3. LP2-induced decreases in strength and rate of contractions of the isolated *Limulus* heart. Whereas the effect on the heart rate is long-lasting, the amplitude starts to increase again 4–5 min after peptide application.

Table II

Peptides isolated and sequenced from Limulus

Name	Sequence	Monoisotopic MH+**	Average MH+	Observed MH+
Lip-HP*	GGRSPSLRLRFamide	1244.73	1245.48	1244.6
LP1	DEGHKMLYFamide	1154.53	1155.32	1155.8 (Avg)
LP2	GHSLLHFamide	809.44	809.95	809.4
LP3	PDHHMMYFamide	1108.45	1109.27	1109.2 (Avg)
LP4	DHGNMLYFamide	1011.44	1012.13	1011.2

* Lip-HP: *Limulus* head peptide (see footnote *; p. 324).
** MH+; protonated molecular ion, nominal mass.

analysis of an aliquot gave the following composition of GGRSPSLRLRFamide: Gly 2.2, Ser 1.9, Leu 2.2, Phe 0.8, Pro 1.0, Arg 3.0. Amino acid analysis of an aliquot of GHSLLHFamide yielded the composition: Gly 1.1, Ser 1.0, Leu 2.0, Phe 0.86, His 1.6. These synthetic peptides co-eluted with their natural congeners when they were rechromatographed on the 2.1 × 220 mm Brownlee column with the ACN/TFA solvent system used with a gradient of 20–50%.

Peptides from the heart

The heart contains less peptide per unit weight than the CNS, but we were still able to purify enough of one Q2-reactive peak to carry out an FABms analysis. This peak showed a prominent protonated molecular ion at an m/z ratio of 809 (the same as LP2), and fragment ions characteristic of the sequence GHSLLHFamide were observed.

Lateral eye extract

HPLC purification of a lateral eye extract, and subsequent analysis by RIA with the Q2 and S253 antisera, revealed no significant immunoreactivity.

Bioactivity of synthetic GGRSPSLRLRFamide and GHSLLHFamide

Concentrations of synthetic GGRSPSLRLRFamide between 2×10^{-8} and 10^{-6} mol/l had no effect on the rate or amplitude of isolated *Limulus* hearts. A slight decrease in amplitude was finally observed at 5×10^{-6} mol/l, but no dose-response curve could be established for this peptide.

Synthetic GHSLLHFamide, on the other hand, produced a dose-dependent decrease in beat amplitude; the threshold was 4×10^{-9} mol/l. Figure 2 shows the dose response relationship for this response; each point represents the average decrease in amplitude from 9–10 experiments with five different hearts. Higher concentrations of GHSLLHFamide (from 2×10^{-8} mol/l) also decreased heart rate (Fig. 3).

5-HT (5-hydroxytryptamine, serotonin) also inhibits the *Limulus* heart, and its effects are blocked by 2-bromo, d-lysergic acid diethylamide (Burgen and Kuffler, 1957; Pax and Sanborn, 1967). We asked whether another lysergic acid analog, methysergide [a 5-HT antagonist on molluscan (Wright *et al.*, 1962) and crustacean (Kerkut and Price, 1964) hearts] might block the effect of

Table III

Comparison of Limulus *head peptide (Lip-HP) with peptides from other species*

Peptide*	Species	Sequence	Reference
Lip-HP	*Limulus polyphemus*	Gly-Gly-Arg-Ser-Pro-Ser-Leu-Arg-Leu-Arg-Phe-amide	This paper
Aea-HP	*Aedes aegypti*	pGlu-Arg-Pro-Pro-Ser-Leu-Lys-Thr-Arg-Phe-amide	(Matsumoto *et al.*, 1989)
NPF	*Helix aspersa*	-Tyr-Ala-Ile-Met-Gly-Arg-Thr-Arg-Phe-amide	(Halton *et al.*, 1992)
PP (C-terminal)	*Alligator mississippiensis*	-Tyr-Leu-Asn-Val-Val-Thr-Arg-Pro-Arg-Phe-amide	(Lance *et al.*, 1984)
—	*Helicoverpa zea*	Gln-Ala-Ala-Arg-Pro-Arg-Phe-amide	(Crim, pers. comm.)
NPFF	*Bos taurus*	Pro-Phe-Trp-Ser-Leu-Ala-Ala-Pro-Gln-Arg-Phe-amide	(Yang *et al.*, 1985)
Chicken brain peptide	*Gallus gallus*	Leu-Pro-Leu-Arg-Phe-amide	(Dockray *et al.*, 1983)

* Abbreviations: Aea-HP, *Aedes aegypti* head peptide; NFP, neuropeptide F; PP, pancreatic polypeptide (NFP and PP sequences are not complete; only the C-terminal is shown.); NPFF, neuropeptide Phe-Phe; (—), no common name given.

Table IV

Sequence homologies of peptides from Limulus, *a chiton, and a sea cucumber*

Species		Sequence
Limulus polyphemus	(LP1)	Asp-Glu-Gly-His-Lys-Met-Leu-Tyr-Phe-amide
	(LP2)	Gly-His-Ser-Leu-Leu-His-Phe-amide
	(LP3)	Pro-Asp-His-His-Met-Met-Tyr-Phe-amide
	(LP4)	Asp-His-Gly-Asn-Met-Leu-Tyr-Phe-amide
*Acanthopleura granulata**		Gly-Gly-Thr-Leu-Leu-Arg-Phe-amide
		Gly-Ser-Leu-Leu-Arg-Phe-amide
*Holothuria glaberrima***		Ser-Gly-Tyr-Ser-Val-Leu-Tyr-Phe-amide
		Gly-Phe-Ser-Lys-Leu-Tyr-Phe-amide

* A chiton; sequence from Greenberg and Price (1992).

** A sea cucumber; sequence from Díaz-Miranda *et al.* (1991).

GHSLLHFamide on *Limulus* heart. Methysergide alone increased the heart rate, but had no effect on the amplitude of beat. After application of methysergide (4×10^{-5} M) for 3 min, the inotropic effect of 5-HT (up to 2×10^{-7} mol/l) was totally blocked. In contrast, GHSLLHFamide, under the same conditions, still produced a dose-dependent decrease in amplitude. 5-HT and the peptide were each tested 10–11 times on 7 different hearts.

Discussion

We have isolated five neuropeptides from CNS extracts of the horseshoe crab *Limulus polyphemus* (Table II). One of these, GGRSPSLRLRFamide (Lip-HP), has 60–67% sequence similarity to another peptide, pQRPPSLKTRFamide (Aea-HP in Table III), which was discovered in the head of the mosquito *Aedes aegypti* (Matsumoto *et al.*, 1989). The identical residues are, furthermore, distributed along the length of the two sequences, and both peptides occur in arthropods. We therefore suppose that Lip-HP and Aea-HP are homologous.

The *Limulus* and mosquito head peptides also share some sequence similarity to the extended family of pancreatic polypeptide-like peptides (NPF and PP in Table III; see Halton *et al.*, 1992), as well as to a mélange of others (Table III). The disparity in the lengths of these peptides, the diversity of the organisms that contain them, and the restriction of the sequence similarities to the C-terminal pentapeptide, all suggest, however, that such similarities may be due to convergence.

The function of neither the horseshoe crab nor the mosquito head peptide is known. But since GGRSPSLRLRFamide had only a very weak cardioinhibitory effect in *Limulus*, with a threshold 5 μM, it is probably not a cardioregulatory agent.

An amidated carboxyl terminal phenylalanine is the only absolutely conserved feature shared by the *Limulus* peptides: DEGHKMLYFamide (LP1), GHSLLHFamide (LP2), PDHHMMYFamide (LP3), and DHGNMLYFamide (LP4). Nevertheless, histidine and tyrosine are commonly exchanged for one another in related proteins (their codons differ at only one position), and methionine-leucine exchanges are also quite frequent, as for example in FMRFamide and FLRFamide. We therefore tentatively propose that these four peptides represent a previously unknown, novel family in arthropods. Because the peptides are of roughly equal abundance, analogy with other peptide families (Greenberg and Price, 1992) suggests that they may even be products of a single precursor.

As one might expect of a "novel" family, the affinities of LP1-4 to other peptides are not obvious. Still, their amino acid sequences are somewhat similar to those of two peptides (GSLLRFamide and GGTLLRFamide) isolated from the granular spiny chiton *Acanthopleura granulata* (Greenberg and Price, 1992), and to another pair (GFSKLYFa and SGYSVLYFa) recently isolated from a sea cucumber, *Holothuria glaberrima* (Díaz-Miranda *et al.*, 1991) (Table IV). But the significance of these similarities is obscure.

One peptide of the proposed new family, GHSLLHFamide, was found in *Limulus* heart extracts. Synthetic GHSLLHFamide decreased the amplitude and rate of heartbeat, and the inotropic effect had a low threshold. The only other known cardioinhibitory transmitter in *Limulus* is 5-HT (Pax and Sanborn, 1967). The action and time course of 5-HT and GHSLLHFamide are quite similar, but whereas the effect of 5-HT can be completely blocked by methysergide, that of GHSLLHFamide was unaffected. We therefore conclude that the peptide does not act by releasing 5-HT from nerve terminals in the heart.

The activities of the other peptides, LP1, LP3, and LP4, are now being assayed on the *Limulus* heart. These experiments may reveal whether the sequence similarities between these peptides and GHSLLHFamide are more important functionally than their differences.

The two antisera used for RIA have quite different specificities for recognizing FaRPs; nevertheless, we are aware that many known FaRPs would not be detected by these antisera. A particular limitation is that the specificity of neither antiserum is determined primarily by the C-terminal RFamide, which is often thought to be the minimal determinant for a peptide to be considered FMRFamide-like. But the antisera do recognize well those peptides that contain the full C-terminal sequence: F(M or L)RFamide, especially when they are extended at the N-terminal. So it is surprising that we could isolate *no* such peptides, especially considering that their presence

has been established in other arthropods. However, because the various FaRPs present in any one species are not expressed at the same level, we may have missed some of the less abundant, but more FMRFamide-related peptides that may be present in *Limulus*. Indeed, evidence from bioassay and immunocytochemistry indicates that peptides more closely related to FMRFamide are present in *Limulus* (Watson *et al.*, 1984; Watson and Groome, 1989; Groome, 1991).

Notwithstanding that FaRPs have been detected immunocytochemically in the lateral eye of the horseshoe crab (Lewandowski *et al.*, 1989), we could detect no immunoreactive fractions in an extract of 50 lateral eyes. We therefore conclude that these peptides are present in the eye in such small amounts, that we are not able to detect them with the S253 and Q2 antisera.

In summary, we have isolated several members of a novel family of peptides, and one of them may be involved in cardioregulation. We have also isolated a close analog of an insect peptide, thereby establishing a pan-arthropodan class of FaRPs. The relationship between these two groups of peptides and those of other phyla are uncertain.

To date, only one other peptide from *Limulus* has been sequenced: proctolin (Groome *et al.*, 1990), which is identical in structure to the peptide originally found in the cockroach (H-Arg-Tyr-Leu-Pro-Thr-OH) by Starrat and Brown (1975). The effect of proctolin on the isolated *Limulus* heart is to increase the amplitude of contraction (Groome *et al.*, 1990).

Acknowledgments

This research was supported by funds from the National Institute of Health (HL28440 to MJG) and the Deutsche Forschungsgemeinschaft (Ga344/2-1 to GG). Peptide sequence analysis and peptide synthesis were provided by the Protein Chemistry Core Facility Interdisciplinary Center for Biotechnology Research, University of Florida. We also thank Lynn Milstead for her assistance in the preparation of figures, and Glen A. Cottrell and two anonymous reviewers for their critical and valuable reviews of the manuscript.

Literature Cited

Bulloch, A. G. M., D. A. Price, A. D. Murphy, T. D. Lee, and H. N. Bowes. 1988. FMRFamide peptides in *Helisoma:* identification and physiological actions at a peripheral synapse. *J. Neurosci.* **8:** 3459–3469.

Burgen, A. S. V., and S. W. Kuffler. 1957. The inhibition of the cardiac ganglion of *Limulus polyphemus* by 5-hydroxytryptamine. *Biol. Bull.* **113:** 336.

Cuthbert, B. A., and P. D. Evans. 1989. A comparison of the effects of FMRFamide-like peptides on locust heart and skeletal muscle. *J. Exp. Biol.* **144:** 395–415.

Díaz-Miranda, L., D. A. Price, M. J. Greenberg, T. D., Lee, K. E. Doble, and J. E. García-Arrarás. 1992. Characterization of two novel neuropeptides from the sea cucumber *Holothuria glaberrima. Biol Bull.* **182:** 241–247.

Dockray, G. J., J. R. Reeve Jr., J. Shively, R. J. Gayton, and C. S. Barnard. 1983. A novel active pentapeptide from chicken brain identified by antibodies to FMRFamide. *Nature* **305:** 328–330.

Greenberg, M. J., and D. A. Price. 1992. Relationships among the FMRFamide-like peptides. *Prog. Brain Res.* **92:** 25–37.

Groome, J. R. 1991. Cardioregulatory peptides in *Limulus:* effects of F1, F2 and an endogenous FMRFamide-like peptide on the neurogenic heart. *Biol. Bull.* **181:** 353.

Groome, J. R., E. K. Tillinghast, M. A. Townley, A. Vetrovs, W. H. Watson, III, D. F. Hunt, P. R. Griffin, J. E. Alexander, and J. Shabanowitz. 1990. Identification of proctolin in the central nervous system of the horseshoe crab, *Limulus polyphemus. Peptides* **11:** 205–211.

Halton, D. W., C. Shaw, A. G. Maule, C. F. Johnston, and I. Fairweather. 1992. Peptidergic messengers: a new perspective of the nervous system of parasitic platyhelminths. *J. Parasitol.* **78:** 179–193.

Holman, G. M., B. J. Cook, and R. J. Nachman. 1986. Isolation, primary structure and synthesis of leucomyosuppressin, an insect neuropeptide that inhibits spontaneous contractions of the cockroach hindgut. *Comp. Biochem. Physiol.* **85C:** 329–333.

Kerkut, G. A., and M. A. Price. 1964. Chromatographic separation of cardiaccelerators (6HT and a mucopeptide) from *Carcinus* heart. *Comp. Biochem. Physiol.* **11:** 45–52.

Lance, V., J. W. Hamilton, J. B. Rouse, J. R. Kimmel, and H. G. Pollock. 1984. Isolation and characterization of reptilian insulin, glucagon, and pancreatic polypeptide: complete amino acid sequence of alligator (*Alligator mississippiensis*) insulin and pancreatic polypeptide. *Gen. Comp. Endocrinol.* **55:** 112–124.

Lewandowski, T. J., II. K. Lehman, and S. C. Chamberlain. 1989. Immunoreactivity in *Limulus:* III. Morphological and biochemical studies of FMRFamide-like immunoreactivity and colocalized substance P-like immunoreactivity in the brain and lateral eye. *J. Comp. Neurol.* **288:** 136–153.

Matsumoto, S., M. R. Brown, J. W. Crim, S. R. Vigna, and A. O. Lea. 1989. Isolation and primary structure of neuropeptides from the mosquito, *Aedes aegypti,* immunoreactive to FMRFamide antiserum. *Insect Biochem.* **19:** 277–283.

Nachman, R. J., G. M. Holman, W. F. Haddon, and N. Ling. 1986. Leucosulfakinin, a sulfated insect neuropeptide with homology to gastrin and cholecystokinin. *Science* **234:** 71–73.

Nichols, R. 1992. Isolation and structural characterization of *Drosophila* TDVDHVFLRFamide and FMRFamide containing neural peptides. *J. Mol. Neurosci.* **3:** 213–218.

Nichols, R., S. A. Schneuwly, and J. E. Dixon. 1988. Identification and characterization of a *Drosophila* homologue to the vertebrate neuropeptide cholecystokinin. *J. Biol. Chem.* **263:** 12,167–12,170.

Pax, R. A., and R. C. Sanborn. 1967. Cardioregulation in *Limulus* III. Inhibition by 5-hydroxytryptamine and antagonism by bromlysergic acid diethylamide and picrotoxin. *Biol. Bull.* **132:** 392–403.

Price, D. A. 1982. The FMRFamide-like peptide of *Helix aspersa. Comp. Biochem. Physiol.* **72C:** 325–328.

Price, D. A., and M. J. Greenberg. 1989. The hunting of the FaRPs: the distribution of FMRFamide-related peptides. *Biol. Bull.* **177:** 198–205.

Price, D. A., C. G. Cobb, K. E. Doble, J. K. Kline, and M. J. Greenberg. 1987. Evidence for a novel FMRFamide-related heptapeptide in the pulmonate snail *Siphonaria pectinata. Peptides* **8:** 533–538.

Price, D. A., W. Lesser, T. D. Lee, K. E. Doble, and M. J. Greenberg. 1990. Seven FMRFamide-related and two SCP-related cardioactive peptides from *Helix. J. Exp. Biol.* **154:** 421–437.

Robb, S., L. C. Packman, and P. D. Evans. 1989. Isolation, primary structure and bioactivity of SchistoFLRFamide, a FMRFamide-like neuropeptide from the locust, *Schistocerca gregaria*. *Biochem. Biophys. Res. Commun.* **160:** 850–856.

Schneider, L. E., and P. H. Taghert. 1988. Isolation and characterization of a *Drosophila* gene that encodes multiple neuropeptides related to Phe-Met-Arg-Phe-NH_2 (FMRFamide). *Proc. Natl. Acad. Sci. USA* **85:** 1993–1997.

Starrat, A. N., and B. E. Brown. 1975. Structure of the pentapeptide proctolin, a proposed neurotransmitter in insects. *Life Sci.* **17(C):** 1253–1256.

Trimmer, B. A., L. A. Kobierski, and E. A. Kravitz. 1987. Purification and characterization of FMRFamide-like immunoreactive substances from the lobster nervous system: isolation and sequence analysis of two closely related peptides. *J. Comp. Neurol.* **265:** 16–26.

Watson, W. H., III, and J. R. Groome. 1989. Modulation of the *Limulus* heart. *Am. Zool.* **29:** 1287–1303.

Watson, W. H., III, J. R. Groome, B. M. Chronwall, J. Bishop, and T. L. O'Donohue. 1984. Presence and distribution of immunoreactive and bioactive FMRFamide-like peptides in the nervous system of the horseshoe crab, *Limulus polyphemus*. *Peptides* **5:** 585–592.

Wright, A. M., M. Moorhead, and J. H. Welsh. 1962. Actions of derivatives of lysergic acid on the heart of *Venus mercenaria*. *Brit. J. Pharmacol.* **18:** 440–450.

Yang, H.-Y. T., W. Fratta, E. A. Majane, and E. Costa. 1985. Isolation, sequencing, synthesis, and pharmacological characterization of two brain neuropeptides that modulate the action of morphine. *Proc. Natl. Acad. Sci. USA* **82:** 7757–7761.

Reference: *Biol. Bull.* **184**: 330–337. (June, 1993)

Endocytosis in Adult Eel Intestine: Immunological Detection of Phagocytic Cells in the Surface Epithelium

SHOUHEI TAMURA, TAKAHIKO SHIMIZU, AND SUSUMU IKEGAMI

Department of Applied Biochemistry, Hiroshima University, 1-4-4 Kagamiyama, Higashi-Hiroshima, Hiroshima 724, Japan

Abstract. This study was undertaken to isolate groups of eel (*Anguilla japonica*) intestinal cells undergoing active endocytosis *in vivo* and to localize these cells within the intestinal epithelium. A monoclonal antibody (8F1) of the immunoglobulin M class containing kappa light chains was raised against such endocytic cells. Ninety-three percent of the 8F1-positive cells absorbed fluorescent isothiocyanate-conjugated dextran from the intestinal lumen *in vivo* during a 30-min incubation, and they retained the ability to absorb dextran *in vitro*. The 8F1-positive cells constitute about 15% of the whole dissociated, macromolecule-absorbing cells. This suggests that other types of endocytic cells exist in the epithelium. The 8F1-positive cell can internalize fixed *Vibrio anguillarum in vivo*. Immunohistochemical observations demonstrated that 8F1-positive cells are very few in number and are located exclusively in the surface epithelium of the intestine. Thus these cells may well be specified phagocytic cells, different from those playing a basic nutritional role.

Introduction

Intestinal cells of adult teleosts are able to internalize intact protein molecules through pinocytosis (Rombout *et al.*, 1985; McLean and Ash, 1987; Georgopoulou *et al.*, 1988). Furthermore, the intestine ingests the bacterium *Vibrio anguillarum*, the causative agent of a widely distributed hermorrhagic septicaemia of teleost fish (Davina *et al.*, 1982; Rombout *et al.*, 1986; Vigneulle and Laurencin, 1991). A variety of hypotheses meant to explain the physiological significance of these observations have been proposed. Ezeasor and Stokoe (1981) and Georgopoulou *et al.* (1986) have suggested that the non-selective absorption of macromolecules may represent an extension of the normal digestive capacity of the fish intestine. On the other hand, Noaillac-Depeyre and Gas (1976) have proposed that endocytosis may be linked to antigen sampling and the subsequent mounting of an immune response in a similar manner to that described for the microfold or "M" cells of mammals (Owen, 1977; Wolf *et al.*, 1981). But since the cytology of the cells engaged in endocytosis is poorly known, the physiological significance of this phenomenon remains largely a matter for conjecture.

Experiments described in this report were therefore designed to isolate groups of cells undergoing active endocytosis *in vivo* and to determine the location of these cells within the intestinal epithelium. The adult eel *Anguilla japonica* was used as the experimental animal. A monoclonal antibody that reacts specifically with a single group of endocytic cells was obtained. Immunohistochemical analysis with this antibody revealed that a very limited number of the endocytic cells in the surface epithelium of the intestine carries the antigen molecules. The antibody-reactive cell retains the ability to internalize macromolecules *in vitro* after dissociation from the intestine.

Materials and Methods

Materials

Adult specimens of both sexes of the eel *Anguilla japonica*, with body weights of 180–220 g, were obtained

Received 9 September 1992; accepted 22 March 1993.

Abbreviations: ASW, artificial seawater; BSA, bovine serum albumin; ELISA, enzyme-linked immunosorbent assay; FCS, fetal calf serum; FDIC, fluorescein isothiocyanate-conjugated-dextran-incorporating cells; FITC, fluorescein isothiocyanate; Ig, immunoglobulin; IMDM, Iscove's modified Dulbecco's medium; PBS, phosphate-buffered saline without divalent cations; TPBS, PBS containing 0.05% Tween 20.

from a local farm and were maintained without food, in plastic aquaria containing artificial seawater (ASW, 20°C), for more than 1 week before use.

Formalin-fixed cells of the bacterium, *Vibrio anguillarum* strain PT-87050, and rabbit antisera reacting specifically with this bacterial strain were gifts from Dr. T. Nakai, Hiroshima University.

Rabbit immunoglobulin (Ig) G was purified from the serum of a rabbit that had been immunized with a cell membrane fraction of the gastrula of the starfish *Asterina pectinifera* (Ikegami *et al.*, 1991).

Administration of macromolecules and particles into the intestinal lumen and fractionation of intestinal cells

Eel intestines were ligated anteriorly and posteriorly and 0.5 ml of a 1-mg/ml concentration of either fluorescein isothiocyanate (FITC)-conjugated dextran (average molecular mass being 70,000, Sigma), rabbit IgG, or formalin-fixed *Vibrio anguillarum* was injected into the central intestinal lumen. As a control, 0.5 ml of phosphate-buffered saline without divalent cations (PBS, Nissui Seiyaku, Tokyo) was injected similarly. The eels were transferred to an aquarium containing ASW (20°C) and kept for 30 min. After death by decapitation, the eels' intestines were immediately excised, cut along their length, and rinsed in 154 m*M* NaCl. Scraped intestinal mucosa were suspended in 5 ml of PBS containing 5 mg of a mixture of collagenase (0.1 unit/mg) and disperse (0.8 unit/mg) (Boehringer-Mannheim, Mannheim, Germany). After pipetting 20 times with a 2-ml pipet, the suspension was incubated at 25°C for 1 h with constant reciprocal shaking. The suspension was passed through a stainless steel filter (75 μm-mesh), and then centrifuged at 400 $\times$ *g* for 10 min. The cell pellet was resuspended in 10 ml of PBS and centrifuged again. This washing process was repeated twice.

The cell pellet was resuspended in PBS at 2.4×10^7/ml. The suspension (0.5 ml) was layered on top of a 12-ml gradient (density: 1.018–1.059 g/ml) of Percoll (Pharmacia), and the cells were separated by centrifugation at 400 $\times$ *g* for 1 min. Twelve 1-ml fractions were collected, and the cell number was counted by trypan blue dye exclusion. The number of cells that incorporated FITC-conjugated dextran was examined with a Leitz Orthoplan fluorescence microscope. Cells that incorporated rabbit IgG or formalin-fixed *Vibrio anguillarum* were detected by immunofluorescence microscopy as described below.

Production and characterization of monoclonal antibody

The cell fraction containing the highest percentage of FITC-conjugated-dextran-incorporated cells (FDIC) was washed three times in PBS and resuspended in PBS at 2.8×10^7/ml. A 6-week-old BALB/c female mouse was injected with 1.4×10^7 cells. Three, seven and twelve weeks later, booster injections of 1.5×10^7, 1.8×10^7, and 4.2×10^7 cells, respectively, were administered. Three days after the final booster, the mouse was sacrificed and its spleen was removed. Monoclonal antibody-producing hybridomas were obtained by fusing cells from the spleen with nonproducer myeloma cell line SP-2/O-Ag-14 by the method of Ikegami *et al.* (1991), except that polyethylene glycol 1500 in 75 m*M* Hepes (Boehringer-Mannheim) was used to induce cell fusion, and that Iscove's modified Dulbecco's medium (IMDM, JRH Biosciences) was used instead of Dulbecco's modification of Eagle's medium. The hybridoma culture supernatants were screened by immunofluorescence microscopy as described below. Hybridomas that showed selective reactivity against live FDIC were expanded and subcloned by transferring a single hybridoma to 100 μl of IMDM containing 10% fetal calf serum (FCS, Hezleton Research Products) and 1×10^5 mouse thymocytes.

Types of H and L chains constituting the monoclonal antibody were determined with a mouse monoclonal antibody isotyping kit (Amersham).

Immunofluorescence staining

For screening hybridomas, FDIC were separated as described above, except that the Percoll gradient had a range of buoyant densities, from 1.040 to 1.097 g/ml. To avoid internalization of antibodies, the following procedures were carried out at 4°C. The cell fractions rich in FDIC were washed several times with PBS and then resuspended in 500 μl of hybridoma culture supernatant or preimmune serum and incubated for 20 min. The cells were then washed twice in PBS. Rhodamine-conjugated goat anti-mouse Ig(G + M) (Tago), diluted 1:100 in PBS (0.5 ml), was added to the cell pellet, and the suspension was incubated for 20 min. The cells were spun down and washed three times with PBS. The cells were resuspended in 10 μl of PBS prior to analysis by double-label immunofluorescence microscopy.

FDIC prepared from intestines that had received an injection of PBS, rabbit IgG or fixed *Vibrio anguillarum*, were fixed with 2% paraformaldehyde in PBS for 20 min at room temperature, and were then spun down. The cells were washed twice in PBS and then immersed in methanol (−20°C) for 5 min. The following procedures were carried out at room temperature. The cells were washed three times with PBS containing 0.05% Tween 20 (TPBS) and then immersed in TPBS containing 10 mg/ml bovine serum albumin (BSA) for 30 min, followed by incubation in a hybridoma culture supernatant for 30 min. After three washes in TPBS, the cells were then incubated for 30 min with rhodamine-conjugated goat anti-mouse Ig(G + M) diluted 1:100 in TPBS, washed again three times, and

incubated for 30 min with rabbit anti-*Vibrio anguillarum* antiserum diluted 1:500 in TPBS containing 0.5 mg/ml BSA. This was followed by three more TPBS washes and incubation for 30 min with FITC-conjugated goat anti-rabbit IgG diluted 1:80 in TPBS. The cells were washed three times in TPBS, mounted, and examined by double-label immuno-fluorescence microscopy.

Cells carrying the antigen molecules were detected histologically as follows. Intestines were excised, washed with PBS, and fixed with 4% paraformaldehyde in PBS overnight. The fixed tissue was immersed in 100% ethanol overnight and then embedded in polyester wax (BDH). Sections 7 μm thick were placed onto glass slides and incubated with an appropriate amount of hybridoma culture supernatant for 30 min, after which they were washed in PBS for 15 min. FITC-conjugated rabbit anti-mouse Ig(G + M) (Cappel), diluted 1:80 in TPBS was then added, in the dark, for 30 min, followed by washing with TPBS for 15 min. Slides were mounted in a solution of 50% (volume by volume) in PBS containing 0.1 *M* *n*-propyl gallate to prevent bleaching (Giloh and Sedat, 1982), sealed, and viewed under a fluorescence microscope. All experiments included negative controls in which FITC-conjugated second antibody was used with primary antibody from preimmune serum.

Eel intestines with *Vibrio anguillarum* injected into the intestinal lumen were processed as described above, except that the sections were treated with the following antibodies successively, each time incubating for 30 min, followed by washing with TPBS for 30 min: an undiluted hybridoma culture supernatant; rhodamine-conjugated goat anti-mouse Ig(G + M) diluted 1:100 in TPBS containing 0.5 mg/ml BSA; rabbit anti-*Vibrio anguillarum* antisera diluted 1:500 in TPBS containing 0.5 mg/ml BSA; and FITC-conjugated goat anti-rabbit IgG. The sections were analyzed by double-label immunofluorography.

Extraction of antigen molecules from FDIC and enzyme-linked immunosorbent assay

The cell fractions rich in FDIC (5.0×10^6 cells; density: 1.040–1.047 g/ml) were centrifuged at $400 \times g$ for 5 min. The cell pellet was resuspended in 500 μl of 0.1 *M* potassium phosphate buffer (pH 7.4) containing 1 m*M* phenylmethylsulfonyl fluoride. The cells were disrupted by freeze-thawing six times, and the lysate was centrifuged at $10{,}000 \times g$ for 30 min at 4°C. The supernatant was separated and its protein content was determined by the protein-dye binding assay (Bradford, 1976), or by the method of Lowry *et al.* (1951) with BSA as the standard. Forty microliters of each of a series of serially diluted supernatants, in PBS, were added to a well of a 96-well microtiter plate (Nunc) for enzyme-linked immunosorbent assay (ELISA) and absorbed overnight at 4°C. ELISA was carried out as described in Ikegami *et al.* (1991), except that horseradish peroxidase linked to goat anti-mouse IgM diluted 1:1000 in TPBS was used to locate the first antibody.

The insoluble fraction of the cell lysate was fixed with 1 ml of 2% paraformaldehyde at room temperature for 20 min, followed by centrifugation at $10{,}000 \times g$ for 30 min. The pellet was washed once with distilled water and then treated with 1 ml of methanol (−20°C) for 5 min. Methanol was removed, and the pellet was washed twice with distilled water. The pellet was resuspended in distilled water to give a suspension of 300 μg BSA-equivalent per ml. Forty microliters each of suspensions serially diluted with distilled water were applied to a well which had been previously coated with 0.002% poly-L-lysine and processed in the same way as described for the soluble fraction.

In vitro *incorporation of FITC-conjugated dextran*

The intestinal mucosa was dispersed and fractionated by Percoll gradient centrifugation (density range: 1.040–1.097 g/ml) as described above. The cell fraction rich in the 8F1 positive cells (density range: 1.040–1.047 g/ml) was collected. The cells (2×10^6) were resuspended in 1 ml of PBS, and the suspension was added to 1 ml of 1 mg/ml FITC-conjugated dextran in PBS. The suspension was incubated for 30 min at 20°C in the dark. The cells were washed three times with PBS and resuspended in 2 ml of PBS (4°C). The following procedure was carried out at 4°C. One milliliter of the hybridoma culture supernatant (8F1) was added to the cell pellet, the suspension was allowed to stand for 20 min, and the cells were then washed three times with PBS. One milliliter of rhodamine-conjugated goat anti-mouse Ig(G + M) diluted at 1:100 in PBS was added to the cells. After standing for 20 min, the cells were collected by centrifugation, washed three time with PBS, and analyzed by double-label immunofluorescence microscopy.

Results

Production of monoclonal antibody and the characterization of the antigen molecule

After extensive screening of the hybridoma cell line culture supernatants, a monoclonal antibody that reacted specifically with the surface of one type of living FDIC was obtained and was designated 8F1. As shown in Figure 1, the cell membrane of an FDIC that had incorporated FITC-conjugated dextran *in vivo* reacted to 8F1 at 4°C.

The lysate of FDIC was separated into soluble and insoluble fractions. An ELISA analysis revealed that the soluble fraction contained the antigen molecules. Under the conditions used in this experiment, the maximal re-

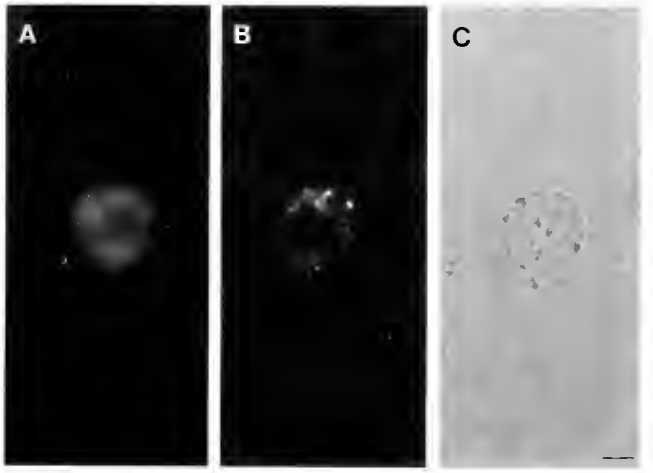

Figure 1. Immunofluorescence micrograph of an intestinal epithelial cell of *Anguilla japonica* incorporating FITC-conjugated dextran *in vivo*. FITC-conjugated dextran (0.5 mg) was injected into the lumen of the intestine. Thirty minutes later, the intestine was excised. The intestinal cells were dissociated, bound to 8F1 antibody at 4°C, and then incubated with rhodamine-conjugated goat anti-mouse Ig(G + M). (A) An endocytic cell, identified by the internal accumulation of FITC-conjugated dextran; (B) the same field showing the 8F1-antigen proteins visualized with the rhodamine-conjugated antibody; (C) the same field observed by brightfield microscopy. Bar, 5 μm.

sponse, which was 1.3 of absorbance at 490 nm, was obtained by applying 3 μg BSA-equivalent of the soluble fraction per well. On the other hand, 6 μg BSA-equivalent of the insoluble fraction per well gave only 15% of the maximum response given by the soluble fraction. When the primary antibody was replaced with preimmune serum, or was omitted, the results were completely negative. We concluded that the antigen molecules were recovered in both soluble and insoluble fractions. When the insoluble fraction was electrophoresed on a reducing sodium dodecyl sulfate-polyacrylamide gel and subsequently analyzed by immunoblot, no 8F1-positive bands were found, whereas proteins of the soluble fraction with apparent molecular masses of 230,000 and 54,000 were stained by 8F1 (data not shown). We must still determine how these soluble 8F1-reactive proteins are related to the antigens located on the cell surface of an FDIC.

The population density of cells harboring 8F1-antigenenic proteins in dissociated intestinal mucosa

FITC-conjugated dextran was introduced into the lumen of the intestine *in vivo*, and the eel was maintained for 30 min before the intestinal tube was excised. The intestinal mucosa were scraped and the cells were dispersed with a mixture of collagenase and disperse. The population density of FDIC was determined by counting fluorescent cells, and 25.5% of the total viable cells were FDIC. Double-label immunofluorescence microscopy, with rhodamine-conjugated goat anti-mouse Ig(G + M) as a second antibody for 8F1, revealed that 15.2% of FDIC (3.9% of the total dissociated cells) and 0.4% of the cells that did not incorporate FITC-dextran (0.3% of the total dissociated cells) were 8F1-positive. When dissociated cells were treated with preimmune mouse serum instead of 8F1, none of the cells observed become fluorescent after the addition of the rhodamine-conjugated secondary antibody (data not shown). These results show that 93% of the 8F1-positive cells were FDIC (Fig. 2).

The dispersed cells were fractionated by Percoll gradient centrifugation. Each cell fraction was fixed, and examined for the presence of 8F1-antigen-containing proteins by immunofluorescence microscopy. There were two groups of FDIC: a comparison with the control tube containing the density marker beads showed that one FDIC fraction had a range of buoyant densities from 1.073 to 1.088 g/ml, and the other FDIC fraction, from 1.040 to 1.047 g/ml. The 8F1-positive cells were found exclusively in the latter fraction (Fig. 3). These results suggested that 8F1 is specific for only one type of endocytic cells in the eel intestine.

The ability of 8F1-positive cells to internalize rabbit IgG and fixed Vibrio anguillarum

The experiments described above were carried out with FITC-conjugated dextran as the ligand for endocytosis. To examine whether the 8F1-positive cell can ingest a proteinaceous ligand as well, 0.5 mg of rabbit IgG was introduced into the intestinal lumen, and the intestine was dissected out 30 min later. The intestinal cells were dispersed, fixed, stained with 8F1, and examined by double immunofluorescence microscopy with FITC-conjugated goat anti-rabbit IgG and rhodamine-conjugated goat anti-mouse Ig(G + M). The majority of 8F1-positive cells incorporated rabbit IgG (Fig. 4). Therefore, the 8F1 positive cells underwent active fluid-phase pinocytosis *in vivo*.

Next we examined whether the 8F1-positive cell could incorporate a particulate ligand. A half milligram of the formalin-fixed bacterium *Vibrio anguillarum* was injected into the lumen of the intestine, and it was processed as described for FITC-conjugated dextran and rabbit IgG. The fixed, dispersed intestinal cells were treated with rabbit anti-*Vibrio anguillarum* antiserum and then analyzed by double immunofluorescence microscopy with FITC-labeled goat anti-rabbit IgG and rhodamine-conjugated goat anti-mouse Ig(G + M). Only the 8F1-positive cells incorporated fixed *Vibrio anguillarum* (Fig. 5). When 0.5 ml of PBS instead of a 0.5-ml suspension of fixed *Vibrio anguillarum* in PBS was introduced into the intestinal lumen and the intestinal cells were processed similarly,

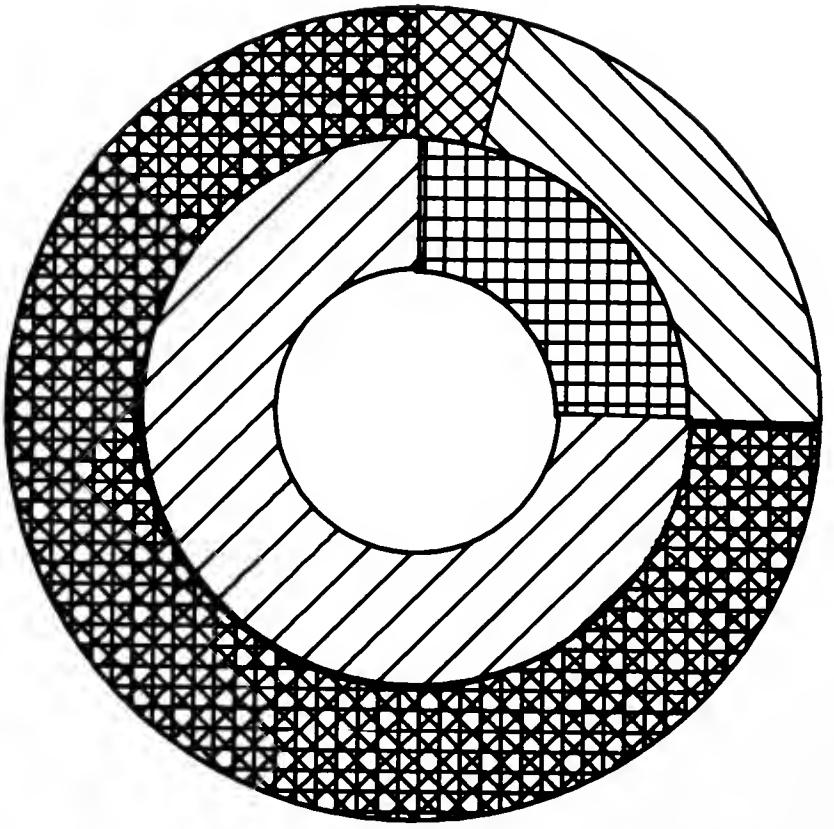

Figure 2. Distribution of 8F1-positive and 8F1-negative FITC-conjugated-dextran-incorporating cells (FDIC) dissociated from the intestine of *Anguilla japonica*. (▦), Percentage of FDIC; (▩), percentage of 8F1-positive FDIC; (▧), percentage of 8F1-negative FDIC; (▨), percentage of cells that did not incorporate FITC-conjugated dextran; (■), percentage of 8F1-positive cells that did not incorporate FITC-conjugated dextran; (■), percentage of 8F1-negative cells that did not incorporate FITC-conjugated dextran.

no specific fluorescence could be detected in the cells after staining.

Localization of 8F1-positive cells in the intestinal epithelium

To localize the 8F1-positive cells in the intestine, the tissue was sectioned and stained with 8F1. Few 8F1-positive cells were present in any villus, and the cells were localized exclusively in the intestinal epithelium (Fig. 6). When a section was stained with the preimmune sera, these cells did not become fluorescent upon the addition of FITC-labeled second antibody (data not shown). When fixed *Vibrio anguillarum* was put in the intestinal lumen, only 8F1-positive cells took up the bacterium; no other cells in the epithelium absorbed this particulate probe under the conditions specified (Fig. 7).

In vitro *uptake of FITC-conjugated dextran by 8F1-positive cells*

To examine whether the 8F1-positive cell could ingest FITC-conjugated dextran *in vitro*, FDIC were prepared, incubated in PBS containing the fluorescent probe for 30 min at 20°C, and then washed extensively. Double immunofluorescence microscopy showed that the 8F1-positive cells took up FITC-conjugated dextran (Fig. 8). When incubation was carried out at 4°C, there was no specific intracellular localization of fluorescent material. These results show that the process of endocytosis is temperature-dependent, and that 8F1 applied to a cell suspension at 4°C complexes with the antigen proteins on the cell surface and remains there without being endocytosed, as is shown in Figure 1.

Discussion

Many reports indicate that enterocytes of teleost fish ingest proteins such as horseradish peroxidase, ferritin, Igs and peptide hormones (Noaillac-Depeyre and Gas, 1976; Rombout *et al.*, 1985; Georgopoulou and Vernier, 1986; Georgopoulou *et al.*, 1986, 1988; McLean and Ash, 1987; Suzuki *et al.*, 1988; Bail *et al.*, 1989; McLean *et al.*, 1990; Moriyama *et al.*, 1990). The experimental fish used in these studies belong to Clupeiformes or to Cyprinbi-

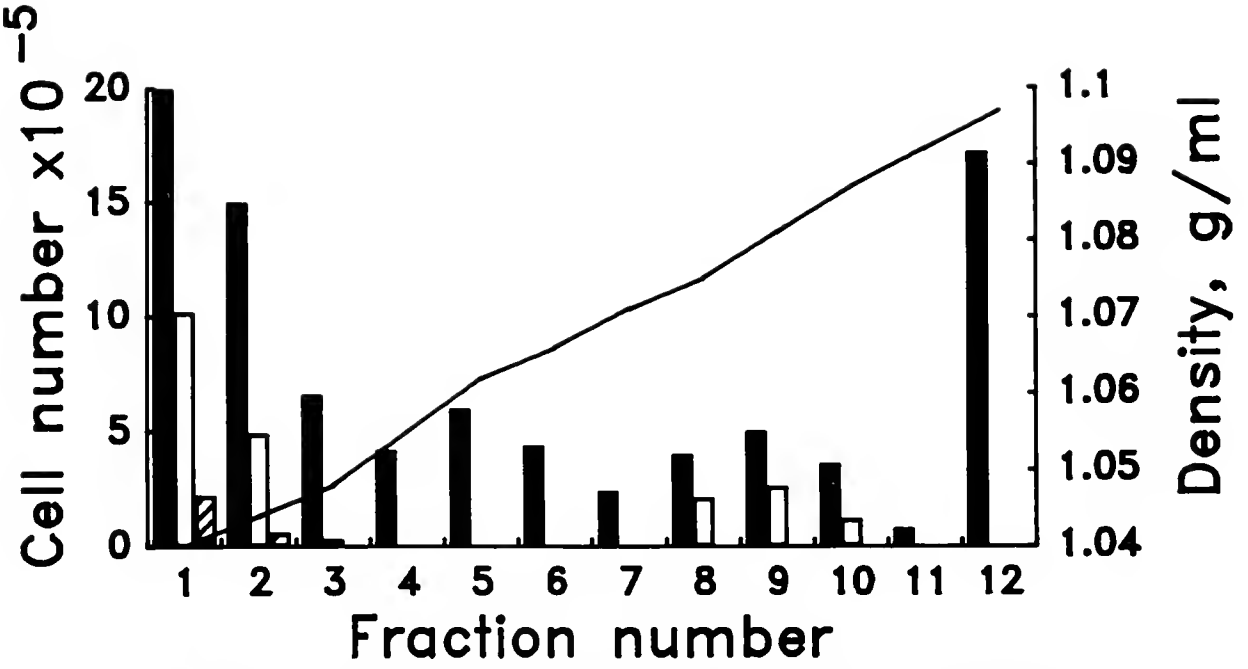

Figure 3. Percoll density-gradient centrifugation of intestinal epithelial cells of *Anguilla japonica*. Procedures for separation are described in Materials and Methods. (■), Number of total cells; (□), number of cells that incorporated FITC-conjugated dextran; (▨), number of 8F1-positive cells; (—), density of Percoll.

formes. Vigneulle and Laurencin (1991) showed that formalin-fixed *Vibrio anguillarum* was ingested by enterocytes of rainbow trout *Oncorhynchys mykiss*, sea bass *Dicentrarchus labrax*, and turbot *Scophthalmus maximus* after oral administration or anal intubation. To our knowledge, the present paper is the first to show that active endocytic cells occur in the intestine of the adult eel. The aim of this study was to prepare monoclonal antibodies to probe for cells undergoing active endocytosis in the eel intestine. We succeeded in obtaining a monoclonal antibody, 8F1, which specifically recognized one type of endocytic cell. We made a survey of cells harboring 8F1-reactive proteins in the histological sections that had been prepared from the intestine of various species belonging to Cluperiformes, Myctophiformes, Cypriniformes, Anguilliformes, Cyprinodontiformes, and Perciformes. Several cells located in the intestinal epithelium of the adult conger eel *Conger myriaster* recognized 8F1, whereas no 8F1-positive cells were found in the intestine of species belonging to other orders than Anguilliformes (manuscript in prep.).

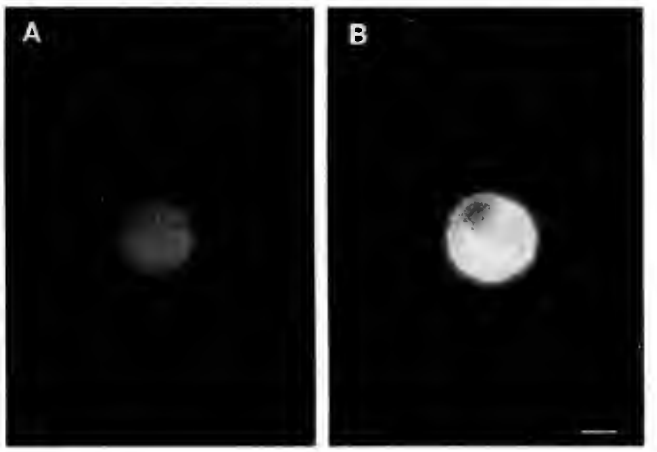

Figure 4. Double-label, immunofluorescence micrograph of an intestinal epithelial cell of *Anguilla japonica* incorporating rabbit IgG *in vivo*. Rabbit IgG (0.5 mg) was injected into the lumen of the intestine. Thirty minutes later, intestinal cells were separated, fixed, and treated with methanol. After being labeled with 8F1, the cells were double-labeled with rhodamine-conjugated goat anti-mouse Ig(G + M) and FITC-conjugated goat anti-rabbit IgG. (A) A cell containing rabbit IgG visualized with the FITC-conjugated antibody; (B) the same cell harboring the 8F1-antigen proteins, identified by the labeling with the rhodamine-conjugated antibody. Bar, 5 μm.

Because the number of 8F1-positive cells in a villus of the eel intestine is very small, such cells are unlikely to play a basic nutritional role. The 8F1-positive cells may be migrating neutrophils or macrophages infiltrated across the blood vessel. But the 8F1-positive cells were found only in the villus epithelium and were absent in the lamina propria, suggesting that they are not such types of leucocytes.

In the intestinal epithelium of mammals, M cells that overlie Peyer's patches have been shown to transport

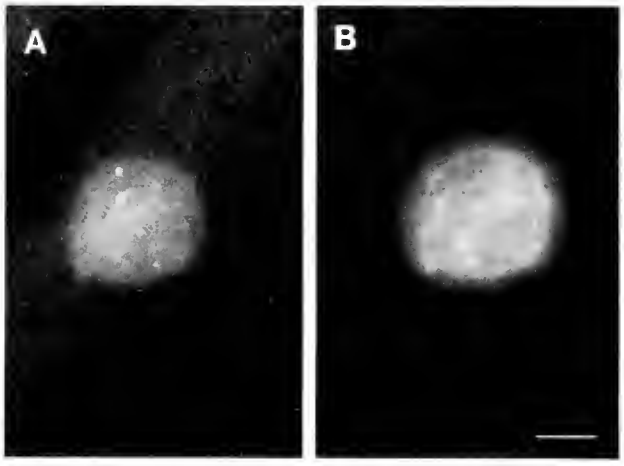

Figure 5. Double-label, immunofluorescence micrograph of an intestinal epithelial cell of *Anguilla japonica* incorporating fixed *Vibrio anguillarum in vivo*. Fixed *Vibrio anguillarum* (0.5 mg) were injected into the lumen of the intestine. Thirty minutes later, intestinal cells were separated, fixed, and treated with methanol. After binding with 8F1 antibody, the cells were labeled with rhodamine-conjugated goat anti-mouse Ig(G + M) and rabbit anti-*Vibrio anguillarum* antisera and finally with FITC-conjugated goat anti-rabbit IgG. (A) A *Vibrio anguillarum*-incorporated cell visualized with anti-*Vibrio anguillarum* antiserum and the FITC-conjugated secondary antibody; (B) the same cell harboring the 8F1-antigen proteins, identified by their labeling with the rhodamine-conjugated antibody. Bar, 5 μm.

macromolecules, such as horseradish peroxidase and ferritin (Bockman and Cooper, 1973; Owen, 1977). Furthermore, viruses (such as reovirus) were phagocytosed into the cells (Wolf *et al.*, 1981; Morrison *et al.*, 1991). Such an endocytic process and the subsequent release of the ingested material into the intercellular space is considered to be the origin of a local IgA immune system (Georgopoulou *et al.*, 1988). It remains to be determined whether the 8F1-positive cell can transfer absorbed material towards the intercellular space and into the circu-

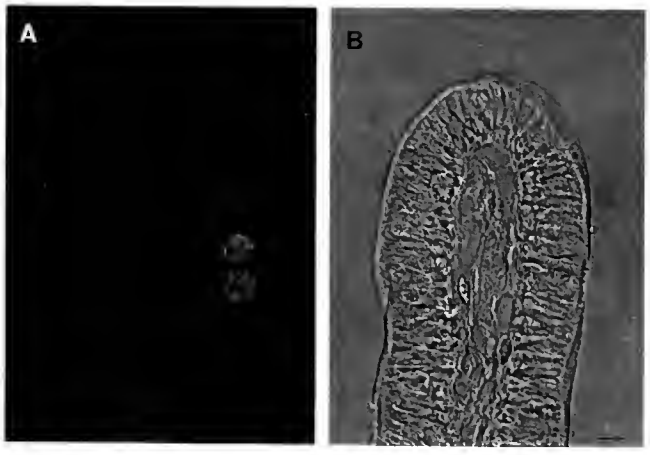

Figure 6. Immunofluorescence micrograph of a section of an intestinal segment of *Anguilla japonica* which was stained with 8F1 and FITC-conjugated rabbit anti-mouse IgG. (A), A section observed by fluorescence microscopy; (B) the same field observed under brightfield microscopy. Bar, 10 μm.

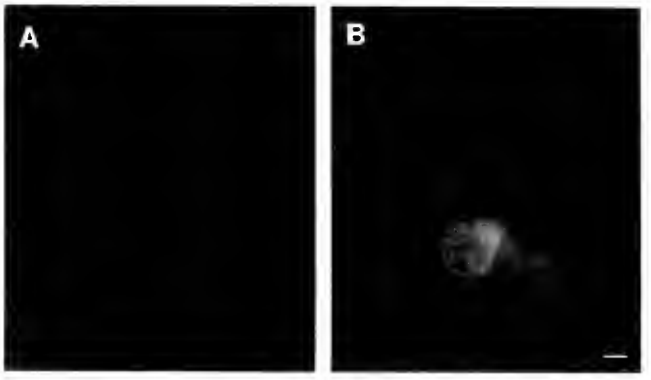

Figure 7. Double-label, immunofluorescence micrograph of a section of an intestinal segment of *Anguilla japonica* incorporating fixed *Vibrio anguillarum in vivo*. Fixed *Vibrio anguillarum* (0.5 mg) were injected into the lumen of the intestine. Thirty minutes later, an intestinal segment was excised and embedded in polyester-wax. Sections (7 μm) were double-labeled with 8F1 antibody and rabbit anti-*Vibrio anguillarum* antibody, with rhodamine-conjugated goat anti-mouse Ig(G + M) and goat FITC-conjugated goat anti-rabbit IgG as second antibodies. (A) A section stained with anti-*Vibrio anguillarum* antibody and the FITC-conjugated secondary antibody; (B) the same field stained with 8F1 and the rhodamine-conjugated second antibody. Bar, 5 μm.

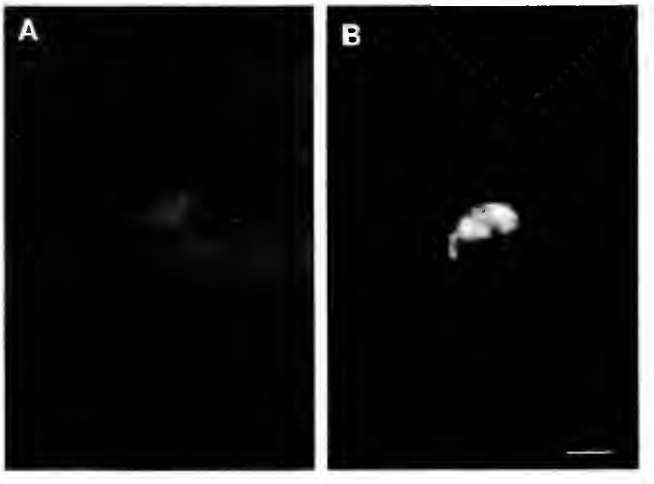

Figure 8. Immunofluorescence micrograph of an intestinal cell of *Anguilla japonica* incorporating FITC-conjugated dextran *in vitro*. Intestinal epithelial cells were dissociated and separated by Percoll density gradient centrifugation. The cell fractions with the range of buoyant densities, 1.040–1.047 g/ml, were collected and incubated with FITC-conjugated dextran for 30 min. They were then immunostained with 8F1 and rhodamine-conjugated goat anti-mouse Ig(G + M). (A) A cell incorporating FITC-conjugated dextran; (B) the same cell harboring the 8F1-antigen proteins, labeled with the rhodamine-conjugated second antibody. Bar, 5 μm.

latory system, thereby triggering local and systemic immune responses. Both histochemical and ultrastructural studies of the 8F1-positive cell are obviously required before the functional resemblance of the cell to M cells of mammals can be discussed.

Acknowledgments

We thank Dr. T. Nakai, Hiroshima University, for the supply of specimen of fixed *Vibrio anguillarum* and antisera for the bacteria. This work was supported in part by grants from the Ministry of Education, Science and Culture of Japan, and from the Japanese Fisheries Agency.

Literature Cited

Bail, P. Y. L., M. F. Sire, and J. M. Vernier. 1989. Intestinal transfer of growth hormone into the circulatory system of the rainbow trout, *Salmo gairdneri*: interference by granule cells. *J. Exp. Zool.* **251:** 101–107.

Bockman, D. E., and M. D. Cooper. 1973. Pinocytosis by epithelium associated with lymphoid follicles in the bursa of fabricius, appendix, and Peyer's patches. An electron microscopic study. *Am. J. Anat.* **136:** 455–478.

Bradford, M. M. 1976. A rapid and sensitive method for the quantification of microgram quantities of protein using the principle of protein-dye binding. *Anal. Biochem.* **72:** 248–254.

Davina, J. H., H. K. Parmentier, and L. P. M. Timmermans. 1982. Effect of oral administration of *Vibrio* bacteria on the intestine of cyprinid fish. *Dev. Comp. Immunol. (Suppl.)* **2:** 157–166.

Ezeasor, D. N., and W. M. Stokoe. 1981. Light and electron microscope studies of the absorptive cells of the intestine, caecea and rectum of the adult rainbow trout *Salmo gairdneri* Rich. *J. Fish Biol.* **18:** 527–544.

Georgopoulou, U., and J. M. Vernier. 1986. Local immunological response in the posterior intestinal segment of the rainbow trout after oral administration of macromolecules. *Dev. Comp. Immunol.* **10:** 529–537.

Georgopoulou, U., M. F. Sire, and J. M. Vernier. 1986. Immunological demonstration of intestinal absorption and digestion of protein macromolecules in the trout (*Salmo gairdneri*). *Cell Tissue Res.* **245:** 387–395.

Georgopoulou, U., K. Dabrowski, M. F. Sire, and J. M. Vernier. 1988. Absorption of intact proteins by the intestinal epithelium of trout, *Salmo gairdneri*. *Cell Tissue Res.* **251:** 145–152.

Giloh, H., and J. W. Sedat. 1982. Fluorescence microscopy: reduced photobleaching of rhodamine and fluorescein protein conjugates by *n*-propyl gallate. *Science* **217:** 1252–1255.

Ikegami, S., T. Mitsuno, M. Kataoka, S. Yajima, and M. Komatsu. 1991. Immunological survey of planktonic embryos and larvae of the starfish *Asterina pectinifera* obtained from the sea, using a monoclonal antibody directed against egg polypeptides. *Biol. Bull.* **181:** 95–103.

Lowry, O. H., N. J. Rosenbrough, A. L. Farr, and R. J. Randall. 1951. Protein measurement with the Folin phenol reagent. *J. Biol. Chem.* **193:** 265–275.

McLean, E., and R. Ash. 1987. The time-course of appearance and net accumulation of horseradish peroxidase (HRP) presented orally to rainbow trout *Salmo gairdneri* (Richardson). *Comp. Biochem. Physiol.* **88A:** 507–510.

McLean, E., A. C. V. D. Meden, and E. M. Donaldson. 1990. Direct and indirect evidence for polypeptide absorption by the teleost gastrointestinal tract. *J. Fish Biol.* **36:** 489–498.

Moriyama, S., A. Takahashi, T. Hirano, and H. Kawauchi. 1990. Salmon growth hormone is transported into the circulation of rainbow trout, *Oncorhynchus mykiss*, after intestinal administration. *J. Comp. Physiol. B* **160:** 251–257.

Morrison, L. A., R. L. Sidman, and B. N. Fields. 1991. Direct spread of reovirus from the intestinal lumen to the central nervous system through vagal autonomic nerve fibers. *Proc. Natl. Acad. Sci. U.S.A.* **88:** 3852–3856.

Noaillac-Depeyre, J., and N. Gas. 1976. Electron microscopic study of gut epithelium of the tench (*Tinca tinca* L.) with respect to its absorptive functions. *Tissue Cell* **8:** 511–530.

Owen, R. L. 1977. Sequential uptake of horseradish peroxidase by lymphoid follicle epithelium of Peyer's patches in the normal unobstructed mouse intestine: an ultrastructural study. *Gastroenterology* **72:** 440–451.

Rombout, J. H. W. M., C. H. J. Lamers, M. H. Helfrich, A. Dekker, and J. J. Taverne-Thiele. 1985. Uptake and transport of intact macromolecules in the intestinal epithelium of carp (*Cyprinus carpio* L.) and the possible immunological implications. *Cell Tissue Res.* **239:** 519–530.

Rombout, J. H. W. H., L. J. Blok, C. H. J. Lamers, and E. Egberts. 1986. Immunization of carp (*Cyprinus carpio*) with a *Vibrio anguillarum* bacterin: indications for a common mucosal immune system. *Dev. Comp. Immunol.* **10:** 341–351.

Suzuki, Y., M. Kobayashi, O. Nakamura, K. Aida, and I. Hanyu. 1988. Induced ovulation of the goldfish by oral administration of salmon pituitary extract. *Aquaculture* **74:** 379–384.

Vigneulle, M., and F. B. Laurencin. 1991. Uptake of *Vibrio anguillarum* bacterin in the posterior intestine of rainbow trout *Oncorhynchus mykiss*, sea bass *Dicentrarchus labrax* and turbot *Scophthalmus maximus* after oral administration or anal intubation. *Dis. Aquat. Org.* **11:** 85–92.

Wolf, J. L., D. H. Rubin, R. Finberg, R. S. Kauffman, A. H. Sharpe, J. S. Trier, and B. N. Fields. 1981. Intestinal M cells: a pathway for entry of reovirus into the host. *Science* **212:** 471–472.

Reference: *Biol Bull* **184**: 338–341. (June, 1993)

The Effect of Depth on the Attachment Force of Limpets

ANDREW M. SMITH*, WILLIAM M. KIER, AND SÖNKE JOHNSEN

Department of Biology, CB # 3280 Coker Hall, University of North Carolina, Chapel Hill, North Carolina 27599-3280

A wide variety of marine animals, including animals as different as cephalopods, echinoderms and fish, use suction adhesion for temporary or long-term attachments (1). One aspect of suction adhesion that has been discussed, but never tested experimentally, is its dependence on depth. The change in hydrostatic pressure with depth may exert a marked effect on the force of attachment produced by suction (2–6). This study was designed to confirm this effect experimentally, using limpets as a test case. Limpets rely on suction to resist dislodgment by predators and crashing waves (7, 8). We measured the suction tenacity of four species of limpets at sea level and at increased ambient pressure in a hyperbaric chamber. Tenacity is defined as the force of attachment divided by the area of the foot contacting the substratum. Change in ambient pressure had a small but significant effect on limpet tenacity. These results show that depth can affect attachment up to a point, but the mechanics of limpet feet appear incapable of producing dramatically larger tenacities.

Increasing hydrostatic pressure raises the upper limit on the force of attachment that a sucker can create (5). This can be explained as follows. A sucker forms an attachment by decreasing the pressure of the water it encloses. This results in a differential between the pressure of the water outside the sucker and the pressure inside. This differential pulls the sucker against the substratum. The pressure outside the sucker is the ambient pressure, which increases by 100 kPa (1 atm) with each 10-m depth increase. The minimum pressure inside the sucker is limited by water's tensile strength. The sucker can reduce the pressure until the tension in the water reaches a critical value, at which point the water cavitates; it undergoes cohesive failure and gas bubbles expand suddenly. The minimum pressure is known as the cavitation threshold. Thus, the greatest possible pressure differential equals the difference between ambient pressure and the cavitation threshold. Because the cavitation threshold is relatively independent of depth, and ambient pressure increases with depth, the maximum possible pressure differential, and thus the force of attachment, increases with depth.

If animals using suction can take advantage of this increased potential, then depth may have a profound impact on the effectiveness of their attachment. The musculature of the sucker and its ability to maintain a seal will determine the extent to which the animal can take advantage of this potential. Each sucker has an intrinsic limit to the pressure differential that it can produce. Once it reaches this limit, it will be unable to generate greater pressure differentials, no matter how much the depth increases (see Fig. 1). This potential limit on the effect of depth on suction adhesion has not been emphasized previously.

We tested the effect of depth on four species of limpets: *Lottia pelta* (Rathke), *Lottia gigantea* Sowerby, *Lottia limatula* (Carpenter), and *Macclintockia scabra* (Gould) (formerly *Collisella scabra*). Chuck Winkler Enterprises (San Pedro, California) supplied limpets for these experiments. The limpets were kept in an artificial seawater aquarium at 21°C.

Tenacity measurements were made with a strain gauge force transducer described in detail previously (7). The transducer was tied in series with monofilament fishing line such that pulling on the line deformed the transducer by three point loading. The force transducer could be attached to the limpet by a Lucite harness glued to the shell. The limpets were allowed 5–15 h to attach to a clear Lucite sheet in the aquarium. The area of the limpet's foot was estimated with calipers as described previously (7). For each force measurement, the force was increased quickly

Received 6 January 1993; accepted 20 March 1993.

* Present address: Laboratoire Arago, 66650 Banyuls-sur-Mer, France.

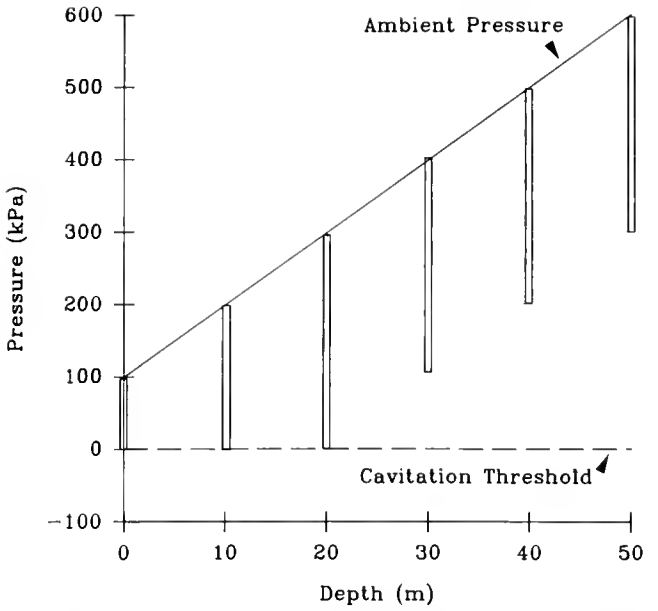

Figure 1. Graph demonstrating the effect of depth on a hypothetical sucker. The maximum possible pressure differential is the difference between ambient pressure and the cavitation threshold. For simplicity, the cavitation threshold is taken to be 0 kPa. The pressure differential created by the sucker is represented by a vertical bar descending from ambient pressure. If the sucker musculature can generate a pressure differential of 300 kPa, then from 0 to 20 m, cavitation limits the sucker and the force of attachment increases with depth. At depths greater than 20 m, the sucker will reach the limit of its musculature before cavitation occurs and the attachment force remains constant despite depth changes.

but steadily until the limpet's attachment failed. The peak force was recorded. Most measurements lasted roughly one second.

Immediately before a tenacity measurement, the limpet was moved by sliding it a few millimeters across the surface to ensure that it was using suction and not a glue-like adhesive (7). Because limpets can use either of these two attachment mechanisms, which have different tenacities, measurements are meaningless unless one knows the attachment mechanism in use (7, 8). We chose to investigate the effects of increased ambient pressure on suction adhesion rather than glue-like adhesion, because increased ambient pressure is not expected to affect glues.

Tenacity measurements at sea level were made in Chapel Hill, North Carolina. Tenacity measurements at increased ambient pressure were made in the hyperbaric chamber operated by the National Oceanographic and Atmospheric Administration National Undersea Research Center (NURC) at the University of North Carolina, Wilmington, North Carolina. Four dives to a pressure of 200 kPa (corresponding to 10 m of water) were made in the chamber. Each dive was approximately one hour in length. In addition, one dive was made to 340 kPa (24 m of water) for approximately 40 min. Two researchers were in the chamber, one to measure foot area and attachment force, the other to videotape the soles of the limpet feet as they were being detached. The limpets were in a 60 × 30 × 30 cm aquarium in the chamber. The force transducer was wired to an amplifier and chart recorder as described previously (7); the amplifier and recorder were both outside the chamber. A VHS video camera in an underwater housing was used with underwater floodlights. The videos were analyzed frame-by-frame after the experiments to determine the mode of failure of the limpet's attachment.

Increased ambient pressure had a small but significant effect on limpet attachment. At sea level, the mean suction tenacity of all four limpet species combined was 50 ± 31 kPa (mean ± S.D., n = 162 trials) (100 kPa = 1 atm). In the hyperbaric chamber, the mean suction tenacity for all four species combined was 59 ± 33 kPa (n = 138). The difference between these means was statistically significant (*t*-test, $P = 0.0094$). Increasing ambient pressure increased the suction tenacity of each of the four species, but this increase was significant only for *L. pelta* (Table I). Further increase of the pressure from 200 kPa to 340 kPa did not affect the limpets' attachment. The mean suction tenacity of all limpets at 200 kPa ambient pressure was 59 ± 34 kPa (n = 115), and the mean suction tenacity of those at 340 kPa was 60 ± 31 kPa (n = 23). There was no significant difference between these means (*t*-test, $P = 0.43$). The tenacity of limpets was consistent among dives. There was no significant variation among the mean tenacities found on the 5 dives (ANOVA, $P > 0.75$). Similarly, there was no significant variation among the mean tenacities measured for each day at sea level (ANOVA, $P > 0.1$). Although not measured quantitatively, the tenacity of limpets using glue-like adhesion did not seem to change with depth. Their shear tenacity, as observed when forcing them to slide slightly to break any glue-like bonds, was not noticeably different at increased pressure relative to their shear tenacity at sea level.

To understand these results, it is helpful to analyze the effect of depth more thoroughly. Cavitation in seawater

Table I

Effect of ambient pressure on suction tenacity, by species

Species	Mean tenacity (kPa)		*P*-value
	Sea level	Hyperbaric	
Lottia gigantea	44 ± 16 (n = 24)	48 ± 36 (n = 28)	0.29
L. limatula	50 ± 29 (n = 73)	54 ± 29 (n = 34)	0.24
L. pelta	46 ± 18 (n = 29)	59 ± 28 (n = 46)	0.012
Macclintockia scabra	59 ± 46 (n = 36)	74 ± 39 (n = 30)	0.084

t-tests were used for comparison of means. Hyperbaric includes ambient pressures of 200 and 340 kPa. Values are mean ± standard deviation.

will not occur until the absolute pressure drops below approximately 20 kPa (9). Thus, at sea level (ambient pressure = 100 kPa) limpets can generate a pressure differential of up to 80 kPa without being limited by cavitation. Greater pressure differentials can occur because seawater can sustain negative pressures, but cavitation becomes possible at pressure differentials greater than 80 kPa.

If the pressure differential acts over the entire area of the foot, then a pressure differential of 80 kPa creates a tenacity of 80 kPa. This probably does not occur, however, because limpets must press the perimeter of their feet down to form a seal. The area that must be in direct contact with the substratum to form a seal reduces the available area over which the pressure differential acts. Thus, a given pressure differential creates lower attachment forces and consequently lower tenacities. Since the area that the pressure acts over can be as small as one half the actual pedal area (7), a pressure differential of 80 kPa might create a tenacity of only 40 kPa. Given these considerations, the tenacity at which cavitation may be limiting ranges from 40 to 80 kPa, depending on the area over which the pressure acts. For this reason we chose 60 kPa as a rough cutoff point; at higher tenacities cavitation may be limiting at sea level.

In 73% of the trials at sea level, the tenacity of limpets on Lucite was less than 60 kPa. Increased depth would probably not have affected these limpets. On the other hand, increased depth may have allowed higher tenacities for the other 27%. This would have led to the increase in the mean for the entire population when tested at depth. Increasing ambient pressure to 200 kPa increased the pressure differential that was possible without cavitation to 180 kPa. Thus, at a depth of 10 m, cavitation would not have been limiting until the tenacity was between 90 to 180 kPa, depending on the area over which the pressure acted. On the videotape of the trials at 200 kPa ambient pressure, cavitation was seen in two cases, at tenacities of 117 and 130 kPa. These two limpets might have been able to take advantage of an even greater increase in ambient pressure.

The extent that limpet tenacity increases with depth depends on the ability of the pedal musculature to produce a larger differential. Because the overall change in tenacity was small and further increase in pressure to 340 kPa did not lead to a further increase in tenacity, it appears that the mechanics of the foot largely determine the tenacity of limpets. Specifically, limpets seem limited in their ability to maintain a seal at the margin of their feet. Analysis of the videotapes of limpets being detached in the hyperbaric chamber showed that most of the attachments failed by the formation of a leak at the foot's margin.

Depth may affect limpets in the field to a larger extent than seen in this study. The suction tenacity of limpets in the field is estimated to be roughly 90 kPa (80 kPa for the species used in this study) (8) as compared to 50 kPa on Lucite at sea level. Because Lucite is smooth, limpets may have greater difficulty preventing the edge of their foot from sliding in towards the center, and thus breaking the seal at the margin. The roughness of many natural substrates may facilitate this seal and allow more limpets to achieve tenacities that are cavitation-limited. Previous data for *Patella vulgata* show that the tenacity on rough slate is 23% higher than on smooth slate and 38% higher than on Lucite (10), although it is uncertain which mechanism these limpets were using. Also, undisturbed mucus at the margin of the foot may help to maintain the seal of limpets that have not been moved prior to the tenacity measurement. Thus, increases in depth may have a larger effect in the field than seen in this experiment.

Another reason for lower tenacity on Lucite is that the Lucite surface affects the limpets' behavior. Limpets are more likely to remain active on Lucite than on natural substrates. Active limpets often do not attach firmly; therefore many of the limpets had low tenacities (below 30 kPa). This clearly diminished the overall effect produced by increased ambient pressure. Differences in activity within the population also probably account for the large standard deviations in the measurements. It is interesting to note that many of the limpets that were firmly attached and not active had tenacities similar to limpets in the field. This demonstrates that it is possible for limpets to achieve high suction tenacities on Lucite, regardless of its smoothness.

Because of surface roughness and a lower level of activity, depth should have a greater effect in the field than in this study. Most likely, a larger percentage of limpets would be cavitation limited and thus affected by depth. This would lead to a greater average increase in tenacity. The data suggest, however, that the pedal musculature is still not capable of large increases in suction tenacity (more than 50%, for example).

A limited effect of depth on suction tenacity is not surprising for intertidal animals that are typically subject to small increases in depth. The limpets used in this study are commonly found in the upper to the middle or lower intertidal (11). There may not be an advantage to increasing the complexity or strength (maximum tensile stress) of their pedal musculature to produce pressure differentials beyond the range that is typically possible for them. Depth changes in the range they experience, however, will have an effect. An animal in the middle to lower intertidal experiences significant depth changes during the day. An increase of 2 m could increase limpet tenacity by 20 kPa (a 25% increase if the tenacity at sea level is 80 kPa).

One of the species used in this study, *L. pelta,* has a broader depth distribution, having a depth range from the intertidal to the subtidal, as low as 50 m (11). This species also experienced the clearest change in tenacity with depth,

although the change was still small. It would be interesting to compare the effect of depth on other subtidal limpets with the results found here for limpets collected from the intertidal. Limpets from the subtidal may have adapted to conditions where the upper limit on tenacity is higher, and they may have the musculature to take advantage of it.

In summary, we have provided experimental confirmation of the effect of depth on suction attachment. We have also demonstrated that intertidal limpets are capable of taking advantage of this effect to a small extent. This study highlights the fact that sucker musculature may limit an animal's ability to take advantage of the effect of depth; this has been overlooked in previous work.

Acknowledgments

We thank Stephen J. Mastro and the staff at NURC-UNC Wilmington, who operated the hyperbaric chamber and provided much technical help. This material is based on a grant from the National Oceanic and Atmospheric Administration (UNCW #9122), a National Science Foundation Graduate Fellowship to A. M. Smith, and a National Science Foundation Presidential Young Investigator Award (DCB-8658069) to W. M. Kier.

Literature Cited

1. **Nachtigall, W. 1974.** *Biological Mechanisms of Attachment. The Comparative Morphology and Bioengineering of Organs for Linkage, Suction, and Adhesion.* Springer-Verlag, New York. 194 pp.
2. **Nixon, M., and P. N. Dilly. 1977.** Sucker surfaces and prey capture. *Symp. Zool. Soc. Lond.* **38:** 447–511.
3. **Able, K. W., and D. E. McAllister. 1980.** Revision of the snailfish genus *Liparis* from arctic Canada. *Can. Bull. Fish. Aquat. Sci.* **208:** 1–58.
4. **Denny, M. 1988.** *Biology and the Mechanics of the Wave-Swept Environment.* Princeton University Press, Princeton. 329 pp.
5. **Kier, W. M., and A. M. Smith. 1990.** The morphology and mechanics of octopus suckers. *Biol. Bull.* **178:** 126–136.
6. **Voight, J. R. 1990.** Population biology of *Octopus digueti* and the morphology of American tropical octopods. Ph.D. Dissertation, University of Arizona, Tucson.
7. **Smith, A. M. 1991.** The role of suction in the adhesion of limpets. *J. Exp. Biol.* **161:** 151–169.
8. **Smith, A. M. 1992.** Alternation between attachment mechanisms by limpets in the field. *J. Exp. Mar. Biol. Ecol.* **160:** 205–220.
9. **Smith, A. M. 1991.** Negative pressure generated by octopus suckers: a study of the tensile strength of water in nature. *J. Exp. Biol.* **157:** 257–271.
10. **Grenon, J. F., and G. Walker. 1981.** The tenacity of the limpet, *Patella vulgata* L.: an experimental approach. *J. Exp. Mar. Biol. Ecol.* **54:** 277–308.
11. **Lindberg, D. R. 1981.** *Acmaeidae: Gastropoda, Mollusca.* Boxwood Press, Pacific Grove. 122 pp.

Reference: *Biol. Bull.* **184**: 342–345. (June, 1993)

Immunological Resorption in *Botryllus schlosseri* (Tunicata) Chimeras is Characterized by Multilevel Hierarchial Organization of Histocompatibility Alleles. A Speculative Endeavor

BARUCH RINKEVICH

Marine Biology Department, National Institute of Oceanography, Tel-Shikmona, P.O.B. 8030, Haifa 31080, Israel

Laboratory studies on chimeras of the tunicate Botryllus schlosseri *revealed the phenomenon of "allogeneic resorption" or "colony resorption," the elimination of one partner in a chimera. A hypothesis outlining the genetic basis of the resorption phenomenon is presented here. It proposes that allogeneic resorption in* Botryllus *is controlled by a polymorphic, ladder-like, tri-level hierarchial system of histocompatibility loci, with codominantly expressed alleles. The relative state of homozygosity at these alleles within each level reflects the state of the hierarchy in the resorption phenomenon. The Fu/HC haplotype of the tunicates serves as the first level, whereas the other two levels are each controlled by specific resorption alleles (Rc/HC) that operate only after a response has failed to occur at previous levels. Some morphologically expressed similarities to murine minor histocompatibility loci (Hh-1 and M1s) are discussed.*

Members of the colonial protochordate *Botryllus schlosseri*, a cosmopolitan, encrusting, subtidal species, have the property of forming either a natural transplantation (vascular anastomosis) or a rejection when confronting conspecific colonies. This histocompatibility character is controlled by a single, highly polymorphic Mendelian locus, with multicodominantly expressed alleles (1–3). This locus, termed the tunicate Fu/HC haplotype (4, 5), resembles in some of its properties the vertebrate MHC, the major histocompatibility complex (3). However, the rules for histocompatibility in *Botryllus* differ significantly from the MHC-dependent graft rejection of vertebrates, in which grafts are accepted only between animals that express the same form of each type of histocompatibility antigens. In tunicates, two colonies sharing at least one allele at the Fu/HC locus may fuse, whereas rejection develops only between colonies that share no allelic determinant at this locus.

In many laboratory studies done with several hundred pairs of fused colonies (chimeras), we have shown (4–12) that once colonies have fused, the chimeras do not survive or grow as well as genetically identical subclones that were left separate. Moreover, fusions usually terminate in the unilateral, morphological elimination of all zooid elements of only one partner within each specific chimera, a phenomenon termed "allogeneic resorption" or "colony resorption" (5). Colony resorption appears to be determined genetically, rather than by relative contribution to the chimera; *i.e.*, when multiple ramets from colony A are allowed to fuse with ramets from colony B, the direction of resorption is usually the same. Progenitor zooids of only one interacting genotype in each pairwise combination are the chimeric survivors.

Our two recent publications (4, 13) have provided some insight into the genetic background governing colony resorption. When pairs of colonies were selected genotypically for "one way allorecognition" (*e.g.*, AA *vs.* AB), the Fu/HC homozygotic partners were resorbed preferentially, but not exclusively [(4) and Y. Saito, unpub.]. This result does not follow the rules underlying MHC-related graft rejection in vertebrates, where the differences in the biochemical composition of the MHC molecules in a similar assay will be recognized only by the homozygotic partner, which will destroy the cells of the heterozygotic individual. In addition, resorption was recorded in chimeras estab-

Received 1 March 1993; accepted 20 March 1993.

lished with colonies that were both homozygous at the Fu/HC locus [*i.e.*, AA *vs.* AA (4, 13)], which implied the involvement of additional genetic elements.

To further analyze this possibility, we established 121 pairs of chimeric partners by fusions of relatives from four generations within a pedigree, all homozygotes (AA line) at their Fu/HC haplotype (13). This was carried out by self- and defined-crosses done in the laboratory on two outbred founder colonies (each AB at the fusibility locus) which were taken from the field. We found that the resorption phenomenon within each generation of colonies is characterized by a linear hierarchy which is expressed by the existence of at least five intermediate hierarchial rungs (*i.e.*, colony A repeatedly resorbs colonies, B, C, D, E; colony B resorbs colonies C, D, E; and so on). Analysis of resorption hierarchies between generations revealed that mother colonies always resorbed their self-crossed offspring. Colonies low in the hierarchy within a specific generation reproducibly resorbed the self-crossed offspring of a superior kin. Chimeras between defined-crossed offspring and self-crossed offspring of different generations revealed nontransitive hierarchies (*i.e.*, colony A resorbs colony B; colony B resorbs colony C; but colony C resorbs colony A) in the resorption; these were correlated with the relative position of each colony in the linear hierarchy established within each generation (major results are schematically illustrated in Fig. 1).

In this essay I speculate on the genetic framework underlying the resorption phenomenon. I propose that allogeneic resorption in *Botryllus* is elicited and controlled by a polymorphic, ladder-like, tri-level hierarchial system of histocompatibility elements (Fig. 1; Table I). Hierarchy

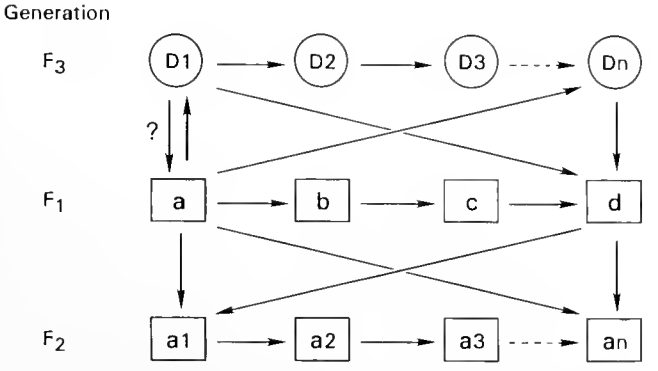

Figure 1. A schematic illustration of the hierarchies in the resorption phenomenon as revealed by a study of three successive generations of *Botryllus schlosseri* colonies, all AA on their Fu/HC locus (13). Squares refer to self-crossed offspring, circles are for the defined-crossed offspring. The arrows point to the inferior partner. Within each generation, colonies of the left side are the most dominant and those of the right side are the subordinates. The question mark refers to a possible additional route of resorption that was not completely verified. The letters a to d refer to specific colonies of the F_1 generation; al to an are the self-crossed offspring of colony a; and Dl to Dn are the defined-crossed F_3 colonies (13).

Table I

A proposed ladder-like, tri-level, hierarchial organization of histocompatibility alleles in Botryllus schlosseri

Level no.	Controlling locus/loci*	Experimental protocol**	Major results***
1	Fu/HC	AX *vs* AA	Heterozygote > homozygote in most cases.
2	Re/HC	CAAs of self-crossing: generations II vs. III. All AA on Fu/HC.	Heterozygote > homozygote.
3	Re/HC	CAAs within generations II, III, IV, respectively. All AA on Fu/HC.	Linear hierarchy (at least 5 intermediate groups) in resorption within each generation. Heterozygote > homozygote?

* Fu/HC = fusibility-histocompatibility locus; Re/HC = resorption-histocompatibility locus or loci.

** CAA = colony allorecognition assay. Generation numbers refer to Rinkevich *et al.* (1993), Figs. 1, 2.

*** From Weissman *et al.* (1990); Rinkevich *et al.* (1993); Y. Saito (unpub.).

in the resorption phenomenon is best explained as being associated with the proportion of homozygosity to heterozygosity among the large numbers of polymorphic histocompatibility loci characterizing the partners within a chimera. Resorption (Fig. 1; Table I) is expressed morphologically in accordance with the following three assumptions:

(1) *The levels.* The Fu/HC haplotype of tunicates is the first level of the theoretical multilevel hierarchial organization of histocompatibility alleles in *Botryllus*, and is the first to be morphologically expressed. This immunological locus encodes three types of cellular interactions: rejection, fusion, and resorption, all observable in Fu/HC disparate *Botryllus* colonies. The second level, which is controlled by specific resorption alleles (Fig. 1, Table I), operates only after the failure of resorption by the first level, is encoded by a different locus or loci, and has no effect on fusion-rejection processes. Similarly, the third level is expressed after lack of a resorption response from the second level.

(2) *Induction.* The resorption initiated by the second level of histocompatibility is elicited or stimulated by a trigger from the alleles of the first level. Moreover, these two levels are not genetically linked and are independently expressed. The same two attributes are relevant to the induction of the third level.

(3) *Re/HC alleles.* Colonies that are heterozygous with respect to the histocompatibility alleles in each of the three levels resorb homozygous colonies. At the first level, AA colonies on the tunicate Fu/HC will be absorbed by AX

colonies. But when both partners in a chimera are homozygotic (*i.e.*, AA *vs.* AA) or heterozygotic (*i.e.*, AB *vs.* AB; AB *vs.* BC) at the Fu/HC locus, the direction of the resorption cannot be determined by this level. At this point, the second level, controlled by the tunicate Re/HC (resorption-histocompatibility loci), is expressed, and the partner which is more heterozygous on this level will be the survivor. As a result, a mother colony will resorb its own self-crossed offspring, or the self-crossed offspring of a kin colony. I also assume that all histocompatibility alleles within each level are codominantly expressed. In any case, the relative state of homozygosity of these alleles within each level is reflected in the state of the resorption hierarchy.

Features of *Botryllus* histocompatibility that are homologous or analogous to vertebrate MHC and non-MHC recognition elements were also sought. An example is the assumption that Fu/HC and Re/HC heterozygotes will resorb Ru/HC and Re/HC homozygotes (Fig. 1; Table I). This is reminiscent of one type of rejection that occurs in the murine immune system; it is called the "hybrid resistance phenomenon" and is controlled by loci designated Hh-1 (14). In this phenomenon, irradiated F_1 heterozygotic mice that have been inoculated with syngeneic (homozygotic) bone marrow cells, reject these cells within a few days of grafting. The result is against the primary genetic rule of vertebrate transplantation: that an F_1 hybrid should not resist grafts from either of its parents.

Also intriguingly similar are the mouse minor lymphocyte stimulating (Mls) genes (15) which can stimulate proliferative responses of T-cells in mixed lymphocyte cultures that contain cells derived from strains identical at the MHC. Mls antigens are encoded by various mouse mammary tumor viruses that have been integrated into the murine germ line as DNA proviruses, but are inherited in a Mendelian fashion [reviewed in (16, 17)].

Below are some of the properties noted in the resorption phenomenon which are also observed in the Mls. As was suggested for the Fu/HC and the Re/HC loci (Fig. 1; Table I), several distinct Mls loci are scattered throughout different chromosomes (17, 18). Contrary to the usual bidirectional mixed lymphocyte reactions (MLRs) elicited by MHC disparaties, many of the Mls responses are unidirectional (18) and thus resemble the hierarchy of the tunicate resorption (13). Mls-specific MLRs (18), like responses elicited by other minor histocompatibility loci in the murine system (19, 20), have quantitative parameters in their expressions similar to the responses obtained in *Botryllus* resorption phenomena (4, 6, 7). Mls specific MLRs also show high polymorphism in the induction of clonal deletion *in vivo* and in T-cell activities *in vitro* (21). As in the *Botryllus* system, the *in vitro* T-cell proliferation that follows the mixing of naive Mls disparate cells, may be measured even without pre-immunizing the animal and *in vivo* challenge (16). Additionally, both the Mls (18) and the resorption (6) systems are characterized by some reciprocal response patterns. Neither the memory components of clonal expansion, nor long-term maintenance of heightened effector functions, were found in these two recognition responses (11, 16–18).

The above analysis of the resorption phenomenon has been studied solely by the assessment of *in vivo* responses of chimeras living in a laboratory setting. These studies (4–13) revealed, for the first time in invertebrates, a second morphologically expressed set of allorecognition responses that are, at least partly, unlinked to the first set of responses, the fusion-rejection processes (1–3). This speculative essay was meant to integrate the accumulated results of the last six years of work on *Botryllus* resorption phenomena into one plausible genetic framework—a hypothesis that will be challenged in further experimental tests. Of course the hypothesis is not perfect; remaining questions will be resolved in future experiments, which will include such diverse approaches as: studies with *Botryllus* inbred lines, *in vitro* experiments on blood cell lines (22), and biochemical and molecular initiatives.

Whether the tunicate resorption phenomenon evolved as a transplantation barrier unique to this group of organisms, or whether it contains an important evolutionary clue that will improve our general understanding of chordate immune systems, it will emerge as a unique example of an allorecognition system aimed at preserving clonal integrity.

Acknowledgments

I am indebted to Irv Weissman for his friendship and insightful, stimulating discussions which motivated me to present this essay. Thanks are also due to S. Sorger and D. Stoner for valuable comments. This study was supported by a Career Development Award from the Israel Cancer Research Fund, USA, by a grant from the United States-Israel Binational Science Foundation, and by a generous grant from S. Price, NAF/IOLR.

Literature Cited

1. **Oka, H., and H. Watanabe. 1960.** Problems of colony specificity in compound ascidians. *Bull. Mar. Biol. Stn. Asamushi* **10:** 153–155.
2. **Sabbadin, A. 1962.** La basi genetishe della capacita di fusione fra colonie in *Botryllus schlosseri* (Ascidiacea). *Red. Accad. Lincei* **32:** 1031–1035.
3. **Scofield, V. L., J. M. Schlumpberger, L. A. West, and I. L. Weissman. 1982.** Protochordate allorecognition is controlled by an MHC-like gene system. *Nature* **295:** 499–502.
4. **Weissman, I. L., Y. Saito, and B. Rinkevich. 1990.** Allorecognition histocompatibility in a protochordate species: is the relationship to MHC semantic or structural? *Immunol. Rev.* **113:** 227–241.
5. **Rinkevich, B., and I. L. Weissman. 1992.** Allogeneic resorption in colonial protochordates: consequences of nonself recognition. *Dev. Comp. Immun.* **16:** 275–286.

6. **Rinkevich, B., and I. L. Weissman. 1987.** A long-term study on fused subclones in the ascidian *Botryllus schlosseri*. the resorption phenomenon (Protochordata: Tunicata). *J. Zool.* **213:** 717–733.
7. **Rinkevich, B., and I. L. Weissman. 1987.** The fate of *Botryllus* (Ascidiacea) larvae cosettled with parental colonies: beneficial or deleterious consequences? *Biol. Bull.* **173:** 474–488.
8. **Rinkevich, B., and I. L. Weissman. 1987.** Chimeras in colonial invertebrates: a synergistic symbiosis or somatic and germ-cell parasitism? *Symbiosis* **4:** 117–134.
9. **Rinkevich, B., and I. L. Weissman. 1989.** Variation in the outcomes following chimera formation in the colonial tunicate *Botryllus schlosseri*. *Bull. Mar. Sci* **45:** 213–222.
10. **Rinkevich, B., and I. L. Weissman. 1990.** *Botryllus schlosseri* (Tunicata) whole colony irradiation: do senescent zooid resorption and immunological resorption involve similar recognition events? *J. Exp. Zool.* **253:** 189–201.
11. **Rinkevich, B., and I. L. Weissman. 1990.** Failure to find alloimmune memory in the resorption phenomenon of *Botryllus* cytomictical chimera. *Eur. J. Immunol.* **20:** 1775–1779.
12. **Rinkevich, B., and I. L. Weissman. 1992.** Chimeras *vs* genetically homogeneous individuals: potential fitness costs and benefits. *Oikos* **63:** 119–124.
13. **Rinkevich, B., Y. Saito, and I. L. Weissman. 1993.** A colonial invertebrate species that displays a hierarchy of allorecognition responses. *Biol. Bull.* **184:** 79–86.
14. **Cudcowich, G. M. 1968.** Hybrid resistance to parental grafts of hematopoietic and lymphoma cells. Pp. 661–691 in *The Proliferation and Spread of Neoplastic Cells*, E. Frei, ed. Williams & Wilkins, Baltimore.
15. **Fenstenstein, H. 1973.** Immunogenetic and biological aspects of *in vitro* lymphocyte allotransplantation (MLR) in the mouse. *Transplant Rev* **15:** 62–88.
16. **Huber, B. T. 1992.** M1s genes and self-superantigens. *TIG* **8:** 399–402.
17. **Coffin, J. M. 1992.** Superantigens and endogenous retroviruses: a confluence of puzzles. *Science* **255:** 411–413.
18. **Abe, R., and R. J. Hodes. 1989.** T-cell recognition of minor lymphocyte stimulating (M1s) gene products. *Ann. Rev. Immunol.* **7:** 683–708.
19. **Graff, R. J., W. K. Silvers, R. E. Billingham, W. H. Hildemann, and G. D. Snell. 1966.** The cumulative effect of histocompatibility antigens. *Transplantation* **4:** 605–617.
20. **Galton, M. 1967.** Factors involved in the rejection of skin transplanted across a weak histocompatibility barrier: gene dosage, sex of recipient, and nature of expression of histocompatibility genes. *Transplantation* **5:** 154–168.
21. **Abe, R., M. Foo-Phillips, L. G. Granger, and O. Kanagawa. 1992.** Characterization of the M1s(f) system. I. A novel "polymorphism" of endogenous superantigens. *J. Immunol* **149:** 3429–3439.
22. **Rinkevich, B., and C. Rabinowitz. 1993.** *In vitro* culture of blood cells from the colonial protochordate *Botryllus schlosseri*. *In Vitro Cell. Dev. Biol* **29A:** 79–85.

INDEX

N

O

P

R

S

T

U

W

Z

CONTENTS